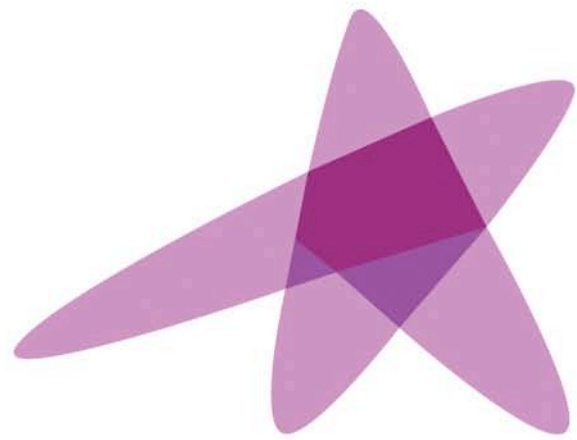


ESTRO

School



ESTRO
School

Advanced Brachytherapy Physics

Treatment Delivery Technologies in Brachytherapy

Prof. Mark J. Rivard, Ph.D., FAAPM

Advanced Brachytherapy Physics, 29 May – 1 June, 2016



Disclosures

The are no conflicts-of-interest to report.

Opinions herein are solely those of the presenter, and are not meant to be interpreted as societal guidance.

Specific commercial equipment, instruments, and materials are listed to fully describe the necessary procedures. Such identification does not imply endorsement by the presenter, nor that these products are necessarily the best available for these purposes.

Learning Objectives

1. Brief history of BT sources and delivery systems
2. LDR BT sources and advancements
3. HDR BT sources and advancements
4. Robotic systems for BT delivery

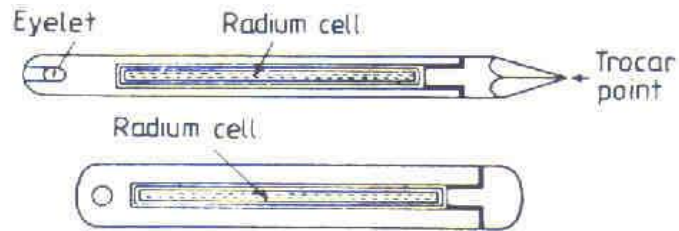
Manually Delivered LDR BT



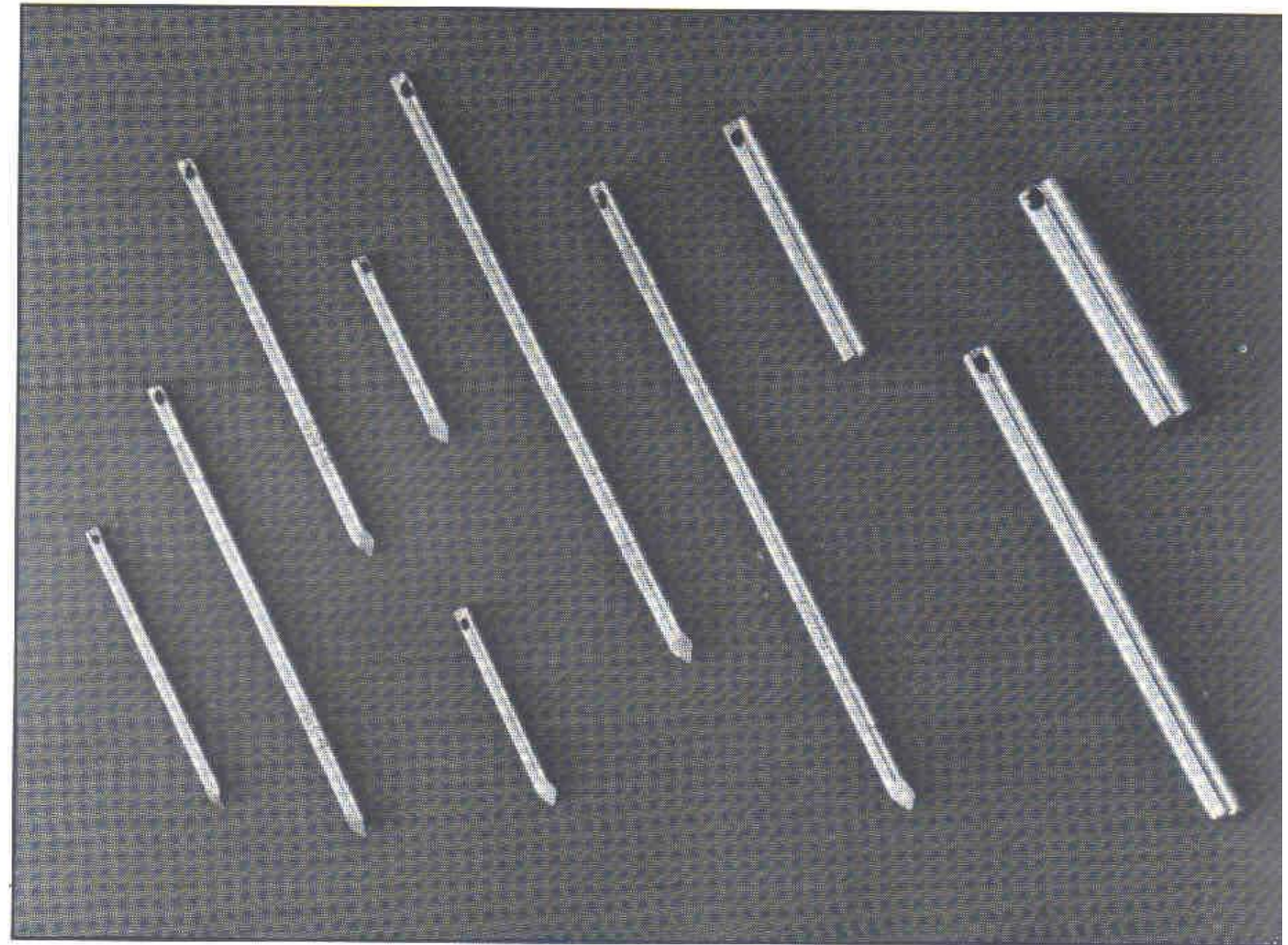
[20.4] Radium plaques being applied in the Skin Department, St. Vincent's Hospital, Melbourne, Australia in 1905¹⁹.

image courtesy of Jack Venselaar

Radium Needles and Tubes



[3.17] Although there was a large range of linear radium sources, tubes and needles, in terms of geometrical and active length and linear activity (milligram radium/cm), the basic design from the early 1920s was essentially that shown in the schematic diagram. Eyelets were used to suture a needle to the patient's tissue to prevent the possibility of its involuntary removal before the end of treatment, or to attach string threads to a tube to enable removal, such as from the uterus or vagina after gynaecological brachytherapy had been completed. Some designs had removable screw-on ends so that different radium cells could be placed in the outer container, depending on the required treatment. Union Minière du Haut Katanga, the Belgian company, supplied such sources in the 1920s, but by the 1950s the Radiochemical Centre, Amersham (later Amersham International), who were then the major supplier of radium sources, had no screw-on end designs and certainly did not supply any radium cells which, because of their very thin walls, were of a much greater hazard than the sealed sources illustrated here. These are the well known G-tubes which were 2 cm geometrical length, and available with different milligram radium contents



such as 10 mg, 15 mg, 20 mg and 25 mg. When radium was replaced by artificially produced radionuclides, such G-tubes then contained caesium-137 with an activity specified in terms of milligram radium equivalent [20.12, 20.56].

Sealed Source Configurations

Physical Forms (schematically)



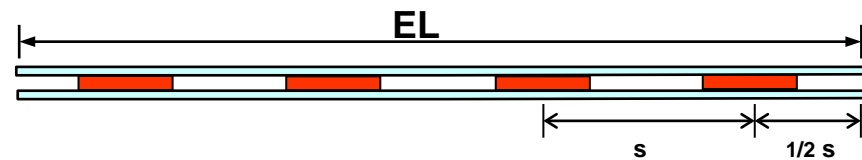
Tube



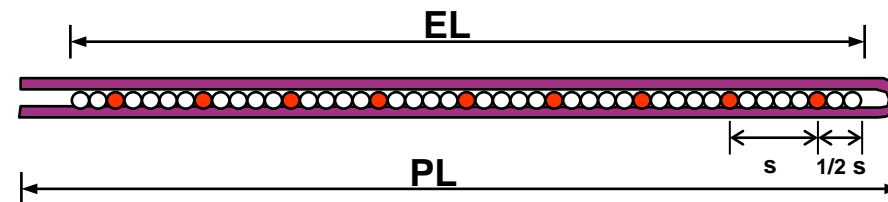
Needle



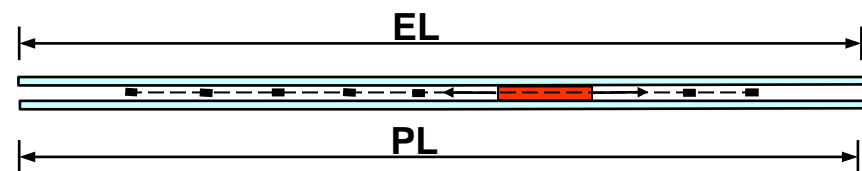
Wire



Seed Ribbon



Source Train

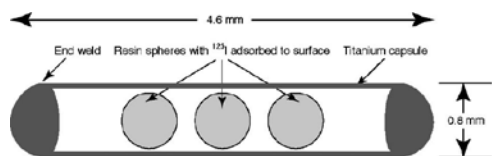


Stepping source

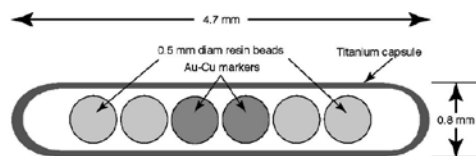
Current LDR Brachytherapy Sources

- Low-energy LDR sources (seeds)
 - ^{125}I and ^{103}Pd most common with ^{131}Cs gaining interest
 - about 4.5 mm long and 0.8 mm diameter capsules
 - treatments either temporary or permanent
 - $0.4 < D_{\text{Rx}} < 2 \text{ Gy/h}$
- High-energy LDR sources (increasingly rarely)
 - ^{137}Cs tubes and ^{192}Ir ribbons or wire
 - treatments mainly temporary (^{137}Cs or ^{192}Ir), or permanent (^{192}Ir)

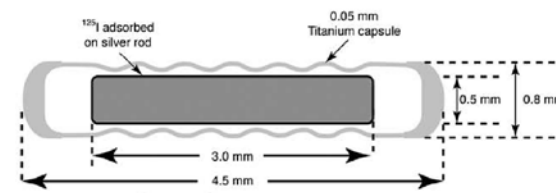
Low-Energy LDR Seeds



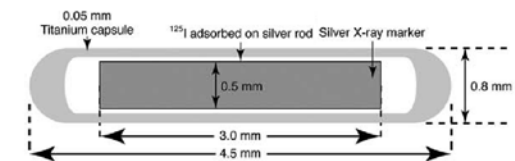
Amersham Health model 6702 source



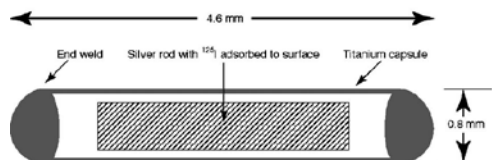
NASI model MED3631-A/M or MED3633 source



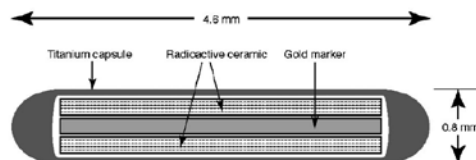
Amersham 6733



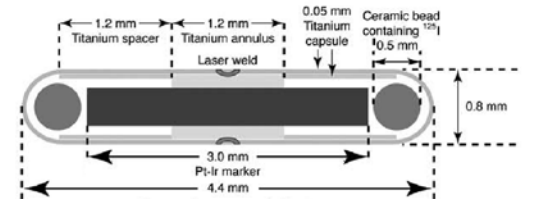
IsoAid Advantage



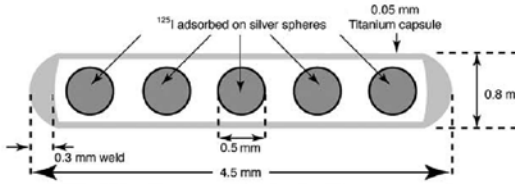
Amersham Health model 6711 source



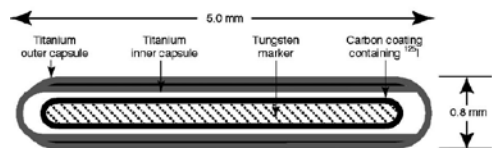
Bebig model I25.S06 source



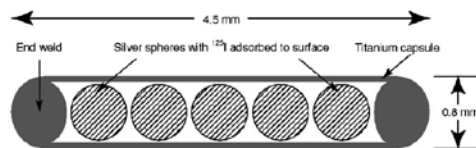
DraxImage LS-1



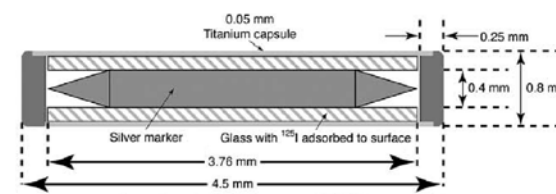
Mills Biopharmaceuticals Prostaseed



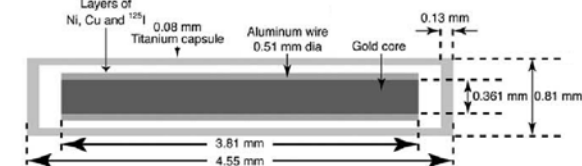
Best model 2301 source



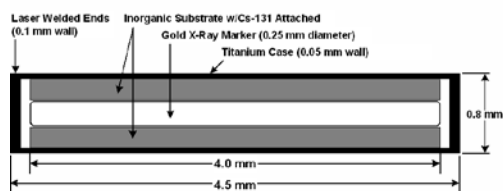
Imagyn model IS-I2501 source



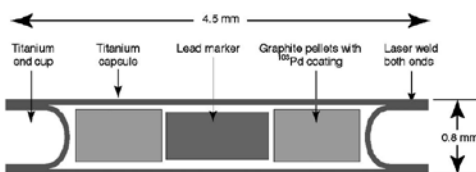
Implant Sciences 3500



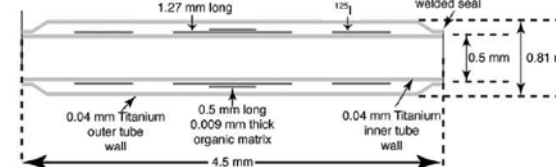
Source Tech Medical STM1251



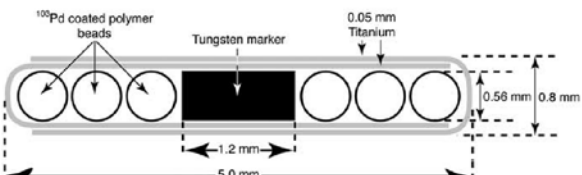
IsoRay model CS-1 Rev2



Theragenics model 200 source

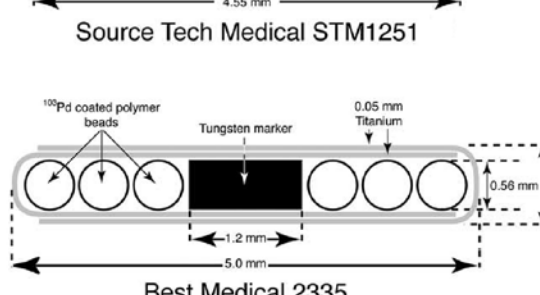
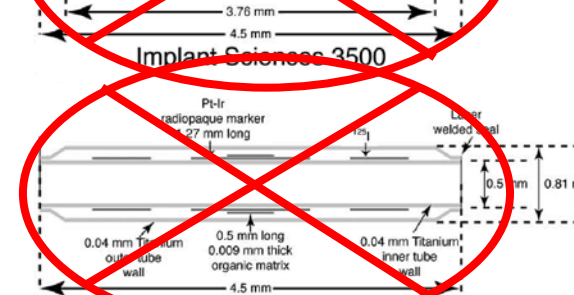
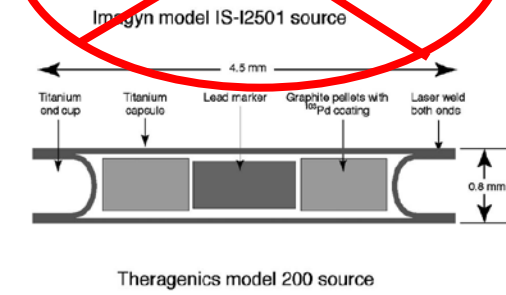
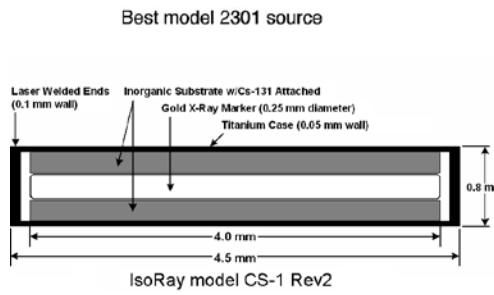
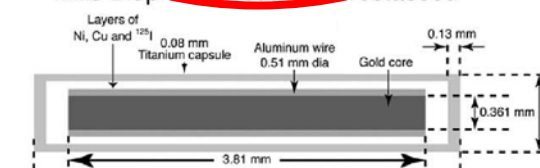
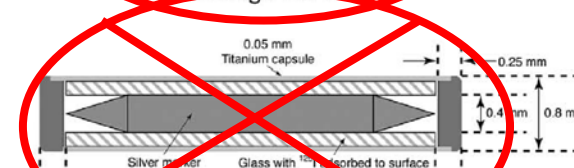
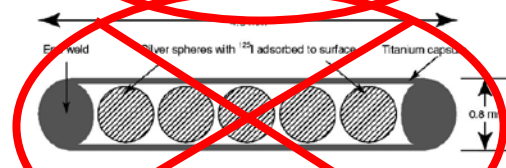
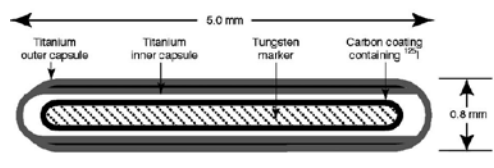
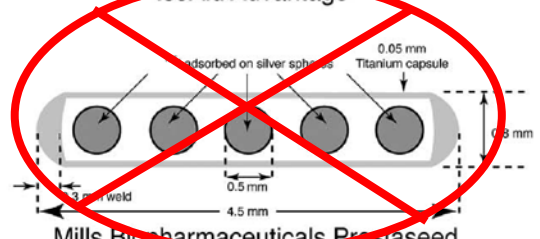
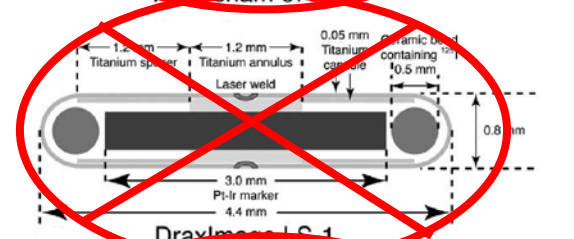
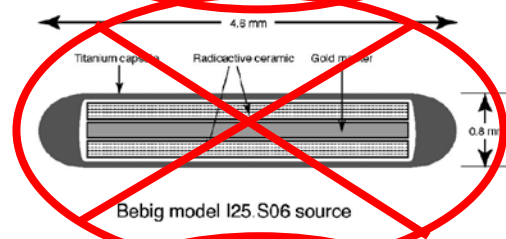
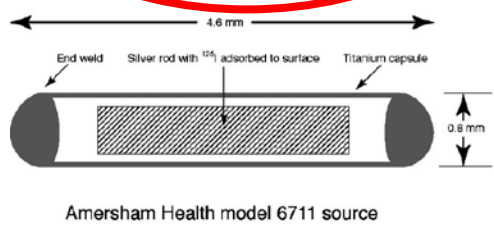
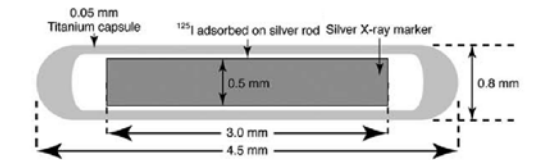
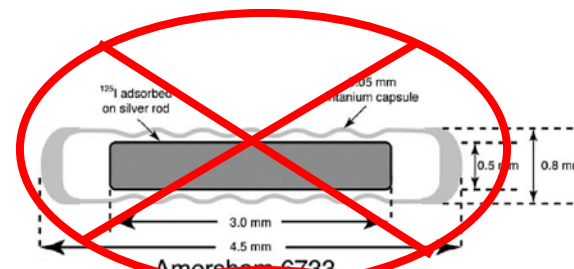
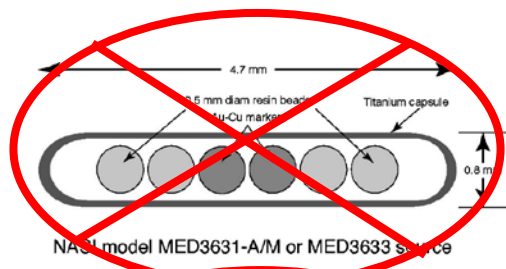
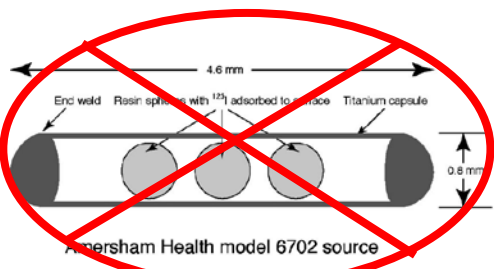


International Brachytherapy InterSource¹²⁵



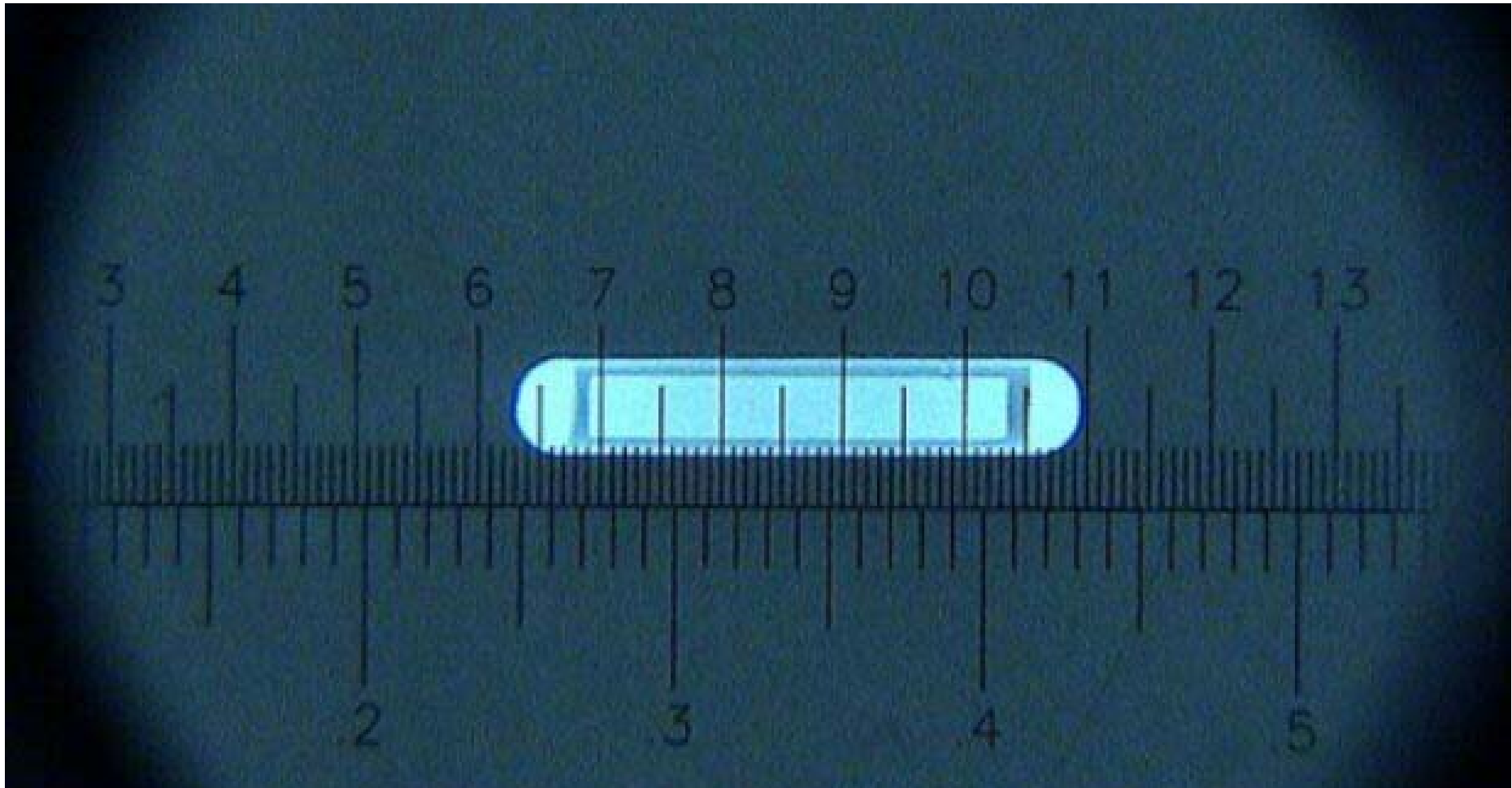
Best Medical 2335

Low-Energy LDR Seeds



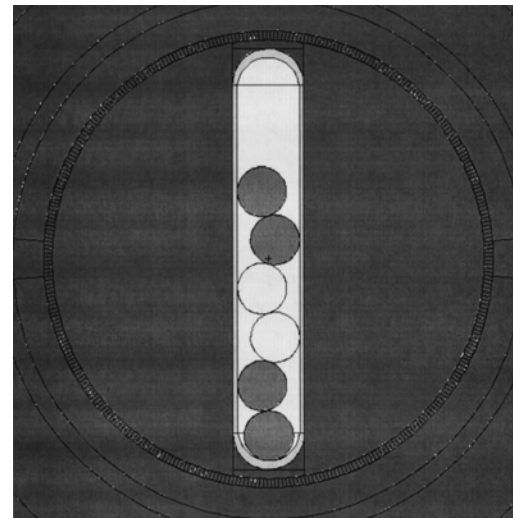
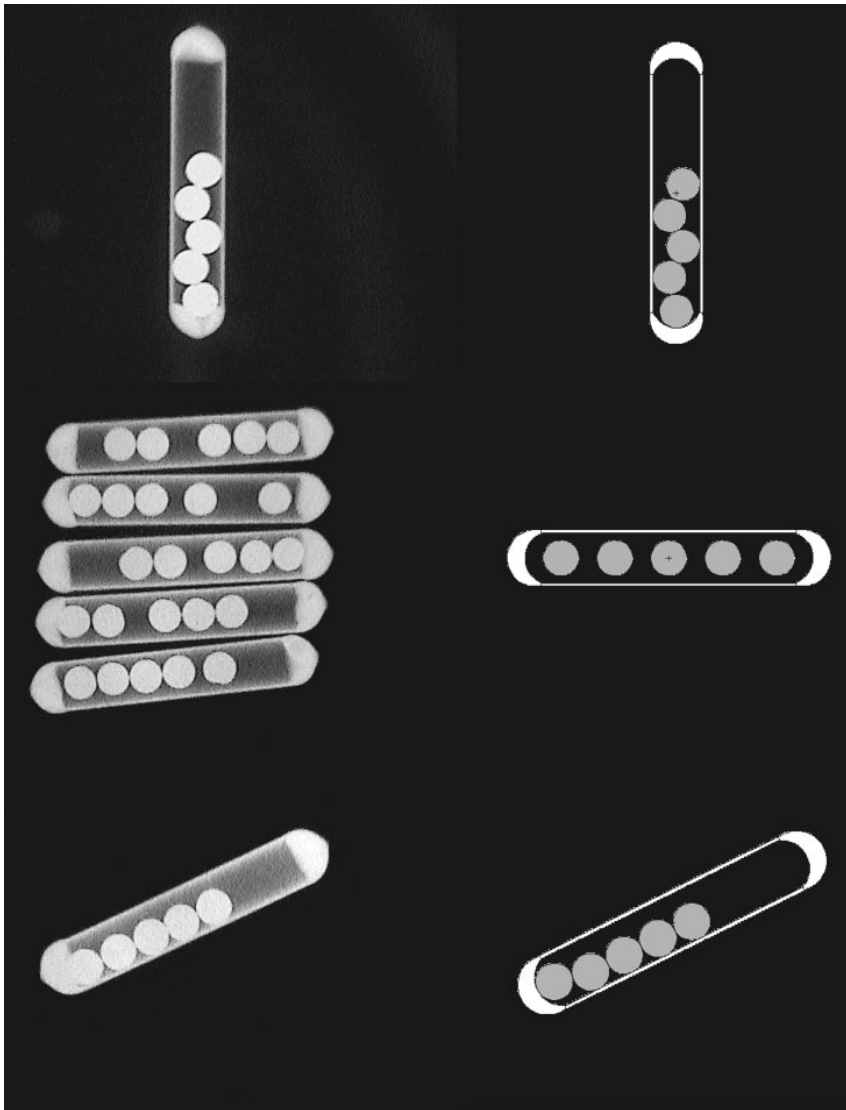
Low-Energy LDR Seeds

Understand the source geometry

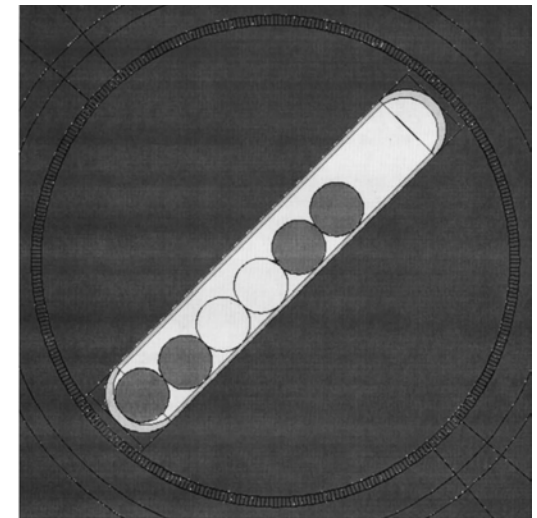


Low-Energy LDR Seeds

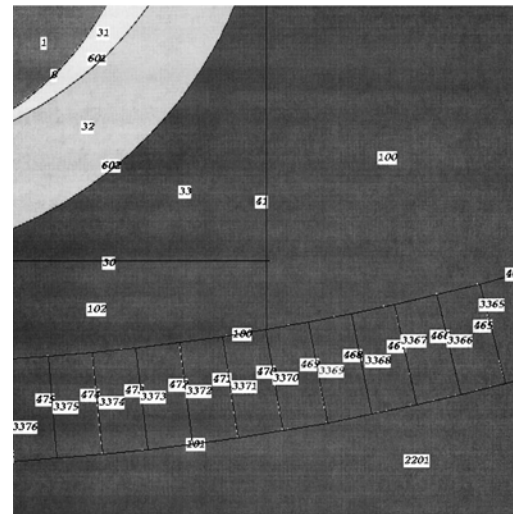
Dynamic source orientation influences some dose distributions



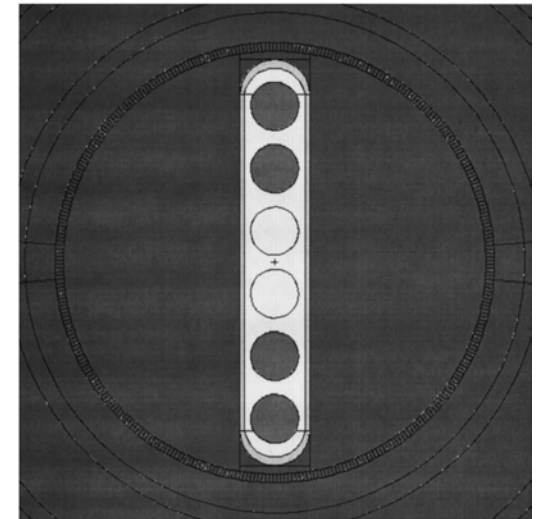
(a)



(b)



(c)



(d)

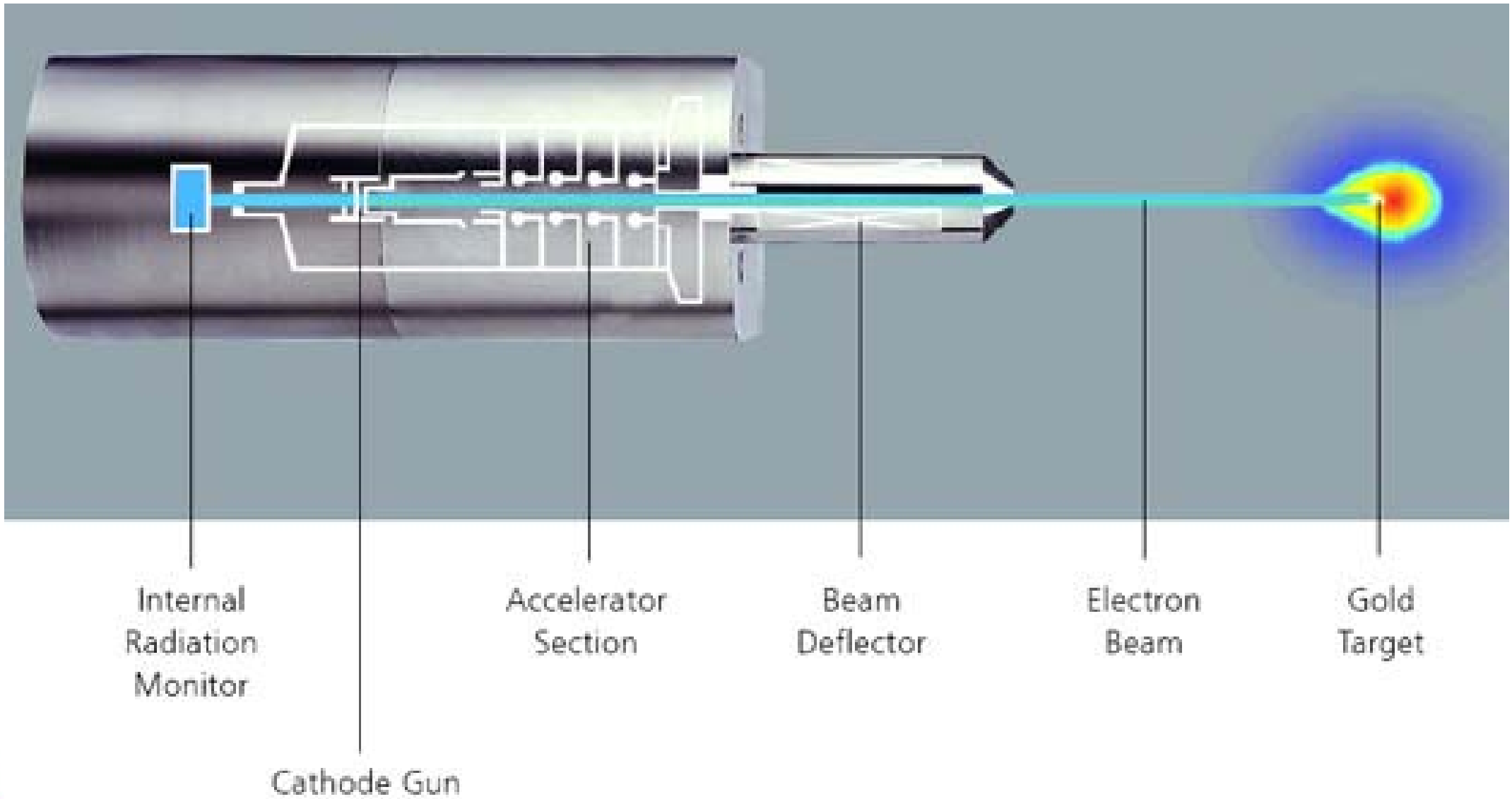
Low-E HDR Brachytherapy Systems

- Low-energy sources for HDR brachytherapy
 - electronic brachytherapy (eBT) can turn on/off
 - similar dose distributions to HDR ^{125}I source
 - independence from a radioactive materials license
 - diminished shielding/licensing/security required
 - potential to replace radionuclide-based brachytherapy like linacs replaced ^{60}Co
- Vendors for eBT brachytherapy systems
 - Carl Zeiss AG (INTRABEAM)
 - Xofigo/iCAD (Axxent)
 - Nucletron/Elekta (esteya)

INTRABEAM System



INTRABEAM X-ray Source



Axxent Controller

touch screen
display

barcode
reader



electrometer



controller
pullback arm

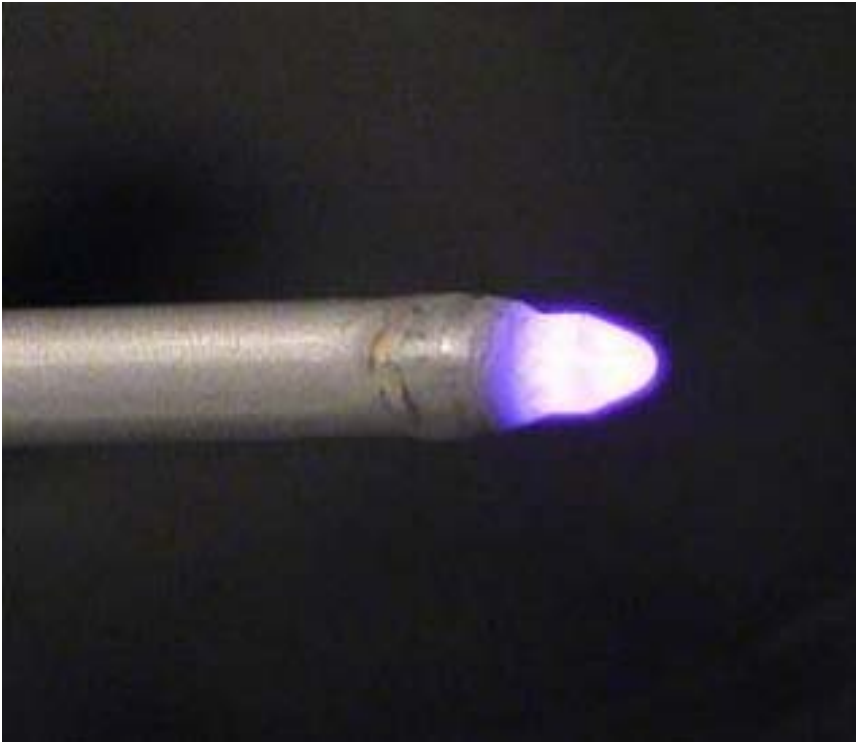
USB port



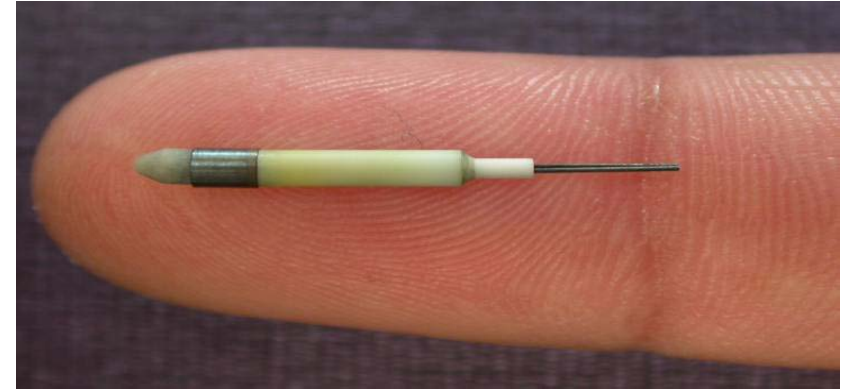
well
chamber



Axxent X-ray Source



light emission from e^-
and x-ray interactions
with anode



x-ray tube size



x-ray source in cooling catheter

esteya System



69.5 kV
10 mm to 30 mm diam.
specific to skin lesions



Medical Physics discussion on eBT

Miniature x-ray tubes will ultimately displace Ir-192 as the radiation sources of choice for high dose rate brachytherapy

Randall W. Holt, Ph.D.

Radiation Oncology Center, Enloe Hospital, Chico, California 95926
(Tel: 530-332-3930, E-mail: randall.holt@enloe.org)

Bruce R. Thomadsen, Ph.D.

Medical Physics, Human Oncology, Engineering Physics and Biomedical Engineering, University of Wisconsin, Madison, Wisconsin 53706
(Tel: 608-263-4183, E-mail: thomadsen@humonc.wisc.edu)

OVERVIEW

Recent advances in the development of miniature x-ray tubes have made electronic brachytherapy a feasible alternative to conventional high dose rate brachytherapy with high activity Ir-192 sources. Because of the obvious radiation safety and security advantages, it is conceivable that the miniature x-ray tube might displace Ir-192 as the source of choice for HDR brachytherapy. This is the proposition debated in this month's Point/Counterpoint.



Arguing for the Proposition is Randall W. Holt, Ph.D. Dr. Holt earned his Ph.D. in Biomedical Engineering at Case Western Reserve University, specializing in 3D-image analysis, after which he received postdoctoral training at the USC Department of Radiation Oncology, specializing in virtual simulation and 3D dosimetry software. Currently Dr. Holt is the Director of

Physics for North Valley Radiation Oncology, which provides a broad range of medical physics services to clinics in Northern California. He is board certified by the ABR in radiation therapy physics.



Arguing against the Proposition is Bruce R. Thomadsen, Ph.D. Dr. Thomadsen earned his M.S. and Ph.D. degrees in Medical Physics at the University of Wisconsin—Madison, where he is currently an Associate Professor in the Department of Medical Physics. He is board certified by the ABR in Radiological Physics, by the ABHP in Comprehensive Health Physics, and by the

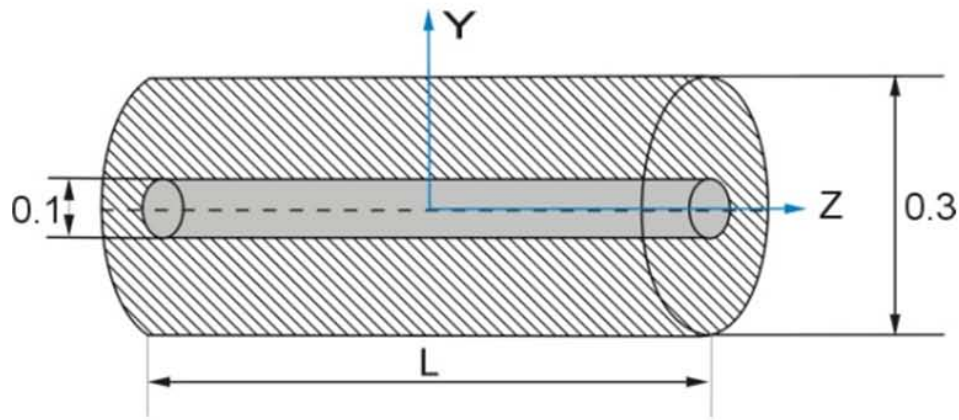
ABMP in Radiation Oncology Physics. His major research interests include all aspects of radiation therapy physics but especially brachytherapy. Dr. Thomadsen currently serves on numerous AAPM committees and task groups and chairs the Radiation Safety Subcommittee and the Special Brachytherapy Modalities Working Group, and is a member of the Board of Editors of *Medical Physics*.

FOR THE PROPOSITION: Randall W. Holt, Ph.D

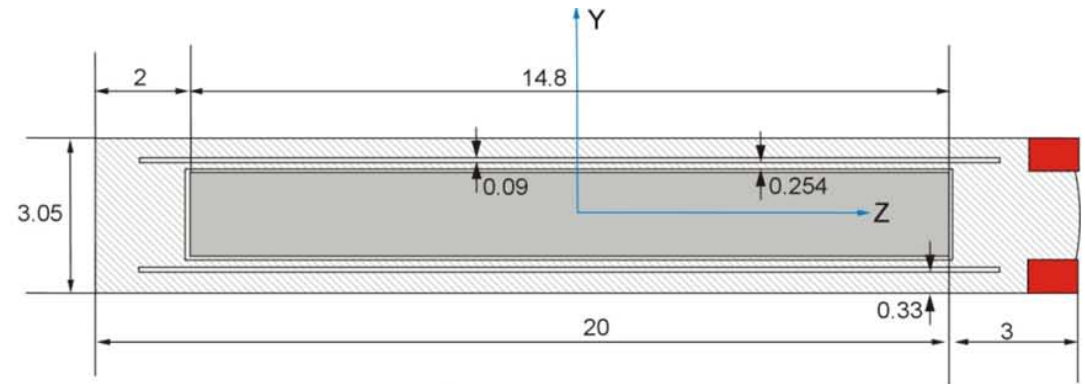
Opening statement

To displace Ir-192, miniature x-ray sources must deliver therapeutic radiation as well as, or potentially better than, Ir-192, under safer conditions, and with favorable economics.

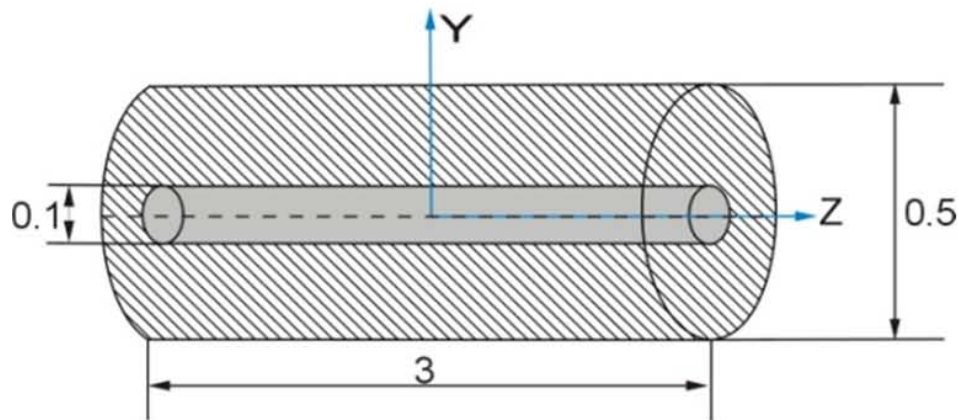
High-Energy LDR Sources



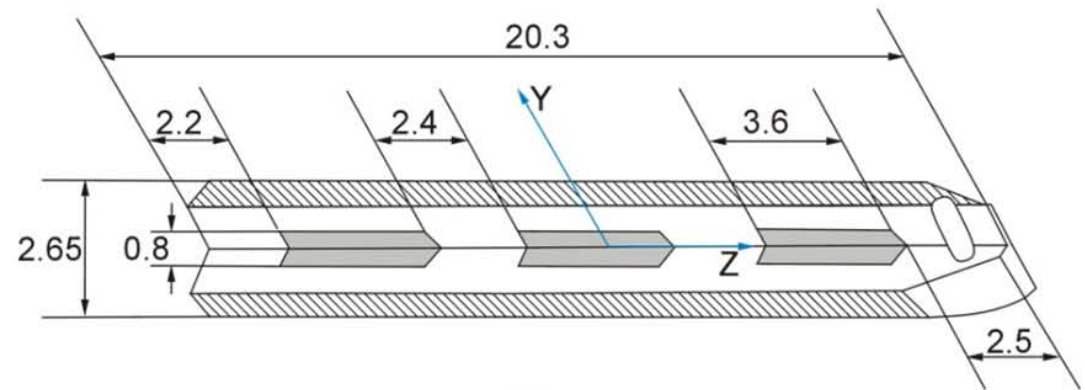
IBt-Bebig LDR ^{192}Ir wires



IPL LDR ^{137}Cs model 67-6520 source

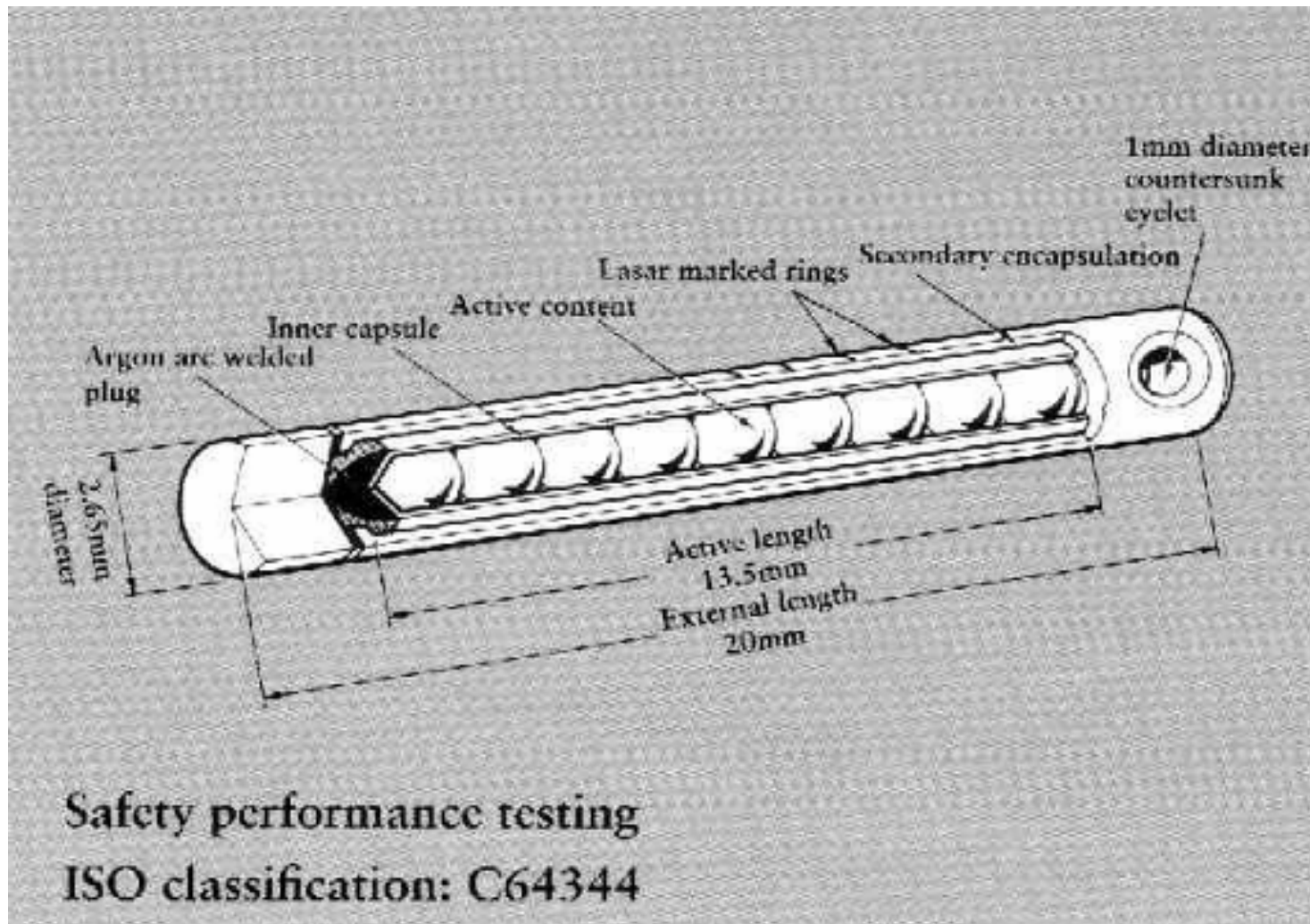


Best Industries LDR ^{192}Ir seed



IBt-Bebig LDR ^{137}Cs model CSM3 source

High-Energy LDR ^{137}Cs Tubes

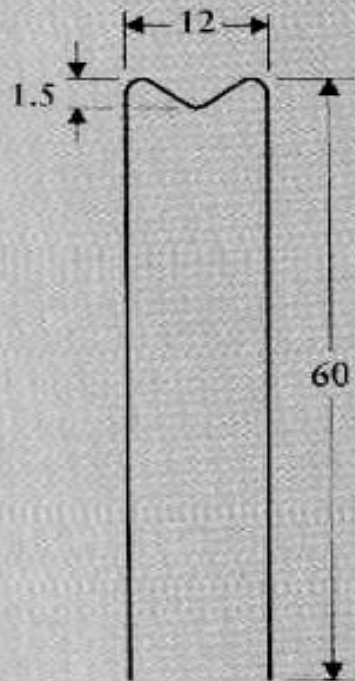


Example of 2 cm tube source
Note difference in active length and external length

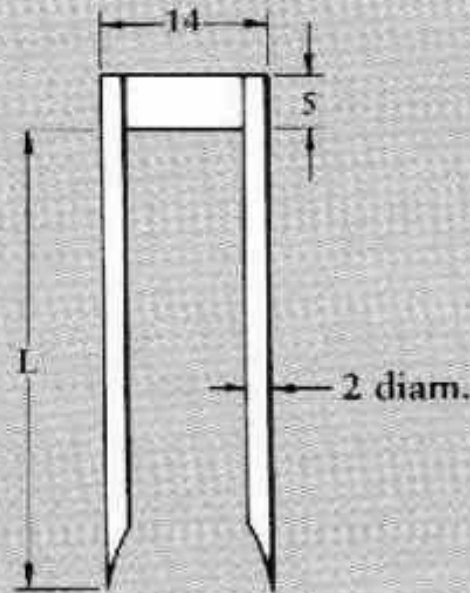
High-Energy LDR ^{192}Ir Hairpins

Special forms of LDR ^{192}Ir sources

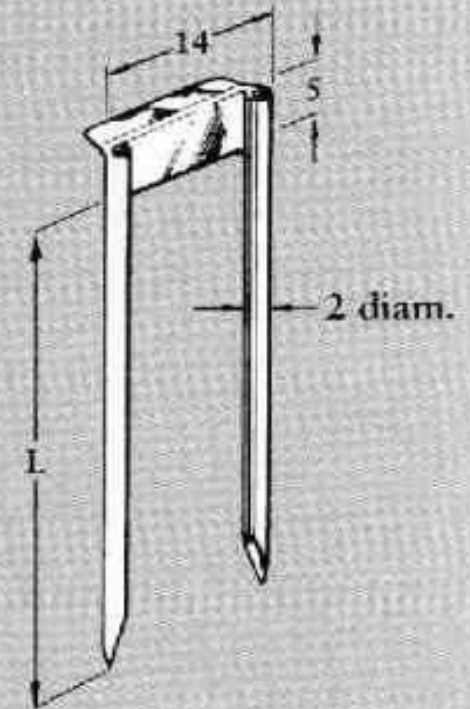
Hairpin
ICW 3040-ICW 3300



Slotted hairpin guide needles
Plain
N474, 476



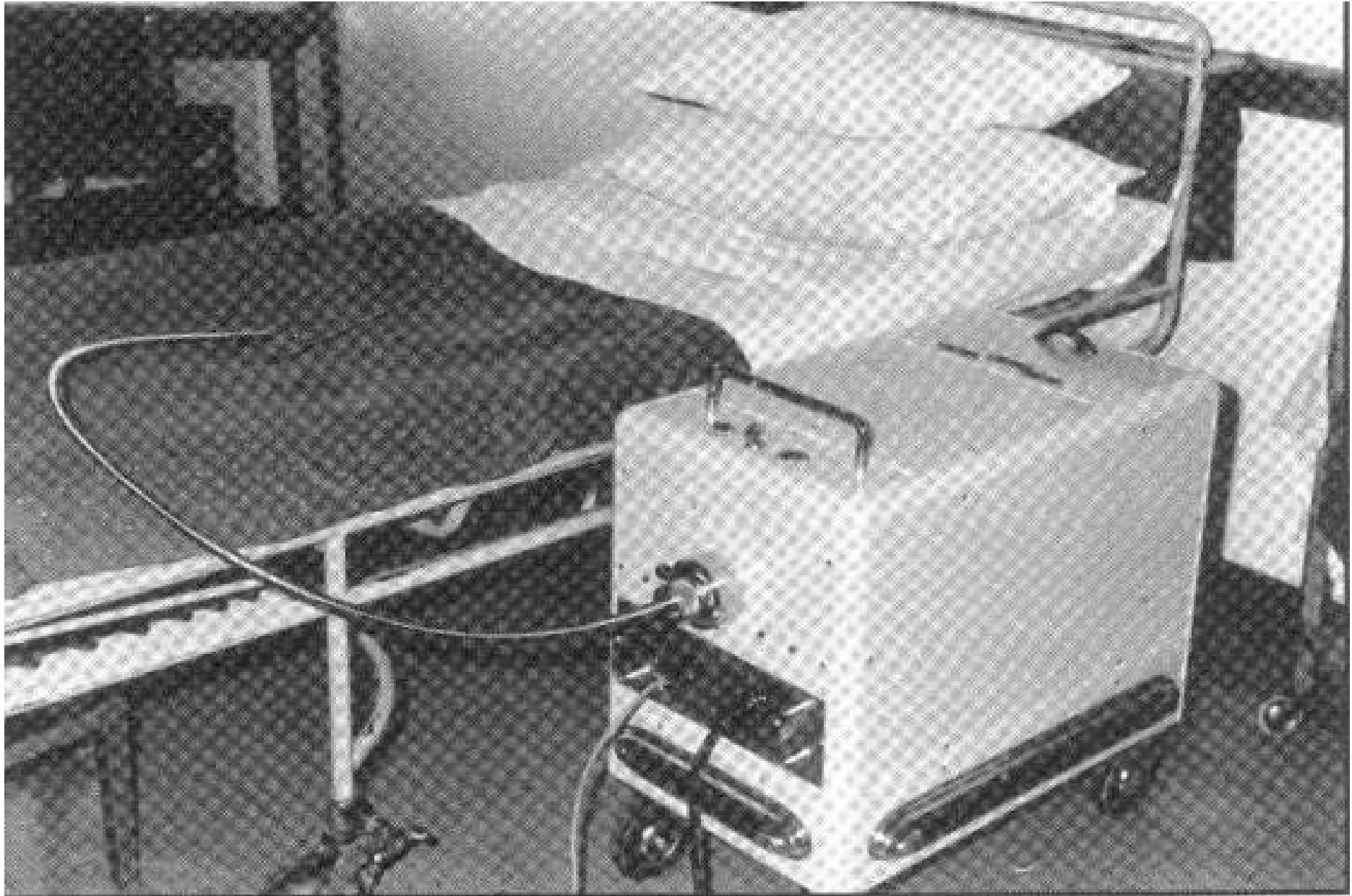
With lip
N484, 486



Left: example of a wire-type source, in “hairpin” form, e.g., for tongue implants

Right: guiding needles for “hairpin”

Remote Afterloading BT

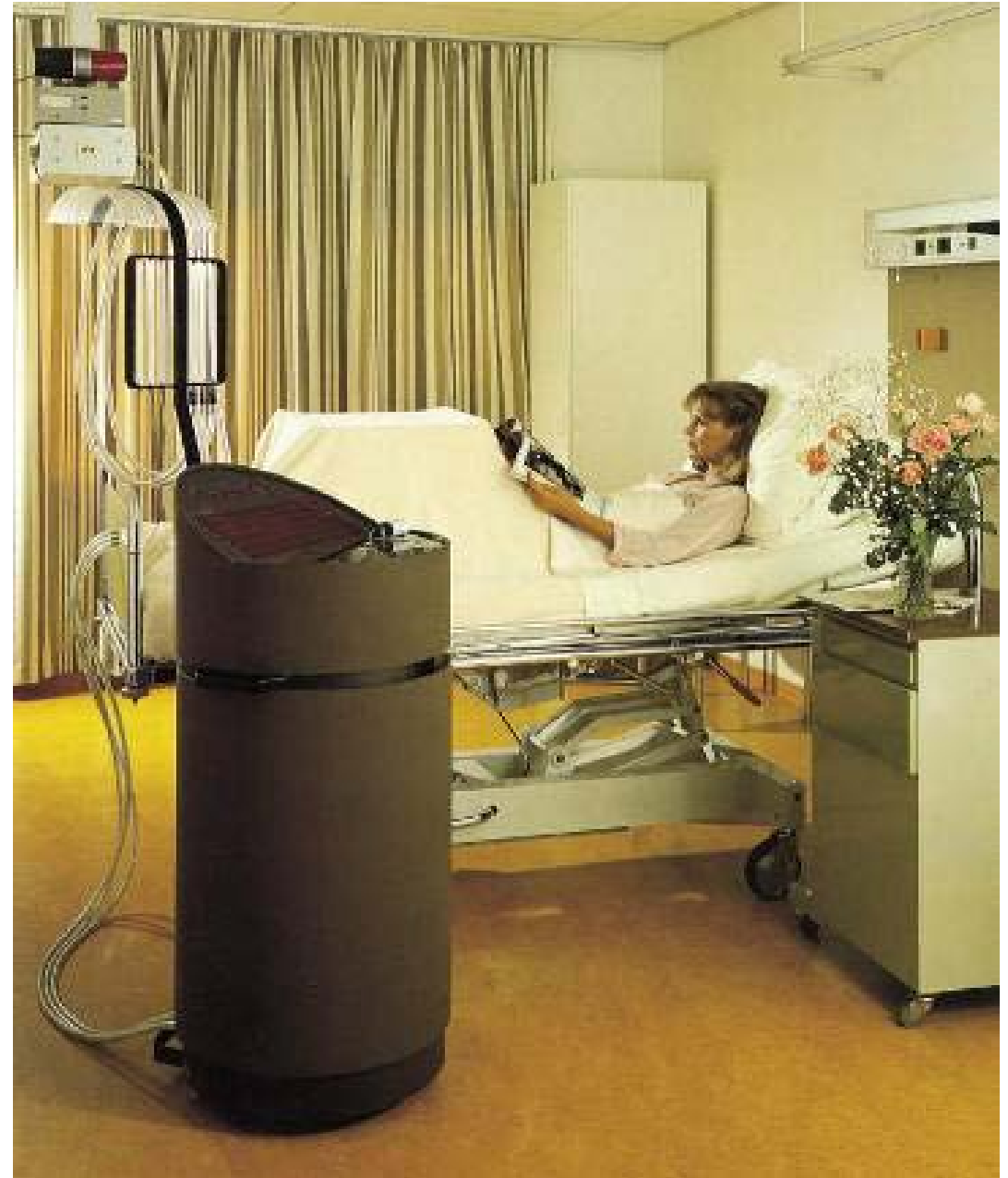


First afterloader ever built

Selectron LDR ^{137}Cs Pellet Afterloaded

3 or 6 channels

**Maximum: 48 sources
(2.5 mm \emptyset pellets)**



Selectron LDR ^{137}Cs Pellet Afterloaded

Afterloader connected to GYN-applicator set

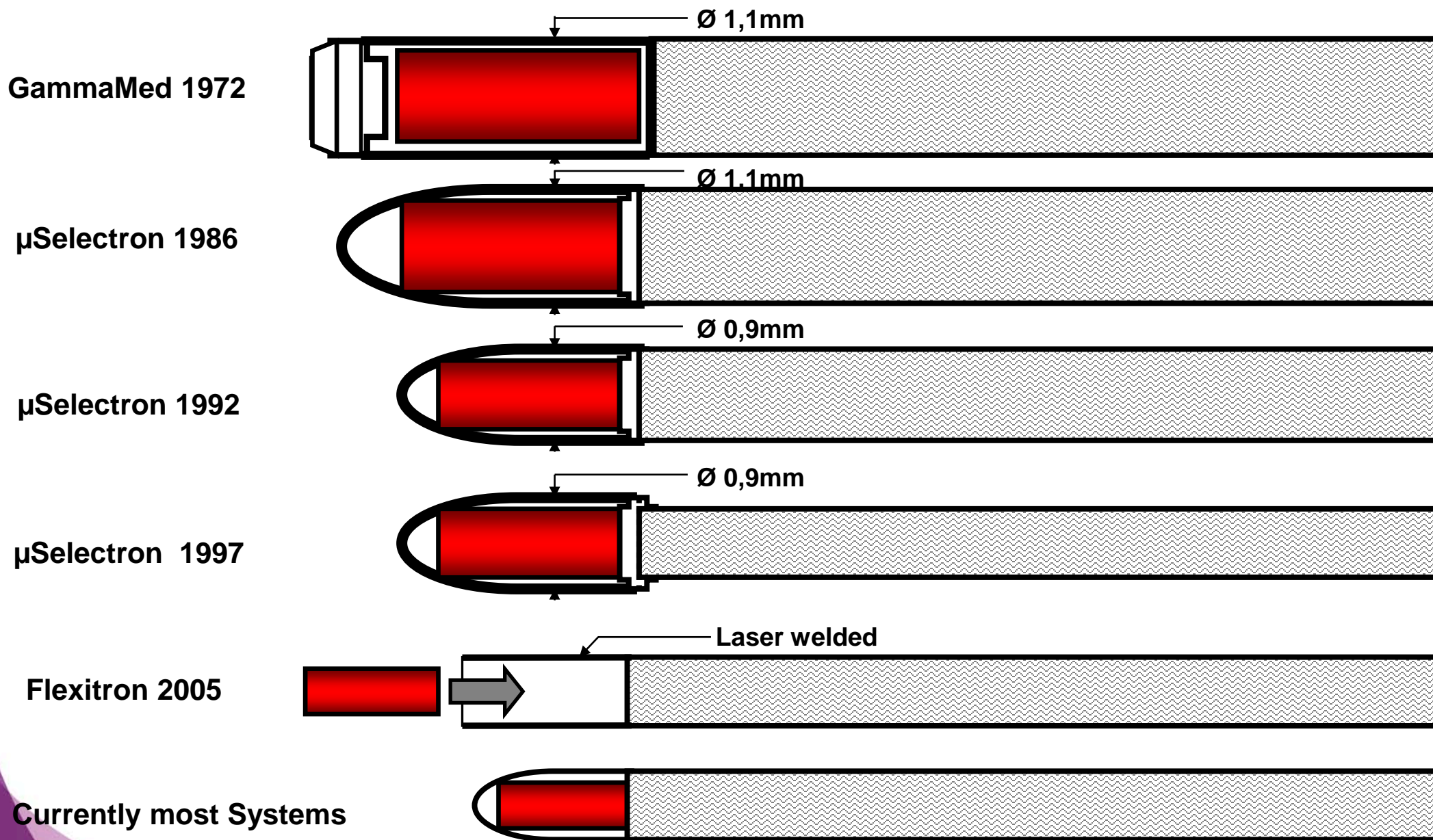


**Source pellets
pneumatically
sorted and
driven to
applicators**

HDR Brachytherapy Systems

- High-energy sources for HDR brachytherapy
 - ^{192}Ir most common with ^{60}Co under development
 - outer diameter ≤ 1 mm
 - treatments from 2 to 20 minutes
 - $D_{\text{Rx}} > 12$ Gy/h or > 0.2 Gy/min.
 - regulatory activity 4 to 12 Ci
 - shielding/licensing required
- Vendors for HDR ^{192}Ir brachytherapy RAUs
 - Nucletron/Elekta (microSelectron + Flexitron)
 - Varian (VariSource + GammaMed)
 - BEBIG (MultiSource)

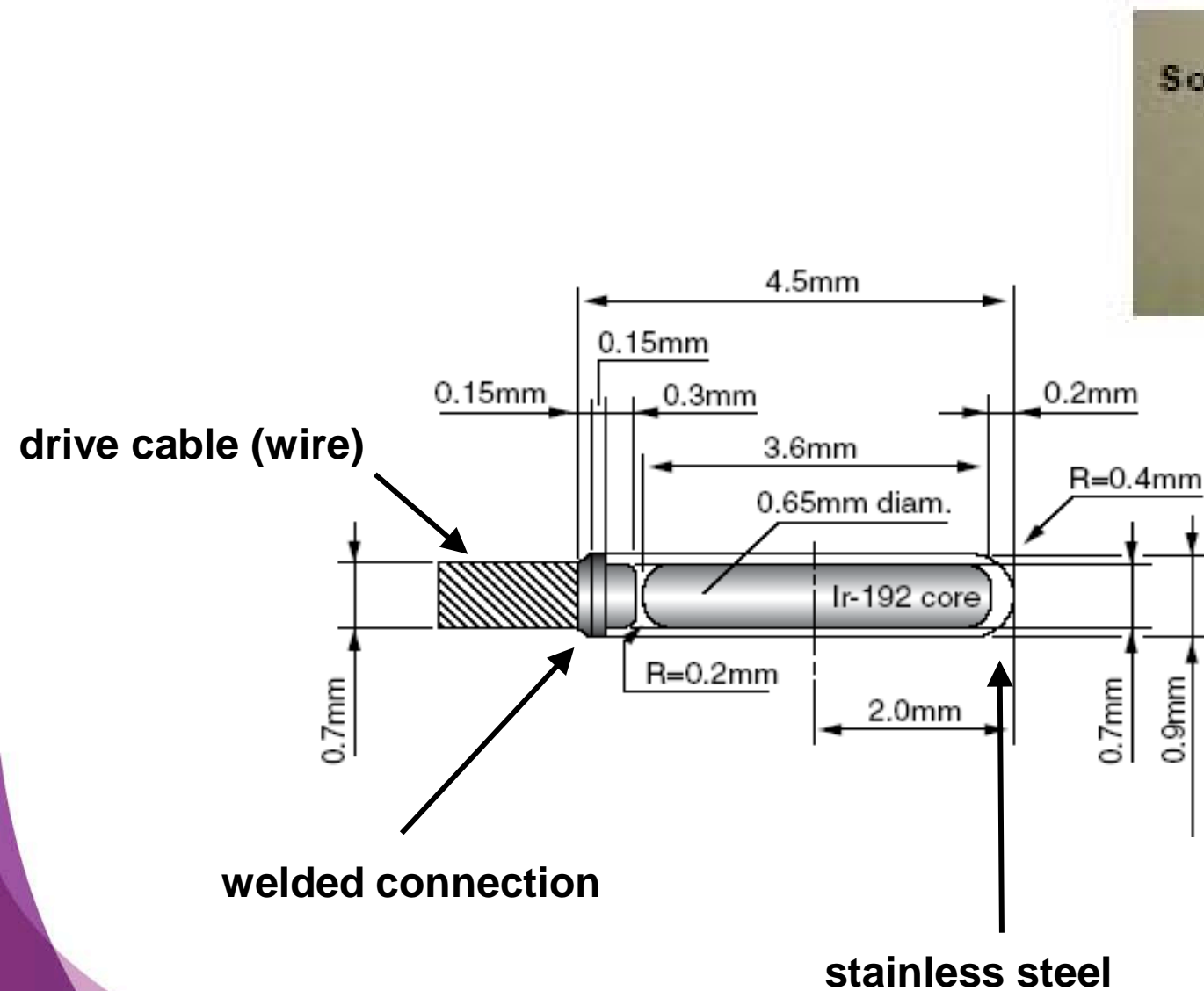
HDR ^{192}Ir Brachytherapy Sources



HDR & PDR have identical dimensions

HDR ^{192}Ir Brachytherapy Sources

Example of miniaturized source welded to the end of a drive cable.



HDR/PDR ^{192}Ir BT Afterloaders: Overview



Varian, GammaMed Plus



Varian, VariSource



BEBIG, MultiSource



Elekta/Nucletron, microSelectron v3



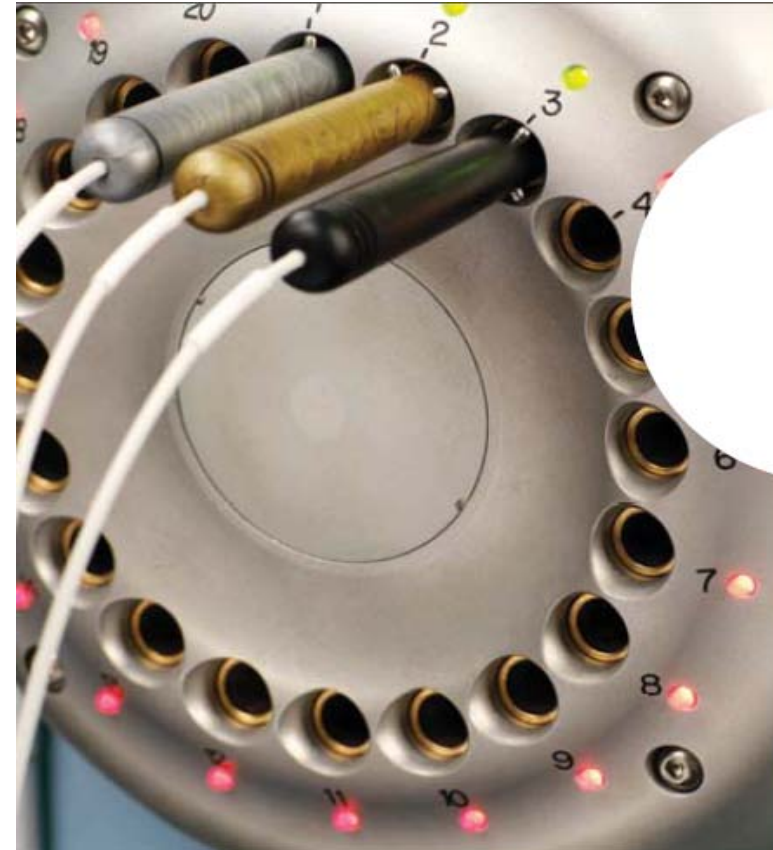
Elekta/Nucletron, Flexitron

Nucletron/Elekta microSelectron



3.5 mm long, 0.9 mm diameter ^{192}Ir source

Varian VariSource



5.0 mm long, 0.59 mm diameter ^{192}Ir source

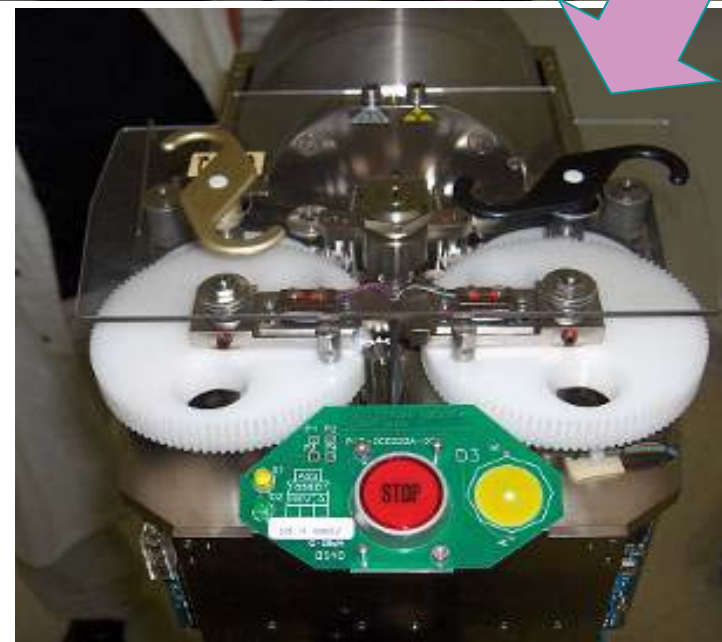


3.5 mm long, 1 mm diameter source
potential for dual HDR ^{192}Ir + ^{192}Ir or HDR ^{192}Ir + ^{60}Co
integrated calibration system for daily verification

Afterloader Head Mechanism



Nucletron, microSelectron v3



Afterloader Properties

TABLE 2.1 Features of Modern HDR and PDR Afterloading Equipment

1. Vendor and Product Specification					
Name of Vendor	Nucletron B.V.	Nucletron B.V.	Eckert & Ziegler BEBIG GmbH	Varian Medical Systems Inc.	Varian Medical Systems Inc.
Website	www.nucletron.com	www.nucletron.com	www.ibt-bebig.eu	www.varian.com	www.varian.com
Name of product(s)	microSelectron Digital 6CH - 18CH - 30CH	Flexitron 40CH	MultiSource: 20 channels (extended to 40 channels in 2011) GyneSource: with 5 channels but same specs as MultiSource	Varisource iX	GammaMedplus iX; GammaMedplus iX 3/24 with 3 channels but same specs
Specify capability for use as HDR and/or PDR	HDR and PDR	HDR and PDR	HDR only	HDR only	HDR for iX models, PDR for non iX models
2. Specifications of Source or Sources					
Single or dual source capability	2 drives	3 drives	Single source	Single source	Single source
Possible types of source (radionuclide), available now and/or under development	¹⁹² Ir	¹⁹² Ir	Co-60: source type Co0.A86 Ir-192: source type Ir2.A85-2	¹⁹² Ir	¹⁹² Ir

(continued)

Refs:

Thomadsen 2000, Achieving Quality in Brachytherapy.

ESTRO Booklet 8 2004, A Practical Guide to QC of Brachytherapy Equipment.

Table taken from Chap. 2 of: Comprehensive Brachytherapy 2013, (Eds. Venselaar, Baltas, Meigooni, Hoskin).

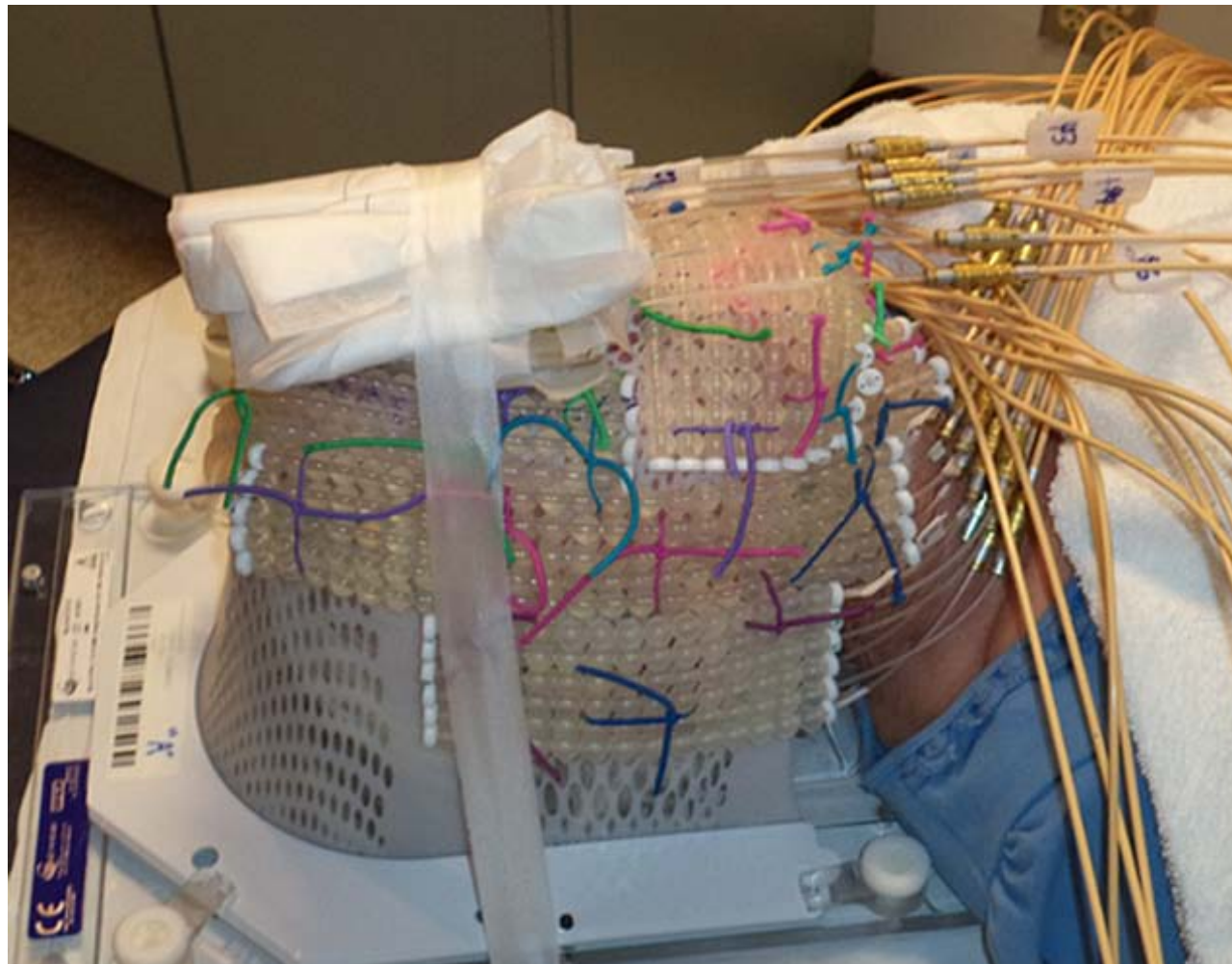
TABLE 2.1 (Continued) Features of Modern HDR and PDR Afterloading Equipment

2. Specifications of Source or Sources					
Maximum source strength for each possible radionuclide, with approval for marketing by authorities	HDR: 57 mGy.h-1 @ 1m (518 GBq (14Ci) of Ir-192) PDR: 10.2 mGy.h-1 @ 1m (92.5 GBq (2.5 Ci) of Ir-192) Maximum storage source capacity: 518 GBq (14 Ci)	HDR: 49 mGy.h-1 @ 1m (444 GBq (12 Ci) of Ir-192) PDR: 10.2 mGy.h-1 @ 1m (92.5 GBq (2.5 Ci) of Ir-192) Maximum storage capacity: 814 GBq (22 Ci) of Ir192	Co0.A86: 22.6 mGy.h-1 @ 1m (2 Ci, 74 GBq) values + 10 % Ir2.A85-2: 40 mGy.h-1 @ 1m (10 Ci, 370 GBq) values +30 % - 10 %	44.8 mGy.h-1 @ 1m (11 Ci, 407 GBq)	61.1 mGy.h-1 @ 1m (15 Ci, 555 GBq) Local regulations may prohibit to install more than 10 Ci
Source outer dimensions for each of the source types (L = length, OD = outer diameter, in mm)	3.5 mm active length x 0.6 mm diameter Source capsule outer diameter: 0.9mm	3.5 mm active length x 0.6 mm diameter Source capsule outer diameter: 0.86 mm	Co0.A86 1.0(OD) x 5(L) mm Ir2.A85-2 0.9(OD) x 5(L) mm	0.59(OD) x 5(L) mm	HDR: 0.9(OD) x 4.52(L) mm; PDR: 0.9(OD) x 2.97(L) mm
Guarantee for the maximum number of source transfers, or source cycles	25,000 cycles	30,000 cycles	Co0.A86 100,000 (>400,000 tested) Ir2.A85-2 25,000	1,000	5,000
3. Specification of Applicators					
Outside diameter of the applicators (needles and/or tubes, in mm)	Needles 1.3 mm Flexibles 4F	Needles 1.3 mm Flexibles 4F	needles 1.5 mm (17G) catheters 1.65mm for both sources	18G (1.27 mm) needles constructed from robust thick wall tubing, 4.7F robust thick walled catheters	17G (1.5 mm) needles, 5F catheters.
Minimum curvature of an applicator (plastic loop radius, e.g. for an 180 degree curve, in mm)	13 mm for all applicators with a fixed geometry and an inner diameter of 2.5 mm or larger; 15 mm for flexible applicators with an inner diameter of 1.5 mm or higher; 20 mm for flexible applicators with an inner diameter of 1.3 mm up to 1.5 mm	13 mm for applicators with a fixed geometry; 15 mm for flexible applicators with an inner diameter of 1.2 mm and outer diameter of 1.5mm or higher;	10 mm (loop of 90°) 15 mm (loop of 180°) for both sources	17 mm	13 mm
4. Source to Cable Attachment					
Method of source attachment to cable	Laser welded to ultra flexible drive wire	Laser welded to ultra flexible drive wire, including weld protection	Laser welded	Embedded in the Nitinol (nickel-titanium) source drive wire	Laser welded to ultraflexible drive cable
5. Source Extension and Movement					
Maximum source extension (in mm from the indexer)	1500 mm	1400 mm	1500 mm	1500 mm	1300 mm
Speed of source movement, in seconds over maximum source extension	500 mm/s, typ. outdrive time 4 s for 1500 mm	1400mm in 3.7 sec	300 mm/s 5 s for 1500 mm	600 mm/s	630 mm/s
6. Number of Channels					
Number of hardware applicator channels	30	40	MultiSource: 20 GyneSource: 5	20	iX model: 24; iX 3/24 model: 3
Maximum number of channels that can be used in one plan/treatment	90	40	MultiSource (2011): 40 GyneSource model: 5	unlimited	unlimited

And 2 pages more.....

(continued)





images courtesy of Ivan Buzurovic

Robotic based Afterloading Technology?



Evolution



Robots!



^{192}Ir ,
 ^{60}Co ,
eBT,
low-E seeds



Robot Definition

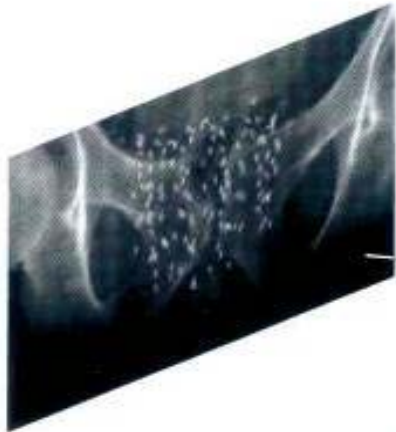
Robot = a reprogrammable multifunctional manipulator designed to move materials, parts, tools, or specialized devices through variable programmed motions for performance of a variety of tasks.

Robotics Institute of America[®]

Commerically Available LDR Robot

A seed afterloader for prostate BT: Robotic Assisted Seed Delivery

- Integrated Work-flow from Preparation and Planning to Treatment Delivery
- Integrated Verification and Quality Assurance
- Real-time adaptation of seed configuration up to the very last moment



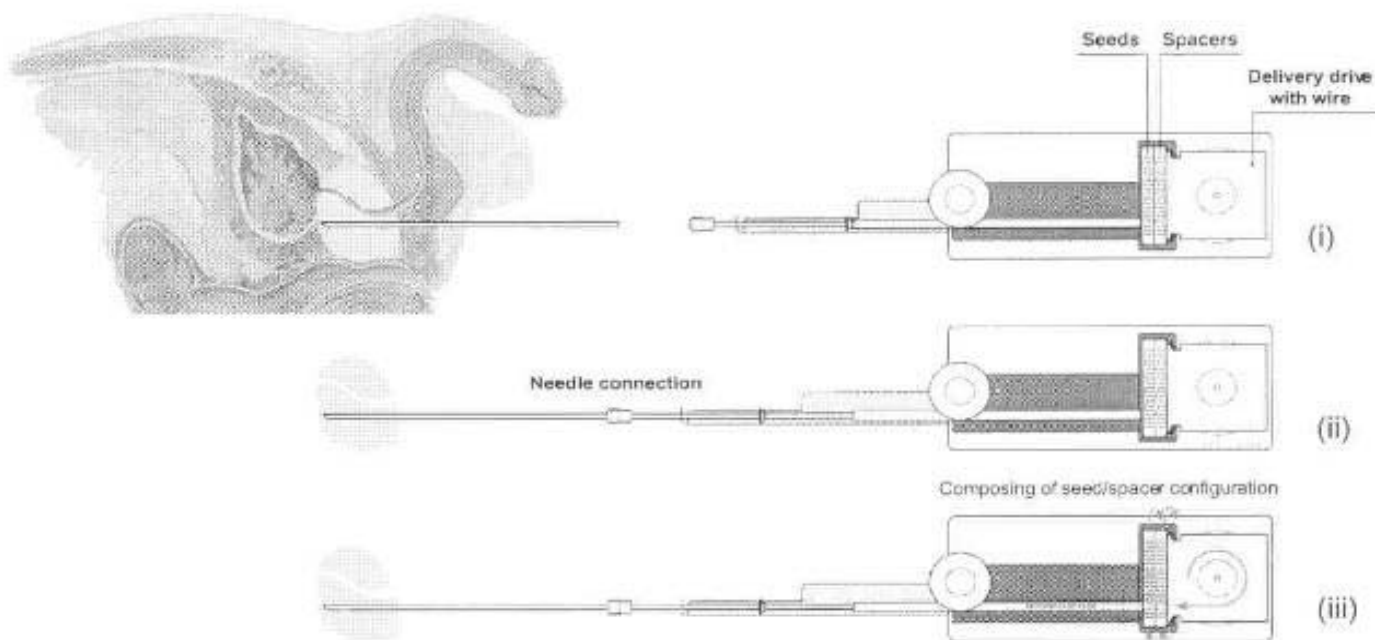
seedSelectron
(by Elekta/Nucletron, The Netherlands)

Commerically Available LDR Robot

A seed afterloader for prostate BT: Robotic Assisted Seed Delivery

Principle of loading of a needle

Application of the seed afterloader



Cassettes with ^{125}I sources and spacers



AAPM/GEC-ESTRO TG-192 Report: Robotic BT

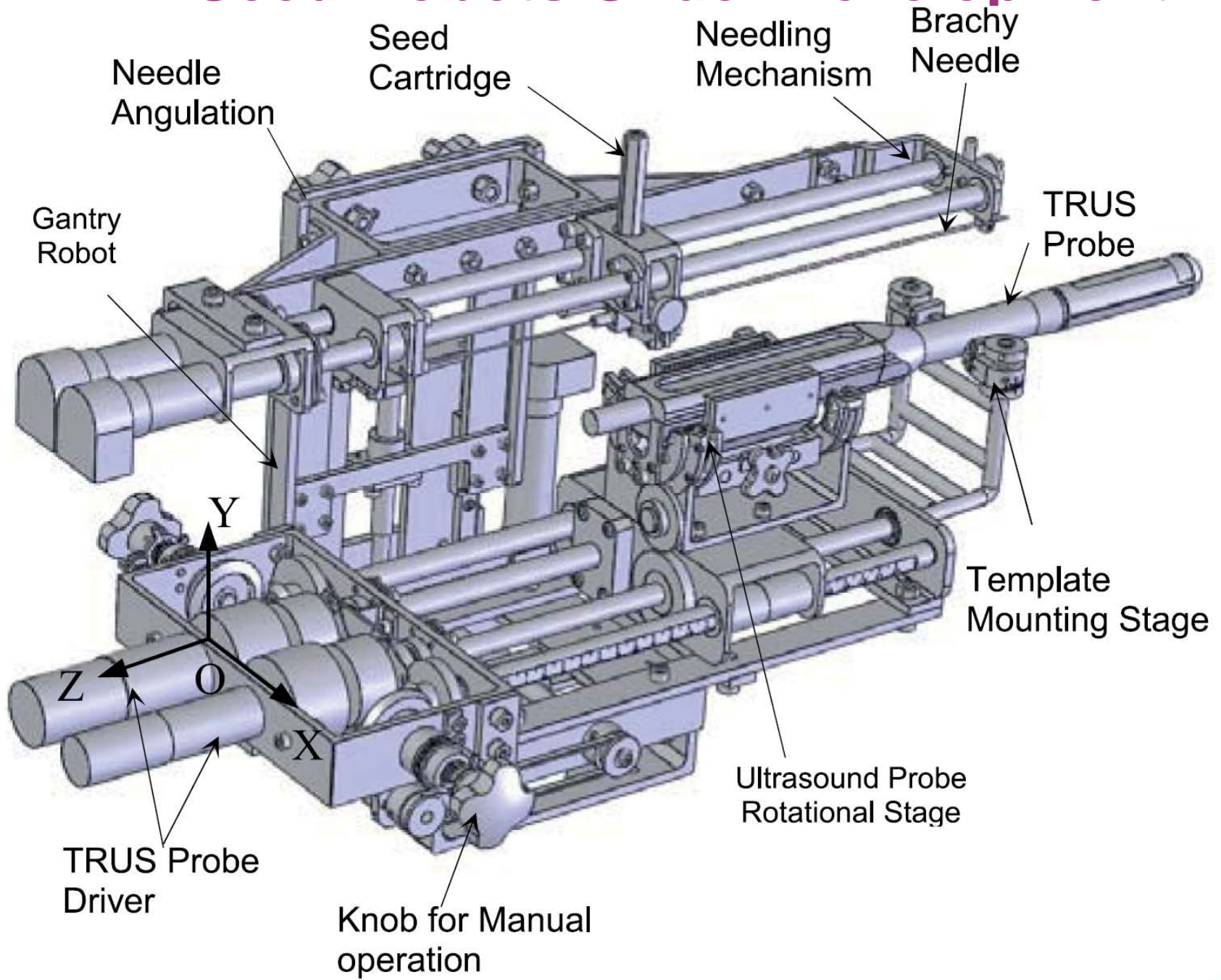
Medical Physics

AAPM and GEC-ESTRO guidelines for image-guided robotic brachytherapy: Report of Task Group 192

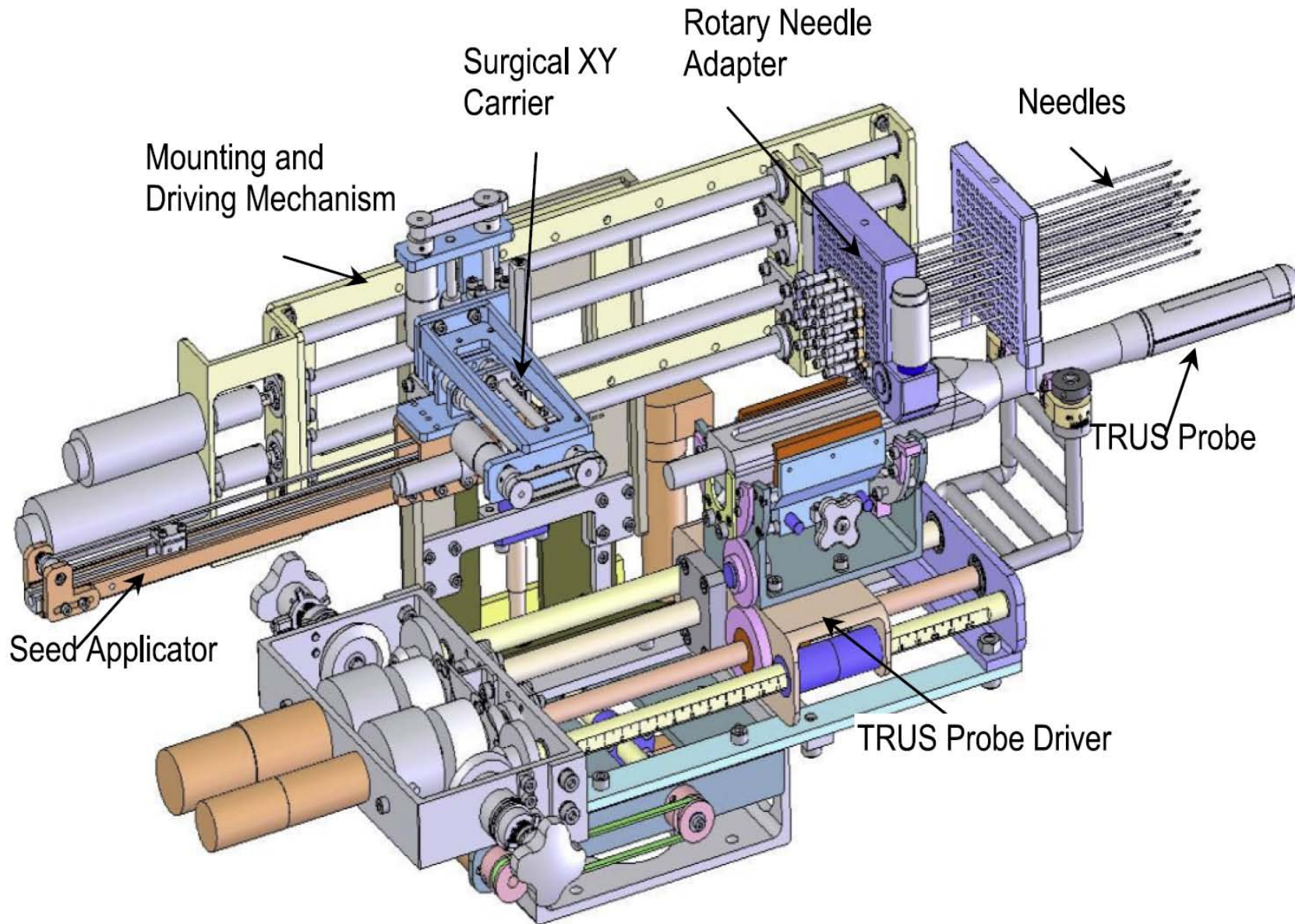
Tarun K. Podder, Luc Beaulieu, Barrett Caldwell, Robert A. Cormack, Jostin B. Crass, Adam P. Dicker, Aaron Fenster, Gabor Fichtinger, Michael A. Meltsner, Marinus A. Moerland, Ravinder Nath, Mark J. Rivard, Tim Salcudean, Danny Y. Song, Bruce R. Thomadsen, and Yan Yu

This is a joint Task Group with the Groupe Européen de Curiethérapie-European Society for Radiotherapy & Oncology (GEC-ESTRO). All developed and reported robotic brachytherapy systems were reviewed. Commissioning and quality assurance procedures for the safe and consistent use of these systems are also provided. Manual seed placement techniques with a rigid template have an estimated in vivo accuracy of 3–6 mm. In addition to the placement accuracy, factors such as tissue deformation, needle deviation, and edema may result in a delivered dose distribution that differs from the preimplant or intraoperative plan. However, real-time needle tracking and seed identification for dynamic updating of dosimetry may improve the quality of seed implantation. The AAPM and GEC-ESTRO recommend that robotic systems should demonstrate a spatial accuracy of seed placement ≤ 1.0 mm in a phantom. This recommendation is based on the current performance of existing robotic brachytherapy systems and propagation of uncertainties. During clinical commissioning, tests should be conducted to ensure that this level of accuracy is achieved. These tests should mimic the real operating procedure as closely as possible.

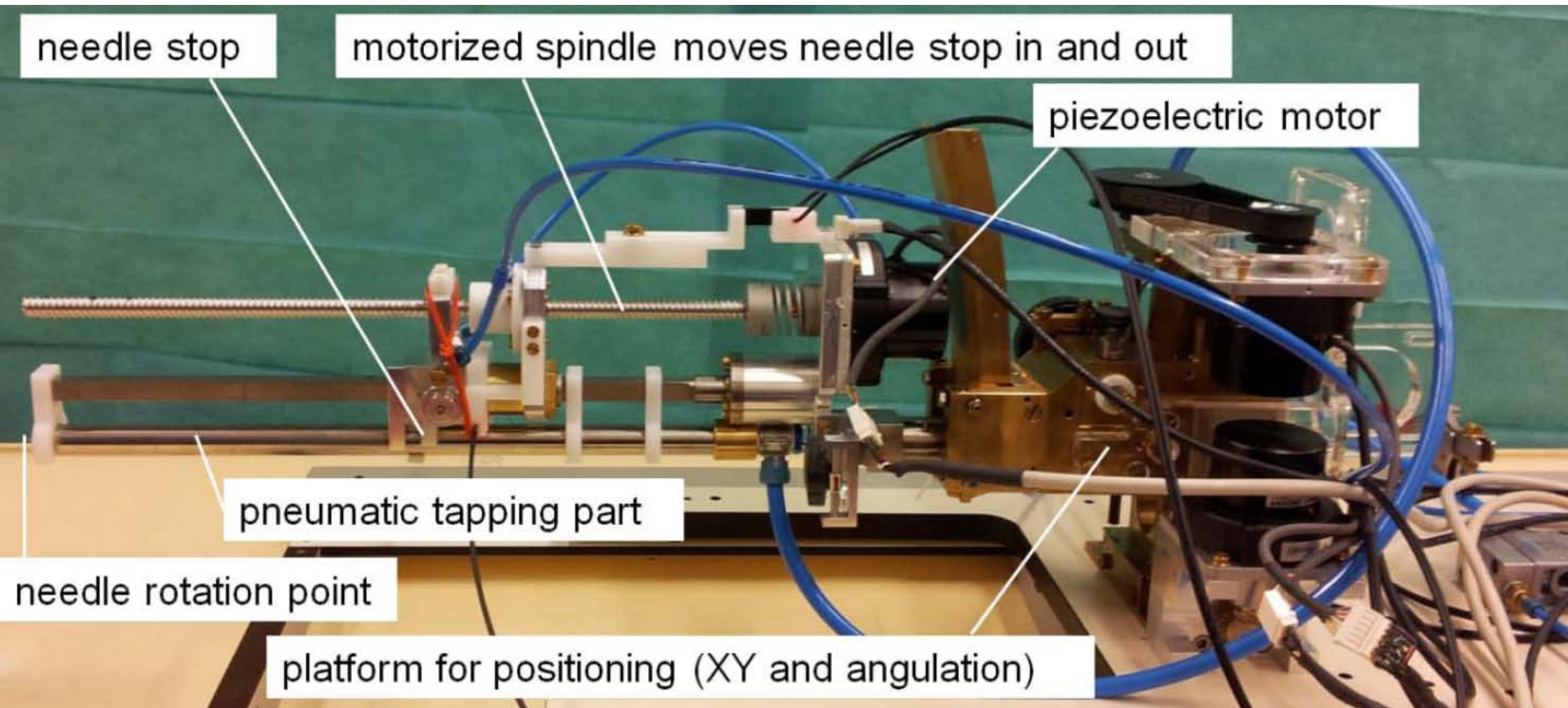
LDR Seed Robots Under Development



LDR Seed Robots Under Development



LDR Seed Robots Under Development



LDR Seed Robots Under Development

Robot-assisted Needle Placement in Open-MRI: System Architecture, Integration and Validation

S.P. DiMaio ^{a,1}, S. Pieper ^b, K. Chinzei ^c, N. Hata ^a, E. Balogh ^d,
G. Fichtinger ^d, C.M. Tempany ^a, R. Kikinis ^a,

^a *Brigham and Women's Hospital, Harvard Medical School*

^b *Isomics Inc.*

^c *National Institute of Advanced Industrial Science and Technology, Japan*

^d *Johns Hopkins University*

MRI-compatible



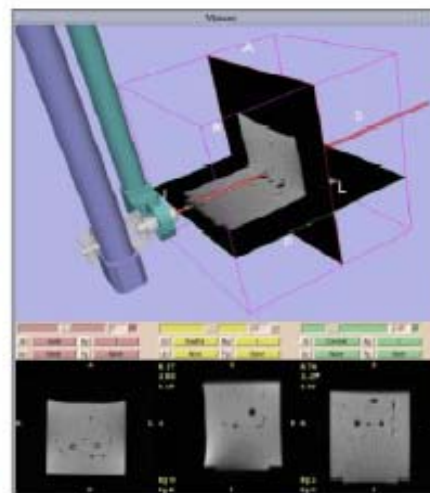
Johns Hopkins Univ.



(a)



(b)



(c)

Figure 3. Phantom experiments: (a) scale models of legs and PVC prostate phantom with embedded targets, (b) patient model and robot placement inside the scanner, with sterile draping, (c) needle trajectories are interactively specified in the planning environment.

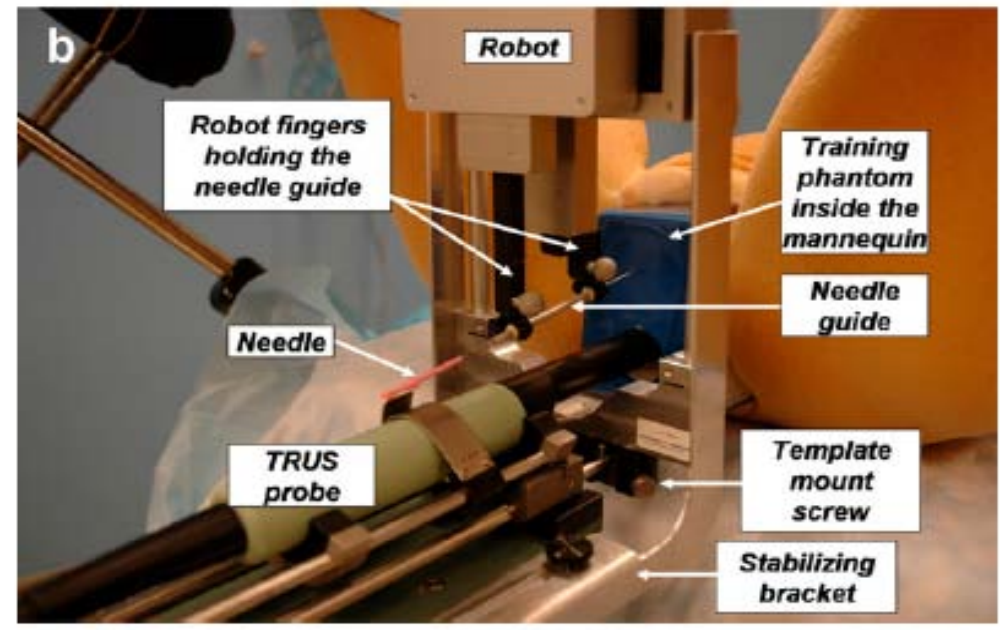
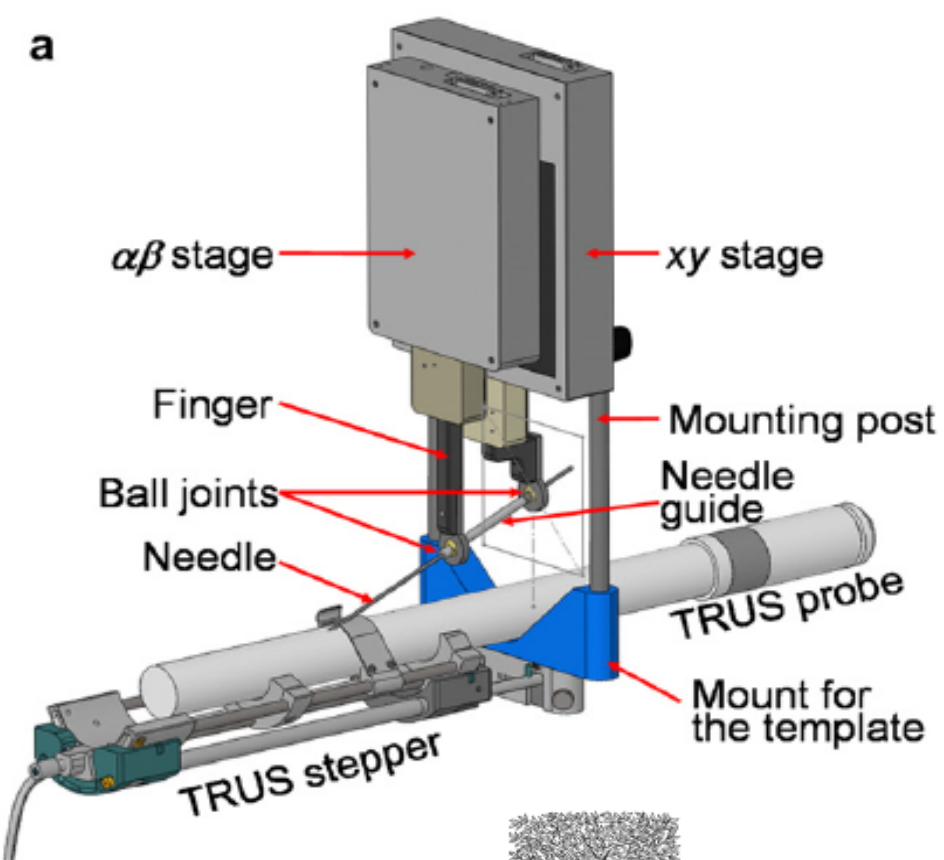


Fig. 1. (a) Computer-generated image of robot positioner mounted onto stepper with ultrasound probe, with depiction of xy and $\alpha\beta$ stages. (b) Photograph of robot positioner on stepper with ultrasound probe in



Robotic needle guide for prostate brachytherapy: Clinical testing of feasibility and performance

Danny Y. Song^{1,*}, Everette C. Burdette^{2,3}, Jonathan Fiene⁴, Elwood Armour¹, Gernot Kronreif⁵, Anton Deguet³, Zhe Zhang⁶, Iulian Iordachita³, Gabor Fichtinger^{3,7}, Peter Kazanzides³

¹Department of Radiation Oncology and Molecular Radiation Sciences, Johns Hopkins University, Baltimore, MD

²Acoustic Medsystems, Inc., Urbana-Champaign, IL

³Computer Science, Johns Hopkins University, Baltimore, MD

⁴Mechanical Engineering and Applied Mechanics, University of Pennsylvania, Philadelphia, PA

⁵Austrian Center for Medical Innovation and Technology, Wiener Neustadt, Austria

⁶Oncology Biostatistics, Johns Hopkins University, Baltimore, MD

⁷Computer Science, Queen's University, Kingston, Ontario, Canada

Summary

- Numerous possibilities for LDR and HDR sources
- Discriminate RAL system features across manufacturers
- Diligence needed by medical physicists to remaining tech savvy
- Future BT developments will grow more complicated with technology
- Medical physicist should decide technology for clinic

Acknowledgements

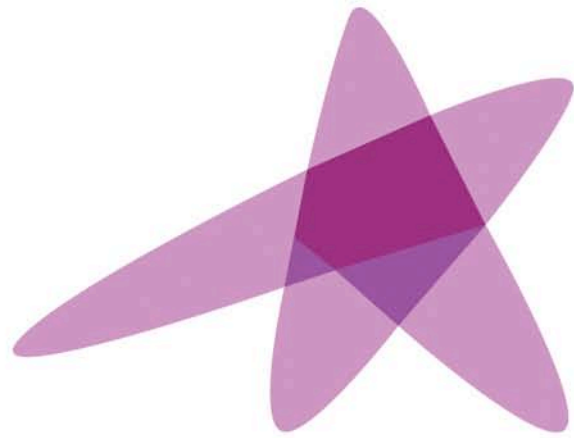
Dimos Baltas, University of Freiburg, Germany

Bruce Thomadsen, University of Wisconsin, USA

Jack Venselaar, Instituut Verbeeten, The Netherlands



Vienna, 29 May – 1 June 2016



ESTRO
School

Advanced Brachytherapy Physics

The Principles of Imaging based Treatment Planning

Dimos Baltas, Ph.D., Prof.

Division of Medical Physics

Department of Radiation Oncology, Medical Center - University of Freiburg

Faculty of Medicine, University of Freiburg, Germany

and

German Cancer Consortium (DKTK), Partner Site Freiburg, Germany

E-mail: dimos.baltas@uniklinik-freiburg.de

List of Content

- **BRT *versus* ERT from Dosimetry Point of View**
- BRT *versus* ERT from RTP-Workflow Point of View
- Introduction to Localisation
- DVH-Evaluation and Prescription
- Introduction to Dynamic and Adaptive Planning

Modern Radiation Therapy

BRT *versus* ERT Similarities and Differences

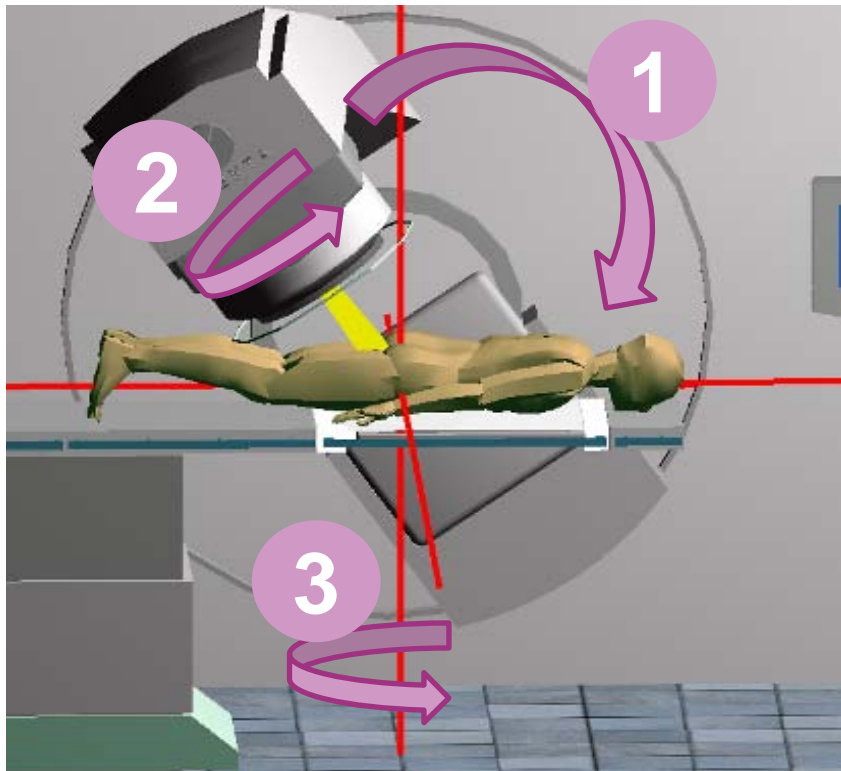
- Dosimetric Kernel
- Delivery Technology
- Dose Distribution

Modern Radiation Therapy

BRT *versus* ERT Similarities and Differences

The Field / Beam:

ERT



BRT



Modern Radiation Therapy

BRT *versus* ERT Similarities and Differences

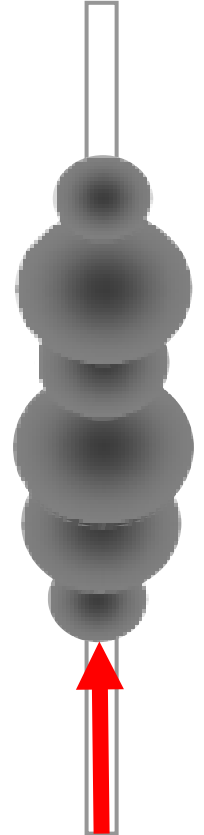
Beam Shaping: Plane

Field

Catheter/Needle/Applicator



MLC
2.5 mm
or
5.0 mm
or
10.0 mm



- 1.0 mm
- 2.5 mm
- 5.0 mm
- 10.0 mm
- ?? mm

MSS

ERT

BRT

Modern Radiation Therapy

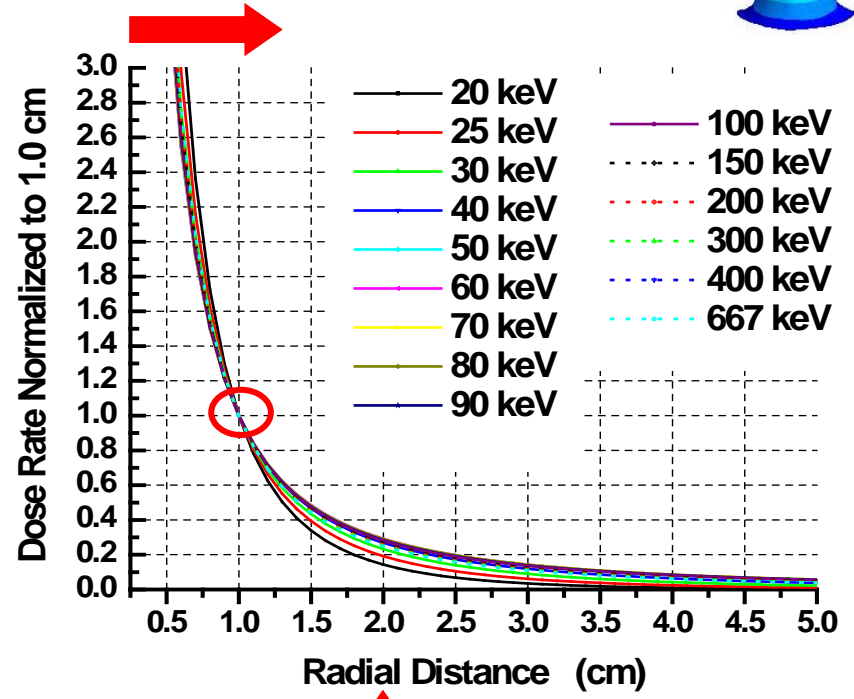
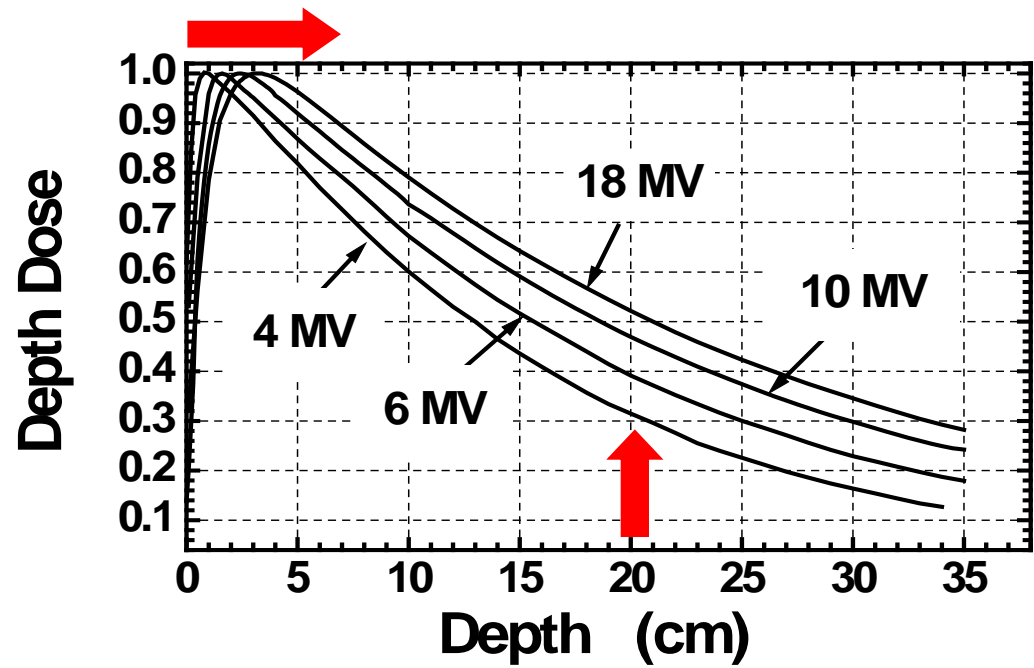
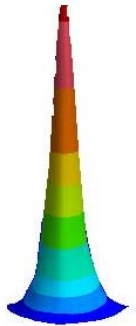
BRT *versus* ERT Similarities and Differences

Dosimetric Kernel

ERT

10 : 1

BRT

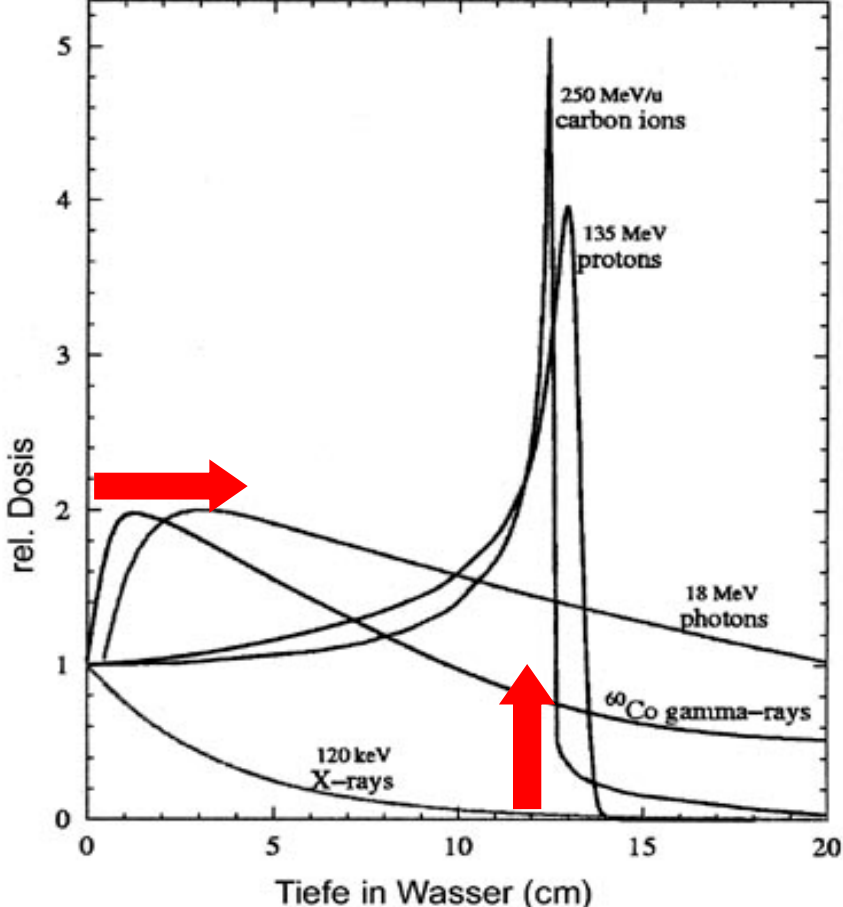


Modern Radiation Therapy

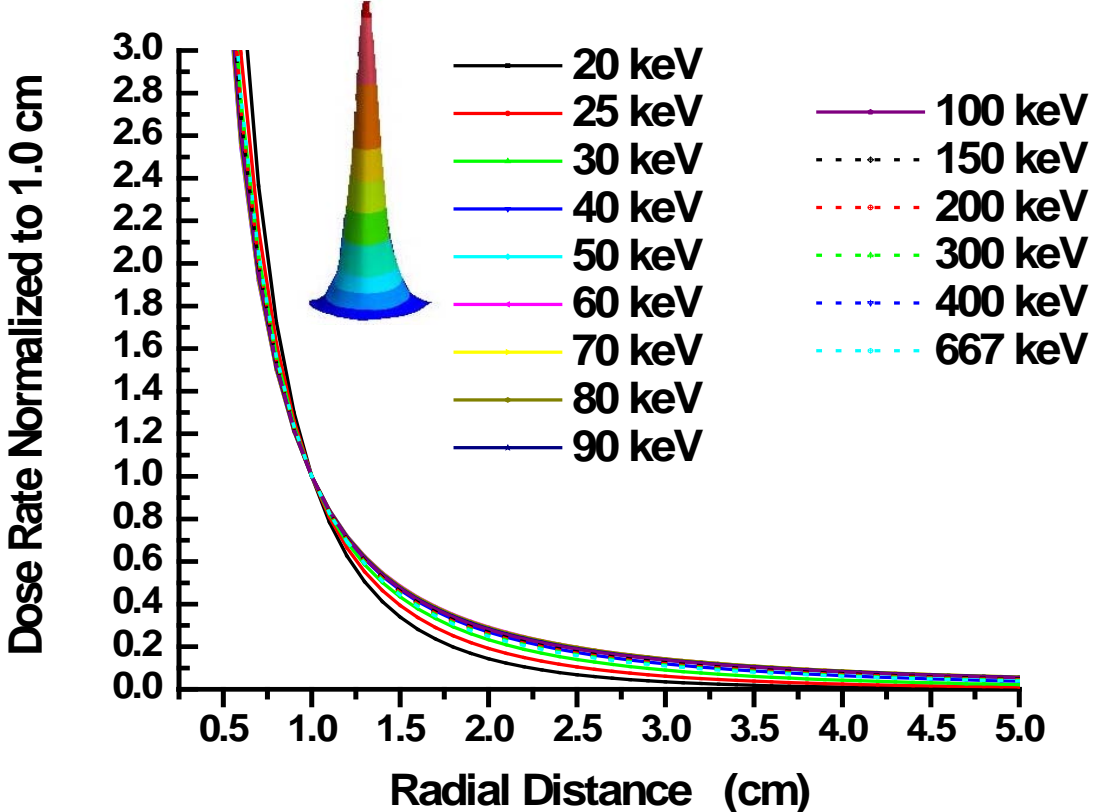
BRT *versus* ERT Similarities and Differences

Dosimetric Kernel

ERT



BRT

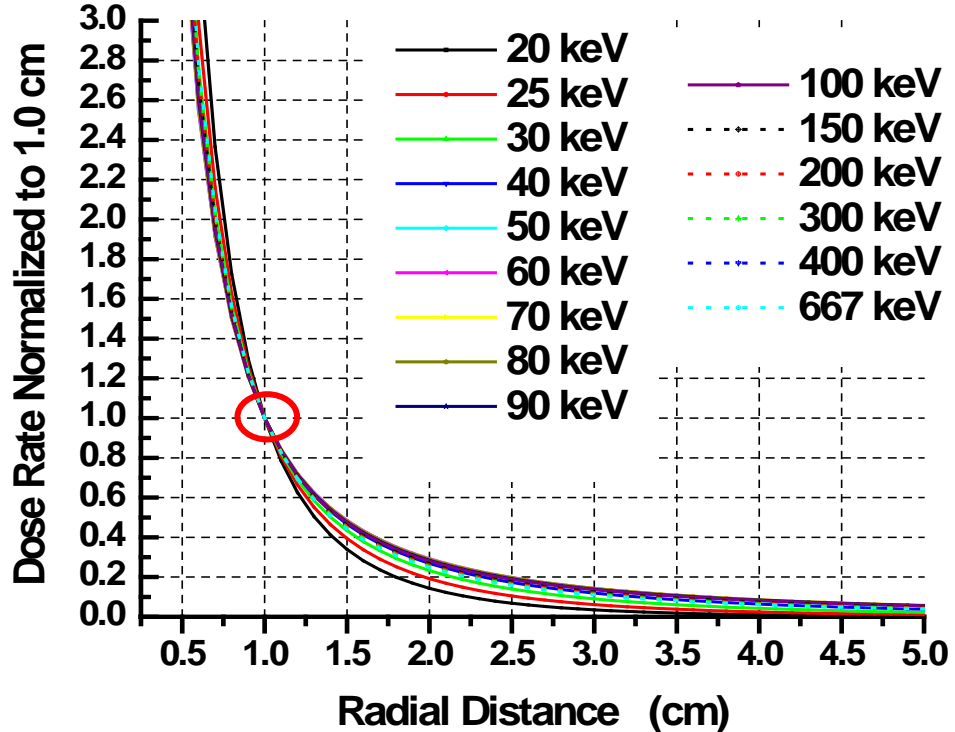
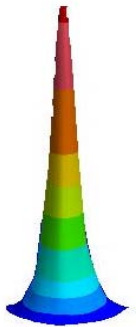


Modern Radiation Therapy

BRT *versus* ERT Similarities and Differences

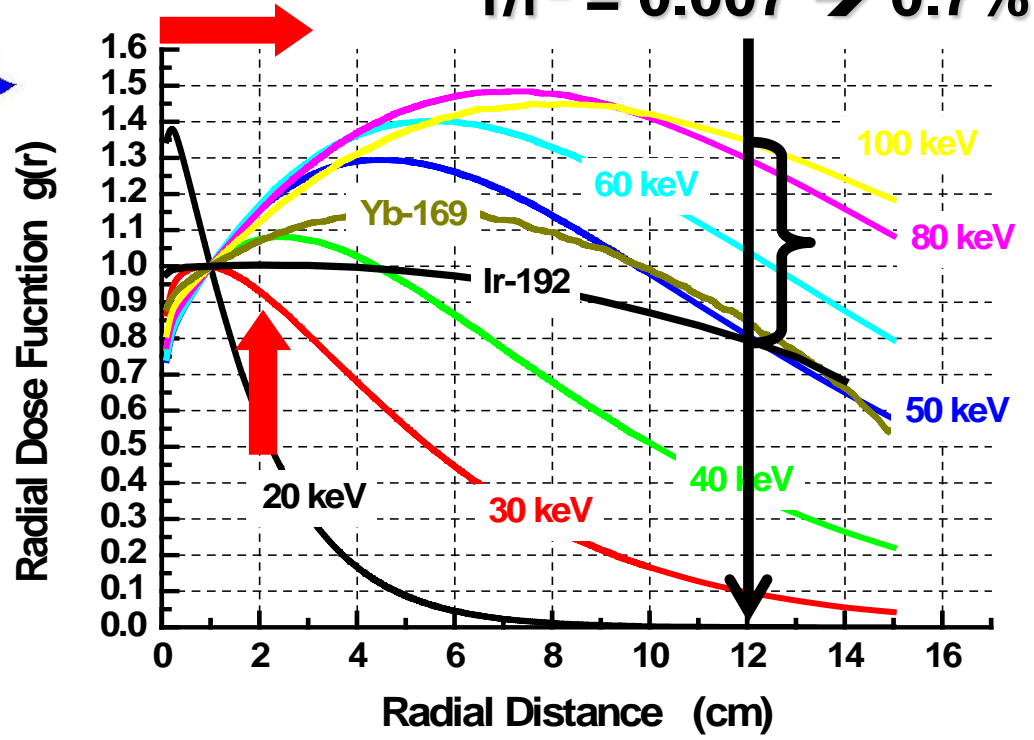
Dosimetric Kernel

BRT



BRT

$1/r^2 = 0.007 \rightarrow 0.7\%$

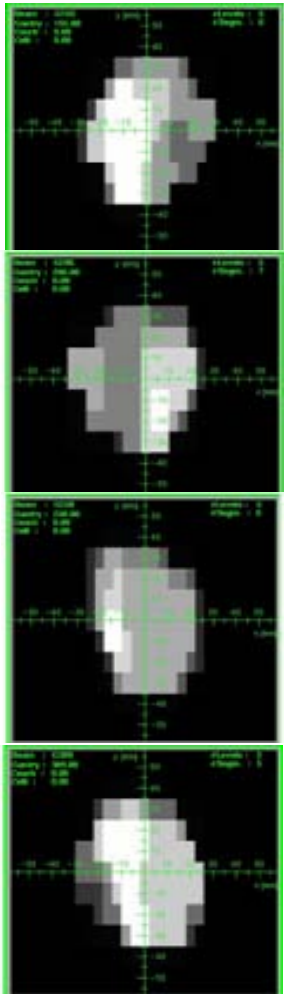


Modern Radiation Therapy

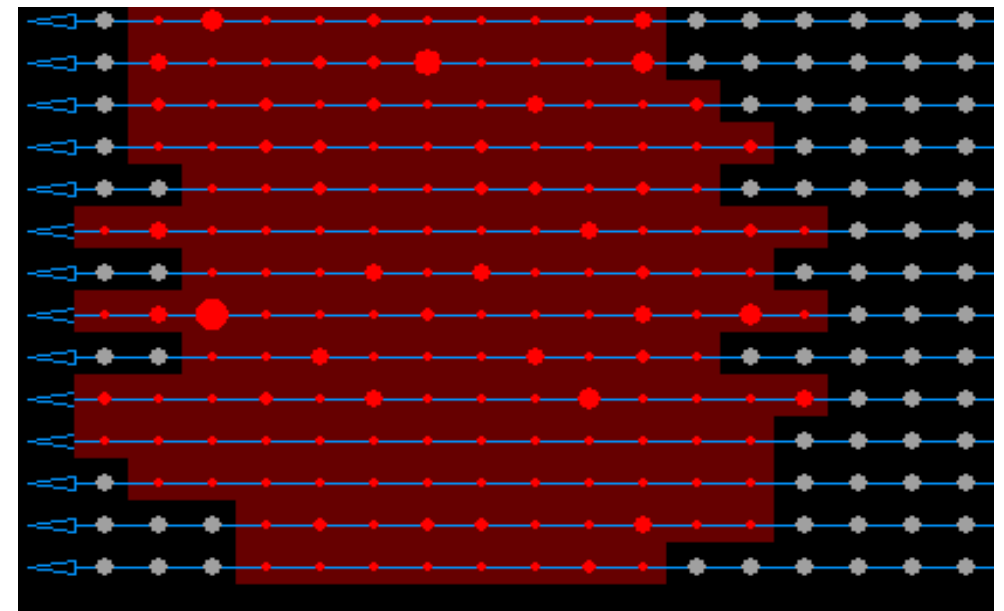
BRT *versus* ERT Similarities and Differences

Delivery Technology: Intensity Modulation (2D)

ERT



BRT



MSS: Step & Shoot

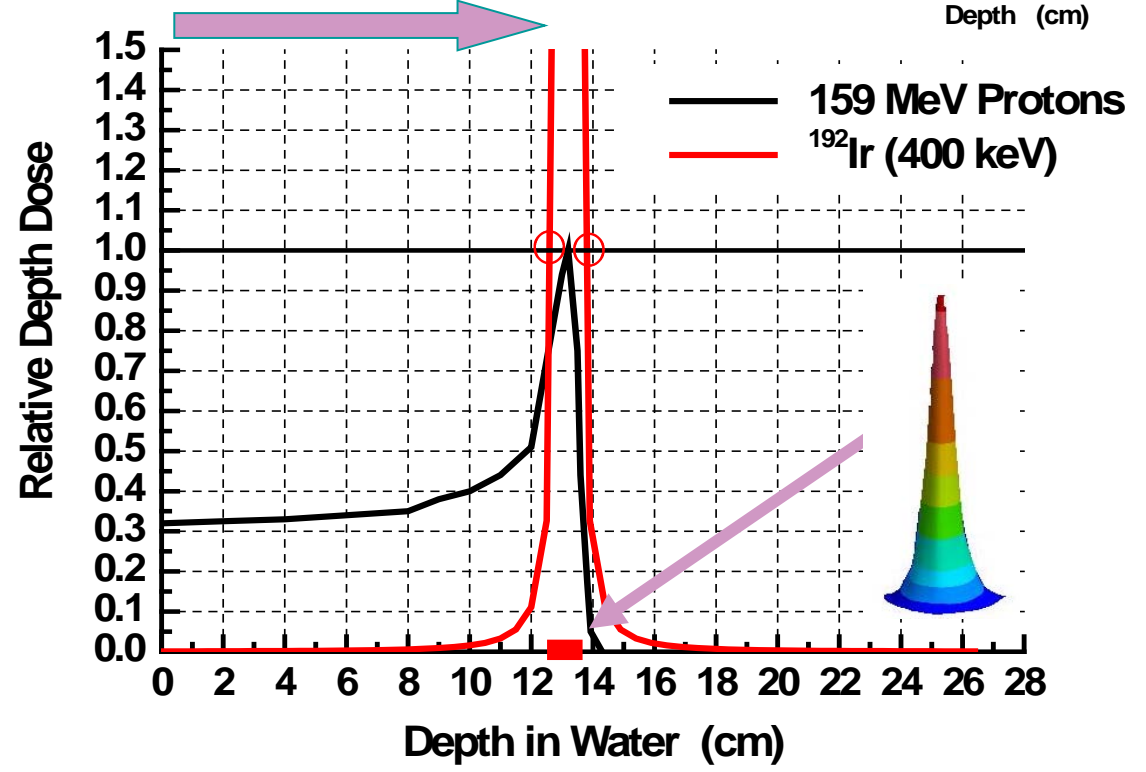
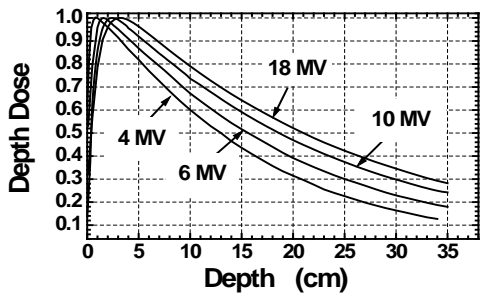
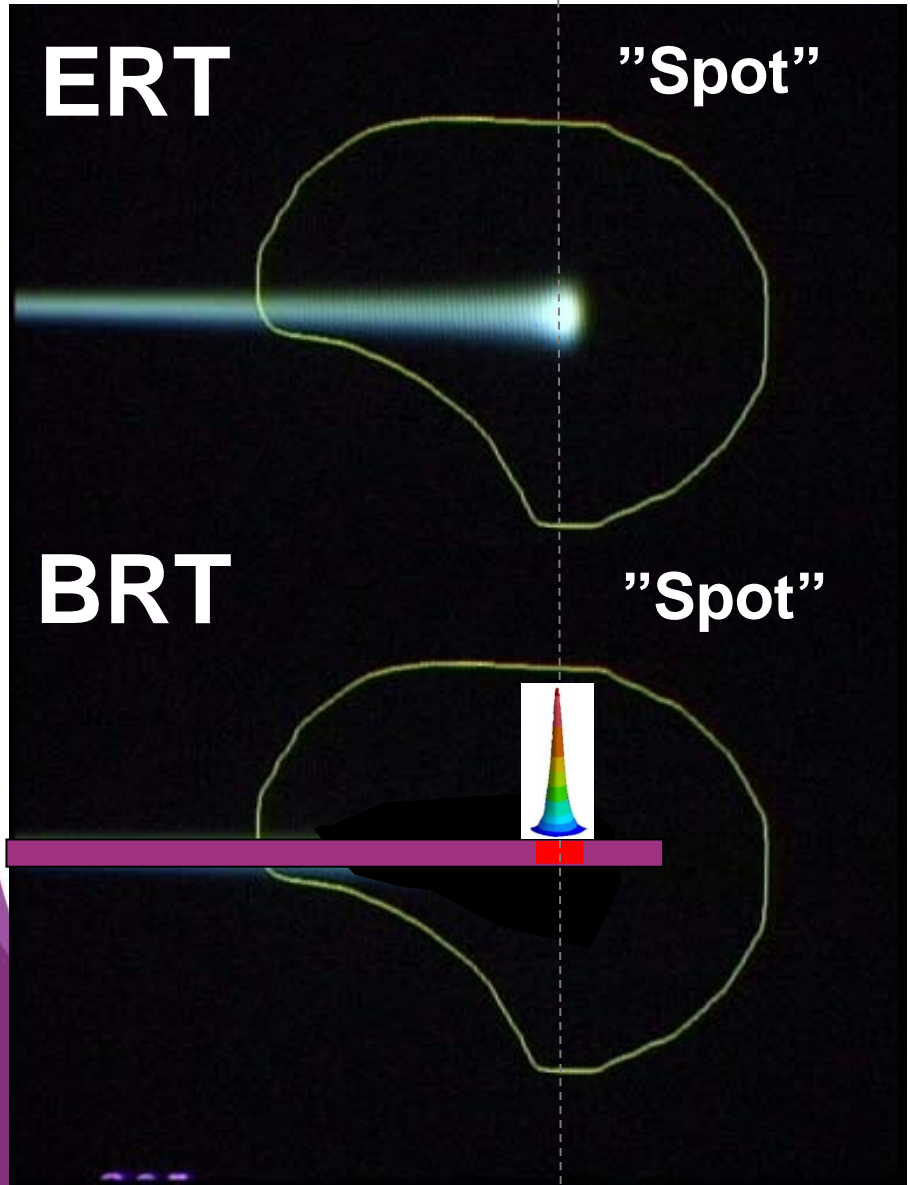
“Bixel” \Leftrightarrow Dwell Position

“MUs” \Leftrightarrow Dwell Time

Modern Radiation Therapy

Delivery Technology

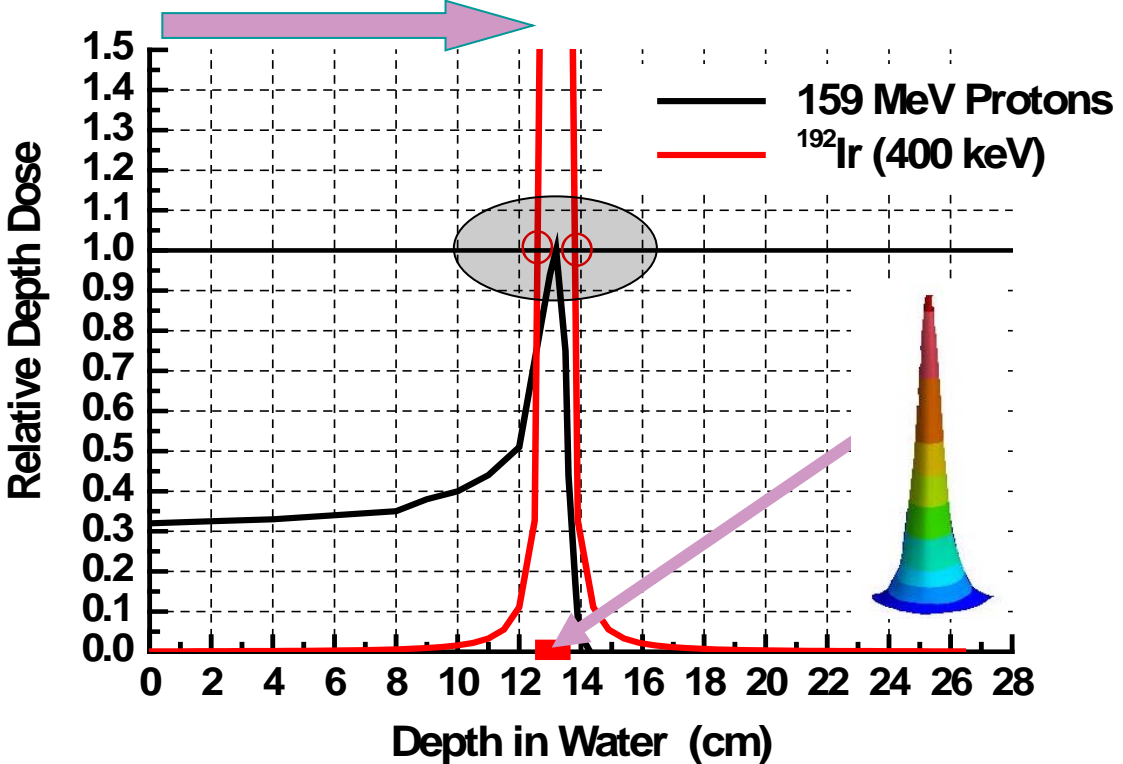
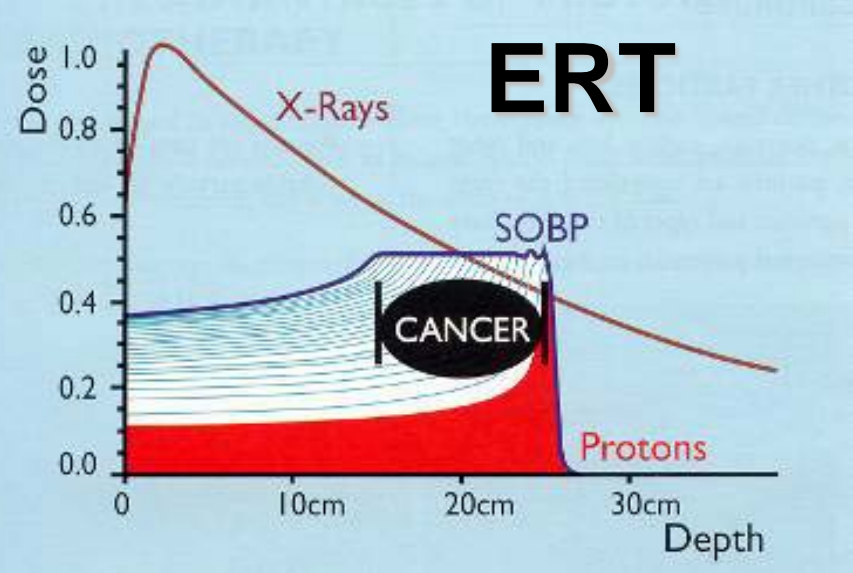
Energy \leftrightarrow Dwell Position (3D)



Modern Radiation Therapy

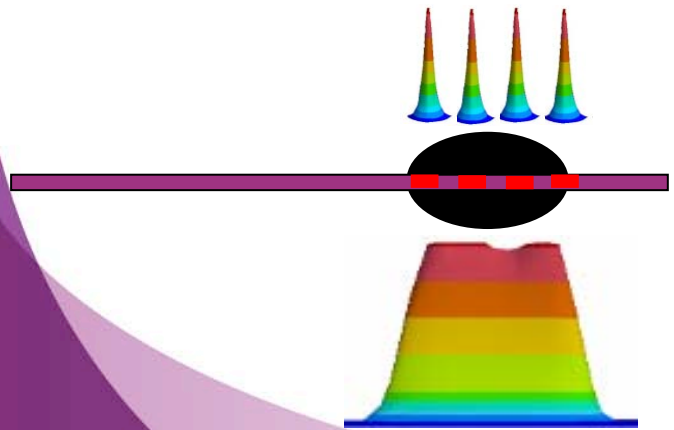
Delivery Technology

Energy \leftrightarrow Dwell Position (3D)



BRT

"Multi-Spots"



Modern Radiation Therapy

BRT *versus* ERT Similarities and Differences

Summary - I

Dosimetric Kernel

→
(Spot)

Particles



Delivery Technology

→
(Modulation, Dose-Volume-Prescription)

IMRT (X, P)



Dose Distribution

→
(Inhomogeneity)

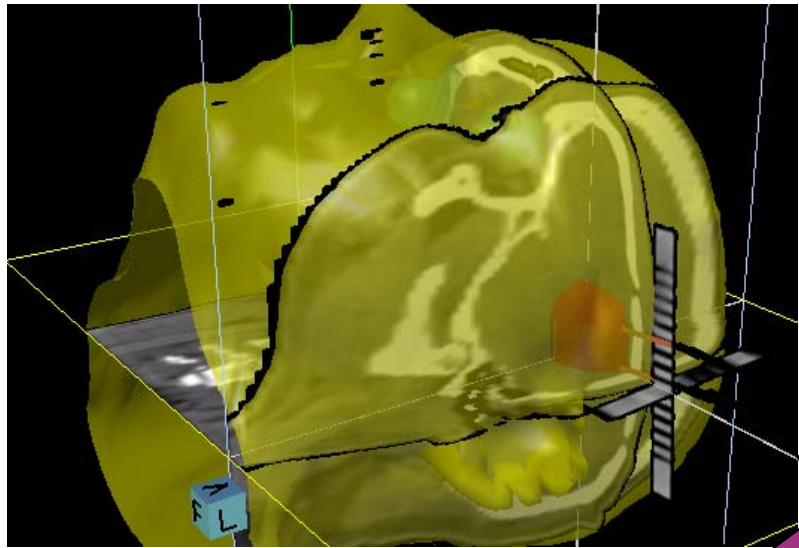
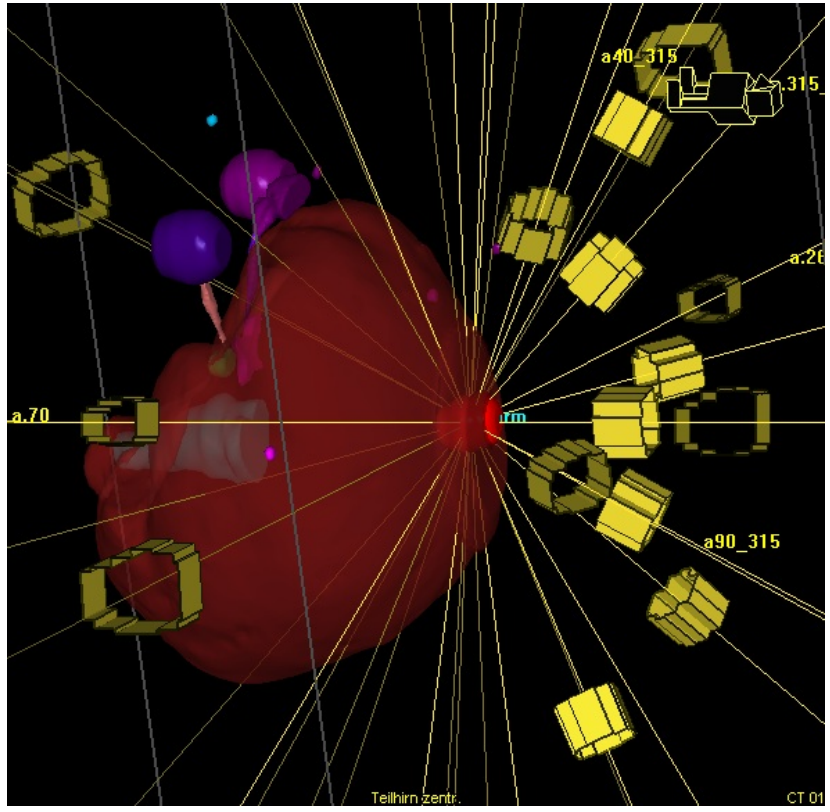
SRS / SBRT



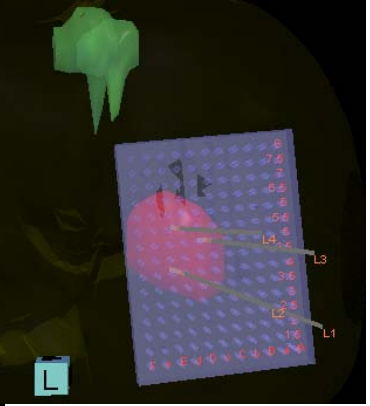
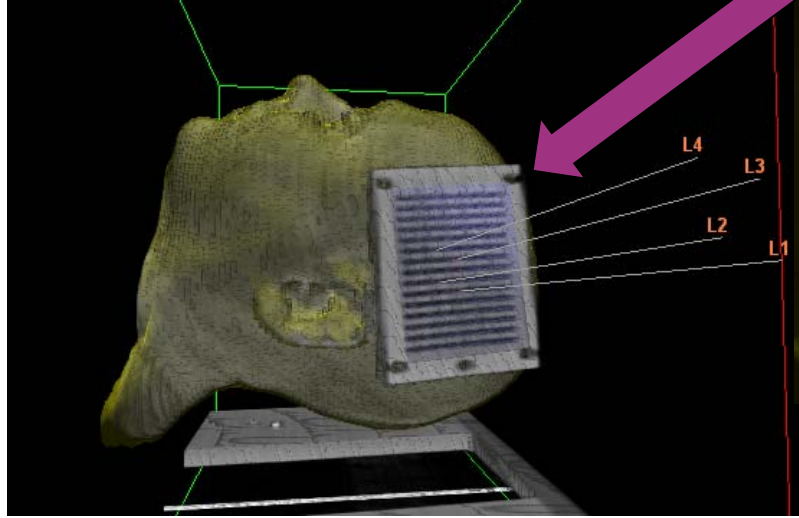
Modern Radiation Therapy

Dose Distribution: Inhomogeneity BRT

SRS



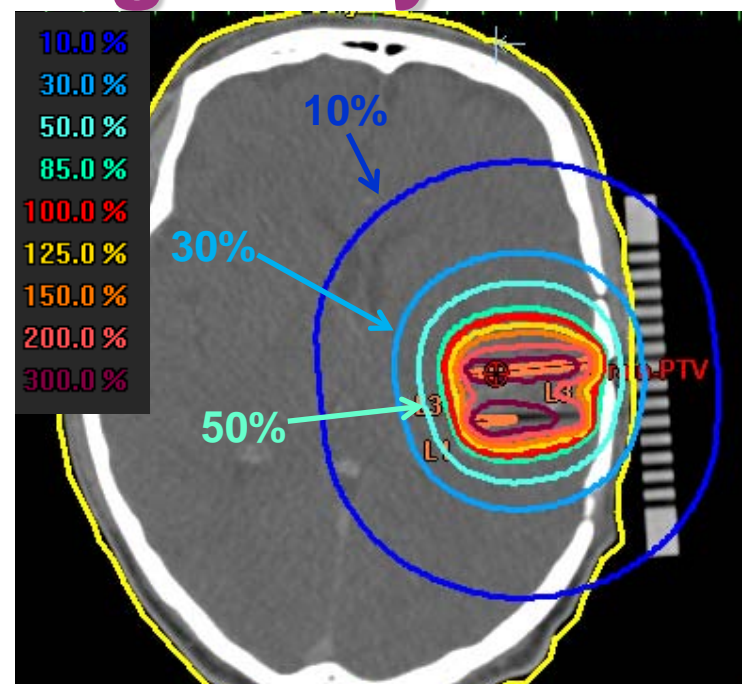
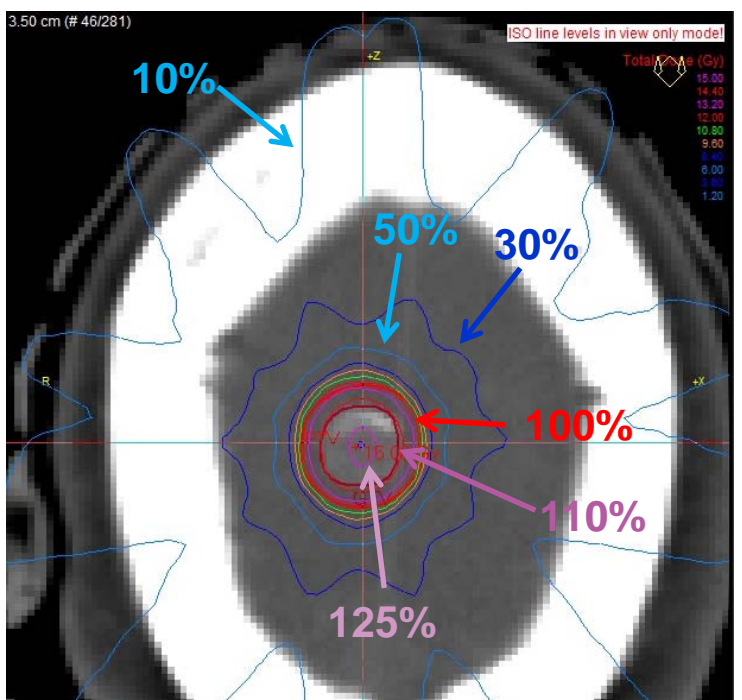
“Beams” &
“MLCs”



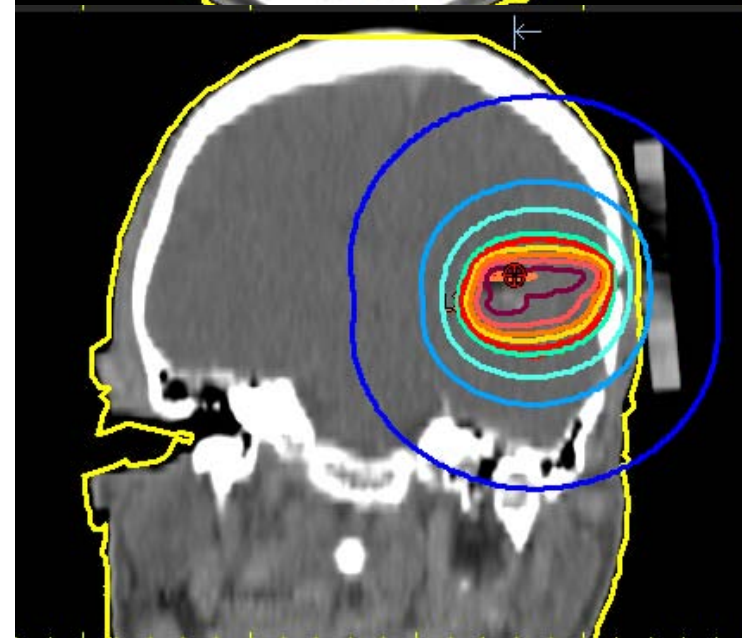
Modern Radiation Therapy

Dose Distribution: Inhomogeneity

SRS



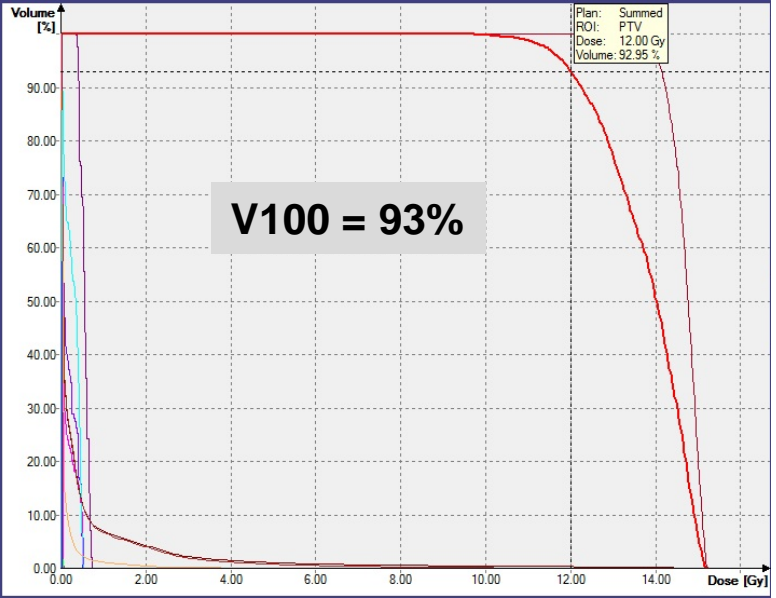
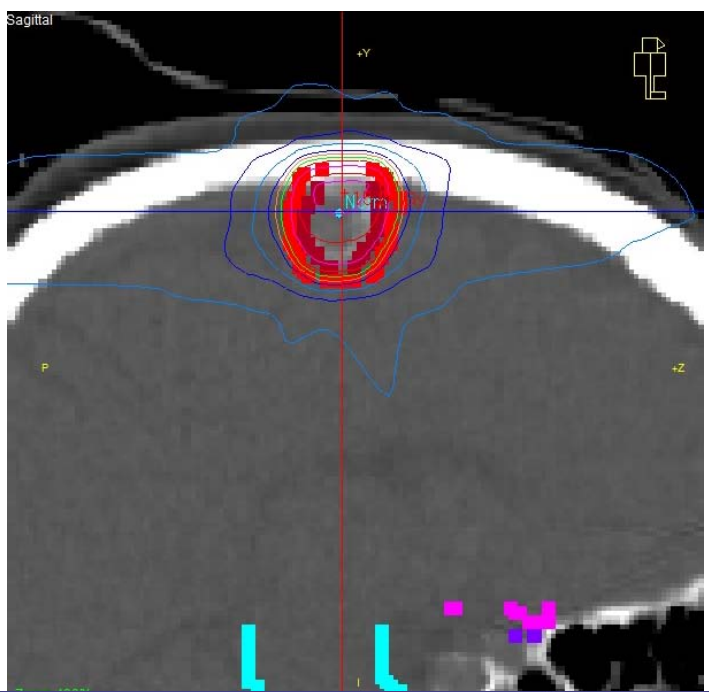
BRT



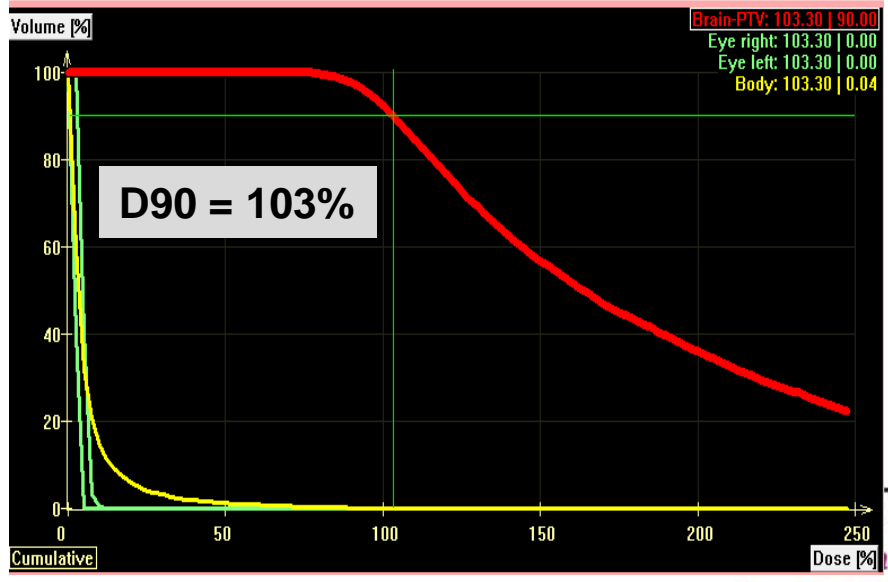
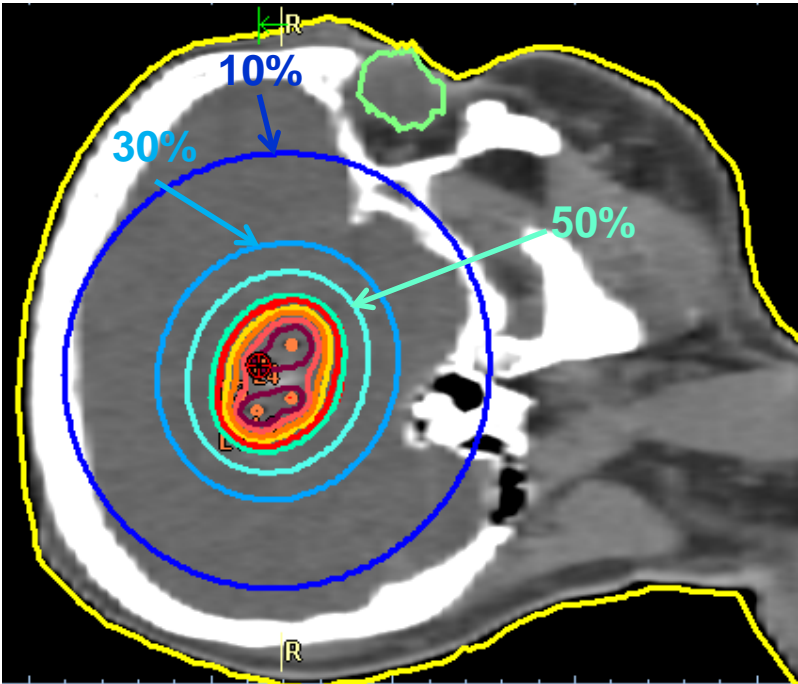
Modern Radiation Therapy

Dose Distribution: Inhomogeneity

SRS



BRT



Modern Radiation Therapy

BRT *versus* ERT Similarities and Differences

Summary - II

Dosimetric Kernel

→
(Spot)

Particles ✓

Delivery Technology

→
(Modulation, Dose-Volume-Prescription)

IMRT (X, P) ✓

Dose Distribution

→
(Inhomogeneity)

SRS / SBRT ✓

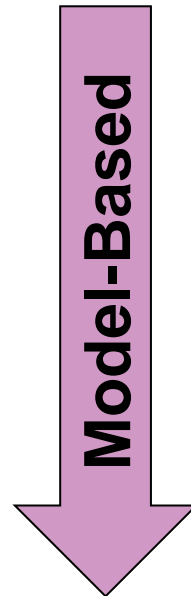
List of Content

- BRT *versus* ERT from Dosimetry Point of View
- **BRT *versus* ERT from RTP-Workflow Point of View**
- Introduction to Localisation
- DVH-Evaluation and Prescription
- Introduction to Dynamic and Adaptive Planning

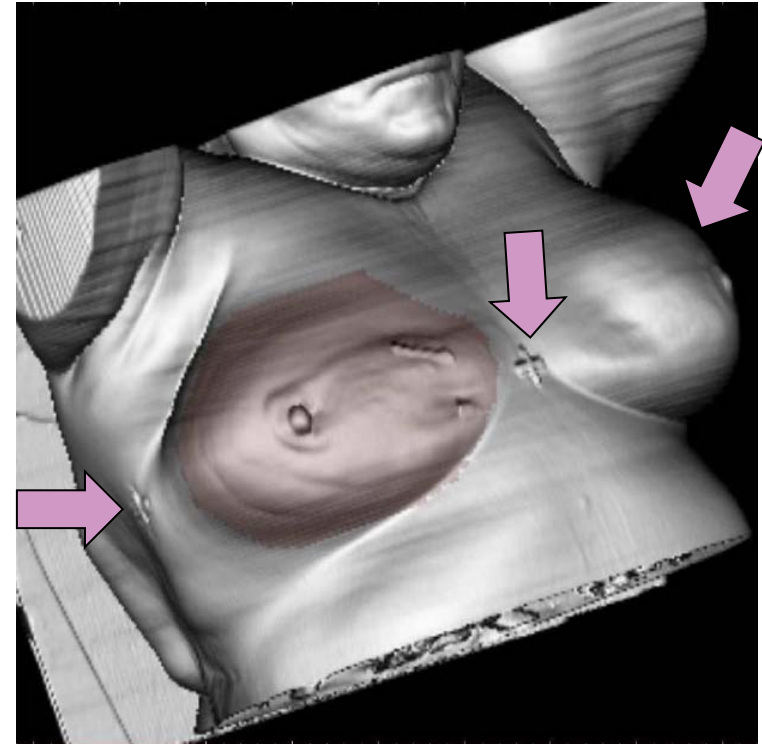
Modern Radiation Therapy

Workflow / Processes in **ERT** Treatment Planning

- Immobilization
- Positioning
- External Coordinate System
- CT-Acquisition
- 3D-Patient Model
- VOI-Definition
- Prescription
- Beam Configuration
- Fluence Adjustment
- DVH-Evaluation
- Treatment Parameters Transfer



3D-Patient Model



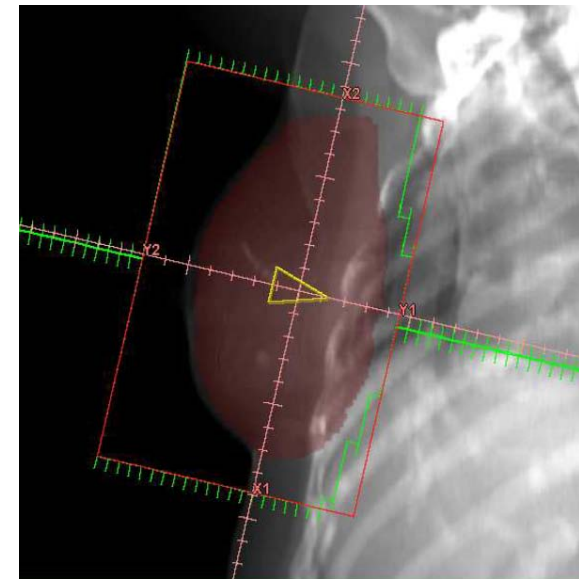
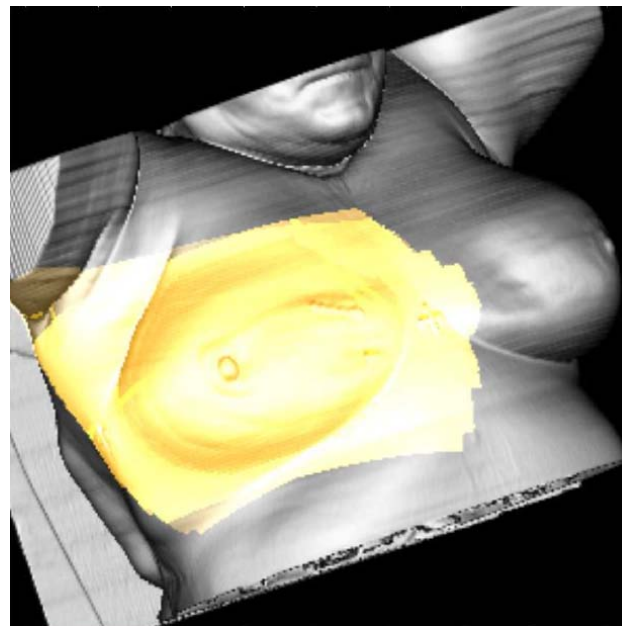
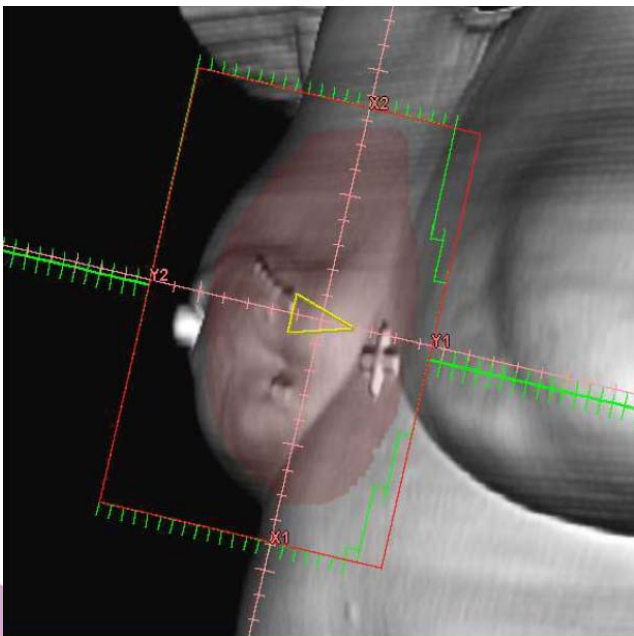
**Reference Point /
Coordinate System**

Modern Radiation Therapy

Workflow / Processes in ERT Treatment Planning

3D-Patient Model: Beam Configuration

- Placement of Beams/Beam Configuration
- Visual Control (BEV, skin projection)
- DRRs

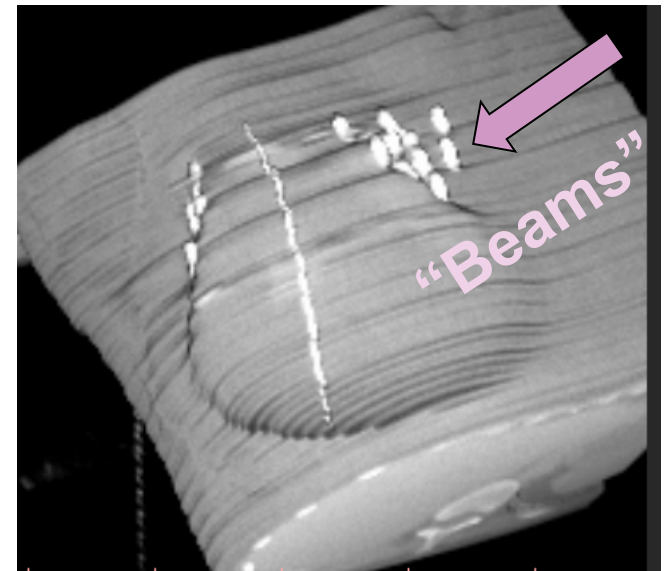


Modern Radiation Therapy

BRT *versus* ERT Similarities and Differences

- Immobilization
- Positioning
- External Coordinate System
- **Implantation (Catheters = Beams)**
- CT-Acquisition
- 3D-Patient Model
- VOI-Definition
- Prescription
- Beam Configuration → **Model-Based** Localisation
- Fluence Adjustment
- DVH-Evaluation
- Treatment Parameters Transfer

3D-Patient Model



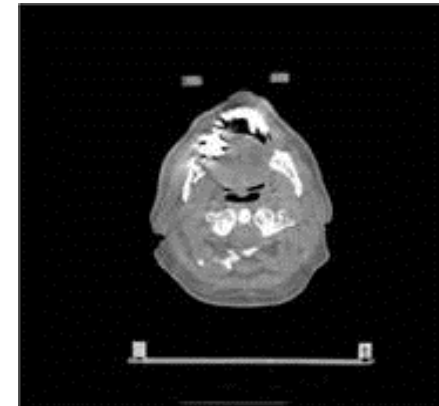
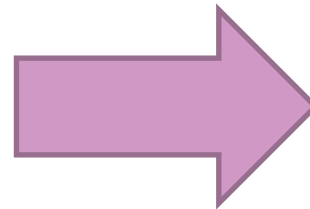
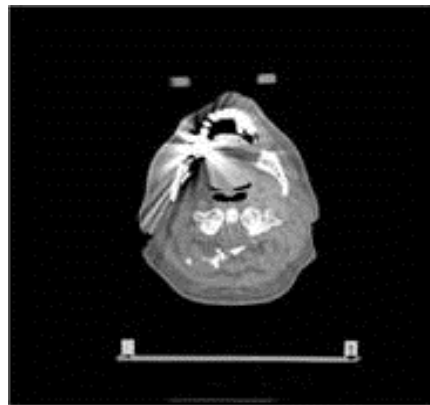
Modern Radiation Therapy

BRT *versus* ERT Similarities and Differences

3D-Patient Model: Anatomy (VOI) Definition

- GTV, CTV, PTV
 - OARs
- w implanted catheters

CT: Artifact Reduction



By Courtesy of Philips CT Imaging

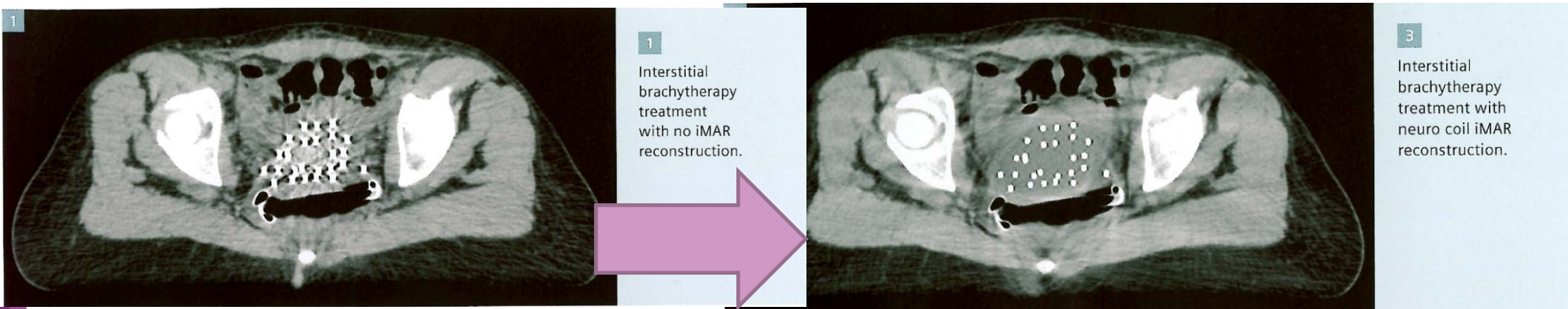
Modern Radiation Therapy

BRT *versus* ERT Similarities and Differences

3D-Patient Model: Anatomy (VOI) Definition

- GTV, CTV, PTV
 - OARs
- ➔ w implanted catheters

CT: Artifact Reduction



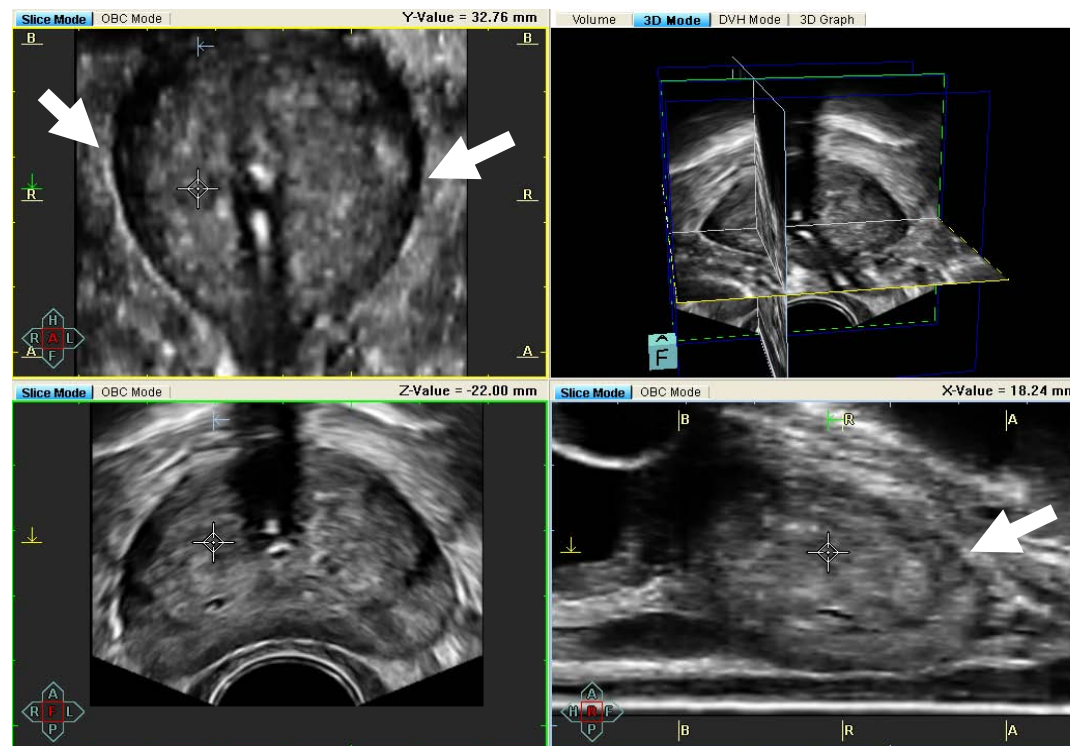
SIEMENS Healthcare, Germany: SOMATOM Definition AS Open – RT Pro edition

Modern Radiation Therapy

BRT *versus* ERT Similarities and Differences

3D-Patient Model: Anatomy (VOI) Definition

- GTV, CTV, PTV
- OARs



**3D-U/S
w/o catheters**

Modern Radiation Therapy

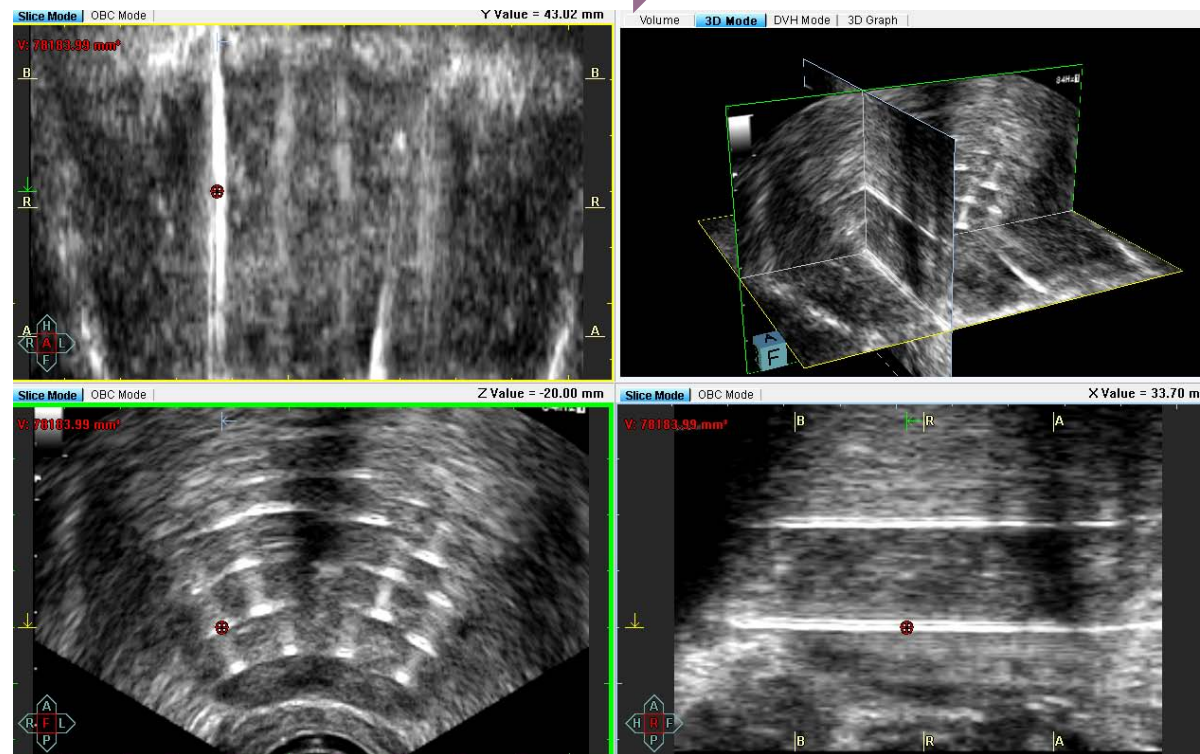
BRT *versus* ERT Similarities and Differences

3D-Patient Model: Anatomy (VOI) Definition

- GTV, CTV, PTV
- OARs



w implanted catheters



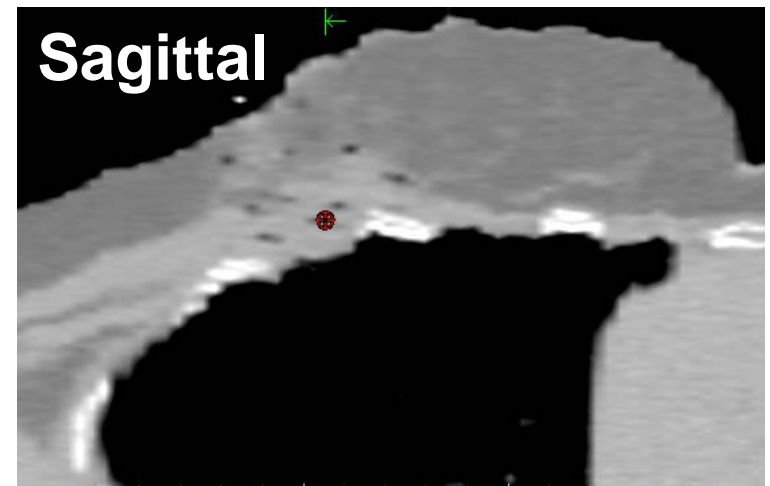
**3D-U/S
with metallic
catheters**

Modern Radiation Therapy

BRT *versus* ERT Similarities and Differences

3D-Patient Model: Catheter (Beam) Configuration

- Localisation of Catheters/Applicators (Beams)
- Visual Control (BEV, skin projection)
- DRRs

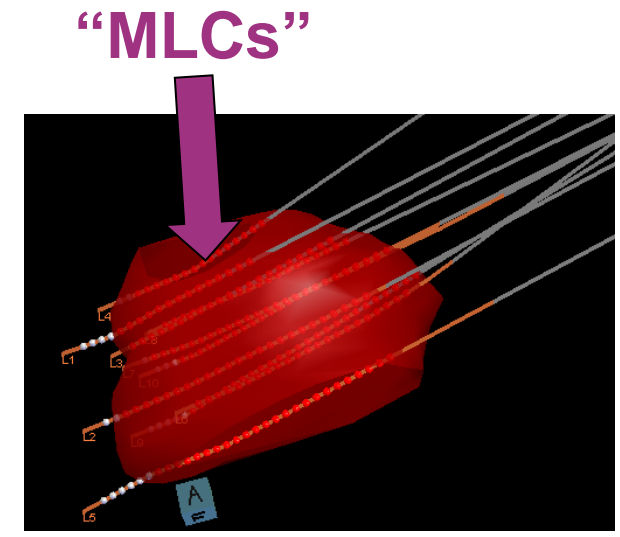
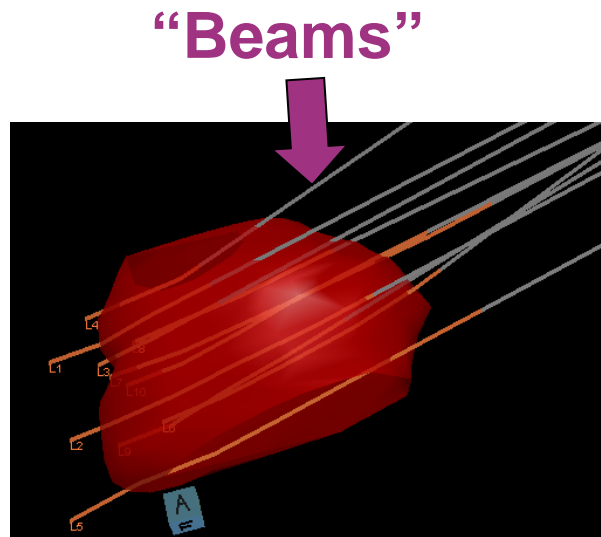


Modern Radiation Therapy

BRT *versus* ERT Similarities and Differences

3D-Patient Model: Catheter (Beam) Configuration

- Localisation of Catheters/Applicators (Beams)
- Visual Control (BEV, skin projection)
- DRRs

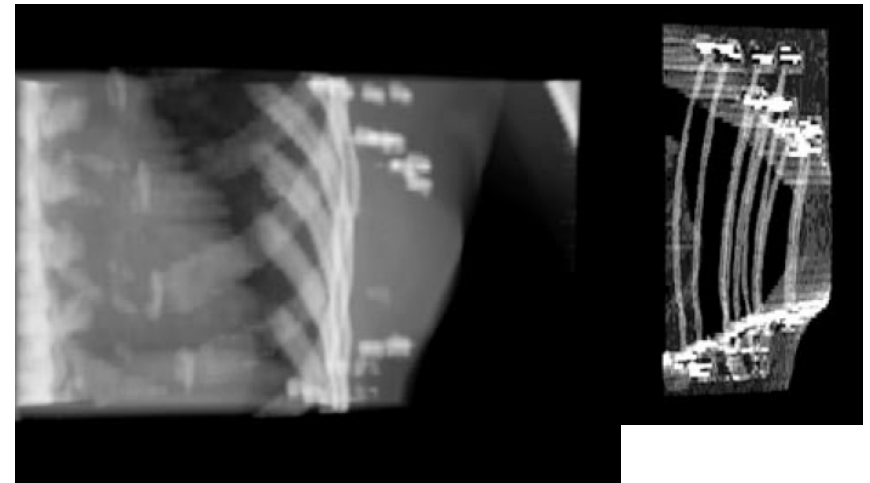
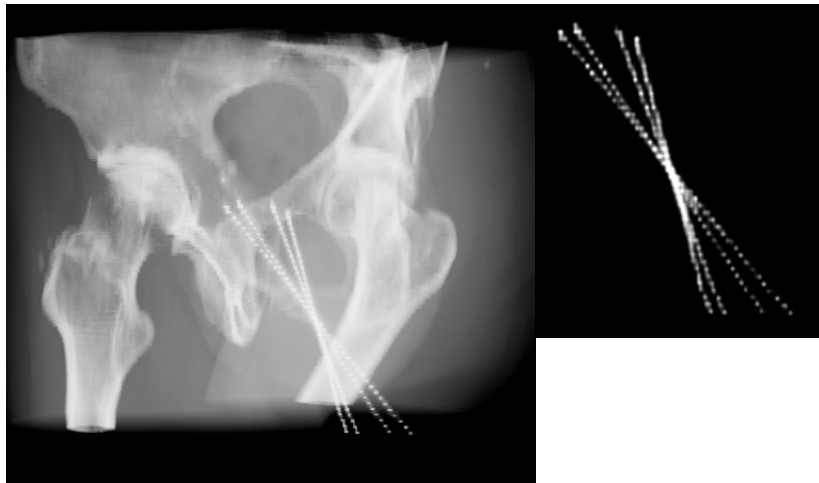


Modern Radiation Therapy

BRT *versus* ERT Similarities and Differences

3D-Patient Model: Catheter (Beam) Configuration

- Localisation of Catheters/Applicators (Beams)
- Visual Control: (BEV, skin projection)
- **DRRs: What is the (analogue of) DRR in BRT?**



Milickovic N., Baltas D, et al. "CT imaging based digitally reconstructed radiographs and their application in brachytherapy", Phys. Med. Biol. 45, 2000

List of Content

- BRT *versus* ERT from Dosimetry Point of View
- BRT *versus* ERT from RTP-Workflow Point of View
- **Introduction to Localisation**
- DVH-Evaluation and Prescription
- Introduction to Dynamic and Adaptive Planning

Modern Brachytherapy Treatment Planning

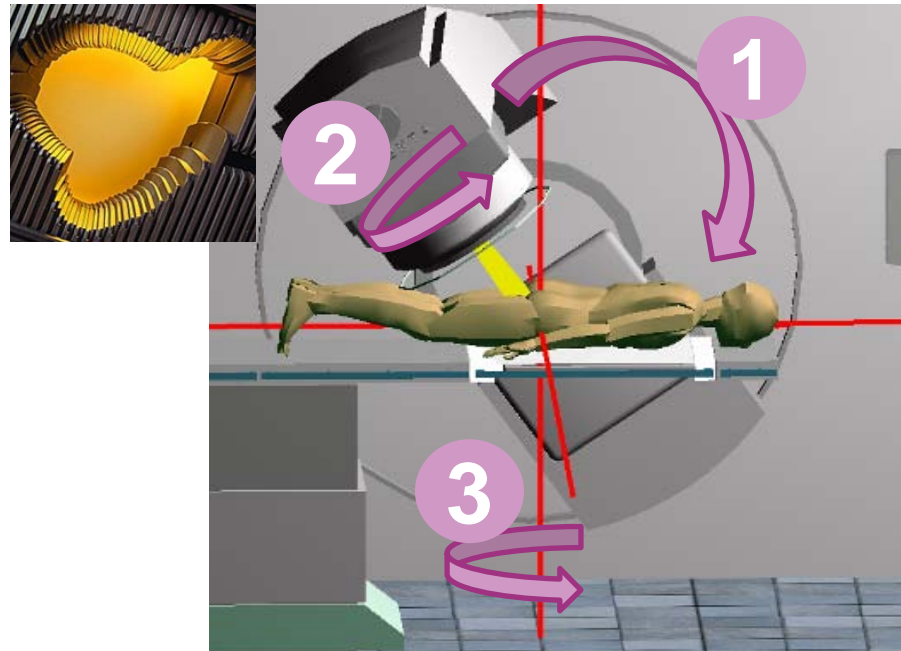
- Immobilization
- Positioning
- External Coordinate System
- **Implantation**
- **Image-Acquisition (CT, MR, U/S, CBCT)**
- 3D-Patient Model
- VOI-Definition
- Prescription
- **Catheters/Applicators (Sources) Localisation**
- **Inverse Optimisation (Intensity modulated)**
- **DVH-Evaluation**
- **Treatment Parameters Transfer**

Modern Brachytherapy Treatment Planning

Catheters/Applicators (Sources) Localisation

In contrast to ERT, where the set-up of the real Beams (irradiation) is based on:

- Immobilization of the patient as in planning process (CT)
- (re)Positioning of the patient using the RP and the Machine Coordinate System (Laser Projection of Isocentre)
→ RP = Laser-Iso
- Imaging-based (2D/3D) verification of Target/Anatomy position
- Fully automatic set-up of the beams and MLC-configurations



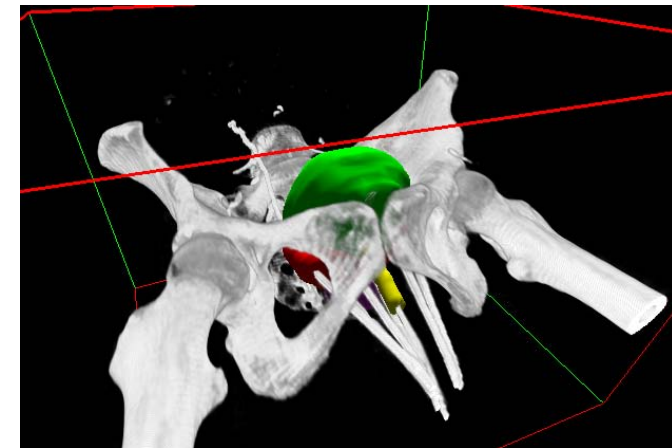
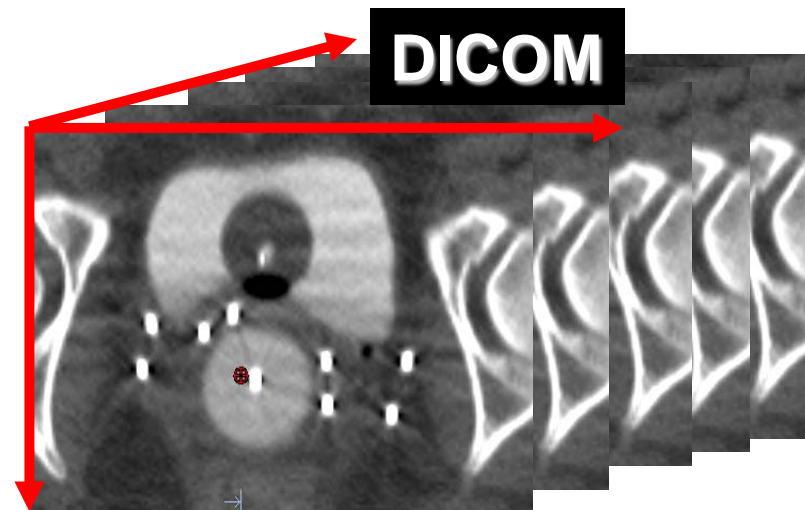
Modern Brachytherapy Treatment Planning

Catheters/Applicators (Sources) Localisation

In contrast to ERT

In BRT the “Beams”, the implanted Catheters/Applicators, have to be firstly localised (reconstructed; definition of their 3D geometry) and registered to the anatomy out of the available imaging data.

Exactly this Co-registration of Anatomy \leftrightarrow Catheters/Applicators replaces the/corresponds to RP \leftrightarrow Laser-Iso Positioning of ERT.



Modern Brachytherapy Treatment Planning

Catheters/Applicators (Sources) Localisation

The actual aim of the Localisation Process is:

to define the 3D-positions of the sources or of the possible source dwell positions and register these to the relevant anatomy (PTV, OARs).

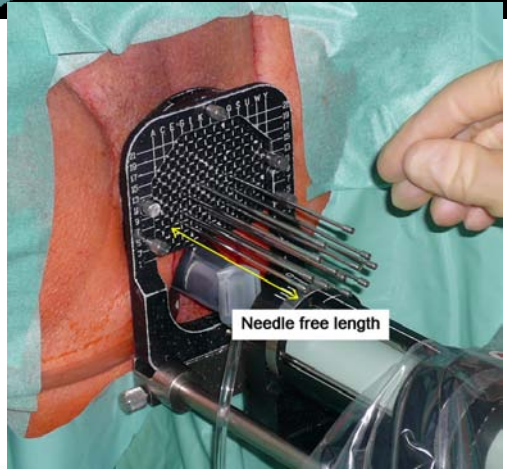
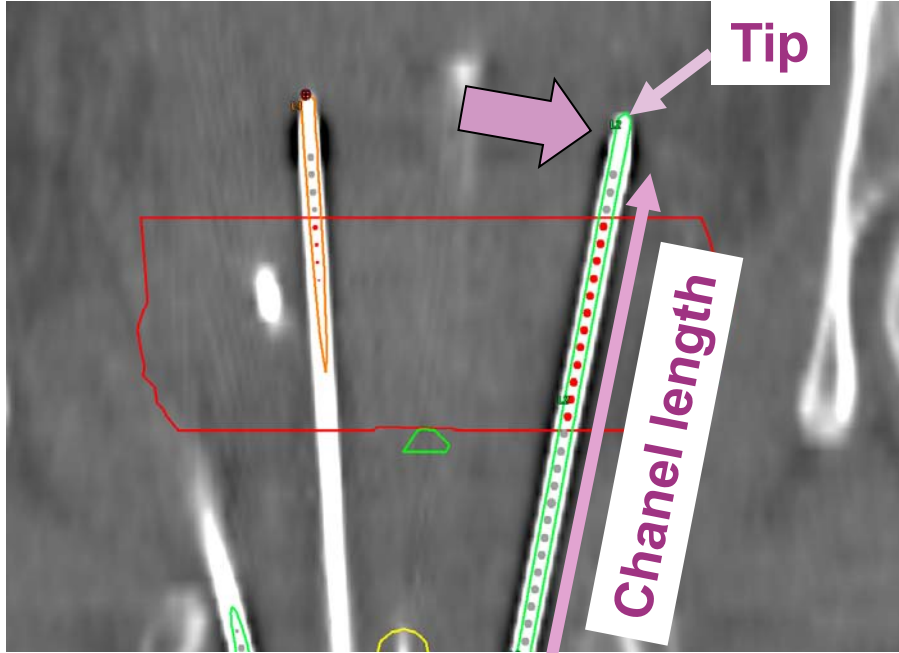
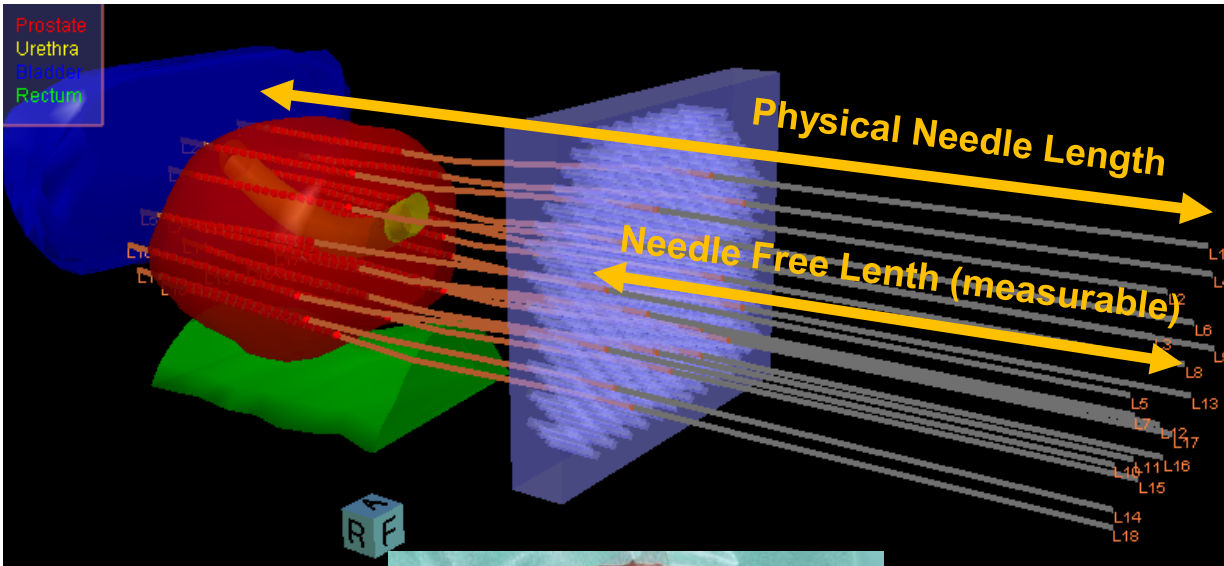
This presumes:

- **Localisation of the implanted Catheters/Needles/ Applicators and**
- **Knowledge of Afterloader and Catheter/Applicator specific Information/Characteristics.**

Modern Brachytherapy Treatment Planning

Catheters/Applicators (Sources) Reconstruction

Knowledge of Afterloader and Catheter/Applicator specific Information/Characteristics

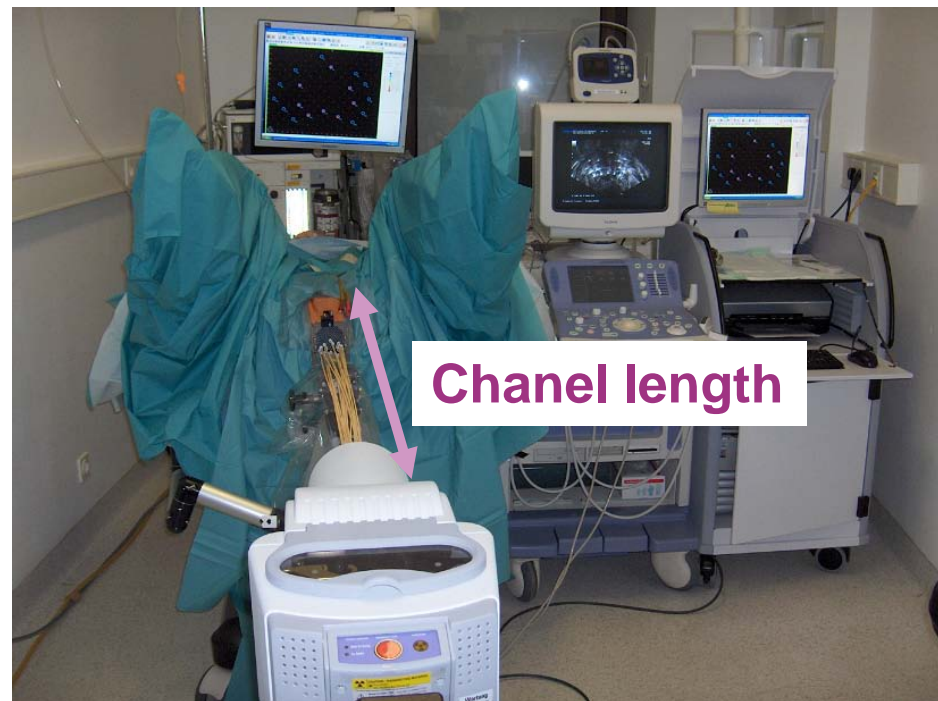
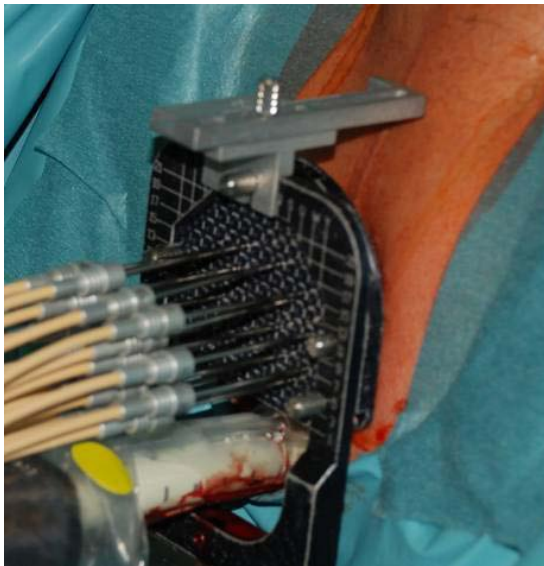


Afterloader

Modern Brachytherapy Treatment Planning

Catheters/Applicators (Sources) Reconstruction

Knowledge of Afterloader and Catheter/Applicator specific Information/Characteristics



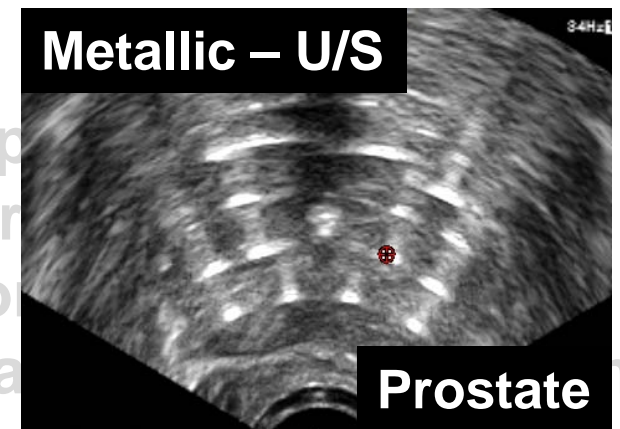
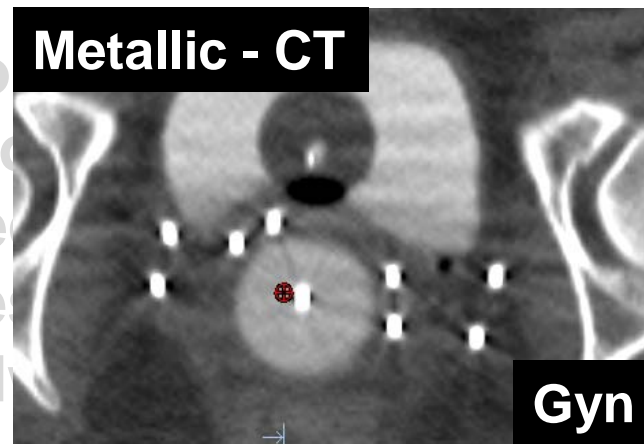
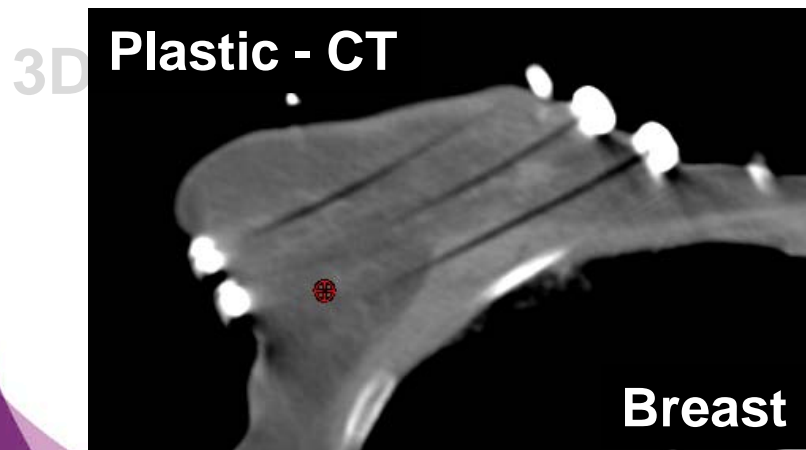
Modern Brachytherapy Treatment Planning

Catheters/Applicators (Sources) Localisation

In general there are exist two methods for the Localisation of the sources/ possible source dwell positions.

Source Path Method

Here the “*finger-print*” of the individual implanted catheters/ applicators on the acquired images is utilized (interstitial implants, endoluminal and simple endocavitary applicators)

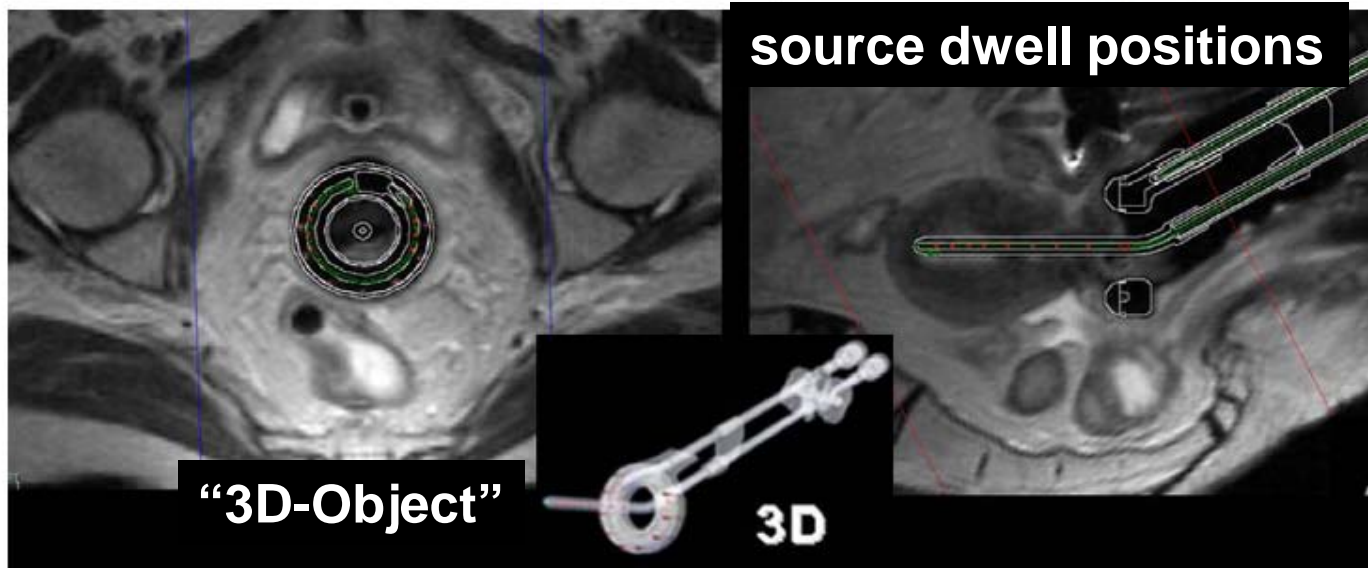


Modern Brachytherapy Treatment Planning

Catheters/Applicators (Sources) Localisation

In general
sources/
imp

Source P
Hel
app
imp



of the

theters/
titial
icators)

Fig. 7. Position of a library applicator (in the middle) in the transversal (left) and sagittal (right) plane.

3D-Applicator Model Method

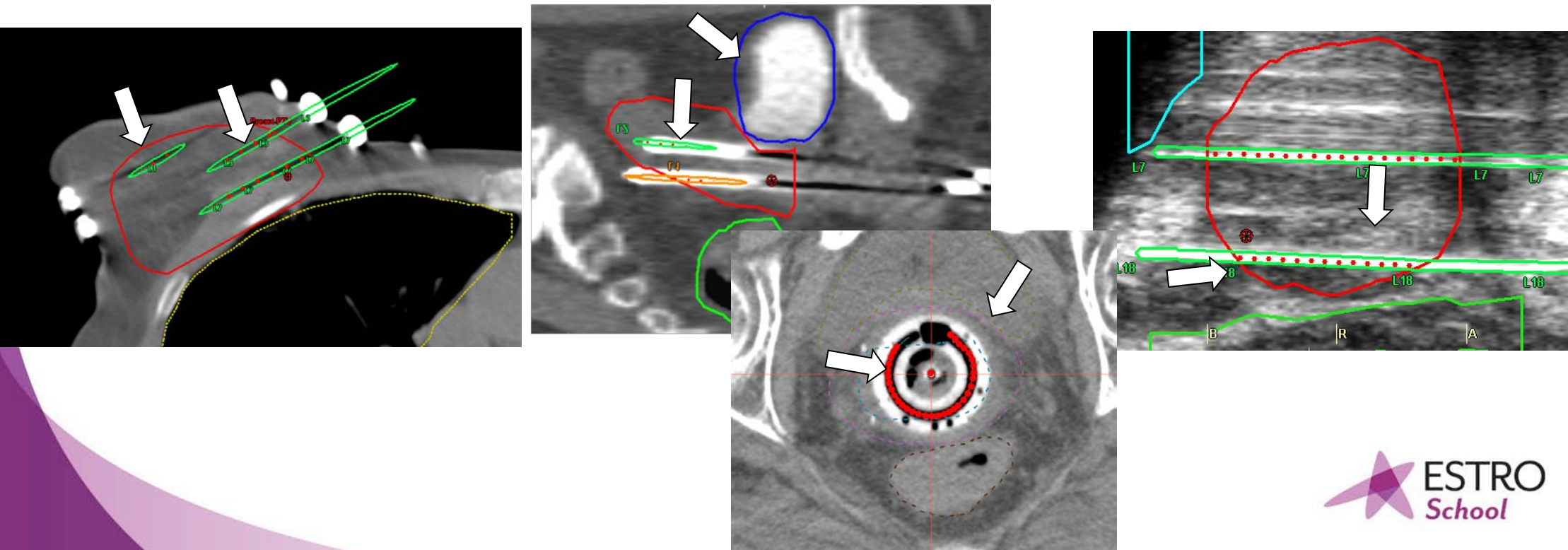
Here the 3D Applicator geometry (rigid) is preexisting and stored as a "3D-Object" including all required information for generation of sources/source dwell positions (source paths, all possible source dwell positions and channel length for each path, ...)

Modern Brachytherapy Treatment Planning

Catheters/Applicators (Sources) Localisation

The actual aim of the Localisation Process is:

to define the 3D-positions of the sources or of the possible source dwell positions and register these to the relevant anatomy (PTV, OARs).



Modern Brachytherapy Treatment Planning

Catheters/Applicators (Sources) Localisation

Session on 3D Imaging Localisation

- 3D imaging modalities and techniques

C. Kirisits

- Catheter/Applicator and source localisation using 3D imaging

M. Rivard

List of Content

- BRT *versus* ERT from Dosimetry Point of View
- BRT *versus* ERT from RTP-Workflow Point of View
- Introduction to Localisation
- DVH-Evaluation and Prescription
- Introduction to Dynamic and Adaptive Planning

Modern Brachytherapy Treatment Planning

- Immobilization
- Positioning
- External Coordinate System
- **Implantation**
- **Image-Acquisition (CT, MR, U/S, CBCT)**
- 3D-Patient Model
- VOI-Definition
- **Prescription**
- Catheters/Applicators (Sources) Localisation
- **Inverse Optimisation (Intensity modulated)**
- **DVH-Evaluation**
- **Treatment Parameters Transfer**

Modern Brachytherapy Treatment Planning

For all further steps in RTP-Workflow in BRT, following is given:

- **3D-Model of the patient anatomy**
 - Target(s)
 - OARs
- **3D-Model of the implant**
 - Catheter and/or applicators
 - (Possible and) active source dwell positions ASDPs
- **Their Co-Registration**
 - DICOM-coordinate system
- **Dwell times for all ASDPs (Optimization, Inverse/Forward)**

Modern Brachytherapy Treatment Planning

For all further steps in RTP-Workflow in BRT, following is presumed:

- **Dose-Calculation Engine**

Monday Session on Dose Calculation

L. Beaulieu, P. Papagiannis and M. Rivard

- **DVH-Calculation Engine**

Tuesday Session on Optimization and Prescription

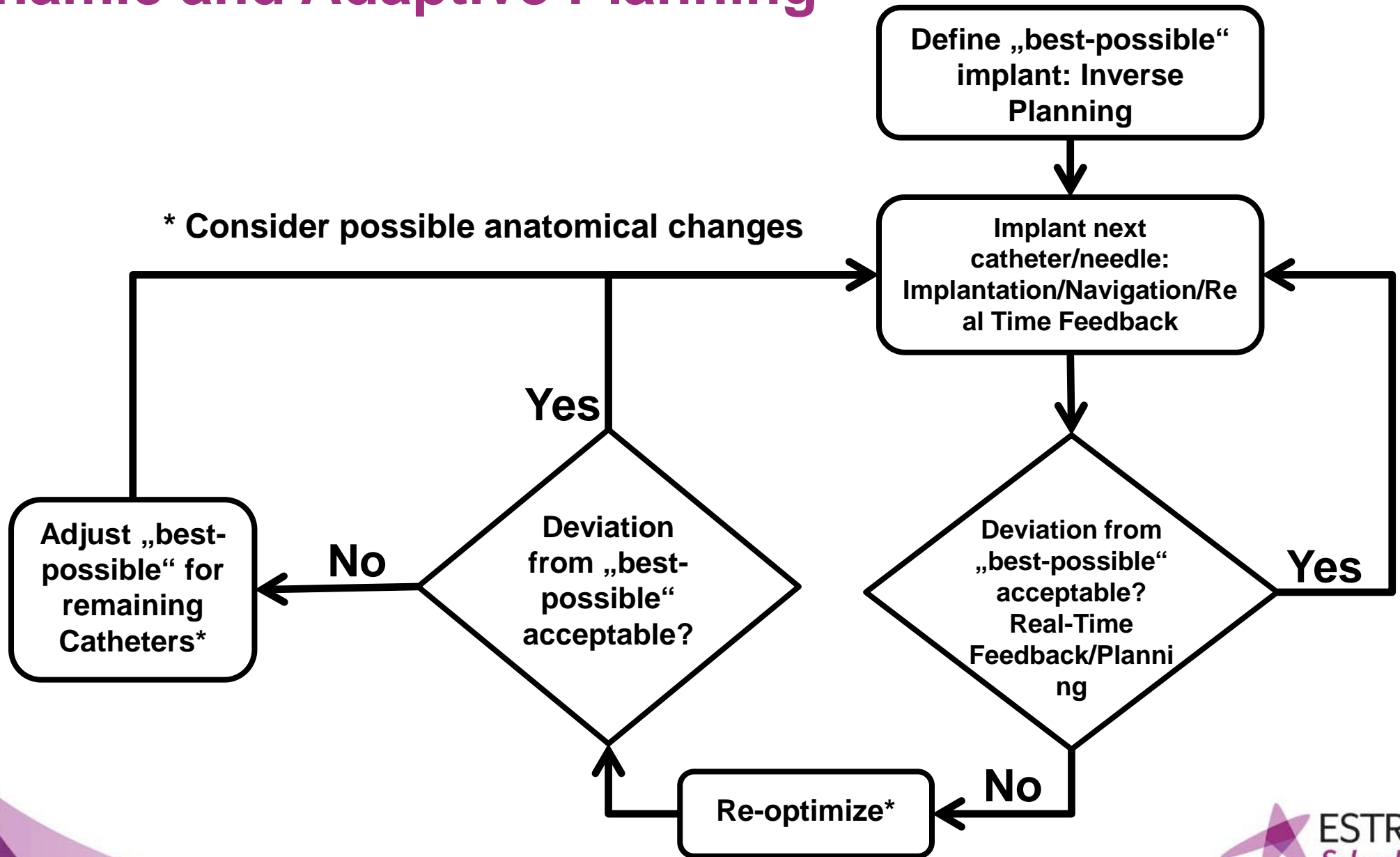
D. Baltas and C. Kirisits

List of Content

- BRT *versus* ERT from Dosimetry Point of View
- BRT *versus* ERT from RTP-Workflow Point of View
- Introduction to Localisation
- DVH-Evaluation and Prescription
- Introduction to Dynamic and Adaptive Planning

Modern Brachytherapy Treatment Planning

Dynamic and Adaptive Planning

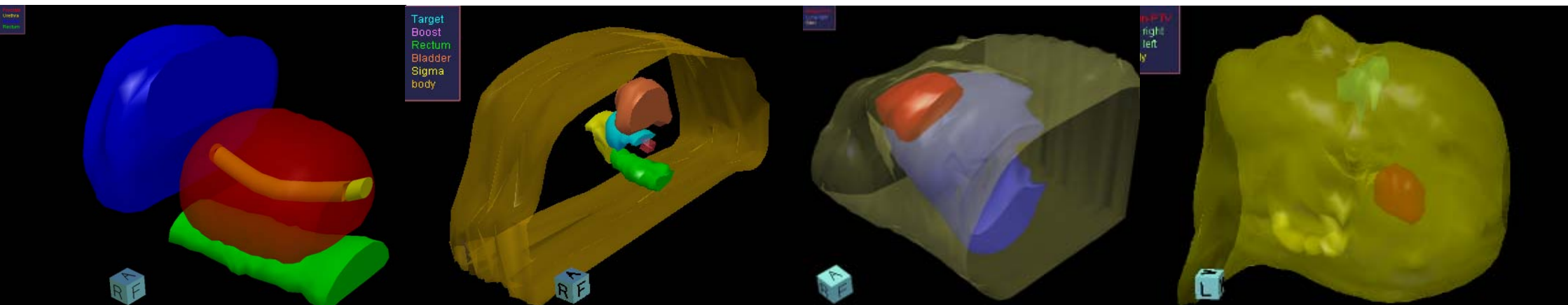


Modern Brachytherapy Treatment Planning

Define “best-possible” = Inverse Planning

It presupposes the availability of:

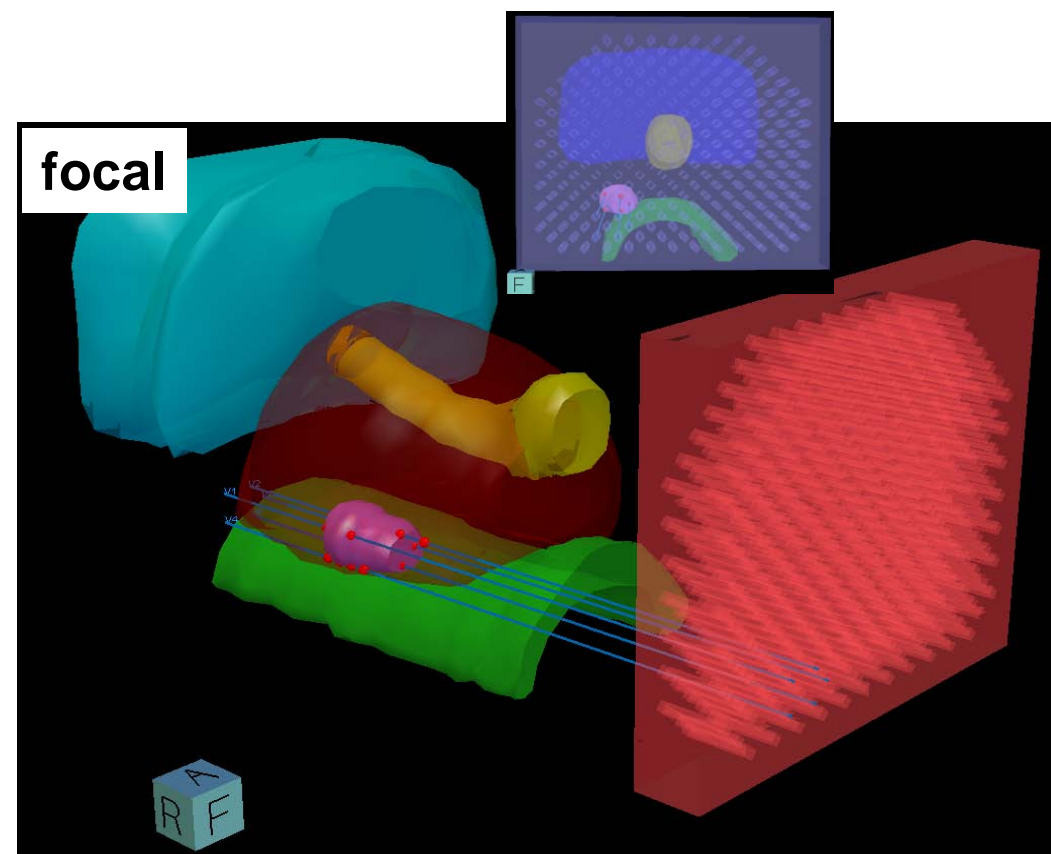
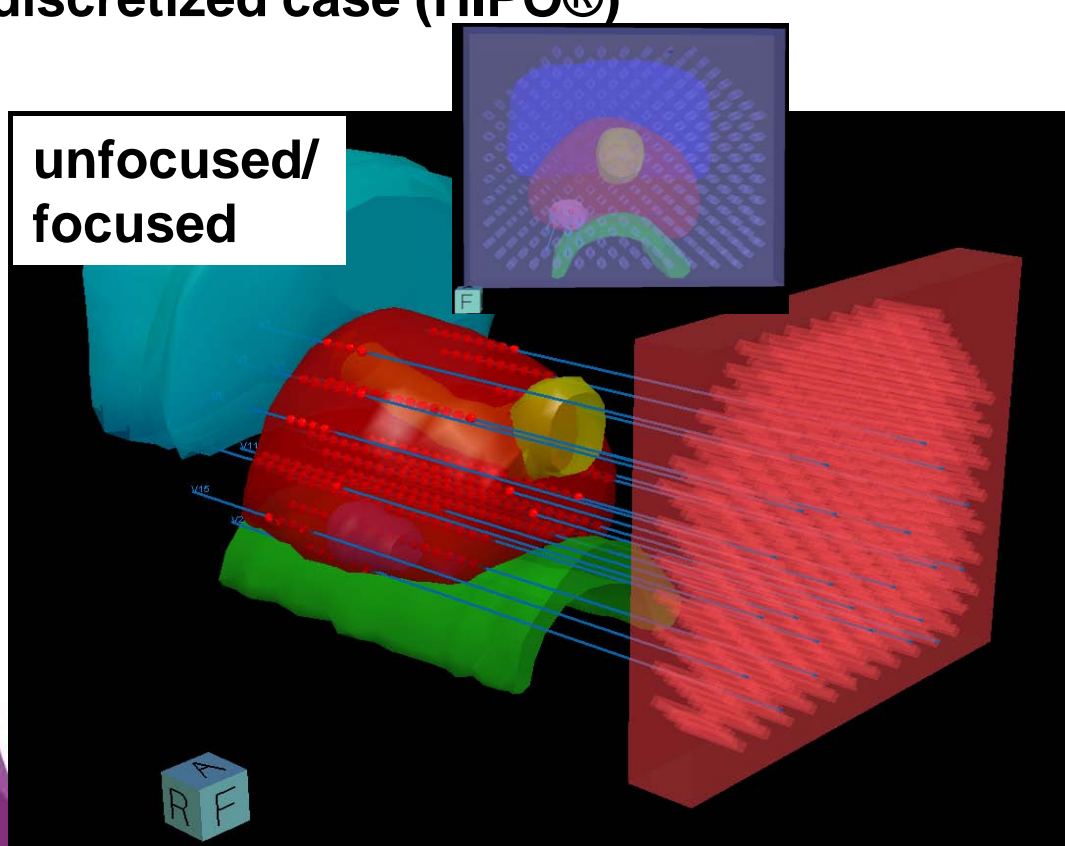
- A complete 3D anatomy model
VOIs: Target(s), OARs } Morphology (3D Imaging)
- The Desired Dose Distribution



Modern Brachytherapy Treatment Planning

Inverse Planning:

The automatic placement of an adequate number of catheters/applicators/needles based on dosimetric objectives and constraints. Consideration of (i) *Medical* (ii) *Anatomical* und (iii) *Technical Implantation* demands/presetting. It is solvable in clinically acceptable time only after *discretisation*. Clinically available for the discretized case (HIPO®)

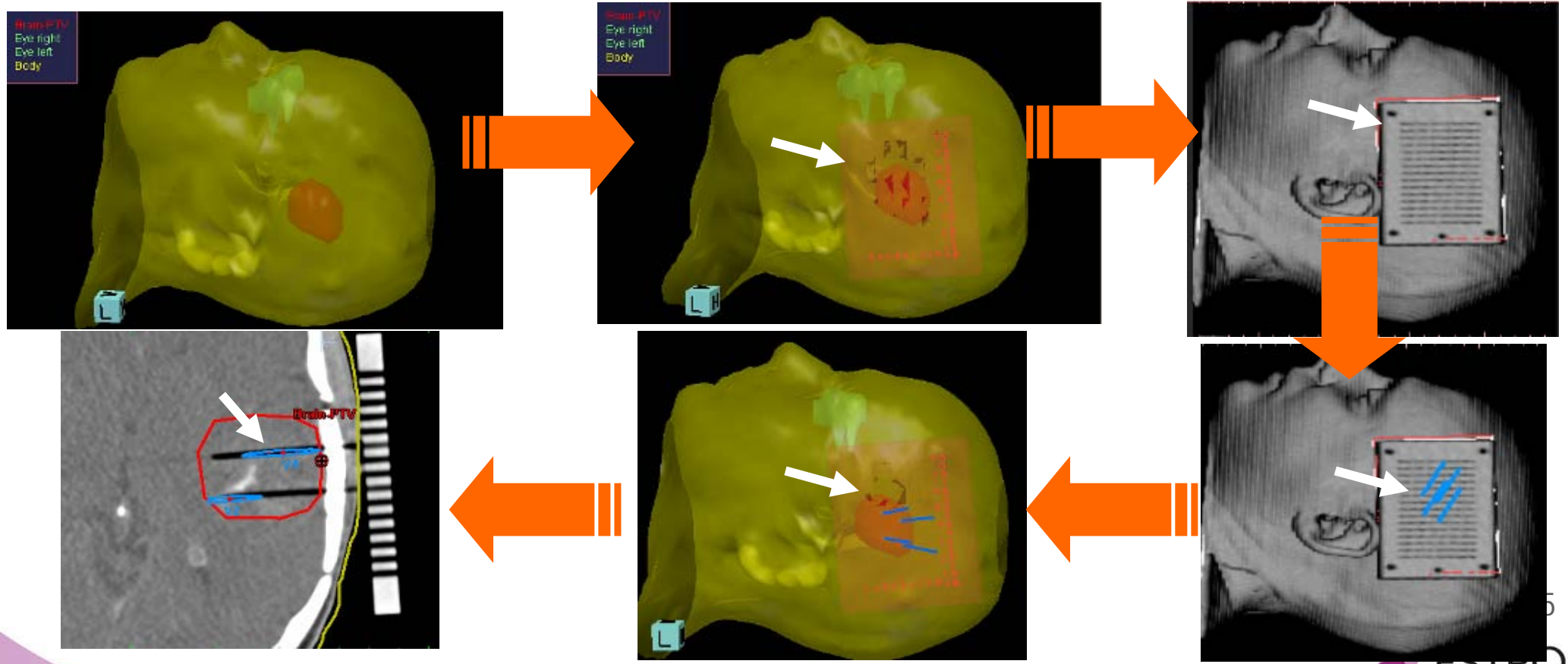


HIPO® by Pi-Medical Ltd. for any localisation template based, combination of „template“ and applicators etc...
IPSA by Nucletron an ELEKTA Company, for permanent prostate implants.

Modern Brachytherapy Treatment Planning

Inverse Planning:

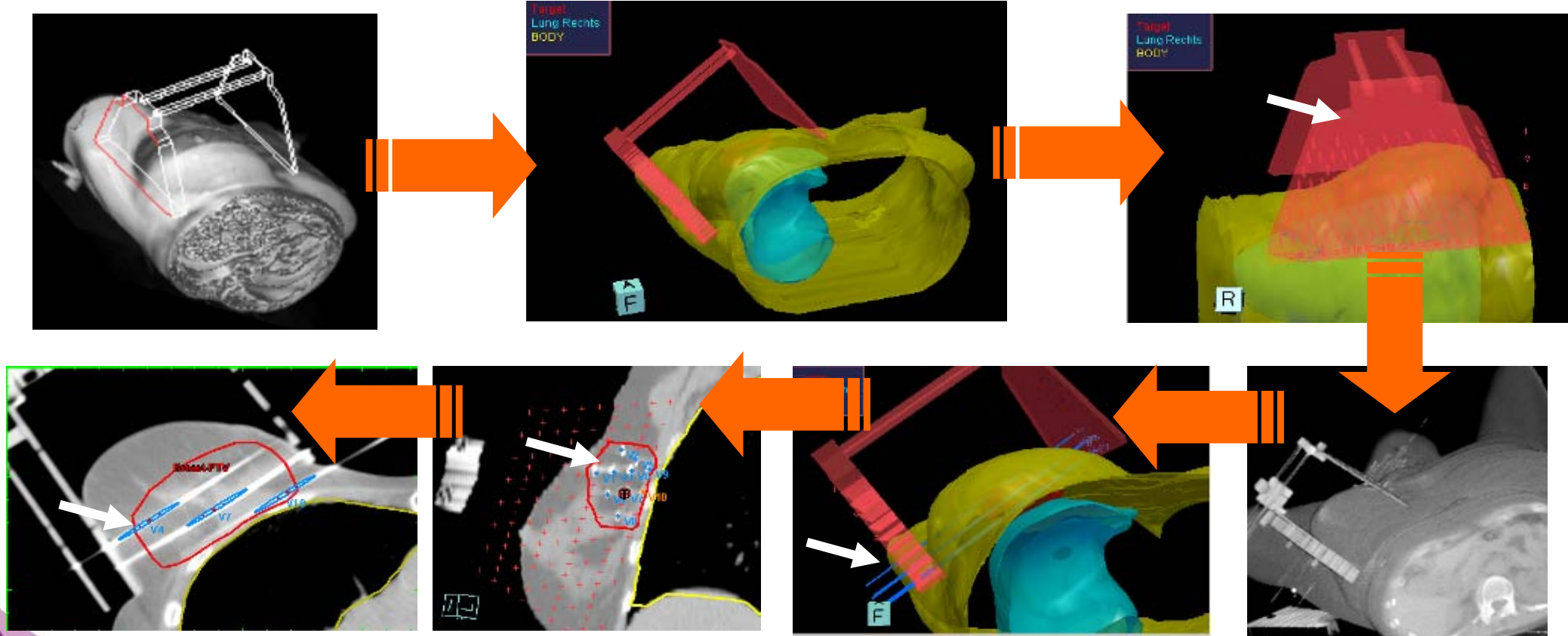
The automatic placement of an adequate number of catheters/applicators/needles based on dosimetric objectives and constraints. Consideration of (i) *Medical* (ii) *Anatomical* und (iii) *Technical Implantation* demands/presetting. It is solvable in clinically acceptable time only after *discretisation*. Clinically available for the discretized case (HIPO®)



Modern Brachytherapy Treatment Planning

Inverse Planning:

The automatic placement of an adequate number of catheters/applicators/needles based on dosimetric objectives and constraints. Consideration of (i) *Medical* (ii) *Anatomical* und (iii) *Technical Implantation* demands/presetting. It is solvable in clinically acceptable time only after *discretisation*. Clinically available for the discretized case (HIPO®)



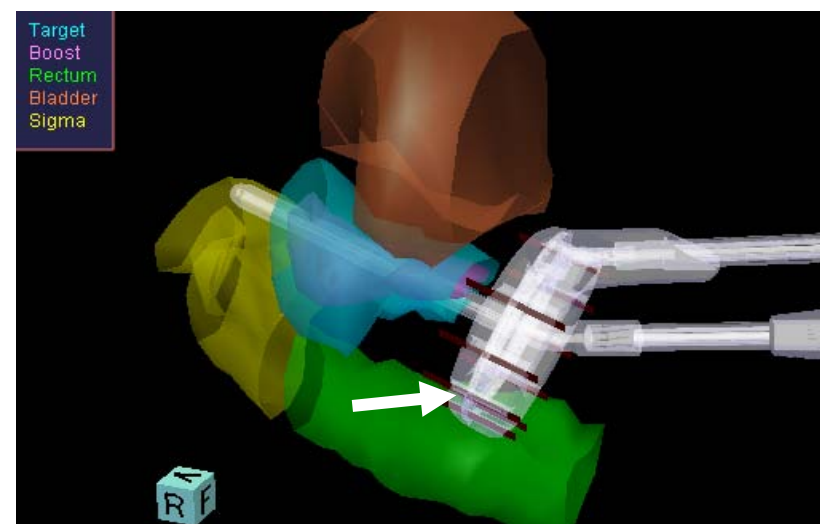
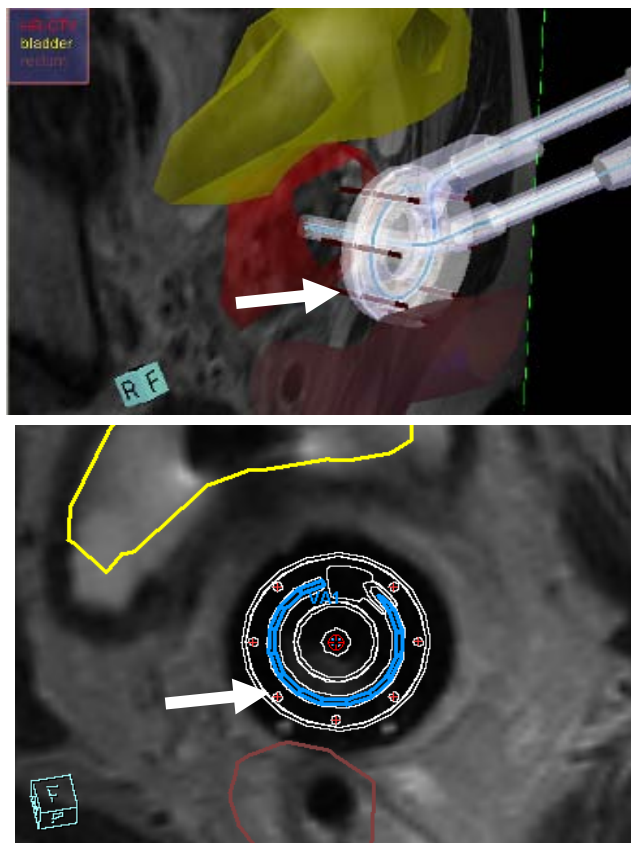
HIPO® by Pi-Medical Ltd. for any localisation template based, combination of „template“ and applicators etc...
IPSA by Nucletron an ELEKTA Company, for permanent prostate implants.



Modern Brachytherapy Treatment Planning

Inverse Planning:

The automatic placement of an adequate number of catheters/applicators/needles based on dosimetric objectives and constraints. Consideration of (i) *Medical* (ii) *Anatomical* und (iii) *Technical Implantation* demands/presetting. It is solvable in clinically acceptable time only after *discretisation*. Clinically available for the discretized case (HIPO®)

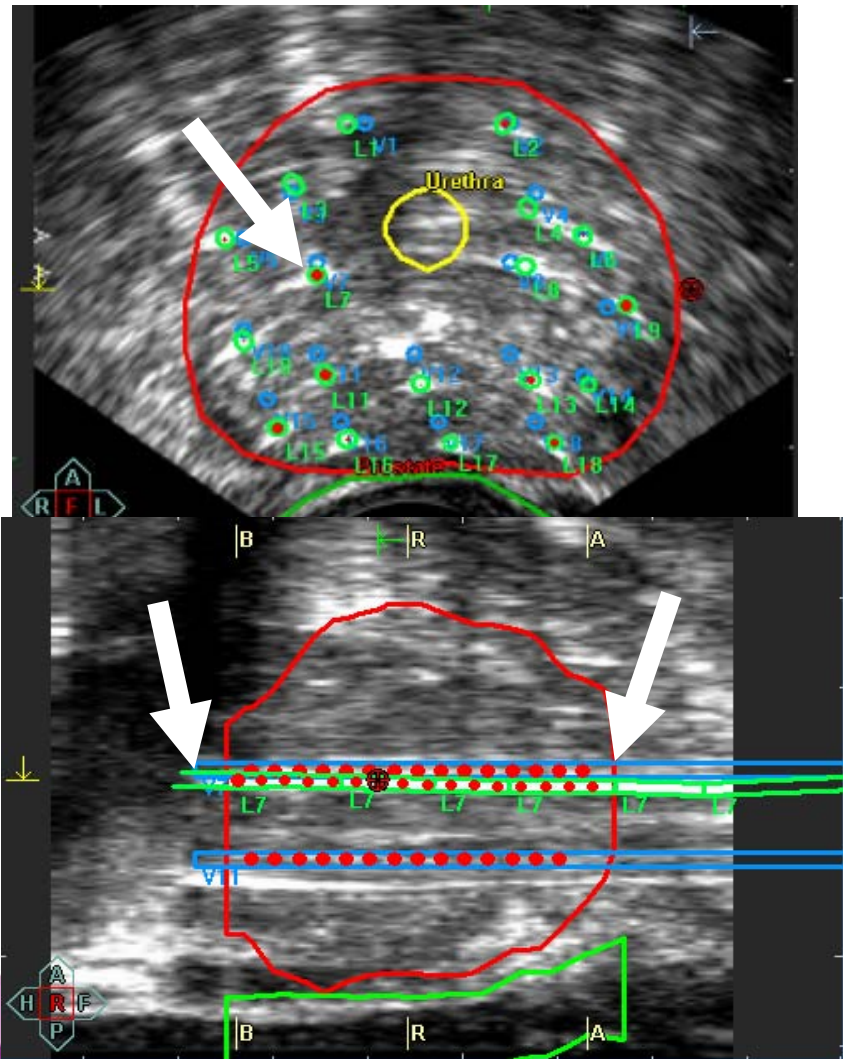


Cervix-Ca: Applicator + Needles
Data by courtesy of University of Vienna

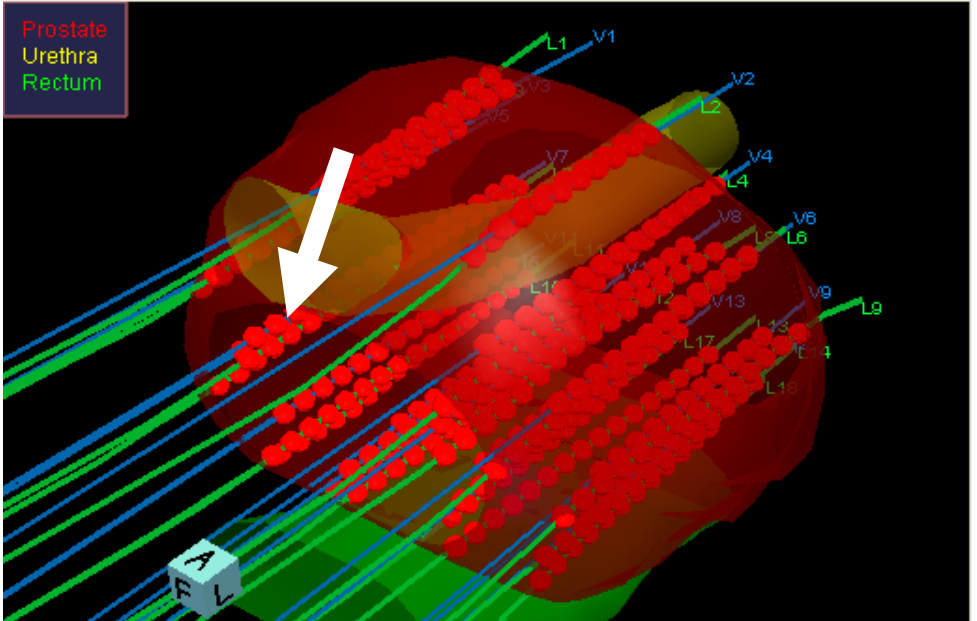
Modern Brachytherapy Treatment Planning

Dynamic and Adaptive Planning:

Adaptation of the implant geometry and of the physical dose distribution during the implantation process for the Occurrence of (i) *Changes in the Anatomy (Morphology)* and (ii) *Deviations in the catheter placement.*



Virtual (inverse planned)
versus
Real (implanted) Catheters

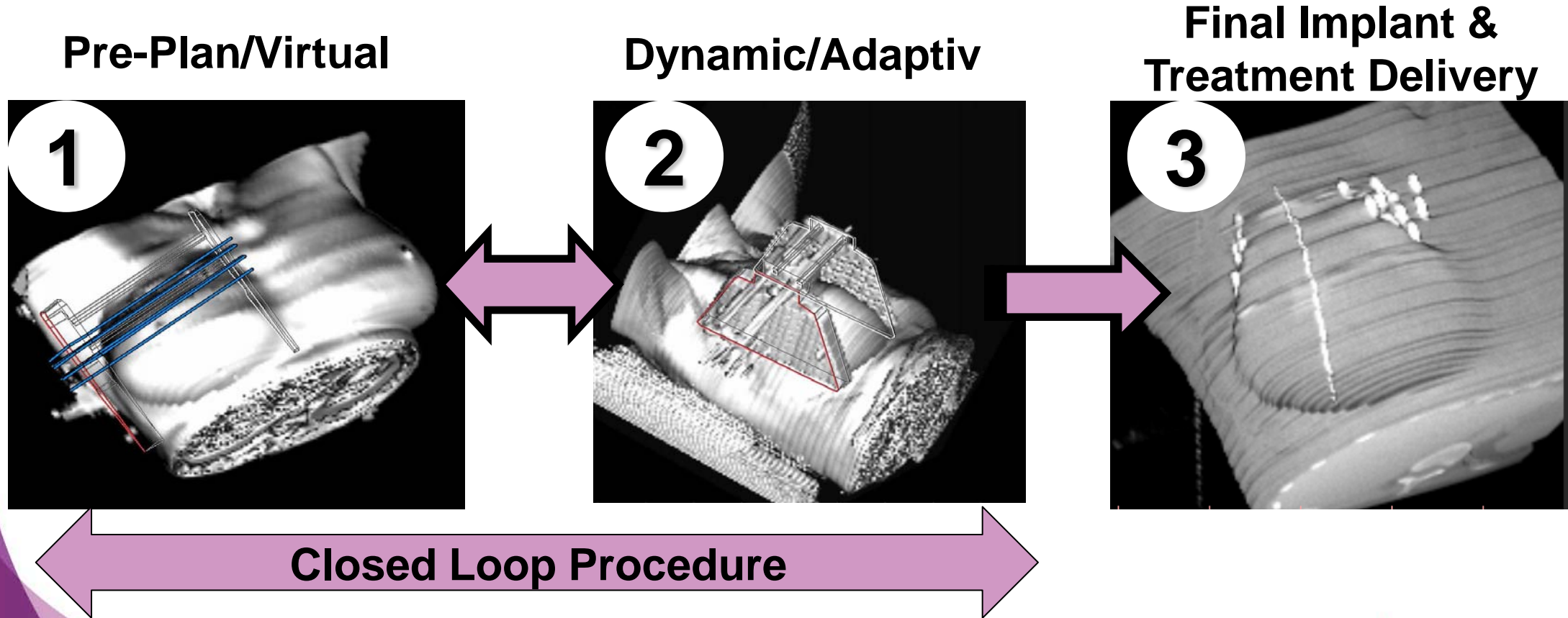


Modern Brachytherapy Treatment Planning

Dynamic and Adaptive Planning:

Adaptation of the implant geometry and of the physical dose distribution during the implantation process for the Occurrence of (i) *Changes in the Anatomy (Morphology)* and (ii) *Deviations in the catheter placement*.

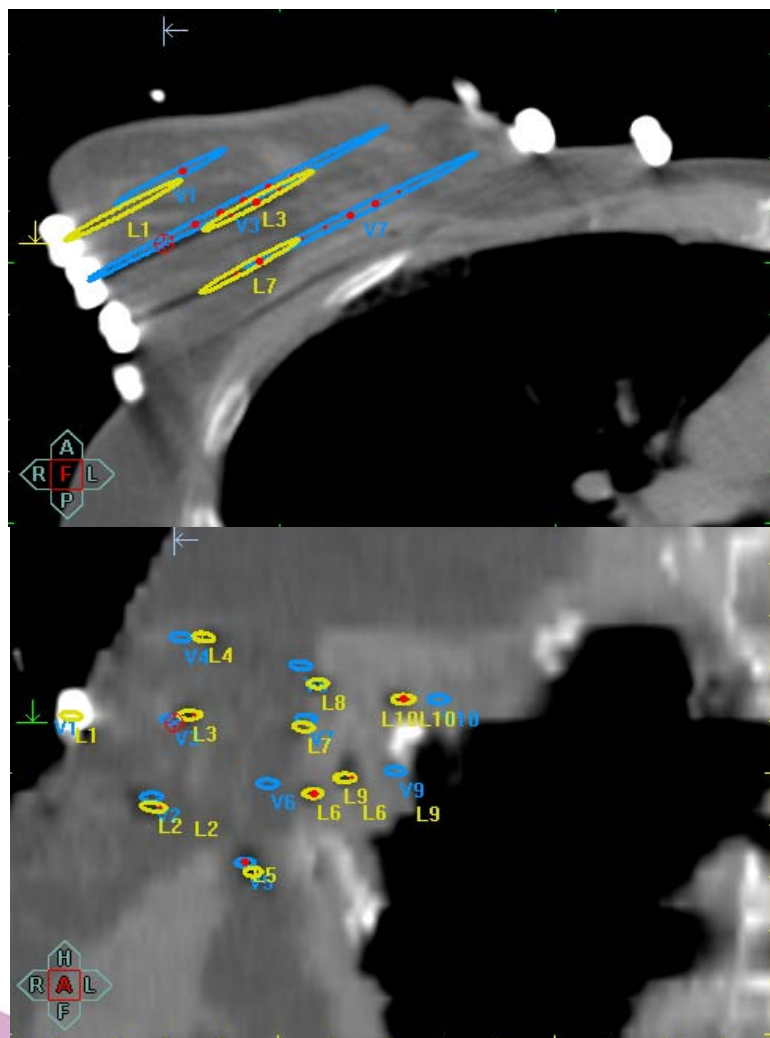
Clinically available for the discretized case (HIPO®)



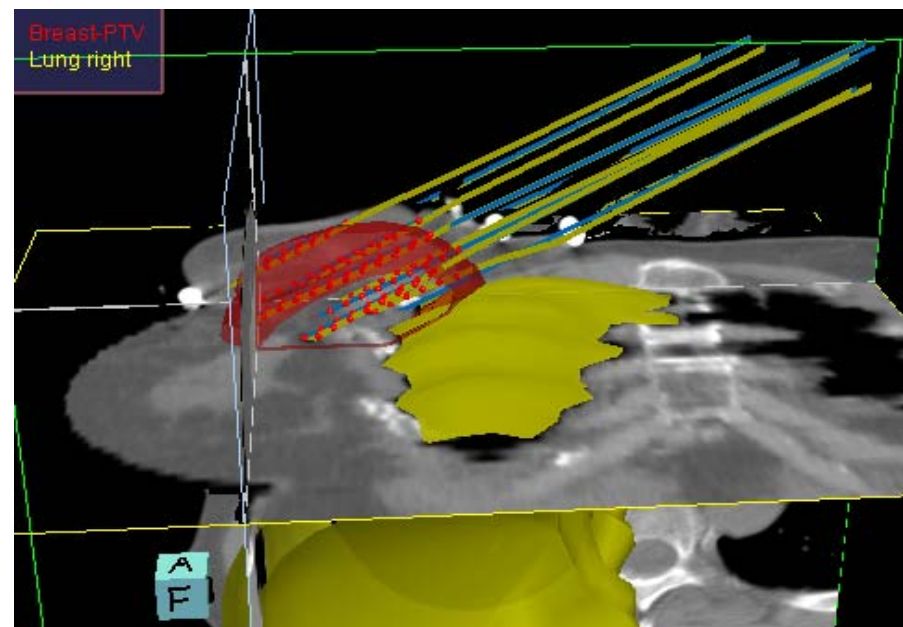
Modern Brachytherapy Treatment Planning

Dynamic and Adaptive Planning:

Adaptation of the implant geometry and of the physical dose distribution during the implantation process for the Occurrence of (i) *Changes in the Anatomy (Morphology)* and (ii) *Deviations in the catheter placement*.



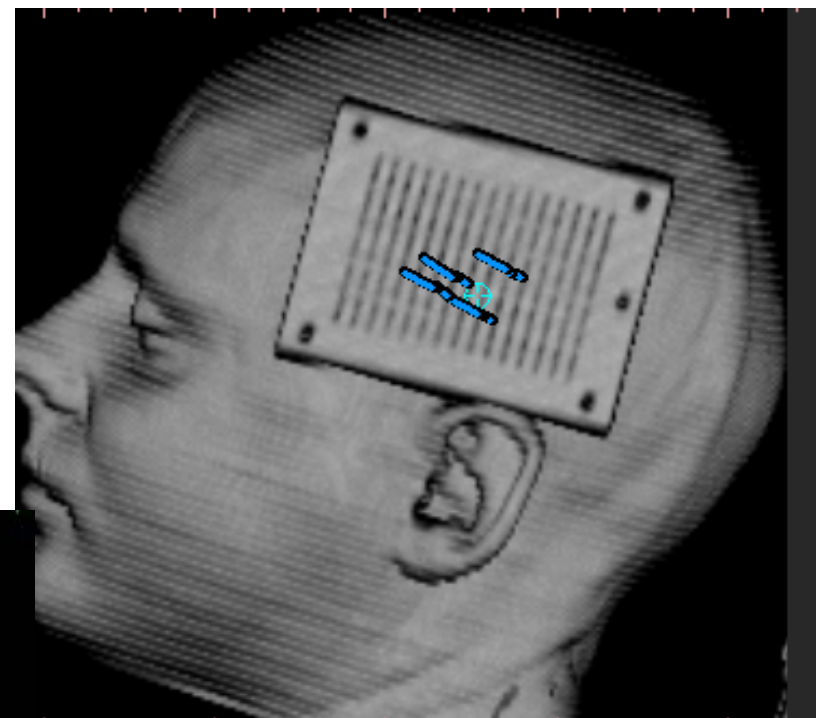
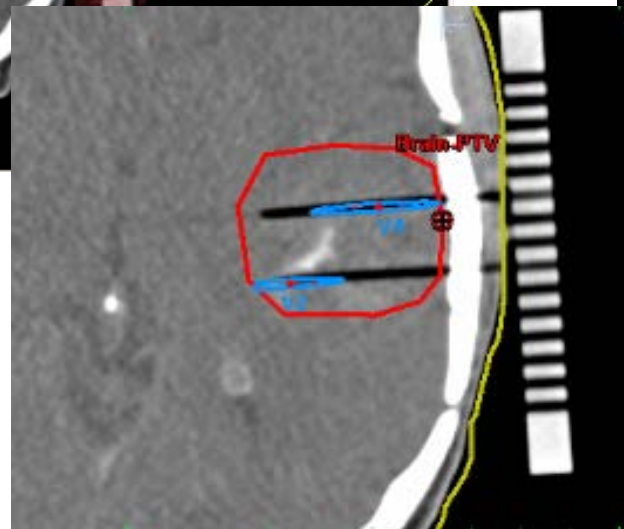
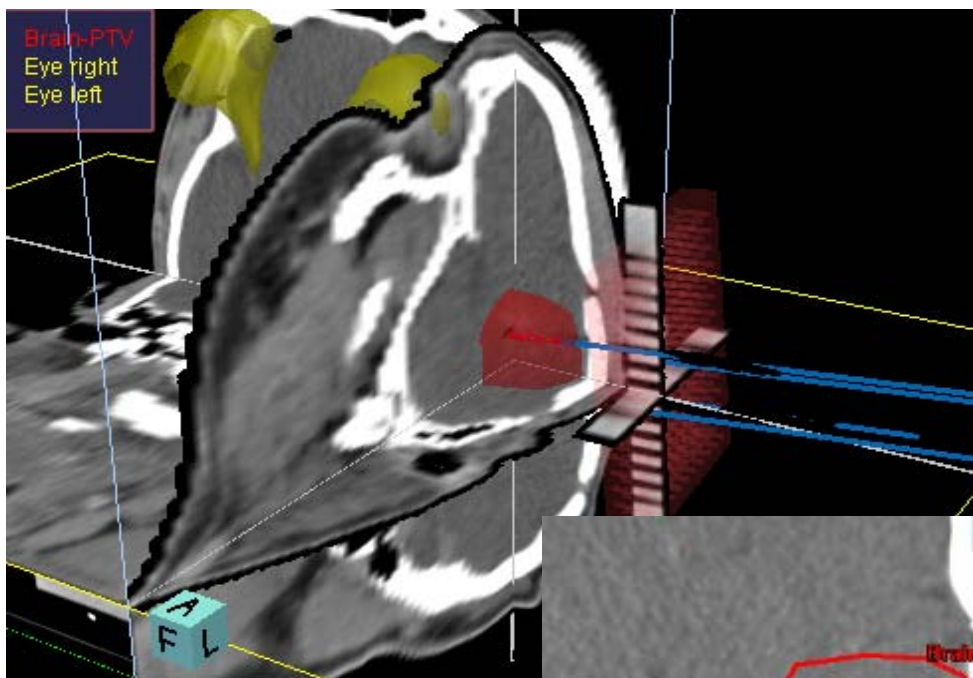
Virtual (inverse planned)
versus
Real (implanted) Catheters



Modern Brachytherapy Treatment Planning

Dynamic and Adaptive Planning:

Adaptation of the implant geometry and of the physical dose distribution during the implantation process for the Occurrence of (i) *Changes in the Anatomy (Morphology)* and (ii) *Deviations in the catheter placement*.



List of Content

- ✓ **BRT *versus* ERT from Dosimetry Point of View**
- ✓ **BRT *versus* ERT from RTP-Workflow Point of View**
- ✓ **Introduction to Reconstruction**
- ✓ **DVH-Evaluation and Prescription**
- ✓ **Introduction to Dynamic and Adaptive Planning**



**Thank you very much
for your Attention !**

Vienna, May 29 – June 1, 2016



**Advanced Brachytherapy
Physics**

3D Imaging modalities and techniques

Christian Kirisits
Chairman of GEC-ESTRO



Disclosure:

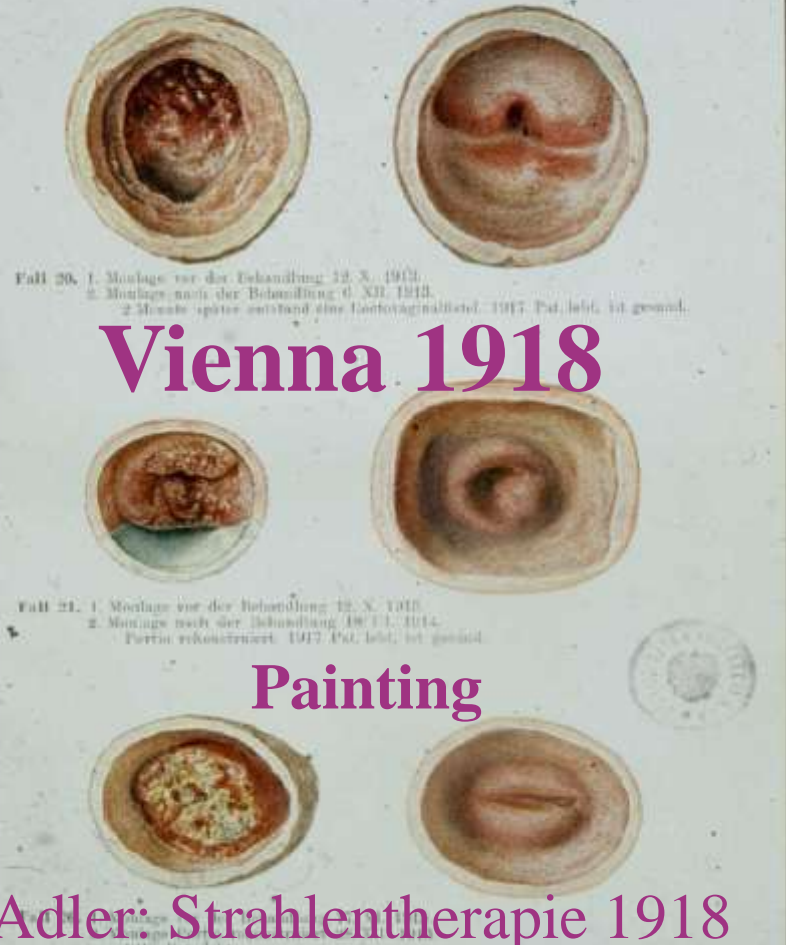
Christian Kirisits reports no conflicts of interest
Christian Kirisits was a consultant to Nucletron, an Elekta
Company
Medical University of Vienna receives financial and
equipment support for training and research activities from
Nucletron, an Elekta Company and Varian Medical

Advanced Brachytherapy Physics, 2016



Clinical Evaluation

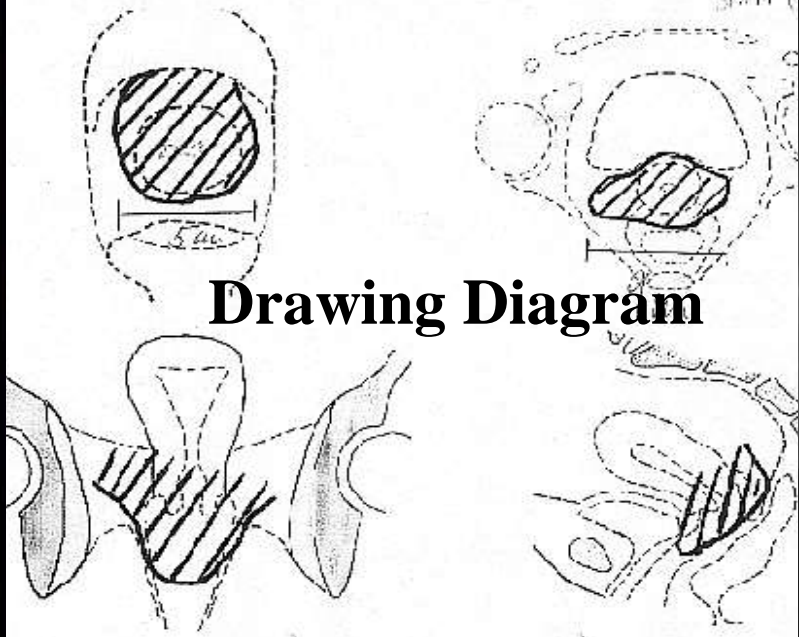
Radiography



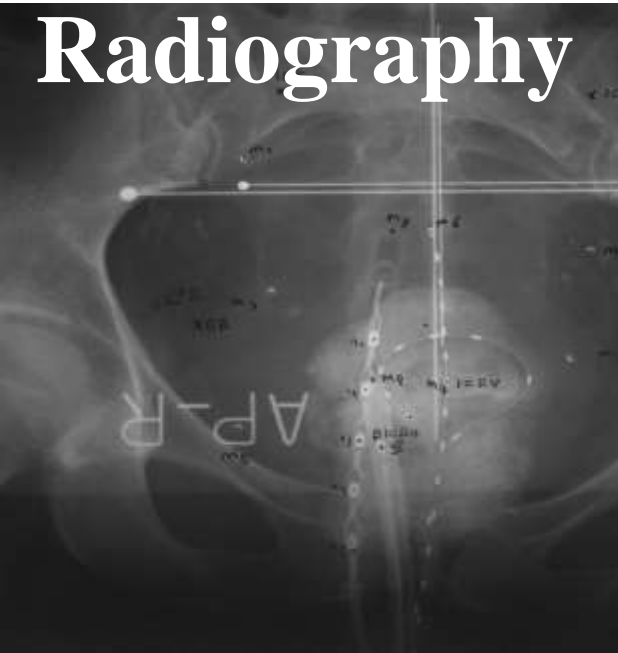
Vienna 1918

Painting

Adler: Strahlentherapie 1918

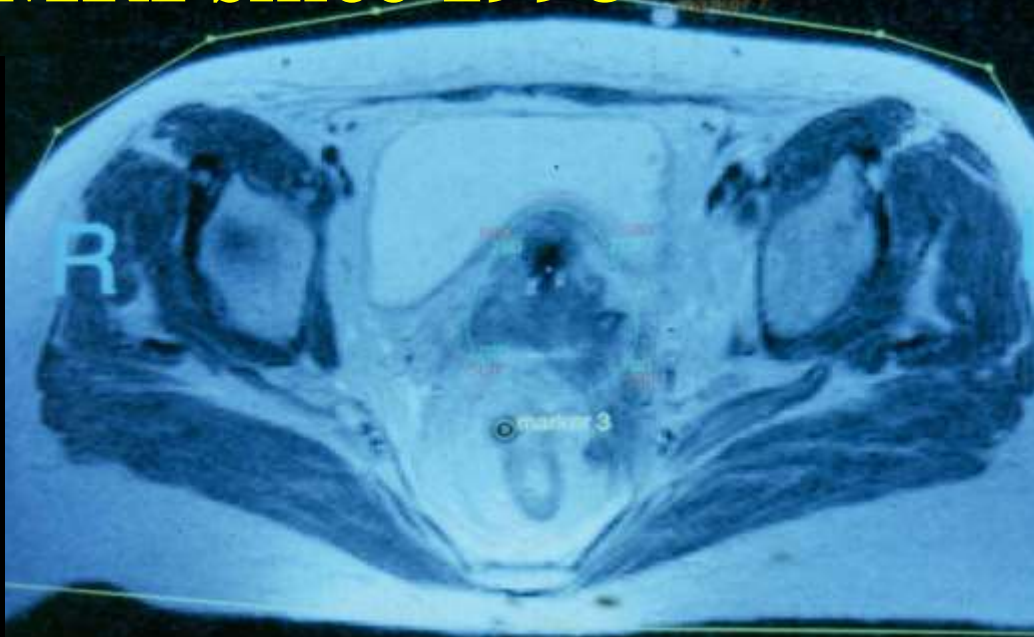


Drawing Diagram



MRI since 1998

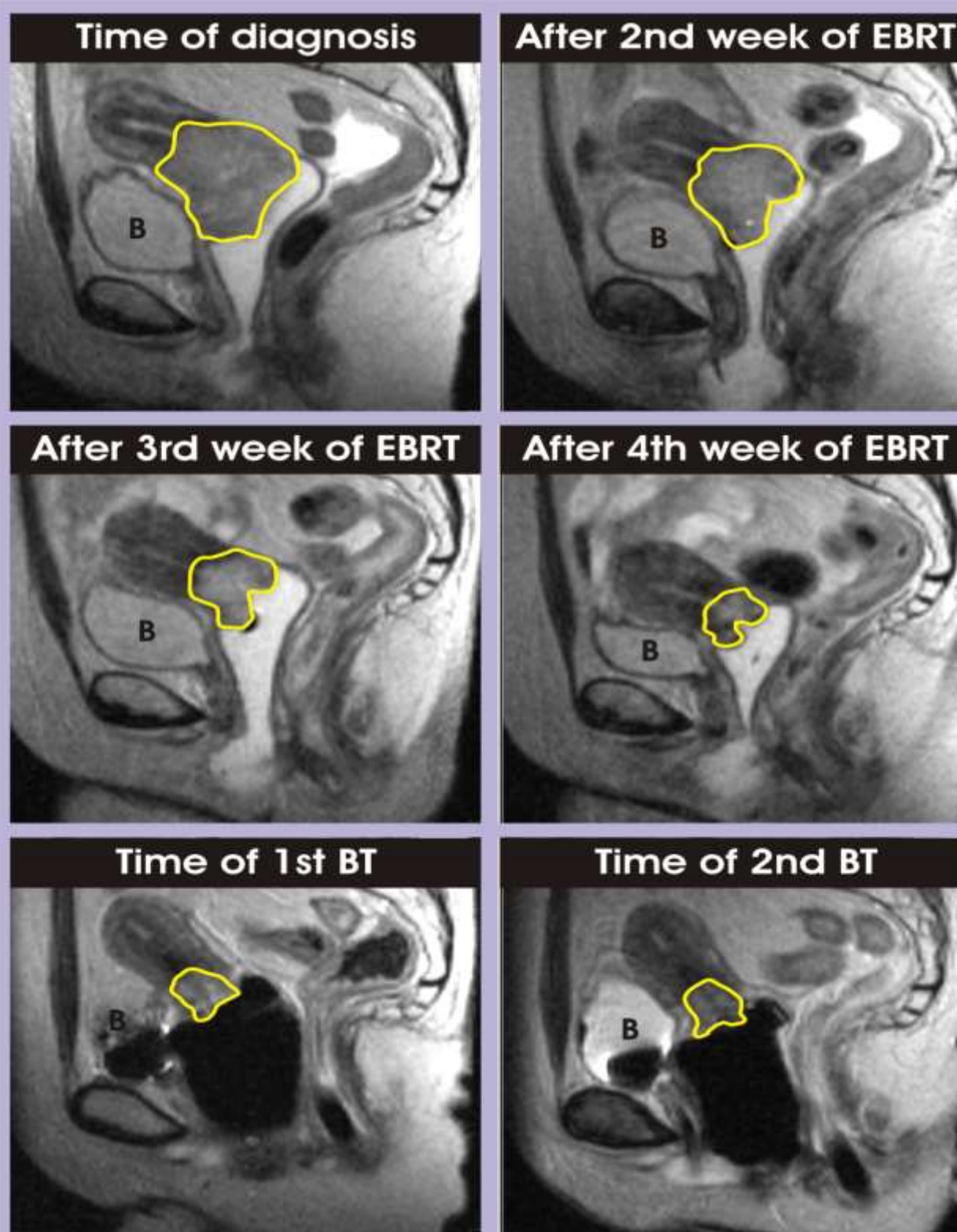
CT since 1983



History of 3D volumetric imaging in brachytherapy

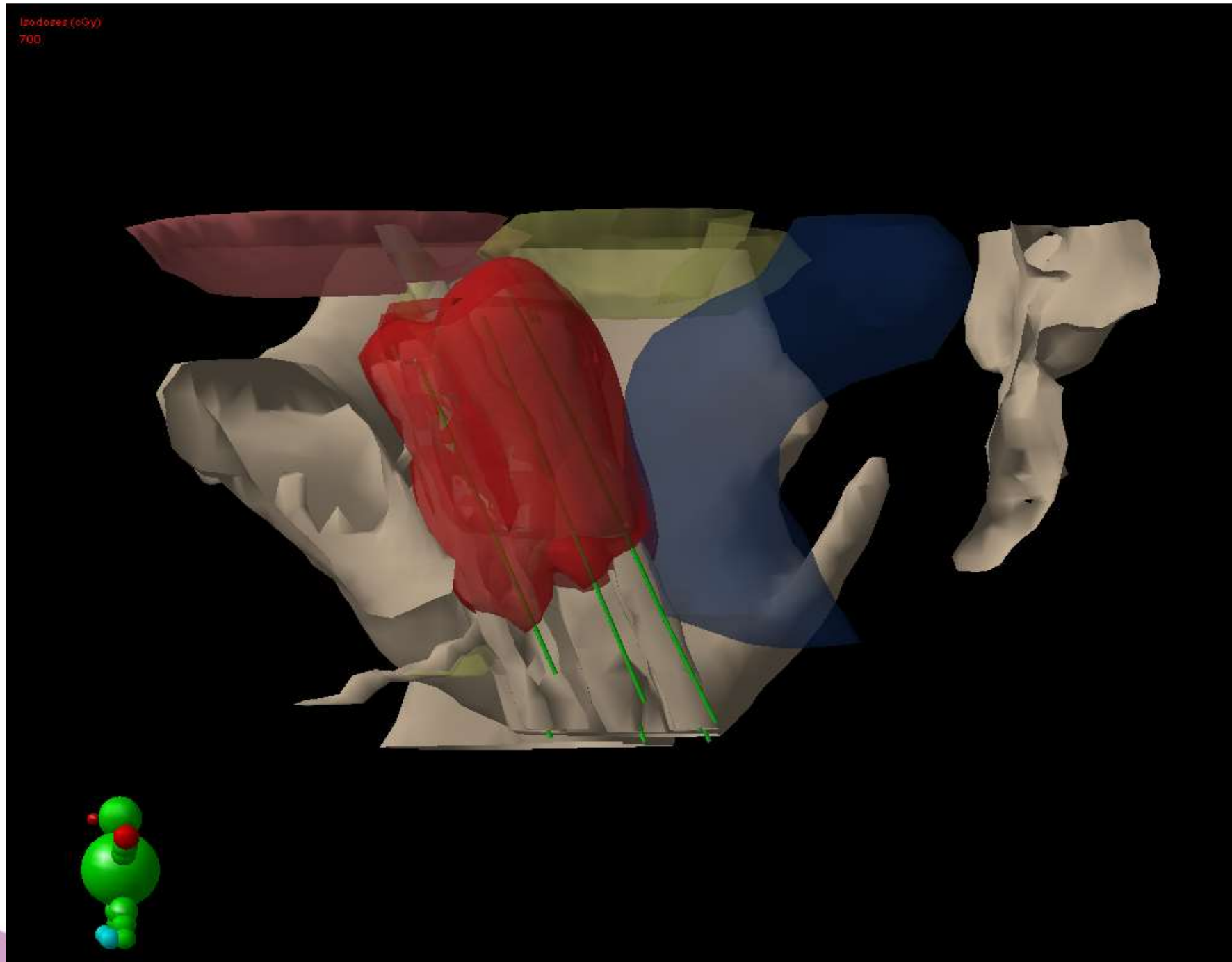
- Long tradition in staging and for GTV/CTV definition
- Projection of isodose distributions on single images
- Treatment planning with contouring, registration of 3D volumetric images with x-ray treatment plans, DVH
- Treatment planning directly on CT/MRI/US
- Image guided adaptive approach for application, planning and verification

Image guided adaptive



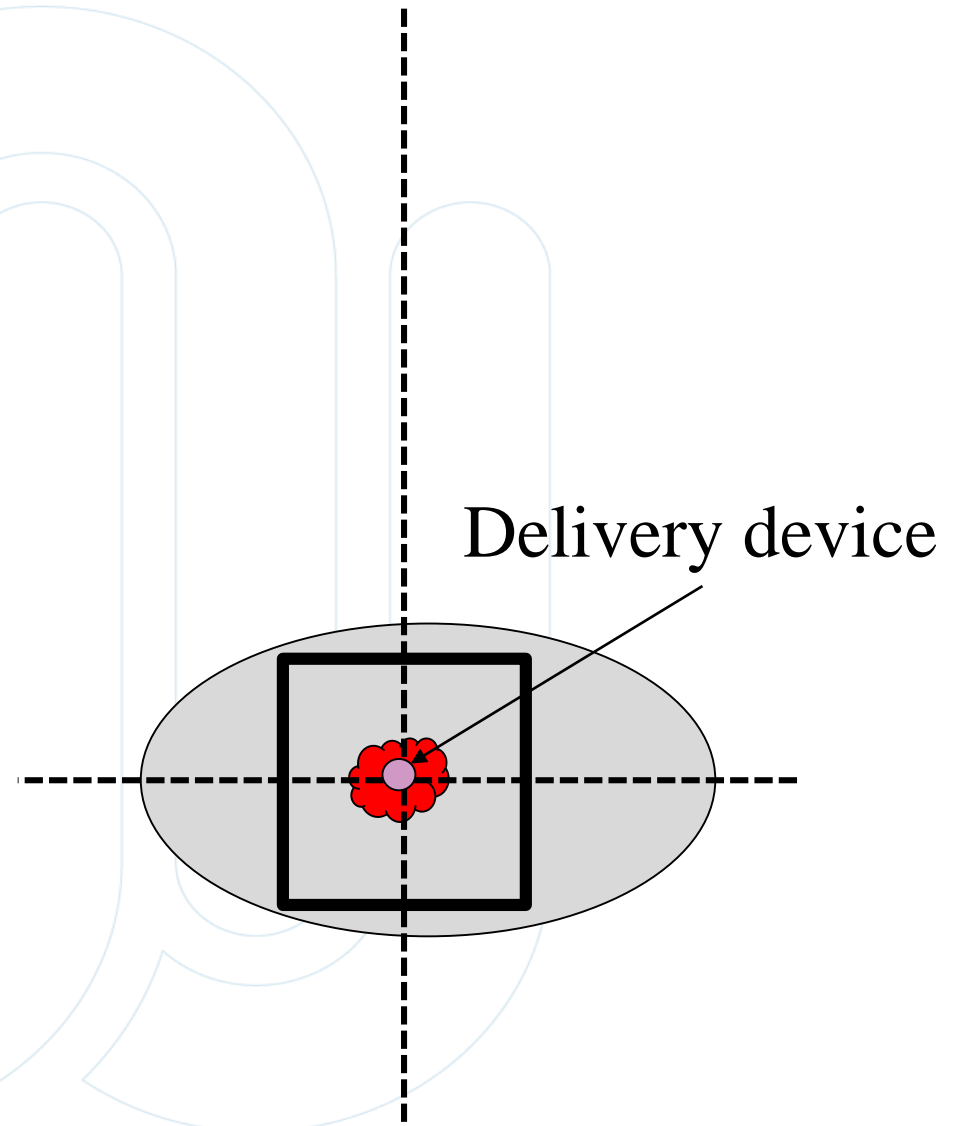
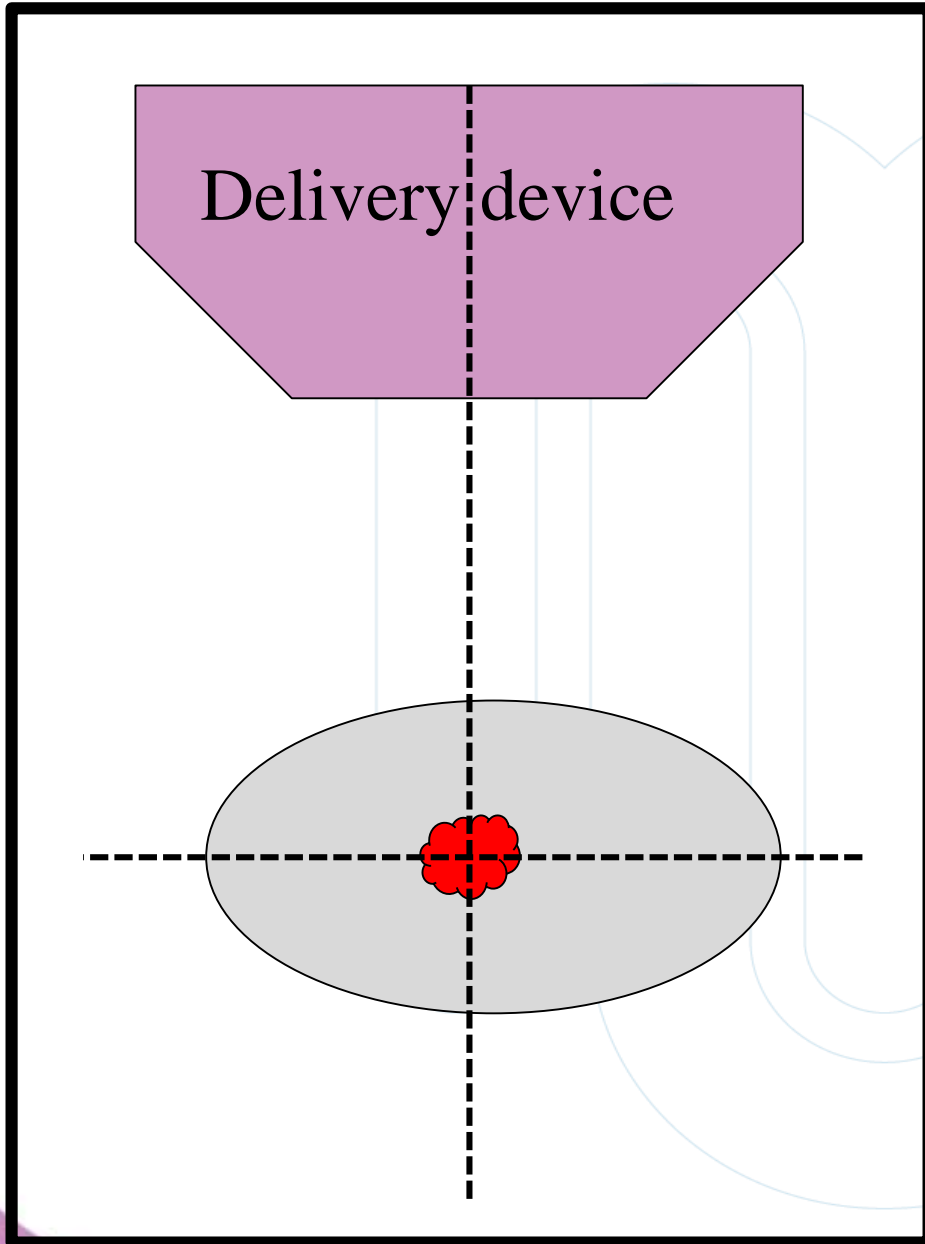
*Dimopoulos et al.
Strahlenther Onkol. 2009*

3D visualisation

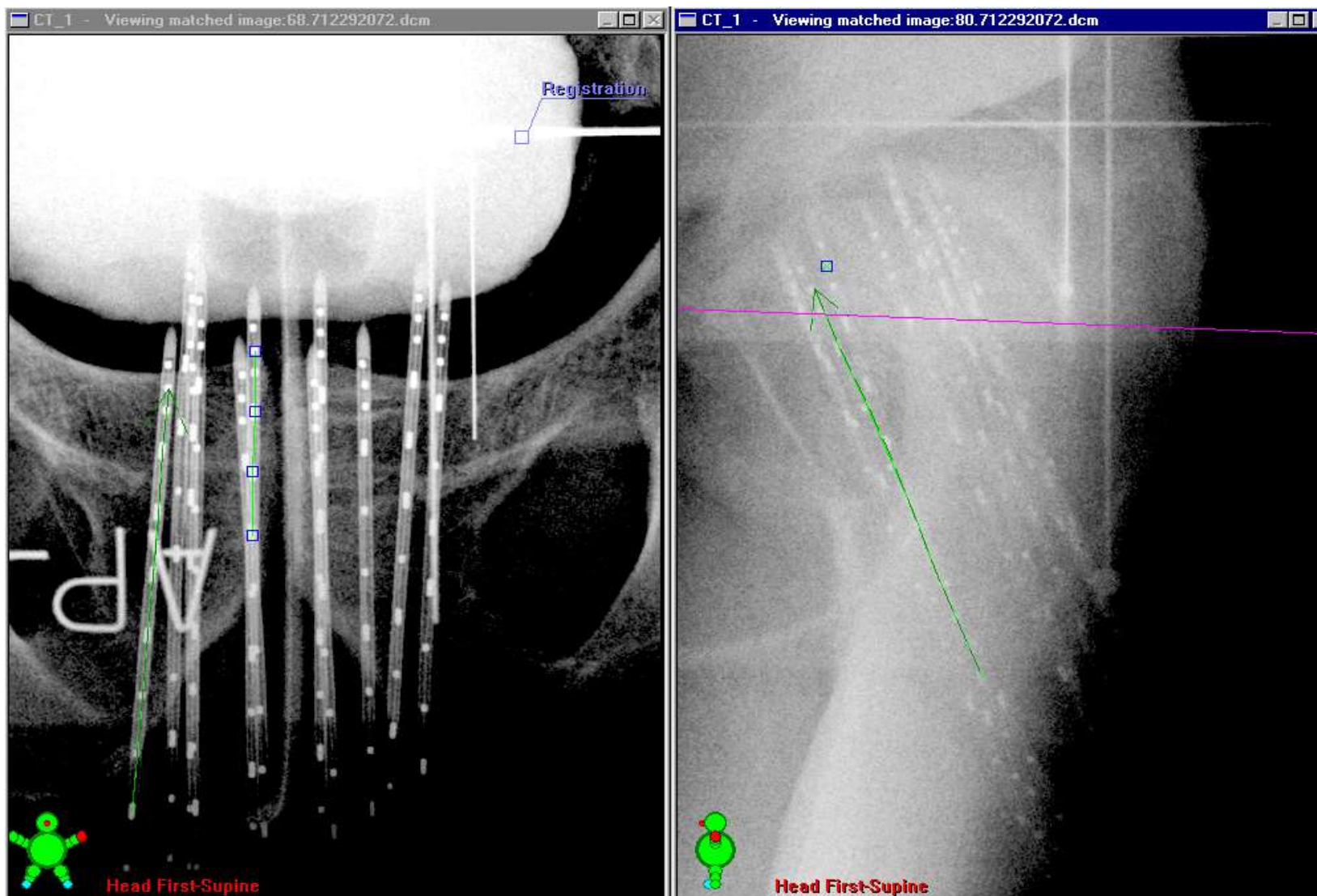


In-room imaging?

Room



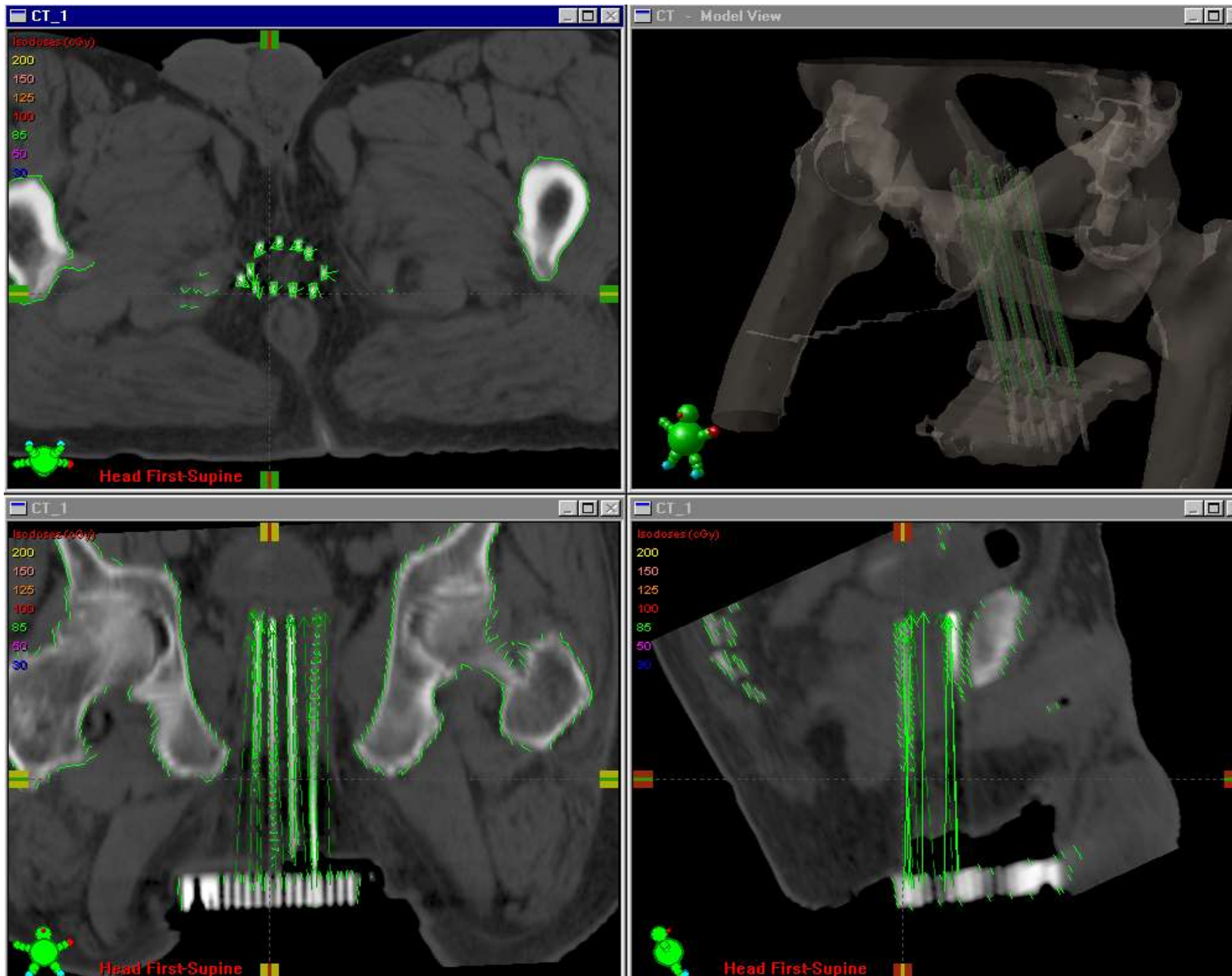
Reconstruction using X-rays



AP radiograph

lateral radiograph

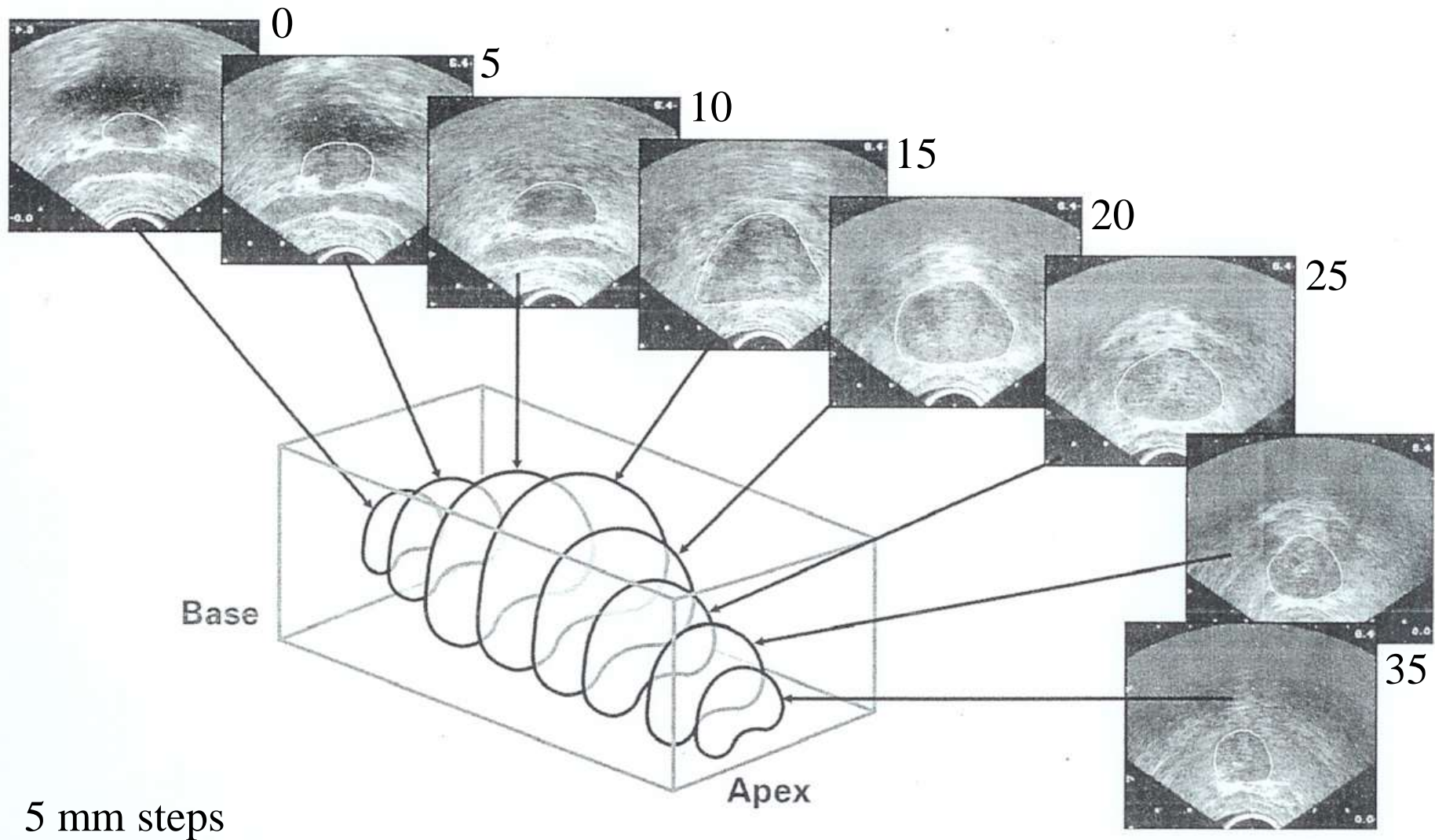
Reconstruction using CT



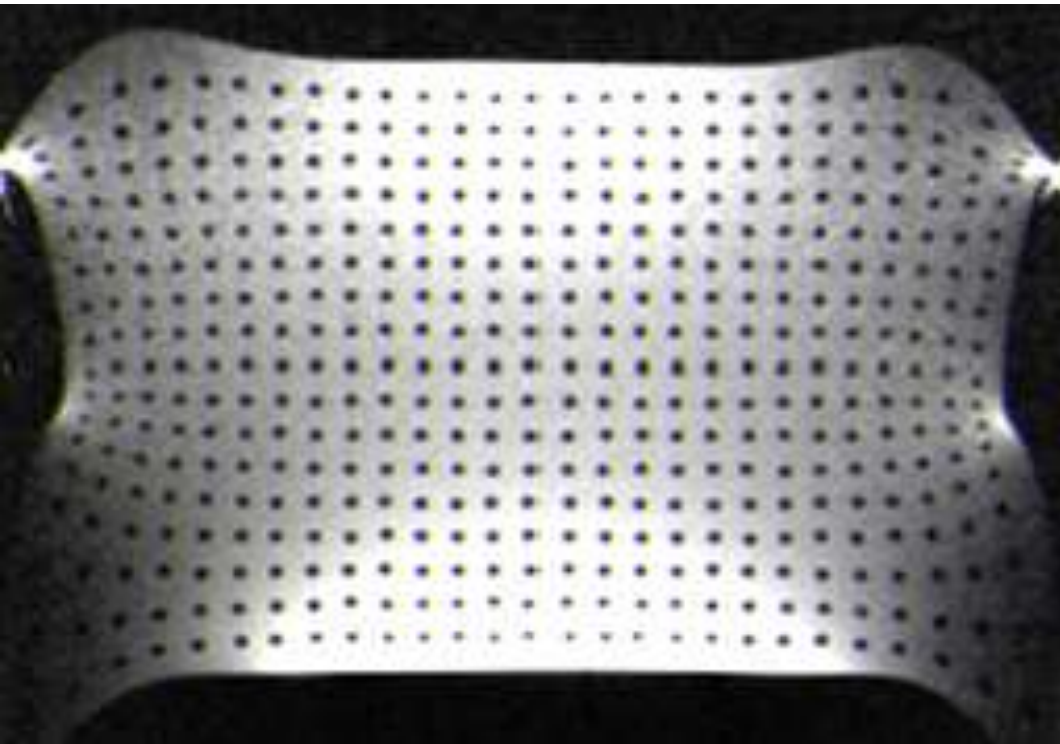
Reconstruction using MRI



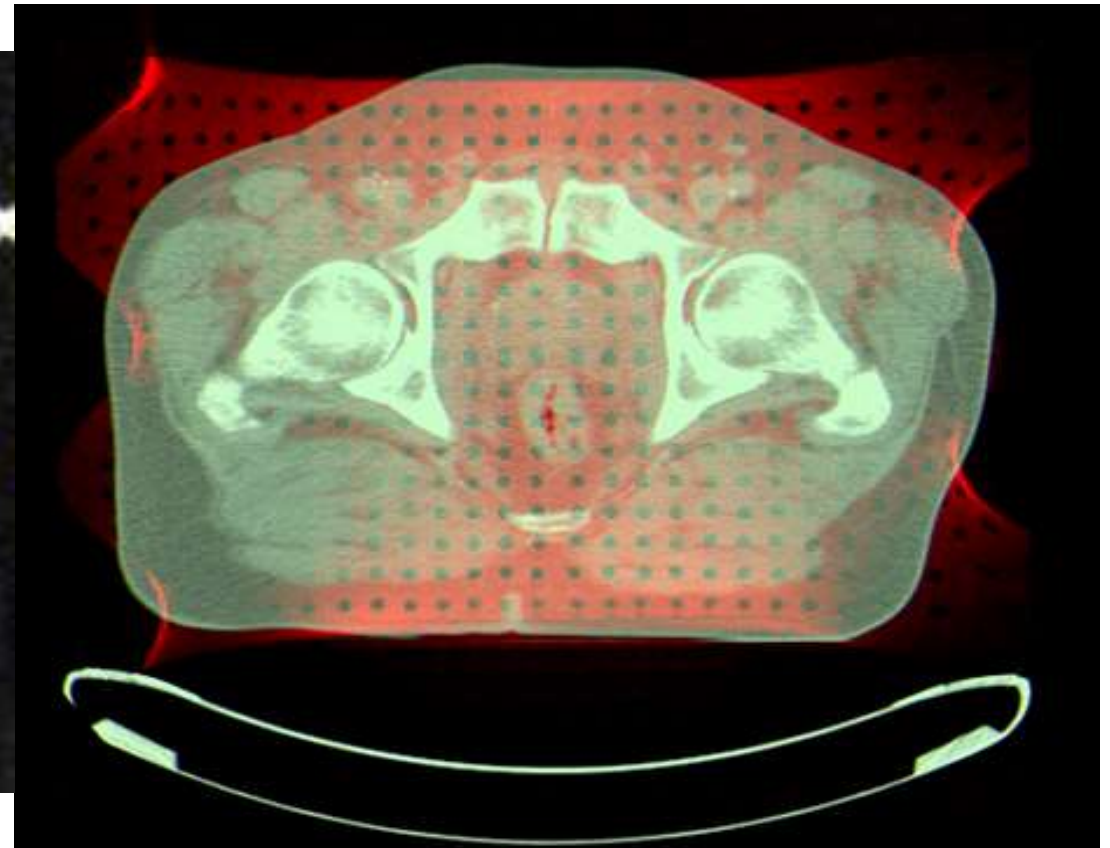
Ultrasound volume study



Geometrical Accuracy (MRI)

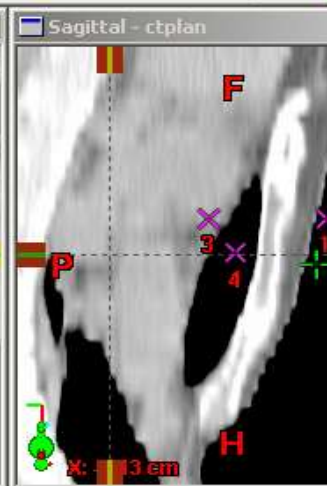
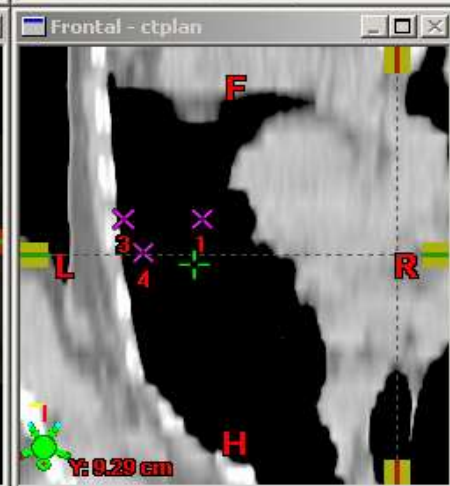
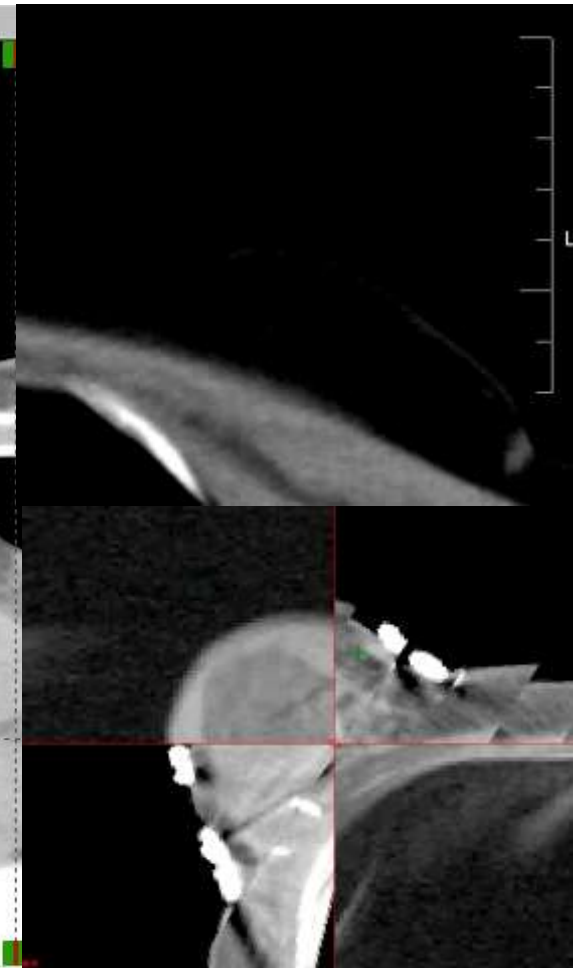
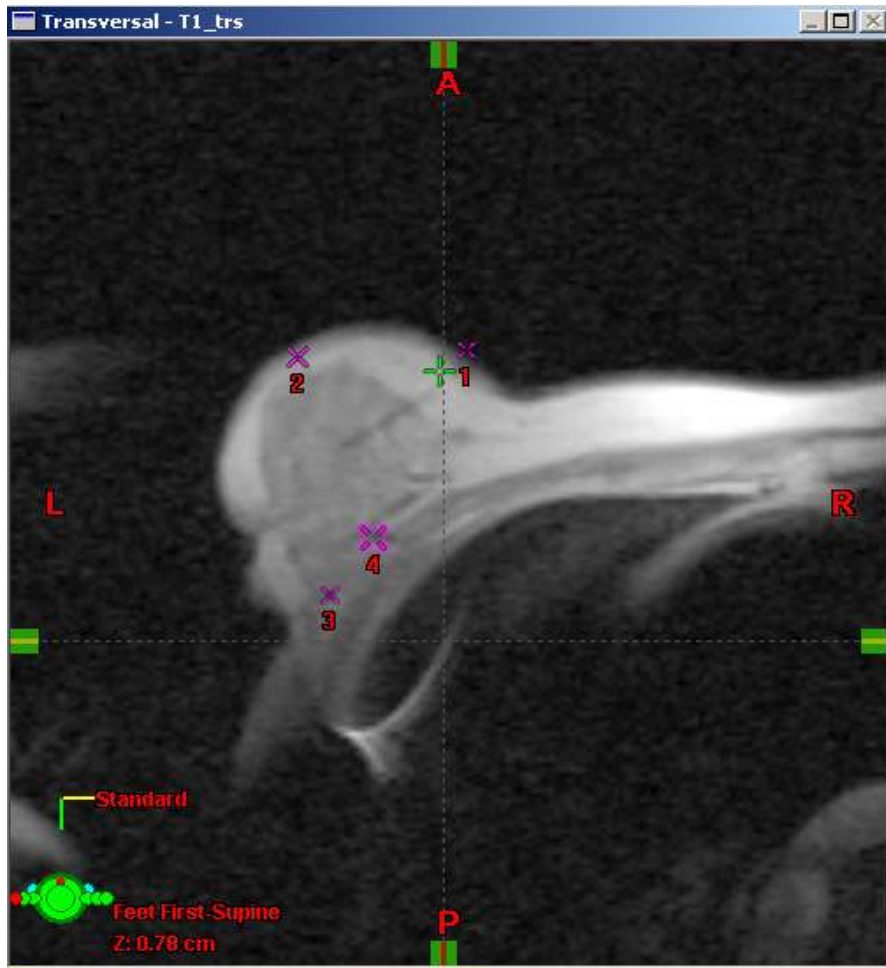


Distortions pronounced
at the periphery of field of view



MRI

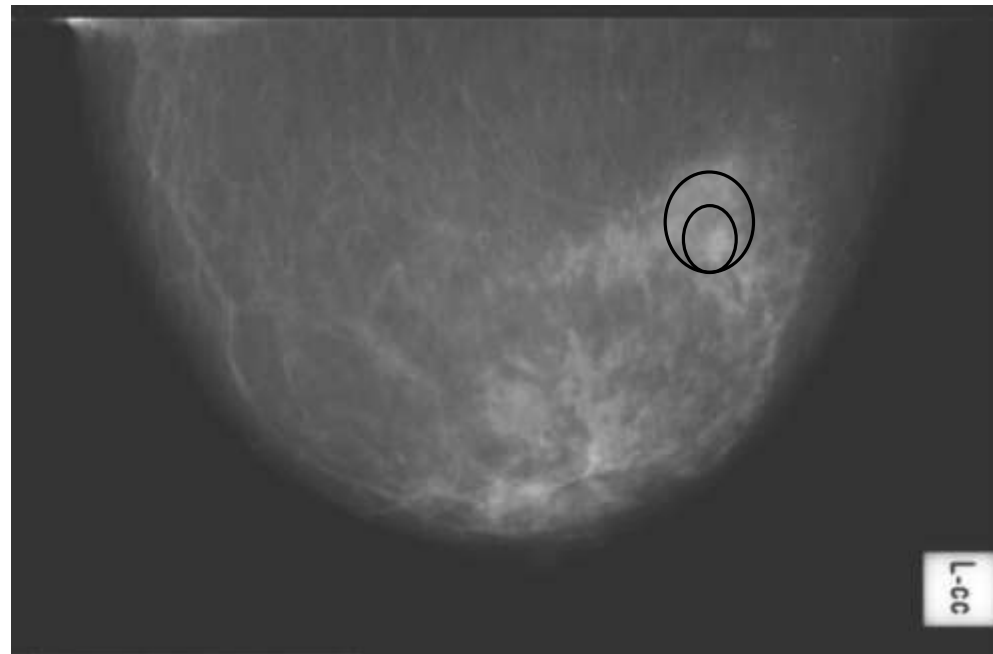
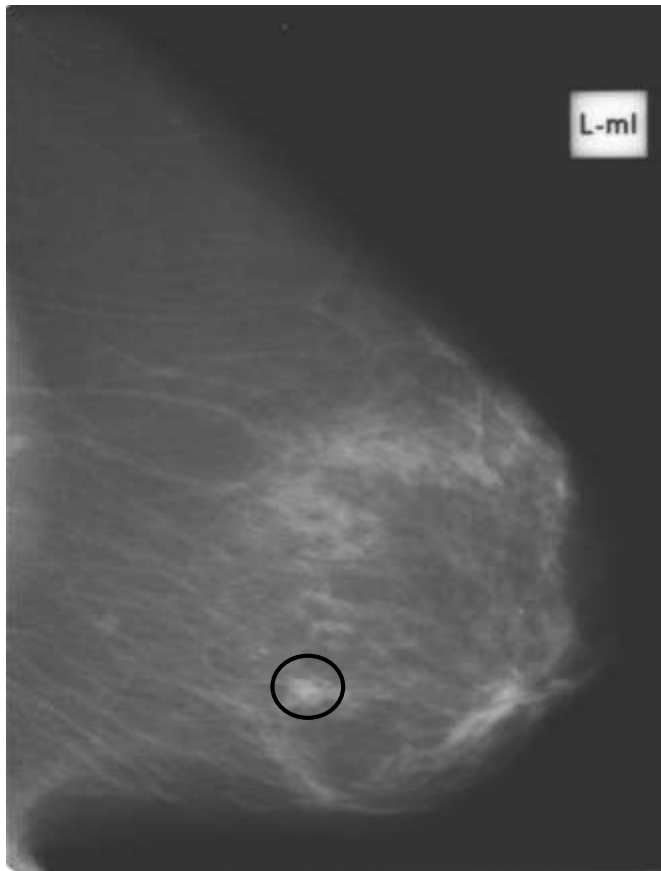
CT



DIAGNOSTIC PART PTV/CTV delineation :

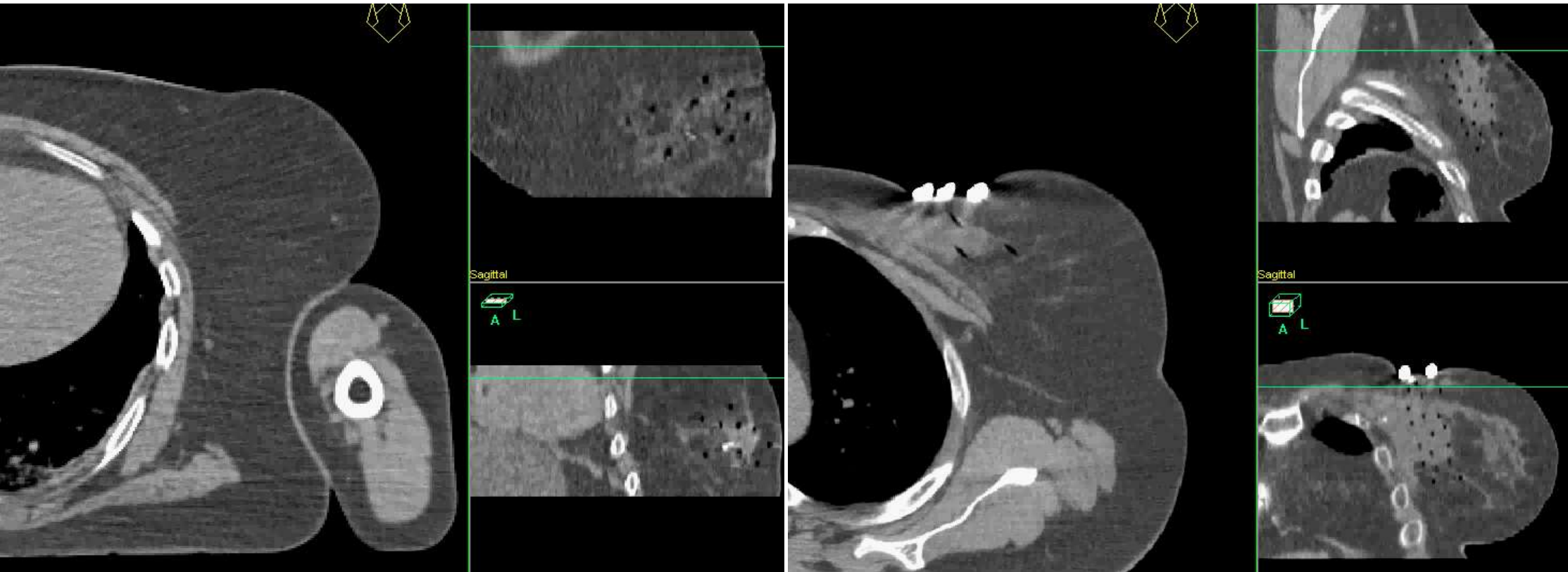
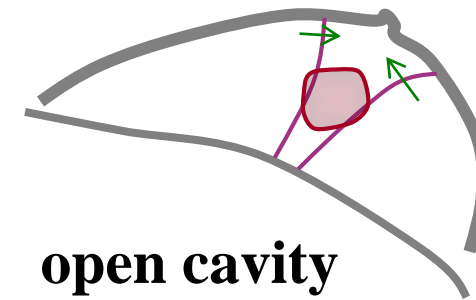
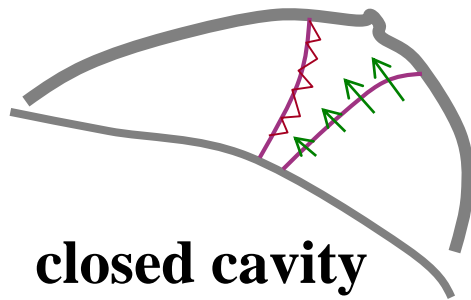
- *Mammography:*
(before surgery)

- tumor size
- localization (quadrant)
- distance to skin/ chest wall



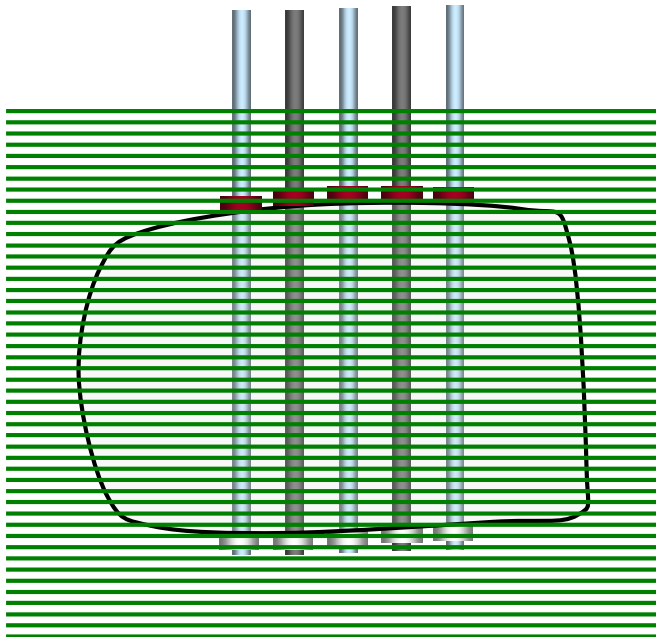
SURGICAL PART PTV/CTV delineation :

- clips

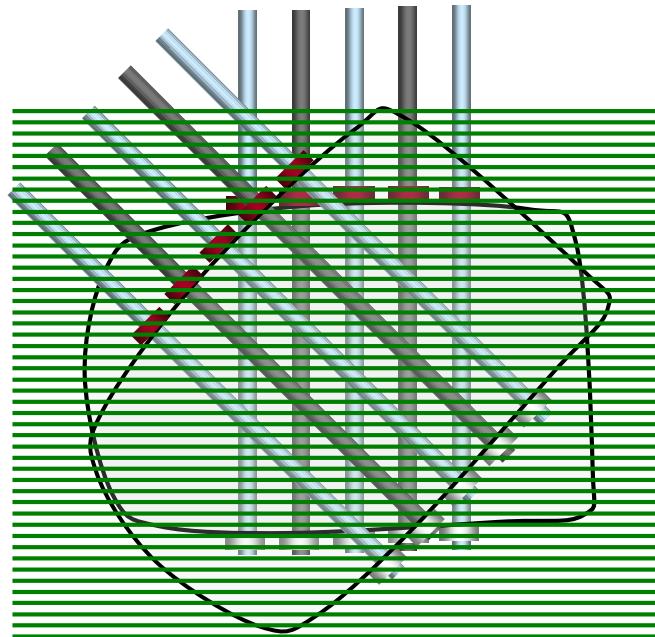


Reconstruction accuracy

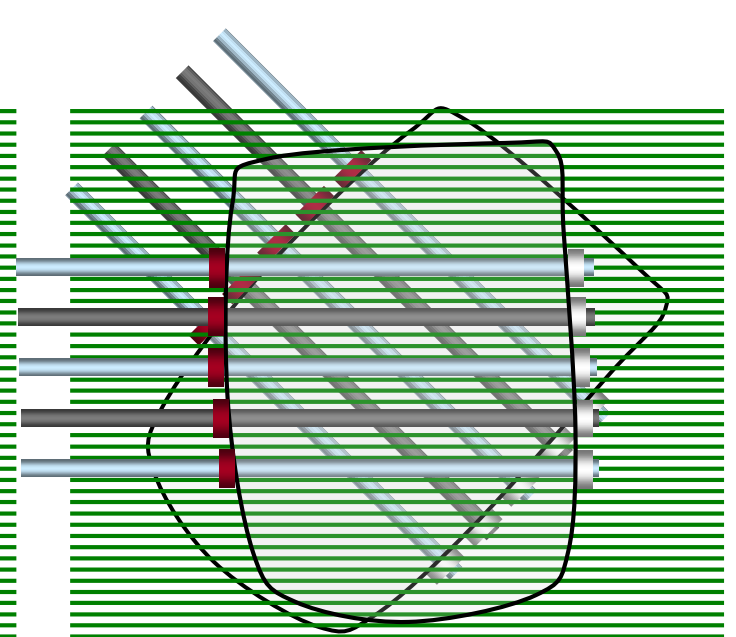
CT scan 2mm slices 0°



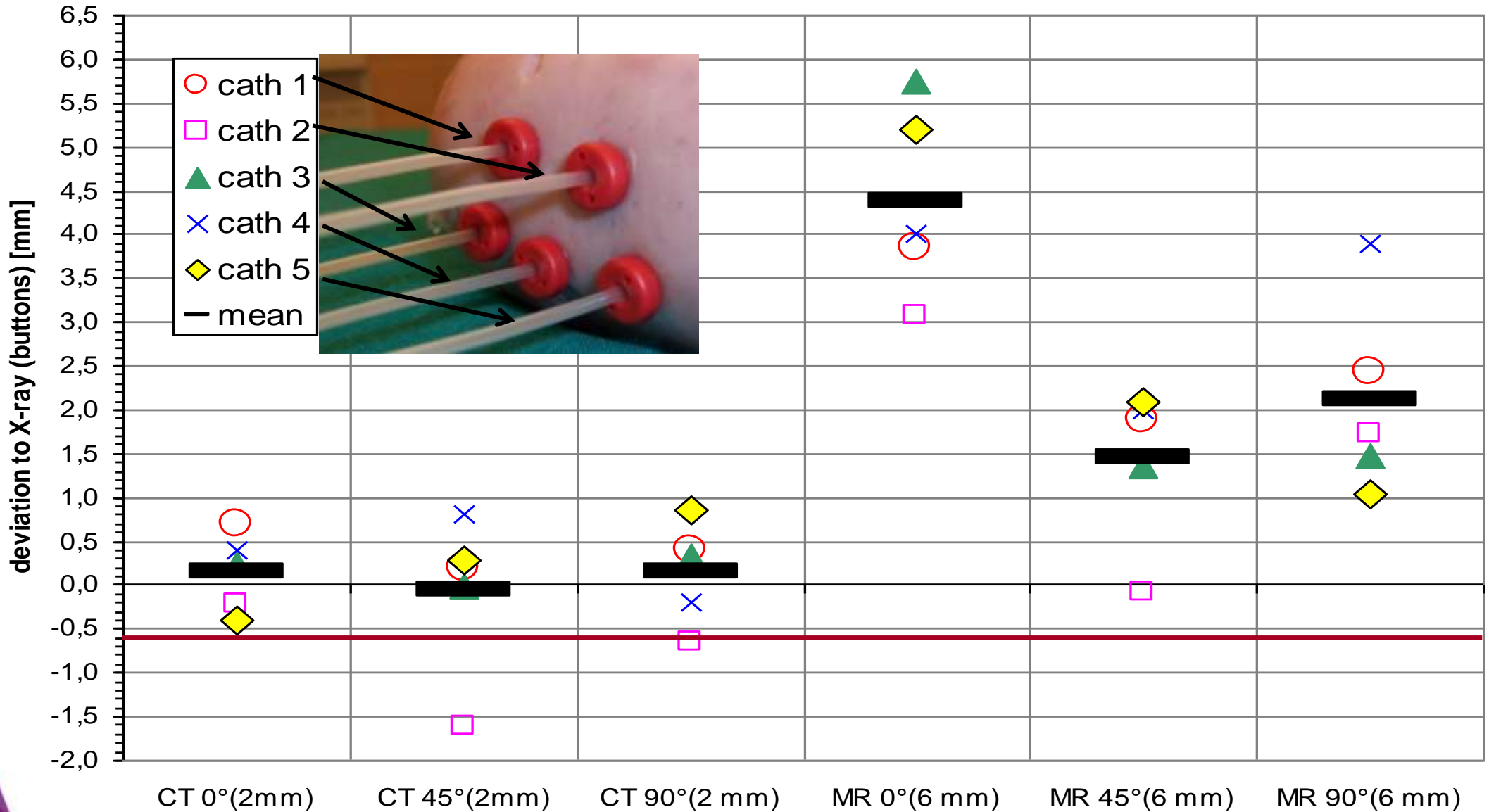
CT scan 2mm slices 45°



CT scan 2mm slices 90°

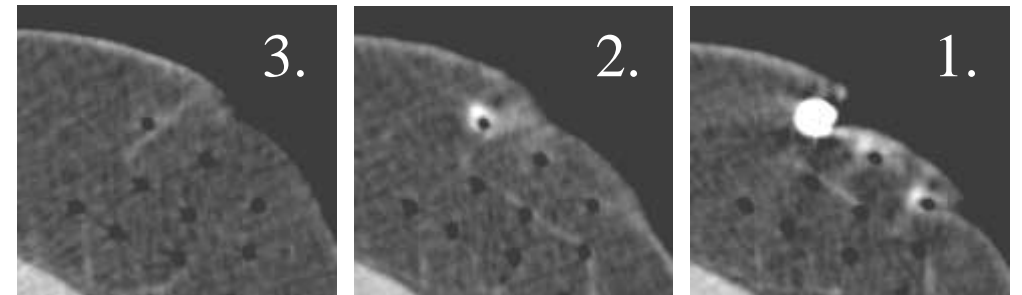
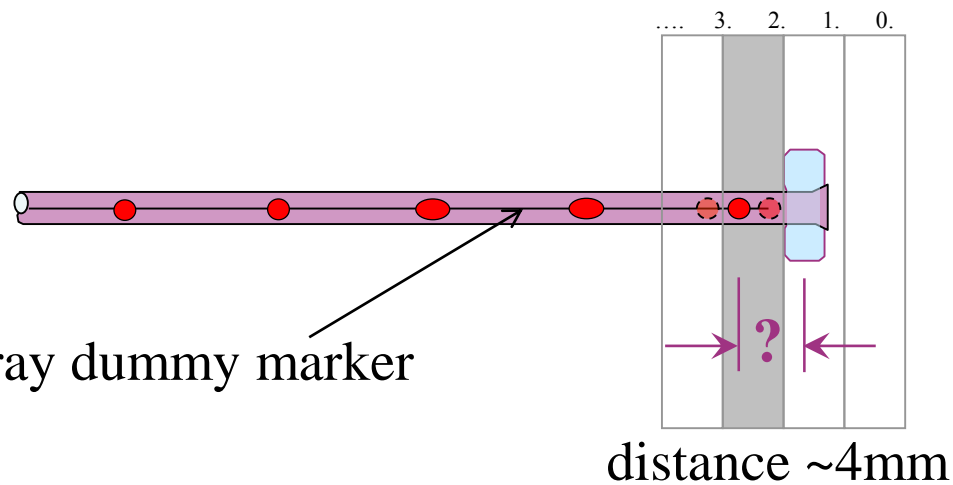
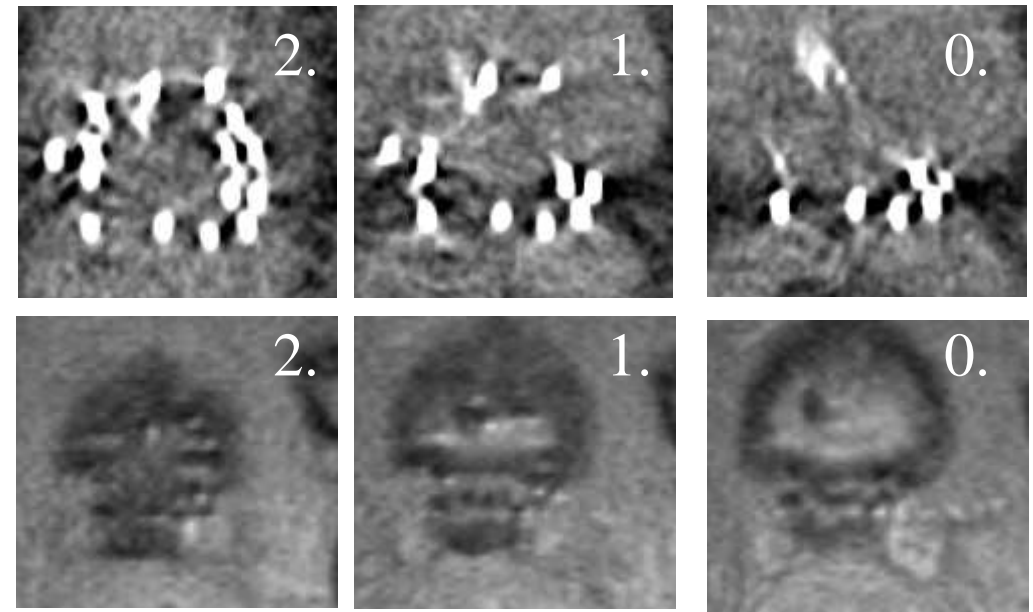
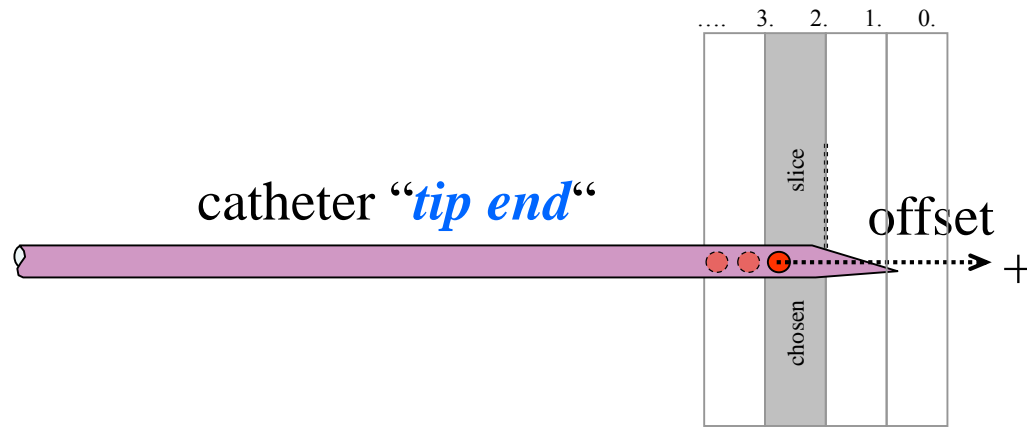


Reconstructed catheter length at the tissue phantom



Direct reconstruction by using CT or MR images

the dwell position problem !



Interstitial Applicator

Know the tool you are using!

Material

Plastic



flexible

Titanium

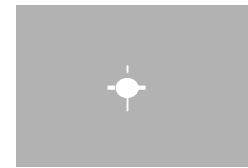


rigid

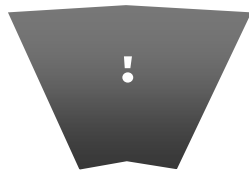
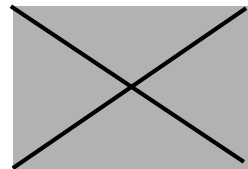
Steel



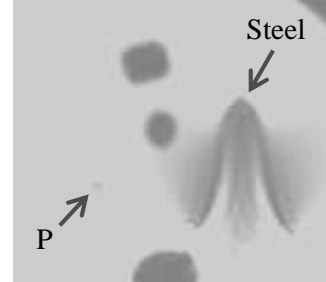
rigid



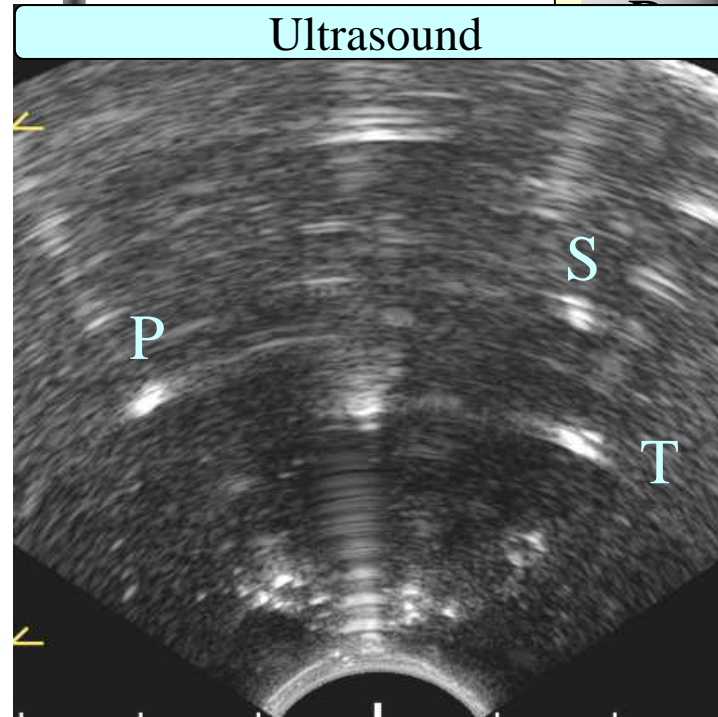
field strength (0.2T, 1.5T, 3T)



Different materials scanned in 0.2 T open MRI



Ultrasound

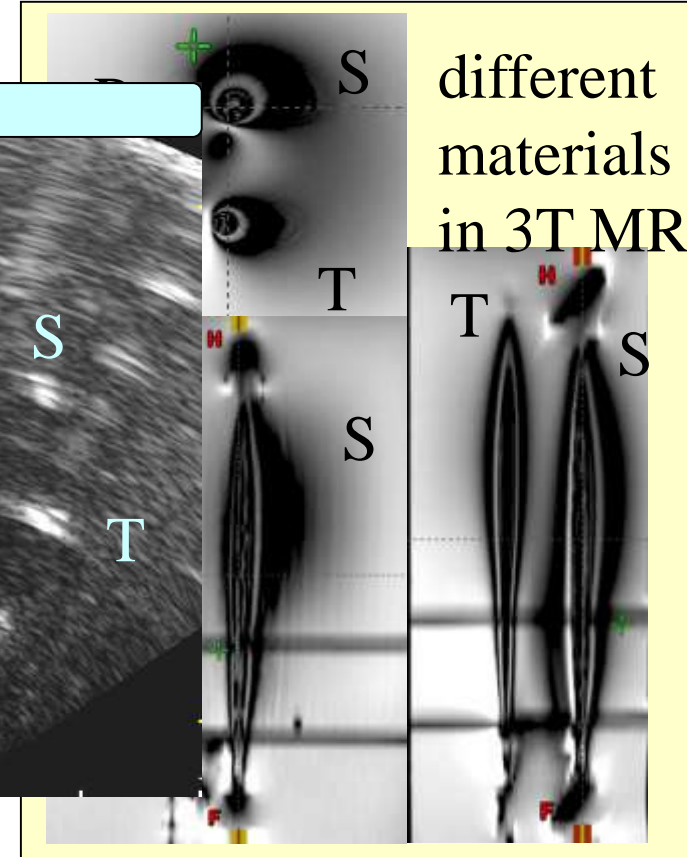


CT

MRI

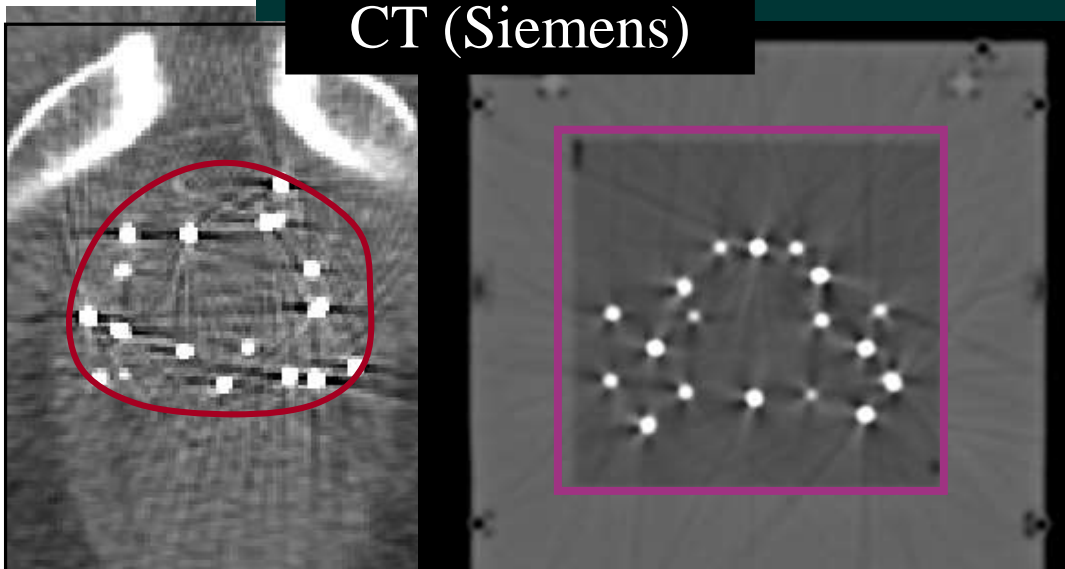
US

different materials in 3T MRI

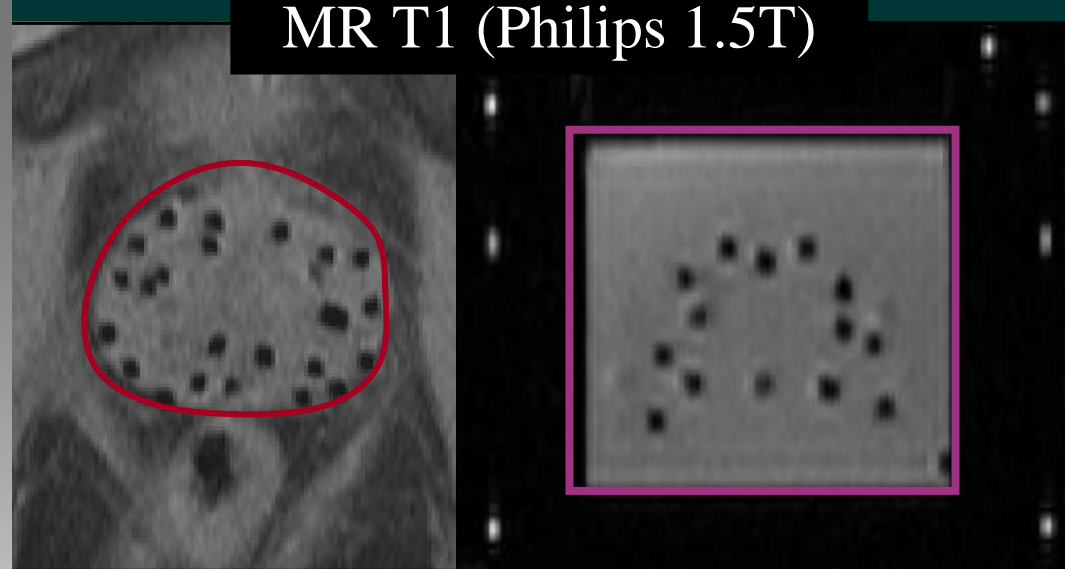


Seed visualisation: prostate vs agarose gel

CT (Siemens)



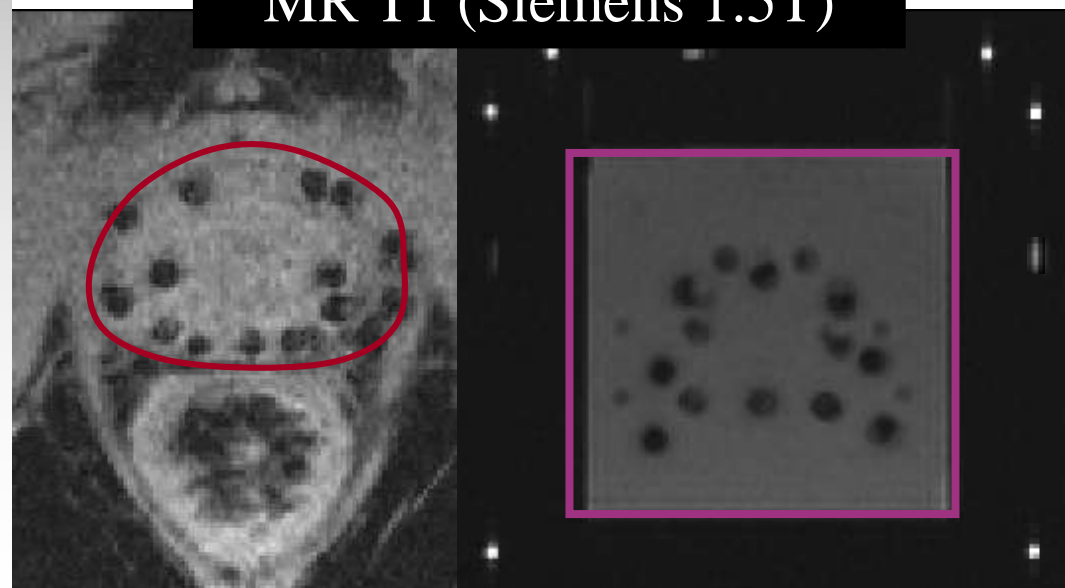
MR T1 (Philips 1.5T)



MR T2 (Philips 1.5T)



MR T1 (Siemens 1.5T)

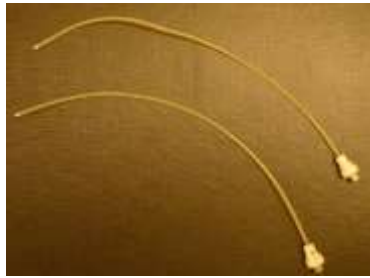


The problem: no visible source channel

How to reconstruct the tandem ring applicator directly on MR Images ?

How to identify the 1st source position of the ring ?

Do we need



to identify the whole source channel (path) ?



The problem: no visible source channel

How to reconstruct the tandem ovoids applicator directly on MR Images ?

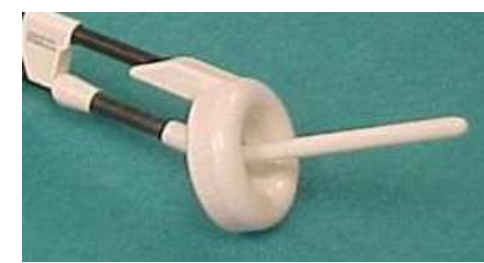
How to identify the 1st source position of the ring ?

Do we need  **to identify the whole source channel (path) ?**



MR markers in Tandem Ovoids provided by Jamema and Umesh, Mumbai

The problem: no visible source channel

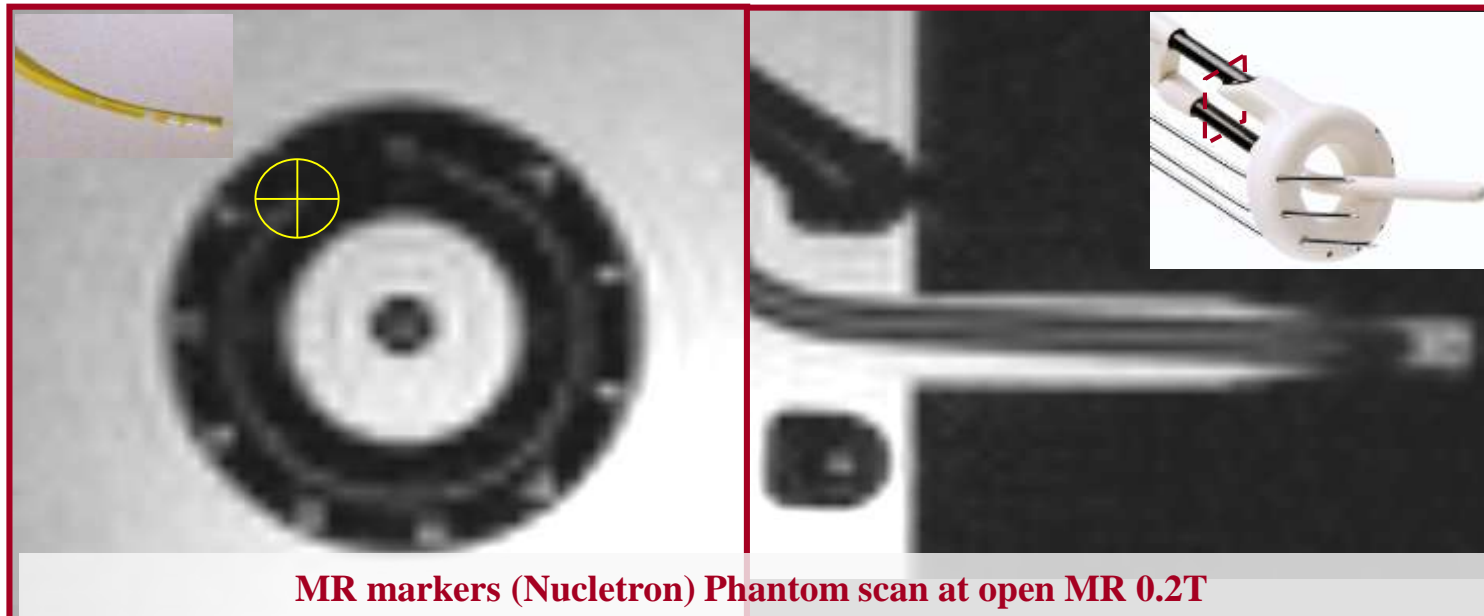
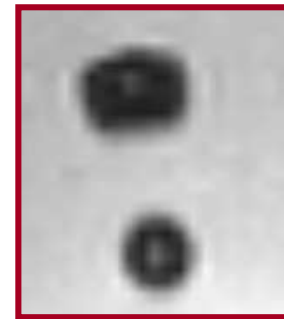


How to reconstruct the tandem ring applicator directly on MR Images ?

How to identify the 1st source position of the ring ?

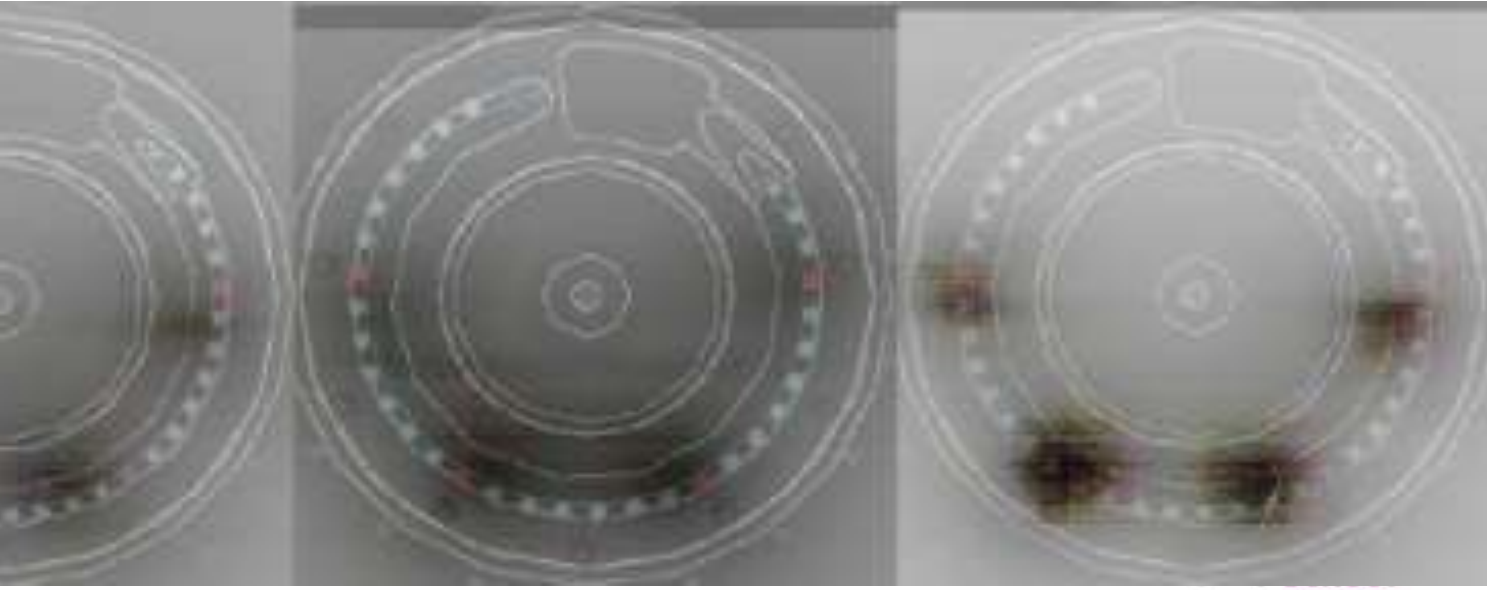
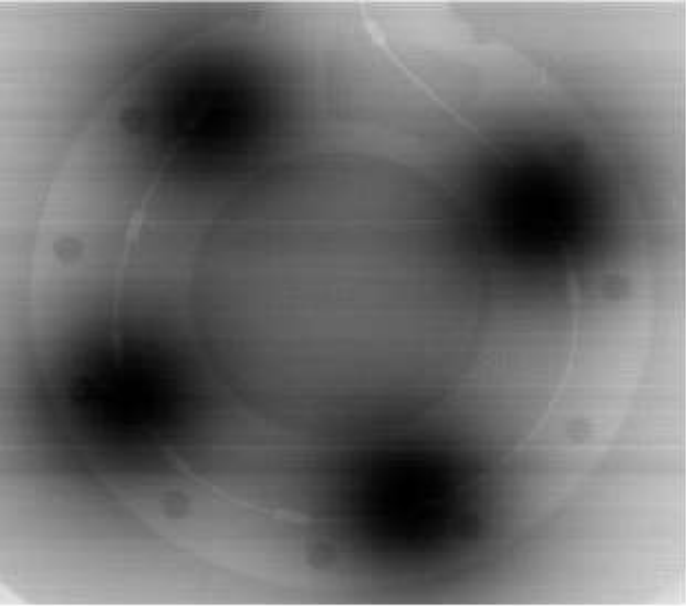
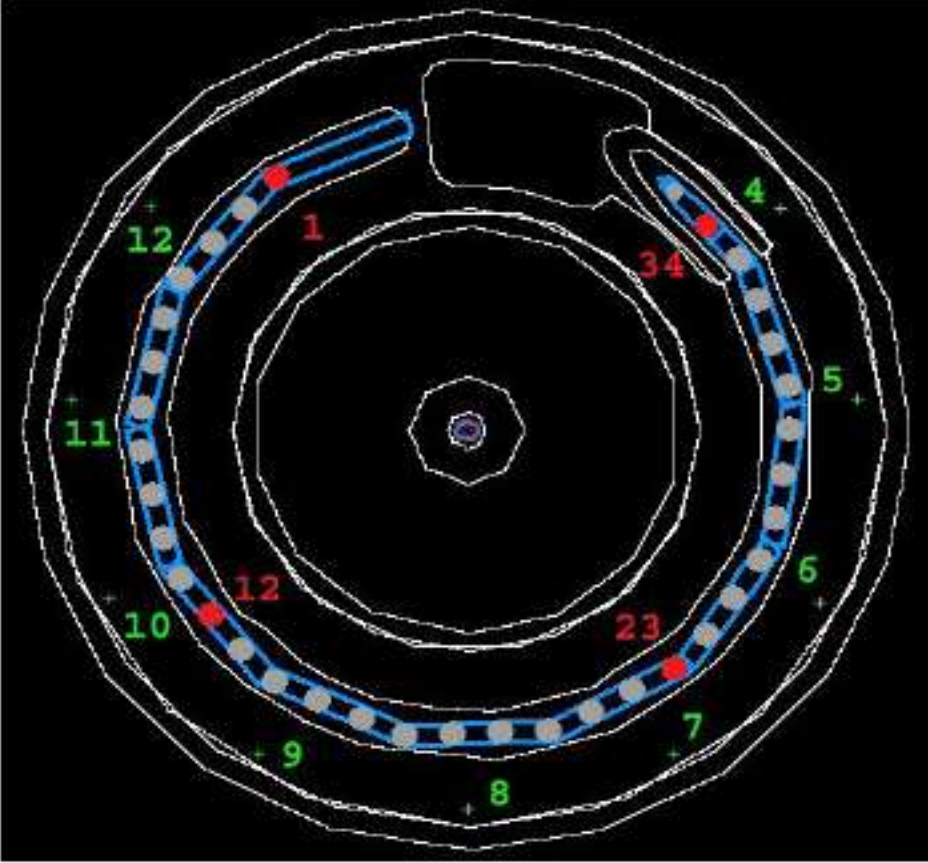
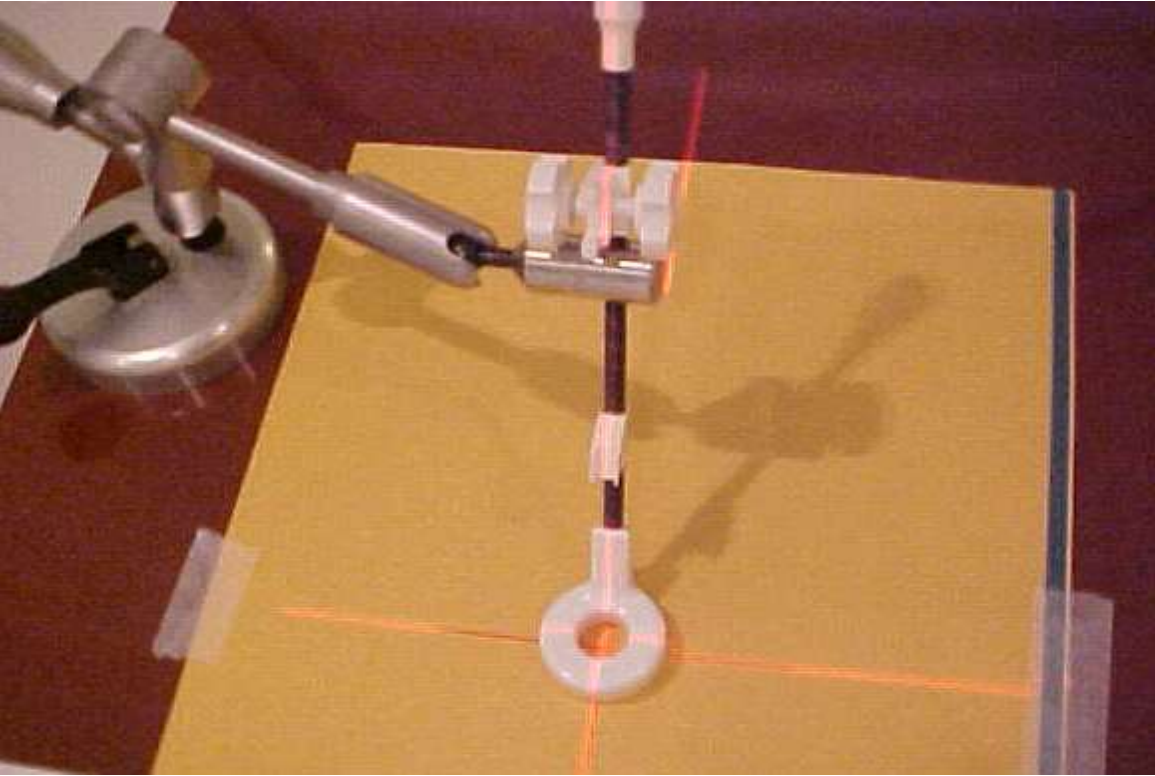
Do we need MR markers to identify the whole source channel (path) ?

•Not necessarily when using the Vienna ring, it helps to provide additional information during the reconstruction process



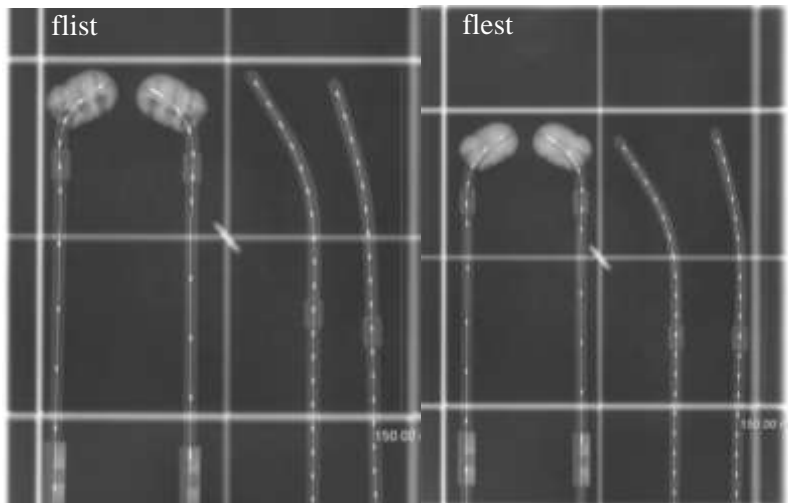
MR markers (Nucletron) Phantom scan at open MR 0.2T

Do acceptance tests and check

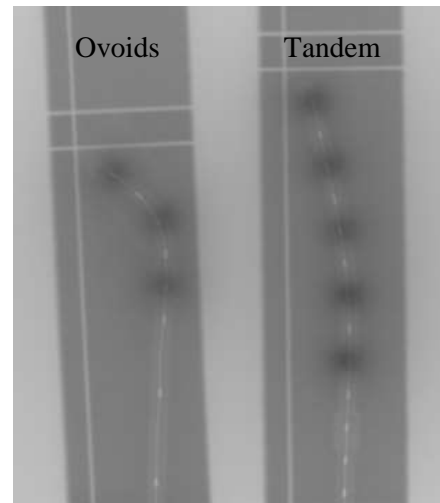


A. De Leeuw et al. Tandem- Ovoids applicator reconstruction on MRI

Radiographs



Auto-Radiography



Template for Reconstruction

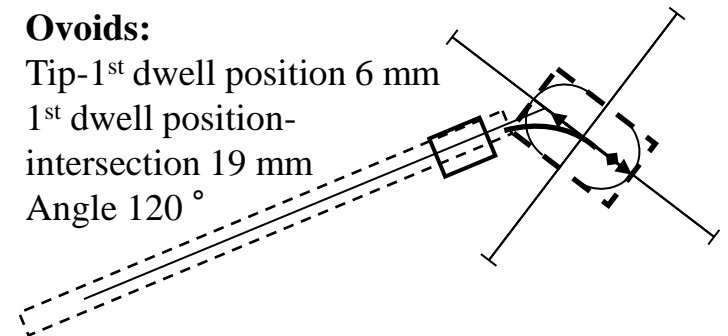
Ovoids:

Tip-1st dwell position 6 mm

1st dwell position-

intersection 19 mm

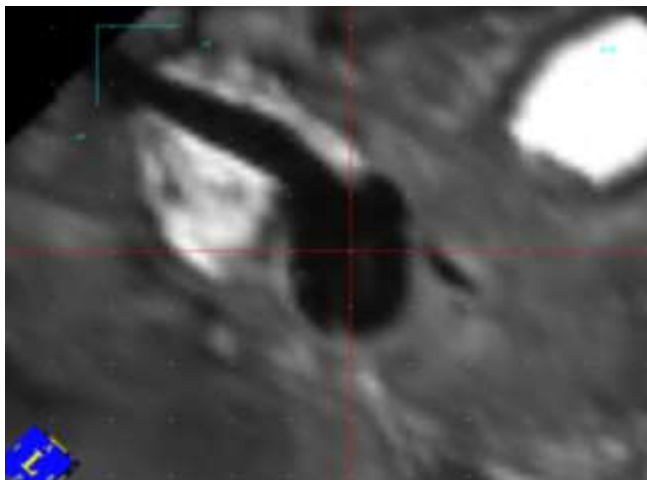
Angle 120°



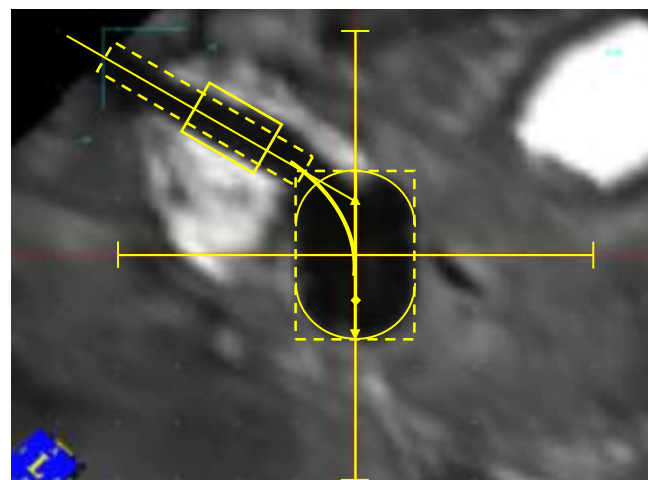
Intrauterine Tandem:

Tip-1st dwell position 7 mm

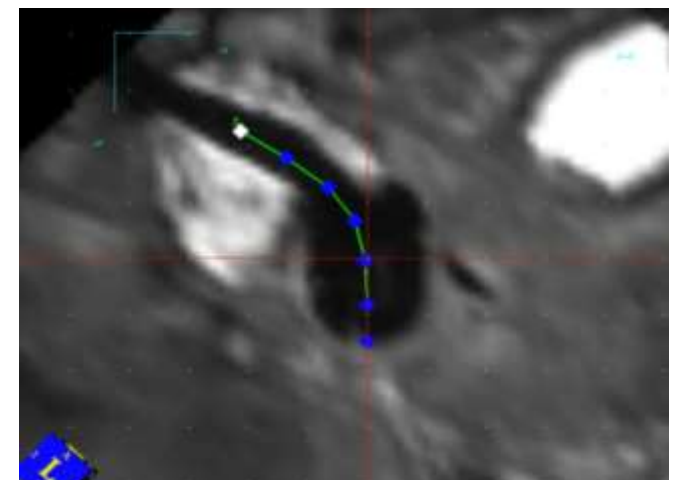
MR Imaging



Template in place

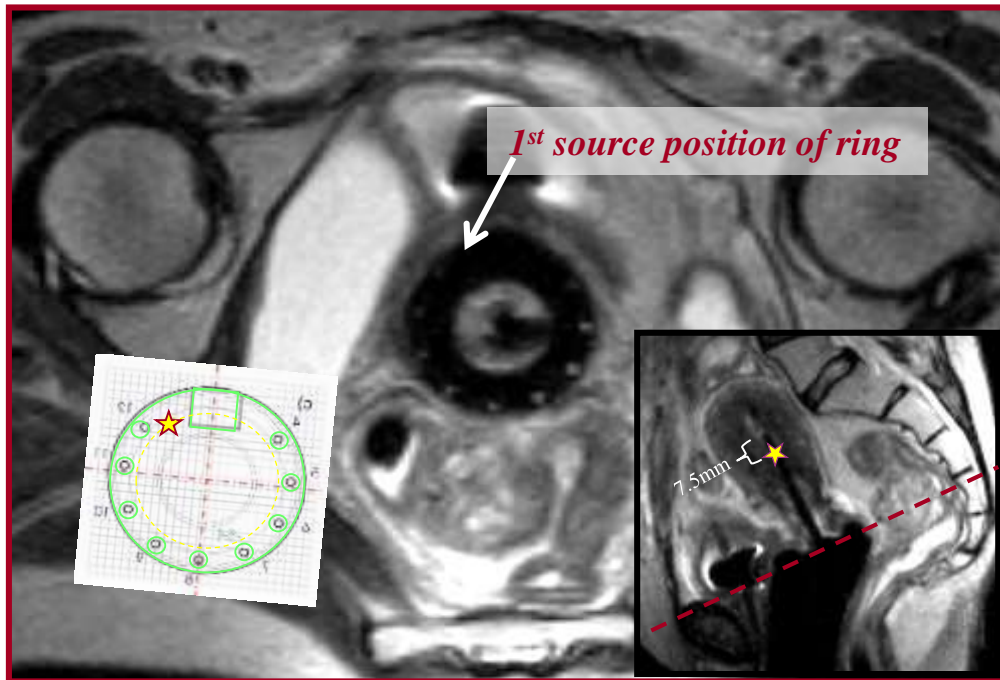


Reconstruction of source path



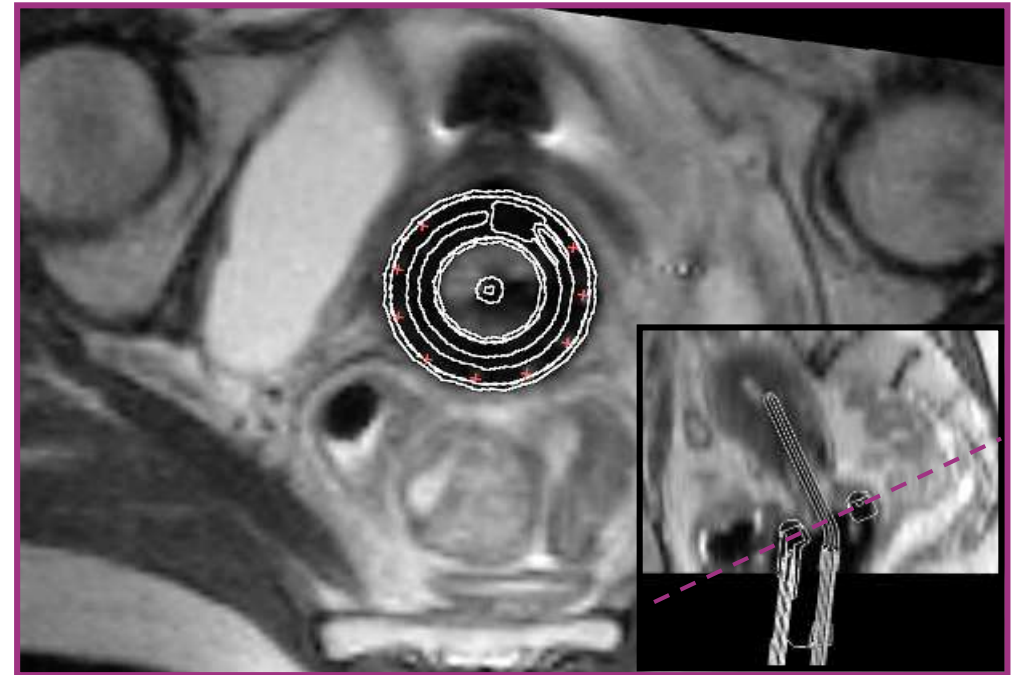
Direct reconstruction of the Vienna applicator on MR images

manual direct



5 – 10 min

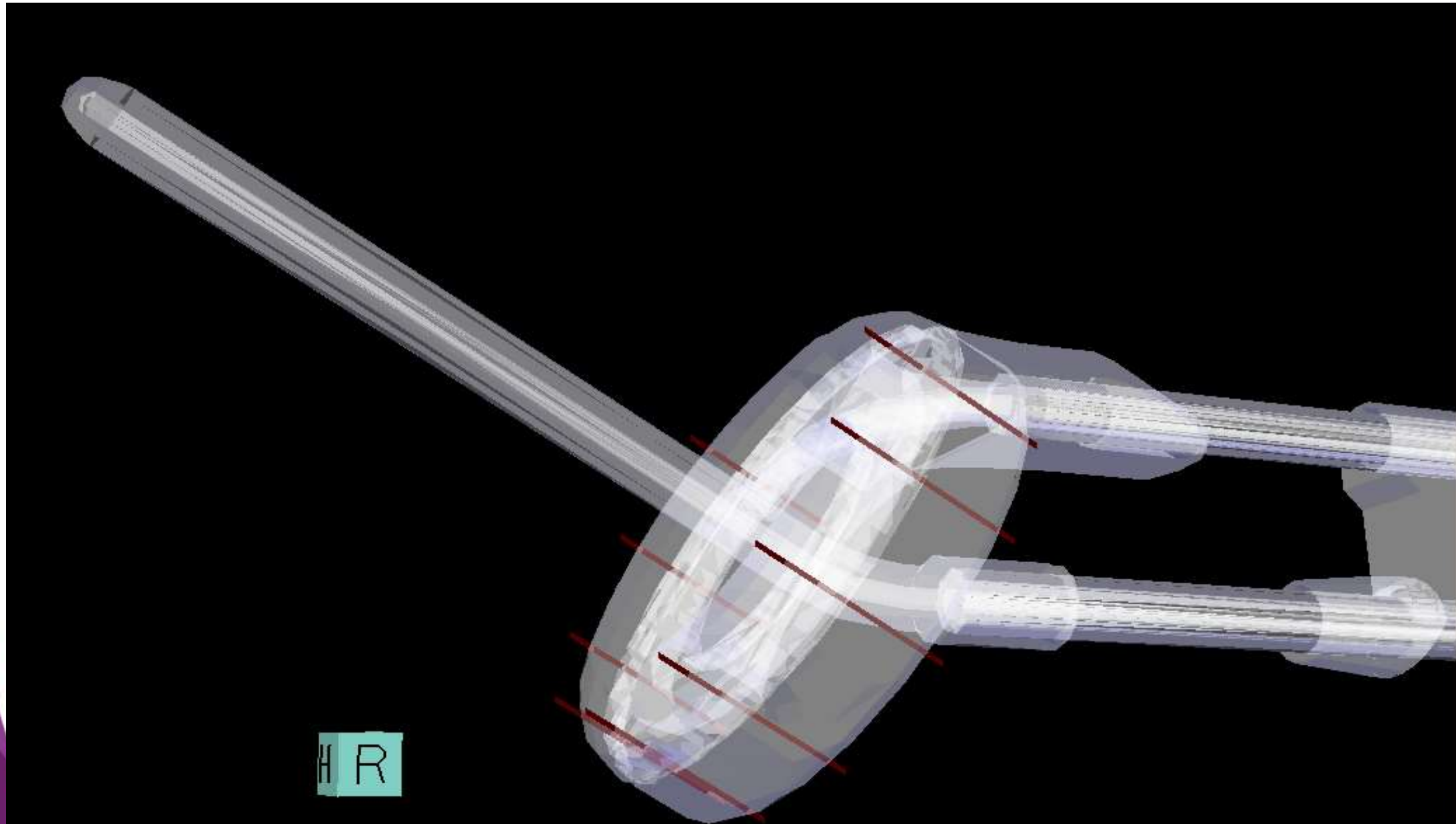
software integrated



less than 5 min

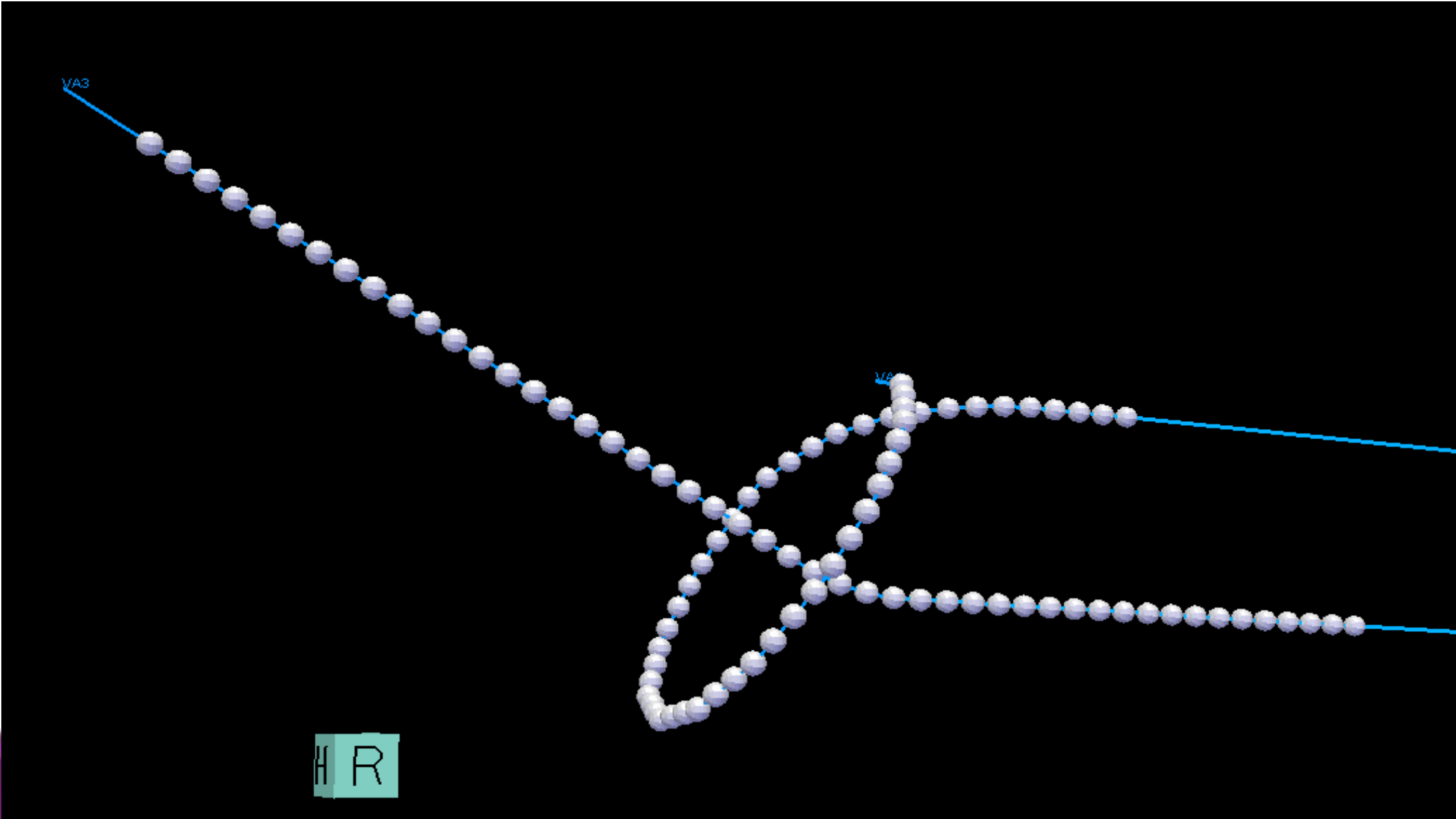
If the relation between applicator shape and the source path is defined once, the reconstruction process can be performed by directly placing the applicator in the MRI dataset.

Applicator surface

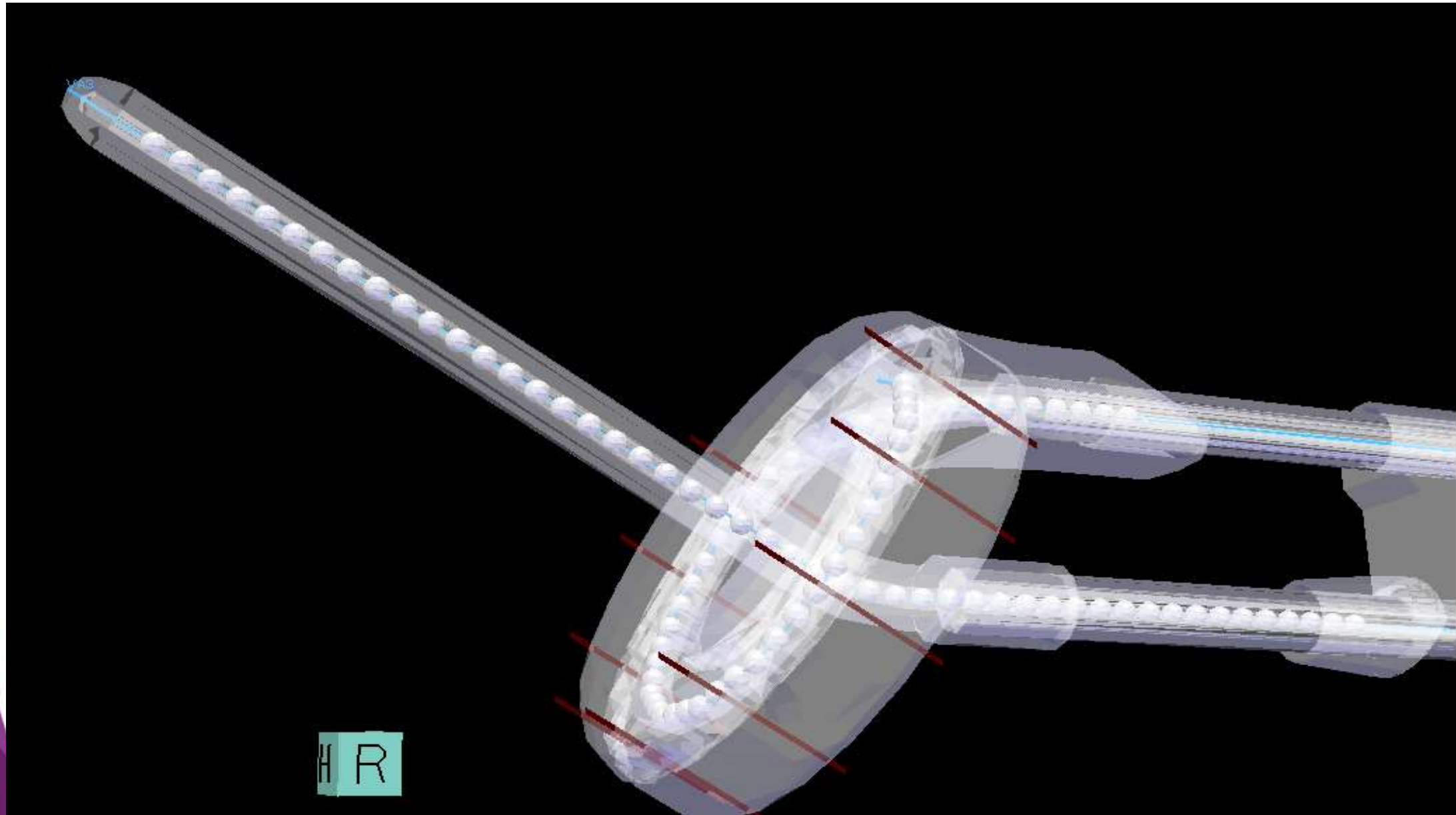


H R

Source path



Applicator + Source path



H R

Reconstruction

Virtual Plan | Live Plan | Post Plan

DB | D=? | SET | 3D | Color | Off | Abs | Update | update

Label | 13 | 4.3

Slice Mode | OBC Mode | Y-Value = 18.903 cm | Volume | 3D Mode | DVH Mode | 3D Graph

Catheter

Auto | Manual
 Applicator | Inverse Plan

Placement | Change type

Adjustment

X: [Left Arrow] [Right Arrow] [Square] [Left Arrow] [Left Arrow]
 Y: [Left Arrow] [Right Arrow] [Square] [Left Arrow] [Left Arrow]
 Z: [Left Arrow] [Right Arrow] [Square] [Left Arrow] [Left Arrow]

Marker

Register [Icon]

Mark | Clear
 Define | Clear all

Modify

Main [mm] Sub [mm]
 [] [] [Apply]

Applicator hole blocking

Block | Free all

#	Hole	Indexer[cm]	Depth[cm]	Free Len.[cm]	Free Len.	Tip-1stSDP[cm]	Activation	Dwell Times	5	10	15
VA1	Ring	99.500				0.770	Unlocked	Unlocked			

Monitoring

Reconstruction

The software interface displays a 3D reconstruction of a catheter system within a patient's anatomical model. The main 3D view shows the catheter's path through the anatomy. Three orthogonal 2D slice views are provided for precise positioning:

- Top View (Y-Z Plane):** Y-Value = 18.903 cm
- Left View (X-Z Plane):** Z-Value = -7.000 cm
- Right View (X-Y Plane):** X-Value = 19.209 cm

The right-hand panel, titled "Catheter", offers control options:

- Mode:** Auto (selected) / Manual
- Applicator:** Inverse Plan
- Actions:** Placement, Change type
- Adjustment:** X, Y, Z axis movement controls.
- Marker:** Register button.
- Modify:** Main [mm] and Sub [mm] input fields with an Apply button.
- Applicator hole blocking:** Block and Free all buttons.

At the bottom, a table provides detailed parameters for the applicator holes:

#	Hole	Indexer[cm]	Depth[cm]	Free Len.[cm]	Free Len.	Tip-1stSDP[cm]	Activation	Dwell Times
VA1	Ring	99.500				0.770	Unlocked	5, 10, 15

Reconstruction

Virtual Plan | Live Plan | Post Plan

DB | SET | 3D | Color | Off | Update | update

Slice Mode | OBC Mode | Y-Value = 18.903 cm | Volume | 3D Mode | DVH Mode | 3D Graph

Slice Mode | OBC Mode | Z-Value = -7.500 cm | Slice Mode | OBC Mode | X-Value = 19.209 cm

Catheter

Auto | Manual
 Applicator | Inverse Plan

Placement | Change type

Adjustment

X: [Left Arrow] [Right Arrow] [Square] [Left Arrow] [Right Arrow]
 Y: [Left Arrow] [Right Arrow] [Square] [Left Arrow] [Right Arrow]
 Z: [Left Arrow] [Right Arrow] [Square] [Left Arrow] [Right Arrow]

Marker

Register [Icon]

Mark | Clear
 Define | Clear all

Modify

Main [mm] Sub [mm]
 [] [] Apply

Applicator hole blocking

Block | Free all

#	Hole	Indexer[cm]	Depth[cm]	Free Len.[cm]	Free Len.	Tip-1stSDP[cm]	Activation	Dwell Times
VA1	Ring	99.500				0.770	Unlocked	Unlocked

Monitoring

Reconstruction

Virtual Plan | Live Plan | Post Plan

DB | SET | 3D | Color | Off | Abs | Update | update

16 | 4.3

Slice Mode | OBC Mode | Y-Value = 18.903 cm | Volume | 3D Mode | DVH Mode | 3D Graph

Slice Mode | OBC Mode | Z-Value = -8.000 cm | Slice Mode | OBC Mode | X-Value = 19.209 cm

Catheter

Auto | Manual

Applicator | Inverse Plan

Placement | Change type

Adjustment

X: [Left Arrow] [Right Arrow] [Square] [Left Arrow] [Right Arrow]

Y: [Left Arrow] [Right Arrow] [Square] [Left Arrow] [Right Arrow]

Z: [Left Arrow] [Right Arrow] [Square] [Left Arrow] [Right Arrow]

Marker

Register [Icon]

Mark | Clear

Define | Clear all

Modify

Main [mm] | Sub [mm] | Apply

Applicator hole blocking

Block | Free all

#	Hole	Indexer[cm]	Depth[cm]	Free Len.[cm]	Free Len.	Tip-1stSDP[cm]	Activation	Dwell Times
VA1	Ring	99.500				0.770	Unlocked	Unlocked

Monitoring

Reconstruction

Virtual Plan | Live Plan | Post Plan

DB | SET | 3D | Color | Off | Abs | Update | update

Slice Mode | OBC Mode | Y-Value = 18.903 cm | Volume | 3D Mode | DVH Mode | 3D Graph

Slice Mode | OBC Mode | Z-Value = -8.500 cm | Slice Mode | OBC Mode | X-Value = 19.209 cm

#	Hole	Indexer[cm]	Depth[cm]	Free Len.[cm]	Free Len.	Tip-1stSDP[cm]	Activation	Dwell Times
VA1	Ring	99.500				0.770	Unlocked	Unlocked

Monitoring

Reconstruction

Virtual Plan | Live Plan | Post Plan

DB | D=? | SET | 3D | Color | Off | Abs | Update | update

18 | 4.3

Y-Value = 18.903 cm | Volume | 3D Mode | DVH Mode | 3D Graph

Slice Mode | OBC Mode | Z-Value = -9.000 cm | Slice Mode | OBC Mode | X-Value = 19.209 cm

#	Hole	Indexer[cm]	Depth[cm]	Free Len.[cm]	Free Len.	Tip-1stSDP[cm]	Activation	Dwell Times
VA1	Ring	99.500				0.770	Unlocked	Unlocked

Monitoring

Reconstruction

Virtual Plan | Live Plan | Post Plan

DB | SET | 3D | Color | Off | Update | update

19 | 4.3

Y-Value = 18.903 cm | Volume | 3D Mode | DVH Mode | 3D Graph

X-Value = 19.209 cm

Z-Value = -9.500 cm

Register | Mark | Clear | Define | Clear all

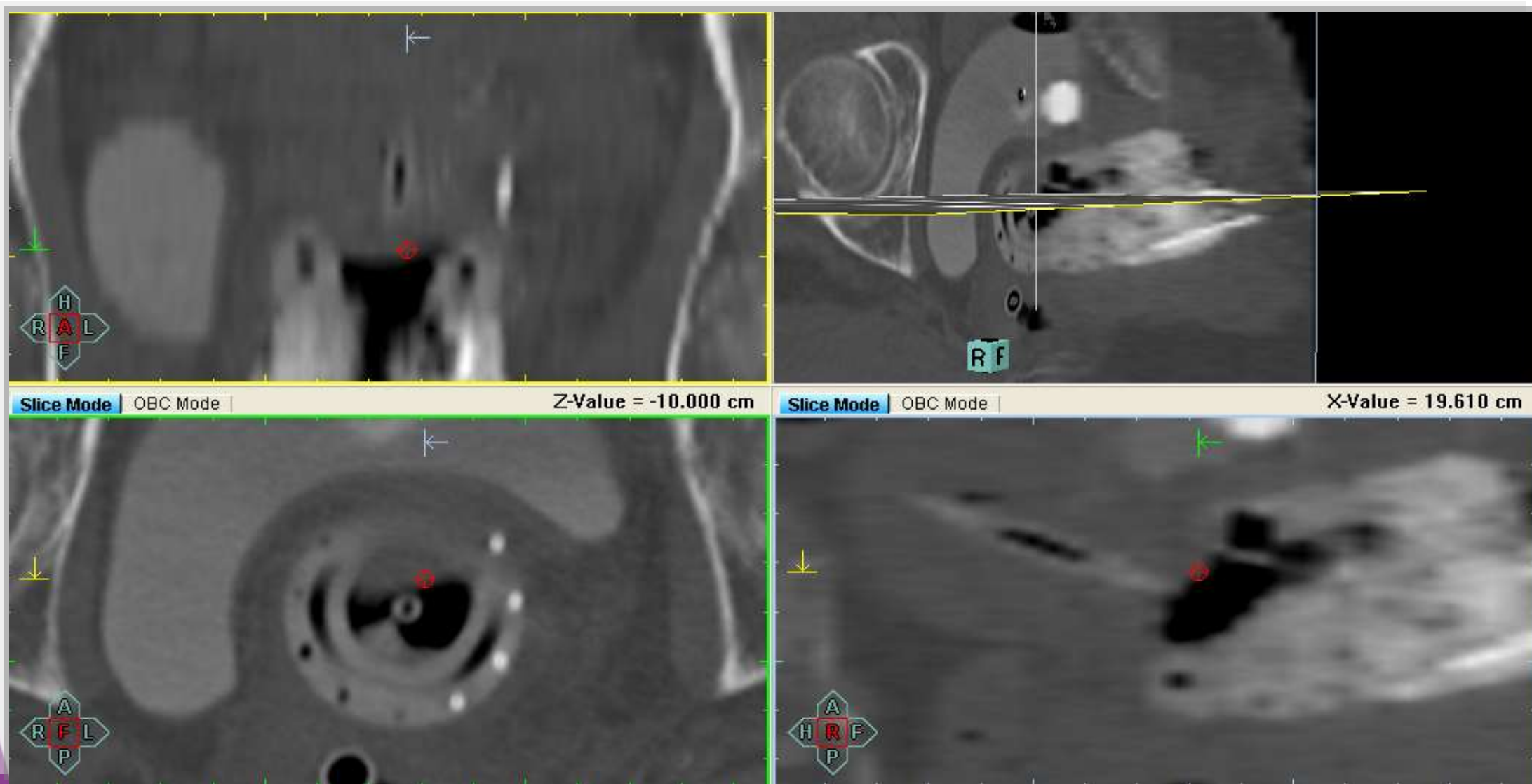
Modify
Main [mm] Sub [mm] Apply

Applicator hole blocking
Block Free all

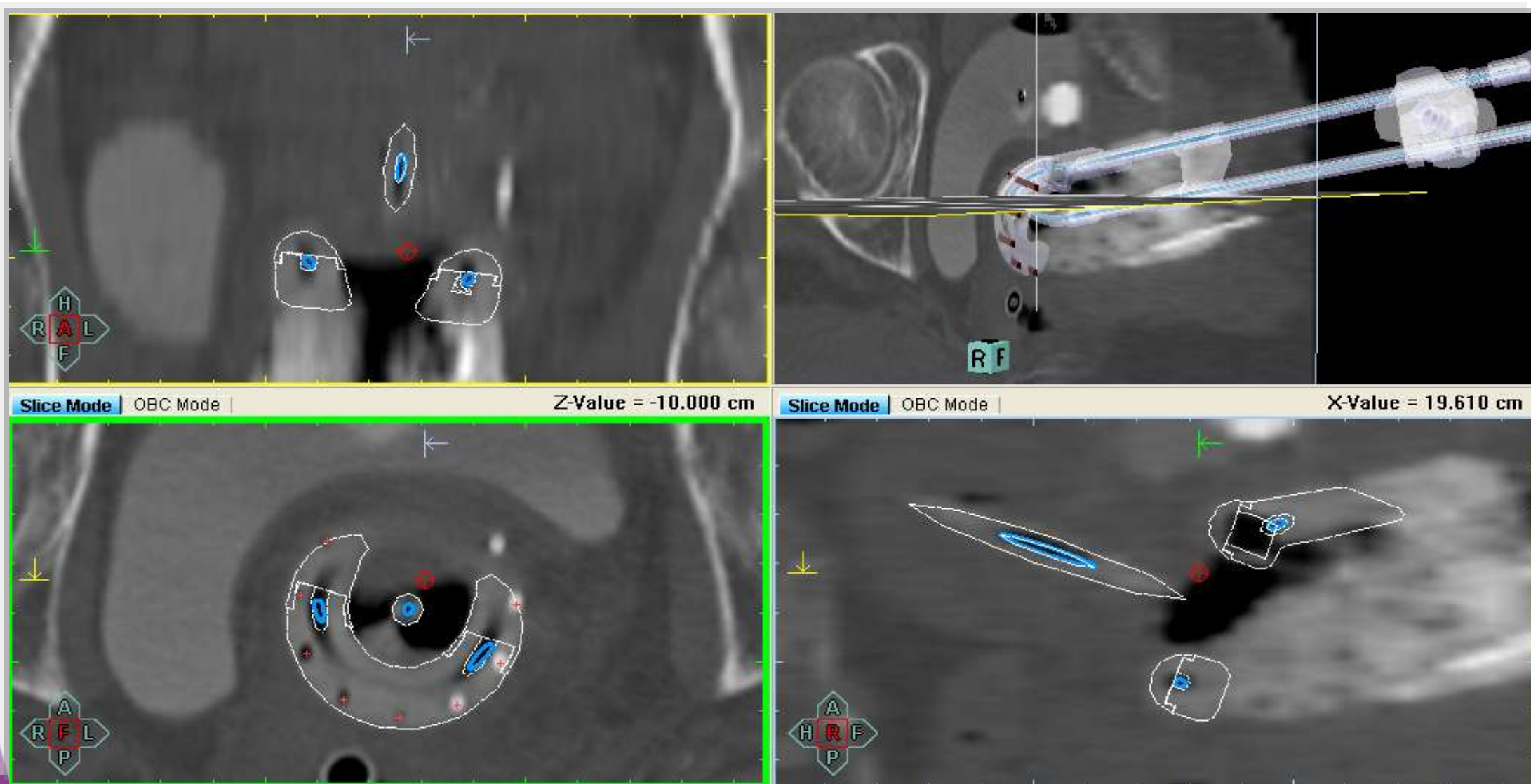
#	Hole	Indexer[cm]	Depth[cm]	Free Len.[cm]	Free Len.	Tip-1stSDP[cm]	Activation	Dwell Times
VA1	Ring	99.500				0.770	Unlocked	Unlocked

Monitoring

Reconstruction



Reconstruction



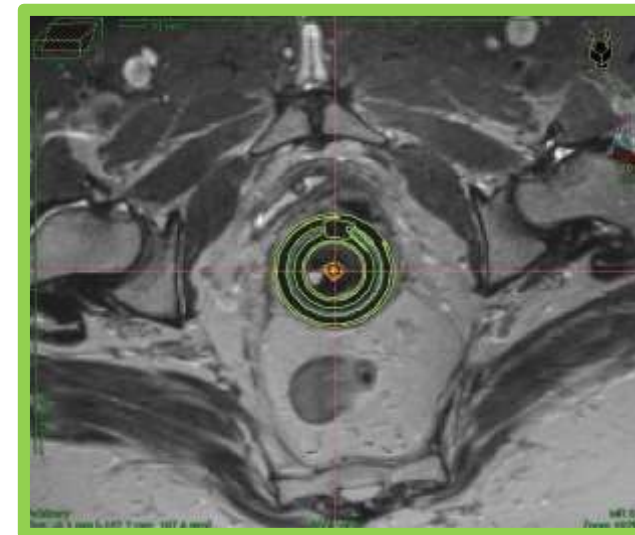
Better accuracy

less time to reconstruct

Treatment Planning directly on MR

Import vendor provided archived applicator into planning images

Can use with 3D SPACE or T2 FSE



Courtesy
B. Erickson
MCW, USA

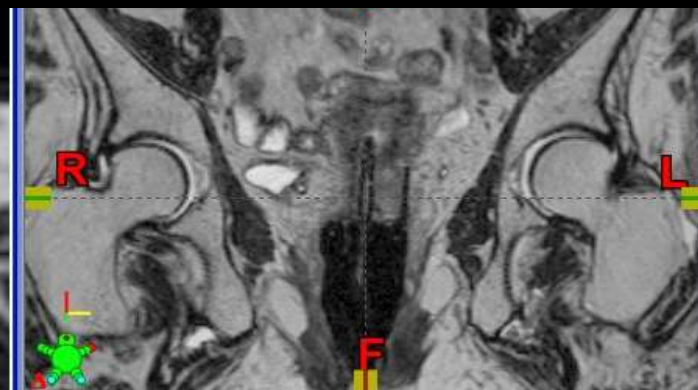
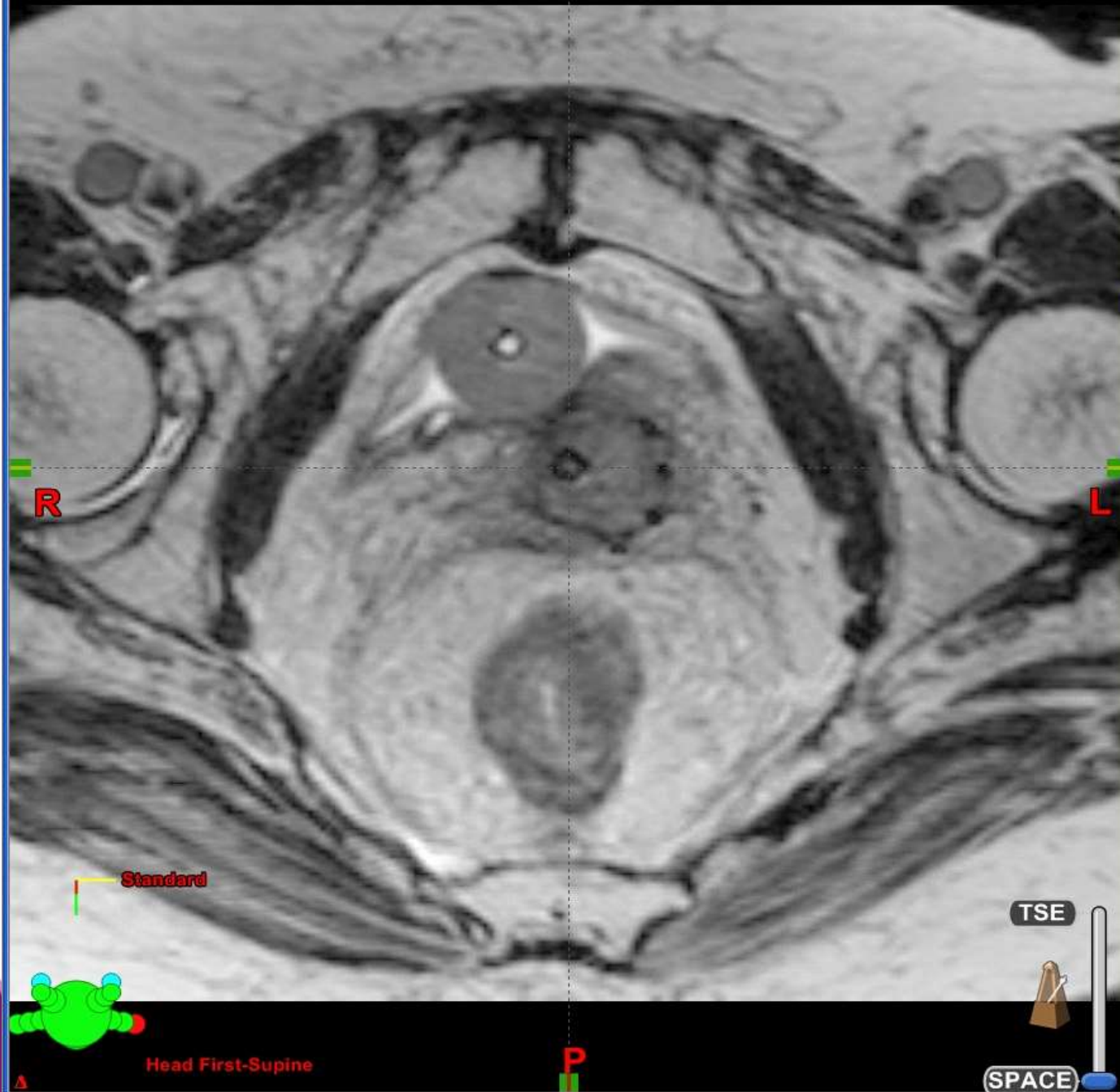
IMAGE FUSION I

- Transversal (Paratransversal) MRI + 3D MR sequence
- Volumes fusion based on **DICOM coordinates**
(patient/applicator/organs should not have moved between MR and CT image acquisitions)

“Standard” T2 FSE: 0.8 x 0.8 mm in-plane pixel size in paratransverse view.



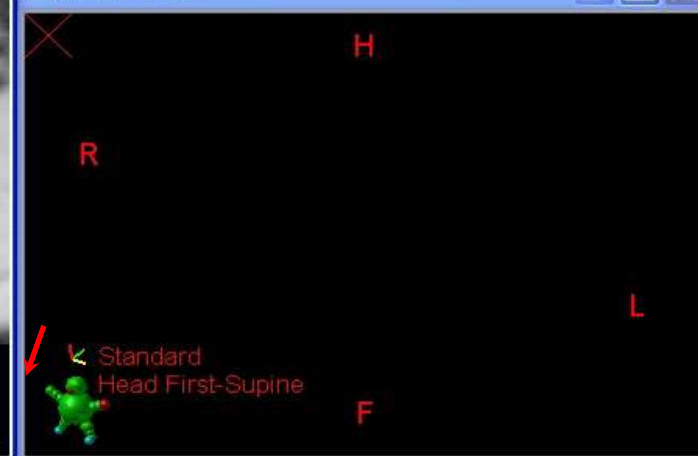
“SPACE / FRFSE”: 1 x 1 mm in-plane pixel, 1 mm slice thickness



TSE - Blended with registered image: ...



Model View



Manual checking of DICOM-coordinates-based registration

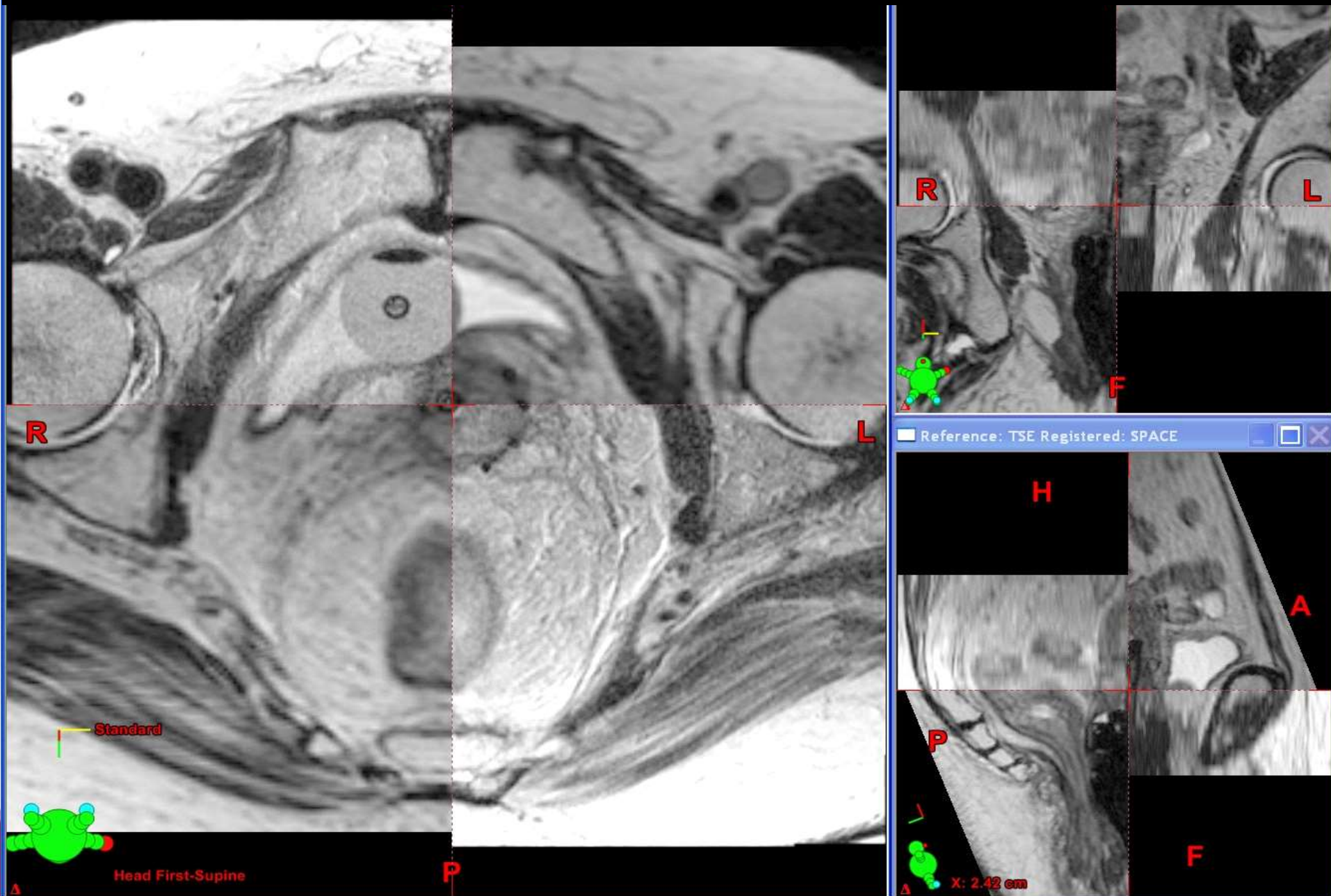


IMAGE FUSION II

- Transversal MRI + CT for better applicator reconstruction
- Volumes fusion based on **DICOM coordinates**
(patient/applicator/organs should not have moved between MR and CT image acquisitions)

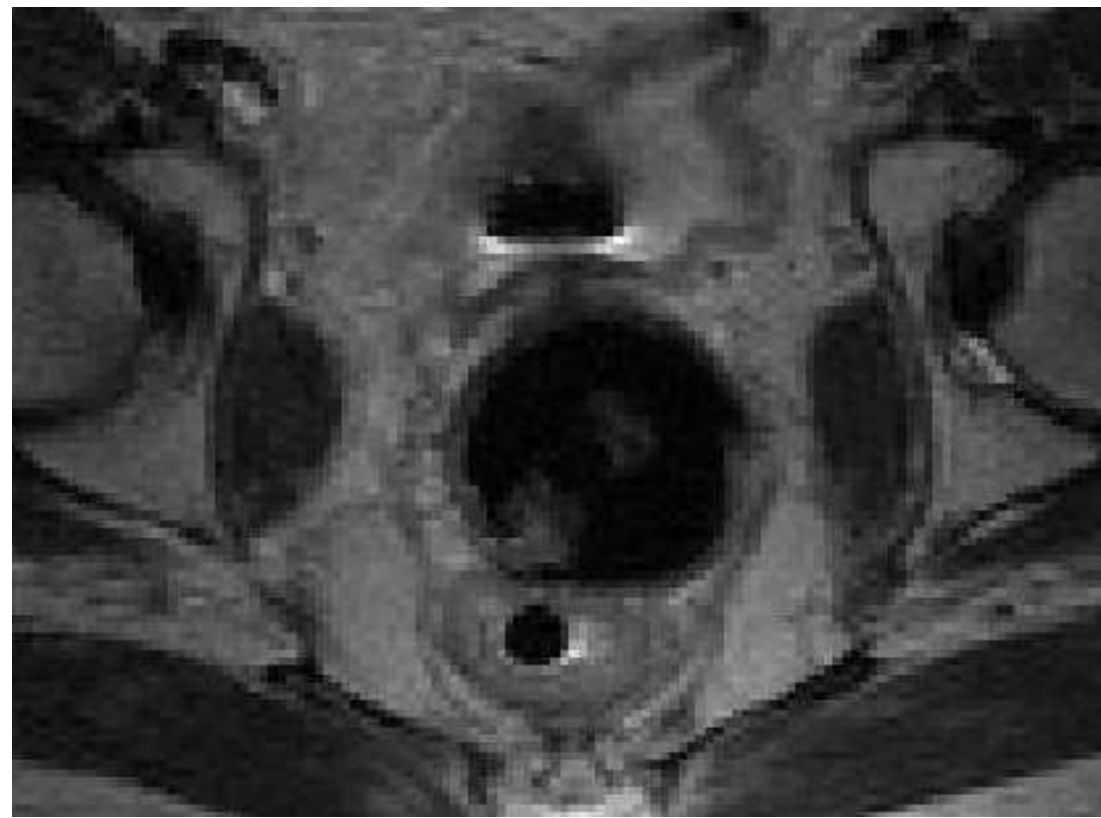
- CT

(better visibility of applicator)

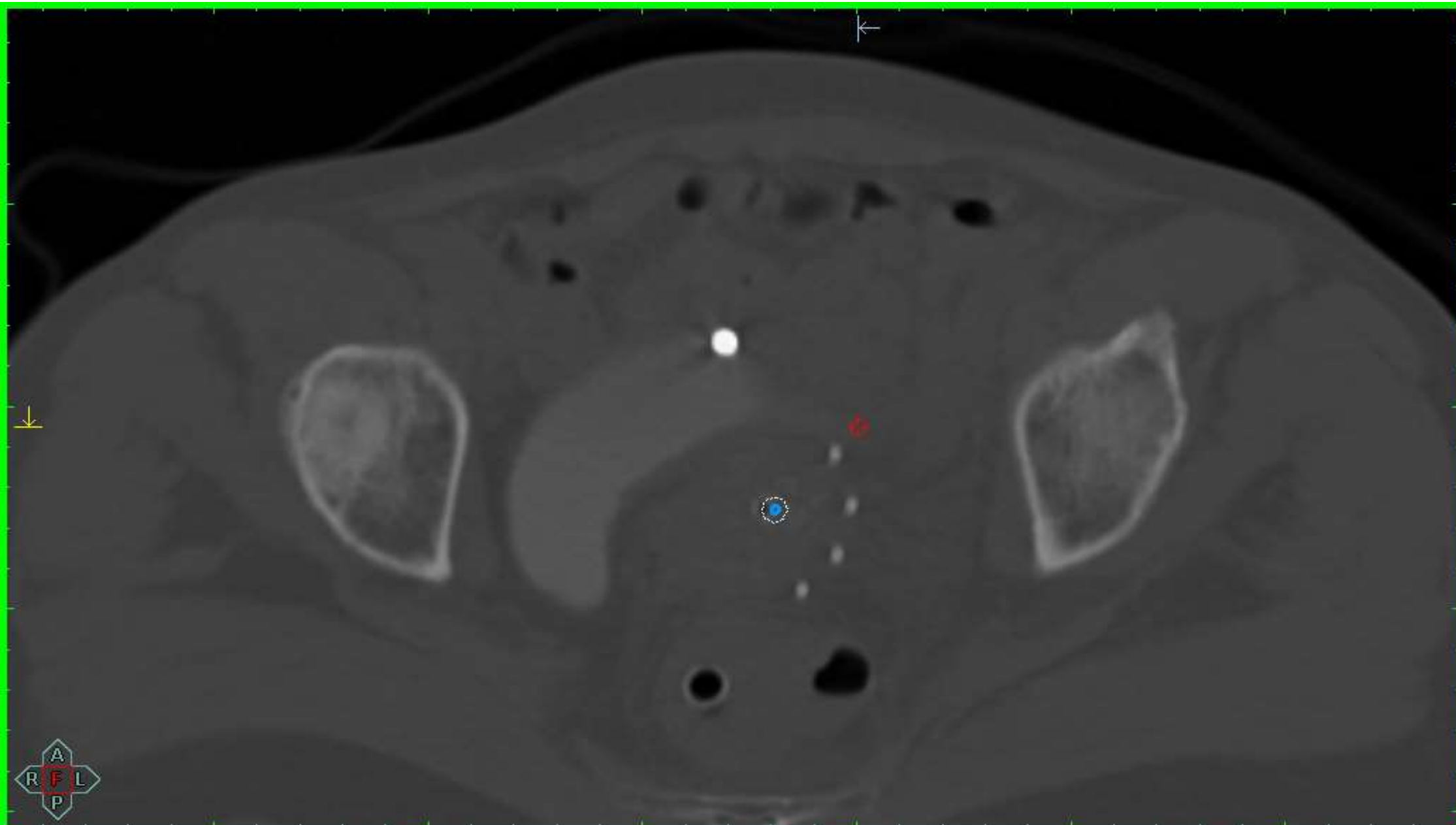


- MR

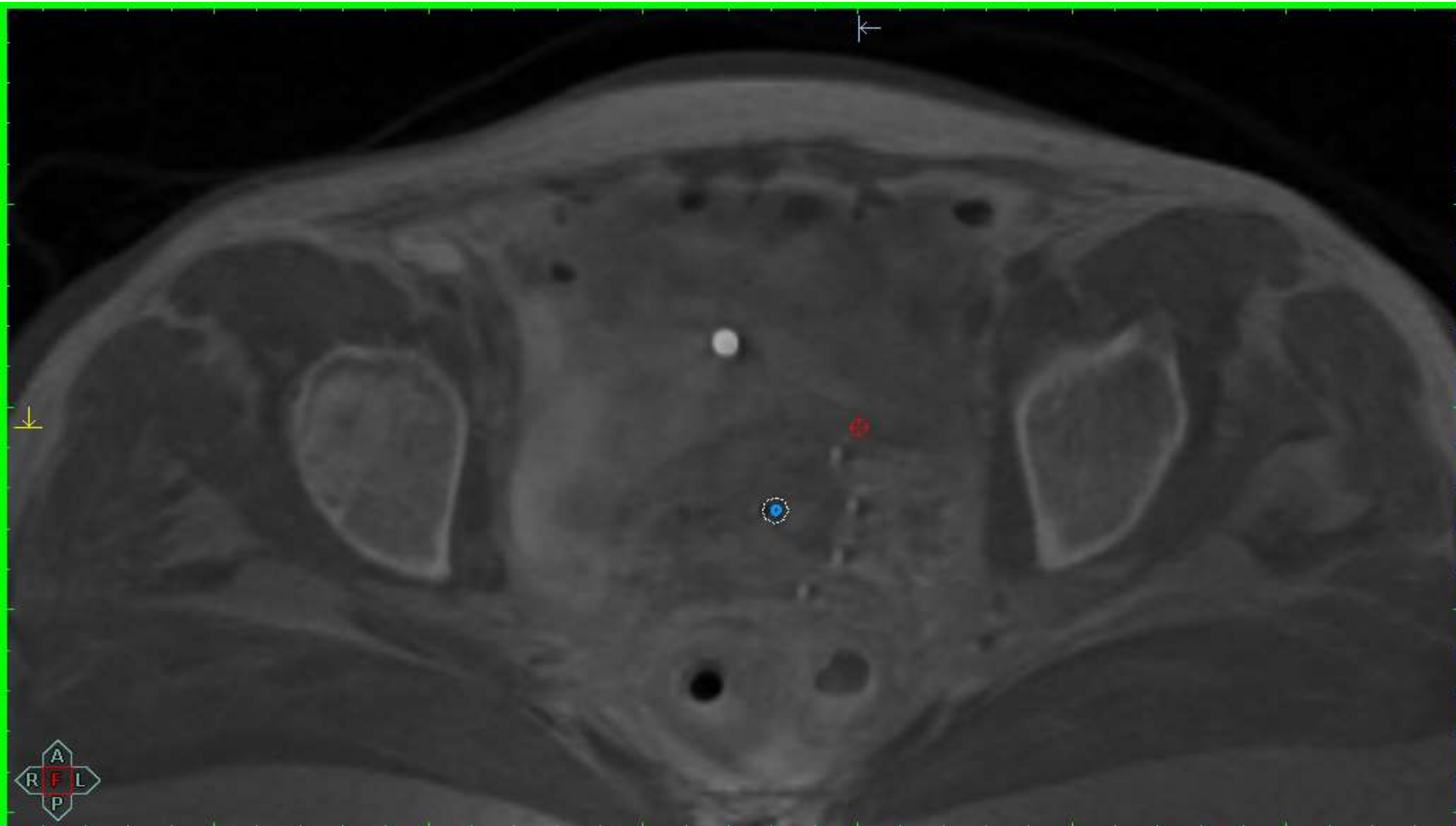
(better visibility of structures)



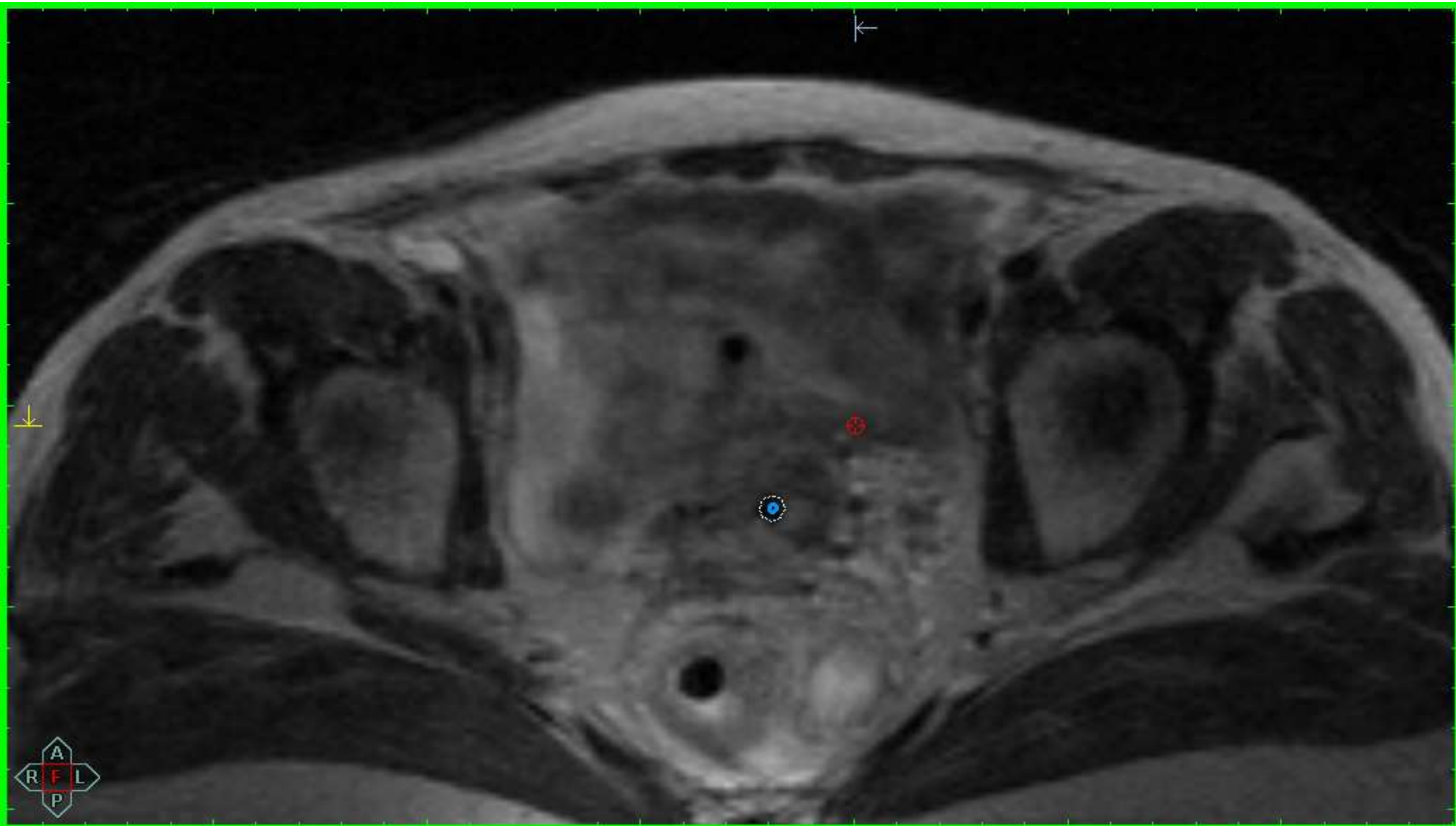
CT / MRI fusion



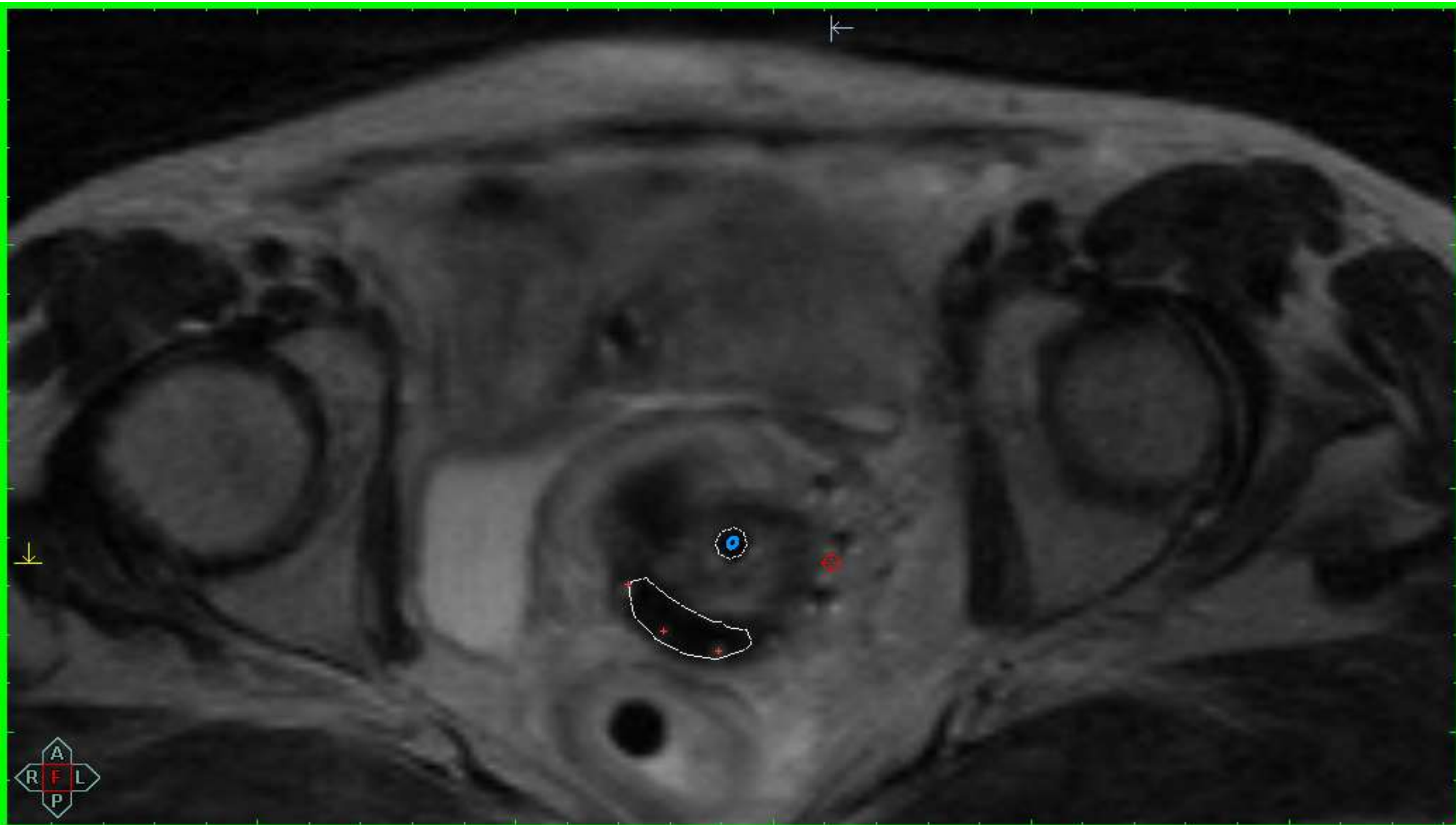
CT / MRI fusion



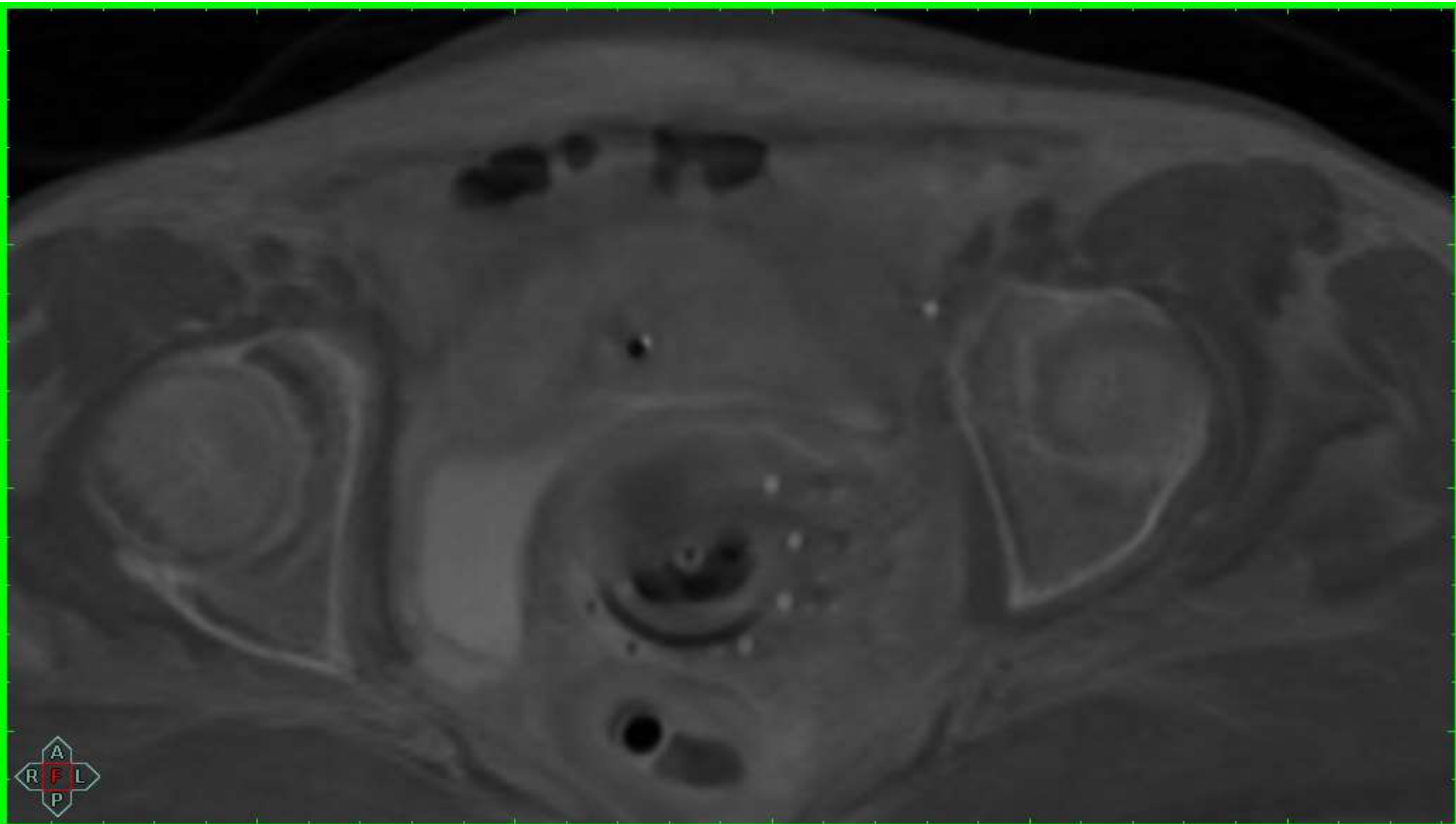
CT / MRI fusion



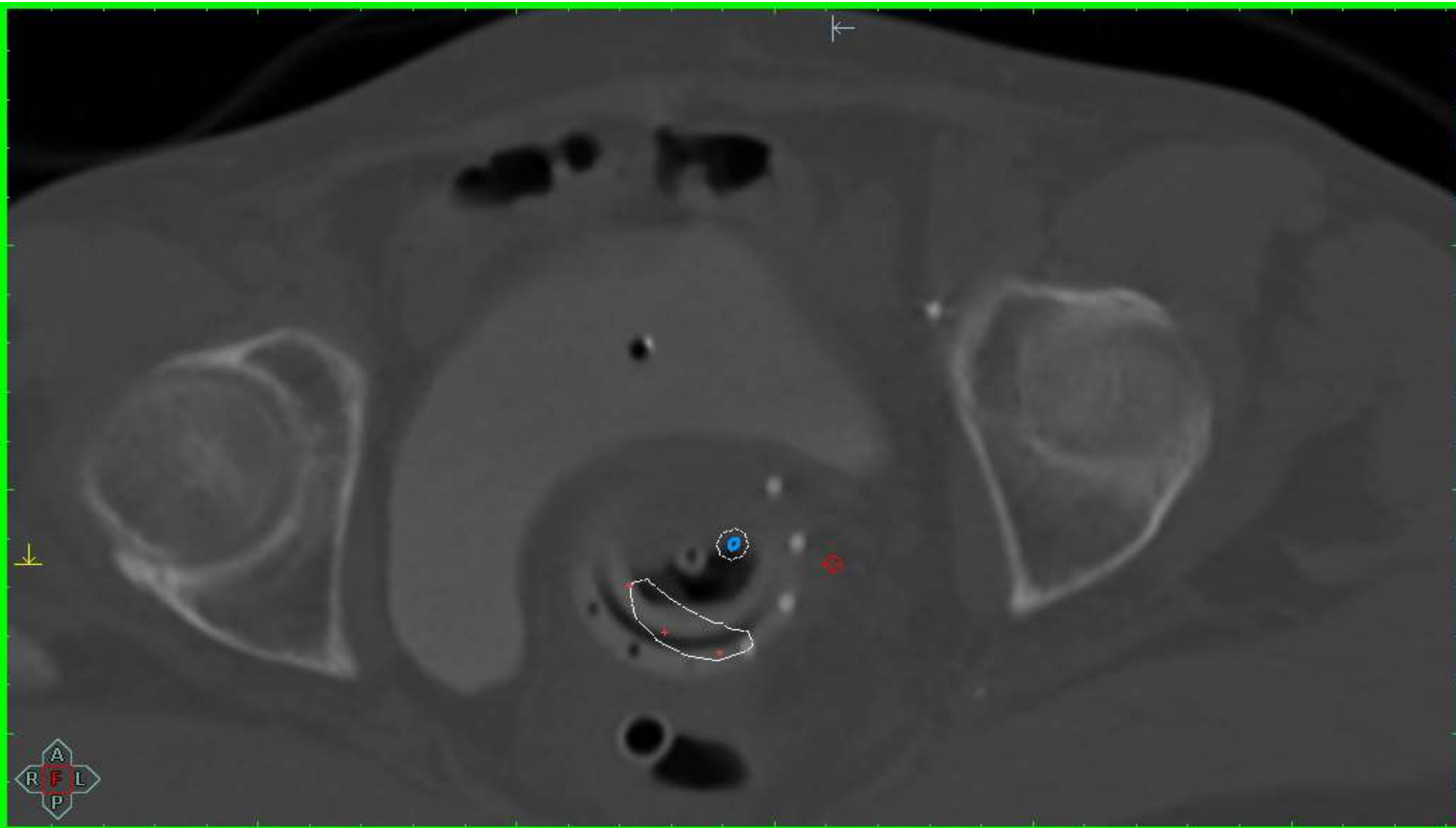
CT / MRI fusion

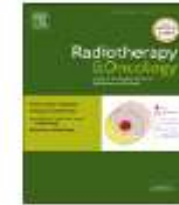


CT / MRI fusion



CT / MRI fusion





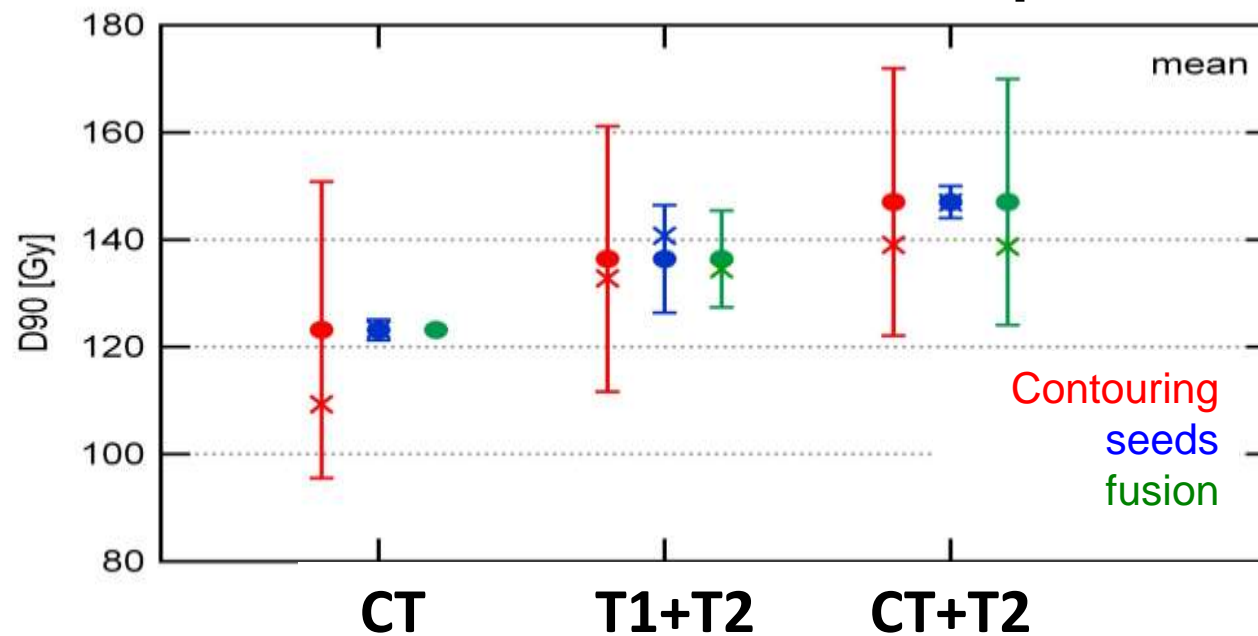
Prostate brachytherapy

Prostate post-implant dosimetry: Interobserver variability in seed localisation, contouring and fusion

Marisol De Brabandere^{a,*}, Peter Hoskin^b, Karin Haustermans^a, Frank Van den Heuvel^a, Frank-André Siebert^c

^aUniversity Hospital Gasthuisberg, Leuven, Belgium; ^bMount Vernon Cancer Centre, Middlesex, UK; ^cUniversity Hospital of Schleswig-Holstein, Kiel, Germany

Mean 3 patients



See also de Brabandere et al. Brachytherapy 2013

Recommendations III

Applicator reconstruction

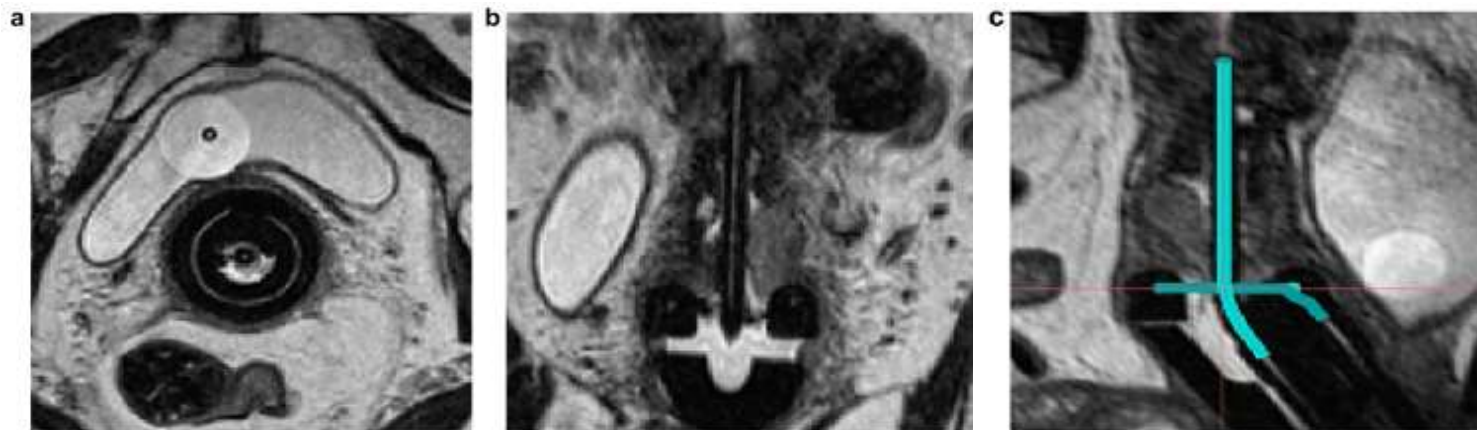


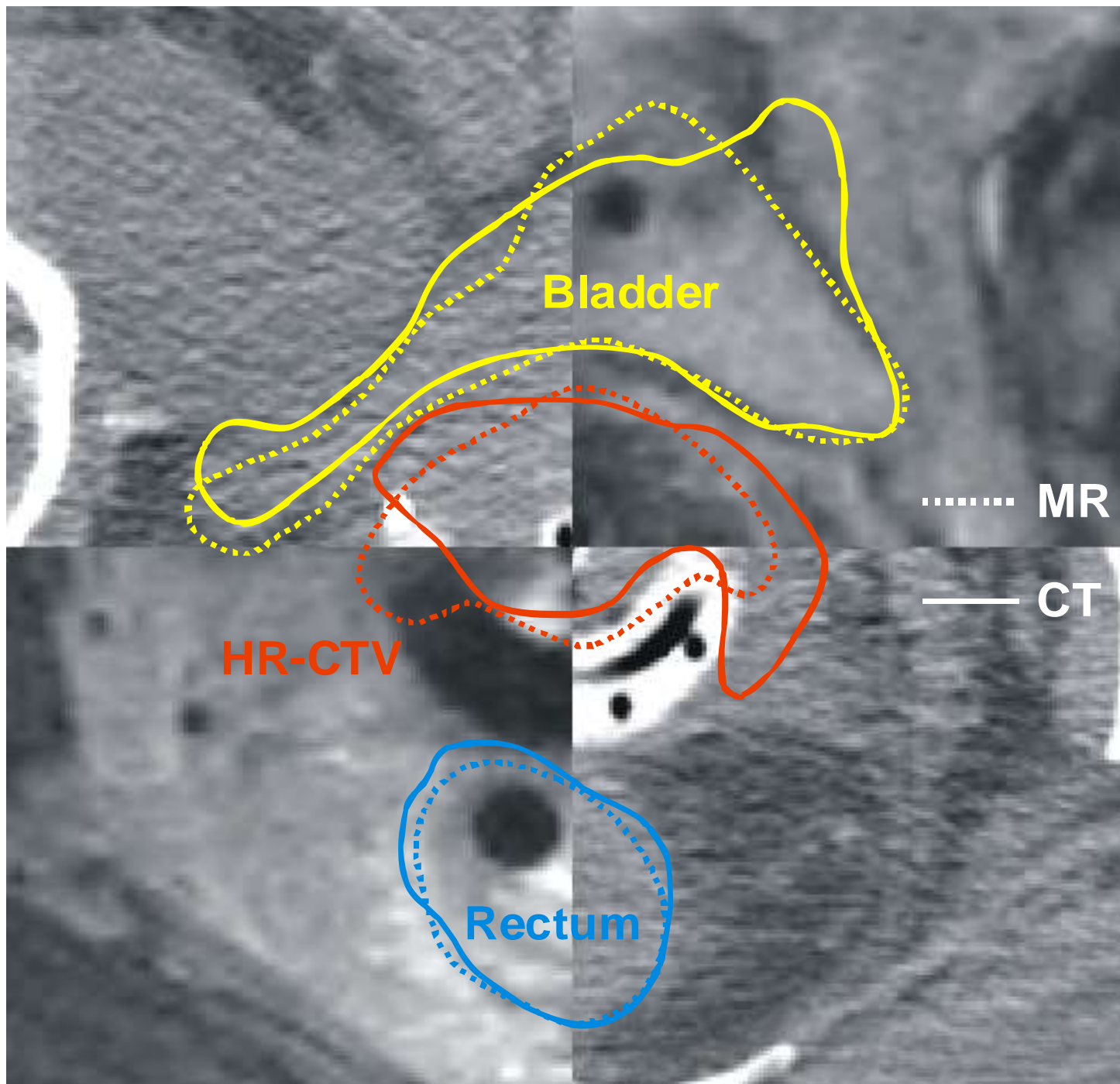
GEC-ESTRO Recommendations

Recommendations from Gynaecological (GYN) GEC-ESTRO Working Group: Considerations and pitfalls in commissioning and applicator reconstruction in 3D image-based treatment planning of cervix cancer brachytherapy

Taran Paulsen Hellebust^{a,*}, Christian Kirisits^b, Daniel Berger^b, José Pérez-Calatayud^c, Marisol De Brabandere^d, Astrid De Leeuw^e, Isabelle Dumas^f, Robert Hudej^g, Gerry Lowe^h, Rachel Wills^h, Kari Tanderupⁱ

- Guidelines for reconstruction of the applicator in 3D image based treatment planning:
 - Applicator commissioning
 - Applicator reconstruction





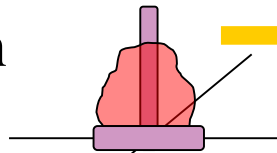
Combined MRI-/CT- guided BT for cervical cancer

4 fractions of BT with 7Gy fraction size, in 2 applications in consecutive weeks
Planning with *Oncentra GYN* treatment planning system (Nucletron)

1st application

MRI- based planning:
3D applicator reconstruction

target delineation



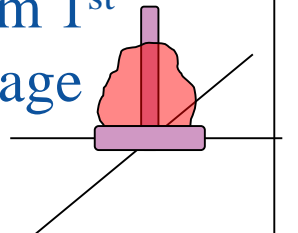
OAR delineation

Dose planning and optimization

2nd application

CT- based planning:
3D applicator reconstruction

Automatic target transfer from 1st
MRI via applicator-based image
registration

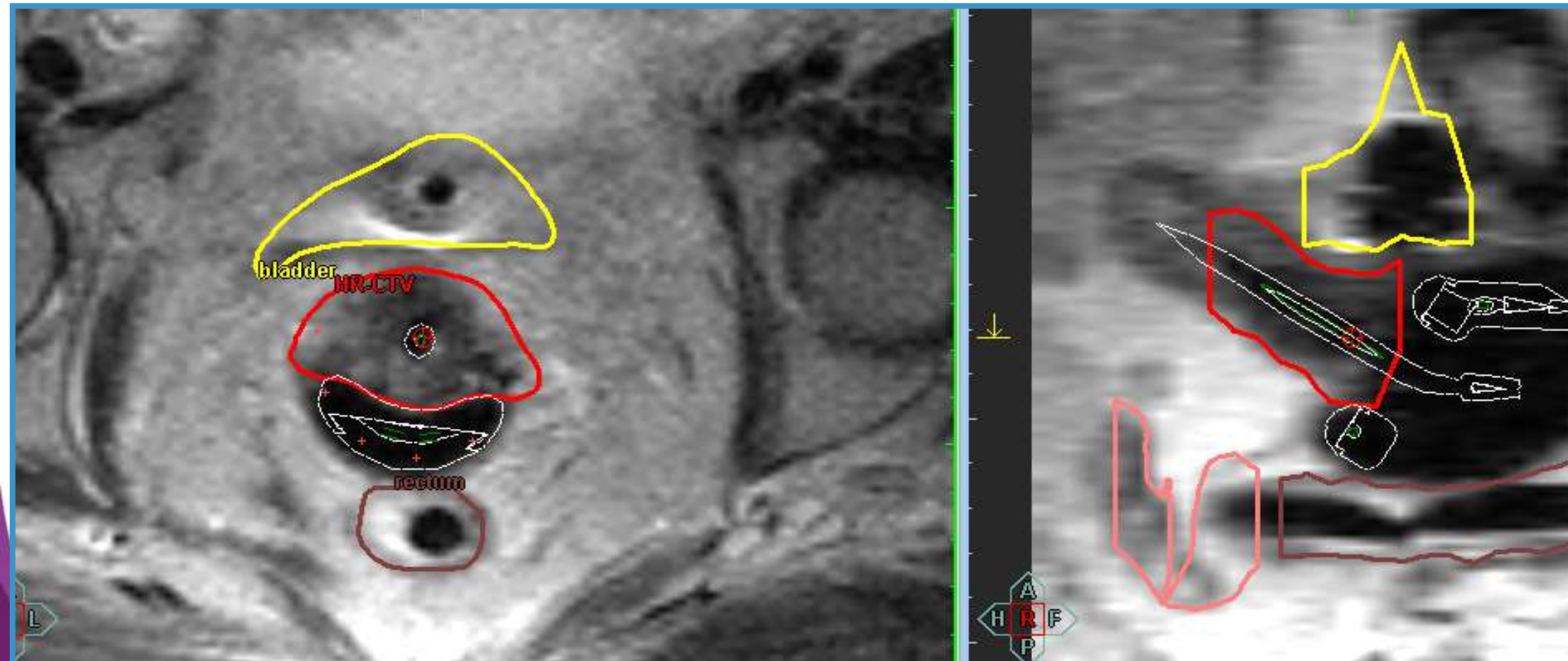


OAR delineation

Dose planning and optimization

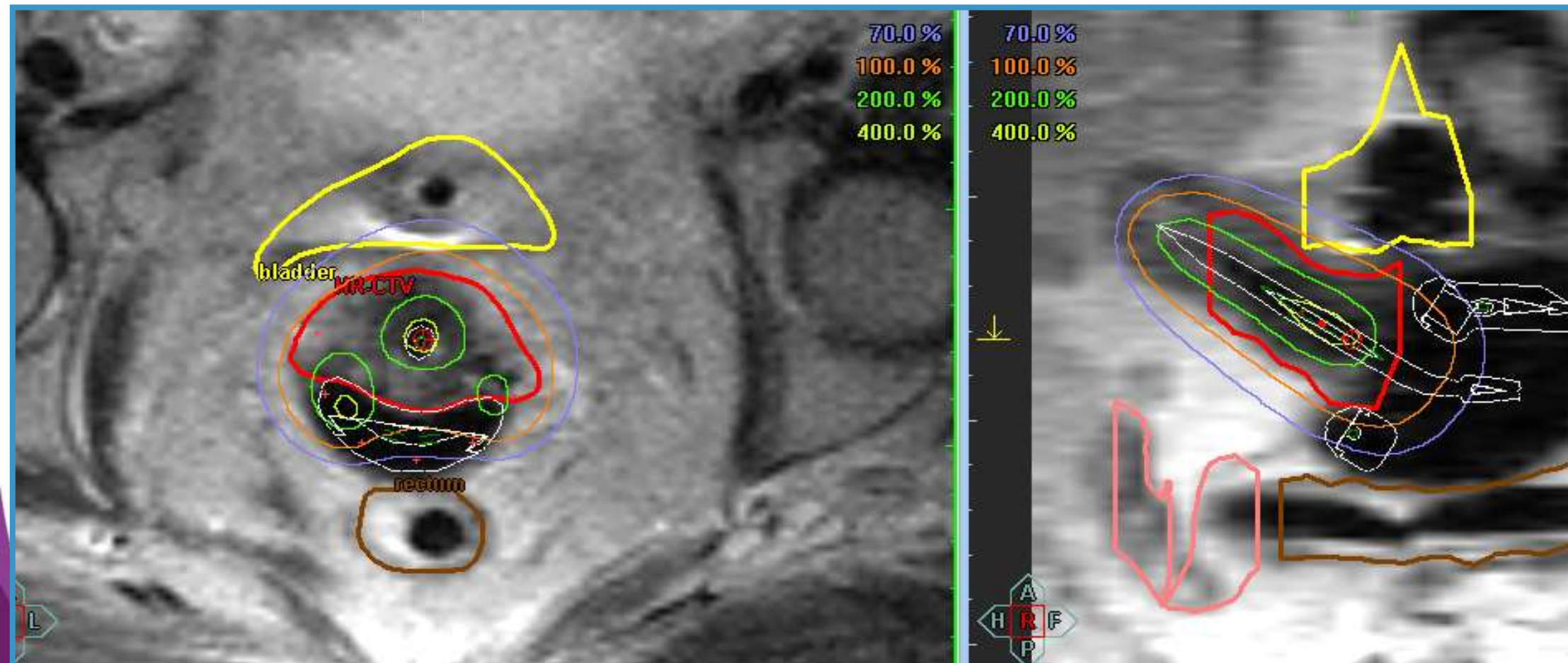
1st application: MRI

Applicator, target (HR CTV), OAR (rectum, bladder, sigmoid)



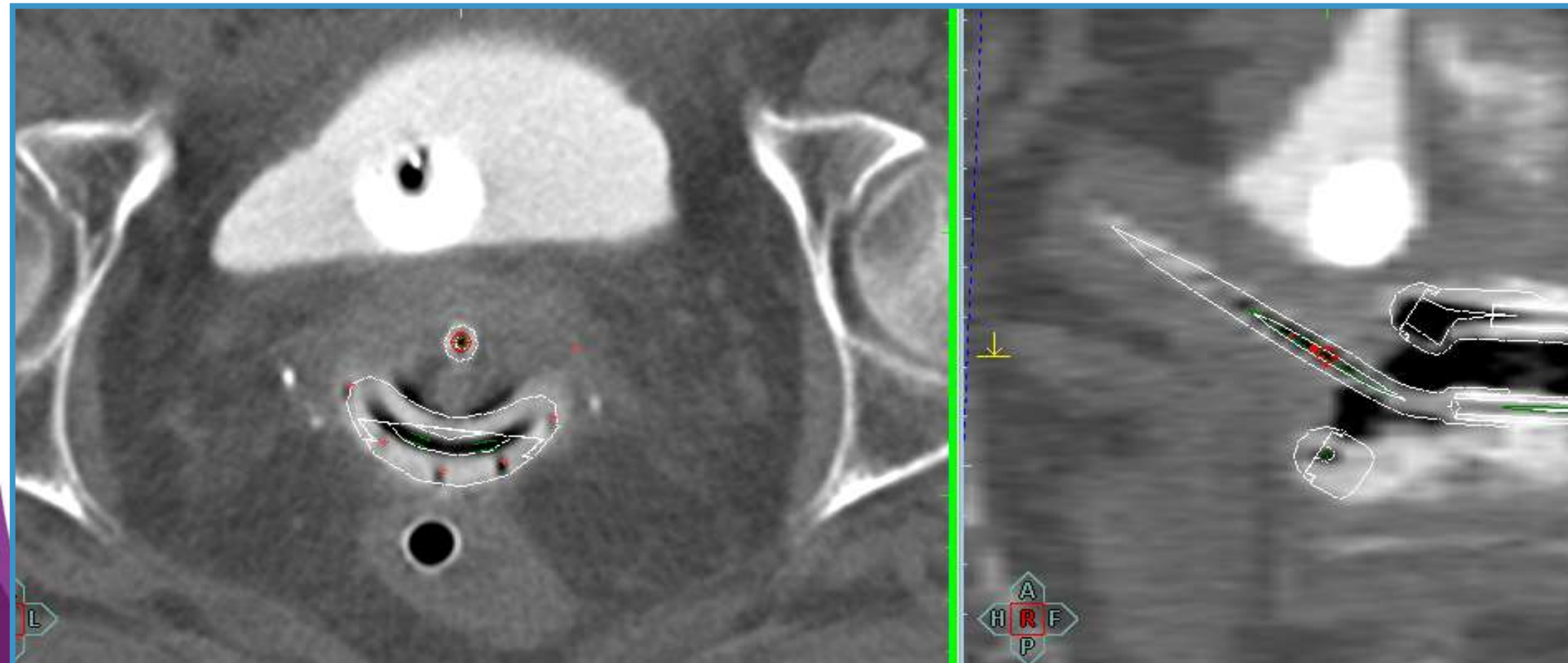
1st application: MRI

Applicator, target (HR CTV), OAR (rectum, bladder, sigmoid)
Dose planning and optimization on target+organ contours



2nd application: CT

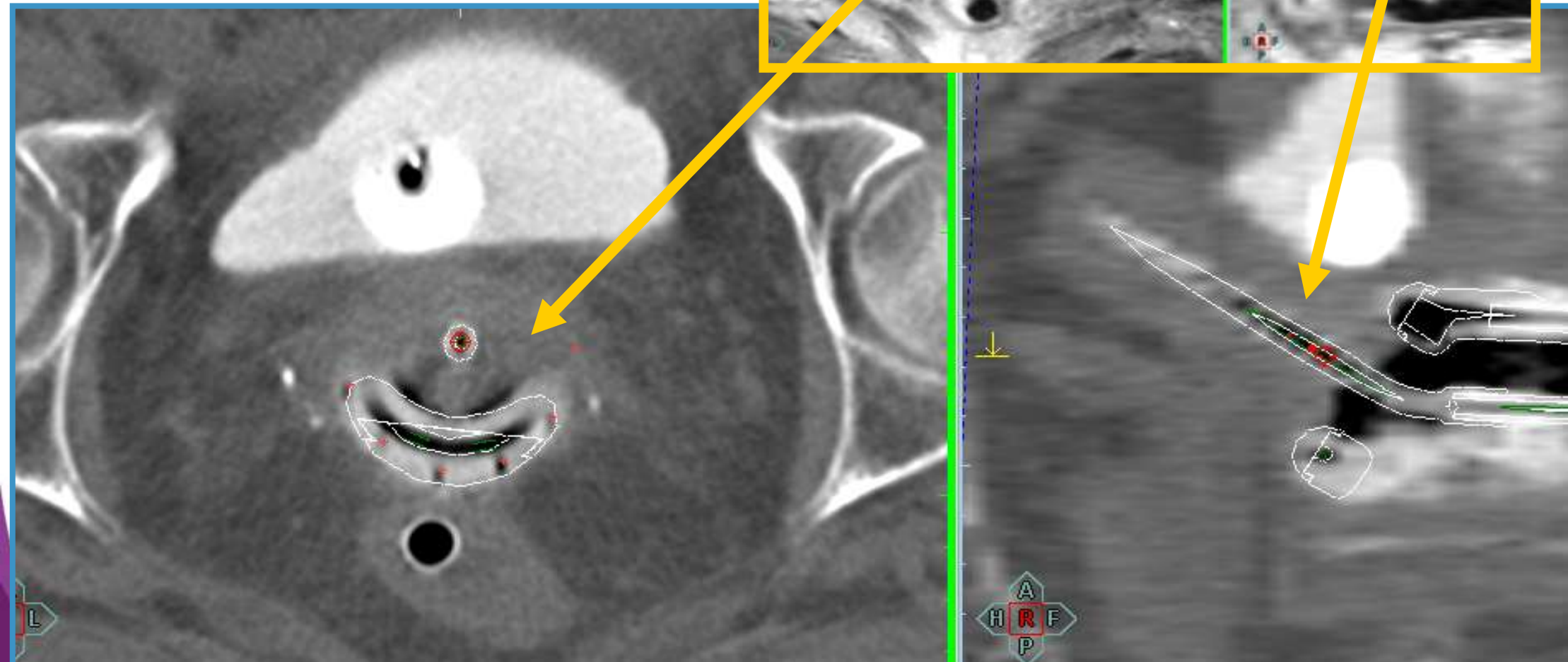
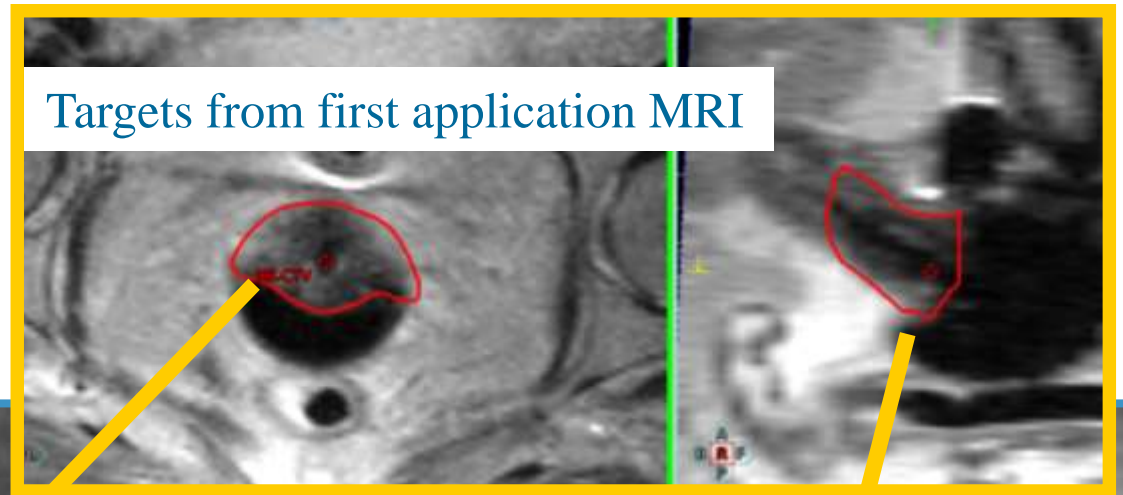
3D applicator reconstruction



2nd application: CT

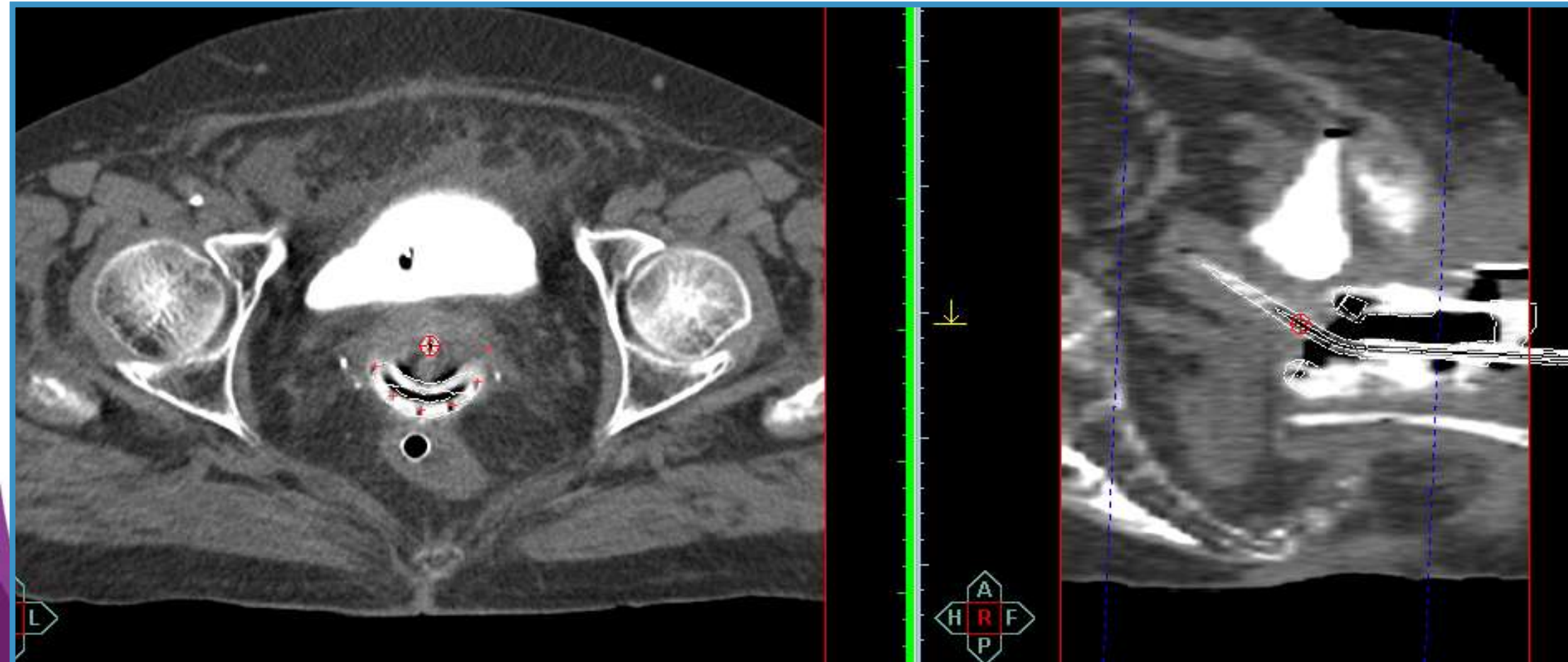
3D applicator reconstruction

Target transfer



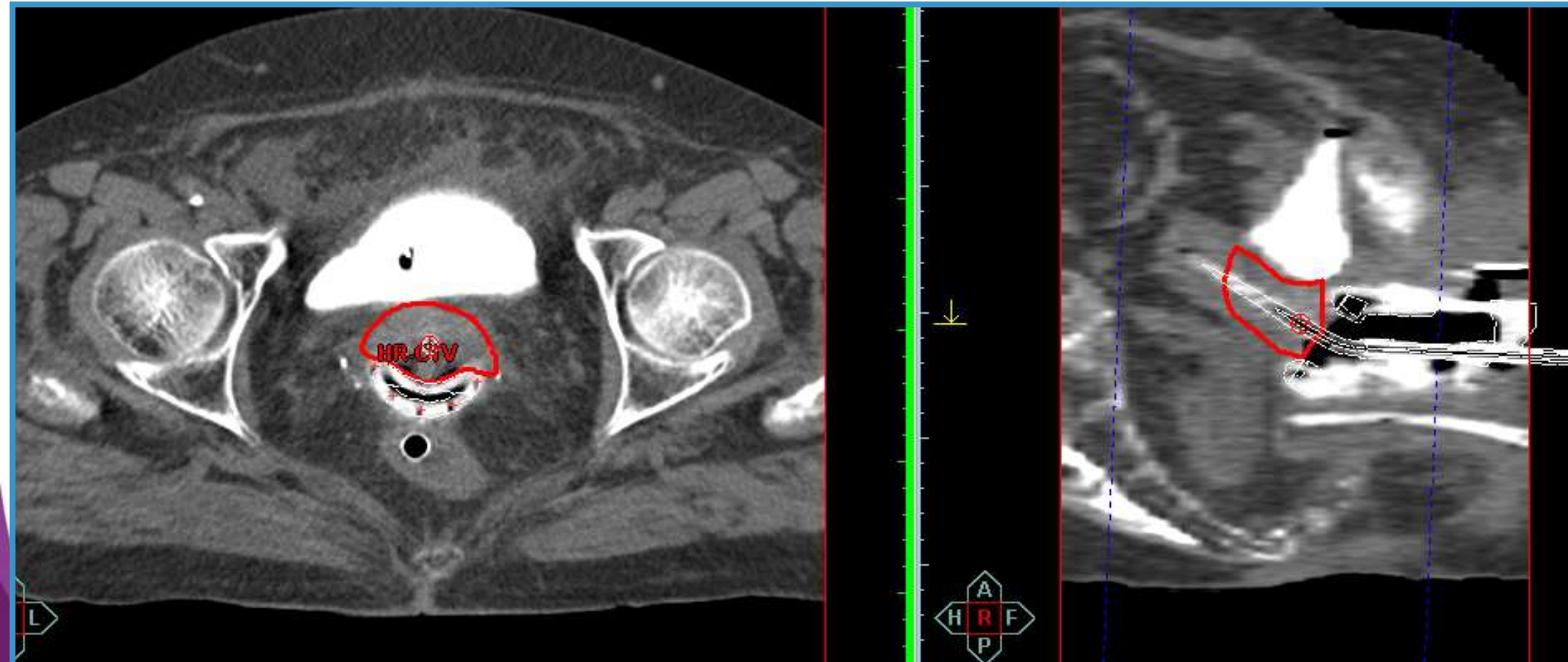
2nd application: CT

Automatic image fusion based on 3D applicator model



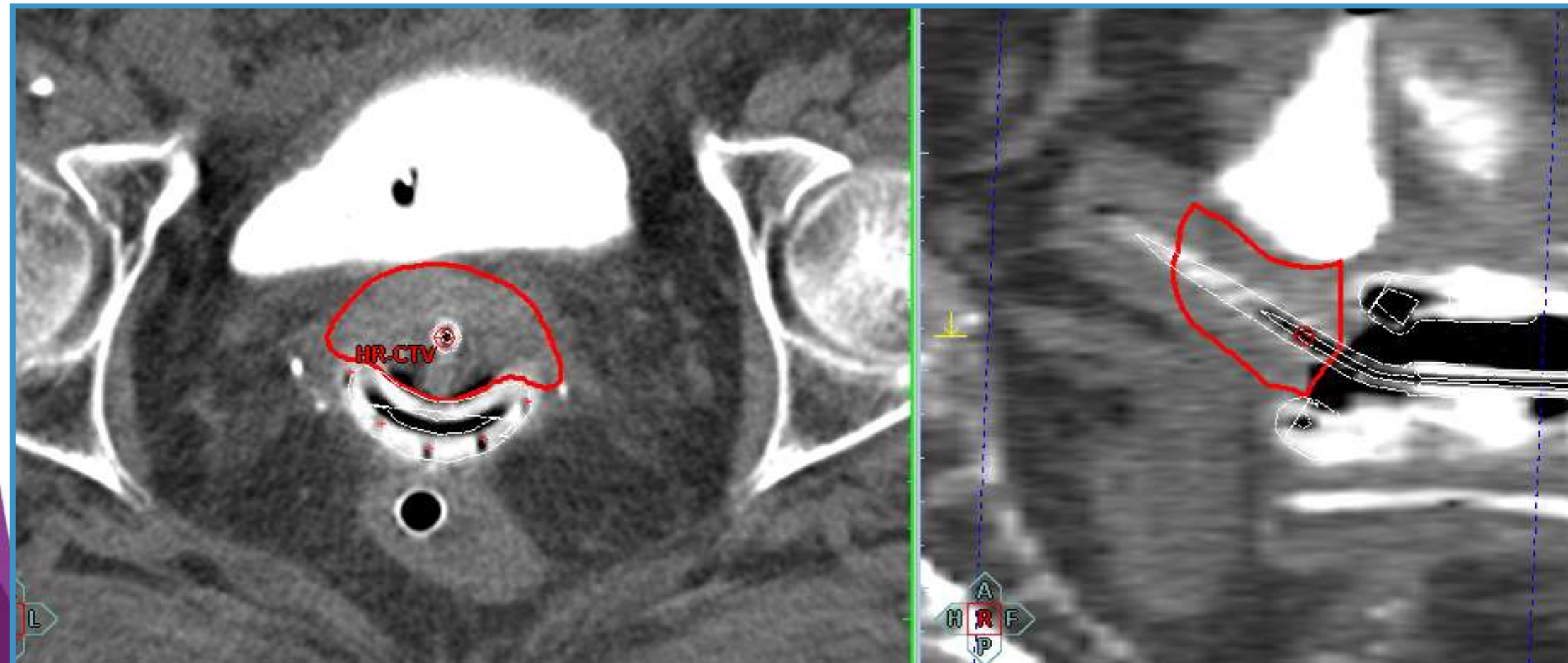
2nd application: CT

Automatic target transfer from MRI to CT with applicator as reference system



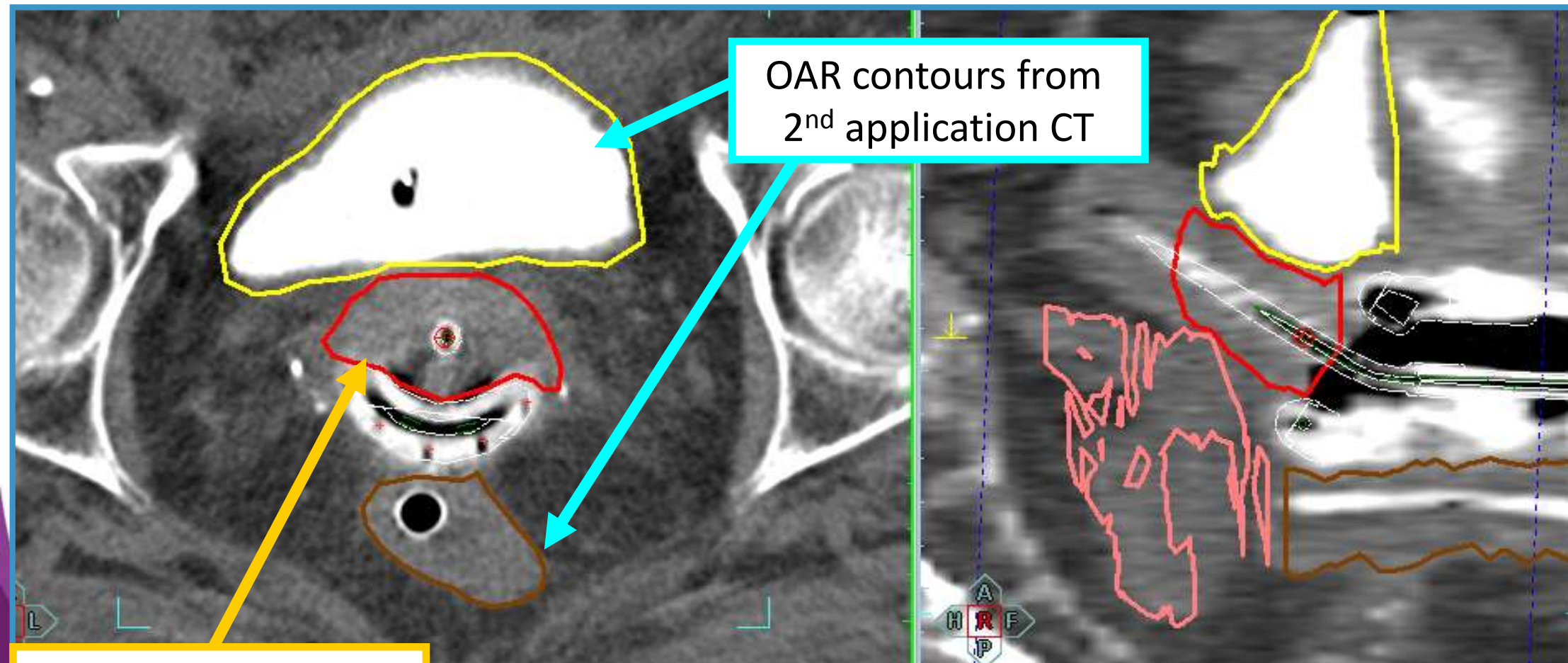
2nd application: CT

Contouring OAR on CT



2nd application: CT

Contouring OAR on CT

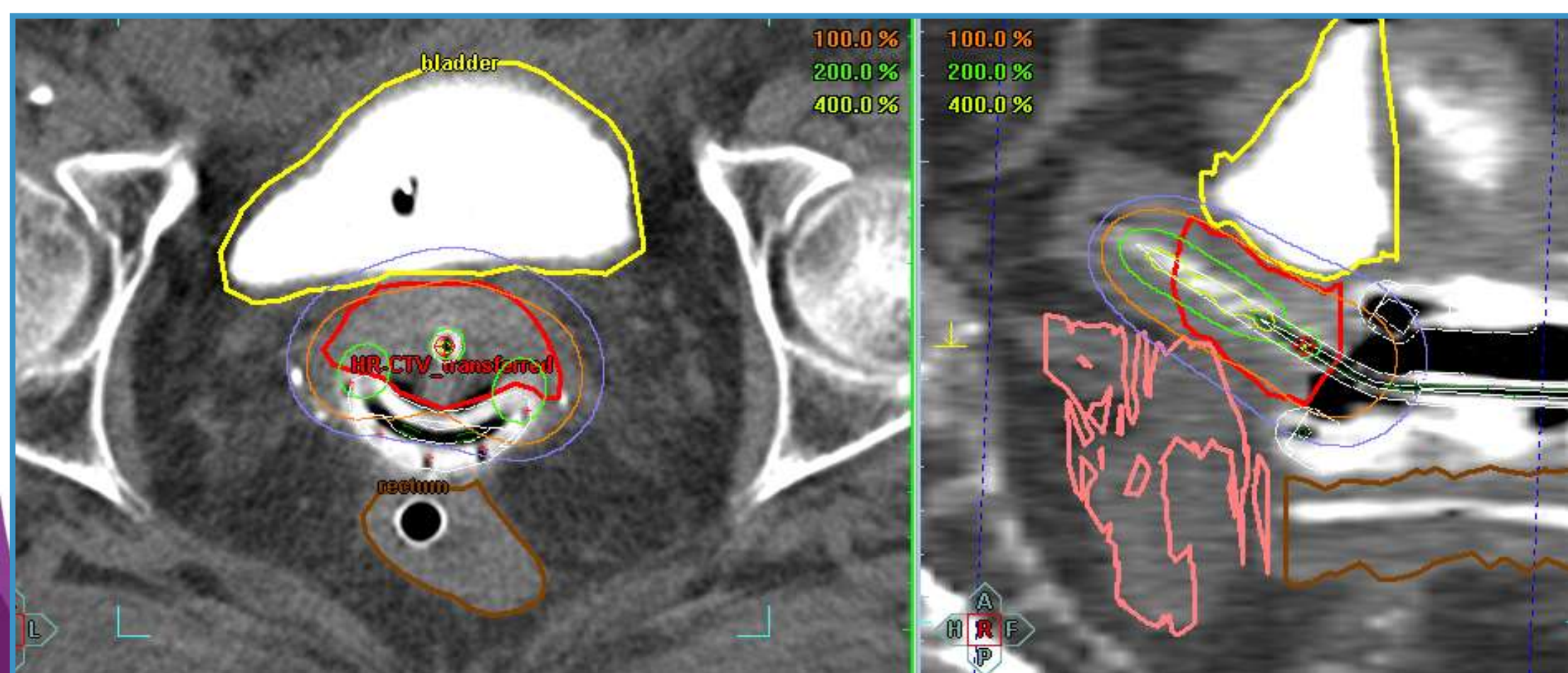


OAR contours from
2nd application CT

Target contour from
1st application MRI

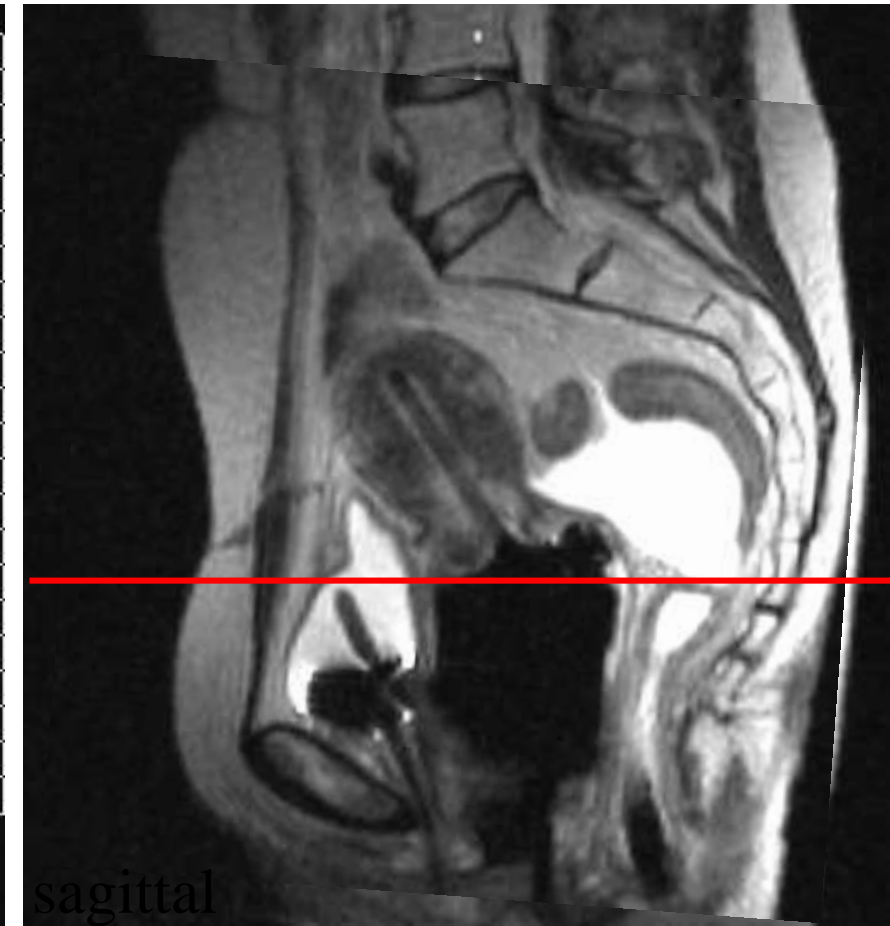
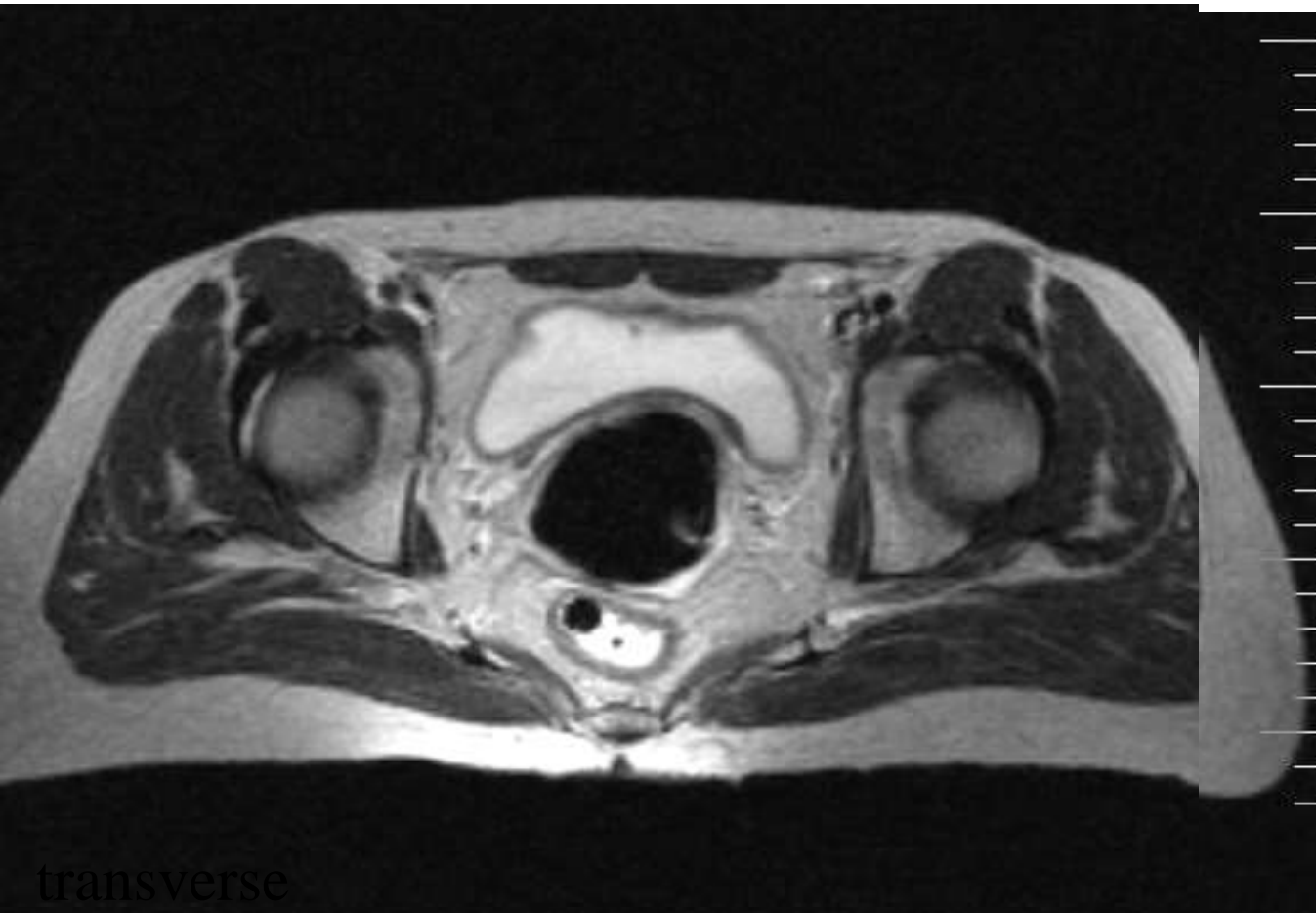
2nd application: CT

Dose planning and optimization based on **copied target** and **individual OAR** contours. All dose constraints for targets and OAR have to be achieved.



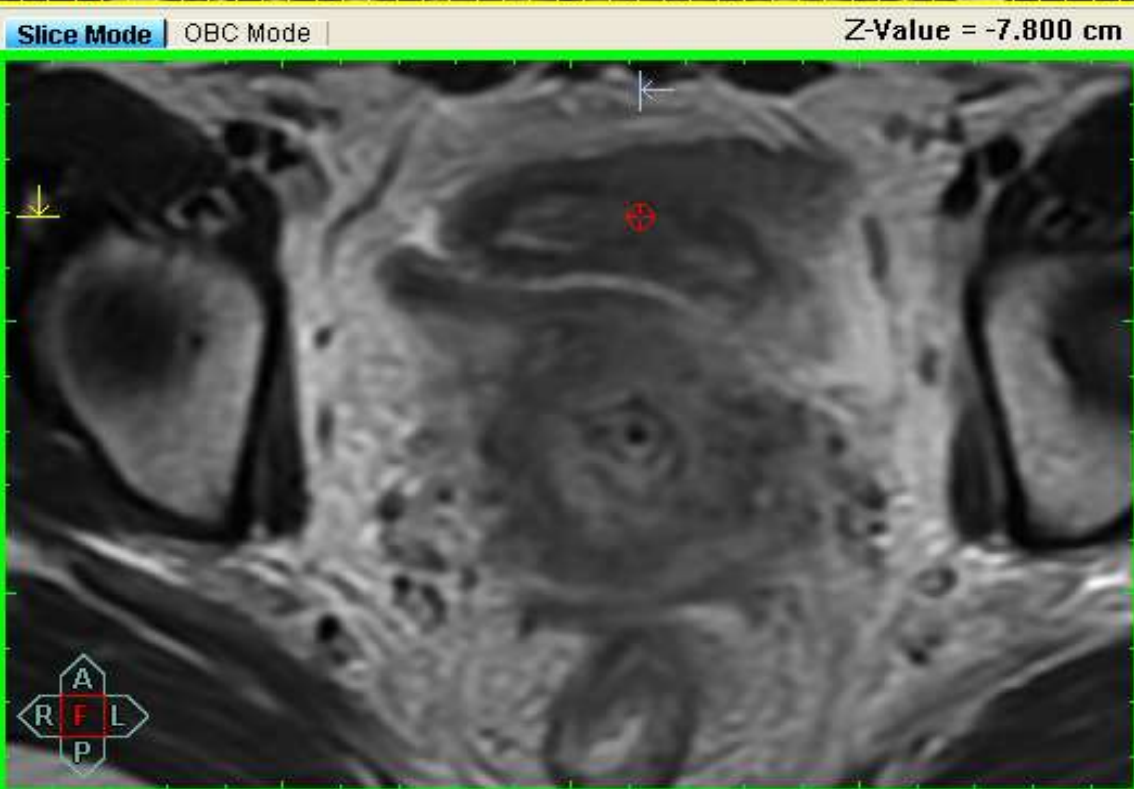
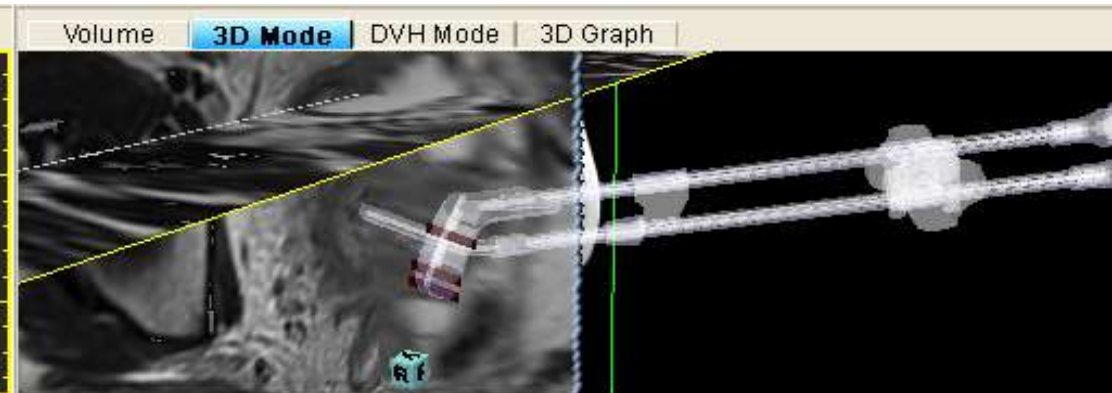
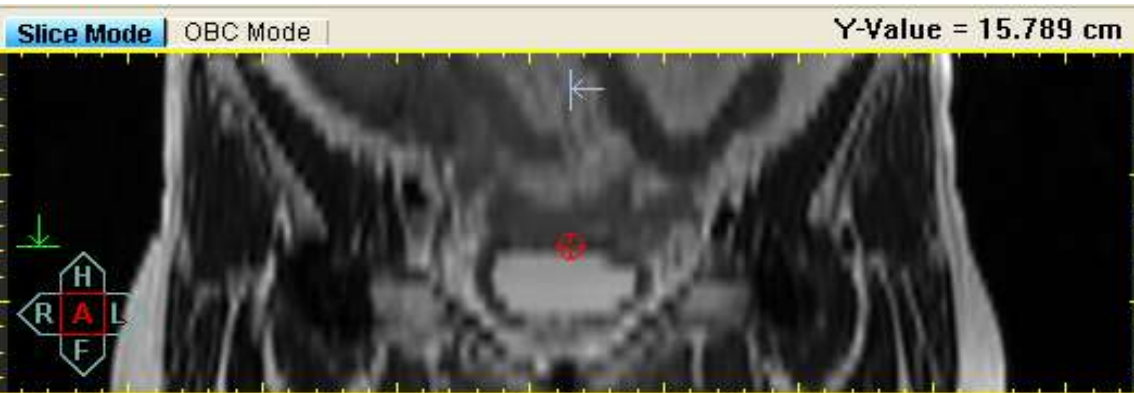
Outlook

Before brachytherapy

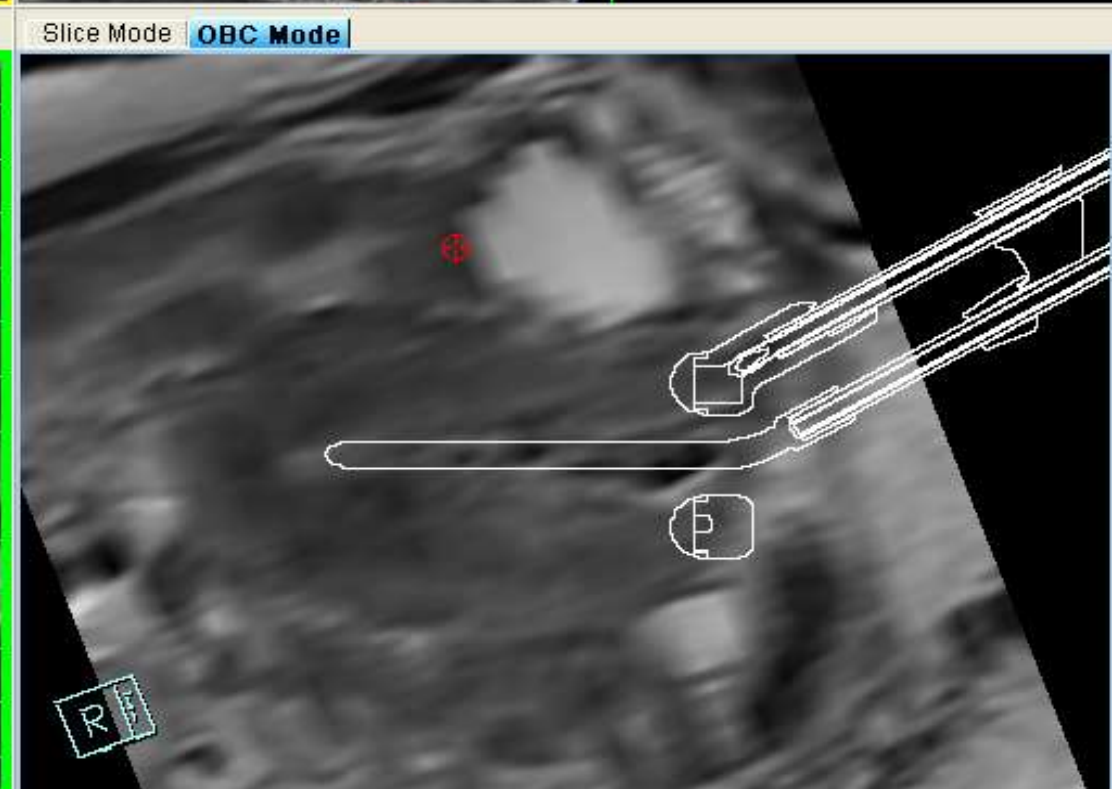
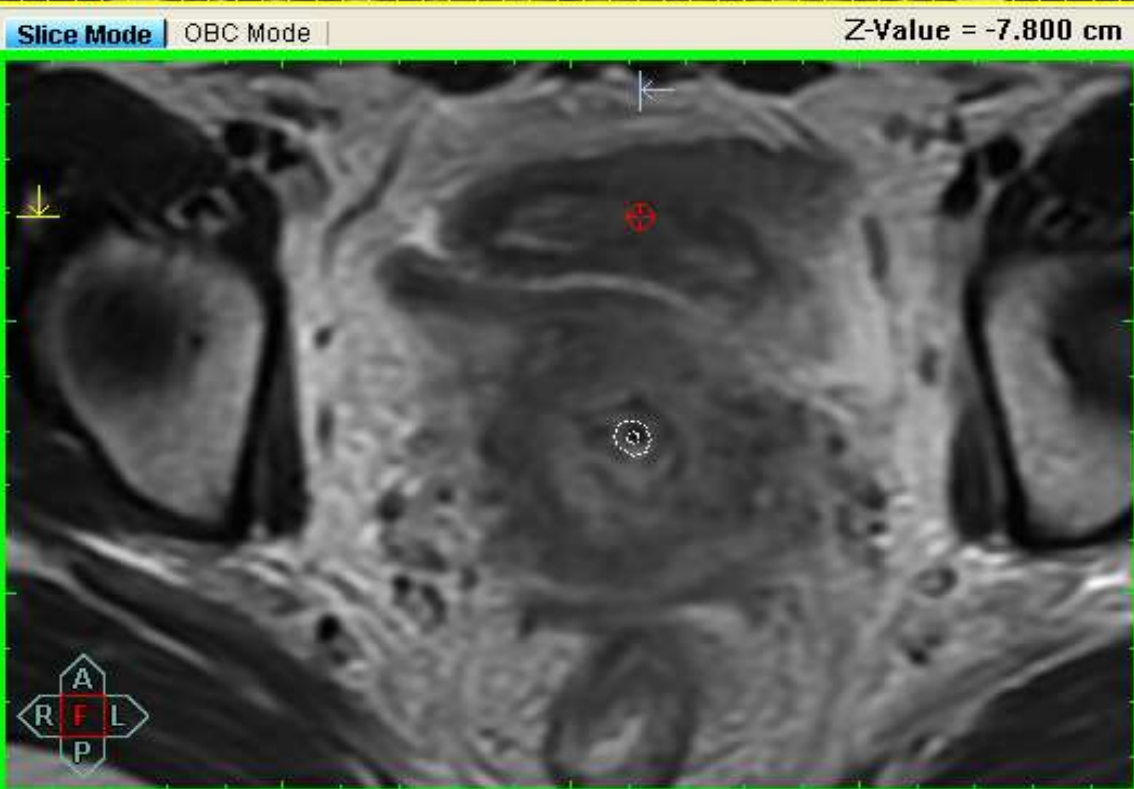
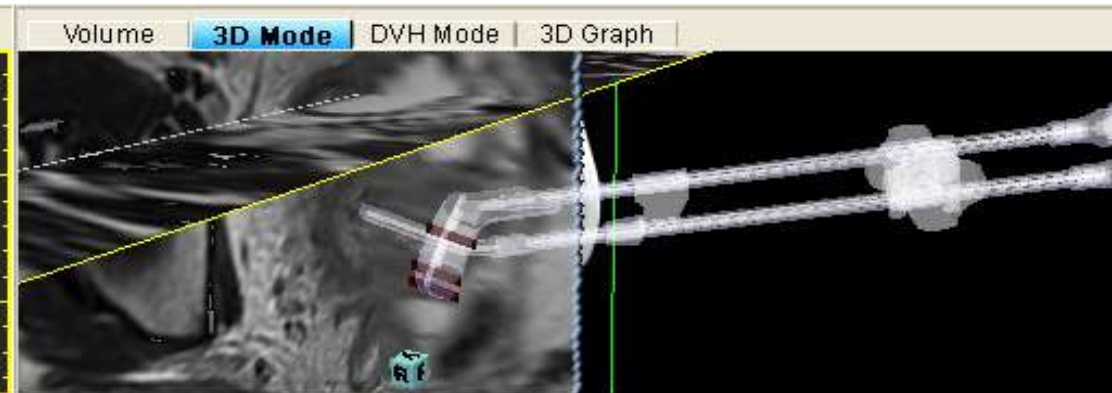
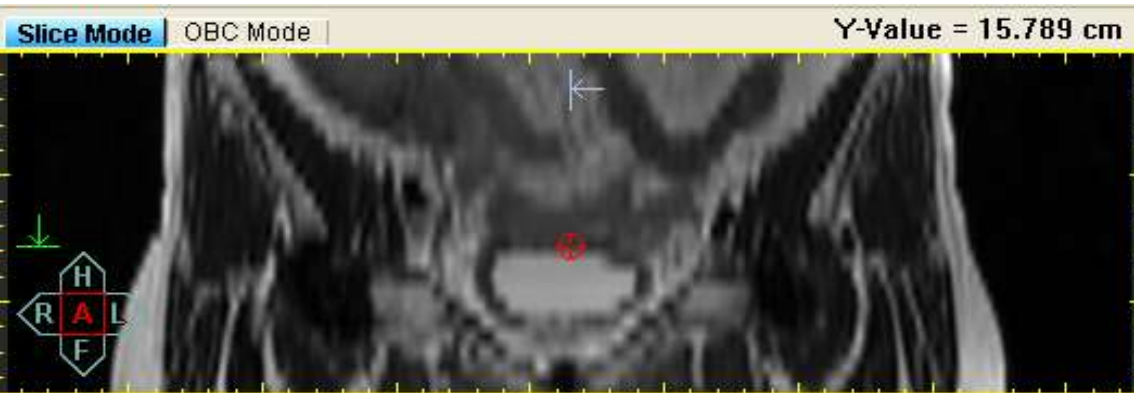


Registration based on bones is not enough

Pre-treatment MRI



Pre-treatment MRI

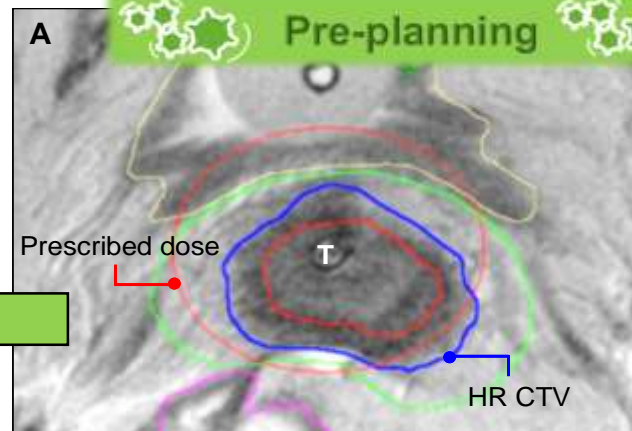
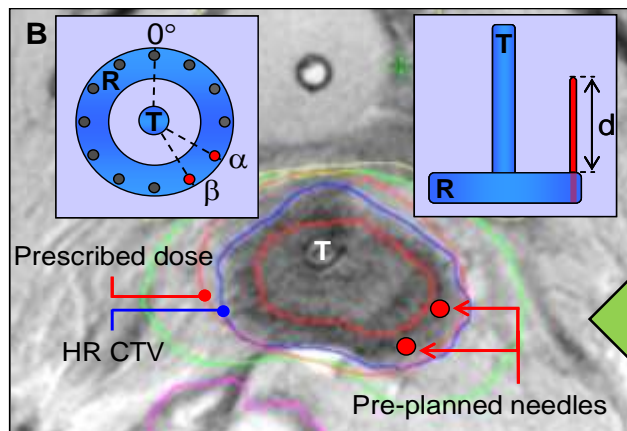


Gyn Pre-planning: Intracavitary / Interstitial Insertion

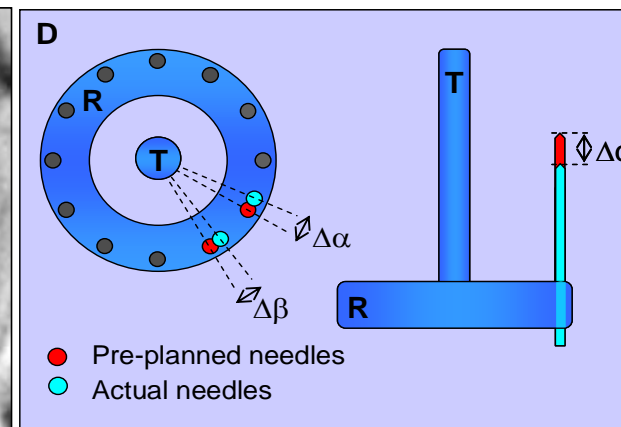
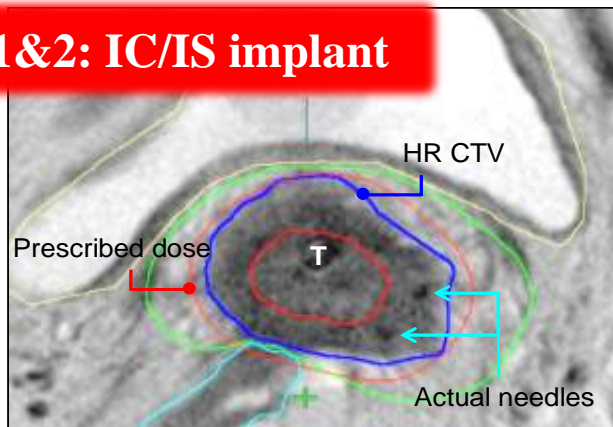
Based on pre-brachytherapy MRI: **With applicator in place**

Cervix cancer
N = 18 pts
IC/IS: 14 pts

Week5: BT 0
(paracervical block)



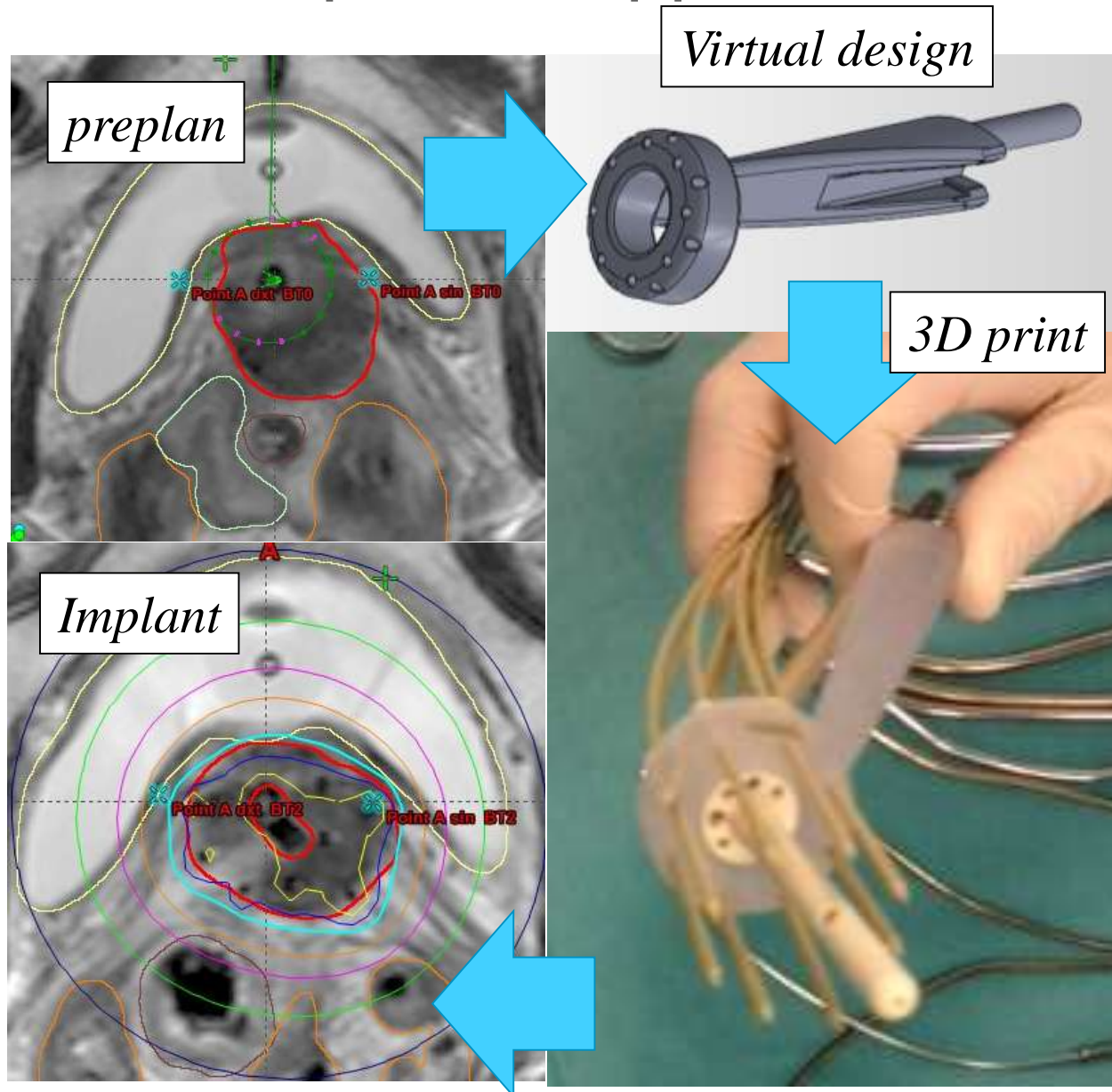
BT 1&2: IC/IS implant



A week later

Petric P, et al. Radiol Oncol 2014

3D printed applicators

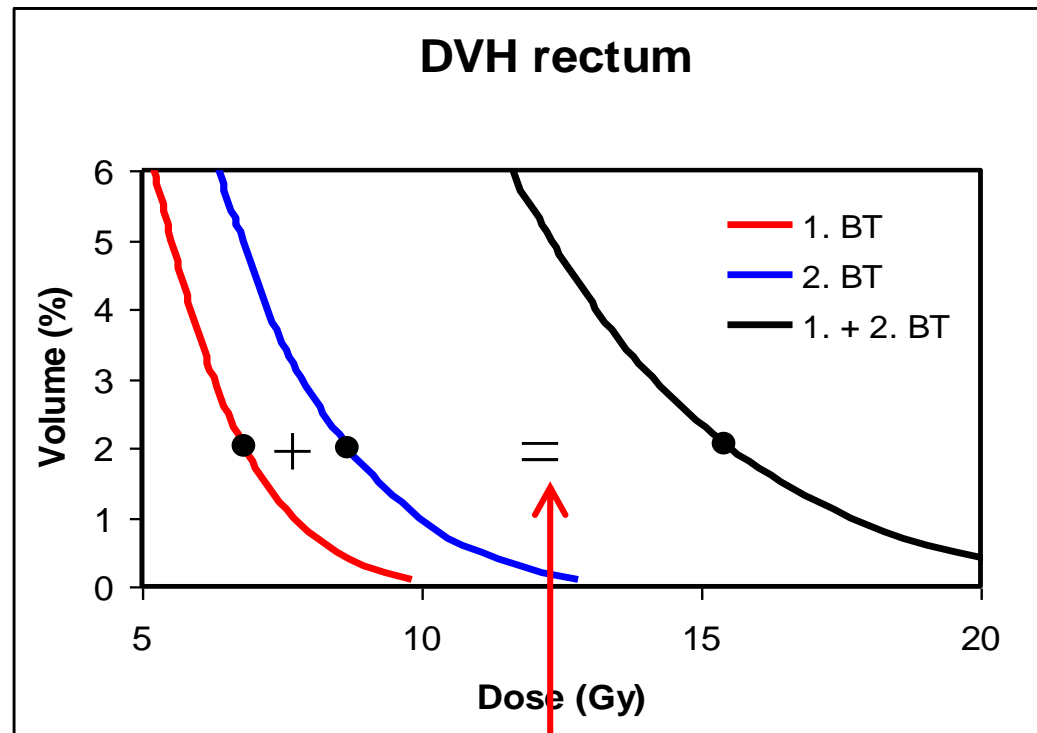


Courtesy – J. Lindegaard, Aarhus &
Lindegaard et al. Radiother Oncol 2016 in press

Deformable registration

- Problem: fusing images (from different modalities), taken at different times in the treatment (before, during, after BT)
 - I) Some organs move and change shape dramatically (sigmoid),
 - II) insertion of applicator changes topography, ...Approximation by rigid registration fails.
- Aim: to register each voxel correctly with the corresponding voxel in a different image set in order to **evaluate the received radiation dose**.
- Currently, especially for the pelvic region and breast it is theoretically not solved how tissue voxels can move, expand and shrink.

Calculation of DVH for several fractions

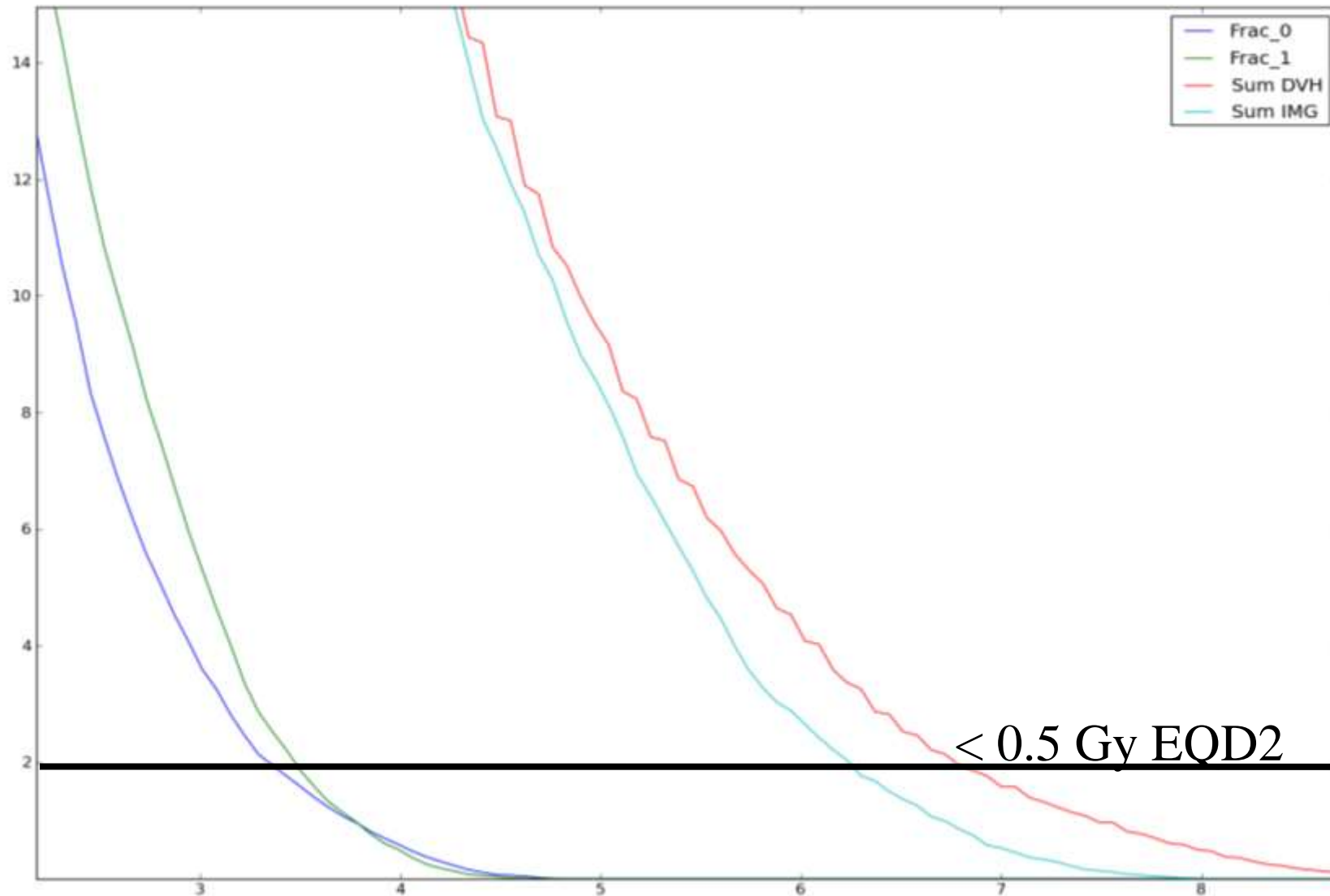


Approximation
Worst case assumption

Provided by K Tanderup

Rectum wall DVH in EQD2

2.5 cm longitudinal shift of whole organ

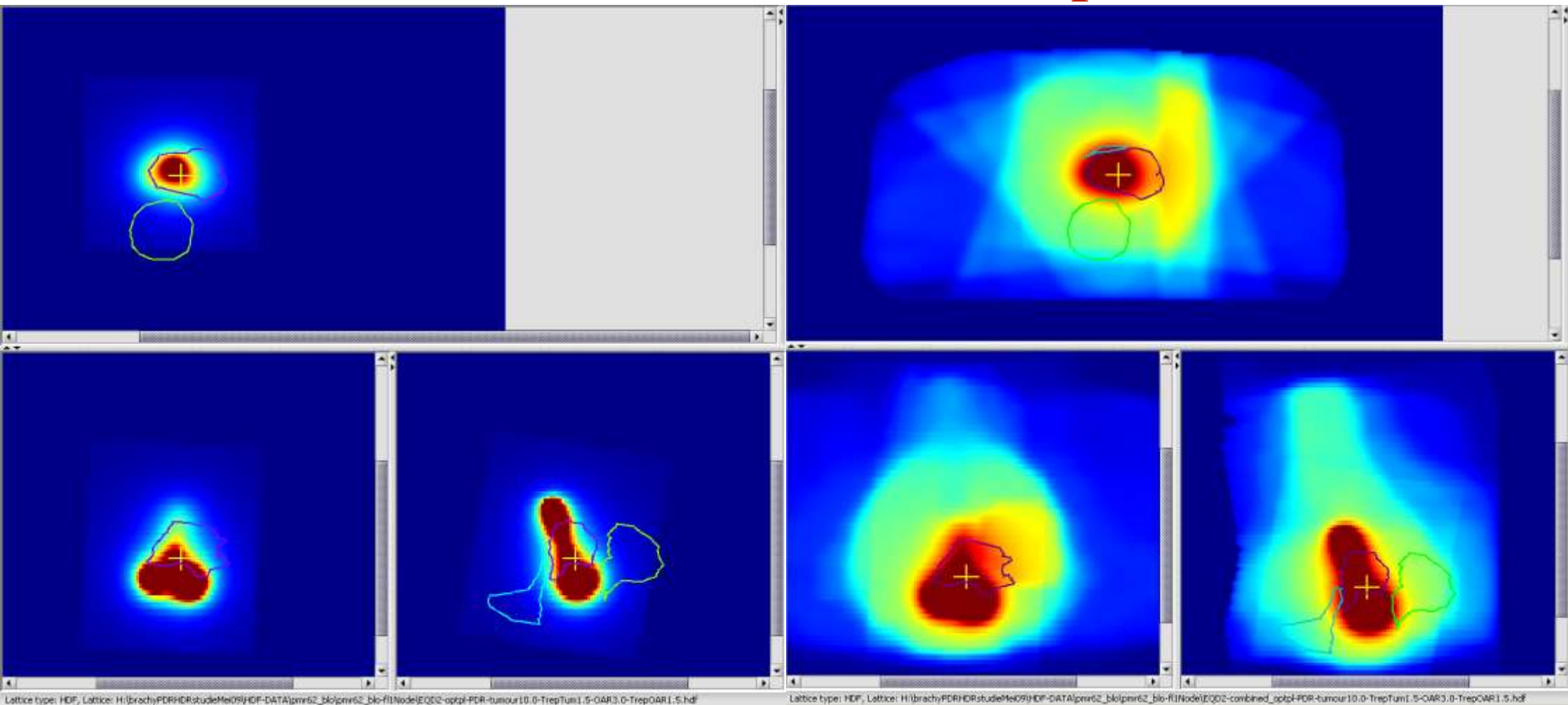


Combination of EBRT and BT

EB + Node Boost

2xF1 optimized PDR

2xF1 optimized PDR



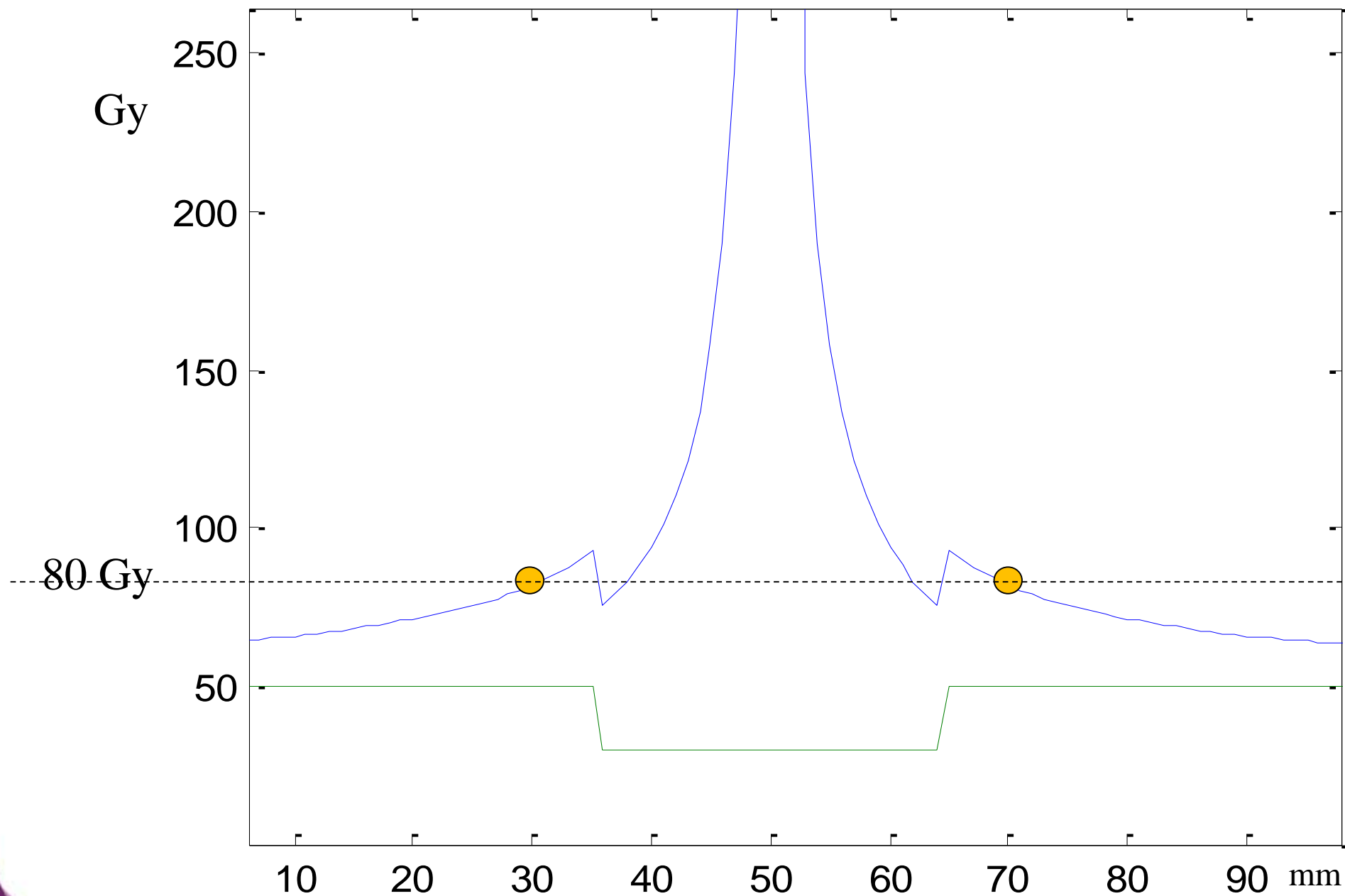
Differences between two methods 'adding 3D Distributions' versus 'adding Parameters'

	HR-CTV		Bladder		Rectum	
	without	with paraBoost	without	with paraBoost	without	with paraBoost
PDR						
avg	1.5%	9.1%	-0.5%	2.4%	-0.2%	0.8%
SD	1.7%	6.2%	1.0%	3.3%	0.6%	1.0%

Is adding parameters a valid approximation?

Yes, provided no EB boost!

3 cm shielding after 30 Gy AP/PA



Group 1 Patient

Group 2 Patient

D2cm³



BT1

BT2



D0.1cm³



BT1

BT2



Deviation when using deformable image registration to conventional DVH summation:

$$D_{2cc} \quad 0.4 \pm 0.3 \text{ Gy}_{\alpha\beta 3} \quad (1.5 \pm 1.8\%)$$

Else Stougård Andersen , Karsten Østergaard Noe , Thomas Sangild Sørensen , Søren Kynde Nielsen , Lars Fokdal , Mer...

Simple DVH parameter addition as compared to deformable registration for bladder dose accumulation in cervix cancer brachytherapy

Radiotherapy and Oncology, Volume 107, Issue 1, 2013, 52 - 57

More literature on deformable image registration for brachytherapy

Dose accumulation during vaginal cuff brachytherapy based on rigid/deformable registration vs. single plan addition.

Sabater S, Andres I, Sevillano M, Berenguer R, Machin-Hamalainen S, Arenas M. Brachytherapy. 2013

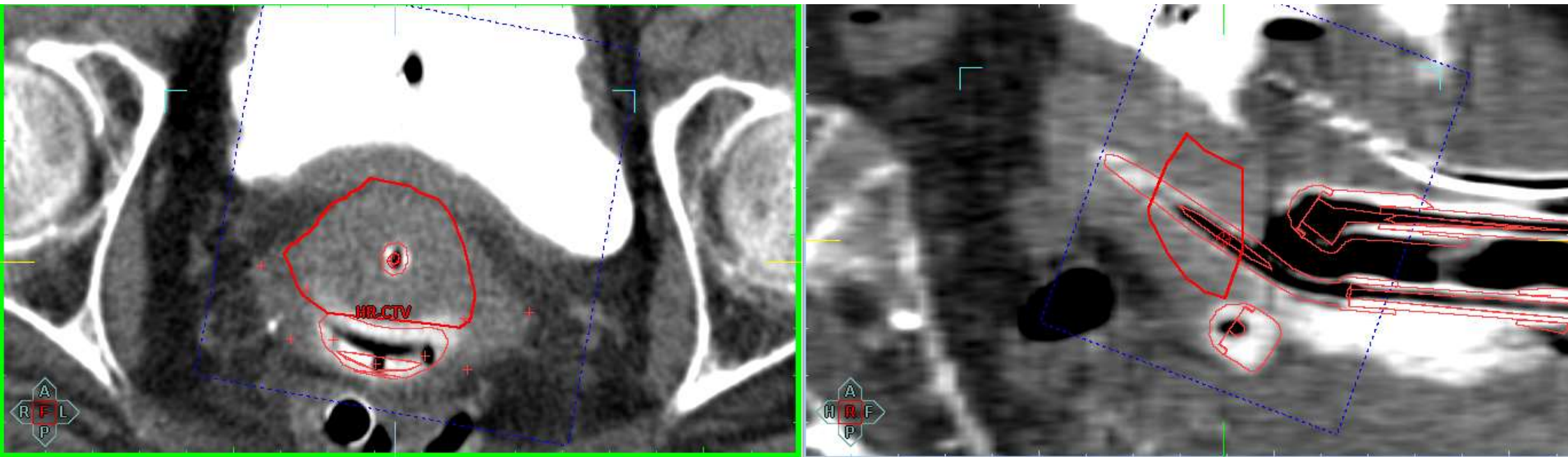
Deformable structure registration of bladder through surface mapping.

Xiong L, Viswanathan A, Stewart AJ, Haker S, Tempany CM, Chin LM, Cormack RA. Med Phys. 2006 Jun;33(6):1848-56.

Image-based dose planning of intracavitary brachytherapy: registration of serial-imaging studies using deformable anatomic templates.

Christensen GE, Carlson B, Chao KS, Yin P, Grigsby PW, Nguyen K, Dempsey JF, Lerma FA, Bae KT, Vannier MW, Williamson JF. Int J Radiat Oncol Biol Phys. 2001 Sep 1;51(1):227-43.

Automatic applicator based fusion and target volume transfer TRUS to CT



Schmid et al. 2016
Nesvacil et al. 2016

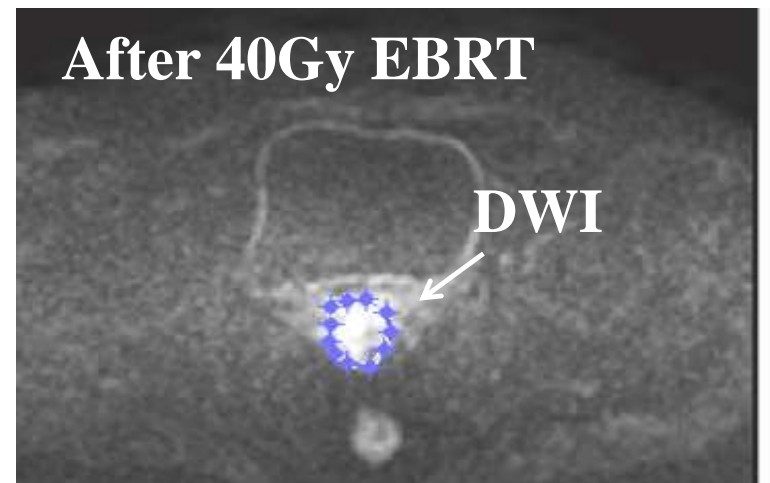
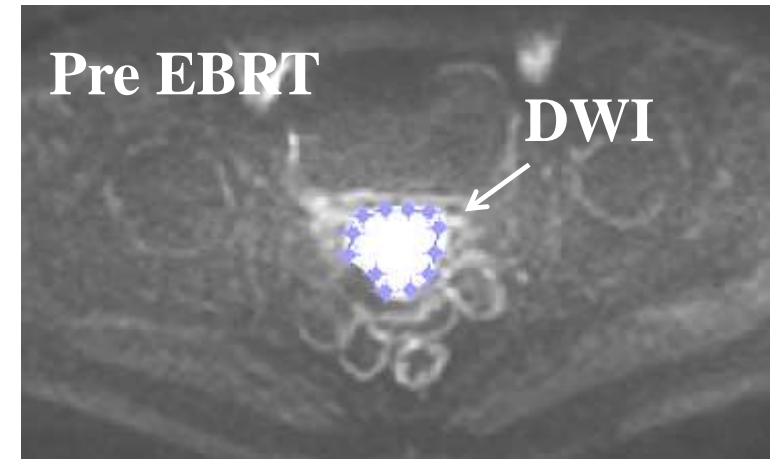
Further improvement with functional imaging?



Functional imaging

- Functional MRI
 - Dynamic contrast enhanced: DCE-MRI
 - Diffusion weighted: DWI
- Repeated tumour imaging during RT
 - Evaluation of response
 - Identification of tumour subvolumes
- Evaluation of residual DWI signal after 40-45Gy EBRT in 53 pts

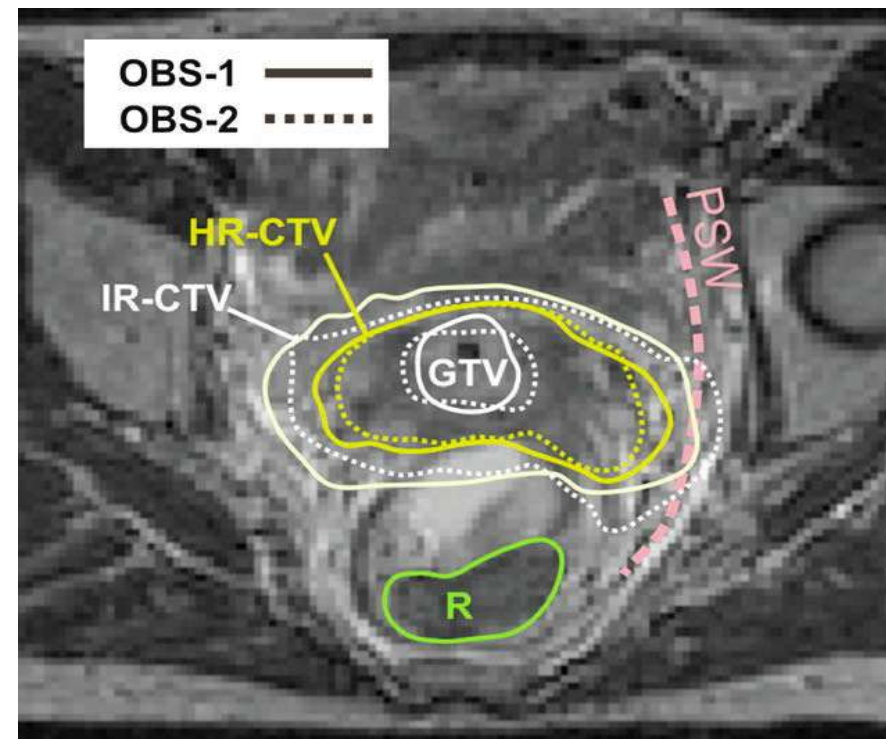
Persistent DWI (25 pts): 8 local failures
No residual DWI (28 pts): 1 local failure



Aarhus University Hospital
Søren Haack, 2012

Interobserver variation Target contouring on MRI

- Two observers
- HR-CTV variations:
 - Extend of vaginal and parametrial involvement
 - Cranial border
- IR-CTV variations:
 - Automargin and insufficient manual editing towards OARs
 - Caudal border

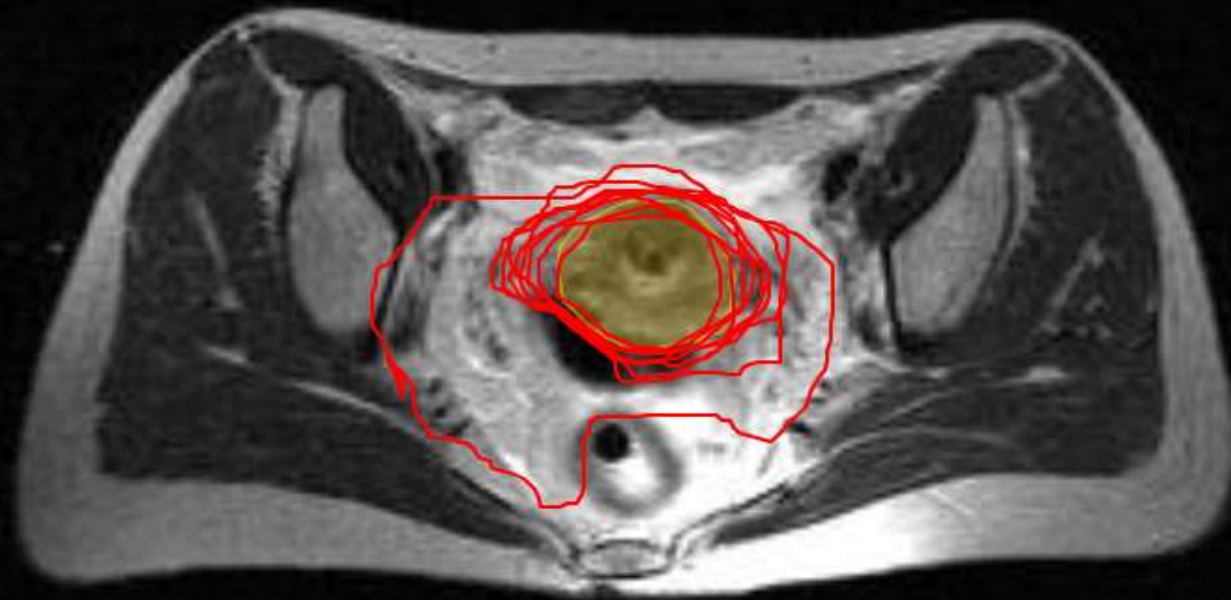


Dimopoulos et al, R&O 2009

Interobserver studies

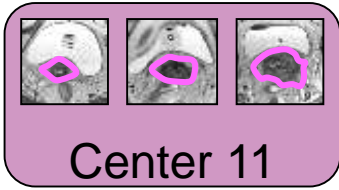
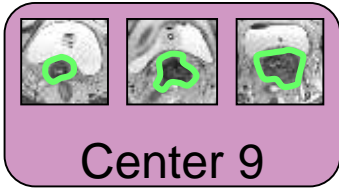
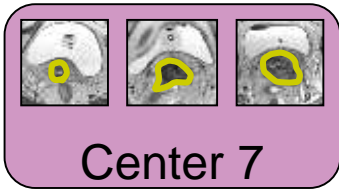
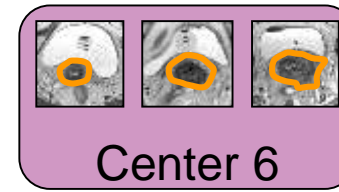
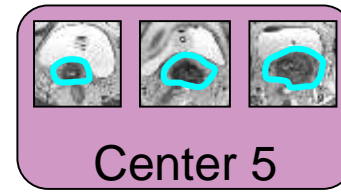
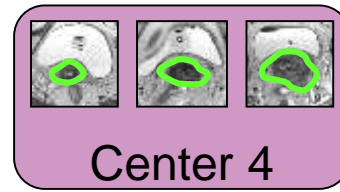
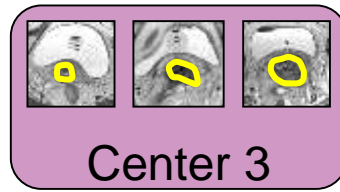
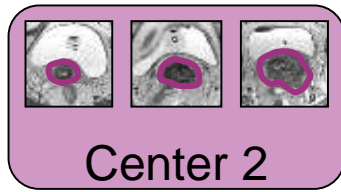
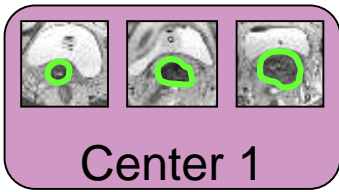
Brachy_pelvis/t2_tse_96_tr

ESTRO ARO Teaching Course
Chandigarh India, 03/2014
The workshops for contouring for all participants



cervix cancer with HRCTV for brachytherapy
random sample of 10 participants

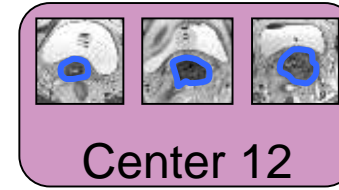
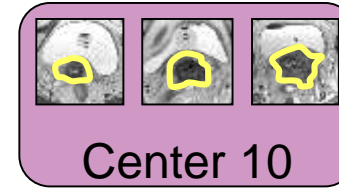
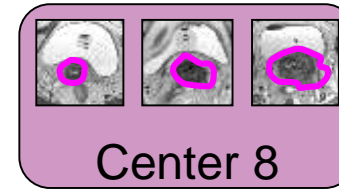
Multicentre study 2 Gyn GEC ESTRO: Interobserver study contouring



Small tumour **Large tumour, good response** **Large tumour, poor response**

EMBRACE ftp server

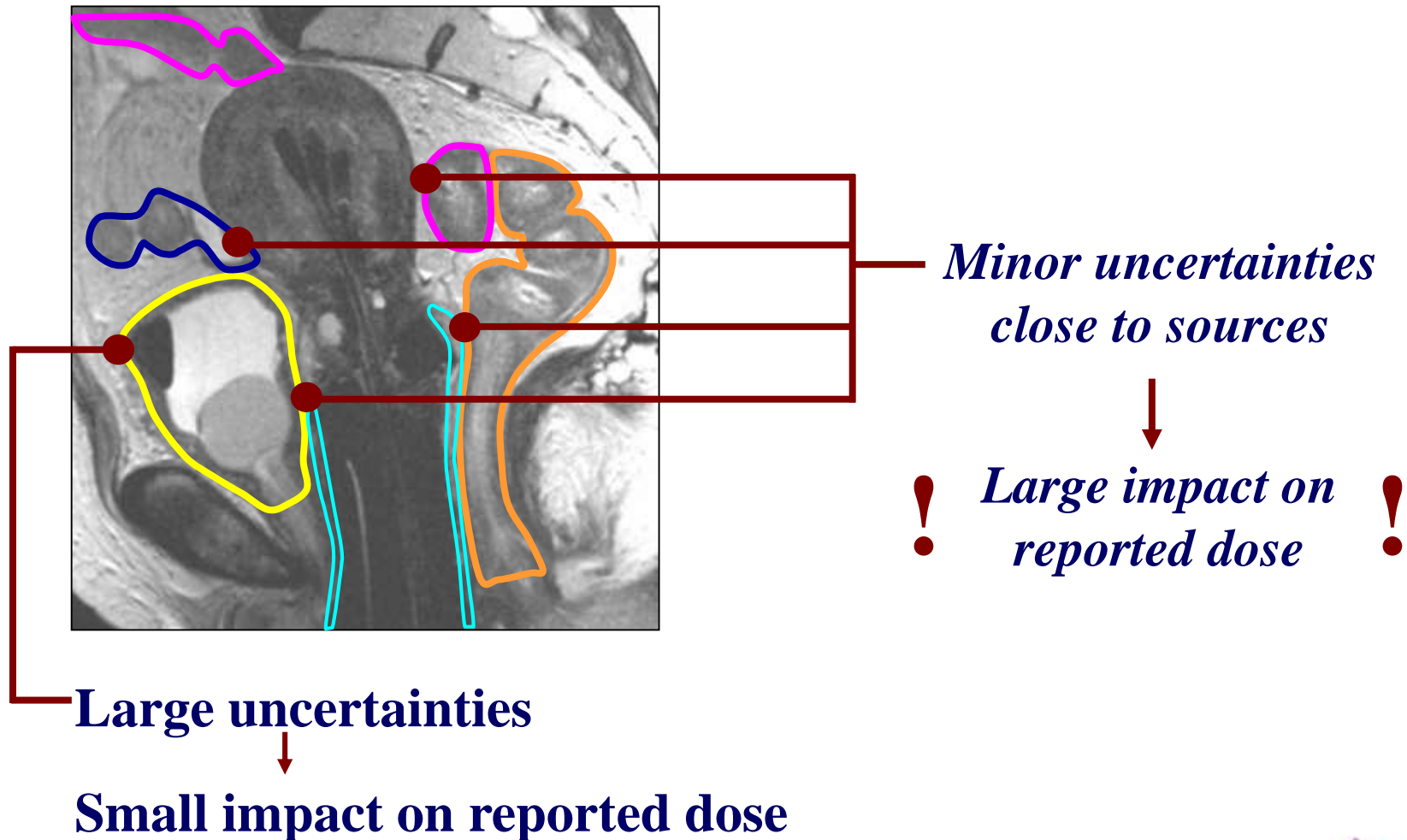
Collected structures data-set



Hellebust et al. 2013
Petric et al. 2013
April issue

Does it matter where we differ?

Yes, it does.



Courtesy of Primoz Petric

Conclusions

QA on imaging techniques

Uncertainties from

Contouring

Reconstruction

Fusion



ESTRO

School



UNIVERSITÉ
LAVAL



CENTRE DE RECHERCHE
SUR LE CANCER
UNIVERSITÉ
LAVAL

Tissue segmentation and characterization

Prof. Luc Beaulieu, Ph.D., FAAPM

*1- Département de physique, de génie physique et d'optique, et
Centre de recherche sur le cancer, Université Laval, Canada*

*2- Département de radio-oncologie et Centre de recherche du CHU
de Québec, CHU de Québec, Canada*

Vienna, May 29 – June 1 2016



Disclosures

- None for this section



Learning Objectives

- Provide an understanding of the challenges of tissue segmentation in brachytherapy
- Present and explain the TG-186 recommendations
- Look at DECT has the next step for tissue segmentation in radiation therapy.

Acknowledgements

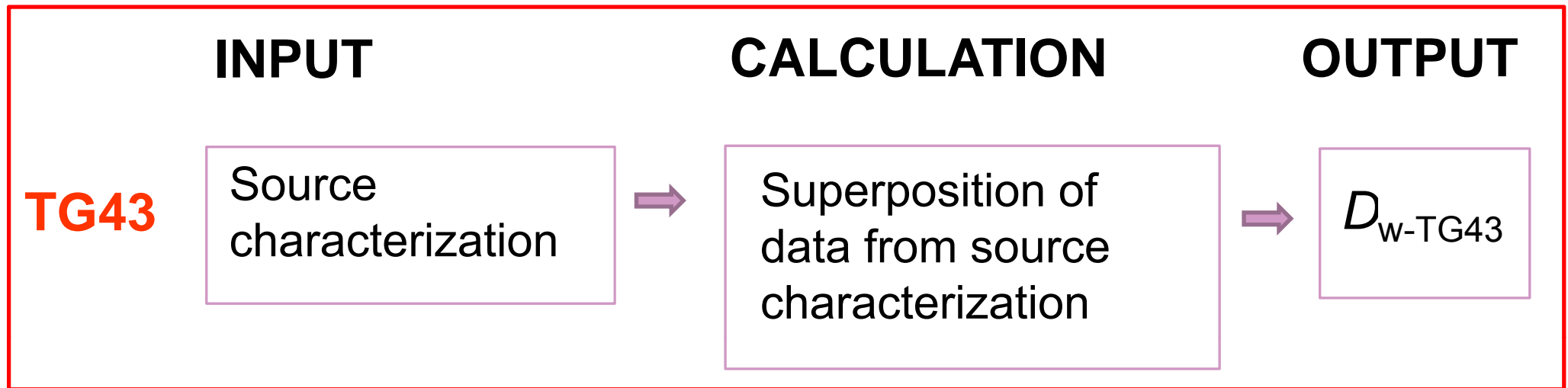
TG-186

- Luc Beaulieu (Chair)
- Å. Carlsson-Tedgren
- Jean-François Carrier
- Steve Davis
- Firas Mourtada
- Mark Rivard
- Rowan Thomson
- Frank Verhaegen
- Todd Wareing
- Jeff Williamson

AAPM/ESTRO/ABG WG

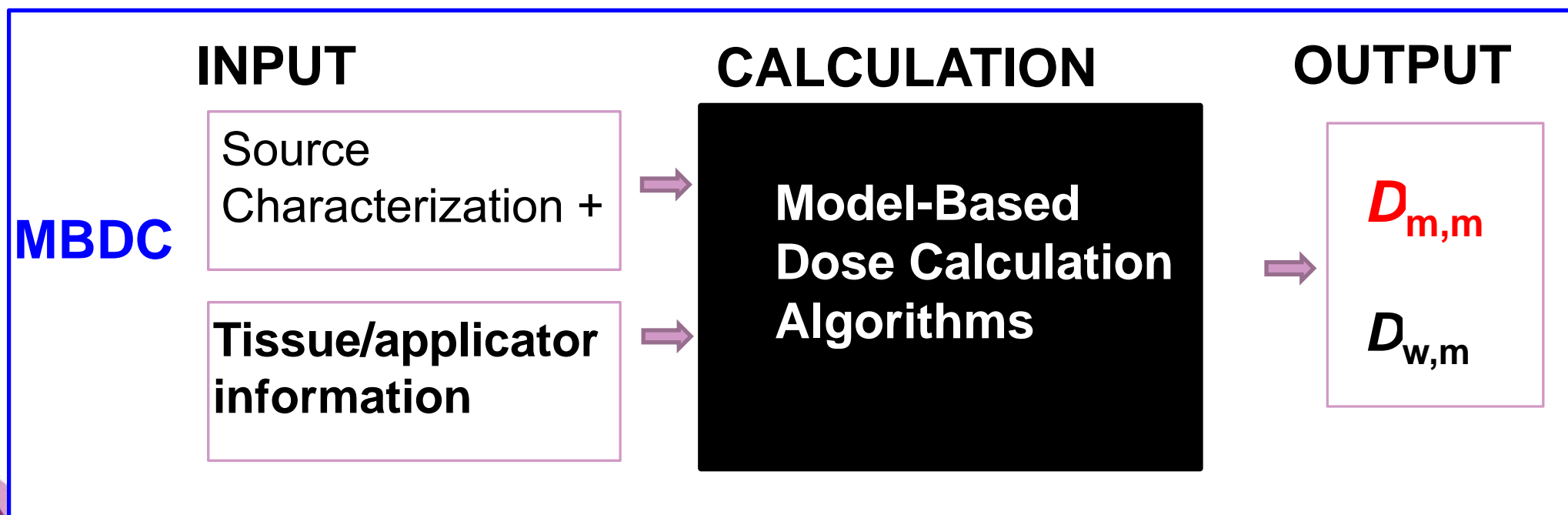
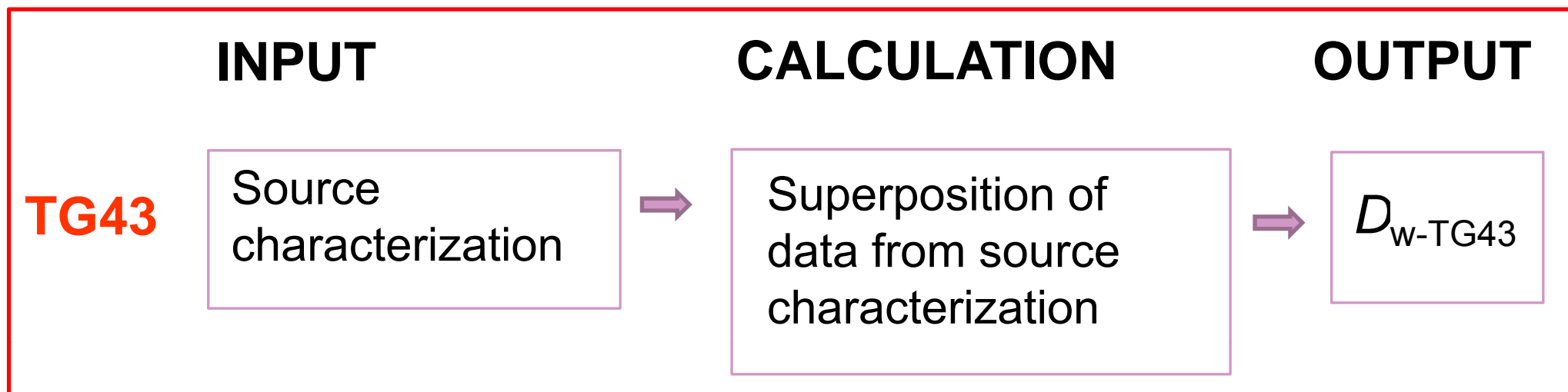
- Luc Beaulieu, CHUQ (Chair)
- Å. Carlsson Tedgren
- A. Haworth
- J. Lief
- Y. Ma
- F. Mourtada
- P. Papagianni
- M.J. Rivard
- F.A. Siebert (Vice-chair)
- R. Smith
- R. S. Sloboda
- R.M. Thomson
- J. Vijande
- F. Verhaegen

Factor-based TG43



There is no tissue segmentation, only organ contouring

Factor-based vs Model-based



Definition of the scoring medium

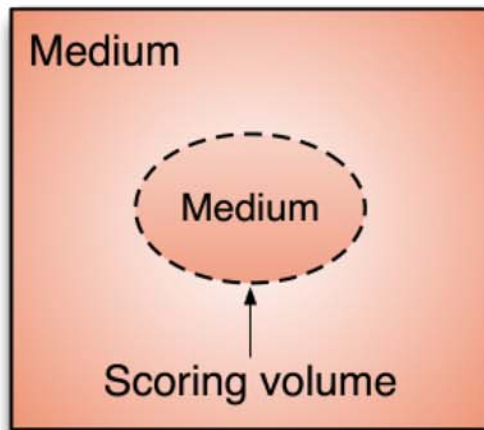
$D_{x,y}$

x : dose specification medium

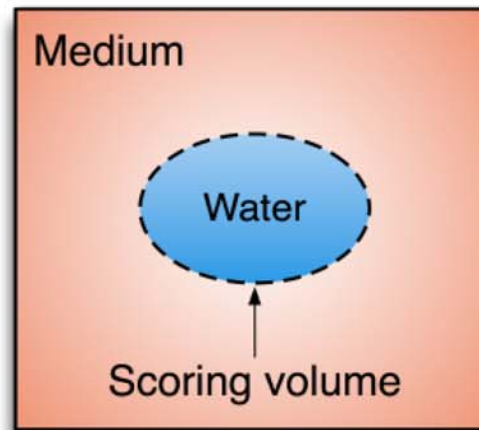
y : radiation transport medium

- x, y : Local medium (m) or water (w)

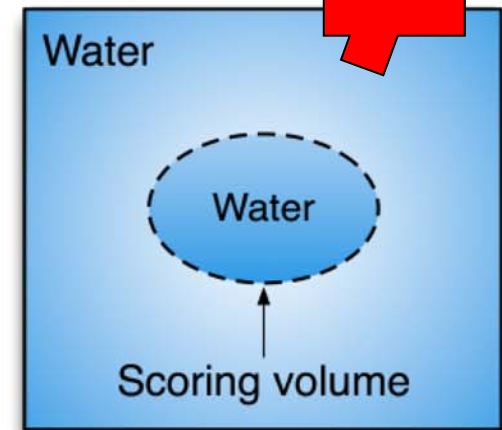
(a) $D_{m,m}$



(b) $D_{w,m}$



(c) $D_{w,w}$



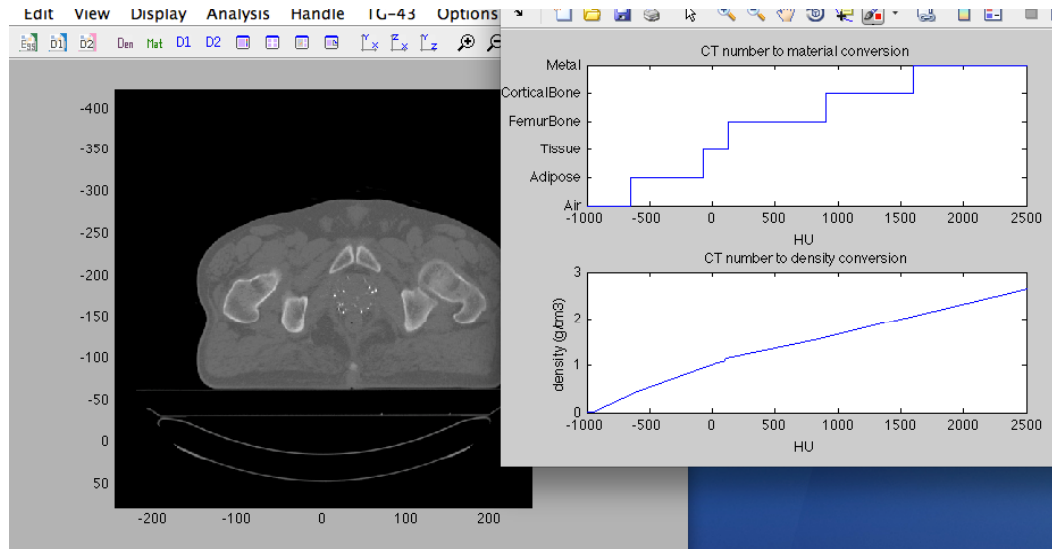
D_{TG43}

On-going Debate

“Results suggest that cells in cancerous and normal soft tissues are generally not radiologically equivalent to either water or the corresponding average bulk tissue”

Thomson, Carlsson, Williamson. PMB 58 (2013)

Procedure: tissue segmentation

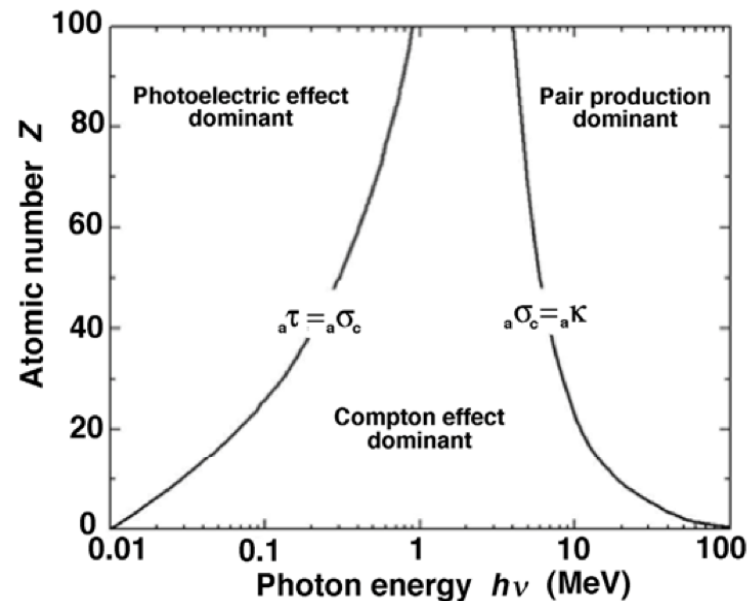


			$(\text{Density})_i,$ $(\text{Medium})_i$	

From F. Verhaegen

Cross section assignments (segmentation)

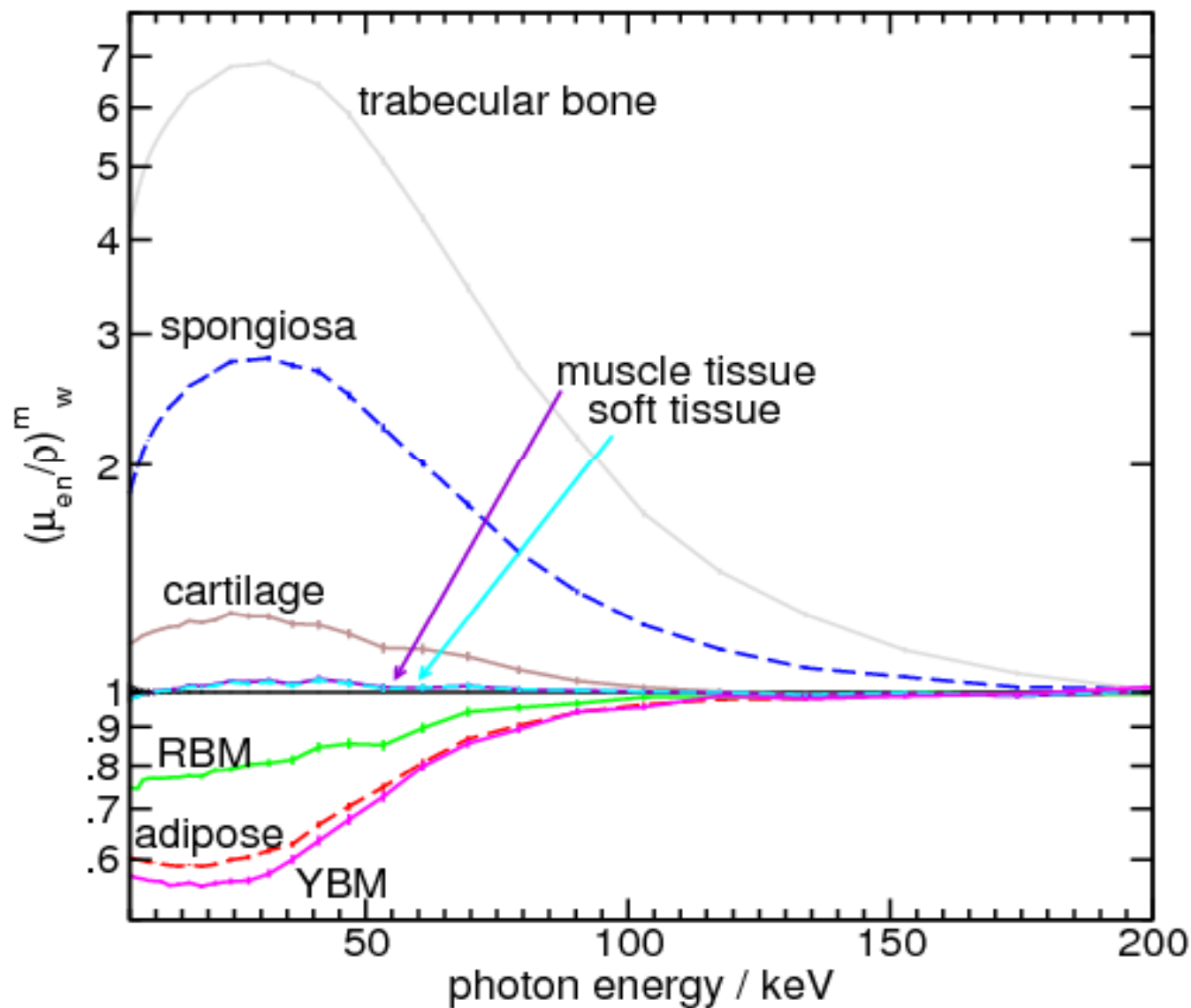
- MDBCA requires assignment of interaction cross section on a voxel-by-voxel basis
- In EBRT one only needs electron densities ρ_e (e^-/cm^3) from CT scan
- In BT (energy range 10-400 keV) the interaction probabilities depend not only on ρ_e but also strongly on atomic number Z



Cross section assignments

- Accurate tissue segmentation, sources and applicators needed: identification (ρ_e, Z_{eff})
 - e.g. in breast: adipose and glandular tissue have significantly different (ρ_e, Z_{eff}); dose will be different
- If this step is not accurate → incorrect dose
 - Influences dosimetry and dose outcome studies
 - Influences dose to organs at risk

Large Cavity Theory Cross Section



TG-186

TG-186 recommendations

- Consensus material definition
- Material assignment method
- CT/CBCT artifact removal

Recommendations

- Extract electron density from CT calibration (see TG53, TG66 ...)
 - Use the density from CT for each voxel
 - Use recommended tissue compositions
 - Organ-based (contoured) assignments
 - Prostate from Woodard et al, BJR 59 (1986) 1209-18
 - All others from ICRU-46 composition
 - From CT calibration: breast, adipose, muscle and bone

TABLE III. Material definitions. Water is given for comparison.

Tissue	% mass					Z > 8	Mass density g cm ⁻³
	H	C	N	O			
Prostate (Ref. 110)	10.5	8.9	2.5	77.4		Na(0.2), P(0.1), S(0.2), K(0.2)	1.04
Mean adipose (Ref. 110)	11.4	59.8	0.7	27.8		Na(0.1), S(0.1), Cl(0.1)	0.95
Mean gland (Ref. 110)	10.6	33.2	3.0	52.7		Na(0.1), P(0.1), S(0.2), Cl(0.1)	1.02
Mean male soft tissue (Ref. 109)	10.5	25.6	2.7	60.2		Na(0.1), P(0.2), S(0.3), Cl(0.2), K(0.2)	1.03
Mean female soft tissue (Ref. 109)	10.6	31.5	2.4	54.7		Na(0.1), P(0.2), S(0.2), Cl(0.1), K(0.2)	1.02
Mean skin (Ref. 109)	10.0	20.4	4.2	64.5		Na(0.2), P(0.1), S(0.2), Cl(0.3), K(0.1)	1.09
Cortical bone (Ref. 109)	3.4	15.5	4.2	43.5		Na (0.1), Mg (0.2), P (10.3), S (0.3), Ca(22.5)	1.92
Eye lens (Ref. 109)	9.6	19.5	5.7	64.6		Na(0.1), P(0.1), S(0.3), Cl(0.1)	1.07
Lung (inflated) (Ref. 109)	10.3	10.5	3.1	74.9		Na(0.2), P(0.2), S(0.3), Cl(0.3), K(0.2)	0.26
Liver (Ref. 109)	10.2	13.9	3.0	71.6		Na(0.2), P(0.3), S(0.3), Cl(0.2), K(0.3)	1.06
Heart (Ref. 109)	10.4	13.9	2.9	71.8		Na(0.1), P(0.2), S(0.2), Cl(0.2), K(0.3)	1.05
Water	11.2			88.8			1.00

Consequences: Uncertainties associated with this process?

- Limited measurements
 - e.g. 1930s' data of prostate from a specimen of 14 year old boy ¹
- Considerable tissue composition variability
 - e.g. Adipose tissue water content between 23% to 78%²
- Patient-specific distribution of tissue types
 - e.g. Breast adipose vs glandular composition: 16% to 68%^{3,4}

1) A. H. Neufeld, Canadian Journal of Research 15B, 132-138 (1937).

2) B. Brooksby, B. W. et al., PNAS 103 (23), 8828-8833 (2006).

3) R. A. Geise and A. Palchevsky, Radiology 198 (2), 347-50 (1996)

4) The Myth of the 50-50 breast, MJ Yaffe et al., Med Phys 36 (2009)

Consequences: Uncertainties associated with this process?

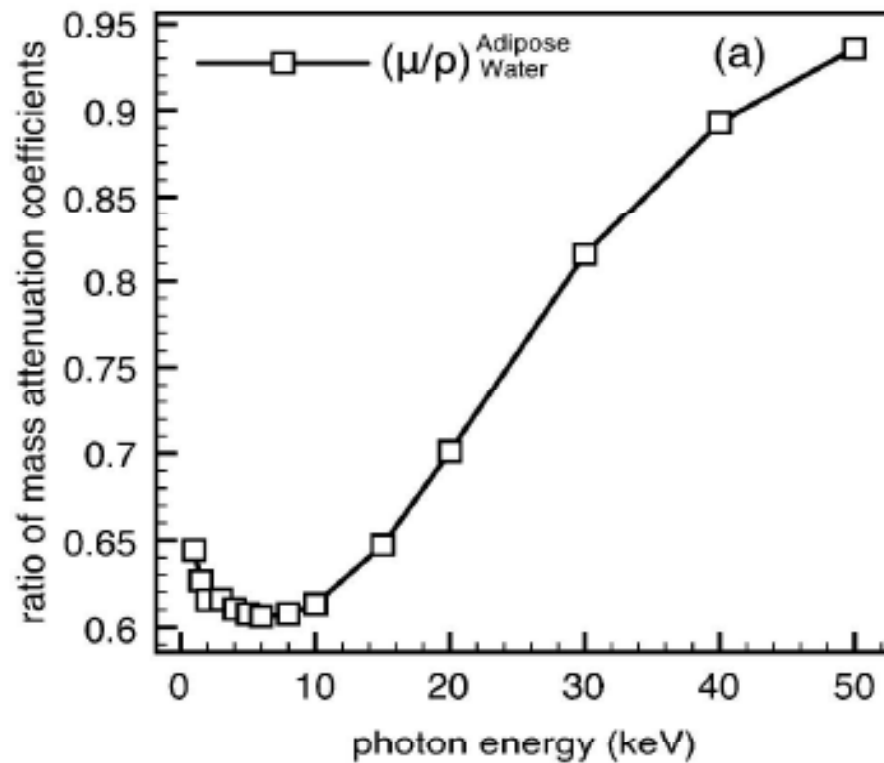
- Human tissues vary from one individual to the other
- Reports (like ICRP 23 or ICRU 44) provides average compositions

(Woodard & White)

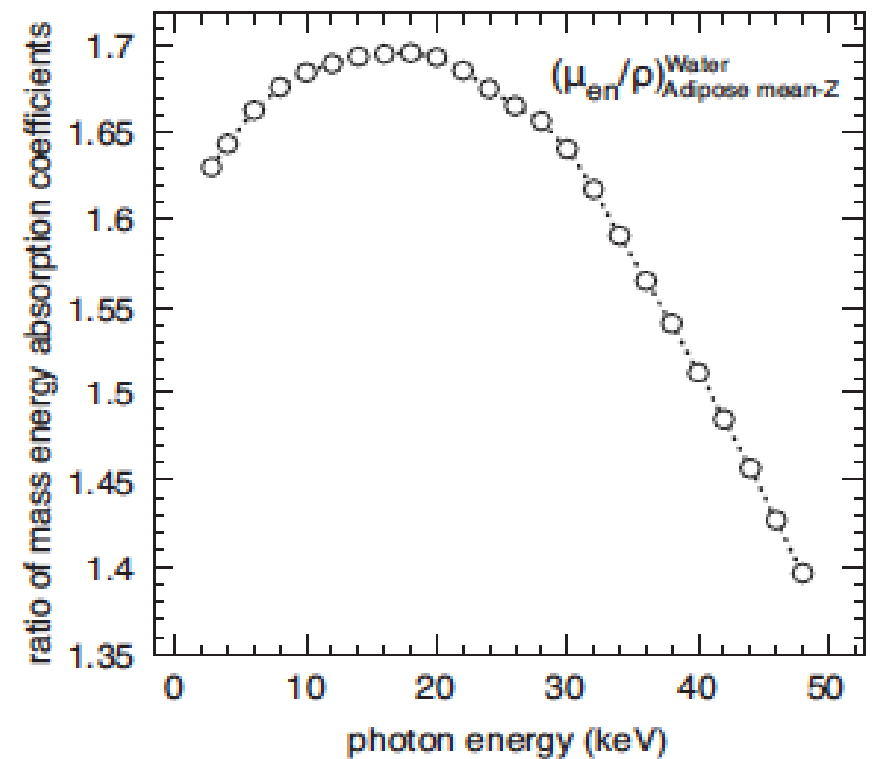
Body tissue	Elemental composition (% by mass)					Densities		
	H	C	N	O	Elements with $Z > 8$	Mass	Electron	
						kg m^{-3}	$\text{el. kg}^{-1} \times 10^{26}$	$\text{el. m}^{-3} \times 10^{26}$
Adipose tissue 1	11.2	51.7	1.3	35.5	Na(0.1), S(0.1), Cl(0.1)	970	3.342	3241
Adipose tissue 2	11.4	59.8	0.7	27.8	Na(0.1), S(0.1), Cl(0.1)	950	3.347	3180
Adipose tissue 3	11.6	68.1	0.2	19.8	Na(0.1), S(0.1), Cl(0.1)	930	3.353	3118

Cross sections

Attenuation



$D_{W,M} / D_{M,M}$



Sensitivity Analysis

TABLE VI. Variations of breast PTV D_{90} with various compositions compared to D_{TG-43} .

Dose calculation method	Mean ΔD_{90} (%)	Absolute uncertainty on ΔD_{90} (%)
MC_{$\rho=1$}		
A30/G70 hi-Z	12.6	0.9
A30/G70 mean-Z	22.1	1.4
A50/G50 mean-Z	26.3	1.8
A70/G30 mean-Z	30.4	2.3
A70/G30 lo-Z	39.8	3.2
MC_{$\rho=CT$}		
Water (ρ_{CT})	3.9	1.5
A30/G70 hi-Z	16.3	1.7
A30/G70 mean-Z	25.8	2.0
A50/G50 mean-Z	29.8	2.6
A70/G30 mean-Z	34.1	2.6
A70/G30 lo-Z	42.9	3.1

Sensitivity Analysis

TABLE VI. Variations of breast PTV D_{90} with various compositions compared to D_{TG-43} .

Dose calculation method	Mean ΔD_{90} (%)	Absolute uncertainty on ΔD_{90} (%)
MC_{$\rho=1$}		
A30/G70 hi-Z	12.6	0.9
A30/G70 mean-Z	22.1	1.4
A50/G50 mean-Z	26.3	1.8
A70/G30 mean-Z	30.4	2.3
A70/G30 lo-Z	39.8	3.2
MC_{$\rho=CT$}		
Water (ρ_{CT})	3.9	1.5
A30/G70 hi-Z	16.3	1.7
A30/G70 mean-Z	25.8	2.0
A50/G50 mean-Z	29.8	2.6
A70/G30 mean-Z	34.1	2.6
A70/G30 lo-Z	42.9	3.1

26% {

Sensitivity Analysis

TABLE VI. Variations of breast PTV D_{90} with various compositions compared to D_{TG-43} .

Dose calculation method	Mean ΔD_{90} (%)	Absolute uncertainty on ΔD_{90} (%)
MC_{$\rho=1$}		
A30/G70 hi-Z	12.6	0.9
A30/G70 mean-Z	22.1	1.4
A50/G50 mean-Z	26.3	1.8
A70/G30 mean-Z	30.4	2.3
A70/G30 lo-Z	39.8	3.2
MC_{$\rho=CT$}		
Water (ρ_{CT})	3.9	1.5
A30/G70 hi-Z	16.3	1.7
A30/G70 mean-Z	25.8	2.0
A50/G50 mean-Z	29.8	2.6
A70/G30 mean-Z	34.1	2.6
A70/G30 lo-Z	42.9	3.1

9%

{

Sensitivity Analysis

“If A80/G20 breast is representative of the average breast cancer patient then our A70/G30 breast results indicate that the compositional uncertainty and the use of breast density from CT data translate into **second order effects** [$\approx \pm 10\%$] compared to effect of going from water to average breast tissue [$\approx 30\%$]”

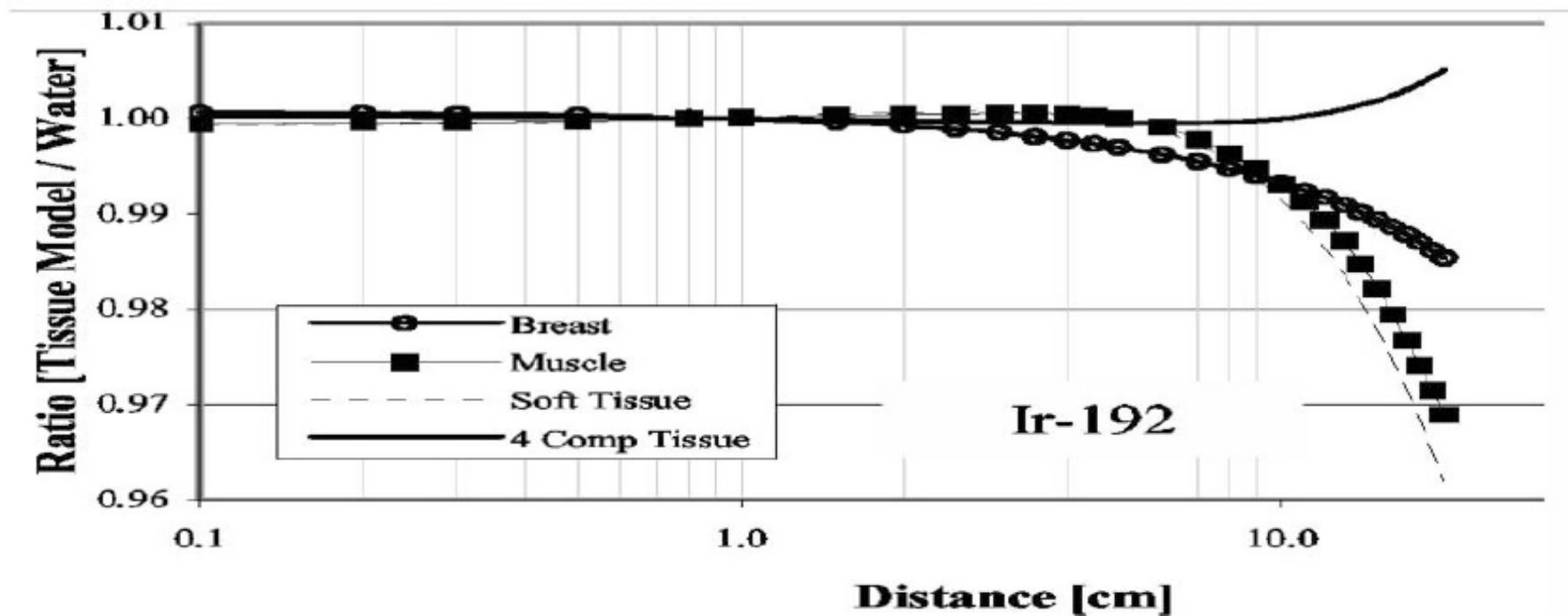
Sensitivity Study: Prostate

- About 3% D90 difference from TG-43
 - Two compositions found in literature disagree...
...**By 3%**
 - Effect of inter-seed attenuation on average also 3-4%

Carrier et al, IJROBP 2007; G. Landry *et al.* Med. Phys. 38 (2011)

Sensitivity Study: ^{192}Ir

- Water vs soft-tissus: almost little effect!



Melhus et al, Med Phys 33 (2006).

From clinical cases: Mikell et al., IJROBP 83 (2012); Desbiens et al, Radiother. Oncol (2013); FA Siebert et al., Brachytherapy 5 (2013)

Recommendations

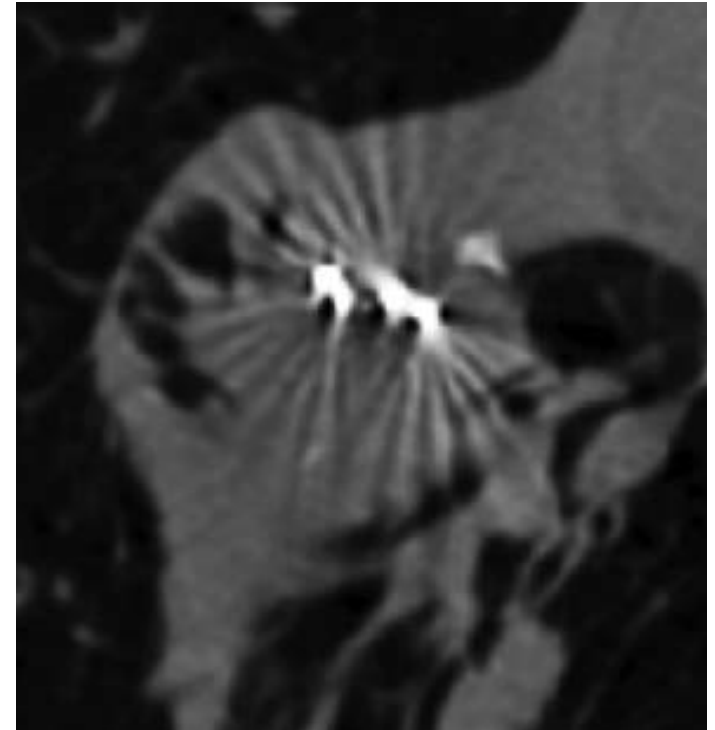
- If artifacts (e.g. from metals)
 - Override the density using the recommended default organ/tissue density
 - Assign tissue composition based on organ contours

TABLE III. Material definitions. Water is given for comparison.

Tissue	% mass					Z > 8	Mass density g cm ⁻³
	H	C	N	O			
Prostate (Ref. 110)	10.5	8.9	2.5	77.4		Na(0.2), P(0.1), S(0.2), K(0.2)	1.04
Mean adipose (Ref. 110)	11.4	59.8	0.7	27.8		Na(0.1), S(0.1), Cl(0.1)	0.95
Mean gland (Ref. 110)	10.6	33.2	3.0	52.7		Na(0.1), P(0.1), S(0.2), Cl(0.1)	1.02
Mean male soft tissue (Ref. 109)	10.5	25.6	2.7	60.2		Na(0.1), P(0.2), S(0.3), Cl(0.2), K(0.2)	1.03
Mean female soft tissue (Ref. 109)	10.6	31.5	2.4	54.7		Na(0.1), P(0.2), S(0.2), Cl(0.1), K(0.2)	1.02
Mean skin (Ref. 109)	10.0	20.4	4.2	64.5		Na(0.2), P(0.1), S(0.2), Cl(0.3), K(0.1)	1.09
Cortical bone (Ref. 109)	3.4	15.5	4.2	43.5		Na (0.1), Mg (0.2), P (10.3), S (0.3), Ca(22.5)	1.92
Eye lens (Ref. 109)	9.6	19.5	5.7	64.6		Na(0.1), P(0.1), S(0.3), Cl(0.1)	1.07
Lung (inflated) (Ref. 109)	10.3	10.5	3.1	74.9		Na(0.2), P(0.2), S(0.3), Cl(0.3), K(0.2)	0.26
Liver (Ref. 109)	10.2	13.9	3.0	71.6		Na(0.2), P(0.3), S(0.3), Cl(0.2), K(0.3)	1.06
Heart (Ref. 109)	10.4	13.9	2.9	71.8		Na(0.1), P(0.2), S(0.2), Cl(0.2), K(0.3)	1.05
Water	11.2			88.8			1.00

Recommendations

- If relevant, artifacts must be removed prior to dose calculations
- Manual override of tissue composition and density is the simplest approach.
- Advanced approaches: if used, must be carefully documented



Sutherland et al, Med. Phys. **38**,
4365 (2012)

Recommendations

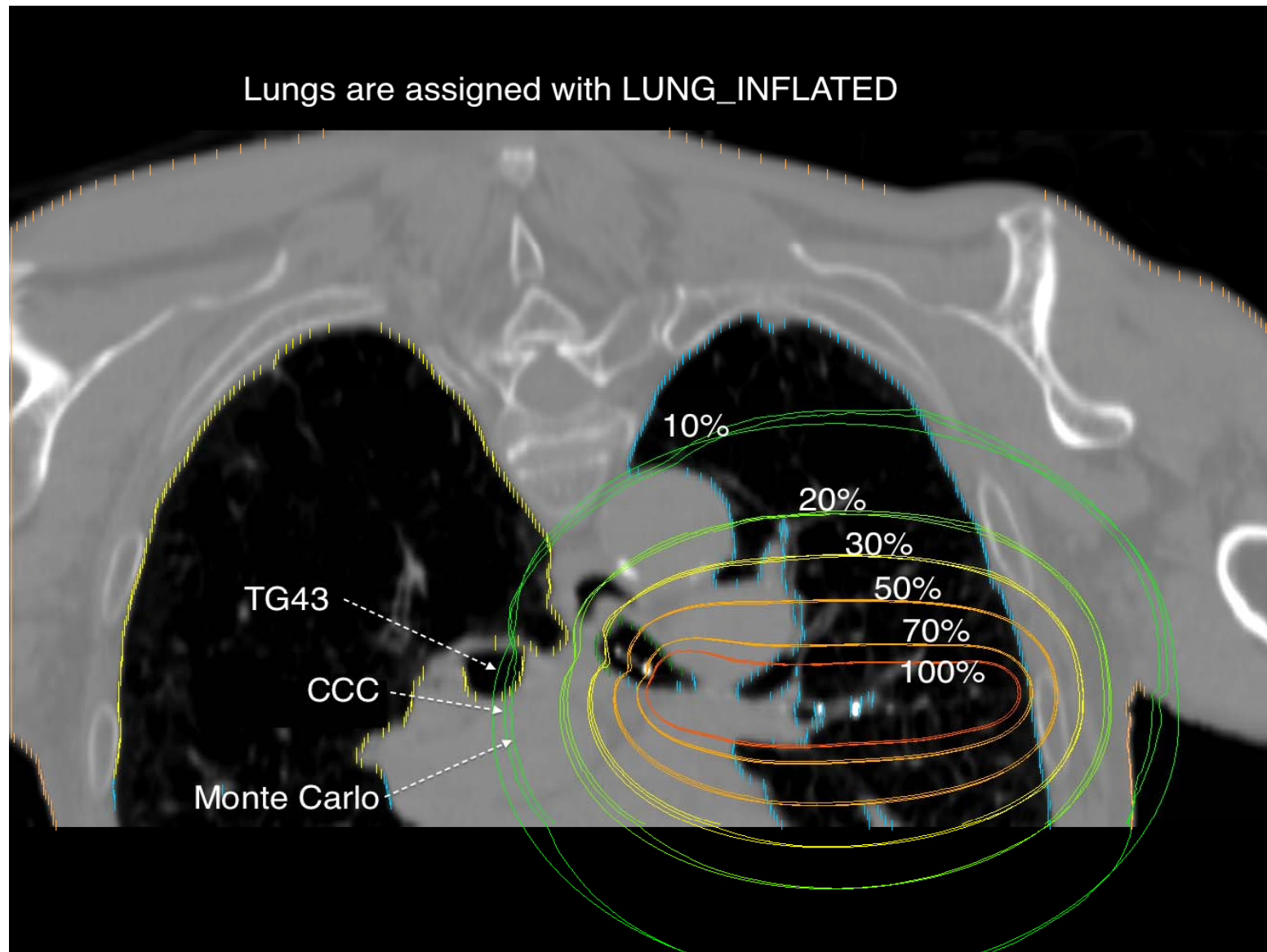
- If no CT (US and MRI)
 - Use contoured organs with recommended tissue compositions
 - For ^{192}Ir , water is a good approximation for soft tissues only.
 - Air, lung, bone, ... should be assigned correctly
 - Could potentially be generated on MRI (Yu et al., IJROBP, In press; DOI: 10.1016/j.ijrobp.2014.03.028)
 - Use accurate source and applicators geometry and composition

Recommendations

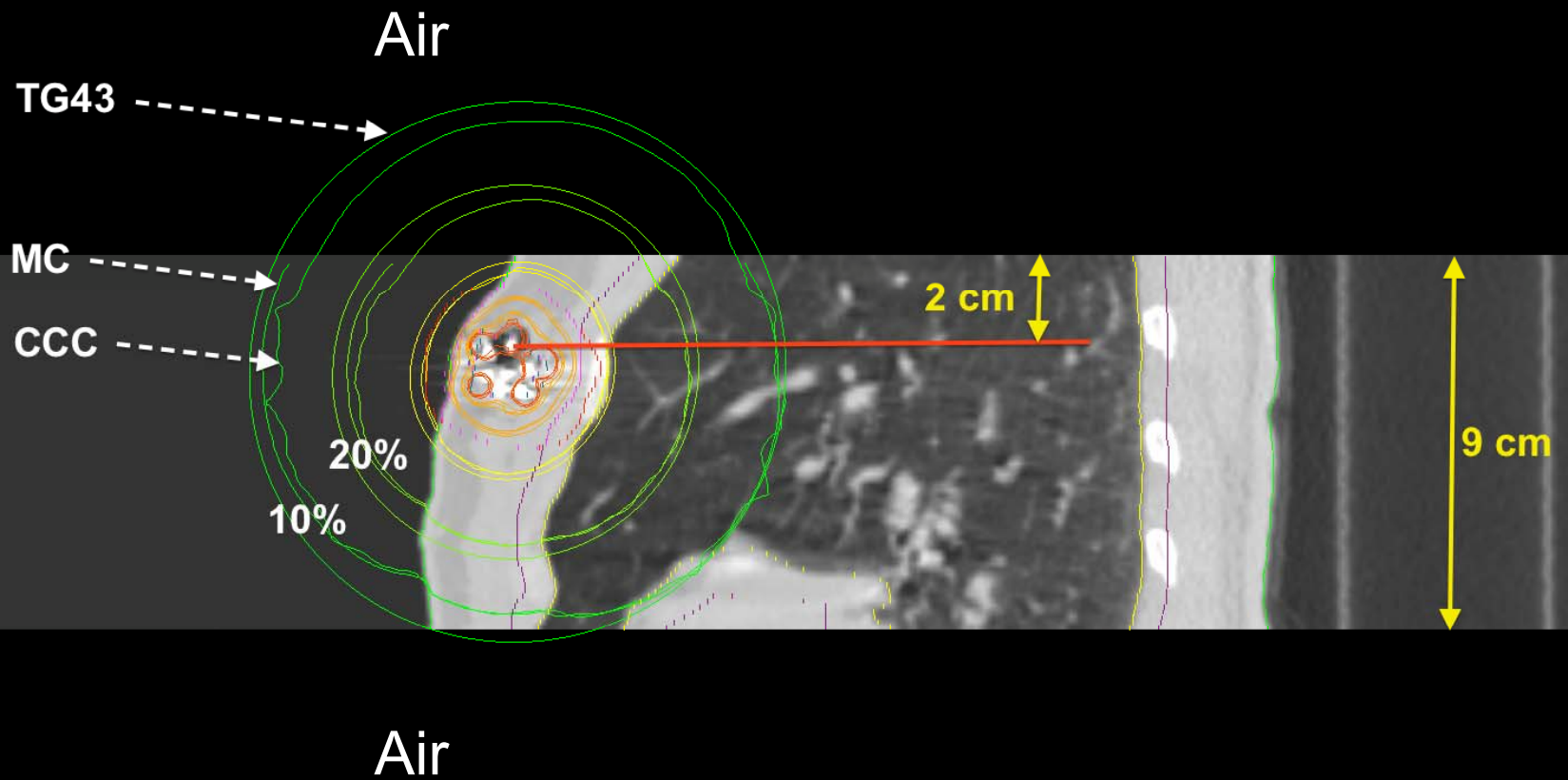
- Requirements from vendors
 - Accurate geometry (information accessible to users for commissioning)
 - Responsible for providing accurate composition of seeds, applicators and shields.
 - To provide a way for the manufacturers (of the above) or alternatively the end users to input such information into the TPS
 - Poke your favorite vendor, this will be critical

Other issues

What is the problem with this figure?



An easier case



Seed/Applicator Model Accuracy Requirements

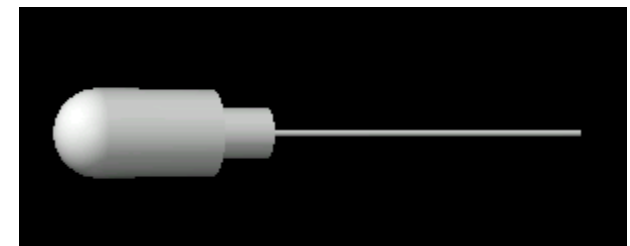
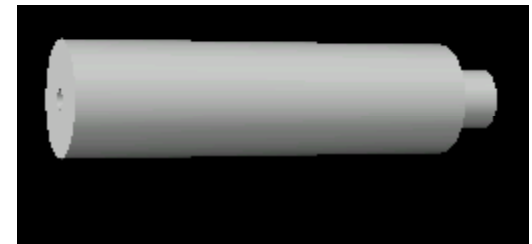
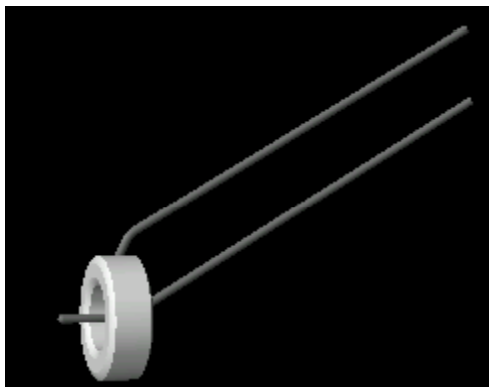
- Patient CT grids (>1 mm voxel) are probably not adequate for accurate modeling on the spatial scale of brachytherapy sources and applicators.
- MBDCA vendors should use analytic modeling schemes or recursively specify meshes with $1\text{--}10\ \mu\text{m}$ spatial resolution.
- Vendors to disclose their geometry, material assignments, and manufacturing tolerances to both end users and TPS vendors (if responsible for data entry and maintenance)

If TPS Applicator Library provided

- Preferred approach
 - Will ease the verification task.
- Vendor must provide visualization or reporting tools to end user to verify the correctness of each included applicator and source model
 - Ideally against independent design specifications.
- In addition, TPS vendors must disclose sufficient information regarding the model or recursive mesh generation to allow verification of the spatial resolution requirement specified in recommendation (2) in TG-186 Section IV-B

TG-186 Section IV.B: Applicators

- “It is the responsibility of the end-user clinical physicist to confirm that MBDCA dose predictions are based upon sufficiently accurate and spatially resolved applicator and source models, including correct material assignments, to avoid clinically significant dose-delivery error prior to implementing the dose algorithm in the clinic.”



Example: Solid Applicator Models in Acuros BV

New Solid Applicator

Part Search:

Afterloader: **GammaMedplus** Vendor: **Varian**

Part Library

Part number	Applicator set	Part name
GM11001000	Flexible Geometry Steel FSD	Right Ovoid - 25 mm, medium
GM11001000	Flexible Geometry Steel FSD	Left Ovoid - 25 mm, medium
GM11001120	Flexible Geometry Titanium FSD - CT/MRI ...	Left Ovoid - 30 mm, large
GM11001120	Flexible Geometry Titanium FSD - CT/MRI ...	Right Ovoid - 30 mm, large
GM11001120	Flexible Geometry Steel FSD	Left Ovoid - 30 mm, large
GM11001120	Flexible Geometry Steel FSD	Right Ovoid - 30 mm, large
GM11003380	Shielded Cylinder Applicator Set	unshielded, 20 mm cylinder
GM11003380	Shielded Cylinder Applicator Set	90x2 shielded (+y, +z quadrant and -y,-z quadrant shield...
GM11003380	Shielded Cylinder Applicator Set	180 degree shielded, (+y half not shielded), 20 mm cyli...
GM11003380	Shielded Cylinder Applicator Set	270 degree shielded, (+y,-z quadrant not shielded), 20 ...
GM11003380	Shielded Cylinder Applicator Set	90 degree shielded, (+y, +z quadrant shielded), 20 mm ...
GM11003390	Shielded Cylinder Applicator Set	90 degree shielded, (+y, +z quadrant shielded), 23 mm ...
GM11003390	Shielded Cylinder Applicator Set	90x2 shielded (+y, +z quadrant and -y,-z quadrant shield...
GM11003390	Shielded Cylinder Applicator Set	270 degree shielded, (+y,-z quadrant not shielded), 23 ...
GM11003390	Shielded Cylinder Applicator Set	180 degree shielded, (+y half not shielded), 23 mm cyli...
GM11003390	Shielded Cylinder Applicator Set	unshielded, 23 mm cylinder
GM11003400	Shielded Cylinder Applicator Set	270 degree shielded, (+y,-z quadrant not shielded), 26 ...
GM11003400	Shielded Cylinder Applicator Set	90 degree shielded, (+y, +z quadrant shielded), 26 mm ...
GM11003400	Shielded Cylinder Applicator Set	180 degree shielded (+y half not shielded) 26 mm cyli...

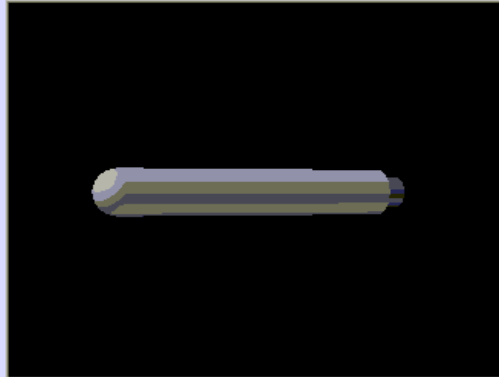
Applicator parts to be added into the current plan

Part number	Applicator set	Part name
GM11003390	Shielded Cylinder Applicator Set	270 degree shielded, (+y,-z quadrant not shielded), 23 ...

Applicator Part Description: Shielded cylinder, 23mm diameter

Applicator Set Description: The Shielded Applicator Set has been developed to treat cancer of the vagina or rectum where partial shielding is required. The 90° and 180° tungsten alloy shielding segments provide a variety of different shielding positions. After insertion, the marking screw allows for external identification of the area being shielded inside.

3D View



Please note that the parts will be placed to the plan according to the active 2D view

OK Cancel

Open Issues: Is there a better approach?

- No simple method to extract Z_{eff} from standard imaging modalities
- Dual/Multi energy CT?

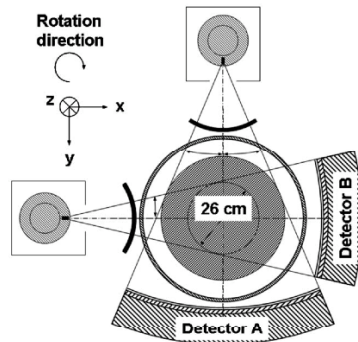
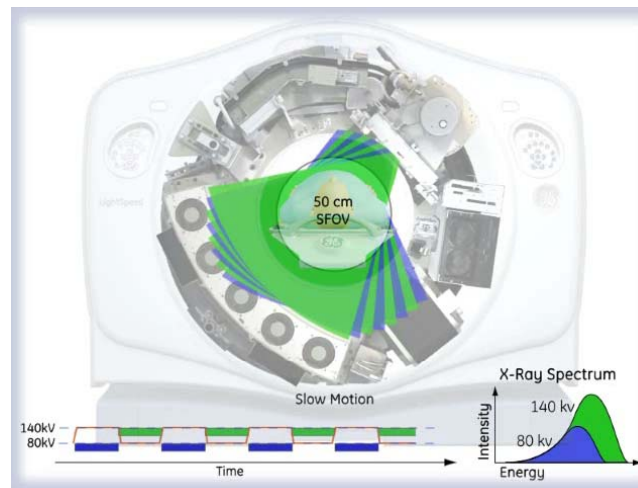


FIG. 1. Technical realization of a DSCT system (SOMATOM Definition, Siemens Healthcare, Forchheim, Germany). One detector (A) covers the entire scan field of view with a diameter of 50 cm, while the other detector (B) is restricted to a smaller, central field of view.

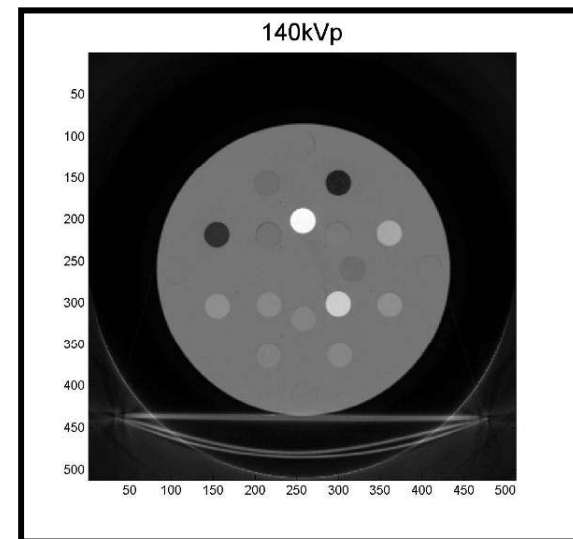
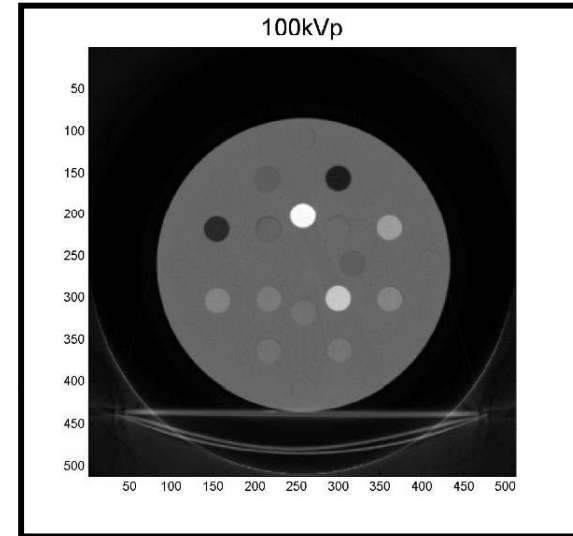


DECT for Brachytherapy and related topics

- Bazalova M et al 2008a Dual-energy CT-based material extraction for tissue segmentation in Monte Carlo dose calculations *Phys. Med. Biol.* 53 2439–56
- Bazalova M et al 2008b Tissue segmentation in Monte Carlo treatment planning: a simulation study using dual-energy CT images *Radiother. Oncol.* 86 93–8
- Goodsitt M M et al 2011 Accuracies of the synthesized monochromatic CT numbers and effective atomic numbers obtained with a rapid kVp switching dual energy CT scanner *Med. Phys.* 38 2222–32
- Heismann B and Balda M 2009 Quantitative image-based spectral reconstruction for computed tomography *Med. Phys.* 36 4471–85
- Heismann B J et al 2003 Density and atomic number measurements with spectral x-ray attenuation method *J. Appl. Phys.* 94 2073–9
- Landry G et al 2010 Sensitivity of low energy brachytherapy Monte Carlo dose calculations to uncertainties in human tissue composition *Med. Phys.* 37 5188–98
- Landry G et al 2011 The difference of scoring dose to water or tissues in Monte Carlo dose calculations for low energy brachytherapy photon sources *Med. Phys.* 38 1526–33
- Mahnken A H et al 2009 Spectral rhoZ-projection method for characterization of body fluids in computed tomography: ex vivo experiments *Acad. Radiol.* 16 763–9
- Landry G et al 2011 Simulation study on potential accuracy gains from dual energy CT tissue segmentation for low-energy brachytherapy Monte Carlo dose calculations *Phys. Med. Biol.* 56 6257–6278
- Bourque AE et al. 2014 A stoichiometric calibration method for dual energy computed tomography. *Phys Med Biol.* 59 2059-88

- Literature is extensive in radiology and DECT is also of interest in hadron therapy (stopping power)

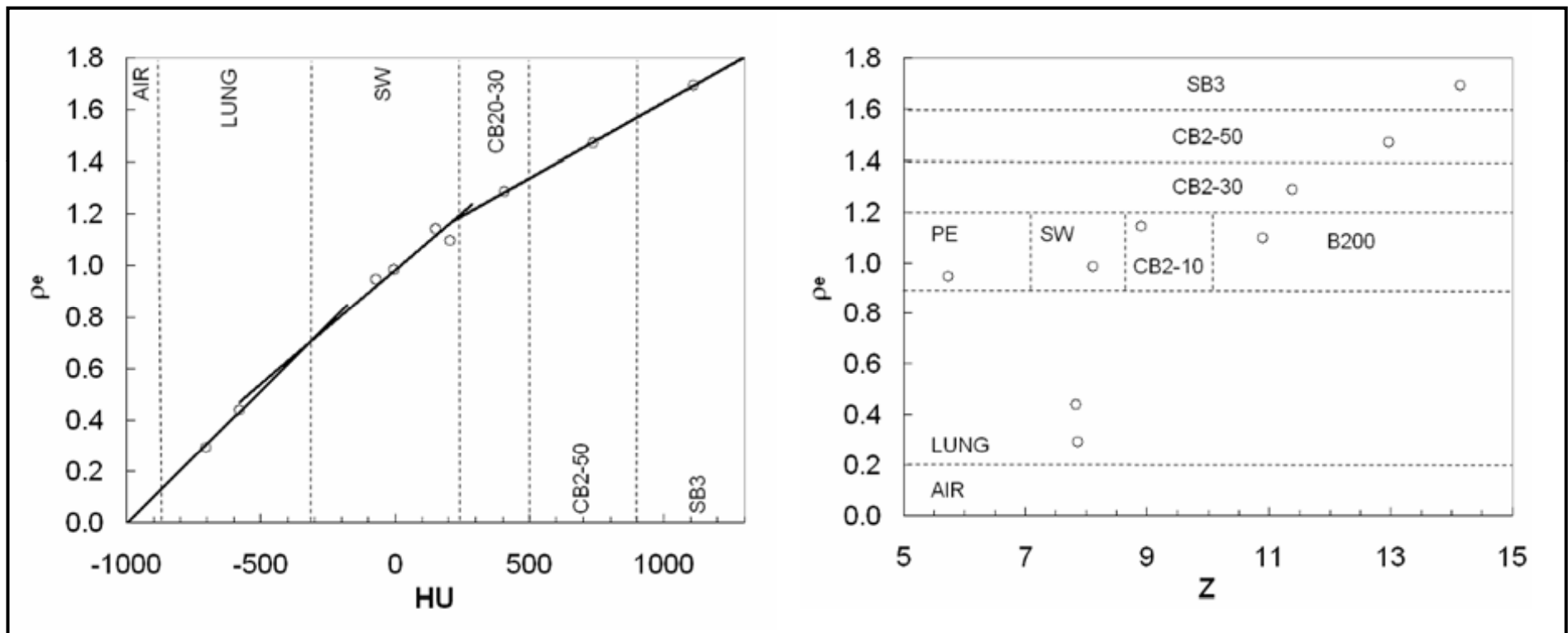
How does it work?



How does it work?

SECT

DECT



Dual-energy x-ray CT material extraction

- CT images are represented by $HU = 1000 \times (\mu / \mu_w - 1)$
 - μ and μ_w are the linear attenuation coefficients of a material and of water
- dual-energy material extraction (DECT) is based on
 - Taking CT images at two tube voltages (e.g. 100 kVp and 140 kVp)
 - The farther apart the energy the better!
 - Parameterization of the linear attenuation coefficient results in ρ_e and Z maps

Linear attenuation coefficient

Describes attenuation of a photon beam

Torikoshi *et al*:

$$\mu(E) = \rho_e \left(Z^4 F(E, Z) + G(E, Z) \right)$$

- $\rho_e = \rho Z/A * N_A =$ electron density
- $Z =$ effective atomic number
- $F(E,Z)$ and $G(E,Z)$ are the photoelectric absorption and scattering terms (Rayleigh and Compton) of μ

For polychromatic x-rays:

$$\mu_j = \rho_e \sum_i \omega_{ji} \left[Z^4 F(E_{ji}, Z) + G(E_{ji}, Z) \right]$$

x-ray spectra represented by weights ω_i at E_i

Linear attenuation coefficient

Having the densities the same material measured at two tube voltages, one can solve for Z:

$$\frac{\mu_1}{\mu_2} - \frac{\sum_i \omega_{1i} [Z^4 F(E_{1i}, Z) + G(E_{1i}, Z)]}{\sum_i \omega_{2i} [Z^4 F(E_{2i}, Z) + G(E_{2i}, Z)]} = 0$$

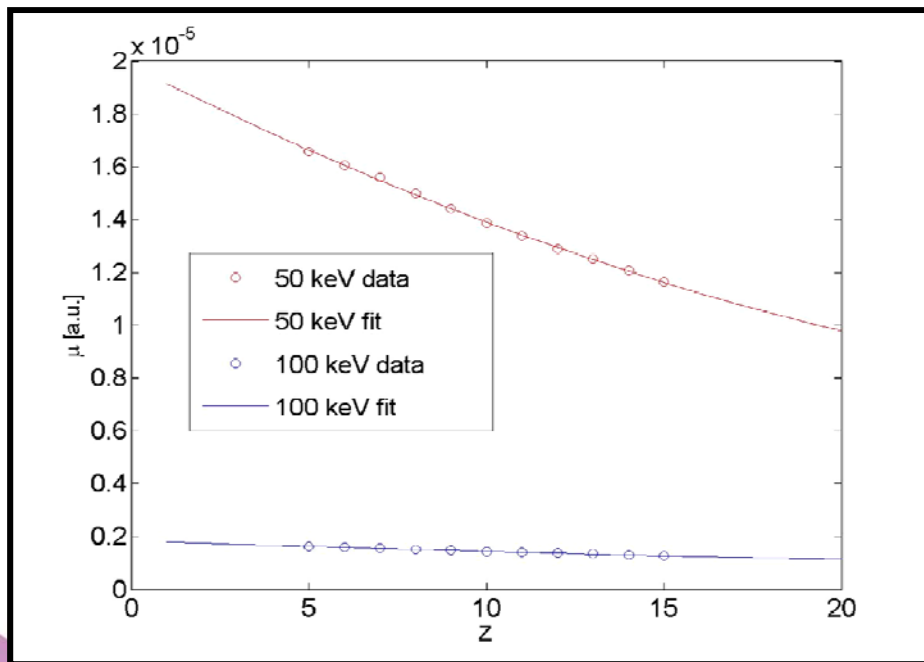
Or, solve for both Z and density simultaneously

$$Z^4 - \frac{\frac{\mu_2}{\mu_{2w}} \sum_i \omega_{2i} [Z_w^4 F(E_{2i}, Z_w) + G(E_{2i}, Z_w)] \sum_i \omega_{1i} G(E_{1i}, Z) - \frac{\mu_1}{\mu_{1w}} \sum_i \omega_{1i} [Z_w^4 F(E_{1i}, Z_w) + G(E_{1i}, Z_w)] \sum_i \omega_{2i} G(E_{2i}, Z)}{\frac{\mu_1}{\mu_{1w}} \sum_i \omega_{1i} [Z_w^4 F(E_{1i}, Z_w) + G(E_{1i}, Z_w)] \sum_i \omega_{2i} F(E_{2i}, Z) - \frac{\mu_2}{\mu_{2w}} \sum_i \omega_{2i} [Z_w^4 F(E_{2i}, Z_w) + G(E_{2i}, Z_w)] \sum_i \omega_{1i} F(E_{1i}, Z)} = 0$$

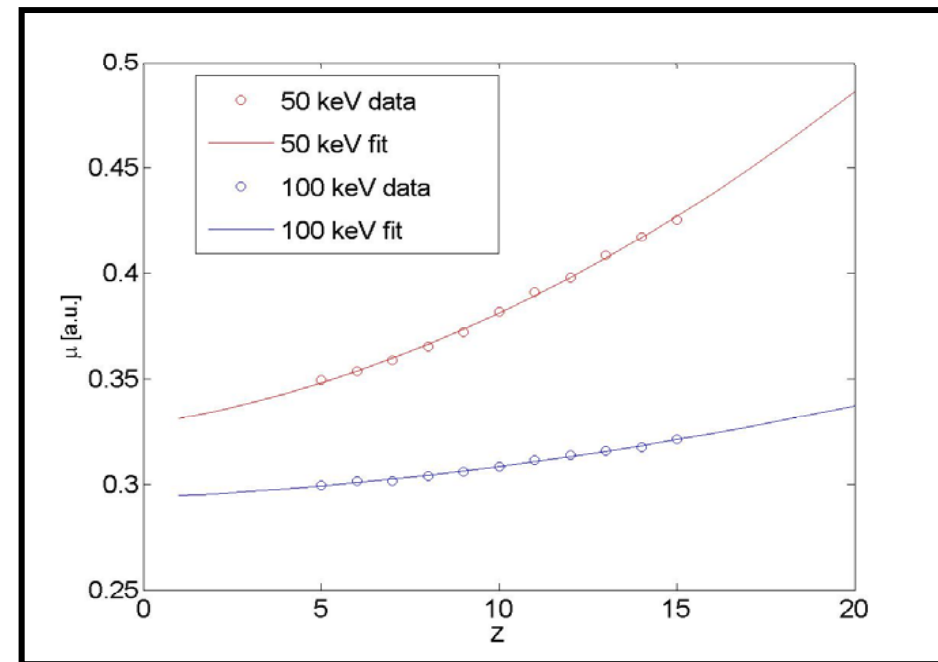
$F(E,Z)$ and $G(E,Z)$ functions

$$\mu = \mu_{\text{photoeffect}} + \mu_{\text{Compton+Rayleigh}}$$

- $(\mu/\rho)_p = Z^5 N_A / A * F(E,Z) \Rightarrow \mu_p = \rho_e Z^4 * F(E,Z)$
- $(\mu/\rho)_{C+R} = Z N_A / A * G(E,Z) \Rightarrow \mu_{C+R} = \rho_e * G(E,Z)$



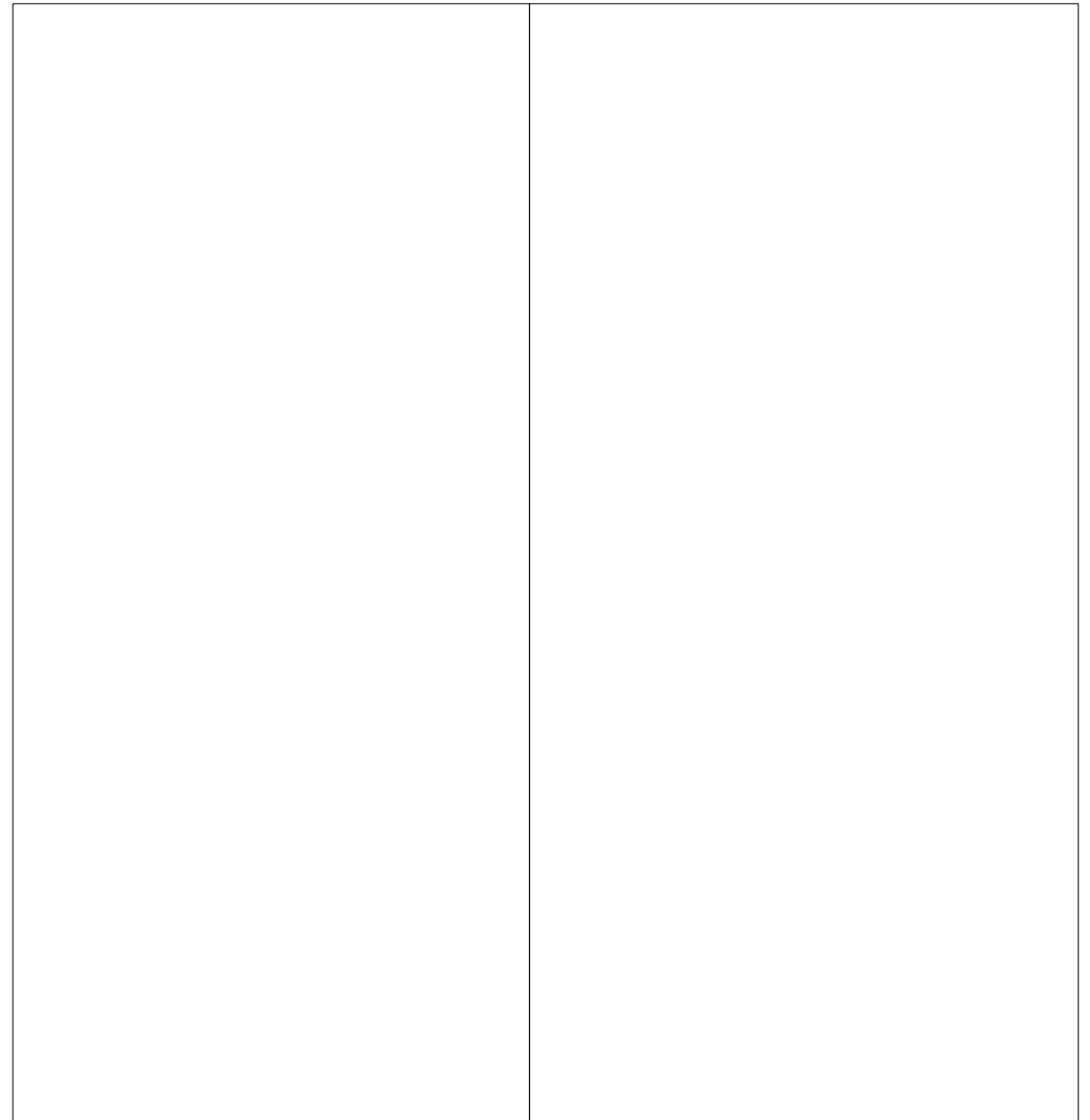
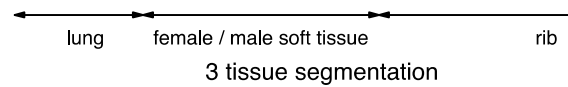
$F(E,Z)$



$G(E,Z)$

Putting these equation to practice

—



Putting these equation to practice

Improved tissue assignment using dual-energy computed tomography in low-dose rate prostate brachytherapy for Monte Carlo dose calculation

Nicolas Côté

*Département de Physique, Université de Montréal, Pavillon Roger-Gaudry (D-428),
2900 Boulevard Édouard-Montpetit, Montréal, Québec H3T 1J4, Canada*

Stéphane Bedwani

*Département de Radio-Oncologie, Centre Hospitalier de l'Université de Montréal (CHUM),
1560 Rue Sherbrooke Est, Montréal, Québec H2L 4M1, Canada*

Jean-François Carrier^{a)}

*Département de Physique, Université de Montréal, Pavillon Roger-Gaudry (D-428),
2900 Boulevard Édouard-Montpetit, Montréal, Québec H3T 1J4, Canada and Département
de Radio-Oncologie, Centre Hospitalier de l'Université de Montréal (CHUM),
1560 Rue Sherbrooke Est, Montréal, Québec H2L 4M1, Canada*

(Received 28 August 2015; revised 9 April 2016; accepted for publication 12 April 2016;
published 29 April 2016)

Putting these equation to practice

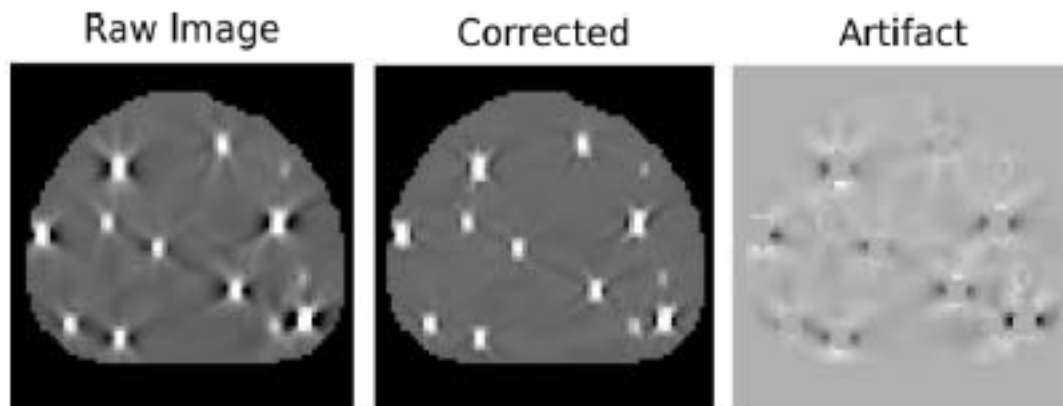
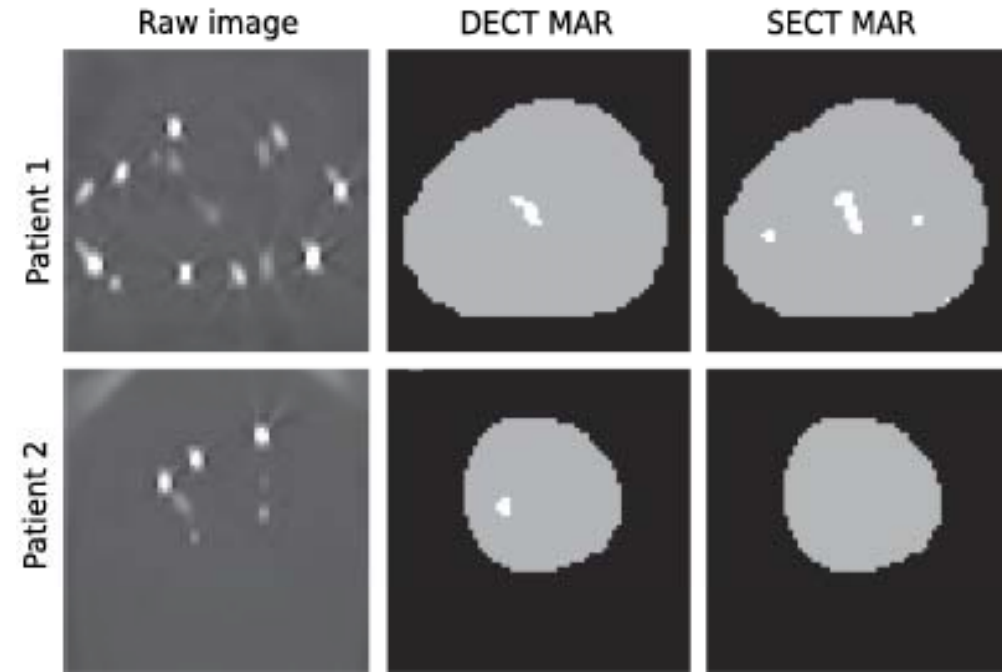


FIG. 3. Raw image at 100 kVp which has been corrected by DECT MAR algorithm. Window level: 461 HU, window width: 1592 HU for both images raw and corrected images. The last image represents the artifact information generated from Eq. (5).

An automatic tissue assignment technique was developed using DECT images. This modality allows for a reduced impact of metallic artifacts, which in turn improves the quality of tissue assignment. Differences in D_{90} were underestimated in the SECT-based approach by up to 2.3% compared with the developed DECT algorithm. Thus, the DECT is a potentially superior method, allowing significant reduction in metallic artifact presentation, and more accurate representation of patient tissue anatomy and density.



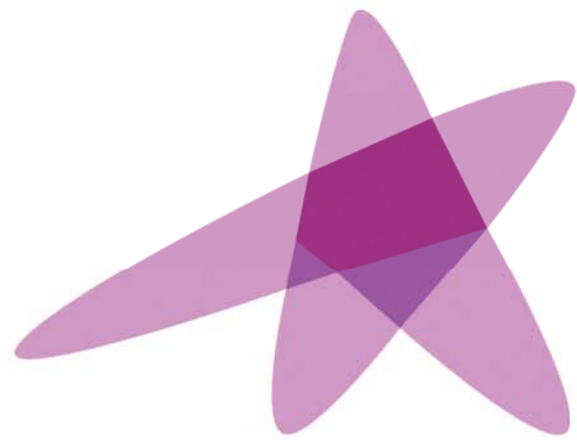
Cote et al, Med Phys 43

Lesson learned?

- DECT calculations for low energy sources within 4% of ground truth
 - 7 tissue bins SECT at <9%; 3 tissue bin (like EBRT) failed!
- DECT very sensitive to noise and motion
 - May make DECT difficult for patient imaging (CT dose / mAs settings)
 - Simultaneous imaging
- Still a very active field of research!

Conclusion

- Voxel-by voxel cross section assignment is a critical step
 - Tissue segmentation; Applicator and source description
 - Follow TG-186 guidelines to ensure centre-to-centre consistency
 - Poke/Question your favorite TPS/Applicator vendor(s)...
- For ^{192}Ir , water is a good representation of soft tissue only
 - Air, bone, metals, ... should be segmented and assigned the right material/density
- Dual-Energy/Multi-Energy-CT should be explored actively
 - Potential accurate solution to (ρ_e, Z_{eff}) assignments
 - Hot research topics



ESTRO

School



UNIVERSITÉ
LAVAL



QA of 3D imaging

Prof. Luc Beaulieu, Ph.D., FAAPM

*1- Département de physique, de génie physique et d'optique, et
Centre de recherche sur le cancer, Université Laval, Canada*

*2- Département de radio-oncologie et Centre de recherche du CHU
de Québec, CHU de Québec, Canada*

Vienna, May 29 – June 1 2016



Disclosures

- None for this section

Learning Objectives

- Defining the role of imaging in brachytherapy
- Identifying the various imaging modality used
- Gives key pointers relative to the content of an efficient QA/QC program
- Provide an overview of topics that need further guidance

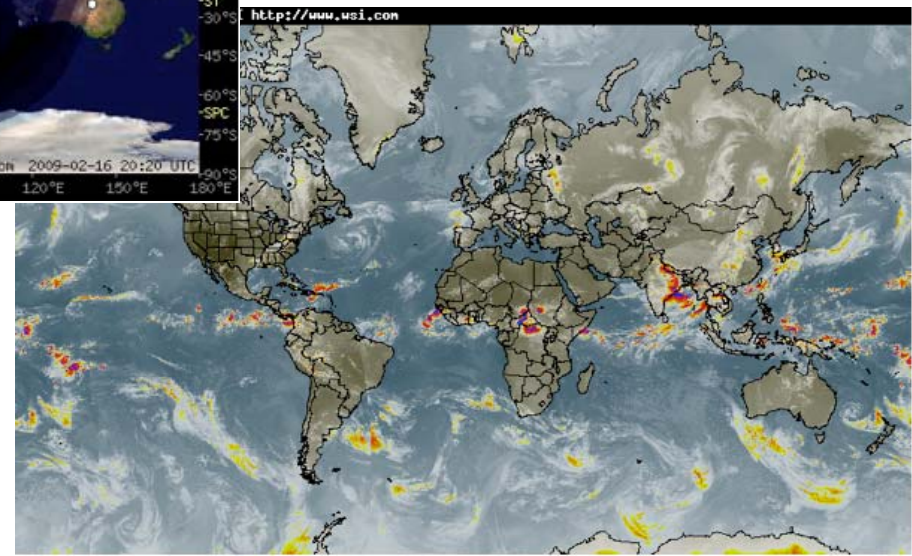
Key References (and refs therein)

- **Comprehensive Brachytherapy: physical and clinical aspect.** JLM Venselaar, D Baltas, AS Meigooni and P.J. Hoskin. CRC Press, Taylor & Francis, 2013.
 - In particular chapter 14. See chapters 4,9,16 and 24.
- **Modern Technology of Radiation Oncology: A Compendium for Medical Physicists and Radiation Oncologists .** J. Van Dyk
 - Vol 3, Chapter 7; Vol 1, Chapter 7; Vol 2, Chapter 2
- **AAPM Report No. 100, “Acceptance Testing and Quality Assurance Procedures for Magnetic Resonance Imaging Facilities”,** E.F. Jackson *et al.*, 2010; Firbank MJ, et al. “Quality assurance for MRI: practical experience”. *Br J Radiol* 73:376-383, 2000; *Physics of MRI*, 1992 AAPM summer school, P. Sprawls and M.J. Bronskill (Eds)
- **Pfeiffer D et al. “AAPM Task Group 128: quality assurance tests for prostate brachytherapy ultrasound systems”. *Med Phys* 2008;35(12):5471–89.**
- **NEMA, NU 2-2001 standard for basic QA/QC of PET; EB Sokole et al., *EJNMI* 2010;37:662-671 and 672-681; Mutic et al, *Phys. Med* 2003;30:2762-92**
- **2013 ESTRO course on Advanced Imaging Physics**

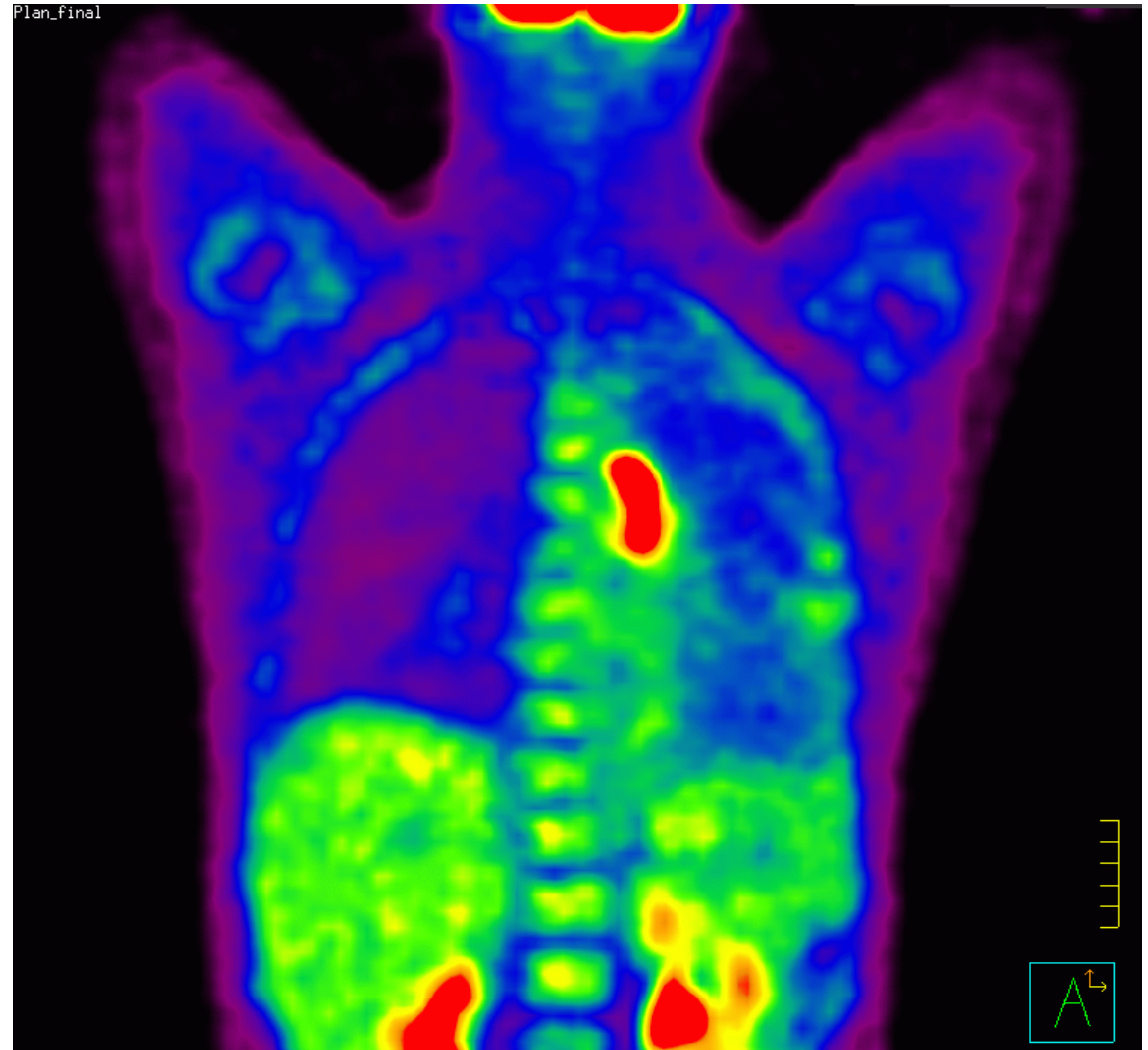
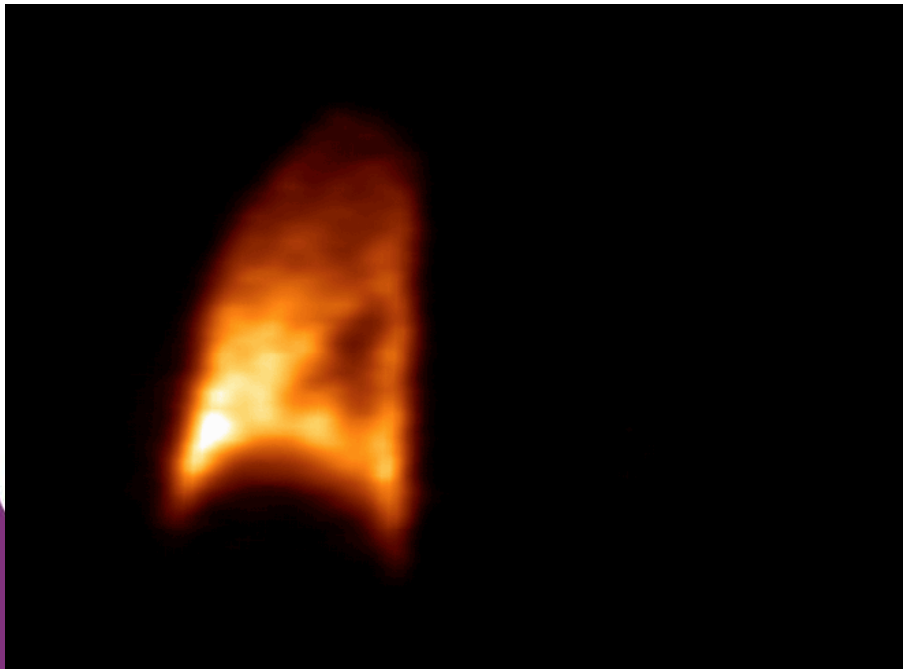
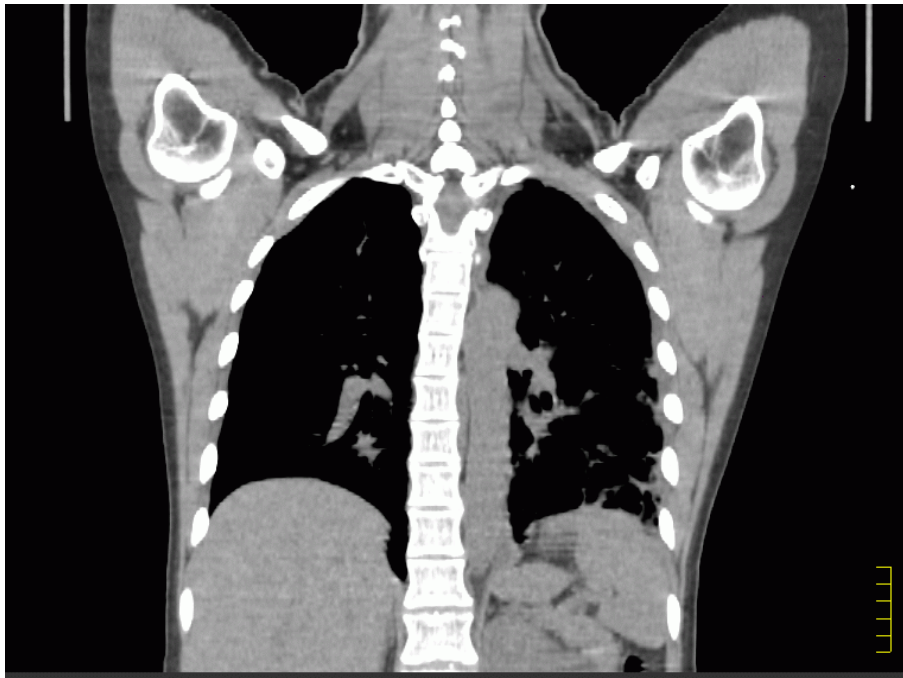
2D vs 3D imaging

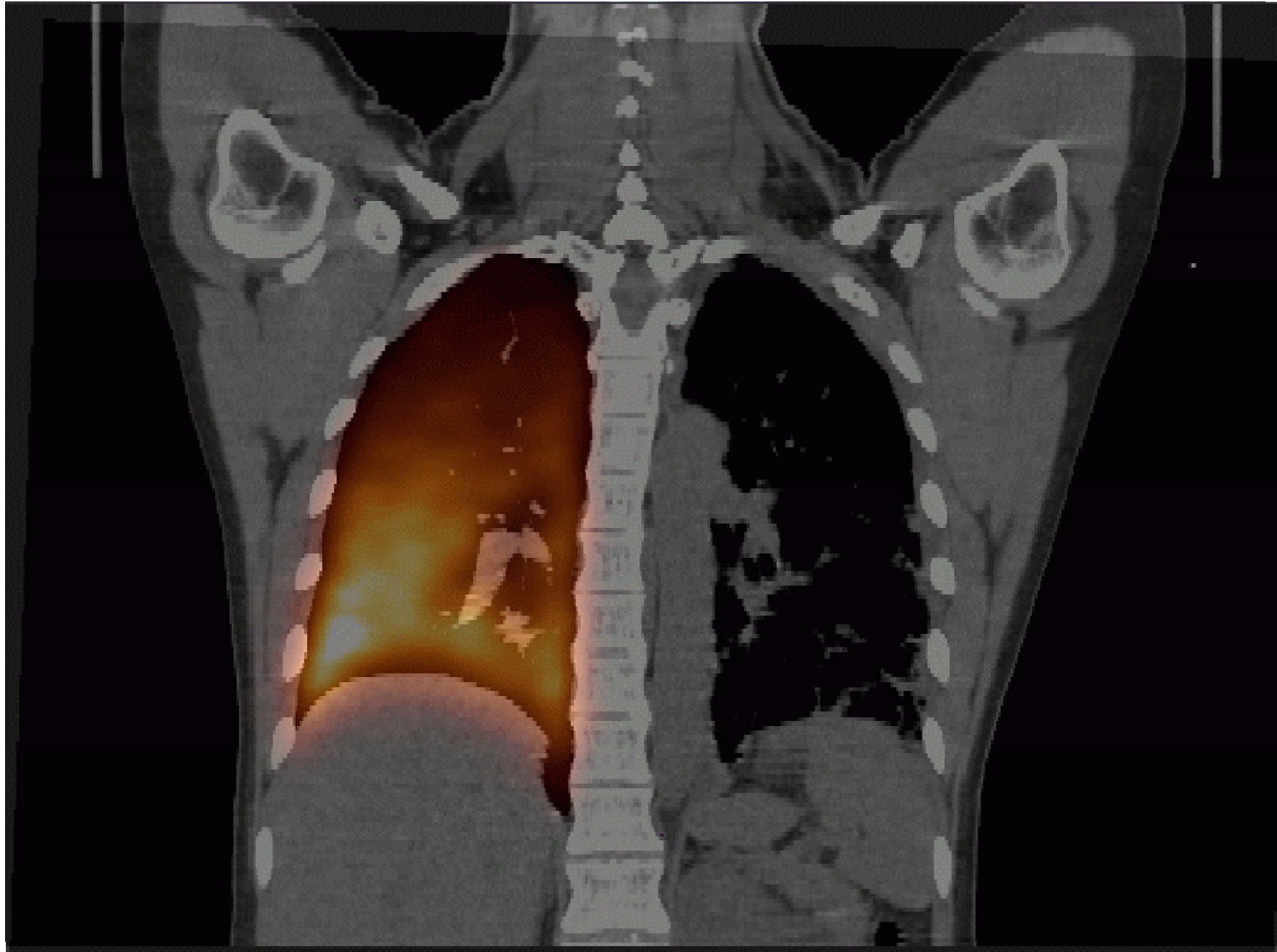


Various ways to look at the world









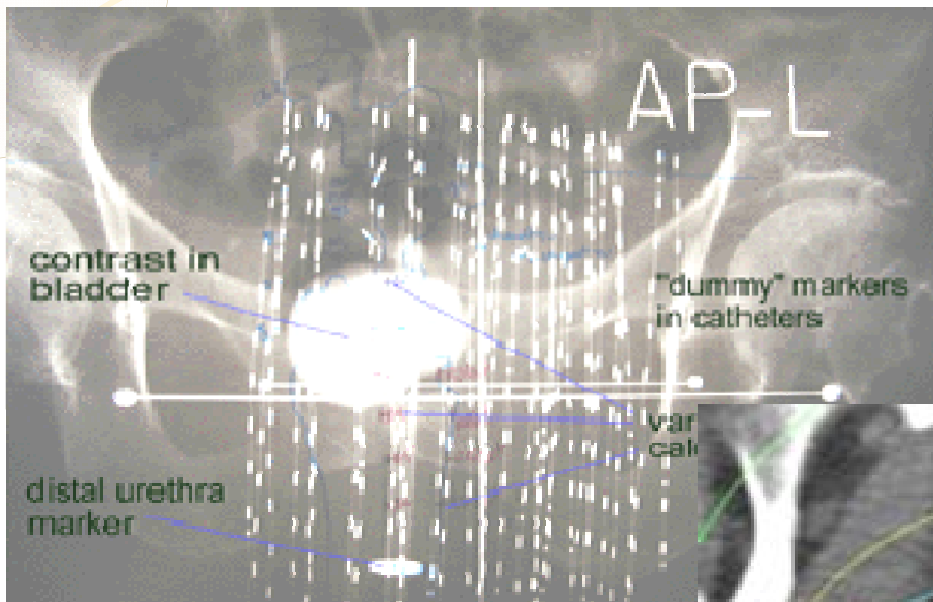
St-Hilaire et al., Radiother Oncol 100 (2011)

New World

- Multiple point of views
 - Do not all agree (Vol!)
- Organ/structure-based planning
 - DVH, max dose constraints
- Heterogeneities
 - Tissues and applicators
- Advanced Tx schemes
 - Source/applicators
 - Functional “planning”
 - Real-time planning
- Dose-outcome revisited?

Old World

- 2D planar views
 - Bones and applicators
- Dose and constraints to points and/or based on applicator, catheter and needle location
- Water-based dosimetry
- Limited in term of new Tx approaches
- Dose-outcome relationship not directly related target doses



Example 1: LDR Prostate Brachytherapy Imaging

- Primary imaging modalities (treatment)
 - Ultrasound
 - Sizing and location
 - Needle guidance
 - Fluoroscopy
 - Intraoperative guidance
 - Plane film
 - Treatment record
 - Source counting
 - Quality assurance tool
 - CT scan
 - Post implant evaluation
 - MRI scan
 - Post implant evaluation
- Additional imaging for diagnosis and staging
 - MRI
 - Dynamic Contrast Enhancement
 - Spectroscopic
 - Diffusion weighting
 - PET / SPECT

doi:10.1016/j.ijrobp.2007.07.2388

QA FOI For non–image-based brachytherapy, the American **CU** Association of Physicists in Medicine Task Group reports **IT** 56 and 59 provide reasonable guidance on procedure-specific process flow and QA.

However, improved guidance is needed even for established procedures such as ultrasound-guided prostate implants.

Adaptive replanning in brachytherapy faces unsolved problems similar to that of image-guided adaptive external beam radiotherapy.

doi:10.1016/j.ijrobp.2007.07.2389

QA FOR RT SUPPLEMENT

QUALITY ASSURANCE ISSUES FOR COMPUTED TOMOGRAPHY–, ULTRASOUND–, AND MAGNETIC RESONANCE IMAGING–GUIDED BRACHYTHERAPY

ROBERT A. CORMACK, PH.D.

This report was intended to indicate the QA concerns arising from the convergence of brachytherapy and imaging—highlighting areas in which technical improvements are needed.

Three-dimensional (3D) image-based brachytherapy creates new error pathways not necessarily addressed in traditional QA aimed at devices, sources, and calculations

Imaging, what for?

- **Localization of sources and applicators**
 - Positions, angles, ...
- **Definition of organs/structures**
 - CTV, PTV, OARs, ...
 - Functional information?
- **Dose calculation**
 - Electron density
 - Materials: tissues, sources, applicators, contrast agent, ...

Demands of 3D dose calculation on QA of imaging



Contents lists available at [ScienceDirect](https://www.sciencedirect.com)

Radiotherapy and Oncology

journal homepage: www.thegreenjournal.com



Original article

Review of clinical brachytherapy uncertainties: Analysis guidelines of GEC-ESTRO and the AAPM[☆]

Christian Kirisits^{a,*}, Mark J. Rivard^b, Dimos Baltas^c, Facundo Ballester^d, Marisol De Brabandere^e, Rob van der Laarse^f, Yury Niatsetski^g, Panagiotis Papagiannis^h, Taran Paulsen Hellebust^{i,j}, Jose Perez-Calatayud^k, Kari Tanderup^l, Jack L.M. Venselaar^m, Frank-André Siebertⁿ

^a Department of Radiotherapy, Comprehensive Cancer Center, Christian Doppler Laboratory for Medical Radiation Research for Radiation Oncology, Medical University of Vienna, Austria; ^b Department of Radiation Oncology, Tufts University School of Medicine, Boston, USA; ^c Department of Medical Physics & Engineering, Sana Klinikum Offenbach, Germany; ^d University of Valencia, Spain; ^e University Hospital Gasthuisberg, Leuven, Belgium; ^f Quality Radiation Therapy, The Netherlands; ^g Nucletron an Elekta Company, The Netherlands; ^h Medical Physics Laboratory, Medical School, University of Athens, Greece; ⁱ Department of Medical Physics, Oslo University Hospital, The Radium Hospital, Oslo, Norway; ^j Department of Physics, University of Oslo, Oslo, Norway; ^k Hospital Universitario La Fe, Valencia, Spain; ^l Aarhus University Hospital, Denmark; ^m Department of Medical Physics and Engineering, Instituut Verbeeten, Tilburg, The Netherlands; ⁿ University Hospital S-H Campus Kiel, Germany

Table 1Example 1 – HDR ¹⁹²Ir BT source for vaginal cylinder applicator.

Category	Typical level (%)	Assumptions
Source strength	2	PSDL traceable calibrations
Treatment planning	3	Reference data with the appropriate bin width
Medium dosimetric corrections	1	Valid for applicator without shielding and if CTV located inside pelvis: an advanced dose calculation formalism should be used if this assumption false
Dose delivery including registration of applicator geometry to anatomy	5	Accurate QA concept for commissioning and constancy checks, especially for source positioning and applicator/source path geometry, appropriate imaging techniques (either small slice thickness, 3D sequences or combination of different slice orientations), applicator libraries (either by using software solutions or manual)
Interfraction/Intrafraction changes between imaging and dose delivery	5*	For one treatment plan per applicator insertion and measures to detect major variations for subsequent fractions
Total dosimetric uncertainty ($k = 1$)	8	For treatment delivered with the same BT source

* Estimated value based on expert discussion.

Table 2Example 2 – HDR ¹⁹²Ir source for intracavitary, image-guided cervical cancer BT.

Category	Typical level (%)	Assumptions
Source strength	2	PSDL traceable calibrations
Treatment planning	3	Reference data with the appropriate bin width
Medium dosimetric corrections	1	Applicator without shielding and CTV inside pelvis (concerning for scatter); an advanced dose calculation formalism should be used if this assumption false
Dose delivery including registration of applicator geometry to anatomy	4	Accurate QA concept for commissioning and constancy checks, especially for source positioning and applicator/source path geometry, appropriate imaging techniques (either small slice thickness, 3D sequences or combination of different slice orientations), applicator libraries (either by using software solutions or manual)
Interfraction/Intrafraction changes (including contouring uncertainties)	11	For one treatment plan per applicator insertion but several subsequent fractions – if only one fraction is applied the remaining uncertainty between imaging and dose delivery should be at least smaller than this interfraction variation
Total dosimetric uncertainty (including contouring uncertainties) ($k = 1$)	12	For treatment delivered with the same BT source – note that in cervix cancer BT, both HDR and PDR schedules consist of several fractions, reducing the random uncertainties (see text)

Table 3
 Example 3 – HDR ¹⁹²Ir BT source for breast balloon applicator.

Category	Typical level (%)	Assumptions
Source strength	2	PSDL traceable calibrations
Treatment planning	3	Reference data with the appropriate bin width
Medium dosimetric corrections	3	Balloon filled with standard level of contrast agent, no consideration or composition of chestwall, lung, or breast
Scatter dosimetric corrections	7	A non-scalar correction for skin dose (and at points in proximity to the surface near the balloon) is needed, and will require an advanced dose calculation formalism to properly account for radiation scatter conditions in the patient. Use of a single prescription point might be not sufficient
Dose delivery including registration of applicator geometry to anatomy	7	Accurate QA concept for commissioning and constancy checks, especially for source positioning and applicator/ source path geometry, appropriate imaging techniques (either small slice thickness, 3D sequences or combination of different slice orientations), applicator characterization
Interfraction/Intrafraction changes between imaging and dose delivery	7*	For one treatment plan per applicator insertion and measures to detect major variations for subsequent fractions
Total dosimetric uncertainty ($k = 1$)	13	For treatment delivered with the same BT source

* Estimated value based on expert discussion.

Table 4
Example 4 – LDR ¹²⁵I sources for permanent prostate BT.

Category	Typical level (%)	Assumptions
Source strength	3	PSDL traceable calibrations
Treatment planning	4	Reference data with the appropriate bin width
Medium dosimetric corrections	5	No consideration is given for calcifications or their composition in the patient
Inter-seed attenuation	4	An advanced dose calculation formalism may indicate source models and orientations cause the largest effects
Treatment delivery imaging	2	US QA performed according to AAPM TG-128
Target contouring uncertainty	2	Using CT or CT + T2 imaging
Anatomy changes between dose delivery and post-implant imaging	7*	Post-implant imaging using CT, with a scalar correction factor for edema correction
Total dosimetric uncertainty ($k = 1$)	11	For treatment delivered without excreted seeds

* Estimated value based on expert discussion.

Table 5
Example 5 – HDR ¹⁹²Ir source for temporary prostate BT.

Category	Typical level (%)	Assumptions
Source strength	2	PSDL traceable calibrations
Treatment planning	3	Reference data with the appropriate bin width
Medium dosimetric corrections	1	Full scatter conditions in the pelvic region and for the prostate location are assumed
US-based Treatment planning and delivery: Catheter reconstruction and source positioning accuracy	2	Assuming usage of dedicated catheter reconstruction tools (catheter free-length measurement based methods) for an accurate (0.7 mm) reconstruction of catheter tip and 1.0 mm source positioning accuracy by the afterloader for straight catheters and transfer tubes
US-based 2D and 3D-imaging overall effect	2	US QA performed according to AAPM TG-128 report
Changes of catheter geometry relative to anatomy between intraoperative treatment planning and intraoperative treatment delivery	2	Assuming that new image acquisition and treatment plan calculation is done always before each fraction. It is also required that no manipulation of the implant and anatomy occurs, as it is the case when removing/manipulating the US-probe or moving the patient from the operation table before treatment delivery
Target contouring uncertainty	2	Using CT or CT + T2 imaging
Total dosimetric uncertainty ($k = 1$)	5	For treatment delivery without patient movement and changes in the lithotomic set-up and with the US probe at the position of the acquisition (transversal plane at the prostate base)

Ultrasounds

- **Intrinsically real-time**
 - **2D+1 and 3D+1**
 - **Standard B-mode is not the only thing you can do**
 - **Elastography, Doppler, CE (micro bubbles), tissue typing and “cell” imaging (apoptosis) -> mpUS!**
 - **STD for prostate seed implant**
 - **Alternative for prostate HDR brachytherapy**
 - **Can be used for applicator insertion guidance**
 - **Can be use for breast brachy insertion**

Ultrasounds

- **But:**
 - **Image visual appearance is very different than CT or MRI**
 - **Needle and catheter localization: YES (but tips difficult)**
 - **Applicator tracking: OK**
 - **Seeds and spacers visualization: Not really**
 - **3D tracked/motorized probe to be favored (imaging reconstruction accuracy)**
 - **No electronic density for dose calculation**
 - **Probe motion inducing organ motion or deformation ?**

Ultrasounds QA/QC program

AAPM Task Group 128: Quality assurance tests for prostate brachytherapy ultrasound systems

Douglas Pfeiffer^{a)}

Imaging Department, Boulder Community Foothills Hospital, Boulder, Colorado 80301

Steven Sutlief

Radiation Therapy, VA Medical Center, VA Puget Sound Health Care System, Seattle, Washington 98108

Wenzheng Feng

Cardiology and Interventional Radiology, William Beaumont Hospital, Royal Oak, Michigan 48073

Heather M. Pierce

CIRS, Inc., Norfolk, Virginia 23513

Jim Kofler

Radiology, Mayo Clinic, Rochester, Minnesota 55905

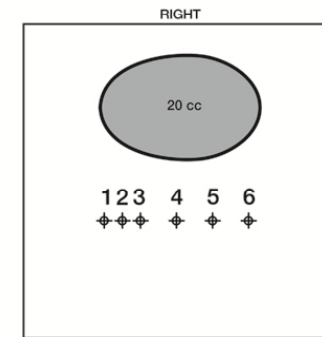
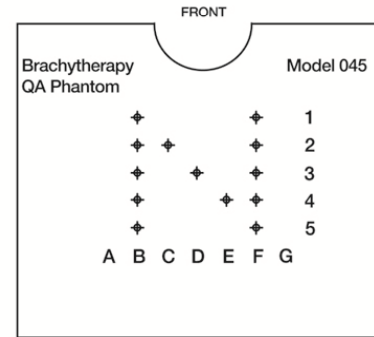
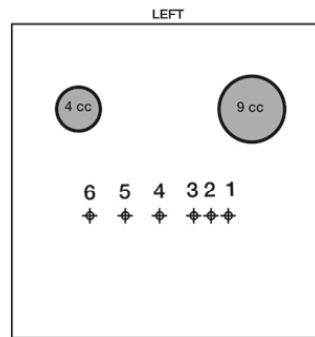
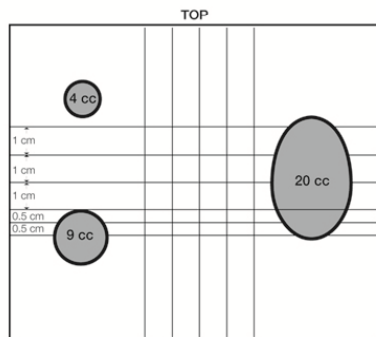
(Received 26 December 2007; revised 27 August 2008; accepted for publication 6 October 2008; published 12 November 2008)

While ultrasound guided prostate brachytherapy has gained wide acceptance as a primary treatment tool for prostate cancer, quality assurance of the ultrasound guidance system has received very little attention. Task Group 128 of the American Association of Physicists in Medicine was created to address quality assurance requirements specific to transrectal ultrasound used for guidance of prostate brachytherapy. Accurate imaging guidance and dosimetry calculation depend upon the quality and accuracy of the ultrasound image. Therefore, a robust quality assurance program for the ultrasound system is essential. A brief review of prostate brachytherapy and ultrasound physics is provided, followed by a recommendation for elements to be included in a comprehensive test phantom. Specific test recommendations are presented, covering grayscale visibility, depth of penetration, axial and lateral resolution, distance measurement, area measurement, volume measurement, needle template/electronic grid alignment, and geometric consistency with the treatment planning computer. © 2008 American Association of Physicists in Medicine.

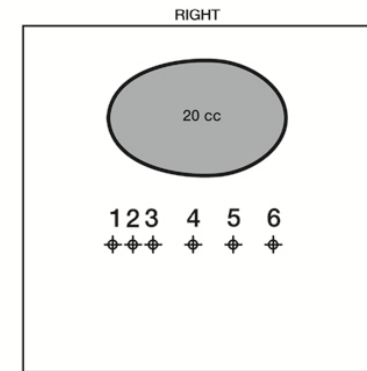
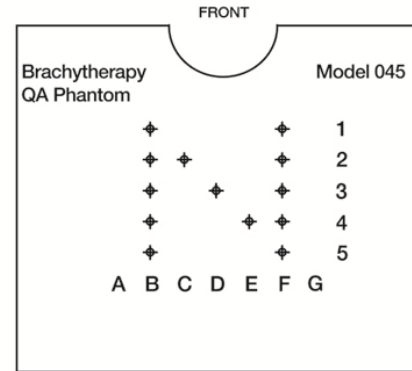
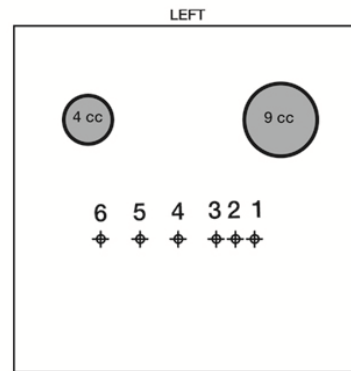
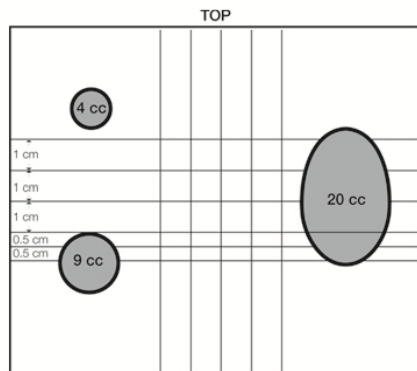
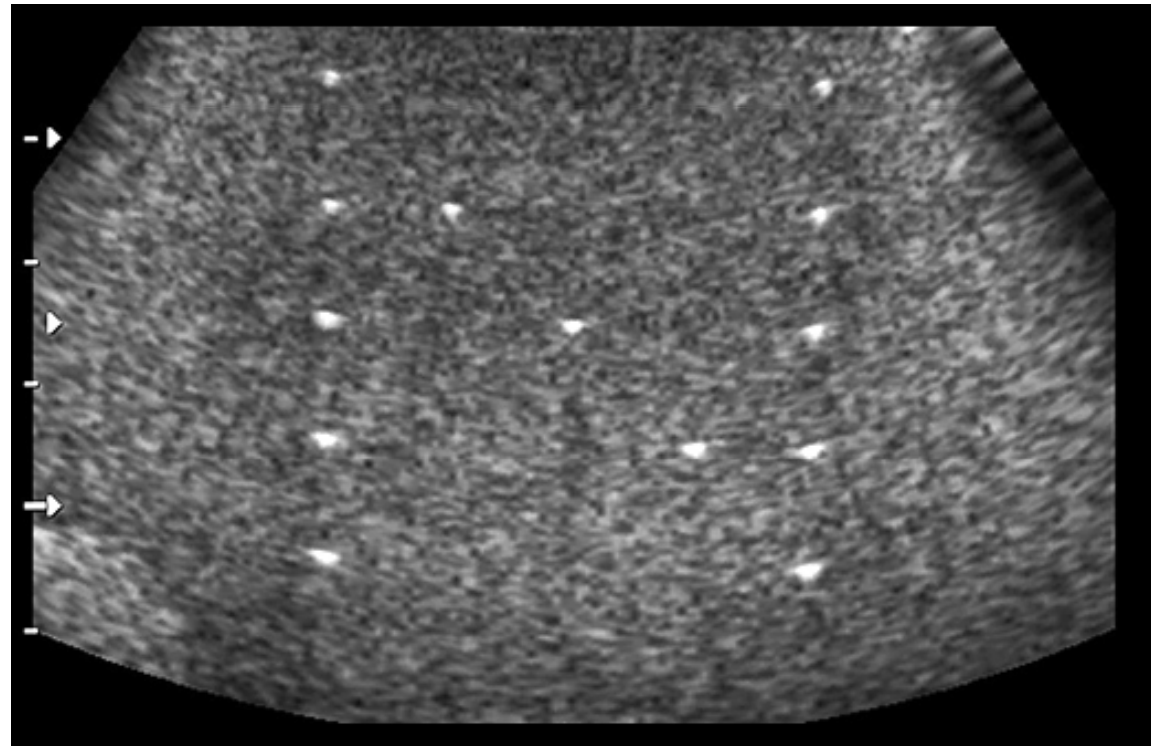
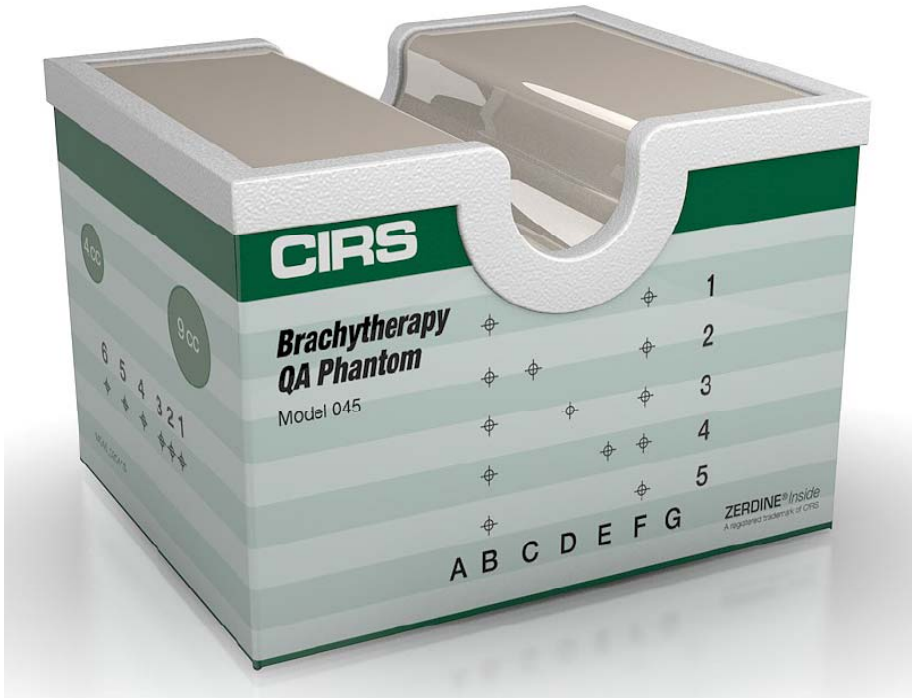
[DOI: [10.1118/1.3006337](https://doi.org/10.1118/1.3006337)]

Key words: prostate, brachytherapy, implant, ultrasound, quality assurance, quality control, phantoms

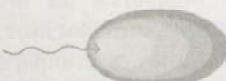
Ultrasounds QA/QC program



Ultrasounds QA/QC program



Ultrasounds QA/QC program

 **Table 7.1**
Ultrasound QA Summary [43].

TEST	BRIEF DESCRIPTION	TOLERANCE	RECOMMENDED FREQUENCY
Grayscale Visibility	Number of gray levels displayed remains consistent from time of purchase	A change of more than 2 levels (or 10%), or fuzzy or blooming text	Annual
Penetration Depth	The depth at which a low contrast object in a phantom can be distinguished	A change of more than 1 cm	Annual
Axial and Lateral Resolution	A filament's width, or graduated spacing measured in a phantom at 1–2 cm and 5–6 cm depths	A change of more than 1 mm	Annual
Axial Distance Measurement Accuracy	Measure known depths in a phantom	The larger of 2 mm or 2%	Annual
Lateral Distance Measurement Accuracy	Measure known depths in a phantom	The larger of 3 mm or 3%	Annual
Area Measurement Accuracy	Use the ultrasound's recommended area measurement tools to measure a known area	Within 5%	Annual
Volume Measurement Accuracy	Use the recommended volume measurement tools to measure a known volume	Within 5%	Annual
Needle Template and Electronic Grid Alignment	Attach template to probe. Insert a needle through a grid hole, into a water bath. Compare to the electronic grid.	3 mm	Annual
Treatment Planning Computer	Measure a known volume in a phantom with planning software	5%	At Acceptance

CT

- **Most commonly available imaging modality for treatment planning in radiation oncology**
 - Relatively fast
 - 3D (and 4D) by collection of 2D slices (partial volume)
 - Electronic density can be obtained (must be calibrated!)
 - Bone, air, bladder, rectum: OK
 - Excellent resolution in the transverse plane
 - Material maps possible for DE/ME-CT
- Resolution limited along the scan axis: needle tips?
- Not very good for soft tissue
- Metal will produce artefacts
- Large patients will create artefacts

CT QA/QC Program

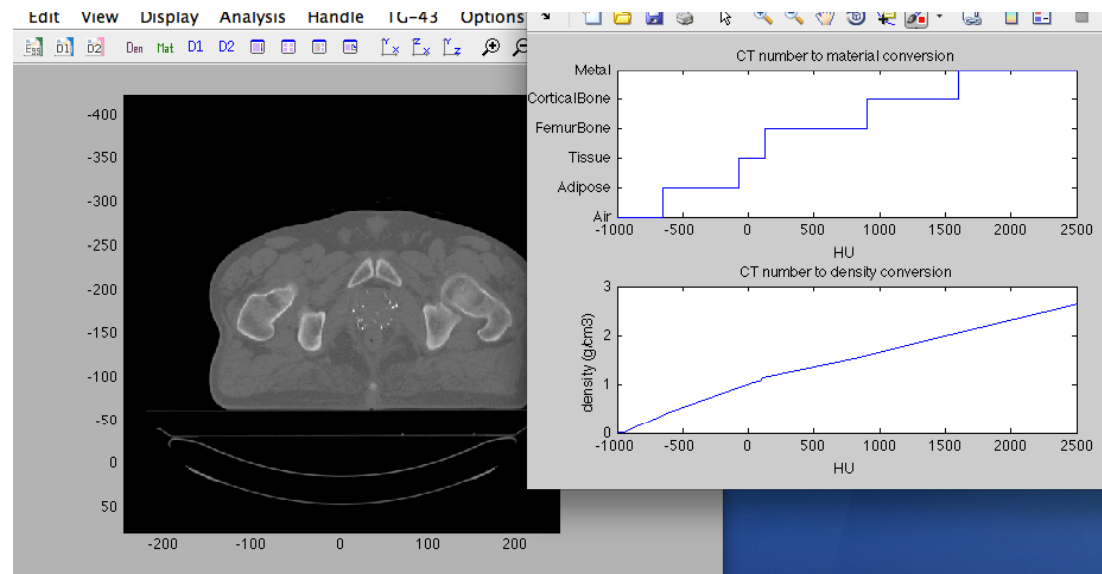
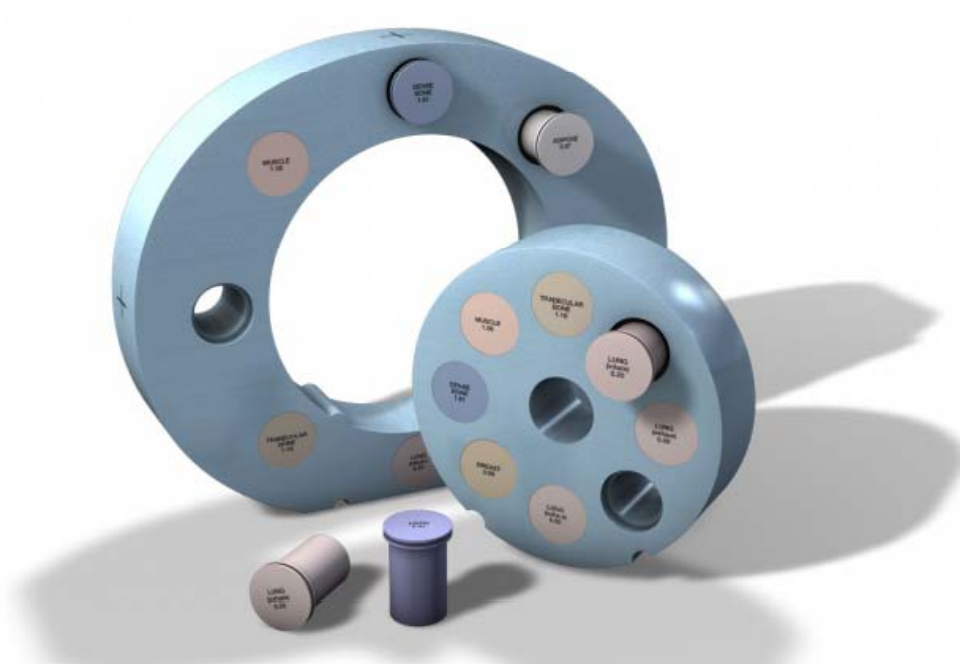
TABLE 14.2 Overview of Tests for CT for Use in Brachytherapy

Check	Frequency	Tolerance
Table vertical and longitudinal motion	Monthly	± 1 mm over the range of table motion
Table indexing and position	Annually	± 1 mm over the scan range
CT number accuracy	Monthly	For water, 0 ± 5 HU (*)
Electron density to CT number conversion	Annually	Consistent with commissioning results
Visibility of clinically applied seeds, tubes, catheters	At commissioning	
Reconstruction of applicators	At commissioning	

Note: Most of the checks taken from Mutic et al. (2003).

*This value is for external beam planning algorithms.

CT QA/QC Program



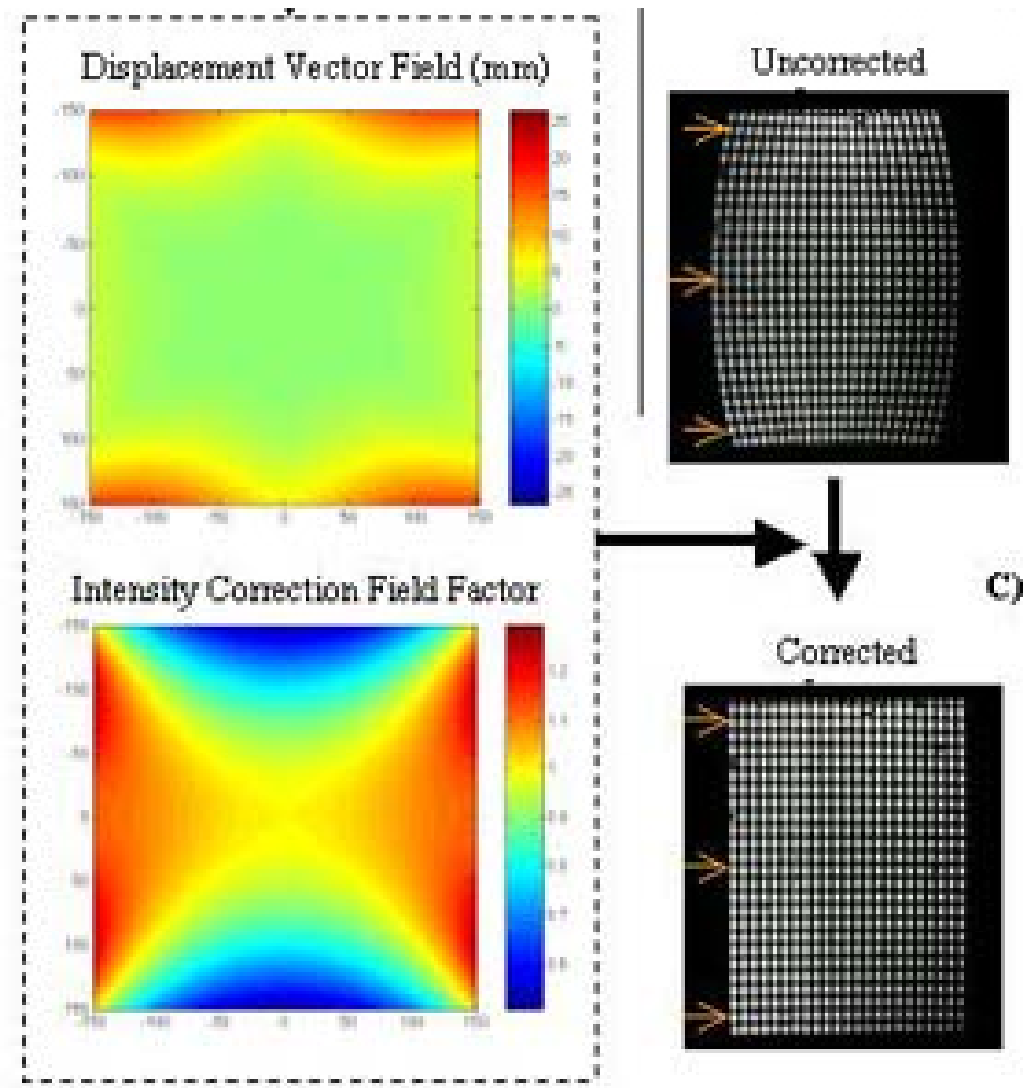
MRI

- **Best soft tissue definition**
 - Gold standard for most pelvic sites
 - 3D image acquisition
 - Good resolution in all planes (isotropic 1 mm voxel size possible!)
 - Large choice of sequences
 - Specific QA/QC to make sure image sets from various sequences are not spatially shifted!
 - Functional MRI possible
 - Specific QA/QC must be implemented
 - Real-time MRI...

MRI

- **Bone/Air definition poor**
- **Must have compatible catheters and applicators**
 - May still need CT to get localization
 - Issue with prosthesis and dental work
- **No electron density (might not be an issue for high energy brachytherapy, ^{192}Ir and over)**
- **Distortions: non-homogeneity of main magnetic field across the volume, spatial non-linearity of gradients.**
- **Voxel size and proton density: related to strength of signals**
- **Partial volume effect**
- **Chemical-shift artefacts; Motion artefacts; Field of view artefacts; RF artefacts**

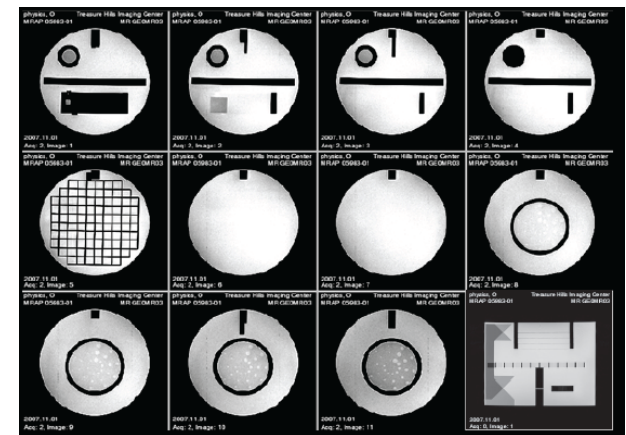
MRI QA/QC Program



MRI QA/QC Program

The ACR magnetic resonance accreditation phantom (ACR MRAP) has been designed to examine a broad range of instrument parameters. These include:

- Geometric Distortion
- Spatial Resolution
- Slice thickness and position
- Interslice Gap
- Estimate of Image Bandwidth
- Low Contrast Detectability
- Image Uniformity
- Signal-to-Noise Ratio (SNR)
- Physical and Electronic Slice Offset
- Landmark



Phantom test guidance for the ACR MRI accreditation program. American College of Radiology, Reston, 1998; MRI quality control manual. American College of Radiology, Reston, 2000

MRI QA/QC Program

TABLE 14.4 Brachytherapy-Specific Checks of MRI

Check	Frequency	Tolerance
Image distortion in all three orthogonal main viewing planes		<2%
Slice thickness test		Within 10% for SE sequences for 5 mm or thicker slices
Check MRI safety of applicator materials	Before first use	
Check of visibility of the clinically applied seeds, tubes, and/or catheters, marker wires	Before first use	
Check of reconstruction of the applicator according to library definition (differences in assumed library data and reality; if not done so for CT)	Before first use	

Note: Details of tests can be found in the recent AAPM update report by Jackson et al. (2010).

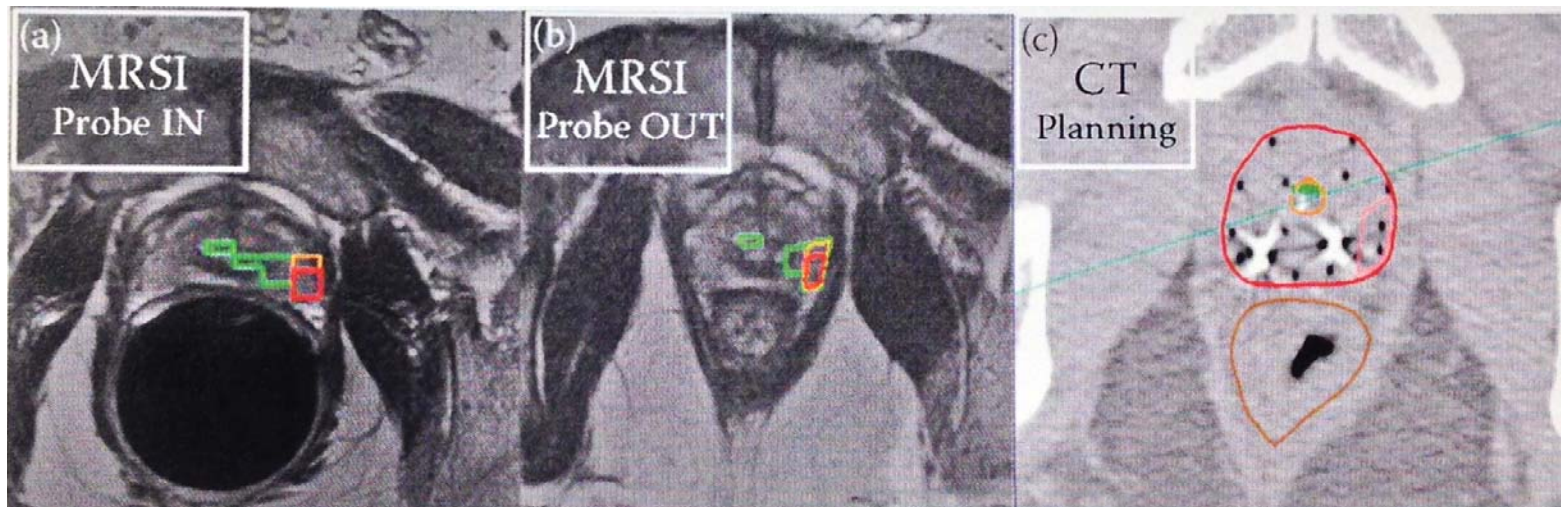
PET/SPECT

- **Functional information**
- **Help in defining targets(?)**
- **Must be used in conjunction with another imaging modality**

- **Flood-field uniformity,**
- **Spatial resolution and linearity**
- **Uncertainty:**
 - **Reconstruction method, attenuation correction, calibrations, noise, scatter, random and dead-time corrections**
 - **patient related: dose, motion, weight, patient activity prior and during uptake, blood glucose level**
 - **Radiotracer: uptake period, injection vs calibration, residual activity in syringe, injection method**
 - **Image analysis: partial volume correction, analysis software, ROI definition, SUV definition**

PET QA/QC program

- NEMA, NU 2-2001 std for basic QA/QC
- EB Sokole et al., EJNNMI 2010;37:662-671 and 672-681
- RT specific: Mutic et al, Phys. Med 2003;30:2762-92
- Related image fusion issues
 - Coordinate system and registration
 - Different image resolution
 - Deformation between imaging modalities (from various origins)



G Reed et al., J. Contemp Brachy 2011;1: 26-31

Unsolved issues

- **True organ/structure shape and volume**
 - May change with time
- **Functional imaging for brachytherapy**
 - How std are SUVs?
- **Deformable registration**
 - Algorithms matter: Kirby N *et al.*, Med Phys 40, 2013.
 - QA/QC program?
- **Real-time procedures**
 - Secondary check of contours, dosimetry, ... ?

Physics Contribution

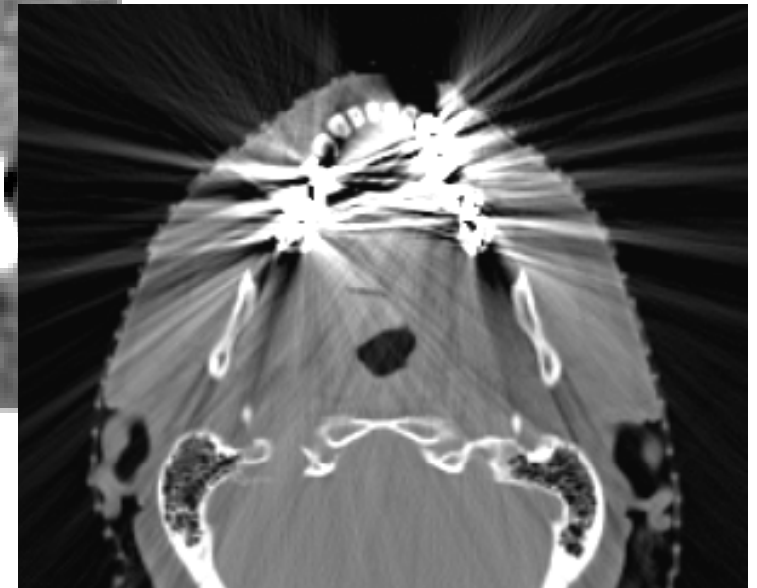
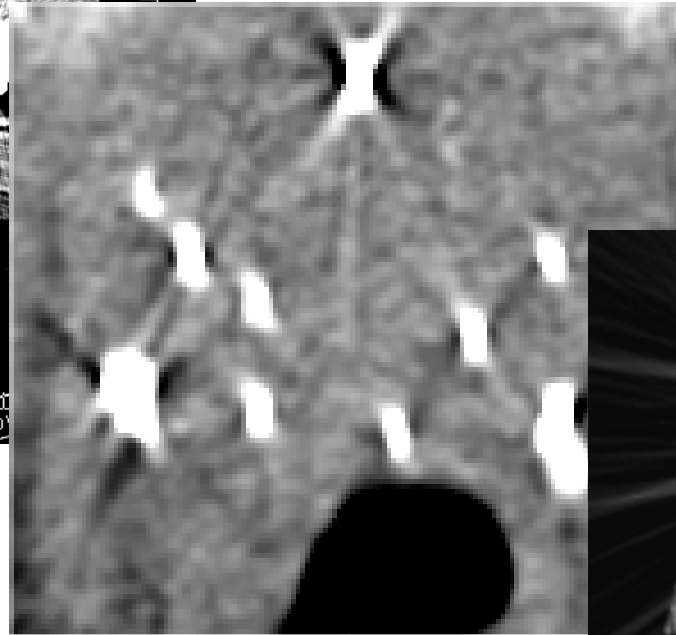
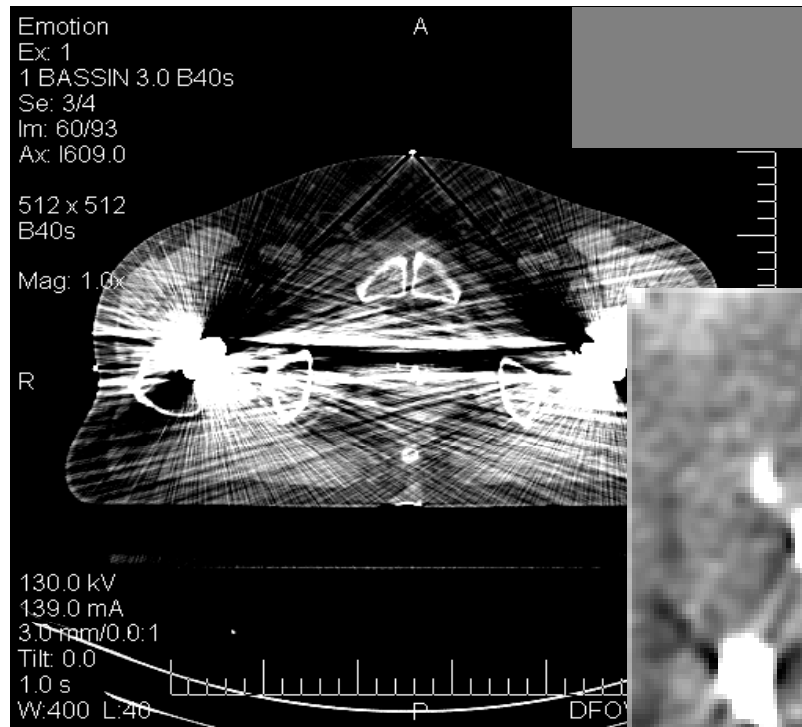
Toward Magnetic Resonance—Only Simulation: Segmentation of Bone in MR for Radiation Therapy Verification of the Head

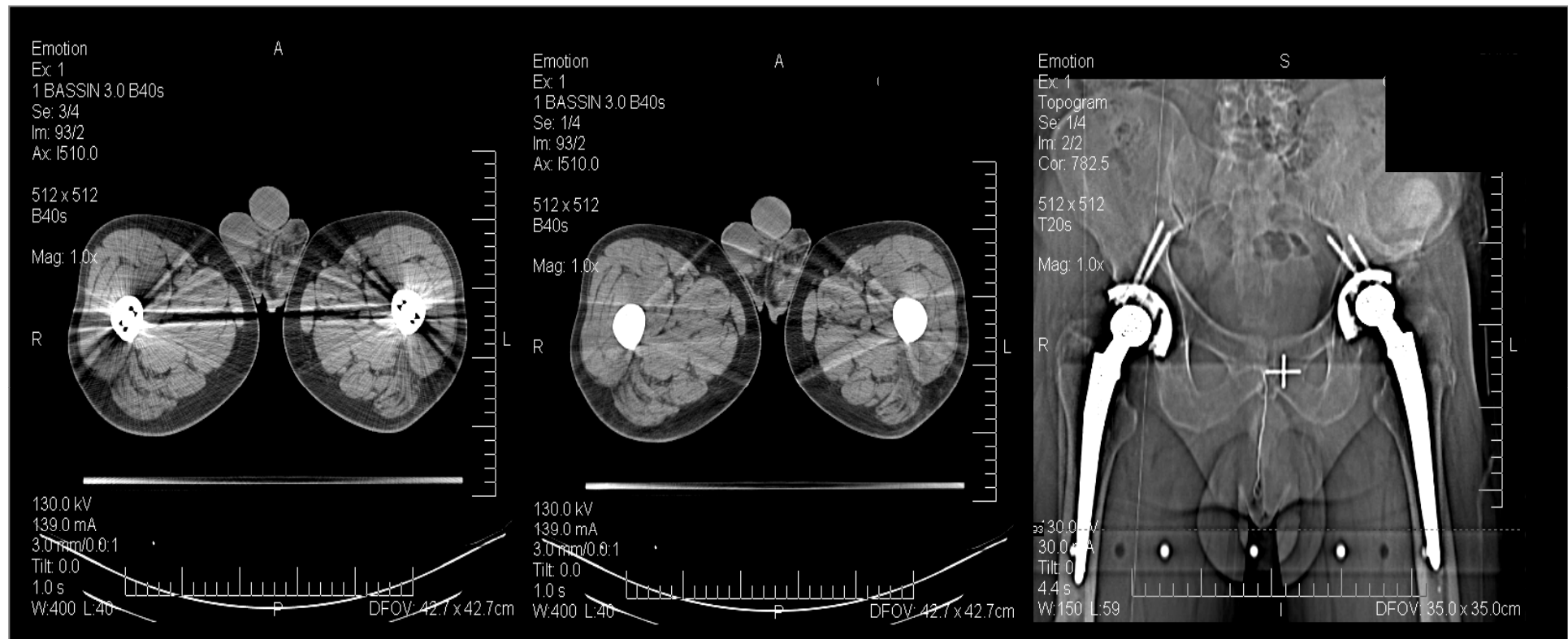
Huan Yu, PhD,^{*} Curtis Caldwell, PhD,^{†,‡,§} Judith Balogh, MD,^{||,¶} and
Katherine Mah, MSc^{*,¶}

*Departments of *Medical Physics and ^{||}Radiation Oncology, Odette Cancer Centre and [‡]Medical Imaging at Sunnybrook Health Science Center, Toronto, ON, Canada; and Departments of [†]Medical Biophysics, [§]Medical Imaging, and [¶]Radiation Oncology, University of Toronto, Toronto, ON, Canada*

Received Nov 8, 2013, and in revised form Feb 10, 2014. Accepted for publication Mar 6, 2014.

CT artefacts





Artefacts

MAR

Topogram

Yazdi M, Gingras L, Beaulieu L. *Int J Radiat Oncol Biol Phys* 2005;62(4):1224–31.

CT artefacts

- **Software solutions available from:**

- **Philips (Big Bore product line) O-MAR**

- <http://www.usa.philips.com/healthcare/product/HCNCTB107/brilliance-ct-big-bore-ct-simulator>

- **GE Smart Metal Artefact Reduction:**

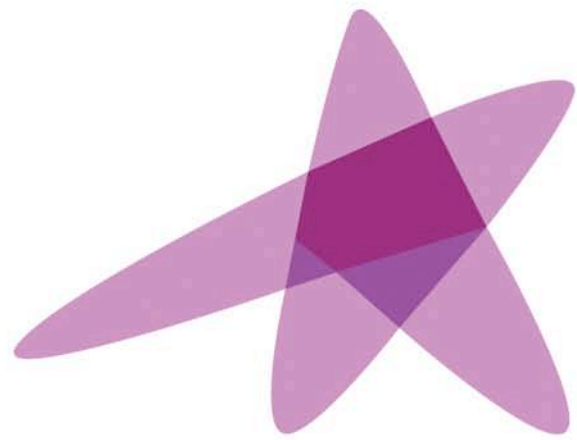
- [http://www3.gehealthcare.com/en/Products/Categories/Computed Tomography/Radiation Therapy Planning/Metal Artifact Reduction](http://www3.gehealthcare.com/en/Products/Categories/Computed_Tomography/Radiation_Therapy_Planning/Metal_Artifact_Reduction)

- **Siemens iMAR - iterative Metal Artifact Reduction:**

- <https://www.healthcare.siemens.com/computed-tomography/options-upgrades/clinical-applications/imar>

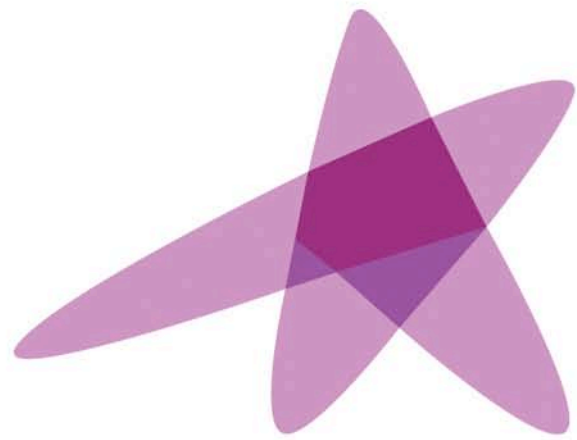
Conclusion

- 3D imaging modalities are essential for modern brachytherapy
- Adequate QA/QC program is necessary for
 - Accurate localization of sources and applicators
 - Contouring (large uncertainties still remaining)
 - Dose calculation
- Brachytherapy moved to 3D is recent but multi-modality imaging is already at our door
 - Deformable registration
 - Quantitative functional imaging



ESTRO

School



ESTRO
School

Advanced Brachytherapy Physics

Catheter/Applicator and Source Localisation using 3D Imaging

Prof. Mark J. Rivard, Ph.D., FAAPM

Advanced Brachytherapy Physics, 29 May – 1 June, 2016

Disclosures

There are no conflicts-of-interest to report.

Opinions herein are solely those of the presenter, and are not meant to be interpreted as societal guidance.

Specific commercial equipment, instruments, and materials are listed to fully describe the necessary procedures. Such identification does not imply endorsement by the presenter, nor that these products are necessarily the best available for these purposes.

Learning Objectives

1. Goal of brachytherapy reconstruction
2. History of reconstruction methods
3. Areas to concern for commissioning
4. Recent literature summary

Goal of Brachytherapy Reconstruction

**accurately identify position of radiation field
relative to tumor (and healthy) tissues**

Goal of Brachytherapy Reconstruction

accurately identify position of radiation field relative to tumor (and healthy) tissues

Tasks of Brachytherapy Reconstruction

**accurately identify position of sources
(markers or applicators) relative to contours**

Historical Reconstructions Methods in Brachytherapy

1. Orthogonal x rays

2. Stereo shifts (table/couch or x-ray tube)

3. Fluoroscopy

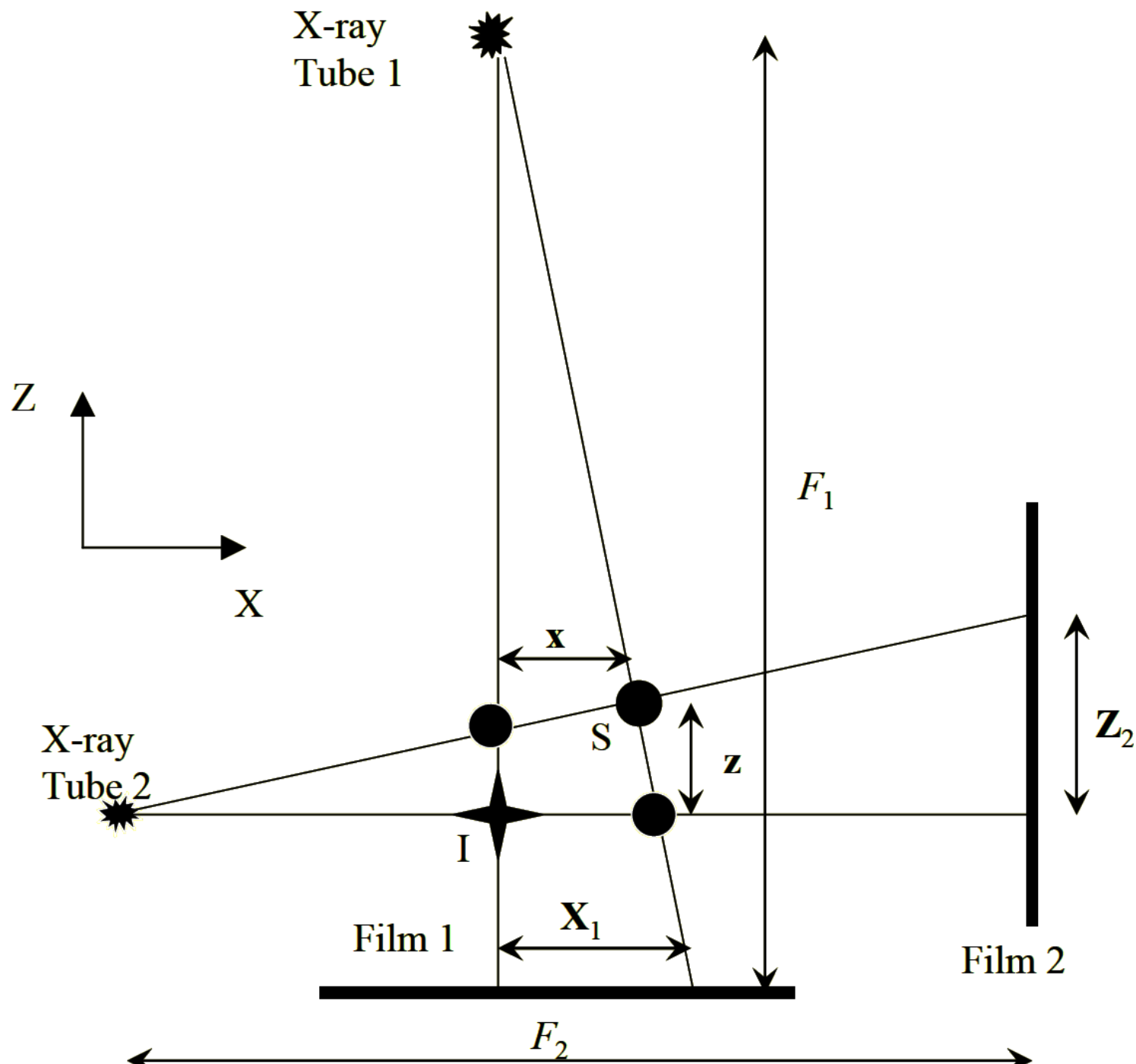
Historical Reconstructions Methods in Brachytherapy

1. Orthogonal x rays

2. Stereo shifts (table/couch or x-ray tube)

3. Fluoroscopy

Orthogonal X Rays for Brachytherapy Reconstructions



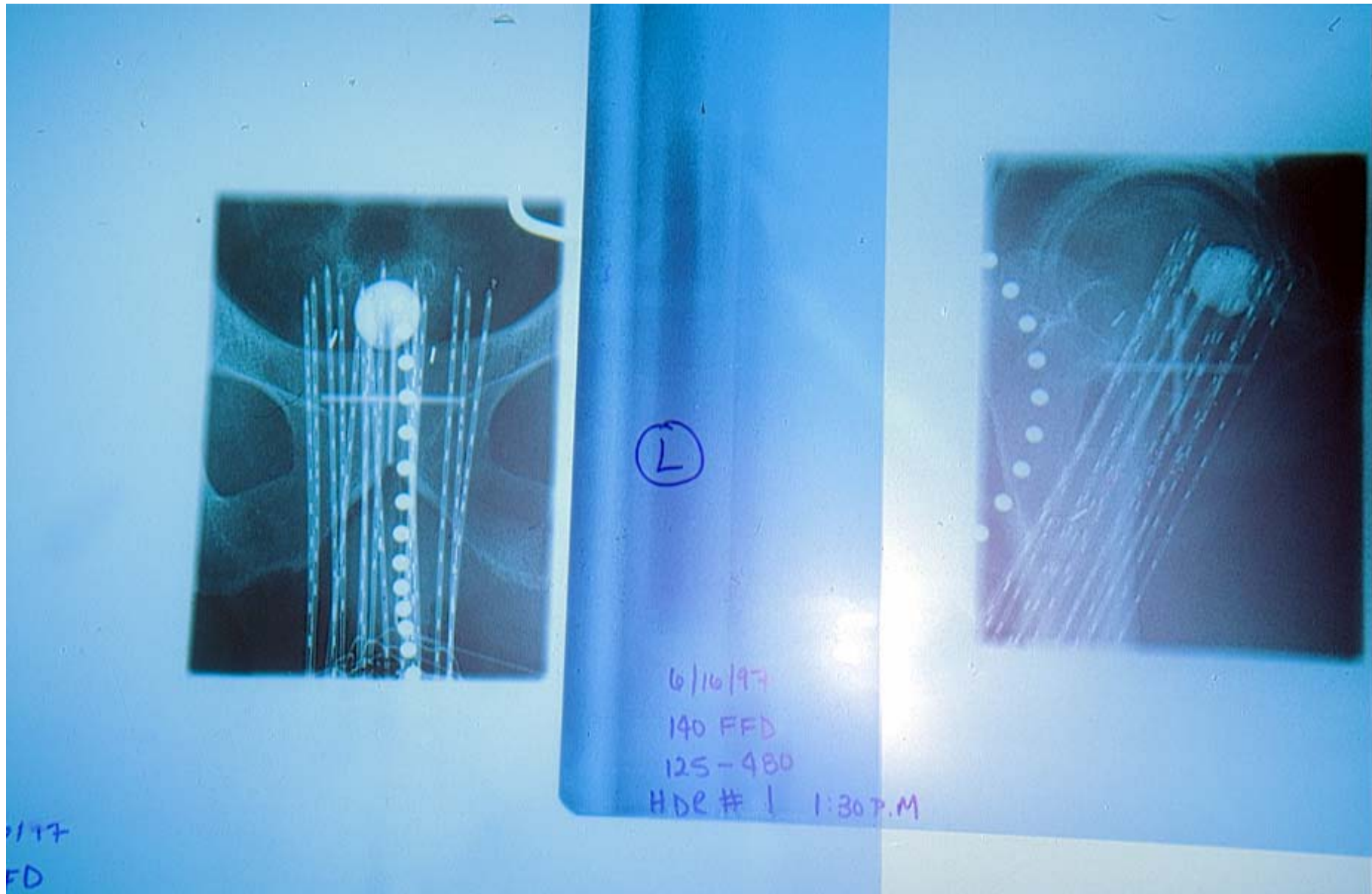
courtesy Eugene Lief, 2005 AAPM + ABS Summer School



courtesy Aronowitz & Rivard, *J. Contemp. Brachy.* 6, 185-190 (2014)



Orthogonal X Rays for Brachytherapy Reconstructions



courtesy Eugene Lief, 2005 AAPM + ABS Summer School

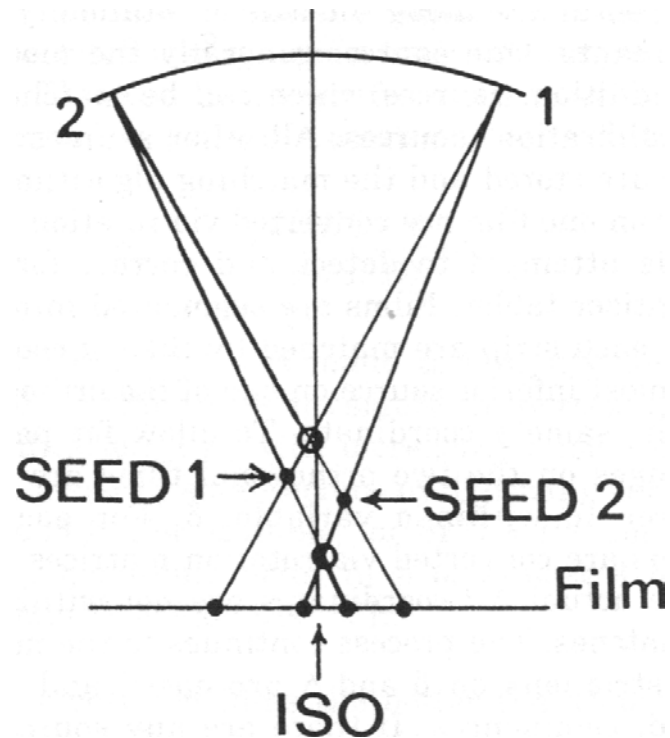
Historical Reconstructions Methods in Brachytherapy

1. Orthogonal x rays

2. Stereo shifts (table/couch or x-ray tube)

3. Fluoroscopy

Stereo Shift Method: Film Based



Properties of treatment planning systems for the following aspects of source localization. A = average magnification; G = geometric reconstruction

1. has the orthogonal film method for point sources
2. has the orthogonal film method for line sources
3. has the stereo shift method for point sources
4. has the stereo shift method for line sources
5. has an automatic source matching algorithm
6. has other localization methods (e.g. isocentric arbitrary angle, reconstruction jigs, etc.)

System	1	2	3	4	5	6
ADAC	A	A	G	G	A	yes
CMS	A	A	G	G	A	no
Theratronics	A,G	A,G	G	G	A	no
GE	A	A	G	G	A	no
ROCS	A	A	A,G	no	no	yes
Nucletron	A	A	A,G	A,G	no	yes
GammaDot	A	A	G	G	no	yes
Prowess	A	A	G	G	no	no

Stereo Shift Method: Film Based

F.M. Khan (1994)
*The Physics of
 Radiation Therapy*

The stereo-shift method of source localization consists of taking two radiographs of the same view but the patient or the x-ray tube is shifted a certain distance (e.g., 20 cm) between the two exposures. The principle of the method is illustrated in Figure 15.20. Suppose both films are AP, parallel to the x - y plane of the patient as the tube is shifted in the y direction between films. A tabletop fiducial marker is used to serve as origin at O . Because the x , y coordinates of a point source or a source end can be obtained from either of the films, the z coordinates can be derived as follows. Let

- P = point to be localized three dimensionally
- y_1 = distance between images of P and O on the first film
- y_2 = distance between images of P and O on the second film
- s = film shift in the origin O due to tube shift
- d = tube shift distance
- F = target-to-film distance
- f = table-to-film distance

From similar triangles APB and CPD

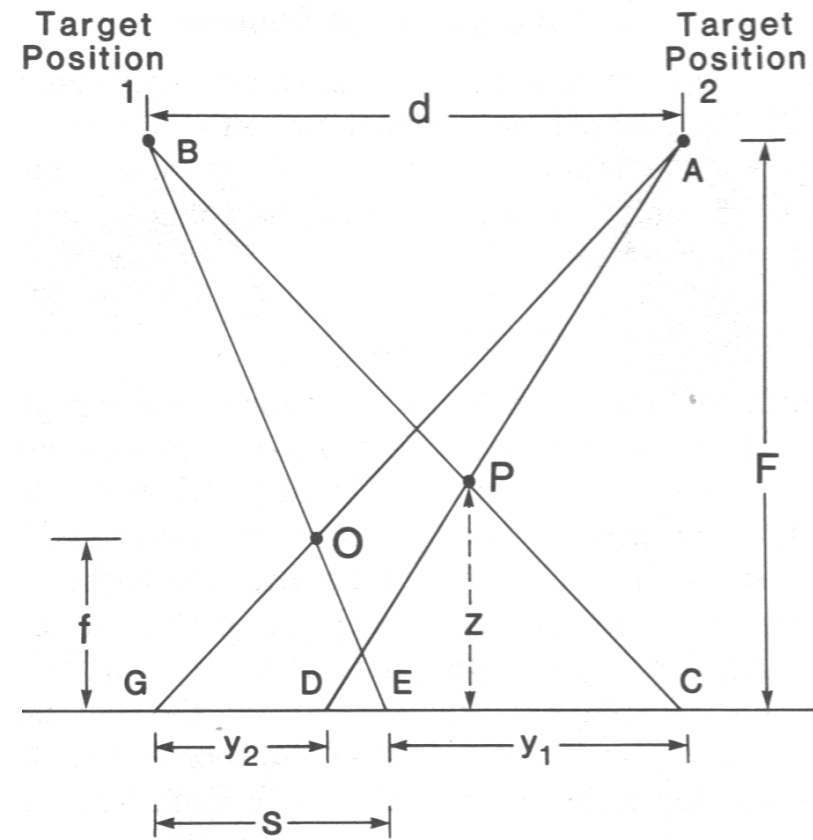
$$\frac{d}{y_1 + s - y_2} = \frac{F - z}{z}$$

Also, from similar triangles AOB and EOG

$$\frac{d}{s} = \frac{F - f}{f}$$

From Equations 15.25 and 15.26, we get

$$z = F \frac{(F - f)(y_2 - y_1) - d \cdot f}{(F - f)(y_2 - y_1) - d \cdot F}$$



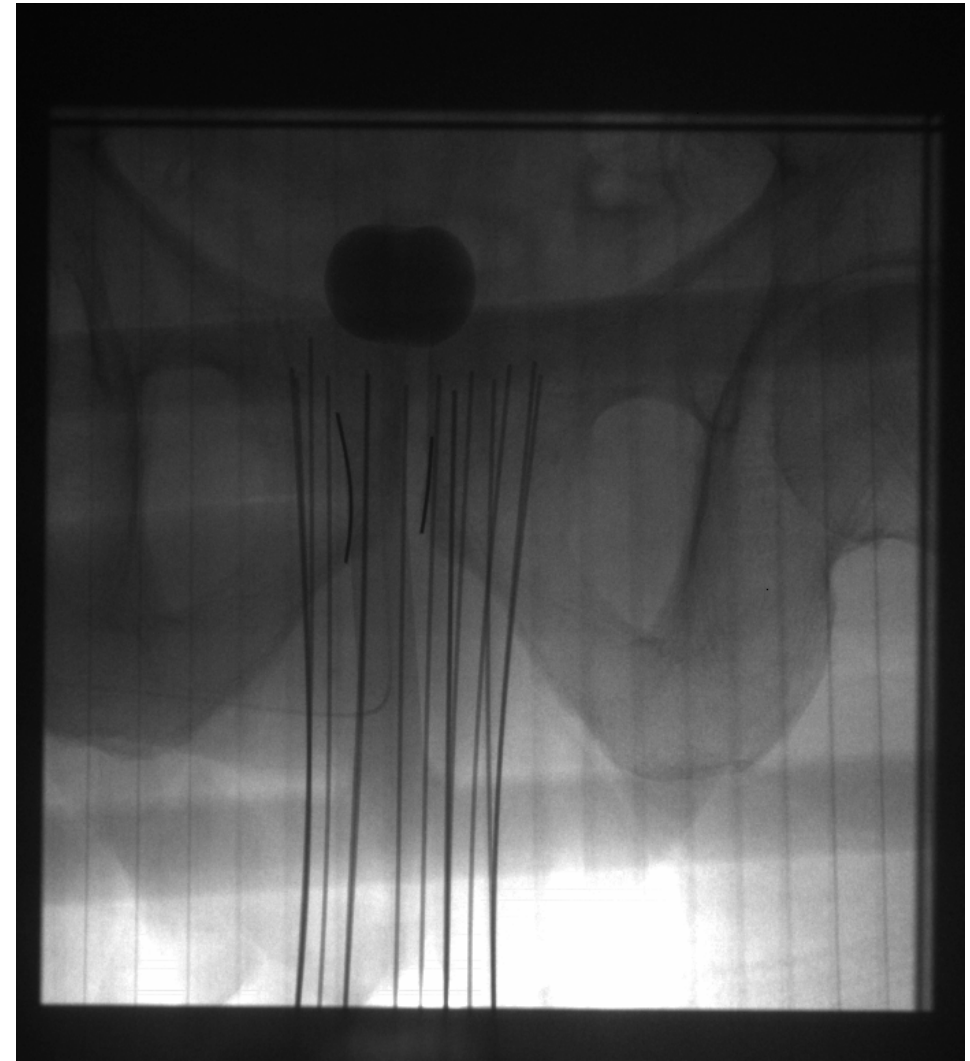
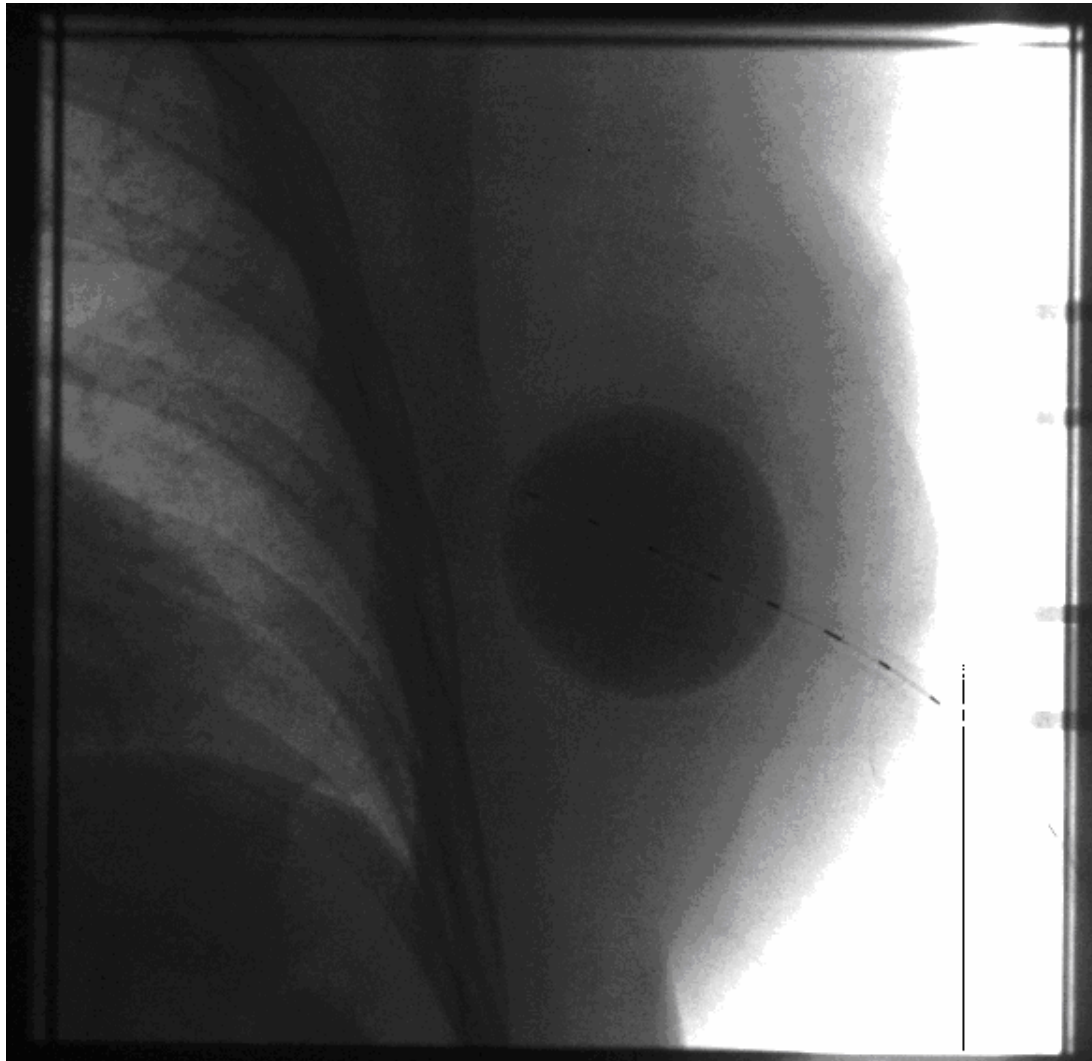
Historical Reconstructions Methods in Brachytherapy

1. Orthogonal x rays

2. Stereo shifts (table/couch or x-ray tube)

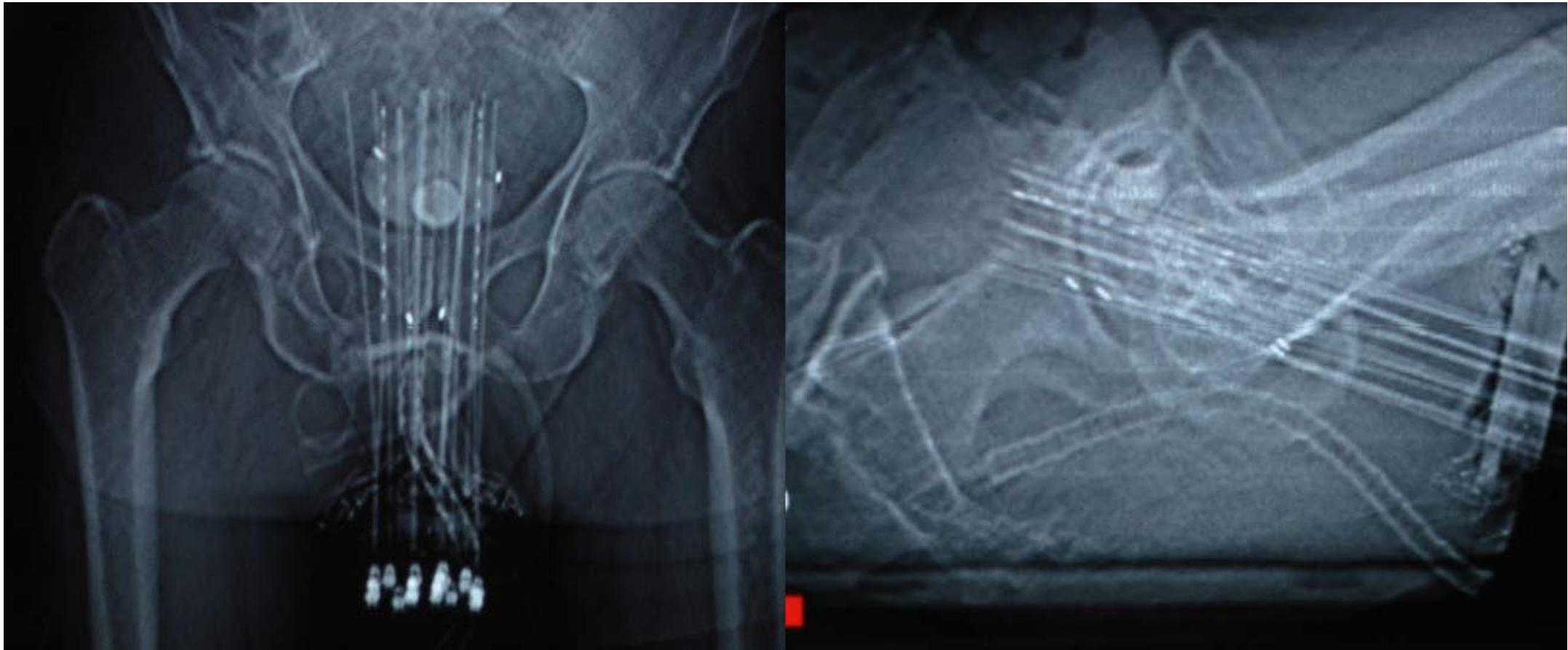
3. Fluoroscopy

Fluoroscopy for Brachytherapy Reconstructions



courtesy Eugene Lief, 2005 AAPM + ABS Summer School

Fluoroscopy for Brachytherapy Reconstructions



AP

LAT

courtesy Eugene Lief, 2005 AAPM + ABS Summer School

Historical Reconstructions Methods in Brachytherapy

1. Orthogonal x rays

Strengths high spatial resolution (< 0.5 mm)
less susceptible to high-Z artifacts than CT

Weaknesses not suitable for dozens of seeds
planar representation of 3D anatomy
limited by magnification uncertainty

2. Stereo shifts (table/couch or x-ray tube)

Strengths good spatial resolution (~ 1 mm)

Weaknesses highly sensitive to uncertainties in shift direction
limited perspective

3. Fluoroscopy

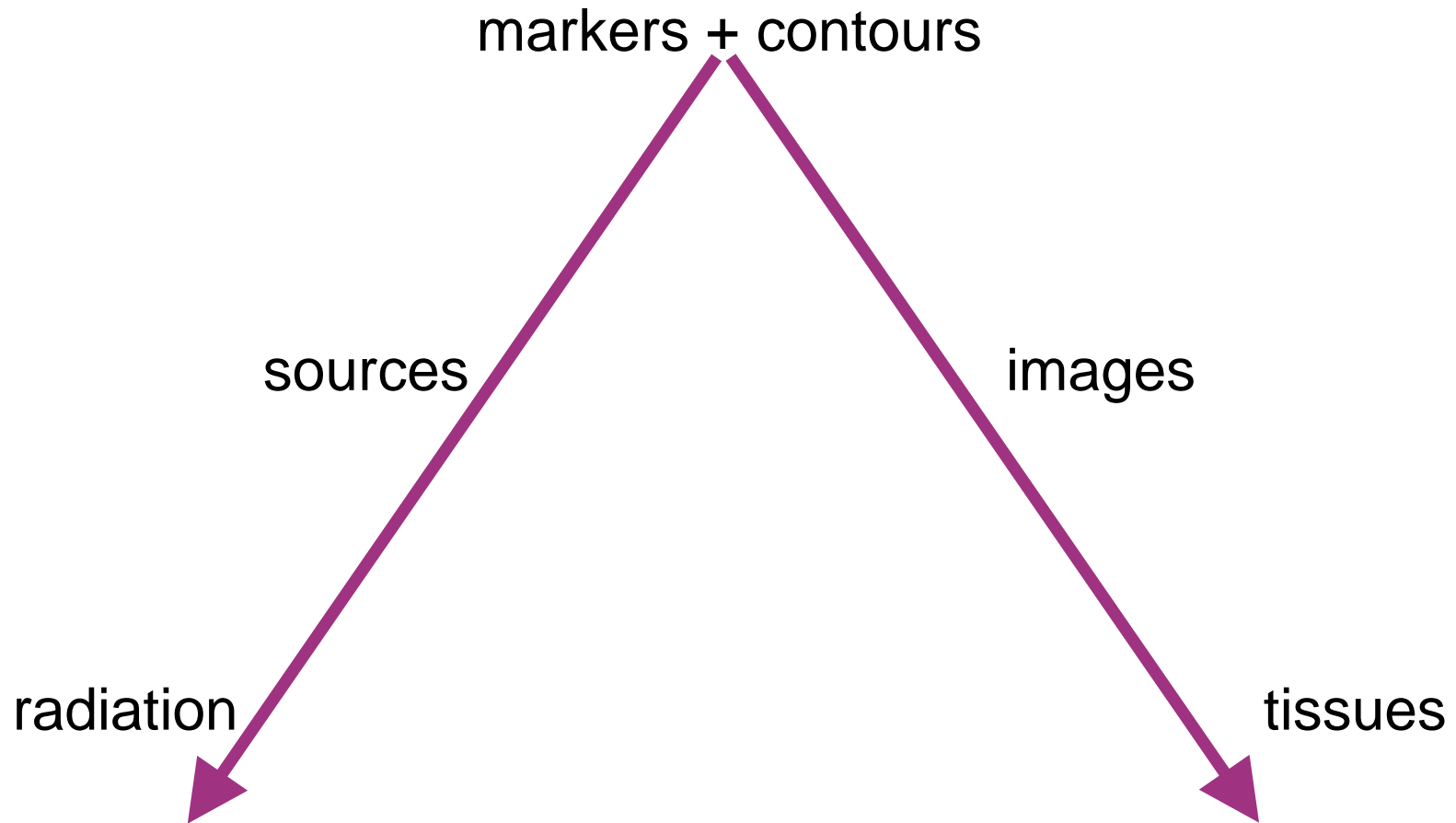
Strengths practical for intraoperative imaging

Weaknesses crude 3D representation

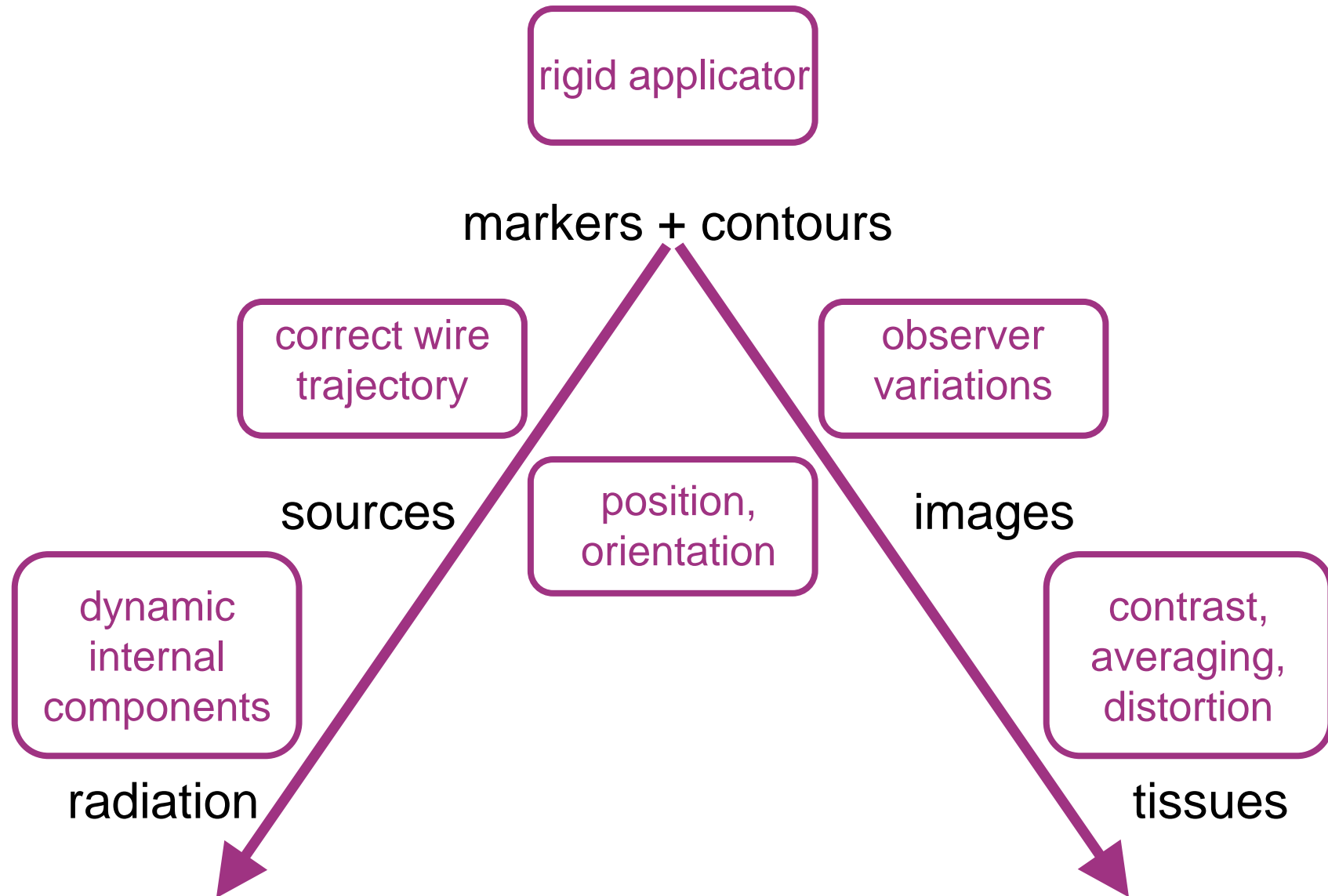
Tasks of Brachytherapy Reconstruction

**accurately identify position of sources
(markers or applicators) relative to contours**

Assumptions of 3D Brachytherapy Reconstruction

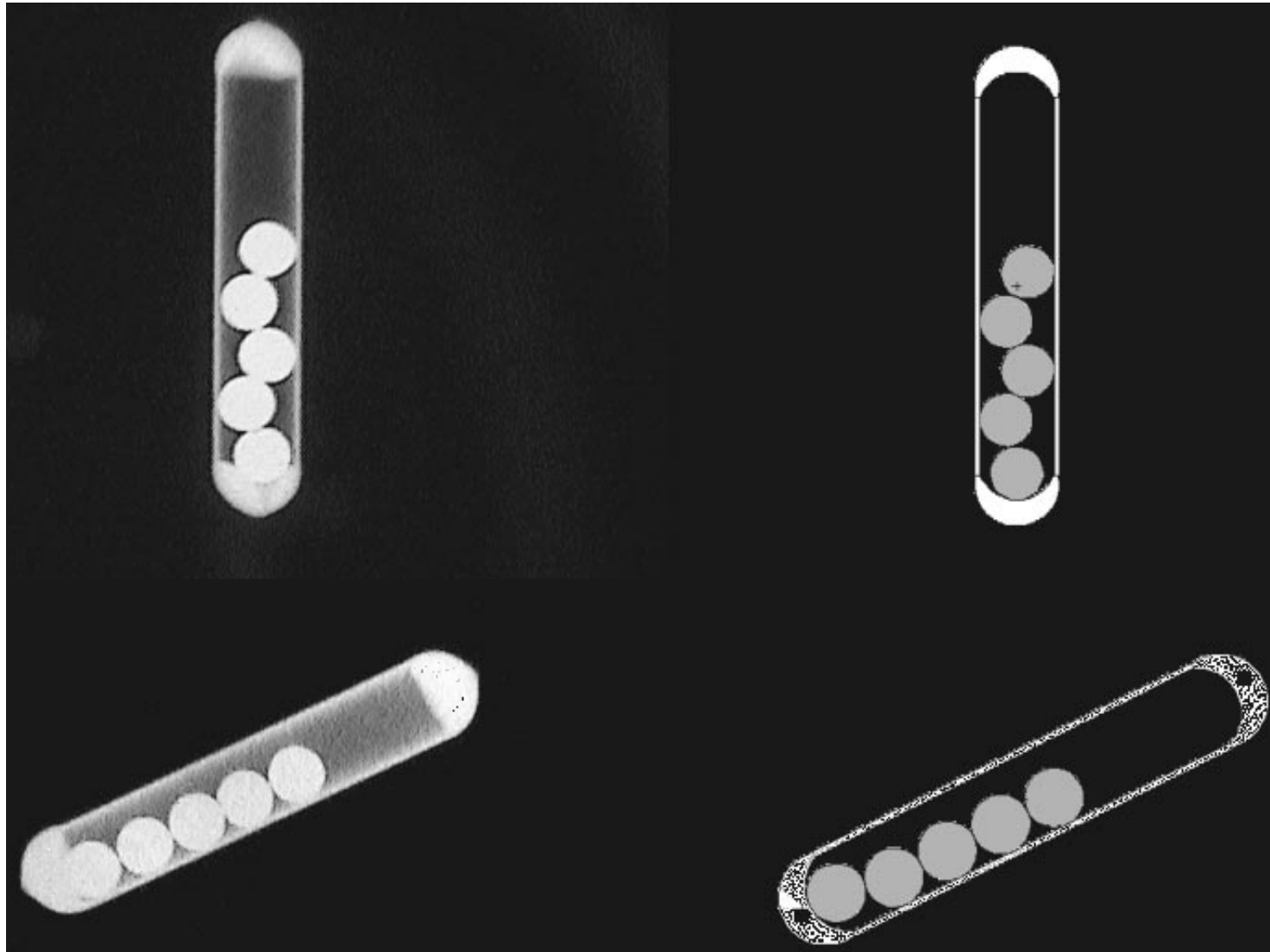


Assumptions of 3D Brachytherapy Reconstruction



Test Assumptions: Reconstruction Commissioning

- source dynamic internal components
 - > 1 mm for some LDR sources



Automatic Seed Reconstruction: Threshold-Based Automatic localization of implanted seeds from post-implant CT images

Haisong Liu¹, Gang Cheng¹, Yan Yu¹, Ralph Brasacchio¹,
Deborah Rubens², John Strang², Lydia Liao² and Edward Messing³

¹ Department of Radiation Oncology, University of Rochester, 601 Elmwood Avenue, Rochester, NY 14642, USA

² Department of Radiology, University of Rochester, 601 Elmwood Avenue, Rochester, NY 14642, USA

³ Department of Urology, University of Rochester, 601 Elmwood Avenue, Rochester, NY 14642, USA

Received 18 December 2002, in final form 5 March 2003

Published 22 April 2003

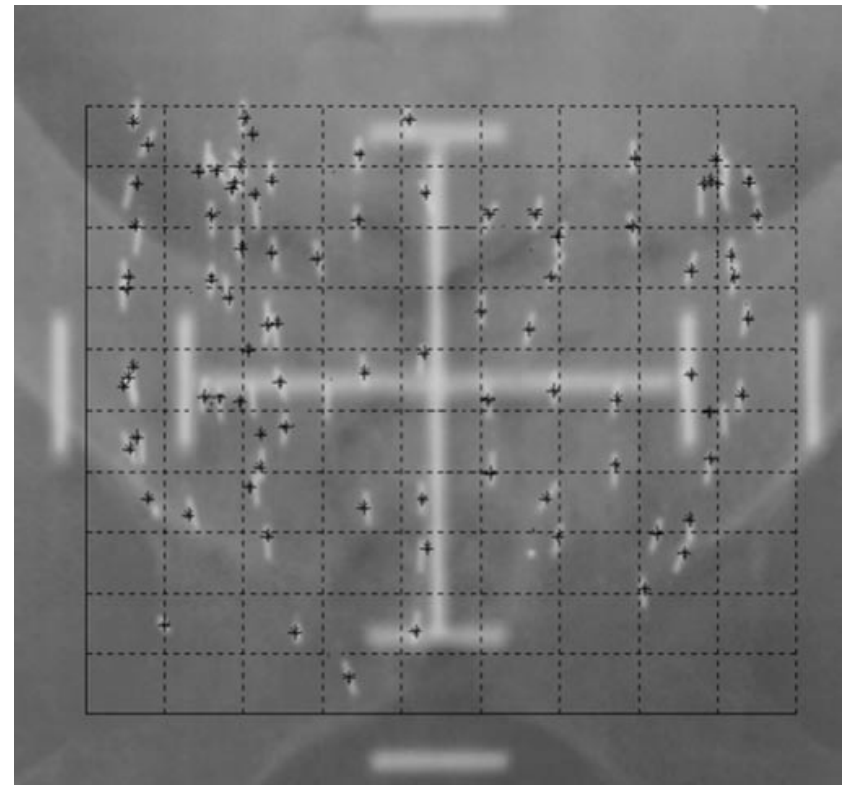
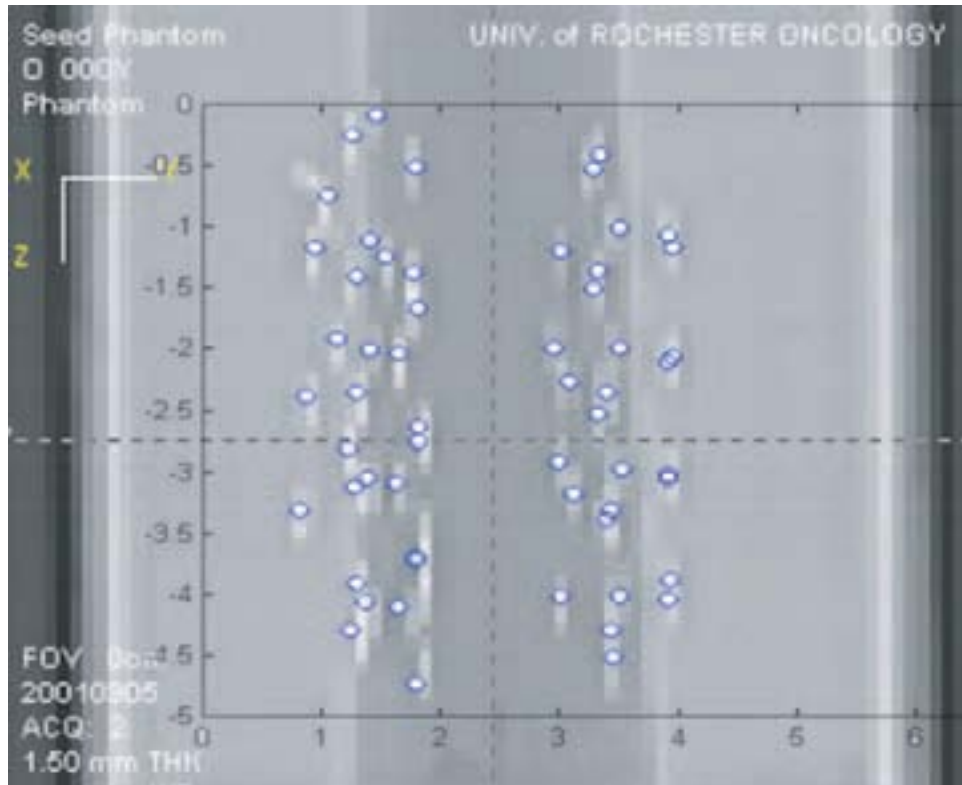
Online at stacks.iop.org/PMB/48/1191

Abstract

An automatic localization method of implanted seeds from a series of post-implant computed tomography (CT) images is described in this paper. Post-implant CT studies were obtained for patients who underwent prostate brachytherapy. Bright areas were segmented using binary thresholding in each CT slice, and geometrical information on these areas was collected. Large areas (possibly containing two connected seeds) were split into smaller ones by geometry-based filtering in each slice. The area connectivity along the longitudinal direction was analysed using a geometry-based connection search algorithm executed on every area slice by slice, so that the connected areas were combined into one object. The weighted centroid of each object was taken as the seed position. This method was tested on a seed-containing prostate phantom as well as using CT studies from patients. Statistical analysis demonstrates that it can achieve above 99% detection rate with reliable localization accuracy and high speed. It is reliable and convenient for localizing implanted seeds on CT and can be used to assist post-implant dosimetry for prostate brachytherapy.

Liu, et al., *Phys. Med. Phys.* 48, 1191-1203 (2003)

Automatic Seed Reconstruction: Threshold-Based



99% seeds identified,
3 mm localization error

Table 1. Distances between corresponding coordinates comparing the two-film technique with the automated method using 1 and 3 mm CT of two patients.

	Minimum (mm)	Maximum (mm)	Average (mm)
1 mm CT vs film (patient 1)	0.17	5.37	2.65
3 mm CT vs film (patient 1)	0.26	6.41	2.99
1 mm CT vs 3 mm CT (patient 1)	0.12	0.32	0.17
3 mm CT vs film (patient 2)	0.26	7.46	3.10

Automatic Seed Reconstruction: Hough Transform

An automatic seed finder for brachytherapy CT postplans based on the Hough transform

E. J. Holupka^{a)} and P. M. Meskell

Department of Radiation Therapy, Beth Israel Deaconess Medical Center, Harvard Medical School, Boston, Massachusetts 02115

E. C. Burdette

Computerized Medical System, Inc., Corporate Park Centre, 2110 Clearlake Boulevard, Suite 102, Champaign, Illinois 61822

I. D. Kaplan

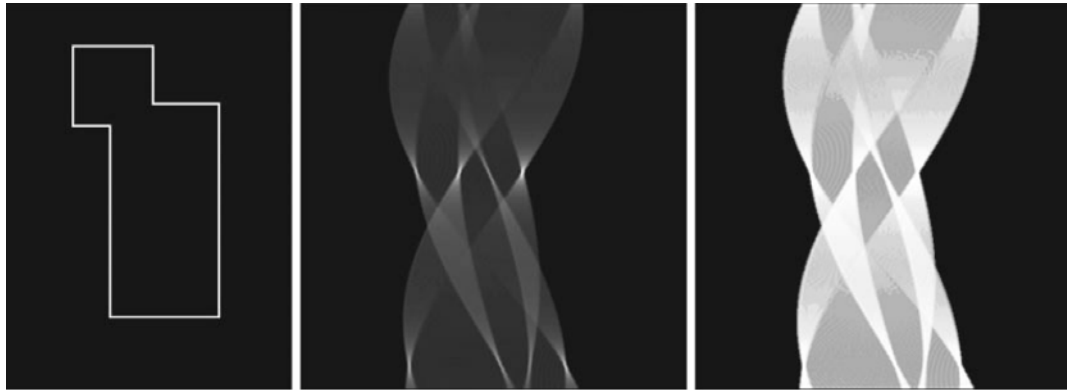
Department of Radiation Therapy, Beth Israel Deaconess Medical Center, Harvard Medical School, Boston, Massachusetts 02115

(Received 1 August 2003; revised 11 June 2004; accepted for publication 12 June 2004; published 27 August 2004)

Purpose: The purpose of the work is to describe a new algorithm for the automatic detection of implanted radioactive seeds within the prostate. The algorithm is based on the traditional Hough transform. A method of quality assurance is described as well as a quantitative phantom study to determine the accuracy of the algorithm. **Methods and Materials:** An algorithm is described which is based on the Hough transform. The Hough transform is a well known transform traditionally used to automatically segment lines and other well defined geometric objects from images. The traditional Hough transform is extended to three-dimensions and applied to CT images of seed implanted prostate glands. A method based on digitally reconstructed radiographs is described to quality assure the determined three-dimensional positions of the detected seeds. Two phantom studies utilizing eight seeds and nine seeds are described. All eight seeds form a contiguous square while the nine seed phantom describes seeds which are placed side-by-side in groups of two and three. The algorithm is applied to the CT scans of both phantoms and the seed positions determined. **Results:** The algorithm has been commercially developed and used to perform post-surgical dosimetric assessment on approximately 1000 patients. Using the described quality assurance tool it was determined that the algorithm accurately determined the seed positions in all 1000 patients. The algorithm was also applied to the eight seed phantom. The algorithm successfully found all eight seeds as well as their seed coordinates. The average radial error was determined to be 0.9 mm. For the nine seed phantom, the algorithm correctly identified all nine seeds, with an average radial error of 3 mm. **Conclusions:** The described algorithm is a robust, accurate, automatic, three-dimensional application for CT based seed determination. © 2004 American Association of Physicists in Medicine. [DOI: 10.1118/1.1778837]

Holupka, et al., *Med. Phys.* 31, 2672-2679 (2004)

Automatic Seed Reconstruction: Hough Transform

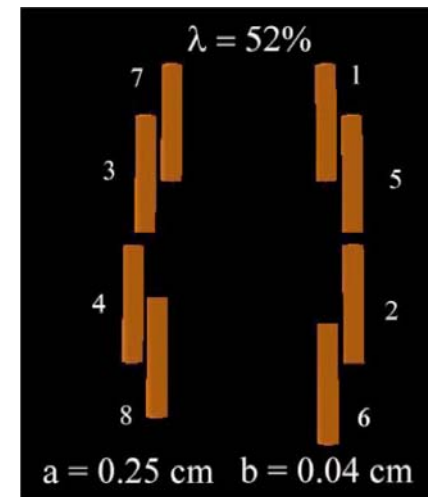


(a)

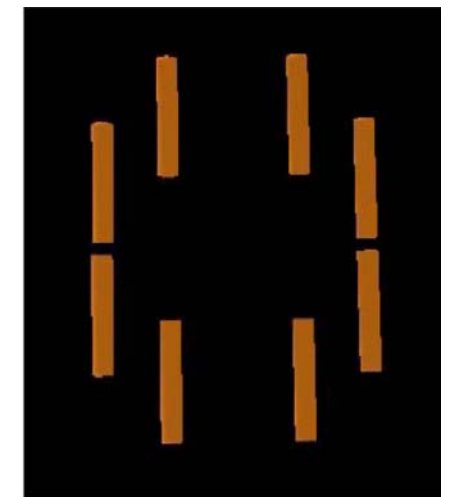
(b)

(c)

- (a) A simple binary image containing lines.
- (b) The Hough transform of the image.
- (c) The Hough transform contrasted to display the underlying structure.



(a)



(b)

- (a) Seed positions as determined by the described algorithm.
- (b) Theoretical seed coordinates. The seeds appear in the inferior to superior direction because the point dose approximation was used and **the true orientation is not needed.**

seed localization error
ranged from 1-3 mm

Seed Reconstruction Uncertainties: CT & MRI

CT- and MRI-based seed localization in postimplant evaluation after prostate brachytherapy

Marisol De Brabandere^{1,*}, Bashar Al-Qaisieh², Liesbeth De Wever³, Karin Haustermans¹, Christian Kirisits⁴, Marinus A. Moerland⁵, Raymond Oyen³, Alex Rijnders⁶, Frank Van den Heuvel¹, Frank-André Siebert⁷

¹Department of Radiation Oncology, University Hospital Gasthuisberg, Leuven, Belgium

²Department of Medical Physics and Engineering, St James's Institute of Oncology, Leeds, United Kingdom

³Department of Radiology, University Hospital Gasthuisberg, Leuven, Belgium

⁴Department of Radiotherapy, Medical University of Vienna, Comprehensive Cancer Center, Vienna, Austria

⁵Department of Radiation Oncology, University Medical Center Utrecht, Utrecht, The Netherlands

⁶Department of Radiation Oncology, Europe Hospitals, Brussels, Belgium

⁷University Hospital of Schleswig-Holstein, Clinic of Radiotherapy, Kiel, Germany

ABSTRACT

PURPOSE: To compare the uncertainties in CT- and MRI-based seed reconstruction in postimplant evaluation after prostate seed brachytherapy in terms of interobserver variability and quantify the impact of seed detection variability on a selection of dosimetric parameters for three postplan techniques: (1) CT, (2) MRI-T1 weighted fused with MRI-T2 weighted, and (3) CT fused with MRI-T2 weighted.

METHODS AND MATERIALS: Seven physicists reconstructed the seed positions on postimplant CT and MRI-T1 images of three patients. For each patient and imaging modality, the interobserver variability was calculated with respect to a reference seed set. The effect of this variability on dosimetry was calculated for CT and CT + MRI-T2 (CT-based seed reconstruction), as well as for MRI-T1 + MRI-T2 (MRI-T1-based seed reconstruction), using fixed CT and MRI-T2 prostate contours.

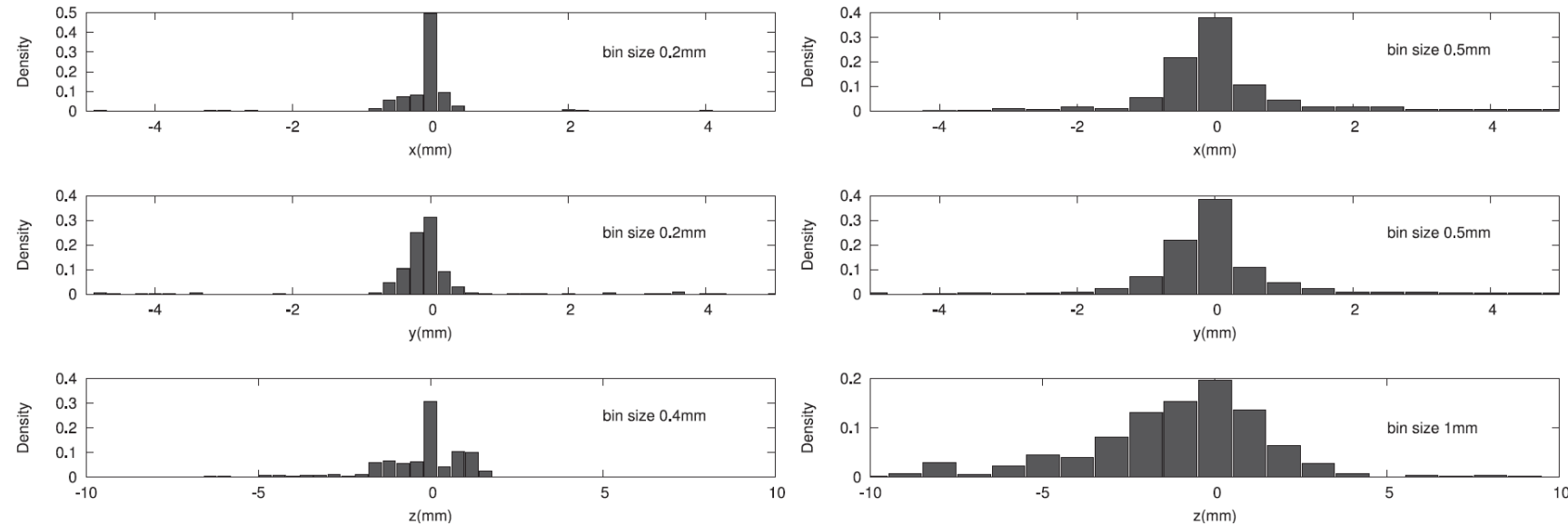
RESULTS: Averaged over three patients, the interobserver variability in CT-based seed reconstruction was 1.1 mm (1 SD_{ref} , i.e., standard deviation with respect to the reference value). The D_{90} (dose delivered to 90% of the target) variability was 1.5% and 1.3% (1 SD_{ref}) for CT and CT + MRI-T2, respectively. The mean interobserver variability in MRI-based seed reconstruction was 3.0 mm (1 SD_{ref}), and the impact of this variability on D_{90} was 6.6% for MRI-T1 + MRI-T2.

CONCLUSIONS: Seed reconstruction on MRI-T1-weighted images was less accurate than on CT. This difference in uncertainties should be weighted against uncertainties due to contouring and image fusion when comparing the overall reliability of postplan techniques. © 2013 American Brachytherapy Society. Published by Elsevier Inc. All rights reserved.

Seed Reconstruction Uncertainties: CT & MRI

CT

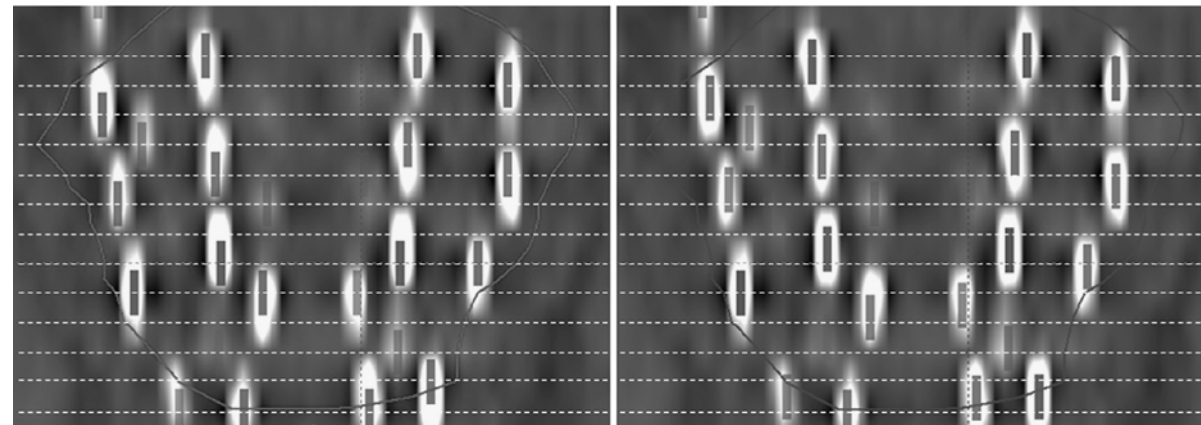
T1



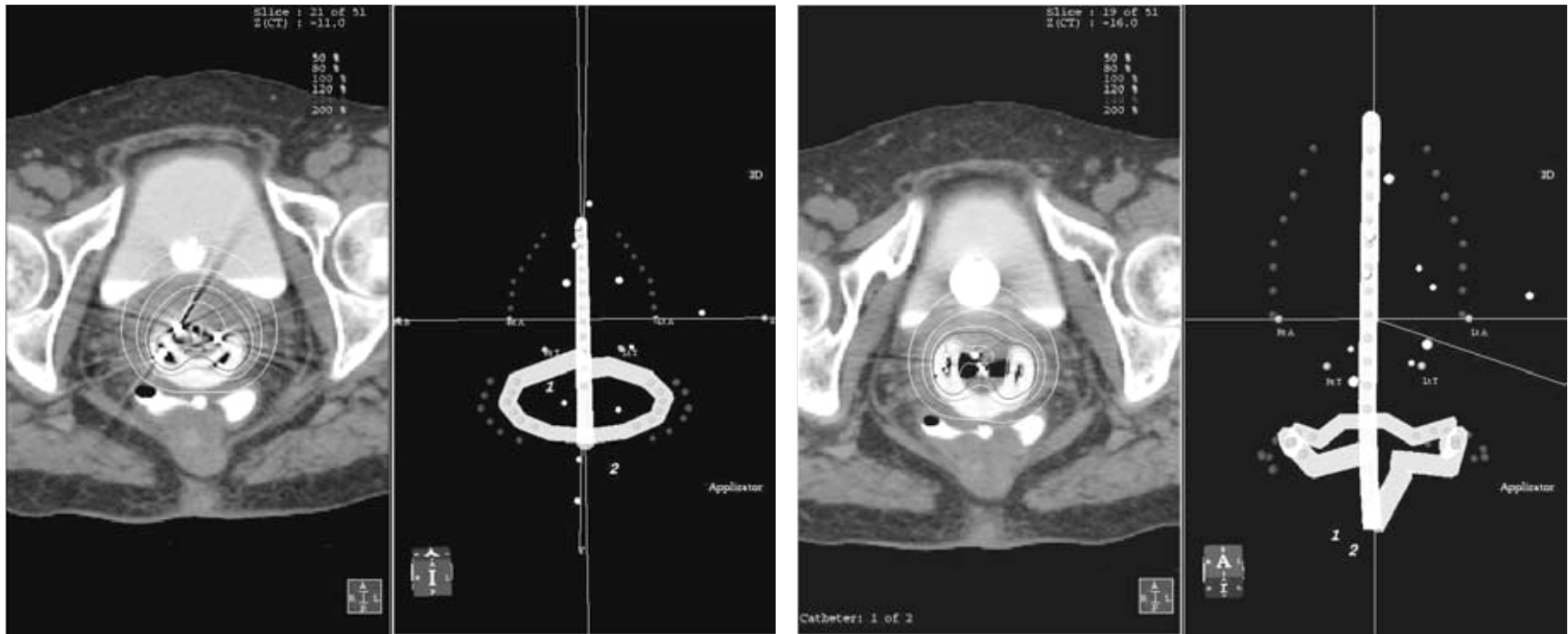
MRI-based seed reconstruction was less accurate than CT, with a mean interobserver variation in seed positioning of 3 mm (1 SD). This resulted in a non-negligible mean interobserver variation in D_{90} of about 7% for T1 + T2.

seed finder tool

seed finder tool + manual corrections (REF)



Applicator Reconstruction Errors



know what to expect,
the ring is circular!

Applicator Reconstruction: ESTRO Recommendations



Contents lists available at ScienceDirect

Radiotherapy and Oncology

journal homepage: www.thegreenjournal.com



GEC-ESTRO Recommendations

Recommendations from Gynaecological (GYN) GEC-ESTRO Working Group: Considerations and pitfalls in commissioning and applicator reconstruction in 3D image-based treatment planning of cervix cancer brachytherapy

Taran Paulsen Hellebust^{a,*}, Christian Kirisits^b, Daniel Berger^b, José Pérez-Calatayud^c, Marisol De Brabandere^d, Astrid De Leeuw^e, Isabelle Dumas^f, Robert Hudej^g, Gerry Lowe^h, Rachel Wills^h, Kari Tanderupⁱ

^aDepartment of Medical Physics, Oslo University Hospital, Norway; ^bDepartment of Radiotherapy and Radiobiology, Medical University of Vienna, Austria; ^cLa Fe University Hospital, Valencia, Spain; ^dDepartment of Radiotherapy, University Hospital Gasthuisberg, Leuven, Belgium; ^eUniversity Medical Centre Utrecht, The Netherlands; ^fDepartment of Radiotherapy, Institut Gustav Roussy, Villejuif, France; ^gDepartment of Radiotherapy, Institute of Oncology Ljubljana, Slovenia; ^hMount Vernon Cancer Center, Northwood, UK; ⁱDepartment of Oncology, Aarhus University Hospital, Denmark

ARTICLE INFO

Article history:

Received 21 April 2010

Received in revised form 7 June 2010

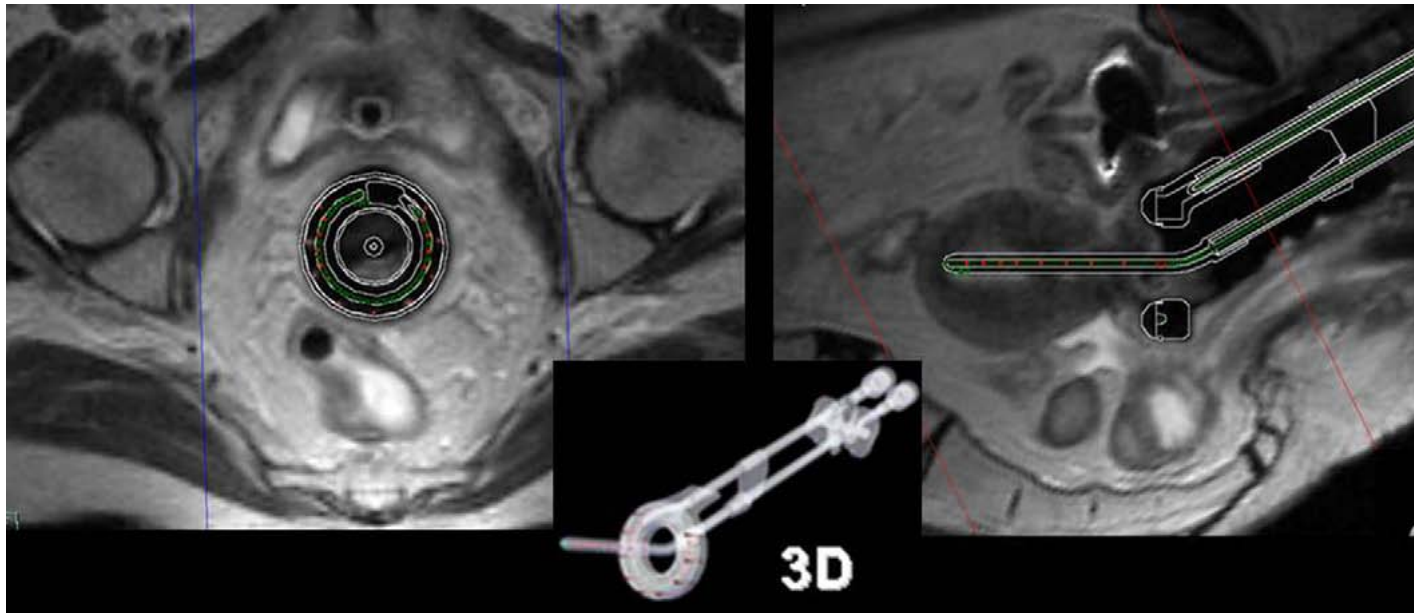
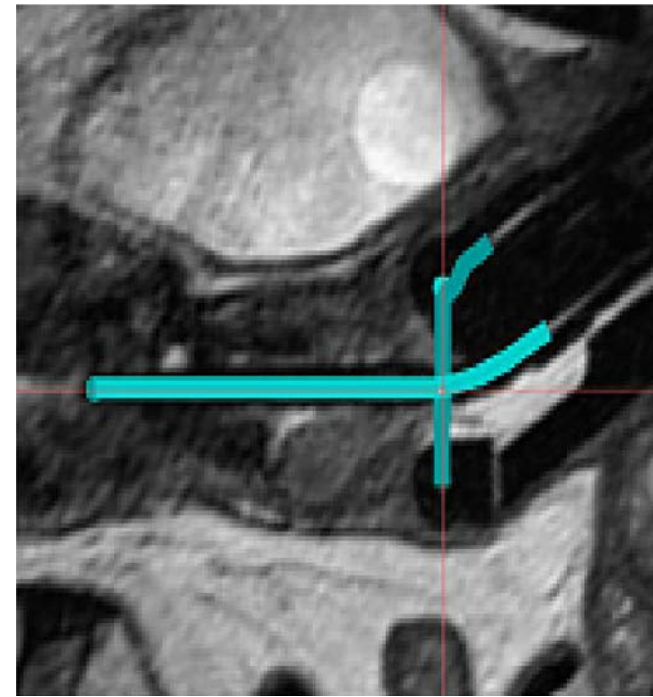
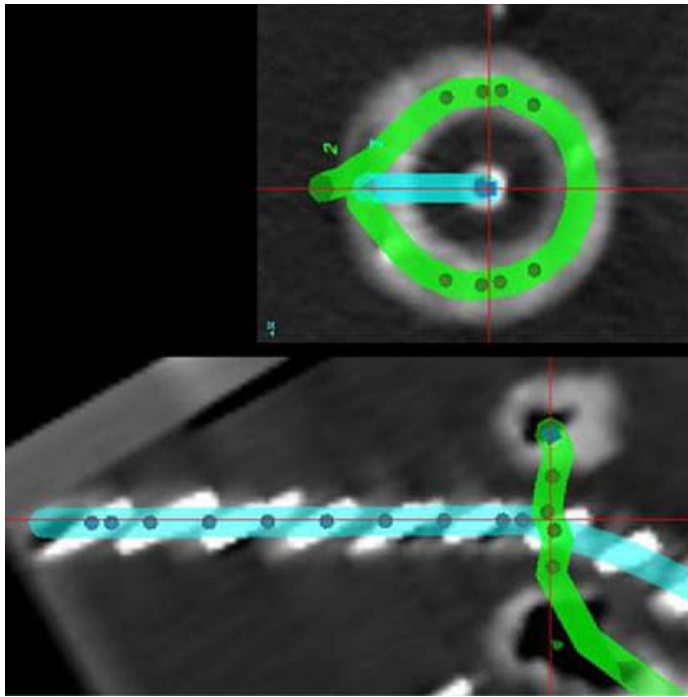
Accepted 8 June 2010

Available online 19 July 2010

ABSTRACT

Image-guided brachytherapy in cervical cancer is increasingly replacing X-ray based dose planning. In image-guided brachytherapy the geometry of the applicator is extracted from the patient 3D images and introduced into the treatment planning system; a process referred to as applicator reconstruction. Due to the steep brachytherapy dose gradients, reconstruction errors can lead to major dose deviations in target and organs at risk. Appropriate applicator commissioning and reconstruction methods must be implemented in order to minimise uncertainties and to avoid accidental errors.

Applicator Reconstruction: ESTRO Recommendations



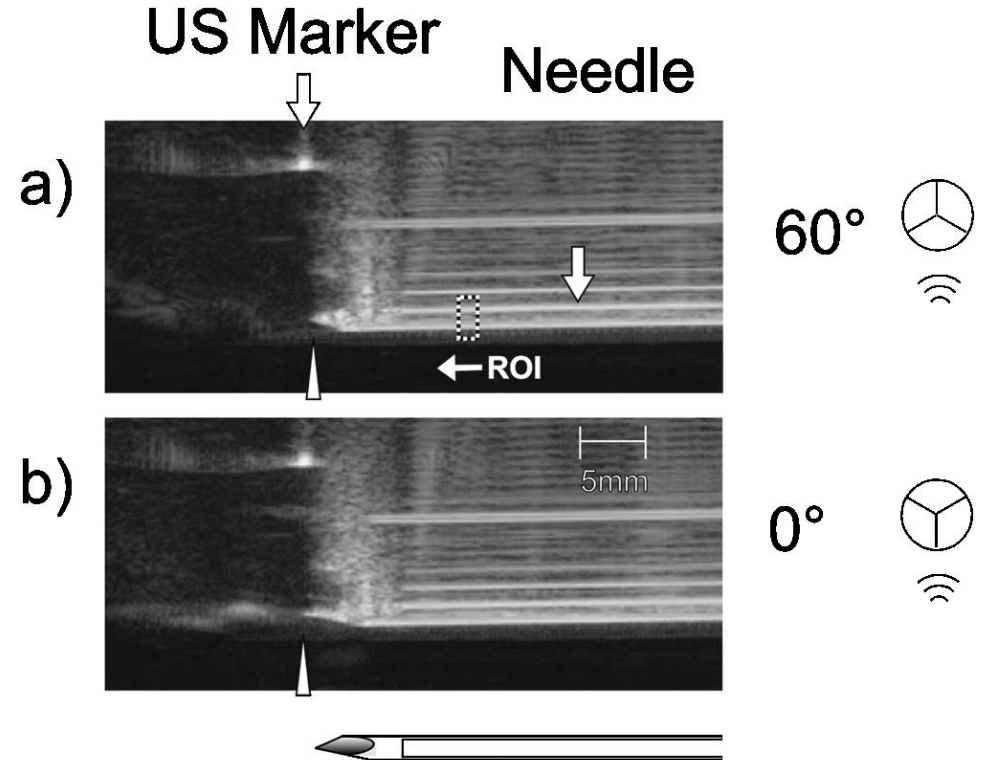
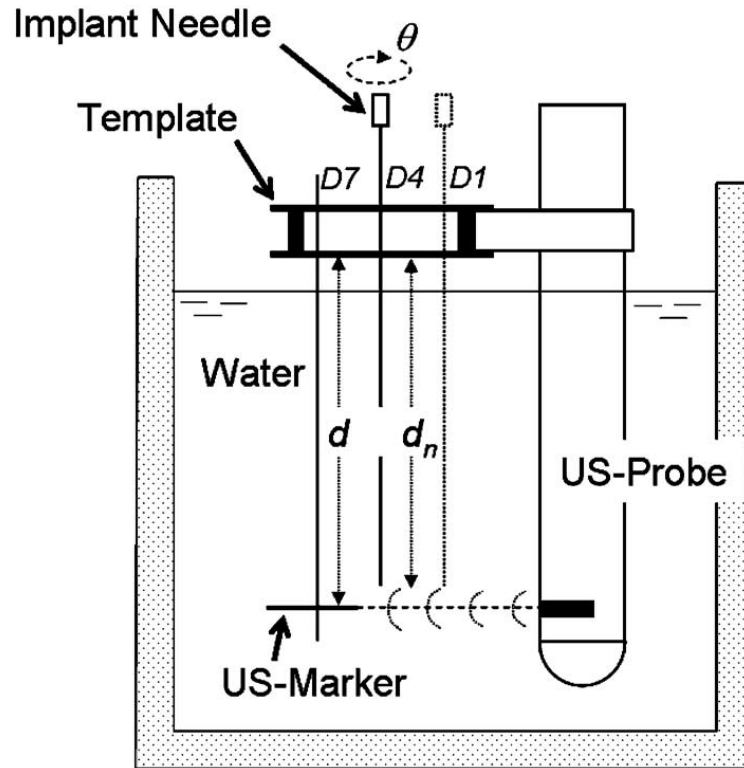
Hellebust, et al., *Radiother. Oncol.* 96, 153-160 (2010)

US Needle Reconstruction Uncertainties: Phantom

Imaging of implant needles for real-time HDR-brachytherapy prostate treatment using biplane ultrasound transducers

Frank-André Siebert,^{a)} Markus Hirt, and Peter Niehoff
Clinic of Radiotherapy, University Hospital of Schleswig-Holstein, Campus Kiel, Kiel 24105, Germany

György Kovács
Interdisciplinary Brachytherapy Unit, University of Lübeck, Lübeck 23538, Germany



0.5 mm needle tip uncertainty,
better accuracy with lower gain

US Needle Reconstruction Uncertainties: Patient

Validation study of ultrasound-based high-dose-rate prostate brachytherapy planning compared with CT-based planning

Deidre Batchelar, Miren Gaztañaga, Matt Schmid, Cynthia Araujo,
François Bachand, Juanita Crook*

Cancer Center for the Southern Interior, British Columbia Cancer Agency, Kelowna, BC, Canada

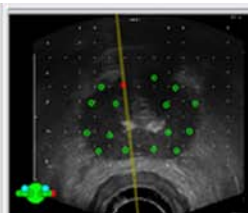
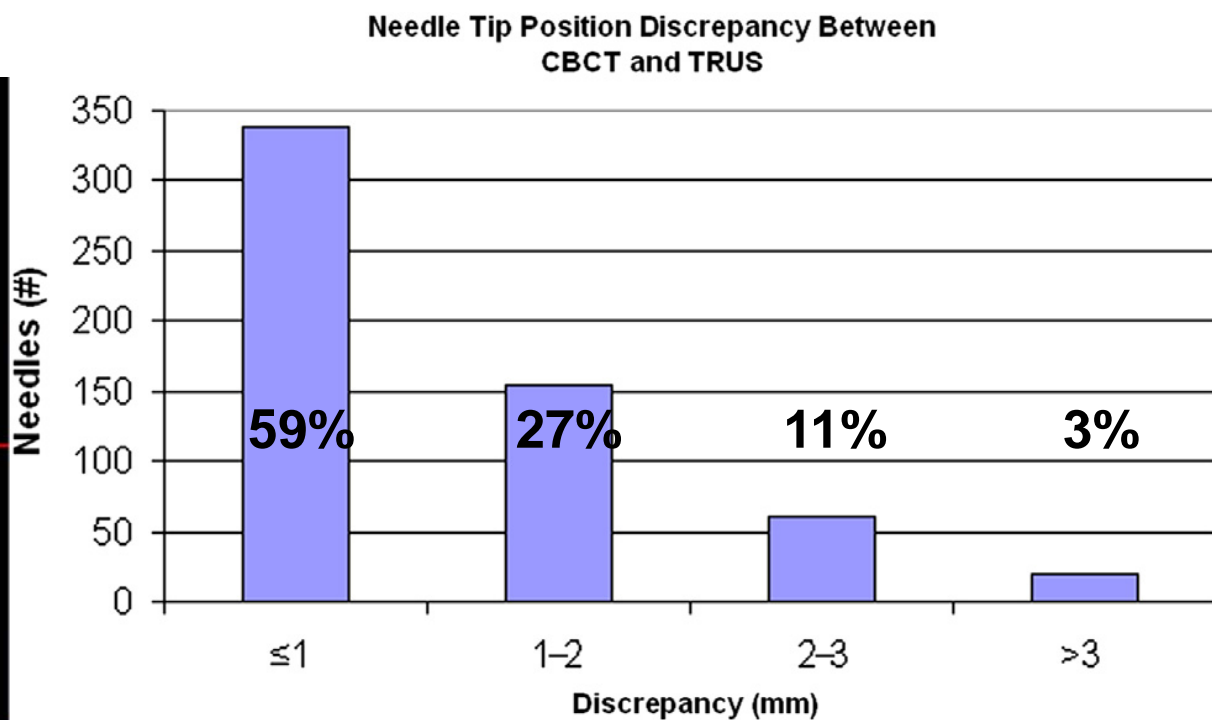
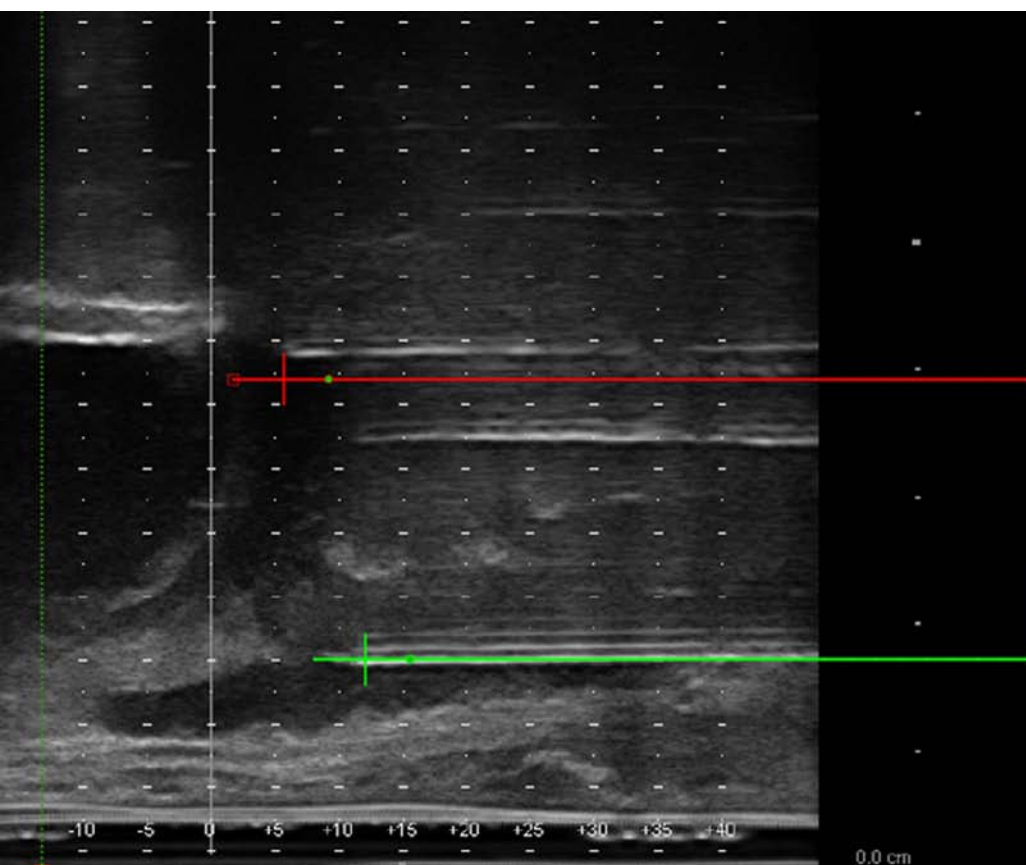
PURPOSE: The use of transrectal ultrasound (TRUS) to both guide and plan high-dose-rate (HDR) brachytherapy (BT) for prostate is increasing. Studies using prostate phantoms have demonstrated the accuracy of ultrasound (US) needle tip reconstruction compared with CT imaging standard. We have assessed the *in vivo* accuracy of needle tip localization by TRUS using cone-beam CT (CBCT) as our reference standard.

METHODS AND MATERIALS: Needle positions from 37 implants have been analyzed. A median of 16 needles (range, 16–18) per implant were inserted, advanced to the prostate base, and their tips identified using live TRUS images and real-time planning BT software. Needle protrusion length from the template was recorded to allow for reverification before capturing images for planning. The needles remained locked in the template, which was fixed to the stepper, while a set of three-dimensional TRUS images was acquired for needle path reconstruction and HDR-BT treatment planning. Following treatment, CBCT images were acquired for subsequent needle reconstruction using a BT Treatment Planning System. The coordinates of each needle tip were recorded from the Treatment Planning System for CT and US and compared.

RESULTS: A total of 574 needle tip positions have been compared between TRUS and CBCT. Of these, 59% agreed within 1 mm, 27% within 1–2 mm, and 11% agreed within 2–3 mm. The discrepancy between tip positions in the two modalities was greater than 3 mm for only 20 needles (3%).

CONCLUSIONS: The US needle tip identification *in vivo* is at least as accurate as CT identification, while providing all the advantages of a one-step procedure. © 2014 American Brachytherapy Society. Published by Elsevier Inc. All rights reserved.

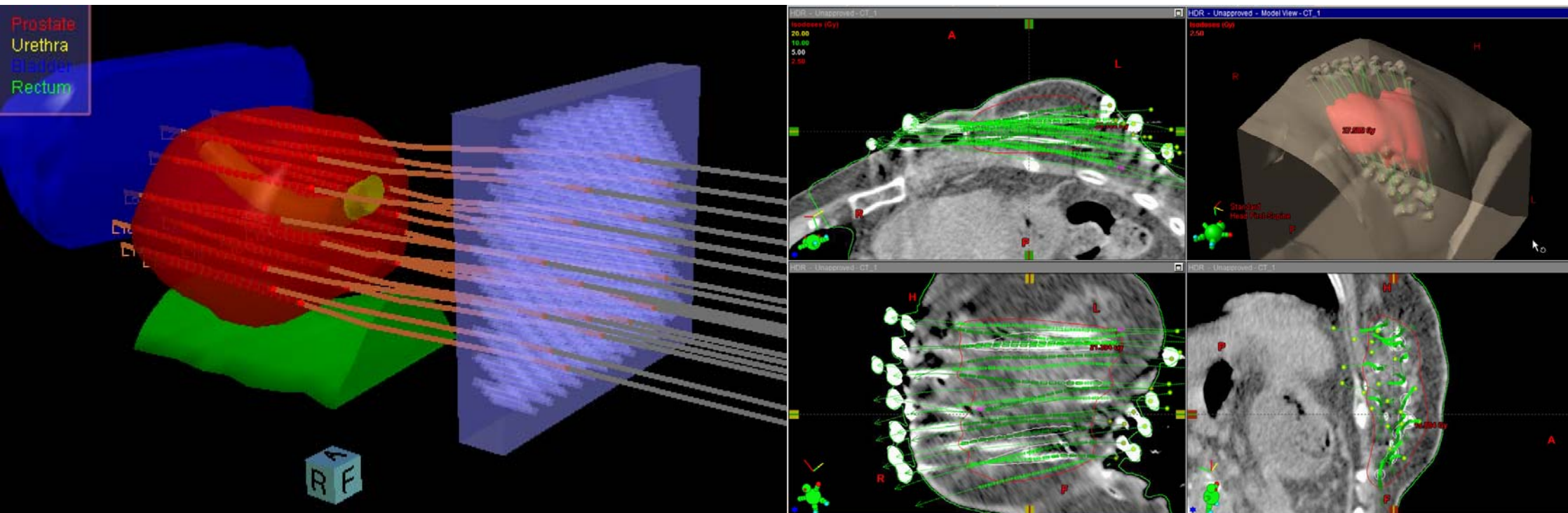
US Needle Reconstruction Uncertainties: Patient



1-3 mm needle tip uncertainty,
comparable accuracy to CT

Test Assumptions: Reconstruction Commissioning

- rigid applicator:
 - required approach for source localization using applicator library
 - consider flexible catheters (HDR prostate and breast) sim-to-treatment



Dosimetric Influence of Reconstruction Errors

Dosimetric impacts of applicator displacements and applicator reconstruction-uncertainties on 3D image-guided brachytherapy for cervical cancer

Joshua Schindel, BS¹, Winson Zhang¹, Sudershan K. Bhatia, MD, PhD, MPH², Wenqing Sun, MD, PhD², Yusung Kim, PhD²

¹Biomedical Engineering Department, ²Radiation Oncology Department, The University of Iowa, Iowa City, USA

Abstract

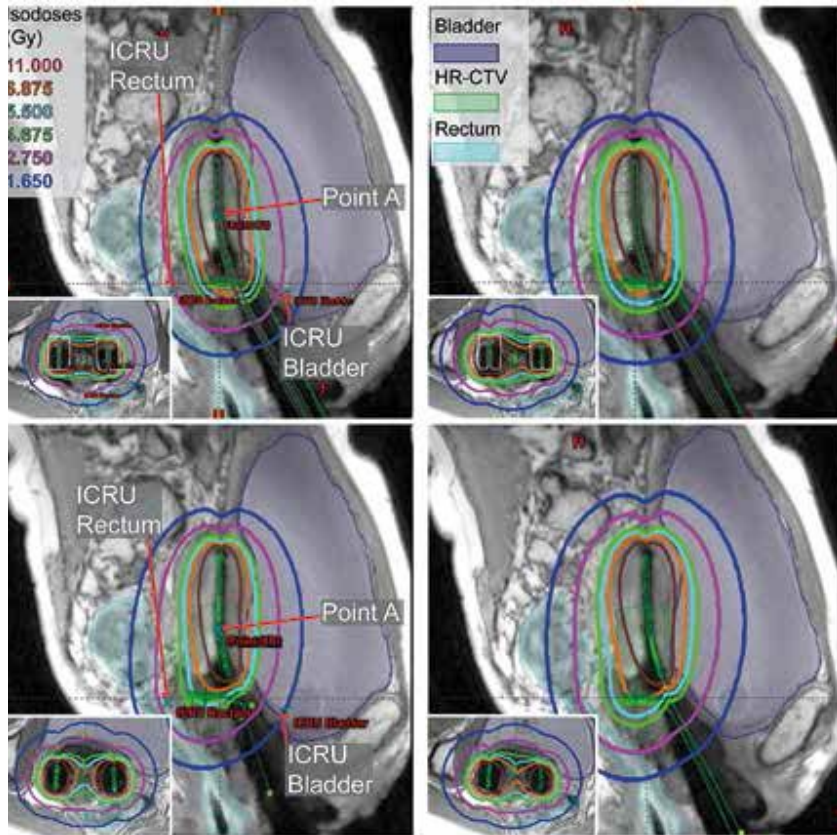
Purpose: To quantify the dosimetric impact of applicator displacements and applicator reconstruction-uncertainties through simulated planning studies of virtual applicator shifts.

Material and methods: Twenty randomly selected high-dose-rate (HDR) titanium tandem-and-ovoid (T&O) plans were retrospectively studied. MRI-guided, conformal brachytherapy (MRIG-CBT) plans were retrospectively generated. To simulate T&O displacement, the whole T&O set was virtually shifted on treatment planning system in the cranial (+) and the caudal (-) direction after each dose calculation. Each shifted plan was compared to an unshifted plan. To simulate T&O reconstruction-uncertainties, each tandem and ovoid was separately shifted along its axis before performing the dose calculation. After the dose calculation, the calculated isodose lines and T&O were moved back to unshifted T&O position. Shifted and shifted-back plan were compared.

Results: Regarding the dosimetric impact of the simulated T&O displacements, rectal D_{2cc} values were observed as being the most sensitive to change due to T&O displacement among all dosimetric metrics regardless of point A ($p < 0.013$) or MRIG-CBT plans ($p < 0.0277$). To avoid more than 10% change, ± 1.5 mm T&O displacements were accommodated for both point A and MRIG-CBT plans. The dosimetric impact of T&O displacements on sigmoid ($p < 0.0005$), bladder ($p < 0.0001$), HR-CTV ($p < 0.0036$), and point A ($p < 0.0015$) were significantly larger in the MRIG-CBT plans than point A plans. Regarding the dosimetric impact of T&O reconstruction-uncertainties, less than ± 3.0 mm reconstruction-uncertainties were also required in order to avoid more than 10% dosimetric change in either the point A or MRIG-CBT plans.

Conclusions: The dosimetric impact of simulated T&O displacements was significantly larger in the MRIG-CBT plans than in the point A plans. Either ± 3 mm T&O displacement or a ± 4.5 mm T&O reconstruction-uncertainty could cause greater than 10% dosimetric change for both point A plans and MRIG-CBT plans.

Dosimetric Influence of Reconstruction Errors



1.5 mm reconstruction error changed dose metrics by 5%

Table 1. The simulated dosimetric impacts of T&O displacements for MRIG-CBT (20 plans) by virtually shifting whole T&O in a treatment planning system

	Simulated dosimetric impacts [%] of T&O displacements for MRIG-CBT plans													
	Caudal T&O shift							Cranial T&O shift						
	-20 mm	-10 mm	-7.5 mm	-6 mm	-5 mm	-3 mm	-1.5 mm	1.5 mm	3 mm	5 mm	6 mm	7.5 mm	10 mm	20 mm
HR-CTV D ₉₀ [%]	23 ± 11	9 ± 5	7 ± 4	9 ± 3	5 ± 3	3 ± 2	2 ± 1	1 ± 1	3 ± 2	5 ± 4	7 ± 5	8 ± 6	11 ± 8	21 ± 16
HR-CTV D ₁₀₀ [%]	20 ± 9	6 ± 9	7 ± 5	6 ± 4	5 ± 4	3 ± 3	2 ± 2	2 ± 1	4 ± 2	6 ± 3	7 ± 4	9 ± 5	11 ± 7	24 ± 11
Rectum D _{2cc} [%]	136 ± 46	50 ± 13	35 ± 8	27 ± 6	22 ± 5	12 ± 3	6 ± 1	6 ± 1	10 ± 2	16 ± 4	19 ± 4	23 ± 5	29 ± 6	47 ± 10
Bladder D _{2cc} [%]	29 ± 10	14 ± 7	11 ± 5	8 ± 5	7 ± 4	4 ± 3	2 ± 1	2 ± 2	5 ± 3	8 ± 6	10 ± 7	13 ± 9	19 ± 13	50 ± 42
Sigmoid D _{2cc} [%]	24 ± 12	12 ± 6	8 ± 5	7 ± 4	5 ± 3	3 ± 2	2 ± 1	1 ± 1	3 ± 2	5 ± 3	5 ± 3	6 ± 4	9 ± 7	13 ± 9
Point A left [%]	28 ± 14	12 ± 8	9 ± 6	7 ± 4	6 ± 4	4 ± 2	2 ± 1	2 ± 1	3 ± 2	5 ± 4	7 ± 4	8 ± 5	11 ± 8	41 ± 31
Point A right [%]	28 ± 17	13 ± 9	10 ± 7	8 ± 5	7 ± 4.5	4 ± 3	2 ± 2	2 ± 2	4 ± 3	8 ± 5	9 ± 7	12 ± 9	17 ± 13	65 ± 53
ICRU rectum [%]	60 ± 53	31 ± 23	23 ± 16	18 ± 12	15 ± 10	9 ± 6	4 ± 3	4 ± 2	8 ± 4	14 ± 6	16 ± 7	20 ± 8	26 ± 9	46 ± 11
ICRU bladder [%]	27 ± 14	14 ± 9	11 ± 6	9 ± 5	7 ± 4	5 ± 3	2 ± 1	3 ± 1	5 ± 3	9 ± 5	10 ± 6	13 ± 8	18 ± 11	35 ± 26
	< 5%	≥ 5%	≥ 10%	≥ 15%										

Table 4. The simulated dosimetric impacts of T&O reconstruction-uncertainties for conventional planning (20 plans)

	Simulated dosimetric impact [%] of T&O reconstruction-uncertainties for conventional point A plans											
	Caudal tandem shift & Anterior ovoid shift						Cranial tandem shift & Posterior ovoid shift					
	-10 mm	-7.5 mm	-6 mm	-4.5 mm	-3 mm	-1.5 mm	1.5 mm	3 mm	4.5 mm	6 mm	7.5 mm	10 mm
HR-CTV D ₉₀ [%]	5 ± 5	4 ± 3	4 ± 3	2 ± 2	2 ± 1	2 ± 2	2 ± 2	4 ± 4	5 ± 5	5 ± 5	6 ± 5	7 ± 5
HR-CTV D ₁₀₀ [%]	8 ± 9	6 ± 5	5 ± 5	3 ± 2	3 ± 2	4 ± 3	3 ± 3	5 ± 5	6 ± 5	8 ± 6	9 ± 7	10 ± 7
Rectum D _{2cc} [%]	19 ± 10	14 ± 8	13 ± 8	11 ± 6	9 ± 6	5 ± 4	7 ± 4	15 ± 8	23 ± 11	33 ± 15	43 ± 22	65 ± 32
Bladder D _{2cc} [%]	10 ± 11	7 ± 6	6 ± 5	5 ± 3	3 ± 3	3 ± 2	2 ± 1	3 ± 2	4 ± 2	5 ± 3	6 ± 4	8 ± 6
Sigmoid D _{2cc} [%]	8 ± 7	7 ± 6	7 ± 7	6 ± 6	5 ± 5	6 ± 6	6 ± 4	8 ± 6	9 ± 6	12 ± 8	12 ± 10	16 ± 13
Point A left [%]	1 ± 1	1 ± 1	2 ± 1	1 ± 2	1 ± 1	1 ± 1	1 ± 1	1 ± 1	1 ± 1	2 ± 2	1 ± 1	2 ± 1
Point A right [%]	1 ± 1	1 ± 1	1 ± 1	1 ± 1	1 ± 1	1 ± 1	1 ± 1	1 ± 1	1 ± 1	2 ± 3	1 ± 1	1 ± 1
ICRU rectum [%]	17 ± 9	12 ± 7	10 ± 7	8 ± 6	6 ± 5	4 ± 4	4 ± 3	9 ± 6	14 ± 7	20 ± 10	25 ± 13	41 ± 26
ICRU bladder [%]	23 ± 23	18 ± 16	14 ± 14	11 ± 10	8 ± 7	5 ± 5	3 ± 3	5 ± 3	7 ± 3	9 ± 4	11 ± 6	15 ± 8

Take Home Message

- BT reconstruction methods have advanced over past 40 years
- 3D imaging datasets permit volumetric rendering not possible with:
 - orthogonal x rays
 - stereo shift planar x rays
 - fluoroscopy
- differing strengths/weaknesses for modern imaging methods
- learn the reconstruction process and datachain
- identify uncertainties at each stage in the reconstruction process

Further Reading

Batchelar, et al. Brachytherapy 2014;13:75-9.

De BraBandere, et al. Brachytherapy 2013;12:580-8.

Hellebust, et al. Radiother Oncol 2010;96:153-60.

Holupka, et al. Med Phys 2004;31:2672-9.

Jain, et al. Med Phys 2005;32:3475-92.

Kim, et al. Med Phys 2004;31:2543-8.

Lam, et al. Phys Med Biol 2004;49:557-69.

Li, et al. Med Phys 2001;28:1410-5.

Liu, et al. Phys Med Biol 2003;48:1191-203.

Milickovic, et al. Med Phys 2000;27:1047-57.

Milickovic, et al. Phys Med Biol 2000;45:2787-800.

Narayanan, et al. Med Phys 2002;29:1572-9.

Narayanan, et al. Phys Med Biol 2004;49:3483-94.

Roué, et al. Radiother Oncol 2006;78:78-83.

Schindel, et al. J Contemp Brachy 2013;5:250-7.

Siebert, et al. Med Phys 2009;36:3406-12.

Todor, et al. Phys Med Biol 2002;47:2031-48.

Venselaar and Perez-Calatayud, 2004. ESTRO Booklet 8.

Acknowledgements

Dimos Baltas, University of Freiburg, Germany

Christian Kirisits, Medical University of Vienna, Austria

Frank-André Siebert, University of Kiel, Germany





ESTRO

School

Advanced Brachytherapy Physics

Vienna, 29 May – 1 June 2016

Objectives/Outline:

To :

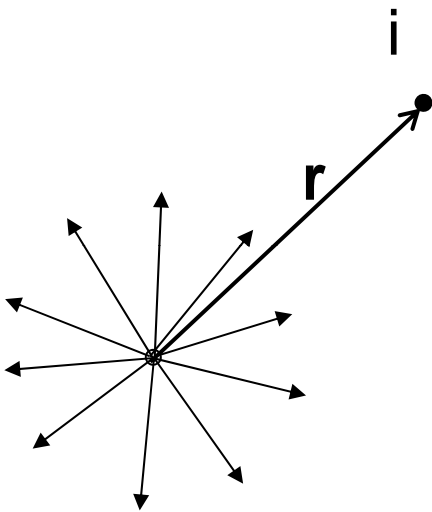
- review the basic principles of the MC method
- outline its implementation for brachy dosimetry (and especially type A and type B uncertainties)

so as to identify:

- its potential to provide reference dose distributions
 - TG-43 uncertainties
 - its potential for clinical implementation

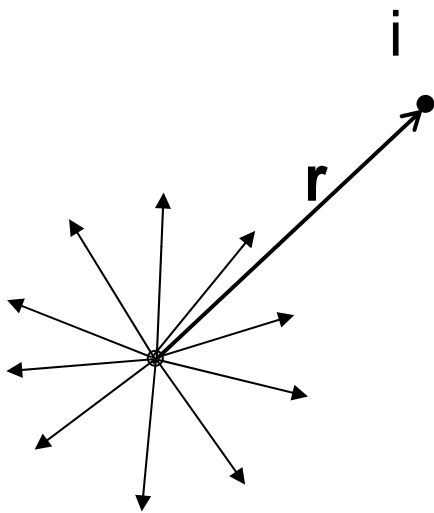
The problem ...

- Let us start from the simplest case (point isotropic monoenergetic photon source in infinite medium of given composition)
- If I know everything there is to know about the source and the medium, can I calculate dose at a point i ...?



The problem ...

- Let us start from the simplest case (point isotropic monoenergetic photon source in infinite medium of given composition)
- If I know everything there is to know about the source and the medium, can I calculate dose at a point i ...?



from initial activity i can calculate the radiant energy rate or the radiant energy over t , R_{pr}

from R_{pr} can calculate energy fluence at any point, $\Psi_{pr_i} = \frac{R_{pr}}{4\pi r_i^2} \exp(-\mu r_i)$

from Ψ_{pr_i} can calculate the TERMA at any point, $T_i = \left(\frac{\mu}{\rho}\right) \Psi_{pr_i}$

i can also calculate the fraction of TERMA that is transferred to kinetic energy of charged particles

\equiv KERMA at any point, $K_{pr_i} = \left(\frac{\mu_{en}}{\rho}\right) \Psi_{pr_i} = \left(\frac{\mu_{en}}{\mu}\right) T_{pr_i}$

The problem ...

For brachytherapy photons:

- secondary e- ranges are small relative to photon m.f.p.
 - e- radiative energy loss is negligible
- CPE can be assumed to exist at all points (except close to a source or high Z materials)

Energy [keV]	CSDA-range electrons [g/cm ²]	$\frac{1}{\mu}$ [cm]
30	1.8E-03	2.5
100	1.2E-02	5.6
350	1.1E-01	8.9
1000	4.4E-01	14

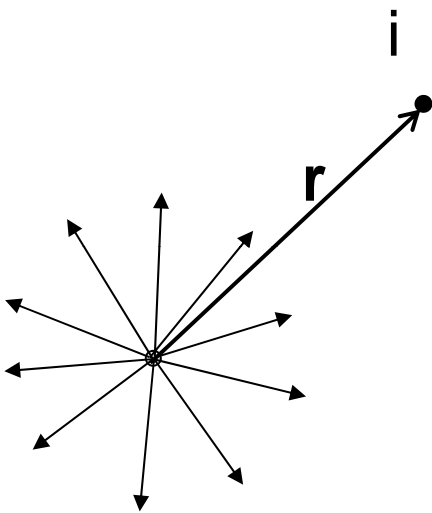
Dose to a point can be approximated by collision KERMA throughout a geometry of mm sized voxel elements

In short, to know the dose distribution one needs to know the energy distribution of fluence, Φ_E , at all points of a geometry:

$$D(\mathbf{r}) = K(\mathbf{r}) = \int_E E \Phi_E(\mathbf{r}) [\mu_{en}(E) / \rho] dE$$

The problem ...

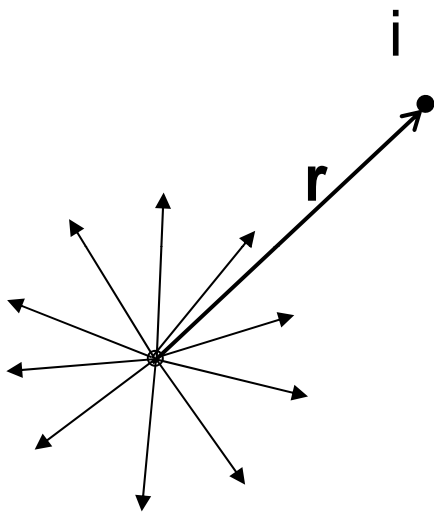
- Let us start from the simplest case (point isotropic monoenergetic photon source in infinite medium of given composition)
- If I know everything there is to know about the source and the medium, can I calculate dose at a point i ...?



$$\text{under CPE : } D_{pr_i} \equiv K_{pr_i} = \left(\frac{\mu_{en}}{\rho}\right) \Psi_{pr_i}$$

- **BUT WHAT ABOUT SCATTER DOSE...?**

The problem ...



- Point isotopic monoenergetic photon source in infinite medium of given composition
- If I know everything there is to know about the source and the medium, can I calculate dose at a point i ...?

$$D_{pr_i} \equiv K_{pr_i} = \left(\frac{\mu_{en}}{\rho}\right) \Psi_{pr_i}$$

For D_{scat} at point i need $\Psi_{E_{sc_i}}$ the depends on:
the probability of a primary photon interacting in one of a number of possible interaction types **at every point of the geometry**,
the probability distribution determining the new direction of a photon and its energy degradation,
the probability this process is repeated due to multiple scattering **at every point of the geometry**

D_{scat} at point i , CANNOT be analytically calculated
NOT because of its stochastic nature, but due to the complexity of the calculation

The problem ...

How important is D_{scat} in brachy ...?

It depends on ENERGY!

Energy [keV]	CSDA-range electrons [g/cm ²]	$\frac{1}{\mu}$ [cm]	$1 - \mu_{\text{en}} / \mu$
30	1.8E-03	2.5	0.56
100	1.2E-02	5.6	0.85
350	1.1E-01	8.9	0.71
1000	4.4E-01	14	0.58

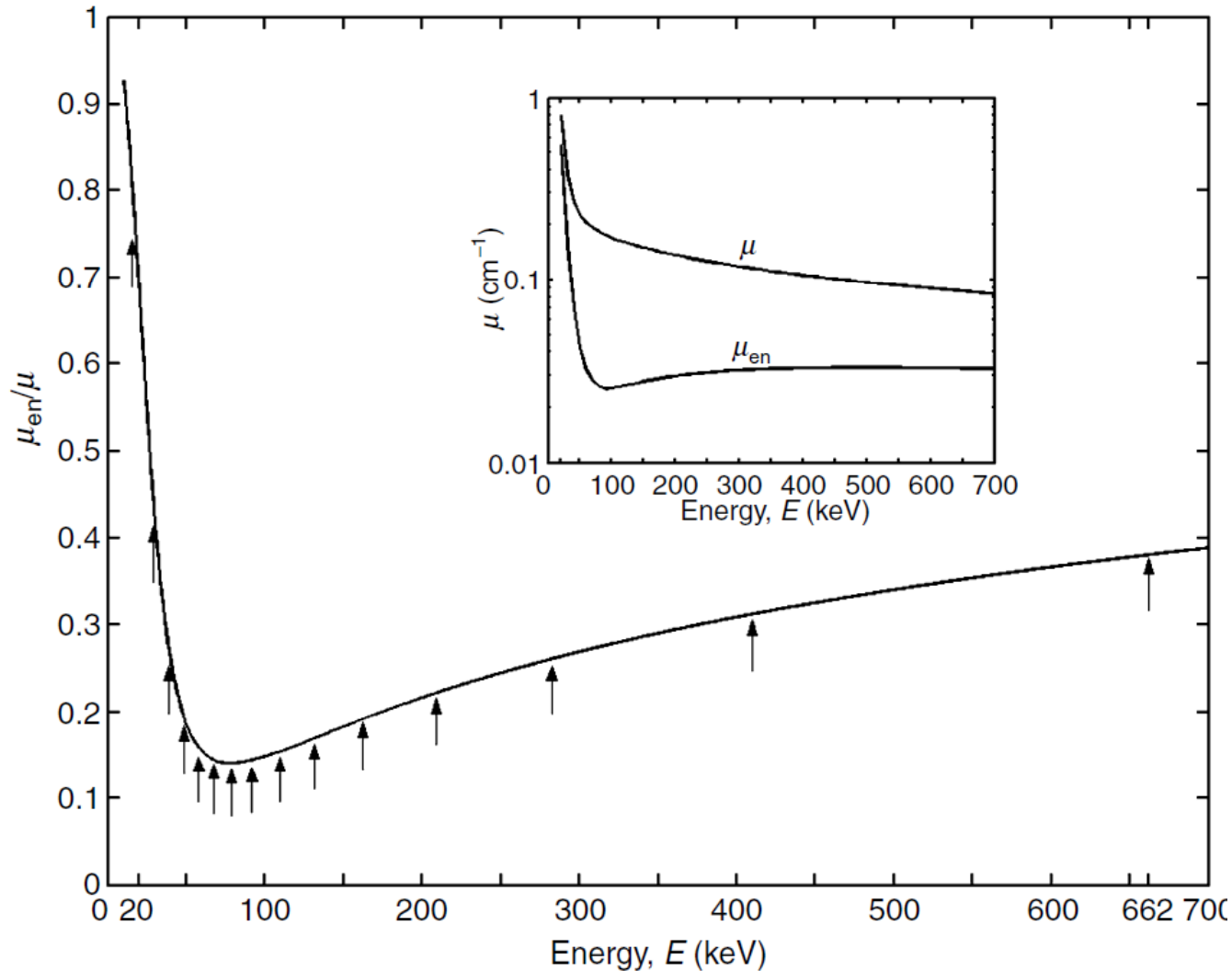


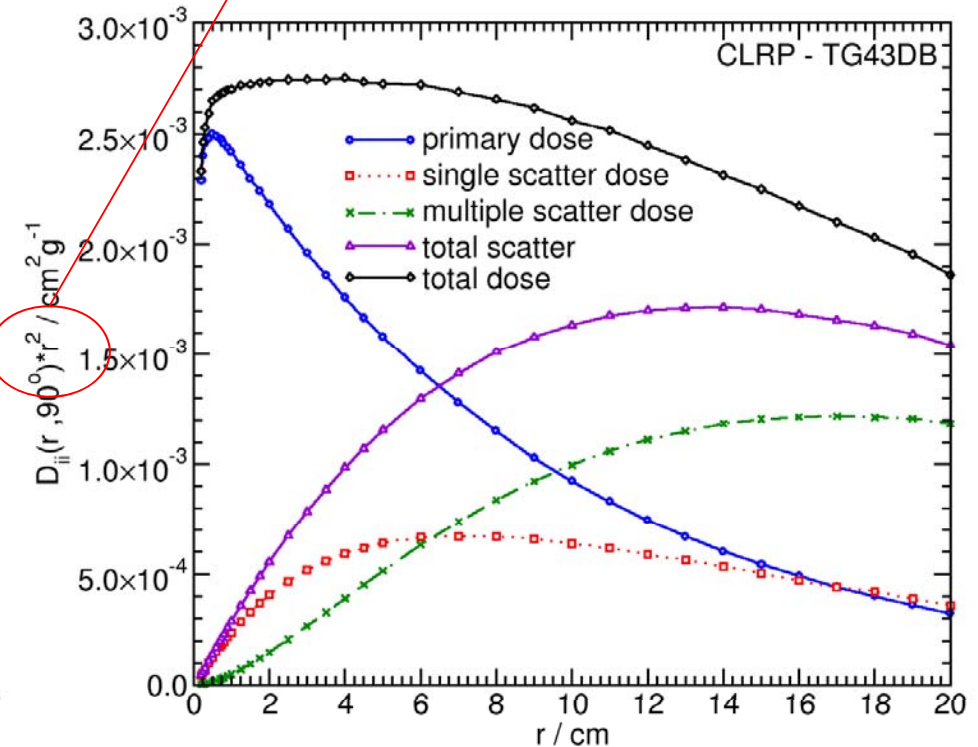
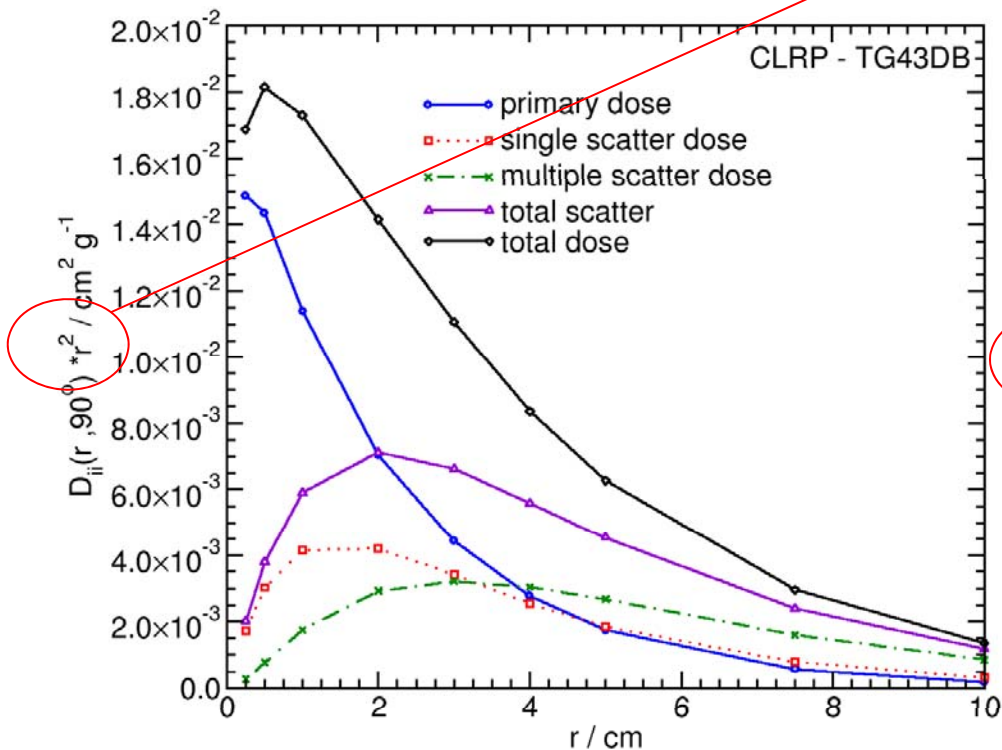
Figure from: Baltas, Sakelliou, Zamboglou (Eds), *The Physics of modern brachytherapy for oncology*, Taylor & Francis Books Inc, 2006

The problem ...

How important is D_{scat} in brachy ...?

It depends on distance from source(s)!

Do not forget: in brachy r^2 reigns!!!



Figures from the Carleton U. TG-43 database available online @:
http://www.physics.carleton.ca/clrp/seed_database

The problem ...

How important is D_{scat} in brachy ...?

It associates the dose distribution with the entire calculation geometry (ρ , Z , dimensions) rather than just the path from a source to a point.

E.g. for dimensions:

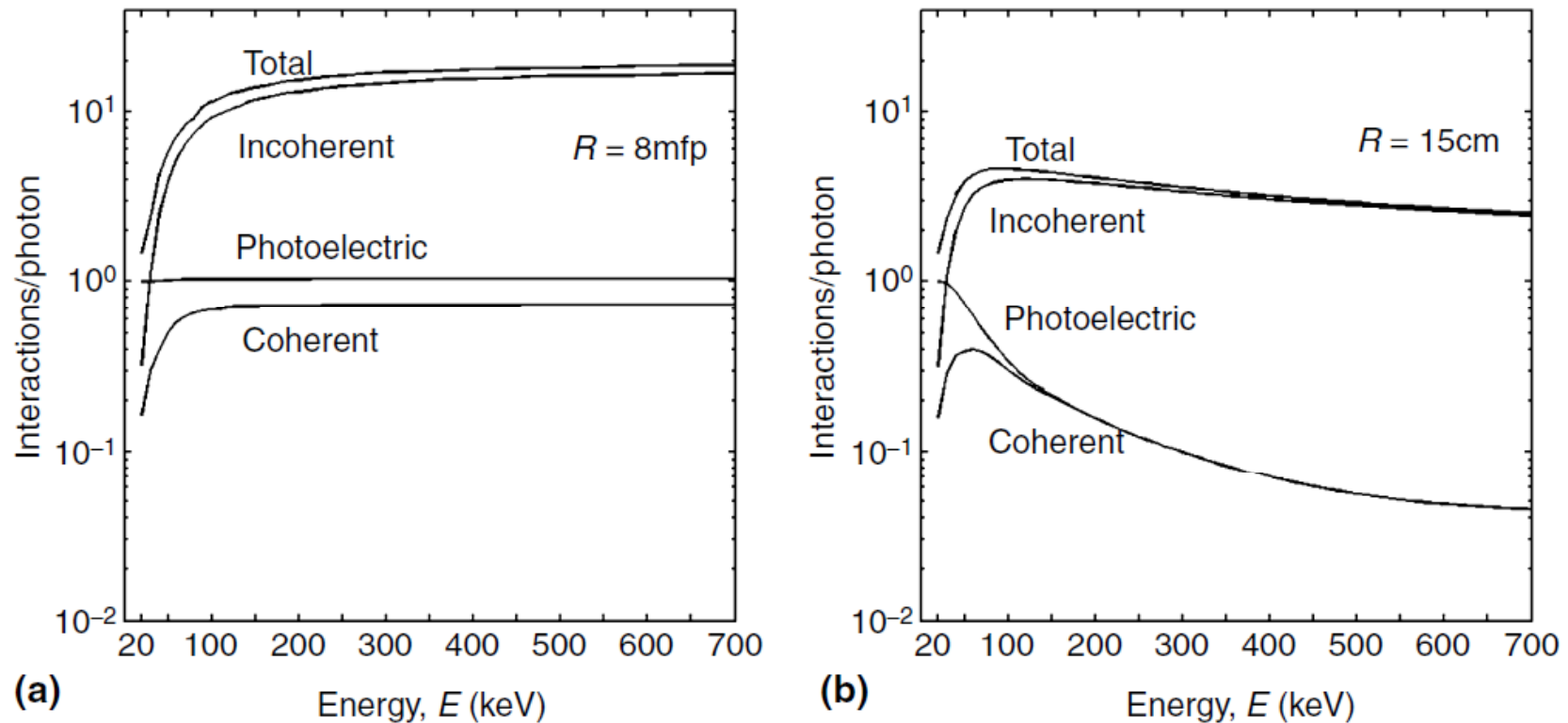


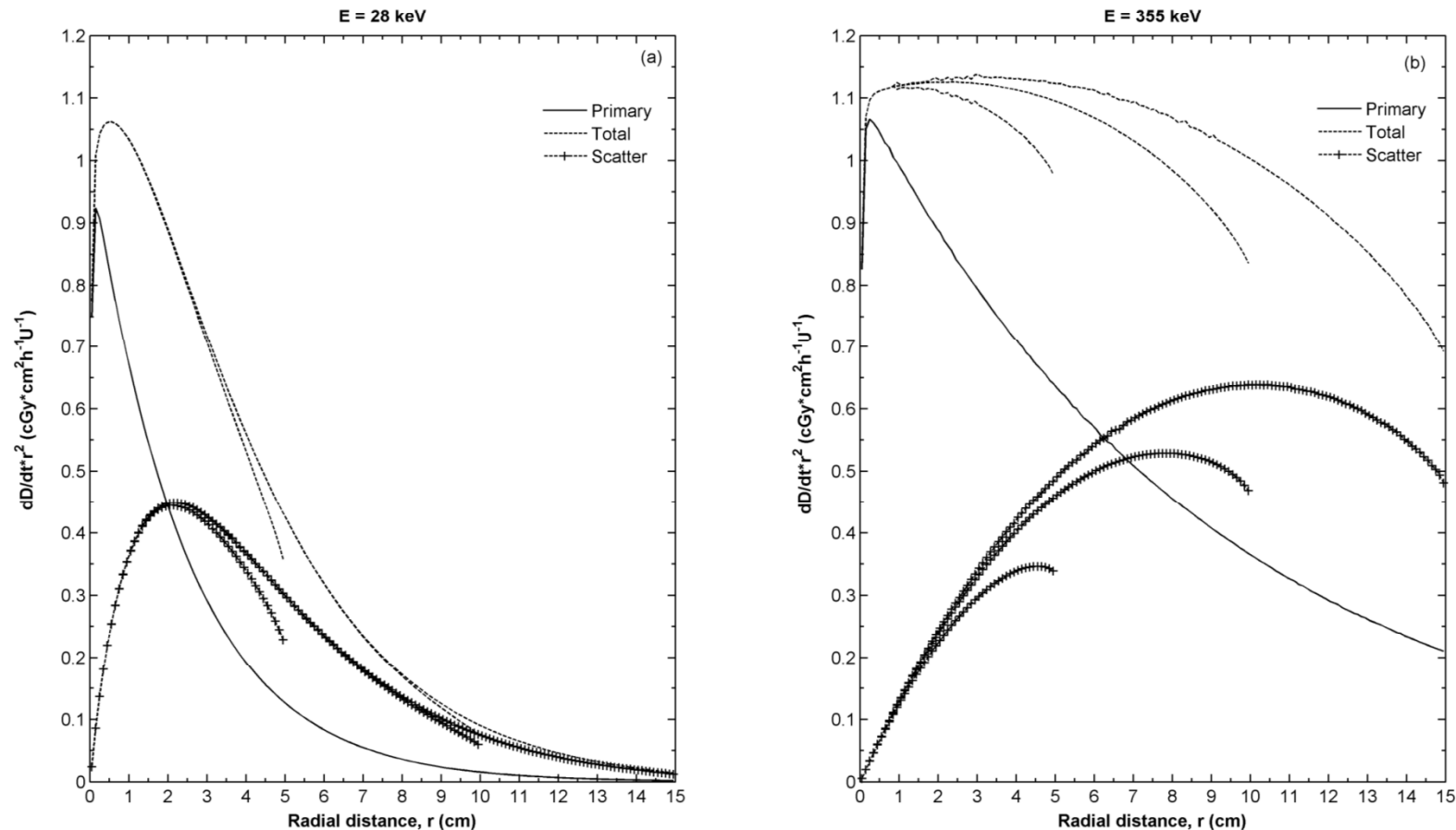
Figure from: Venselaar, Baltas, Meigooni, Hoskin (Eds), *Comprehensive Brachytherapy: physical and clinical aspects*. CRC Press, Taylor & Francis, © 2013

The problem ...

How important is D_{scat} in brachy ...?

It associates the dose distribution with the entire calculation geometry (ρ , Z , dimensions) rather than just the path from a source to a point.

E.g. for dimensions:



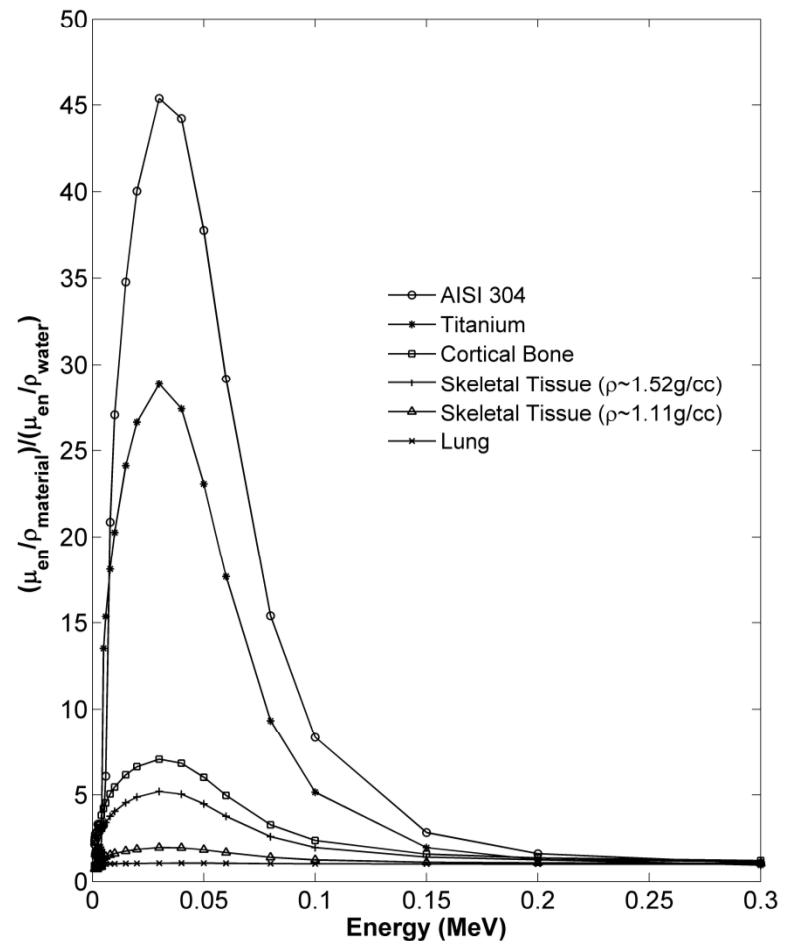
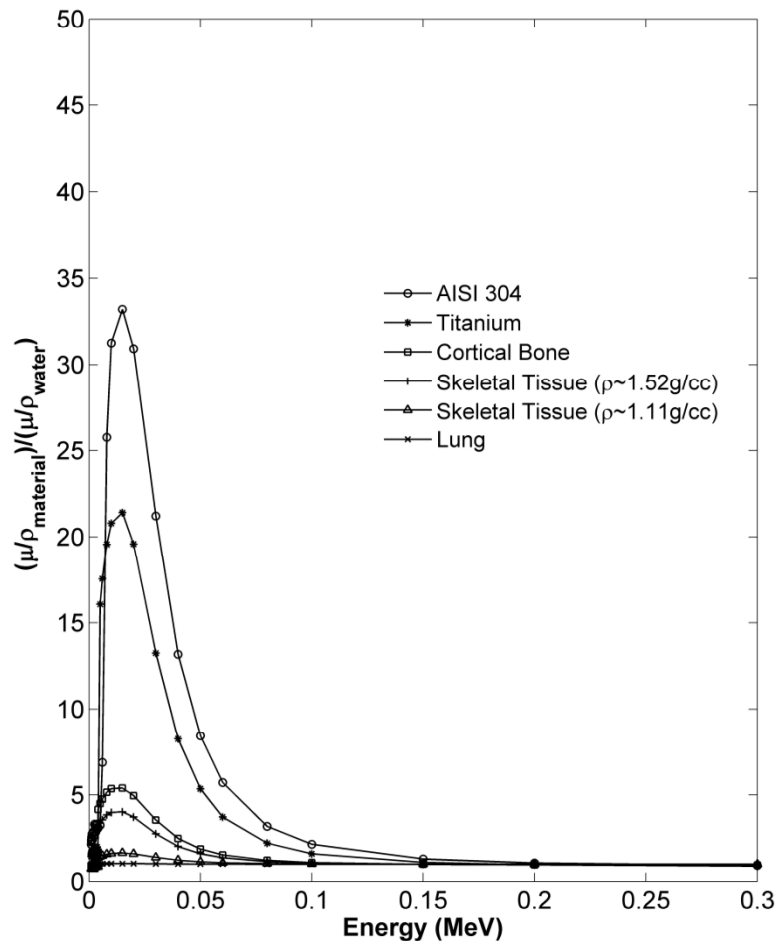
Figures from: Papagiannis, Pantelis, Karaiskos, Br J Radiol (2014) 87: 20140163

The problem ...

How important is D_{scat} in brachy ...?

It associates the dose distribution with the entire calculation geometry (ρ , Z , dimensions) rather than just the path from a source to a point.

E.g. for materials:



The MC method ...

Since we know the Physics underlying radiation transport through matter (probabilities for interaction: site, type and associated energy/direction distributions), can't we reproduce (simulate) all possible photon tracks?

Could I then calculate any related quantity at all points...?



The MC method ...

The Central Limit Theorem: the sum of a **large** number of identical, independent random variables is approximately **normally** distributed.

So, if I want to calculate an unknown quantity, m , and k is a random variable of expectation value $E(k)=m$ and variance $\text{Var}(k)=b^2$.

If k_1, k_2, \dots, k_N are N RANDOMLY selected values of k ,

then: $\sum_{i=1}^N k_i$ is normally distributed with $E\left(\sum_{i=1}^N k_i\right)=Nm$ and $V\left(\sum_{i=1}^N k_i\right)=Nb^2$

or equivalently: $P(Nm - 3b\sqrt{N} < \sum_{i=1}^N k_i < Nm + 3b\sqrt{N}) \approx 0.997$

or: $P\left(-\frac{3b}{\sqrt{N}} < \frac{1}{N}\sum_{i=1}^N k_i - m < \frac{3b}{\sqrt{N}}\right) \approx 0.997$

So, if I want to estimate the photon fluence (or any related quantity) at point r , I can average the contribution of N photon tracks RANDOMLY sampled from the probability distribution of all possible tracks

The MC method ...

Do I know the probability distribution of possible tracks?

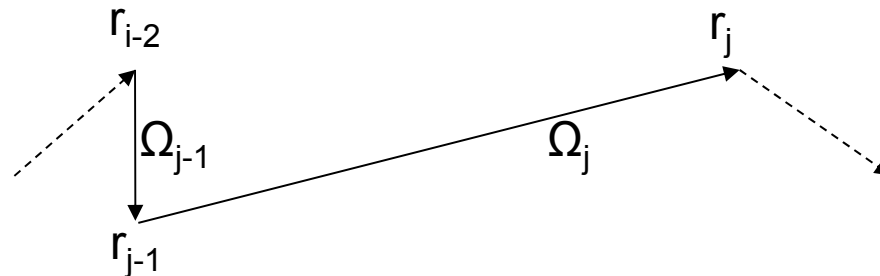
A photon “moves” from phase space element to phase space element.

A photon track is composed of the sequential phase space elements or photon states, $\mathbf{S}_j(\mathbf{r}_j, E_j, \boldsymbol{\Omega}_j)$ just before each interaction j .

The probability of occurrence of each photon state j only depends on the probability of occurrence of state $j-1$.

Or in other words: the probability that the photon interacts at \mathbf{r}_{j-1} , the probability that a specific kind of interaction occurs and the probability that during this interaction the photon is scattered in direction $\boldsymbol{\Omega}_j$ with energy E_j given $\boldsymbol{\Omega}_{j-1}$ and E_{j-1} .

These probability distributions are known in Physics....!



Hence, the only component missing is a method to RANDOMLY sample from the above, known, probability distributions.

The MC method ...

How do I sample RANDOMLY from a known probability distribution?

There are numerous mathematical methods. In example:

Inversion theorem

Let x be a continuous random variable distributed over the interval $[a, b]$ with a probability density function $f(x)$ and a cumulative probability distribution function $F(x)$ that is invertible. Given a random number, r , in the interval $[0, 1]$, a value x^* of x can be randomly selected according to:

$$r = F(x^*) = \int_a^{x^*} f(x) dx$$

Let x be a discrete random variable taking N values, x_i of probability, P_i so that: $\sum_{i=1}^N P_i = 1$

Given a random number, r , in the interval $[0, 1]$, a value x^* of x can be randomly selected according to:

$$x^* = x_j \text{ where } j = \min \left\{ j : r < \sum_{i=1}^j P_i \right\}$$

The MC method ...

Simple examples:

Choosing emission direction for a mono-energetic point source.

The emission is isotropic and the probability of emission into a solid angle element $d\Omega$ equals the fraction of this solid angle in the 4π geometry so that:

$$p(\theta, \phi)d\theta d\phi = \frac{d\Omega}{4\pi} = \frac{\sin\theta d\theta d\phi}{4\pi}$$

$$p(\theta)d\theta = \frac{\sin\theta d\theta}{2} \quad \text{and} \quad r = P(\theta^*) = \int_0^{\theta^*} \frac{\sin\theta d\theta}{2} \Rightarrow r = \frac{1 - \cos\theta^*}{2} \Rightarrow \cos\theta^* = 1 - 2r$$

$$p(\phi)d\phi = \frac{d\phi}{2\pi} \quad \text{and} \quad r' = P(\phi^*) = \frac{1}{2\pi} \int_0^{\phi^*} d\phi \Rightarrow \phi^* = 2\pi r'$$

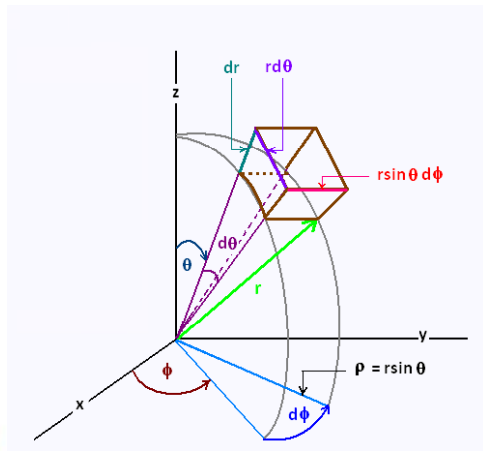
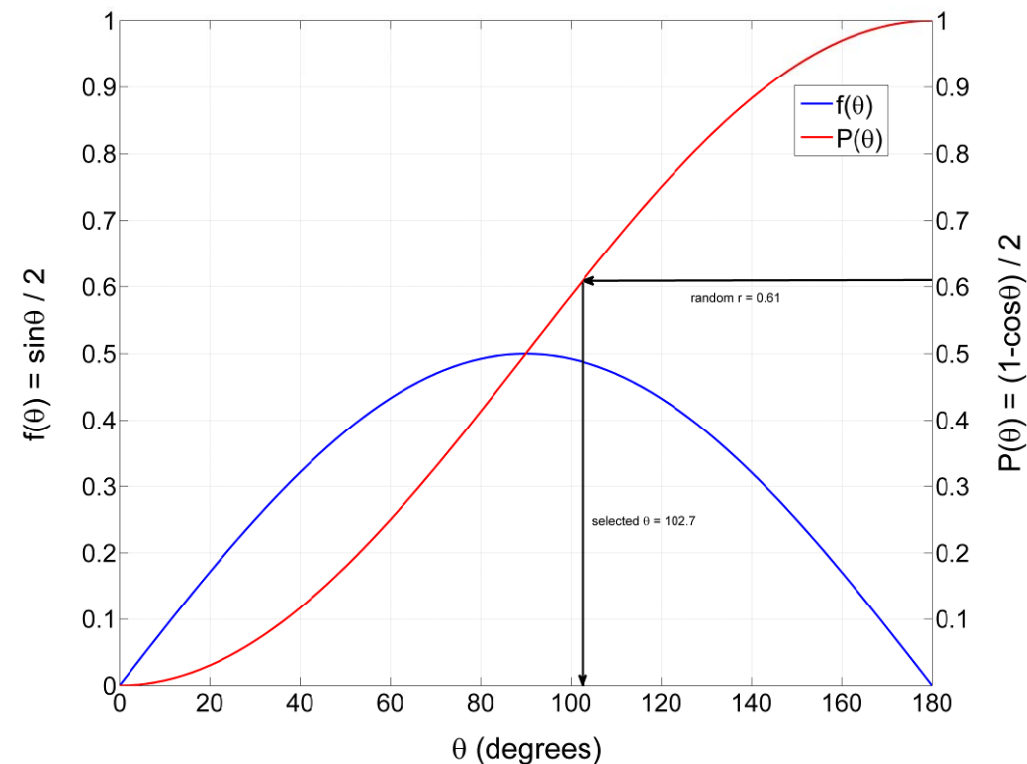


Figure from: Venselaar, Baltas, Meigooni, Hoskin (Eds),
Comprehensive Brachytherapy: physical and clinical
aspects. CRC Press, Taylor & Francis, © 2013



The MC method ...

Choosing interaction site.

The probability that a photon interacts within dx after travelling a distance x is $\mu \exp(-\mu x)$ so that:

$$r = P(x) = \int_0^{x^*} \mu \exp(-\mu x) dx \Rightarrow r = -\exp(-\mu x^*) + 1 \Rightarrow x^* = -\frac{1}{\mu} \ln(1-r) = -\frac{1}{\mu} \ln(r)$$

Choosing interaction type.

Interaction type is a discrete random variable of i values so that

$$P_i = \mu_i / \mu_{\text{total}}$$

So given r , I choose interaction j so that:

$$j = \min \left\{ j : r < \sum_{i=1}^j P_i \right\}$$

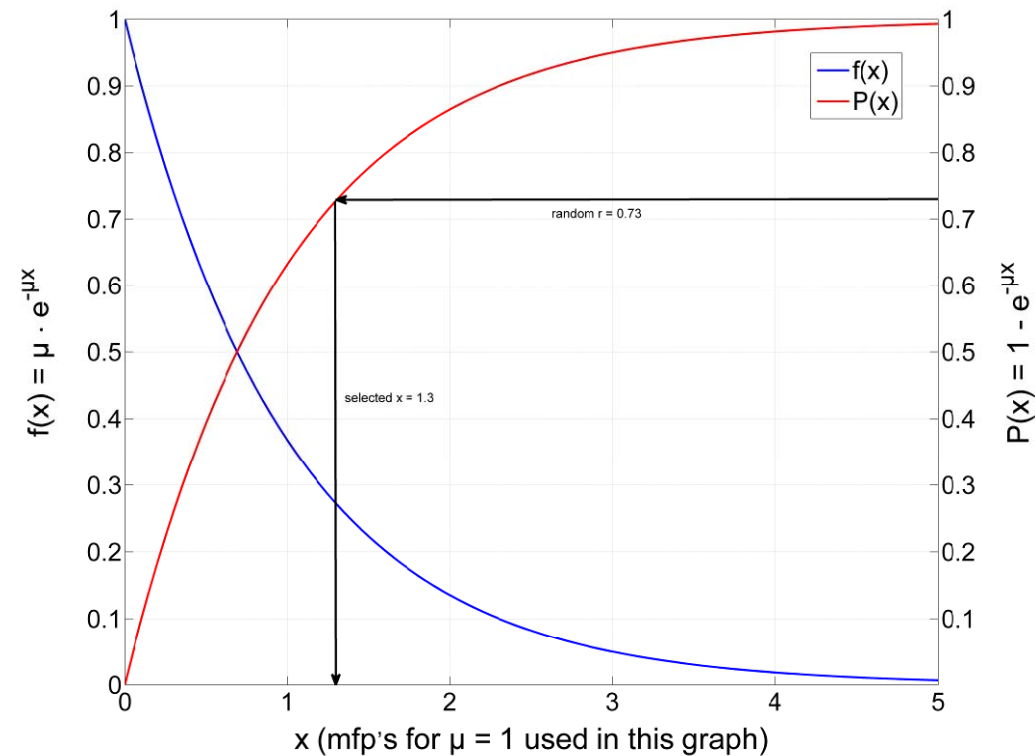
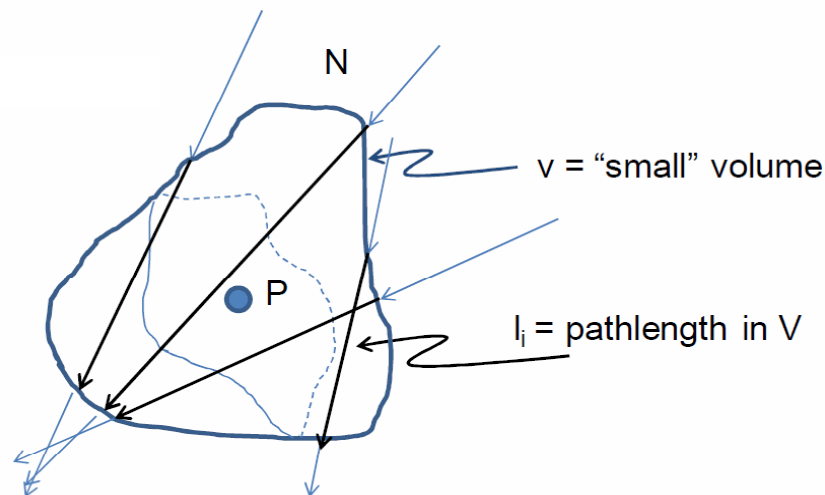


Figure from: Venselaar, Baltas, Meigooni, Hoskin (Eds),
Comprehensive Brachytherapy: physical and clinical
aspects. CRC Press, Taylor & Francis, © 2013

The MC method ...

- Similar procedures (available in the literature from the 50's) are used for sampling randomly from the probability distributions for every process involved in photon transport.
- MC is a statistical method to approximate dose at all points of a geometry
- The method inherently accounts for real sources, inhomogeneities, and phantom dimensions according to input data.
- The collision KERMA can be calculated within voxels by scoring the energy transferred to charged particles from interactions within the voxel and weighing by voxel mass ($dm = \rho dV$) (analogue MC).
- Alternatively, photon energy fluence can be scored in each voxel and weighed by μ_{en}/ρ to obtain collision KERMA (track length estimator).

$$\Phi = \lim_{\substack{N \rightarrow \infty \\ V \rightarrow 0}} \left\{ \frac{1}{V} \sum_{i=1}^N l_i \right\}$$



The MC method ...

MC simulations for single source dosimetry are ALWAYS a set of **2 MC** simulations

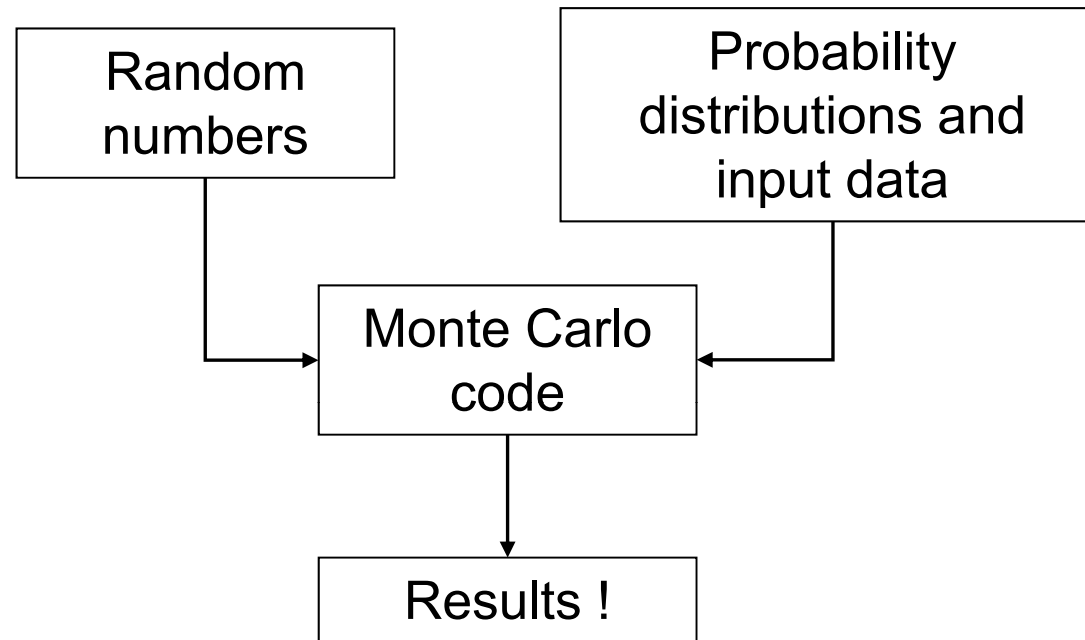
one for the distribution of energy absorbed
at all points of the geometry per starting particle
and

one for the air kerma of the source per starting particle

In multiple source MC dosimetry (e.g. a clinical case) results from single source positions can be weighed by t_i , summed and multiplied by TRAK ($S_K * t_{tot}$)

The MC method ...

The general outline of a MC code is:



The questions then are:

1. What is the accuracy of the method?
2. How efficient can the method be?

Type A uncertainty

➤ Recall that : $P\left(-\frac{3b}{\sqrt{N}} < \frac{1}{N} \sum_{i=1}^N k_i - m < \frac{3b}{\sqrt{N}}\right) \approx 0.997$

b, the stdev of unknown quantity m is not known but for $N \gg \bar{k} = \frac{1}{N} \sum_{i=1}^N k_i$ approximates m and the square root of the variance $Var(k) = \frac{1}{N-1} \sum_{i=1}^N (k_i - \bar{k})^2 \approx \bar{k}^2 - \bar{k}^2$ approximates b.

$\sqrt{\frac{Var(k)}{N}}$ therefore forms precision confidence interval (k=3) of our tally and it must be as low as possible.

➤ Type A uncertainty decreases $\sim 1/\sqrt{N}$

➤ type A uncertainty decreases as voxel size increases for analogue MC (at the expense of volume averaging)

➤ the only other way to decrease type A would be to reduce Var(k) which is in essence an efficiency gain and will be discussed later

Type A uncertainty

- TG-43 U1* suggests that enough histories, N , should be used to ensure that dosimetry results have relative uncertainties $<2\%$ at $r < 5$ cm
- AAPM/ESTRO** recommendations are MC Type A uncertainties ($k=1$) $<0.1\%$ for distances < 5 cm and Type A uncertainties ($k=1$) $<0.2\%$ for distances <10 cm
- TG-138 (AAPM/ESTRO)*** suggests MC type A $<0.1\%$ when feasible

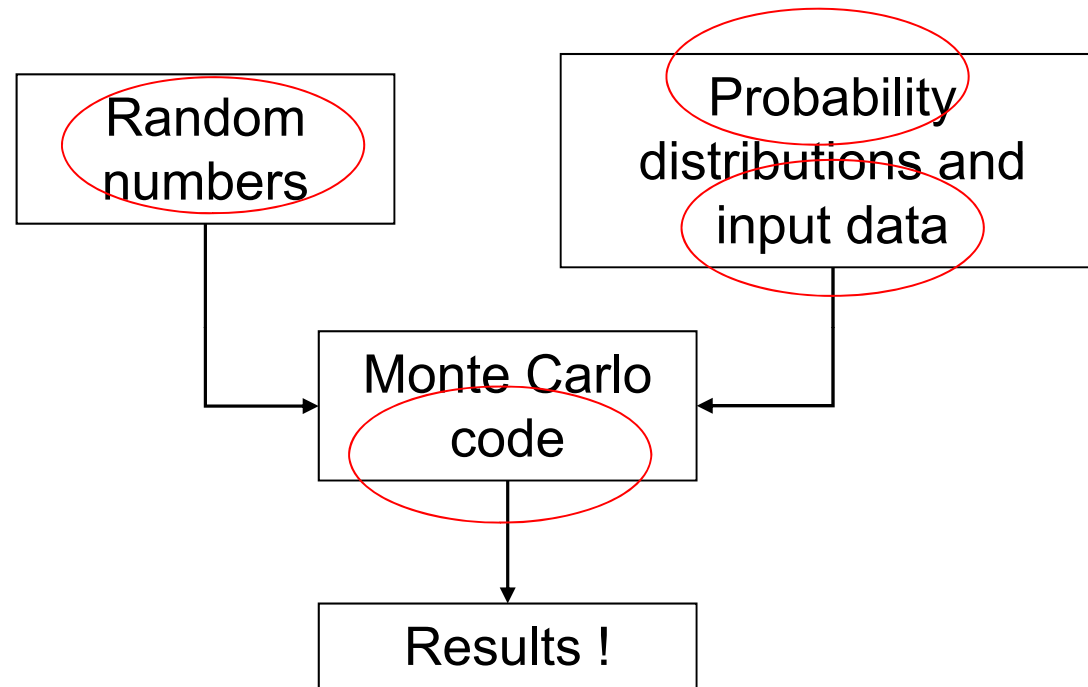
* Rivard et al., 2004. Update of AAPM Task Group No. 43 Report: A revised AAPM protocol for brachytherapy dose calculations. Med. Phys. 31(3), p.633.

** Perez-Calatayud et al., 2012. Dose calculation for photon-emitting brachytherapy sources with average energy higher than 50 keV: report of the AAPM and ESTRO. Med. Phys. 39(5), p.2904

*** DeWerd et al., 2011. A dosimetric uncertainty analysis for photon-emitting brachytherapy sources: report of AAPM Task Group No. 138 and GEC-ESTRO. Med. Phys. 38(2), pp. 782

Type B uncertainty

All other aspects of the simulation contribute to type B uncertainty



Type B uncertainty ... random number generator

Pseudo random number generators are used, e.g. Lehmer type, multiplicative-congruential of the form:

$$r_{n+1} = Br_n \text{ mod } 2^M$$

with B, M and r_0 (the “seed” of the sequence) appropriately selected.

- These generators are generally robust in benchmarked and extensively used codes
- These generators are periodic with a period of 2^M . Exceeding this period might underestimate result variance
- If you are using different simulations to estimate $\text{Var}(k)$ make sure the seed is different

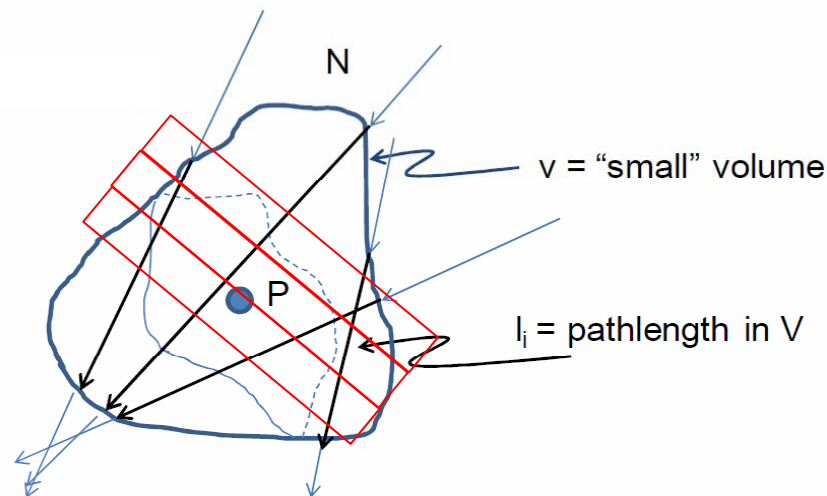
Type B uncertainty ... code

- What MC code should I use? / Should I prepare my own?
- Codes benchmarked and extensively used in the literature: PTRAN, MCNP, GEANT4, PENELOPE, and EGS.
- TG-43U1*: Monte Carlo codes not previously used in brachytherapy dosimetry, should be more rigorously tested and documented in the peer-reviewed literature before proposing to use their results clinically.
- TG-43U1*: “regardless of the transport code chosen and its pedigree, all investigators should assure themselves that they are able to reproduce previously published dose distributions for at least one widely used brachytherapy source model. This exercise should be repeated whenever new features of the code are explored, upon installing a new code version, or as part of orienting a new user.”

Type B uncertainty ... scoring

- CPE can be assumed and only photons need be simulated
Photon-only simulation introduces errors >2% @ distances at or below 1.6, 3, and 7mm for Ir-192, Cs-137, and Co-60 sources, respectively (Perez-Calatayud et al. 2012) but this is source specific and clinically irrelevant in most cases.
- Scoring cell dimensions are important! See Taylor et al. (2007) for details and Rivard et al. (2004) and Perez-Calatayud et al. (2012) for recommendations
 - For analogue MC increasing voxel size will reduce type A but increase volume averaging
 - For track length estimators reducing voxel thickness while preserving surface will reduce volume averaging without affecting type A

$$\Phi = \lim_{\substack{N \rightarrow \infty \\ V \rightarrow 0}} \left\{ \frac{1}{V} \sum_{i=1}^N l_i \right\}$$



Type B uncertainty ... cross sections

- Probability distributions are in the form of a **cross section data base**.
- Total partial and differential photon cross sections are required including atomic form factors $F(x, Z)$ and incoherent scatter factors $S(x, Z)$
- These cross sections must be: complete (in terms of E, Z) self-consistent and up to date/accurate.
- Self-consistency is also required with mass energy absorption data used for kerma calculation from energy fluence

- Up to date cross sections are used in all current versions of benchmarked MC codes: EPDL97 (LLNL) in the ENDL or ENDF/B-VI formats or the DLC-146 format (ORNL) or XCOM (NIST) database. Mass energy-absorption coefficients for water by Seltzer and Hubbell (available on line at NIST).
Data readily available online through NIST (<http://www.nist.gov/pml/data/xraycoef/>)

- TG-138 (AAPM/ESTRO) cites ~1% cross section type B that contributes to dosimetric uncertainty at $r=5$ cm about 0.76 % (low E) and 0.12% (high E)

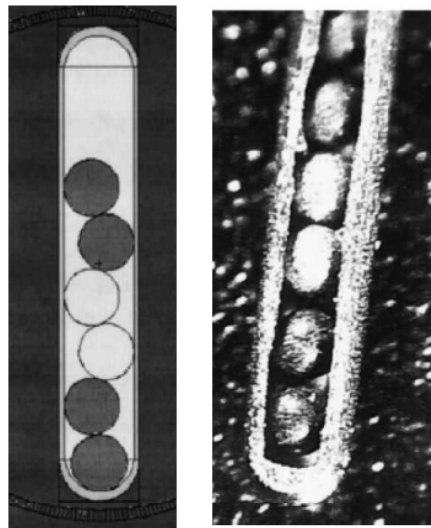
Type B uncertainty ... input

Source geometry

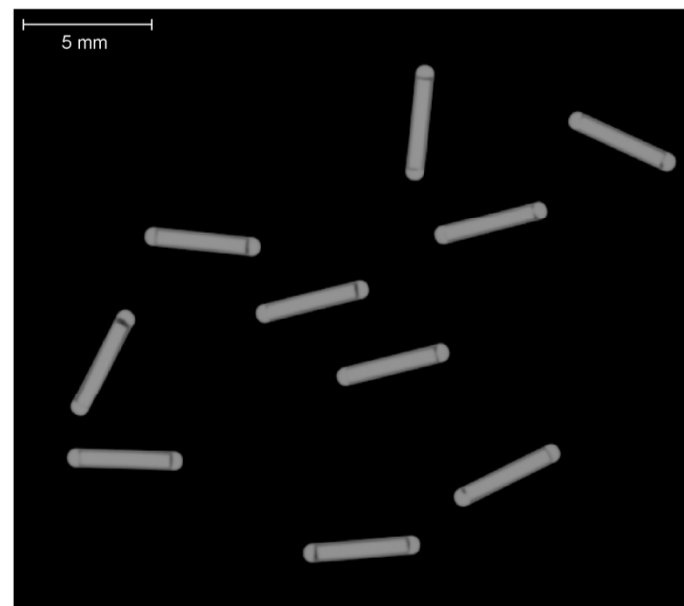
- Information is required on geometry, materials, density, elemental composition, and dimensions.
- The uncertainty of this information is more crucial for low energy sources
- For reference dosimetry of new sources geometry and dimensions should be verified experimentally in a sample of sources.
- If the source includes parts of non-negligible mobility, MC should be performed for different configurations and results averaged.



e microscopy (6711)



seed cut out view
(3631 A/M)



contact tr. radiography
(IsoSeed I25.S17plus)

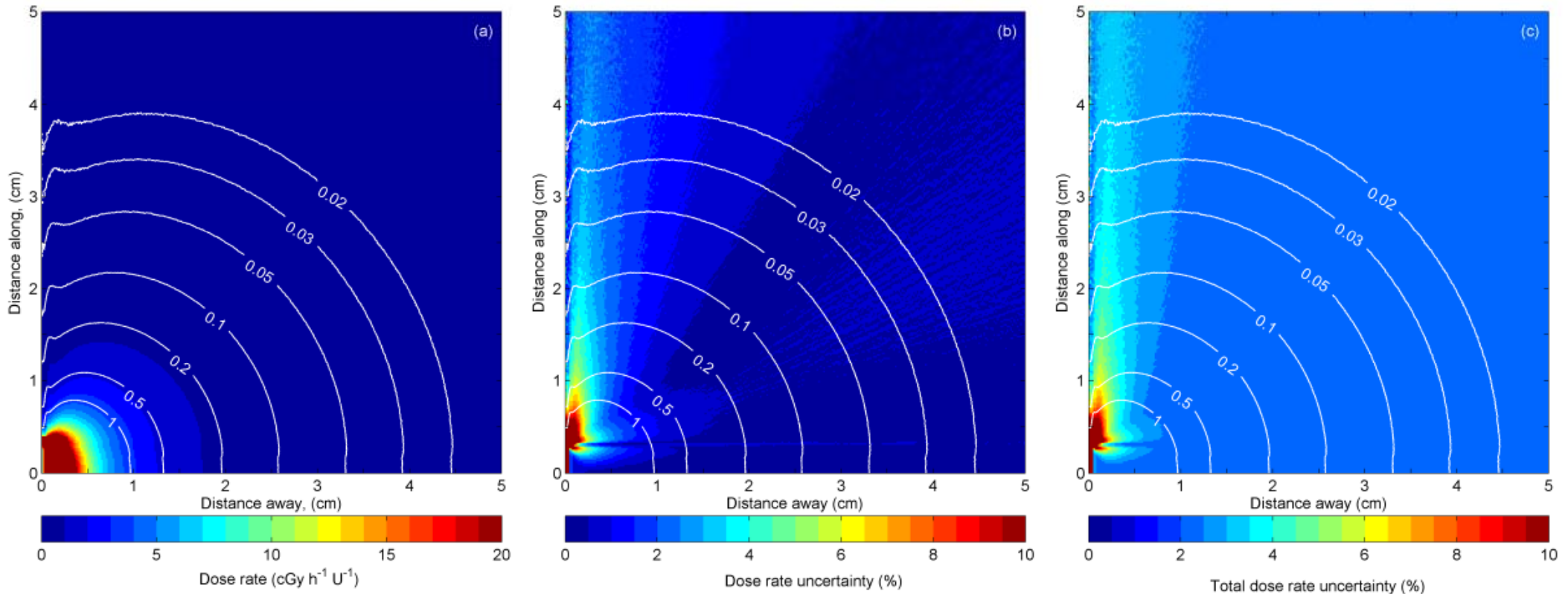
Pics from: Rogers & Cygler (Eds), *Clinical dosimetry measurements in radiotherapy* (2009 AAPM Summer School), Monograph No. 34, Medical Physics Publishing 2011

Pantelis et al, *J Contemp Brachytherapy* 5(4), 240 (2013)

Type B uncertainty ... input

Source geometry

➤ Besides verified, the uncertainty in construction details (tolerances) must be included in the uncertainty budget. In example: uncertainty map for an I-125 seed



MC dose rate distr.

IsoSeed I25.S17plus:
% uncert.: geo. + type A

% uncert.: geo. + type A + cross secs.

Type B uncertainty ... input

➤ Phantom geometry (for single source dosimetry)

Remember dose from scatter depends on geometry dimensions...!
or patient segmentation and source/applicator position (for patient dosimetry)

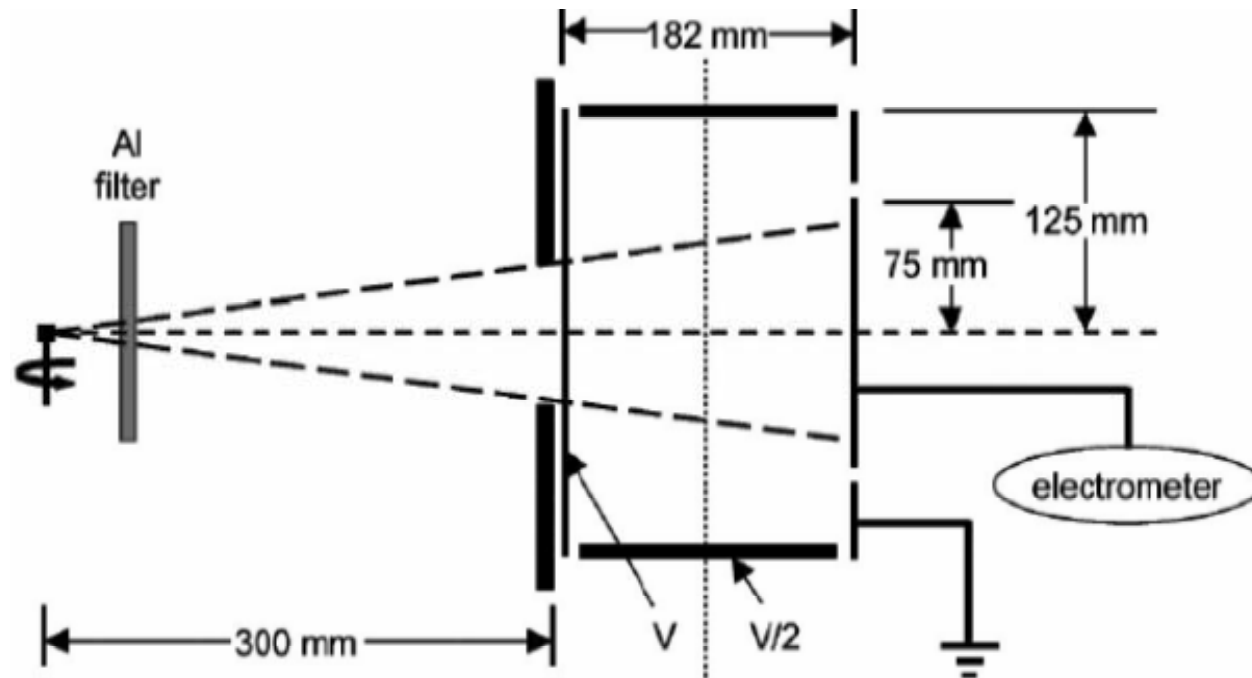
➤ Geometry in simulation for S_K (for single source dosimetry)

In order to comply with the definition of S_K :

- Air (point) detector at large distance from the source in vacuo
- Photon emissions of energy lower than $\delta=5$ keV (i.e. characteristic x-rays of Ti encapsulation following photoelectric absorption of ^{125}I photons) must be suppressed.

Geometry for actual measurement of S_K

For low energy sources, simulations must also account for the WAFAC - 7.6° half angle.



- Due to polar angle averaging, S_K increases for sources with radioactivity distributed over cyl. ends, leading to Λ_{WAFAC} lower than Λ_{point} results.
- This effect depends on the ratio of marker diameter to marker length.
- Differences between Λ_{WAFAC} and Λ_{point} range from non-detectable to 3.5%.

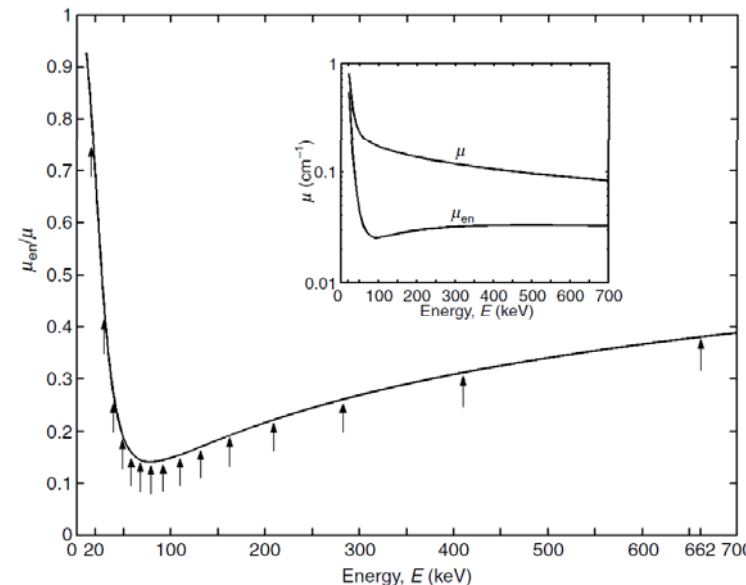
How efficient can MC be ...?

Traditionally, MC was said to be too slow for clinical use and therefore reserved for high quality single source dosimetry in reference conditions that was then partitioned to TG-43 quantities and used in TPS for treatment planning purposes.

How efficient can MC be ...?

Traditionally, MC was said to be too slow for clinical use and therefore reserved for high quality single source dosimetry in reference conditions that was then partitioned to TG-43 quantities and used in TPS for treatment planning purposes.

- Total t_{CALC} scales with N , which is determined by the level of desired type A uncertainty which is proportional to $\sqrt{\text{Var}(k)/N}$
- MC for Brachy enjoys t_{CALC}/N reduction from photon only tracking (20%-70%)
- In brachy however, t_{CALC}/N is large when multiple scattering occurs



How efficient can MC be ...?

t_{CALC} scales with N , type A uncertainty scales with $\sqrt{\frac{\text{Var}(k)}{N}}$

➤ The only means to decrease t_{CALC} for a given level of type A uncertainty is variance reduction.

➤ Variance reduction:

- Simple techniques: geom. truncation, E cut off, phase space files*, analytical primary scatter separation (PSS), ...

(* Pantelis et al. On source models for ^{192}Ir HDR brachytherapy dosimetry using model based algorithms Phys. Med. Biol. 61, 2016)

- Elaborate techniques**: techniques to bias the sampling distributions while using correction factors to eliminate the biasing effect in the sample mean of the quantity of interest

(** see Sheikh-Bagheri, D., Kawrakow, I., Walters, B., and Rogers, D.W.O. 2006. Monte Carlo simulations: Efficiency improvement techniques and statistical considerations. Integrated New Technologies into the Clinic: Monte Carlo and Image-Guided Radiation Therapy—Proceedings of the 2006 AAPM Summer School)

Monte Carlo for TPS?

- t_{CALC} reductions from: photon only tracking (20%-70%), track length scoring (20-30), pre-calculated source phase space (30%-40%), variance reduction (40-60) + (inherent) parallelization and reduction of t_{CALC}/N from availability of multi-core processors have facilitated clinically viable calculation times:
 - ✓ sub-minute to minutes for LDR applications
 - MCPI (GEPTS): Chibani & Williamson 2005 Med Phys 32, 3688
 - BRACHYDOSE (EGSnrc): Thomson et al 2010 Med. Phys. 37, 3910
 - ALGEBRA (GEANT4): Afsharpour et al. 2012 Phys Med Biol 57, 3273
 - ✓ 2.5–17 minutes for 40^3 – 140^3 2mm voxels for HDR rectal application
 - BRACHYGUI (PTRAN) Poon et al 2008 J Phys Conf Ser 102, 012018.

- further reduction of t_{CALC}/N from GPU implementation might do the trick:
 - ✓ sub-sec for single source, 2 sec for HDR+shield implant
 - Hissoiny et al, Med. Phys. 39 (2012)
- ✓ Tian et al, “Monte Carlo dose calculations for high-dose–rate brachytherapy using GPU-accelerated processing,” *Brachytherapy* 15(3), pp. 387 (2016).

Monte Carlo: summary

- !Monte Carlo based TPS not clinically available for brachytherapy yet!
- MC is the gold standard for single source dosimetry in brachytherapy (TG-43 data)
- Several public domain codes are available that have been extensively benchmarked, and ample literature/experience/recommendations are available
- Type B uncertainties associated with MC results for single source dosimetry are (mainly) user-related
- MC is inherently associated with a level of type A uncertainty

Other uses...?

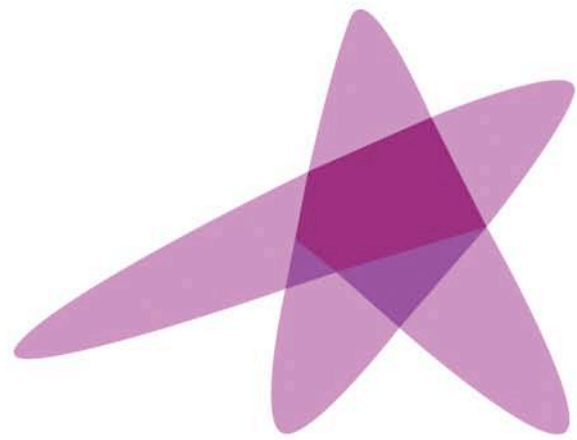
- MC for TPS
- MC for benchmarking TPS dose calculations
- MC for the calculation of experimental dosimetry corrections

Further reading ...

- J. Seco, F. Verhaegen (Eds), Monte Carlo Techniques in Radiation Therapy. CRC Press, Taylor & Francis, © 2013
- Venselaar, Baltas, Meigooni, Hoskin (Eds), Comprehensive Brachytherapy: physical and clinical aspects. CRC Press, Taylor & Francis, © 2013
- Rivard, M.J. et al., 2004. Update of AAPM Task Group No. 43 Report: A revised AAPM protocol for brachytherapy dose calculations. Medical Physics, 31(3), p.633.
- Perez-Calatayud, J. et al., 2012. Dose calculation for photon-emitting brachytherapy sources with average energy higher than 50 keV: report of the AAPM and ESTRO. Medical physics, 39(5), pp.2904–29.

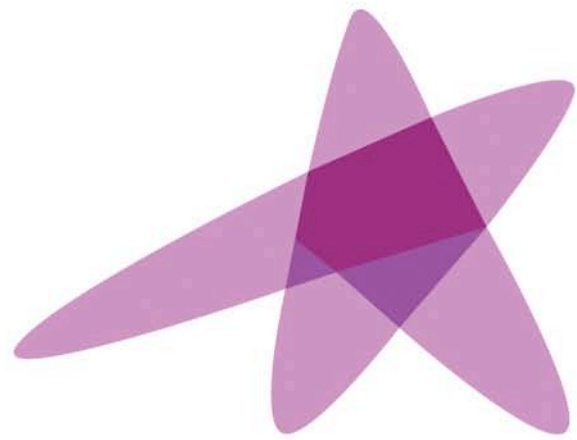
and references therein

- references cited herein



ESTRO

School



ESTRO
School

Advanced Brachytherapy Physics

Background and Details on TG-43 Based Dosimetry

Prof. Mark J. Rivard, Ph.D., FAAPM

Advanced Brachytherapy Physics, 29 May – 1 June, 2016



Disclosures

The are no conflicts-of-interest to report.

Opinions herein are solely those of the presenter, and are not meant to be interpreted as societal guidance.

Specific commercial equipment, instruments, and materials are listed to fully describe the necessary procedures. Such identification does not imply endorsement by the presenter, nor that these products are necessarily the best available for these purposes.

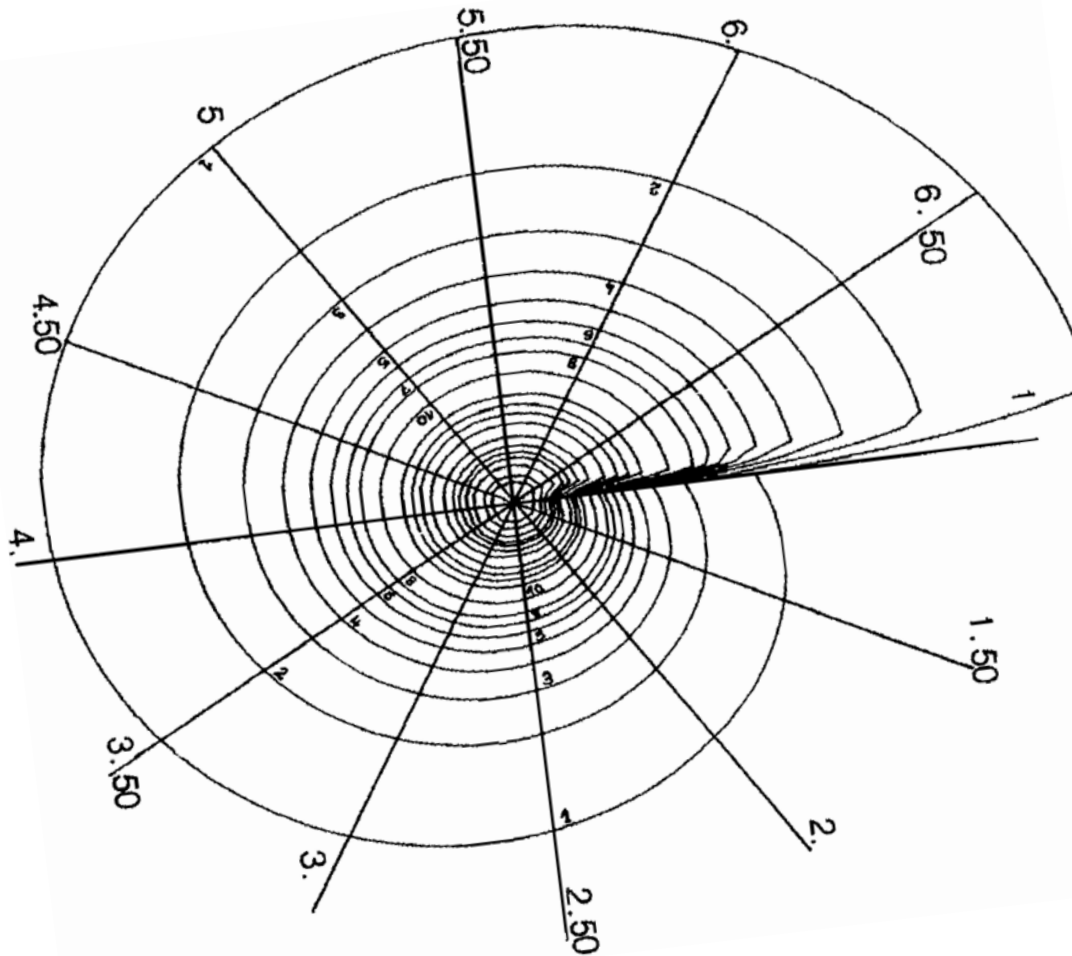
Learning Objectives

1. Review need for international BT dosimetry formalism
2. Explore the TG-43 BT dosimetry formalism
3. Example calculations and TPS source commissioning

Brachytherapy Dosimetry?



Brachytherapy Dosimetry?



Dutreix, et al., Dosimétrie en Curiethérapie (Paris, 1982).

Brachytherapy Dosimetry!

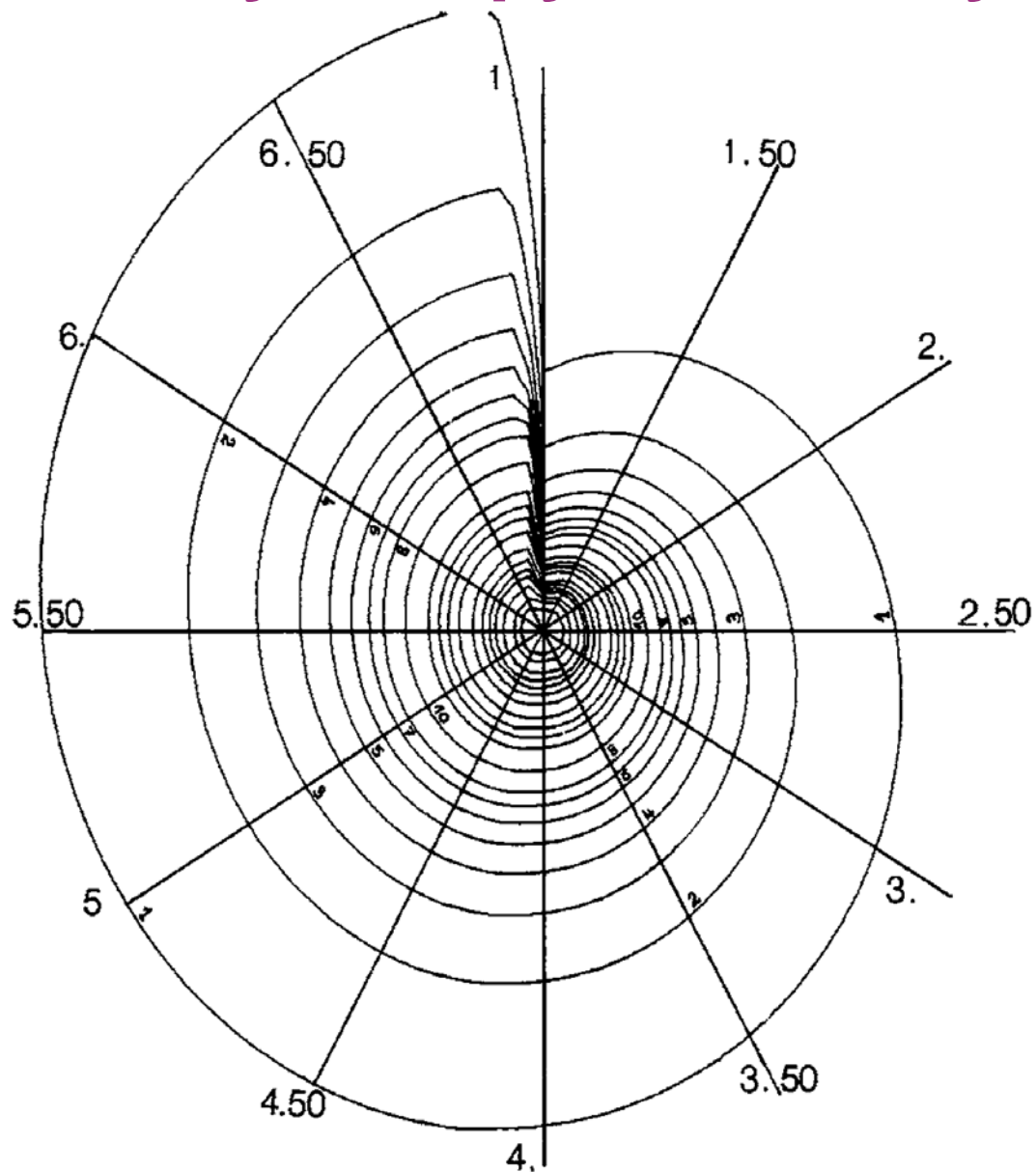


FIG. 1. The escargot diagram in the Paris system is a tool for manual calculation of the dose rate at points at distances in the plane transversal to the source. The curves represent the dose rate in cGy h^{-1} for sources of 1 up to 7 cm length and a linear strength of $1 \text{ mR h}^{-1} \text{ m}^2 \text{ cm}^{-1}$

Why Follow the TG-43 Dose Calculation Formalism?

- Accurate interpolation of dose distribution is achieved because geometric dependence of dose falloff (as function of r and θ) is accounted for. This allows use of a limited dataset while providing robust dose calculation.
- Analytic, uniform approach to brachytherapy dose calculation is readily available, thereby promoting consistent clinical practice worldwide.

Rivard, et al., *Med. Phys.* 31, 633-674 (2004)

Perez-Calatayud, et al., *Med. Phys.* 38, 2904-2929 (2012)



Low-Energy BT Dosimetry Report

Medical Physics

Update of AAPM Task Group No. 43 Report:

A revised AAPM protocol for brachytherapy dose calculations

Since publication of the TG-43 protocol in 1995, significant advances have taken place in the field of permanent source implantation and brachytherapy dosimetry. To accommodate these advances, the AAPM deemed it necessary to update this protocol for the following reasons:

- (a) eliminate minor inconsistencies and omissions in the original TG-43 formalism and its implementation.
- (b) incorporate subsequent AAPM recommendations, addressing requirements for acquisition of dosimetry data as well as clinical implementation. These recommendations, e.g., elimination of A_{app} (see Appendix E) and description of minimum standards for dosimetric characterization of low-energy photon-emitting brachytherapy sources, needed to be consolidated in one convenient document.
- (c) critically reassess published brachytherapy dosimetry data for the ^{125}I and ^{103}Pd source models introduced both prior and subsequent to publication of the TG-43 protocol in 1995, and to recommend consensus datasets where appropriate.
- (d) develop guidelines for determination of reference-quality dose distributions by experimental and Monte Carlo methods, and promote consistency in derivation of parameters used in TG-43 formalism.

High-Energy BT Dosimetry Report

Medical Physics

Dose calculation for photon-emitting brachytherapy sources with average energy higher than 50 keV: Report of the AAPM and ESTRO

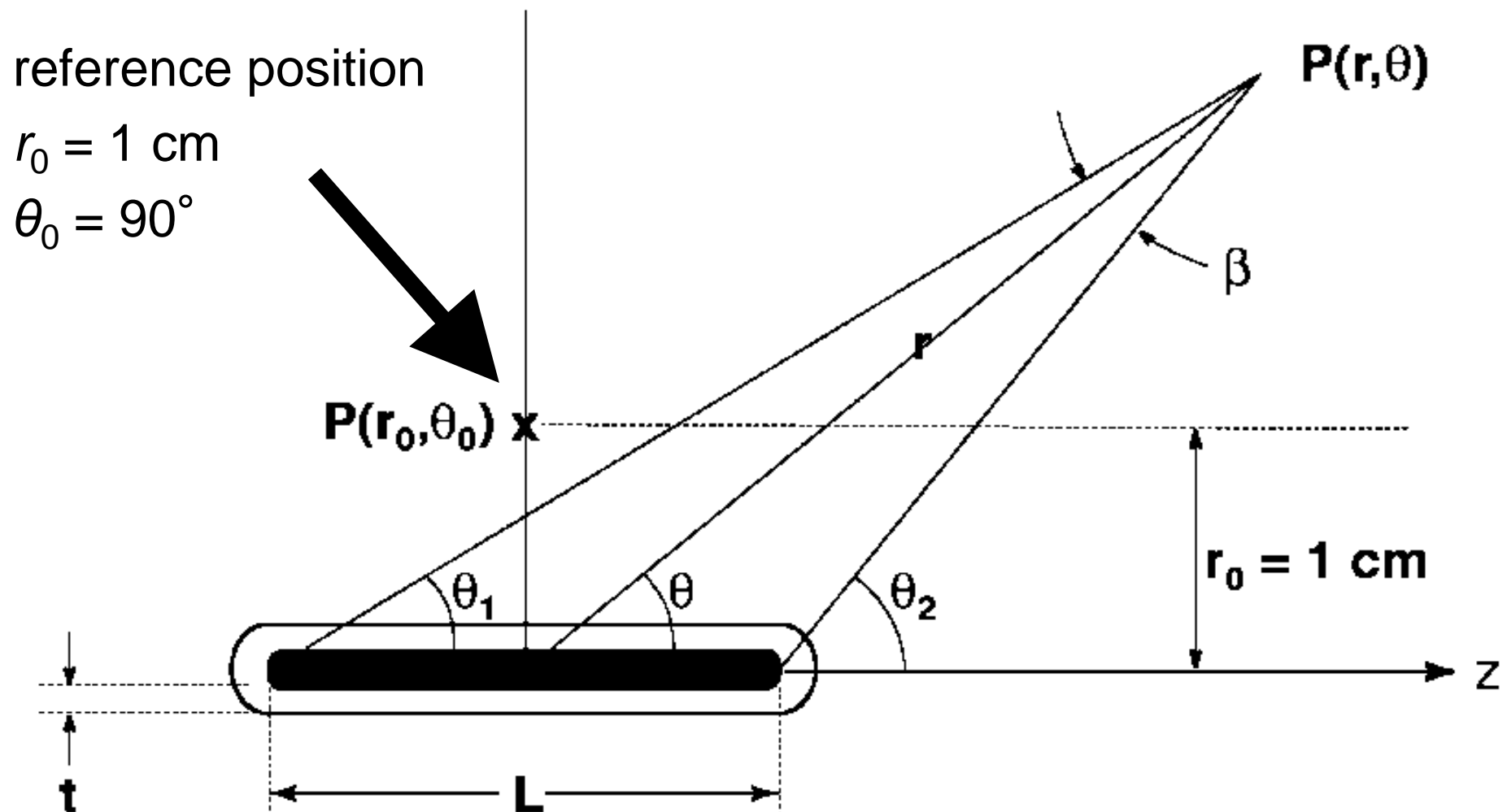
Purpose: Recommendations of the AAPM and ESTRO on dose calculations for high energy (avg energy > 50 keV) photon-emitting brachytherapy sources are presented, including physical characteristics of specific ^{192}Ir , ^{137}Cs , and ^{60}Co .

Methods: This report was prepared by the High Energy Brachytherapy Source Dosimetry (HEBD) Working Group, and includes considerations for applying the TG-43U1 formalism to high-E photon-emitting sources with particular attention to phantom size effects, interpolation accuracy dependence on dose calculation grid size, and dosimetry parameter dependence on active length.

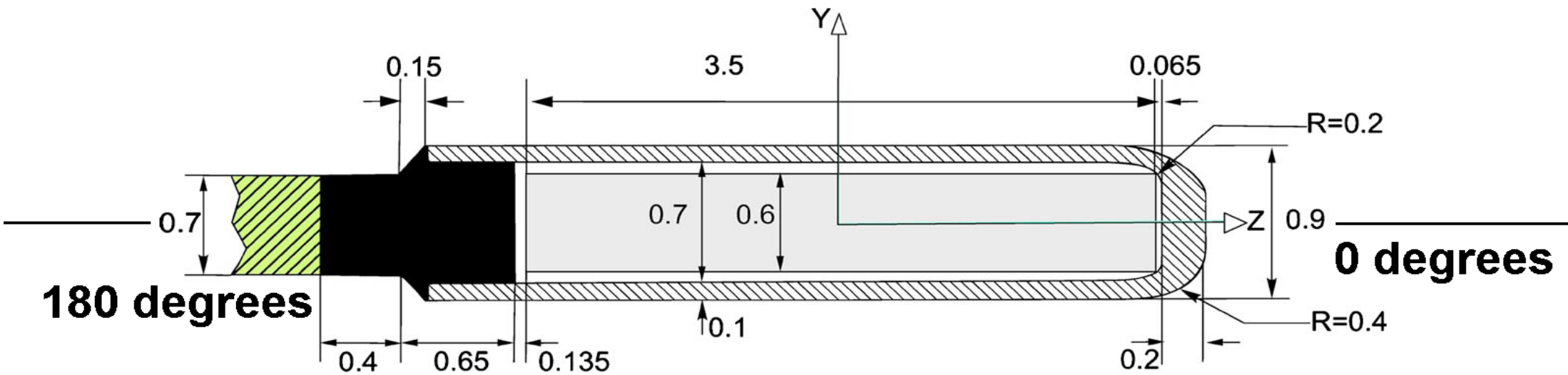
Results: Consensus datasets for commercially available sources are provided, along with recommended methods for evaluating these datasets. Recommendations on dosimetry characterization methods, mainly using experimental procedures and Monte Carlo, are established and discussed. Included are methodological recommendations on detector choice, detector energy response characterization and phantom materials, and measurement specification methodology. Uncertainty analyses are discussed and recommendations are given for sources without consensus datasets.

Conclusions: Recommended consensus datasets for high-energy sources are derived for sources that were commercially available as of January 2010. Data are presented according to the AAPM TG-43U1 formalism, with modified interpolation and extrapolation techniques of the AAPM TG-43U1S1 report for the 2D anisotropy function and radial dose function.

BT Dose Calculation Geometry



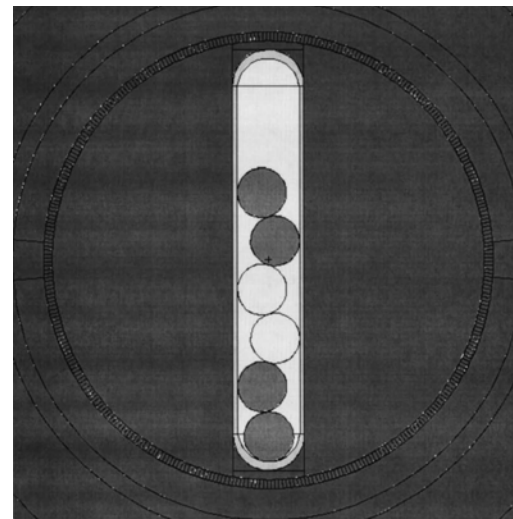
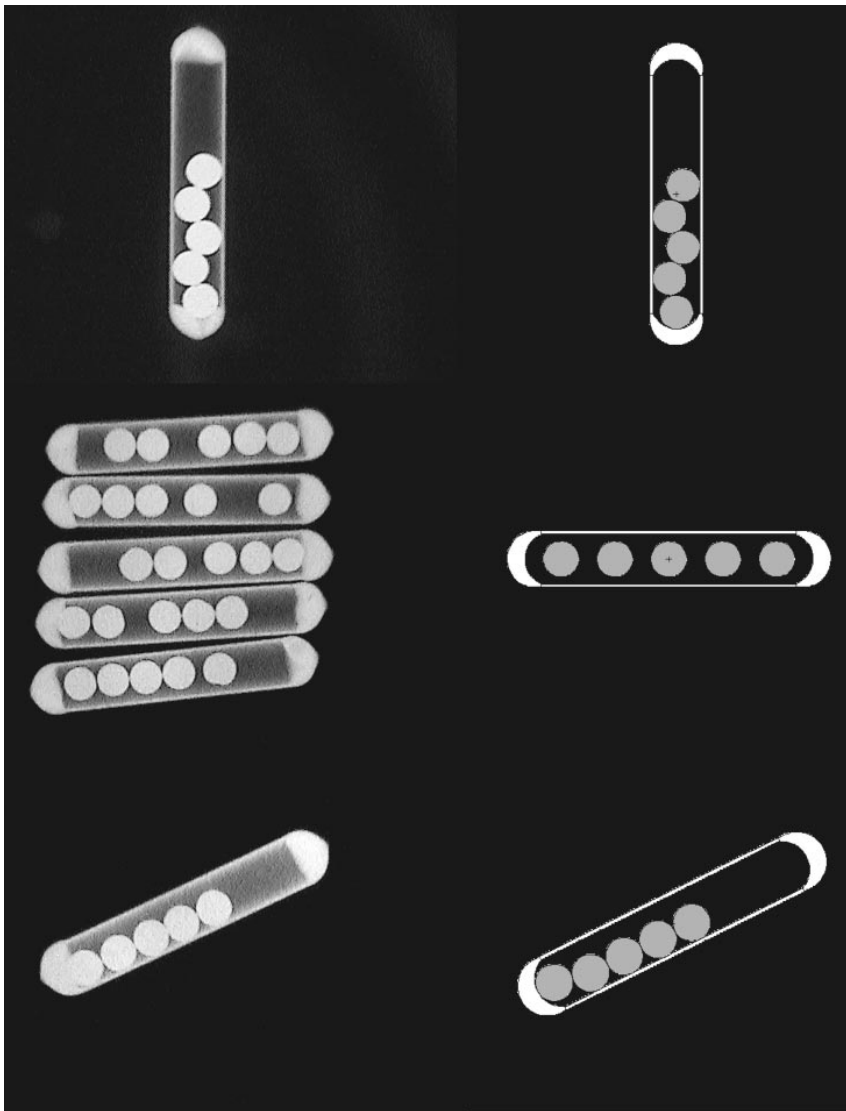
Origin and Angular Notation



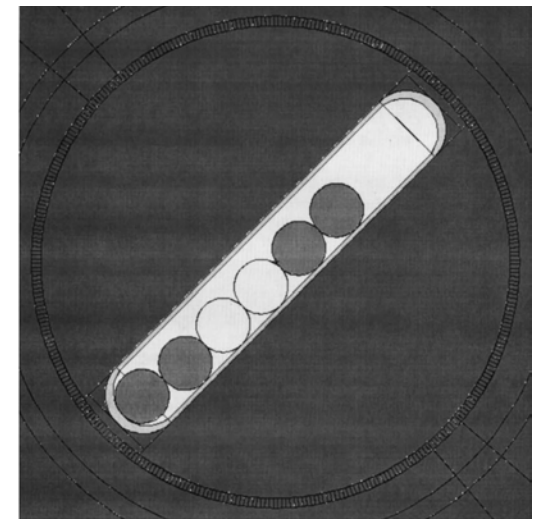
dimensions need to be in centimeters (cm), not millimeters

Low-Energy LDR Seeds

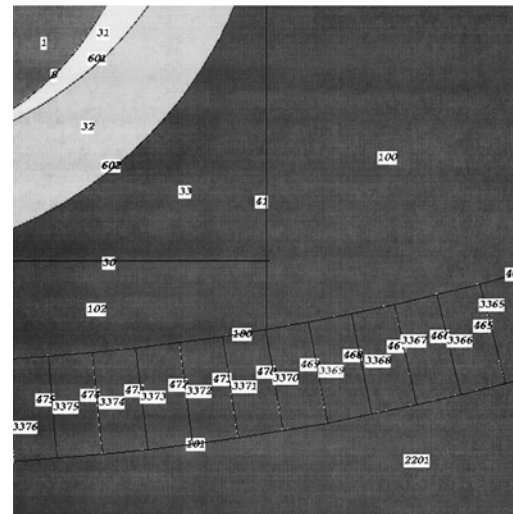
Dynamic source orientation influences some dose distributions



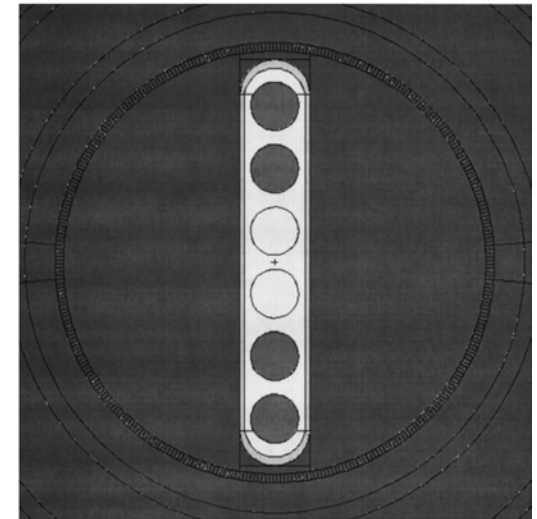
(a)



(b)



(c)



(d)

TG-43 2D Formalism

$$\dot{D}(r, \theta) = S_K \Lambda \frac{G(r, \theta)}{G(r_0, \theta_0)} g_L(r) F(r, \theta)$$

$\dot{D}(r, \theta)$ dose rate to water at point P(r,θ)

S_K air kerma strength

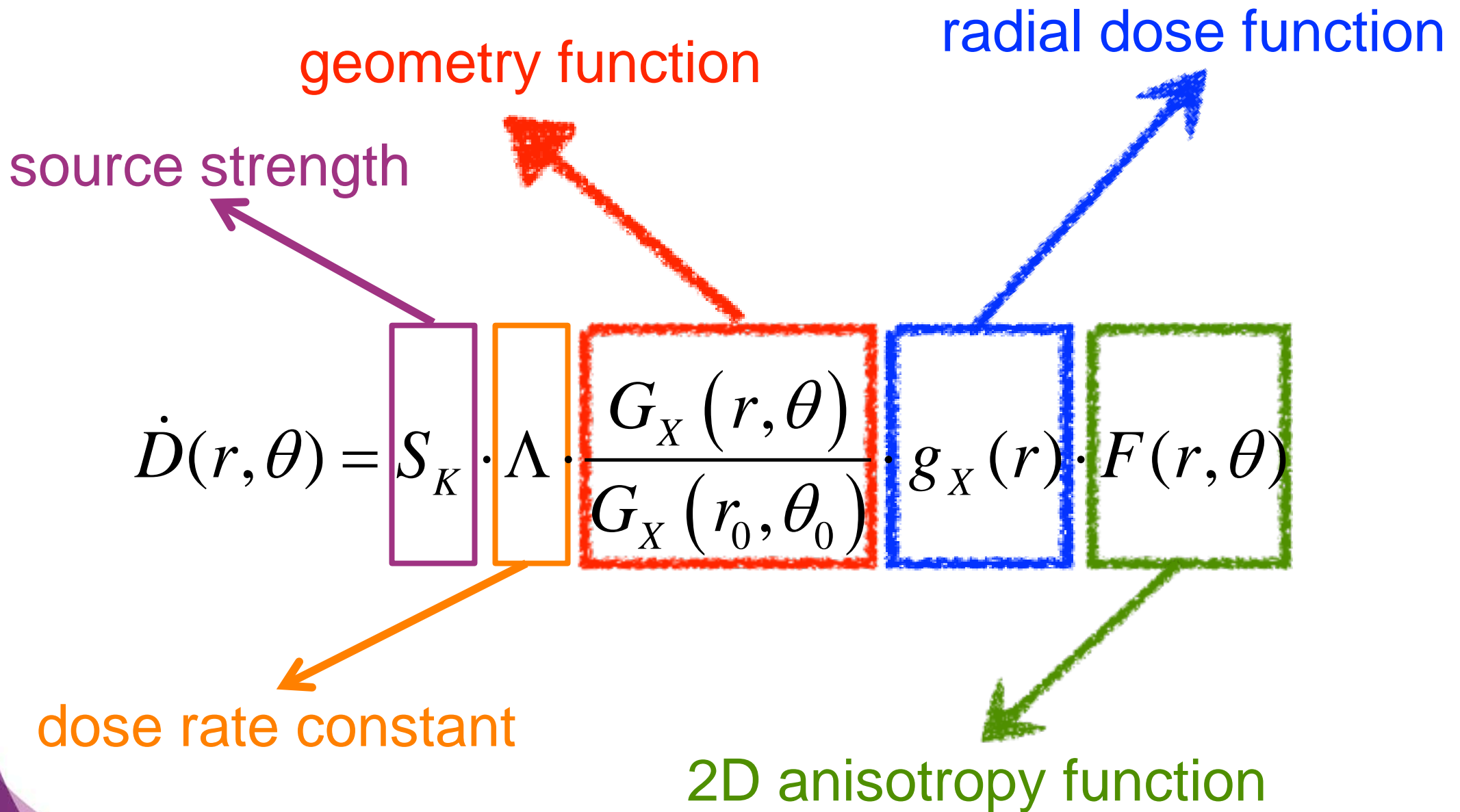
Λ dose rate constant

$G_L(r, \theta)$ geometry function (line-source approximation)

$g_L(r)$ radial dose function

$F(r, \theta)$ 2D anisotropy function

TG-43 2D Formalism



TG-43 1D Formalism: Comparisons

BAD
$$\dot{D}(r) = S_K \cdot \Lambda \cdot \frac{G_L(r, \theta_0)}{G_L(r_0, \theta_0)} \cdot g_P(r) \cdot \phi_{an}(r)$$

BAD
$$\dot{D}(r) = S_K \cdot \Lambda \cdot \left(\frac{r_0}{r}\right)^2 \cdot g_L(r) \cdot \phi_{an}(r)$$

GOOD
$$\dot{D}(r) = S_K \cdot \Lambda \cdot \left(\frac{r_0}{r}\right)^2 \cdot g_P(r) \cdot \phi_{an}(r)$$

BEST
$$\dot{D}(r) = S_K \cdot \Lambda \cdot \frac{G_L(r, \theta_0)}{G_L(r_0, \theta_0)} \cdot g_L(r) \cdot \phi_{an}(r)$$

TG-43 1D Formalism

$$\dot{D}(r) = S_K \Lambda \left(\frac{r_0}{r} \right)^2 g_P(r) \phi_{an}(r)$$

$\dot{D}(r)$	dose rate to water at point P(r,θ)
S_K	air kerma strength
Λ	dose rate constant
$1/r^2$	geometry function (point-source approximation)
$g_P(r)$	radial dose function
$\phi_{an}(r)$	1D anisotropy function

BT Source Strength

$$S_K = \dot{K}_\delta(d) d^2$$

$$1 \text{ U} = 1 \mu\text{Gy h}^{-1} \text{ m}^2$$

reference air kerma rate (RAKR)

ICRU 38, ICRU 60

Rivard, et al., *Med. Phys.* 31, 633-674 (2004)

Perez-Calatayud, et al., *Med. Phys.* 38, 2904-2929 (2012)

Dose Rate Constant

$$\dot{D}(r_0, \theta_0) = S_K \cdot \Lambda \quad \frac{\dot{D}(r_0, \theta_0)}{S_K} = \Lambda$$

$$\frac{\Lambda_L}{G_L(r_0, \theta_0)} = \frac{\Lambda_{L_{\text{REF}}}}{G_{L_{\text{REF}}}(r_0, \theta_0)}$$

$$\Lambda_{\text{Ir-192}} = 1.120 \times G_L(r_0, \theta_0) [\text{cGy h}^{-1} \text{U}^{-1}]$$

$$\Lambda_{\text{Co-60}} = 1.094 \times G_L(r_0, \theta_0) [\text{cGy h}^{-1} \text{U}^{-1}]$$

HEBD Dose Rate Constants

Source Name (Manufacturer)	${}_{CON}\Lambda$ [cGy·h ⁻¹ ·U ⁻¹]	Statistical uncertainty ($k = 1$)	${}_{CON}\Lambda/G_L(r, \theta)$ [cGy·cm ² ·h ⁻¹ ·U ⁻¹]
mHDR-v1 (Nucletron)	1.116	0.9%	1.127
mHDR-v2 (Nucletron)	1.109	1.1%	1.121
VS2000 (Varian)	1.100	0.6%	1.123
Buchler (E&Z BEBIG)	1.117	0.4%	1.119
GammaMed HDR 12i (Varian)	1.118	0.4%	1.129
GammaMed HDR Plus (Varian)	1.117	0.4%	1.128
GI192M11 (E&Z BEBIG)	1.110	0.4%	1.121
Ir2.A85-2 (E&Z BEBIG)	1.109	1.2%	1.120
M-19 (SPEC)	1.114	0.2%	1.125
Flexisource (Isodose Control)	1.113	1.0%	1.124

Geometry Function

$$G(r, \theta) = \frac{\arctan [L/(2r \sin \theta) + \cot \theta] + \arctan [L/(2r \sin \theta) - \cot \theta]}{Lr \sin \theta}$$

$$G_L(r, \theta) = \begin{cases} \frac{\beta}{Lr \sin \theta} & \text{if } \theta \neq 0^\circ \\ (r^2 - L^2/4)^{-1} & \text{if } \theta = 0^\circ \end{cases}$$

$$G(r, \theta_0) = \frac{2 \arctan (L/2r)}{[Lr]}$$

Rivard, et al., *Med. Phys.* 26, 2445-2450 (1999)

Rivard, et al., *Med. Phys.* 31, 633-674 (2004)

HEBD Radial Dose Functions

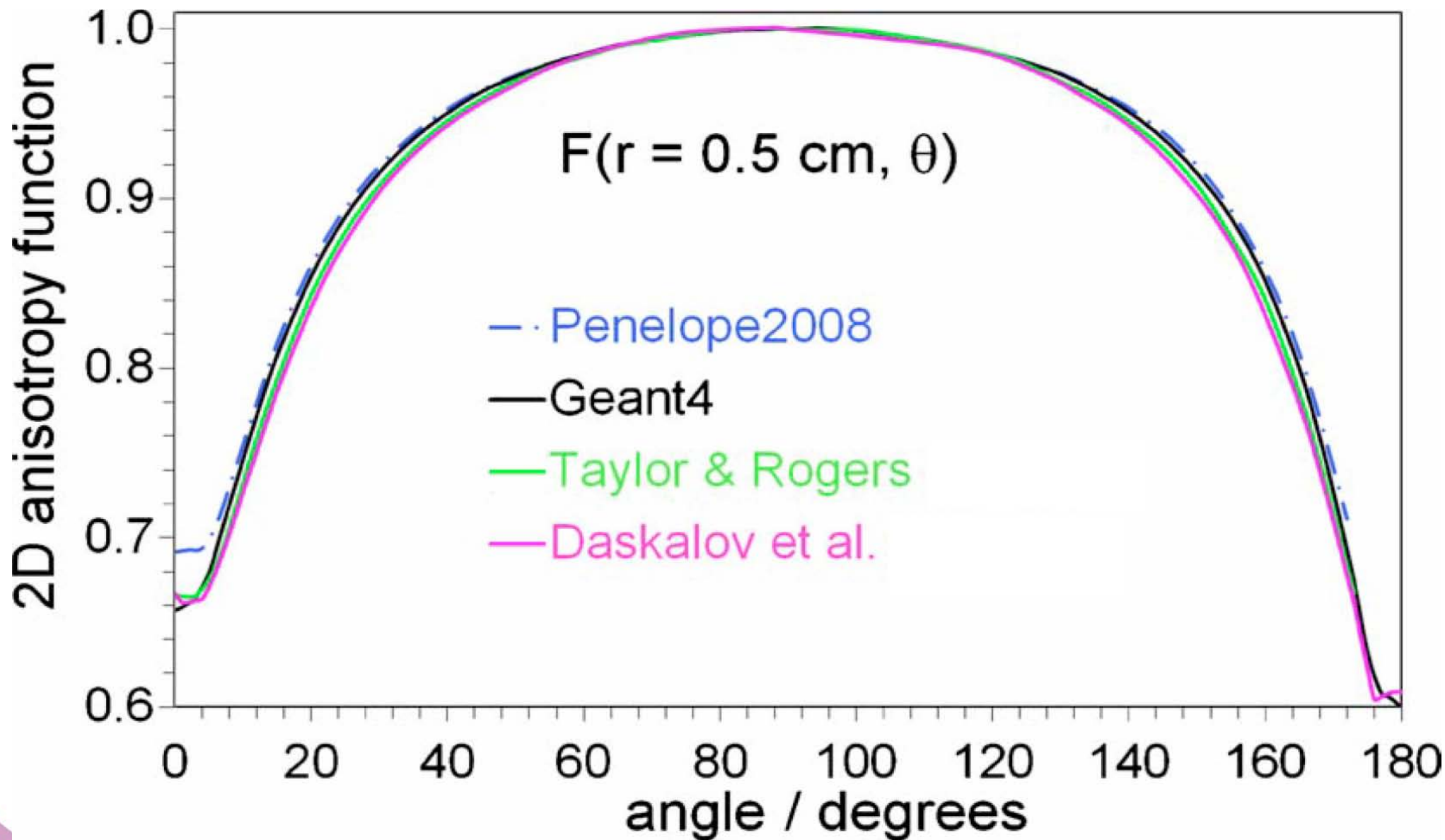
r [cm]	$g_L(r)$									
	Nucletron mHDR-v1	Nucletron mHDR-v2	Varian VS2000	E&Z BEBIG Buchler	Varian GammaMed HDR 12i	Varian GammaMed HDR Plus	E&Z BEBIG GI192M11	E&Z BEBIG Ir2.A85-2	SPEC M-19	Isodose Control Flexisource
	$L = 0.35$ cm	$L = 0.35$ cm	$L = 0.5$ cm	$L = 0.13$ cm	$L = 0.35$ cm	$L = 0.35$ cm	$L = 0.35$ cm	$L = 0.35$ cm	$L = 0.35$ cm	$L = 0.35$ cm
0.00	<u>[0.991]</u>	<u>1.276</u>	<u>0.986</u>	<u>1.023</u>	<u>0.992</u>	<u>0.998</u>	<u>0.990</u>	<u>0.990</u>	<u>0.993</u>	<u>0.991</u>
0.06		1,276								
0.08		1,199								
0.10		1,110								
0.15		1,018								
0.20	[0.991]	1,001	0.986	1.023	0.992	0.998				
0.25	[0.992]	0.995	0.991	1.018	0.992	0.997	0.990	0.990	0.993	0.991
0.50	[0.997]	0.997	0.997	1.002	0.994	0.996	0.996	0.996	0.995	0.997
0.75	[0.999]	0.998	0.999	0.999	0.997	0.998	0.998	0.998	0.998	0.998
1	1	1	1	1	1	1	1	1	1	1
1.5	[1.002]	1,003	1.005	1.003	1.004	1.003	1.003	1.002	1.001	1.002
2	[1.004]	1,005	1.010	1.004	1.006	1.006	1.004	1.004	1.005	1.004
3	[1.006]	1,008	1.012	1.008	1.008	1.006	1.005	1.005	1.008	1.005
4	[1.006]	1,007	1.013	1.007	1.005	1.004	1.004	1.003	1.003	1.003
5	[1.001]	1,003	1.011	1.002	0.999	0.999	0.999	0.999	0.999	0.999
6	[0.993]	0.996	1.003	0.995	0.991	0.993	0.992	0.991	0.994	0.991
8	[0.970]	0.972	0.982	0.971	0.968	0.968	0.968	0.968	0.969	0.968
10	[0.934]	0.939	0.949	0.941	0.936	0.935	0.935	0.935	0.939	0.935

2D Anisotropy Function

$$F(r,\theta) = \frac{\dot{D}(r,\theta) G_X(r,\theta_0)}{\dot{D}(r,\theta_0) G_X(r,\theta)}$$

- $F(r,\theta)$ is always unity for a perfect point source
- $F(r,\theta) = 1$ at θ_0
- $F(r,\theta)$ accounts for dose-rate variation over angles due to differing attenuation by source capsule, internal components, ...
- Must know source orientation use 2D formalism
 - otherwise, use the 1D formalism

HEBD 2D Anisotropy Function: HDR ^{192}Ir



HEBD 2D Anisotropy Function (upper)

θ (deg)	r (cm)									
	0	0.06	0.08	0.10	0.15	0.20	0.25	0.30	0.35	0.40
0	<u>0.951</u>	<u>0.951</u>	<u>0.934</u>	<u>0.917</u>	<u>0.874</u>	<u>0.831</u>	0.787	0.744	0.714	0.692
2	<u>0.947</u>	<u>0.947</u>	<u>0.930</u>	<u>0.914</u>	<u>0.871</u>	<u>0.829</u>	0.786	0.744	0.714	0.693
4	<u>0.944</u>	<u>0.944</u>	<u>0.927</u>	<u>0.910</u>	<u>0.869</u>	<u>0.827</u>	0.785	0.744	0.714	0.694
6	<u>1.059</u>	<u>1.059</u>	<u>1.033</u>	<u>1.008</u>	<u>0.944</u>	<u>0.881</u>	0.817	0.754	0.721	0.707
8	<u>0.999</u>	<u>0.999</u>	<u>0.980</u>	<u>0.961</u>	<u>0.914</u>	<u>0.866</u>	0.819	0.772	0.744	0.730
10	<u>1.007</u>	<u>1.007</u>	<u>0.989</u>	<u>0.971</u>	<u>0.927</u>	<u>0.882</u>	0.837	0.793	0.766	0.755
12	<u>1.007</u>	<u>1.007</u>	<u>0.991</u>	<u>0.975</u>	<u>0.936</u>	<u>0.897</u>	0.858	0.819	0.791	0.780
14	<u>1.158</u>	<u>1.158</u>	<u>1.129</u>	<u>1.100</u>	<u>1.027</u>	0.954	0.881	0.830	0.811	0.804
16	<u>1.269</u>	<u>1.269</u>	<u>1.230</u>	<u>1.192</u>	<u>1.094</u>	0.997	0.900	0.851	0.832	0.825
18	<u>1.378</u>	<u>1.378</u>	<u>1.330</u>	<u>1.281</u>	<u>1.159</u>	1.037	0.915	0.867	0.850	0.844
20	<u>1.784</u>	<u>1.784</u>	<u>1.678</u>	<u>1.572</u>	1.306	1.041	0.933	0.885	0.868	0.861
22	<u>1.784</u>	<u>1.784</u>	<u>1.679</u>	<u>1.575</u>	1.313	1.050	0.942	0.893	0.881	0.875
26	<u>1.704</u>	<u>1.704</u>	<u>1.610</u>	<u>1.516</u>	1.281	1.046	0.953	0.920	0.906	0.900
30	<u>1.089</u>	<u>1.089</u>	<u>1.119</u>	1.149	1.225	1.049	0.961	0.932	0.923	0.919
32	<u>1.157</u>	<u>1.157</u>	<u>1.167</u>	1.178	1.203	1.039	0.966	0.939	0.931	0.927
36	<u>1.181</u>	<u>1.181</u>	<u>1.176</u>	1.170	1.156	1.023	0.971	0.949	0.944	0.941
40	<u>0.954</u>	<u>0.954</u>	1.053	1.152	1.109	1.016	0.974	0.961	0.955	0.953
50	<u>1.037</u>	<u>1.037</u>	1.071	1.104	1.047	0.999	0.981	0.976	0.974	0.973
60	<u>1.008</u>	1.008	1.041	1.062	1.013	0.998	0.993	0.987	0.986	0.985
70	<u>1.078</u>	1.078	1.023	1.026	1.001	0.997	0.996	0.995	0.994	0.994
80	<u>1.020</u>	1.020	1.005	1.007	1.000	1.002	1.003	0.998	0.998	0.998

HEBD 2D Anisotropy Function (lower)

θ (deg)	r (cm)									
	0	0.06	0.08	0.10	0.15	0.20	0.25	0.30	0.35	0.40
100	<u>1.012</u>	1.012	1.002	1.008	0.996	0.995	0.999	0.999	0.999	0.999
110	<u>1.069</u>	1.069	1.029	1.025	1.006	0.994	0.996	0.995	0.994	0.994
120	<u>1.004</u>	1.004	1.049	1.060	1.020	0.999	0.992	0.988	0.986	0.986
130	<u>1.056</u>	<u>1.056</u>	1.080	1.105	1.047	1.003	0.985	0.976	0.975	0.974
132	<u>1.043</u>	<u>1.043</u>	1.077	1.111	1.058	1.002	0.982	0.974	0.972	0.970
134	<u>1.021</u>	<u>1.021</u>	1.078	1.135	1.068	1.007	0.982	0.971	0.968	0.967
136	<u>1.011</u>	<u>1.011</u>	1.075	1.138	1.076	1.014	0.979	0.967	0.964	0.963
138	<u>1.080</u>	<u>1.080</u>	1.113	1.146	1.098	1.016	0.977	0.963	0.961	0.958
140	<u>0.983</u>	<u>0.983</u>	1.068	1.153	1.113	1.020	0.982	0.961	0.956	0.954
144	<u>1.184</u>	<u>1.184</u>	<u>1.176</u>	1.169	1.151	1.033	0.978	0.951	0.945	0.942
148	<u>1.140</u>	<u>1.140</u>	<u>1.155</u>	1.169	1.204	1.031	0.976	0.942	0.932	0.928
150	<u>1.099</u>	<u>1.099</u>	<u>1.128</u>	1.158	1.232	1.052	0.967	0.930	0.923	0.920
154	<u>1.631</u>	<u>1.631</u>	<u>1.554</u>	<u>1.477</u>	1.285	1.093	0.959	0.914	0.904	0.899
158	<u>1.725</u>	<u>1.725</u>	<u>1.636</u>	<u>1.547</u>	1.324	1.101	0.947	0.896	0.879	0.873
160	<u>1.741</u>	<u>1.741</u>	<u>1.649</u>	<u>1.558</u>	1.329	1.099	0.937	0.880	0.863	0.858
162	<u>1.515</u>	<u>1.515</u>	<u>1.452</u>	<u>1.389</u>	<u>1.230</u>	1.072	0.914	0.862	0.846	0.840
164	<u>1.382</u>	<u>1.382</u>	<u>1.331</u>	<u>1.280</u>	<u>1.153</u>	1.025	0.898	0.843	0.826	0.820
166	<u>1.961</u>	<u>1.961</u>	<u>1.845</u>	<u>1.729</u>	<u>1.439</u>	1.150	0.860	0.819	0.804	0.797
168	<u>1.036</u>	<u>1.036</u>	<u>1.016</u>	<u>0.996</u>	<u>0.946</u>	<u>0.895</u>	0.845	0.794	0.779	0.770
170	<u>0.894</u>	<u>0.894</u>	<u>0.884</u>	<u>0.874</u>	<u>0.850</u>	<u>0.825</u>	<u>0.801</u>	0.776	0.752	0.741
172	<u>0.880</u>	<u>0.880</u>	<u>0.870</u>	<u>0.860</u>	<u>0.835</u>	<u>0.810</u>	<u>0.786</u>	<u>0.761</u>	0.736	0.711
174	<u>0.626</u>	<u>0.626</u>	<u>0.627</u>	<u>0.627</u>	<u>0.628</u>	<u>0.629</u>	<u>0.630</u>	<u>0.631</u>	<u>0.632</u>	<u>0.633</u>
176	<u>0.575</u>	<u>0.575</u>	<u>0.575</u>	<u>0.576</u>	<u>0.577</u>	<u>0.579</u>	<u>0.580</u>	<u>0.582</u>	<u>0.583</u>	<u>0.585</u>
178	<u>0.536</u>	<u>0.536</u>	<u>0.537</u>	<u>0.537</u>	<u>0.539</u>	<u>0.540</u>	<u>0.542</u>	<u>0.543</u>	<u>0.545</u>	<u>0.546</u>
180	<u>0.497</u>	<u>0.497</u>	<u>0.498</u>	<u>0.499</u>	<u>0.500</u>	<u>0.502</u>	<u>0.503</u>	<u>0.504</u>	<u>0.506</u>	<u>0.507</u>

Example Dosimetry Parameter Dataset

1	r [cm]	$g_L(r)$	$g_P(r)$	r [cm]	$\phi(r)$	$F(r,8)$	0	10	20	30	40	50	60	70	80
2	0.10	0.990	0.582	0.25	1.164	0.05							1.067	0.996	0.985
3	0.25	1.021	0.889	0.5	0.973	0.075					1.050	1.006	0.994	0.996	0.996
4	0.50	1.030	0.998	1.0	0.933	0.1				1.046	0.996	0.990	0.993	0.988	0.999
5	1.00	1.000	1.000	1.5	0.931	0.15			1.039	0.978	0.958	0.977	0.988	0.987	0.996
6	1.50	0.943	0.949	2.0	0.931	0.2		0.987	0.921	0.940	0.960	0.975	0.984	0.988	0.997
7	2.00	0.872	0.879	2.5	0.932	0.25	0.494	0.574	0.785	0.899	0.943	0.967	0.986	0.995	1.000
8	2.50	0.795	0.803	3.0	0.934	0.5	0.610	0.513	0.679	0.808	0.892	0.944	0.974	0.990	0.997
9	3.00	0.717	0.724	3.5	0.935	1	0.580	0.561	0.705	0.813	0.885	0.933	0.967	0.987	0.997
10	3.50	0.643	0.650	4.0	0.937	2	0.652	0.626	0.743	0.830	0.893	0.934	0.967	0.987	0.997
11	4.00	0.573	0.579	4.5	0.938	5	0.690	0.700	0.789	0.854	0.905	0.941	0.968	0.986	0.996
12	4.50	0.508	0.513	5.0	0.938	10	0.709	0.742	0.815	0.872	0.912	0.947	0.972	0.990	0.997
13	5.00	0.448	0.453	6.0	0.939										
14	6.00	0.347	0.351	7.0	0.942	$\Lambda = 1.011$									
15	7.00	0.265	0.268	10.0	0.948	$L = 3.7 \text{ mm or } 0.37 \text{ cm}$									
16	8.00	0.201	0.203												
17	9.00	0.151	0.153												
18	10.00	0.114	0.115												

prefer societal-recommended datasets

otherwise use AAPM/RPC Registry data and original pubs

websites (ESTRO, Univ. Carleton, etc) also post datasets

HEBD 2D Along-Away QA Table

z (cm)	y (cm)											
	0	0.25	0.5	0.75	1	1.5	2	3	4	5	6	7
7	0.01690	0.01709	0.01724	0.01749	0.01772	0.01800	0.01797	0.01713	0.01564	0.01385	0.01209	0.01044
6	0.0227	0.0231	0.0235	0.0239	0.0243	0.0246	0.0244	0.0226	0.01996	0.01719	0.01455	0.01226
5	0.0320	0.0328	0.0337	0.0345	0.0351	0.0353	0.0345	0.0306	0.0259	0.0213	0.01750	0.01432
4	0.0487	0.0505	0.0524	0.0540	0.0549	0.0542	0.0513	0.0426	0.0338	0.0265	0.0208	0.01656
3	0.0819	0.0886	0.0936	0.0965	0.0967	0.0910	0.0813	0.0604	0.0440	0.0324	0.0244	0.01875
2	0.1776	0.2006	0.214	0.214	0.204	0.1704	0.1360	0.0853	0.0557	0.0384	0.0277	0.0207
1.5	0.311	0.364	0.382	0.362	0.324	0.241	0.176	0.0993	0.0614	0.0410	0.0290	0.0215
1	0.707	0.859	0.818	0.682	0.542	0.340	0.223	0.1124	0.0662	0.0431	0.0301	0.0220
0.5	3.45	3.47	2.19	1.354	0.885	0.446	0.264	0.1219	0.0694	0.0445	0.0308	0.0224
0		15.5	4.29	1.953	1.109	0.497	0.281	0.1254	0.0705	0.0449	0.0310	0.0225
-0.5	2.62	3.47	2.20	1.355	0.885	0.447	0.264	0.1219	0.0694	0.0445	0.0308	0.0224
-1	0.608	0.849	0.816	0.681	0.543	0.340	0.223	0.1124	0.0662	0.0431	0.0301	0.0220
-1.5	0.274	0.355	0.380	0.361	0.323	0.242	0.1764	0.0993	0.0614	0.0410	0.0290	0.0215
-2	0.1587	0.1927	0.212	0.213	0.203	0.1703	0.1361	0.0853	0.0558	0.0384	0.0277	0.0207
-3	0.0745	0.0840	0.0915	0.0955	0.0962	0.0907	0.0812	0.0605	0.0440	0.0324	0.0244	0.01875
-4	0.0422	0.0472	0.0507	0.0531	0.0543	0.0540	0.0512	0.0426	0.0338	0.0265	0.0208	0.01656
-5	0.0279	0.0304	0.0324	0.0337	0.0346	0.0351	0.0343	0.0306	0.0259	0.0213	0.01750	0.01432
-6	0.0200	0.0213	0.0225	0.0233	0.0238	0.0244	0.0242	0.0225	0.01994	0.01717	0.01455	0.01226
-7	0.01500	0.01576	0.01647	0.01697	0.01735	0.01780	0.01786	0.01708	0.01561	0.01384	0.01207	0.01044

HEBD Reference Data

	^{192}Ir	^{137}Cs	^{60}Co
Half-life	73.81 days	30.07 yr	5.27 yr
Type of disintegration	β^- (95.1%), EC (4.9%)	β^- (100%)	β^- (100%)
Maximum x-ray energy (keV)	78.6	37.5	8.3
Gamma energy-range (keV)	110.4–1378.2	661.6	1173.2–1332.5
Mean x-ray and gamma energy (keV)	350.0	613.0	1252.9
Maximum β^- ray energies (keV)	81.7 (0.103%) 258.7 (5.6%) 538.8 (41.43%) 675.1 (48.0%)	514.0 (94.4%) 1175.6 (5.6%)	318.2 (99.88%) 1491.4 (0.12%)
Mean β^- ray energy (keV)	180.7	188.4	96.5
Air-kerma rate constant, $\Gamma_{\delta = 10 \text{ keV}}$ ($\mu\text{Gy m}^2 \text{ h}^{-1} \text{ MBq}^{-1}$)	0.1091	0.0771	0.3059
Specific activity (GBq mg^{-1})	341.0	3.202	41.91

NNDC photon spectrum <http://www.nndc.bnl.gov/nudat2/>

H_2O @ 0.998 g/cm^3 (22° C)

dry air (0% humidity)

Perez-Calatayud, et al., *Med. Phys.* 39, 2904-2929 (2012)

Locale for Dosimetry Parameter Datasets

- HEBD Report (AAPM+GEC-ESTRO) Med. Phys. 2012
- IROC Houston website (Brachytherapy Source Registry)
(rpc.mdanderson.org/RPC/BrachySeeds/Source_Registry.htm)
- ESTRO website
<http://www.estro.org/about/governance-organisation/committees-activities/tg43>
- University of Carleton website
http://www.physics.carleton.ca/clrp/seed_database

Data Interpolation/Extrapolation Methods

Parameter	$r < r_{\min}$ Extrapolation	$r_{\min} < r \leq r_{\max}$ Interpolation	$r > r_{\max}$ Extrapolation
$g_L(r)$	Nearest neighbor or zeroth-order extrapolation	Linear using datapoints immediately adjacent to the radius of interest	Linear using data of last two tabulated radii
$F(r, \theta)$	Nearest neighbor or zeroth-order extrapolation	Bilinear	Nearest neighbor or zeroth-order extrapolation

TG-43 Dataset Resolution

JOURNAL OF APPLIED CLINICAL MEDICAL PHYSICS, VOLUME 16, NUMBER 4, 2015

Brachytherapy treatment planning commissioning: effect of the election of proper bibliography and finite size of TG-43 input data on standard treatments

Christian N. Valdés,^{1a} Gustavo H. Píriz,² Enrique Lozano,³

Departamento de Física Médica,¹ Centro Oncológico de Antofagasta, Antofagasta, Chile;

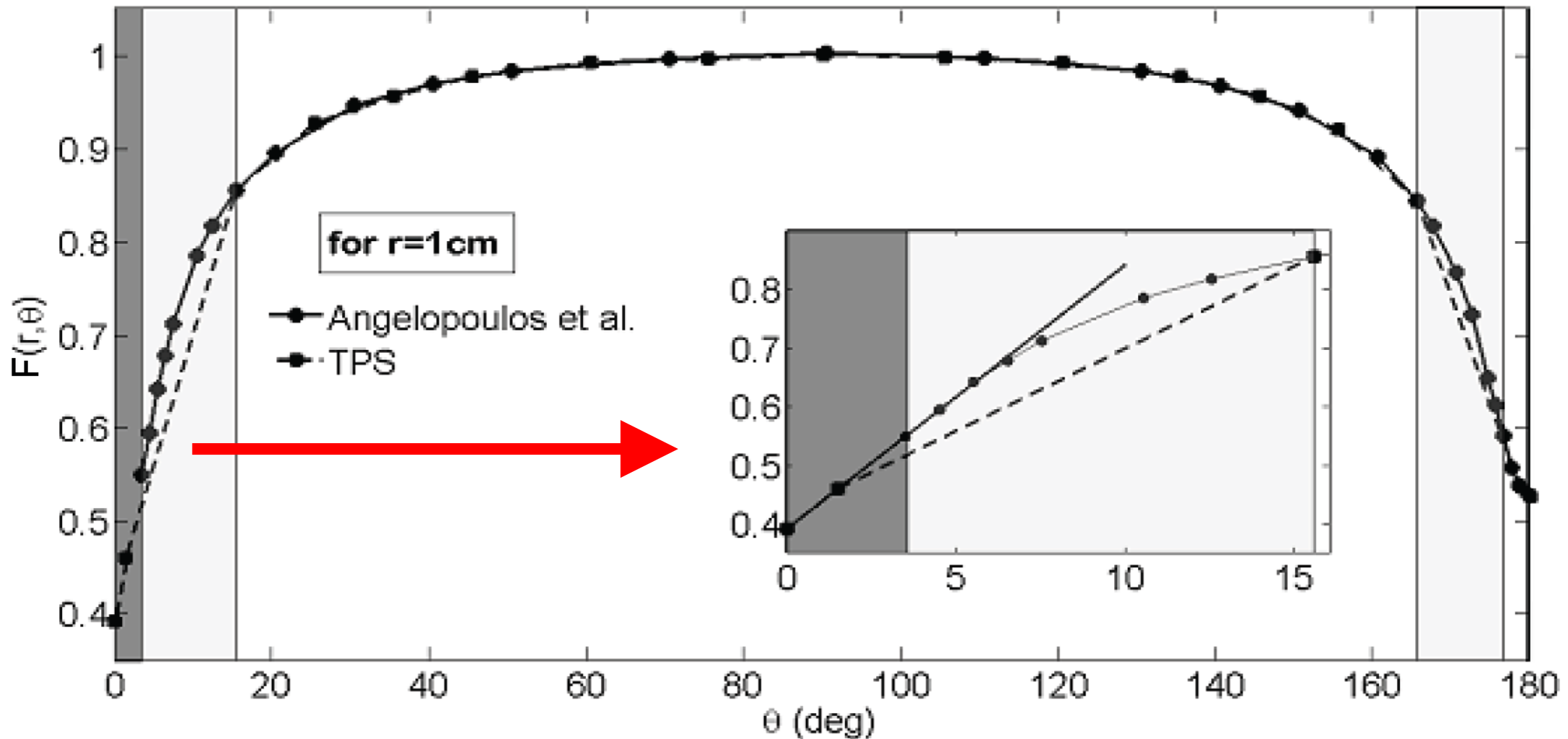
Departamento de Física Médica,² Centro de Oncología ONCOSUR, Florida, Uruguay;

Departamento de Física Médica,³ Instituto Nacional del Cáncer, Santiago, Chile

cvalcort@gmail.com

The aim of this work is to evaluate performance of a commercial BT TPS with vendor TG-43 data, analyze possible discrepancies with respect to a proper reference source and its implications for standard treatments, and judge the effectiveness of certain widespread recommended quality controls to find potential errors related with interpolations of TG-43 tables.

TG-43 Dataset Resolution



differences > 2% encompassed ~17% of surrounding source volume

Monte Carlo Uncertainty Analysis: HDR ^{192}Ir

Component	$\dot{D}(1 \text{ cm}, \theta_0)$		$\dot{D}(5 \text{ cm}, \theta_0)$		s_K	
	Type A	Type B	Type A	Type B	Type A	Type B
Source geometry		0.46%		0.46%		0.46%
Capsule geometry		0.01%		0.01%		0.01%
Dynamic source design		0.4%		0.08%		0.04%
^{192}Ir photon spectrum		1.0%		1.0%		1.0%
MC physics		0.05%		0.05%		0.05%
Phantom composition		0.01%		0.05%		0.01%
Phantom cross sections		0.013%		0.067%		0.001%
Dose calculation (μ_{en}/ρ)		1.0%		1.0%		1.0%
Tally volume averaging		0.2%		0.4%		0.02%
Tally statistics	0.03%		0.03%		0.03%	
Quadrature sum	0.03%	1.54%	0.04%	1.50%	0.03%	1.49%
Total ($k=1$) uncertainty		1.54%		1.50%		1.49%

Example TLD Uncertainty Analysis: ¹²⁵I

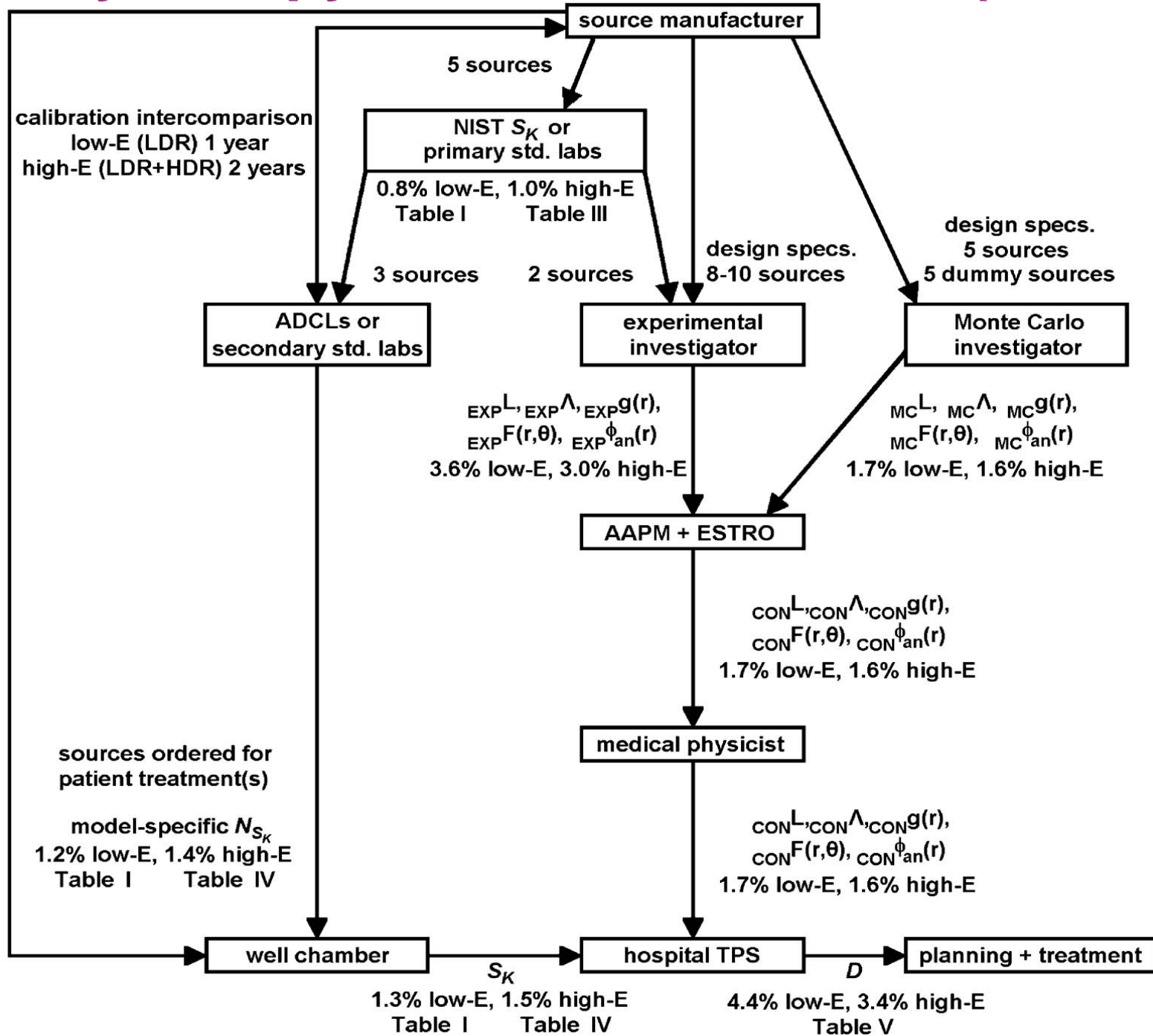
TABLE II. Uncertainty determinations in experimental measurements of dose rate constant.

Component of uncertainty	Type A(%)	Type B(%)
Repetitive TLD measurements	4.6	
TLD dose calibration (including uncertainty in linac calibration)		2.0
Correction for energy dependence of LiF		5.0
Correction for solid water to liquid water conversion factor		3.0
Seed and TLD positioning		1.0
Quadrature combination	4.6	6.2
Total uncertainty (1σ)		7.7
NIST uncertainty		0.5
Total combined uncertainty		7.7

Example MC Uncertainty Analysis: ^{131}Cs

Component	$\dot{d}(1 \text{ cm}, \theta_0)$		$\dot{d}(5 \text{ cm}, \theta_0)$		s_K	
	A	B	A	B	A	B
Source:capsule geometry		0.16%		0.16%		0.16%
Dynamic internal components		0.02%		0.05%		0.02%
Source radiation spectrum		0.1%		0.7%		0.2%
Phantom composition		0.01%		0.02%		0.01%
Physics of Monte Carlo code		0.3%		0.7%		0.3%
Cross-sections in phantom		0.2%		0.9%		0.2%
μ_{en}/ρ for dose calculation		1.2%		1.2%		1.2%
Tally volume averaging		0.006%		<0.001%		<0.001%
Tally statistics	0.02%		0.04%		0.03%	
Quadrature sum	0.02%	1.3%	0.04%	1.8%	0.03%	1.3%
Total ($k=1$) uncertainty		1.3%		1.8%		1.3%

Brachytherapy Dose Uncertainties (TG-138)



DeWerd, et al., *Med. Phys.* 38, 782-801 (2011)

Measurement Uncertainty in RAKR and Dose

Measurement description	Quantity (units)	Relative propagated uncertainty (%)
ADCL calibration	$S_{K,NIST}$ (U)	1.1
ADCL well ion chamber calibration	$S_{K,NIST}/I_{ADCL}$ (U/A)	1.2
ADCL calibration of source from manufacturer	$S_{K,ADCL}$ (U)	1.3
ADCL calibration of clinic well ion chamber	$S_{K,ADCL}/I_{CLINIC}$ (U/A)	1.4
Clinic measures source air-kerma strength	$S_{K,CLINIC}$ (U)	1.5
Expanded uncertainty ($k=2$)	$S_{K,CLINIC}$ (U)	2.9

Uncertainty component	Relative propagated uncertainty (%)	
	<i>high-E</i>	
S_K measurements from row 5 of Tables I and IV	1.5	
Measured dose	3.0	
Monte Carlo dose estimate	1.6	
TPS interpolation uncertainties	2.6	
Total dose calculation uncertainty	3.4	
Expanded uncertainty ($k=2$)	6.8	

Summary

- BT dosimetry in the clinic generally follows the TG-43 formalism
 - Luc will next show you its limitations and advancements in accuracy
- uniform BT (over time and space) requires standardization
 - consistent formalism (and formats)
 - consistent dosimetry parameters
 - consistent reference data
 - consistent TPS approach
- HDR/LDR and HE/LE have different planning approaches
- medical physicist must know the data trail and commission the source(s)

Further Reading

Ballester, et al. Med Phys 2009;36:4250-6.

Beaulieu, et al. Med Phys 2012;39:6208-36.

Butler, et al. Med Phys 2008;35:3860-5.

DeWerd, et al. Med Phys 2011;38:782-801.

Granero, et al. Med Phys 2011;38:487-94.

Kirisits, et al. Radiat Oncol 2014;110:199-212.

Nath, et al. Med Phys 1995;22:209-34.

Perez-Calatayud, et al. Med Phys 2012;39:2904-29.

Rivard, Med Phys 1999;26:2445-50.

Rivard, Appl Radiat Isot 2001;55:755-82.

Rivard, et al. Med Phys 2004;31:633-74.

Rivard, et al. Nuc Sci Engin 2005;149:101-6.

Rivard, et al. Med Phys 2007;34:2187-205.

Rivard, et al. Med Phys 2009;36:1968-75.

Rivard, et al. Med Phys 2009;36:2136-53.

Thomadesn, et al. Med Phys 2008;35:4708-23.



ESTRO

School



UNIVERSITÉ
LAVAL



CENTRE DE RECHERCHE
SUR LE CANCER
UNIVERSITÉ
LAVAL

Limitations of TG-43 based dosimetry: TG-43 versus the “true” dose distribution

Prof. Luc Beaulieu, Ph.D., FAAPM

1- Département de physique, de génie physique et d'optique, et Centre de recherche sur le cancer, Université Laval, Canada

2- Département de radio-oncologie et Centre de recherche du CHU de Québec, CHU de Québec, Canada

Vienna, May 29 – June 1 2016



Disclosures

- None for this section

Key References

- Comprehensive Brachytherapy: physical and clinical aspect. JLM Venselaar, D Baltas, AS Meigooni and P.J. Hoskin. CRC Press, Taylor & Francis, 2013.
 - In particular: Chapters 5, 7 and 10
- The physics of modern brachytherapy for oncology. D Baltas, L Sakelliou et N Zamboglou. Taylor & Francis Series in Medical Physics and Biomedical Engineering, 2007.
- The physics of radiation therapy, FM Khan, 4ed, 2009.
- Brachytherapy physics, 2ed, AAPM monograph #31, 2005.
- J. Pouliot and L Beaulieu, Chapter 13, Liebel and Philips Textbook of Radiation Oncology, 3rd Ed, 2010
- Perez-Calatayud JJ, Ballester FF, Das RKR, Dewerd LAL, Ibbott GSG, Meigooni ASA, et al. Dose calculation for photon-emitting brachytherapy sources with average energy higher than 50 keV: Report of the AAPM and ESTRO. Med Phys 2012;39(5):2904–29.
- Rivard MJ, Coursey BM, DeWerd LA, Hanson WF, Saiful Huq M, Ibbott GS, et al. Update of AAPM Task Group No. 43 Report: A revised AAPM protocol for brachytherapy dose calculations. Med Phys 2004;31(3):633–74.

Key References

- Rivard MJ, Venselaar JLM, Beaulieu L. **The evolution of brachytherapy treatment planning.** *Med Phys* 2009;36:2136–53.
- Beaulieu L, Carlsson Tedgren A, Carrier J-F, Davis SD, Mourtada F, Rivard MJ, et al. **Report of the Task Group 186 on model-based dose calculation methods in brachytherapy beyond the TG-43 formalism: Current status and recommendations for clinical implementation.** *Med Phys* 2012;39(10):6208–36.
- Papagiannis P, Pantelis E, Karaiskos P. **Current state of the art brachytherapy treatment planning dosimetry algorithms.** *Br J Radiol* 2014;87(1041):20140163.
- Ma Y, Lacroix F, Lavallée M-C and Beaulieu L. **Validation of the Oncentra Brachy Advanced Collapsed cone Engine for a commercial ^{192}Ir source using heterogeneous geometries.** *Brachytherapy* 2015;14:939–52
- Ballester F et al. **A generic high-dose rate ^{192}Ir brachytherapy source for evaluation of model-based dose calculations beyond the TG-43 formalism.** *Med. Phys.* 2015;42:3048–61

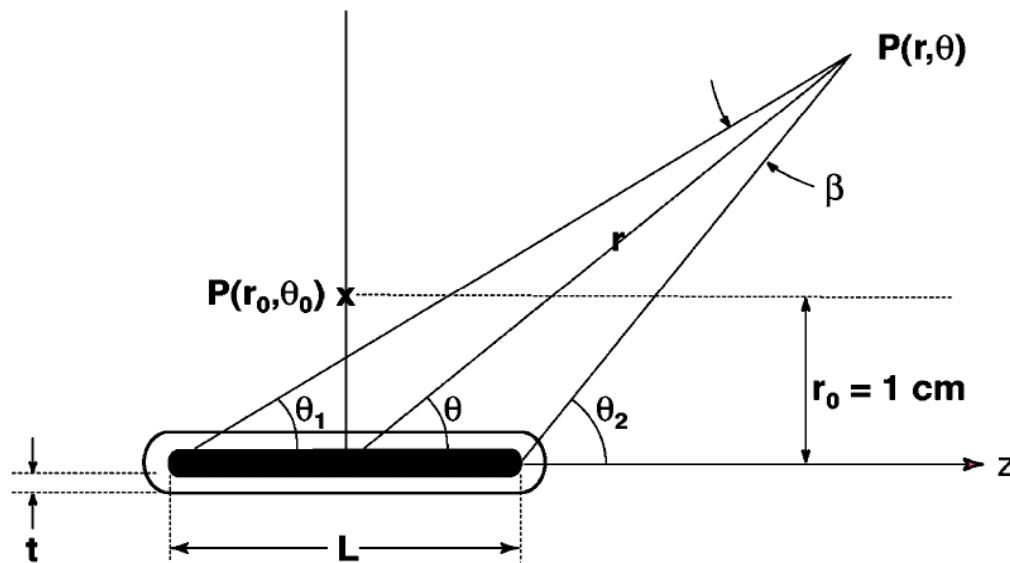
Learning Objectives

- Review the limitations of TG43
- Understand how these limitations translate to clinical tumor sites and brachytherapy procedures (relative to MC)
- Be able to anticipate potential TG43 failures

TG-43: Brachytherapy Dosimetry

Update of AAPM Task Group No. 43 Report: A revised AAPM protocol for brachytherapy dose calculations

$$\dot{D}(r, \theta) = S_K \cdot \Lambda \cdot \frac{G_L(r, \theta)}{G_L(r_0, \theta_0)} \cdot g_L(r) \cdot F(r, \theta)$$



The good!

- Each source model is specifically taken into account
- S_k (and RAKR) link to a primary standard!
- The values of the various parameters are compiled following a rigorous process
 - Process includes a review and consensus by a group of experts
- Analytical formulation leads to fast dose computation
 - Hundreds of thousands of iterations possible in a few seconds

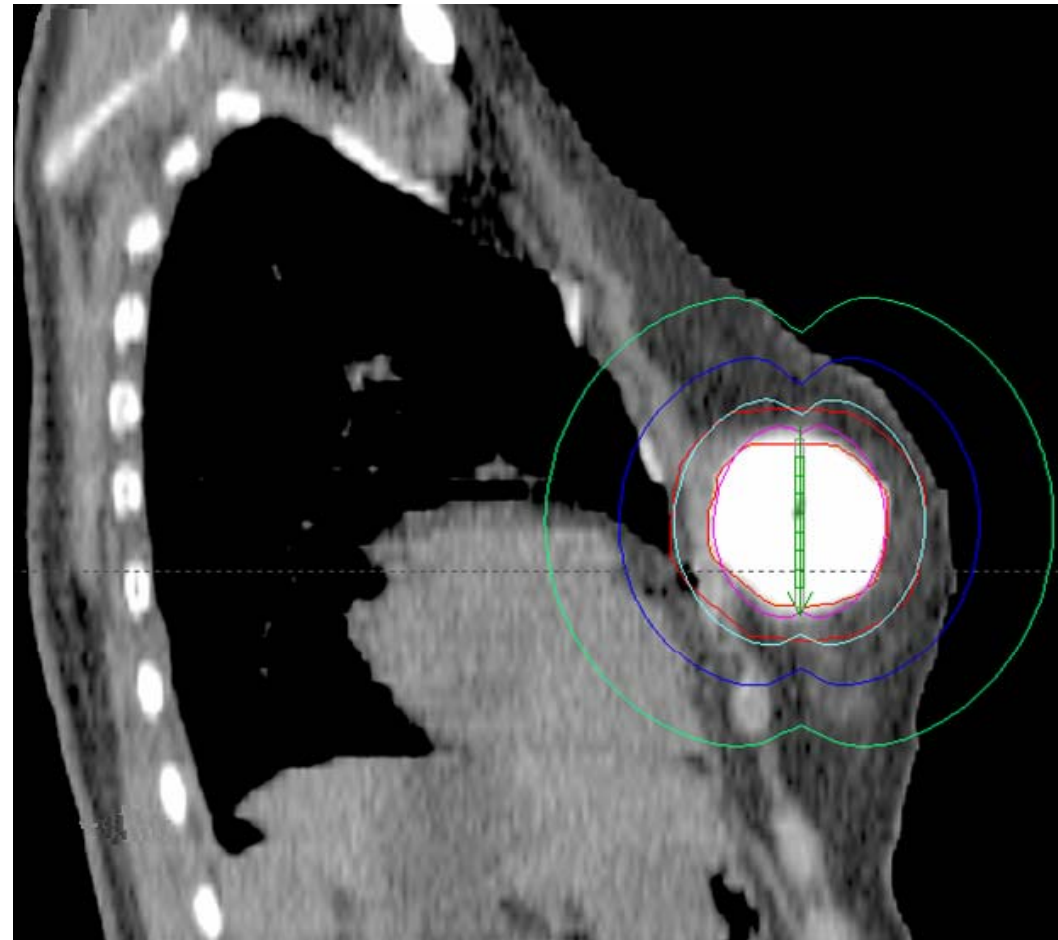
What's all the fuss about?



TG-43: Brachytherapy Dosimetry



≠



The limitations

- Homogeneous water medium assumed
- Full scatter condition assumed
 - 5 cm beyond the last position of interest for low energy seed (15 cm geometry)
 - 20 cm beyond the last position of interest for $E > 50$ keV (40 cm radius geometry)
- No electrons (Dose vs Kerma)
 - Dose may not be related to photon fluence close to the source (e.g. ^{60}Co)
- Full 3D source geometry not taken into account
 - Close to the source
 - Extended line sources, ...
 - Shielded applicators or directional sources

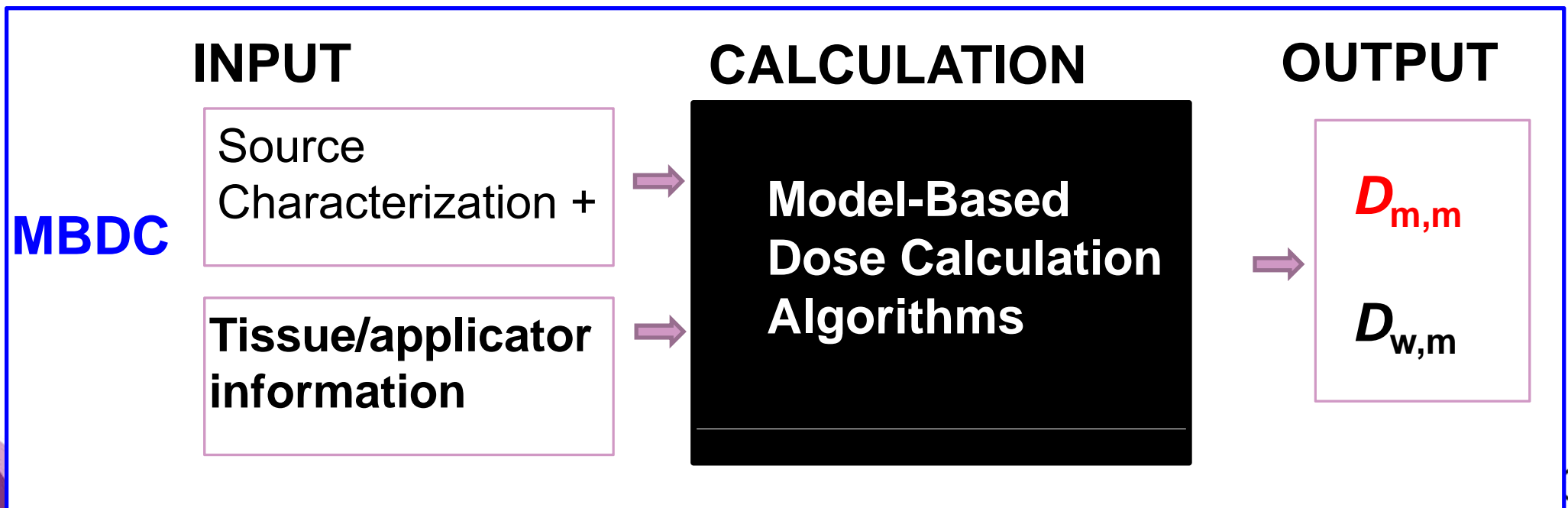
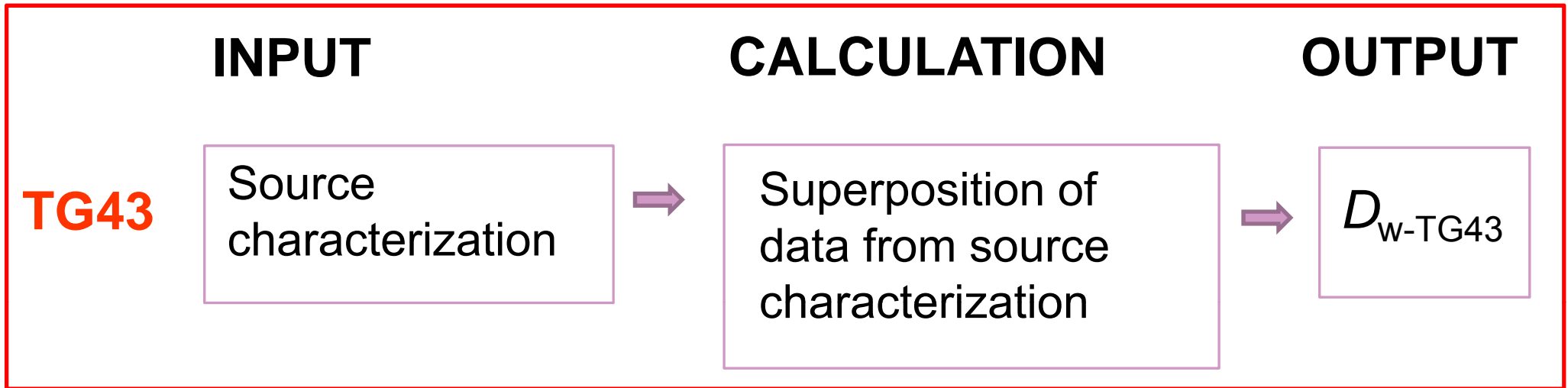
Why should you care?

Significant dose differences expected

$\geq 10\%$ or more relative to TG-43

Dose is the fundamental quantity in RT

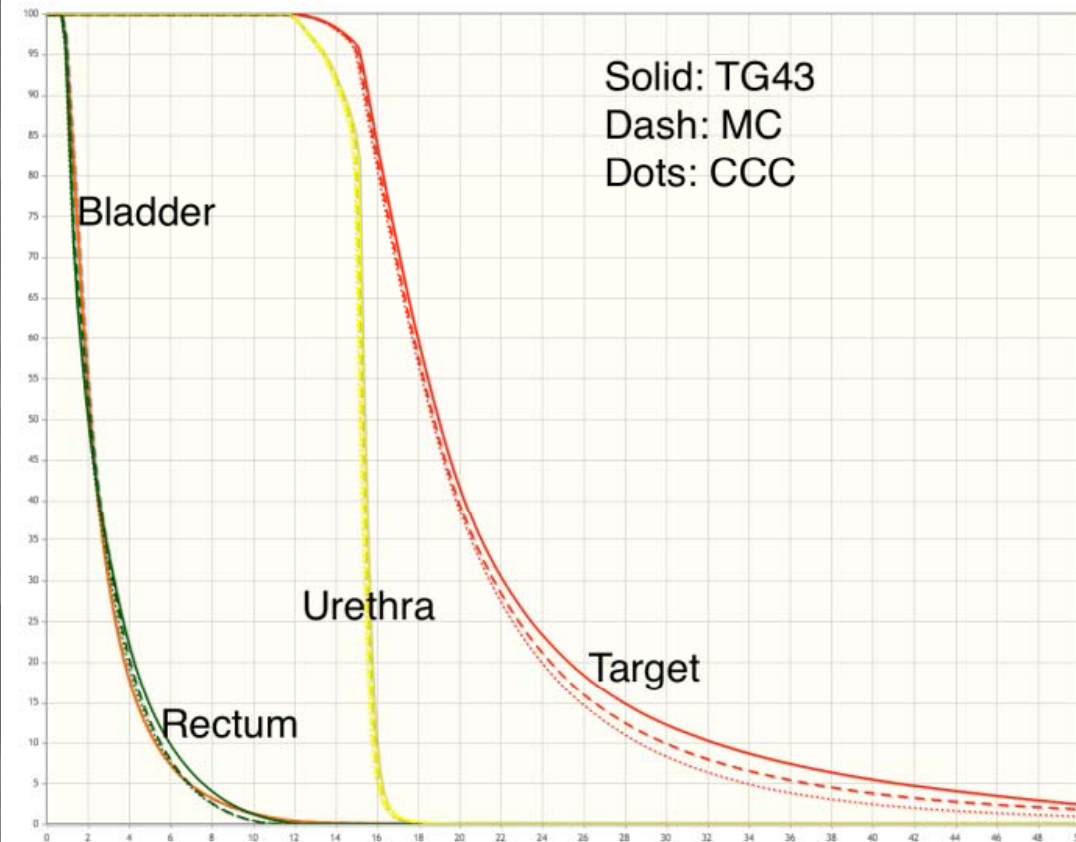
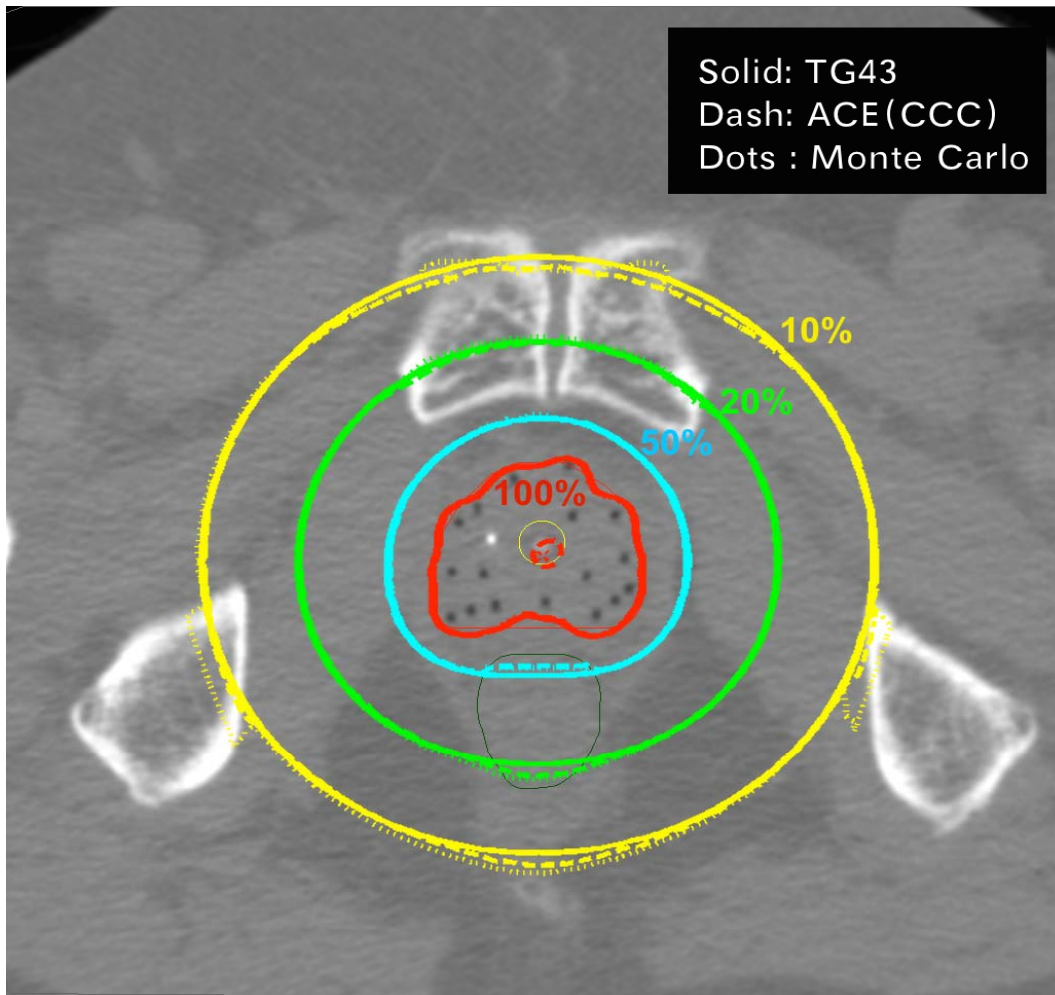
Factor-based vs Model-based



Sensitivity of Anatomic Sites to Dosimetric Limitations of Current Planning Systems

anatomic site	photon energy	absorbed dose	attenuation	shielding	scattering	beta/kerma dose
prostate	high					←
	low	XXX	XXX	XXX		
breast	high				XXX	
	low	XXX	XXX	XXX		
GYN	high			XXX		
	low	XXX	XXX			
skin	high			XXX	XXX	
	low	XXX		XXX	XXX	
lung	high				XXX	XXX
	low	XXX	XXX		XXX	
penis	high				XXX	
	low	XXX			XXX	
eye	high			XXX	XXX	XXX
	low	XXX	XXX	XXX	XXX	

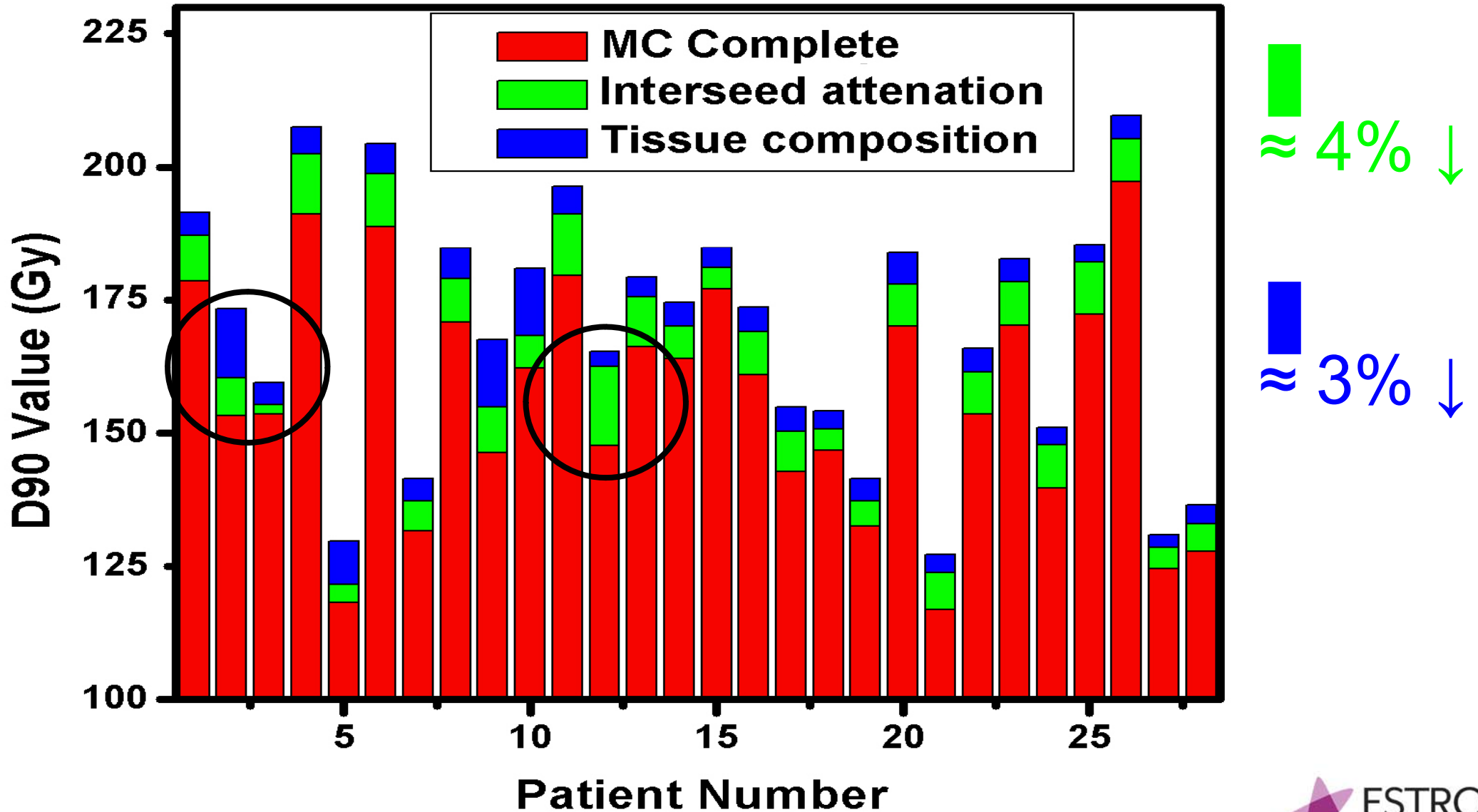
Prostate HDR Brachytherapy



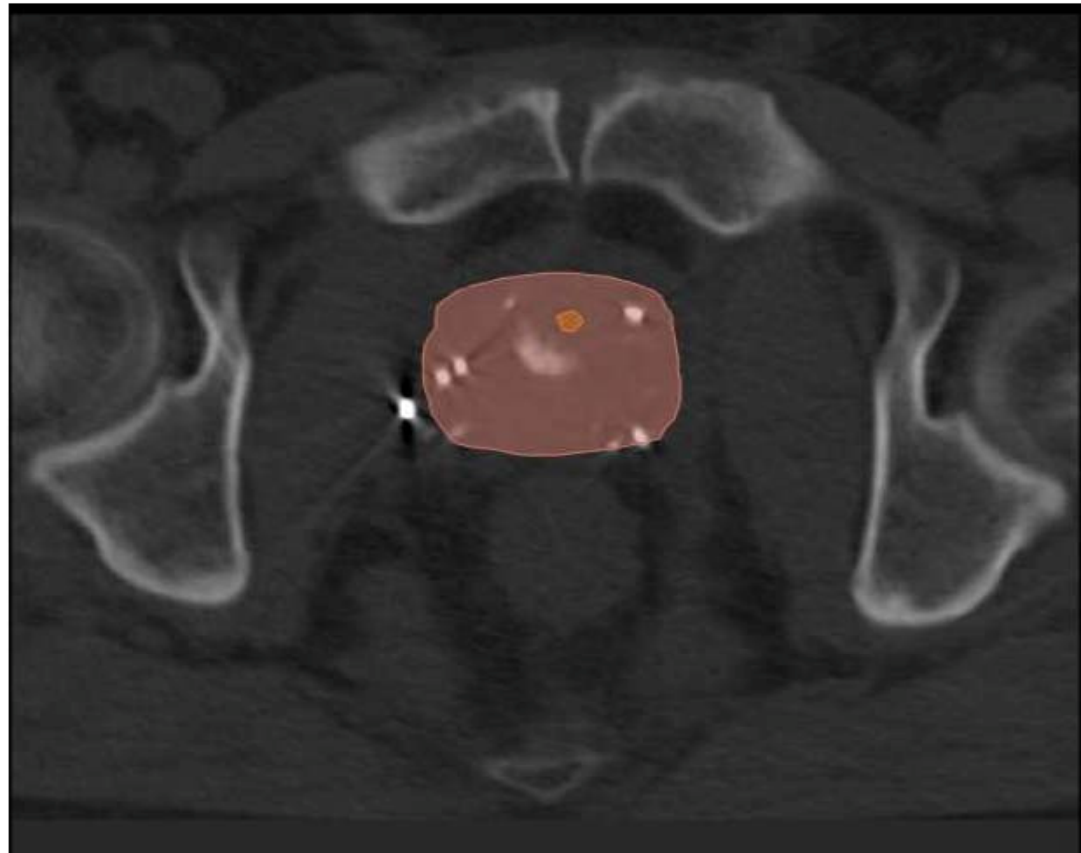
17 catheters; rectum set to air!

Ma et al, Brachytherapy 2015

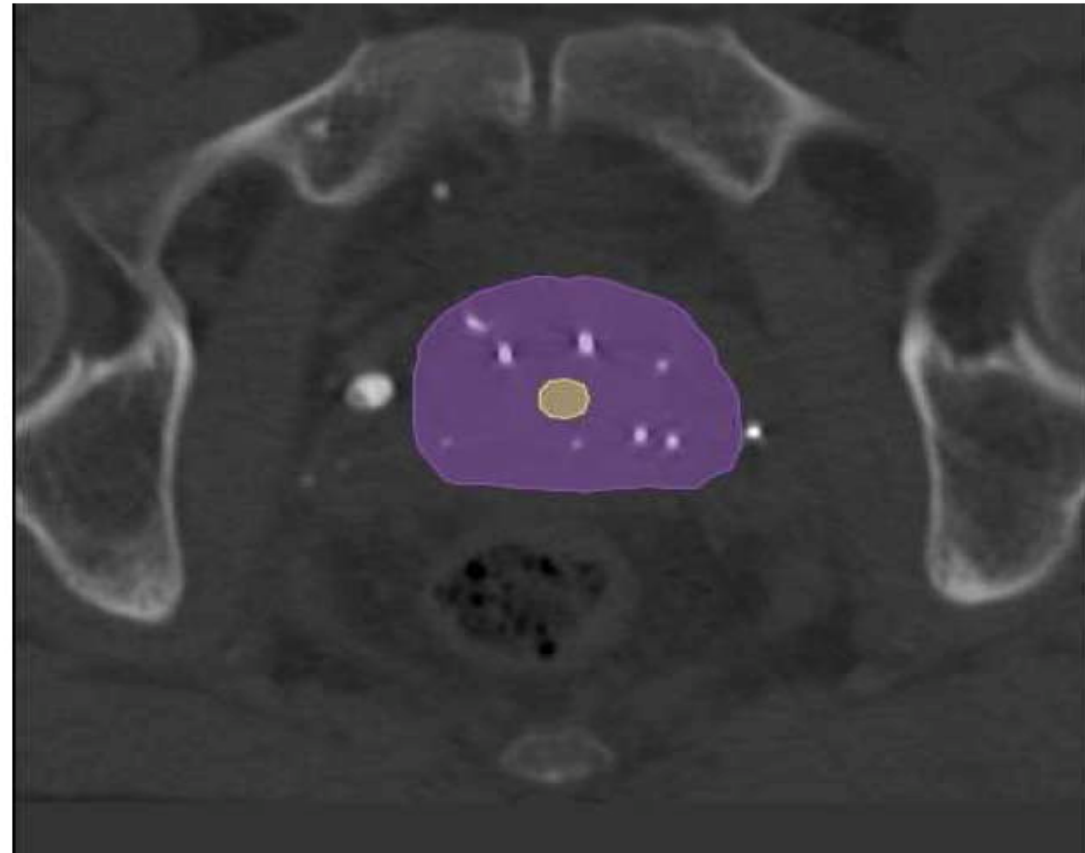
Prostate LDR Brachytherapy



Calcifications



(g) Significant calcification



(h) Typical patient

Average of 42 selected patients with visible calcifications

	D_Water [%]	D_Calci [%]	D_Full_MC [%]
D10	98,7 ± 0,4	94,8 ± 08,8	92,3 ± 08,4
D90	98,4 ± 0,4	88,6 ± 12,1	86,8 ± 09,2
V100	99,6 ± 1,1	93,5 ± 18,4	93,8 ± 17,7
V150	99,1 ± 0,6	92,1 ± 12,0	90,7 ± 10,2
V200	97,2 ± 1,1	84,9 ± 13,3	80,8 ± 12,6

TABLE: Dosimetrics indices table relative to the TG43 algorithm

Summary for Prostate Brachytherapy

- Minimal impact for HDR brachytherapy
 - CTV-PTV
 - OARs: rectum, bladder, urethra
- Important effect for seed implants
 - D90: -7% average due to ISA and tissues
 - Calcifications: -10% average on D90 (large std.)

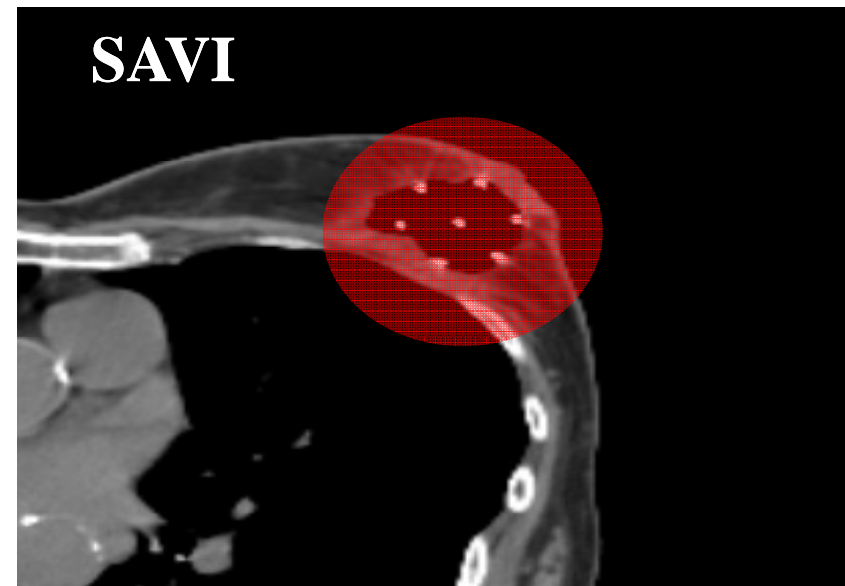
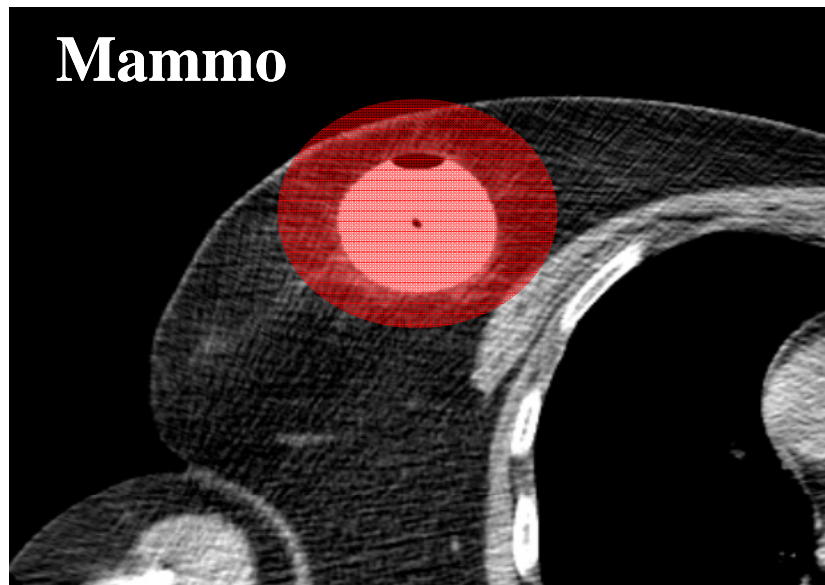
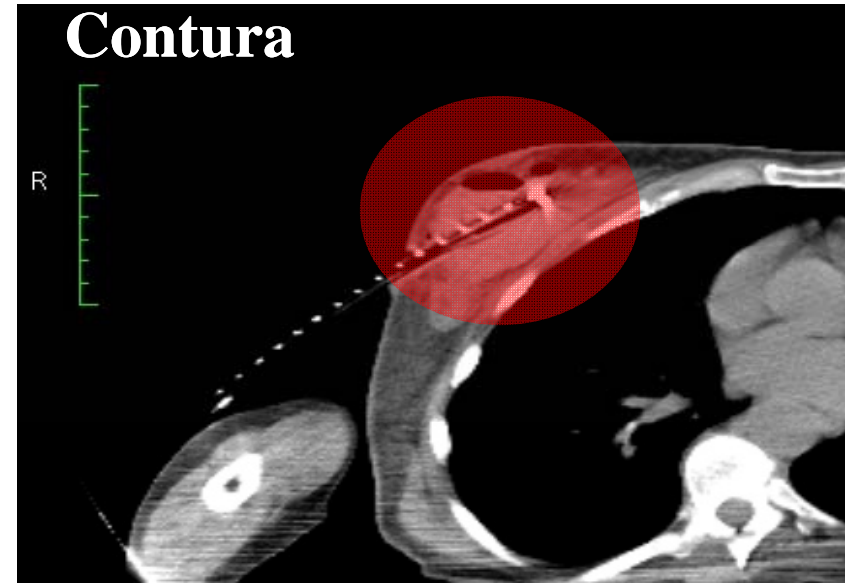
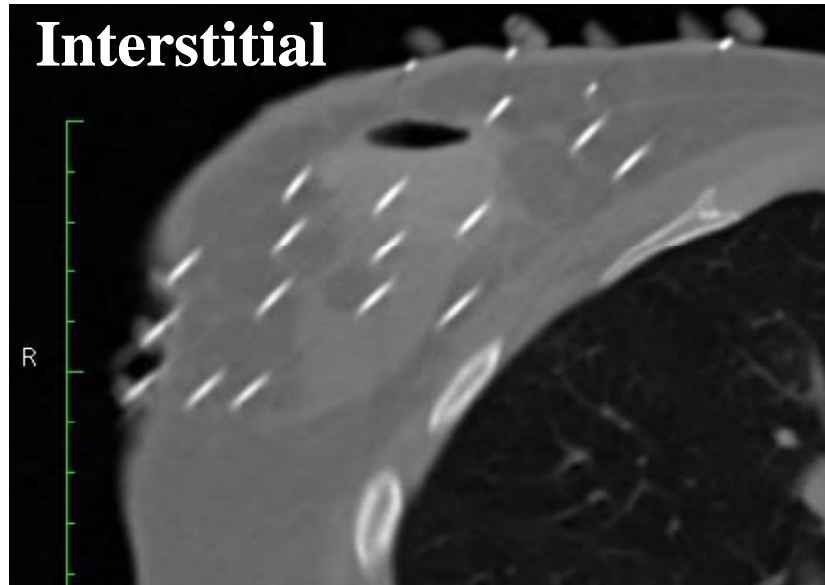
Sensitivity of Anatomic Sites to Dosimetric Limitations of Current Planning Systems

anatomic site	photon energy	absorbed dose	attenuation	shielding	scattering	beta/kerma dose
prostate	high					
	low	XXX	XXX	XXX		
breast	high				XXX	←
	low	XXX	XXX	XXX		
GYN	high			XXX		
	low	XXX	XXX			
skin	high			XXX	XXX	
	low	XXX		XXX	XXX	
lung	high				XXX	XXX
	low	XXX	XXX		XXX	
penis	high				XXX	
	low	XXX			XXX	
eye	high			XXX	XXX	XXX
	low	XXX	XXX	XXX	XXX	

Various Approaches



Various Approaches



Contrast

TABLE II. Percentage reduction ($\Delta\%$) in dose rate at 1 cm from the balloon due to contrast, relative to water, for the various balloon diameters.

Balloon diameter (cm)	$\Delta\%$				
	5% contrast	10% contrast	15% contrast	20% contrast	25% contrast
4	-0.8%	-1.6%	-2.4%	-3.2%	-4.0%
5	-1.0%	-1.6%	-2.7%	-3.8%	-4.9%
6	-1.4%	-2.9%	-4.3%	-5.4%	-5.7%

Contrast effects on dosimetry of a partial breast irradiation system

Bassel Kassas,^{a)} Firas Mourtada, John L. Horton, and Richard G. Lane
The University of Texas MD Anderson Cancer Center, Box 94, 1515 Holcombe Boulevard, Houston, Texas 77030

(Received 24 February 2004; revised 6 April 2004; accepted for publication 22 April 2004; published 17 June 2004)

Papagiannis, Pantelis, Karaiskos, Br J Radiol, 87, 20141063 (2014)



Contrast recommendations were made!

Air

Dosimetric effects of an air cavity for the SAVI™ partial breast irradiation applicator

Susan L. Richardson^{a)}

Department of Radiation Oncology, Washington University School of Medicine, St. Louis, Missouri 63110

Ramiro Pino

Department of Radiation Oncology, The Methodist Hospital, Houston, Texas 77030 and Texas Cancer Clinic, San Antonio, Texas 78240

(Received 8 July 2009; revised 3 June 2010; accepted for publication 5 June 2010; published 12 July 2010)

Purpose: To investigate the dosimetric effect of the air inside the SAVI™ partial breast irradiation device.

Methods: The authors have investigated how the air inside the SAVI™ partial breast irradiation device changes the delivered dose from the homogeneously calculated dose. Measurements were made with the device filled with air and water to allow comparison to a homogenous dose calculation done by the treatment planning system. Measurements were made with an ion chamber, TLDs, and film. Monte Carlo (MC) simulations of the experiment were done using the EGSnrc suite. The MC model was validated by comparing the water-filled calculations to those from a commercial treatment planning system.

Results: The magnitude of the dosimetric effect depends on the size of the cavity, the arrangement of sources, and the relative dwell times. For a simple case using only the central catheter of the largest device, MC results indicate that the dose at the prescription point 1 cm away from the air-water boundary is about 9% higher than the homogeneous calculation. Independent measurements in a water phantom with a similar air cavity gave comparable results. MC simulation of a realistic multidwell position plan showed discrepancies of about 5% on average at the prescription point for the largest device.

Conclusions: The dosimetric effect of the air cavity is in the range of 3%–9%. Unless a heterogeneous dose calculation algorithm is used, users should be aware of the possibility of small treatment planning dose errors for this device and make modifications to the treatment delivery, if necessary. © 2010 American Association of Physicists in Medicine. [DOI: [10.1118/1.3457328](https://doi.org/10.1118/1.3457328)]

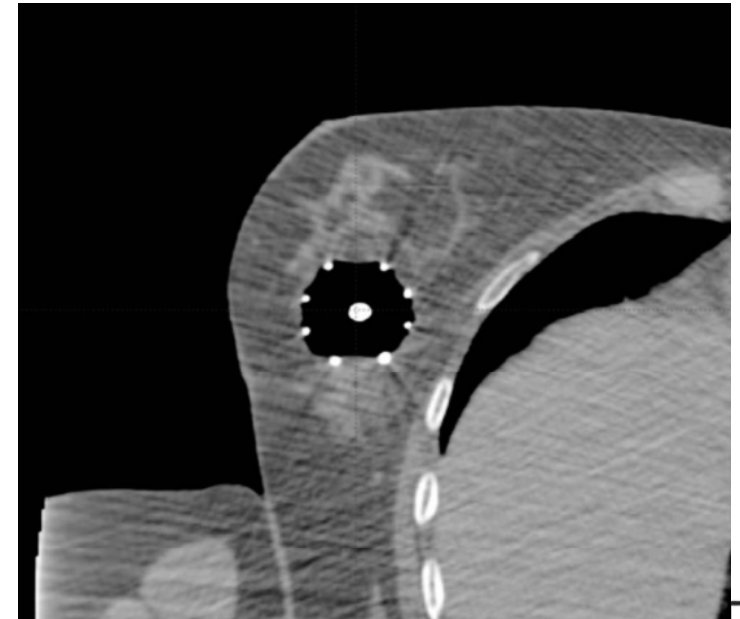


TABLE II. Comparison between MC doses calculated at selected distances from the edge of the device using different sized devices for single and multidwell position plans with and without air cavity present. The treatment planning benchmark is shown for comparison to the MC in water. The percent difference represents the absolute difference between the MC in water and MC in air calculation.

Six-strut device								
Distance (cm)	Single-dwell positions				Multiple dwell positions			
	TPS dose	MC water	MC air	Absolute % difference	TPS dose	MC water	MC air	Absolute % difference
1.0	340.2	340.2	352.4	3.6	360.8	369.4	381.2	3.2
1.5	232.6	232.9	241.9	2.7	243.6	245.0	252.6	2.1
2.0	168.8	169.2	177.2	2.3	177.2	178.0	183.9	1.6
3.0	100.0	102.0	106.4	1.3	106.1	106.0	110.7	1.3
4.0	65.6	67.2	70.1	0.9	70.2	71.8	76.5	1.3
5.0	46.0	47.4	49.5	0.6	49.4	51.4	58.2	1.9
10.0	12.3	14.6	15.3	0.2	13.4	14.3	15.5	0.3

0-4%

Eight-strut device								
Distance (cm)	Single-dwell positions				Multiple dwell positions			
	TPS dose	MC water	MC air	Absolute % difference	TPS dose	MC water	MC air	Absolute % difference
1.0	340.2	348.8	369.7	6.0	334.1	346.1	362.1	4.6
1.5	249.6	254.8	272.0	4.9	239.6	245.9	259.8	4.0
2.0	190.9	196.8	210.7	4.0	180.2	183.8	194.4	3.1
3.0	121.3	125.7	134.8	2.6	112.6	117.5	118.6	0.3
4.0	83.2	86.6	92.6	1.7	76.6	80.8	83.9	0.9
5.0	60.1	62.8	67.2	1.3	55.1	57.6	60.1	0.7
10.0	17.1	20.2	21.6	0.4	15.6	16.4	21.5	1.5

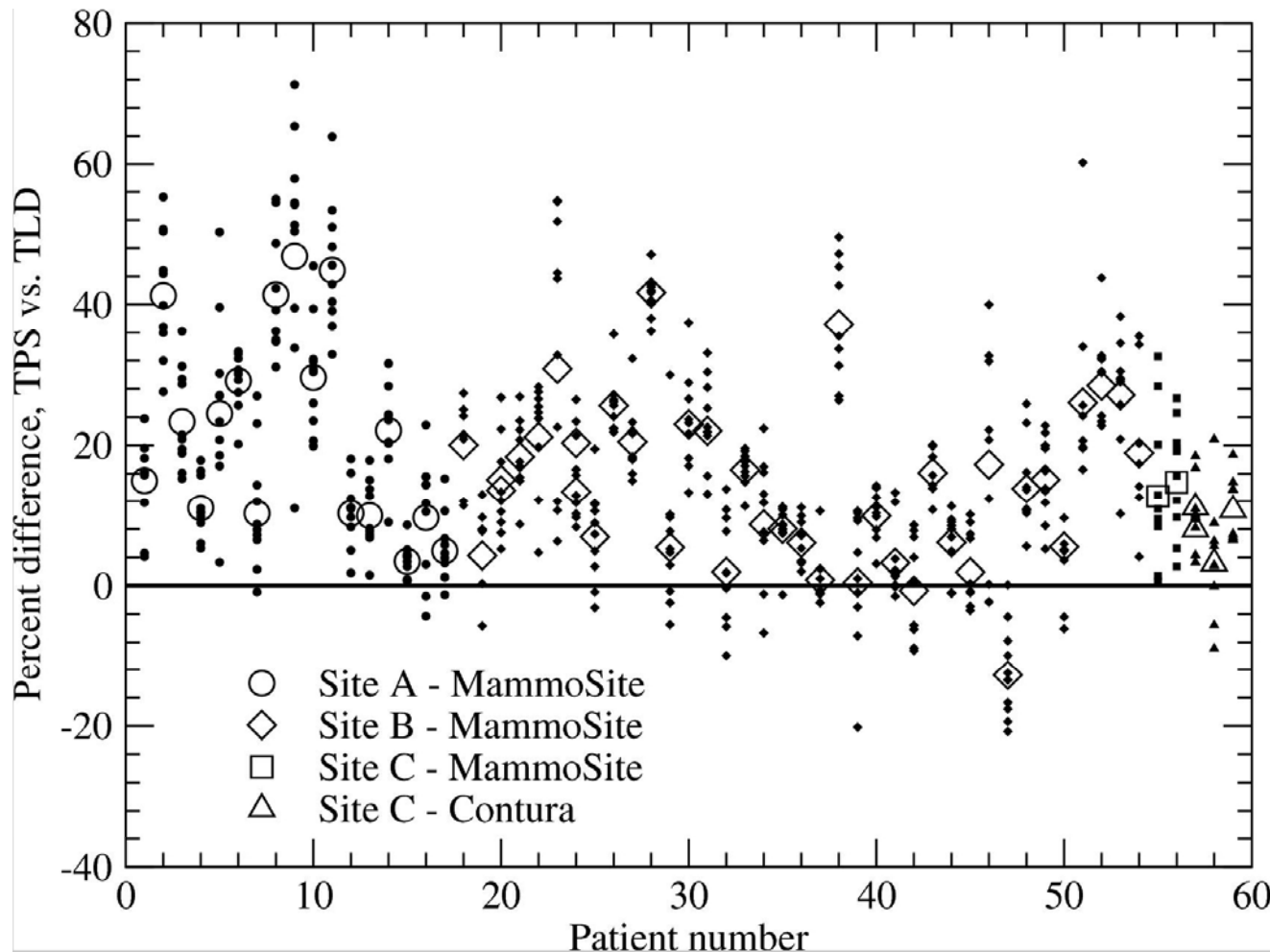
0-6%

Ten-strut device								
Distance (cm)	Single-dwell positions				Multiple dwell positions			
	TPS dose	MC water	MC air	Absolute % difference	TPS dose	MC water	MC air	Absolute % difference
1.0	340.3	345.4	373.9	8.3	371.5	370.8	402.7	8.6
1.5	258.2	263.3	285.7	6.5	265.2	263.2	275.9	3.4
2.0	202.2	208.1	226.6	5.3	201.2	199.2	202.9	1.0
3.0	132.9	137.0	149.5	3.6	128.5	129.8	112.6	4.6
4.0	93.2	96.7	105.8	2.6	89.0	91.6	81.6	2.7
5.0	68.3	71.1	78.0	2.0	64.8	66.1	60.3	1.6
10.0	20.0	23.1	25.2	0.6	18.7	19.8	21.3	0.4

0-9%



Skin Doses: study on 59 patients



TLD skin dose meas.

- TPS-TLD: -13% to 47%
- Average: 16% overestimation
- MC or Acuros: < 5%

Balloon-Based Accelerated Partial Breast Irradiation With Contura™: Comparison Between Conventional TG-43 and Brachyvision Acuros™ Dose Calculation Methods

Ruben Ter-Antonyan, PhD¹, Paul W. Read, MD, PhD¹, Bernard F. Schneider, MD, PhD¹, Anneke T. Schroen, MD, MPH², Stanley H. Benedict, PhD¹, Bruce P. Libby, PhD¹. ¹Radiation Oncology, University of Virginia Health System, Charlottesville, VA; ²Surgery, University of Virginia Health System, Charlottesville, VA.

- 5 Contura patients

	TG-43	Acuros™	Difference
PTV_eval D95 (cGy)	322.7	311.9	(3.4 ± 0.5) %
PTV_eval D1 (cGy)	816.4	806.6	(1.2 ± 0.6) %
PTV_eval D _{min} (cGy)	238.4	254.1	(-7.1 ± 7.1) %
PTV_eval V150 (cm ³)	26.5	24.0	(9.2 ± 1.3) %
Skin D _{max} (cGy)	439.0	420.1	(4.6 ± 1.2) %
Skin D _{mean} (cGy)	242.8	226.6	(6.7 ± 0.6) %
Skin D _{skin_pt} (cGy)	297.1	278.1	(6.7 ± 1.7) %

Comparison between Two Dose Calculation Methods, Acuros and TG43: Implications for Accelerated Partial Breast Irradiation

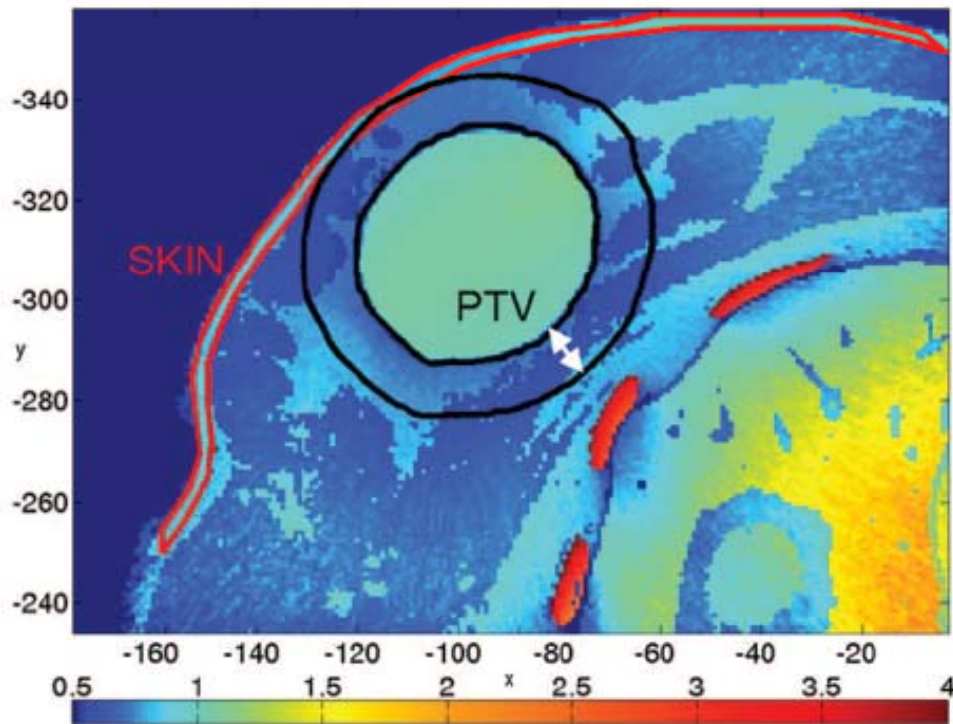
*Jill P. Heffernan, M.D., Lynn Gilbert, C.M.D., Douglas W. Arthur, M.D.,
Dorin A. Todor, Ph.D. Radiation Oncology, Virginia Commonwealth
University, Richmond, VA.*

- 30 patients evaluated Skin_{max}, Rib_{max}, D90, V100, V150, V200
- Variety of applicators including interstitial
 - Results for interstitial were within 3% or 3cc
- Balloon based:
 - Skinmax – 8% including >10% if only using central lumen/single dwell
 - Ribmax- 5% on average
 - Target coverage less (3.5% – 8%)
 - Larger balloons had greater differences in V100, etc.

TG-186 Heterogeneous Model ($D_{m,m}$)



(b) Dose ratio: Heterogenous Model $D_{m,m}$ / TG-43 MC



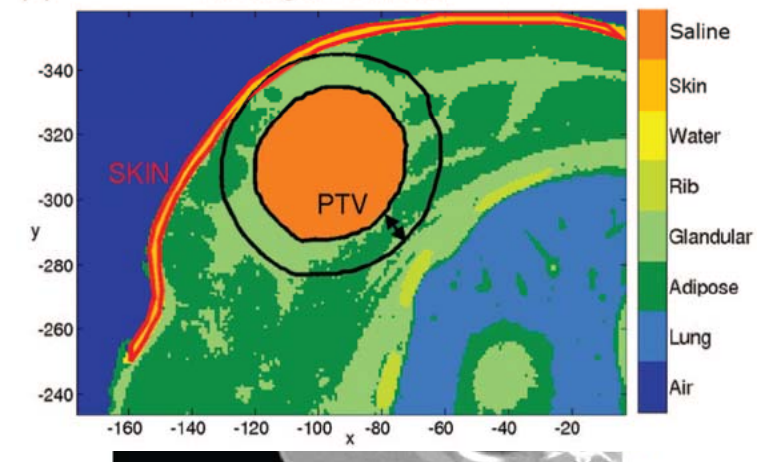
TG-186 < TG-43

TG-186 > TG-43

- Large DVH decreases in $D_{m,m}$ compared to TG-43
- Higher calculated rib dose

DVH	% differences range
D_{90}	-36% to -33%
V_{100}	-54% to -29%
V_{200}	-97% to -25%
$D_{0.2cc}$ (Skin)	-19% to 0%

(e) Heterogenous Model



Summary for Breast Brachytherapy

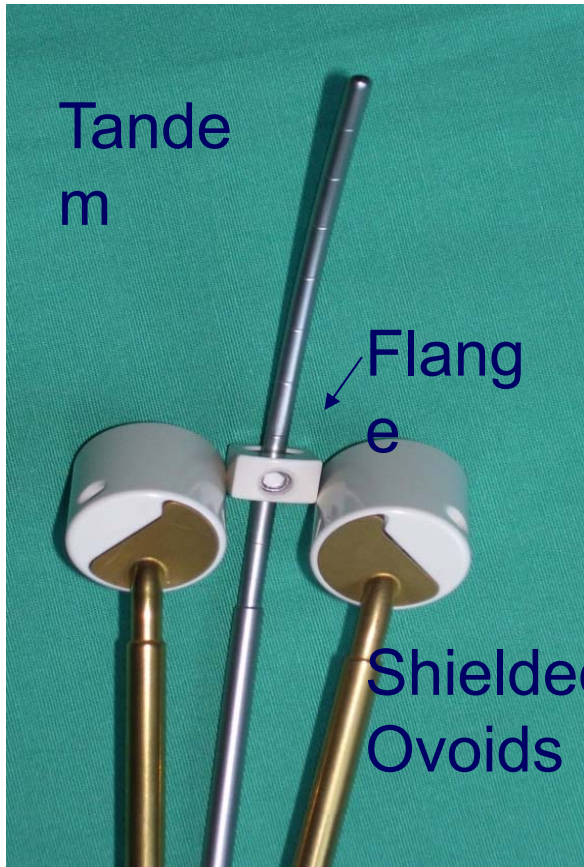
- The experts agree that in using TG43 for ^{192}Ir procedures:
 - If you are using high levels of contrast – your overall dose is decreased
 - Skin dose is over-estimated (~ 4-10%)
 - Dose to ribs is under-estimated (~ 5 -7%)
 - Dose coverage is probably slightly over-estimated
- If you use seeds or electronic brachytherapy sources
 - Very large effect due to breast composition (adipose and glandular tissues)
 - Very large effect from bones (ribs)

Sensitivity of Anatomic Sites to Dosimetric Limitations of Current Planning Systems

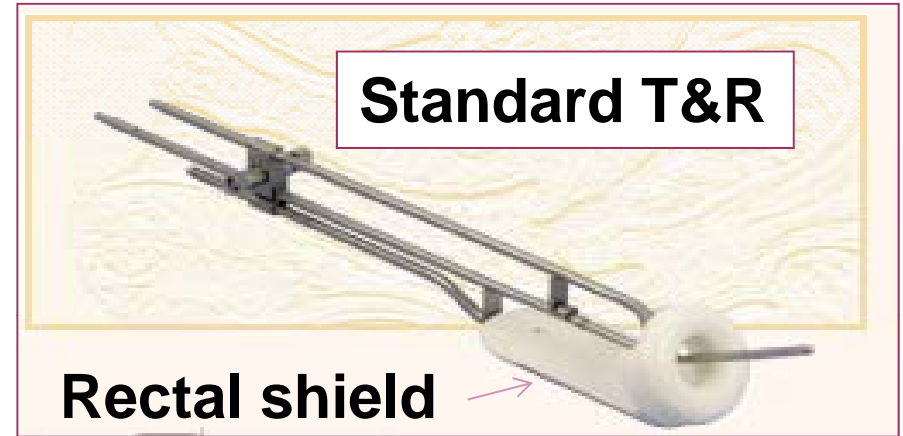
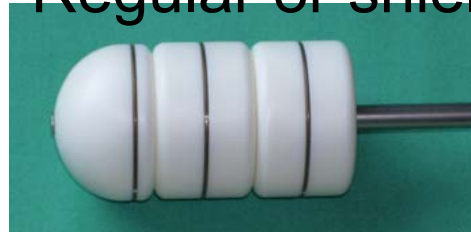
anatomic site	photon energy	absorbed dose	attenuation	shielding	scattering	beta/kerma dose
prostate	high					
	low	XXX	XXX	XXX		
breast	high				XXX	
	low	XXX	XXX	XXX		
GYN	high			XXX		←
	low	XXX	XXX			
skin	high			XXX	XXX	
	low	XXX		XXX	XXX	
lung	high				XXX	XXX
	low	XXX	XXX		XXX	
penis	high				XXX	
	low	XXX			XXX	
eye	high			XXX	XXX	XXX
	low	XXX	XXX	XXX	XXX	

GYN Standard Applicators too many to list

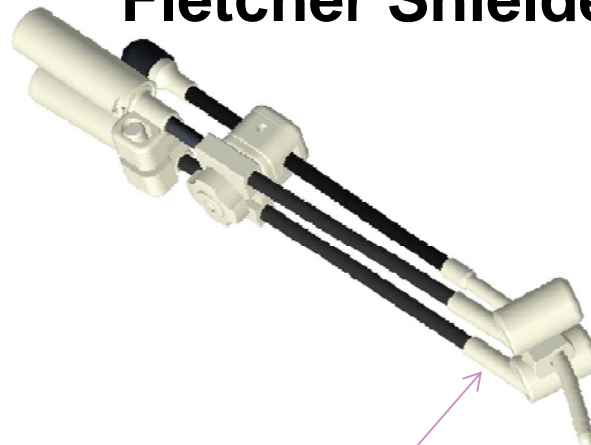
Fletcher-Williamson T&O



Standard Cylinder
Regular or shielded

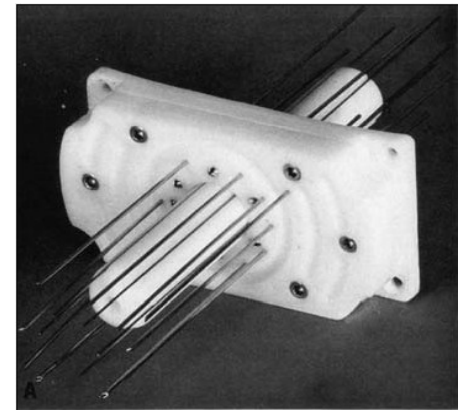


Fletcher Shielded

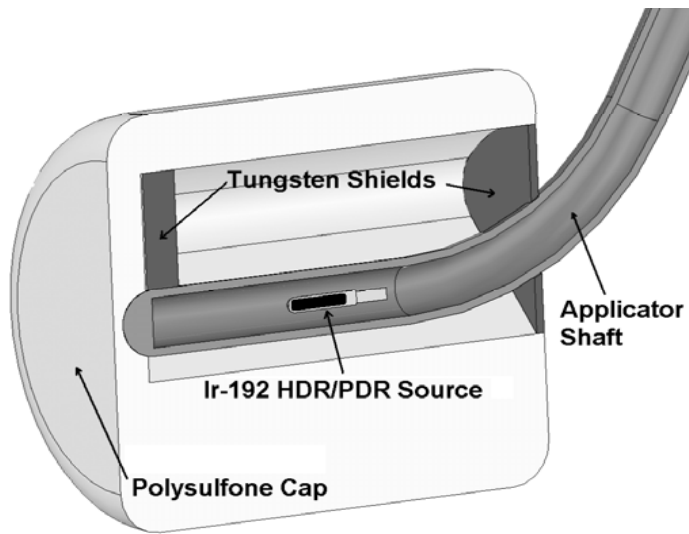


Shielded ovoids

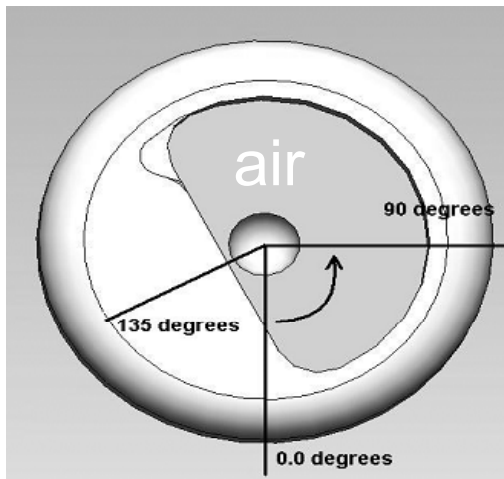
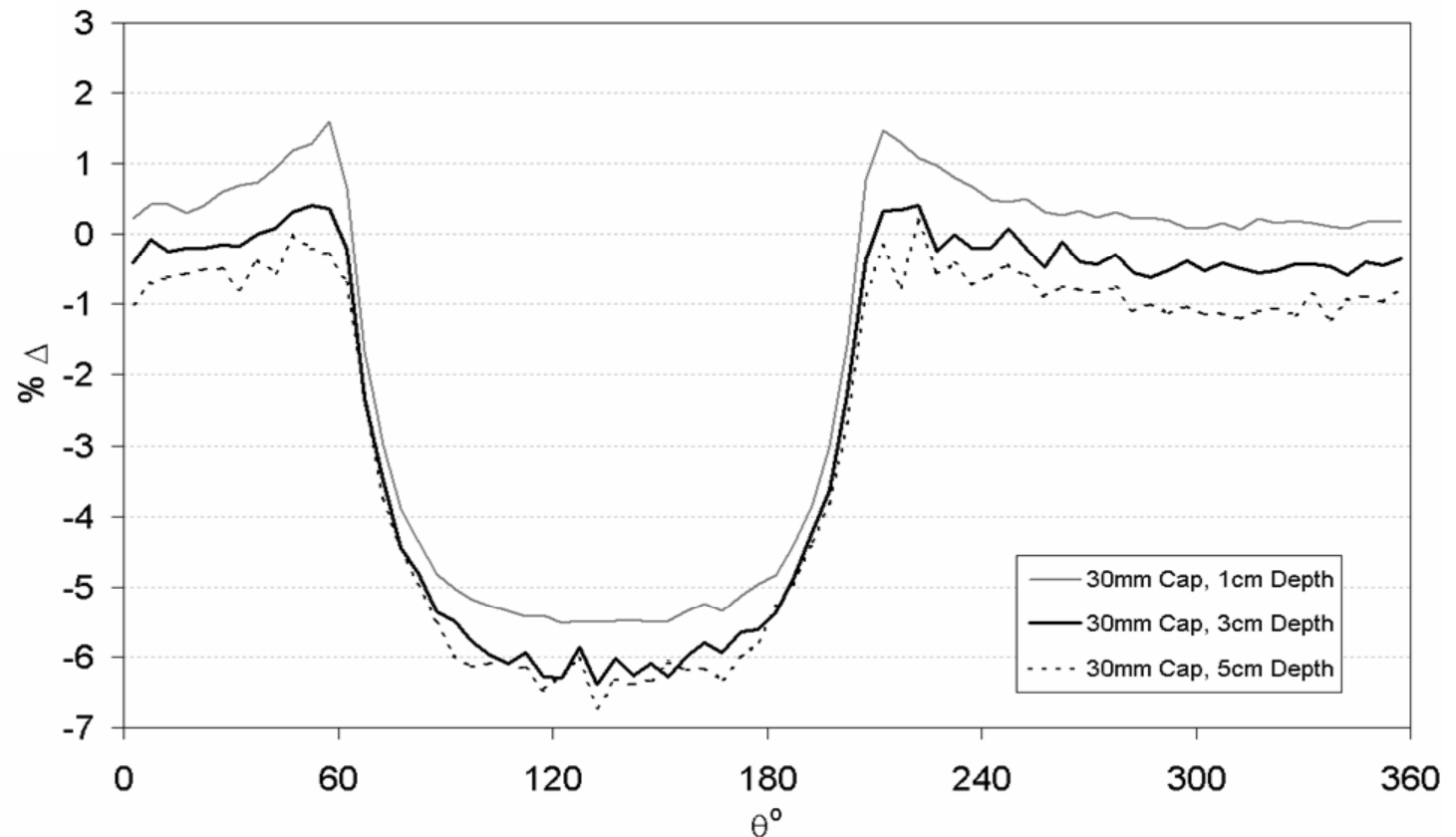
Interstitial



Shielded applicators with cap



MCNPX 2.5 simulations compared with TG-43 predicted doses (Plato TPS)



Attenuation of intracavitary applicators in ^{192}Ir -HDR brachytherapy

Sung-Joon Ye,^{a)} Ivan A. Brezovich, Sui Shen, Jun Duan, Richard A. Popple,
and Prem N. Pareek

*Department of Radiation Oncology, University of Alabama School of Medicine, 1824 6th Avenue South,
Birmingham, Alabama 35294*

TABLE I. Elemental compositions and densities of the ^{192}Ir source and applicator components used in the Monte Carlo simulations.

Component	Material	Atomic composition	Density (g/cm^3)
Active wire	Iridium metal	1.0 Ir	22.42
Encapsulation	Stainless steel	[0.02 Si, 0.18 Cr	8.02
Uterine tube	Stainless steel	0.02 Mn, 0.67 Fe, 0.11 Ni]	8.02
Vaginal cylinder	Polysulfone	0.41 H, 0.5 C, 0.07 O, 0.02 S	1.40

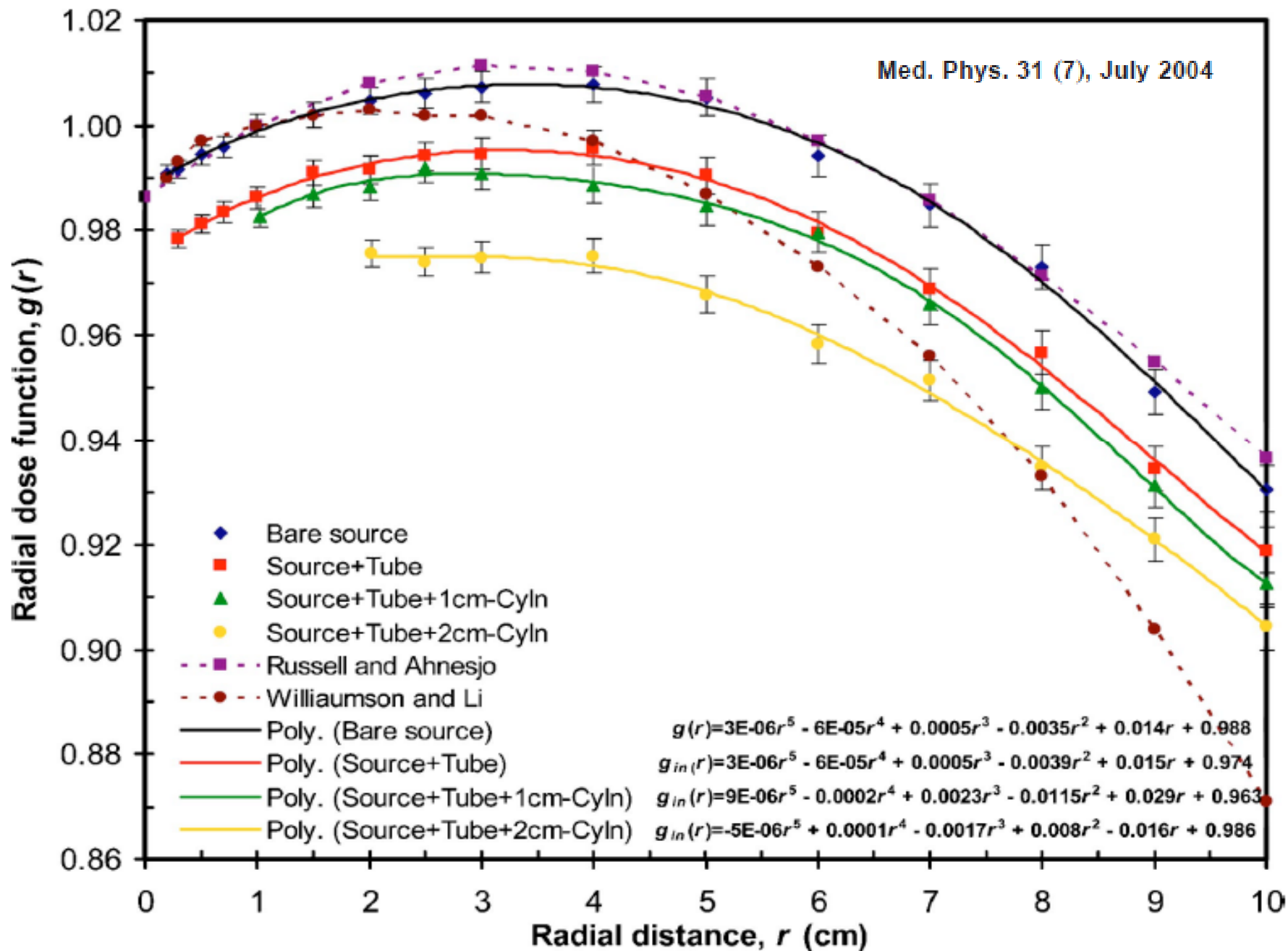


FIG. 5. Radial dose functions calculated for a bare source and a source embedded in various cylindrical applicators and their comparisons to published data. Fifth-order polynomial fittings to our calculated radial dose functions are also presented.

Impact of Heterogeneity-Based Dose Calculation Using a Deterministic Grid-Based Boltzmann Equation Solver for Intracavitary Brachytherapy

Justin K. Mikell, B.S.,^{*,||} Ann H. Klopp, M.D., Ph.D.,[†] Graciela M.N. Gonzalez, M.P.H.,[‡] Kelly D. Kisling, M.S.,^{§,||} Michael J. Price, Ph.D.,^{**} Paula A. Berner, B.S.,^{*} Patricia J. Eifel, M.D.,[†] and Firas Mourtada, Ph.D.^{§,¶,††}

Departments of ^{*}Radiation Physics, [†]Radiation Oncology, [‡]Biostatistics, [§]Radiation Physics—Patient Care, and [¶]Experimental Diagnostic Imaging, The University of Texas MD Anderson Cancer Center, Houston, Texas; ^{||}University of Texas Graduate School of Biomedical Sciences at Houston, Houston, Texas; ^{**}Department of Physics and Astronomy, Louisiana State University and Agricultural and Mechanical College, Baton Rouge, Louisiana, and Mary Bird Perkins Cancer Center, Baton Rouge, Louisiana; and ^{††}Department of Radiation Oncology, Helen F. Graham Cancer Center, Newark, Delaware

Summary

This study investigated the use of a grid-based Boltzmann solver (GBBS) for cervical cancer patients treated with unshielded CT/MR applicators. The GBBS was found to have minimal impact on clinical dosimetric parameters for these patients. GBBS differences from standard TG-43 dose estimates were mainly due to source, boundary, and applicator model differences. CT-to-material mapping of rectal and balloon contrast did not impact clinical dosimetry. Rectal dose parameters may be affected by incorrectly mapping packing material.

Purpose: To investigate the dosimetric impact of the heterogeneity dose calculation Acuros (Transpire Inc., Gig Harbor, WA), a grid-based Boltzmann equation solver (GBBS), for brachytherapy in a cohort of cervical cancer patients.

Methods and Materials: The impact of heterogeneities was retrospectively assessed in treatment plans for 26 patients who had previously received ¹⁹²Ir intracavitary brachytherapy for cervical cancer with computed tomography (CT)/magnetic resonance-compatible tandems and unshielded colpostats. The GBBS models sources, patient boundaries, applicators, and tissue heterogeneities. Multiple GBBS calculations were performed with and without solid model applicator, with and without overriding the patient contour to 1 g/cm³ muscle, and with and without overriding contrast materials to muscle or 2.25 g/cm³ bone. Impact of source and boundary modeling, applicator, tissue heterogeneities, and sensitivity of CT-to-material mapping of contrast were derived from the multiple calculations. American Association of Physicists in Medicine Task Group 43 (TG-43) guidelines and the GBBS were compared for the following clinical dosimetric parameters: Manchester points A and B, International Commission on Radiation Units and Measurements (ICRU) report 38 rectal and bladder points, three and nine o'clock, and D_{2cm3} to the bladder, rectum, and sigmoid.

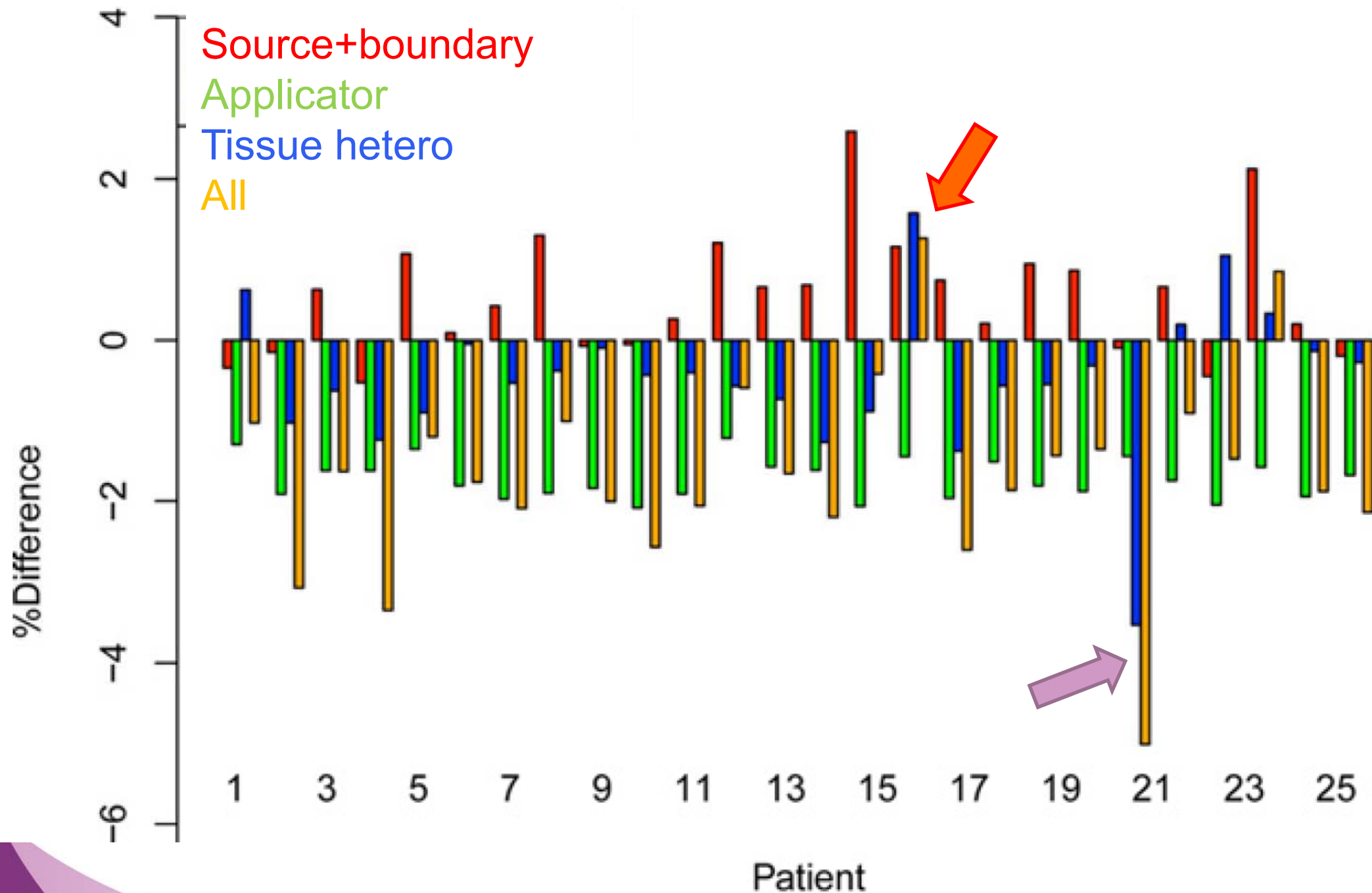
Results: Points A and B, D_{2 cm³} bladder, ICRU bladder, and three and nine o'clock were within 5% of TG-43 for all GBBS calculations. The source and boundary and applicator account for most of the differences between the GBBS and TG-43 guidelines. The D_{2cm3} rectum ($n = 3$), D_{2cm3} sigmoid ($n = 1$), and ICRU rectum ($n = 6$) had differences of >5% from TG-43 for the worst case incorrect mapping of contrast to bone. Clinical dosimetric parameters were within 5% of TG-43 when rectal and balloon contrast were mapped to bone and radiopaque packing was not overridden.

Conclusions: The GBBS has minimal impact on clinical parameters for this cohort of patients with unshielded applicators. The incorrect mapping of rectal and balloon contrast does not have a significant impact on clinical parameters. Rectal parameters may be sensitive to the mapping of radiopaque packing. © 2012 Elsevier Inc.

- ✓ VS-2000 source
- ✓ Applicator part #: AL07334001

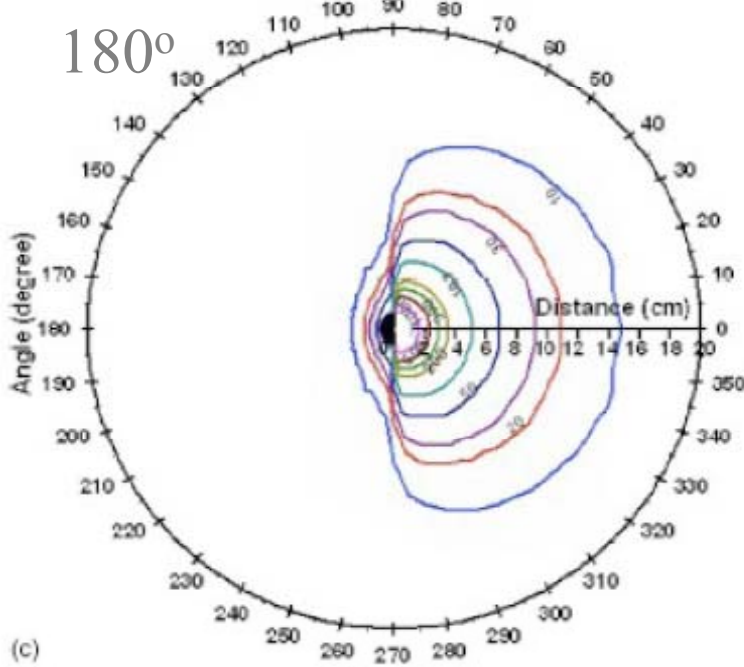
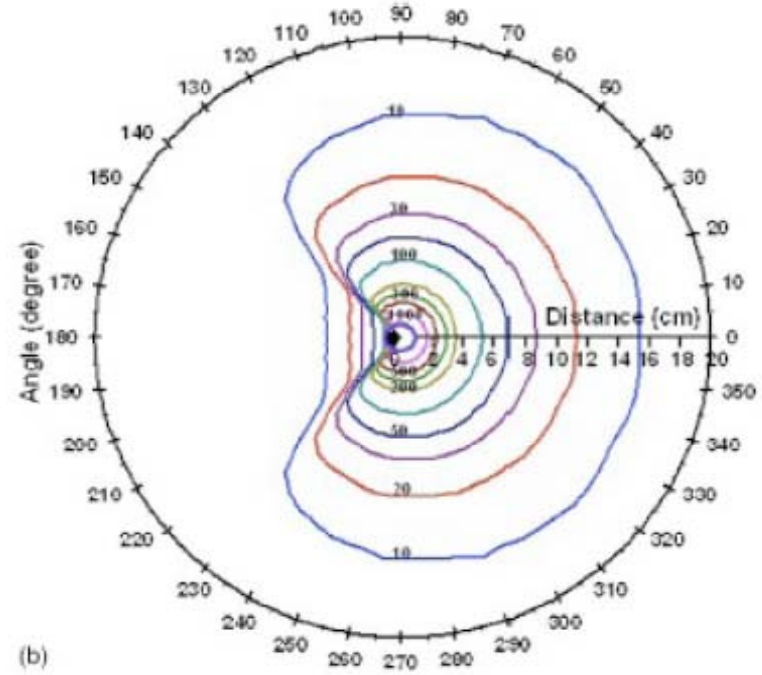
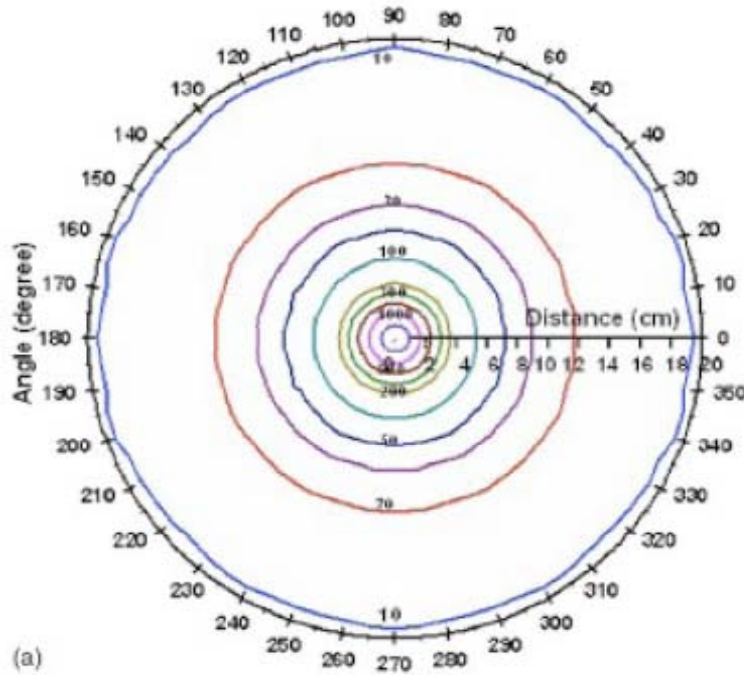


ICRU Rectal Point Dose Impact of GBBS relative to TG-43

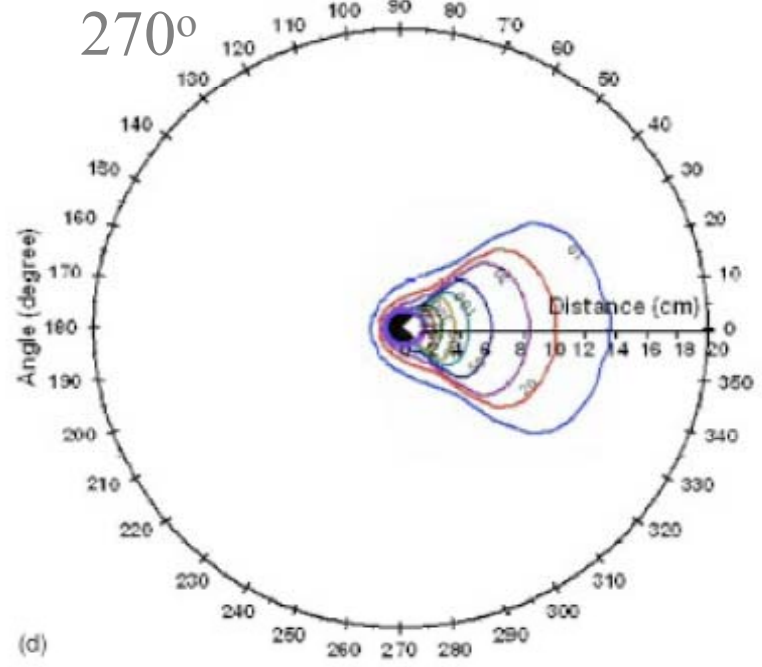


TG43

90°

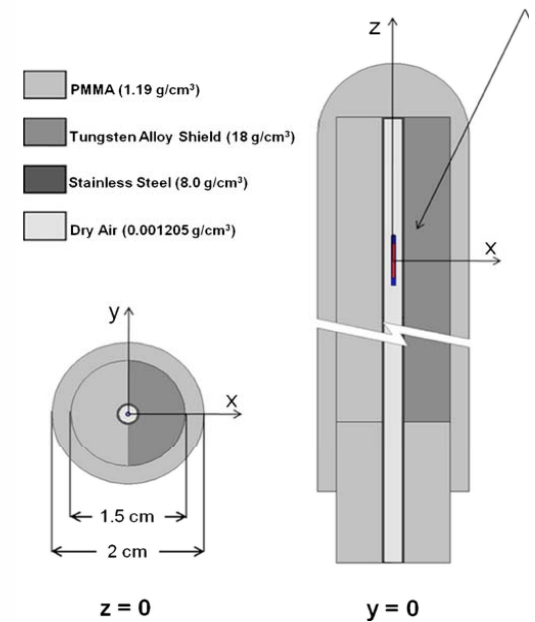
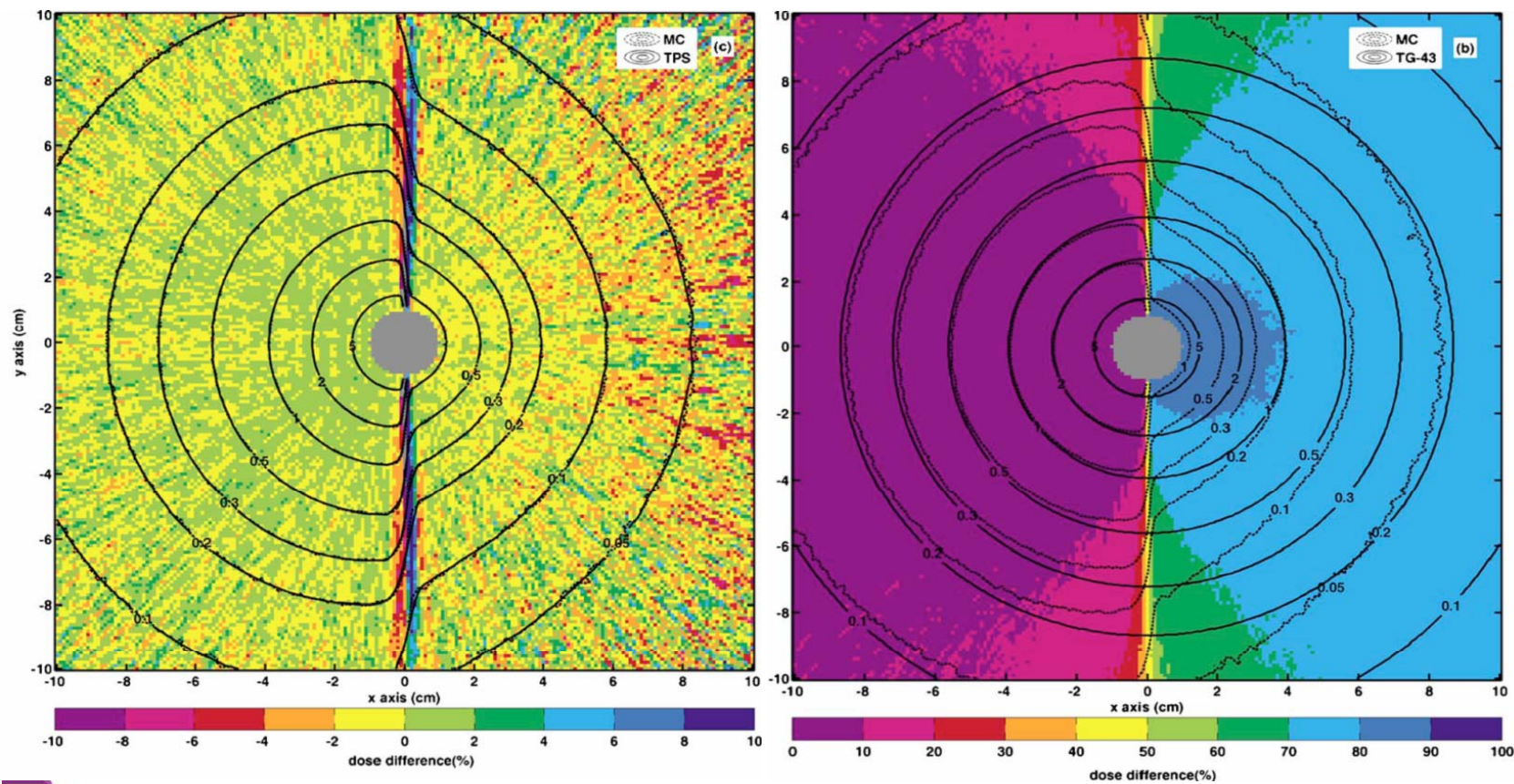


270°

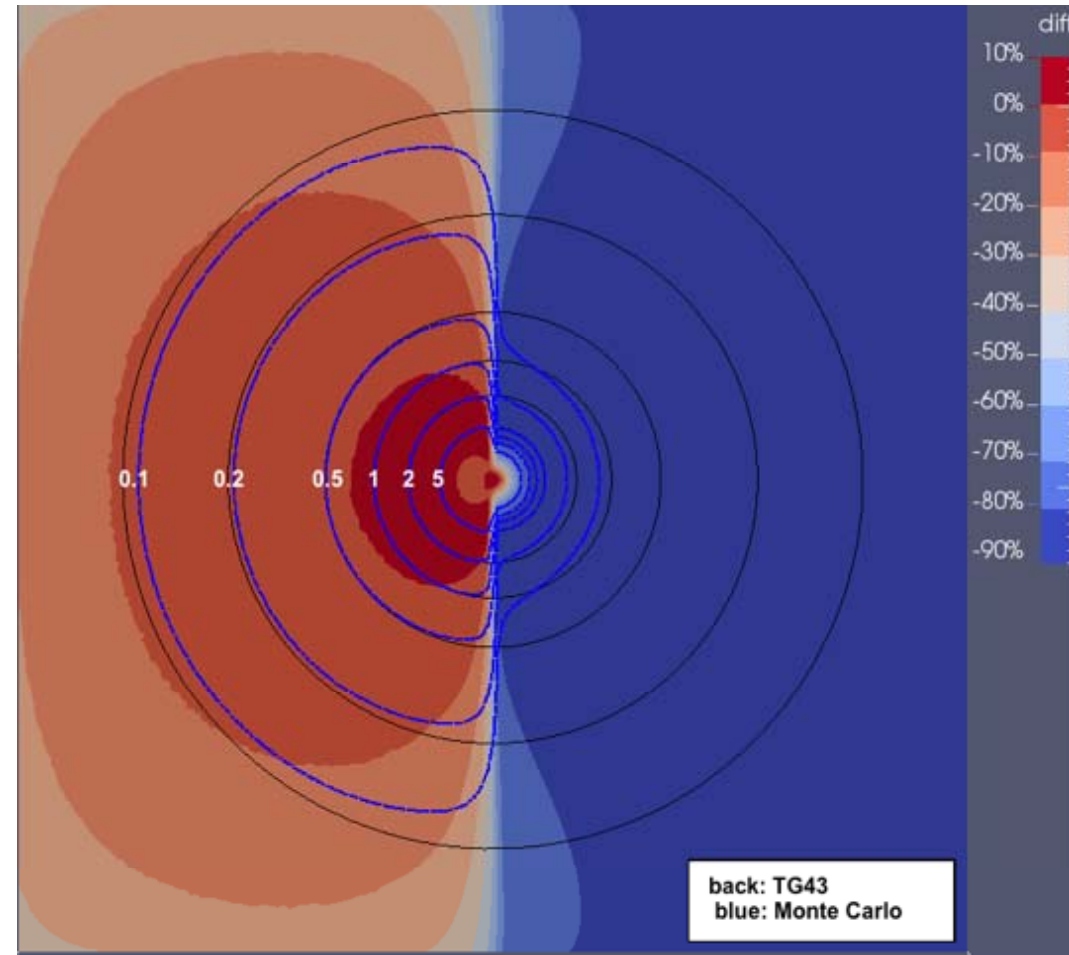
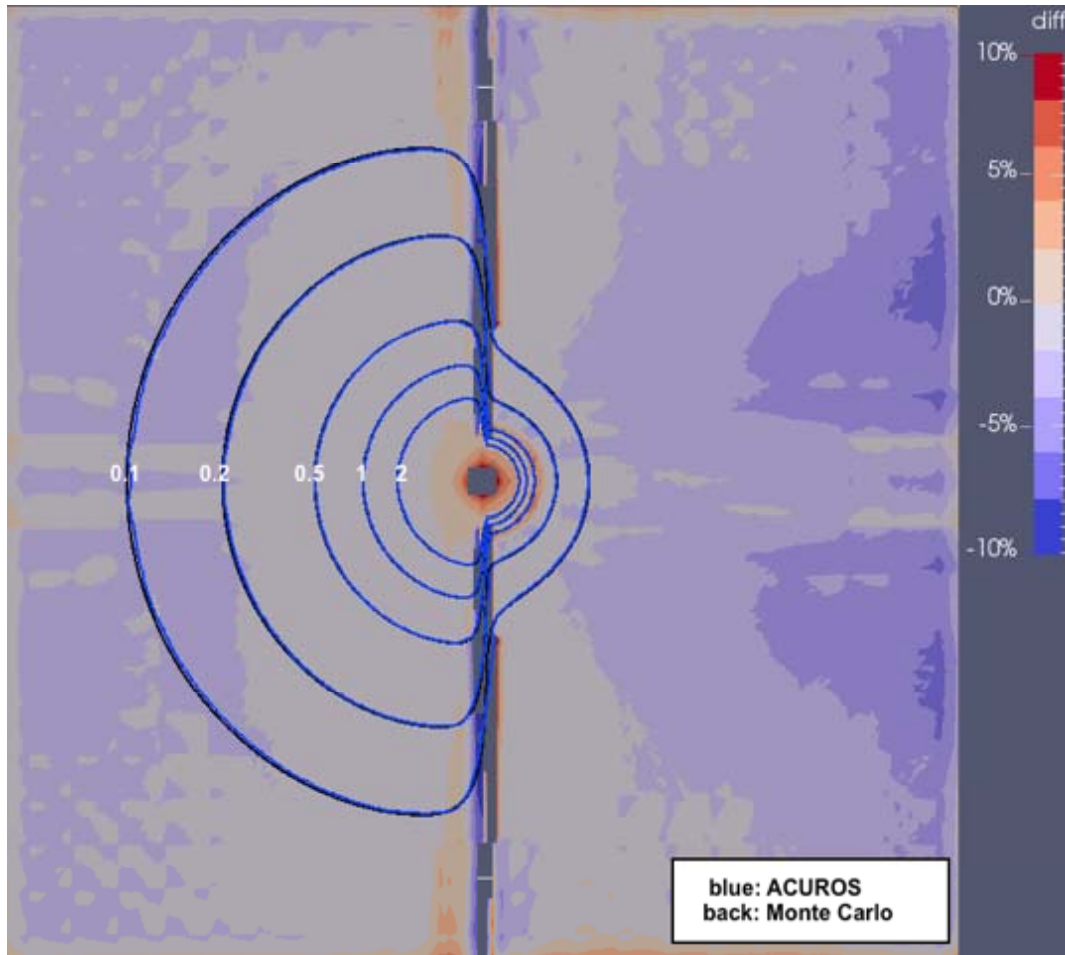


Shielded Geometry

Petrokokkinos *et al.*, MedPhys 38, 1981-1992 (2011)



WG Shielded Applicator Test Case



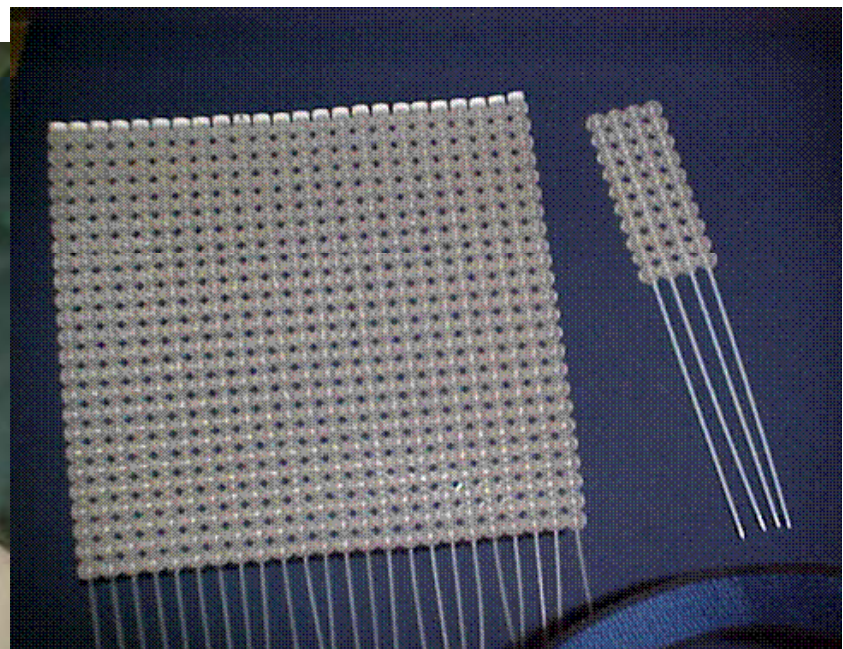
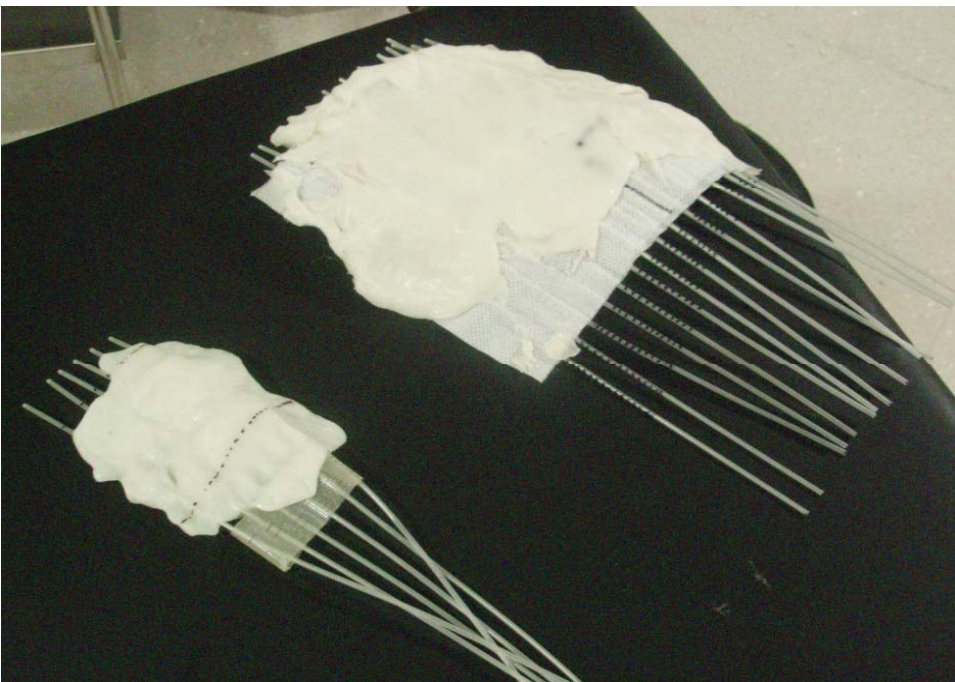
Summary for GYN Brachytherapy

- The new brachy dose calculation algorithms provide more accurate dose distributions for GYN brachytherapy than the standard TG-43.
- Unshielded GYN CT/MR applicators impact is within $\pm 5\%$
- Shielded Applicator can significantly reduces dose to OARs

Sensitivity of Anatomic Sites to Dosimetric Limitations of Current Planning Systems

anatomic site	photon energy	absorbed dose	attenuation	shielding	scattering	beta/kerma dose
prostate	high					
	low	XXX	XXX	XXX		
breast	high				XXX	
	low	XXX	XXX	XXX		
GYN	high			XXX		
	low	XXX	XXX			
skin	high			XXX	XXX	←
	low	XXX		XXX	XXX	
lung	high				XXX	XXX
	low	XXX	XXX		XXX	
penis	high				XXX	
	low	XXX			XXX	
eye	high			XXX	XXX	XXX
	low	XXX	XXX	XXX	XXX	

HDR ^{192}Ir Skin Molds/Flaps



HDR ^{192}Ir Shielded (Leipzig) Applicators

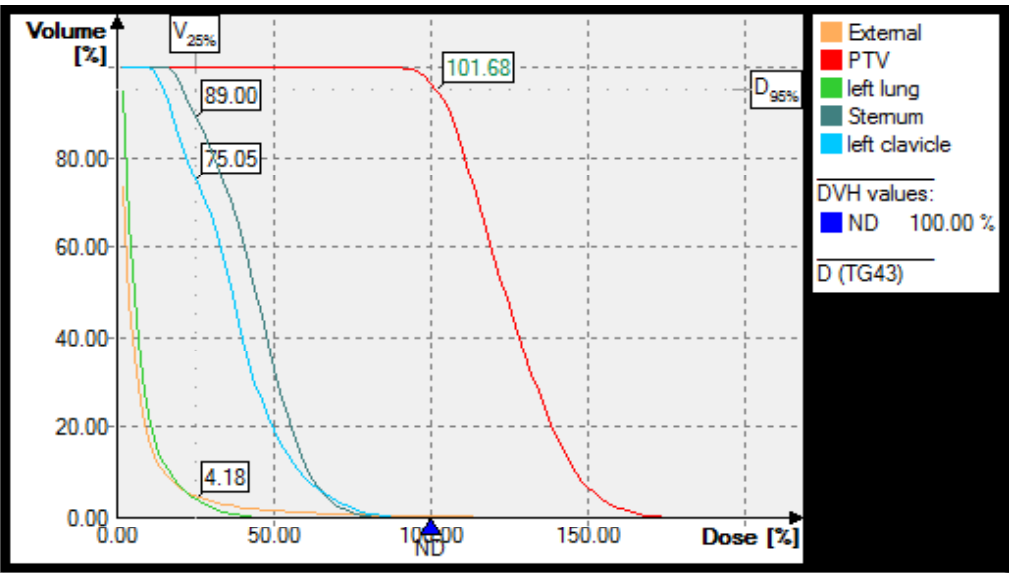
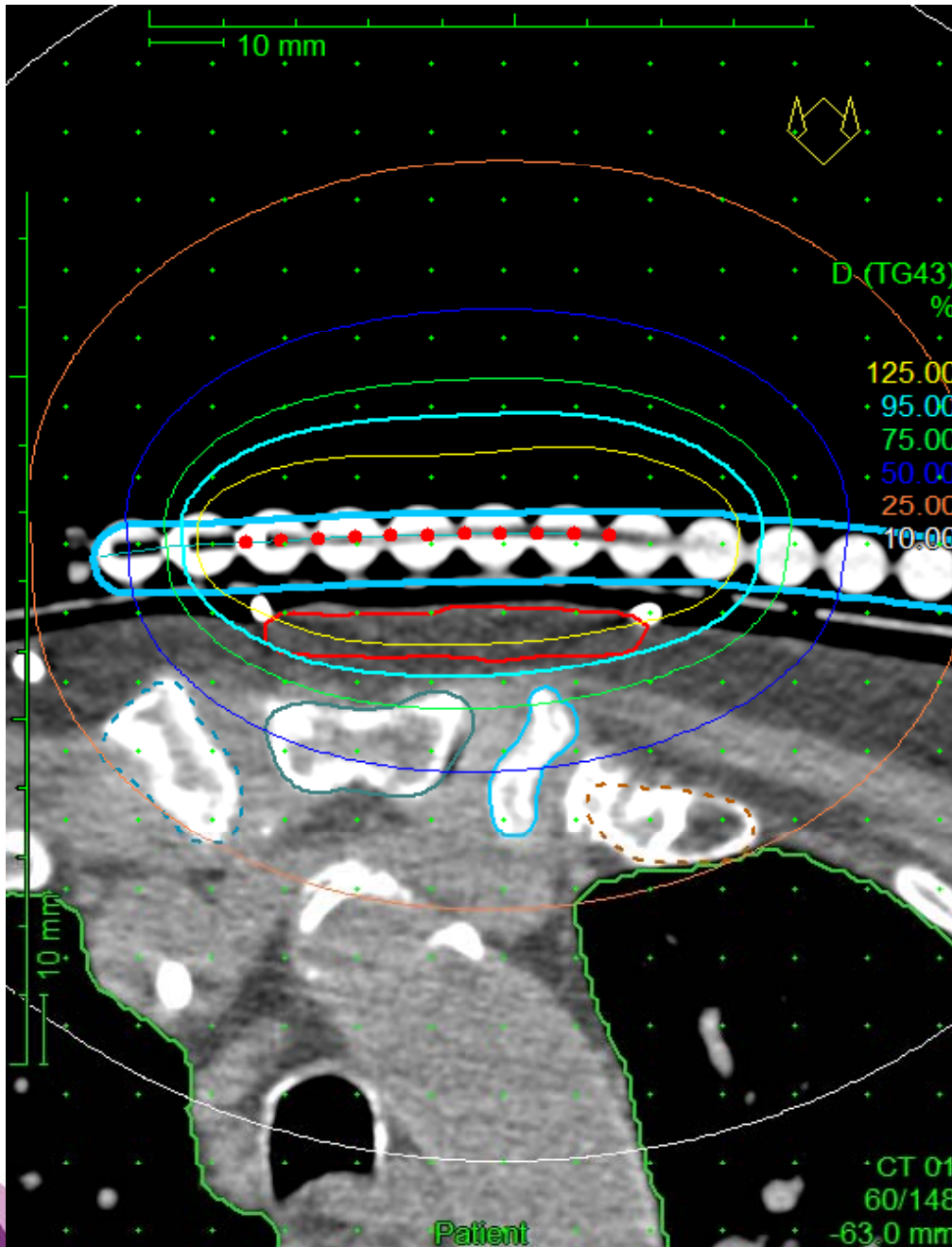


Cup-shaped of tungsten
Horizontal and Vertical
Diameters 1 cm, 2 cm, 3 cm

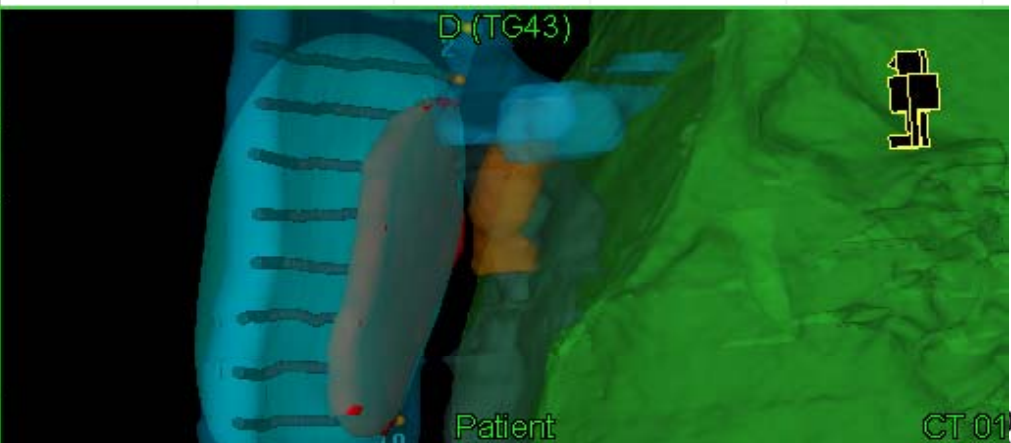


Plastic cap 1 mm, to reduce
skin dose due to electrons.

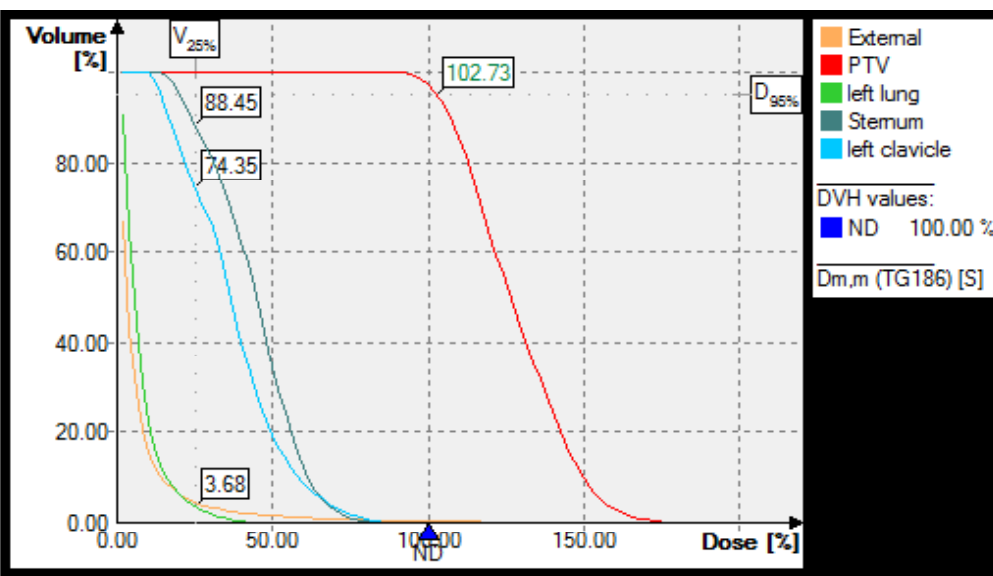
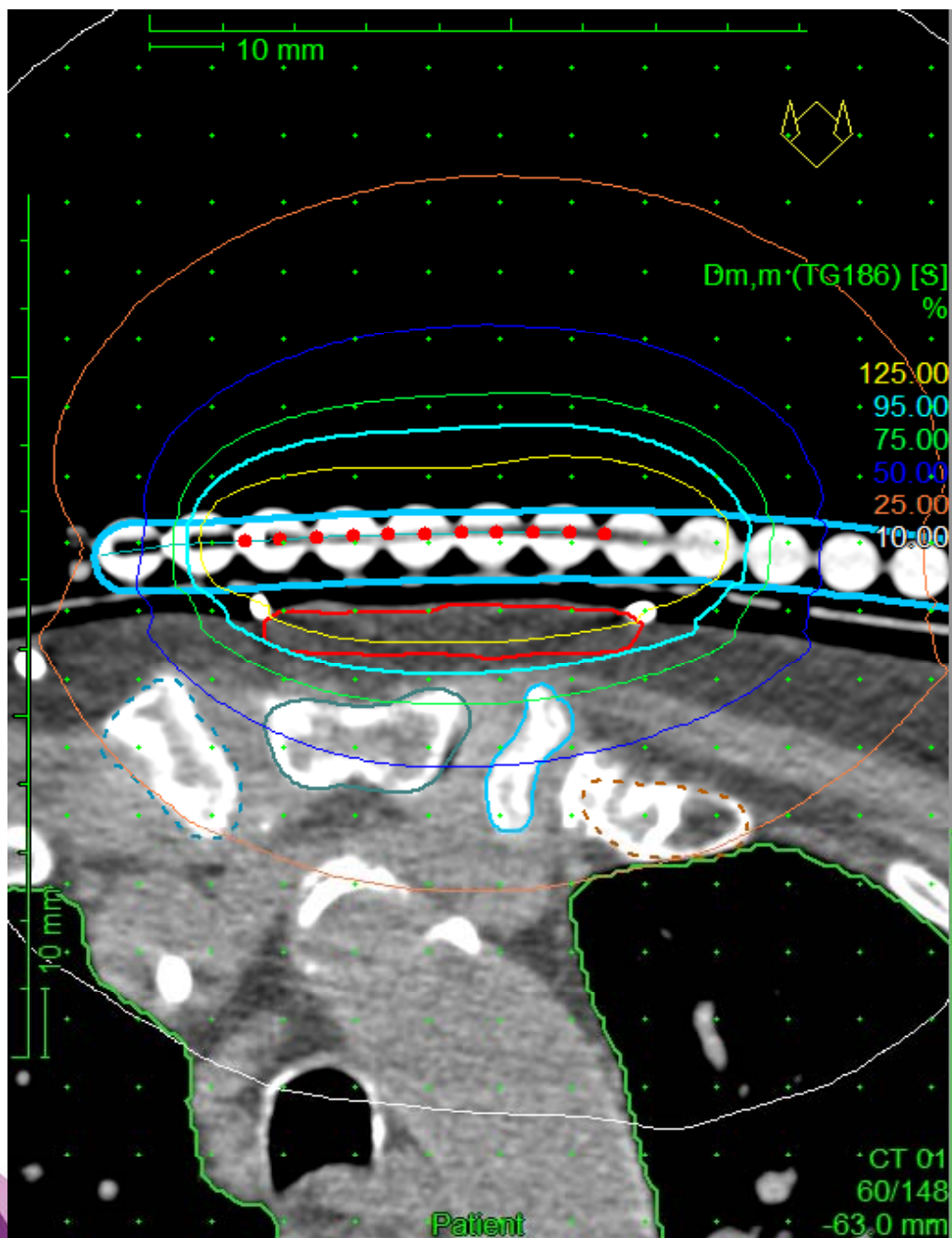
Oncentra[®] ACE TG-43



ROI	Dose [%]	Dose [Gy]	Volume [%]	Volume [ccm]
left lung	42.01	1.6804	0.24	2.00
Sternum	65.03	2.6011	5.69	2.00
left clavicle	48.71	1.9484	21.14	2.00
left lung	25.00	1.0000	4.18	34.51
Sternum	25.00	1.0000	89.00	31.31
left clavicle	25.00	1.0000	75.05	7.10
PTV	101.68	4.0673	95.00	19.74



Oncentra[®] ACE TG-186



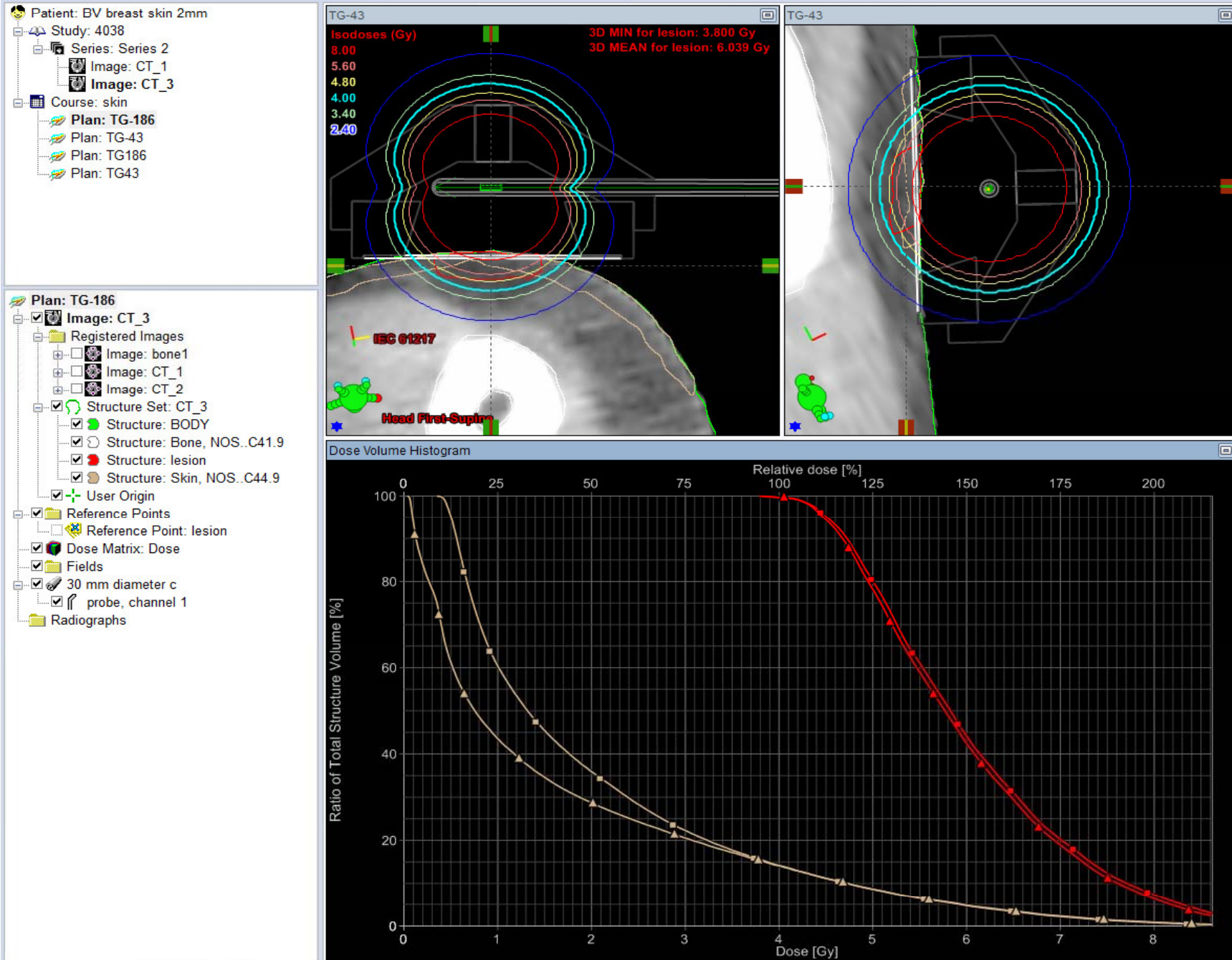
ROI	Dose [%]	Dose [Gy]	Volume [%]	Volume [ccm]
left lung	39.93	1.5970	0.24	2.00
Sternum	65.36	2.6145	5.69	2.00
left clavicle	48.85	1.9538	21.14	2.00
left lung	25.00	1.0000	3.68	30.37
Sternum	25.00	1.0000	88.45	31.12
left clavicle	25.00	1.0000	74.35	7.03
PTV	102.73	4.1093	95.00	19.74



Oncentra[®] ACE Skin Mold Differences

target	TG-43 D_{95} (Gy)	TG-186 D_{95} (Gy)	TG-43 Dose (%)	TG-186 Dose (%)
PTV	4.07	4.11	101.7	102.7
no big deal for skin mold				
ROI	TG-43 V_{25} (cm ³)	TG-186 V_{25} (cm ³)	TG-43 V_{25} (%)	TG-186 V_{25} (%)
sternum	31.31	31.12	89.00	88.45
clavicle	7.10	7.03	75.05	74.35
lung	34.51	30.37	4.18	3.68

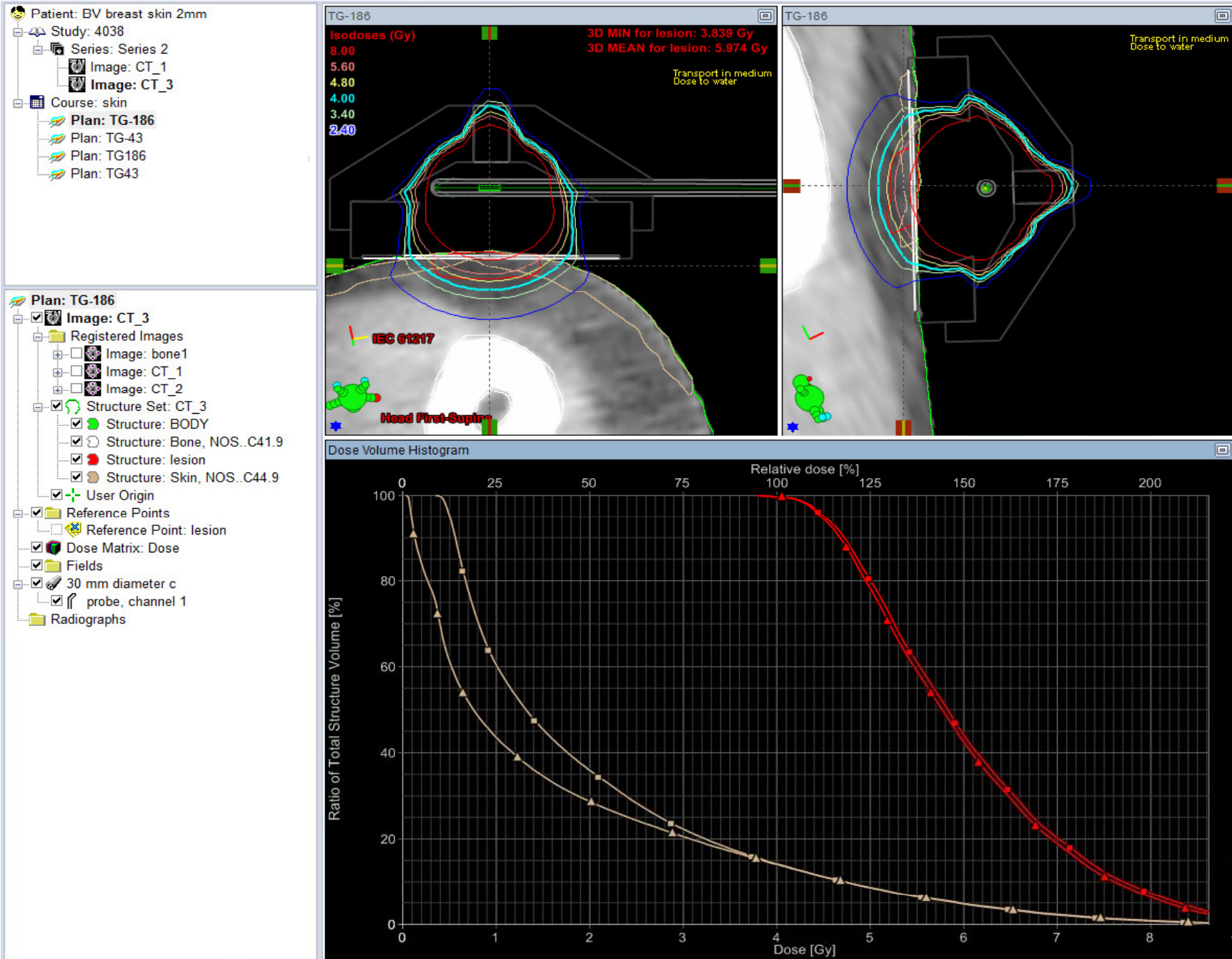
Acuros™ BV TG-43



ESTRO

courtesy R. Park

Acuros™ BV TG-186



ESTRO

courtesy R. Park

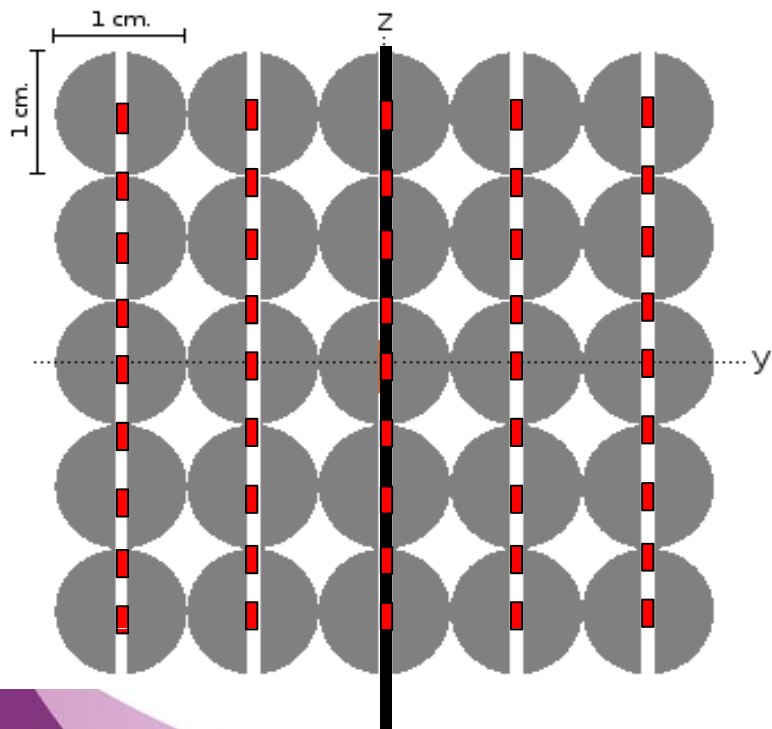
Acuros™ BV Shielded Applicator

target	TG-43 D_{95} (Gy)	TG-186 D_{95} (Gy)	TG-43 Dose (%)	TG-186 Dose (%)
PTV	4.50	4.50	100.0	100.0
collimation is important				
ROI	TG-43 V_{25} (cm ³)	TG-186 V_{25} (cm ³)	TG-43 V_{25} (%)	TG-186 V_{25} (%)
skin	3.97	2.88	60.1	43.7
bone	3.32	5.85	3.88	6.83

Comparing TG-43 and MC for Skin BT

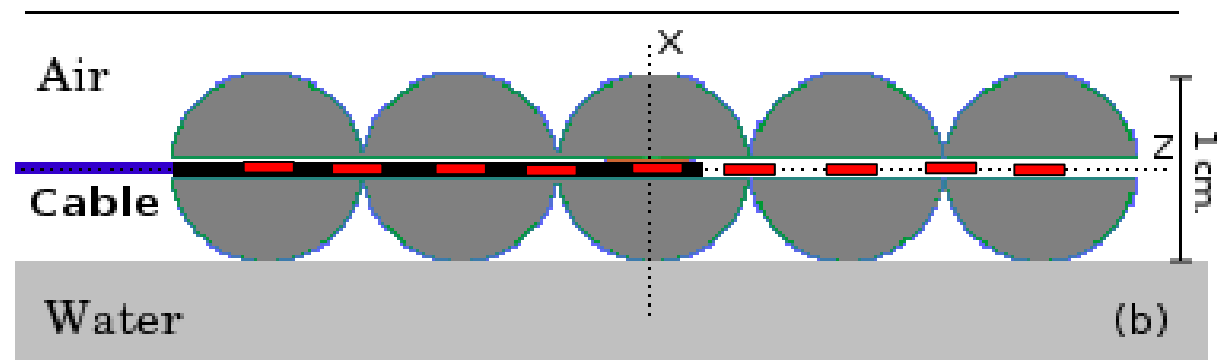
Dosimetry comparison between TG-43 and Monte Carlo calculations using the Freiburg flap for skin high-dose-rate brachytherapy

Javier Vijande^{1,2,*}, Facundo Ballester¹, Zoubir Ouhib³, Domingo Granero⁴,
M. Carmen Pujades-Claumarchirant⁵, Jose Perez-Calatayud⁵



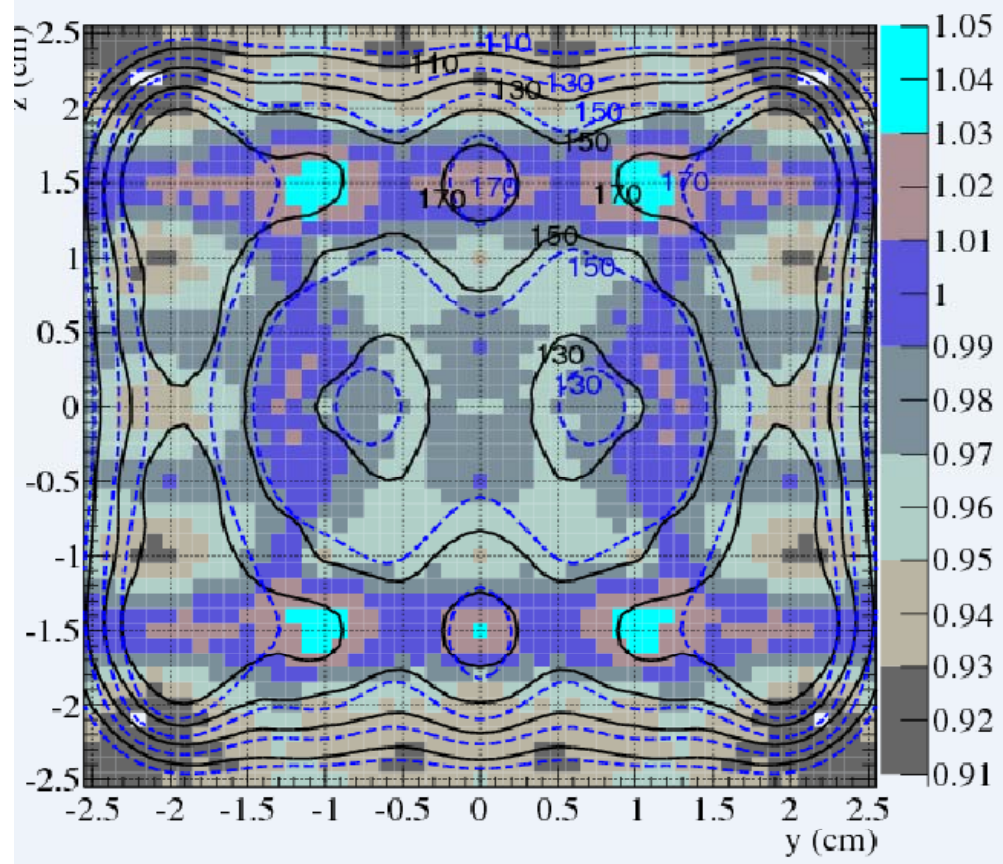
⇒ evaluate scatter defect, air gap

⇒ 5x5 cm² clinical mesh



Comparing TG-43 and MC for Skin BT

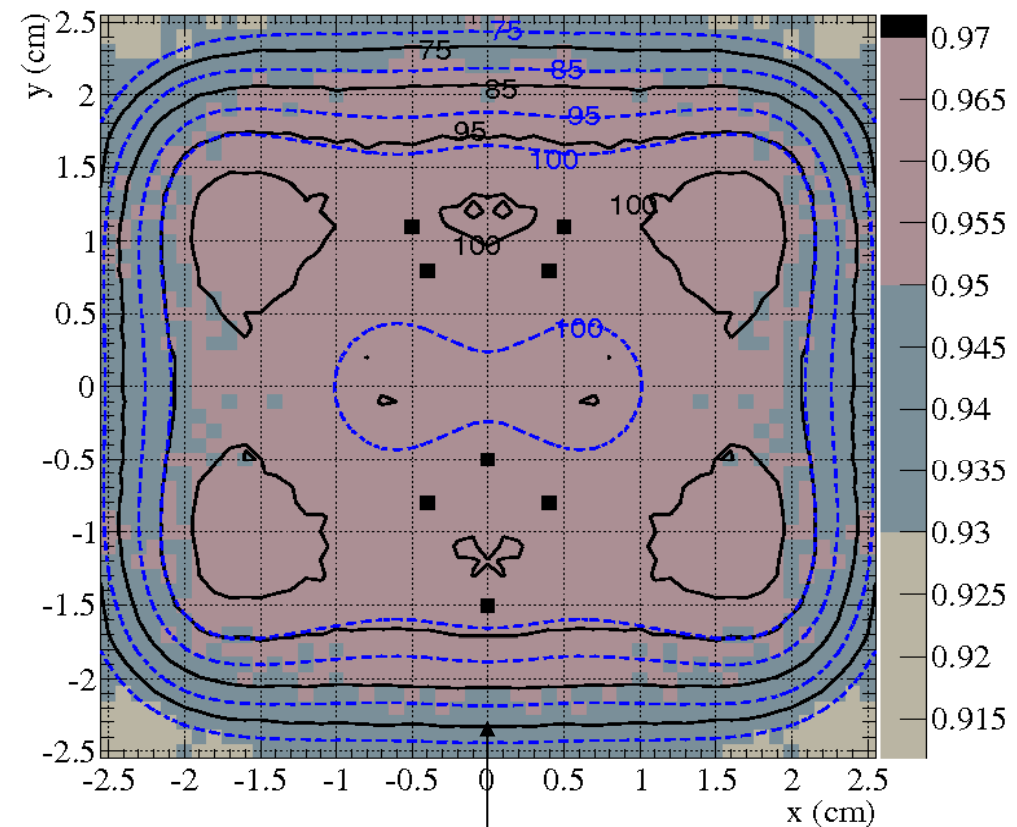
Monte Carlo (MCFF) / TG-43



surface

+5% to -7%

over/under dose compensation between adjacent spheres



5 mm depth

-4% to -7%



Summary for Skin Brachytherapy

- Challenges due to irregular surface
 - Interplay between scatter and shielding effects
- Departure from TG43 calculated dose depends on shielding and/or presence of air gaps
 - Small for PTV with unshielded geometry
 - Need further dose recalculation studies of (large) patient cohorts

Sensitivity of Anatomic Sites to Dosimetric Limitations of Current Planning Systems

anatomic site	photon energy	absorbed dose	attenuation	shielding	scattering	beta/kerma dose
prostate	high					
	low	XXX	XXX	XXX		
breast	high				XXX	
	low	XXX	XXX	XXX		
GYN	high			XXX		
	low	XXX	XXX			
skin	high			XXX	XXX	
	low	XXX		XXX	XXX	
lung	high				XXX	XXX
	low	XXX	XXX		XXX	
penis	high				XXX	←
	low	XXX			XXX	
eye	high			XXX	XXX	XXX
	low	XXX	XXX	XXX	XXX	

Penil brachytherapy

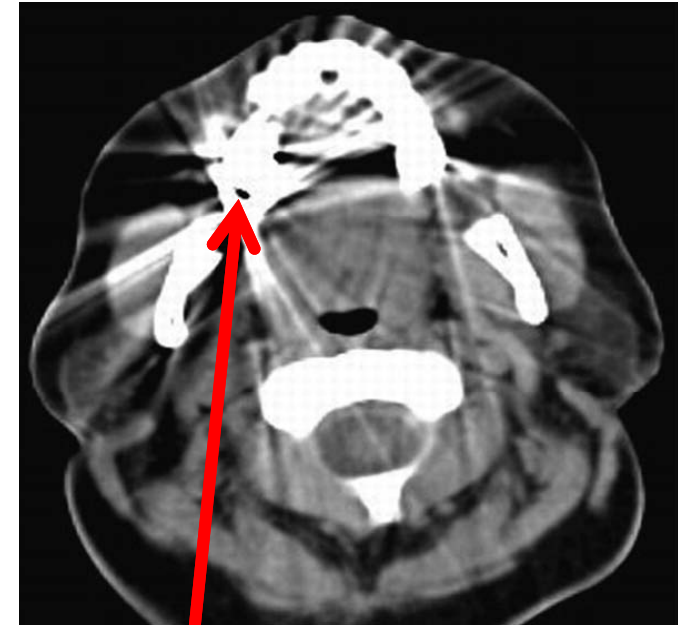
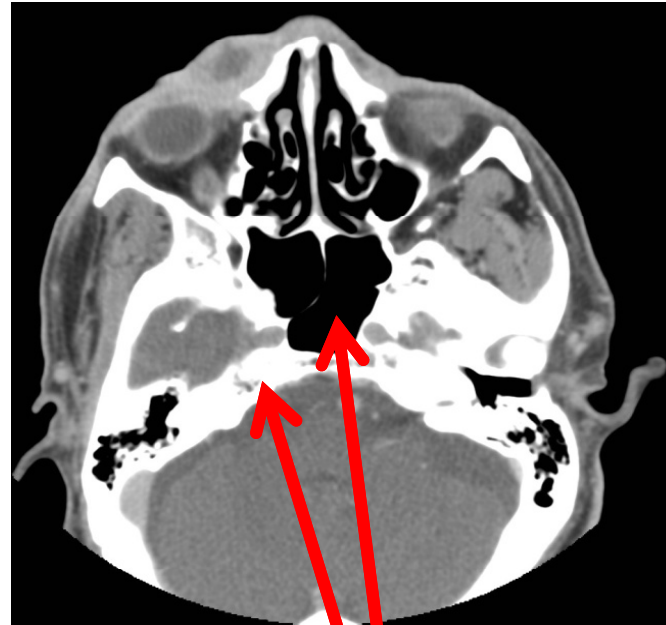
			PTV						Urethra							
	GTV V100 [SD]		V100 [SD]		V150 [SD]		V200 [SD]		D 1cc [SD]		D 0.5 cc [SD]		D 0.1 cc [SD]		Dmax [SD]	
TG43	99.2	[1.7]	74.3	[15.0]	20.7	[2.8]	8.9	[0.9]	6.9	[2.2]	31.6	[14.1]	76.5	[5.3]	88.8	[9.4]
Monte Carlo	97.0	[3.0]	70.0	[14.1]	18.6	[2.3]	8.7	[1.1]	7.2	[3.1]	36.2	[13.8]	68.5	[4.5]	85.0	[9.0]
MC - TG43 dose difference (Gy)	-2.3		-4.3		-2.0		-0.3		0.4		4.6		-8.1		-3.7	
MC - TG43 dose difference (%)	-2.3		-5.8		-9.7		-2.9		5.1		14.6		-10.6		-4.2	

Carlone et al, World Brachy Congress 2016

Head and Neck?

anatomic site	photon energy	absorbed dose	attenuation	shielding	scattering	beta/kerma dose
prostate	high					
	low	XXX	XXX	XXX		
breast	high				XXX	
	low	XXX	XXX	XXX		
GYN	high			XXX		
	low	XXX	XXX			
skin	high			XXX	XXX	
	low	XXX		XXX	XXX	
lung	high				XXX	XXX
	low	XXX	XXX		XXX	
penis	high				XXX	
	low	XXX			XXX	
eye	high			XXX	XXX	XXX
	low	XXX	XXX	XXX	XXX	

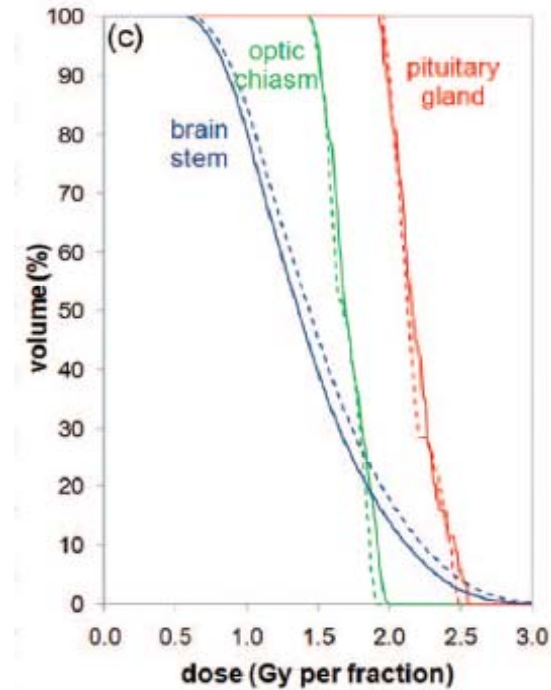
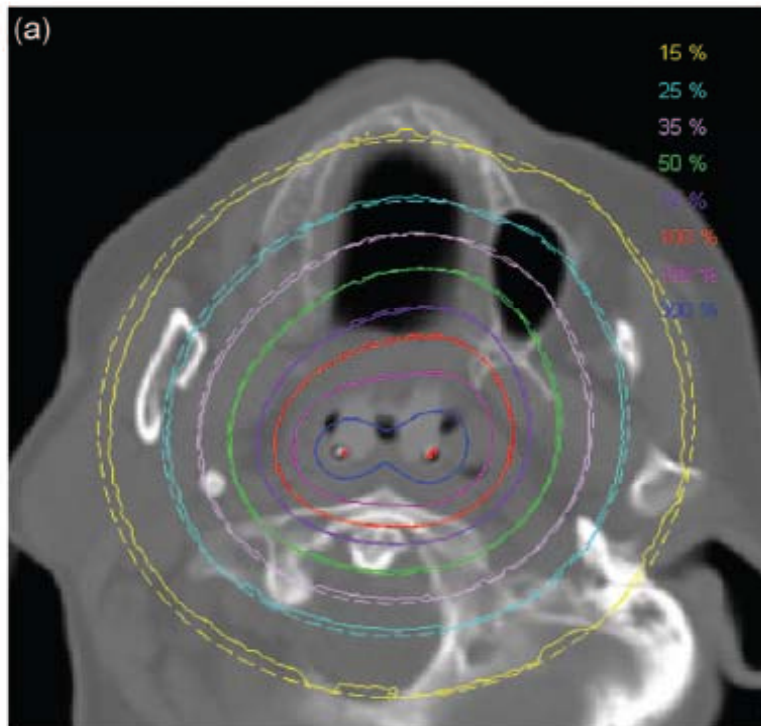
Geometry



- Scatter condition
- Bone and air cavity
- Tooth filling

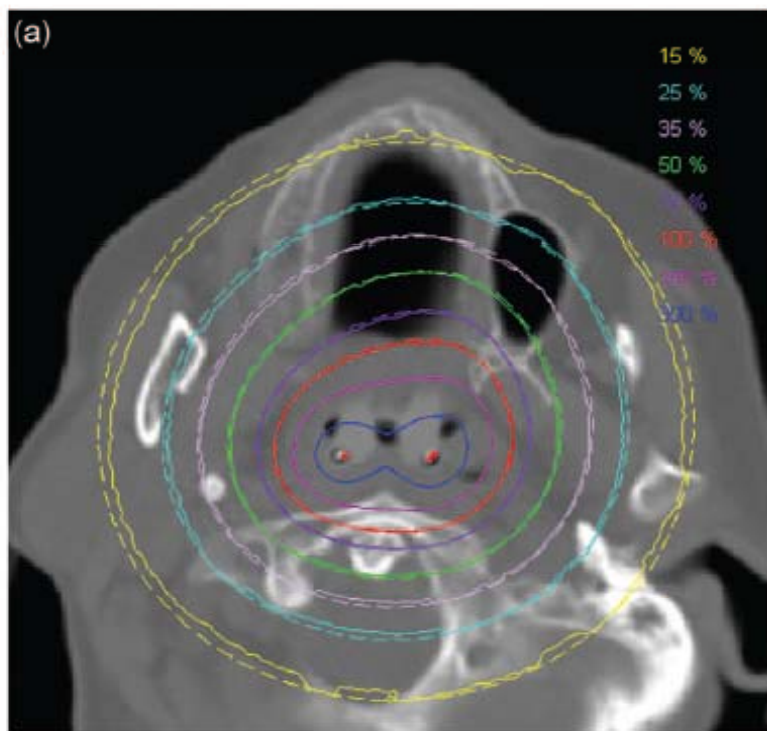
TG43 vs MC

Poon *et al*, Med Phys 36 (2009)



MC = solid lines; TG43= dashed lines

TG43 vs MC



- Target dose unaffected
 - Dominated by primary
- $D_{TG43} > D_{MC}$ brain stem
 - Screening by bones
- $D_{TG43} > D_{MC}$ close to skin

Poon *et al*, Med Phys 36 (2009)

AcurosBV vs TG43

Siebert *et al*, J Contemp Brachytherapy 2013

- 49 consecutive patients, 2001-2009
 - floor of mouth carcinoma
 - larynx carcinoma
 - parotid carcinoma
- 2.5 Gy/Fx
- BV 8.8 and Acuros 1.3.1

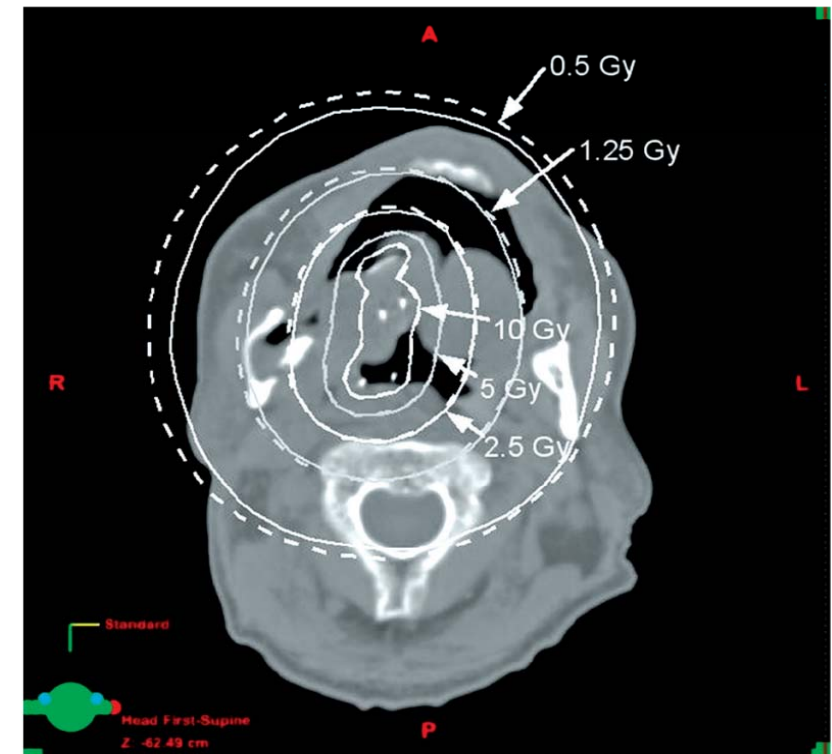


Fig. 1. Transversal CT slice of a patient with mandibular cancer with infiltration of the floor-of-mouth and tongue using a single prescription dose of 2.5 Gy. Dotted isodose lines represent doses of TG-43 formalism, whereas straight lines show isodose lines of computations of the GBBS algorithm

AcurosBV vs TG43

Siebert *et al*, J Contemp Brachytherapy 2013

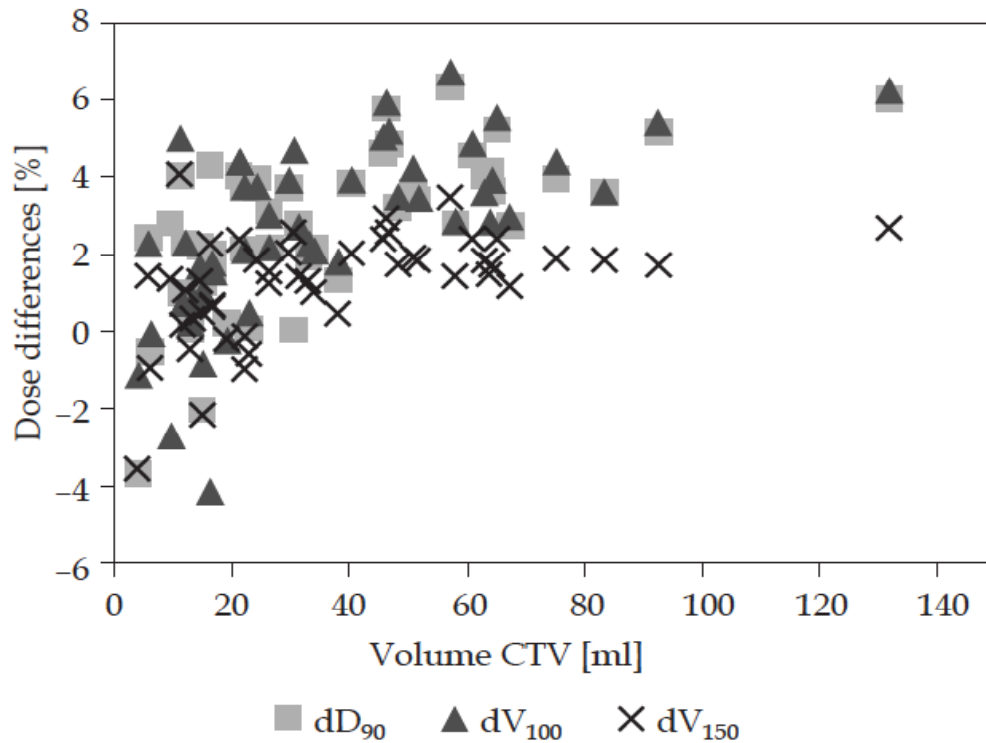
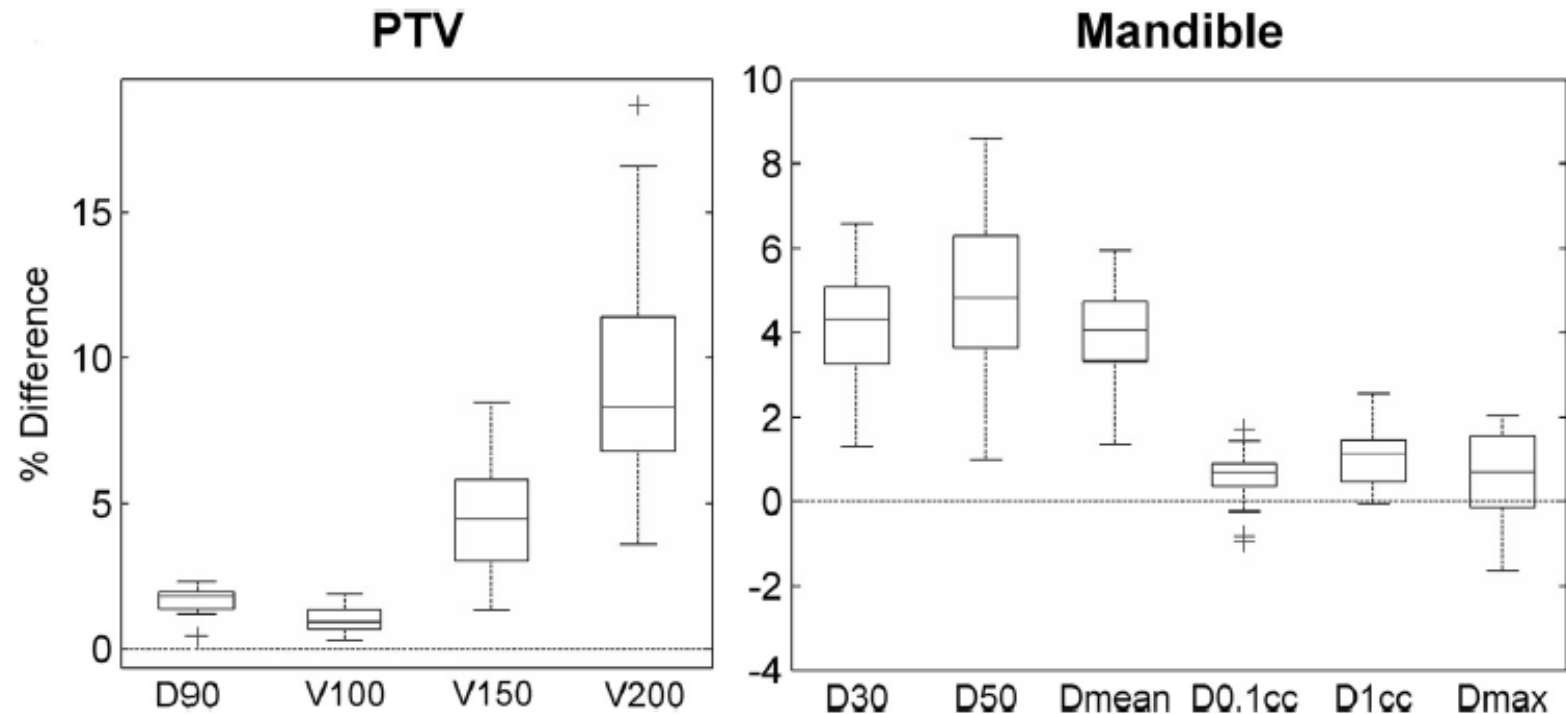
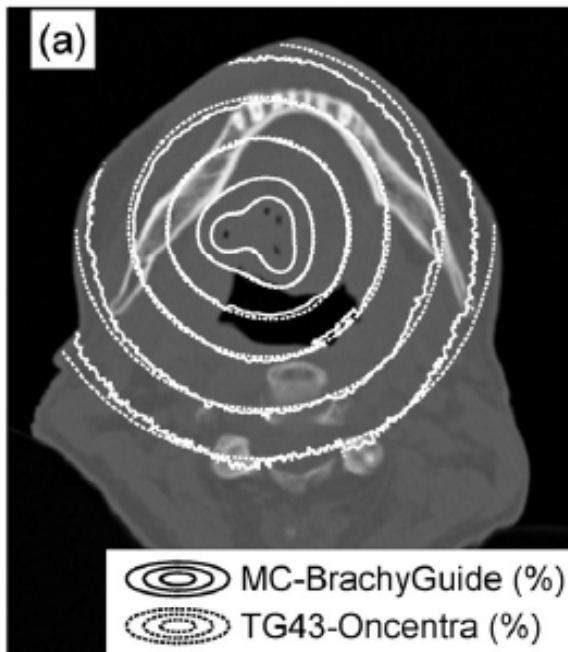


Fig. 2. Dose differences in percent between TG-43 formalism and the GBBS (TG-43 minus GBBS) for D_{90} , V_{100} and V_{150} of the CTV versus volume of the CTV. A positive dose difference means that TG-43 result was larger than the GBBS results

- $D_{TG43} > D_{MC}$ by $\approx 3\%$
 - CTV D_{90} and V_{100}
 - Range -4% to +7%
- Larger volumes lead to larger differences
 - Primary vs scatter contributions to total dose important

MC vs TG43: Study from 22 patients



Summary for H&N Brachytherapy

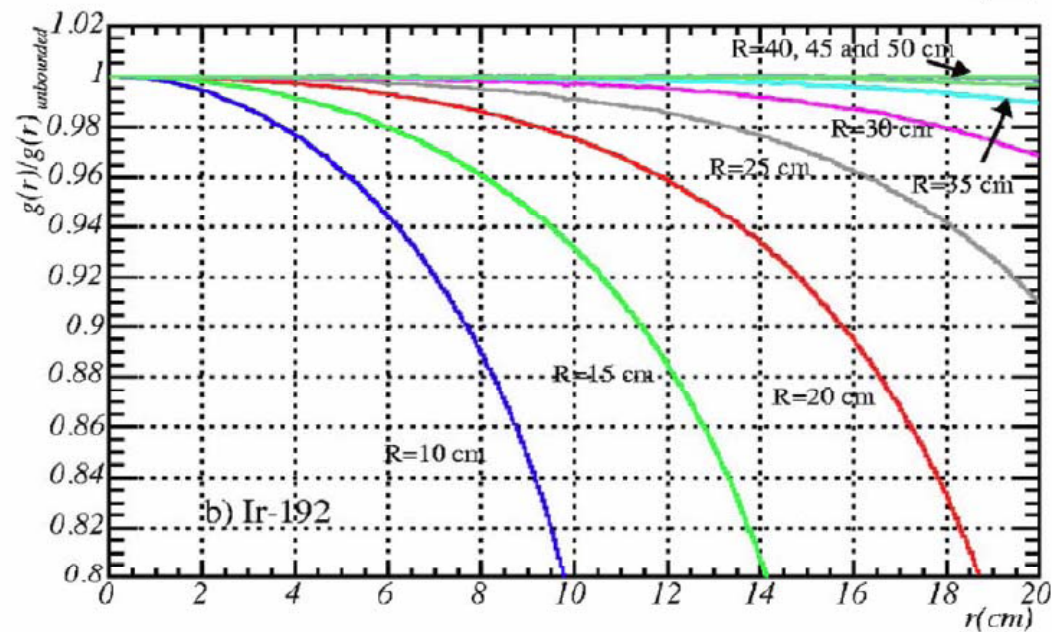
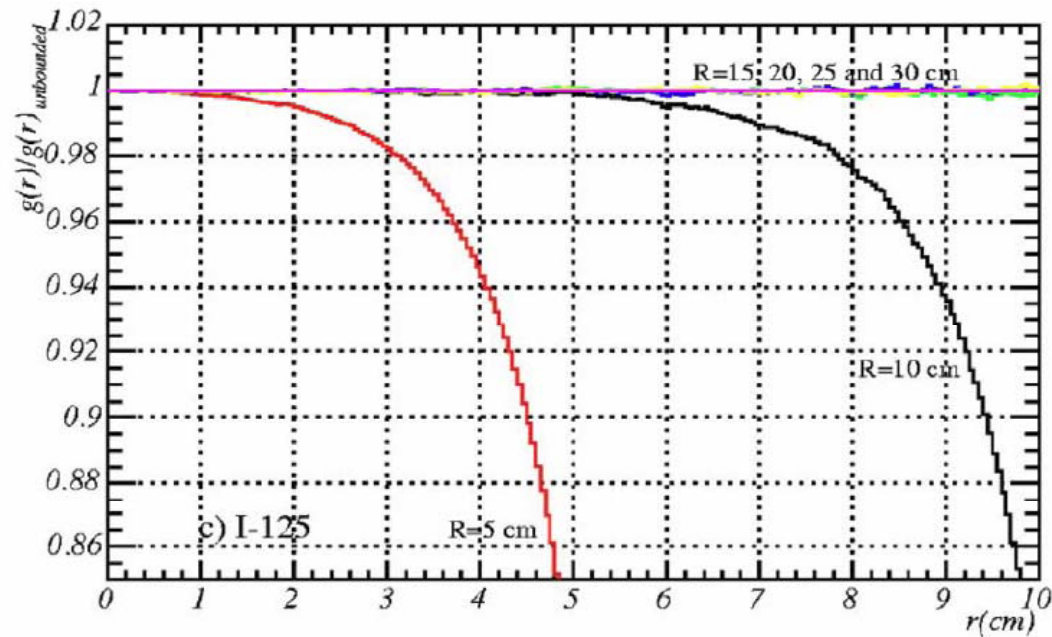
- Differences small on average for CTV/PTV
 - Over and under dosage is patient specific(!)
 - Effects greater at distance from CTV
- OARs
 - Indices statistically different for mandible, parotid, skin, spinal cord.
 - But absolute difference small in most cases.

How Important in the clinic?

Site / Application	Importance
Shielded Applicators	Huge
Eye plaque	-10 to -30% (TG129)
Breast Brachy	-5% to -40%
Prostate Brachy	-2 to -15% on D90
GYN	Depends on applicators
H&N	-4% to +7%

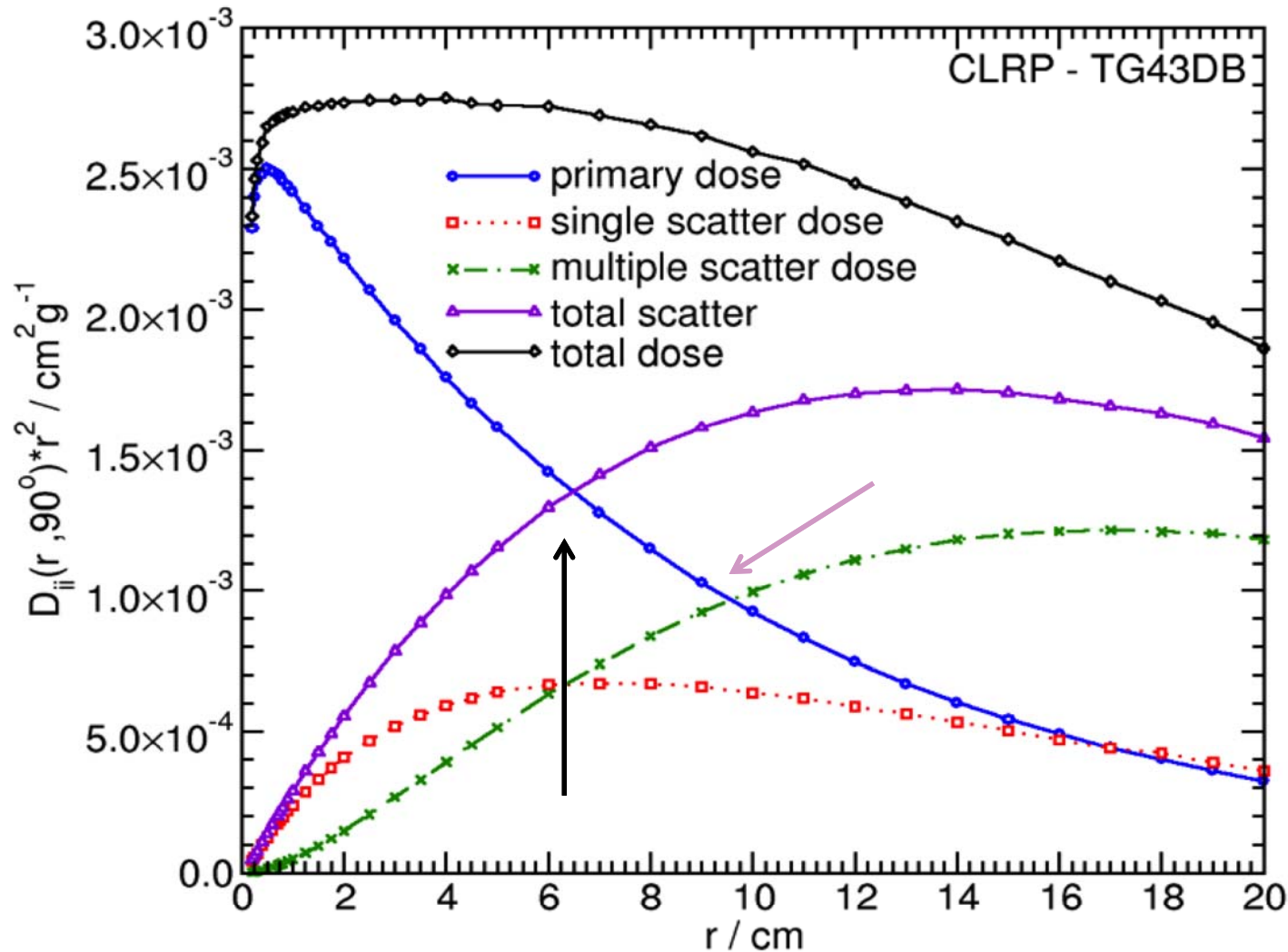
Back to Physics!

Importance of the Physics: Scatter Conditions



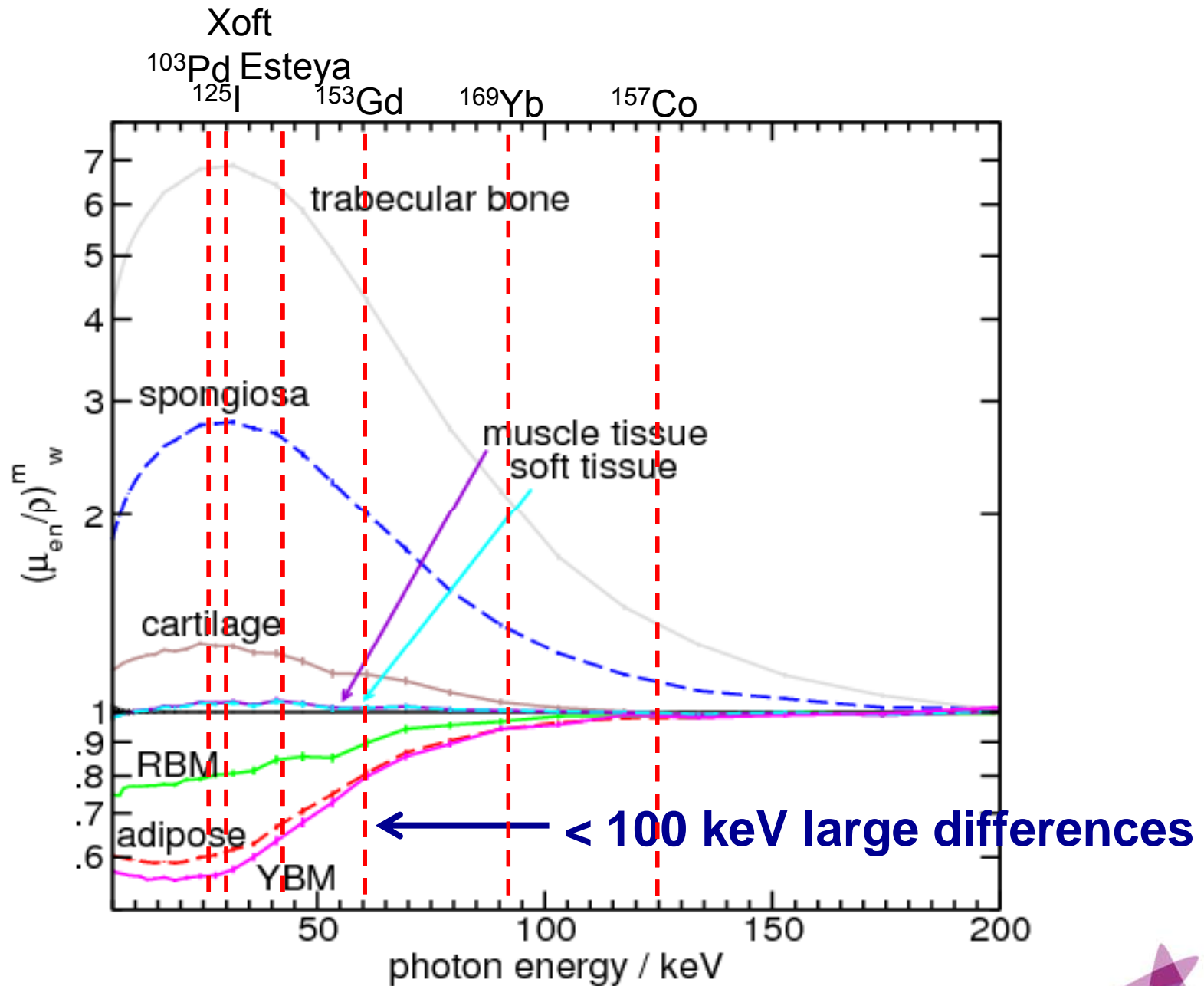
Primary vs. Scatter

Primary dominate total dose for the first 6 cm



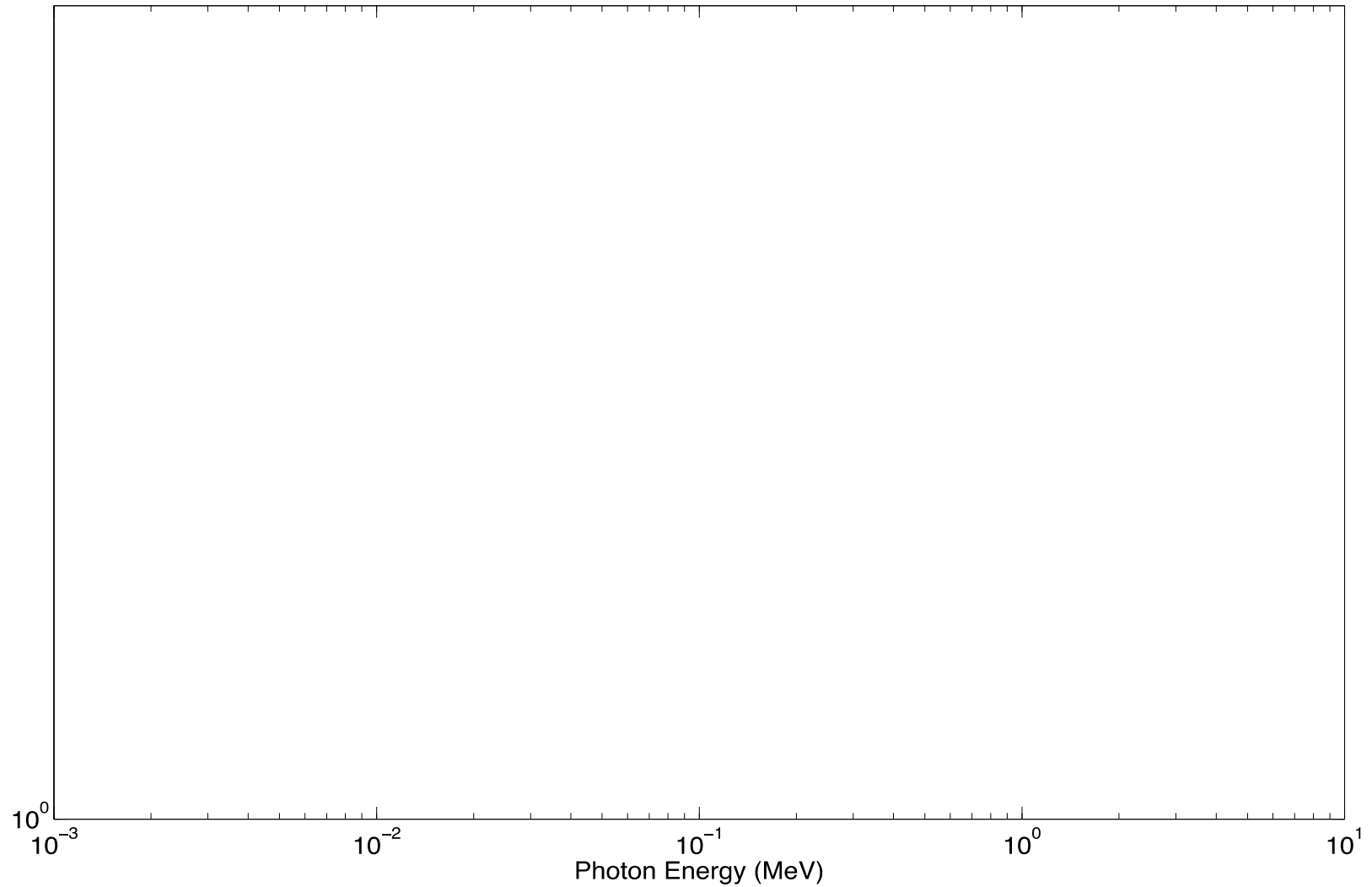
Source: <http://www.physics.carleton.ca/clrp>

Importance of the Physics: Water vs Tissues



TG-186

Importance of the Physics: Attenuation by Metals



From NIST website

Rule of thumb

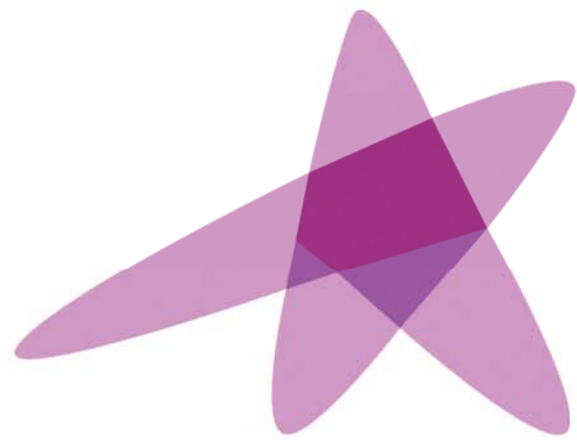
Energy Range	Effect
^{192}Ir	Scatter condition
	Shielding (applicator related)
$^{103}\text{Pd}/^{125}\text{I}/\text{eBx}$	Absorbed dose (μ_{en}/ρ)
	Attenuation (μ/ρ)
	Shielding (applicator, source)

Remember

- TG-43 is still the recommended STD for:
 - Prescription dose levels
 - Dose planning/optimization
- Beyond TG43
 - Follow TG-186 recommendations
 - For tissue assignments
 - For dose reporting
 - **ATTN to physics!**

Conclusion

- TG43 presents limitation for many clinical sites
 - From a few % to many tens of % for shielded geometries
- Algorithms desperately needed for low energy brachytherapy: seeds or eBx
 - Much larger effects expected
- New approaches depend on going beyond TG43
 - Shielded and directional applicators
 - Directional sources
 - eBx and low energy brachytherapy.



ESTRO

School

Advanced Brachytherapy Physics

Vienna, 29 May – 1 June 2016

Dosimetry using the Advanced Collapsed cone Engine (ACE)

P. Papagiannis, PhD
Medical Physics Laboratory
Medical School
National & Kapodistrian University of Athens

(no conflict of interest to disclose)

Dosimetry using the Advanced Collapsed cone Engine (ACE)

Method used since decades in external beam RT
(for a review see: Ahnesjö and Aspradakis 1999 Phys. Med. Biol.
44(11) R99)

Method for brachy outlined in a series of publications:

- ✓ Russell KR & Ahnesjö A 1996 Phys Med Biol 41(6):1007
- ✓ Carlsson AK & Ahnesjö A 2000 Med Phys 27(10):2320
- ✓ Carlsson ÅK & Ahnesjö A 2000 Phys Med Biol 45(2):357–82
- ✓ Carlsson AK & Ahnesjö A. 2003 Med Phys 30(8):2206.
- ✓ Russell KR et al 2005 Med Phys 32(9):2739
- ✓ Carlsson Tedgren A & Ahnesjö A 2008 Med Phys 35(4):1611

and implemented for ^{192}Ir dosimetry in Oncentra Brachy:

- ✓ user manuals
- ✓ white paper by Elekta: ACE Advanced Collapsed cone Engine

Objectives/Outline:

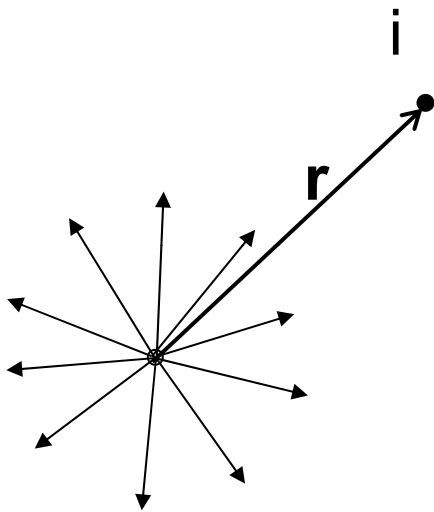
To :

- review the basic principles of the method
 - outline its implementation

so as to identify:

- strengths and weaknesses
- analogies and differences between (current/future) commercially available MBDCAs
 - potential improvements over TG-43
- potential shortcomings relative to reference dose distributions

The method ...



- Let us start again from the simplest case (point isotropic monoenergetic photon source in infinite medium of given composition)
- at any point I know more than D_{prim} :

$$R \rightarrow \Psi_i = \frac{R}{4\pi r_1^2} \exp(-\mu r_1)$$

$$T_i = \left(\frac{\mu}{\rho}\right) \Psi_i$$

$$\text{under CPE : } D_{prim_i} \equiv K_i = \left(\frac{\mu_{en}}{\rho}\right) \Psi_i = \left(\frac{\mu_{en}}{\mu}\right) T_i$$

$$S_i = T_i - K_i = \left(\frac{\mu - \mu_{en}}{\rho}\right) \Psi_i = \left(1 - \frac{\mu_{en}}{\mu}\right) T_i = \left(\frac{\mu}{\mu_{en}} - 1\right) D_{prim_i}$$

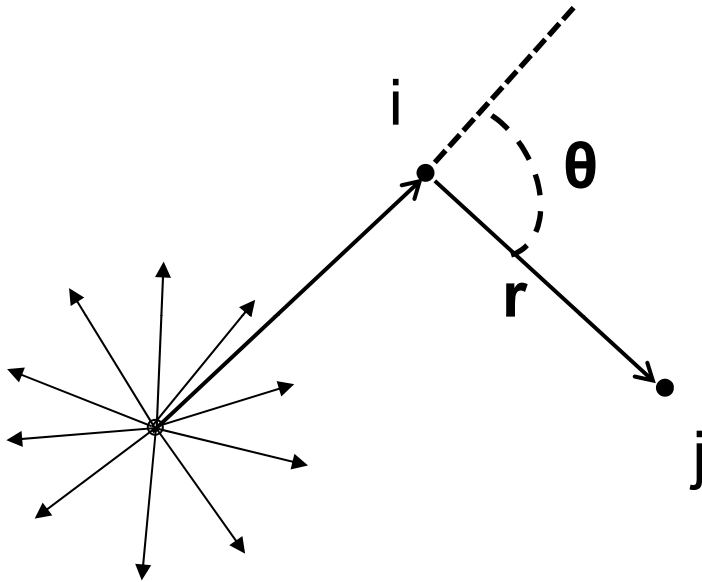
- If I know the spectrum of the source I know the amount of energy per unit mass scattered in first interactions of primary photons, S_{1sc}

The method ...

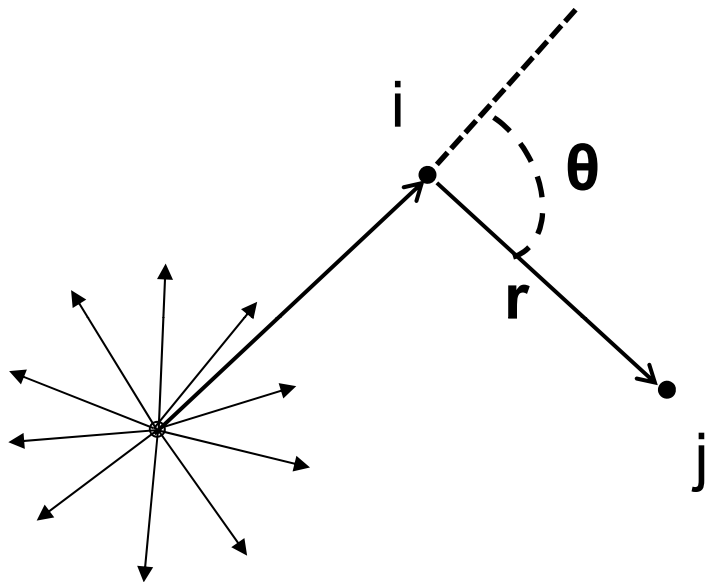
- I know S_{isc} at each point

$$S_{1sc_i} = T_i - K_i = \left(\frac{\mu - \mu_{en}}{\rho}\right)\Psi_i = \left(1 - \frac{\mu_{en}}{\mu}\right)T_i = \left(\frac{\mu}{\mu_{en}} - 1\right)D_{prim_i}$$

- I need a way to distribute this energy to all other points ...



The method ...



- I know S_{1sc} at each point

$$S_{1sc_i} = T_i - K_i = \left(\frac{\mu - \mu_{en}}{\rho}\right)\Psi_i = \left(1 - \frac{\mu_{en}}{\mu}\right)T_i = \left(\frac{\mu}{\mu_{en}} - 1\right)D_{prim_i}$$

- I need a way to distribute this energy to all other points ...

- Suppose $h_{1sc,j} \equiv h_{1sc}(r, \theta) = \frac{\varepsilon(r, \theta)}{R_{1sc} dV}$

is the fraction of 1sc energy released at a point (@ the origin) that is absorbed @ (r, θ) , per unit of volume

- Can I calculate $h_{1sc}(r, \theta)$?

- From 1st principles:

$$h_{1sc}(r, \theta) = \frac{\varepsilon(r, \theta)}{R_{1sc} dV} = \frac{d\sigma(\theta)/d\Omega}{\sigma} \frac{1}{r^2} \exp(-\mu_{1sc, \theta} r) \mu_{en1sc, \theta}$$

- Since I know the spectrum of 1sc photons, I can calculate $h_{1sc}(r, \theta)$

The method ...

- It is more efficient to use MC to calculate $h_{1sc_i}(r, \theta)$ and fit an analytical expression

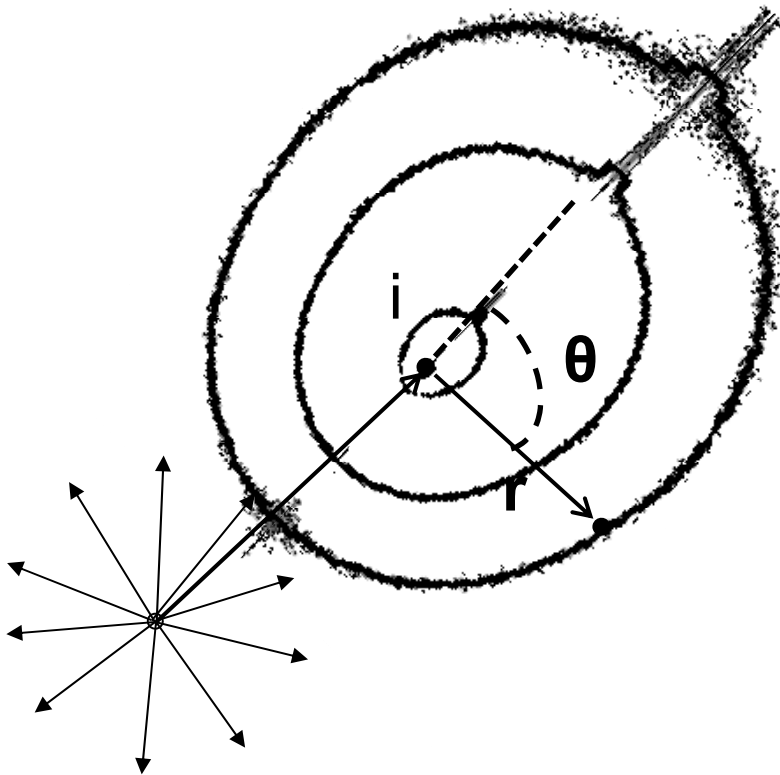
$$\begin{aligned}
 h_{1sc}(r, \theta) &= \frac{\varepsilon(r, \theta)}{\overline{R_{1sc}} dV} = \frac{dR_{1sc}(\theta)}{\overline{R_{1sc}}} \frac{1}{r^2 d\Omega} \exp(-\mu_{1sc, \theta} r) \mu_{en1sc, \theta} = \\
 &= \frac{dR_{1sc}(\theta)}{E(1 - \frac{\mu_{en}}{\mu})} \frac{1}{r^2 d\Omega} \exp(-\mu_{1sc, \theta} r) \mu_{en1sc, \theta} = \\
 &= \frac{B_{\theta} \exp(-b_{\theta} r)}{r^2}
 \end{aligned}$$

where:

$$B_{\theta} = \frac{dR_{1sc}(\theta)}{E(1 - \frac{\mu_{en}}{\mu})} \frac{1}{d\Omega} \mu_{en1sc, \theta}$$

$$b_{\theta} = \mu_{1sc, \theta}$$

- What material should I choose for the calculation of h...?



The method ...is ready!

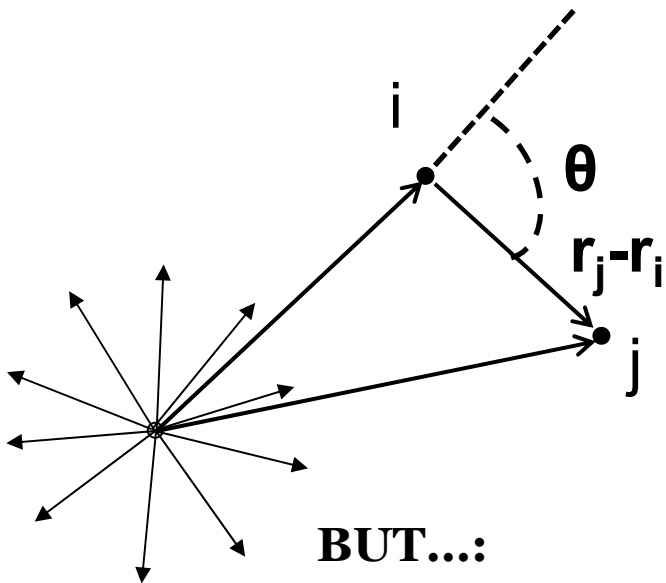
(and it's convolution/superposition)

- I can calculate D_{1sc} @ any point from any point, e.g.:

$$D_{1sc i \rightarrow j} = \frac{1}{\rho_j} R_{1sc, i} h_j = \frac{1}{\rho_j} S_{1sc, i} \rho_i dV h(\vec{r}_j - \vec{r}_i, \theta) = \\ = \frac{\rho_i}{\rho_j} S_{1sc, i} h(\vec{r}_j - \vec{r}_i, \theta) dV$$

and the total dose to j would be:

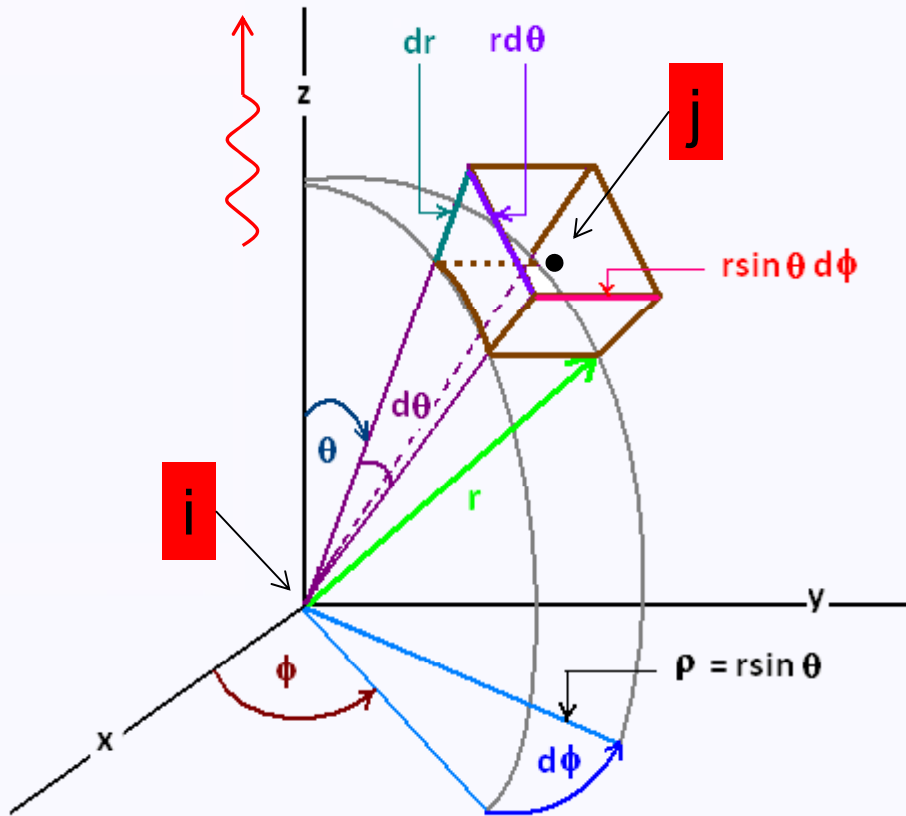
$$D_{1sc j} = \iiint_V \frac{\rho_i}{\rho_j} S_{1sc, i} h_j dV$$



BUT...:

1. I need to be efficient (reduce the # of the N^6 evaluations required) & work with finite voxels
2. I need to account for inhomogeneities
3. I need to account for higher order of scatter (D_{2sc} , D_{3sc} , ..., D_{msc})
4. I need to work with real sources
5. I need to account for finite patient dimensions

1. I need to be efficient



- It is inherently beneficial to work in spherical coordinates to lift the kernel singularity since:
 $dV = dS dr = r^2 d\Omega dr = r^2 \sin\theta d\theta d\phi dr$

$$D_{1sc i \rightarrow j} = \iiint_V \frac{\rho_i}{\rho_j} S_{1sc,i} h_j dV =$$

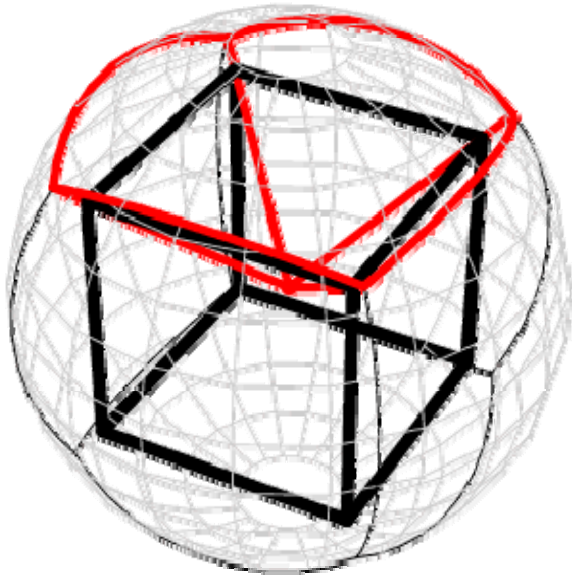
$$\frac{\rho_i}{\rho_j} \int \int \int S_{1sc,i} \frac{B_\theta \exp(-b_\theta r)}{r^2} r^2 \sin\theta d\theta d\phi dr$$

- Instead of evaluating ALL directions around a scerma generating point, I can DISCRETIZE space using a number M of solid angle elements, $\Delta\Omega_M$, defined by $(\theta_o, \phi_o)_M$, and assume scerma does not vary with θ within $\Delta\Omega$ (i.e. on dS for a given r)

$$D_{1sc i \rightarrow j} = \iint_{\Delta\Omega} \int \frac{\rho_i}{r \rho_j} S_{1sc,i} B_\theta \exp(-b_\theta r) d\Omega dr =$$

$$\Delta\Omega \frac{\rho_i}{\rho_j} S_{1sc,i} B_{\theta_0} \int_r \exp(-b_{\theta_0} r) dr$$

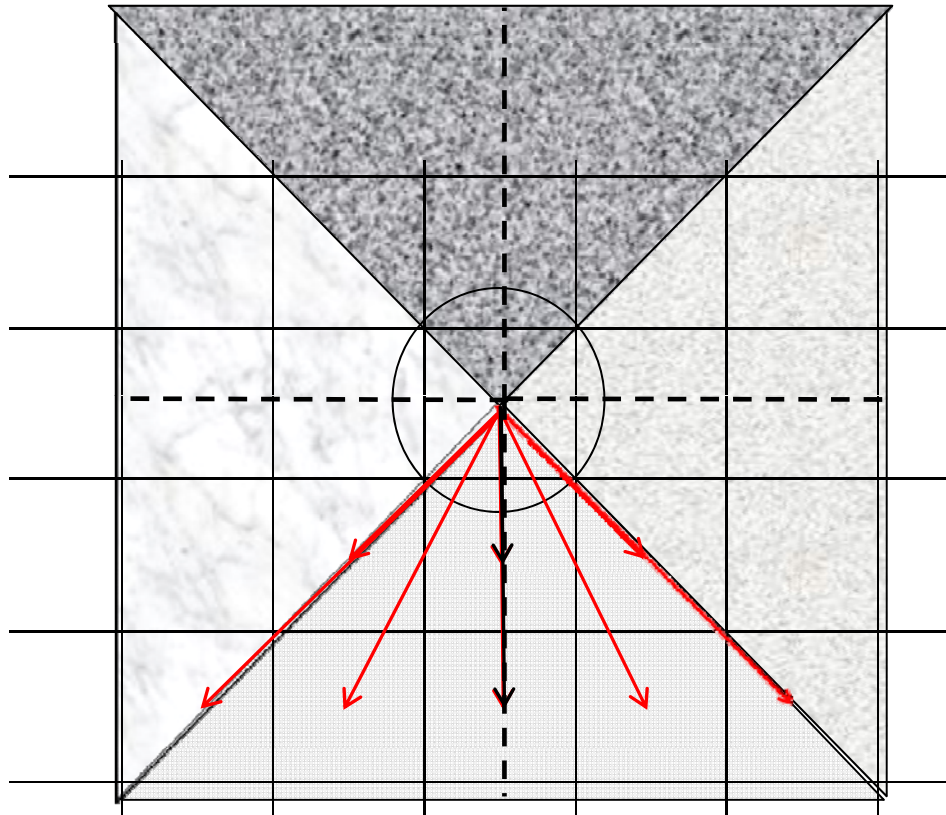
1. I need to be efficient



An oversimplified example:
one solid angle element per cubic voxel side

$$M=6, \Delta\Omega=2\pi/3$$

1. I need to be efficient



Our oversimplified example on a plane (one array of voxels or one image):

scerma does not vary with θ within $\Delta\Omega \rightarrow$ less fitting for B_θ, b_θ

BUT

- I still need to evaluate $D_{i \rightarrow j}$ for all points j at different radial distance

OR

- I could evaluate $D_{i \rightarrow j}$ only for j at exactly θ_o, φ_o

Hence each **cone** defined by $\Delta\Omega$ is **collapsed** to its main axis and scerma from each point is transported along lines defined by the directions from volume discretization in $\Delta\Omega$ (order of evaluations required $\sim MN^4$)

1. I need to be efficient

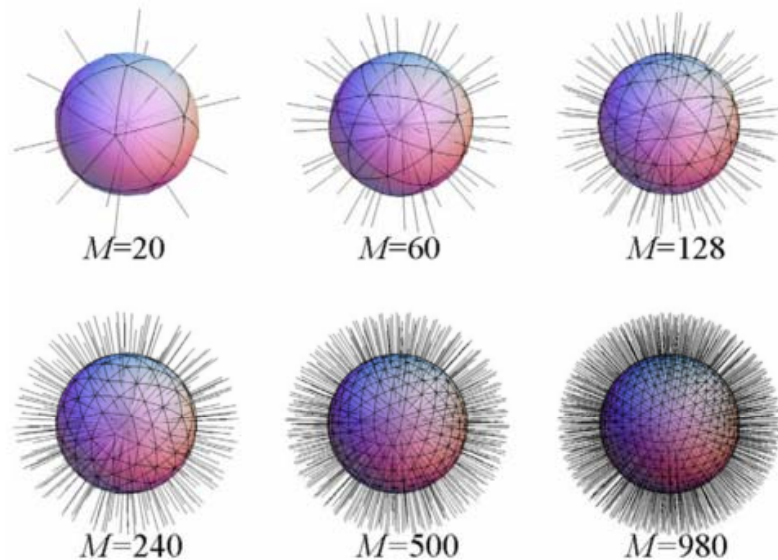


Figure from: Carlsson & Ahnesjö
Med. Phys. 35 (4) 1611 (2008)

Can the CC method be both efficient AND accurate...?

- At the limit of fine discretization ($M \rightarrow N^3$, $\Delta\Omega \rightarrow d\Omega$) the collapsed cone method can be exact (but inefficient)

1. I need to be efficient

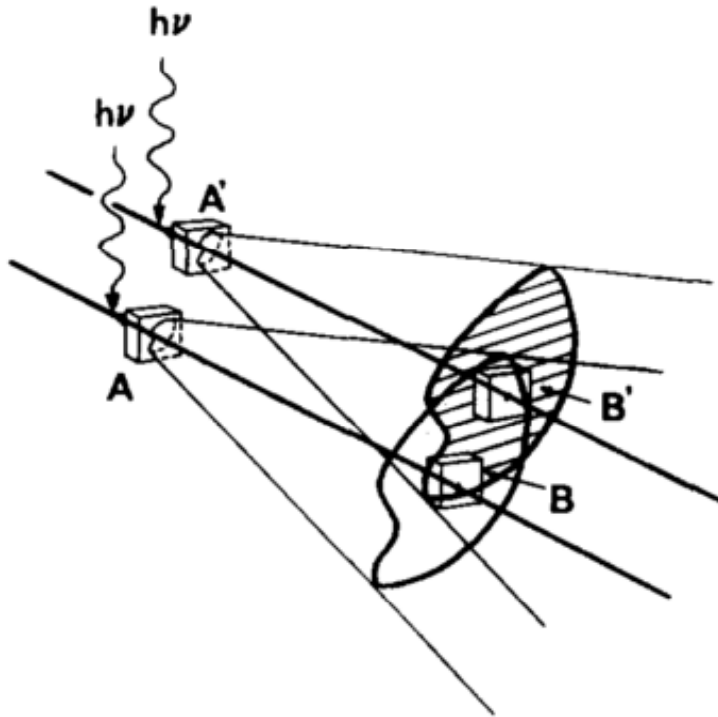
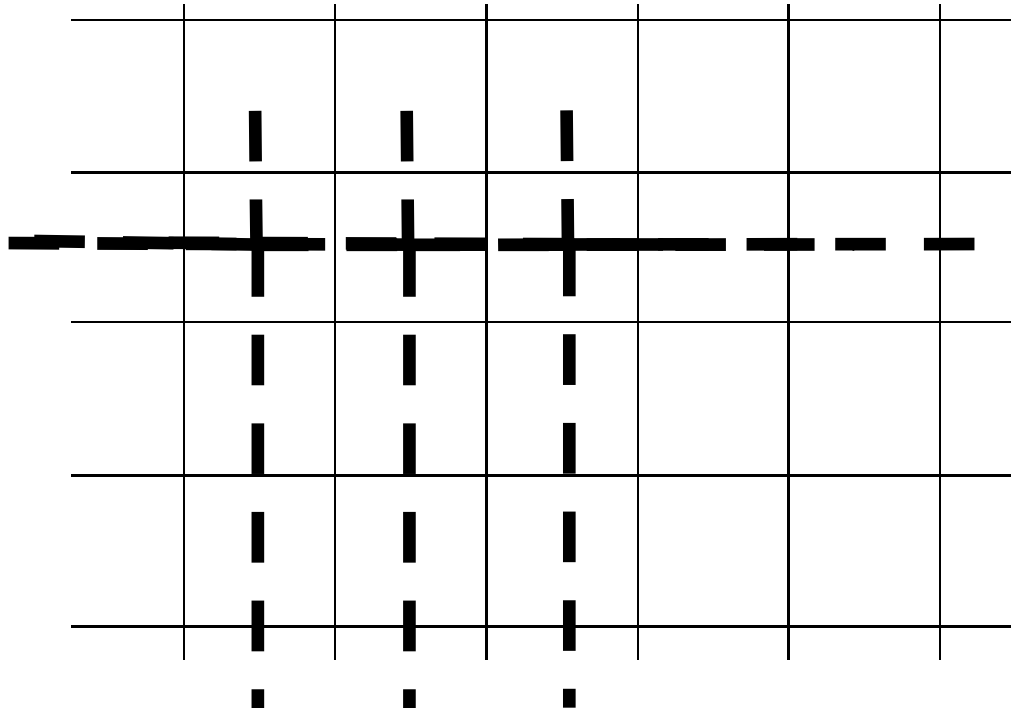


Figure from: Ahnesjö
Med. Phys. 16, 577 (1989)

Can the CC method be both efficient AND accurate...?

- I can reduce the number of directions since scerma from voxel A not distributed to voxel B' due to the CC approximation will be compensated by scerma from another point A' along the same transport direction

1. I need to be efficient

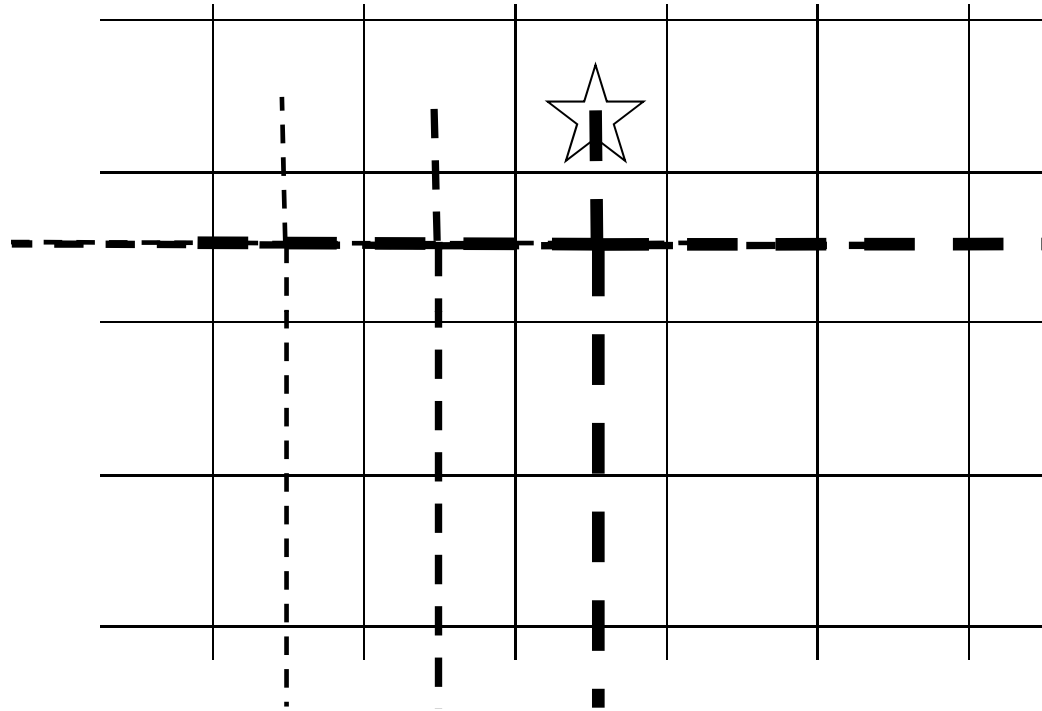


Can the CC method be both efficient AND accurate...?

YES if I optimize the number of directions

- Optimization criterion...?

1. I need to be efficient



Can the CC method be both efficient AND accurate...?

YES if I optimize the number of directions

Optimization criterion...?

- THE SCERMA GRADIENT!!!

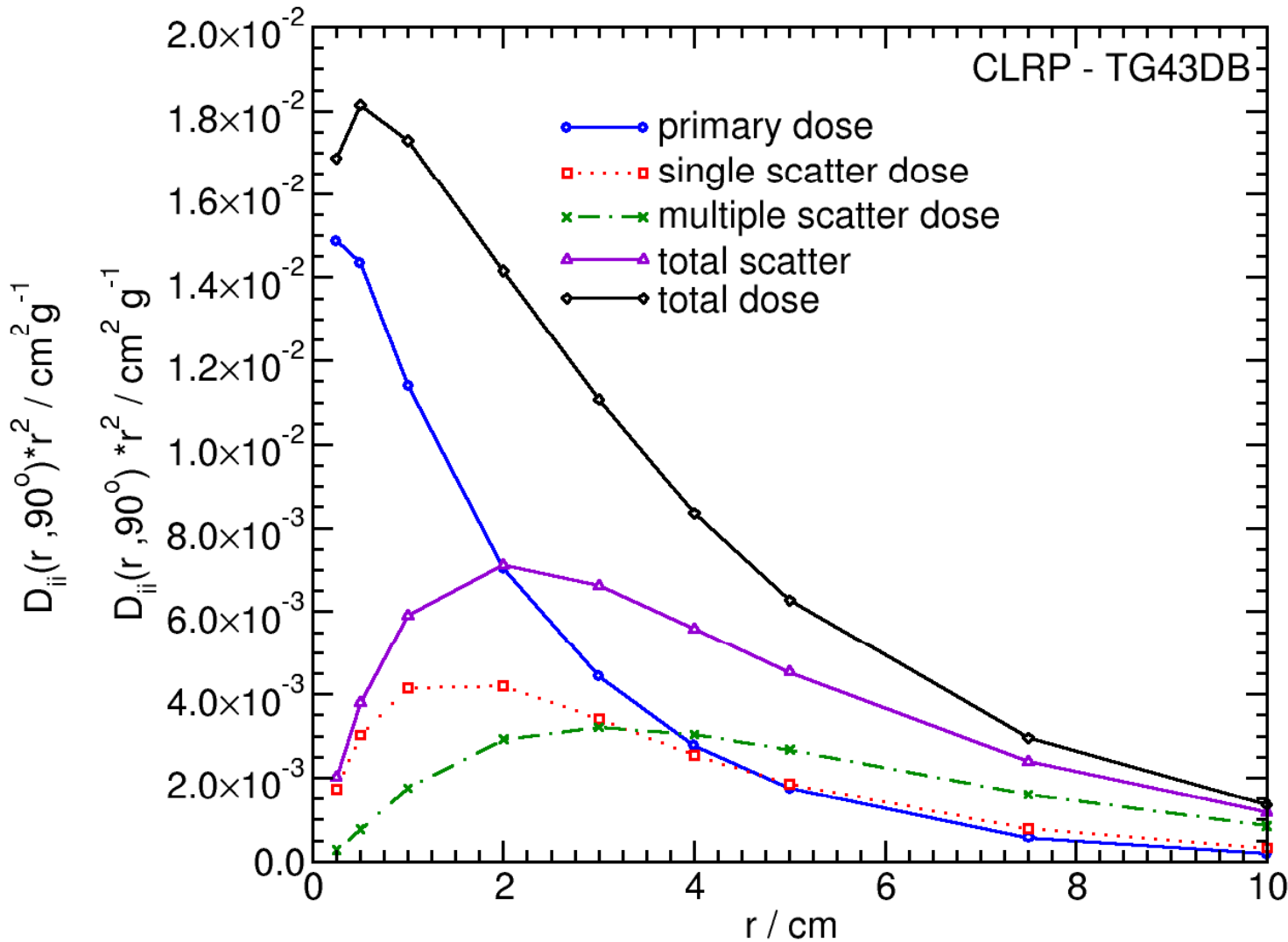
1. I need to be efficient

Can the CC method be both efficient AND accurate...?

The less scerma varies the more I can reduce the number of directions
(increase of efficiency) without a considerable loss of accuracy

Which cases are less/more forgiving...?

1. I need to be efficient



Can the CC method be both efficient AND accurate...?

The less scatter varies the more I can reduce the number of directions (increase of efficiency) without a considerable loss of accuracy

Which cases are less/more forgiving...?

1. I need to be efficient

Can the CC method be both efficient
AND accurate...?

**The less scerma varies the more I
can reduce the number of
directions** (increase of efficiency)
without a considerable loss of
accuracy

The approximation by CC that scerma is
transported linearly will only break
down at increased distances where
 $r^2\Delta\Omega = \Delta S \gg$
unless resolution is coarse
(voxel cross section $\sim \Delta S$)

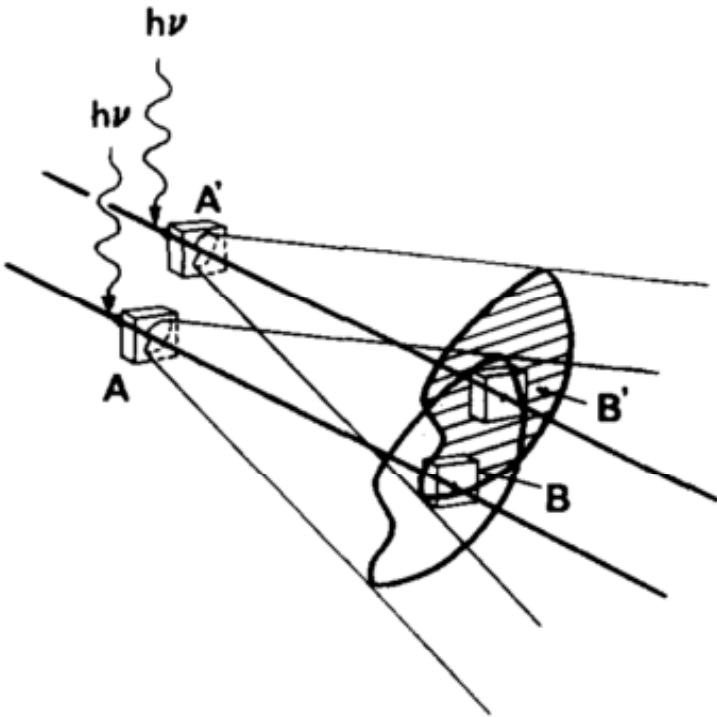
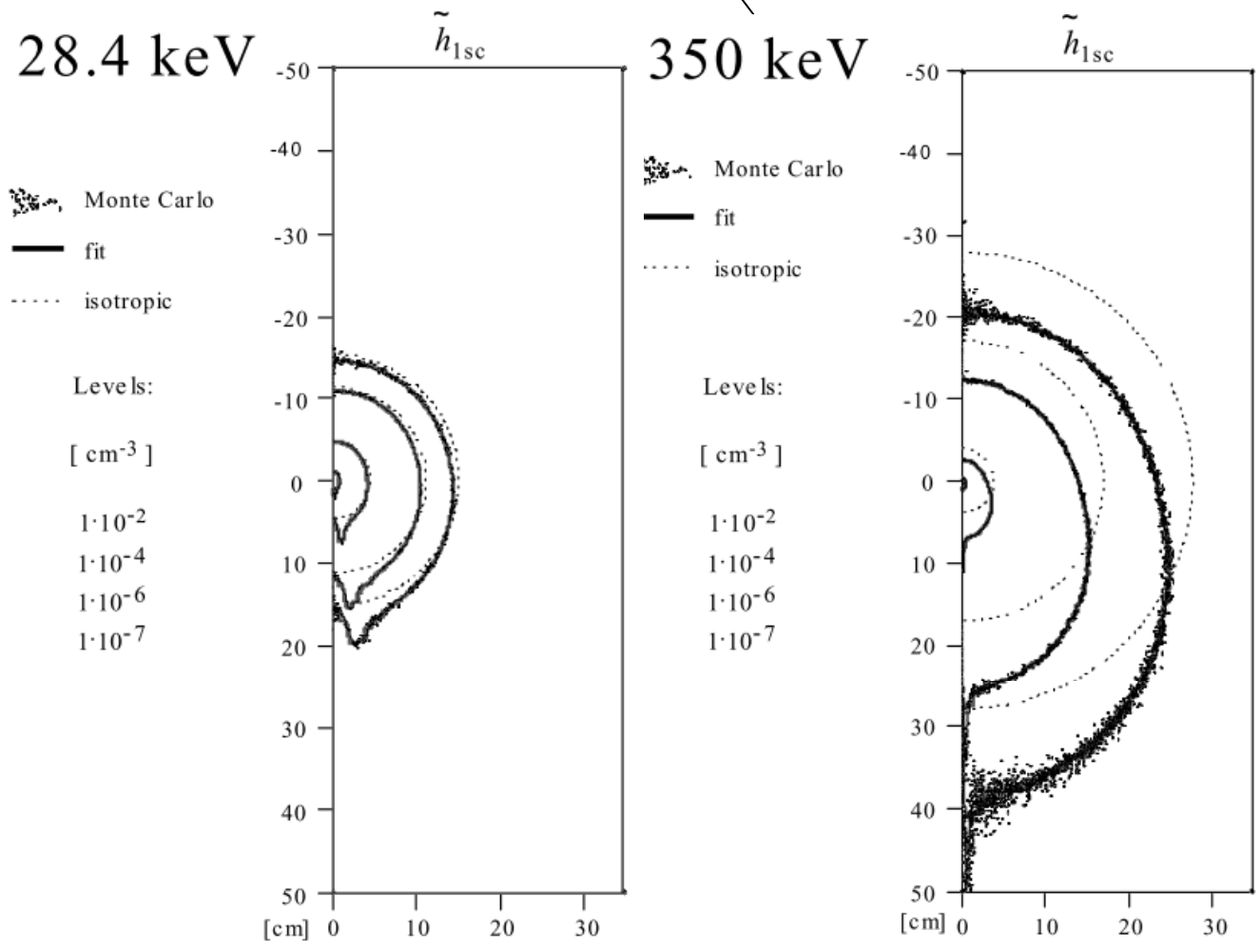


Figure from: Ahnesjö
Med. Phys. 16, 577 (1989)

1. I need to be efficient

Can the CC method be both efficient AND accurate...?



The less scerma varies the more I can reduce the number of directions (increase of efficiency) without a considerable loss of accuracy

The approximation by CC that scerma is transported linearly will only break down (ray artefacts) at increased distances where $r^2\Delta\Omega = \Delta S \gg$
How increased ...?

It depends on how rapidly the kernel decreases with distance.

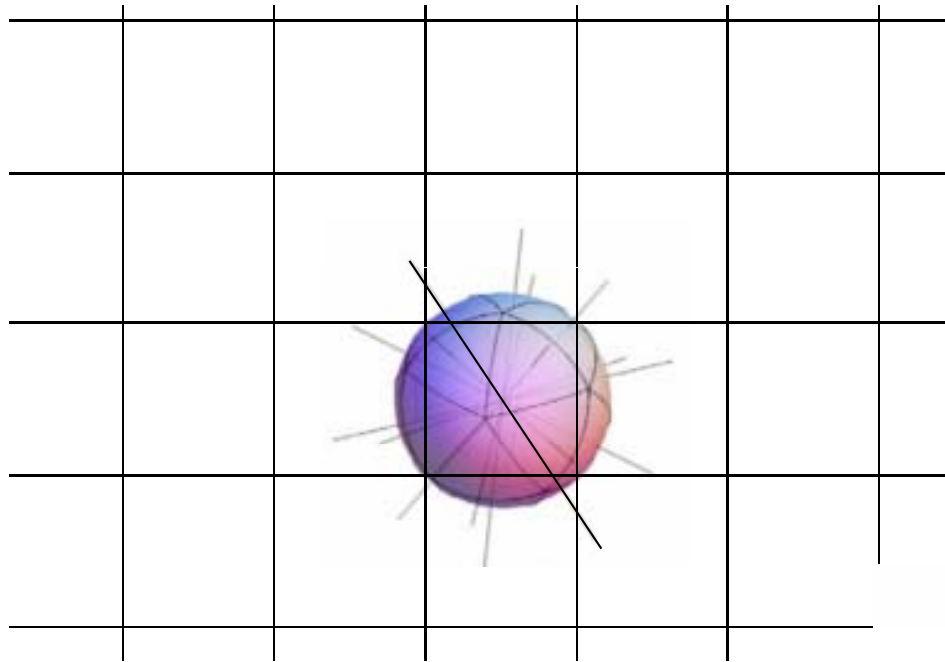
Rapidly decreasing kernels are more forgiving.

1. I need to be efficient

All that is missing then is:

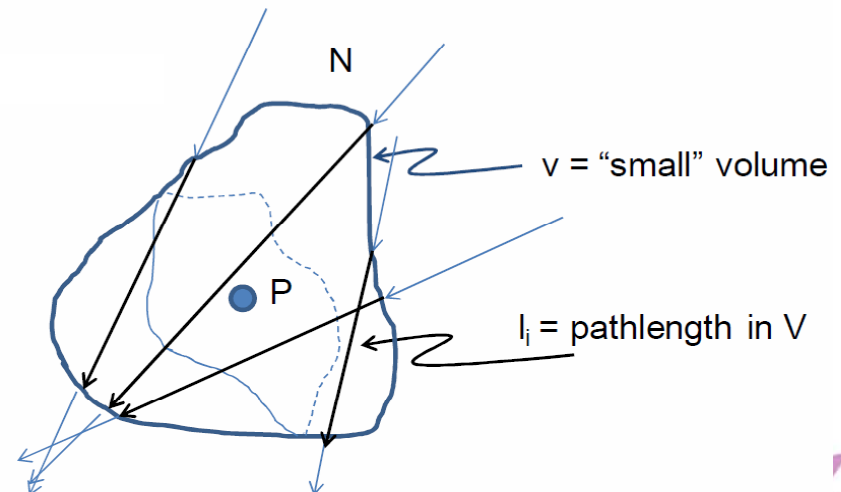
- a method to define a grid of transport lines along the discretization directions
and
- a set of recursive equations to calculate stepwise on each transport line and not from point to point

1. I need to be efficient

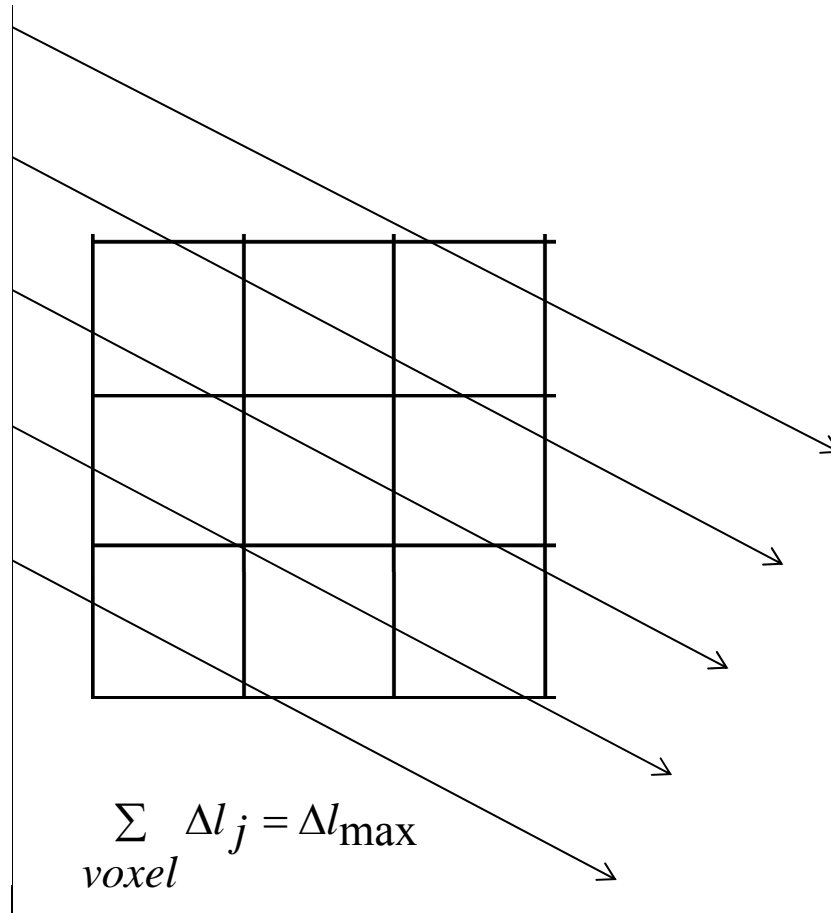


Method to define a grid of transport lines along the discretization directions

$$\Phi = \lim_{\substack{N \rightarrow \infty \\ V \rightarrow 0}} \left\{ \frac{1}{V} \sum_{i=1}^N l_i \right\}$$

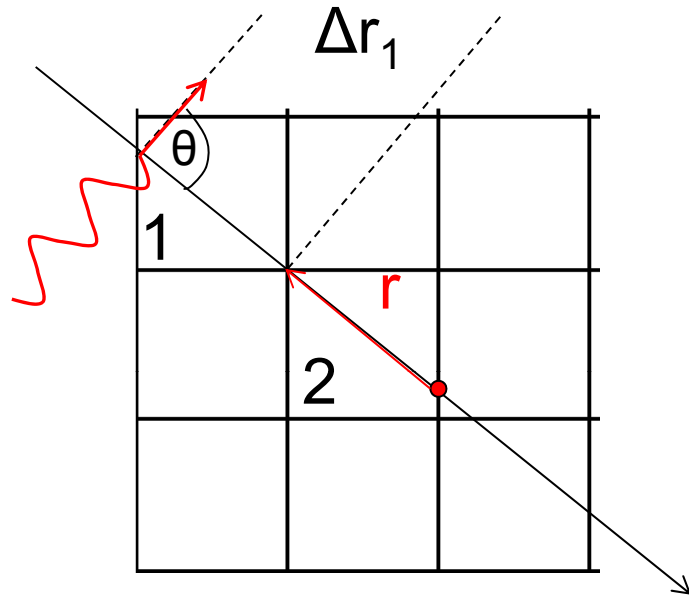


1. I need to be efficient



Method to define a grid of transport lines along the discretization directions

1. I need to be efficient



Dose **from** points along Δr_1 in voxel 1, **to** voxel 2 :

$$D_{1sc1 \rightarrow 2} = \iint_{\Delta\Omega} \int \frac{\rho_1}{r \rho_2} S_{1sc,1} B_\theta \exp(-b_\theta r) d\Omega dr =$$

$$\Delta\Omega \frac{\rho_1}{\rho_2} S_{1sc,1} B_\theta \int_r^{r+\Delta r_1} \exp(-b_\theta r') dr =$$

$$\Delta\Omega \frac{\rho_1}{\rho_2} S_{1sc,1} \frac{B_\theta}{b_\theta} \exp(-b_\theta r) [1 - \exp(-b_\theta \Delta r_1)]$$

Equations for the transport of scerma generated at each point along a transport line

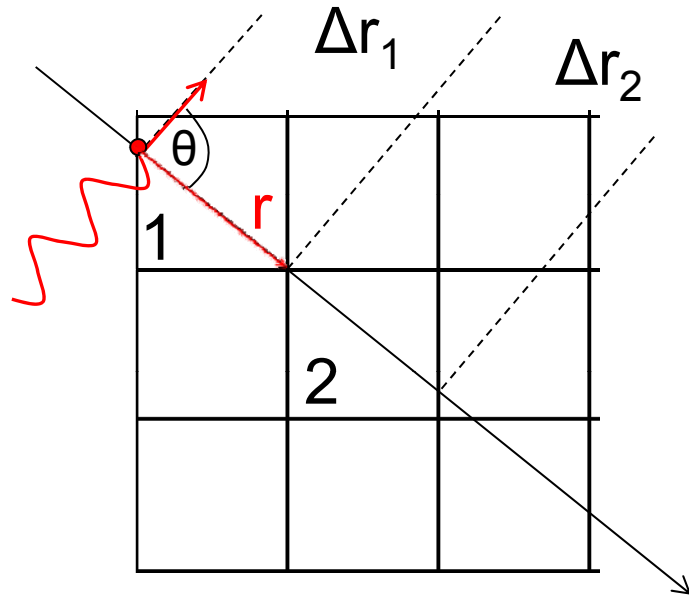
Under the collapsed cone approximation:

- Scerma does not vary with θ within $\Delta\Omega$ (B_θ , b_θ constant along transport line) and scerma generated, emitted and absorbed along transport line

and assuming:

- Scerma generated per unit r is constant within the same voxel (scerma does not vary considerably within voxels)

1. I need to be efficient



Averaging scerma from voxel 1, over points **within Δr2** in voxel 2 :

$$\overline{D_{1sc1 \rightarrow 2}} = \frac{\int_r^{r+\Delta r_2} D_{1sc1 \rightarrow 2} dr'}{\Delta r_2} = \frac{\Delta \Omega \frac{\rho_1}{\rho_2} S_{1sc,1} \frac{B\theta}{b\theta} [1 - \exp(-b\theta \Delta r_1)] \int_r^{r+\Delta r_2} \exp(-b\theta r') dr'}{\Delta r_2} =$$

$$\Delta \Omega \frac{\rho_1}{\rho_2} S_{1sc,1} \frac{B\theta}{b\theta^2 \Delta r_2} \exp(-b\theta r) [1 - \exp(-b\theta \Delta r_1)] [1 - \exp(-b\theta \Delta r_2)]$$

Equations for the transport of scerma generated at each point along a transport line

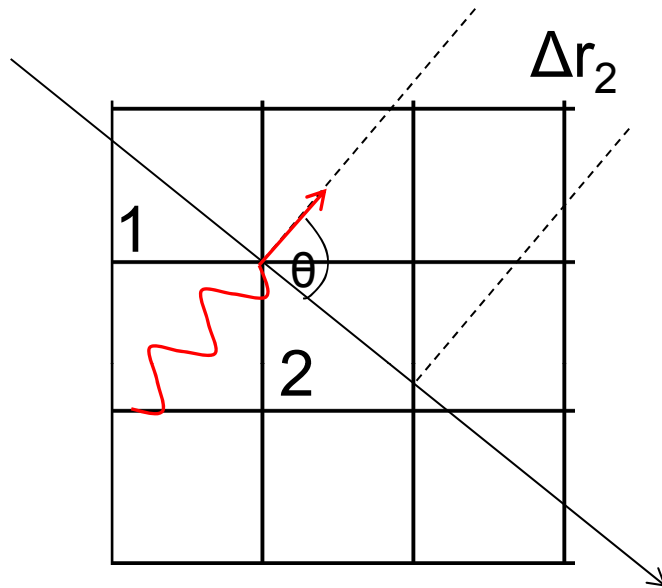
Under the collapsed cone approximation:

- Scerma does not vary with θ within $\Delta\Omega$ ($B\theta$, $b\theta$ constant along transport line) and scerma generated, emitted and absorbed along transport line

and assuming:

- Scerma generated per unit r is constant within the same voxel (scerma does not vary considerably within voxels)

1. I need to be efficient



Scerma **from** points along Δr_2 in voxel 2, **to** voxel 2:

$$D_{1sc2 \rightarrow 2} = \iint_{\Delta\Omega} \int_0^r \frac{\rho^2}{r \rho^2} S_{1sc,2} B\theta \exp[-b\theta(r-r')] d\Omega dr' =$$

$$\Delta\Omega S_{1sc,2} B\theta \int_0^r \exp[-b\theta(r-r')] dr' =$$

$$\Delta\Omega S_{1sc,2} \frac{B\theta}{b\theta} [1 - \exp(-b\theta r)]$$

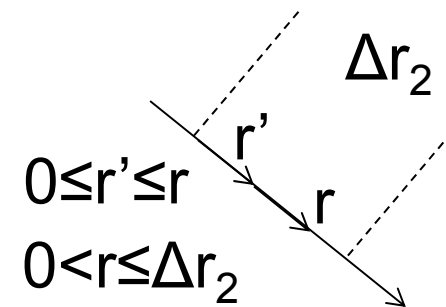
Equations for the transport of scerma generated at each point along a transport line

Under the collapsed cone approximation:

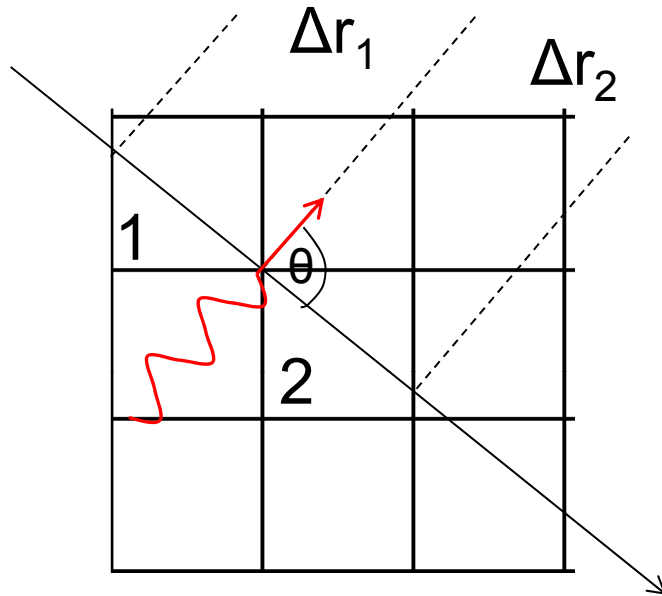
- Scerma does not vary with θ within $\Delta\Omega$ ($B\theta$, $b\theta$ constant along transport line) and scerma generated, emitted and absorbed along transport line

and assuming:

- Scerma generated per unit r is constant within the same voxel (scerma does not vary considerably within voxels)



1. I need to be efficient



Averaging scerma from voxel 2, over points **within Δr2** in voxel 2 :

$$\overline{D_{1sc2 \rightarrow 2}} = \frac{\int_0^{\Delta r_2} D_{1sc2 \rightarrow 2} dr}{\Delta r_2} = \frac{\Delta \Omega S_{1sc,2} \frac{B\theta}{b\theta} \int_0^{\Delta r_2} [1 - \exp(-b\theta r)] dr}{\Delta r_2} =$$

$$\Delta \Omega S_{1sc,2} \frac{B\theta}{b\theta^2} \frac{\{b\theta \Delta r_2 - [1 - \exp(-b\theta \Delta r_2)]\}}{\Delta r_2}$$

Equations for the transport of scerma generated at each point along a transport line

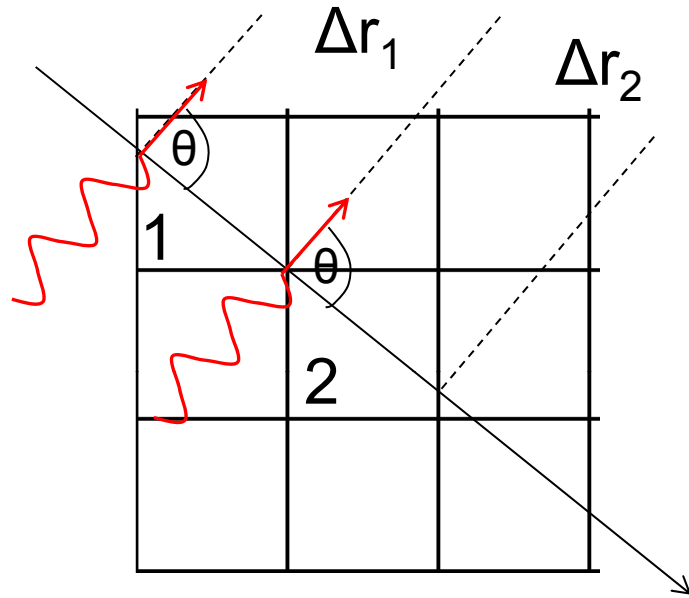
Under the collapsed cone approximation:

- Scerma does not vary with θ within $\Delta\Omega$ ($B\theta$, $b\theta$ constant along transport line) and scerma generated, emitted and absorbed along transport line

and assuming:

- Scerma generated per unit r is constant within the same voxel (scerma does not vary considerably within voxels)

1. I need to be efficient



Overall, exiting voxel 2:

$$\overline{D_{1sc2}} = \overline{D_{1sc1 \rightarrow 2}} + \overline{D_{1sc2 \rightarrow 2}} =$$

$$\Delta\Omega \rho_1 S_{1sc,1} \frac{B\theta}{b\theta^2} [1 - \exp(-b\theta \Delta r_1)] \exp(-b\theta r) \frac{1}{\rho_2 \Delta r_2} [1 - \exp(-b\theta \Delta r_2)] + \Delta\Omega S_{1sc,2} \frac{B\theta}{b\theta^2} \frac{\{b\theta \Delta r_2 - [1 - \exp(-b\theta \Delta r_2)]\}}{\Delta r_2}$$

Equations for the transport of scerma generated at each point along a transport line

Under the collapsed cone approximation:

- Scerma does not vary with θ within $\Delta\Omega$ ($B\theta$, $b\theta$ constant along transport line) and scerma generated, emitted and absorbed along transport line

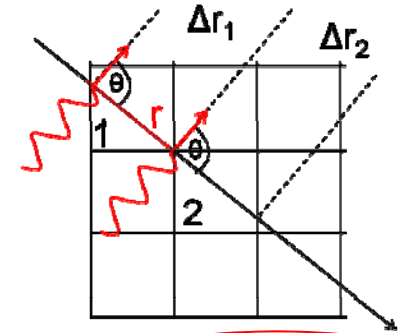
and assuming:

- Scerma generated per unit r is constant within the same voxel (scerma does not vary considerably within voxels)

1. I need to be efficient

Equation for the transport of scerma generated at each point along a transport line

$$\overline{D_{1sc1}} = \overline{D_{1sc0 \rightarrow 1}} + \overline{D_{1sc1 \rightarrow 1}} = 0 + S_{1sc,1} \frac{B\theta}{b\theta^2} \Delta\Omega \frac{\{b\theta\Delta r_1 - [1 - \exp(-b\theta \Delta r_1)]\}}{\Delta r_1}$$



$$\overline{D_{1sc2}} = \overline{D_{1sc1 \rightarrow 2}} + \overline{D_{1sc2 \rightarrow 2}} = \rho_1 S_{1sc,1} \frac{B\theta}{b\theta^2} \Delta\Omega [1 - \exp(-b\theta \Delta r_1)] \exp(-b\theta \Delta r_1) \frac{[1 - \exp(-b\theta \Delta r_2)]}{\rho_2 \Delta r_2} + \Delta\Omega S_{1sc,2} \frac{B\theta}{b\theta^2} \frac{\{b\theta\Delta r_2 - [1 - \exp(-b\theta \Delta r_2)]\}}{\Delta r_2}$$

$$\overline{D_{1sc3}} = \overline{D_{1sc1 \rightarrow 3}} + \overline{D_{1sc2 \rightarrow 3}} + \overline{D_{1sc3 \rightarrow 3}} = \dots$$

$$\overline{D_{1sc_i}} = \sum_i \overline{D_{1sc_{i-1} \rightarrow i}} + \overline{D_{1sc_i \rightarrow i}} = \sum_1^{i-1} \{\rho_{i-1} S_{1sc,i-1} \frac{B\theta}{b\theta^2} \Delta\Omega [1 - \exp(-b\theta \Delta r_{i-1})]\} \exp(-\sum_1^{i-1} b\theta \Delta r_i) \frac{[1 - \exp(-b\theta \Delta r_i)]}{\rho_i \Delta r_i} + \Delta\Omega S_{1sc,i} \frac{B\theta}{b\theta^2} \frac{\{b\theta\Delta r_i - [1 - \exp(-b\theta \Delta r_i)]\}}{\Delta r_i}$$

1. I need to be efficient

An efficient algorithm for the calculation of dose from 1st scatter:

- Calculate S_{1sc} distr., from D_{prim} distr.
 - Choose $\Delta\Omega$: optimal number of directions
- Construct lattice of transport lines (B_θ , b_θ per $\Delta\Omega$, relative to direction of primaries)
- Ray-trace along each transport line for Δr_i and iteratively calculate D_i
 - Sum D_i from all transport lines

Input:

- D_{prim} distr.
- Source primary spectrum for calculating S_{1sc}
 - 1st scatter kernel
 - Individual voxel density data

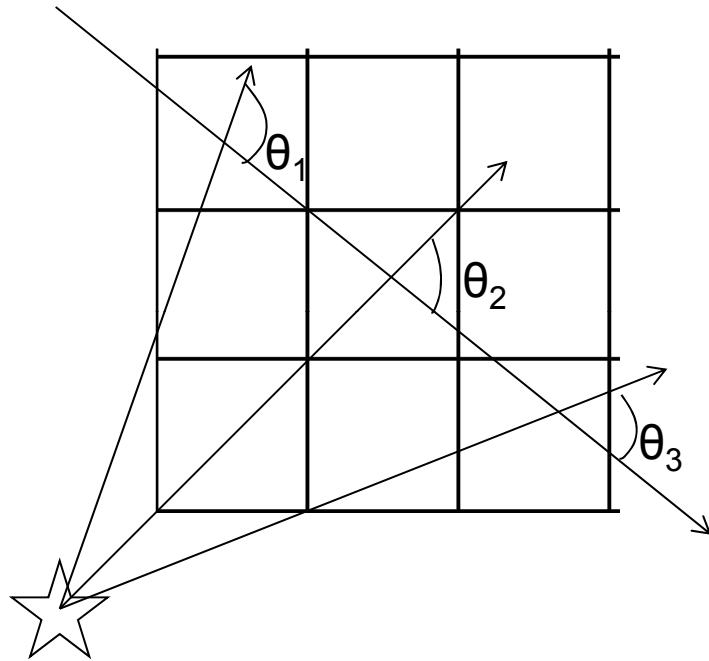
Assumptions:

CC:

- S_{1sc} does not vary with θ within $\Delta\Omega$ (B_θ , b_θ constant along transport line)
- S_{1sc} generated, emitted and absorbed along transport line and:
 - S_{1sc} generated per unit r is constant within the same voxel (scatter does not vary considerably within voxels)

$$\overline{D_{1sc i}} = \sum_i \overline{D_{1sc i-1 \rightarrow i}} + \overline{D_{1sc i \rightarrow i}} = \sum_1^{i-1} \{ \rho_{i-1} S_{1sc, i-1} \frac{B_\theta}{b_\theta^2} \Delta\Omega [1 - \exp(-b_\theta \Delta r_{i-1})] \} \exp(-\sum_1^{i-1} b_\theta \Delta r_i) \frac{[1 - \exp(-b_\theta \Delta r_i)]}{\rho_i \Delta r_i} + \Delta\Omega S_{1sc, i} \frac{B_\theta}{b_\theta^2} \frac{\{ b_\theta \Delta r_i - [1 - \exp(-b_\theta \Delta r_i)] \}}{\Delta r_i}$$

1. I need to be efficient



Implementation corrections:

- S_{isc} does not vary with θ within $\Delta\Omega$ ($B\theta$, $b\theta$ constant along transport line)
 - $b\theta$ evaluated recursively as a moving average of previous and current step
- S_{isc} generated per unit r is constant within the same voxel (scerma does not vary considerably within voxels)
 - in high scerma gradient regions scerma is estimated piecewise from a log-linear interpolation over r

2. inhomogeneities

$$D_{1scj} = \iiint_V \frac{\rho_i}{\rho_j} S_{1sc,i} h_j dV$$

$$\begin{aligned} h_{1sc}(r, \theta) &= \frac{\varepsilon(r, \theta)}{\bar{R}_{1sc} dV} = \frac{dR_{1sc}(\theta)}{\bar{R}_{1sc}} \frac{1}{r^2 d\Omega} \exp(-\mu_{1sc, \theta} r) \mu_{en1sc, \theta} \\ &= \frac{dR_{1sc}(\theta)}{E(1 - \frac{\mu_{en}}{\mu})} \frac{1}{r^2 d\Omega} \exp(-\mu_{1sc, \theta} r) \mu_{en1sc, \theta} \\ &= \frac{B_{\theta} \exp(-b_{\theta} r)}{r^2} \end{aligned}$$

$$B_{\theta} = \frac{dR_{1sc}(\theta)}{E(1 - \frac{\mu_{en}}{\mu})} \frac{1}{d\Omega} \mu_{en1sc, \theta}$$

$$b_{\theta} = \mu_{1sc, \theta}$$

Medium can be of varying density
What changes...?

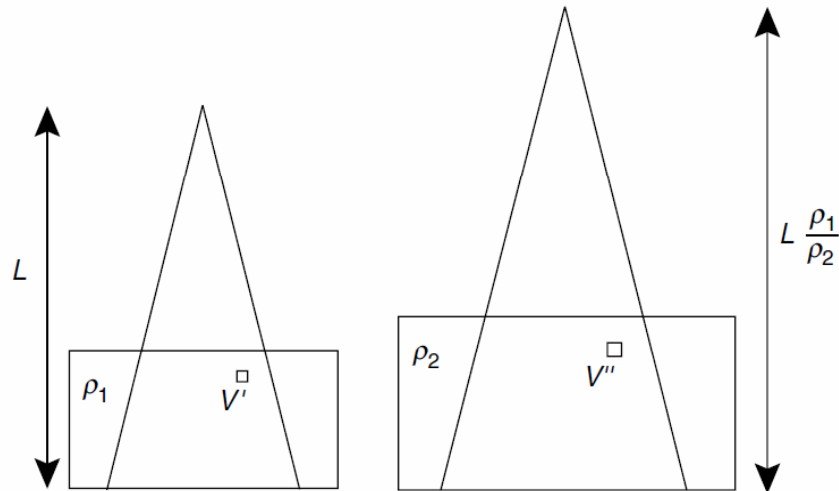
Our basic equation already accounts for:

- Density @ scatter release voxel
- Density @ energy absorption voxel

The kernel also changes ...!

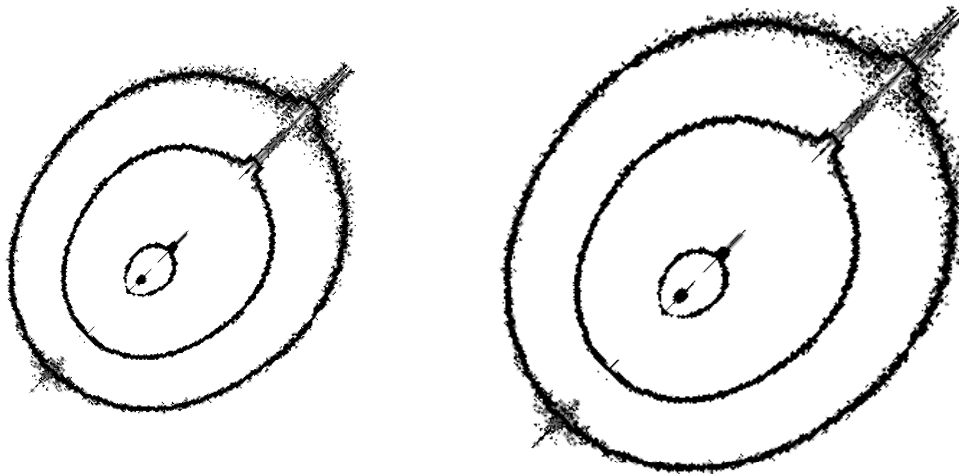
2. inhomogeneities

Medium can be of varying density

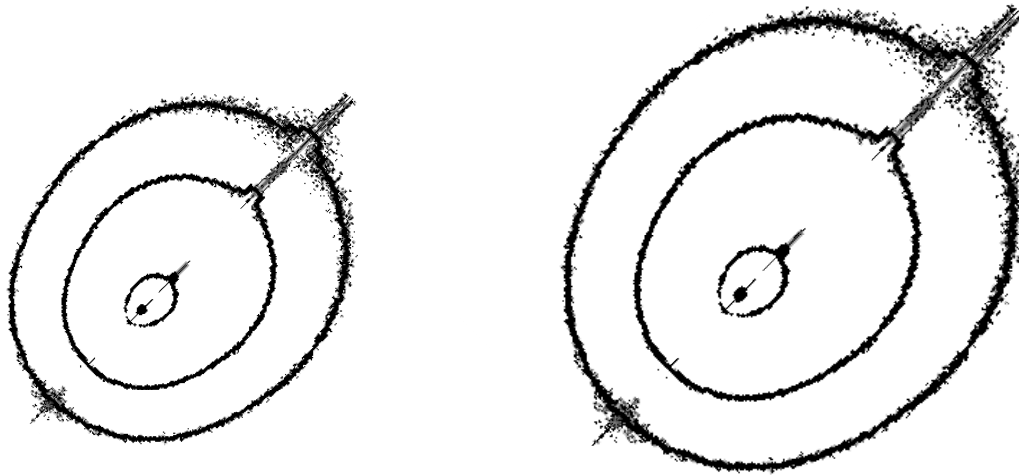


So if we also scale all distances with density we solve the problem and our method is in accordance with O'Connor's theorem:

When considering two media of different densities but the same atomic composition exposed to the same beam, the dose at corresponding points in the two media will be the same provided that all geometric distances in the two media are scaled inversely with density



2. inhomogeneities



Medium can be of varying density

This affects only the exponential attenuation term in our recursive equation which now has to be:

$$\exp(-b\theta \sum_{i=1}^{i-1} \rho_i \Delta r_i)$$

2. inhomogeneities

$$\begin{aligned}
 h_{1sc}(r, \theta) &= \frac{\varepsilon(r, \theta)}{\bar{R}_{1sc} dV} = \frac{dR_{1sc}(\theta)}{\bar{R}_{1sc}} \frac{1}{r^2 d\Omega} \exp(-\mu_{1sc, \theta} r) \mu_{en1sc, \theta} \\
 &= \frac{dR_{1sc}(\theta)}{E(1 - \frac{\mu_{en}}{\mu})} \frac{1}{r^2 d\Omega} \exp(-\mu_{1sc, \theta} r) \mu_{en1sc, \theta} \\
 &= \frac{B_{\theta} \exp(-b_{\theta} r)}{r^2}
 \end{aligned}$$

$$B_{\theta} = \frac{dR_{1sc}(\theta)}{E(1 - \frac{\mu_{en}}{\mu})} \frac{1}{d\Omega} \mu_{en1sc, \theta}$$

$$b_{\theta} = \mu_{1sc, \theta}$$

**Medium can be of varying material
(different elemental composition
and Zeff)**

This affects cross sections
and hence B_{θ}, b_{θ}

Can't we scale the kernel?

Yes and different approaches have
appeared in the literature.

ACE scales attenuation and absorption
voxel-wise according to:

$$b_{\theta_m} = b_{\theta} \frac{\rho_m}{\rho_w} \left[\frac{\mu_{1sc, \theta}}{\rho} \right]_w^m = b_{\theta} \eta_{1sc}$$

$$B_{\theta_m} = B_{\theta} \frac{\rho_m}{\rho_w} \left[\frac{\mu_{en1sc, \theta}}{\rho} \right]_w^m = b_{\theta} \chi_{1sc}$$

2. inhomogeneities

ACE scales attenuation and absorption voxel-wise according to:

$$b_{\theta m} = b_{\theta} \frac{\rho_m}{\rho_w} \left[\frac{\mu_{1sc, \theta}}{\rho} \right]_w^m = b_{\theta} \eta_{1sc}$$
$$B_{\theta m} = B_{\theta} \frac{\rho_m}{\rho_w} \left[\frac{\mu_{en1sc, \theta}}{\rho} \right]_w^m = b_{\theta} \chi_{1sc}$$

Medium can be of varying material (different elemental composition and Zeff)

The same recursive equation applies

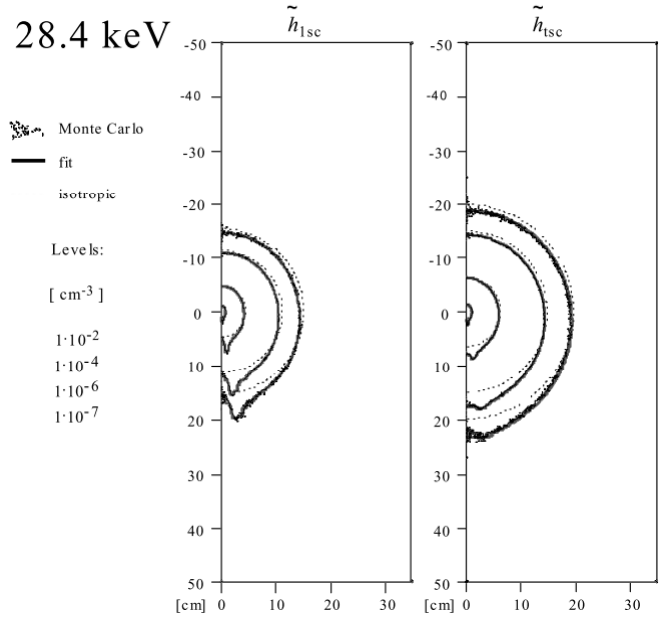
BUT:

- additional input is required to calculate η_{1sc} , χ_{1sc} : the energy spectrum of 1sc photons generated at each point.

This is taken from calculations in water so:

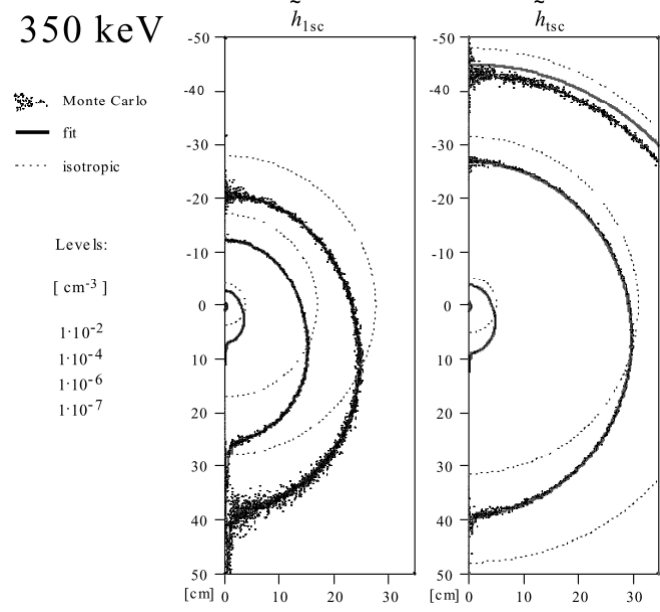
- the scaling is APPROXIMATE and its accuracy deteriorates as materials yield different 1sc spectrum from water (as Z increases due to coherent & photoelectric phenomena-x ray fluorescence and S(x,Z))

3.



scatter

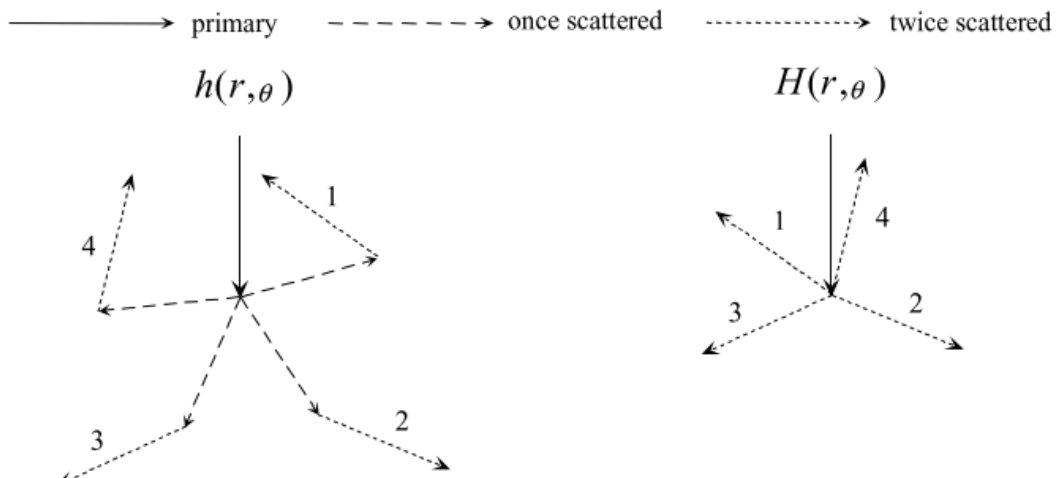
Instead of using h_{1sc} with S_{1sc} obtained from D_{prim} , to obtain D_{1sc} couldn't I distribute S_{1sc} due to ALL orders of scattering in a single step using a different kernel, i.e. h_{msc} ...?



I could, but it is NOT a good idea due to:

- h_{msc} reducing less than h_{1sc} with $r \rightarrow$ ray artefacts
- accuracy close to boundaries of finite geometries (discussed in the following)

3. Higher order of scatter



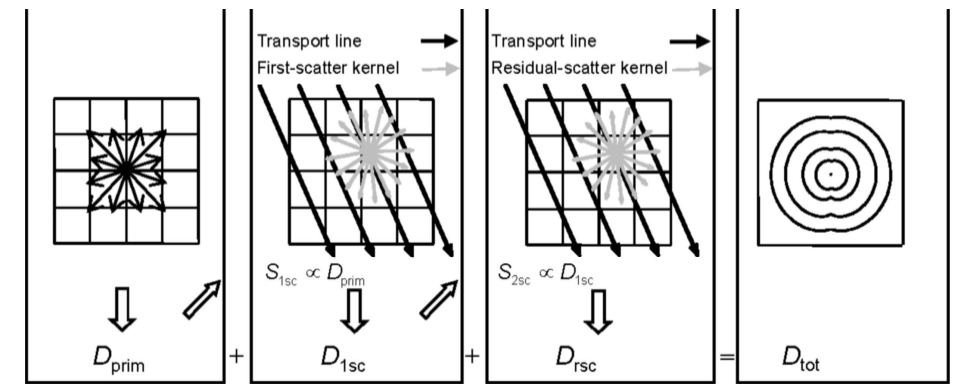
- Primary photons forced to interact
- Once scattered photons and all subsequent particles transported
- Scoring of dose mediated by
 - once-scattered photons: h_{1sc}
 - all scatter generations : h_{isc}

- Primary photons forced to interact
- Once scattered photons started but forced to interact without transport
- Twice scattered photons and all subsequent particles transported
- Scoring of dose mediated by multiply-scattered photons: H_{msc}

I have to repeat the method 2 times:

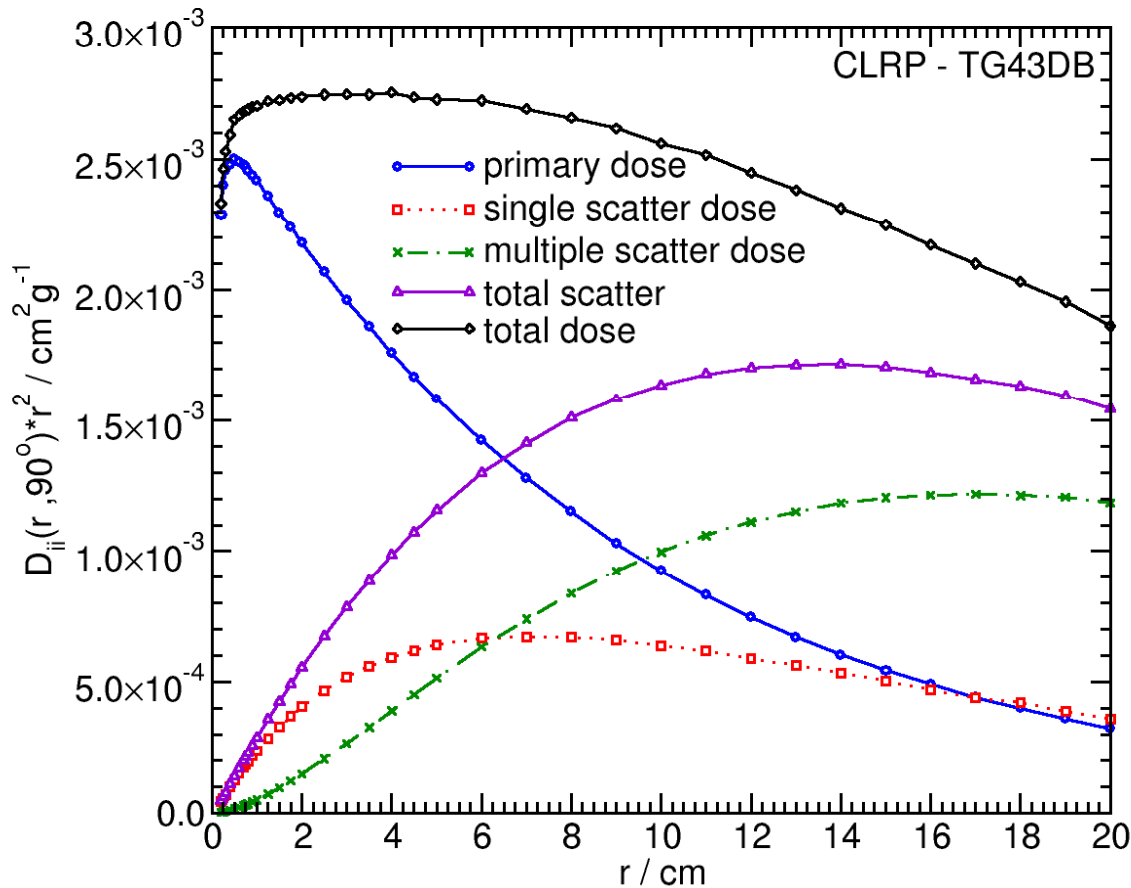
$$D_{prim} \rightarrow S_{1sc} \rightarrow \text{CC with } h_{1sc} \rightarrow D_{1sc}$$

$$D_{1sc} \rightarrow S_{2sc} \rightarrow \text{CC with } H_{msc} \rightarrow D_{msc}$$



3. Higher order of scatter

I have to repeat the method 2 times:



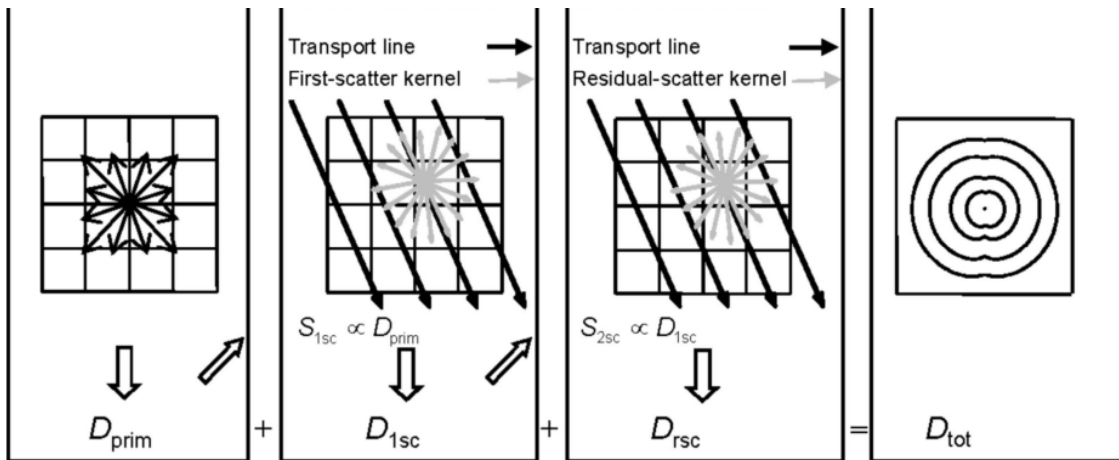
- The second step is approximate in that I do not know the orientation of H_{msc} I can assume it is isotropic or align it with h_{1sc}
 - Calculation time increases to $(M_{1sc} + M_{msc})N^3$
 - Required M_{msc} is $< M_{1sc}$ since the gradient of D_{1sc} is considerably less than that of D_{prim}

3. Higher order of scatter

I have to repeat the method 2 times:

$$D_{\text{prim}} \rightarrow S_{1\text{sc}} \rightarrow \text{CC with } h_{1\text{sc}} \rightarrow D_{1\text{sc}}$$

$$D_{1\text{sc}} \rightarrow S_{2\text{sc}} \rightarrow \text{CC with } H_{\text{msc}} \rightarrow D_{\text{msc}}$$



An analogous recursive equation applies with the difference that H_{msc} is better fit by a bi-exponential function

$$H_{\text{msc}}(r, \theta) = \frac{C\theta \exp(-c\theta r) + D\theta \exp(-d\theta r)}{r^2}$$

Additional input is required to calculate inhomogeneity corrections: the energy spectrum of msc photons generated at each point

4. real sources

Input must now be source specific:

- Primary dose distribution
- Distribution of primary photon energy spectrum
- Distribution of 1sc photon energy spectrum
- Distribution of msc photon energy spectrum

μ/ρ , μ_{en}/ρ data for the calculation of scerma, as well as 1sc & msc kernels, must be weighed over the appropriate energy spectra

Implementation detail:

Primary dose distribution is fit by an analytical expression

$$\frac{K_{\text{prim}}(\mathbf{x})}{R} = \underbrace{\gamma_c(r, \theta, \nu)}_{\substack{\text{V ave.} \\ \text{correction}}} \cdot \underbrace{\frac{\psi(\theta)}{4 \cdot \pi \cdot r^2}}_{\substack{\Psi_E \text{ anis.} \\ \text{correction}}} \cdot \left(\frac{\bar{\mu}_{\text{en}}(\mathbf{x})}{\rho} \right)_{\text{med}} \cdot e^{\underbrace{-m(\theta)}_{\substack{\text{Att. anis.} \\ \text{Correction due to} \\ \Psi_E \text{ diffs over } \theta}} \sum_{i \in \text{rayline to } \mathbf{x}} (\bar{\mu}/\rho)_i \cdot \rho_i \cdot \Delta r_i$$

This allows calculations @ resolution different than that used in the MC simulation to derive the primary dose distribution

5. finite patient dimensions

Kernel data are traditionally calculated in full scatter geometries (8mfp)

This overestimates msc dose close to the edges of a bounded geometry

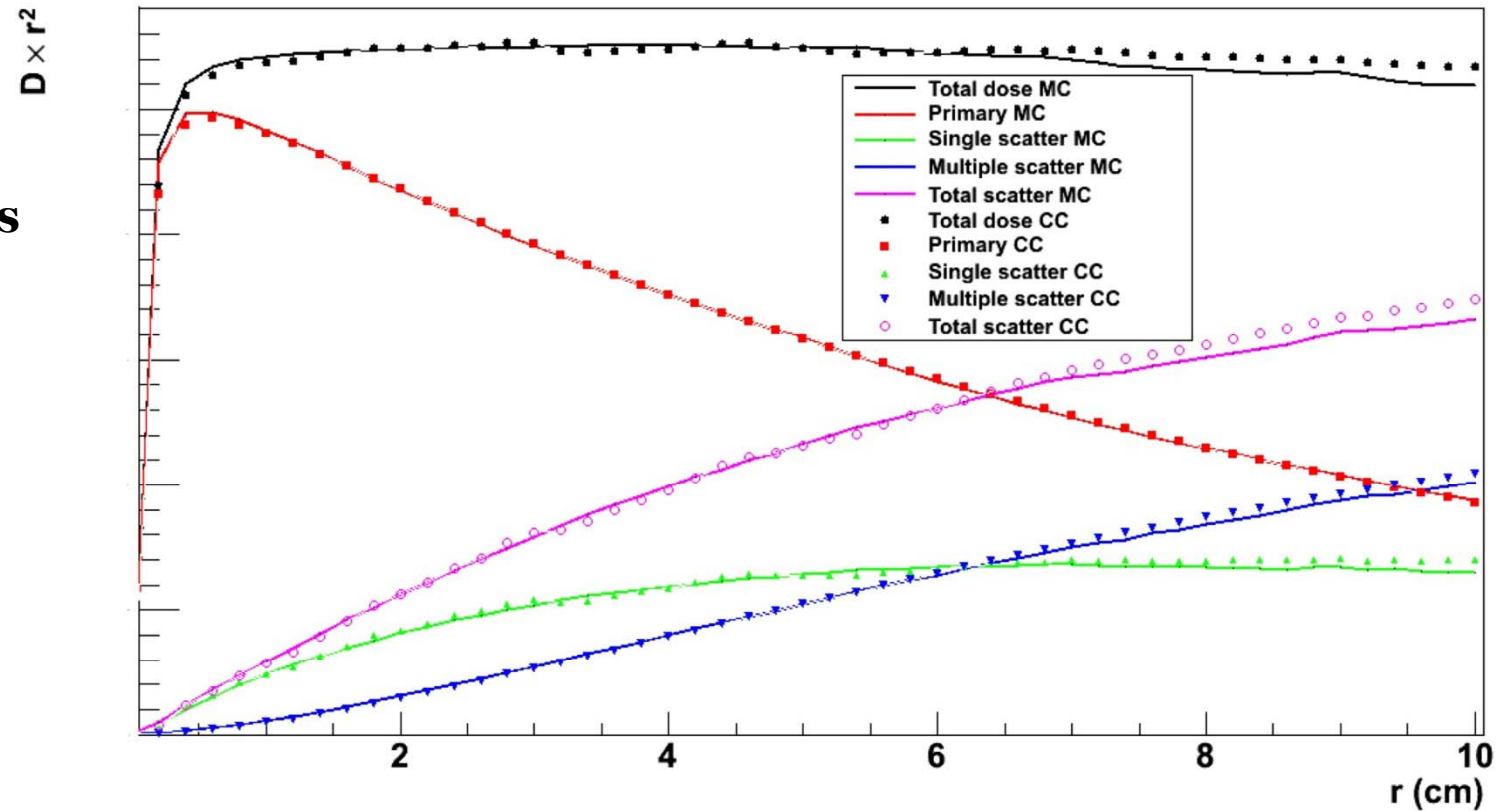


Figure : unpublished data, courtesy of L. Beaulieu

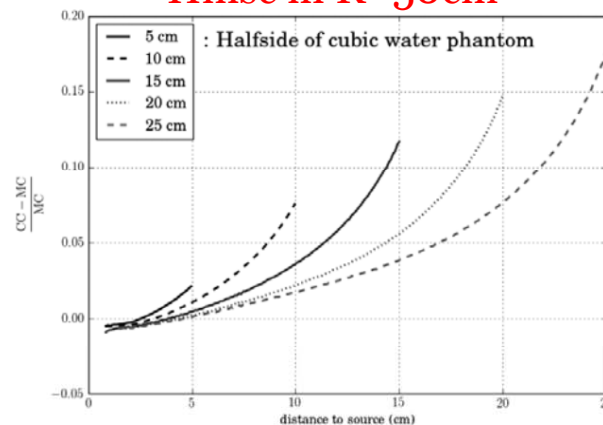
5. finite patient dimensions

Kernel data are traditionally calculated in full scatter geometries (8mfp)

This overestimates msc dose close to the edges of a bounded geometry

Differences could be lifted if a msc kernel calculated in a phantom of equal dimensions to the geometry was used.

Diff. phantoms,
Hmsc in R=50cm



Diff. phantoms
Hmsc in R=10cm

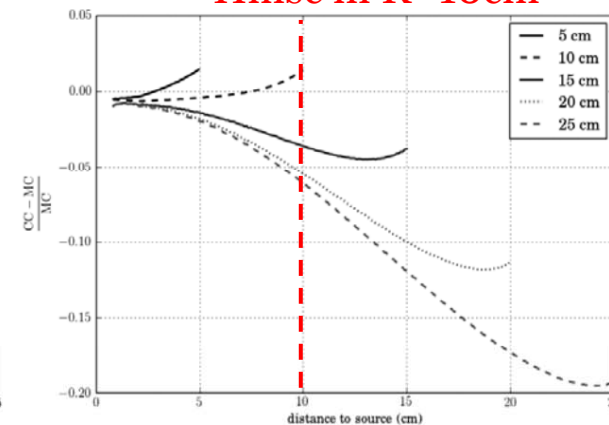
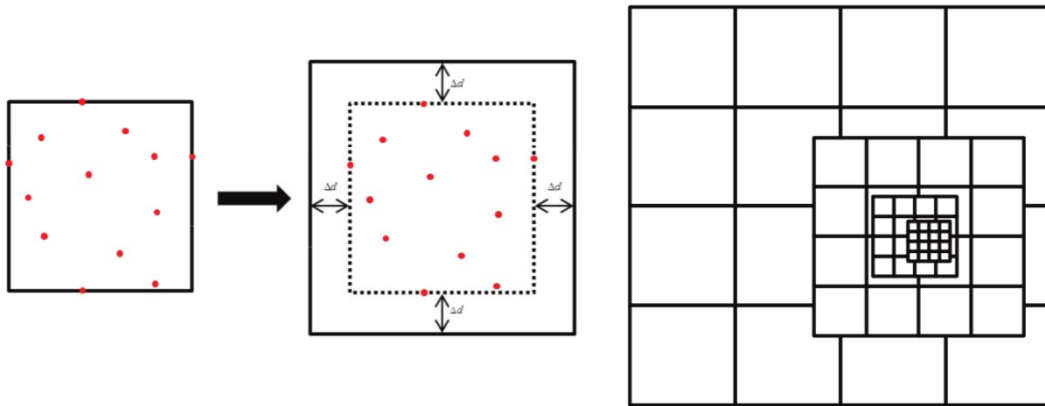


Figure 3. (left): Dose differences between CC and MC as function of the distance from a centrally positioned ^{192}Ir source obtained in cubic water phantoms of halvesides 5 cm, 10 cm, 15 cm, 20 cm and 25 cm. A multiple-scatter point kernel that was generated in a water sphere of outer radii 50 cm was used with CC for all the distributions. (right): Dose differences between CC and MC as function of the distance from a centrally positioned ^{192}Ir source obtained in cubic water phantoms of halvesides 5 cm, 10 cm, 15 cm, 20 cm and 25 cm. A multiple-scatter point kernel that was generated in a water sphere of outer radii 10 cm was used with CC for all the distributions.

Important implementation details



Accuracy Level	Voxel size (cm)			
	0.1	0.2	0.5	1.0
Standard	1	8	20	50
High	8	20	35	50
High (single dwell position)	10	20	50	100

Accuracy level	Number of transport directions for first and residual scatter dose calculations				
	1 dwell position	2-50 dwell positions	51-150 dwell positions	151-300 dwell positions	>300 dwell positions
Standard	320 and 180	320 and 180	240 and 128	200 and 80	180 and 72
High	1620 and 240	720 and 240	500 and 200	320 and 180	240 and 128

All calculation settings are preset!

- The user only selects between two options denoted as: standard and high accuracy levels.
 - These options control:
 - the extent of each of the 4 regions in the multiresolution Cartesian calculation grid used
 - the number of directions for 1sc and msc dose calculations.
- Material assignment is ROI based (TG-186 + applicator materials) otherwise water is considered **within** the patient external contour
- Density can be uniform (ROI based) or HU based (ICRP 44/46 data + method in Knöös et al. Radiother. Oncol. 5, 337, 1986)

In short:

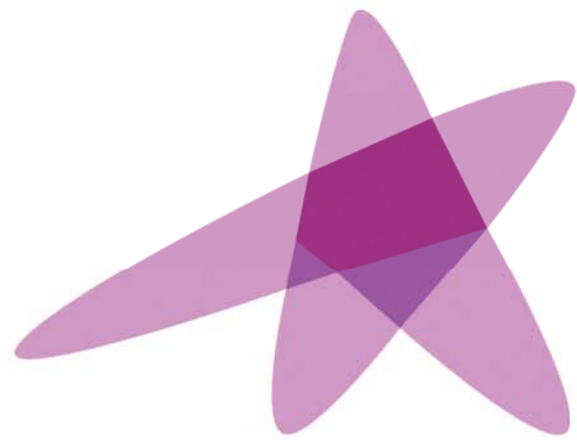
	ACE (Oncentra Brachy)
Long heritage	√
Angular discretization	adaptive (“accuracy” selection & # sources)
Spatial discretization	adaptive multi-resolution Cartesian grid (“accuracy” selection)
Pre-calculated data as input	Primary dose for source model, energy spectra, kernels
Energy discretization	-
Primary scatter separation	√
Ray-tracing for primary	√
Successive scattering	Prim. dose → 1 st scatter SCERMA → multiple scatter SCERMA

In short:

	ACE (Oncentra Brachy)
Applicator libraries	√
Pre-fixed calculation settings to optimize t vs. accuracy	√
Type A uncertainty (through pre-calculated data)	√
Type B uncertainty	√ cross sections, ray effects, spectral changes in low E/high Z, approx. inhomogeneity correction, ray trace in high scatter gradients, kernel tilting, use of geometry specific kernels
Where to look for type Bs:	high gradients such as very close to the source(s), away from implant, close to geom. boundaries, high Z inhomogeneities

In short:

	ACE (Oncentra Brachy)
Material definition	individual voxel density from CT + user defined (ROI based) materials from list based on TG186 (ICRU 46, Woodard & White 1986) dens. based in future version?
Dose reporting medium	local medium
Dose calculation grid	geometry defined by imaging
Use in plan optimization	X



ESTRO

School

Advanced Brachytherapy Physics

Vienna, 29 May – 1 June 2016

Dosimetry using a Grid-Based Boltzmann equation Solver (Acuros)

P. Papagiannis, PhD
Medical Physics Laboratory
Medical School
National & Kapodistrian University of Athens

(no conflict of interest to disclose)

Dosimetry using a Grid-Based Boltzmann equation Solver (Acuros)

- GBBS algorithms used primarily for neutron transport and shielding problems
- Method evaluated for brachy in the literature as early as 2000
 - The first GBBS algorithm incorporated in a commercially available ^{192}Ir brachytherapy TPS was Acuros
 - Acuros is based on the Attila GBBS developed at Los Alamos National Laboratory, optimized for brachytherapy and later also for external beam therapy.

Method can be reviewed in a number of publications:

- ✓ Daskalov GM et al 2000 Med. Phys. 27(10):2307
- ✓ Daskalov GM et al, 2002 Med. Phys. 29(2): 113
- ✓ Gifford K A et al, 2006 Phys. Med. Biol., 51(9): 2253
- ✓ Gifford et al 2008 Med. Phys. 35(6): 2279

+

- ✓ BV-Acuros user manual

Objectives/Outline:

To :

- review the basic principles of the method
 - outline its implementation

so as to identify:

- strengths and weaknesses
- analogies and differences between (current/future) commercially available MBDCAs
 - potential improvements over TG-43
- potential shortcomings relative to reference dose distributions

The basic idea ...

Remember, if I know the energy distribution of fluence, Φ_E , at all points of a geometry, I know the dose distribution!

$$D(\mathbf{r}) = K(\mathbf{r}) = \int_E E \Phi_E(\mathbf{r}) [\mu_{\text{en}}(E) / \rho] dE$$

Can't I formulate an equation describing Φ_E , at my simple problem (point isotropic source in infinite homogeneous medium) and solve it...?

The basic equation is the LBTE

Let $\Phi_{\Omega, E}(\vec{r}, E, \hat{\Omega})$ be the angular fluence ($d\Phi/d\Omega dE = dN/dAd\Omega dE$) denoting the number of photons in phase space element $(\vec{r}, E, \hat{\Omega})$, i.e. passing through a voxel of area dA normal to $\hat{\Omega}$ located at \vec{r} , with $\hat{\Omega}$ within Ω and $\Omega + d\Omega$ and E between E and $E + dE$.

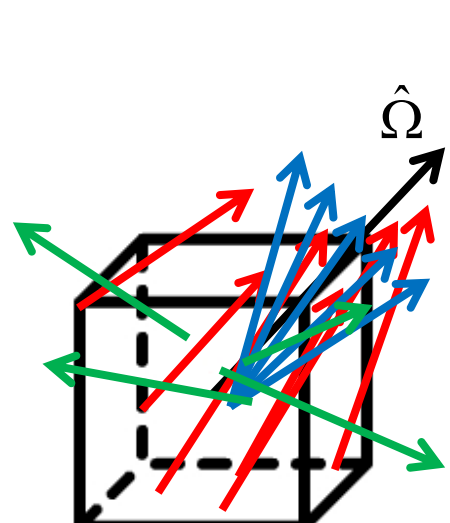
At any part of this “phase space”, conservation of E dictates particle density balance.

The net flow of photons through a phase space cell equals:

photons scattered in it
from all others (E', Ω')

+ photons emitted by a source
in it

- photons absorbed or
scattered out of it


$$\hat{\Omega} \cdot \nabla \Phi_{\Omega, E}(\vec{r}, E, \hat{\Omega}) =$$
$$q_{scat}(\vec{r}, E, \hat{\Omega})$$
$$+ \frac{q_p(E, \hat{\Omega})}{4\pi} \delta(\vec{r} - \vec{r}_p)$$
$$- \mu_t(\vec{r}, E) \Phi_{\Omega, E}(\vec{r}, E, \hat{\Omega})$$

L.B.T.E.

The LBTE

Rearranging the equation, and dropping notation for angular Φ and E distr. of Φ (these can be discerned by the argument):

$$\hat{\Omega} \cdot \vec{\nabla} \Phi(\vec{r}, E, \hat{\Omega}) + \mu_t \Phi(\vec{r}, E, \hat{\Omega}) = q_{scat} + \sum_{p=1}^P \frac{q_p}{4\pi} \delta(\vec{r} - \vec{r}_p)$$

Where:

μ_t is the total linear interaction coefficient

q_p is the primary photon density due to any of P point sources present at a phase space cell

q_{scat} is the scatter photon density

OK...!

Can I solve the LBTE for Φ ...?

The LBTE

$$\hat{\Omega} \cdot \vec{\nabla} \Phi(\vec{r}, E, \hat{\Omega}) + \mu_t \Phi(\vec{r}, E, \hat{\Omega}) = q_{scat} + \sum_{p=1}^P \frac{q_p}{4\pi} \delta(\vec{r} - \vec{r}_p)$$

There is no analytical (closed form) solution of the LBTE.

This is because it is an equation of 6 variables which is integro-differential since the scatter source is:

$$q_{scat}(\vec{r}, E, \hat{\Omega}) = \int_0^\infty \int_{4\pi} \mu_s(\vec{r}, E' \rightarrow E, \hat{\Omega} \cdot \hat{\Omega}') \Phi(\vec{r}, E', \hat{\Omega}') d\hat{\Omega}' dE'$$

i.e. : I must integrate for the scatter source and this depends on the solution itself at all other (E', Ω') points of the phase space...!

The only option is to solve the equation numerically (and this is exactly what Acuros and similar algorithms do) by:

- separating variables: $\Phi(\vec{r}, E, \hat{\Omega}) = \Phi(\vec{r}, E) Y(\hat{\Omega}) = \Phi(\vec{r}) f(E) Y(\hat{\Omega})$
- solve the LBTE iteratively:
 - make initial guess for $\Phi(\vec{r})$
- approximate integration for the scatter source by summation over discrete E, Ω elements
- approximate derivatives by finite differences over discrete space elements
 - correct initial guess, and continue until a convergence criterion is met

The method

Let us take a closer look at q_{scat} :

$$q_{\text{scat}}(\vec{r}, E, \hat{\Omega}) = \int_0^{\infty} \int_{4\pi} \mu_s(\vec{r}, E' \rightarrow E, \hat{\Omega} \cdot \hat{\Omega}') \Phi(\vec{r}, E', \hat{\Omega}') d\hat{\Omega}' dE'$$

The probability of a photon scattering from Ω' to Ω (for a given energy) depends only on $\cos\theta \in [-1, 1]$, where θ is the scattering angle

and

the number of photons scattered in a given direction (for a given energy) depends on the solid angle element around the direction: $\sin\theta d\theta d\varphi$

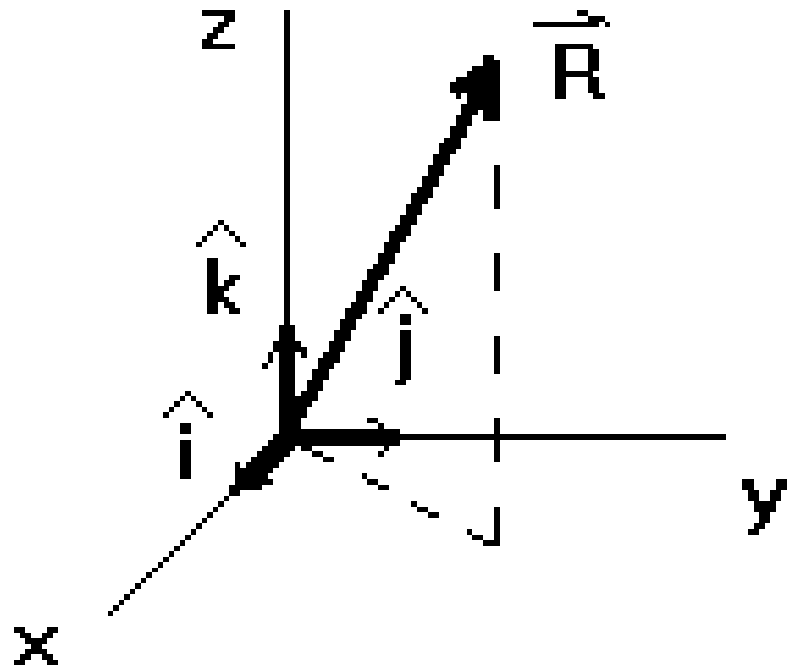
or

the area on the unit sphere defined by the solid angle around the direction

Hence, I can expand q_{scat} in an infinite series of spherical harmonics.

WHAT...???!?!?

The method



It would not strike you as odd that
any function in \mathbb{R}^3
can be expanded as a 3 term series

provided the basis for this expansion is
orthogonal, e.g.:

$$\hat{i} \cdot \hat{j} = \hat{j} \cdot \hat{k} = \hat{k} \cdot \hat{i} = 0$$

$$\hat{i} \cdot \hat{i} = \hat{j} \cdot \hat{j} = \hat{k} \cdot \hat{k} = 1$$

\hat{i} , \hat{j} , and \hat{k} are said to form an orthogonal basis

Many orthogonal bases exist!

The method

Many orthogonal bases exist

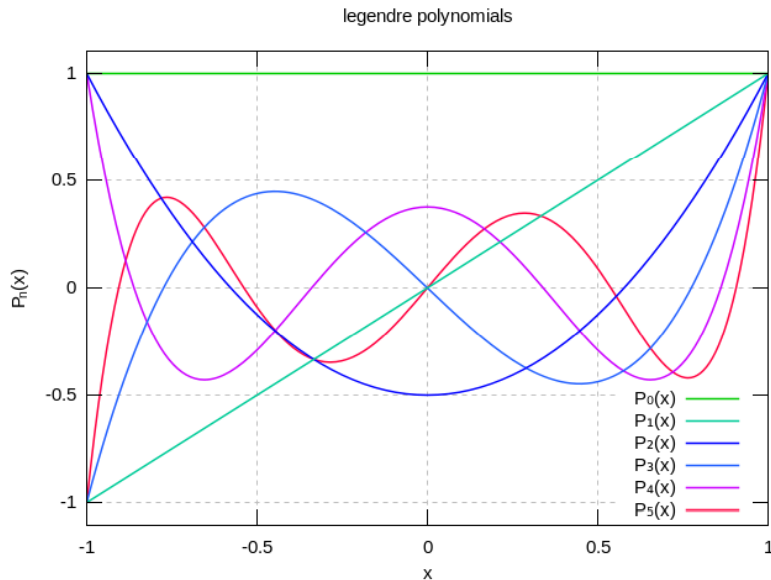
In example:

- Legendre polynomials, $P_n(x)$, are a series of functions that exhibit orthogonality

for $-1 \leq x \leq 1$:

$$\int_{-1}^1 P_m(x) P_n(x) dx = \frac{2}{2n+1} \delta_{mn}$$

and therefore they can be used to expand any function defined in $[-1,1]$ in an infinite series:



$$f(x) = \sum_{n=0}^{\infty} w_n P_n(x),$$

$$w_n = \int_{-1}^1 f(x) P_n(x) dx$$

$$\mu_S(\vec{r}, E' \rightarrow E, \hat{\Omega} \cdot \hat{\Omega}') = \sum_{n=0}^{\infty} \frac{2n+1}{4\pi} \mu_{S,n}(\vec{r}, E' \rightarrow E) P_n(\hat{\Omega} \cdot \hat{\Omega}'),$$

$$\mu_{S,n}(\vec{r}, E' \rightarrow E) = 1/2 \int_{-1}^1 \mu_S(\vec{r}, E' \rightarrow E, \hat{\Omega} \cdot \hat{\Omega}') P_n(\hat{\Omega} \cdot \hat{\Omega}') d(\hat{\Omega} \cdot \hat{\Omega}')$$

The method

- We can truncate the expansion of μ_s up to N (N=3 is adequate for ^{192}Ir anisotropic scattering)

$$\mu_s(\bar{r}, E' \rightarrow E, \hat{\Omega} \cdot \hat{\Omega}') = \sum_{n=0}^{N=3} \frac{2n+1}{4\pi} \mu_{s,n}(\bar{r}, E' \rightarrow E) P_n(\hat{\Omega} \cdot \hat{\Omega}'),$$
$$\mu_{s,n}(\bar{r}, E' \rightarrow E) = 1/2 \int_{-1}^1 \mu_s(\bar{r}, E' \rightarrow E, \hat{\Omega} \cdot \hat{\Omega}') P_n(\hat{\Omega} \cdot \hat{\Omega}') d(\hat{\Omega} \cdot \hat{\Omega}')$$

Note that truncation pertains to the detail in the description of scatter cross section in spherical coordinates and that we have NOT discretized in direction

The method

Many orthogonal bases exist

In example:

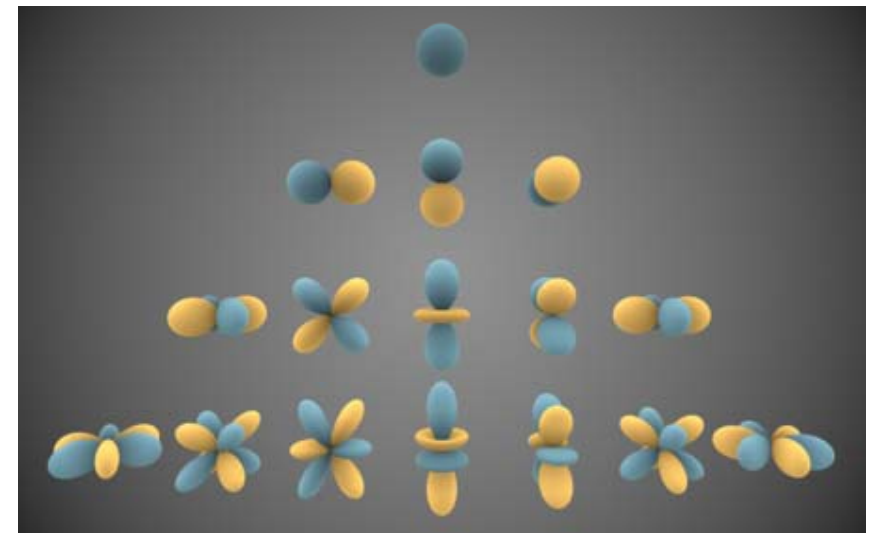
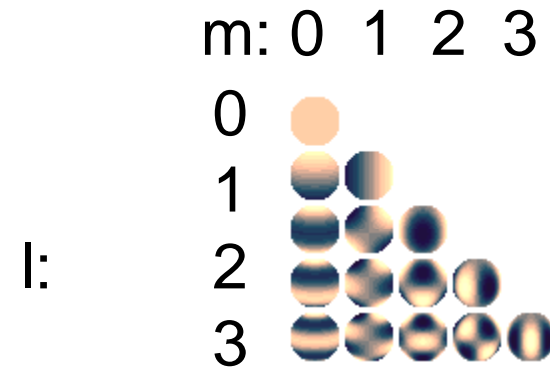
➤ Spherical harmonics, $Y_l^m(\theta, \phi)$, are a series of functions defined on the surface of a sphere that exhibit orthogonality:

$$\int_0^{2\pi} \int_0^\pi Y_l^m(\theta, \phi) \bar{Y}_{l'}^{m'}(\theta, \phi) \sin \theta d\theta d\phi = \frac{1}{2\pi} \int_{-1}^1 \int_0^{2\pi} Y_l^m(\theta, \phi) \bar{Y}_{l'}^{m'}(\theta, \phi) d(\cos \theta) d\phi = \delta_{mm'} \delta_{ll'}$$

and therefore they can be used to expand any function defined on the surface of a sphere in an infinite series:

$$f(\theta, \phi) = \sum_{l=0}^{\infty} \sum_{m=-l}^l C_{l,m} Y_l^m(\theta, \phi),$$

$$C_{l,m} = \iint_{\Omega} f(\theta, \phi) Y_l^m(\theta, \phi) d\Omega$$



Various types of spherical harmonics are available.

A particular set, of order $l=N$ (orthogonal basis) + the corresponding weights of a function are called a **quadrature set of order N**.

The method

Many orthogonal bases exist

In example:

➤ Spherical harmonics, $Y_l^m(\theta, \phi)$, are a series of functions defined on the surface of a sphere that exhibit orthogonality:

$$\int_{2\pi} \int_{\pi} Y_l^m(\theta, \phi) \bar{Y}_{l'}^{m'}(\theta, \phi) \sin \theta \, d\theta \, d\phi =$$

$$\int_{2\pi} \int_{-1}^1 Y_l^m(\theta, \phi) \bar{Y}_{l'}^{m'}(\theta, \phi) \, d(\cos \theta) \, d\phi = \delta_{mm'} \delta_{ll'}$$

and therefore they can be used to expand any function defined on the surface of a sphere in an infinite series:

$$f(\theta, \phi) = \sum_{l=0}^{\infty} \sum_{m=-l}^l C_{l,m} Y_l^m(\theta, \phi),$$

$$C_{l,m} = \iint_{\Omega} f(\theta, \phi) Y_l^m(\theta, \phi) \, d\Omega$$

$$\Phi(\vec{r}, E', \hat{\Omega}') = \sum_{l=0}^{\infty} \sum_{m=-l}^l \Phi_{l,m}(\vec{r}, E') Y_l^m(\hat{\Omega}'),$$
$$\Phi_{l,m}(\vec{r}, E') = \iint_{4\pi} \Phi(\vec{r}, E', \hat{\Omega}') Y_l^m(\hat{\Omega}') \, d\Omega'$$

The method

OK.

Let us agree that instead of :

$$q_{scat}(\vec{r}, E, \hat{\Omega}) = \int_0^{\infty} \int_{4\pi} \mu_s(\vec{r}, E' \rightarrow E, \hat{\Omega} \cdot \hat{\Omega}') \Phi(\vec{r}, E', \hat{\Omega}') d\hat{\Omega}' dE'$$

q_{scat} can be written as :

$$q_{scat}(\vec{r}, E, \hat{\Omega}) = \int_0^{\infty} \sum_{l=0}^{\infty} \sum_{m=-l}^l \mu_{s,l}(\vec{r}, E' \rightarrow E) \Phi_{l,m}(\vec{r}, E') Y_l^m(\theta, \phi) dE',$$

$$\mu_{s,l}(\vec{r}, E' \rightarrow E) = 1/2 \int_{-1}^1 \mu_s(\vec{r}, E' \rightarrow E, \hat{\Omega} \cdot \hat{\Omega}') P_l(\hat{\Omega} \cdot \hat{\Omega}') d(\hat{\Omega} \cdot \hat{\Omega}')$$

$$\Phi_{l,m}(\vec{r}, E') = \iint_{4\pi} \Phi(\vec{r}, E', \hat{\Omega}') Y_l^m(\hat{\Omega}') d\Omega'$$

is there a benefit?

The method

- We have separated r and E , from direction variables and turned integration to summation for direction in the scatter source

$$\hat{\Omega} \cdot \vec{\nabla} \Phi_{\Omega, E}(\vec{r}, E, \hat{\Omega}) + \mu_t \Phi_{\Omega, E}(\vec{r}, E, \hat{\Omega}) = q_{scat} + \sum_{p=1}^P \frac{q_p}{4\pi} \delta(\vec{r} - \vec{r}_p) \quad (1)$$

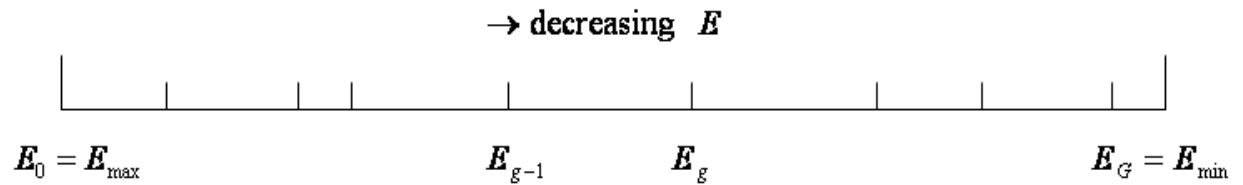
$$q_{scat}(\vec{r}, E, \hat{\Omega}) = \int_0^{\infty} \sum_{l=0}^{\infty} \sum_{m=-l}^l \mu_{s,l}(\vec{r}, E' \rightarrow E) \Phi_{l,m}(\vec{r}, E') Y_l^m(\theta, \phi) dE' \quad (2)$$

$$\mu_{s,l}(\vec{r}, E' \rightarrow E) = \frac{1}{2} \int_{-1}^1 \mu_s(\vec{r}, E' \rightarrow E, \hat{\Omega} \cdot \hat{\Omega}') P_l(\hat{\Omega} \cdot \hat{\Omega}') d(\hat{\Omega} \cdot \hat{\Omega}') \quad (3)$$

$$\Phi_{l,m}(\vec{r}, E') = \iint_{4\pi} \Phi(\vec{r}, E', \hat{\Omega}') Y_l^m(\hat{\Omega}') d\Omega' \quad (4)$$

Let us continue with E ...

The method



- Energy is divided in $g=1, \dots, G$ **groups** of width ΔE_g so that energy decreases as group order decreases

$$\hat{\Omega} \cdot \vec{\nabla} \Phi_g(\vec{r}, \hat{\Omega}) + \mu_{t,g} \Phi_g(\vec{r}, \hat{\Omega}) = q_{scat,g} + \sum_{p=1}^P \frac{q_{p,g}}{4\pi} \delta(\vec{r} - \vec{r}_p) \quad (1)$$

$$q_{scat,g}(\vec{r}, \hat{\Omega}) = \sum_{l=0}^{\infty} \sum_{m=-l}^l \sum_{g'=1}^G \mu_{s,l,g' \rightarrow g}(\vec{r}) \Phi_{l,m,g'}(\vec{r}) Y_l^m(\theta, \phi) \quad (2)$$

Our equations become:

$$\mu_{s,l,g' \rightarrow g}(\vec{r}) = \frac{\int_{E_{g'}}^{E_{g'-1}} \int_{E_g}^{E_{g-1}} \mu_{s,l}(\vec{r}, E' \rightarrow E) \Phi(\vec{r}, E') dE' dE}{\int_{E_g}^{E_{g-1}} \Phi(\vec{r}, E) dE} \quad (3)$$

$$\Phi_{l,m,g}(\vec{r}) = \int_{E_g}^{E_{g-1}} \Phi_{l,m}(\vec{r}, E) dE = \int_{E_g}^{E_{g-1}} \iint_{4\pi} \Phi(\vec{r}, E', \hat{\Omega}') Y_l^m(\hat{\Omega}') d\Omega' dE \quad (4)$$

$$\mu_{t,g}(\vec{r}) = \frac{\int_{E_g}^{E_{g-1}} \mu_t(\vec{r}, E) \Phi(\vec{r}, E) dE}{\int_{E_g}^{E_{g-1}} \Phi(\vec{r}, E) dE} \quad (5)$$

The method

➤ Up to now, our set of equations is EXACT
but we need to separate r from E to solve it iteratively

$$\hat{\Omega} \cdot \vec{\nabla} \Phi_g(\vec{r}, \hat{\Omega}) + \mu_{t,g} \Phi_g(\vec{r}, \hat{\Omega}) = q_{scat,g} + \sum_{p=1}^P \frac{q_{p,g}}{4\pi} \delta(\vec{r} - \vec{r}_p) \quad (1)$$

$$q_{scat,g}(\vec{r}, \hat{\Omega}) = \sum_{l=0}^{\infty} \sum_{m=-l}^l \sum_{g'=1}^G \mu_{s,l,g' \rightarrow g}(\vec{r}) \Phi_{l,m,g'}(\vec{r}) Y_l^m(\theta, \phi) \quad (2)$$

$$\mu_{s,l,g' \rightarrow g}(\vec{r}) = \frac{\int_{E_{g'-1}}^{E_{g-1}} \int_{E_g}^{E_{g-1}} \mu_{s,l}(\vec{r}, E' \rightarrow E) \Phi(\vec{r}, E') dE' dE}{\int_{E_g}^{E_{g-1}} \Phi(\vec{r}, E) dE} \quad (3)$$

$$\Phi_{l,m,g}(\vec{r}) = \int_{E_g}^{E_{g-1}} \Phi_{l,m}(\vec{r}, E) dE = \int_{E_g}^{E_{g-1}} \iint \Phi(\vec{r}, E', \hat{\Omega}') Y_l^m(\hat{\Omega}') d\Omega' dE \quad (4)$$

$$\mu_{t,g}(\vec{r}) = \frac{\int_{E_g}^{E_{g-1}} \mu_t(\vec{r}, E) \Phi(\vec{r}, E) dE}{\int_{E_g}^{E_{g-1}} \Phi(\vec{r}, E) dE} \quad (5)$$

The method

➤ if we define a spectral weighting factor: $f(E)$ so that: $\Phi(\vec{r}, E) = \Phi(\vec{r}) f(E)$, $\int f(E) dE = 1$

$$\hat{\Omega} \cdot \vec{\nabla} \Phi_g(\vec{r}, \hat{\Omega}) + \mu_{t,g} \Phi_g(\vec{r}, \hat{\Omega}) = q_{scat,g} + \sum_{p=1}^P \frac{q_{p,g}}{4\pi} \delta(\vec{r} - \vec{r}_p) \quad (1)$$

Our equations
become:

$$q_{scat,g}(\vec{r}, \hat{\Omega}) = \sum_{l=0}^{\infty} \sum_{m=-l}^l \sum_{g'=1}^G \mu_{s,l,g' \rightarrow g}(\vec{r}) \Phi_{l,m,g'}(\vec{r}) Y_l^m(\theta, \phi) \quad (2)$$

$$\mu_{s,l,g' \rightarrow g}(\vec{r}) = \int_{E_{g'}}^{E_{g-1}} \int_{E_g}^{E_{g-1}} \mu_{s,l}(\vec{r}, E' \rightarrow E) f(E') dE dE' \quad (3)$$

$$\Phi_{l,m,g}(\vec{r}) = \int_{E_g}^{E_{g-1}} \Phi_{l,m}(\vec{r}) f(E) dE = \int_{E_g}^{E_{g-1}} \iint_{4\pi} \Phi(\vec{r}, \hat{\Omega}') f(E) Y_l^m(\hat{\Omega}') d\Omega' dE \quad (4)$$

$$\mu_{t,g}(\vec{r}) = \int_{E_g}^{E_{g-1}} \mu_t(\vec{r}, E) f(E) dE \quad (5)$$

➤ All that is left then is to discretize direction and space and solve iteratively!

The method

$$\Phi(\vec{r}, E) = \Phi(\vec{r}) f(E), \quad \int_E f(E) dE = 1$$

The importance of $f(E)$:

The spectral weighting factor connects photon fluence to energy fluence at any point of a geometry and hence depends on the actual geometry and its physical properties.

However, as G increases, and ΔE_G become narrow, the energy group cross sections $\mu_{t,g}$, $\mu_{s,g}$, approximate the continuous $\mu_t(E)$, $\mu_s(E)$ and do not depend heavily on $f(E)$.

This means that generic multi group cross sections (of $\Delta E_G \ll$) are used with **analytic or semi-analytic $f(E)$ appropriate for the problem at hand.**

The method

Let us make the final step:

We ask our equations to hold for a number of directions M determined by a **quadrature set \mathbf{S}_N** of order N (Discrete Ordinates Method-DOM)
(M is linked to N in a different way for different quadrature sets)

$$\hat{\Omega} \cdot \bar{\nabla} \Phi_{g,n}(\bar{r}) + \mu_{t,g} \Phi_{g,n}(\bar{r}) = q_{scat,g,n} + \sum_{p=1}^P \frac{q_{p,g,n}}{4\pi} \delta(\bar{r} - \bar{r}_p), \quad \Phi_{g,n}(\bar{r}) = \Phi_g(\bar{r}, \hat{\Omega}_n) \quad (1)$$

$$q_{scat,g,n}(\bar{r}, \hat{\Omega}) = \sum_{l=0}^{\infty} \sum_{m=-l}^l \sum_{g'=1}^G \mu_{s,l,g' \rightarrow g}(\bar{r}) \Phi_{l,m,g'}(\bar{r}) Y_l^m(\theta, \phi) \quad (2)$$

$$\mu_{s,l,g' \rightarrow g}(\bar{r}) = \int_{E_{g'}}^{E_{g'-1}} \int_{E_g}^{E_{g-1}} \mu_{s,l}(\bar{r}, E' \rightarrow E) f(E') dE dE' \quad (3)$$

$$\Phi_{l,m,g}(\bar{r}) = \int_{E_g}^{E_{g-1}} \Phi_{l,m}(\bar{r}) f(E) dE = \int_{E_g}^{E_{g-1}} \iint_{4\pi} \Phi(\bar{r}, \hat{\Omega}') f(E) Y_l^m(\hat{\Omega}') d\Omega' dE = \int_{E_g}^{E_{g-1}} \sum_{n=1}^N \Phi_{g,n}(\bar{r}) f(E) Y_l^m(\hat{\Omega}_n) w_n dE \quad (4)$$

$$\mu_{t,g}(\bar{r}) = \int_{E_g}^{E_{g-1}} \mu_t(\bar{r}, E) f(E) dE \quad (5)$$

The method ... is ready

I have GxM equations of the form (1) @ each voxel (GxMxN_{vox} in total)

- begin with E1 (highest energy group)
- make an initial guess for $\Phi_{1,n}(\vec{r})_{iter=0}$
- • calculate cross sections from (3) & (5)
- calculate the expansion from (4)
- use these in (2) to calculate $q_{scat,1,n}$
- solve (1) for $\Phi_{1,n}(\vec{r})_{iter=1}$
- if convergence criterion not met, re-iterate
- if convergence criterion met, proceed with g=2

$$\hat{\Omega} \cdot \vec{\nabla} \Phi_{g,n}(\vec{r}) + \mu_{t,g} \Phi_{g,n}(\vec{r}) = q_{scat,g,n} + \sum_{p=1}^P \frac{q_{p,g,n}}{4\pi} \delta(\vec{r} - \vec{r}_p) \quad (1)$$

$$q_{scat,g,n}(\vec{r}, \hat{\Omega}) = \sum_{l=0}^{\infty} \sum_{m=-l}^l \sum_{g'=1}^G \mu_{s,l,g' \rightarrow g}(\vec{r}) \Phi_{l,m,g'}(\vec{r}) Y_l^m(\theta, \phi) \quad (2)$$

$$\mu_{s,l,g' \rightarrow g}(\vec{r}) = \int_{E_{g'}}^{E_{g'-1}} \int_{E_g}^{E_{g-1}} \mu_{s,l}(\vec{r}, E' \rightarrow E) f(E') dE dE' \quad (3)$$

$$\Phi_{l,m,g}(\vec{r}) = \int_{E_g}^{E_{g-1}} \sum_{n=1}^N \Phi_{g,n}(\vec{r}) f(E) Y_l^m(\hat{\Omega}_n) w_n dE \quad (4)$$

$$\mu_{t,g}(\vec{r}) = \int_{E_g}^{E_{g-1}} \mu_t(\vec{r}, E) f(E) dE \quad (5)$$

BUT...:

1. **I need to be efficient** (t~ GxMxN_{vox}x#iters.x order of legendre exp.) **& work with finite voxels**
2. **I need to account for inhomogeneities**
3. **I need to work with real sources**
4. **I need to account for finite patient dimensions**

1. I need to be efficient

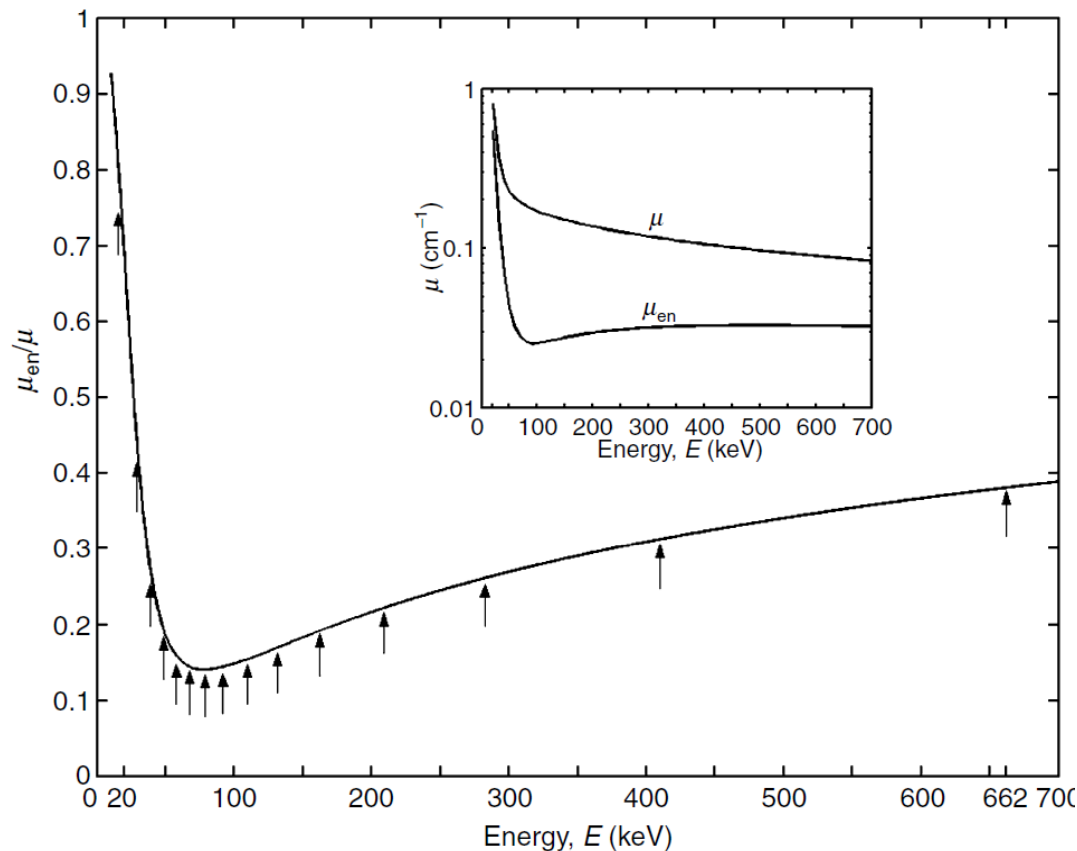
The iterations are needed because I do not know q_{scat} within the energy group
i.e. scattering events with minimal energy transfer

When do I expect delays in convergence?

1. I need to be efficient

The iterations are needed because I do not know q_{scat} within the energy group
i.e. scattering events with minimal energy transfer

When do I expect delays in convergence?



Multiple scattering with minimal energy transfer that occurs in the ^{192}Ir energy range
as well as
coherent scattering that is significant at low energies and high Z materials,
delay convergence

Algorithms to force convergence are used
(DSA-Diffusion synthetic acceleration)

1. I need to be efficient

The multigroup (G), DOM (S_N), cross section expansion (P_N) method converges to an analytic solution of the LBTE for $G, N \rightarrow \text{infinity}$

and

no volume averaging is expected for fine spatial discretization ($N_{\text{vox}} \rightarrow \text{infinity}$)

BUT

I need to be efficient

and since $t \sim G \times M \times N_{\text{vox}}$ (\times #iters. \times order of legendre exp.),

even if I have the perfect finite differencing algorithm for solving the system of equations,

I need to reduce G, M, N_{vox} !!!

1. I need to be efficient, angular discretization

Guess what happens when I reduce M (order of S_N) ...

RAY EFFECTS...!

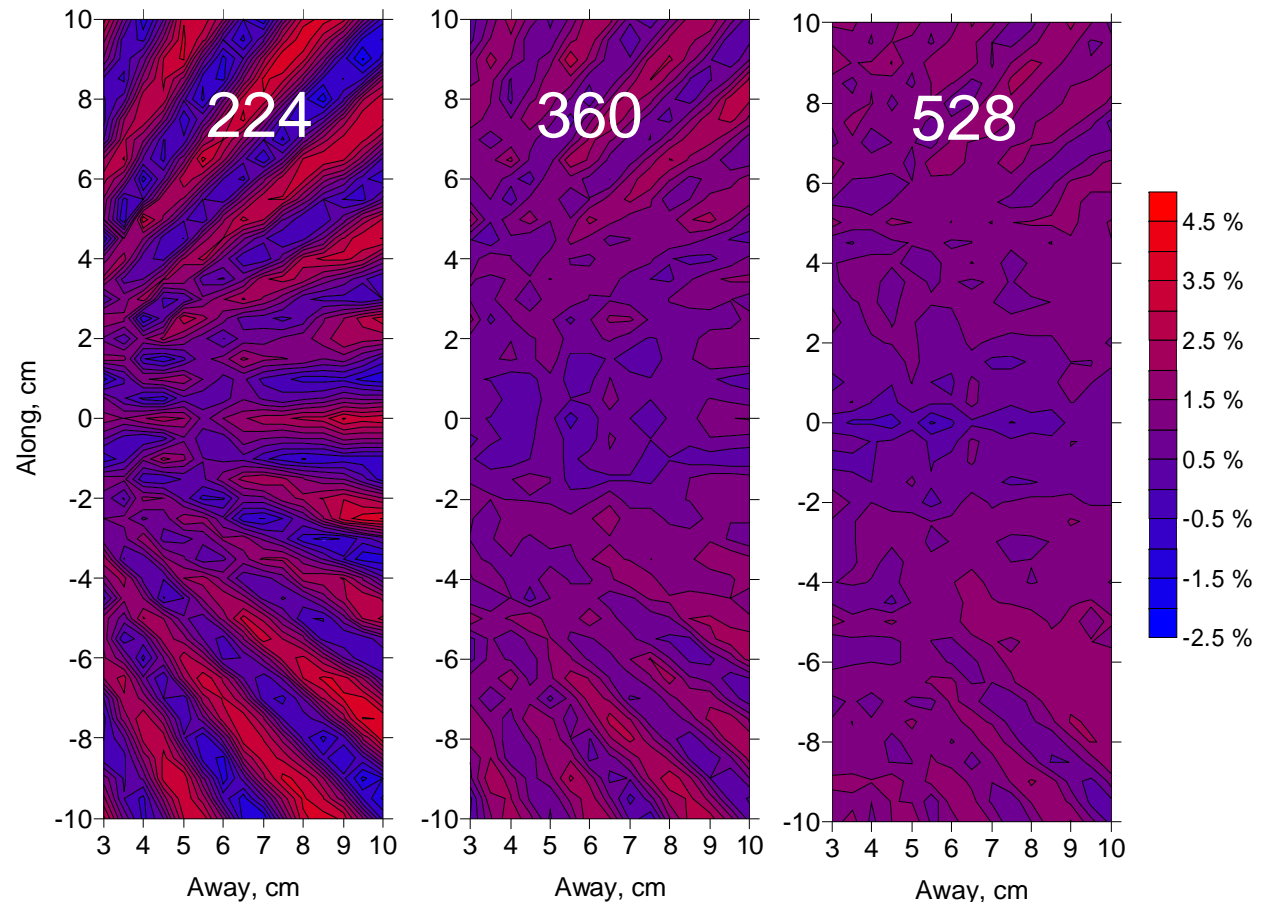


Figure from: Venselaar, Baltas, Meigooni, Hoskin (Eds), *Comprehensive Brachytherapy: physical and clinical aspects*. CRC Press, Taylor & Francis, © 2013

1. I need to be efficient, angular discretization

- discretization artifacts or “rays”: an artificial buildup of particle fluence along the finite number of directions used

↑ with high gradients of scatter fluence, at points where primary dose is small
↓ with ↑ $N_{\text{directions}}$ & voxel size at the expense of calculation time and potential volume averaging

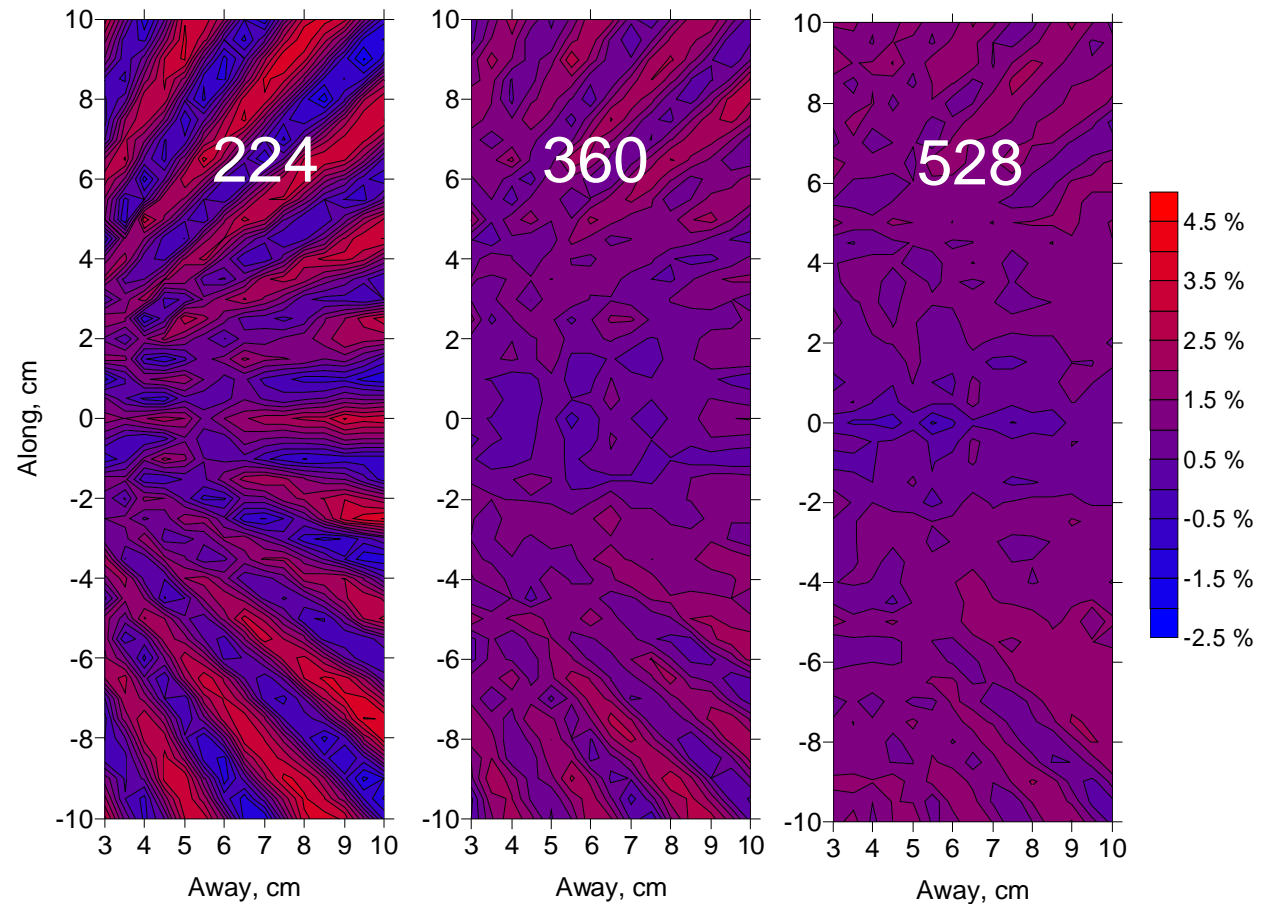


Figure from: Venselaar, Baltas, Meigooni, Hoskin (Eds), *Comprehensive Brachytherapy: physical and clinical aspects*. CRC Press, Taylor & Francis, © 2013

1. I need to be efficient, angular discretization

How can I relax the demand on S_N without ray effects?

The LBTE is linear so assuming:

$$\Phi_g(\vec{r}, \hat{\Omega}) = \sum_{p=1}^P \Phi_{p,g}^{unc}(\vec{r}, \hat{\Omega}) + \Phi_g^{coll}(\vec{r}, \hat{\Omega})$$

For any direction, we can split our system of equations in two:

$$\hat{\Omega} \cdot \vec{\nabla} \Phi_g^{unc} + \sigma_{t,g} \Phi_g^{unc} = \sum_{p=1}^P \frac{q_{p,g}}{4\pi} \delta(\vec{r} - \vec{r}_p) \quad (1)$$

$$\hat{\Omega} \cdot \vec{\nabla} \Phi_g^{coll} + \sigma_{t,g} \Phi_g^{coll} = q_g^{scat,coll} + \sum_{p=1}^P q_{p,g}^{scat,unc} \quad (2)$$

Equation (1) for the primary (uncollided) part of the fluence can be analytically solved!!!

I can ray-trace the solution for the spectrum of primary photons through the geometry and arrive at very quick and accurate: initial guess $\Phi_{1,n}(\vec{r})_{iter=0}$ and $q_{scat,1,n}$

Then I proceed to solve the system of equations (2) for the collided fluence to refine my solution with the higher orders of scatter

This is known as the 1st scatter source method

1. I need to be efficient, angular discretization

- Acuros uses the first scatter source method **so the photon spectrum exiting a source needs to be known**
- Acuros uses Triangular-Chebyshev quadrature sets for angular discretization and the integration for the generation of the scattering source
 - The angular discretization scheme is adaptive with S_N order ranging from $N=4$ (24 discrete directions) to 30 (960 discrete directions) varying both within an energy group ($g \rightarrow g$) and between energy groups ($g \rightarrow g'$)

Guess which energies are given larger N ...!

1. I need to be efficient, energy discretization

Remember: Energy discretization is realistic if cross sections do not vary considerably within each group and appropriate $f(E)$ is very important

Acuros (for ^{192}Ir) uses an adaptive $G=37$ group cross section set.

For the uncollided component all 37 groups are used, with $f(E) = 1/\Delta E_g$

For the collided (scattered) component, this group is collapsed applying an appropriate (proprietary) energy weighting function $f(E)$.

Acuros uses cross section generated by CEPXS, a multigroup-Legendre cross-section generating code.

CEPXS does not include coherent scattering and uses the Klein-Nishina incoherent scattering cross sections.

1. I need to be efficient, spatial discretization

For spatial discretization, Acuros partitions the computational volume (the CT image series) into variable sized Cartesian elements.

Computational element size varies based on material properties and the gradient of the scatter photon fluence.

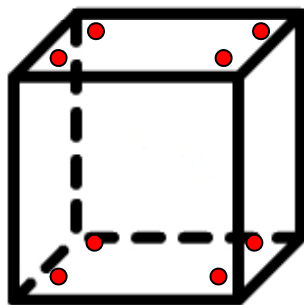
The spatial derivatives in the LBTEs are replaced by finite differences at multiple points within each computational element

Supplementary equations are used to describe fluence variation between these points and preserve particle balance (DFEM - linear discontinuous Galerkin finite-element method)

Hence the angular fluence is known everywhere in each element, not only at the points where spatial derivatives are evaluated

BUT

spatial discretization errors can ensue at points in high fluence gradients



$$\frac{\partial \Phi_{m,g}(x_i)}{\partial x} = \frac{\Phi_{m,g}(x_{i+1}) - \Phi_{m,g}(x_{i-1})}{\Delta x_i}$$

2. inhomogeneities

The method inherently accounts for inhomogeneities assuming material properties are constant within each computational element
(!!! restriction on computational element size !!!)

through:

- $\mu_{t,g}$, $\mu_{s,l,g}$
- primary fluence ray tracing
 - dose calculation

$$D(\vec{r}) = \frac{1}{\rho(\vec{r})} \sum_{g=1}^G \mu_{en,g}(\vec{r}) \left\{ \sum_{p=1}^P \Phi_{p,g}^{unc}(\vec{r}) + \Phi_g^{coll}(\vec{r}) \right\} \quad D(\vec{r}) = \frac{1}{\rho_{water}} \sum_{g=1}^G \mu_{en,g}^{water}(\vec{r}) \left\{ \sum_{p=1}^P \Phi_{p,g}^{unc}(\vec{r}) + \Phi_g^{coll}(\vec{r}) \right\}$$

(note that D is calculated as a post processing operation)

3. real sources

Input must now be source specific:

- Energy distribution of primary fluence (in essence the source phase space file)

Acuros uses effective sources:
pre-calculated source specific phase space file

+

a number of points within the source volume for ray tracing the primary fluence in the geometry

Brachy sources are small BUT the number of point sources used for ray tracing can be important

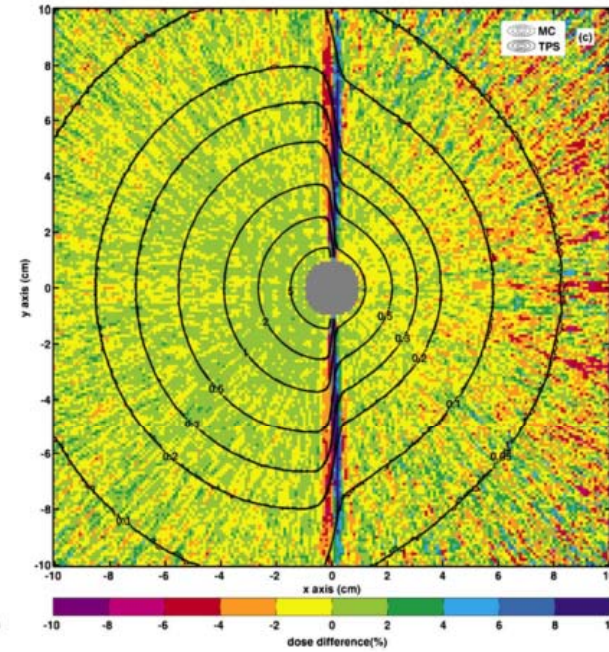
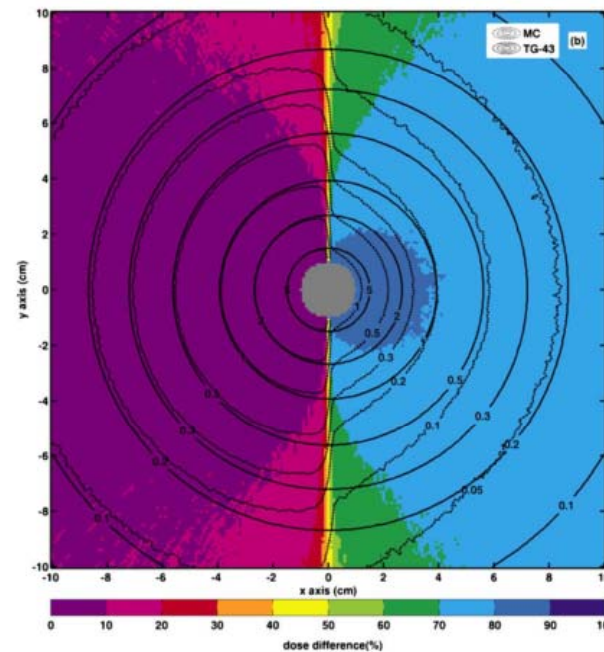
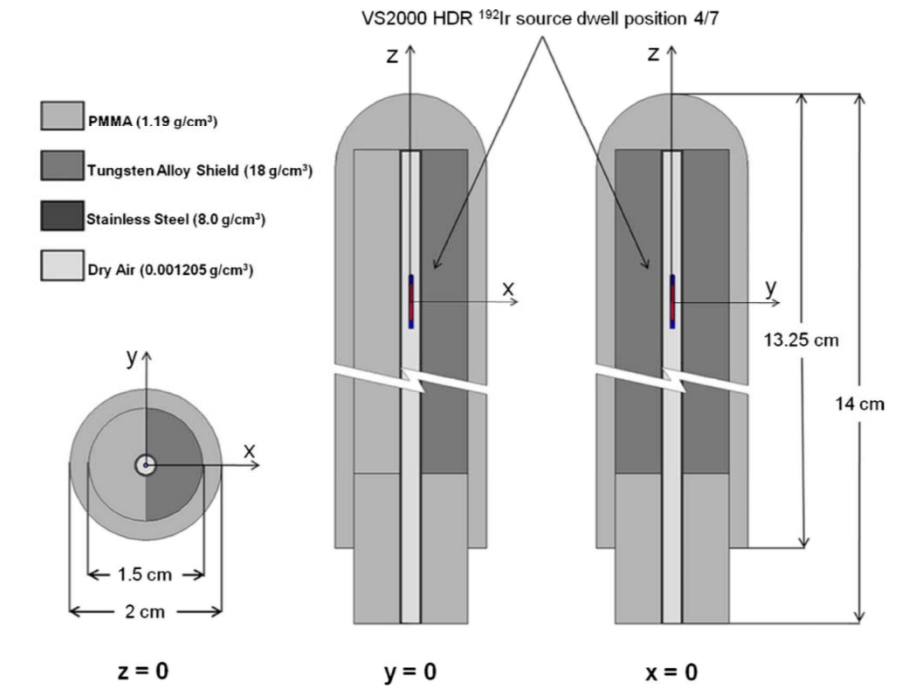


Figure from: L. Petrokokkinos et al. Med. Phys. 38 1981 (2011)

4. finite patient dimensions

Inherently taken into account

(there is no geometry specific input to the method apart from $f(E)$ and the method accounts for geometry specific scatter conditions)

Important implementation details

All calculation settings are preset!

- user specifies D output grid (affects t) and resolution (affects t & accuracy)
- D calculation grid is automatically defined as the D output grid +10 cm in all directions, unless CT image boundary is reached
 - Density is HU based through a user editable calibration
- Material assignment is based on a density lookup table and data from ICRP 23 (1975)

In short:

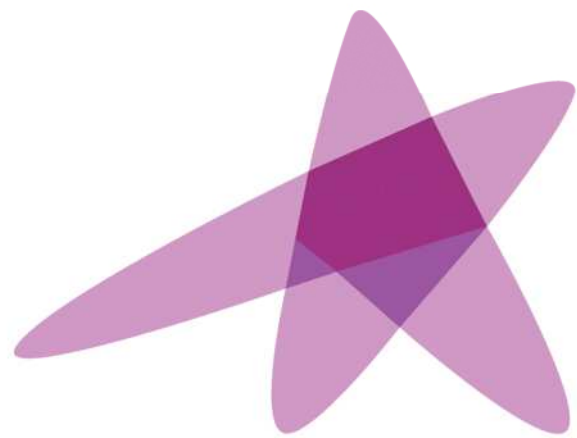
	ACE (Oncentra Brachy)	Acuros (BrachyVision)
Long heritage	√	√
Angular discretization	adaptive (“accuracy” selection & # sources)	adaptive (24 to 960 auto. varying within/between energy groups)
Spatial discretization	adaptive multi-resolution Cartesian grid (“accuracy” selection)	adaptive multi-resolution Cartesian grid (auto. based on scatter fluence gradient)
Pre-calculated data as input	Primary dose for source model, energy spectra, kernels	Phase space file for source model
Energy discretization	-	37 groups (adaptive for the scatter fluence using an appropriate energy weighting function $f(E)$)
Primary scatter separation	√	√
Ray-tracing for primary	√	√
Successive scattering	Prim. dose → 1 st scatter SCERMA → multiple scatter SCERMA	Prim. fluence → 1 st scatter source

In short:

	ACE (Oncentra Brachy)	Acuros (BrachyVision)
Applicator libraries	√	√
Pre-fixed calculation settings to optimize t vs. accuracy	√	√
Type A uncertainty (through pre-calculated data)	√	√
Type B uncertainty	√ cross sections, ray effects, spectral changes in low E/high Z, approx. inhomogeneity correction, ray trace in high scatter gradients, kernel tilting, use of geometry specific kernels	√ cross sections, ray effects, E and spatial discretization, ray trace in high scatter gradients
Where to look for type Bs:	high gradients such as very close to the source(s), away from implant, close to geom. boundaries, high Z inhomogeneities	high gradients such as very close to the source(s), away from implant

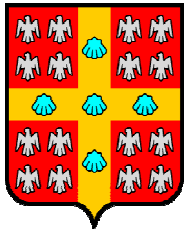
In short:

	ACE (Oncentra Brachy)	Acuros (BrachyVision)
Material definition	individual voxel density from CT + user defined (ROI based) materials from list based on TG186 (ICRU 46, Woodard & White 1986) CT based in future version	CT based: individual voxel density from CT + material from density look up table based on ICRP 23 1975
Dose reporting medium	local medium	originally water now both water and local medium
Dose calculation grid	geometry defined by imaging	(user defined) output grid + 10cm (unless end of CT image is met)
Use in plan optimization	X	X (?)



ESTRO

School



UNIVERSITÉ
LAVAL



Commissioning and Evaluation of Dose Calculation Algorithms

Prof. Luc Beaulieu, Ph.D., FAAPM

*1- Département de physique, de génie physique et d'optique, et
Centre de recherche sur le cancer, Université Laval, Canada*

*2- Département de radio-oncologie et Centre de recherche du CHU
de Québec, CHU de Québec, Canada*

Vienna, May 29 – June 1 2016



Disclosures

- Elements from TG-186 and of the AAPM/ESTRO/ABG Working Group on Model-based Dose Calculation Algorithms will be presented.
 - WG is working with all brachytherapy TPS vendors.

Acknowledgements AAPM/ESTRO/ABG WG

- Luc Beaulieu, CHUQ (Chair)
- Å. Carlsson Tedgren
- A. Haworth
- J. Lief
- Y. Ma
- F. Mourtada
- P. Papagianni
- M.J. Rivard
- F.A. Siebert (Vice-chair)
- R. Smith
- R. S. Sloboda
- R.M. Thomson
- J. Vijande
- F. Verhaegen

Key References

- Comprehensive Brachytherapy: physical and clinical aspect. JLM Venselaar, D Baltas, AS Meigooni and P.J. Hoskin. CRC Press, Taylor & Francis, 2013.
- Brachytherapy physics, 2ed, AAPM monograph #31, 2005.
- Beaulieu L, Carlsson Tedgren A, Carrier J-F, Davis SD, Mourtada F, Rivard MJ, et al. Report of the Task Group 186 on model-based dose calculation methods in brachytherapy beyond the TG-43 formalism: Current status and recommendations for clinical implementation. *Med Phys* 2012;39(10):6208–36.
- Rivard MJ, Coursey BM, DeWerd LA, Hanson WF, Saiful Huq M, Ibbott GS, et al. Update of AAPM Task Group No. 43 Report: A revised AAPM protocol for brachytherapy dose calculations. *Med Phys* 2004;31(3):633–74.
- Rivard, Beaulieu, and Mourtada. *Med Phys* 2010;37:2645-58

Learning Objectives

- TPS Commissioning.
- Commissioning of dose calculation:
 - TG43
 - Review TG186 commissioning requirements
 - Overview of the Commissioning under the AAPM-ESTRO-ABG Working Group on Model-based dose calculation algorithm

Commissioning

Google:

“Process by which an equipment, facility, or plant (which is installed, or is complete or near completion) is tested to verify if it functions according to its design objectives or specifications”

Basics

- General software functions (manufac. specs.)
- Training
- Integration into IT environment
- Acceptance testing plans (annual!)
 - Applicators' library (dimension, ...)
 - Input source strength (each source change)
 - Volume rendering (DVHs!)
 - Transfer to TCS
 - Reports
- ...

TPS Commissioning Guidelines

Consider AAPM Task Group Reports and Guidance

TG-53 QA for Clinical Radiotherapy Treatment Planning (1998)

TG-56 Code of Practice for Brachytherapy (1997)

TG-59 High Dose Rate Tx Delivery (1998)

Consider AAPM Summer School texts

1994 Chapters 28, 30, 31, 32

2005 Chapters 6, 7, 11, 22, 32, 48

Consider Bruce Thomadsen's 1999 text

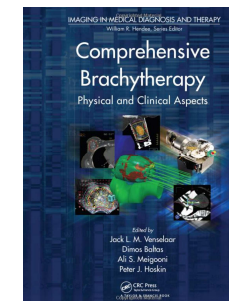
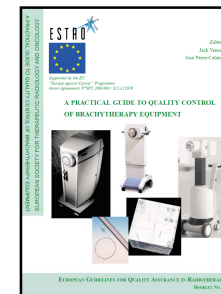
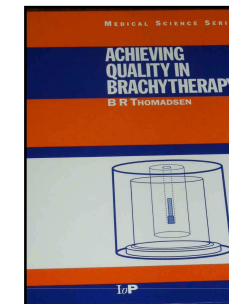
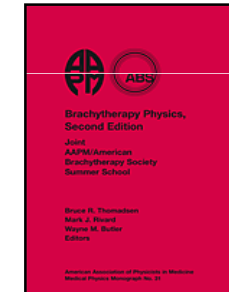
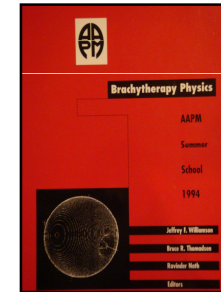
Achieving Quality in Brachytherapy

Consider 2004 ESTRO Booklet 8 text

A Practical Guide to Quality Control of Brachytherapy Equipment

Consider 2013 CRC press book

Comprehensive Brachytherapy: physical and clinical aspect



AAPM TG-53 TPS Commissioning

TABLE A5-3. Source Library Information

Radionuclide	Active length
Source type	Overall length
Model number/vendor	Capsule thickness
Source strength	Capsule composition
Source strength units	Filtration
Name	Algorithm type
Coding	Algorithm parameters
Availability	Anisotropy correction
Decay constant	Other features
Half life	

2004 ESTRO Booklet 8

A PRACTICAL GUIDE TO QUALITY CONTROL OF BRACHYTHERAPY EQUIPMENT
EUROPEAN SOCIETY FOR THERAPEUTIC RADIOLOGY AND ONCOLOGY

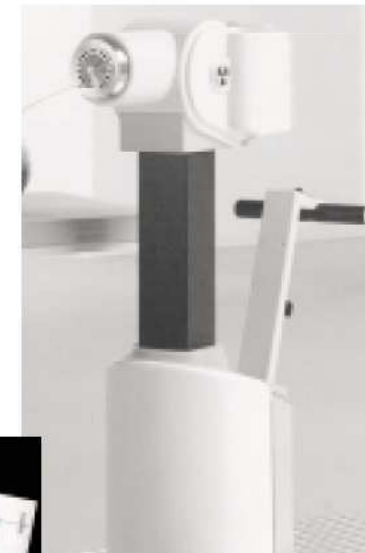
ESTRO 



*Supported by the EU
"Europe against Cancer" Programme
Grant Agreements N°SPC.2002480 / S12.322029*

*Edited by
Jack Venselaar
José Pérez-Calatayud*

A PRACTICAL GUIDE TO QUALITY CONTROL OF BRACHYTHERAPY EQUIPMENT



Chapter 9.2 on TPS Commissioning

9.2 Physicists tasks at commissioning and continued use of a BT TPS

Dose calculation algorithms

Source data

Basic dose calculations

Documentation of dose distributions

Influence of source manipulations

Influence of shields, missing tissue and tissue inhomogeneities

Dose volume histograms

Optimisation routines

Reconstruction techniques

Chapter 9.2 on TPS Commissioning

9.2.6 *Influence of shields, missing tissue, and inhomogeneities* (abridged)

Presently, only simple correction algorithms are applied in some TPS. The effect of these algorithms must be verified and documented.

yes

Published shielding or tissue inhomogeneity data are based on MC.

yes

Validation of these MC data should be done by comparing with measured data, such as those obtained using TLD or small ionisation chambers.

ouch!

Algorithms are under development to account for scatter conditions and tissue inhomogeneities.

yes

Validation of these algorithms should be done in a similar way to the method used for checking the shielding algorithms.

ouch!

AAPM TG-53 TPS Commissioning

TABLE A5-5. Brachytherapy Dose Calculation Issues

Confirmation of dose model input data (**from publications**) for each source type. The basic **literature datasets** selected for use and comparisons should be identified.

Comparison of single point, 2-D and 3-D dose distributions with **hand calculations** for a single source, for each source type in the source library.

Comparison of point, 2-D and 3-D dose distributions with **hand calculations** for multiple source configurations, for at least one source type.

Any **applicator shielding effects** included or neglected should be explained and documented.

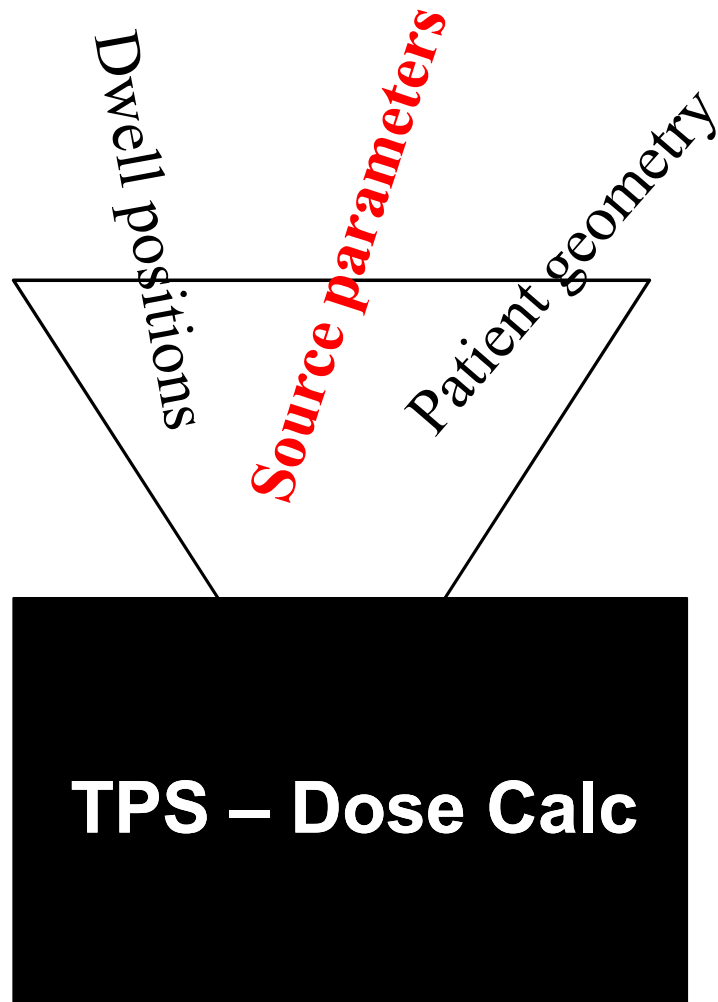
Verify correct behavior of dose calculations, sometimes **including tissue multiple scattering and attenuation**, at selected distances from the source.

Let's take a step back...



**KEEP
CALM
AND
TRUST THE
MEDICAL PHYSICIST**

TG 43 Ingredients



Dose parameters,
DVHs, isodoses

Before Starting

Get TG 43 parameters for sources used in your clinic

1- Concensus data sets

AAPM Publications such as TG43U1/S1

2- RPC and Original Publications

- <http://rpc.mdanderson.org/RPC/home.htm>

Joint AAPM/RPC Registry of Brachytherapy Sources Meeting the AAPM Dosimetric Prerequisites

Source Registry	Prerequisites	Dosimetry Datasets	Application for Registry
Registry Policy	Disclaimer	3 rd Party Checks	AAPM Publications

125 I Sources		
Manufacturer	Sources	Model
Amersham	OncoSeed	6711
Amersham	ThinSeed	9011
BEBIG GmbH	IsoSeed@I-125	I25.S06
Best Medical International Inc	Best@ I-125 Source	2301
IsoAid, LLC	Advantage I-125	IAI-125A
Core Oncology, Inc.	ProstaSeed®	125SL 125SH
Nucletron	SelectSeed I-125	130.002
Bard Urological Division	125 Implant Seeds	STM1251
Theragenics Corporation®	I-Seed I-125	I25.S06
Theragenics	I-Seed I-125	AgX100

103 Pd Sources		
Manufacturer	Sources	Model
Best Medical International Inc	Best Palladium - 103	2335
IsoAid, LLC	Advantage Pd-103	IAPd-103A
Theragenics Corporation®	TheraSeed®	200

131 Cs Sources		
Manufacturer	Sources	Model
IsoRay Medical Inc.	Proxcelan	Cs - 1

192 Ir HDR Sources		
Manufacturer	Sources	Model
Mallinckrodt Diagnostica, The Netherlands	Nucletron mHDR	V-1 ("Classic")
AEA Technology QSA, Inc	Nucletron mHDR	V-2
Varian Oncology Systems	Varian HDR	VS2000

2- RPC and Original Publications

- <http://rpc.mdanderson.org/RPC/home.htm>

Joint AAPM/RPC Registry of Brachytherapy Sources Meeting the AAPM Dosimetric Prerequisites

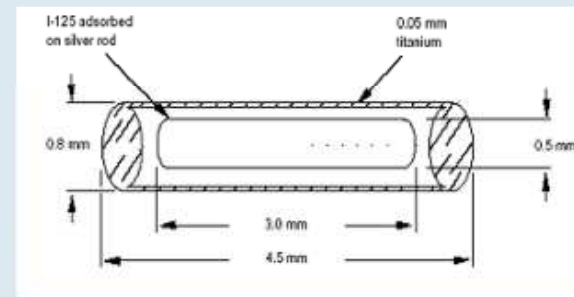
Source Registry	Prerequisites	Dosimetry Datasets	Application for Registry
Registry Policy	Disclaimer	3 rd Party Checks	AAPM Publications

125 I Sources		
Manufacturer	Sources	Model
Amersham	OncoSeed	6711

103 Pd Sources		
Manufacturer	Sources	Model
Best Medical International	Best Brachytherapy	2225

OncoSeed ¹²⁵I Model 6711

GE Healthcare, Medi-Physics Inc.
Arlington Heights, IL 60004
<http://www.amershamhealth-us.com/>
distributed by: Oncura Inc.
(877) 639-8060

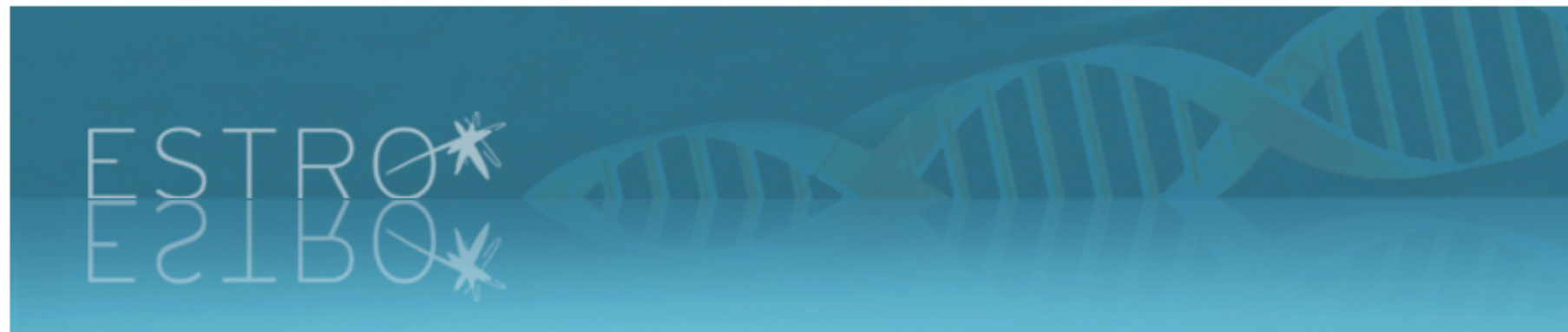


- Williamson J. F., Coursey B. M., DeWerd L. A., Hanson W. F., Nath R., Ibbott G. S., "Guidance to users of Nycomed Amersham and North American Scientific, Inc., I-125 Interstitial Sources: Dosimetry and calibration changes: recommendations of the American Association of Physicists in Medicine Radiation Therapy Committee Ad Hoc Subcommittee on Low-Energy Seed Dosimetry" *Med. Phys.* **36**: 570-573, 1999.
- James Dolan , Zuofeng Li, Jeffrey F. Williamson., "Monte Carlo and experimental dosimetry of an ¹²⁵I brachytherapy seed" *Med. Phys.* **33**: 4675-4684, 2006.
- Other relevant dosimetry publications are listed in the TG-43 Protocol

added to Registry March 1,2001; Updated Dec. 13, 2006

3- ESTRO and Carleton websites

- <http://www.estro.org/estroactivities/Pages/TG43BTDOSMETRICPARAMETERS.aspx>
- http://www.physics.carleton.ca/clrp/seed_database/



TG43 HOME PAGE

General information

By clicking here you will be taken to a page that contains dosimetry data for selected photon emitting brachytherapy sources which are most commonly used in the European area. Most of them have a world wide spread. The focus is on high energy photon emitting sources used in manual and remotely controlled afterloading brachytherapy technique: caesium-137, iridium-192 and cobalt-60, and one caesium-131 source. See Section 5.1 "High Energy Sources" in [General Dosimetry Data](#).

Furthermore, full data sets are included in some iodine-125 and palladium-103 seed sources which comply with the dosimetric prerequisites of the AAPM TG-43 subcommittee. See Section 5.2 in [General Dosimetry Data](#) and also Rivard et al 2004.

Data sets of photon emitting sources, containing dosimetric parameters and reference data for brachytherapy applications, are presented following the dosimetry formalism recommended by the AAPM TG-43. The data sets include:

- General information,
- Links to the abstracts of the original publications,
- Source design,
- Dose rate table (along-away),
- Geometry function,
- Dose rate constant,
- Radial dose function,
- Anisotropy function and, if available, anisotropy factor

TG43 - Working Group 4

[General Dosimetry Data](#)

[BT Dosimetric Parameters](#)

BRAPHYQS Working Group

[Membership](#)

[Work Packages](#)

[Meetings and Reports](#)

[Publications](#)

[BRAPHYQS Home Page](#)

Contacts

[Working Group Co-ordinator](#)

[ESTRO Co-ordinator](#)

Brachytherapy Seed Data:

For the current list of seeds covered by TG-43 and the Joint AAPM/RPC brachytherapy source registry please visit the [RPC](#) website.

¹²⁵I Seeds:

- Amersham, EchoSeed, [6733](#)
- Amersham, OncoSeed, [6702](#)
- Amersham, OncoSeed, [6711](#)
- BEBIG GmbH, IsoSeed, [I25.S17](#)
- BEBIG GmbH/ Theragenics Co., IsoSeed, [I25.S06](#)

- Bacon Co., Braquibac, [Braquibac](#)
- Best Industries, Best I-125, [2301](#)
- DRAXIMAGE, BrachySeed, [LS-1](#)
- IBt, InterSource, [1251L](#)
- Imagyn, IsoStar, [IS-12501](#)
- Implant Sciences, IPlant, [3500](#)
- IsoAid, Advantage, [IA1-125A](#)
- Mills Bio. Pharm., ProstaSeed, [125SL](#)
- NASI, Prospera, [Med3631 - ideal](#)
- Nucletron, SelectSeed, [130.002*](#)
- STM, Implant, [STM1251](#)
- Syncor, PharmaSeed, [BT-125-1](#)
- Syncor, PharmaSeed, [BT-125-2](#)

¹⁰³Pd Seeds:

- BEBIG GmbH, IsoSeed, [Pd-103](#)
- Best Industries, BestPd-103, [2335](#)
- DRAXIMAGE, BrachySeed, [Pd-1](#)
- IBt, InterSource, [1031L](#)
- IBt, OptiSeed, [1032P](#)

- IsoAid, Advantage, [IAPd-103A](#)
- NASI, Prospera Pd-103, [Med3633 - ideal](#)
- Syncor, PharmaSeed, [BT-103-3](#)
- Theragenics Co., TheraSeed, [200](#)

¹⁹²Ir HDR Seeds:

- Amersham, Buchler, [HDR*](#)
- BEBIG GmbH, GI192M11, [HDR*](#)
- GammaMed, 12i, [HDR*](#)
- GammaMed, Plus, [HDR*](#)
- Isodose Control, Flexisource, [HDR*](#)
- Nucletron, microSelectron-[HDR*](#) v1 (classic)
- Nucletron, microSelectron-[HDR*](#) v2
- S.P.E.C. Inc., Co., M19, [HDR*](#)
- Varian, VariSource (classic), [HDR*](#)
- Varian, VariSource VS2000, [HDR*](#)

¹⁹²Ir PDR Seeds:

- GammaMed, 12i, [PDR*](#)
- GammaMed, Plus, [PDR*](#)
- Nucletron, microSelectron-[PDR*](#) v1
- Nucletron, microSelectron-[PDR*](#) v2

¹⁶⁹Yb HDR Seeds:

- Implant Sciences Corporation, 4140, [HDR*](#)

* Primary and Scatter Separated (PSS) dose data available

Example of Dosimetry Parameter Dataset

View TG43 data

General information

Treatment machine name: Clinique mHDR v2 Source name: 192-Ir-mHDR-v2

TG43 dosimetry data

Dose Rate Constant, Λ : 1.1080 cGy/h/U, where U = cGy cm²/h

Radial Dose Function, $g(r)$

r (mm)	$g(r)$
0.0	1.0080
5.0	1.0000
10.0	1.0000
15.0	1.0030
20.0	1.0070
25.0	1.0080
30.0	1.0080
35.0	1.0067
40.0	1.0040
45.0	1.0002
50.0	0.9950
55.0	0.9884
60.0	0.9810
65.0	0.9732
70.0	0.9640

2D Anisotropy Function, $F(r, \theta)$

r (mm)	θ (degrees)												
	0.0	5.0	10.0	15.0	20.0	25.0	30.0	35.0	40.0	45.0	50.0	55.0	60.0
0.0	0.7910	0.7950	0.7850	0.8370	0.8760	0.9083	0.9360	0.9442	0.9589	0.9694	0.9724	0.9780	0.984
5.0	0.6670	0.6710	0.7270	0.7863	0.8360	0.8749	0.9040	0.9262	0.9433	0.9564	0.9672	0.9770	0.984
10.0	0.6310	0.6610	0.7270	0.7893	0.8390	0.8752	0.9020	0.9250	0.9429	0.9575	0.9693	0.9778	0.984
15.0	0.6339	0.6751	0.7378	0.7981	0.8449	0.8796	0.9058	0.9264	0.9460	0.9601	0.9691	0.9773	0.984
20.0	0.6450	0.6840	0.7450	0.8017	0.8460	0.8803	0.9070	0.9270	0.9481	0.9612	0.9679	0.9767	0.985
25.0	0.6535	0.6920	0.7516	0.8065	0.8492	0.8809	0.9066	0.9282	0.9492	0.9624	0.9696	0.9778	0.985
30.0	0.6600	0.7000	0.7580	0.8122	0.8540	0.8820	0.9060	0.9296	0.9497	0.9634	0.9723	0.9794	0.985
35.0	0.6676	0.7084	0.7642	0.8175	0.8587	0.8837	0.9062	0.9303	0.9497	0.9636	0.9733	0.9797	0.984
40.0	0.6765	0.7170	0.7703	0.8222	0.8631	0.8859	0.9073	0.9304	0.9494	0.9630	0.9725	0.9789	0.983
45.0	0.6862	0.7259	0.7762	0.8266	0.8674	0.8885	0.9090	0.9300	0.9488	0.9619	0.9705	0.9771	0.981
50.0	0.6960	0.7350	0.7820	0.8309	0.8720	0.8915	0.9110	0.9293	0.9478	0.9604	0.9680	0.9749	0.979

Close

Example of Dosimetry Parameter Dataset

1	r [cm]	$g_L(r)$	$g_P(r)$	r [cm]	$\phi(r)$	$F(r,8)$	0	10	20	30	40	50	60	70	80
2	0.10	0.990	0.582	0.25	1.164	0.05							1.067	0.996	0.985
3	0.25	1.021	0.889	0.5	0.973	0.075					1.050	1.006	0.994	0.996	0.996
4	0.50	1.030	0.998	1.0	0.933	0.1				1.046	0.996	0.990	0.993	0.988	0.999
5	1.00	1.000	1.000	1.5	0.931	0.15			1.039	0.978	0.958	0.977	0.988	0.987	0.996
6	1.50	0.943	0.949	2.0	0.931	0.2		0.987	0.921	0.940	0.960	0.975	0.984	0.988	0.997
7	2.00	0.872	0.879	2.5	0.932	0.25	0.494	0.574	0.785	0.899	0.943	0.967	0.986	0.995	1.000
8	2.50	0.795	0.803	3.0	0.934	0.5	0.610	0.513	0.679	0.808	0.892	0.944	0.974	0.990	0.997
9	3.00	0.717	0.724	3.5	0.935	1	0.580	0.561	0.705	0.813	0.885	0.933	0.967	0.987	0.997
10	3.50	0.643	0.650	4.0	0.937	2	0.652	0.626	0.743	0.830	0.893	0.934	0.967	0.987	0.997
11	4.00	0.573	0.579	4.5	0.938	5	0.690	0.700	0.789	0.854	0.905	0.941	0.968	0.986	0.996
12	4.50	0.508	0.513	5.0	0.938	10	0.709	0.742	0.815	0.872	0.912	0.947	0.972	0.990	0.997
13	5.00	0.448	0.453	6.0	0.939										
14	6.00	0.347	0.351	7.0	0.942										
15	7.00	0.265	0.268	10.0	0.948										
16	8.00	0.201	0.203												
17	9.00	0.151	0.153												
18	10.00	0.114	0.115												

$\Lambda = 1.011$

$L = 3.7 \text{ mm or } 0.37 \text{ cm}$

From M. Rivard

$$\begin{aligned}
 \text{1D b): } \dot{D}(r, \theta) &= S_k \cdot \Lambda \cdot \left(\frac{r_0}{r} \right)^2 \cdot g_P(r) \cdot \phi(r) \\
 &= 0.4 \cdot 1.011 \cdot (1/2)^2 \cdot 0.879 \cdot 0.931
 \end{aligned}$$

Notes

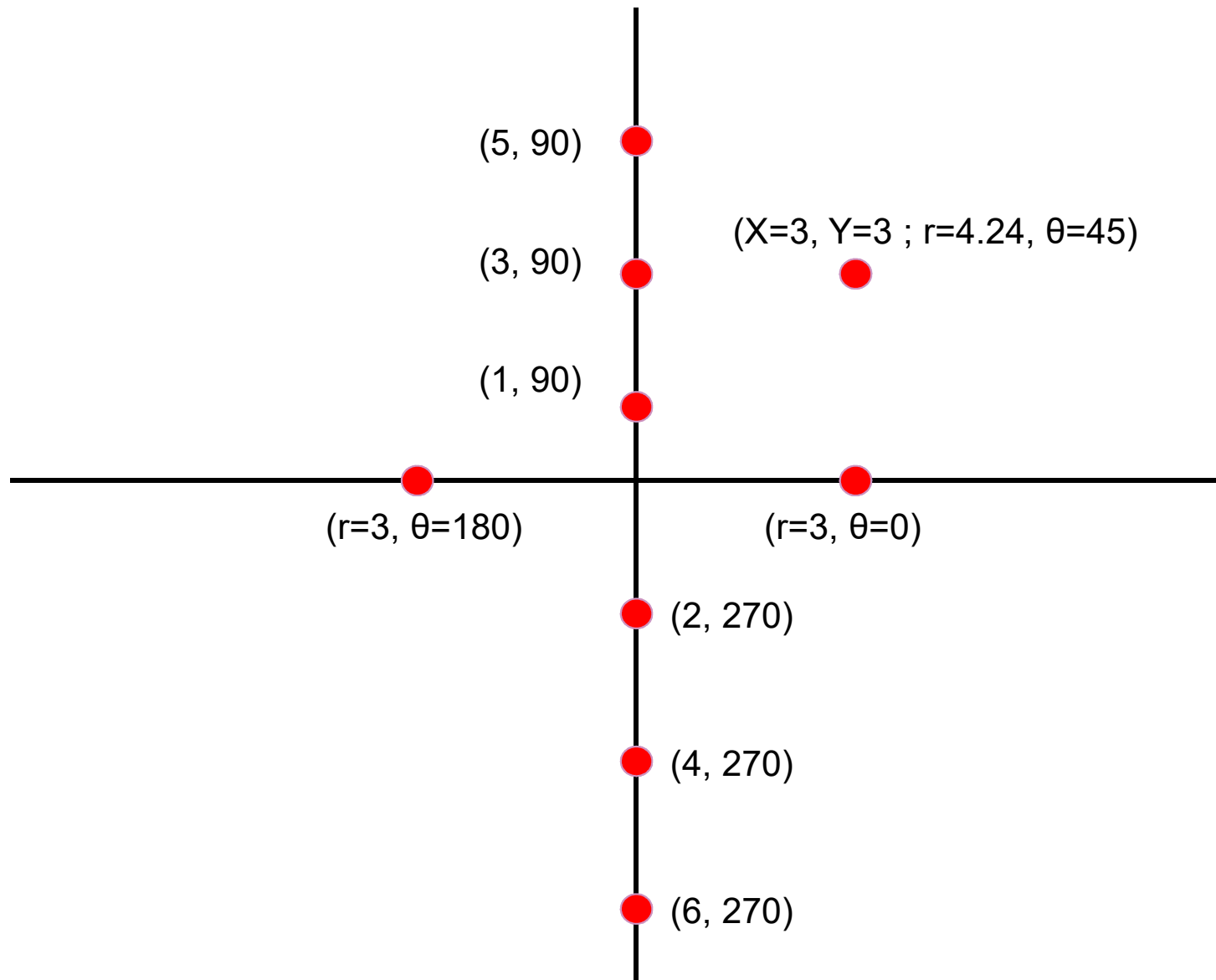
1. S_k is in unit of $\text{cGy cm}^2 \text{ h}^{-1}$ (or U)
2. At $(r=r_0, \theta = \theta_0)$, $\dot{D}_0(1, 90) = S_k \Lambda$.
3. If $t_{\text{tx}} \gg t_{1/2}$ $D = \dot{D}_0 / \lambda = \dot{D}_0 t_{1/2} / \ln 2$.
4. If $t_{\text{tx}} \ll t_{1/2}$ ($< 0.05 t_{1/2}$) $D = \dot{D}_0 t_{\text{tx}}$

Before Starting Tx

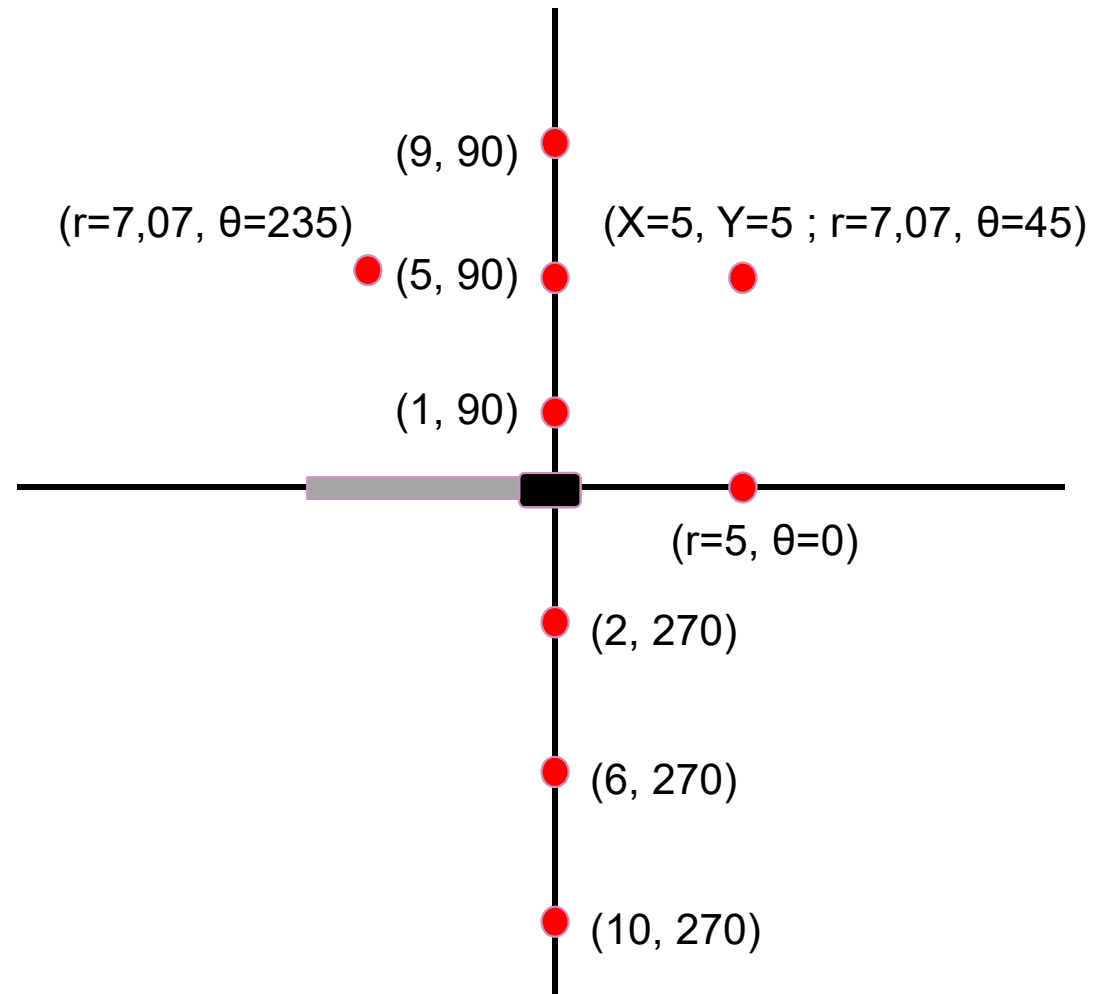
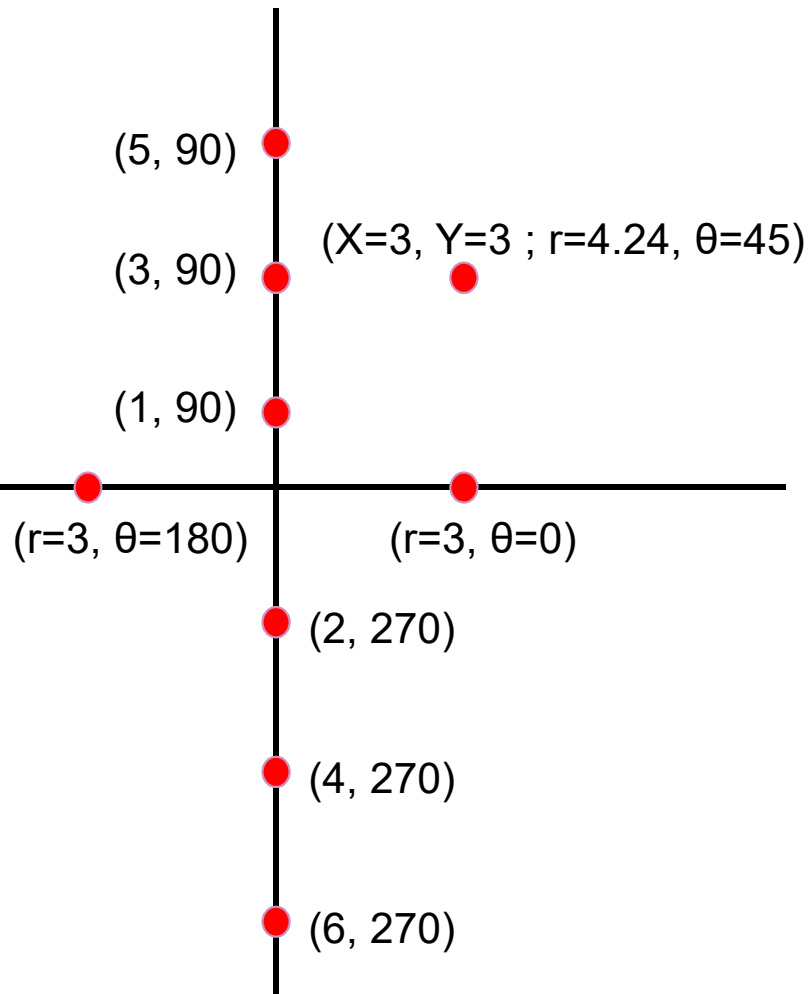
Source Strength

- Certificate
- Well-Chamber measurements (NIST- tracable)

Test configuration: LDR seeds



Low energy seeds vs ^{192}Ir



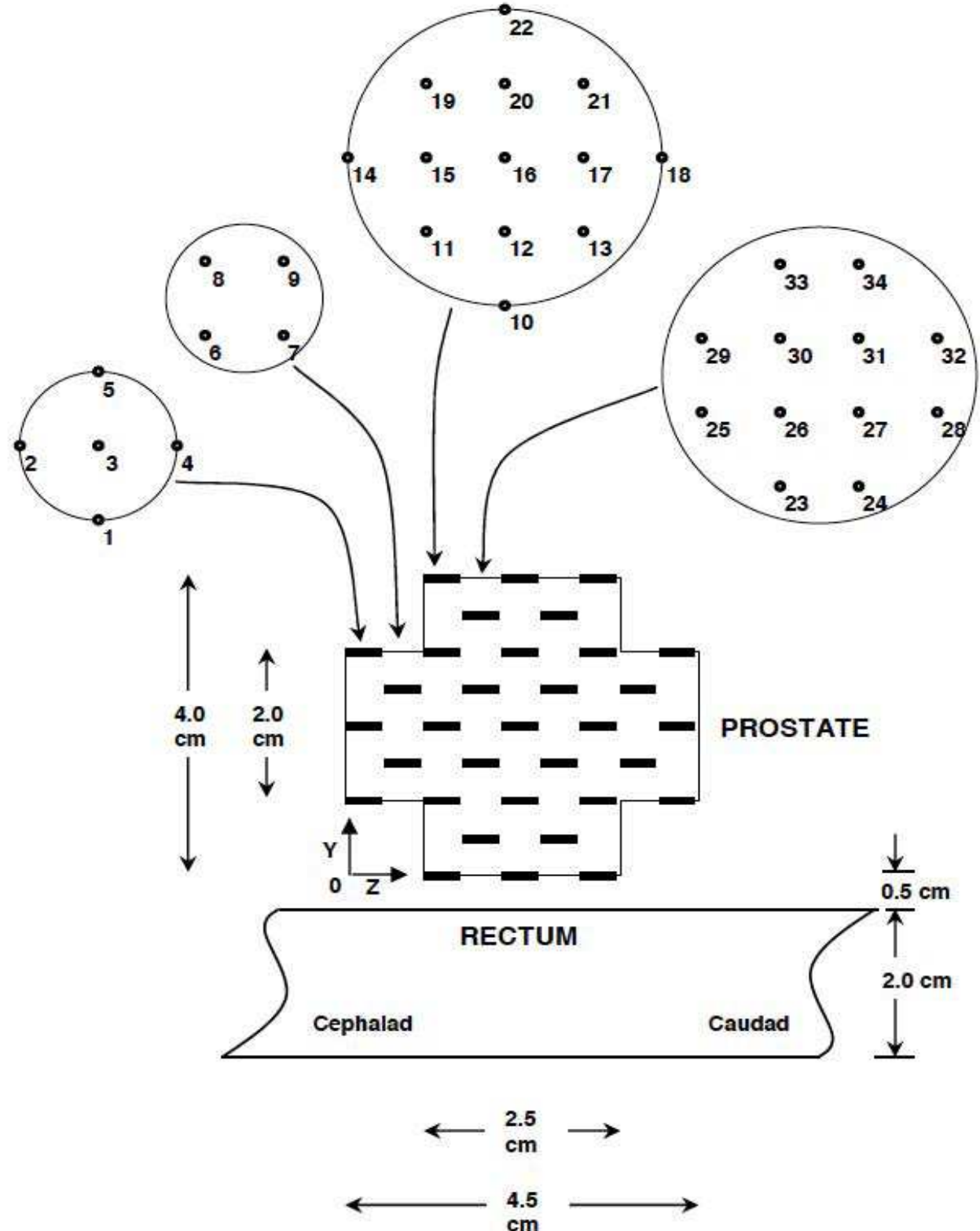
Report Sheet

	r (cm)	Theta	Hand Calc	TPS	Difference
1	1	90			
2	2	270			
3	3	90			
4	4	270			
5
6	4.24	45			
...					

Validation Before Tx

- Hand Calculations versus TPS
 - Various distances from the source
 - $< 1\%$
- More complex geometries / multiple sources (e.g. RTOG 0232)
 - Make an excel spreadsheet
 - MathLab routines
 - Python / C++ ...
 - $< 2\%$

Possible validation by QARC/RPC

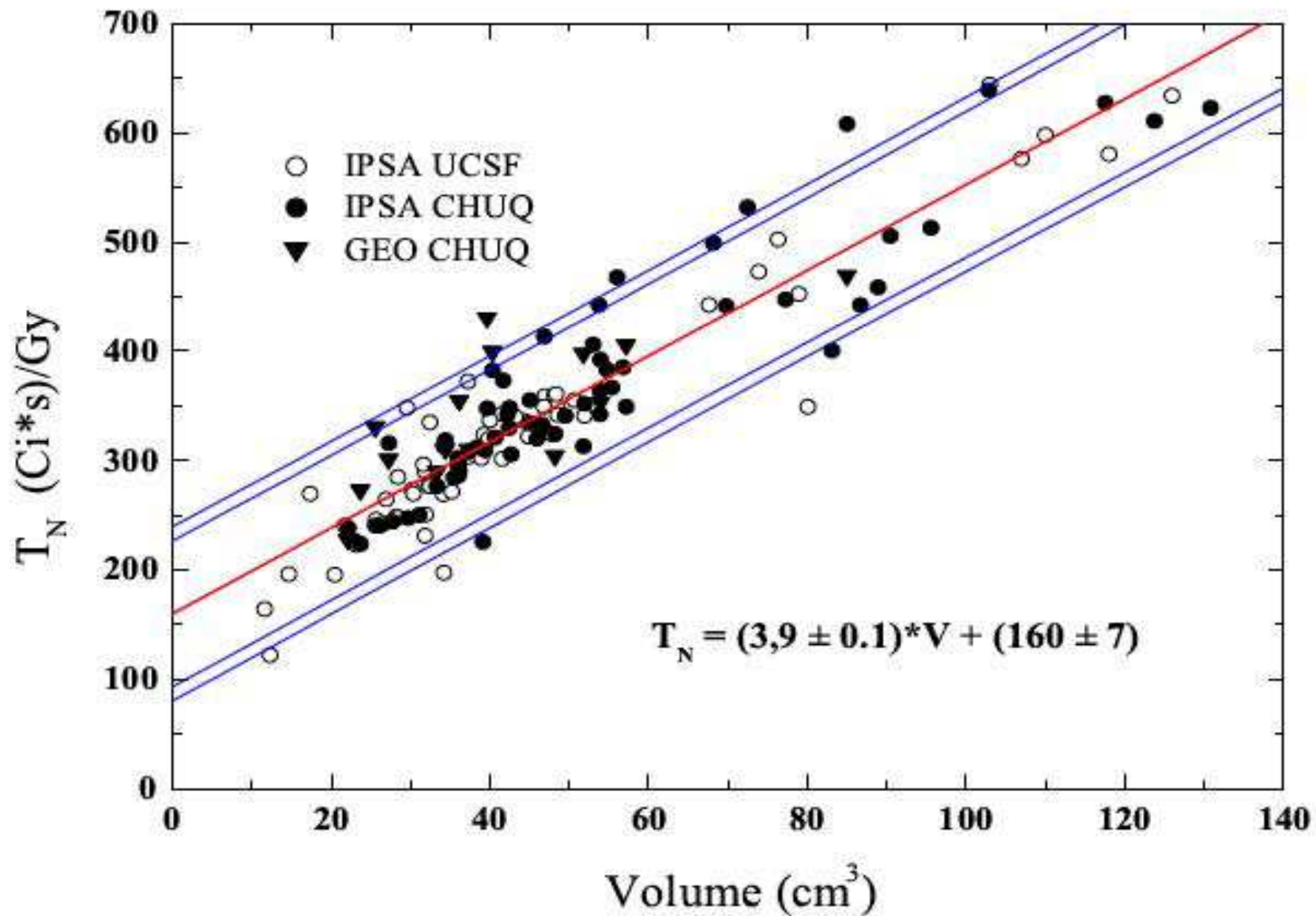


When to Perform

- After each source change (HDR)
- Adopting a new source model (e.g. LDR)
- Any change in your system
 - New software version
 - New hardware
- New consensus data set
- ...At least once a year

Validation related to Tx

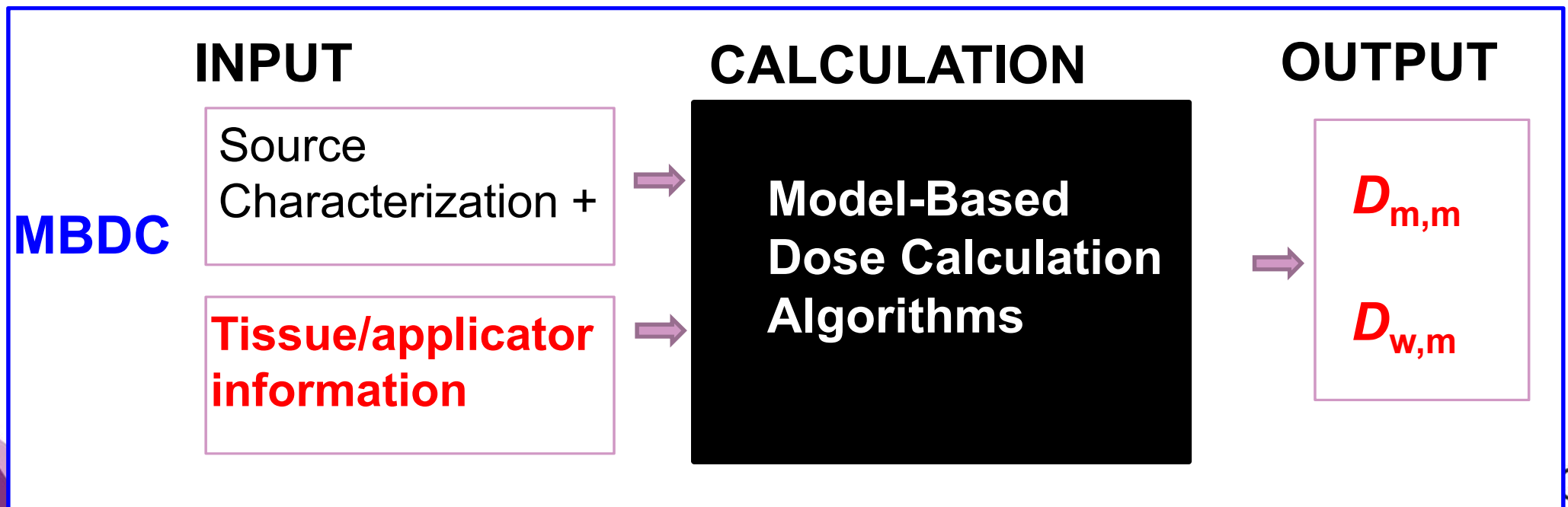
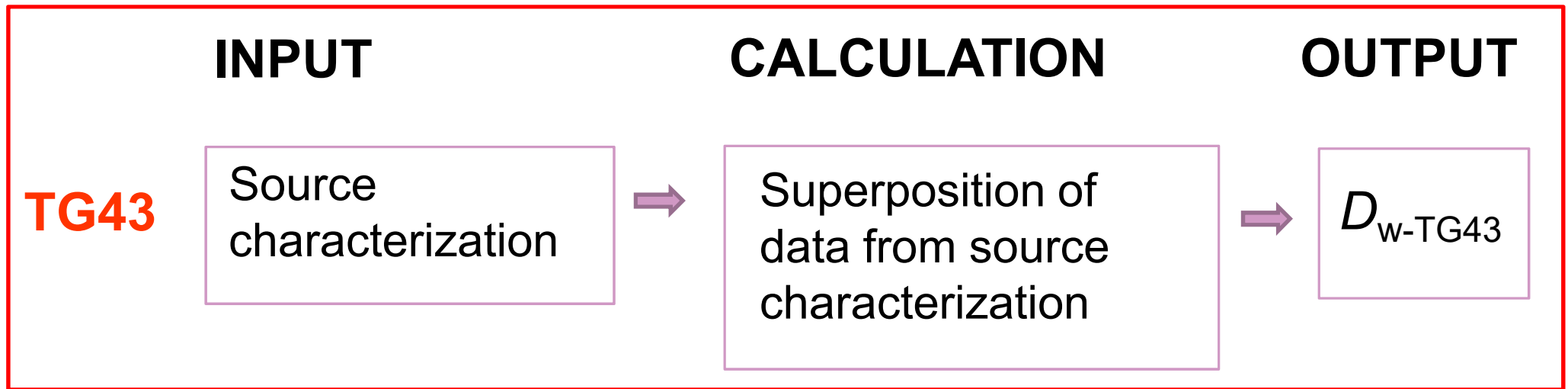
- Should an independant verification be performed?
 - **YES**
 - Second, validated TPS (reading DICOM-RT)
 - Home-made validated TG43 implementation (MathLab/C++/VB + DICOM-RT import)
 - Nomogram type chart



C. Tremblay, MS thesis, 2003

Going Beyond TG43

Factor-based vs Model-based



Report of the Task Group 186 on model-based dose calculation methods in brachytherapy beyond the TG-43 formalism: Current status and recommendations for clinical implementation

Luc Beaulieu^{a)}

Département de Radio-Oncologie et Centre de Recherche en Cancérologie de l'Université Laval, Centre hospitalier universitaire de Québec, Québec, Québec G1R 2J6, Canada and Département de Physique, de Génie Physique et d'Optique, Université Laval, Québec, Québec G1R 2J6, Canada

Åsa Carlsson Tedgren

Department of Medical and Health Sciences (IMH), Radiation Physics, Faculty of Health Sciences, Linköping University, SE-581 85 Linköping, Sweden and Swedish Radiation Safety Authority, SE-171 16 Stockholm, Sweden

Jean-François Carrier

Département de radio-oncologie, CRCHUM, Centre hospitalier de l'Université de Montréal, Montréal, Québec H2L 4M1, Canada and Département de physique, Université de Montréal, Montréal, Québec H3C 3J7, Canada

Stephen D. Davis

Department of Medical Physics, University of Wisconsin-Madison, Madison, Wisconsin 53705 and Department of Medical Physics, McGill University Health Centre, Montréal, Québec H3G 1A4, Canada

Firas Mourtada

Radiation Oncology, Helen F. Graham Cancer Center, Christiana Care Health System, Newark, Delaware 19899

Mark J. Rivard

Department of Radiation Oncology, Tufts University School of Medicine, Boston, Massachusetts 02111

Rowan M. Thomson

Carleton Laboratory for Radiotherapy Physics, Department of Physics, Carleton University, Ottawa, Ontario K1S 5B6, Canada

Frank Verhaegen

Department of Radiation Oncology (MAASTRO), GROW, School for Oncology and Developmental Biology, Maastricht University Medical Center, Maastricht 6201 BN, the Netherlands and Department of Medical Physics, McGill University Health Centre, Montréal, Québec H3G 1A4, Canada

Todd A. Wareing

Transpire Inc., 6659 Kimball Drive, Suite D-404, Gig Harbor, Washington 98335

Jeffrey F. Williamson

Department of Radiation Oncology, Virginia Commonwealth University, Richmond, Virginia 23298

(Received 7 May 2012; revised 26 July 2012; accepted for publication 2 August 2012; published 25 September 2012)

The charge of Task Group 186 (TG-186) is to provide guidance for early adopters of model-based dose calculation algorithms (MBDCAs) for brachytherapy (BT) dose calculations to ensure practice uniformity. Contrary to external beam radiotherapy, heterogeneity correction algorithms have only recently been made available to the BT community. Yet, BT dose calculation accuracy is highly dependent on scatter conditions and photoelectric effect cross-sections relative to water. In specific situations, differences between the current water-based BT dose calculation formalism (TG-43) and MBDCAs can lead to differences in calculated doses exceeding a factor of 10. MBDCAs raise three major issues that are not addressed by current guidance documents: (1) MBDCA calculated doses are sensitive to the dose specification medium, resulting in energy-dependent differences between dose calculated to water in a homogeneous water geometry (TG-43), dose calculated to the local medium in the heterogeneous medium, and the intermediate scenario of dose calculated to a small volume of water in the heterogeneous medium. (2) MBDCA doses are sensitive to voxel-by-voxel interaction cross sections. Neither conventional single-energy CT nor ICRU/ICRP tissue composition compilations provide useful guidance for the task of assigning interaction cross sections to each voxel. (3) Since each patient-source-applicator combination is unique, having reference data for each possible combination to benchmark MBDCAs is an impractical strategy. Hence, a new commissioning process is required. TG-186 addresses in detail the above issues through the literature review

Report of the Task Group 186 on model-based dose calculation methods in brachytherapy beyond the TG-43 formalism: Current status and recommendations for clinical implementation

1. recommendations to MBDCA early-adopters to evaluate:

- phantom size effect
- inter-seed attenuation
- material heterogeneities within the body
- interface and shielded applicators

2. commissioning process to maintain inter-institutional consistency

3. patient-related input data

4. research is needed on:

- tissue composition standards
- segmentation methods
- CT artifact removal

Approved by

ESTRO (BRAPHYQS, EIR)

AAPM (BTSC, TPC)

ABS (U.S. Phys Cmte)

ABG (Australia)

MBDCAs

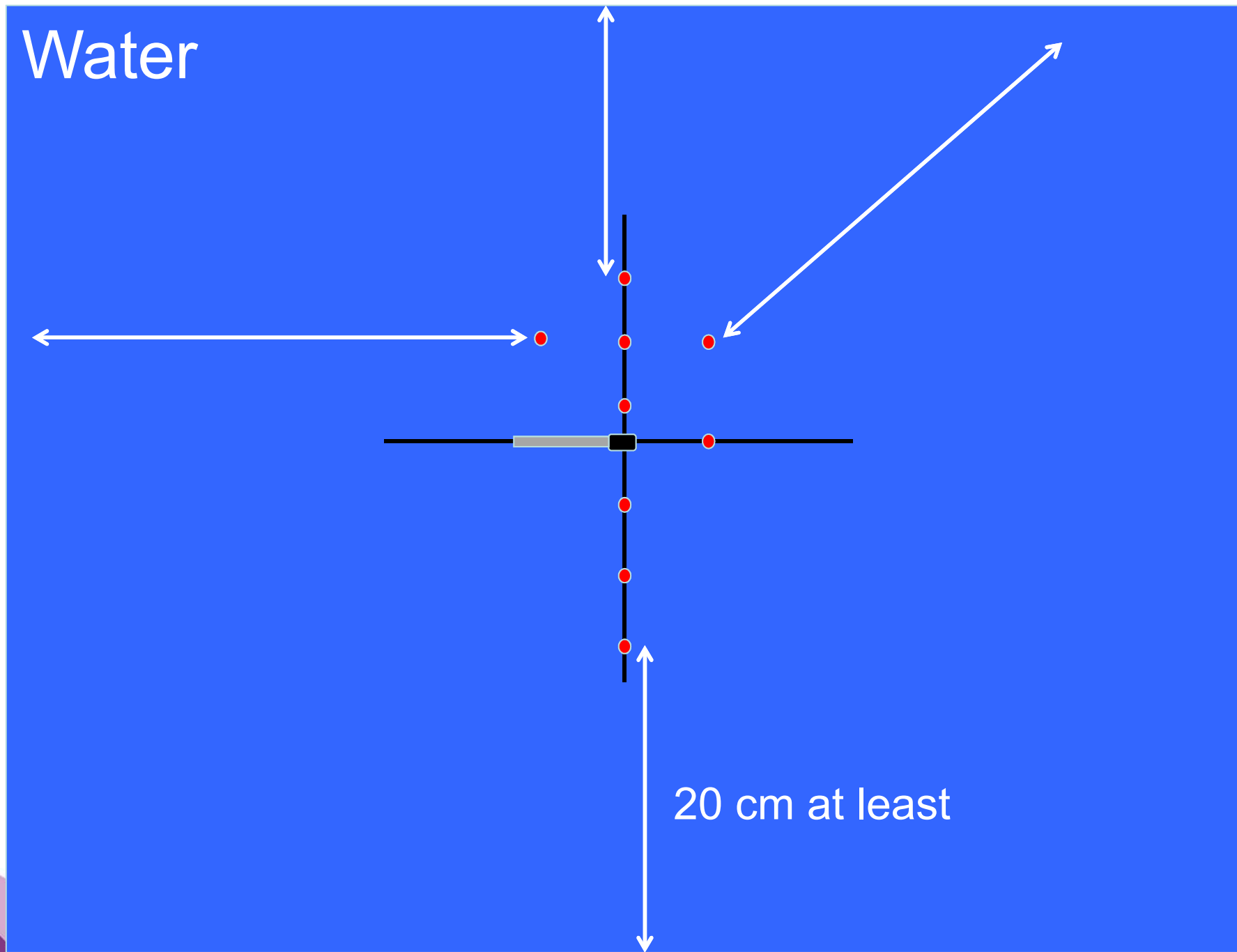
- Software commissioning guidance (TG186):

Level	Source Positions	Phantom	Benchmark Dose Distribution
1	single	H ₂ O full scatter	TG43
2	single, multiple	virtual geometry mimicking clinical scenario	MC derived from same geometry

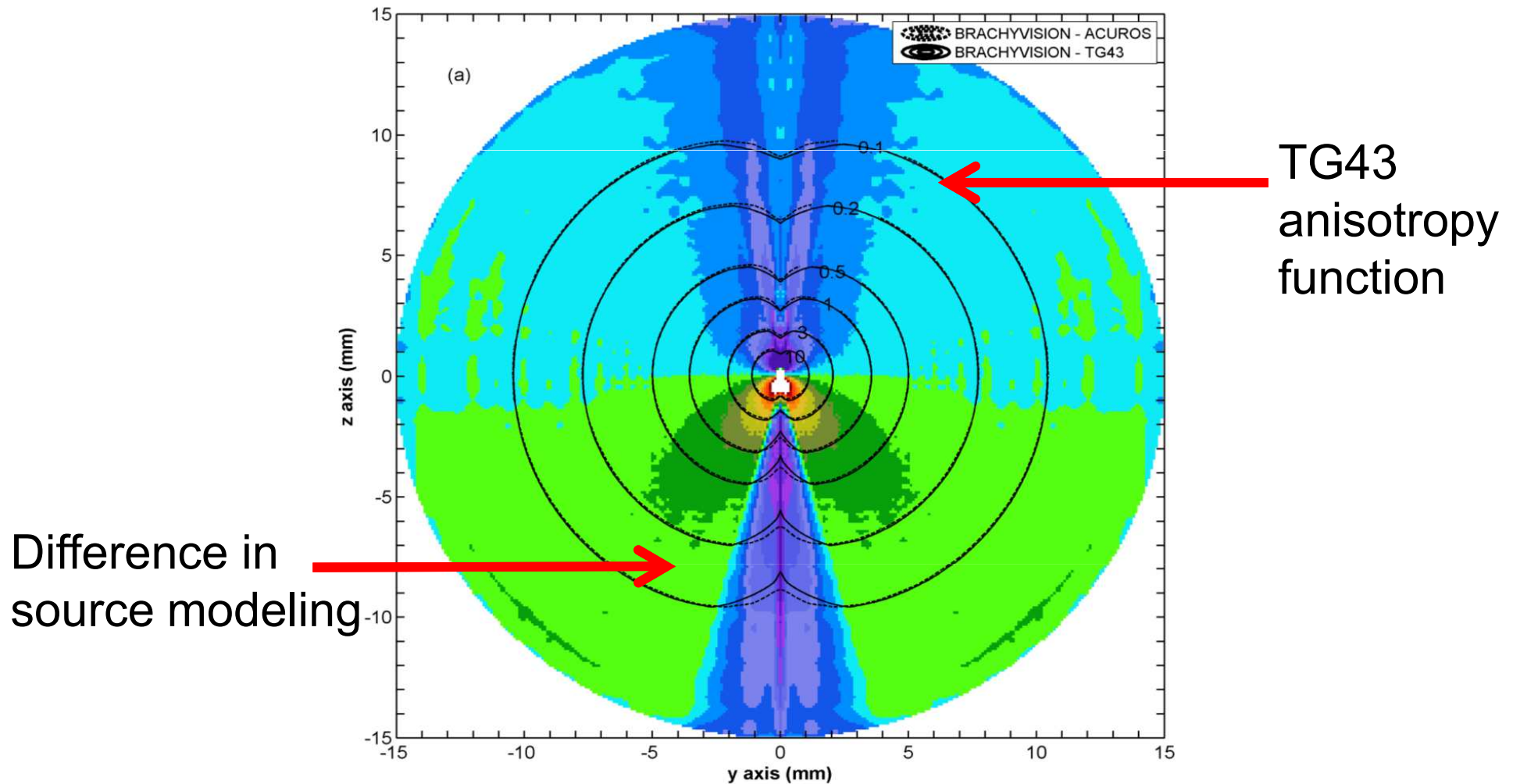
TG186 Commissioning Proposal

- Level 1: MBDCA should fall back to TG43 in well controlled conditions
 - Full scatter: $R-r \geq 5$ cm or 20 cm
 - All water
 - From TG43 expect $< 2\%$...

^{192}Ir Test Geometry for MBDCA

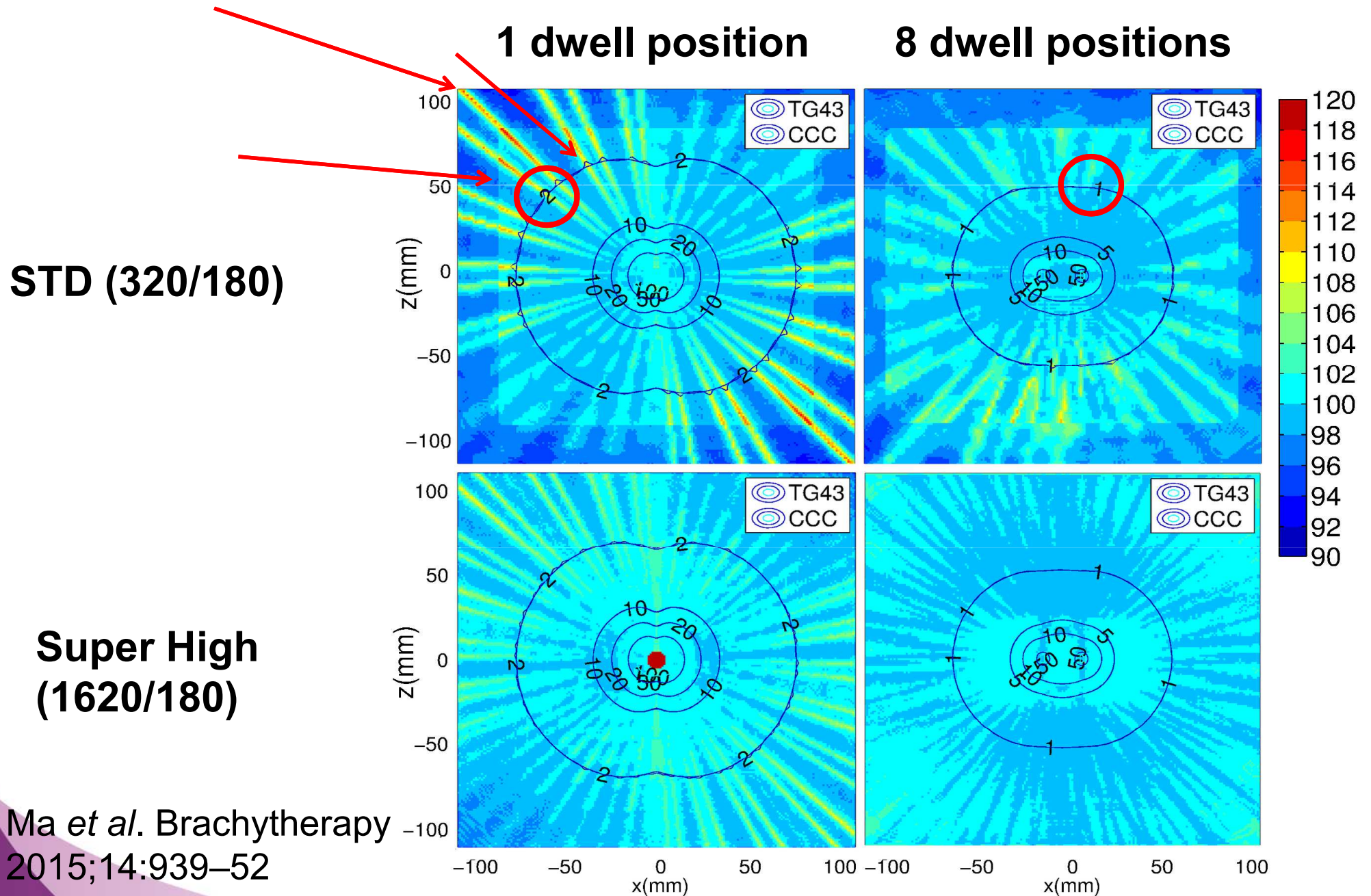


Acuros vs TG43: TG-43 conditions (L1)



Papagiannis P, Pantelis E, Karaiskos P. **Current state of the art brachytherapy treatment planning dosimetry algorithms.** Br J Radiol 2014;87(1041):20140163.

ACE vs TG43: TG-43 conditions (L1)



Lessons Learned

- Single source geometry is a difficult problem (gradients, ...)
- Go back to the physics and understand your model-based algorithm strength and limitation
- Set proper evaluation tolerances
 - $<2\%$ for doses $>10\%$ of the prescription dose.

Specific commissioning process

- **MBDCA specific tasks**

“Currently, only careful comparison to Monte Carlo with or w/o experimental measurements can fully test the advanced features of these codes”.



Your choice of pain...

Commissioning 2 MBDCA

- Your clinical TPS
- and a MC TPS

Performing measurements

- But you cannot beat the house...

TABLE V. Propagation of best practice uncertainties ($k=1$ unless stated otherwise) in dose at 1 cm on the transverse plane associated with source-strength measurements at the clinic, brachytherapy dose measurements or simulation estimates, and treatment planning system dataset interpolation for low-energy (*low-E*) and high-energy (*high-E*) brachytherapy sources as relating to values presented in Fig. 1.

Row	Uncertainty component	Relative propagated uncertainty (%)	
		<i>low-E</i>	<i>high-E</i>
1	S_K measurements from row 5 of Tables I and IV	1.3	1.5
2	Measured dose	3.6	3.0
3	Monte Carlo dose estimate	1.7	1.6
4	TPS interpolation uncertainties	3.8	2.6
5	Total dose calculation uncertainty	4.4	3.4
	Expanded uncertainty ($k=2$)	8.7	6.8

TG138: DeWerd et al, Med. Phys. 38 (2011)

Specific commissioning process

This is not sustainable for the clinical physicists

Vision 20/20 Paper: 2010

TABLE I. Status of MBDCAs that can account for radiation scatter conditions and/or material heterogeneities and were useable in brachytherapy treatment planning systems as of 12 May 2010.

MBDCA system	Sponsor(s)	Radiation type	Clinical use	FDA/CE mark status	Release date
PLAQUE SIMULATOR	Astrahan	$^{125}\text{I} + ^{103}\text{Pd}$ photons	Y	N	1990
Collapsed cone	Ahnesjö, Russell, and Carlsson	^{192}Ir photons	N	N	1996
BRACHYDOSE	Yegin, Taylor, and Rogers	0.01–10 MeV photons	N	N	2004
MCPI	Chibani and Williamson	$^{125}\text{I} + ^{103}\text{Pd}$ photons	N	N	2005
GEANT4/DICOM-RT	Carrier <i>et al.</i>	Any	N	N	2007
Scatter correction	Poon and Verhaegen	^{192}Ir photons	N	N	2008
Hybrid TG-43:MC	Price and Mourtada, and Rivard <i>et al.</i>	Any	Y	Y	2009
ACUROS	Transpire/Varian	^{192}Ir photons	Y	Y	2009

V. NEEDED INFRASTRUCTURE

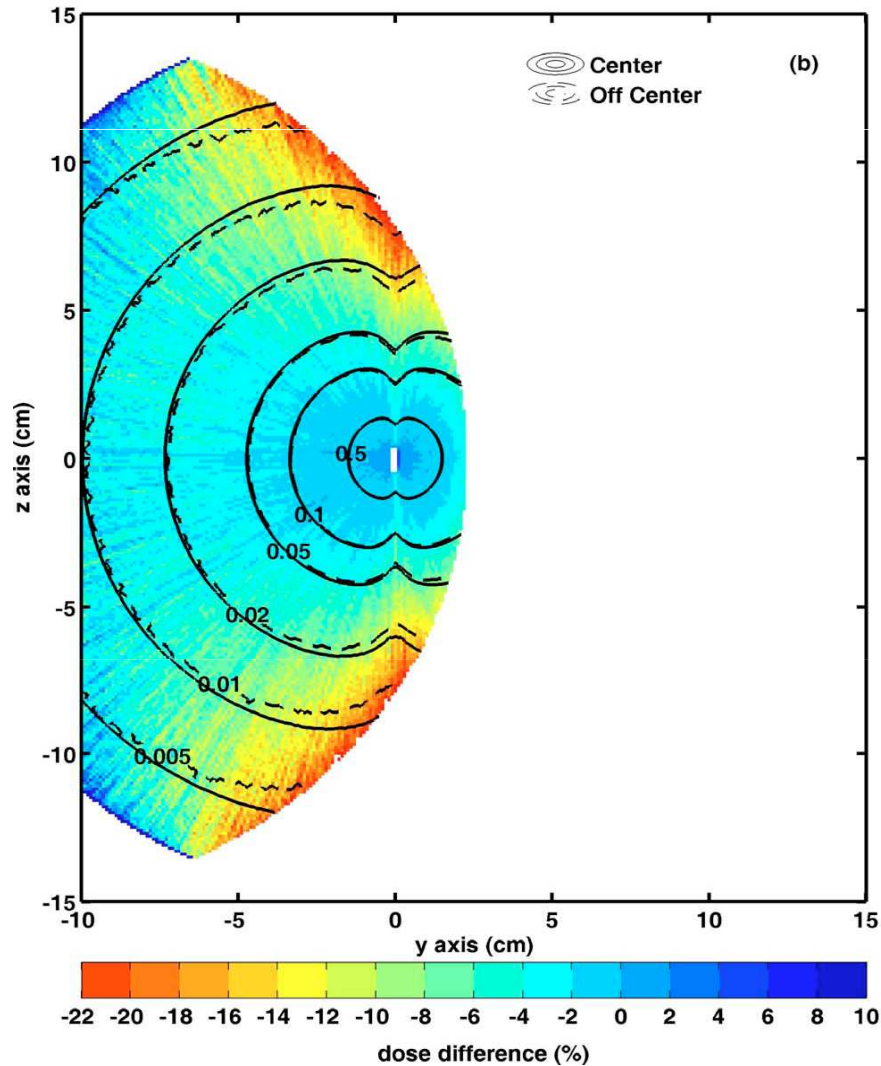
While MBDCAs are expected to produce more accurate dosimetric results than the current TG-43 formalism, the authors feel that the medical community should not immediately replace the current approach without careful consideration for widespread integration. **Assessment of the current infrastructure is needed** before assigning new resources, with opportunity for further cooperation of national and international professional societies.

V.A. Centralized dataset management

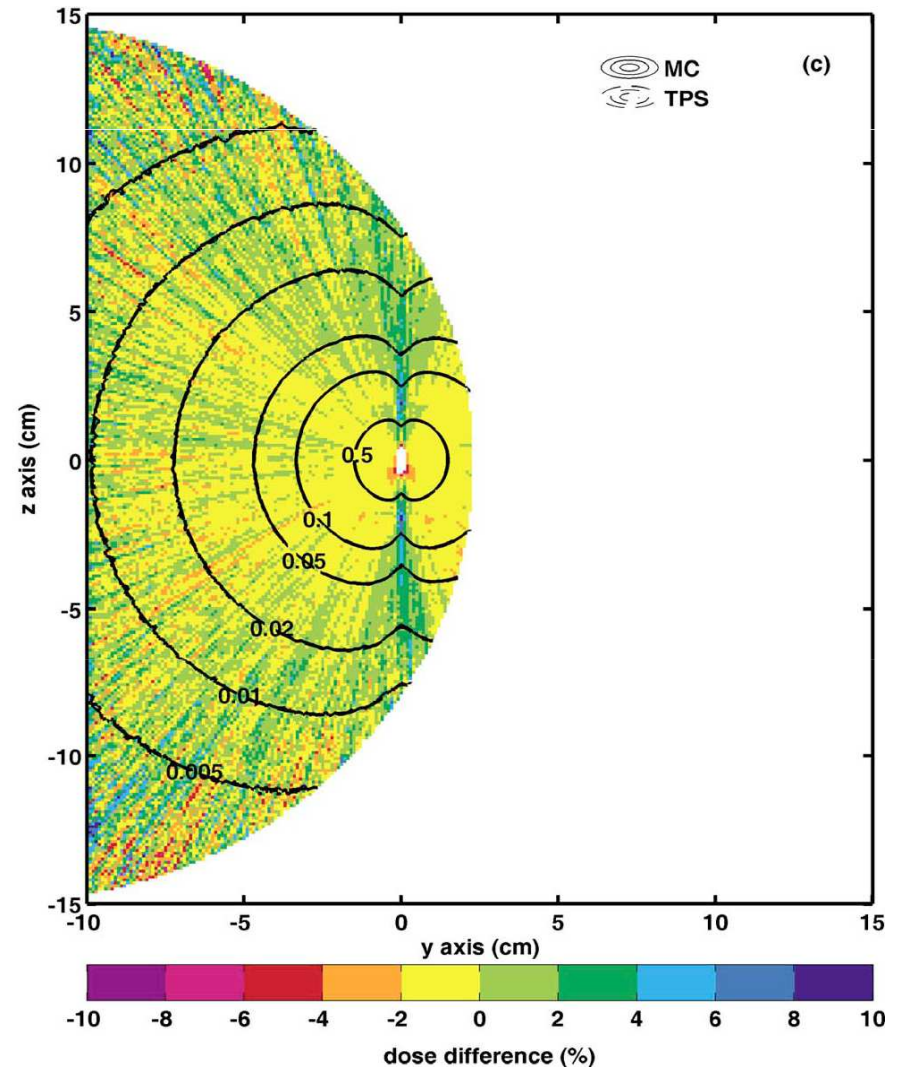
Societal recommendations and reference data do the clinical physicist no good if they cannot be readily implemented. Having quantitative data available beyond the scientific, peer-reviewed literature may be accomplished through **expansion of the joint AAPM/RPC Brachytherapy Source Registry**. An independent repository such as the Registry to house the reference data would facilitate this process—especially **with international accessibility**.

Offset Source Geometry

test of scatter conditions



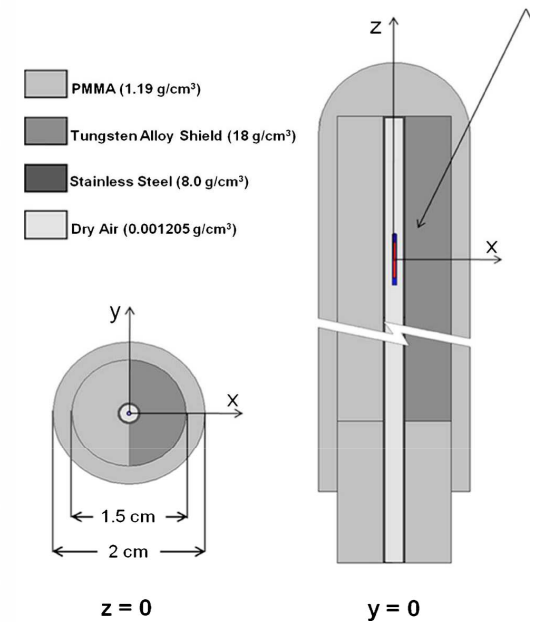
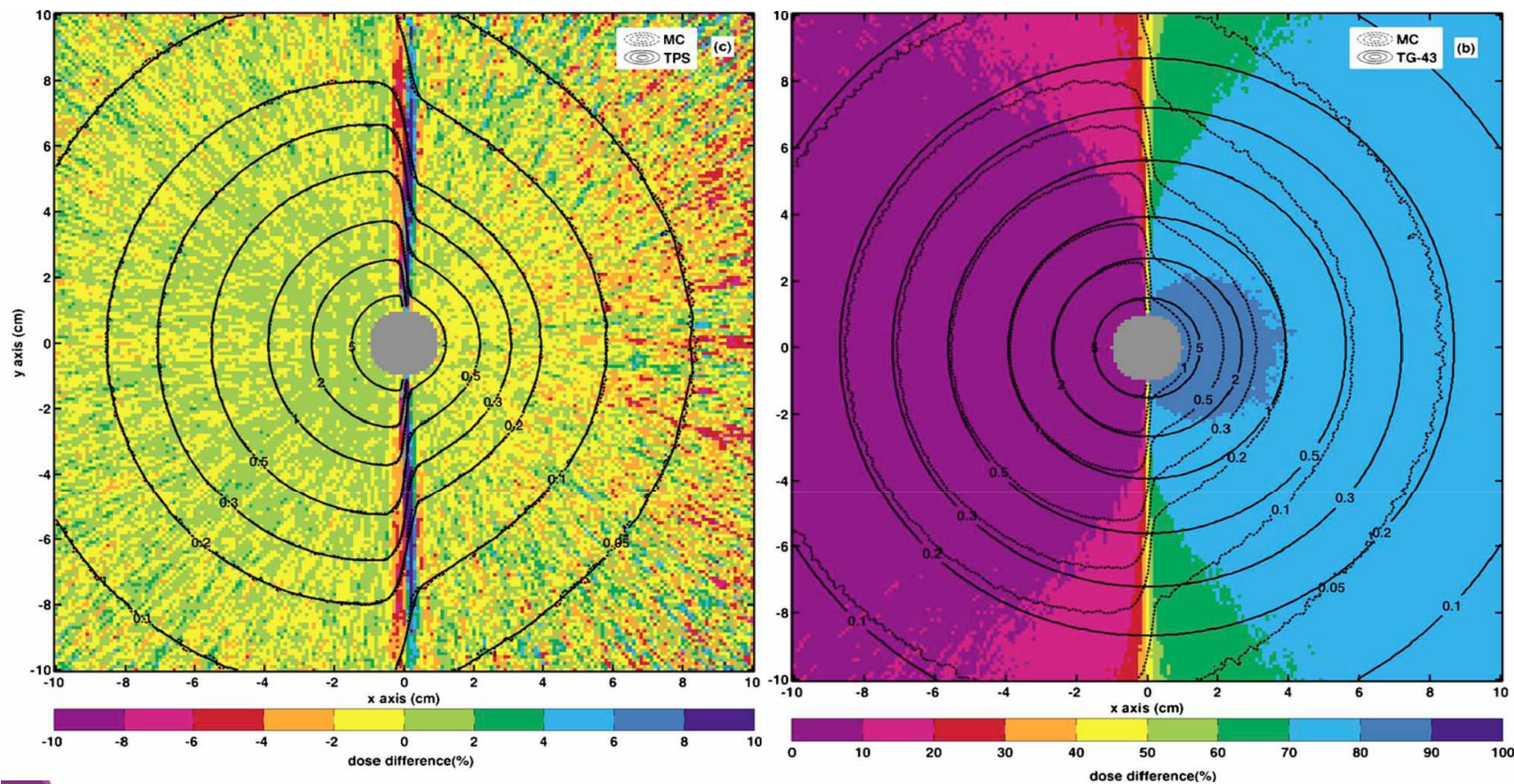
HDR ^{192}Ir benchmark for Acuros BV



Need Standardized MBDCA Benchmarks

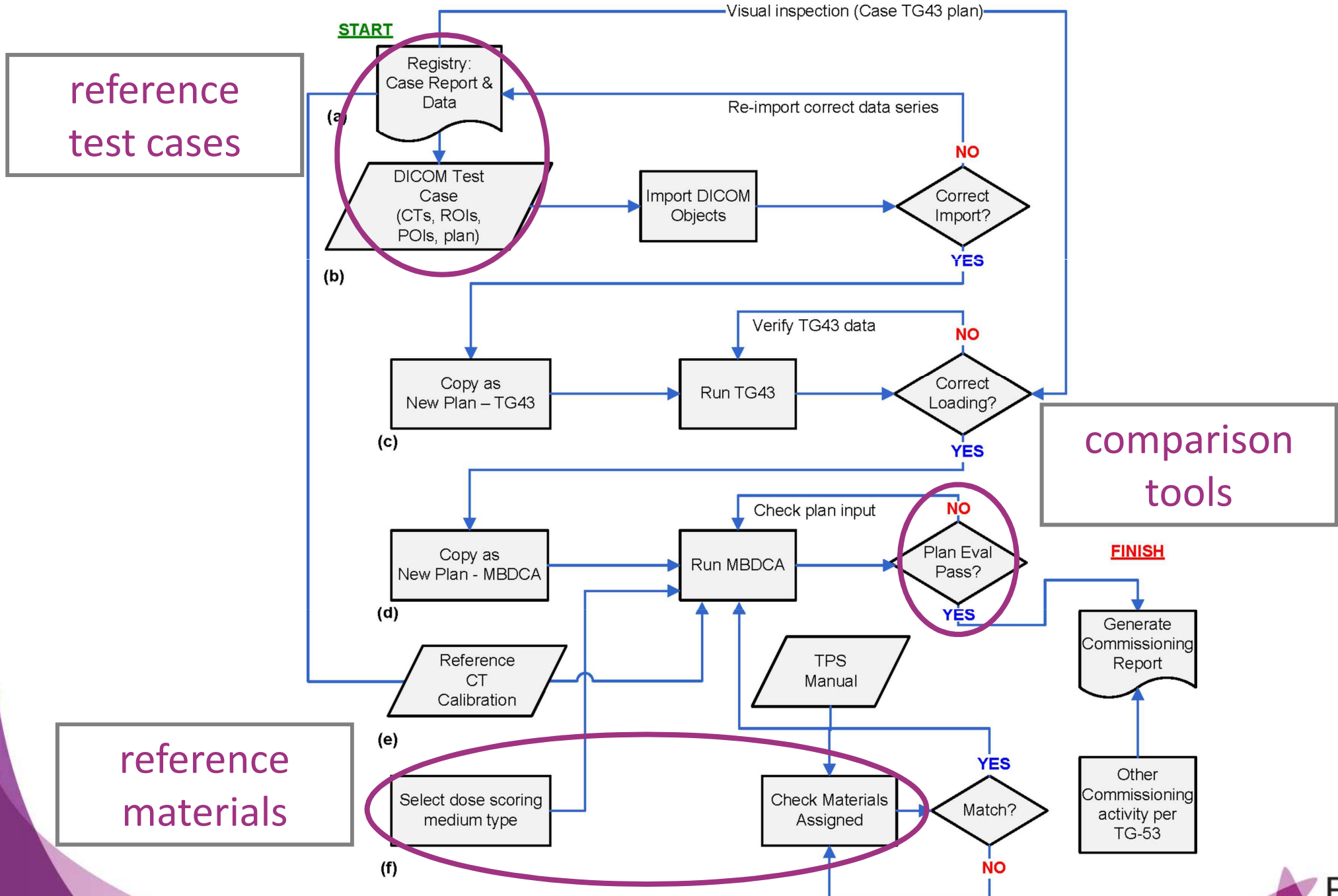
Excellent reference HDR ^{192}Ir benchmarks in *MedPhys*

➤ Acuros BrachyVision



Petrokokkinos *et al.*, *MedPhys* 38, 1981-1992 (2011)

MBDCA Commissioning Workflow



Beaulieu, et al., *Med. Phys.* 39, 6208-6236 (2012)

TG-186 Recommended Materials

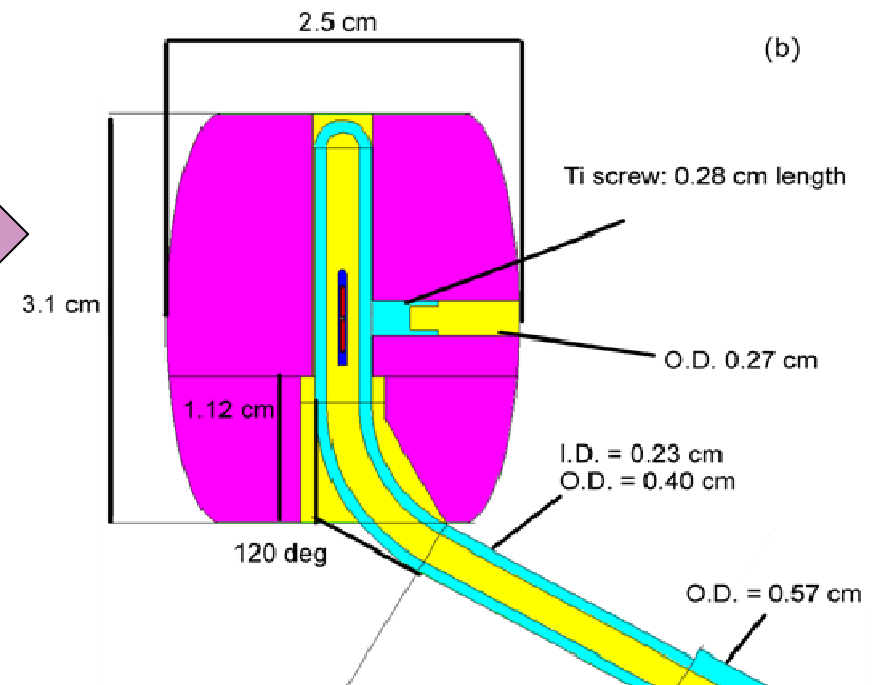
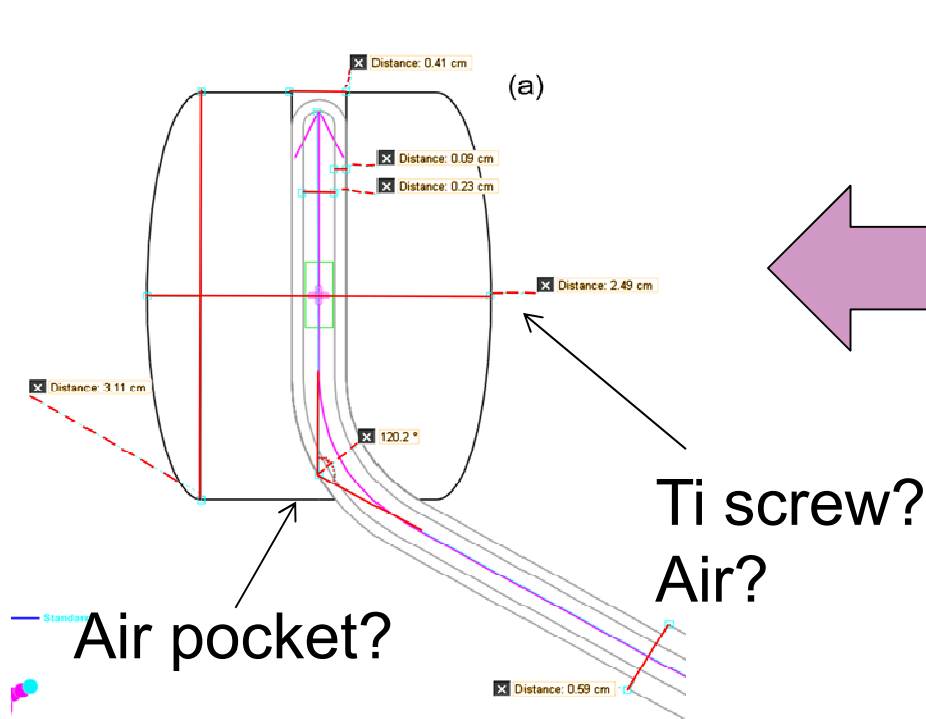
TABLE III. Material definitions. Water is given for comparison.

Tissue	% mass					Z > 8	Mass density g cm ⁻³
	H	C	N	O			
Prostate (Ref. 110)	10.5	8.9	2.5	77.4	Na(0.2), P(0.1), S(0.2), K(0.2)	1.04	
Mean adipose (Ref. 110)	11.4	59.8	0.7	27.8	Na(0.1), S(0.1), Cl(0.1)	0.95	
Mean gland (Ref. 110)	10.6	33.2	3.0	52.7	Na(0.1), P(0.1), S(0.2), Cl(0.1)	1.02	
Mean male soft tissue (Ref. 109)	10.5	25.6	2.7	60.2	Na(0.1), P(0.2), S(0.3), Cl(0.2), K(0.2)	1.03	
Mean female soft tissue (Ref. 109)	10.6	31.5	2.4	54.7	Na(0.1), P(0.2), S(0.2), Cl(0.1), K(0.2)	1.02	
Mean skin (Ref. 109)	10.0	20.4	4.2	64.5	Na(0.2), P(0.1), S(0.2), Cl(0.3), K(0.1)	1.09	
Cortical bone (Ref. 109)	3.4	15.5	4.2	43.5	Na (0.1), Mg (0.2), P (10.3), S (0.3), Ca(22.5)	1.92	
Eye lens (Ref. 109)	9.6	19.5	5.7	64.6	Na(0.1), P(0.1), S(0.3), Cl(0.1)	1.07	
Lung (inflated) (Ref. 109)	10.3	10.5	3.1	74.9	Na(0.2), P(0.2), S(0.3), Cl(0.3), K(0.2)	0.26	
Liver (Ref. 109)	10.2	13.9	3.0	71.6	Na(0.2), P(0.3), S(0.3), Cl(0.2), K(0.3)	1.06	
Heart (Ref. 109)	10.4	13.9	2.9	71.8	Na(0.1), P(0.2), S(0.2), Cl(0.2), K(0.3)	1.05	
Water	11.2			88.8		1.00	

TG-186 Recommended Materials

- Commercial MDBCAs for ^{192}Ir sources
 - Soft tissue assignments not an issue and water is ok
 - Air, lung (inflated), (cortical) bone must be considered.
 - TG-186 recommends using ICRU Report 46 compositions
 - Applicator geometries and compositions are given by the vendors' library of applicators ...

Applicator Geometry & Composition Verification



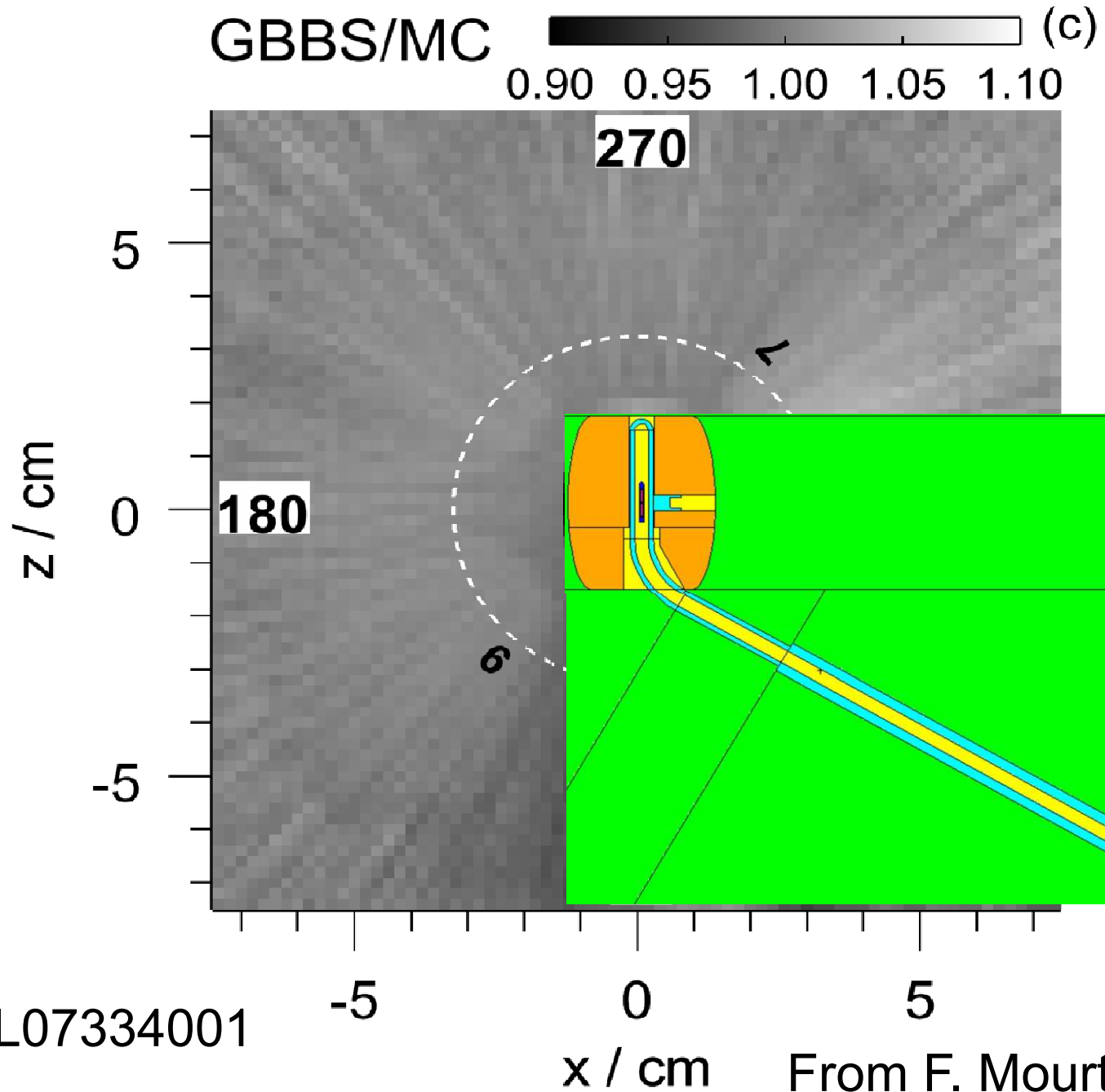
**In house MC model derived
from physical verification
and vendor CAD**

Brachytherapy 10 (3): S36, 2011

**BV TPS
Applicator
Library-
Solid Model**
part #: AL07334001

From F. Mourtada

Results - CT/MR ovoid dosimetry



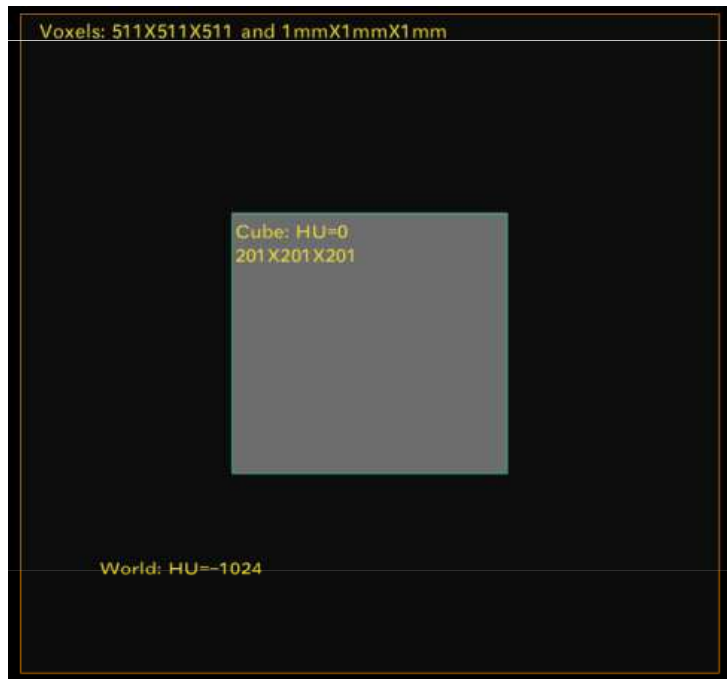
part #: AL07334001

WG Charges

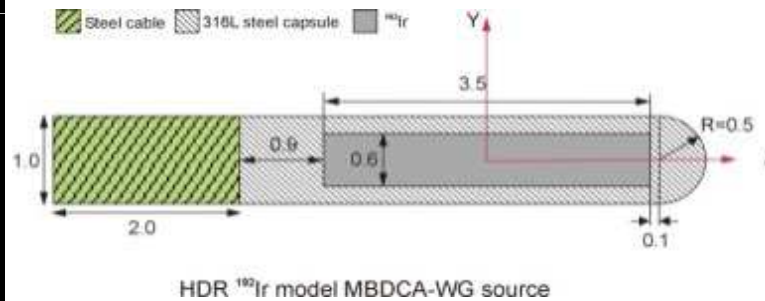
- Develop a limited number (approximately 5) of well-defined test case plans and perform MBDCA dose calculations and comparisons.
- Identify the best venue for housing the reference plans/data, and put in place in collaboration with identified partners of the Registry.
- *Propose to the community well-defined prerequisites for test case plans to be submitted to the Registry.*
- *Develop a review process for evaluation as new reference data meeting the prerequisites.*
- Engage the vendors to promote uniformity of practice.

TPS Commissioning Phantom: AAPM+ESTRO+ABG

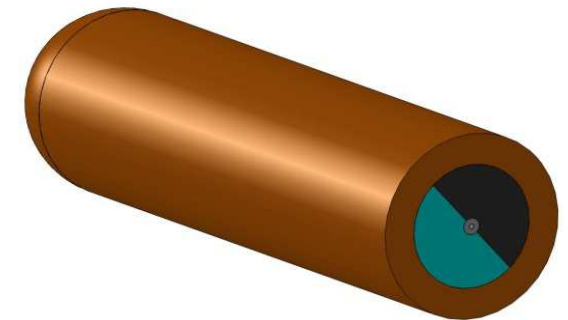
DICOM (512 mm)³
1 mm voxels



Generic source
HDR ¹⁹²Ir



W-alloy Shielded
GYN applicator



Monte Carlo codes:

- ALGEBRA
- BrachyDose
- Geant4
- MCNP5
- MCNP6
- Penelope

TPS:

- BRACHYVISION
(Acuros BV)
- ONCENTRABRACHY
(Collapsed-Cone)

Level 1 Dosimetry Benchmark

Medical Physics

A generic high-dose-rate ^{192}Ir brachytherapy source for evaluation of model-based dose calculations beyond the TG-43 formalism

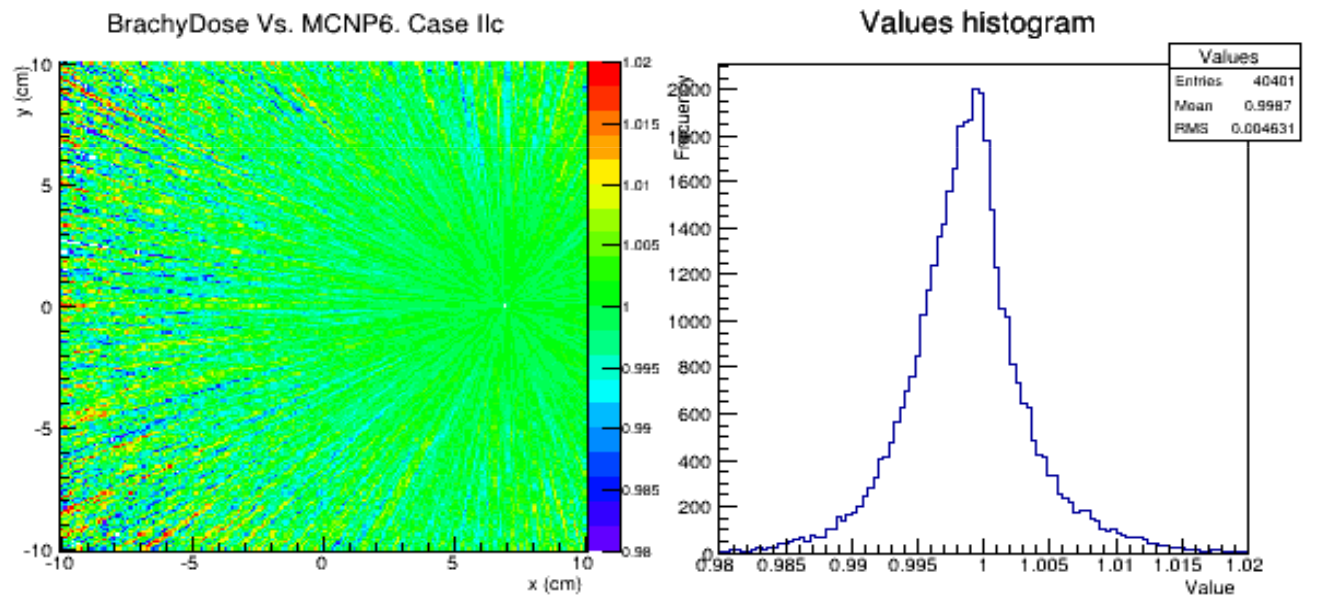
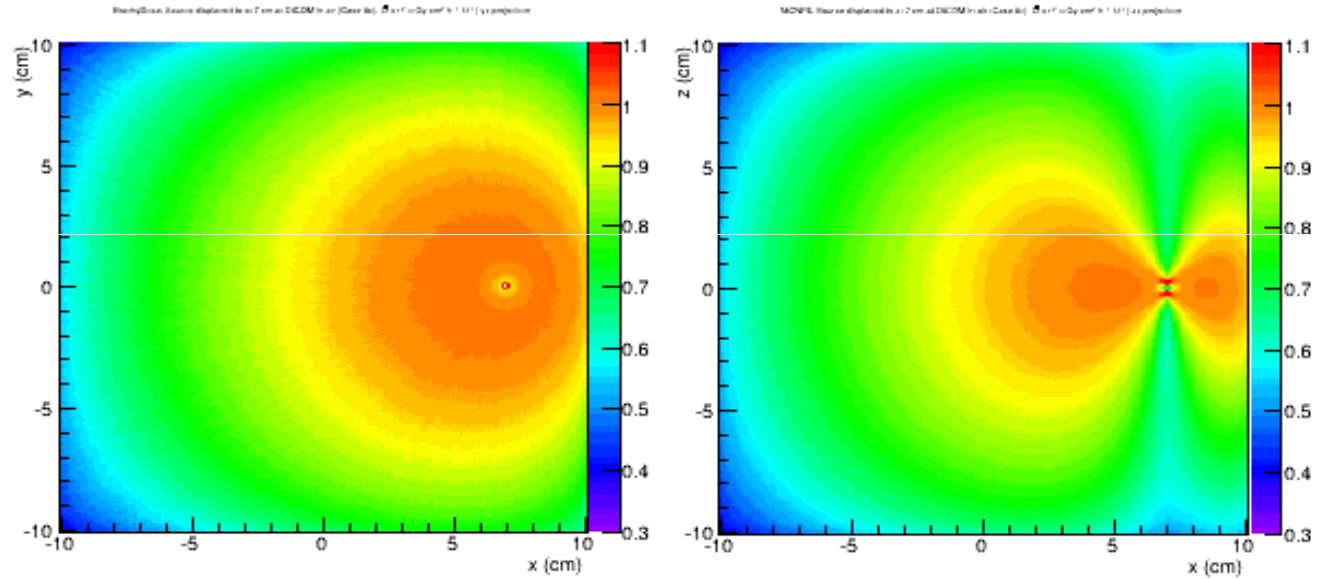
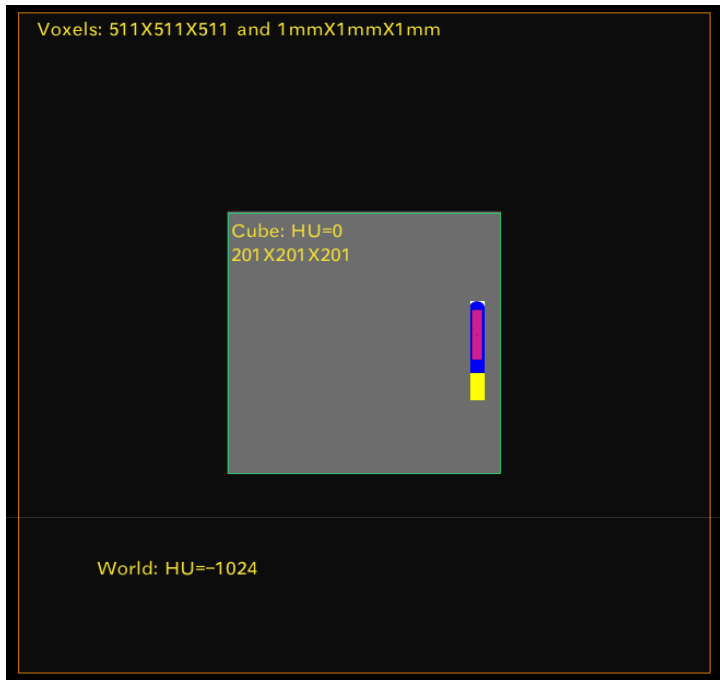
Ballester, Carlsson Tedgren, Granero, Haworth, Mourtada, Paiva Fonseca, Zourari, Papagiannis, Rivard, Siebert, Sloboda, Smith, Thomson, Verhaegen, Vijande, Ma, and Beaulieu

Conclusions: A hypothetical, generic HDR ^{192}Ir source was designed and implemented in two commercially available TPSs employing different MBDCAs. Reference dose distributions for this source were benchmarked and used for evaluation of MBDCA calculations employing a virtual, cubic water phantom in the form of a CT DICOM image series. Implementation of a generic source of identical design in all TPSs using MBDCAs is an important step toward supporting univocal commissioning procedures and direct comparisons between TPSs.

Ballester *et al.*, *Med. Phys.* 42, 3048-3062 (2015)

L2: Offset Source Geometry

test of scatter conditions



L2: Shielded GYN Applicator

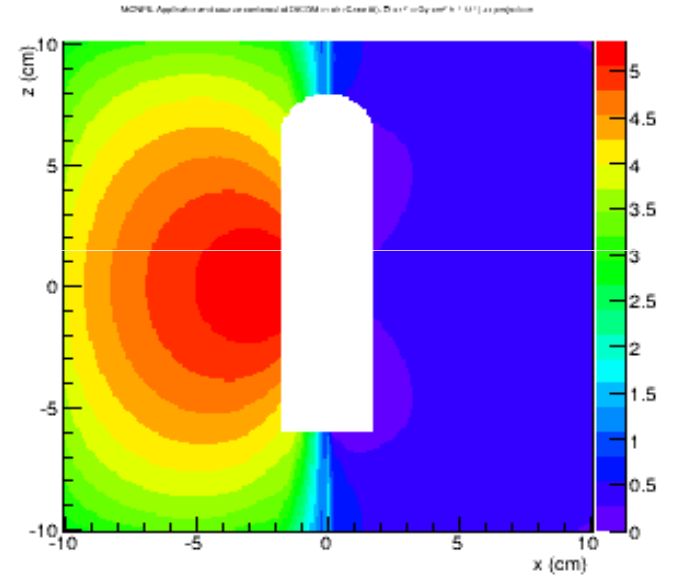
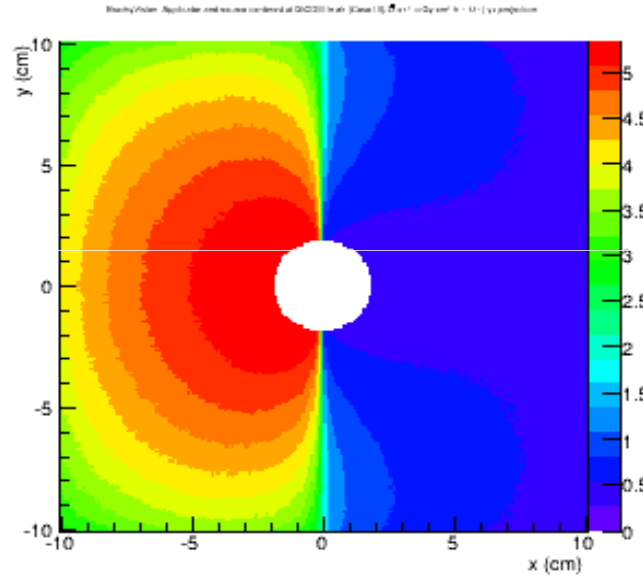
test of shielding

Voxels: 511X511X511 and 1mmX1mmX1mm

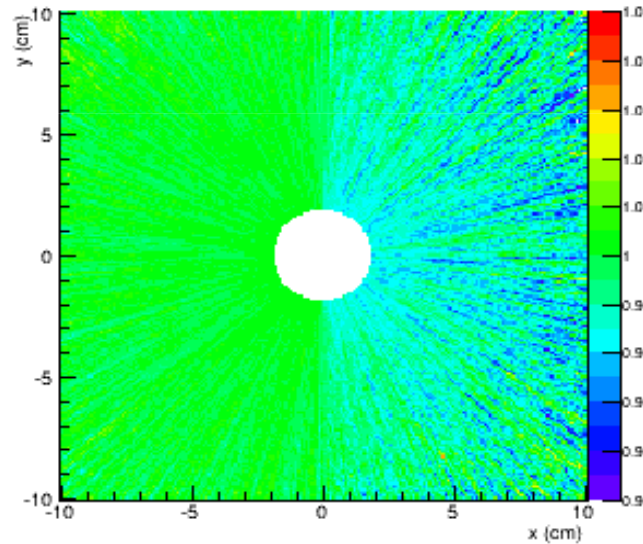
Cube: HU=0
201 X 201 X 201



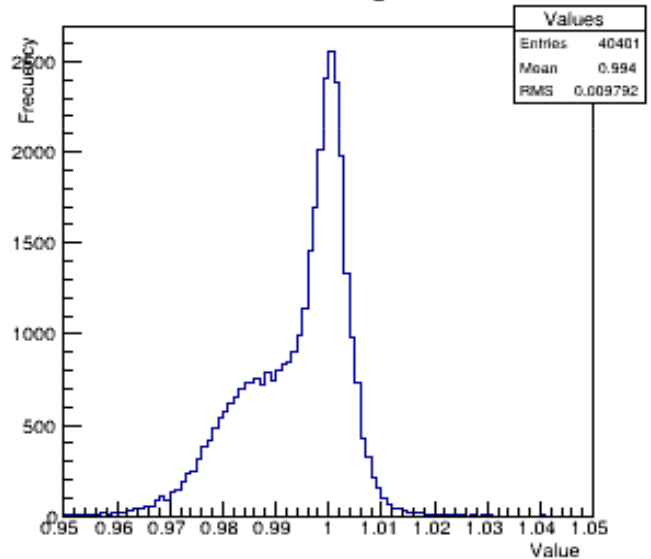
World: HU=-1024



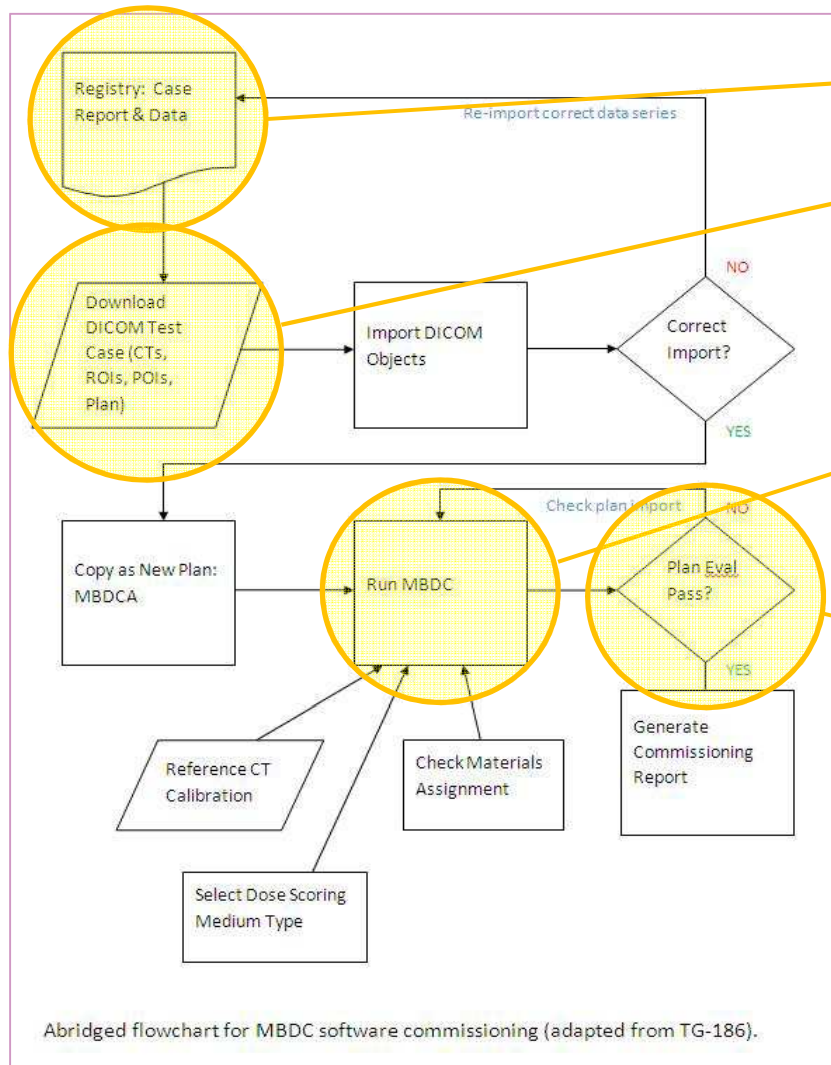
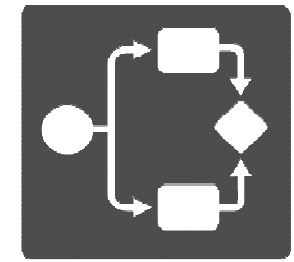
BrachyDose Vs. MCNP6. Case III



Values histogram



Commissioning Workflow



1. Access the Registry
2. Download a test case plan and MC reference dose distribution (DICOM)
3. Calculate dose locally using the plan and MBDCA
4. Compare and evaluate MBDCA and reference dose distributions

Supporting Infrastructure



MD Anderson

IROC Houston Quality Assurance Center

Search IROC Houston by Google



Tel: 713-745-8989

[Home](#) [Credentialing](#) [Participating Institutions](#) [IROC'S New Participant Demographics Form](#) [Facility Questionnaire](#)

Model Based Dose calculations

Reference dataset(DICOM archive) generated with MC simulation. Users may import these archives into TPS for benchmarking.

- [Reference Data](#)

TPS-specific seed DICOM archive. Users may start TPS calculation simply by importing these archives. CT images, RP and RS files are contained.

- [Elekta Database](#)
- [Varian Database](#)

Supporting Infrastructure



IMAGING AND
RADIATION ONCOLOGY CORE
Global Leaders in Clinical Trial Quality Assurance

MD Anderson

IROC Houston Quality Assurance Center

Search IROC Houston by Google



Tel: 713-745-8989

[Home](#) [Credentialing](#) [Participating Institutions](#) [IROC'S New Participant Demographics Form](#) [Facility Questionnaire](#)

Reference Data

This folder contains the reference datasets. The reference datasets are based on MCNP6 simulations.

Elekta Reference Data:

- [Case 1](#)
- [Case 2](#)
- [Case 3](#)
- [Case 4](#)

Varian Reference Data:

- [Case 1](#)
- [Case 2](#)
- [Case 3](#)
- [Case 4](#)

Supporting Infrastructure



Search IROC Houston by Google



Tel: 713-745-8989

Home **Credentiali**



Search IROC Houston by Google



Tel: 713-745-8989

Home **Credentialing**

Participating Institutions

IROC'S New Participant
Demographics Form

Facility Questionnaire

This folder contains:

- **User Guide**
- **Case I**
- **Case II**
- **Case III**
- **Case IV**
- **WG Source I**

Varian Source Database

This folder contains datasets created with the Varian TPS, BrachyVision.

- **User Guide**
- **Case I**
- **Case II**
- **Case III**
- **Case IV**

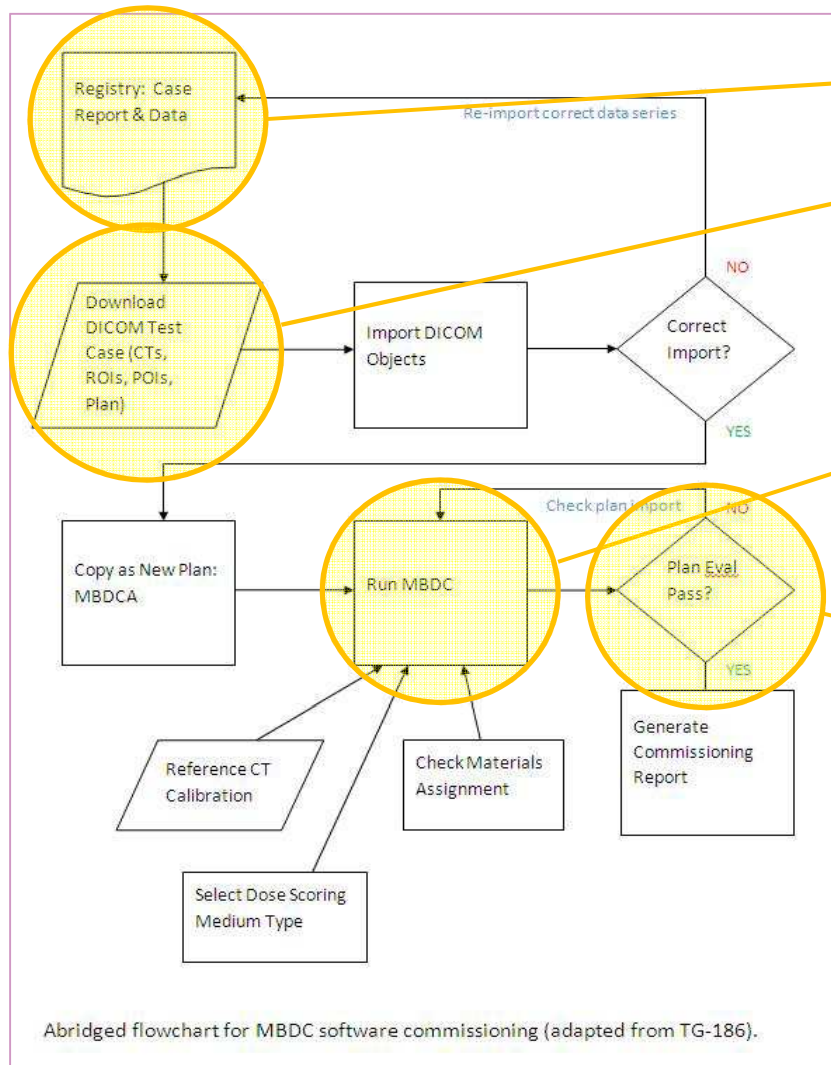
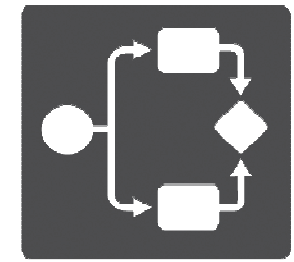
User Guide for ACE[®] Testing (version 26 April 2016)

User Guide for Elekta Brachytherapy ACE[®] Algorithm Testing

Contents

- I Introduction**
- II Test Case Import**
 - A. Accessing the Test Case Repository**
 - B. Downloading the Test Cases**
 - C. Importing a Test Case into OCB**
 - a. Importing ACE[®] Images, Plan, Structure Set & Dose Data
 - b. Importing MCNP6 Plan & Dose Data
- III Dose Calculation**
 - A. Process Overview**
 - B. Test Case 1**
 - a. Selecting the Plan & Setting the Virtual Source
 - b. Setting the Source Dwell Time
 - c. Setting the Dose Calculation Accuracy & Performing the Calculation
 - d. Creating a 3D Dose Distribution
 - C. Test Case 2**
 - a. Selecting the Plan & Setting the Virtual Source
 - b. Setting the Source Dwell Time
 - c. Setting the Dose Calculation Accuracy & Performing the Calculation
 - d. Creating a 3D Dose Distribution
 - D. Test Case 3**
 - a. Selecting the Plan & Setting the Virtual Source
 - b. Setting the [Source Dwell Time](#)
 - c. Setting the Dose Calculation Accuracy & Performing the Calculation
 - d. Creating a 3D Dose Distribution
 - E. Test Case 4**
 - a. Selecting the Plan & Setting the Virtual Source
 - b. Setting the Source Dwell Time
 - c. Setting the Dose Calculation Accuracy & Performing the Calculation
 - d. Creating a 3D Dose Distribution

Commissioning Workflow

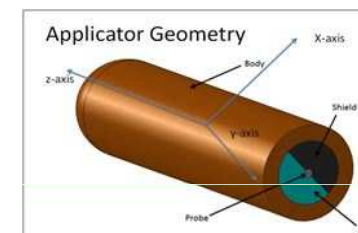


1. Access the Registry
2. Download a test case plan and MC reference dose distribution (DICOM)
3. Calculate dose locally using the plan and MBDCA
4. Compare and evaluate MBDCA and reference dose distributions

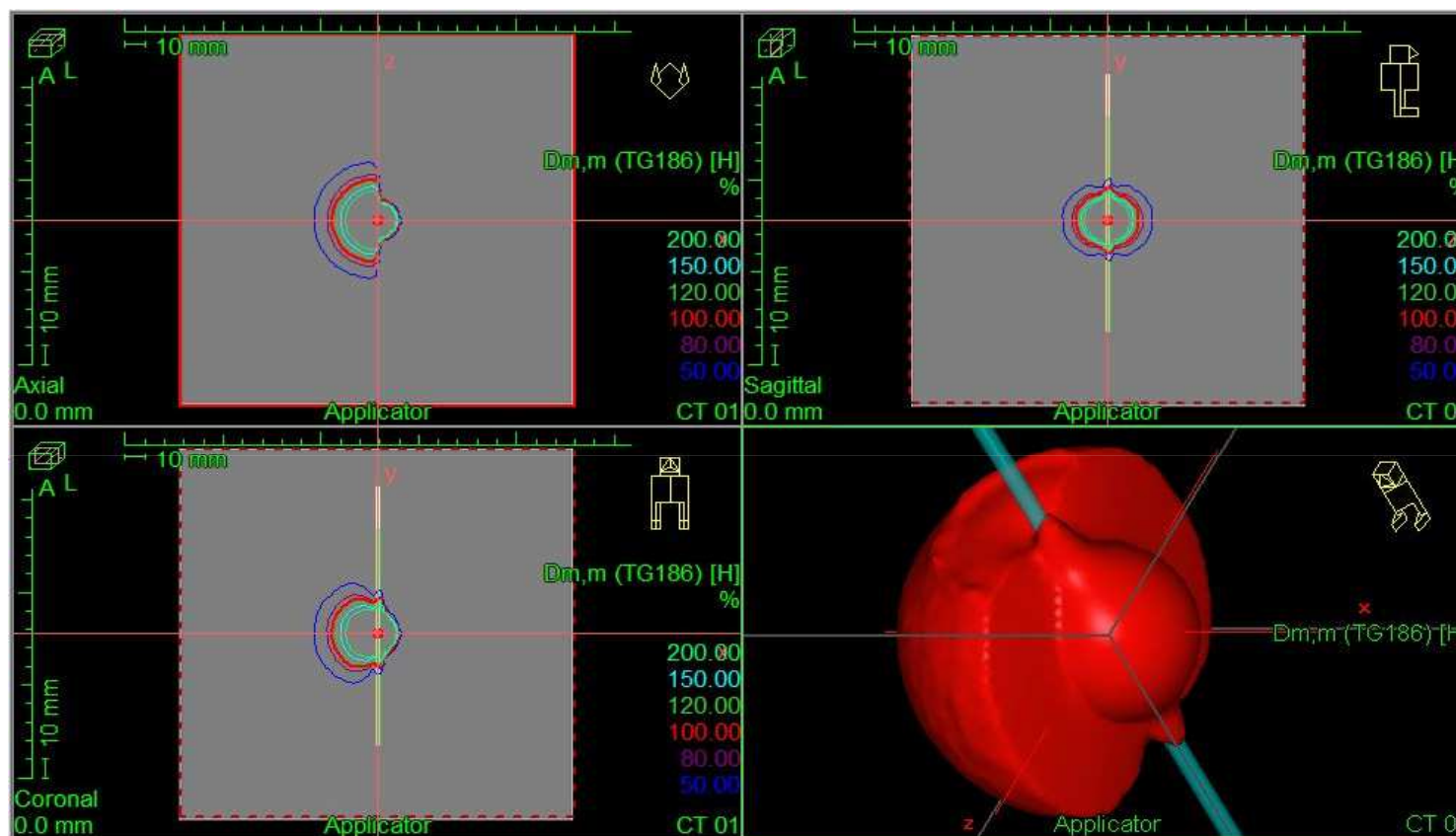
Commissioning Process



- Main steps:
 - Calculate dose locally using the MBDCA



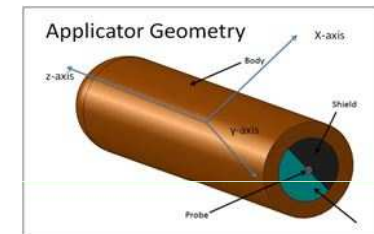
Level 2



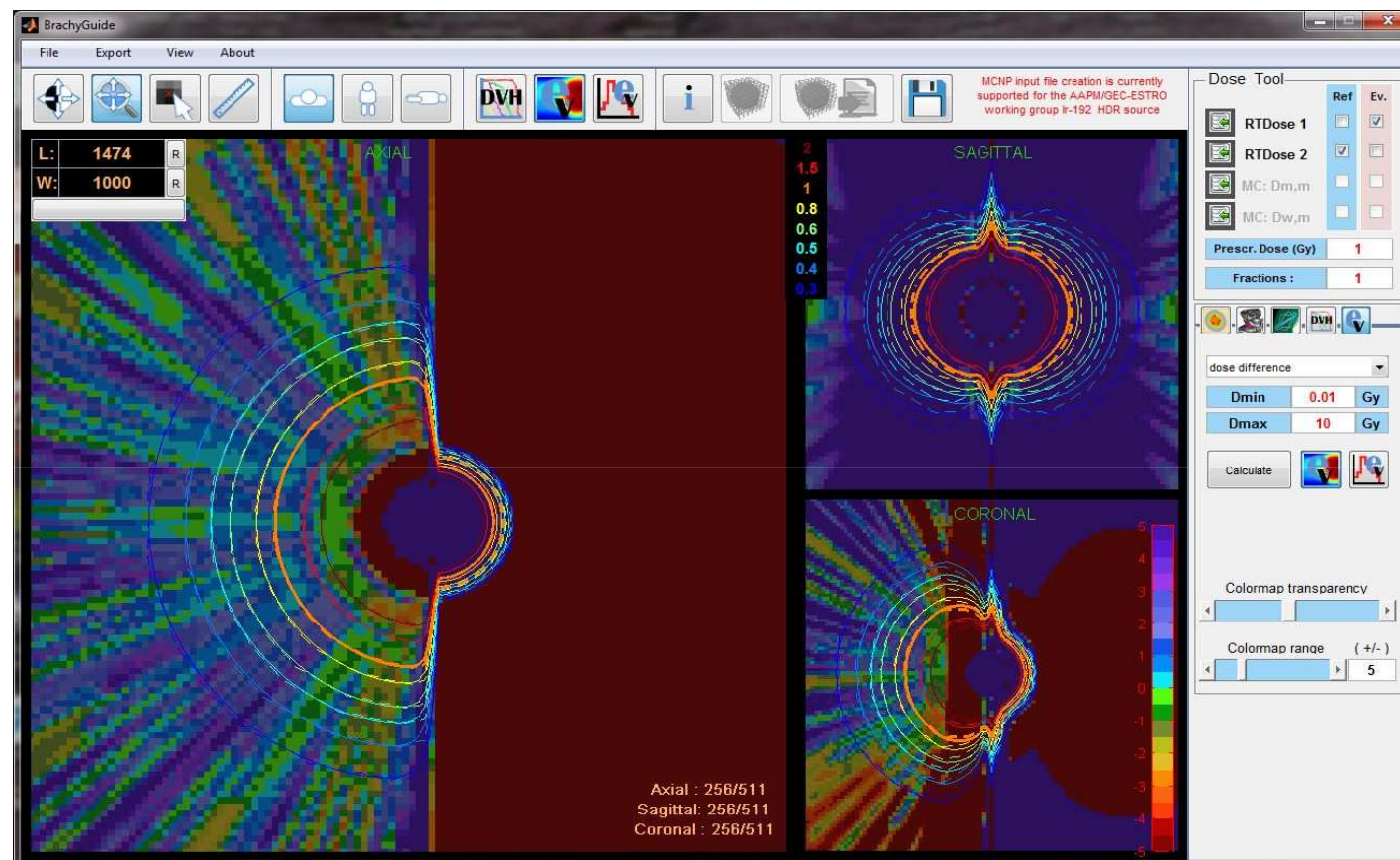
Commissioning Process



- Main steps:
 - Compare & evaluate MBDCA and ref. doses



Level 2



BrachyGuide
P. Papagiannis
et al.

Take Home Message: Commissioning

- TG43 remains the reference dose engine for prescription, planning and optimization
 - Advanced dose engine for dose recalculation
- TG-186 recommendations include:
 - TPS acceptance testing & commissioning
 - tissue & material assignments
 - dose reporting approaches
- New commissioning infrastructure available soon
 - Bypass the need for a second model-based TPS
 - Watch for WCB 2016 announcement!

Vienna, May 29 – June 1, 2016



**Advanced Brachytherapy
Physics**

Dose plan evaluation

Christian Kirisits
Medical University of Vienna



Disclosure:

Christian Kirisits reports no conflicts of interest
Christian Kirisits was a consultant to Nucletron, an Elekta Company
Medical University of Vienna receives financial and equipment support for training and research activities from Nucletron, an Elekta Company and Varian Medical

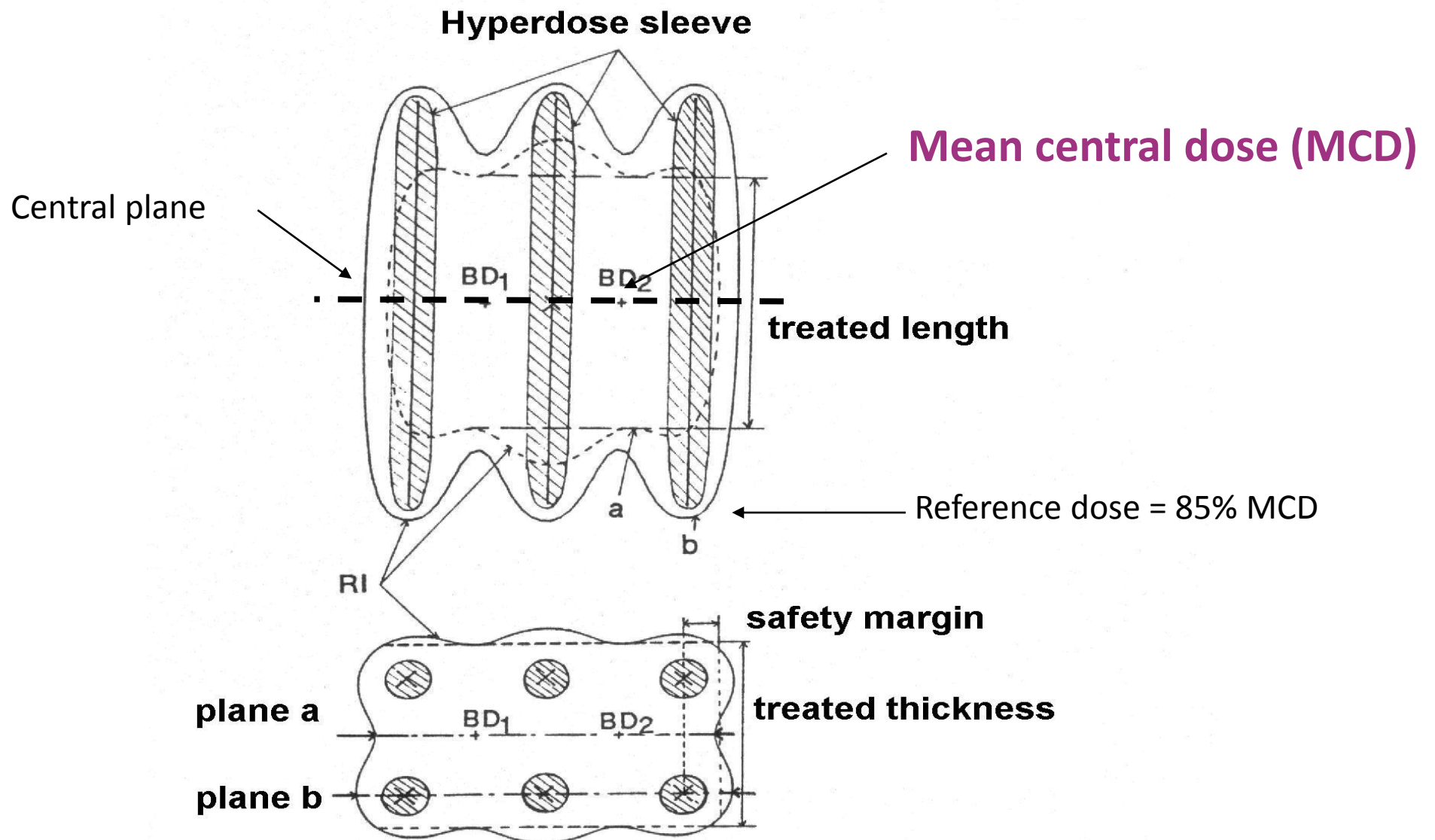
Advanced Brachytherapy Physics, 2016



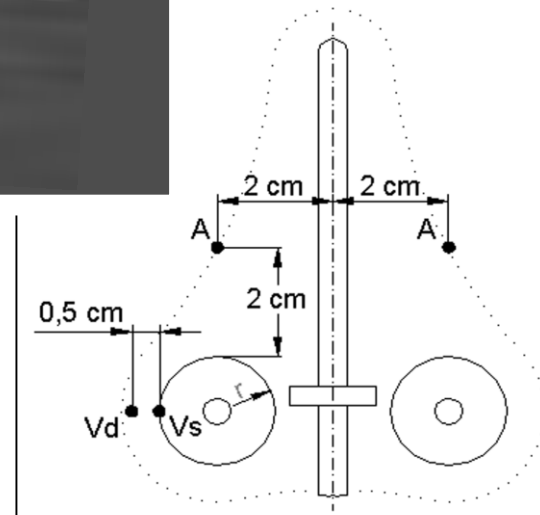
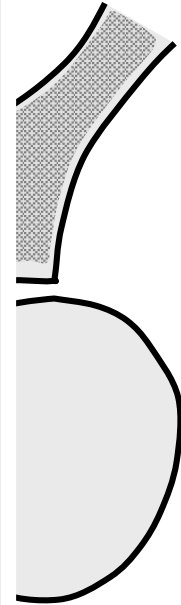
How to evaluate a treatment plan?

Dose points and volumes (dimensions)

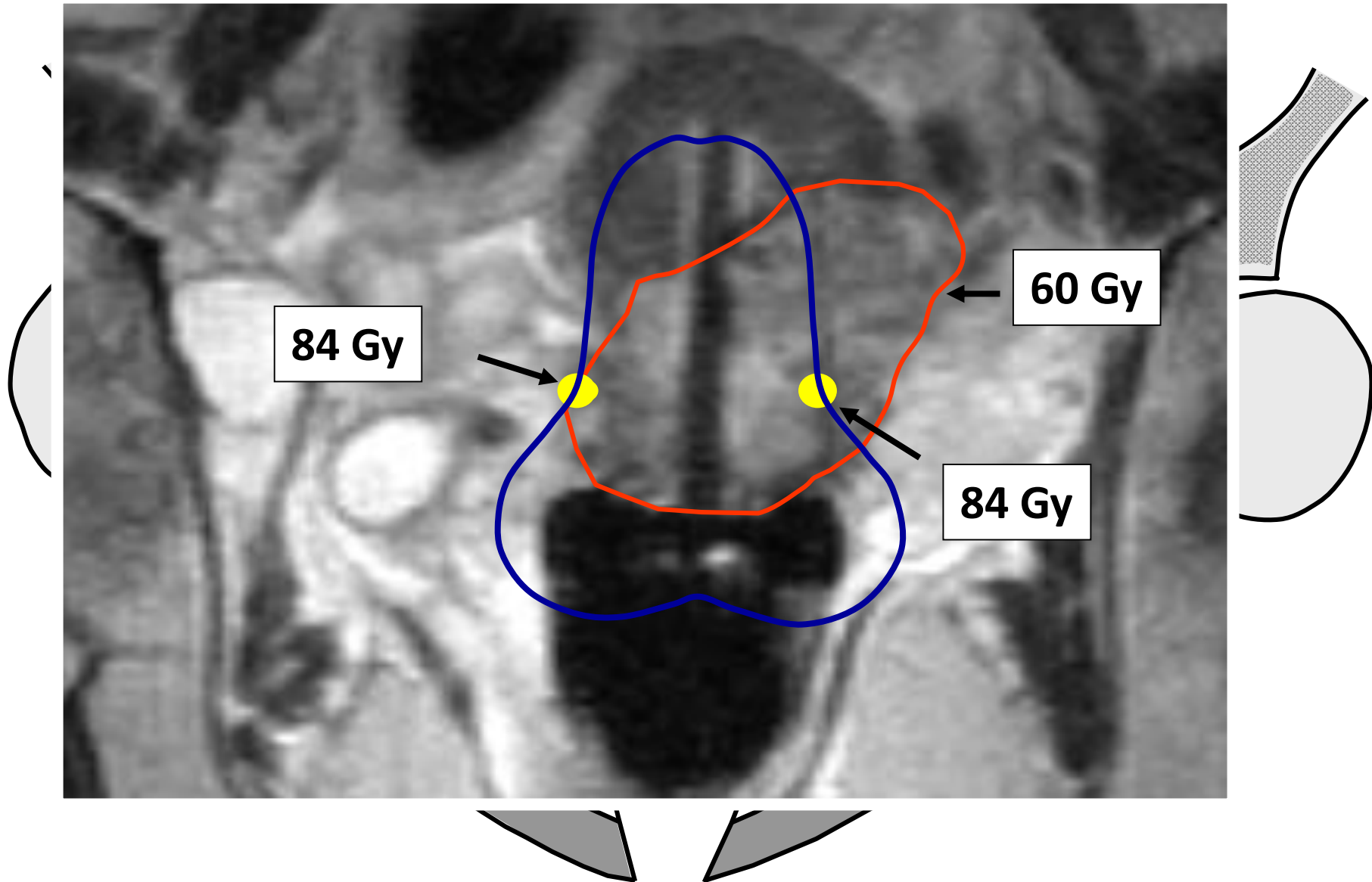
ICRU 58



Point A



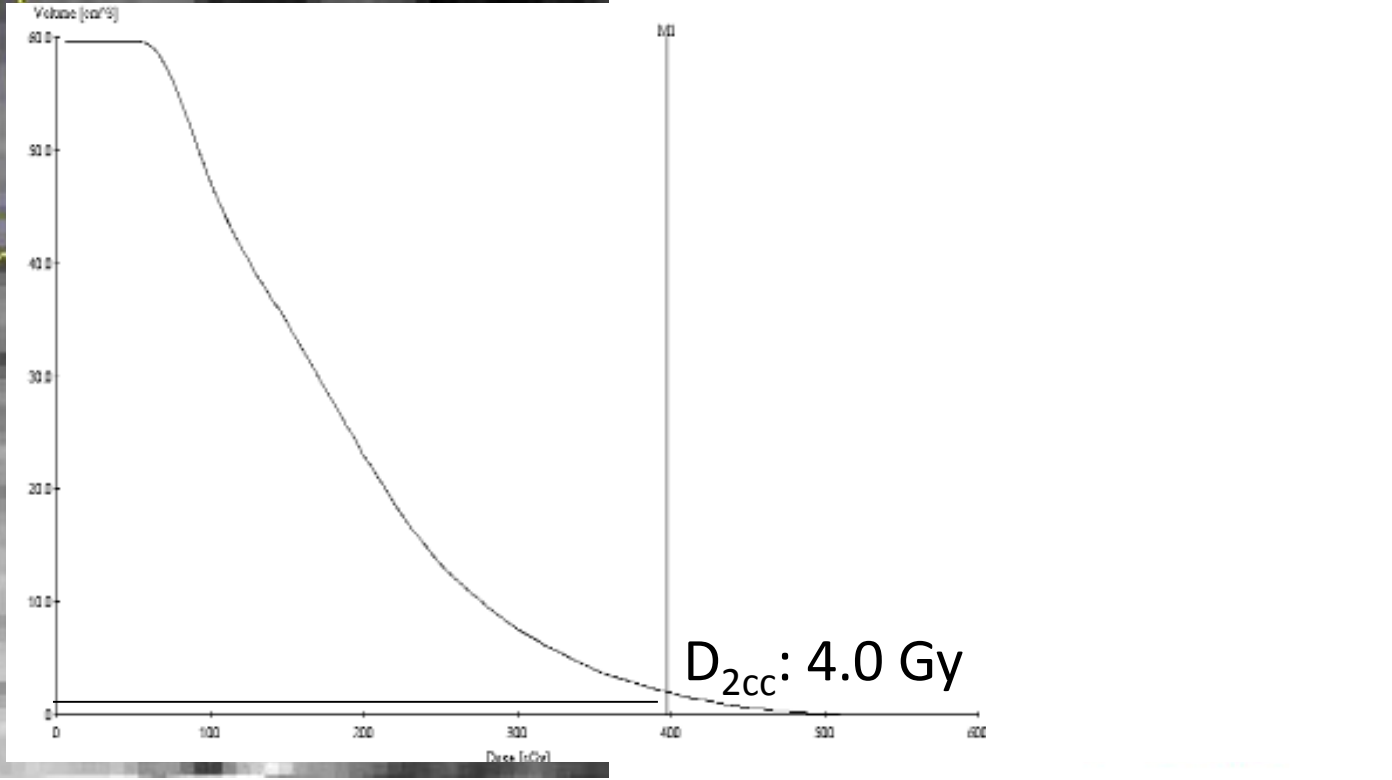
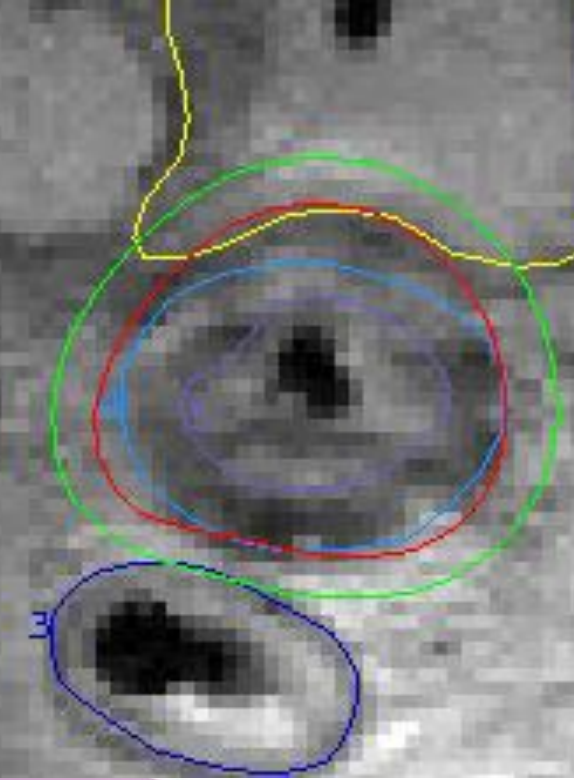
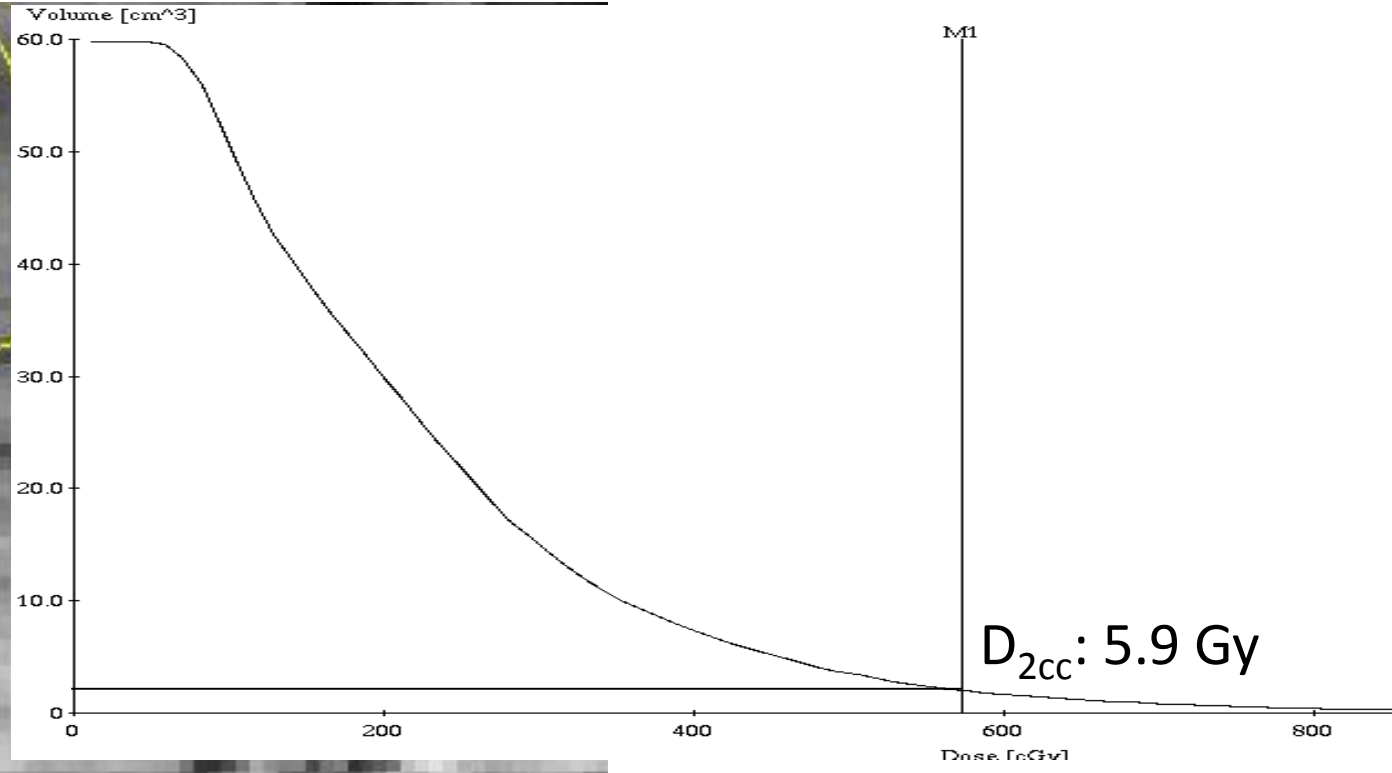
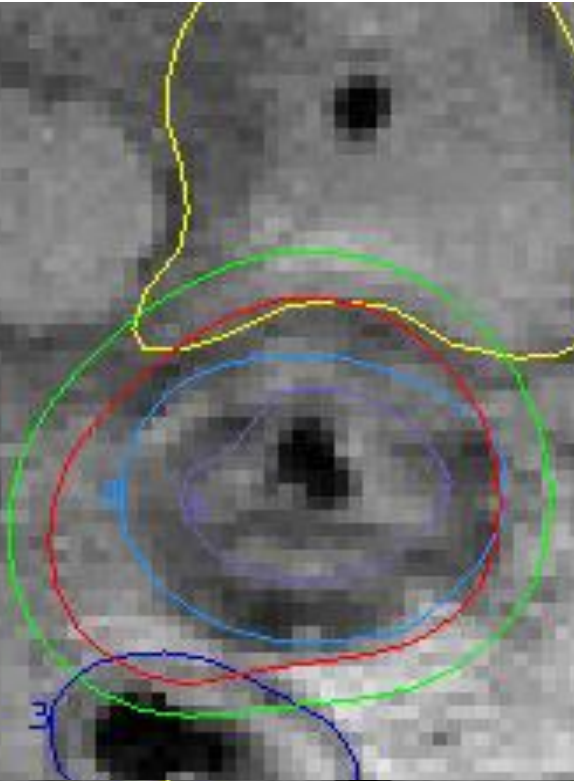
Point A / target dose



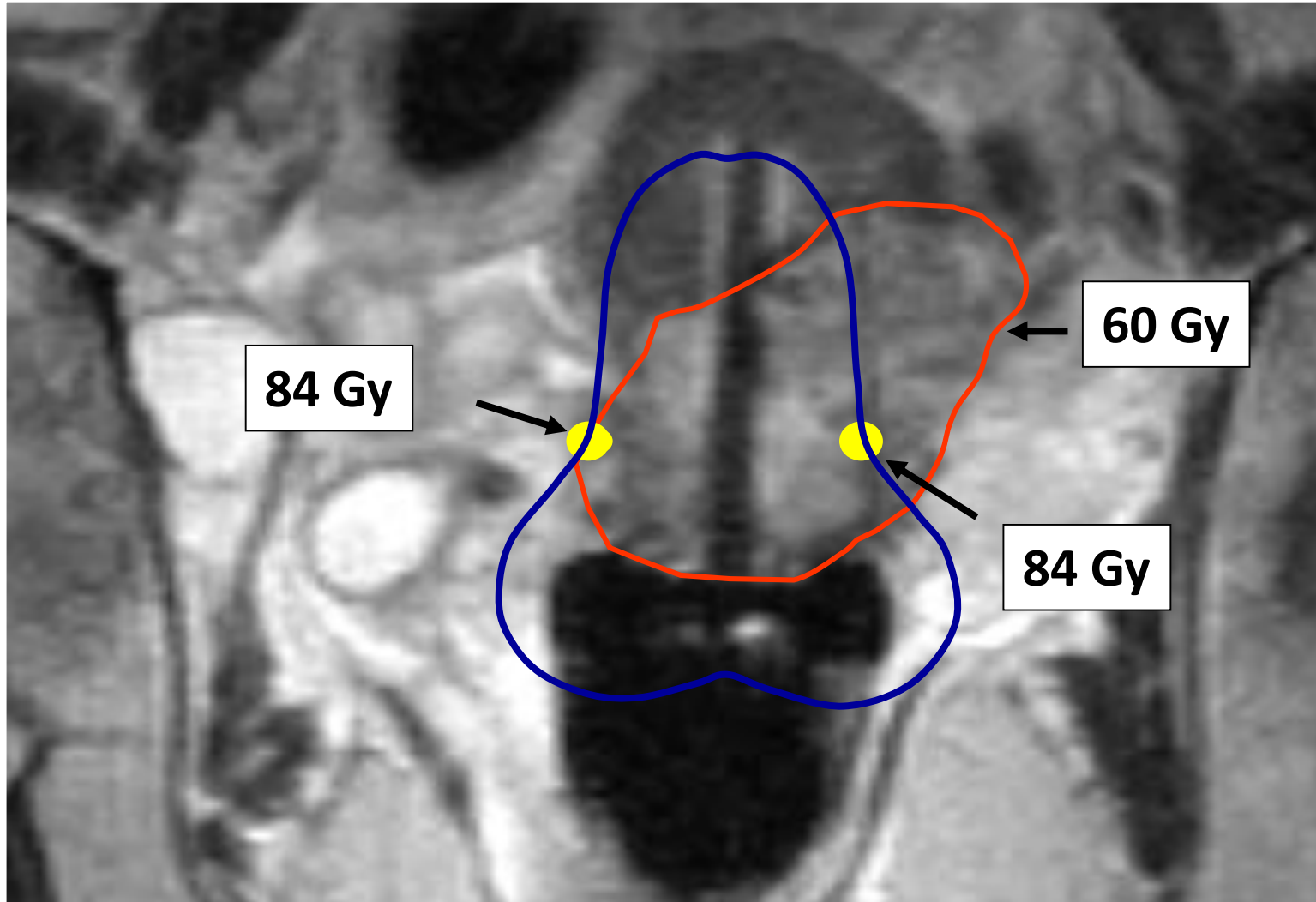
How to evaluate a treatment plan?

Dose points

Dose distribution

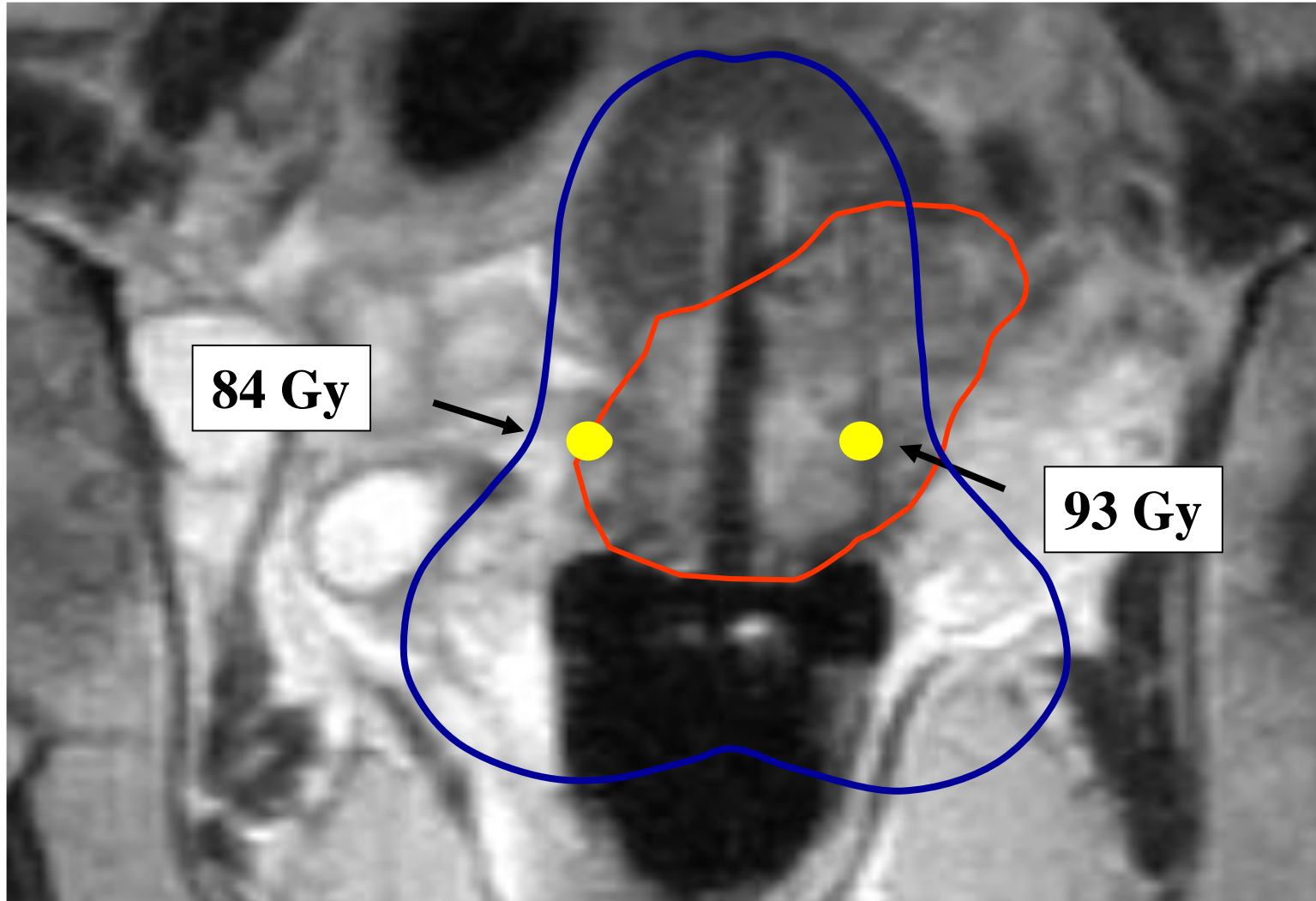


Point A / target dose



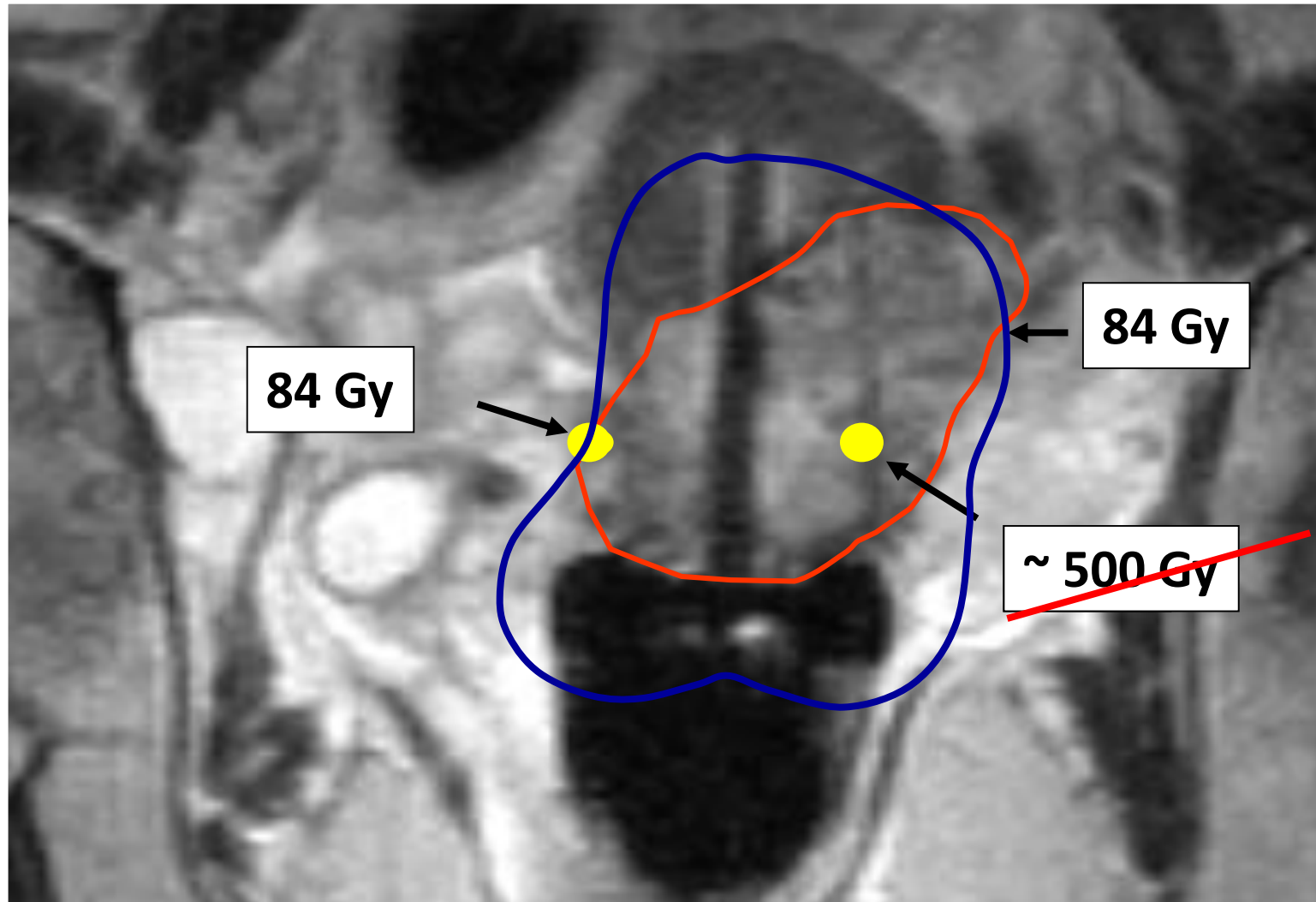
D90 = 65 Gy EQD2

Point A / target dose



D90 = 75 Gy EQD2

Point A / target dose



D90 = 90 Gy EQD2

How to evaluate a treatment plan?

Dose points

Dose distribution

Dose volume histogram parameters

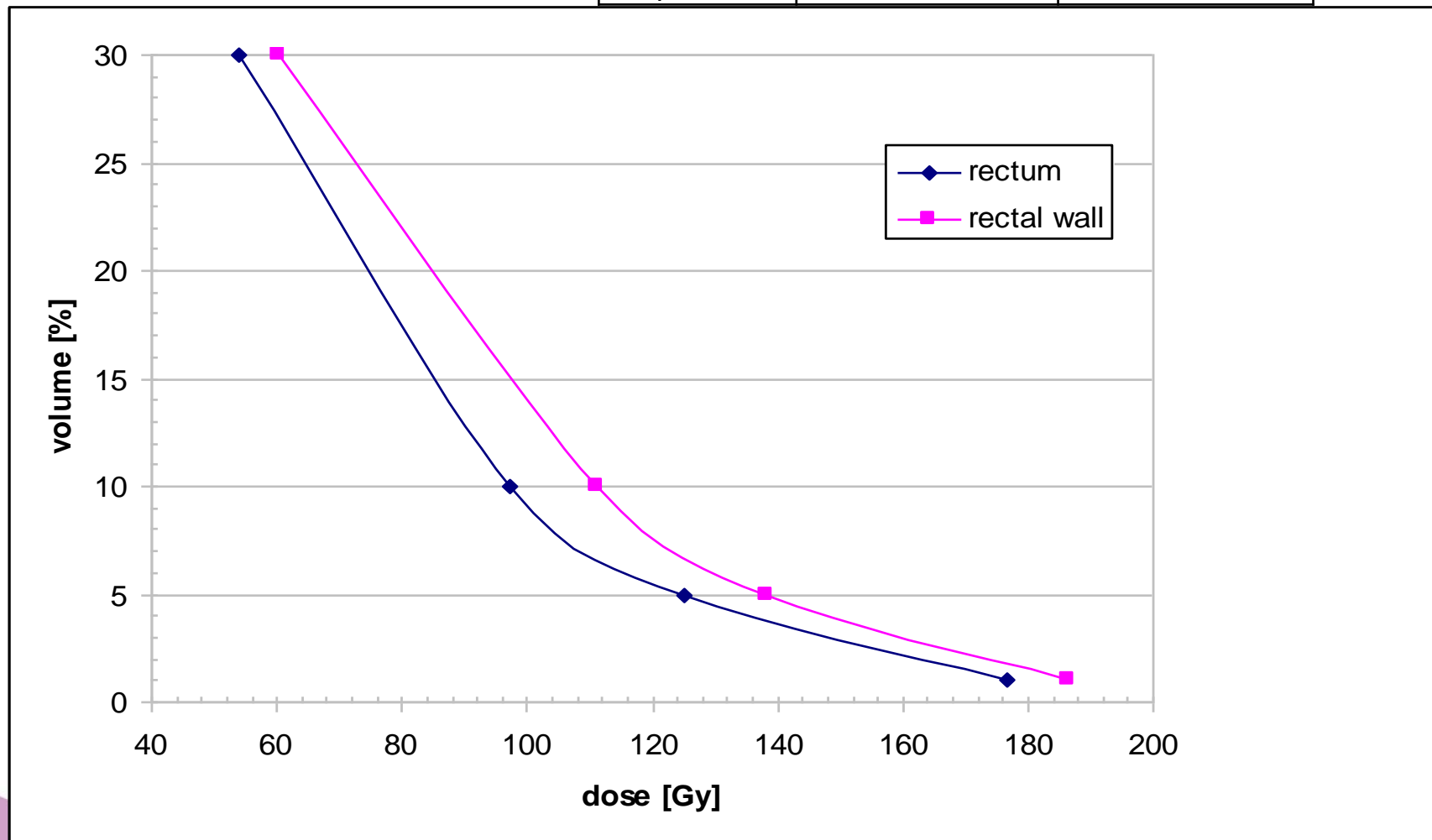
Absolute or Relative Dose Volume Parameters?

Organ or Organ Wall?

DVH

relative Volume

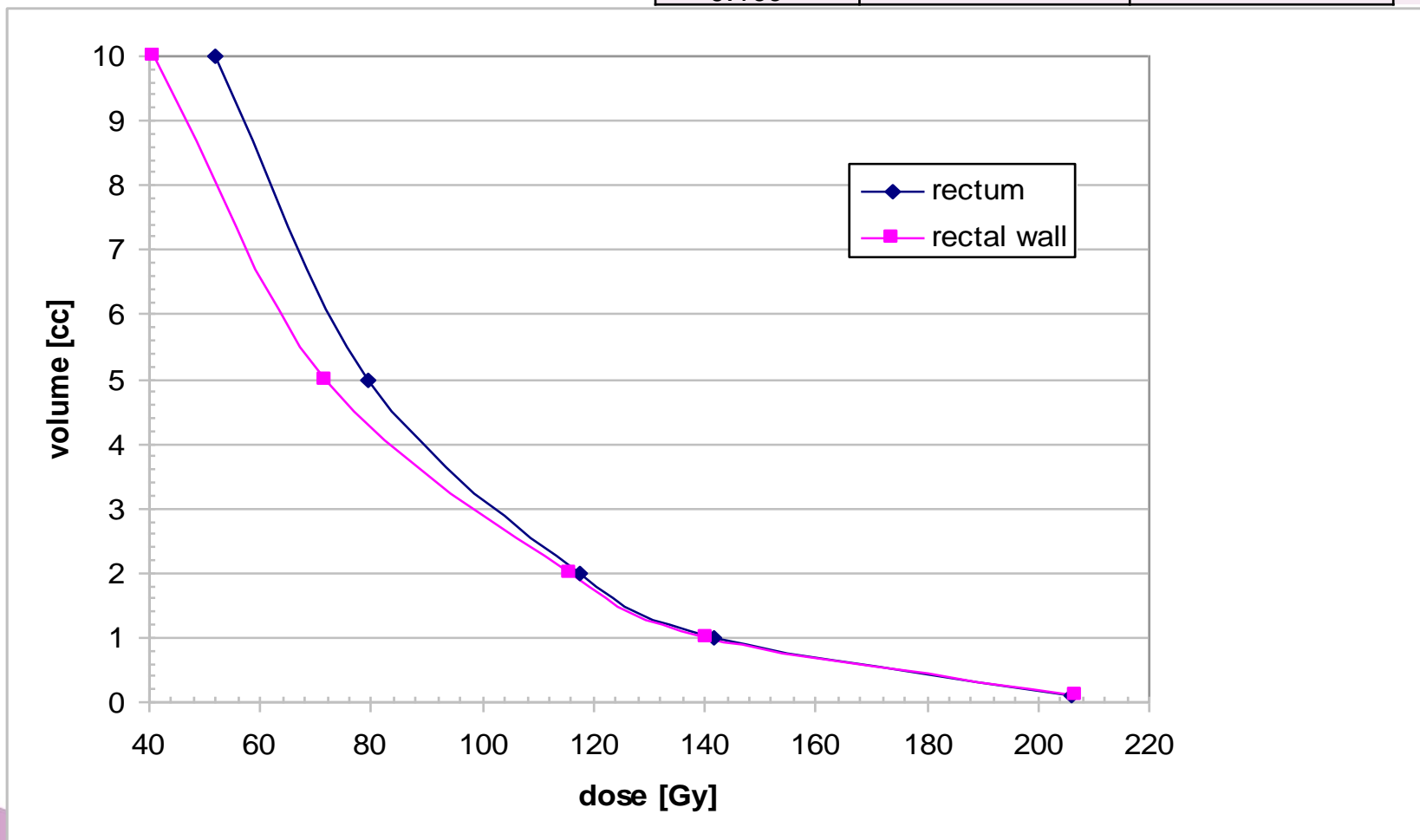
	Wall	Total	deviation
Volume	22 cm ³	34 cm ³	
D ₃₀	60.5 Gy	53.8 Gy	-12.4 %
D ₁₀	111.1 Gy	97.3 Gy	-14.1 %
D ₅	138.4 Gy	125.0 Gy	-10.7 %
D ₁	186.4 Gy	176.5 Gy	-5.4 %



DVH

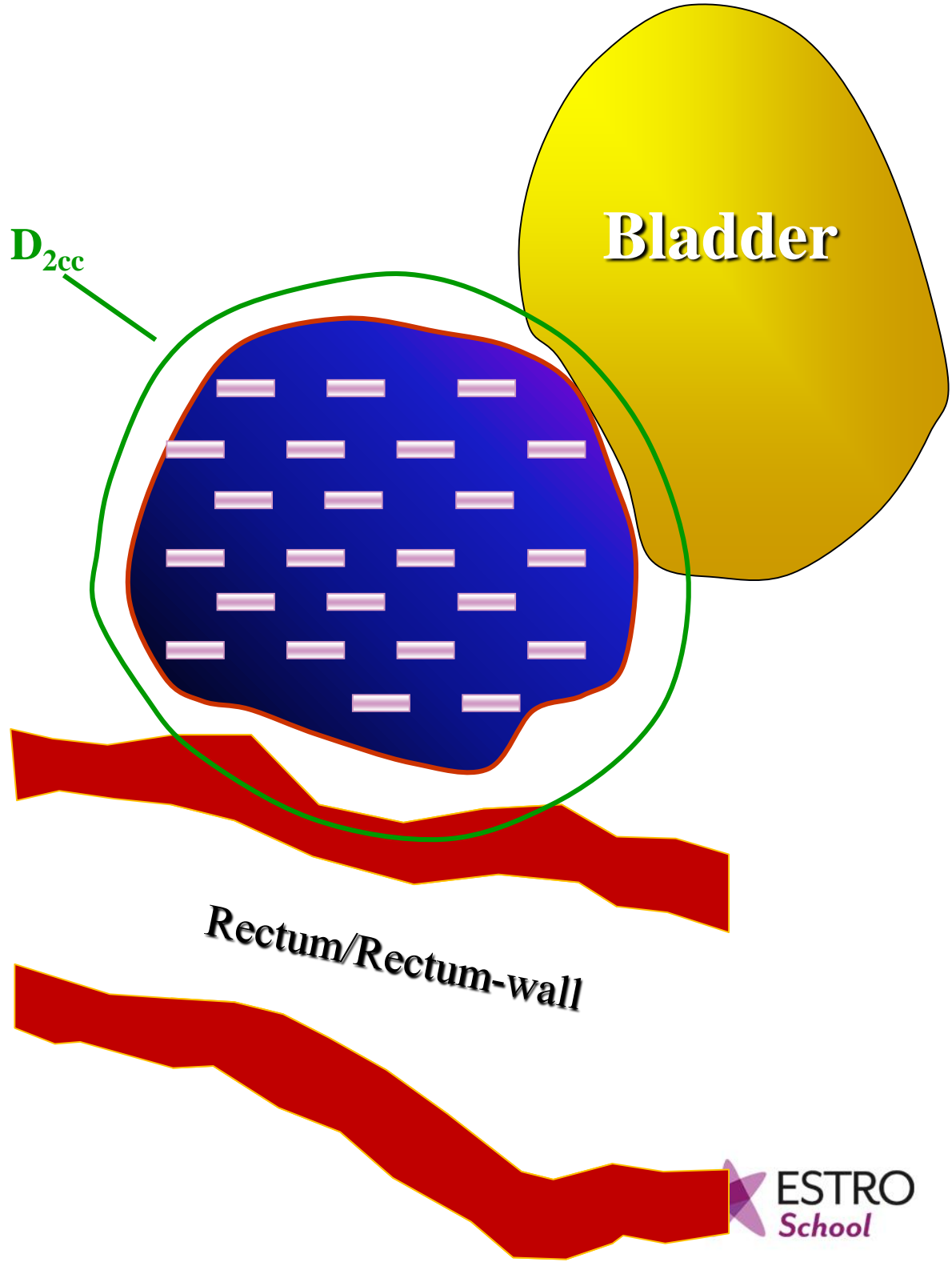
absolute Volume

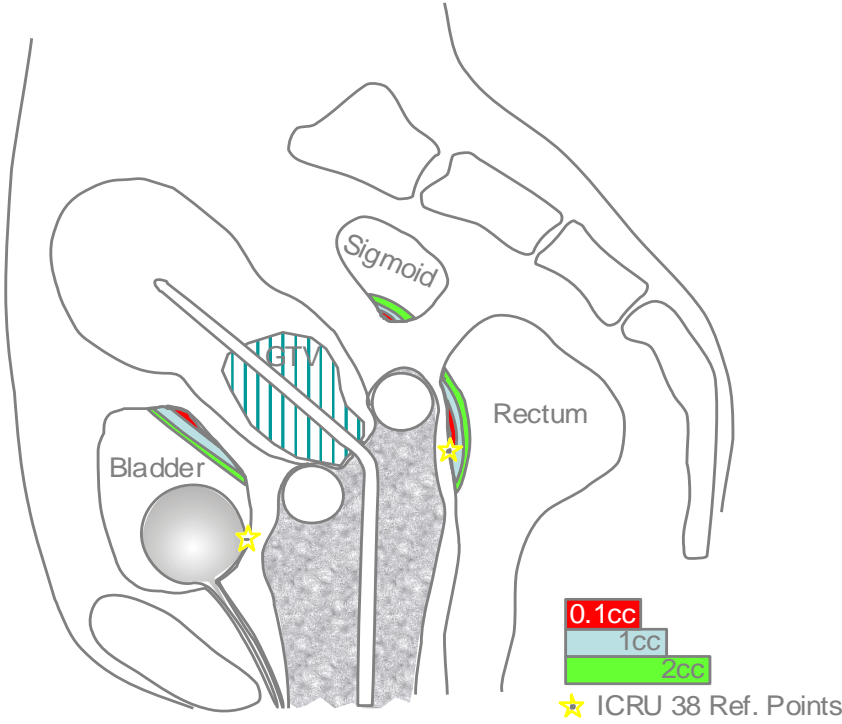
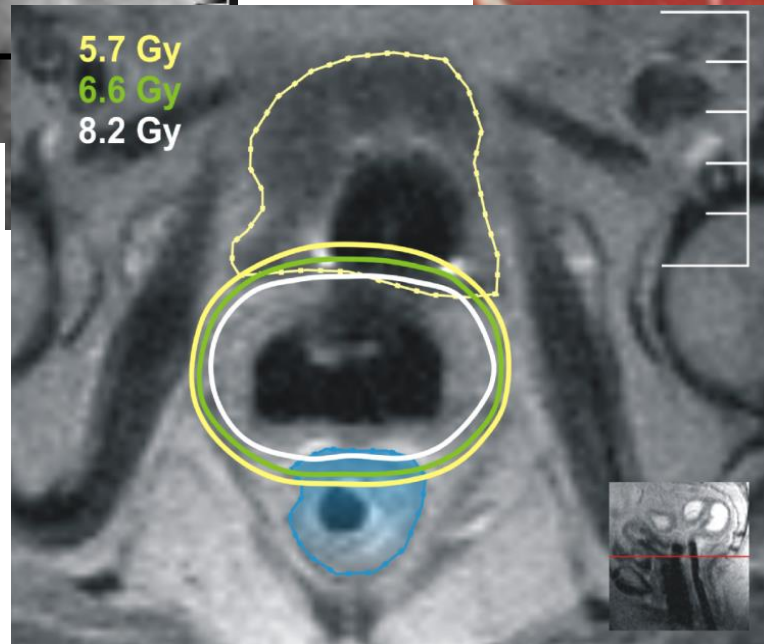
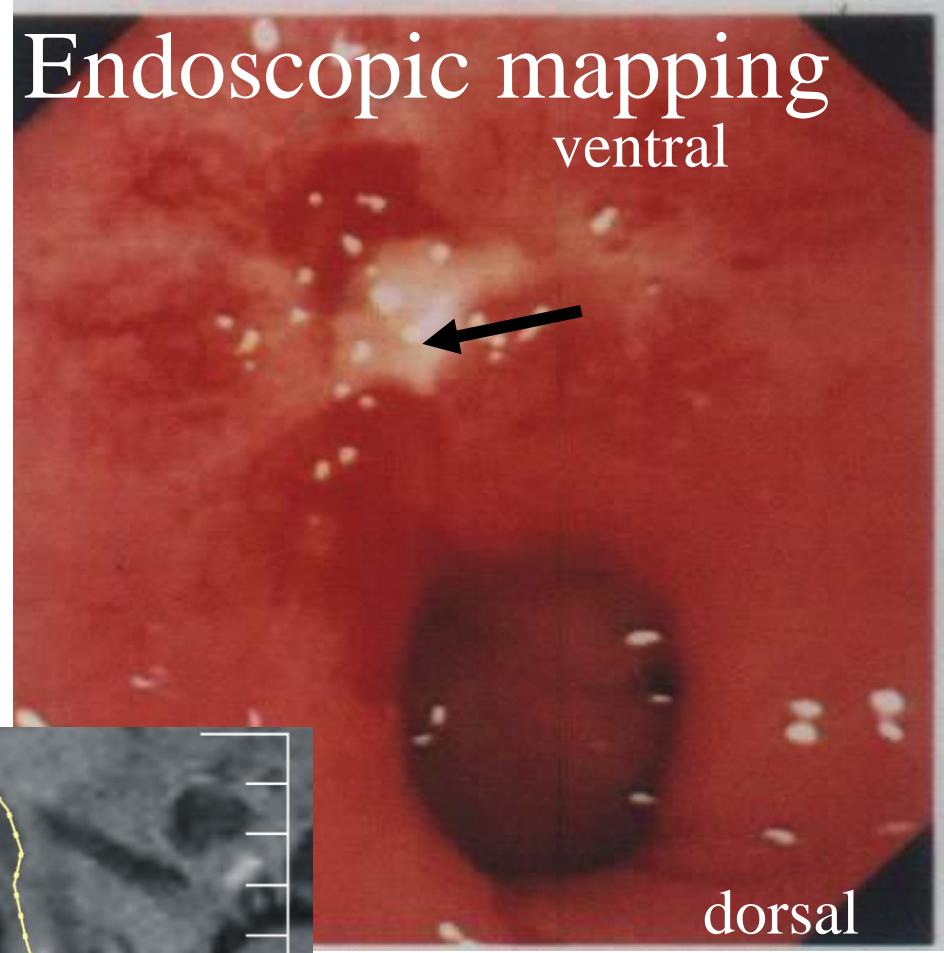
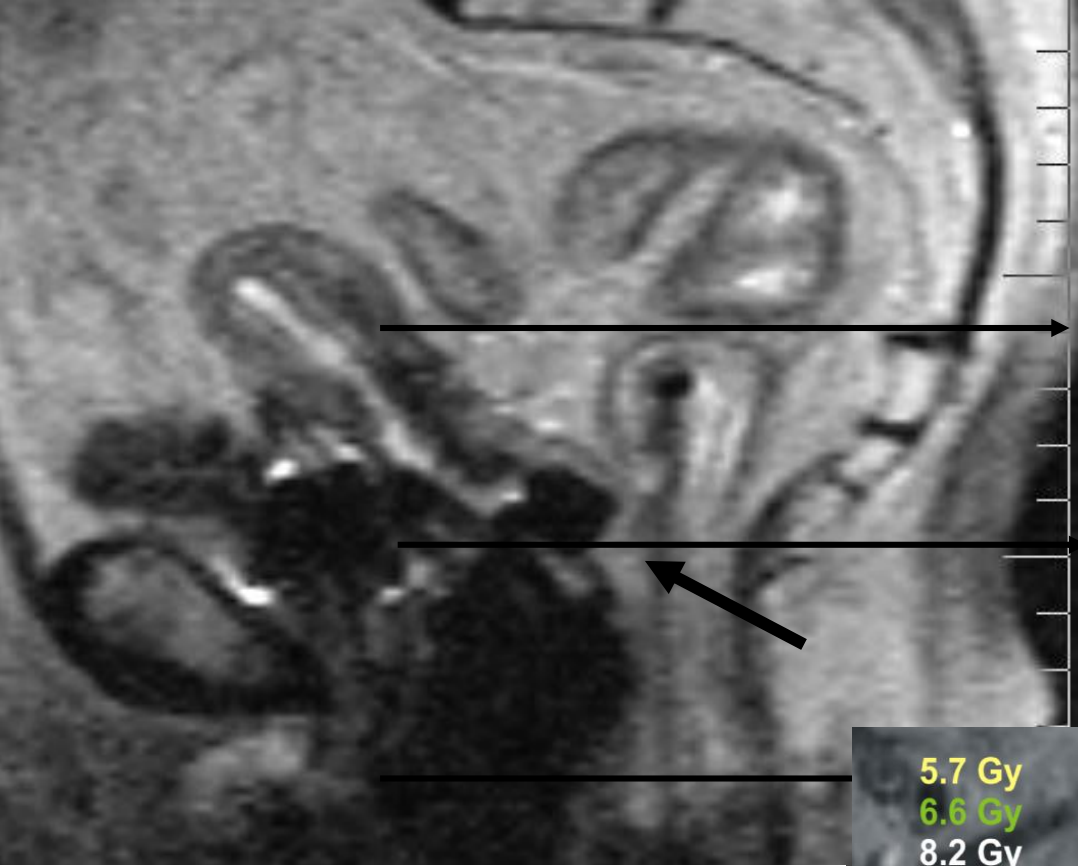
	Wall	Total	deviation
Volume	22 cm ³	34 cm ³	
D _{10cc}	40.9 Gy	52.0 Gy	21.4 %
D _{5cc}	71.6 Gy	79.2 Gy	9.6 %
D _{2cc}	115.7 Gy	117.7 Gy	1.7 %
D _{1cc}	140.3 Gy	141.6 Gy	0.9 %
D _{0.1cc}	206.7 Gy	206.0 Gy	-0.4 %



Parameter	Rectal whole organ		deviation
Volume	28 cm ³	46 cm ³	
D2cc	131 cm ³	131 cm ³	0%
D0.1cc	234 cm ³	234 cm ³	0%
D10	116 cm ³	95 cm ³	-22%
D5	143 cm ³	122 cm ³	-17%
V100	5%	3%	-62%
V100	1,3 cm ³	1,3 cm ³	0%

	Rectal wall		
Volume	20 cm ³	27 cm ³	
D2cc	128 cm ³	128 cm ³	0%
D0.1cc	241 cm ³	241 cm ³	0%
D10	128 cm ³	117 cm ³	-10%
D5	161 cm ³	146 cm ³	-10%
V100	7%	5%	-37%
V100	1,5 cm ³	1,4 cm ³	-1%





$$D_{2cc} = 81 \text{ Gy EQD}_2$$

$$D_{0.1cc} = 108 \text{ Gy EQD}_2$$

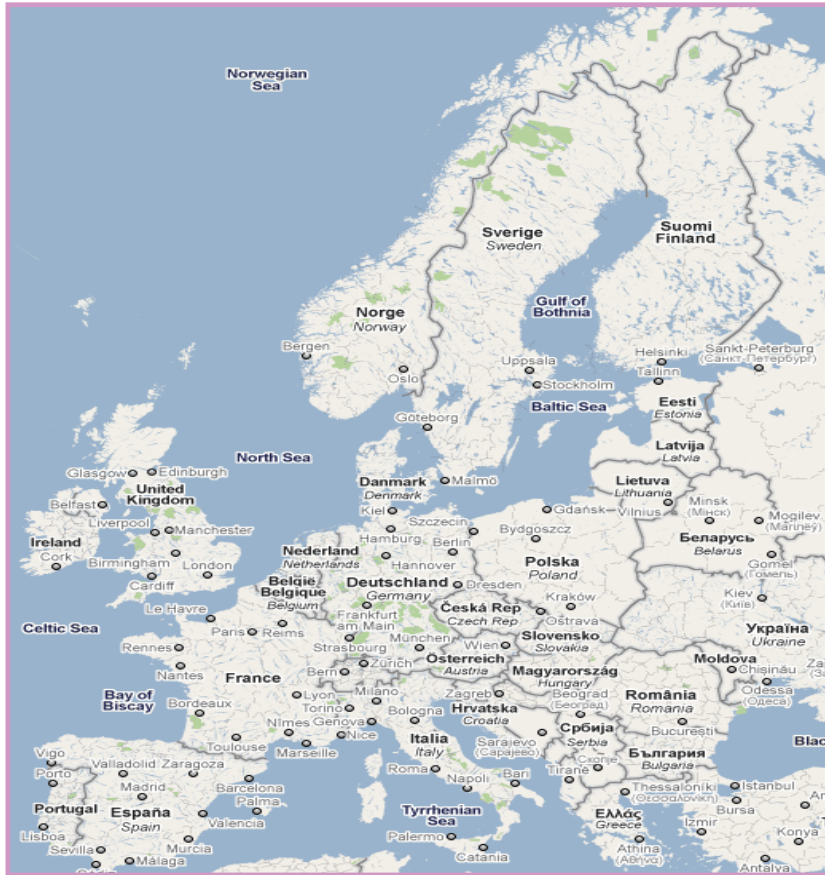
Pötter et al. Radiother & Oncol 2005
 Georg et al. Radiother & Oncol 2009





EMBRACE

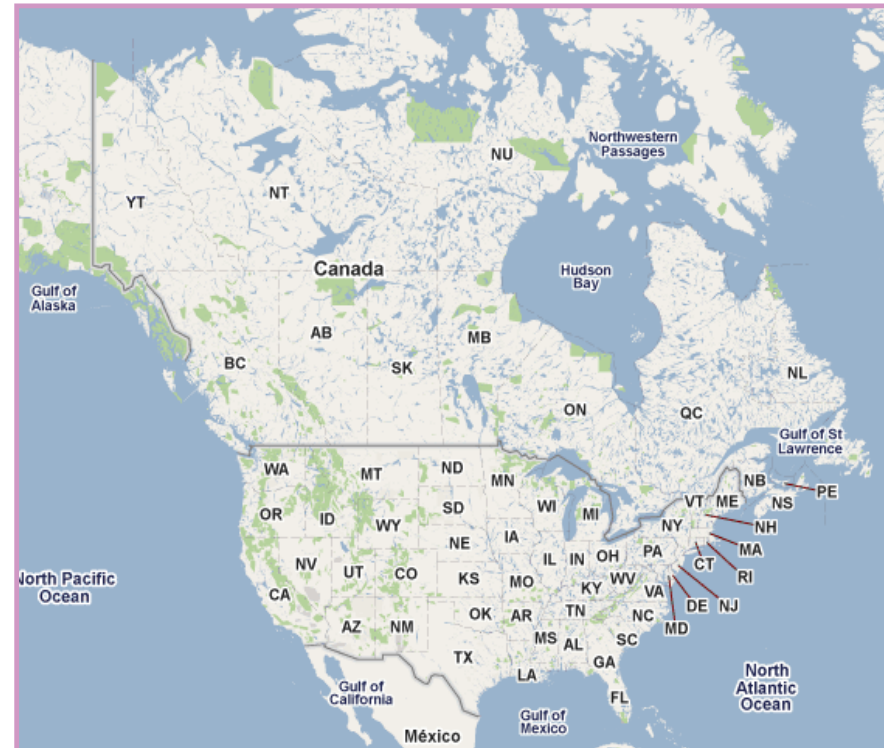
Vienna
 Aarhus
 Utrecht
 Leiden
 Leuven
 Ljubljana
 London
 Arnhem
 Pamplona
 Paris
 Kaposvar
 Maastricht
 Trondheim
 Leeds
 Oslo
 Amsterdam
 Kuopio
 Cambridge



24 Active Centers
 > 1400 patients

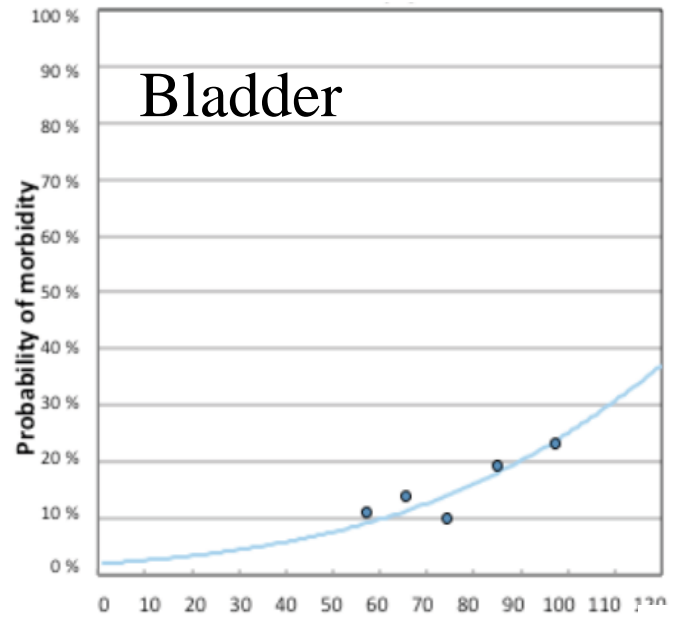


Mumbai
 Chandigarh

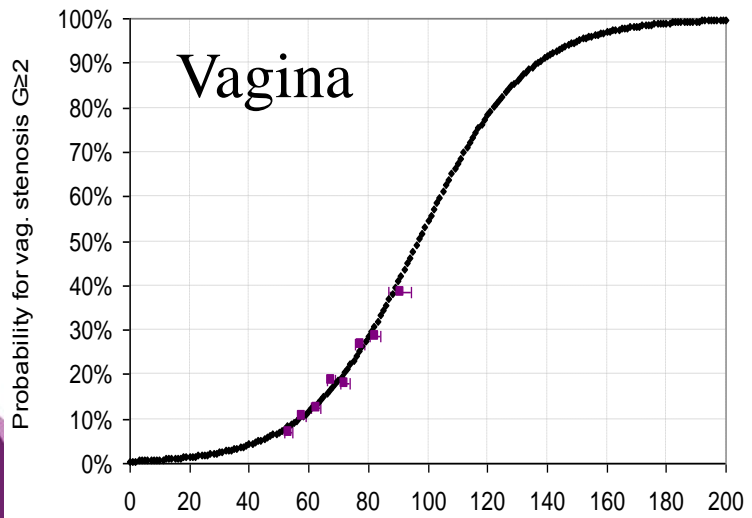


Milwaukee
 Edmonton
 Iowa
 BCU

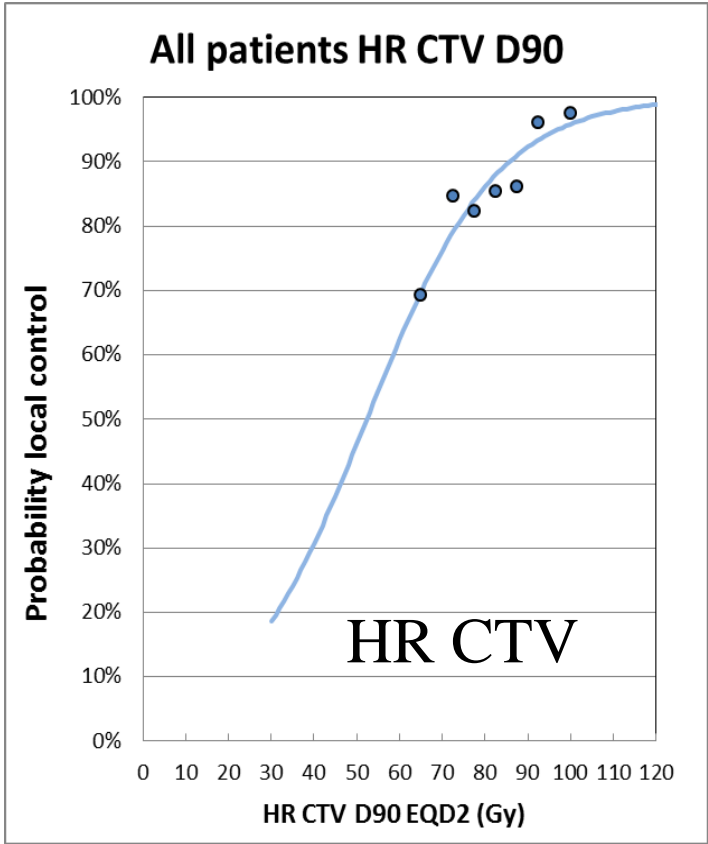
Preliminary dose response studies EMBRACE and retro-EMBRACE



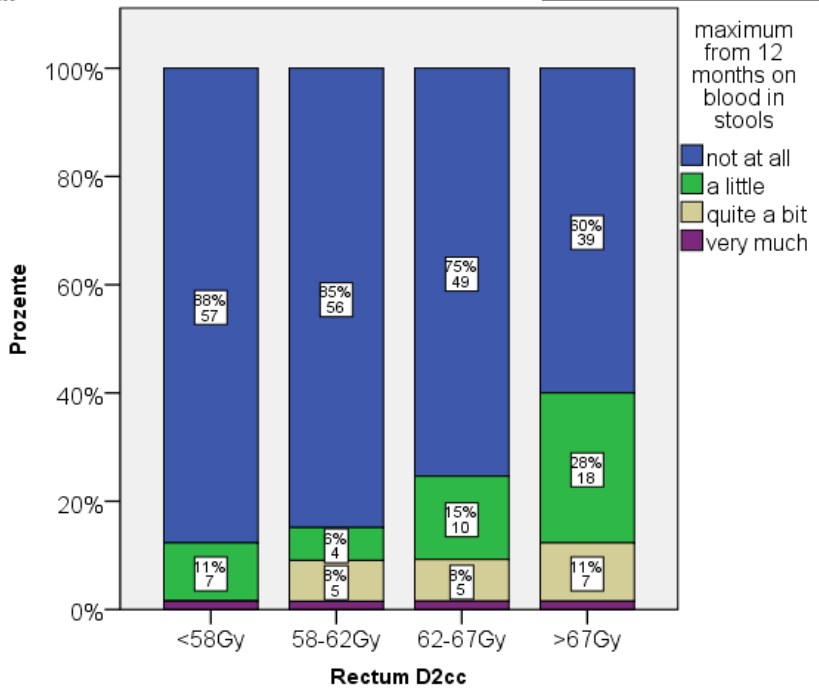
Dose response curve



Dose to the ICRU rectal point in Gy (EQD2)



GI



Do we need more than one dose parameter?

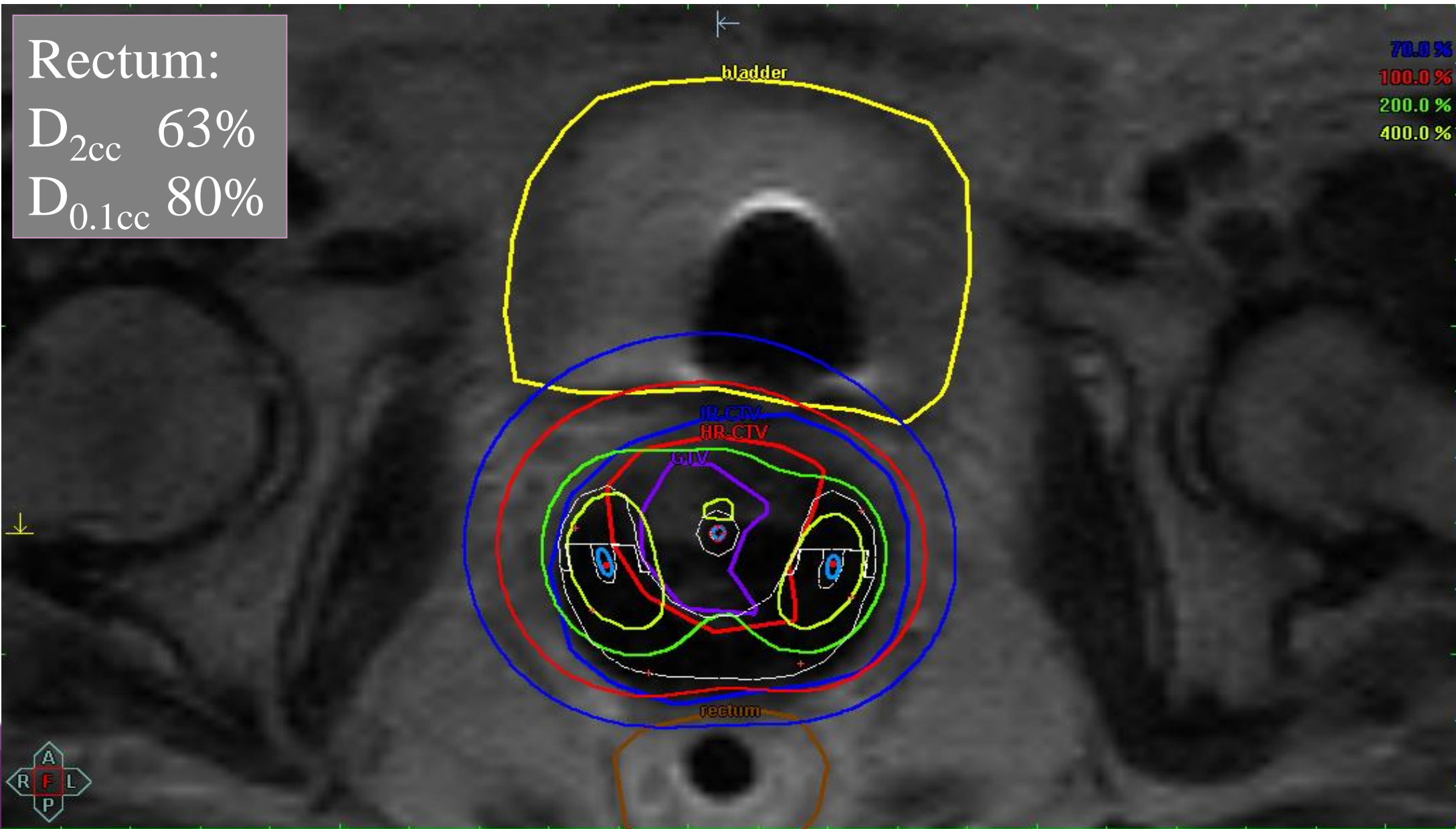
	EBRT	HDR boost	HDR mono
EBRT	70 Gy	35.7 Gy 13 fr.	0
BT	0 Gy	2 x 8.5 Gy	4 x 9.5 Gy
EQD2	70 Gy	??80 Gy??	??95 Gy??
D_{2cc}	70 Gy	2 x 5.4 Gy	4 x 6.0 Gy
EQD2	70 Gy	59 Gy	43 Gy
$D_{0.1cc}$	70 Gy	2 x 7.3 Gy	4 x 8.2 Gy
EQD2	70 Gy	71 Gy	73 Gy
	1.0	1.2	1.7

Typical dose distribution

Rectum:

D_{2cc} 63%

$D_{0.1cc}$ 80%

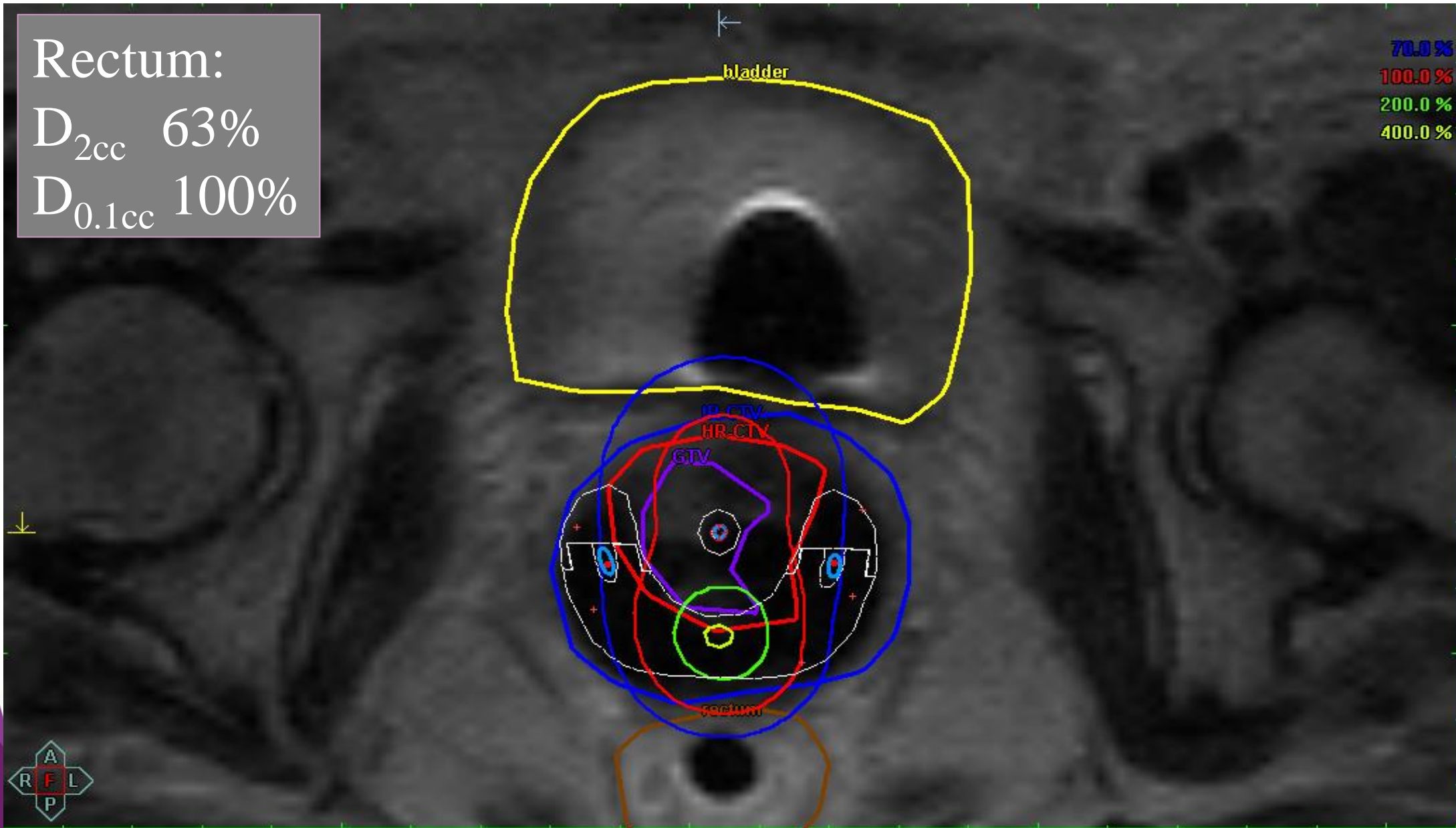


Optimized only based on limited parameter set

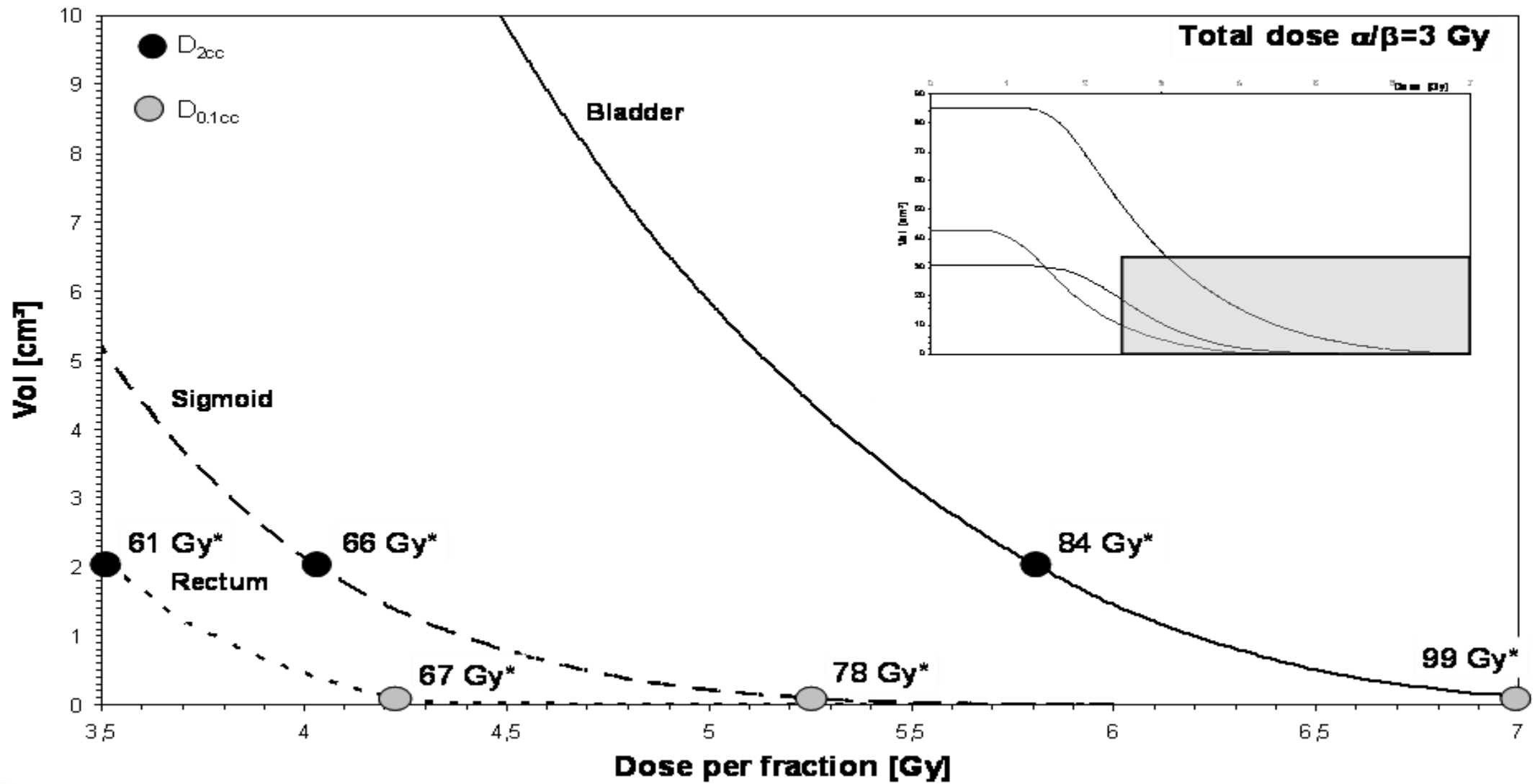
Rectum:

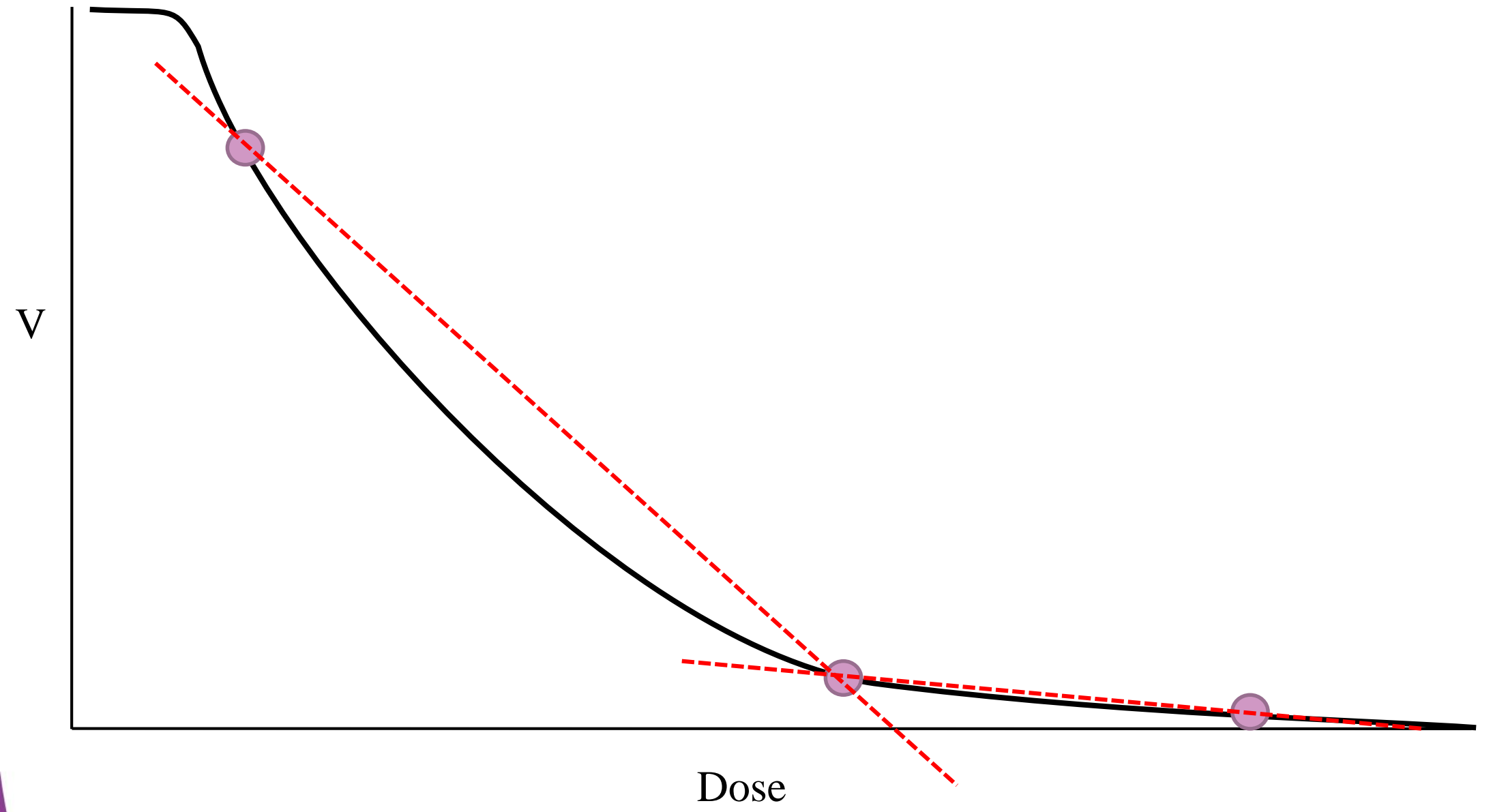
D_{2cc} 63%

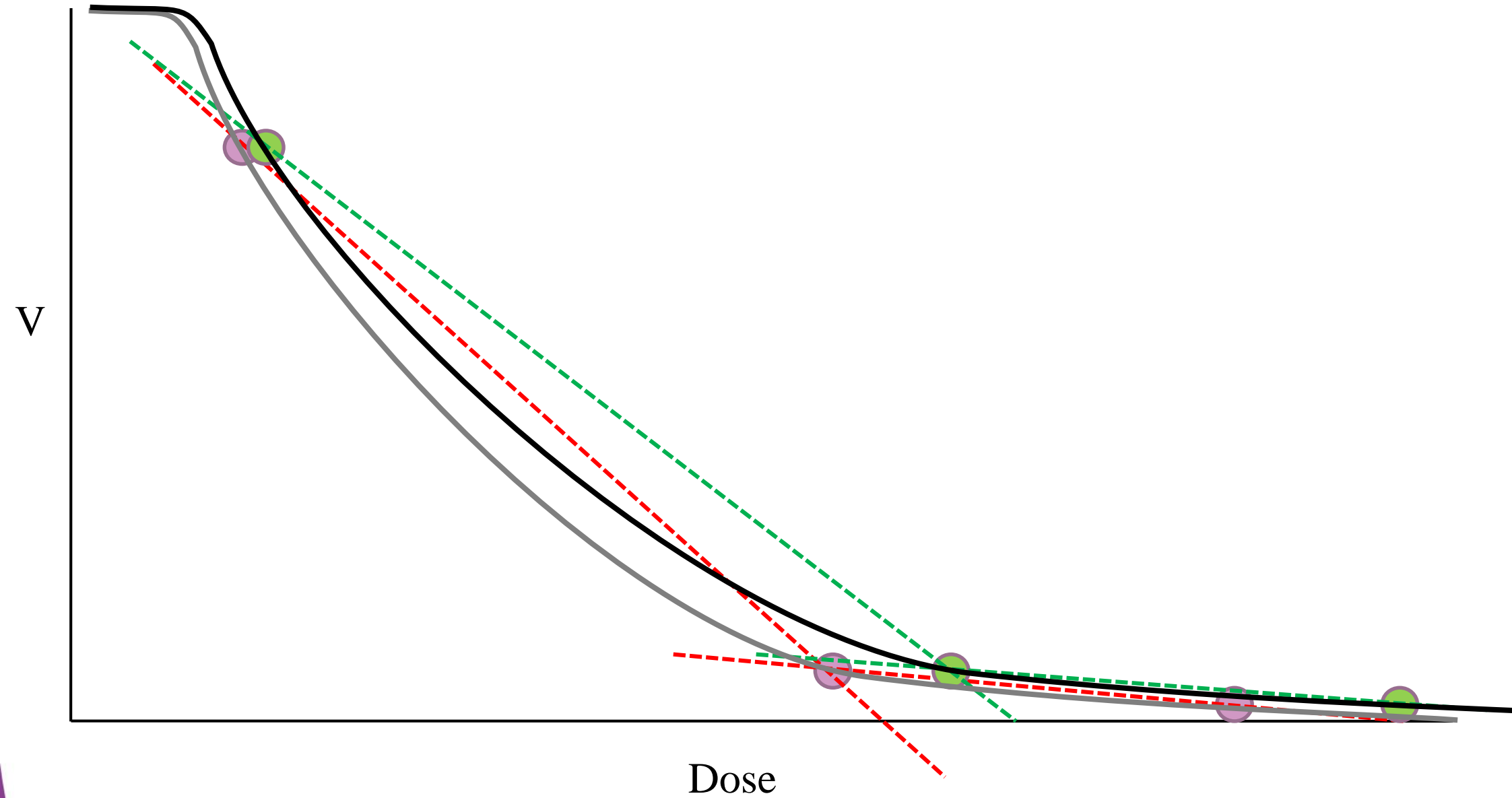
$D_{0.1cc}$ 100%

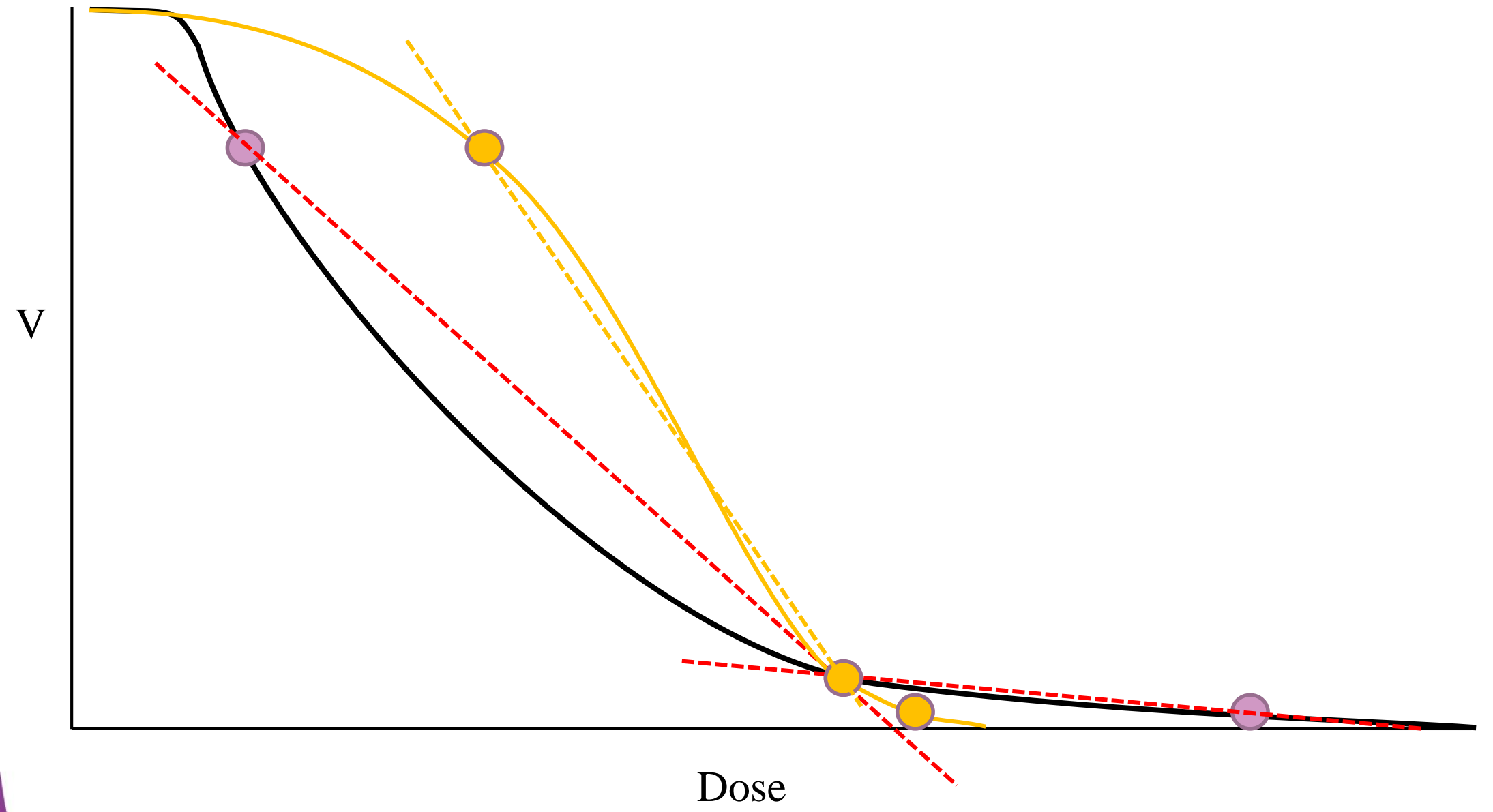


DVH for OAR

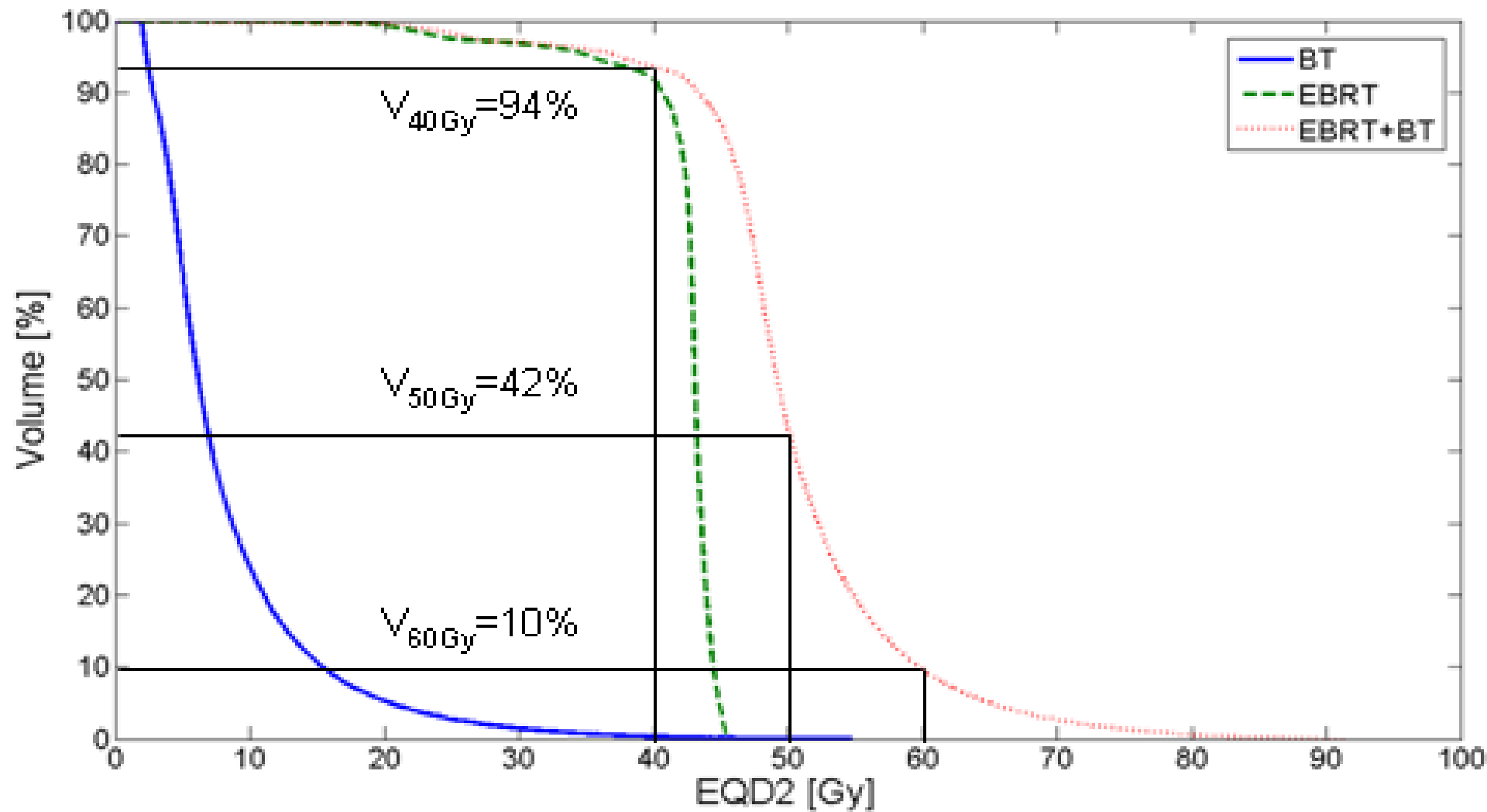






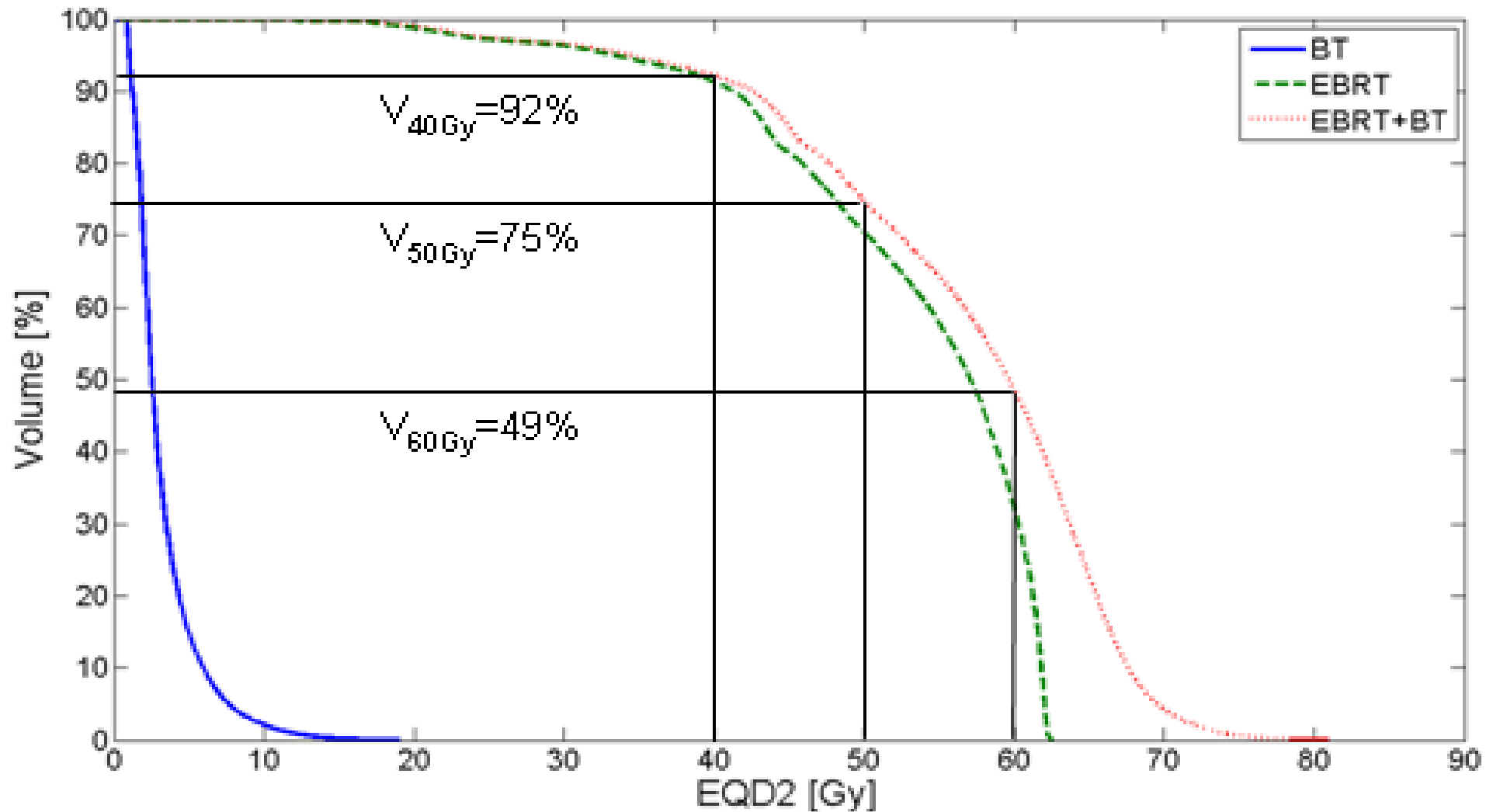


Rectum DVH: 45 Gy whole pelvis EBRT plus 4 fractions of HDR brachytherapy (total target dose 85Gy EQD2)



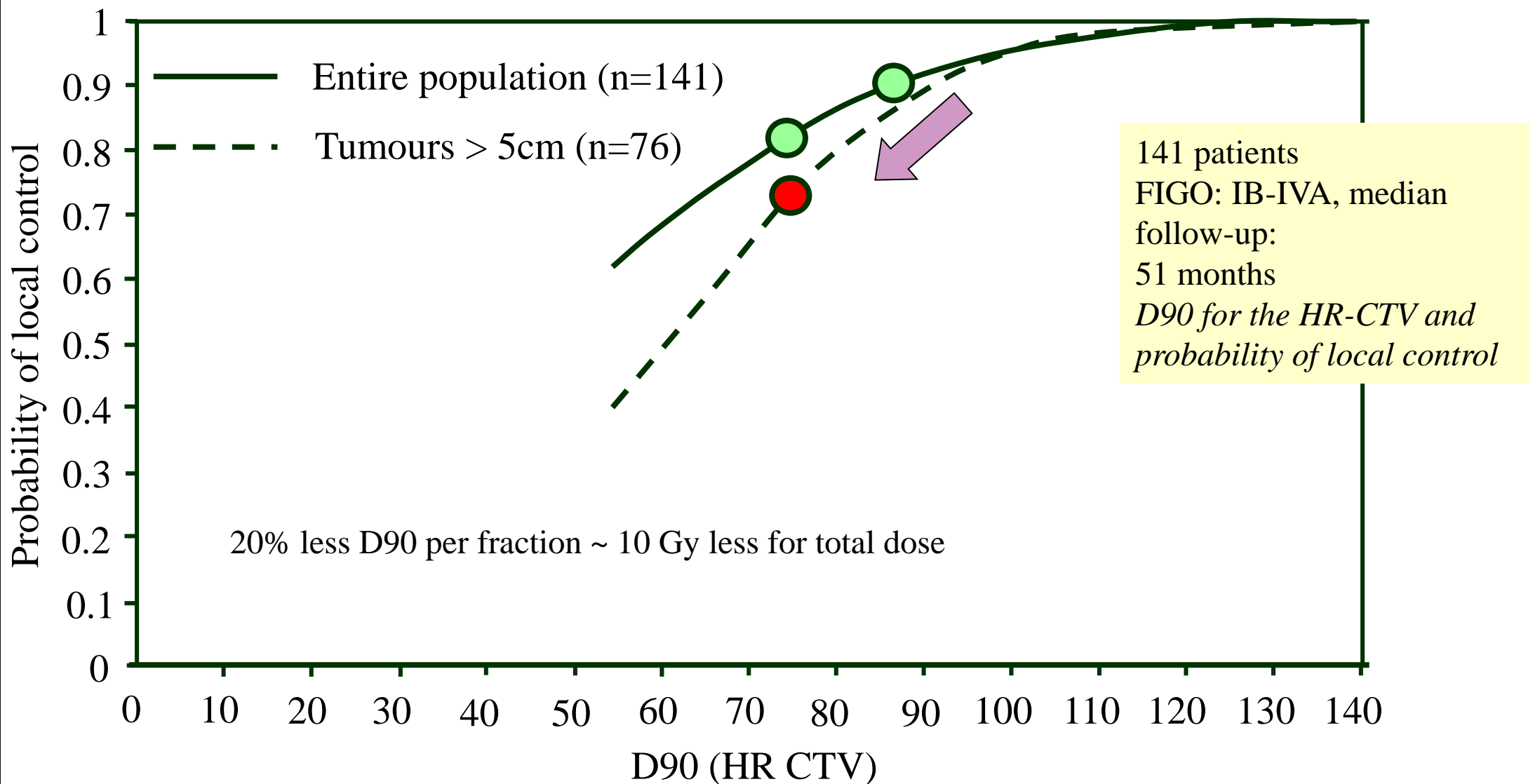
From upcoming ICRU report 88

Rectum DVH: 45 Gy whole pelvis EBRT plus 15 Gy EBRT tumor boost plus 2 fractions of HDR brachytherapy (total target dose 85Gy EQD2)

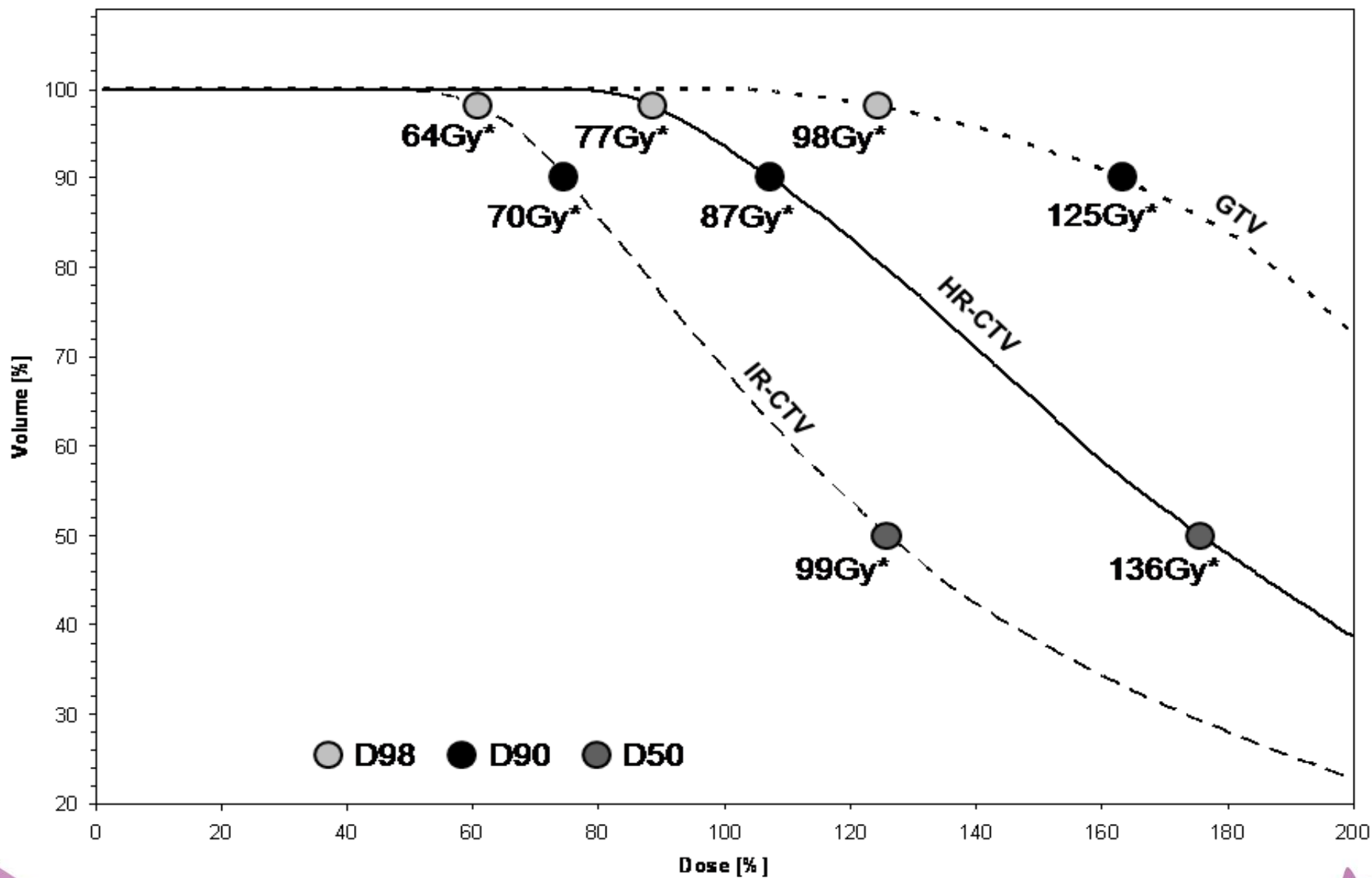


From upcoming ICRU report 88

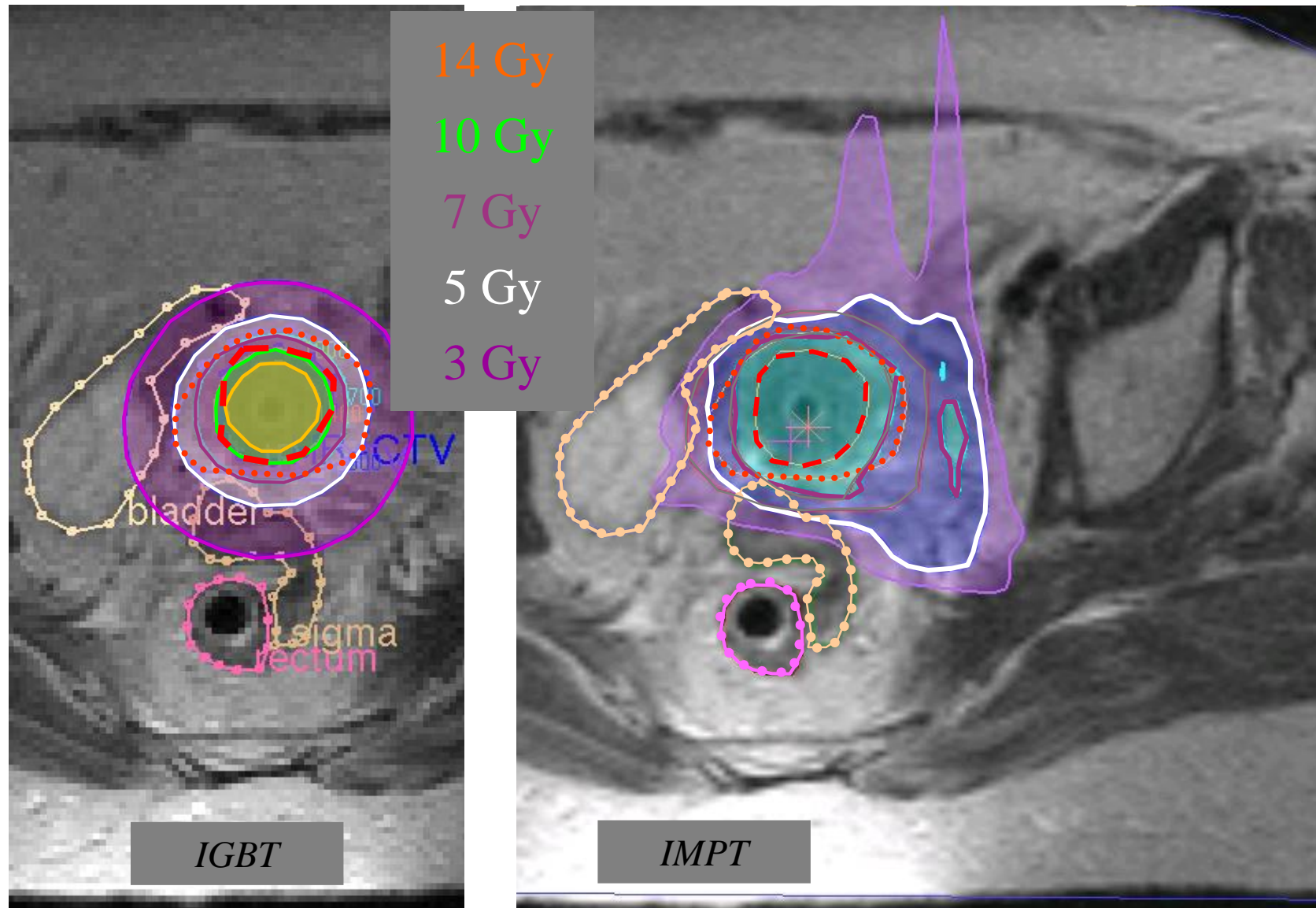
LINKING DVH PARAMETERS TO CLINICAL OUTCOME for TARGET/TUMOUR



DVH for target volumes



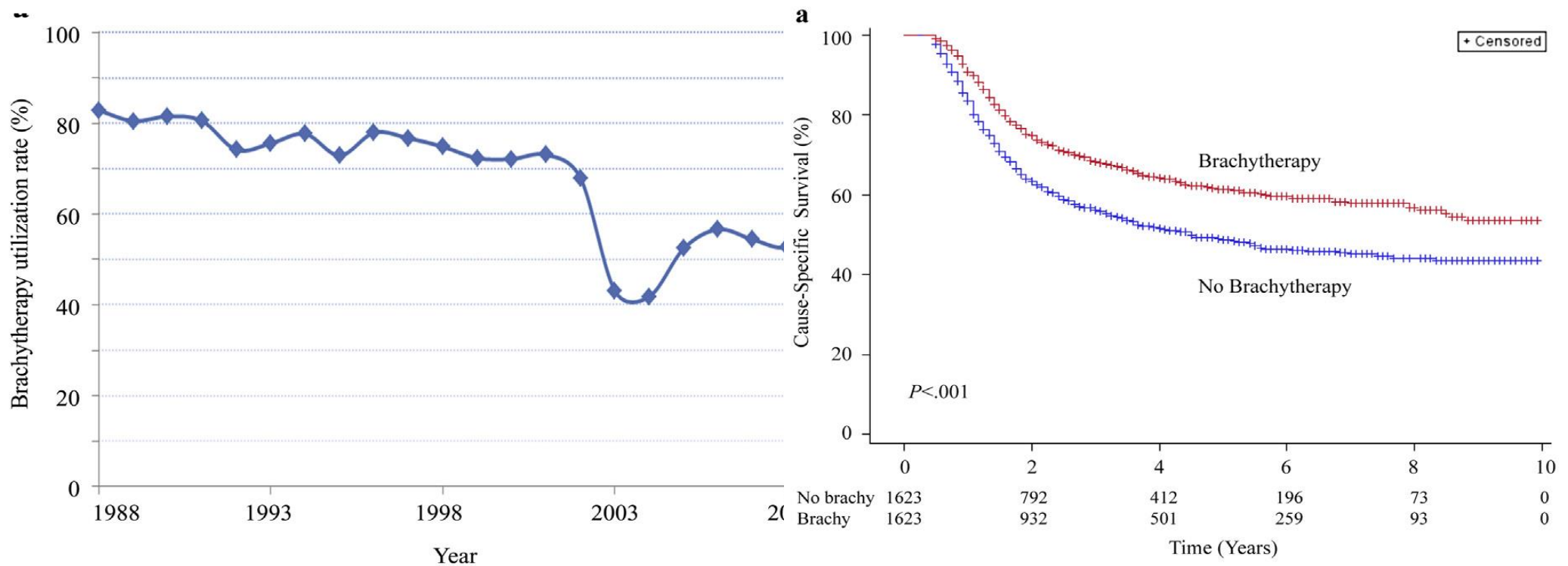
Can we reach the same dose levels by keeping OAR constraints with EBRT?



Georg et al. – IJROBP 2008

Trends in the Utilization of Brachytherapy in Cervical Cancer in the United States

Hahn K, Milosevic M, Fyles, A, Pintilie M, Viswanathan A
 Int J Radiat Oncol Biol Phys 2013



How to evaluate a treatment plan?

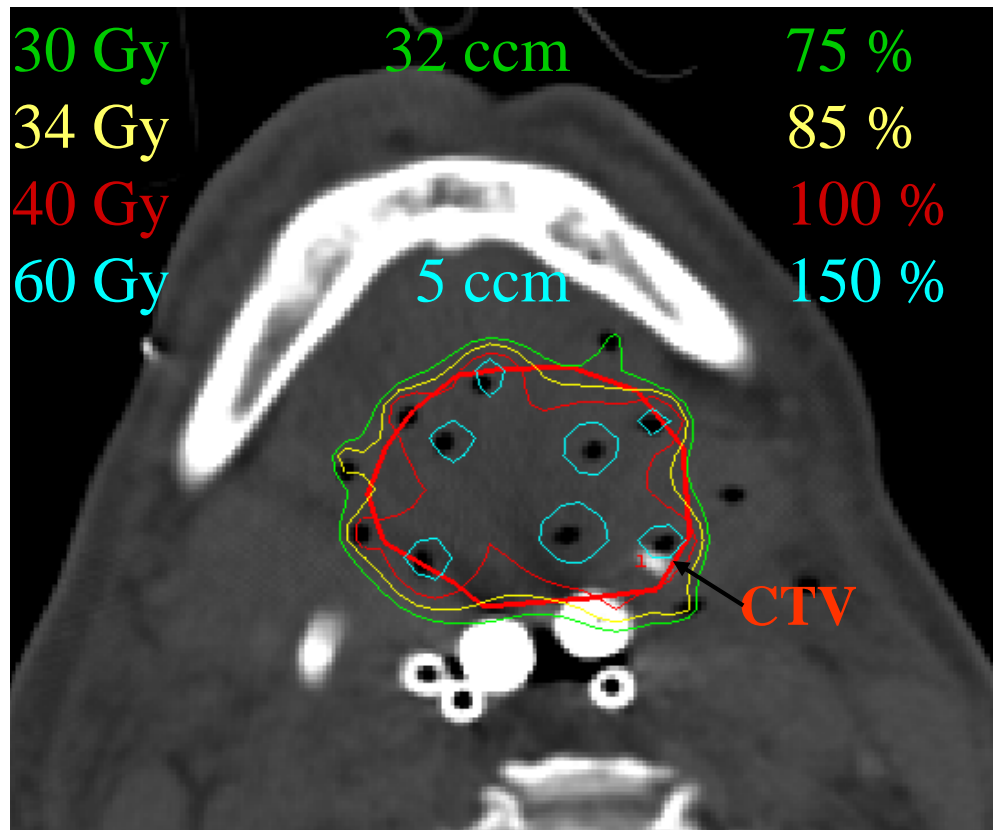
Dose points

Dose distribution

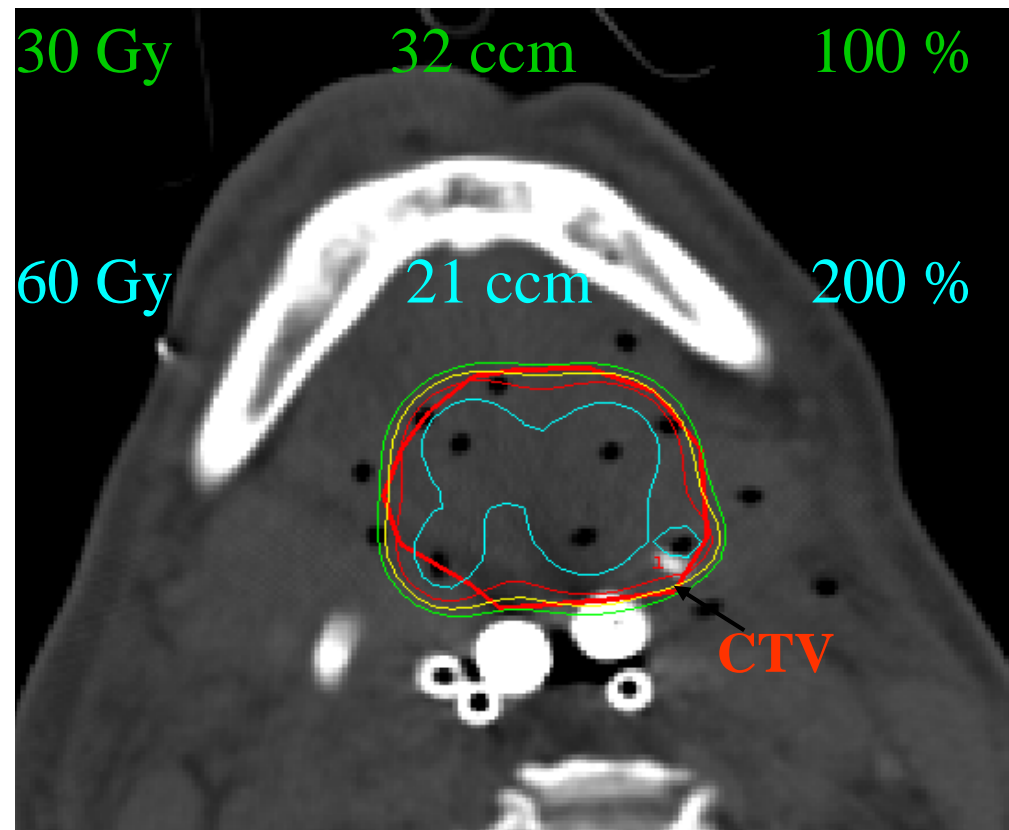
Dose volume histogram parameters

More than one DVH parameter

Dose-volume relationships for interstitial implants

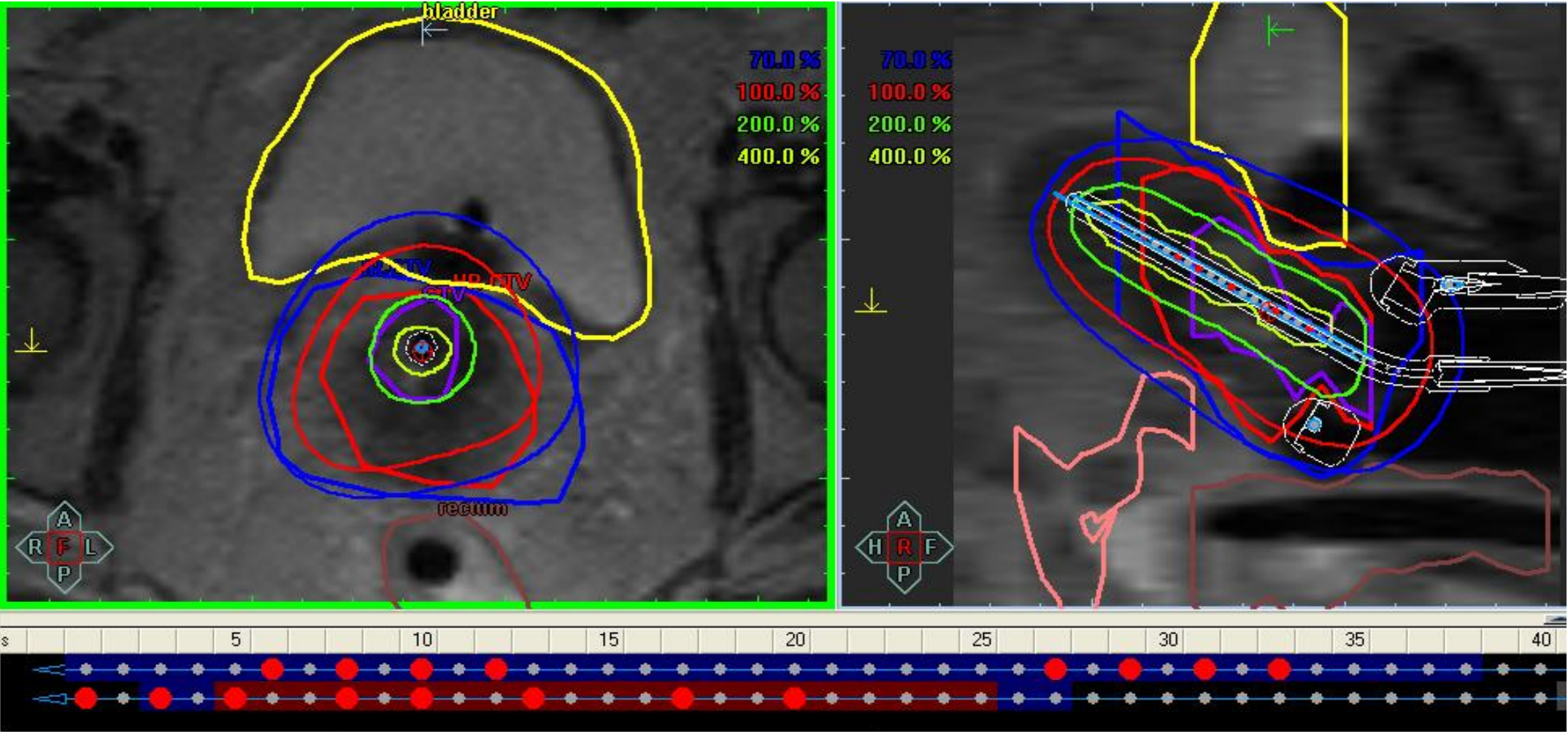


Minimum target dose
Reference dose (85% ICRU58)
Mean central dose
High dose volume

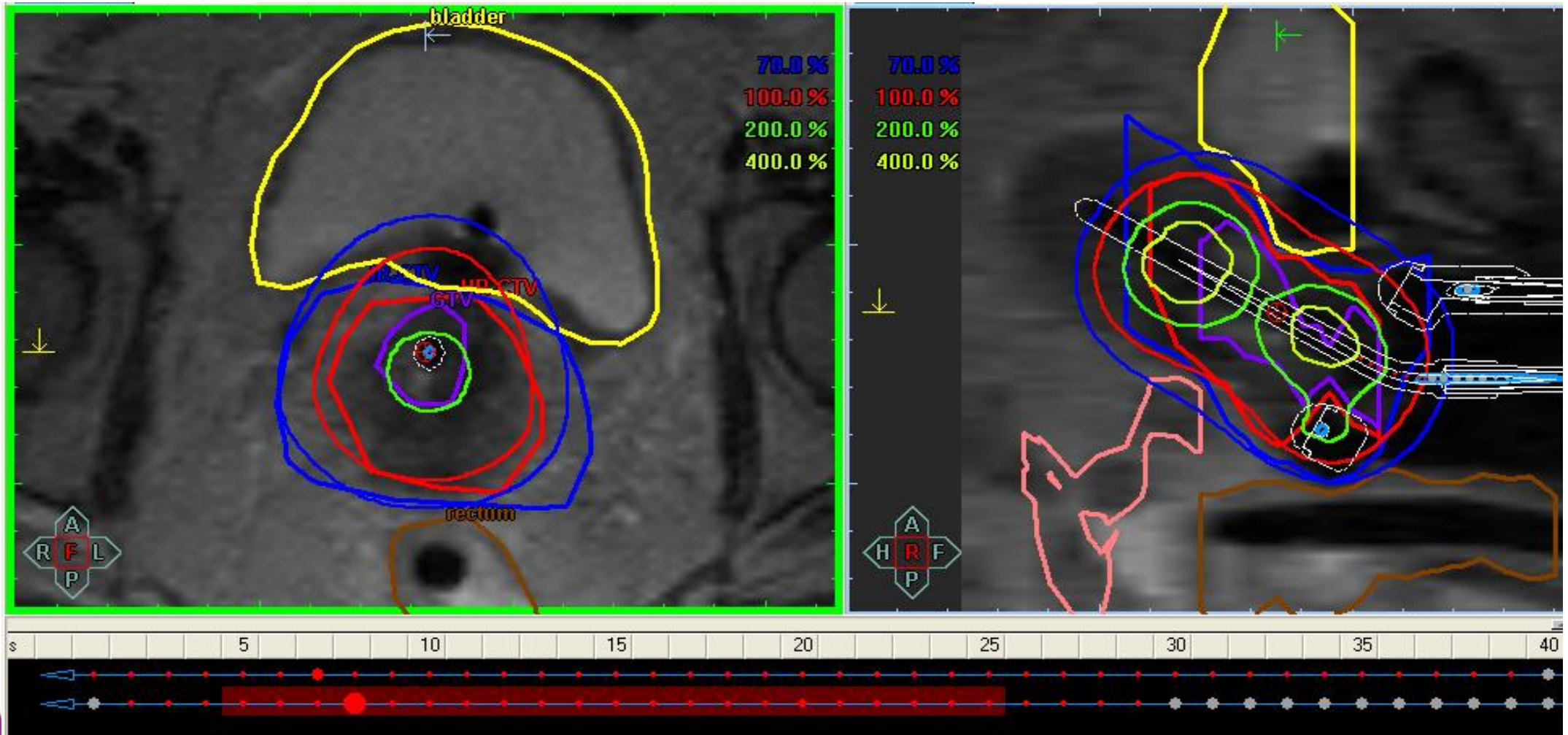


Minimum target dose
High dose volume

Standard loading

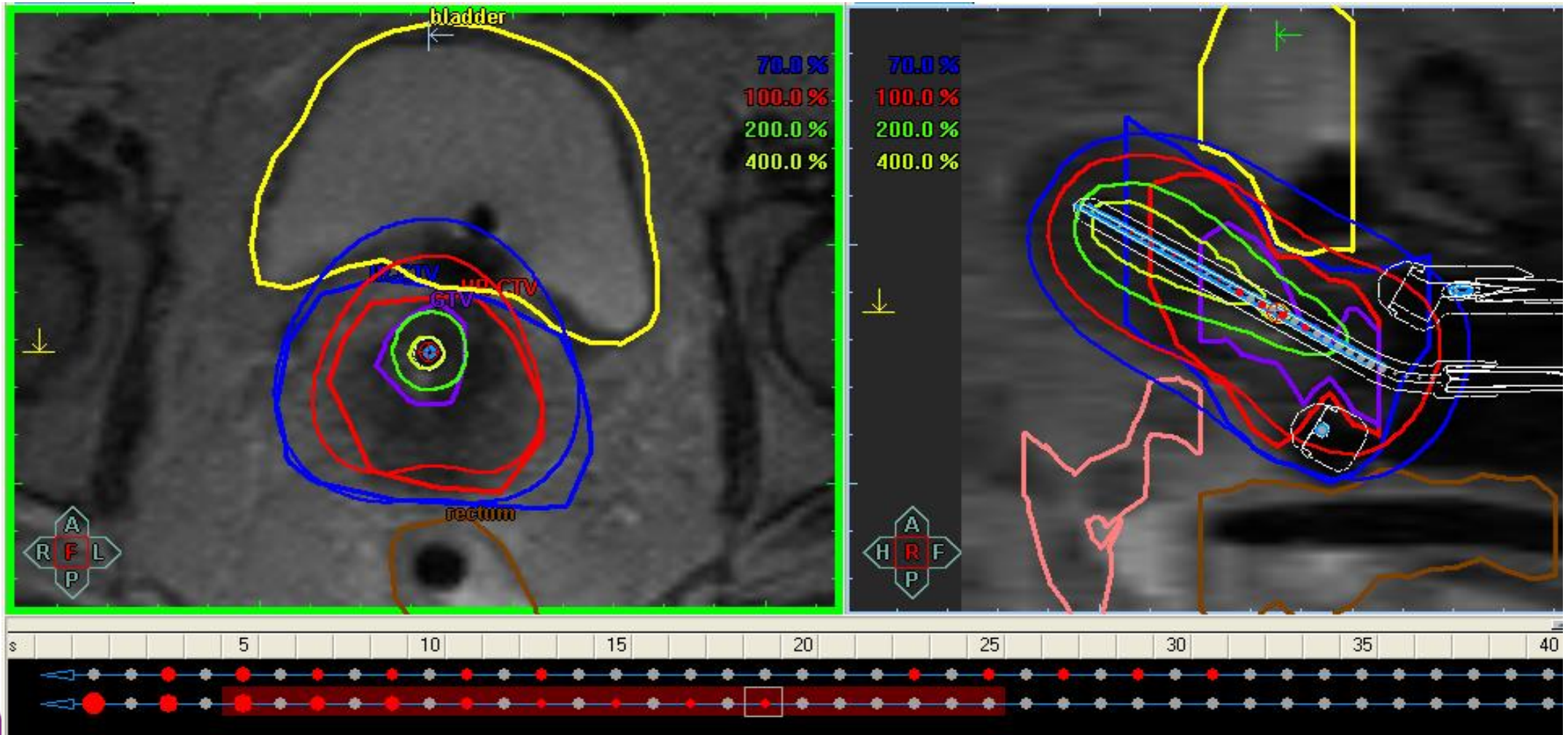


Inverse optimization without thinking

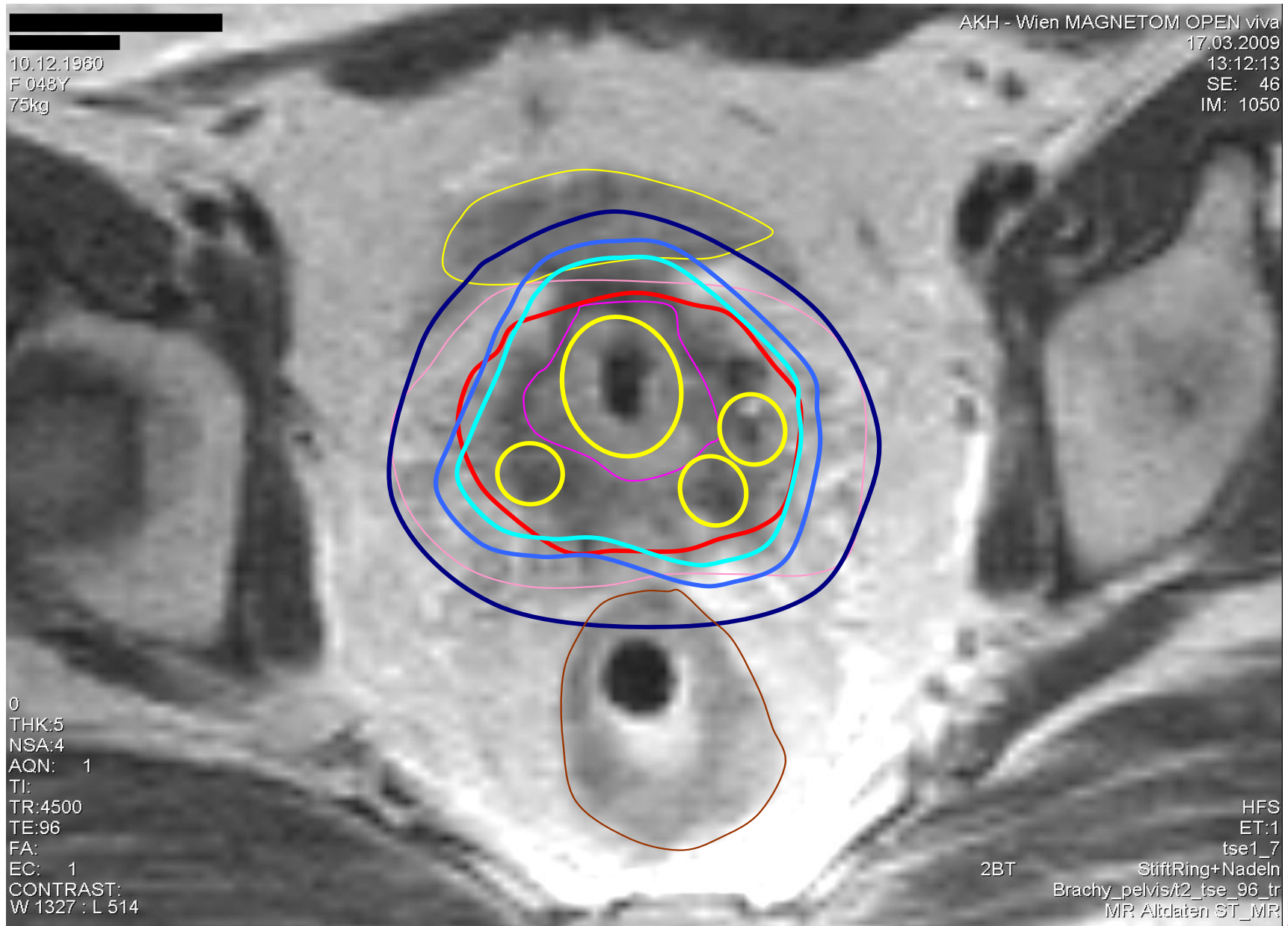


Inverse optimization

Taking into account experience from manual opt.



Spatial dose distribution



Limitations

DVH parameters

Spatial dose distribution (Hot spots)

Dwell time distribution to take into account

not contoured structures

parametrial tissue

vagina

nerves

vessels

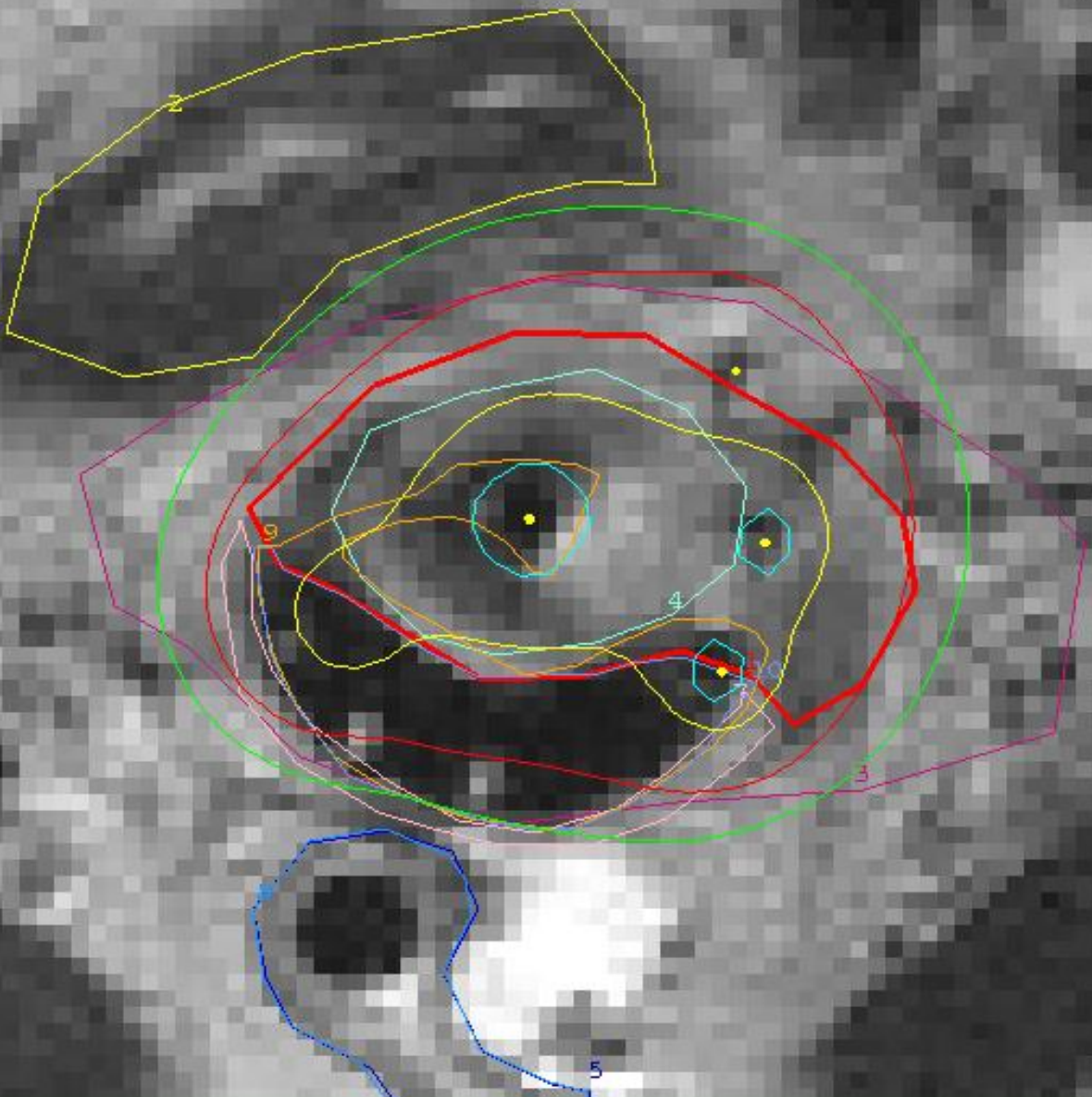
ureter

HR-CTV (1)
bladder (2)
IR-CTV (3)
rectum (5)
vaginal wall (7)
rectosigmoid (8)
app (9)
app_down (10)

slice : 11 of 24
CT) : 5.9

Manual optimization

100 %
200 %
400 %



Catheter: 1 of 6

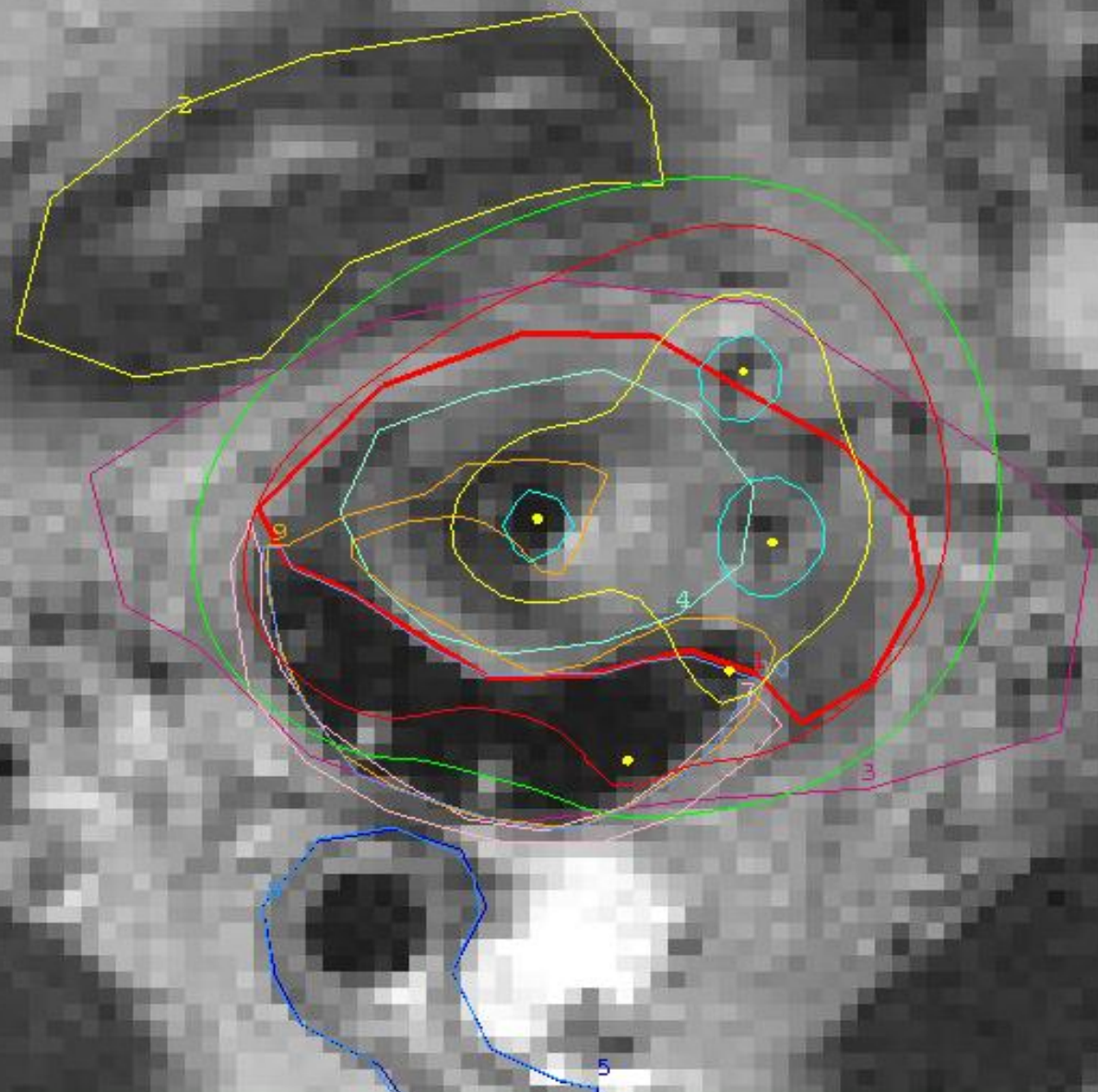


HR-CTV (1)
bladder (2)
IR-CTV (3)
rectum (5)
anal wall (7)
rectosigmoid (8)
app (9)
app_down (10)

Slide : 11 of 24
CT) : 5.9

Inverse optimization

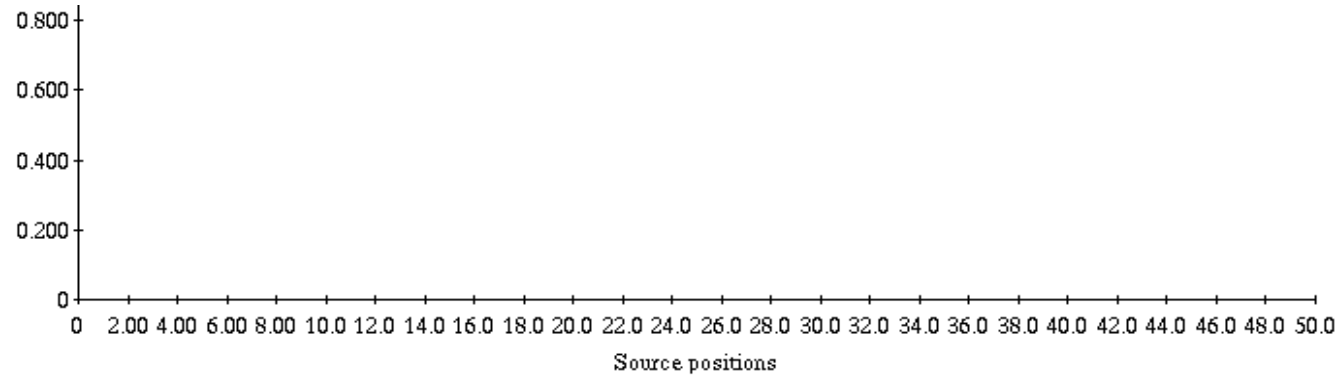
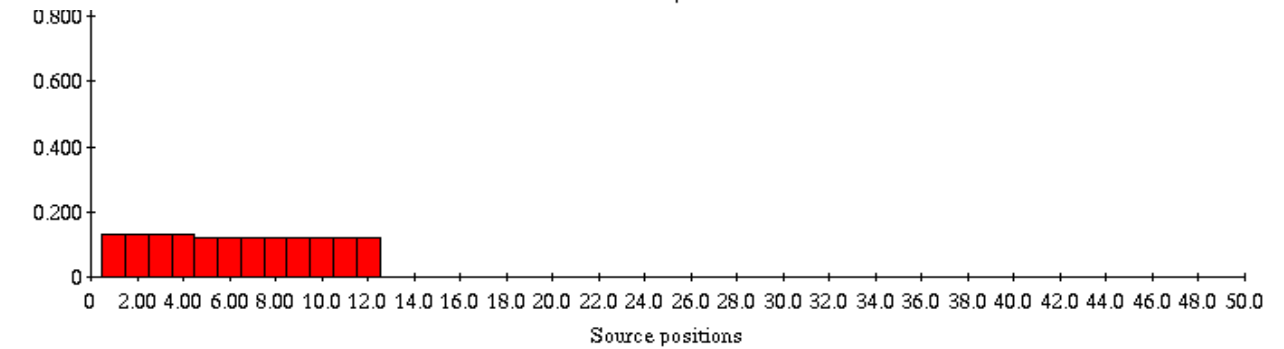
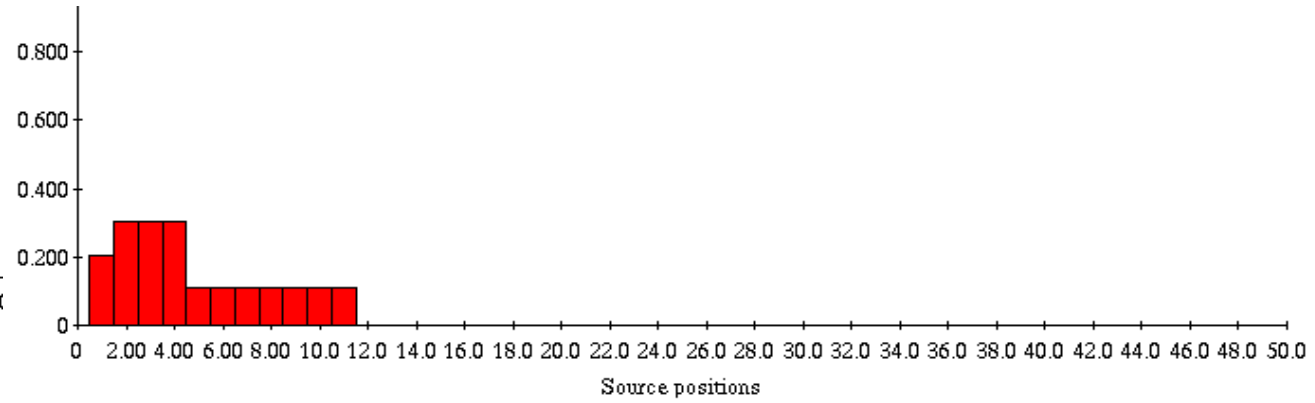
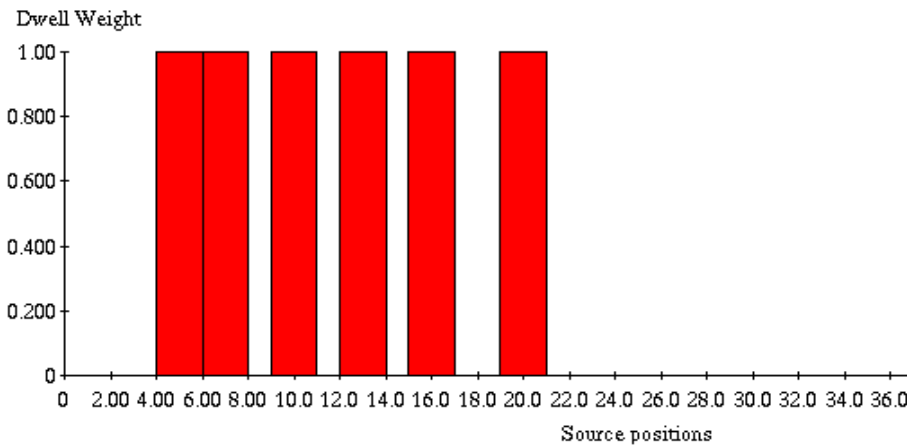
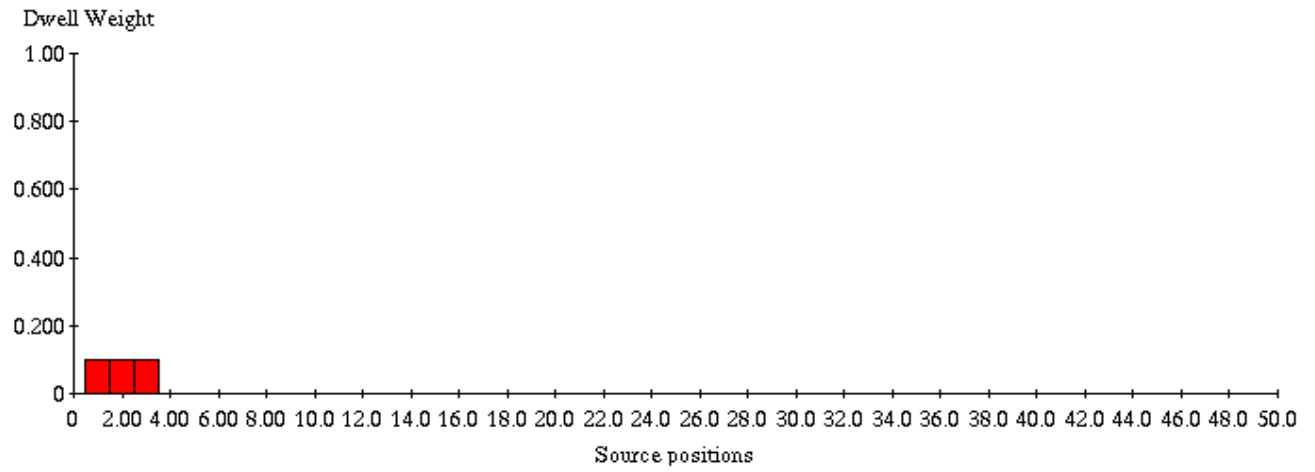
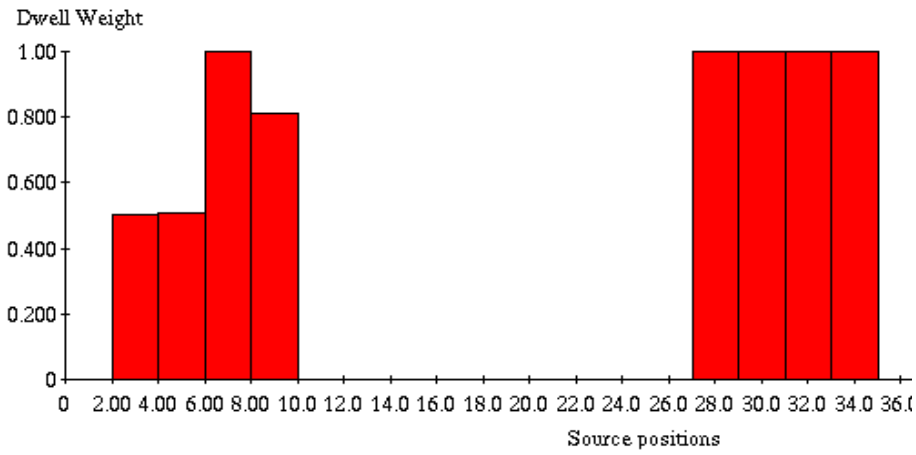
100
200
400



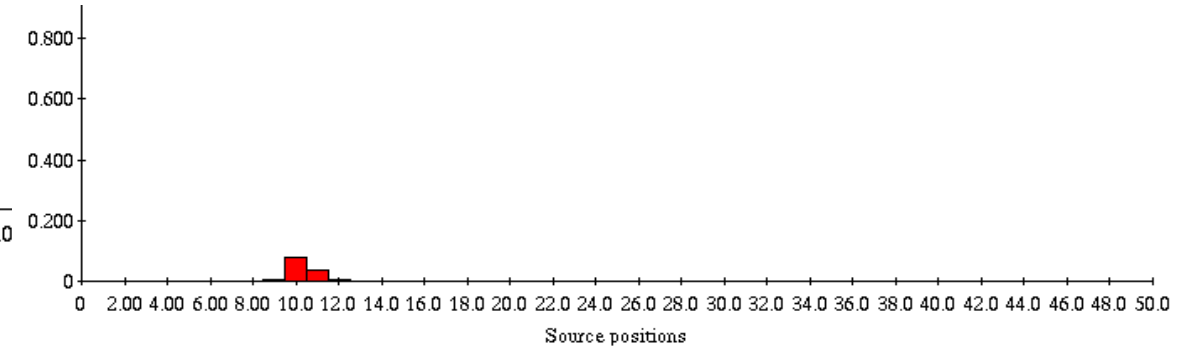
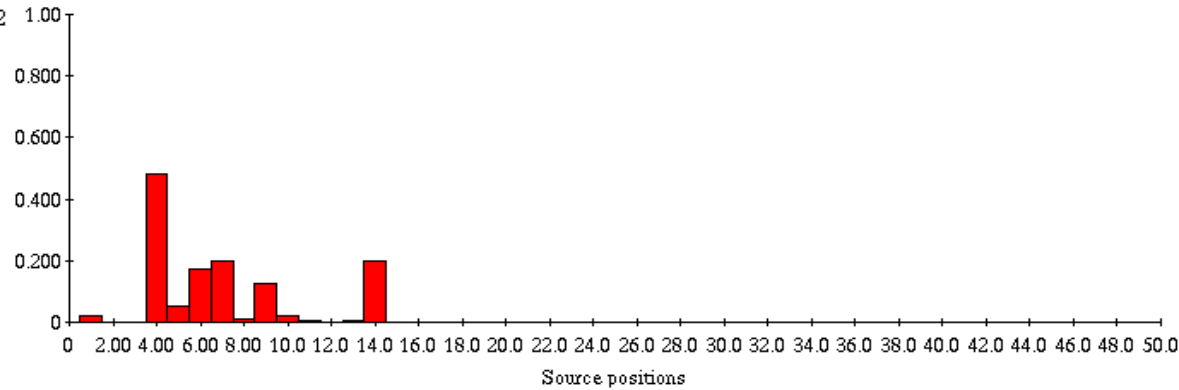
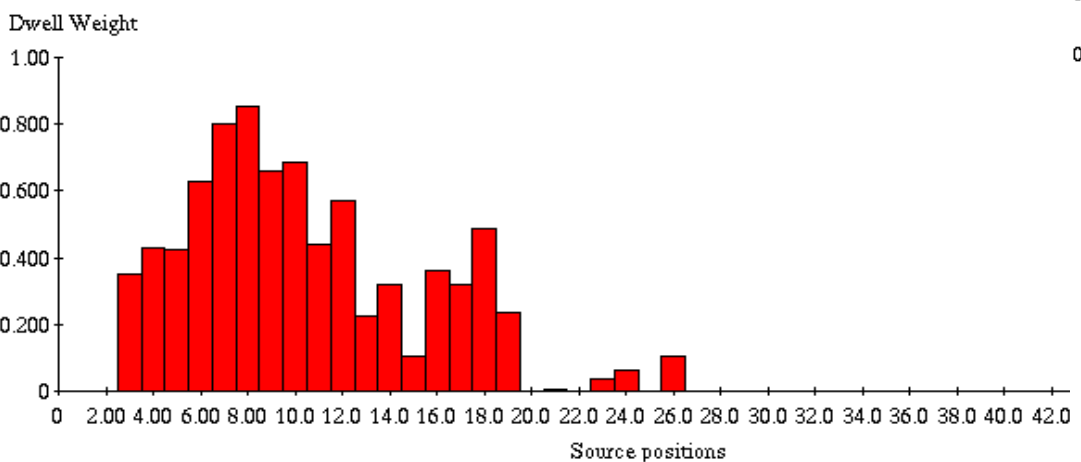
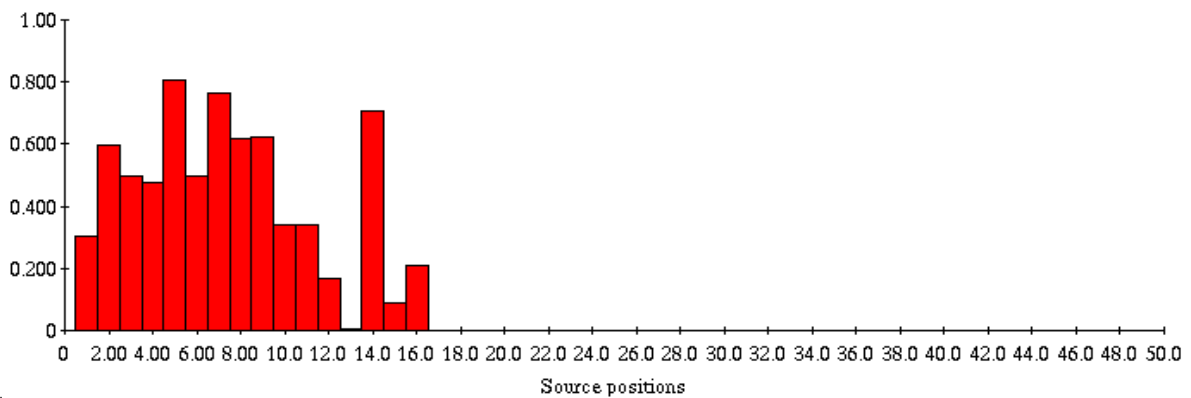
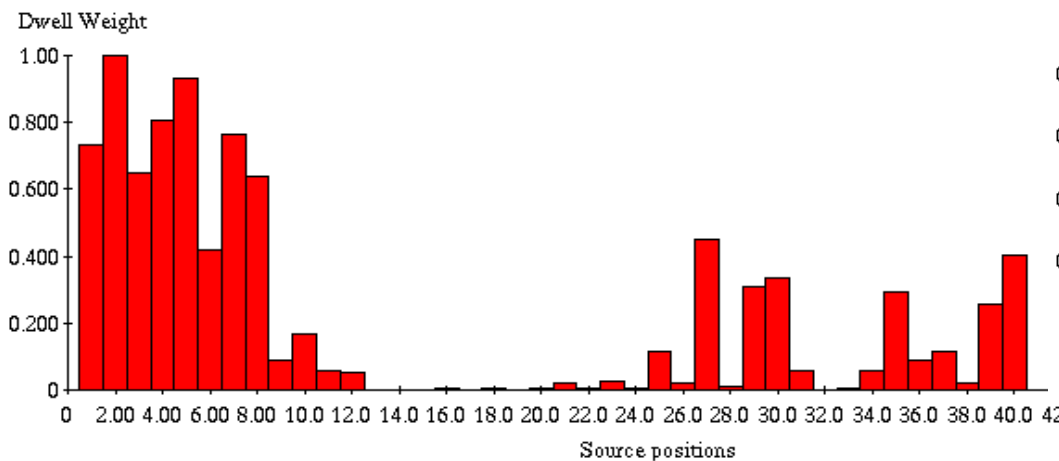
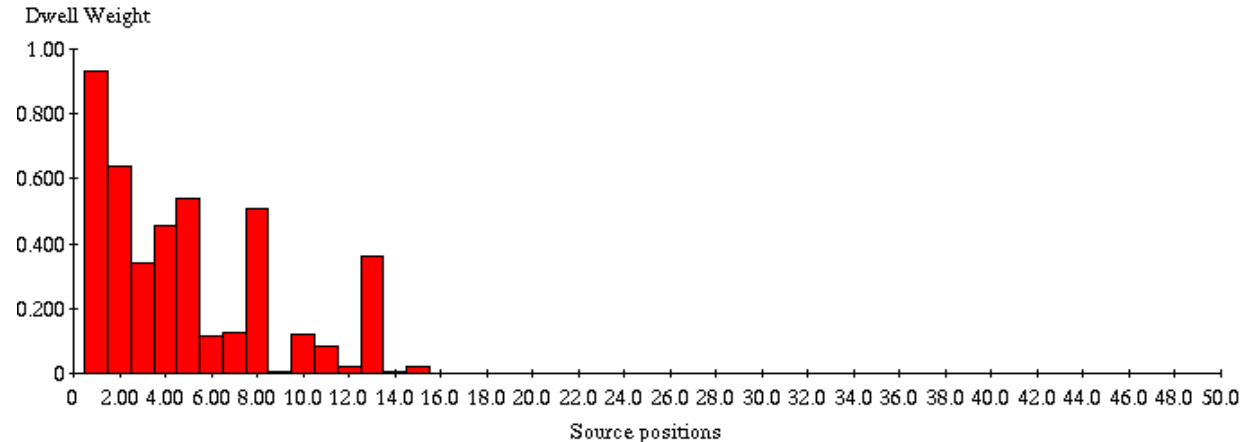
Catheter: 1 of 6



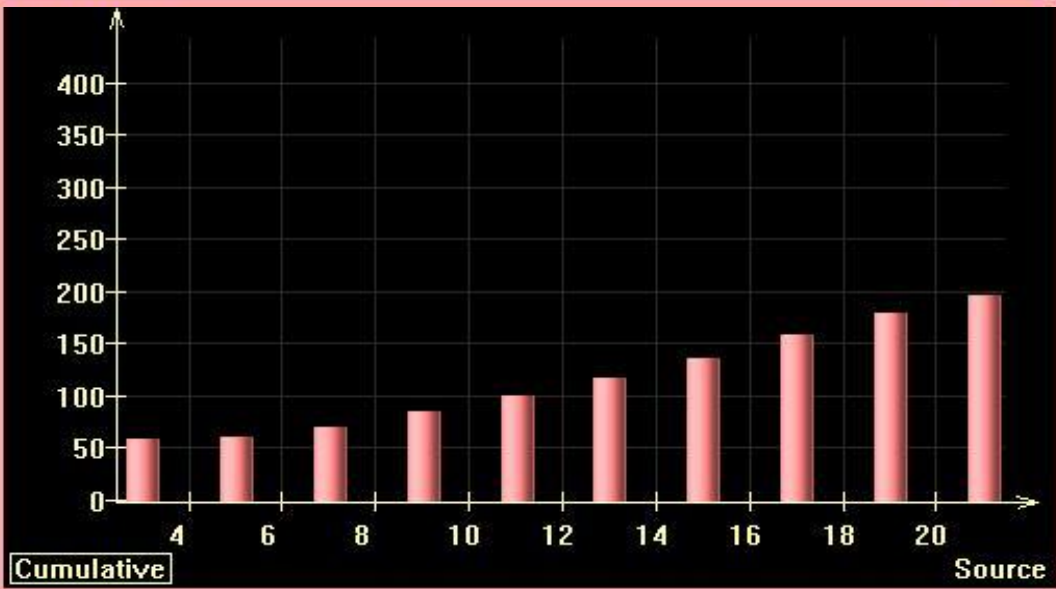
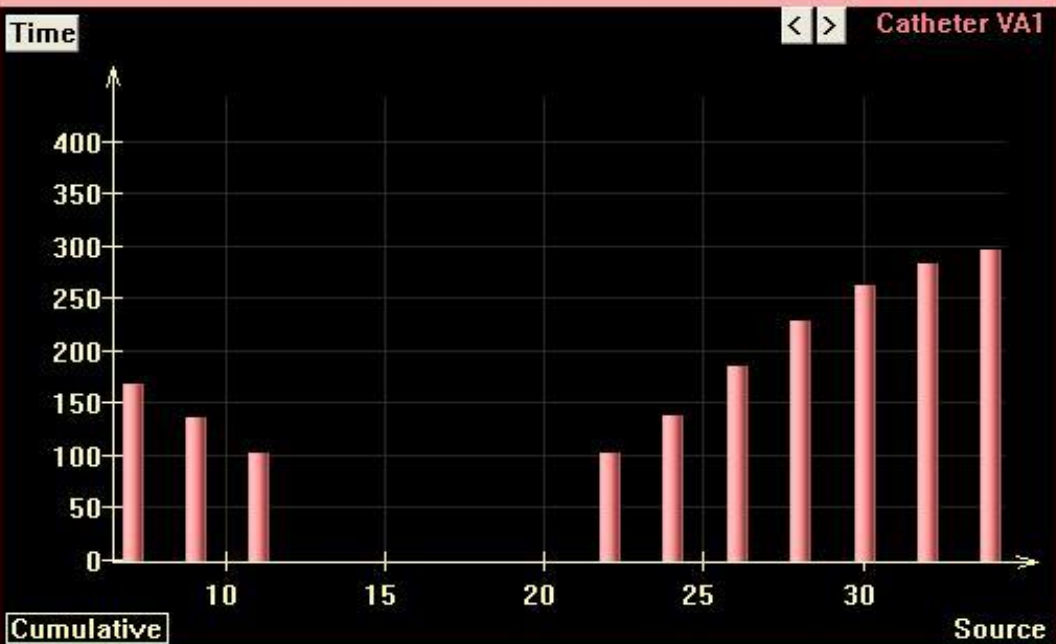
Manual plan



IPSA

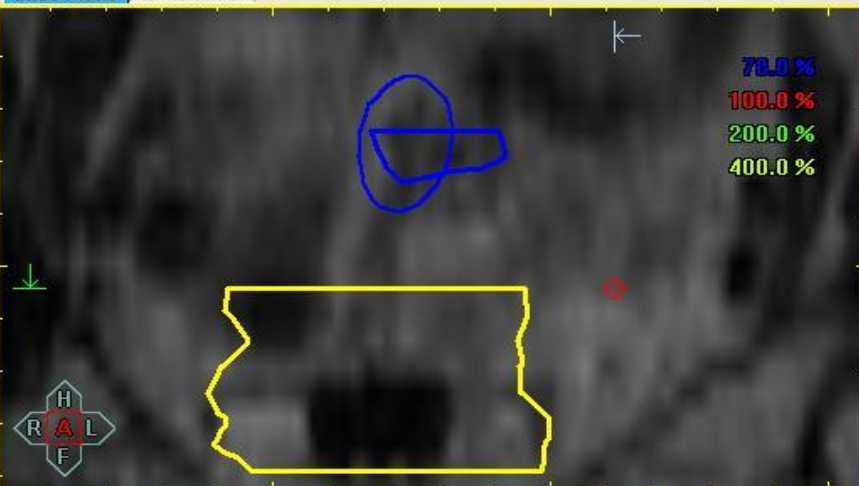


HIPO with dwell time gradient restriction





Slice Mode OBC Mode Y-Value = 17.705 cm



Volume 3D Mode DVH Mode 3D Graph



Optimization

! Not Optimized !

Geometrical
 Manual Graphical
 Inverse Optimization

DVHO settings

Dose sampling settings
Optimization settings

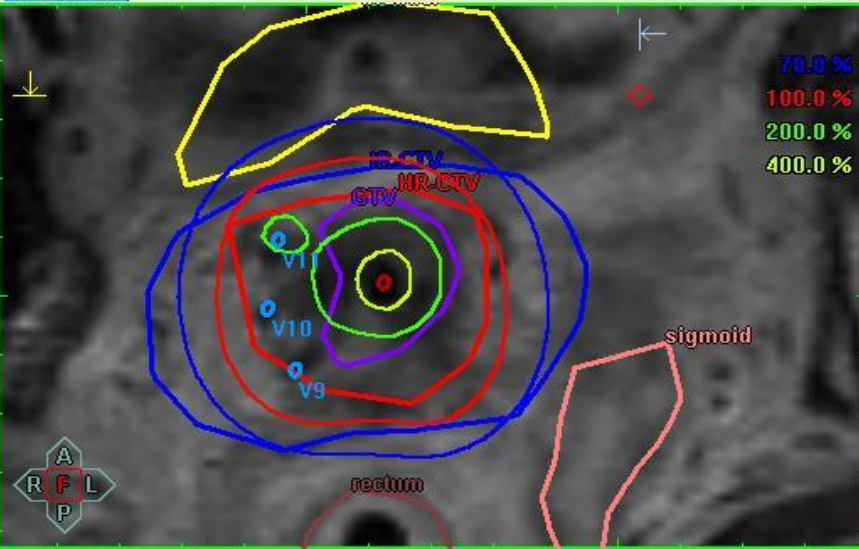
Consider Predelivered
Show last Protocol

Optimize

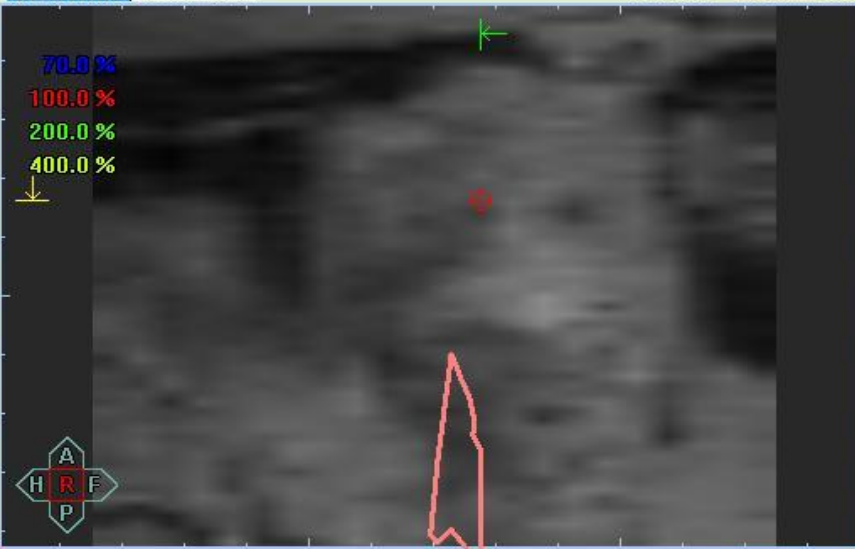
History

Activate
Undo

Slice Mode OBC Mode Z-Value = -6.000 cm



Slice Mode OBC Mode X-Value = 22.283 cm



#	Hole	Indexer[cm]	Depth[cm]	Free Len.[cm]	Free Len.	Tip-1stSDP[cm]	Activation	Dwell Times	5	10	15
VA1	Ring	99.500				0.770	Locked	Locked	●	●	●
VA3	Int	99.500				0.750	Locked	Locked	●	●	●
V9	L4	94.600	3.456	18.544		0.600	Unlocked	Unlocked	●	●	●
V10	L3	94.600	2.685	19.315		0.600	Unlocked	Unlocked	●	●	●
V11	L2	94.600	3.177	18.823		0.600	Unlocked	Unlocked	●	●	●

How to evaluate a treatment plan?

Dose points

Dose distribution

Dose volume histogram parameters

More than one DVH parameter

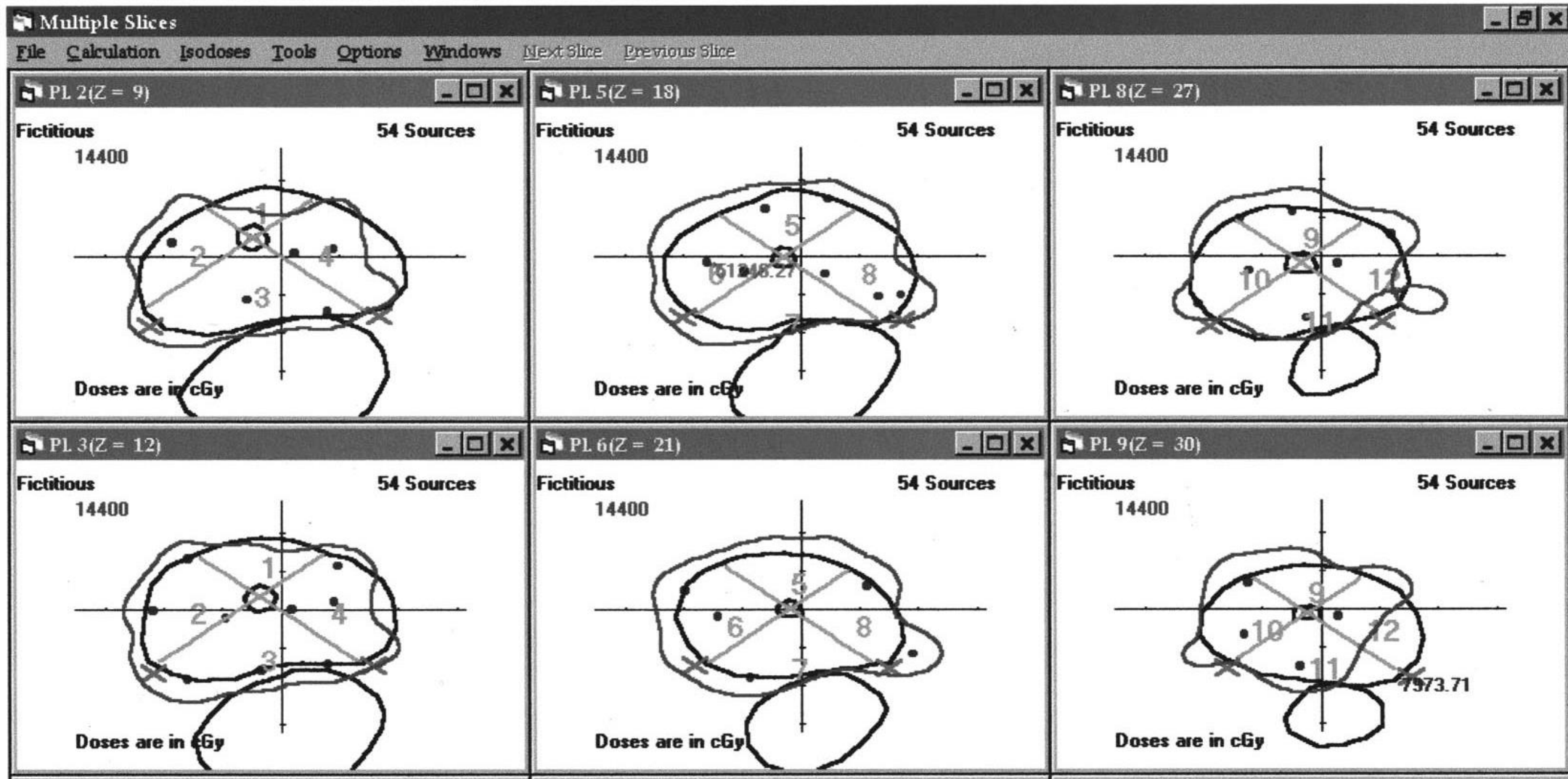
Spatial dose distribution and anatomy

How to evaluate a treatment plan?

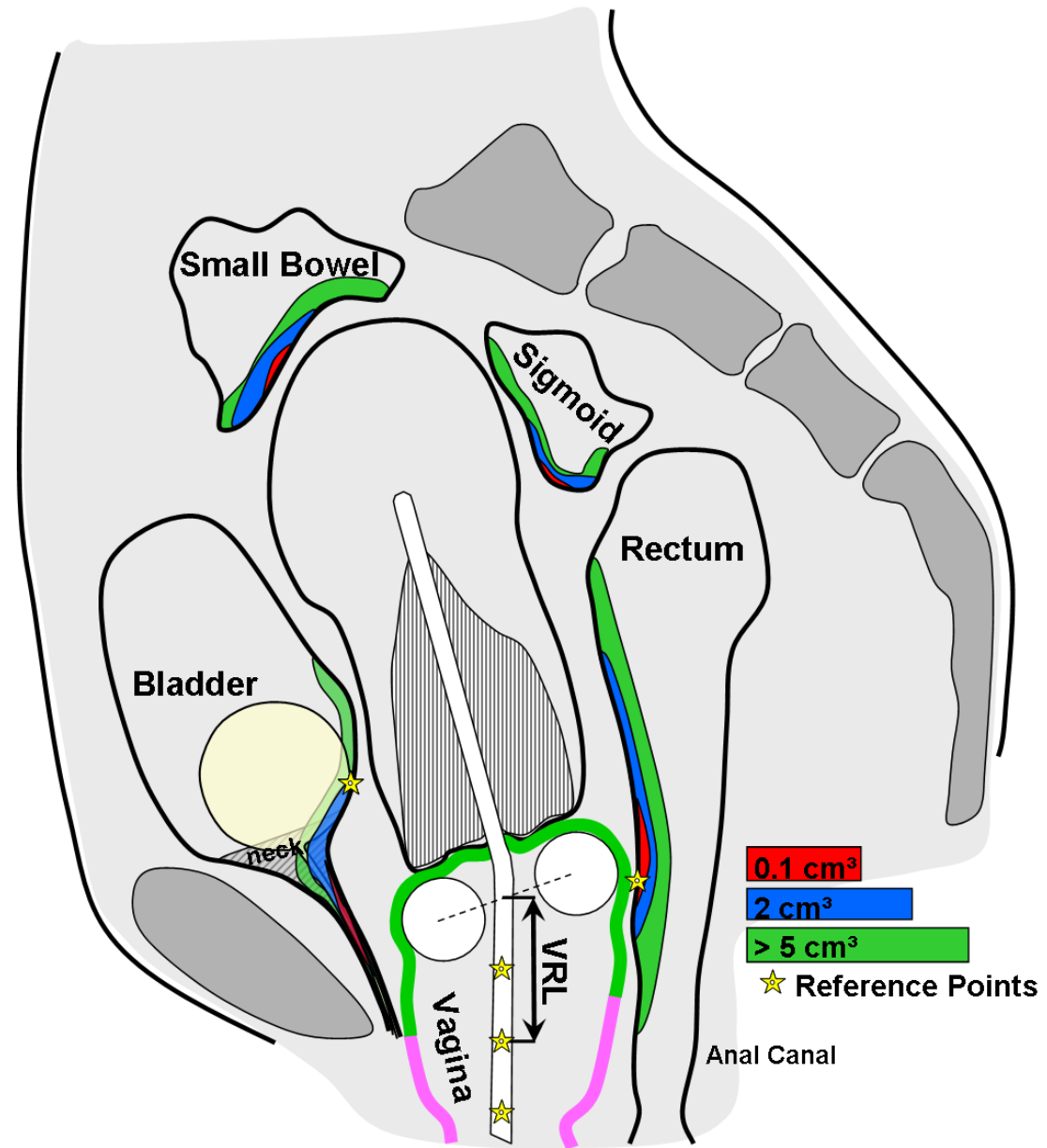
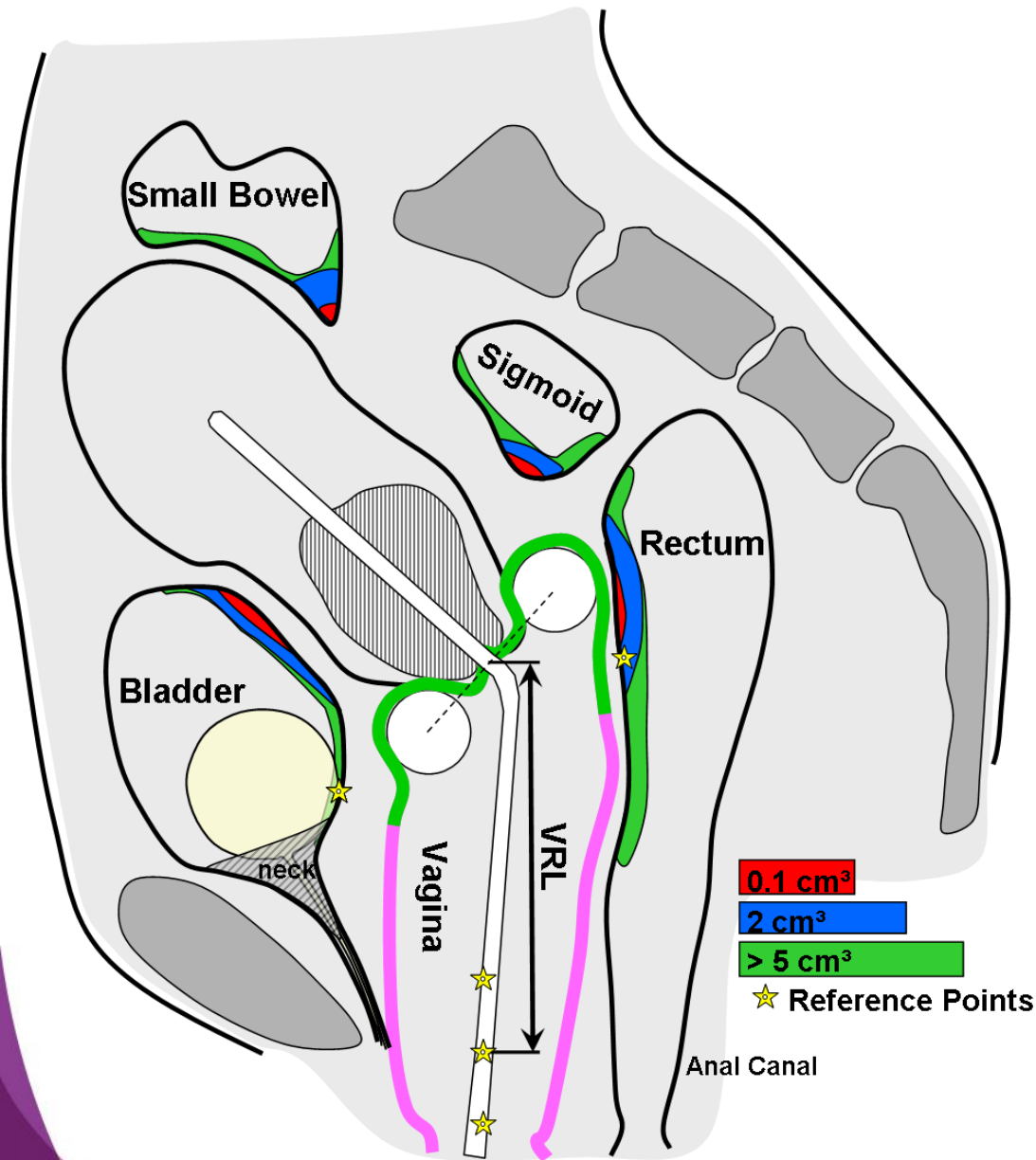
Slides on multi-sector prostate dosimetry

Sector analysis of prostate implants

Bice WS, Prestidge BR, Sarosdy MF.
Medical Physics 28, 2561 (2001)



Points AND Volumes!



From upcoming ICRU 88 report

Dose to skin

$D_{\max} < 100 \% \text{ or } 120 \% \text{ or } 140 \%$

J.A. Vargo, V. Verma, H. Kim, R. Kalash, D.E. Heron, R. Johnson, S. Beriwal Extended (5-year) Outcomes of Accelerated Partial Breast Irradiation Using MammoSite Balloon Brachytherapy: Patterns of Failure, Patient Selection, and Dosimetric Correlates for Late Toxicity. *Int J Radiat Oncol Biol Phys*, 81 (2014)

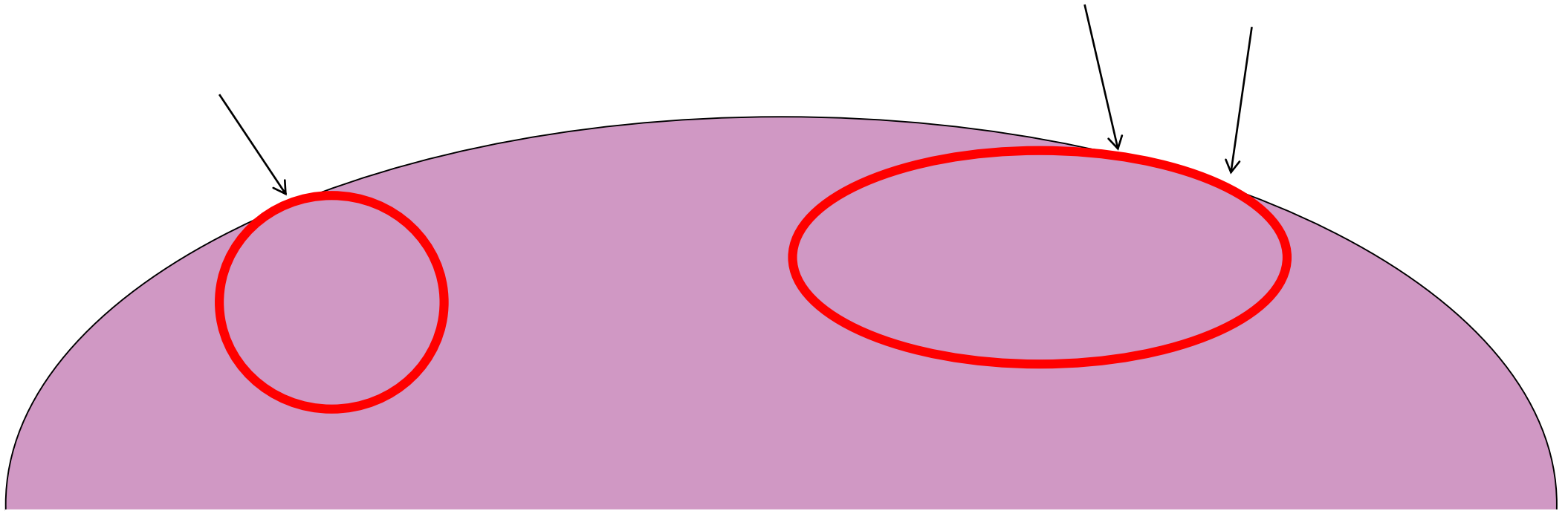
L.W. Cuttino, J. Heffernan, R. Vera et al. Association between maximal skin dose and breast brachytherapy outcome: A proposal for more rigorous dosimetric constraints. *Int J Radiat Oncol Biol Phys*, 81 (2011)

D.W. Arthur, F.A. Vicini, D.A. Todor et al. Contura multi-lumen balloon breast brachytherapy catheter: Comparative dosimetric findings of a phase 4 trial. *Int J Radiat Oncol Biol Phys*, 86 (2013)

$D_{\max} < 70 \% \text{ within GEC ESTRO and European Trials}$

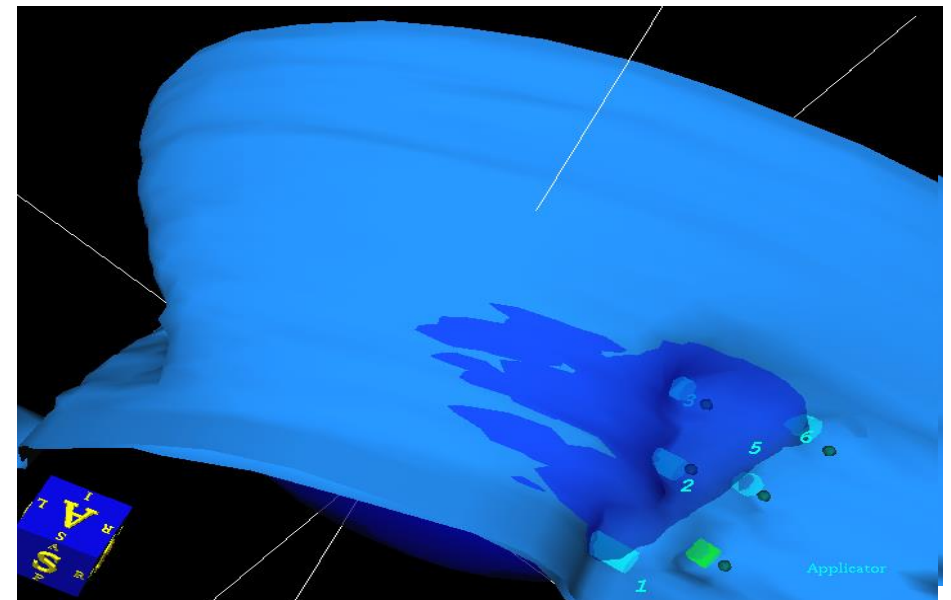
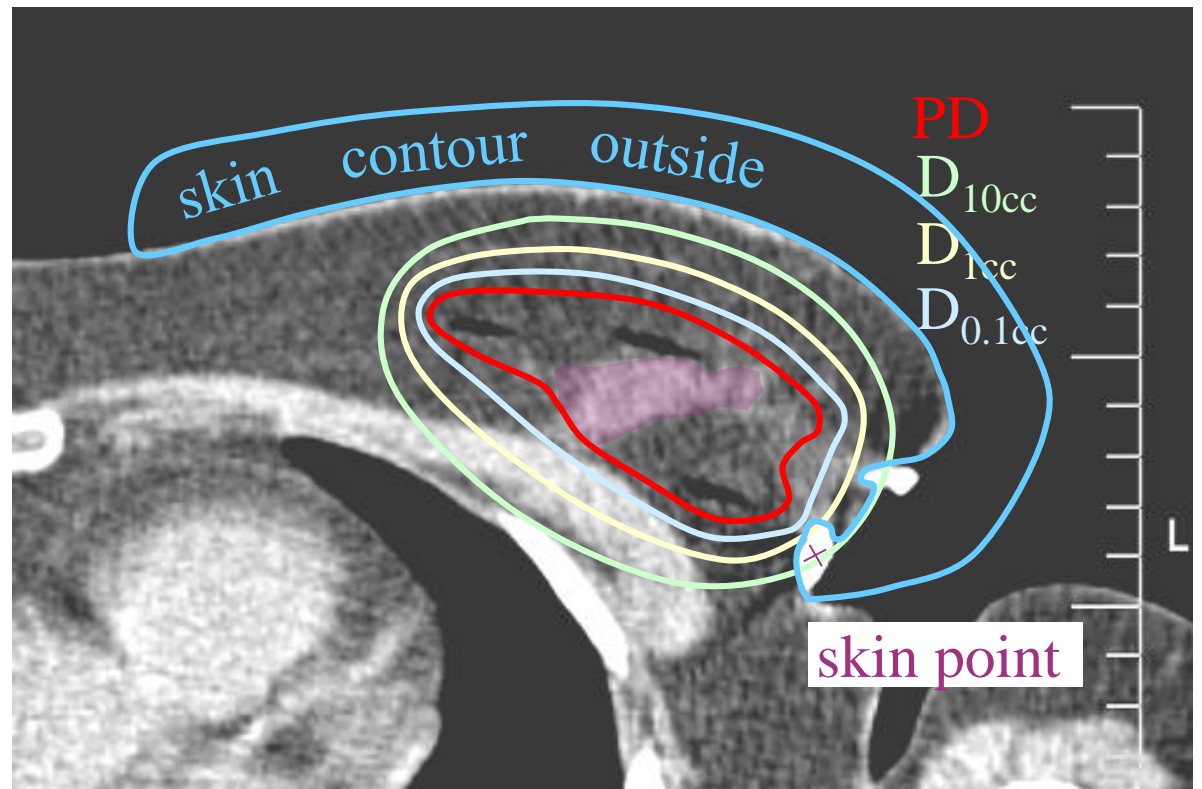
T. Major, C. Polgar, K. Lövey, G Fröhlich. Dosimetric characteristics of accelerated partial breast irradiation with CT image--based multicatheter interstitial brachytherapy: a single institution's experience. *Brachytherapy* (2011)

Dose to skin – only D_{\max} counts?



Dose to skin

skin parameter	mean	std
Vol	534 ± 275	
D0,1cc	66 ± 21	
D1cc	46 ± 8	
D10cc	30 ± 4	
max.skin_point	57 ± 46	
DVH_max	108 ± 54	
mamille	17 ± 4	
skin data of 23 patients Dose in cGy, Vol in cm ³ and Areas in cm ²		
Area of D0.1cc	1 ± 1	
Area of D1cc	5 ± 3	
Area of D10cc	26 ± 11	



Berger et al. Brachytherapy 2008

How to evaluate a treatment plan?

Dose points

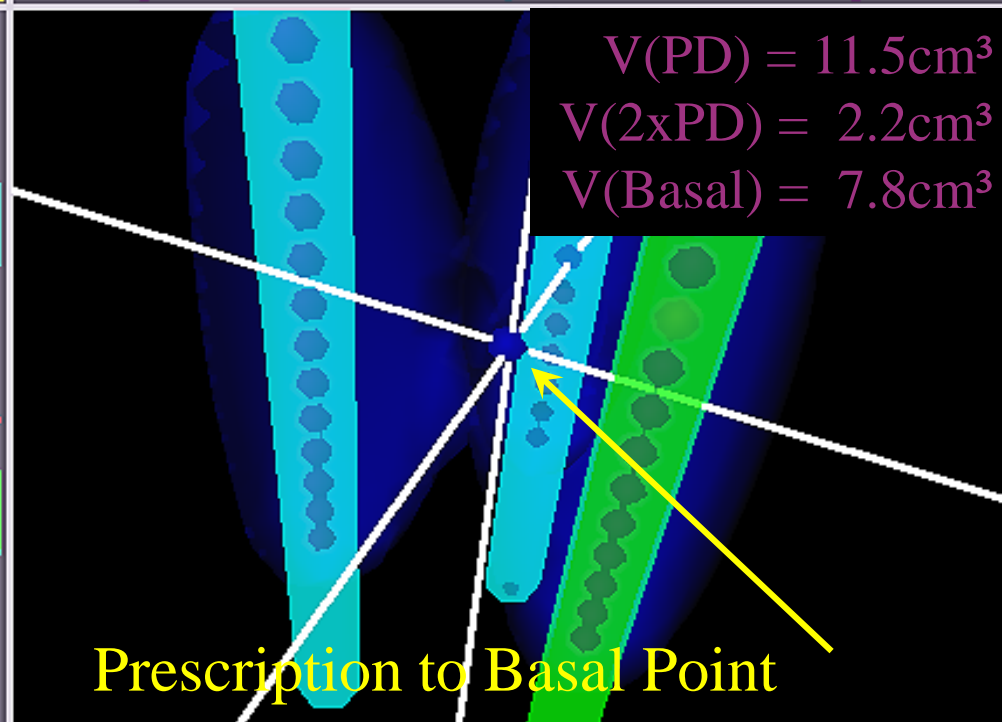
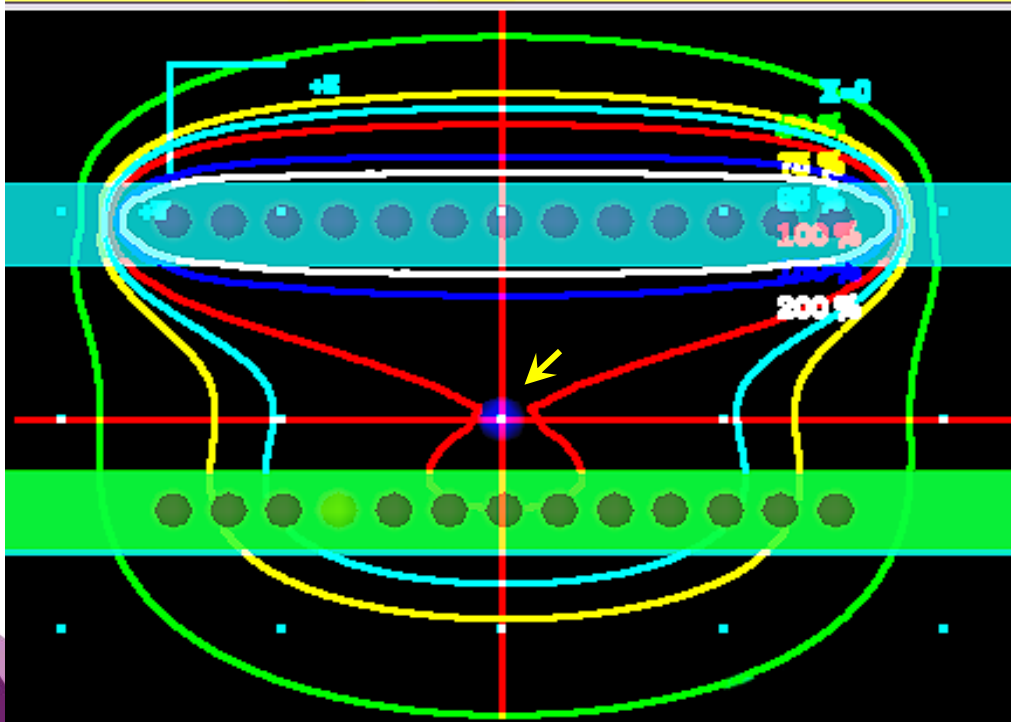
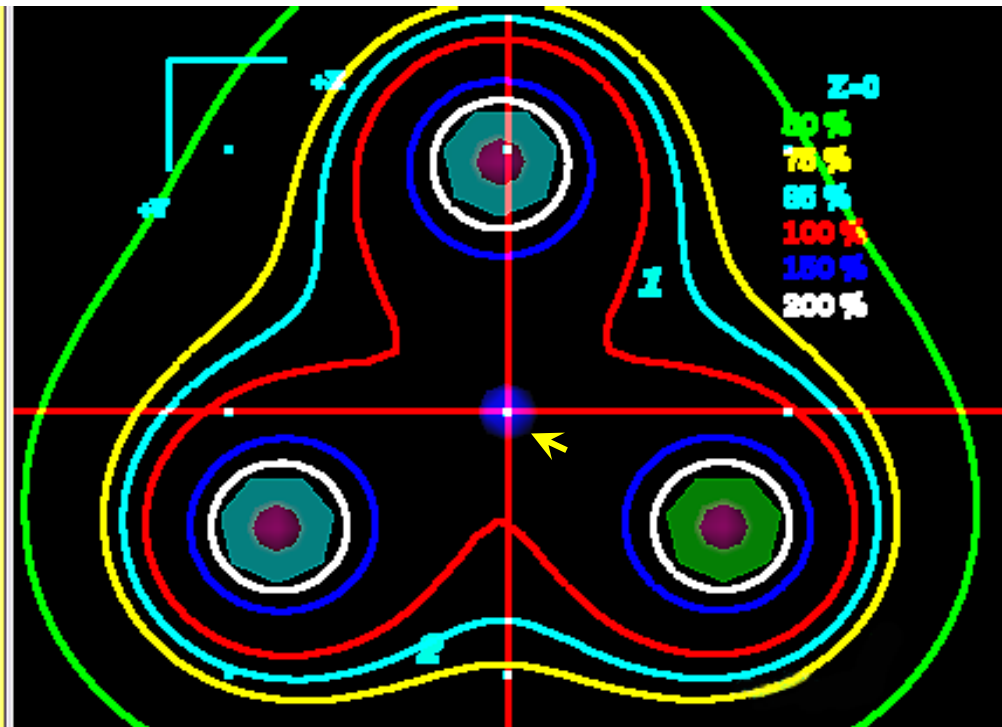
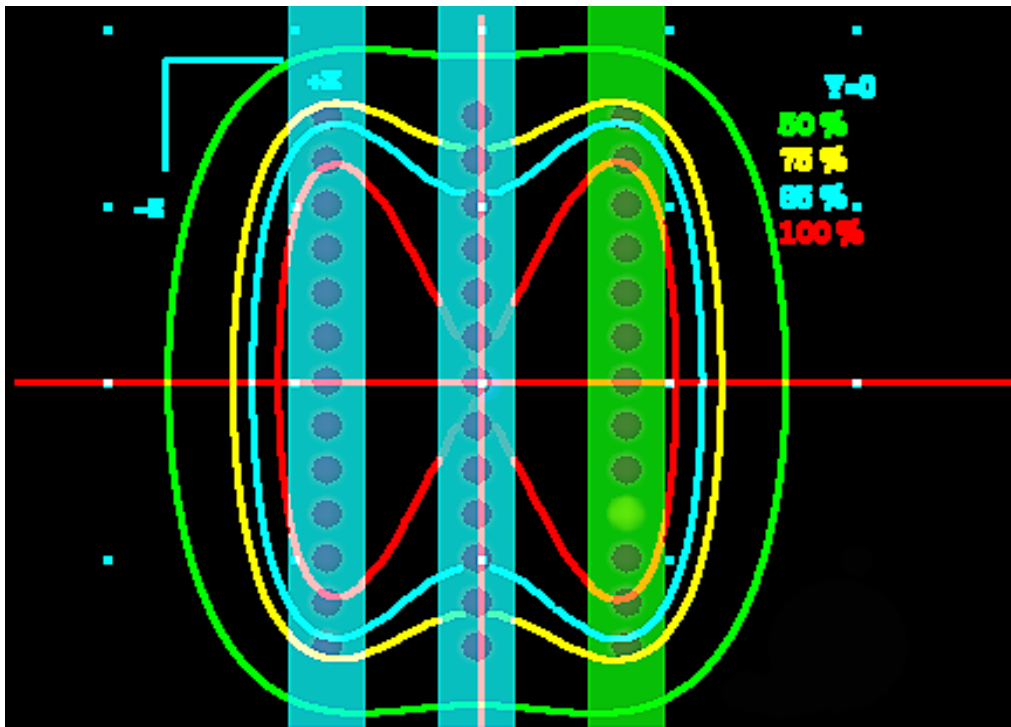
Dose distribution

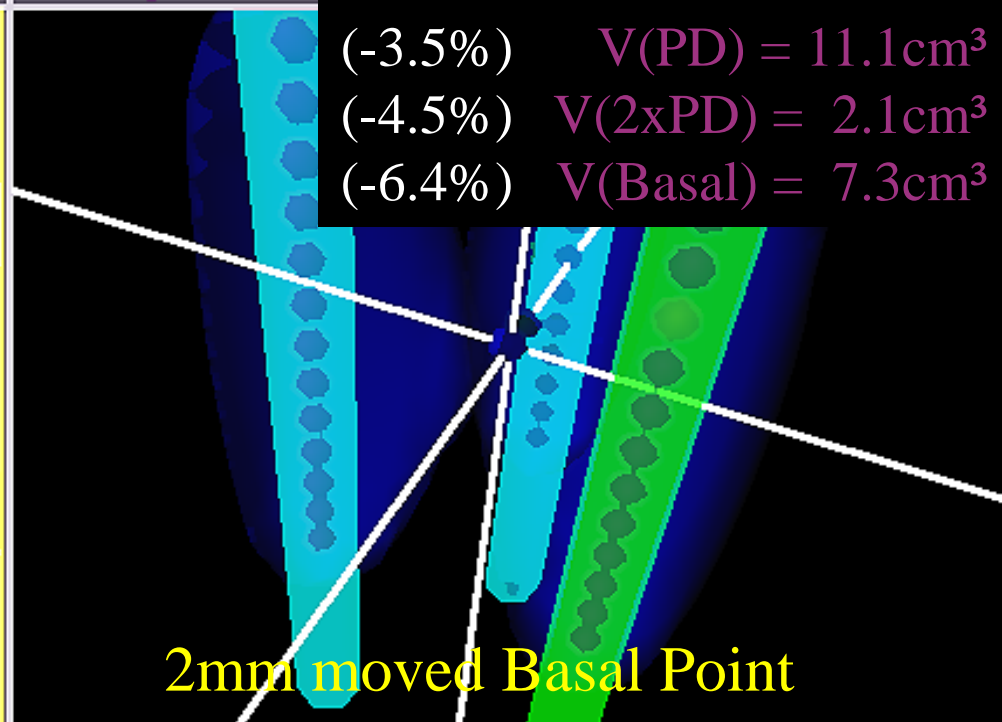
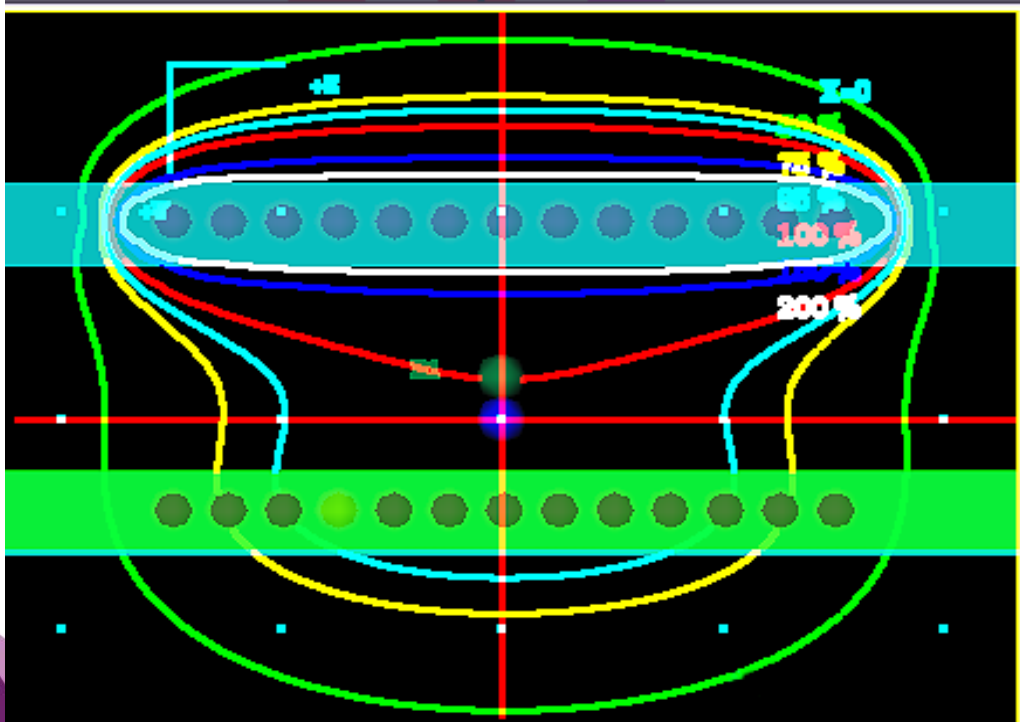
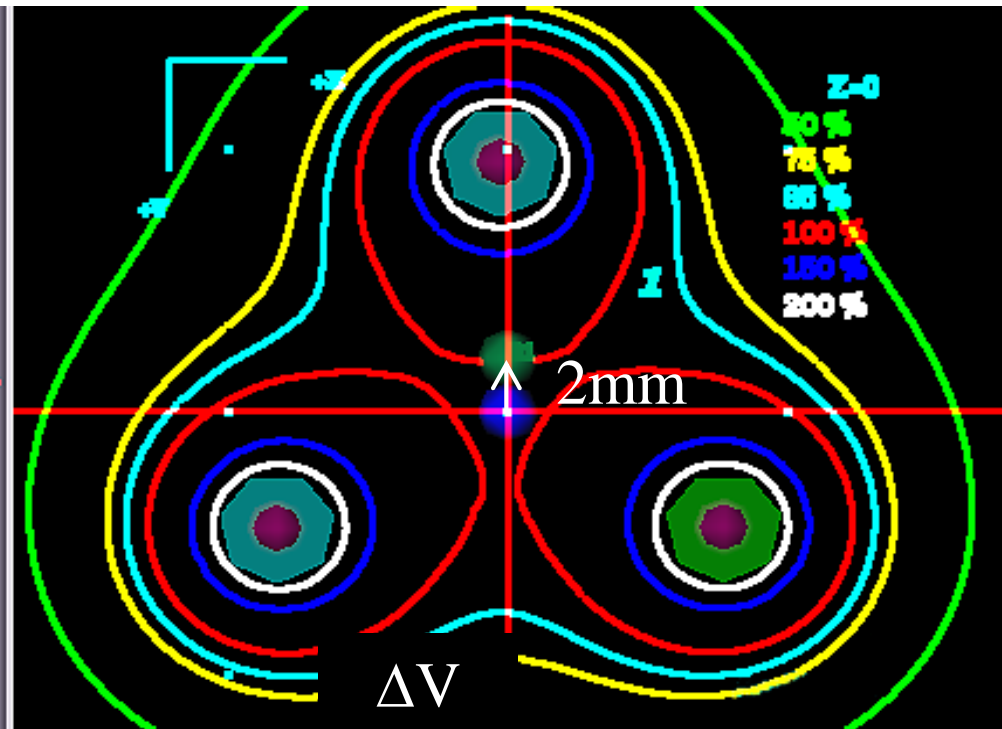
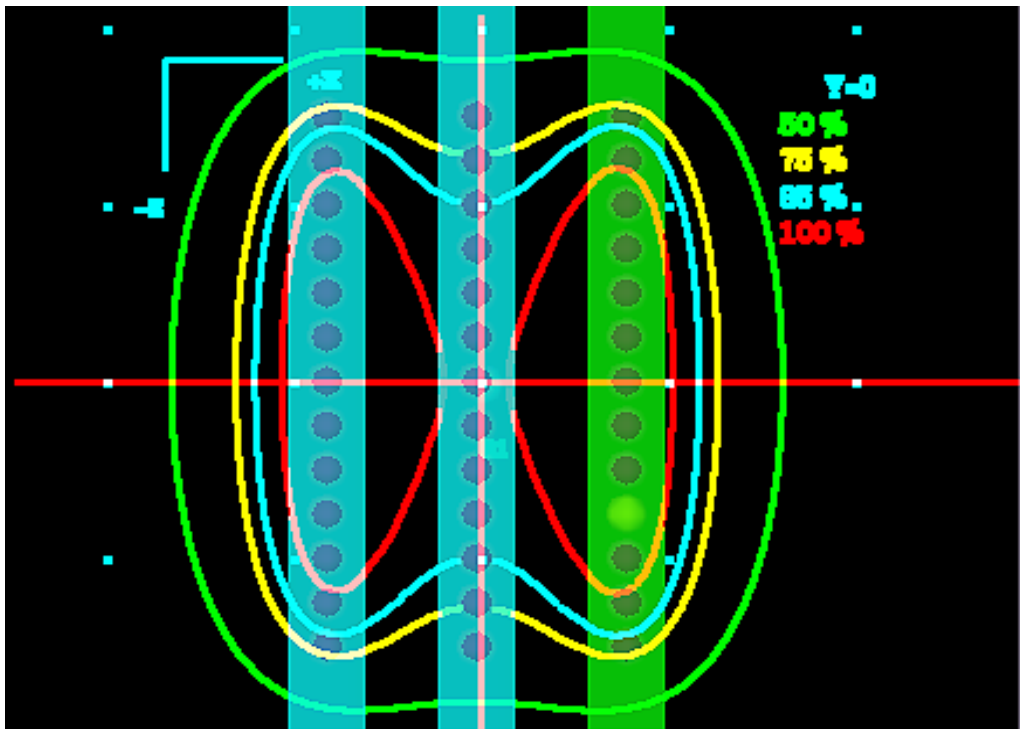
Dose volume histogram parameters

More than one DVH parameter

Spatial dose distribution and anatomy

Anatomy, topography and morphology
(functional imaging)

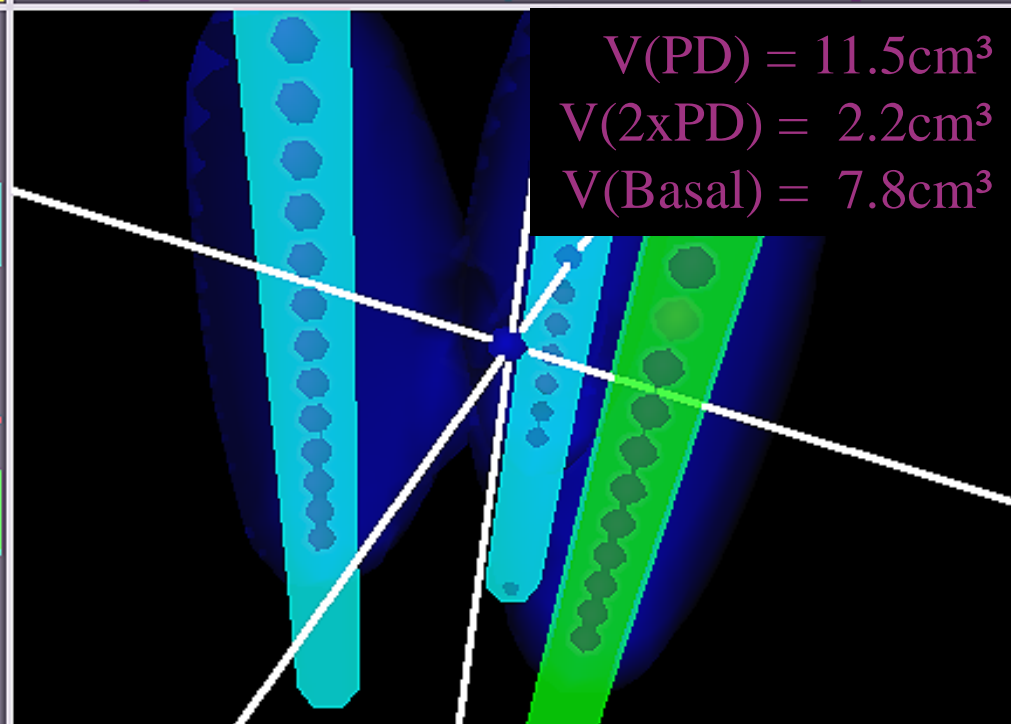
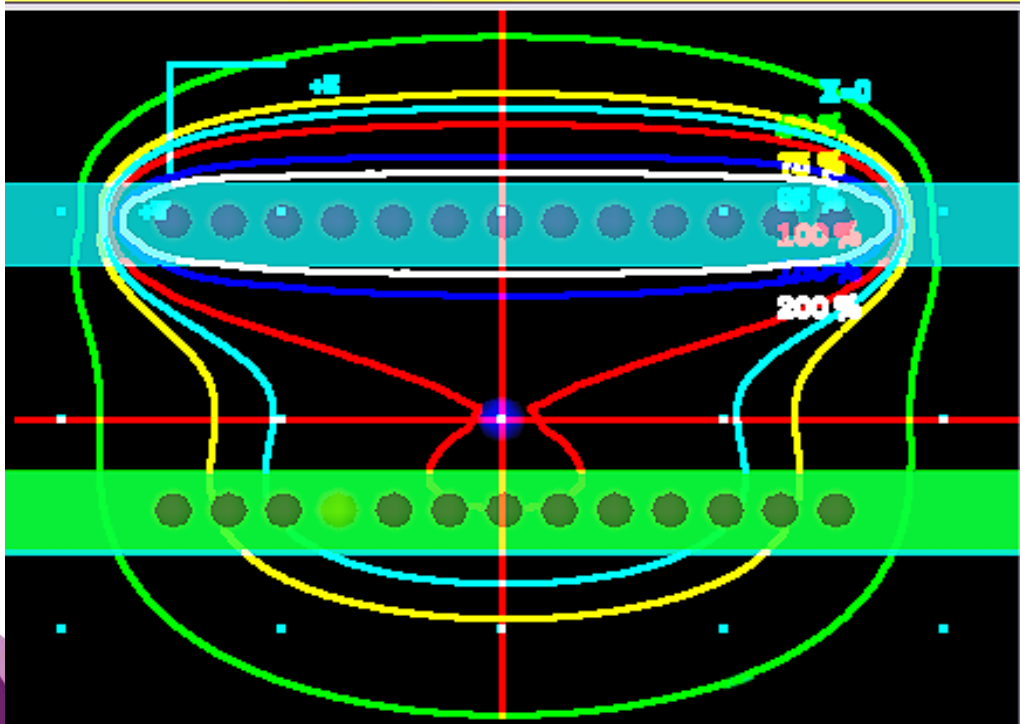
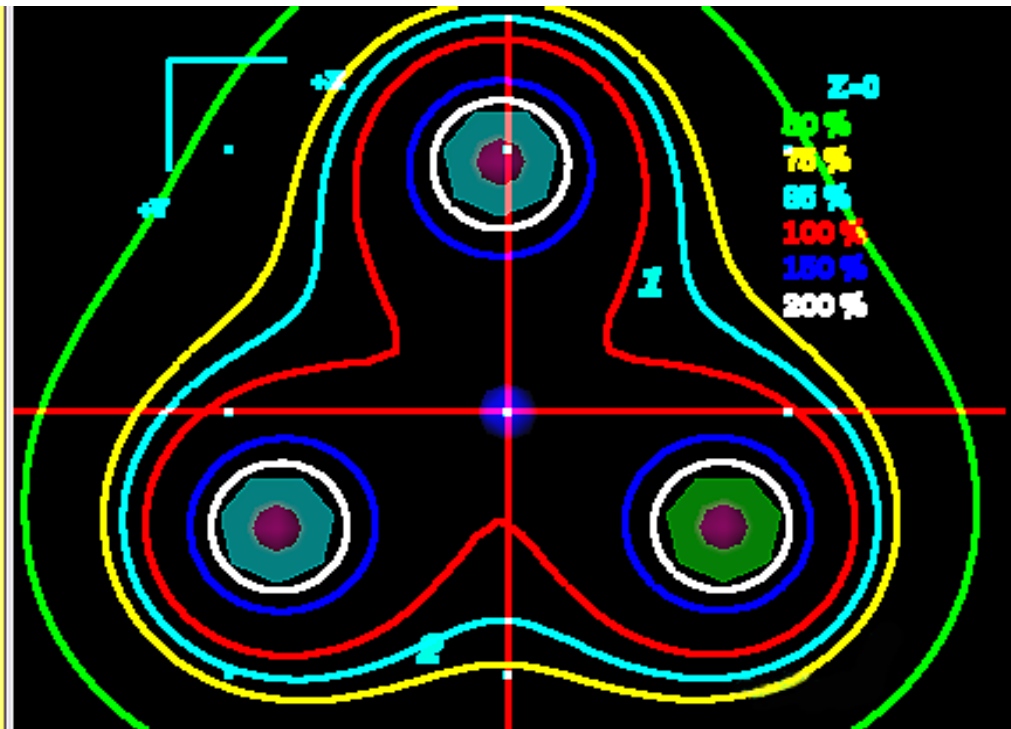
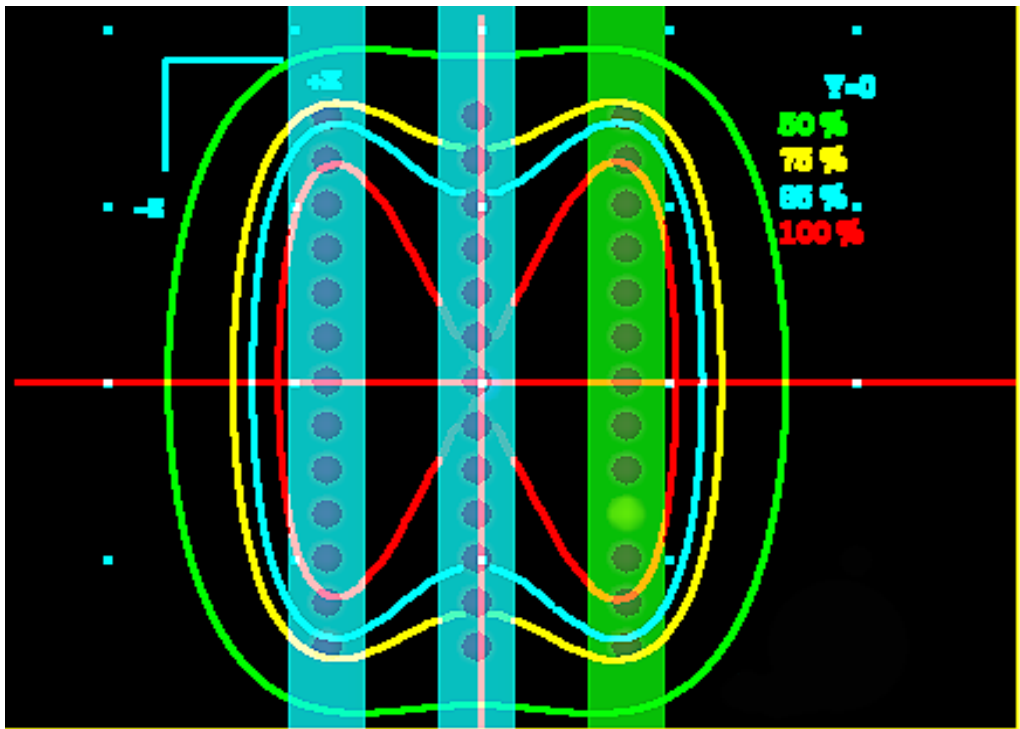


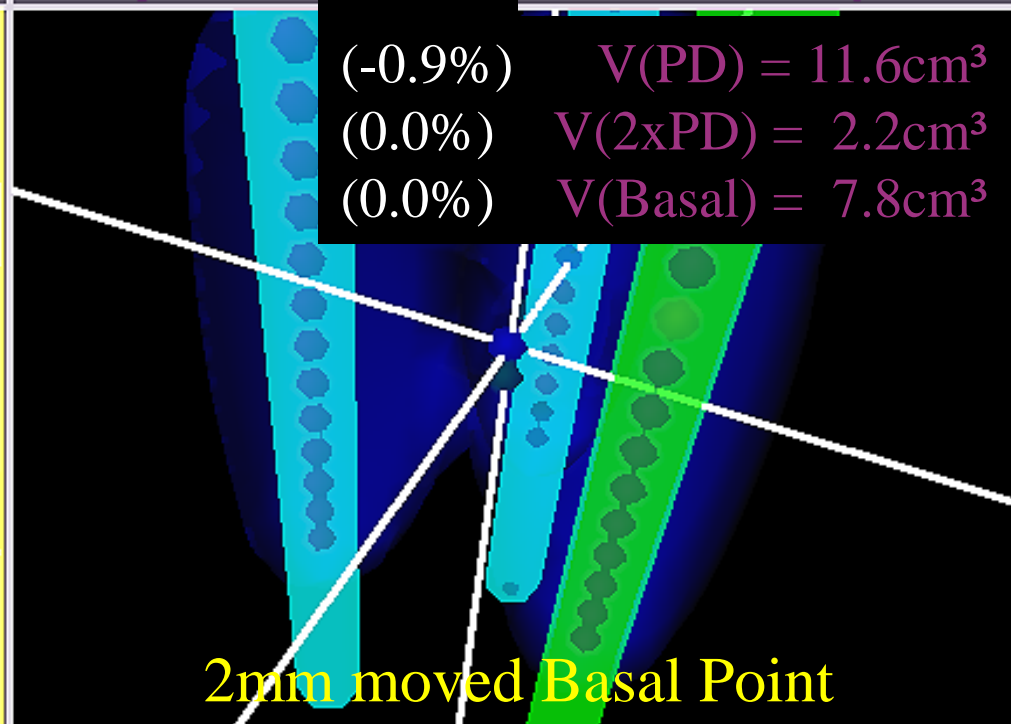
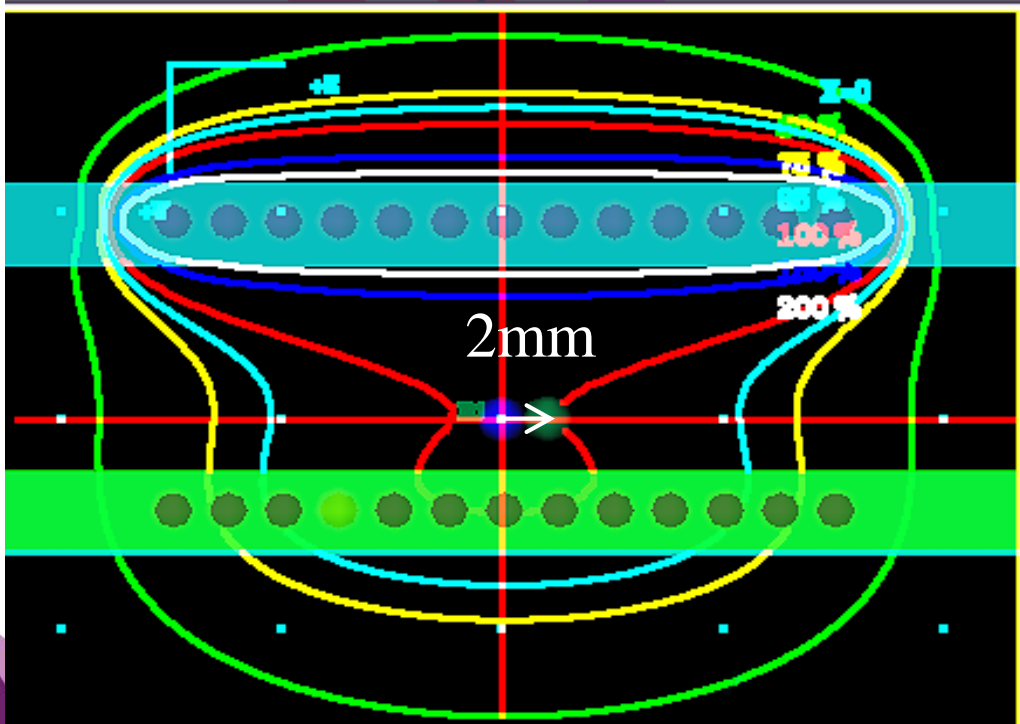
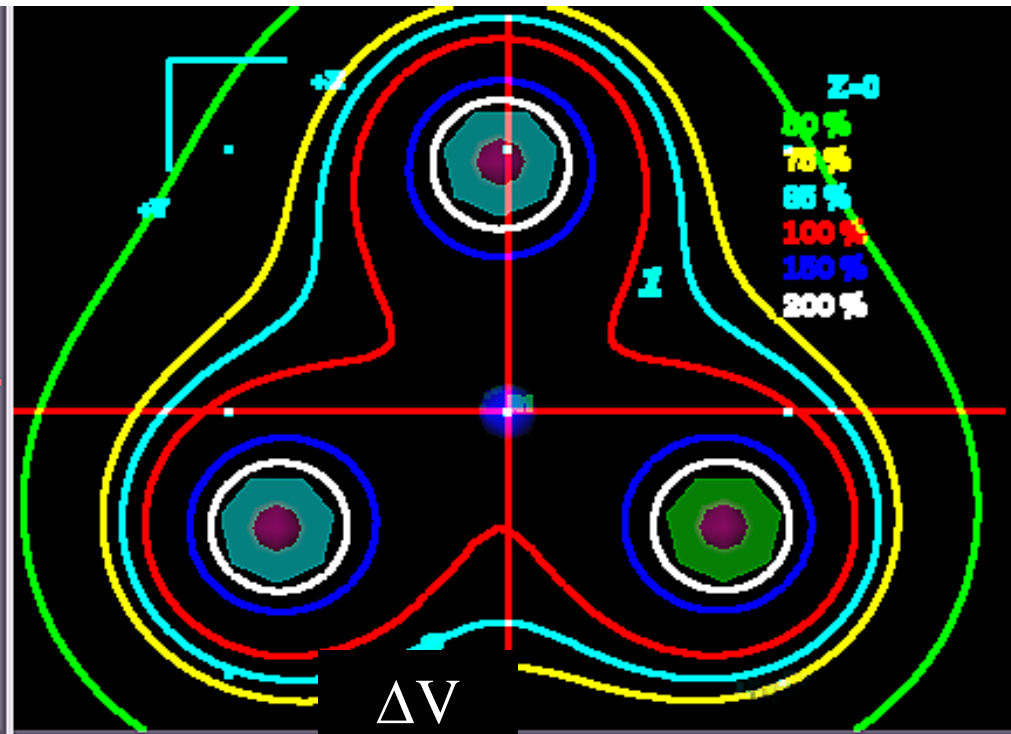
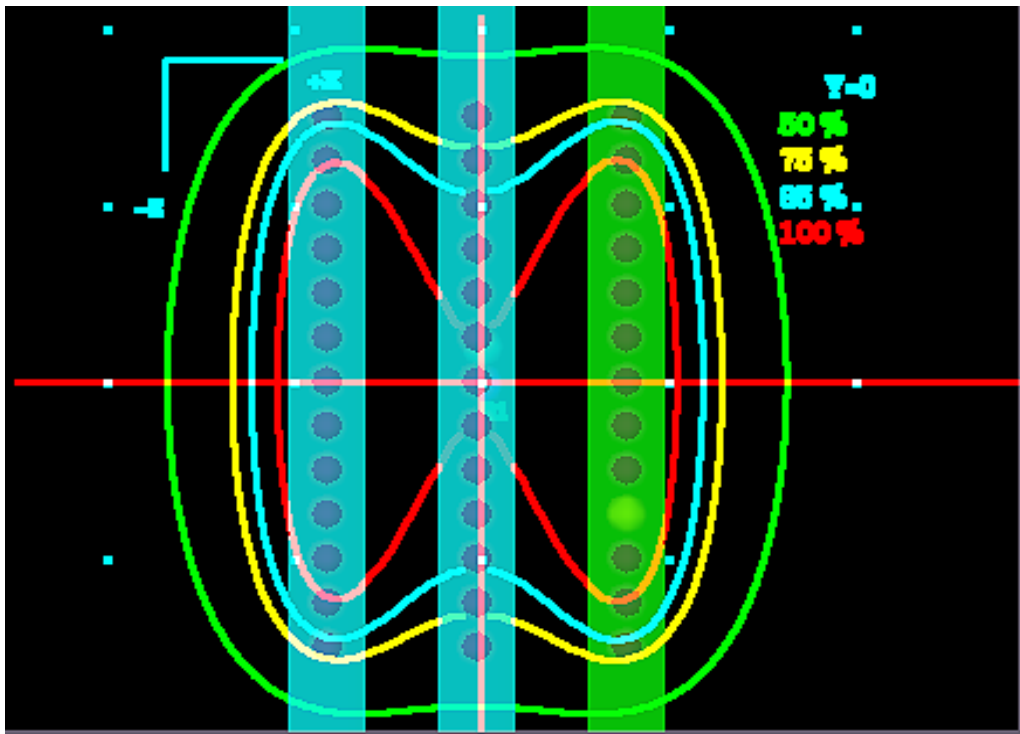


ΔV

(-3.5%)	$V(\text{PD}) = 11.1\text{cm}^3$
(-4.5%)	$V(2\times\text{PD}) = 2.1\text{cm}^3$
(-6.4%)	$V(\text{Basal}) = 7.3\text{cm}^3$

2mm moved Basal Point

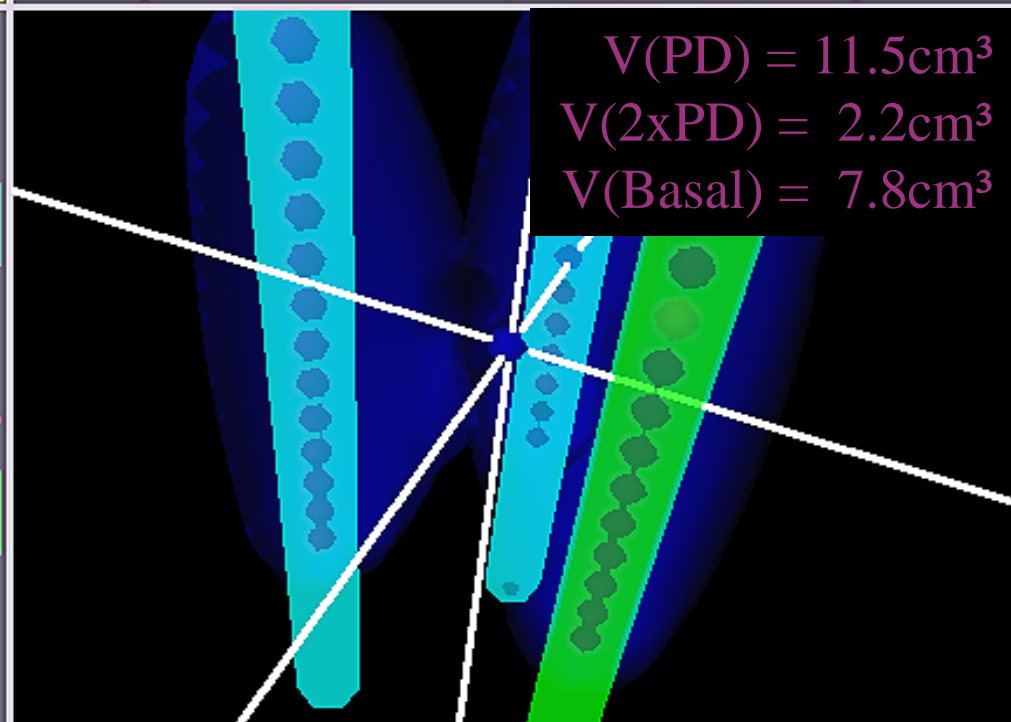
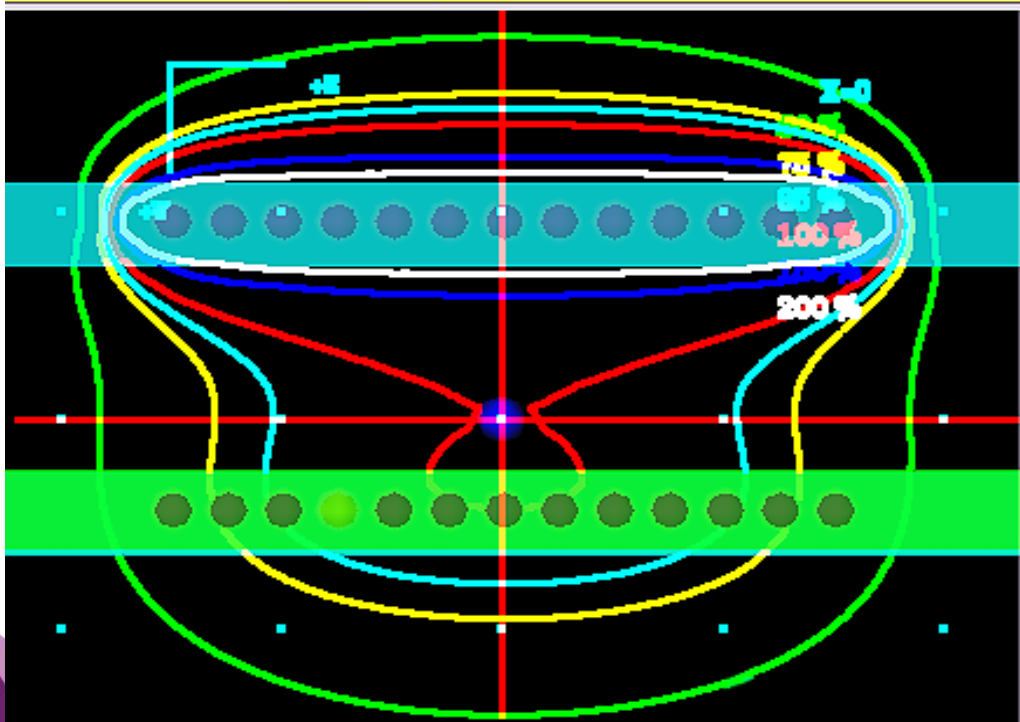
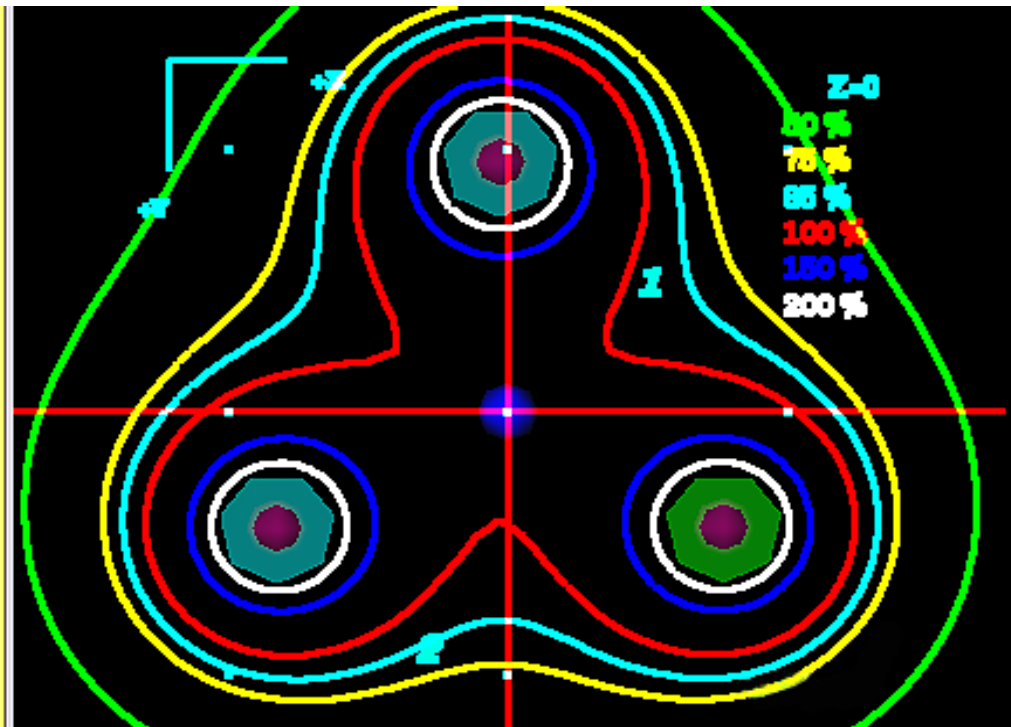
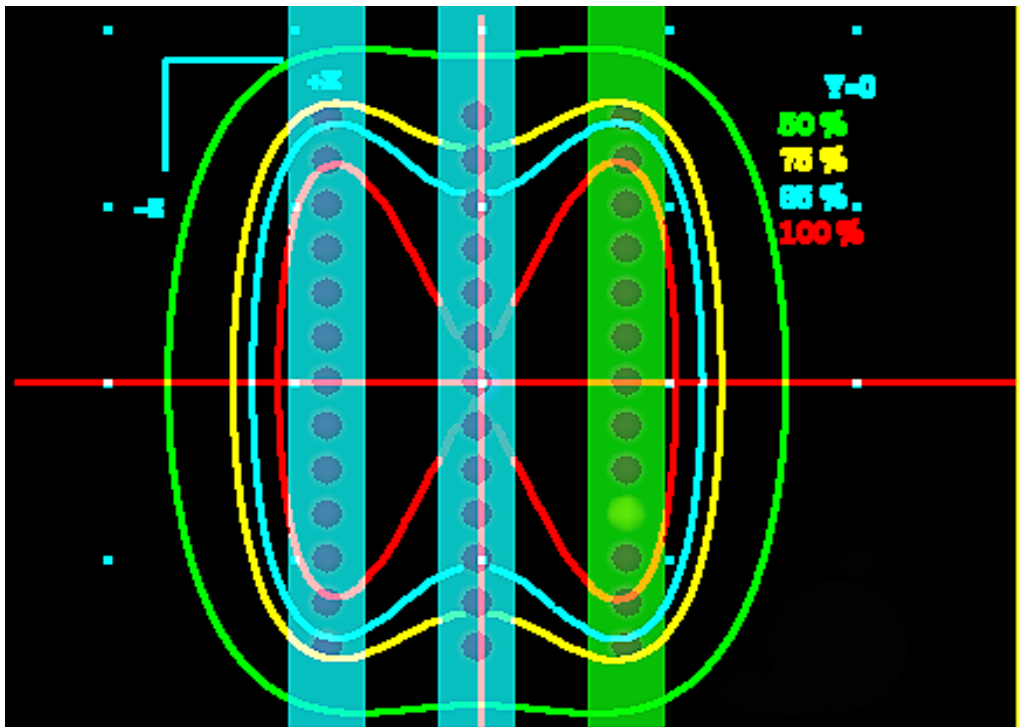


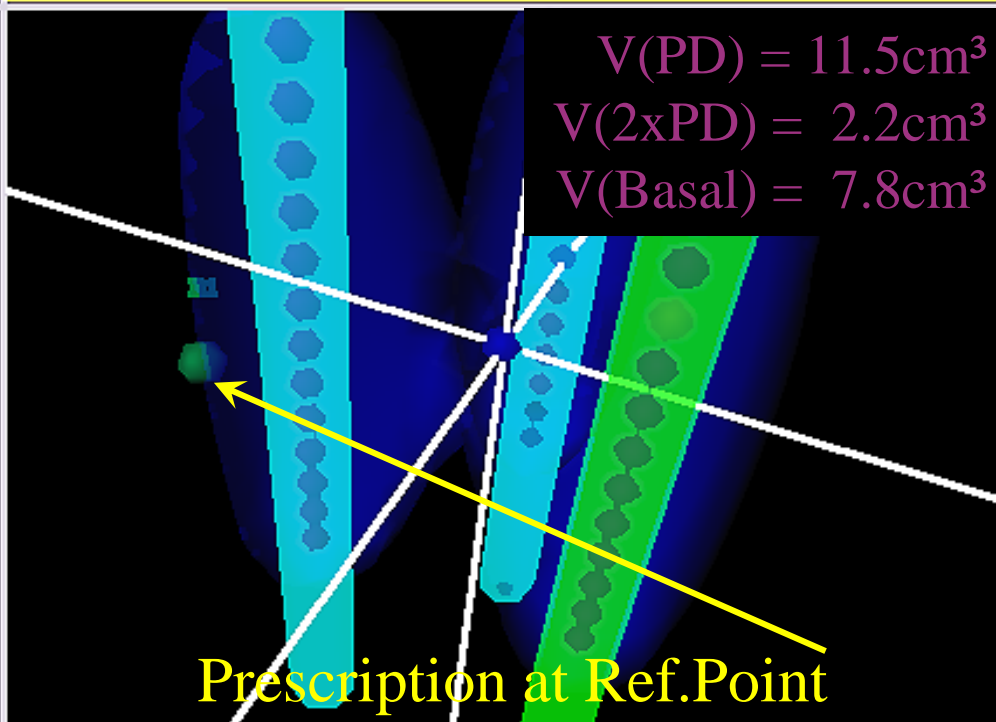
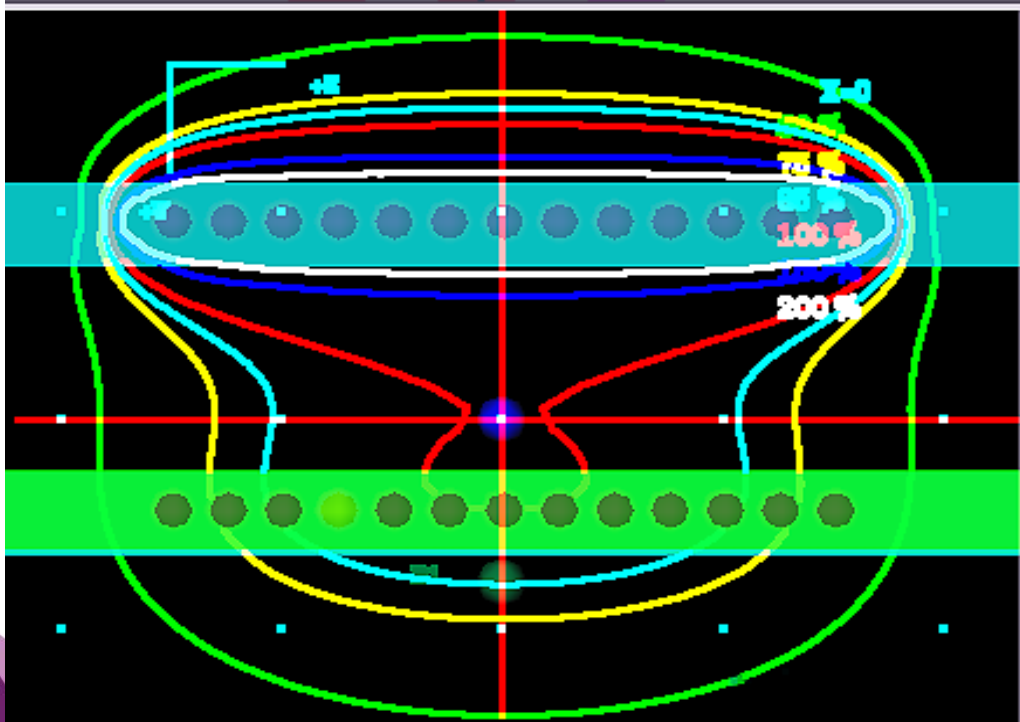
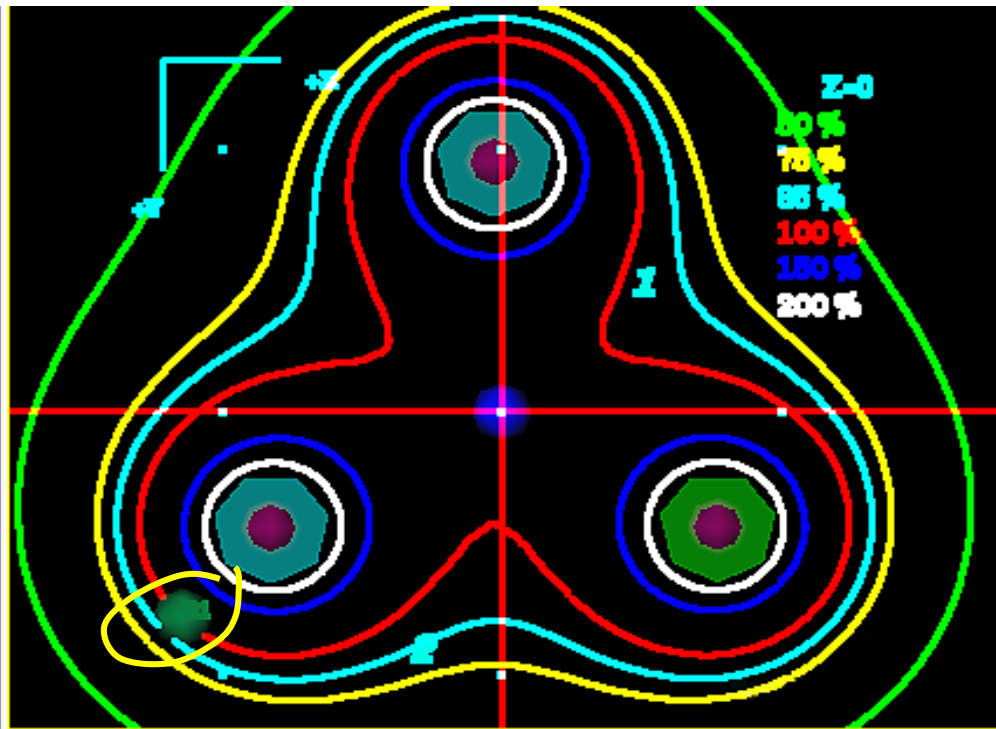
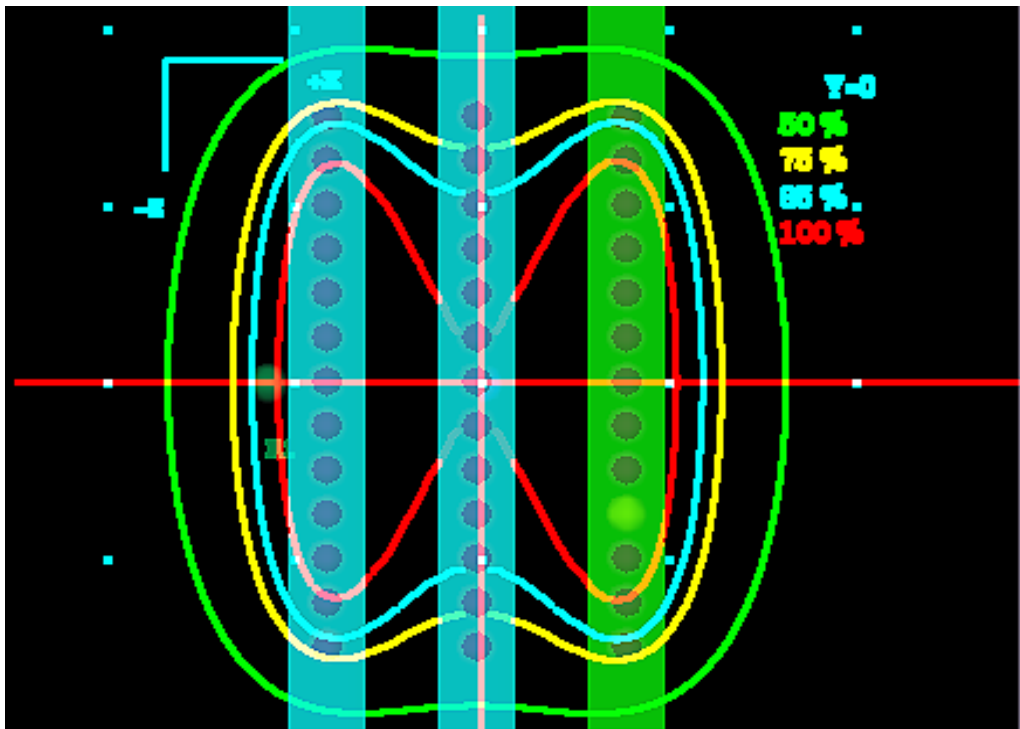


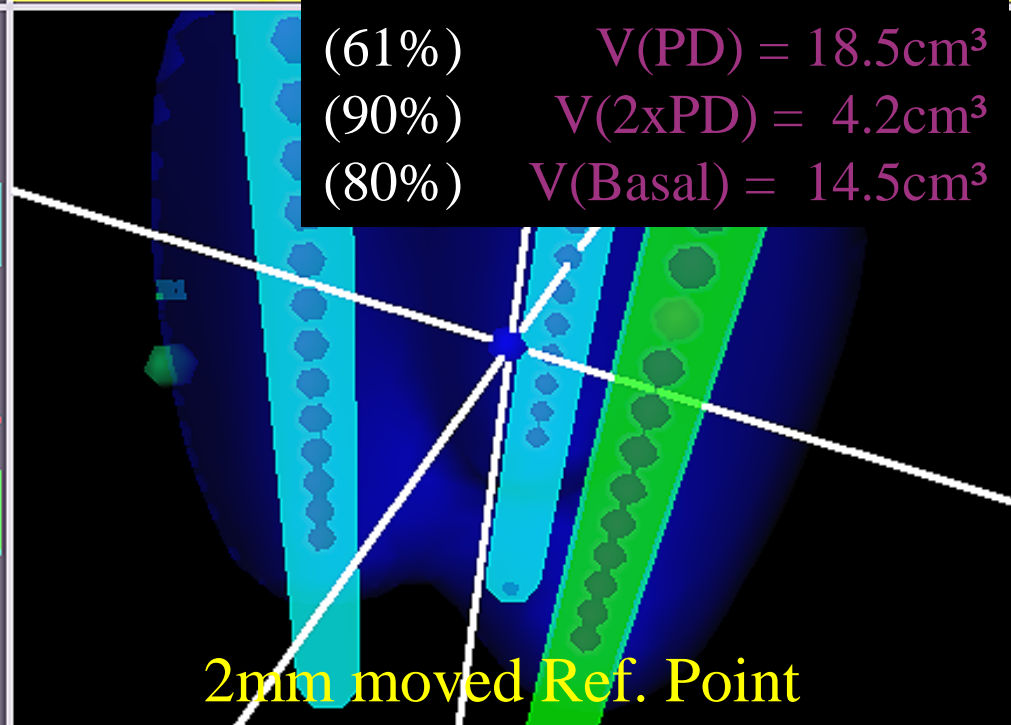
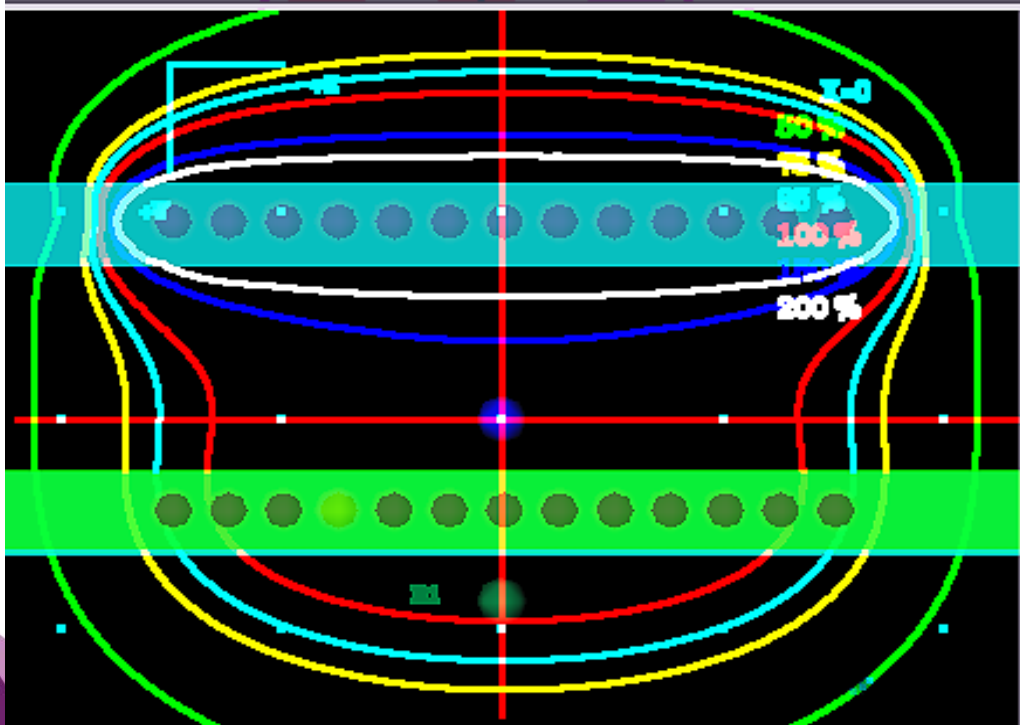
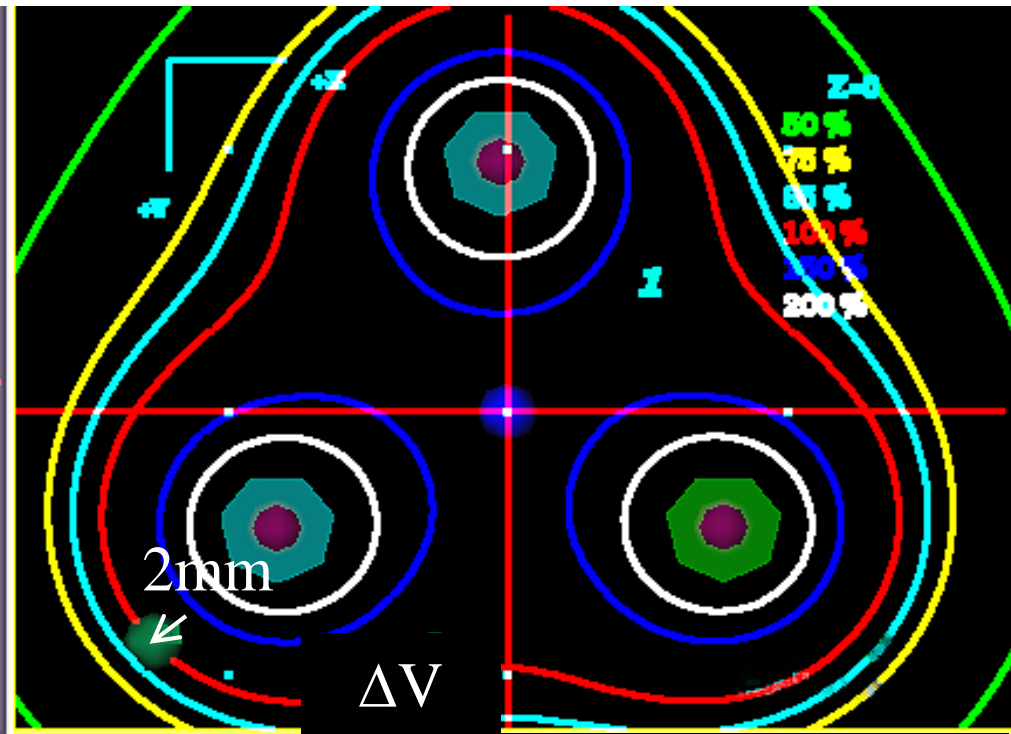
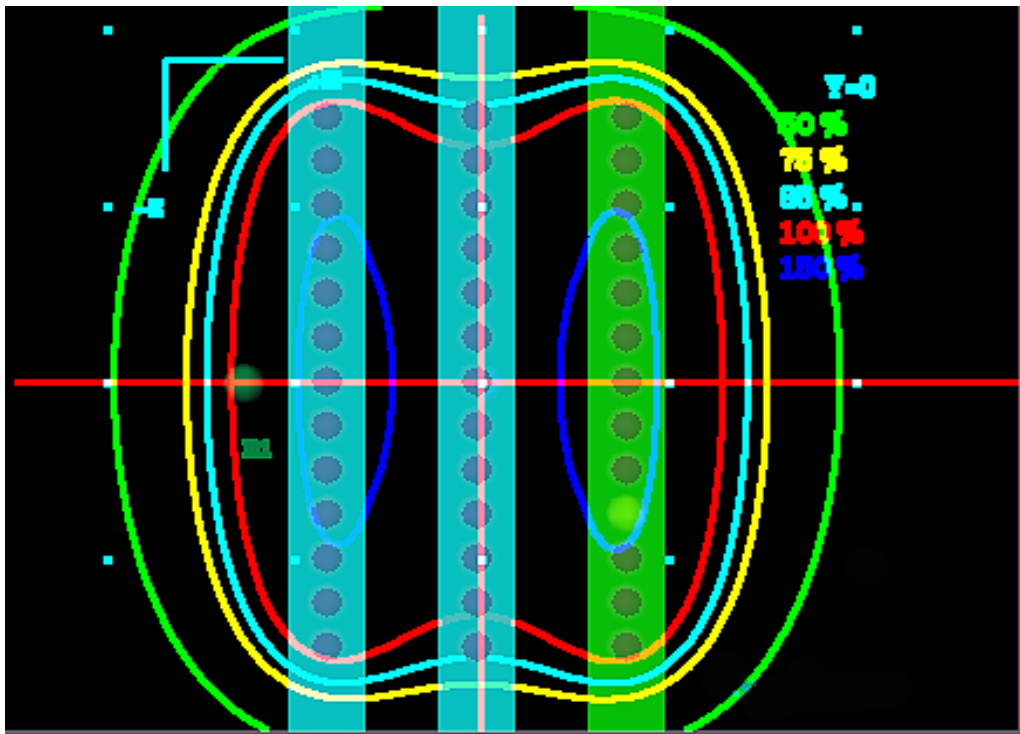
ΔV

(-0.9%)	$V(\text{PD}) = 11.6\text{cm}^3$
(0.0%)	$V(2\times\text{PD}) = 2.2\text{cm}^3$
(0.0%)	$V(\text{Basal}) = 7.8\text{cm}^3$

2mm moved Basal Point







2mm moved Ref. Point

Vienna, May 29 – June 1 2016



**Advanced Brachytherapy
Physics**

Prescribing and reporting

Christian Kirisits
Medical University of Vienna



Disclosure:

Christian Kirisits reports no conflicts of interest
Christian Kirisits was a consultant to Nucletron, an Elekta Company
Medical University of Vienna receives financial and equipment support for training and research activities from Nucletron, an Elekta Company and Varian Medical

Advanced Brachytherapy Physics, 2016



Summary on

GYN recommendations

Prostate recommendations

Endovascular (intraluminal) recommendations

Outlook on

Breast

Recommendations for gynaecological brachytherapy

GYN GEC ESTRO recommendations I (Haie-Meder et al.) - contouring

GYN GEC ESTRO recommendations II (Pötter et al.) - dose parameters

GYN GEC ESTRO recommendations III (Hellebust et al.) - reconstruction

GYN GEC ESTRO recommendations IV (Dimopoulos et al.) - imaging

ABS recommendations on GYN general (Viswanathan and Thomadsen, ABS Cervical Cancer Recommendations Committee) -general

ABS recommendations on GYN HDR (Viswanathan et al.)

ABS recommendations on GYN PDR (Lee et al.)

ICRU/GEC-ESTRO 89 report (coordinators: R. Pötter and C. Kirisits,

committee members: B. Erickson, C. Haie-Meder, J. Lindegaard, E. van Limbergen, J. Rownd, K. Tanderup, B. Thomadsen)

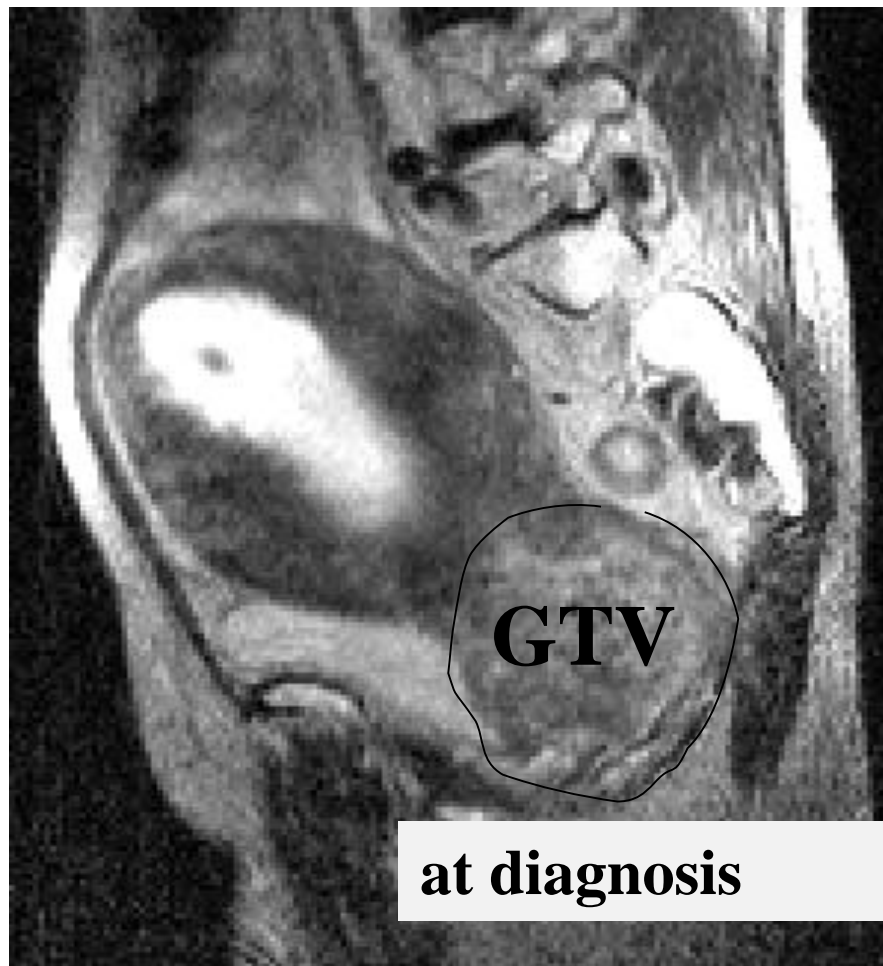
Table of Contents for ICRU/GEC-ESTRO 89

- 1 - INTRODUCTION**
 - 2 - PREVENTION, DIAGNOSIS, PROGNOSIS, TREATMENT AND OUTCOME**
 - 3 - BRACHYTHERAPY TECHNIQUES AND SYSTEMS**
 - 4 - BRACHYTHERAPY IMAGING FOR TREATMENT PLANNING**
 - 5 - TUMOR AND TARGET VOLUMES AND ADAPTIVE RADIOTHERAPY**
 - 6 - ORGANS AT RISK-AND-MORBIDITY-RELATED CONCEPTS AND VOLUMES**
 - 7 - RADIOBIOLOGICAL CONSIDERATIONS**
 - 8 - DOSE AND VOLUME PARAMETERS FOR PRESCRIBING, RECORDING, AND REPORTING OF BRACHYTHERAPY ALONE AND COMBINED WITH EXTERNAL BEAM RADIOTHERAPY**
 - 9 - 3D VOLUMETRIC DOSE ASSESSMENT**
 - 10 - RADIOGRAPHIC DOSE ASSESMENT**
 - 11 - SOURCES AND DOSE CALCULATION**
 - 12 - TREATMENT PLANNING**
 - 13 - SUMMARY OF THE RECOMMENDATIONS**
- APPENDIX – EXAMPLES, SPREADSHEETS, DRAWINGS**

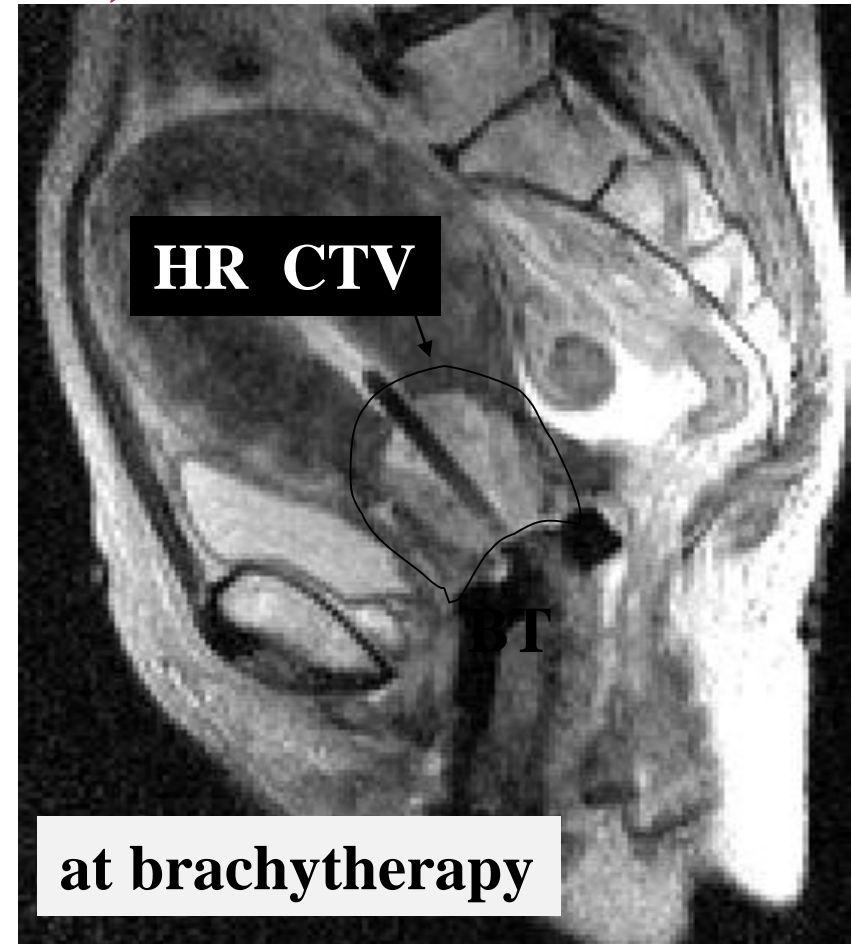
Target definition

Advanced disease, significant remission after EBRT:

Change of GTV/CTV with time (4D RT) (FIGO IIB)

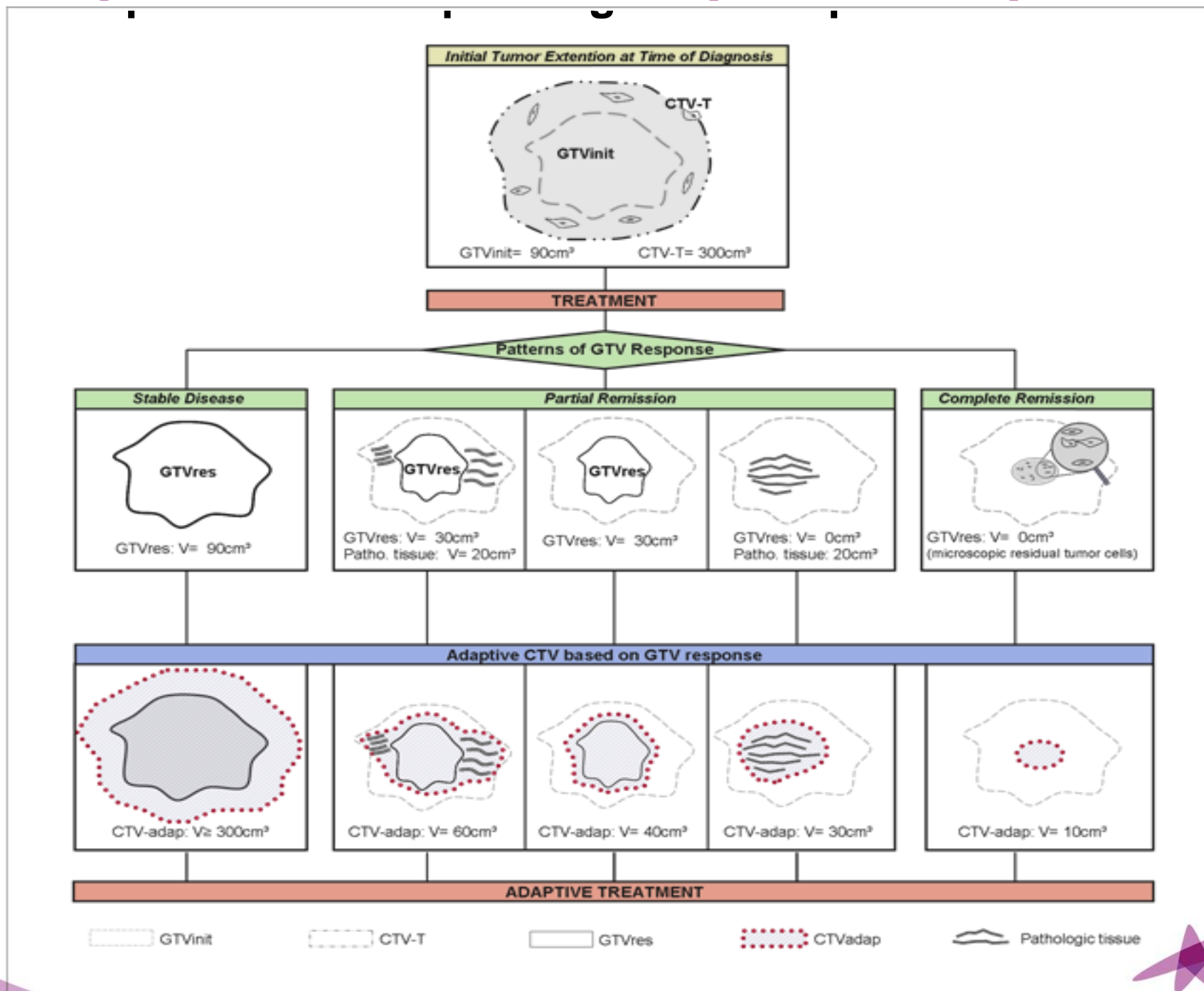


**Tumor Extension
before EBT**

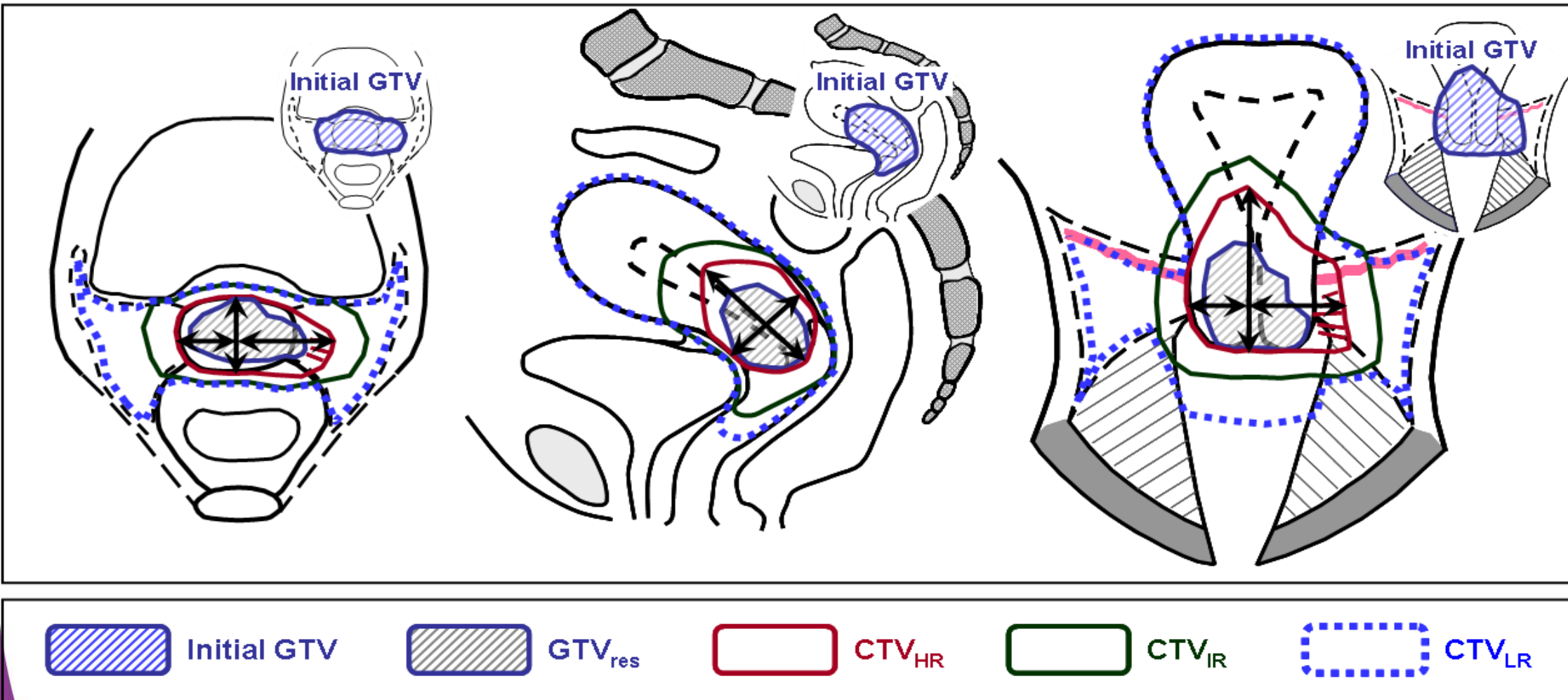


**Target Volume of BT
Based on dimensions and
Topography at time of BT**

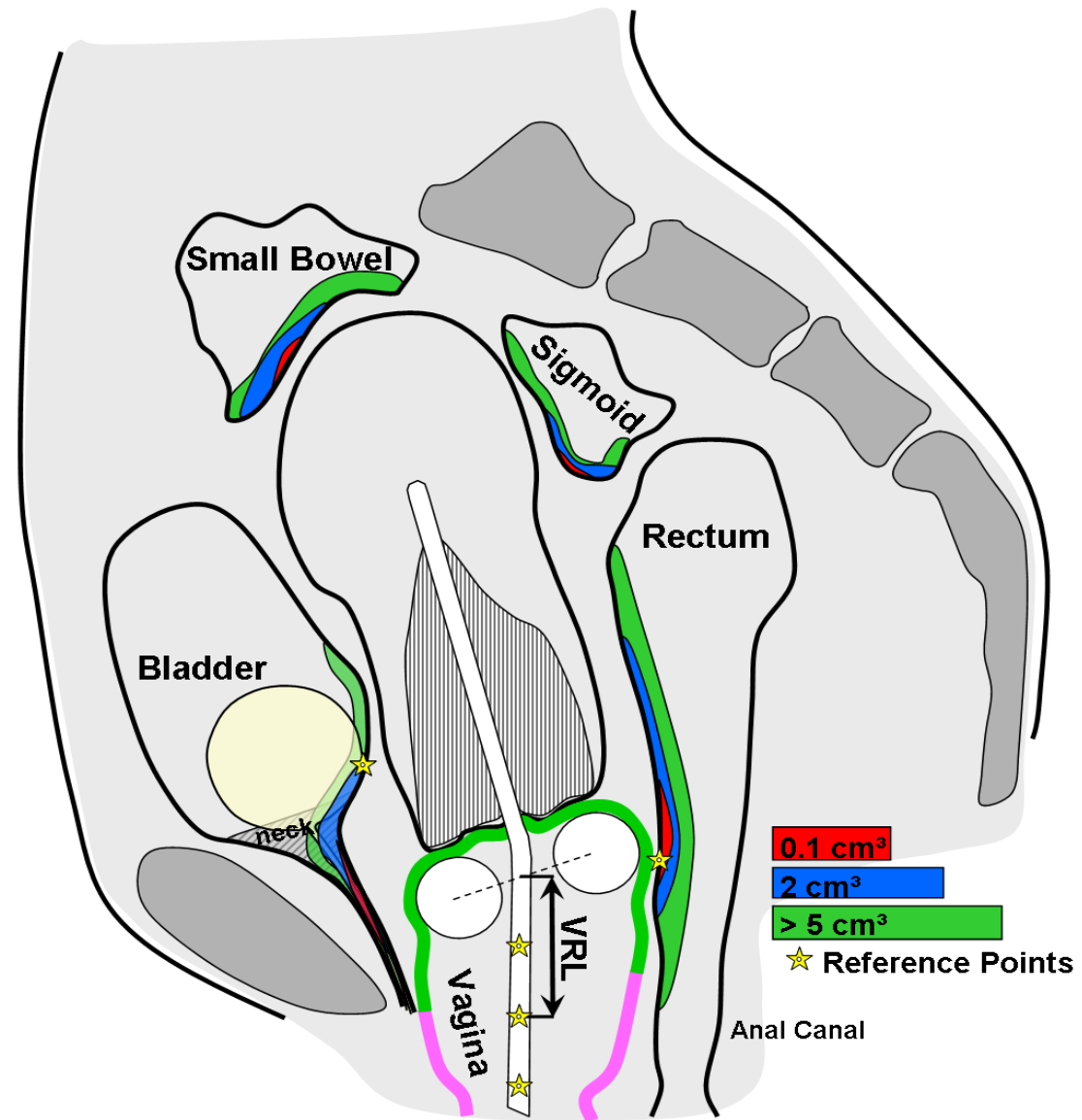
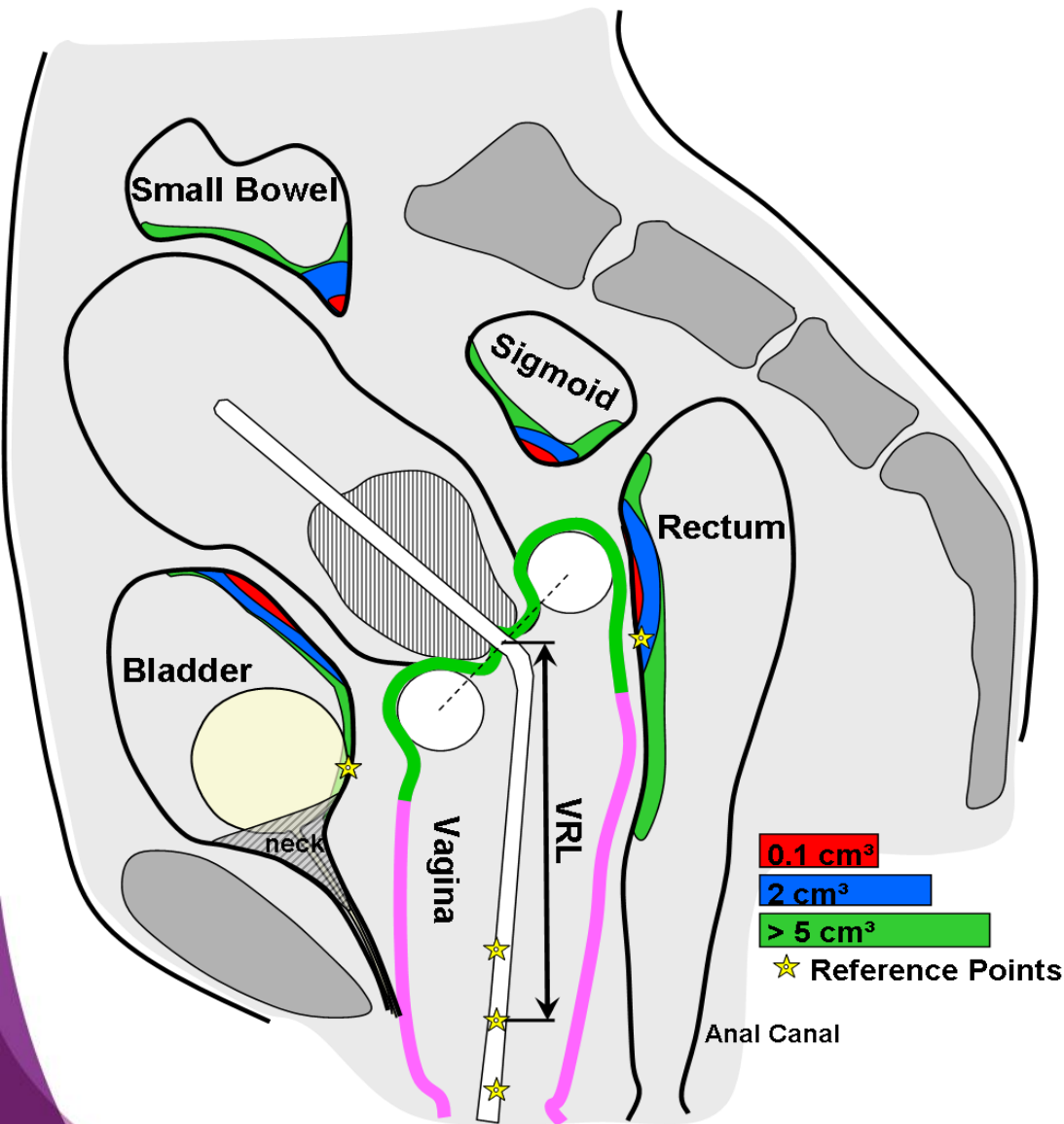
Various patterns of tumor response adapted CTV



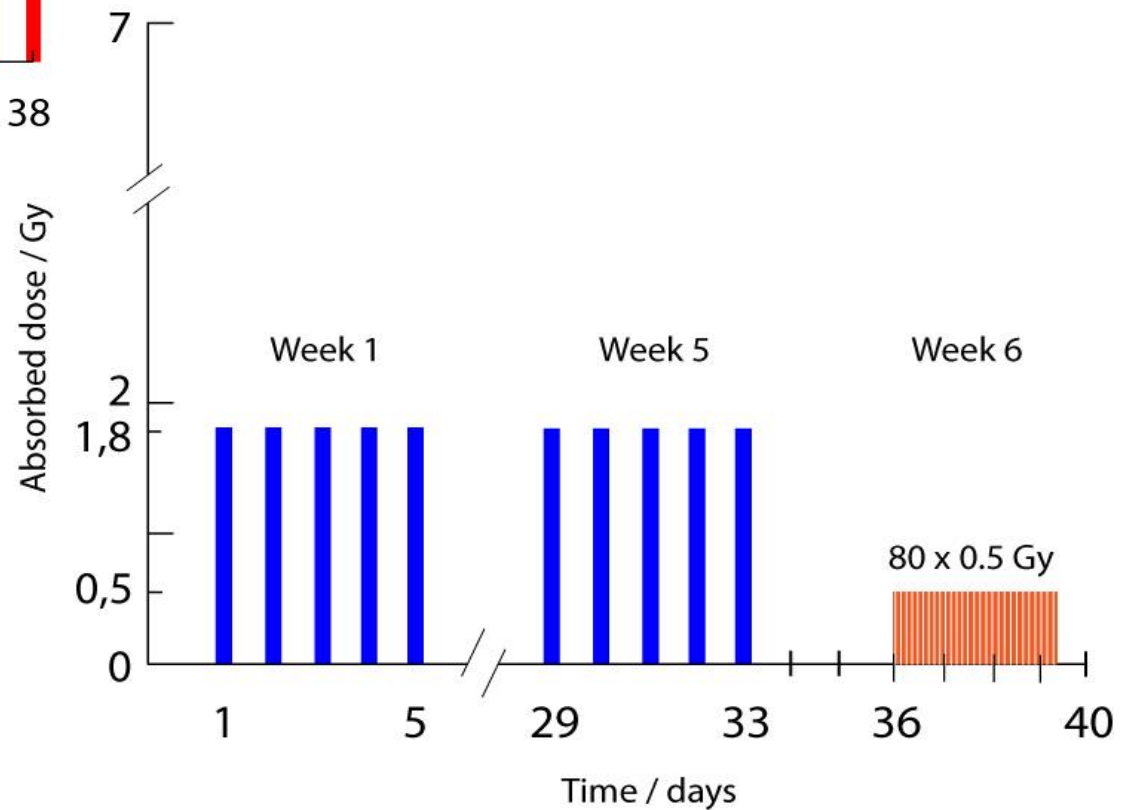
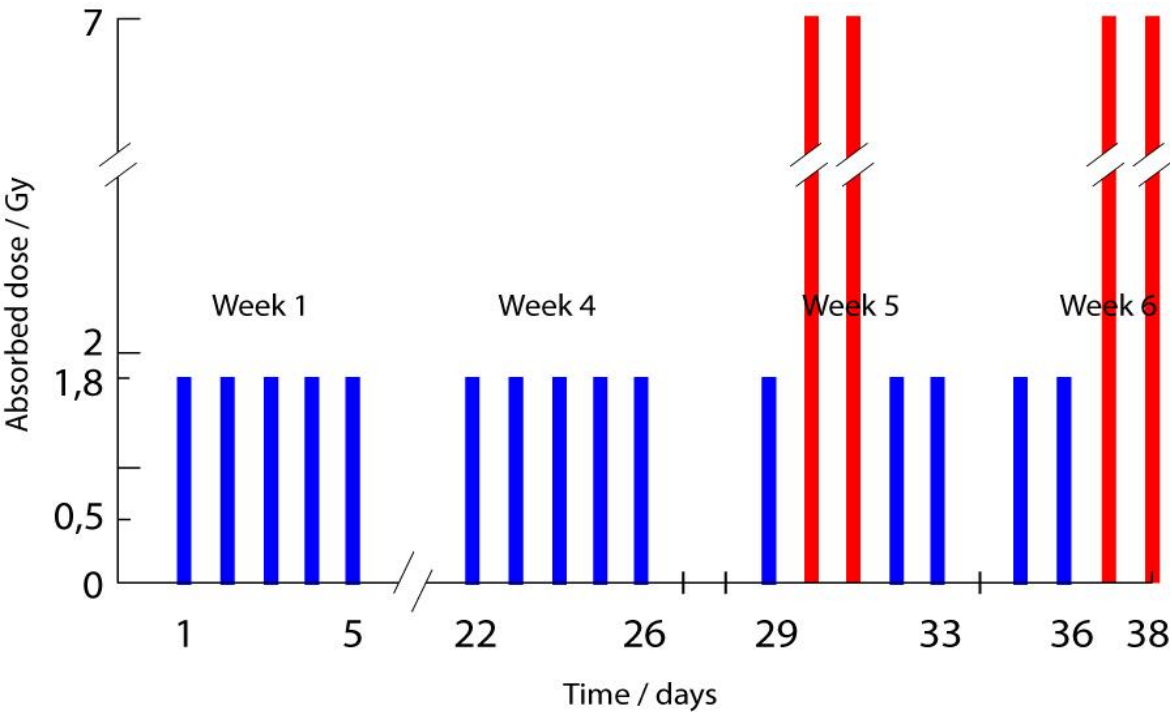
Various patterns of tumor response adapted CTV



OAR concept and related volumes



Radiobiology: Time-dose pattern



General principles for assessment and reporting of physical and equieffective EBRT and BT dose (all reporting levels)

Physical dose and number of fractions is assessed for target, OARs, dose points:

- BT
- EBRT

Total equieffective dose (EQD2) is calculated according to the linear quadratic model through the following steps:

- BT EQD2 for each fraction
- Total BT EQD2
- Total EBRT EQD2
- Accumulated total EBRT+BT EQD2*

**Based on current assumptions outlined in chapter 9*

Reporting of radiobiological parameters:

α/β values for tumour and OARs*

In addition $T_{1/2}$ and recovery model for LDR and PDR treatments*

*At present: $\alpha/\beta=3$ Gy for late effects in OAR and 10 Gy for tumour, and $T_{1/2}=1.5$ h

Radiotherapy & Oncology

Volume 105, Issue 2 , Pages 266-268, November 2012

Bioeffect modeling and equieffective dose concepts in radiation oncology – Terminology, quantities and units

Søren M. Bentzen, Wolfgang Dörr, Reinhard Gahbauer, Roger W. Howell, Michael C. Joiner, Bleddyn Jones, Dan T.L. Jones, Albert J. van der Kogel, André Wambersie, Gordon Whitmore

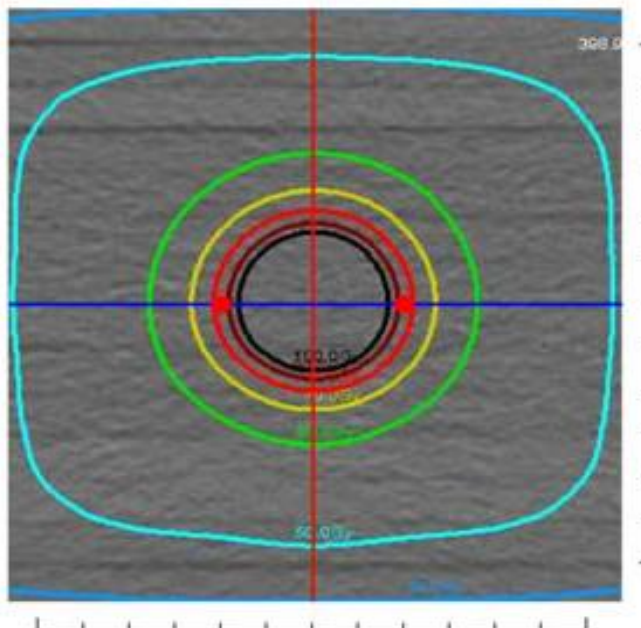
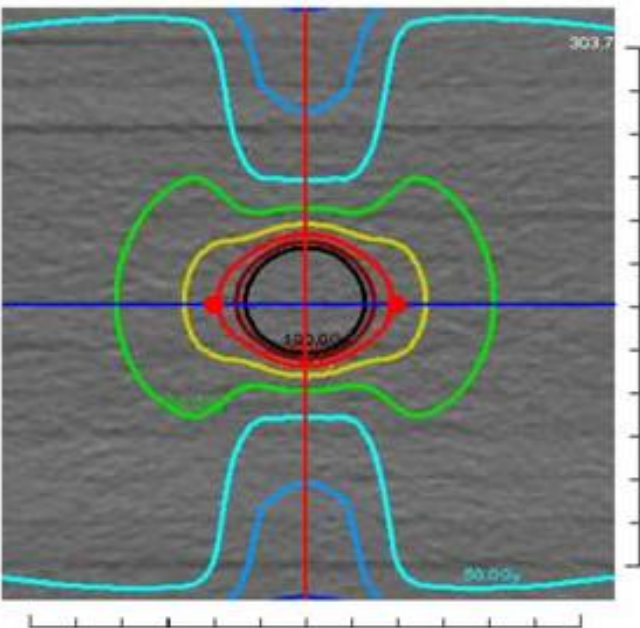
Filling the gap in central shielding: threedimensional analysis of the EQD2 dose in radiotherapy for cervical cancer with the central shielding technique

Tomoaki Tamaki, Tatsuya Ohno, Shin-ei Noda, Shingo Kato, Takashi Nakano

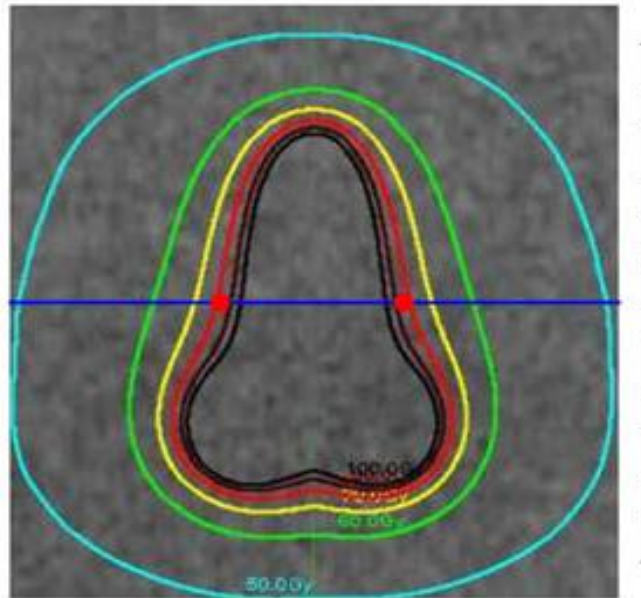
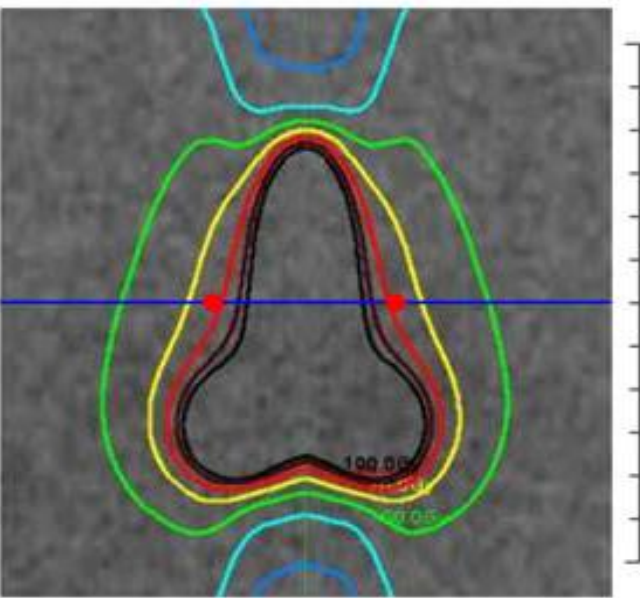
Axial plane

With CS

Without CS



Coronal plane

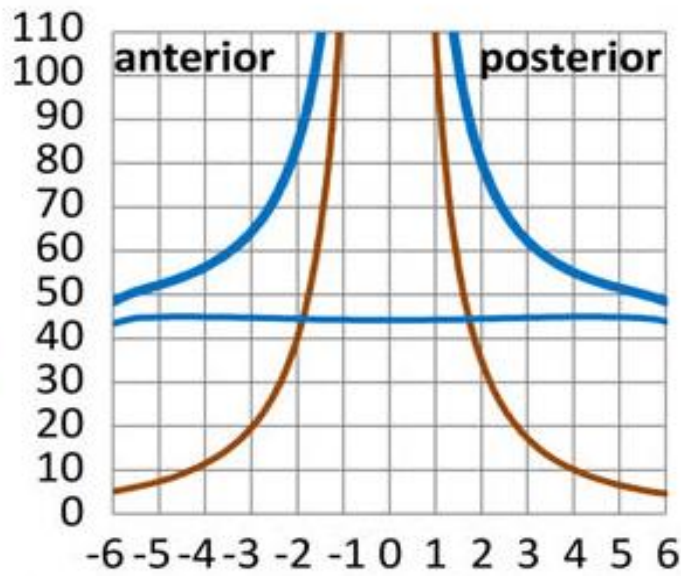
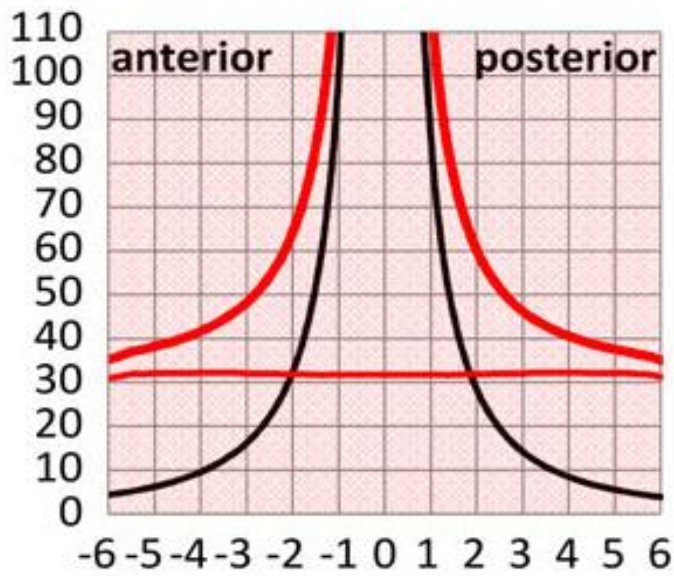
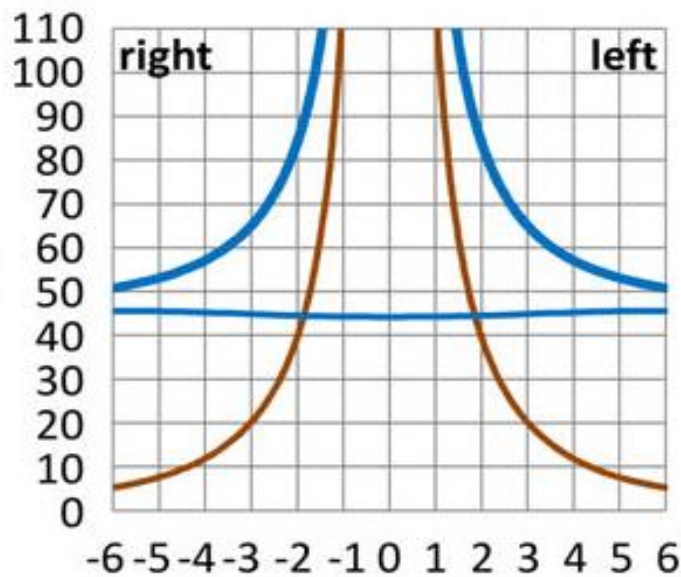
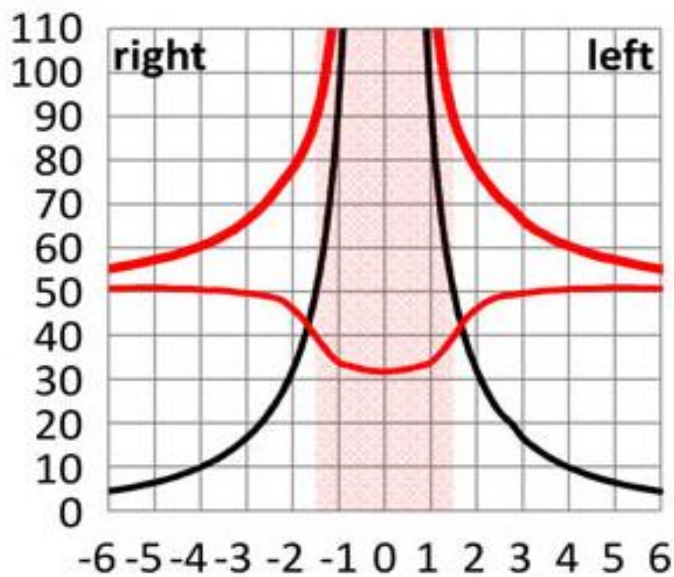


Journal of Radiation Research, 2015, pp. 1-7

Isodose lines: (EQD₂)

- 100 Gy
- - - 90 Gy
- - - 80 Gy
- - - 70 Gy
- - - 60 Gy
- - - 50 Gy
- - - 40 Gy
- - - 30 Gy

● Point A



Distance from the center on the right-left axis (cm)

Distance from the center on the anterior-posterior axis (cm)

— Total Dose — Brachytherapy
— WP + CS Shielded by CS

— Total Dose — Brachytherapy
— WP

See also Abe al.

FROM PLANNING AIMS TO PRESCRIPTION

Traditional concepts:

“when prescribing to a target, the prescription dose is the planned dose to cover this target as completely as possible.”

or

prescription to a 100% isodose which is “to cover” the target volume”

Need for common terminology according to ICRU reports on proton treatment and IMRT

Planning aim dose

- Set of dose and dose/volume constraints for a treatment

Prescribed dose

- Finally accepted treatment plan (which is assumed to be delivered to an individual patient)

Delivered dose

- Actually delivered dose to the individual patient

Need for common terminology according to ICRU reports on proton treatment and IMRT

Example:

~~Previously: 4x7 Gy ~ 84 Gy EQD2 prescribed, D90 was mean 93 Gy~~

Planning aim was to deliver 4 x 7 Gy ~ 84 Gy, $D_{2\text{cm}^3}$ for rectum, sigmoid < 70 Gy EQD2, bladder < 90 Gy EQD2

Prescribed dose was mean 93 Gy \pm 13 Gy (1SD) EQD2 to D_{90} HR CTV

Delivered dose ? *Depending on variations and uncertainties – on average no systematic deviation from prescribed dose*

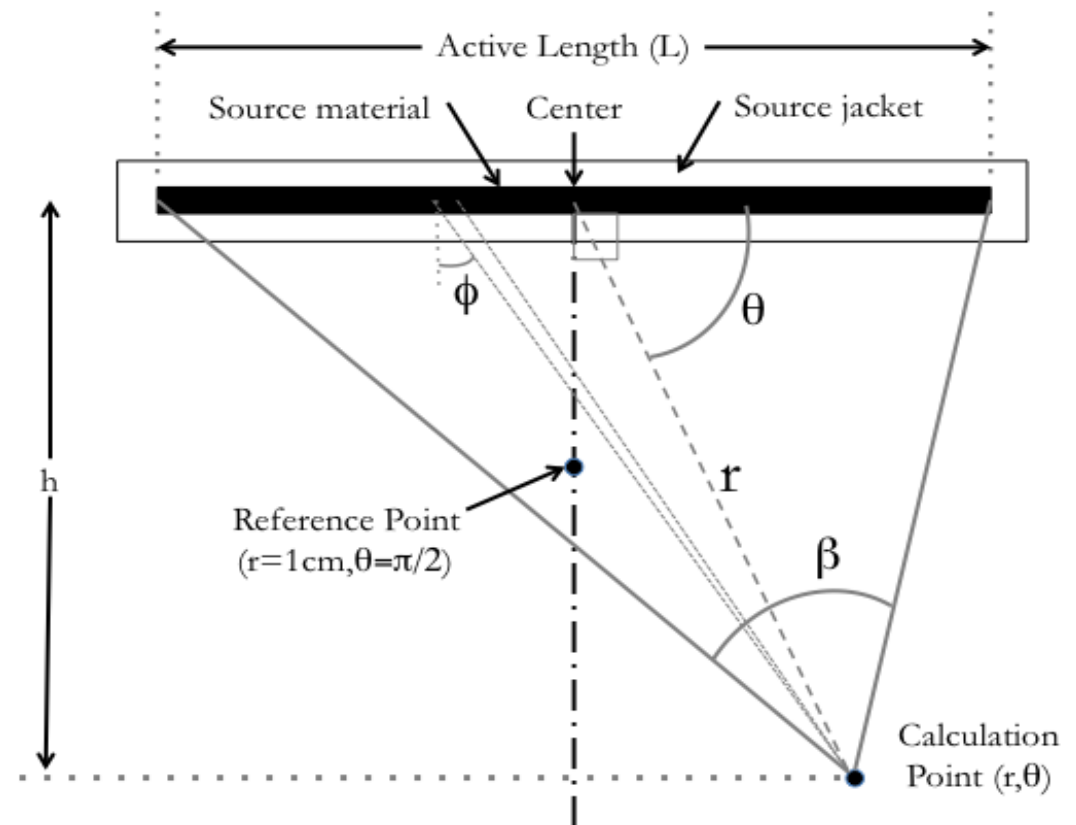
Level 1 - *Minimum standard for reporting*

Source and dose calculation:

Radionuclide and source model

Source strength

Dose calculation algorithm



Level 1 - *Minimum standard for reporting*

Comprehensive clinical gynecologic examination

Volumetric imaging (MRI, CT, US, PET CT) at time of diagnosis and BT
FIGO/TNM stage

Baseline morbidity and QoL assessment

Schematic 3D documentation on a clinical diagram indicating dimensions
and volumes for:

- GTV_{init} (GTV at diagnosis)
- GTV_{res} (GTV at brachytherapy)
- CTV_{HR} (GTV_{res} (plus residual pathologic tissue plus whole cervix))
- (CTV_{IR} : GTV_{init} and CTV_{HR} plus safety margin if used for prescription)

Level 1 - *Minimum standard for reporting*

Dose reporting:

TRAK

Point A dose

Recto-vaginal reference point dose

$D_{0.1\text{cm}^3}$, $D_{2\text{cm}^3}$ for bladder, rectum

or

Bladder reference point for radiographs

Level 2 - *Advanced standard for reporting*

All that is reported in level 1 plus:

3D delineation of volumes (on volumetric images with applicator and on clinical diagrams):

GTV_{res}

CTV_{HR}

(CTV_{IR} if used for prescription)

With maximum width, height, thickness and with volume

Level 2 - *Advanced standard for reporting*

All that is reported in level 1 plus:

Dose reporting for defined volumes:

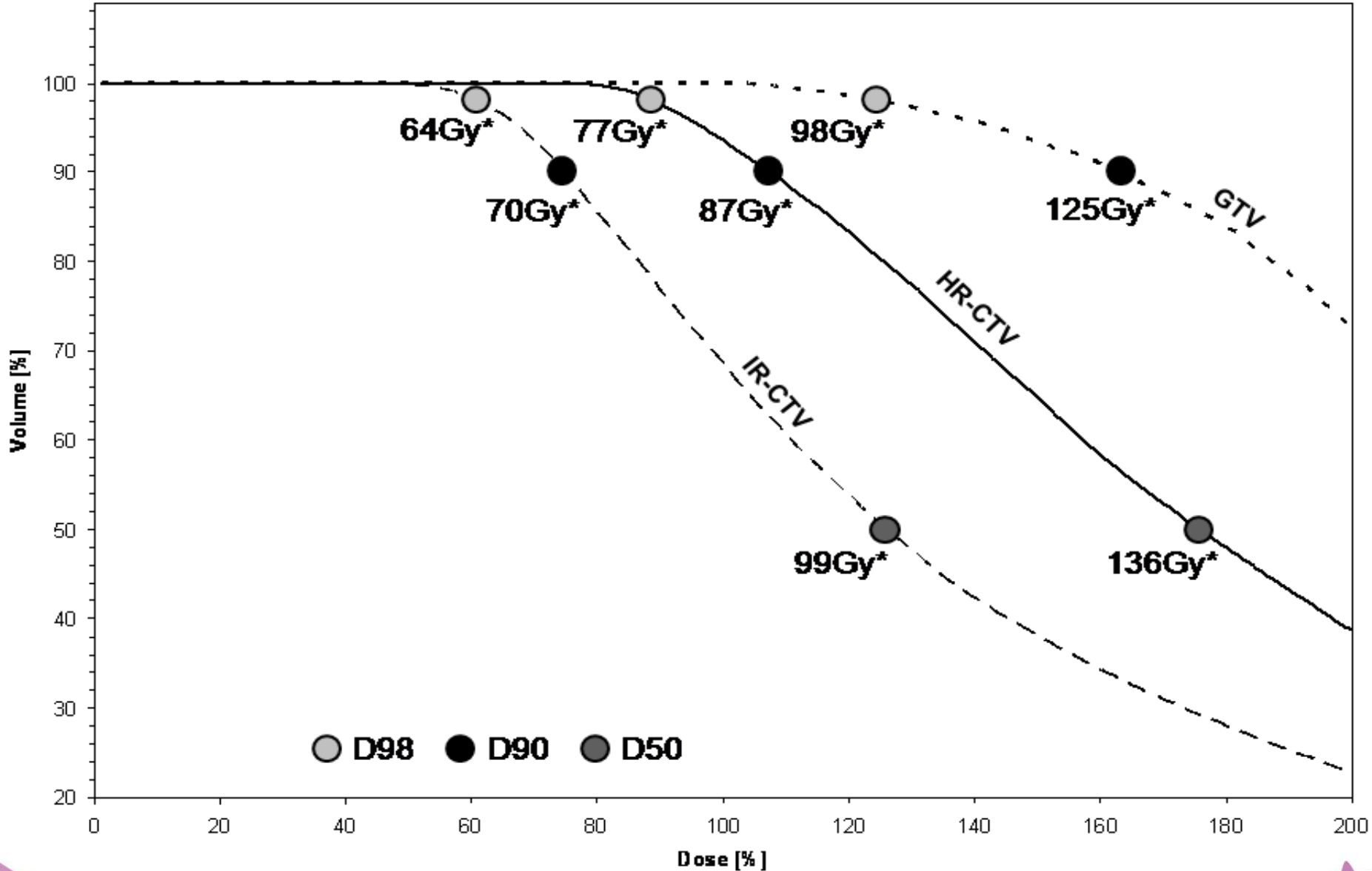
D_{98} , D_{90} , D_{50} for CTV_{HR}

(D_{98} , D_{90} for CTV_{IR} if used for prescription)

D_{98} for GTV_{res}

D_{98} for pathological Lymph nodes

DVH for target volumes



Level 2 - *Advanced standard for reporting*

All that is reported in level 1 plus:

Dose reporting OARs:

Bladder reference point dose

$D_{0.1\text{cm}^3}$, $D_{2\text{cm}^3}$ for sigmoid*

$D_{2\text{cm}^3}$ bowel (if fixed)*

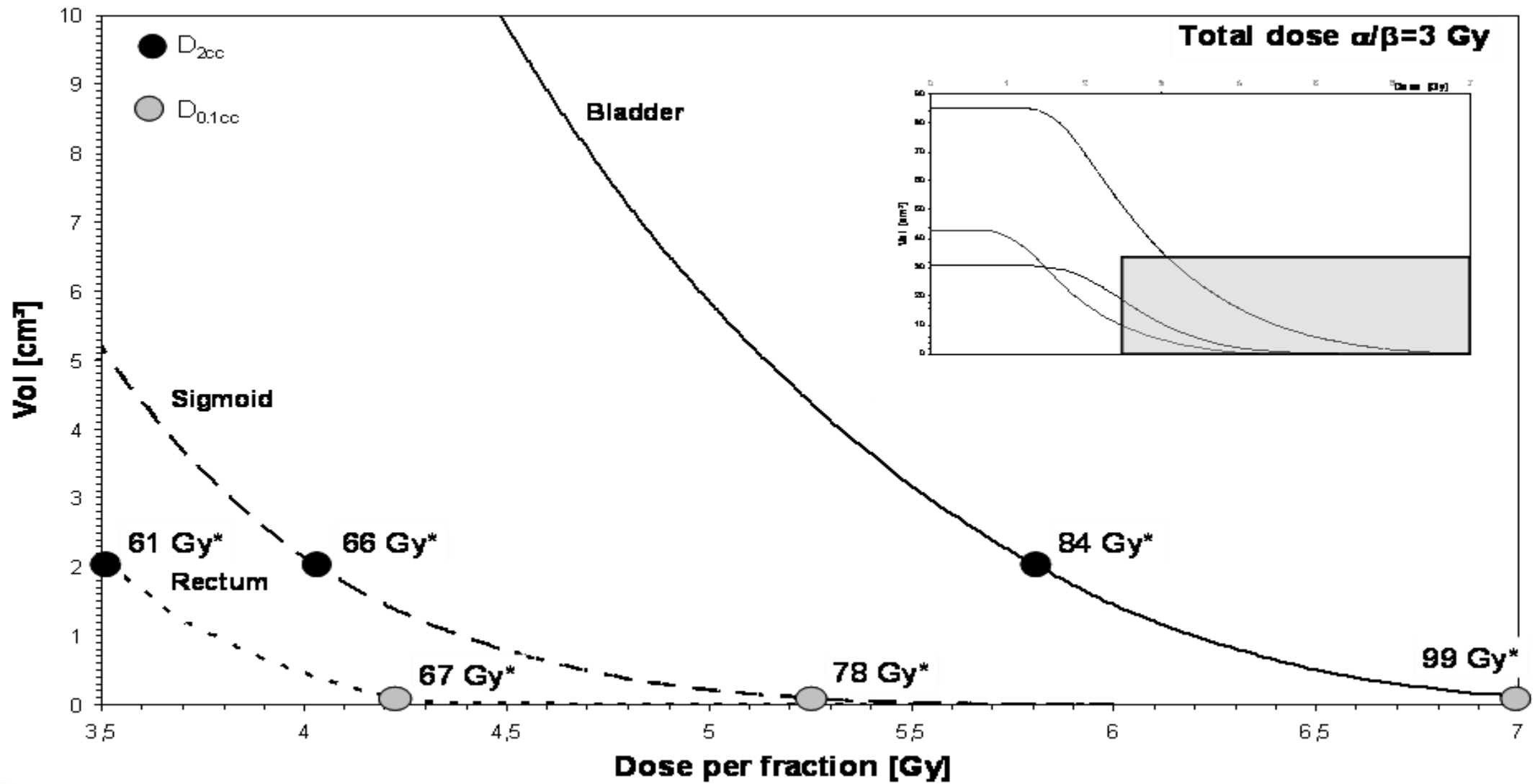
Intermediate and low dose parameters in bladder, rectum, sigmoid, bowel

(e.g. $V_{25\text{Gy}}$, $V_{35\text{Gy}}$, $V_{45\text{Gy}}$ or $D_{98\%}$, $D_{50\%}$, $D_{2\%}$)

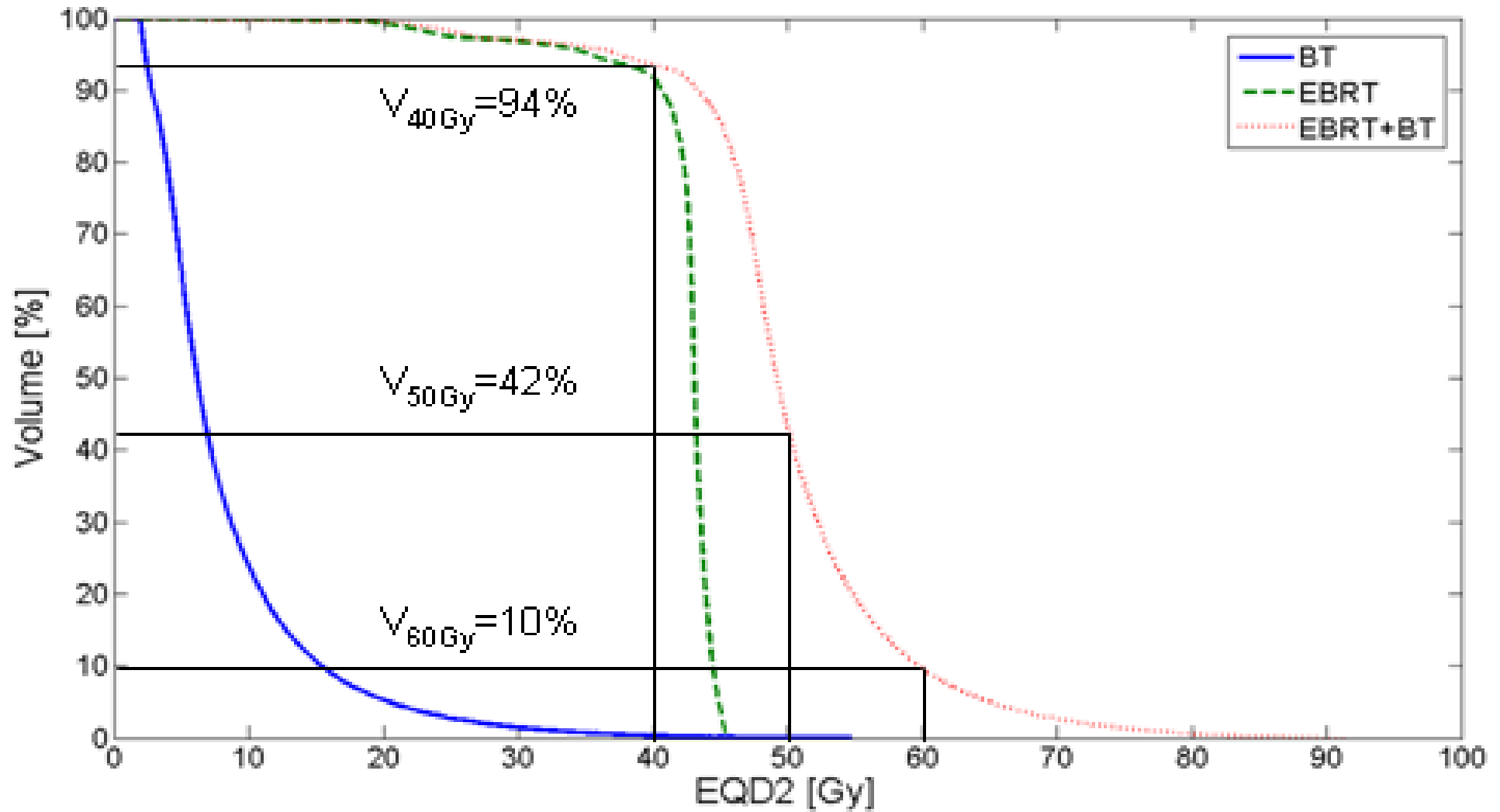
Vaginal point doses at level of sources (lateral at 5 mm)**

Lower and mid vagina doses (PIBS, PIBS $\pm 2\text{cm}$)**

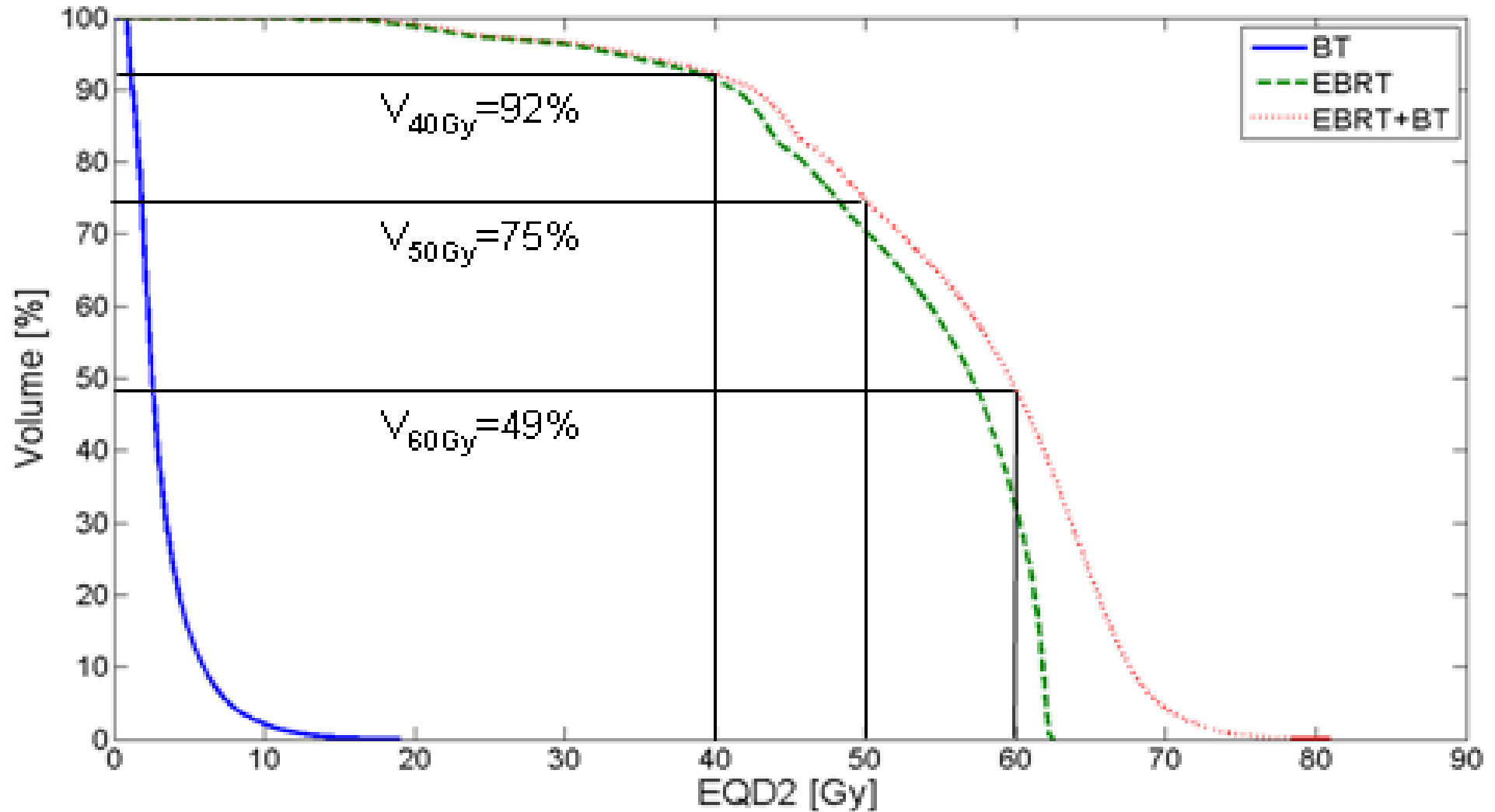
DVH for OAR



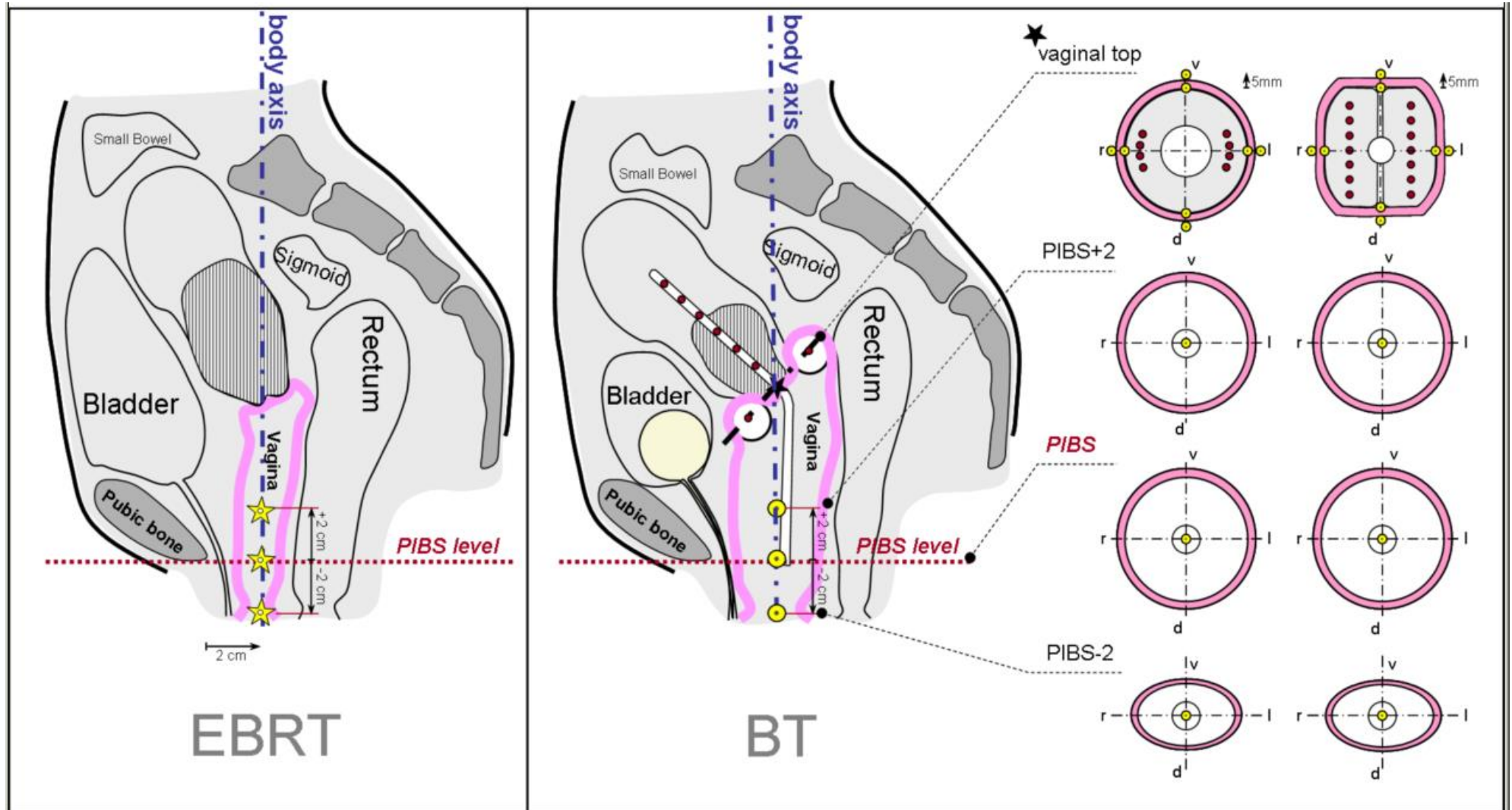
45 Gy whole pelvis EBRT plus 4 fractions of HDR brachytherapy (total target dose 85Gy EQD2)



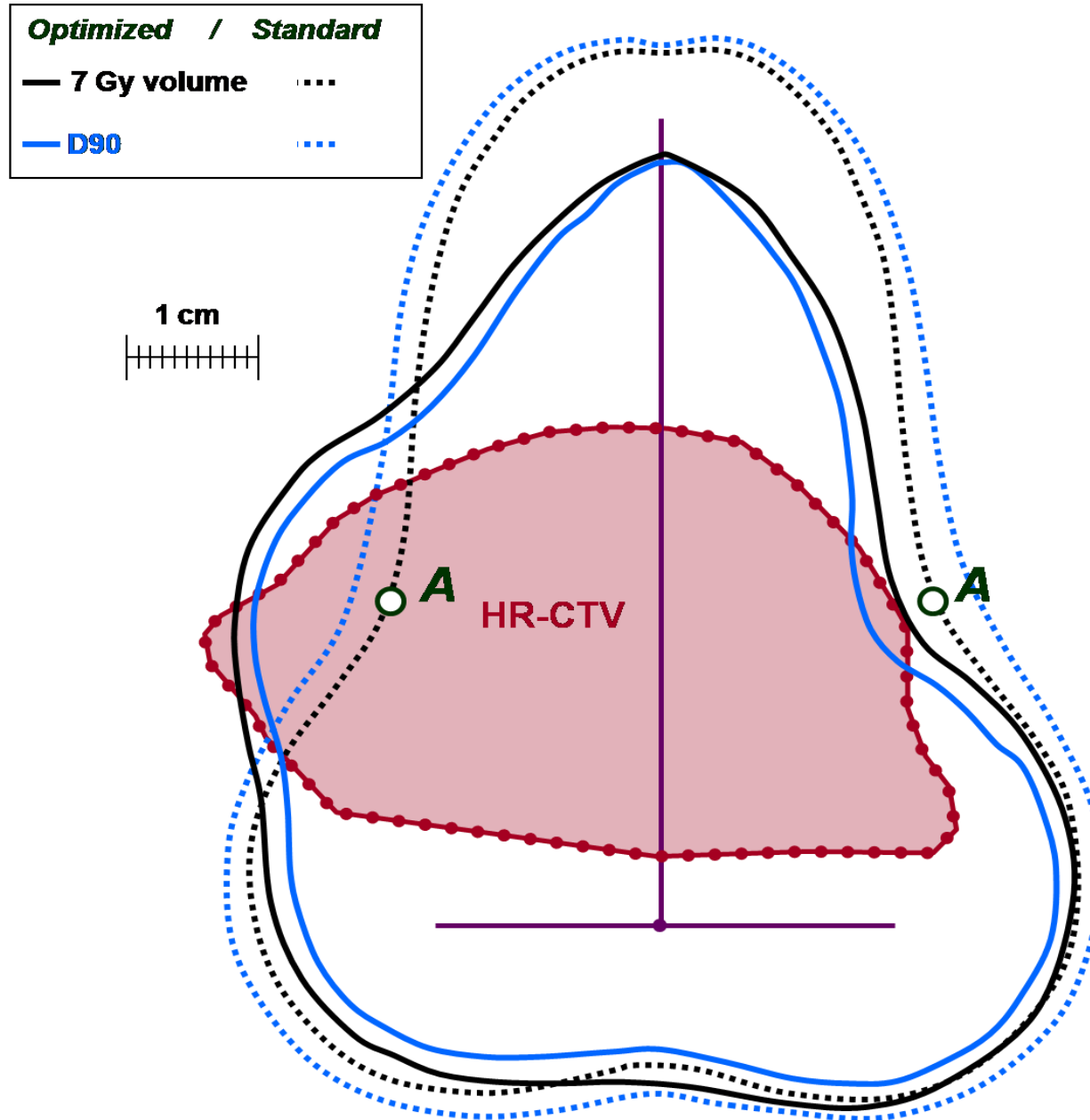
*45 Gy whole pelvis EBRT plus 15 Gy EBRT tumor boost plus
2 fractions of HDR brachytherapy (total target dose 85Gy EQD2)*



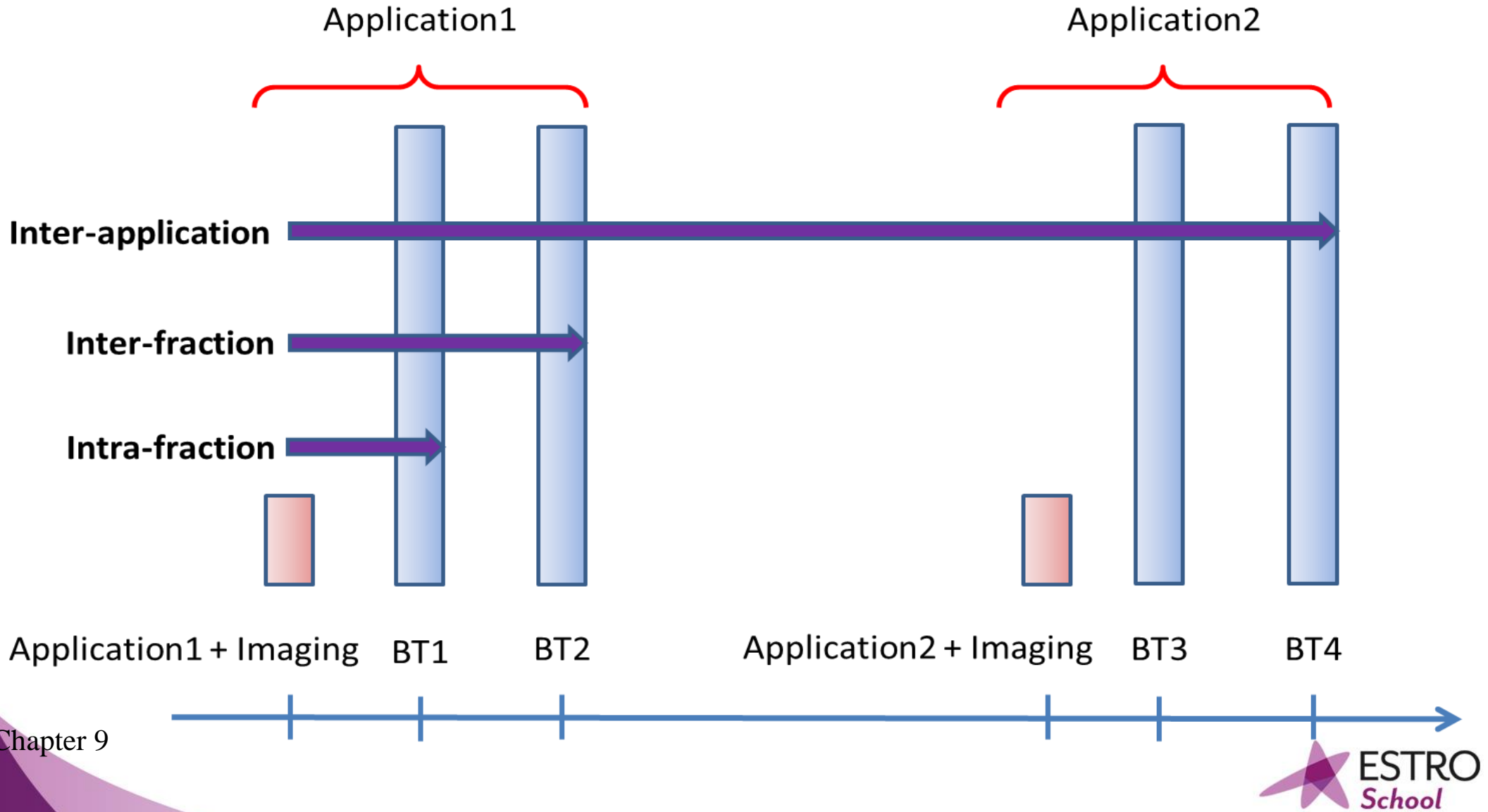
Vaginal Reference Points



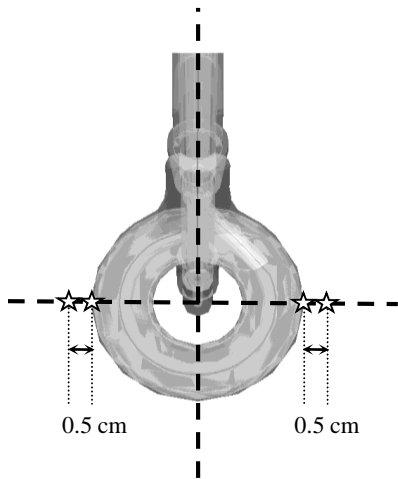
Isodose (surface) volume



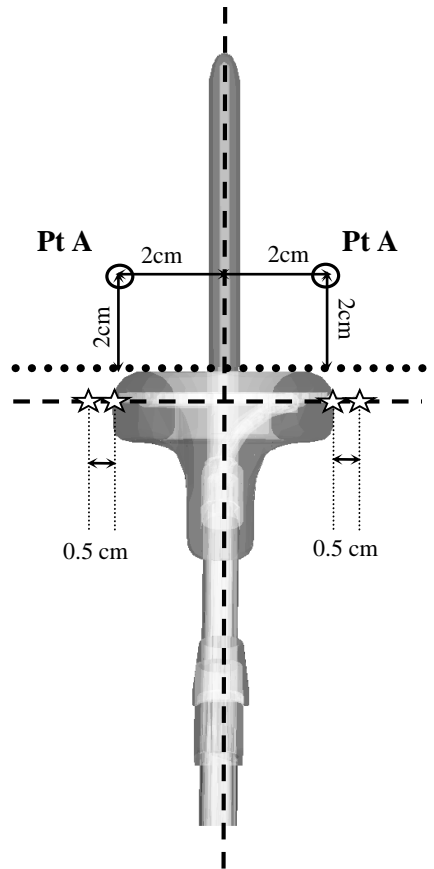
Terminology for fractionated dose delivery



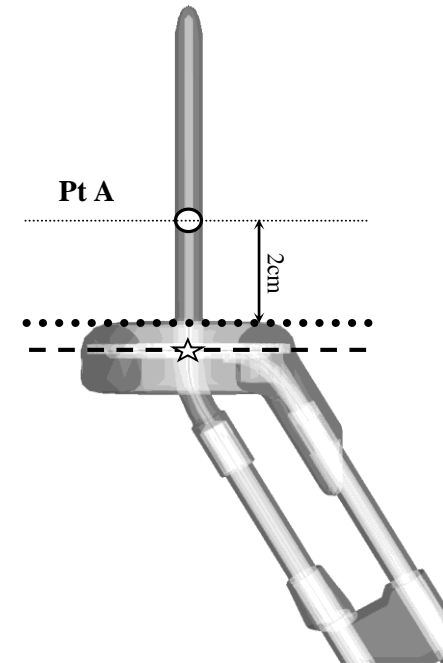
Point A



axial

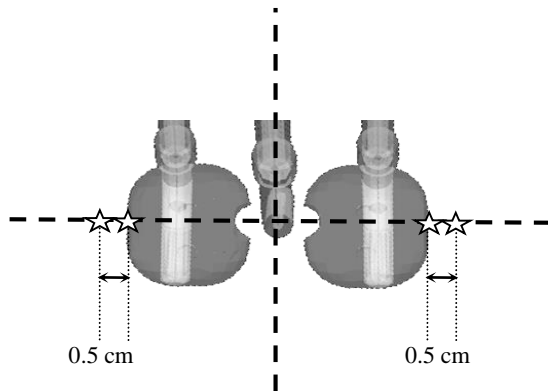


coronal

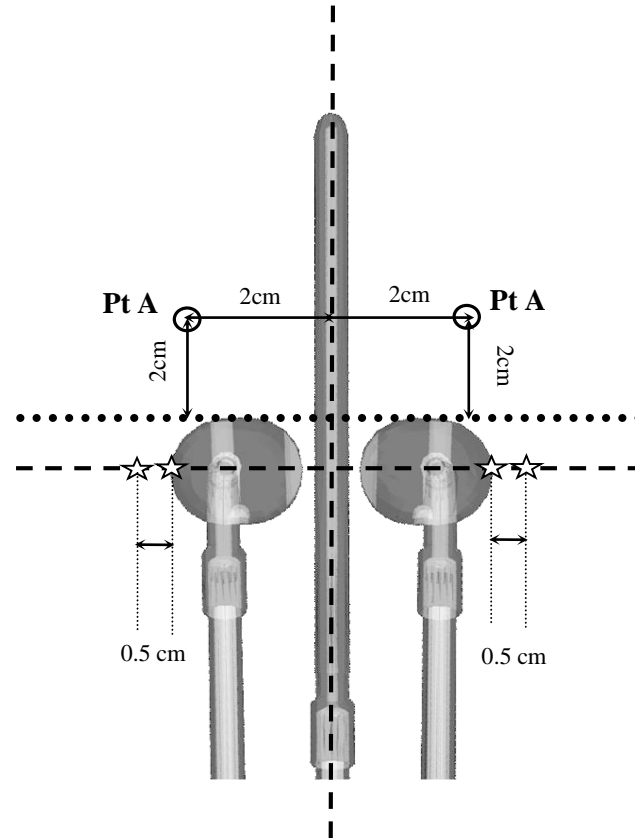


sagittal

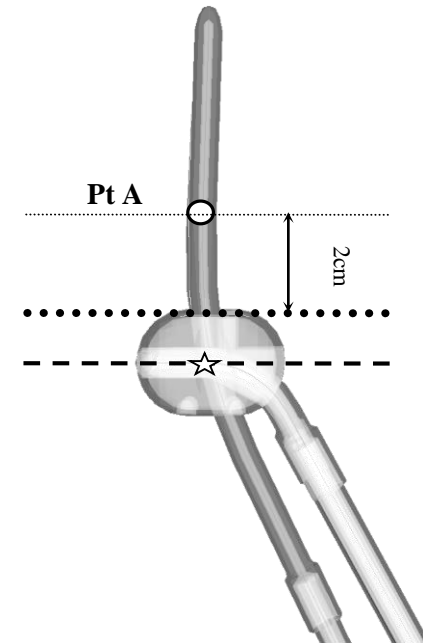
Point A



axial

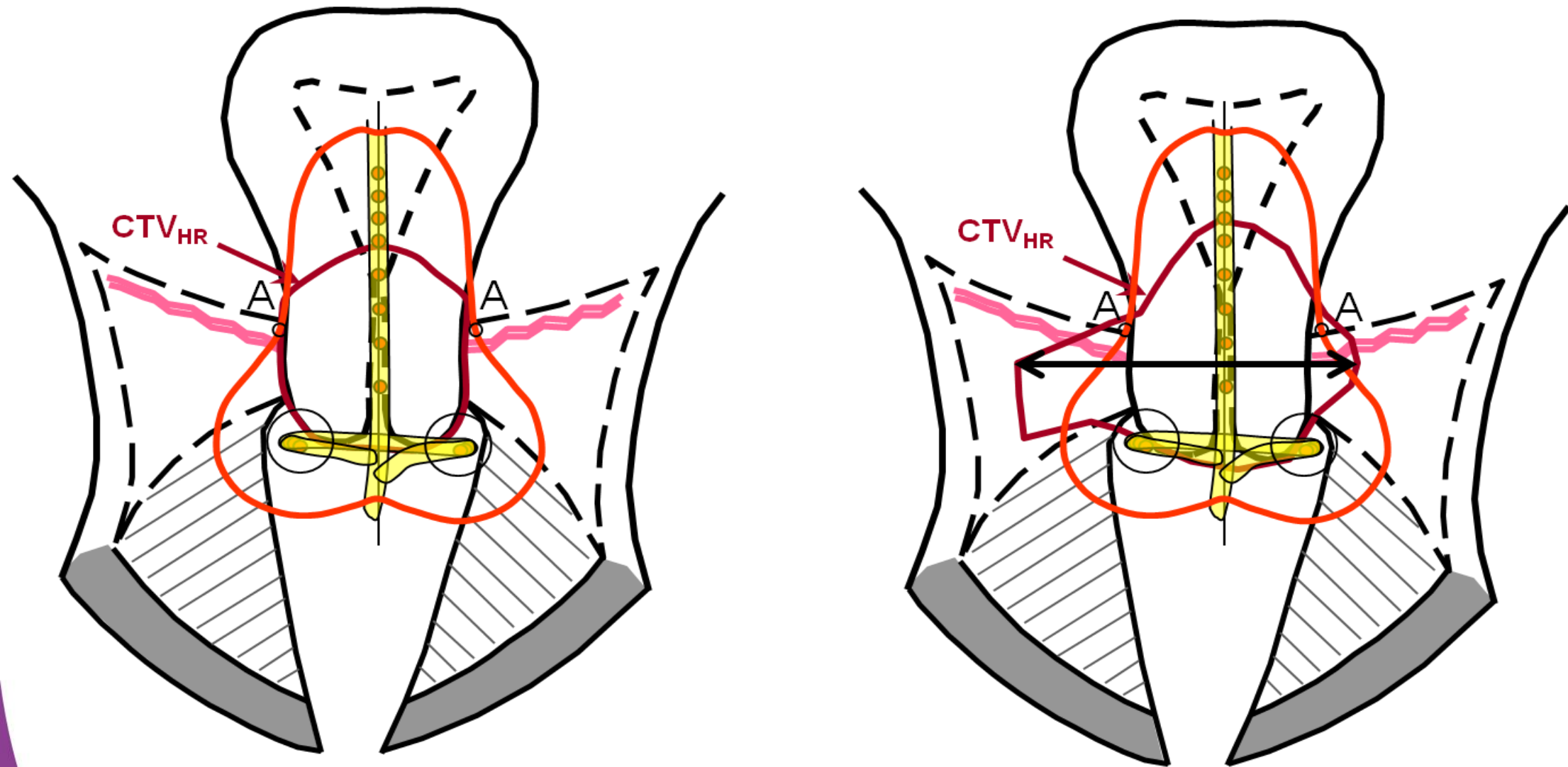


coronal

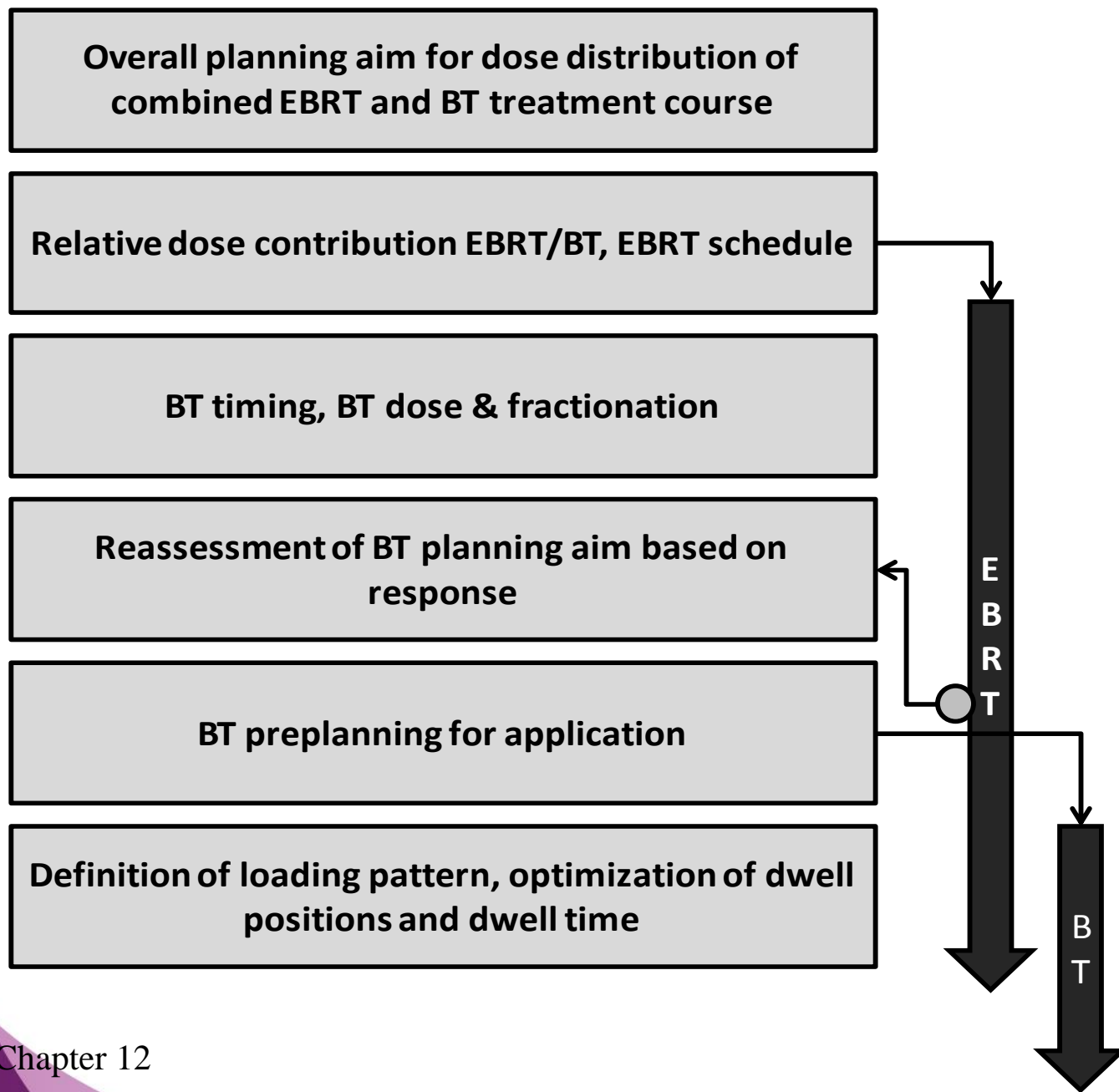


sagittal

Dose estimation in case of radiographs

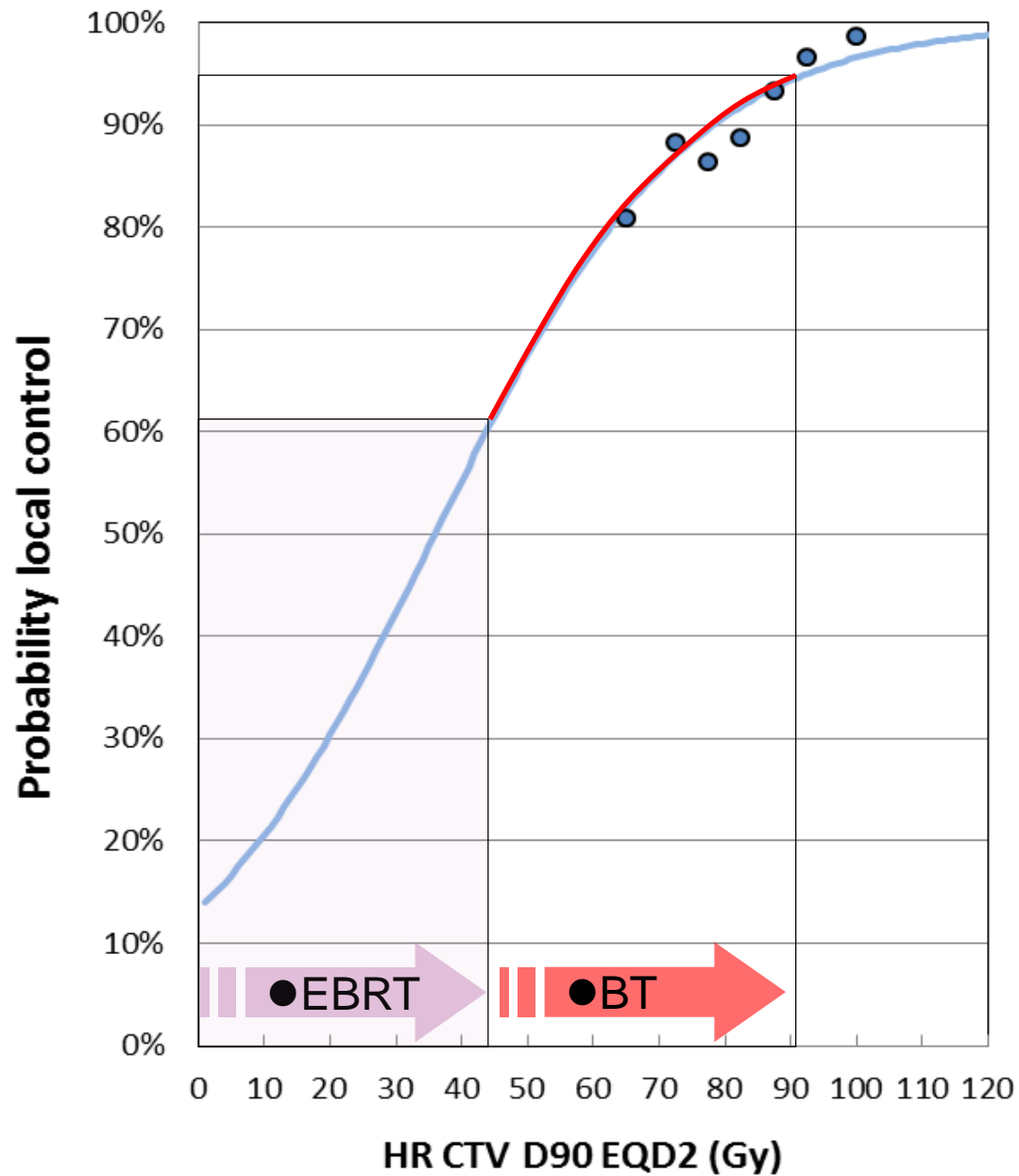


Treatment planning



Dose-response for local control

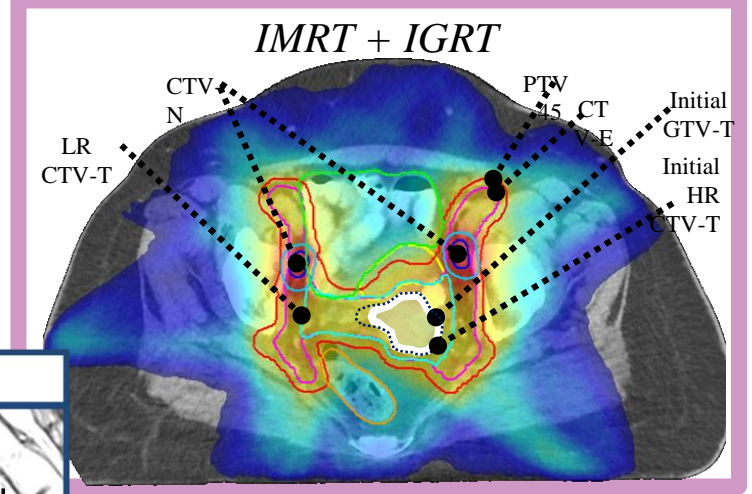
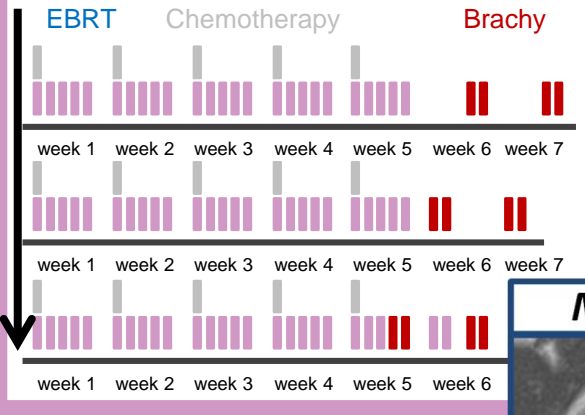
RETRO
EMBRACE



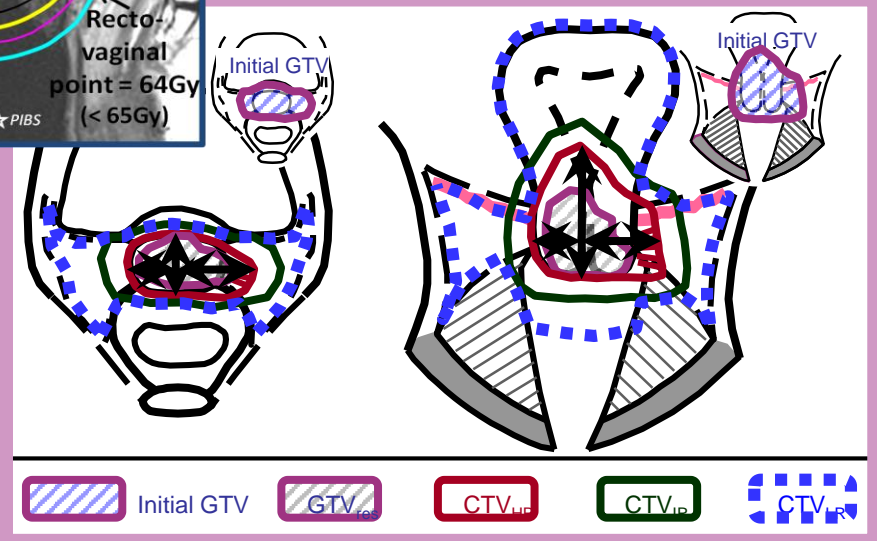
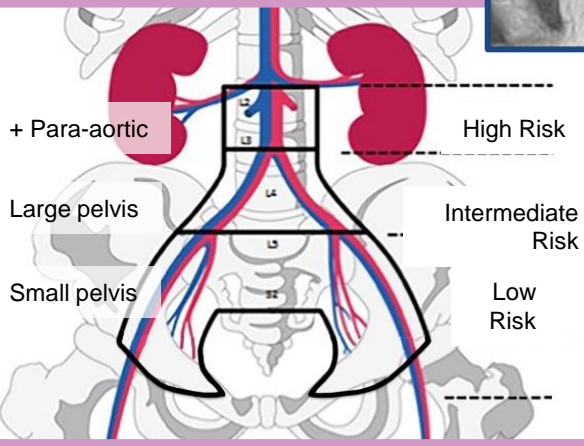
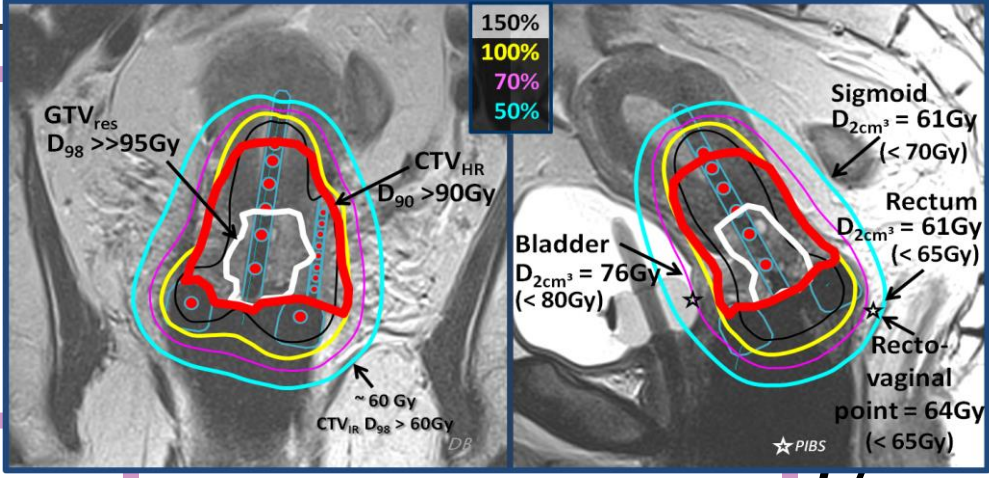
Tanderup
ESTRO 2nd Forum
Geneve, 2013
&
Radiother Oncol 2016

EMBRACE II

RChTh + BT in < 50 days



MRI guided adaptive brachytherapy (IGABT)



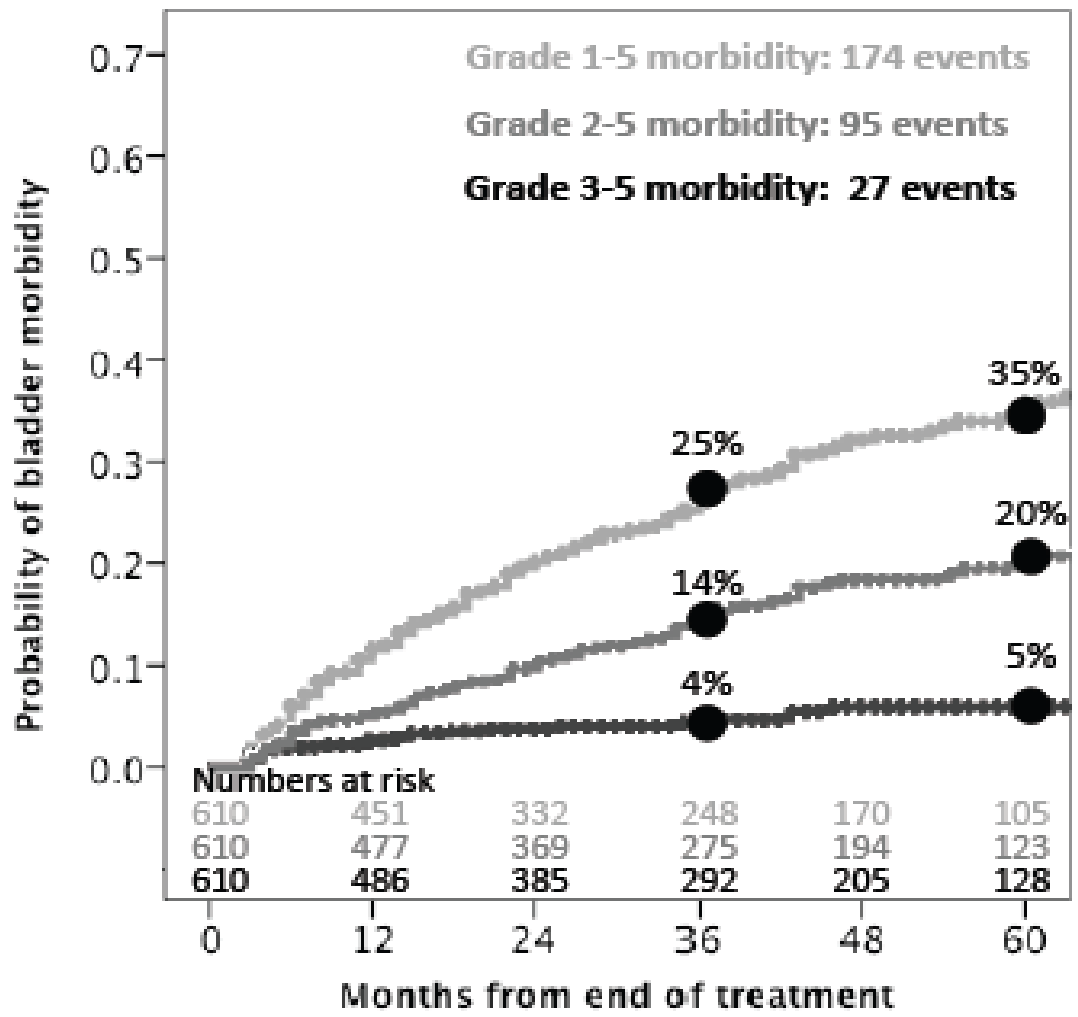
Nodal CTV-E based on Risk Group

Residual GTV-T, Adaptive HR CTV-T, IR CTV-T

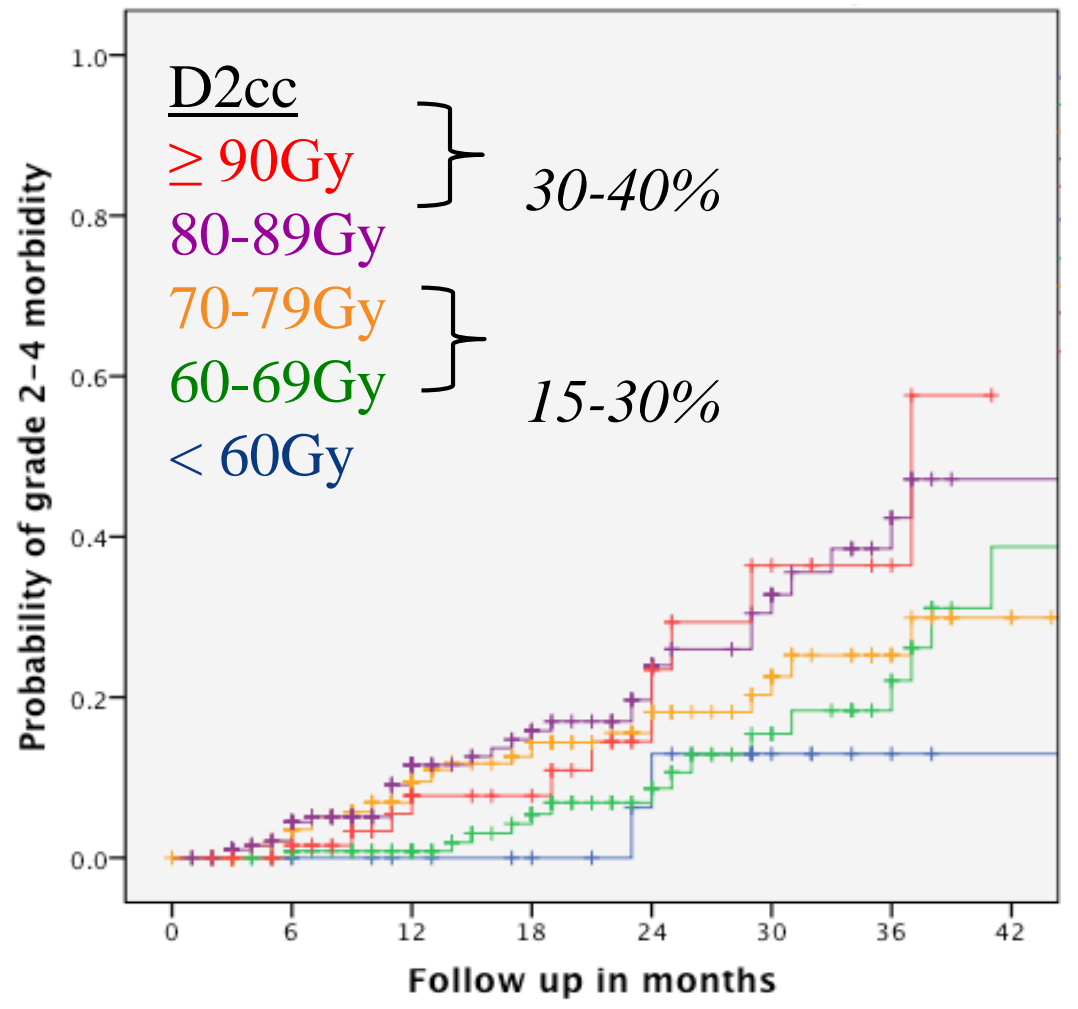
EMBRACE II - dose prescription protocol

	D90 CTV _{HR} EQD2 ₁₀	D98 CTV _{HR} EQD2 ₁₀	D98 GTV EQD2 ₁₀	D98 CTV _{IR} EQD2 ₁₀	Point A EQD2 ₁₀
Planning Aims	> 90 Gy < 95 Gy	> 75 Gy	>95 Gy	> 60 Gy	> 65 Gy
Limits for Prescribed Dose	> 85 Gy	-	>90 Gy	-	-

RETRO EMBRACE



EMBRACE



Fokdal, submitted

EMBRACE II - dose prescription protocol

	Bladder $D_{2\text{cm}^3}$ EQD2 ₃	Rectum $D_{2\text{cm}^3}$ EQD2 ₃	Recto- vaginal point EQD2 ₃	Sigmoid/ Bowel $D_{2\text{cm}^3}$ EQD2 ₃
Planning Aims	< 80 Gy	< 65 Gy	< 65 Gy	< 70 Gy*
Limits for Prescribed Dose	< 90 Gy	< 75 Gy	< 75 Gy	< 75 Gy*

* for the sigmoid/bowel structures these dose constraints are valid in case of non-mobile bowel loops resulting in the situation that the most exposed volume is located at a similar part of the organ

Example

			Planning aim	Prescribed dose
CTV _{HR}	D ₉₀	EQD2 ₁₀	≥ 90 Gy	92.3 Gy
Bladder	D _{2cm³}	EQD2 ₃	≤ 80 Gy	80.6 Gy
Rectum	D _{2cm³}	EQD2 ₃	≤ 65 Gy	64.3 Gy
Sigmoid	D _{2cm³}	EQD2 ₃	≤ 70 Gy	51.7 Gy

Conclusion

Concepts and terminology for
prescribing
recording and reporting

In a level concept:

- Level 1 - *Minimum standard for reporting*
- Level 2 - *Advanced standard for reporting*
- Level 3 - *Research oriented reporting*

GEC/ESTRO recommendations on high dose rate afterloading brachytherapy for localised prostate cancer: an update.

Radiotherapy and Oncology 107 (2013) 325–332



ELSEVIER

Contents lists available at SciVerse ScienceDirect

Radiotherapy and Oncology

journal homepage: www.thegreenjournal.com



GEC/ESTRO recommendations

GEC/ESTRO recommendations on high dose rate afterloading brachytherapy for localised prostate cancer: An update

Peter J. Hoskin ^{a,*}, Alessandro Colombo ^b, Ann Henry ^c, Peter Niehoff ^d, Taran Paulsen Hellebust ^e, Frank-Andre Siebert ^f, Gyorgy Kovacs ^g

Planning aim dose

Prescription dose

Table 3

Reporting parameters for HDR prostate brachytherapy.

1. External beam dose
2. Implant technique; number of catheters;
3. Total reference air kerma (TRAK). Total source exposure
4. Pattern of dwell times for each applicator
5. CTV: D90, V100, V150, V200
6. PTV (if defined): D90, V100, V150, V200
7. Organs at risk:
 - a. Rectum: D2 cc, D0.1 cc
 - b. Urethra: D0.1 cc, D10, D30

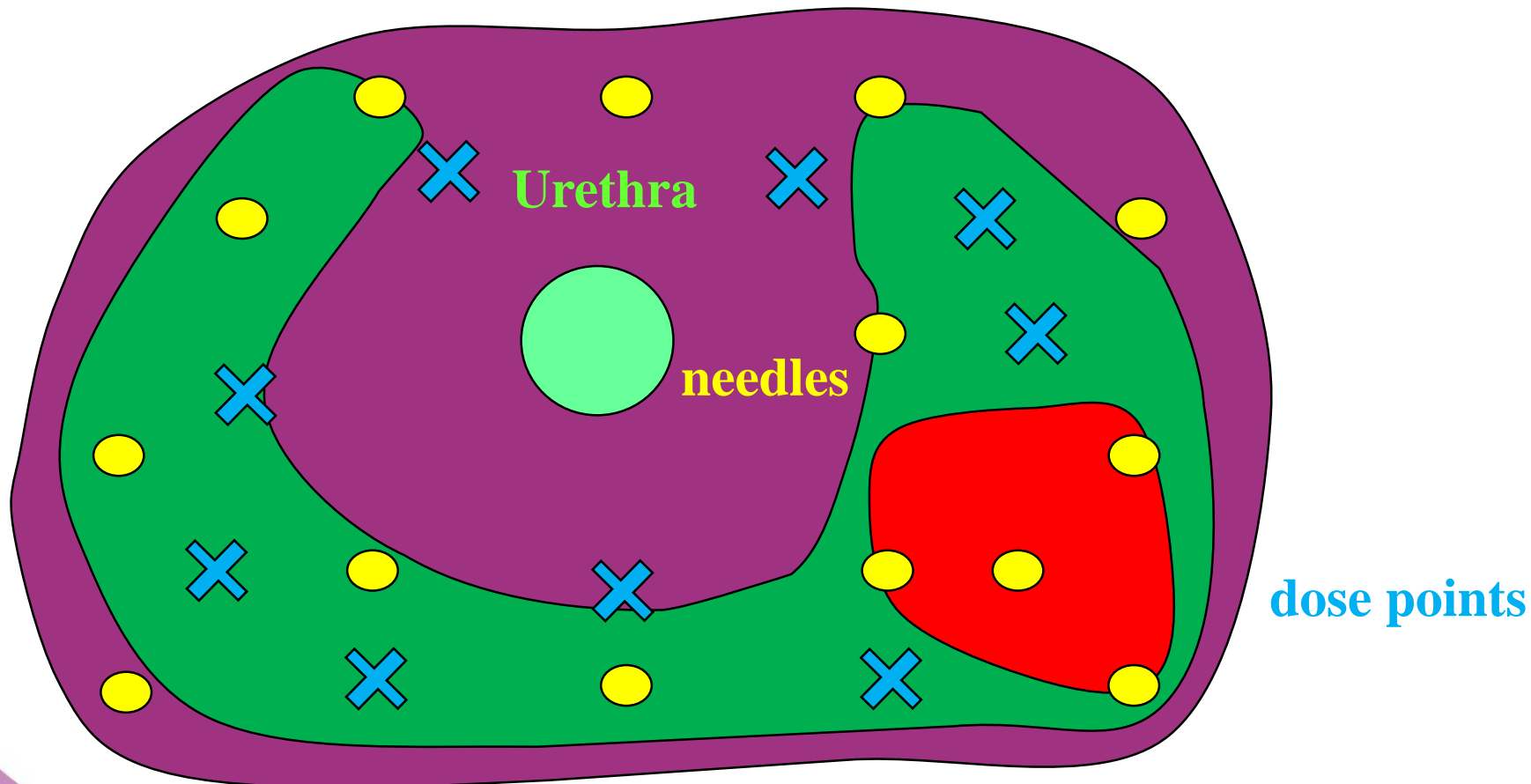
Other volumes which may be recorded but are not considered mandatory: GTV, subvolumes within CTV/PTV and Penile bulb.

Definition of target volumes / planning aim dose

CTV1 Prostate

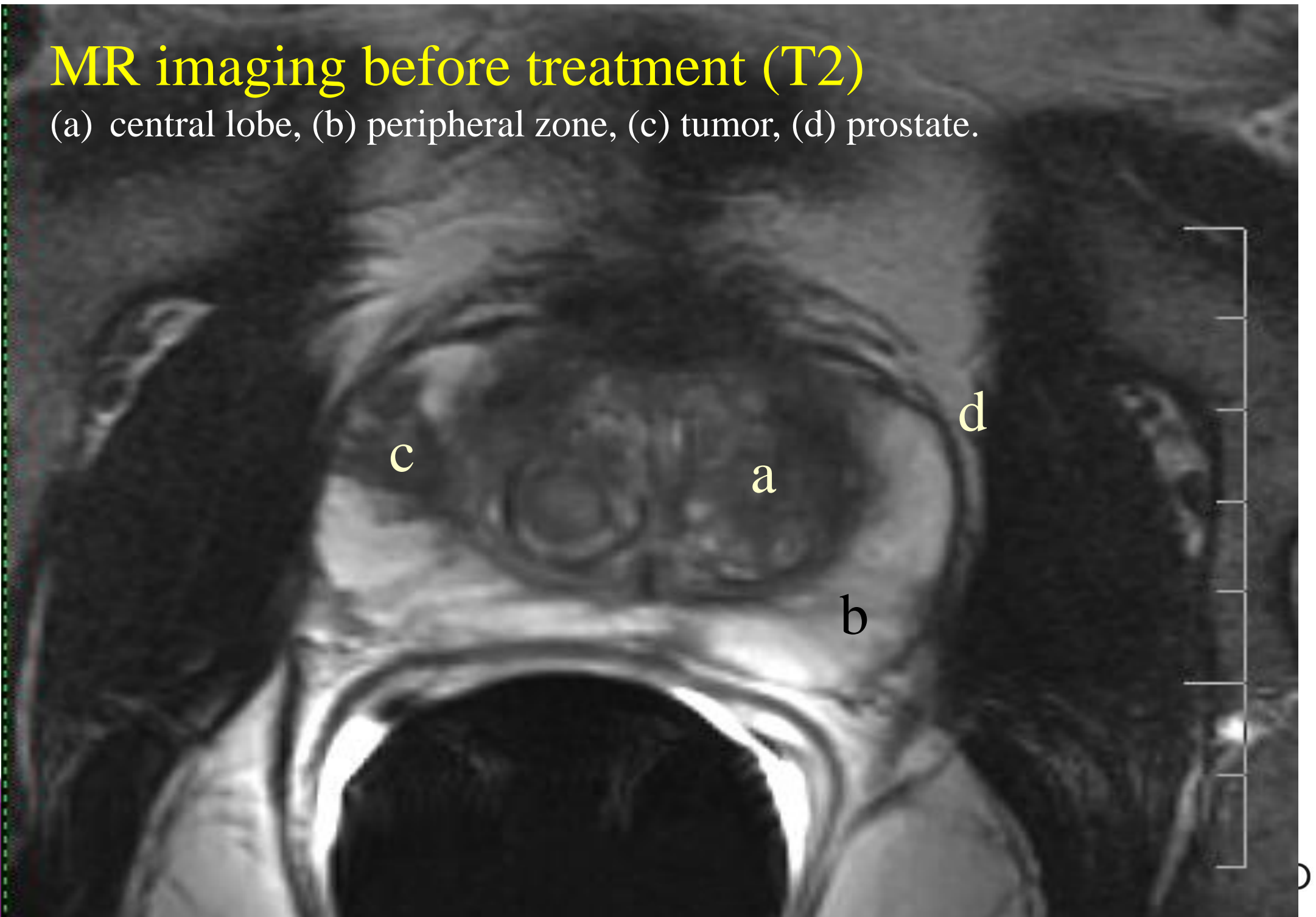
CTV2 Peripheral zone

CTV3 Suspected tumor location (if available)



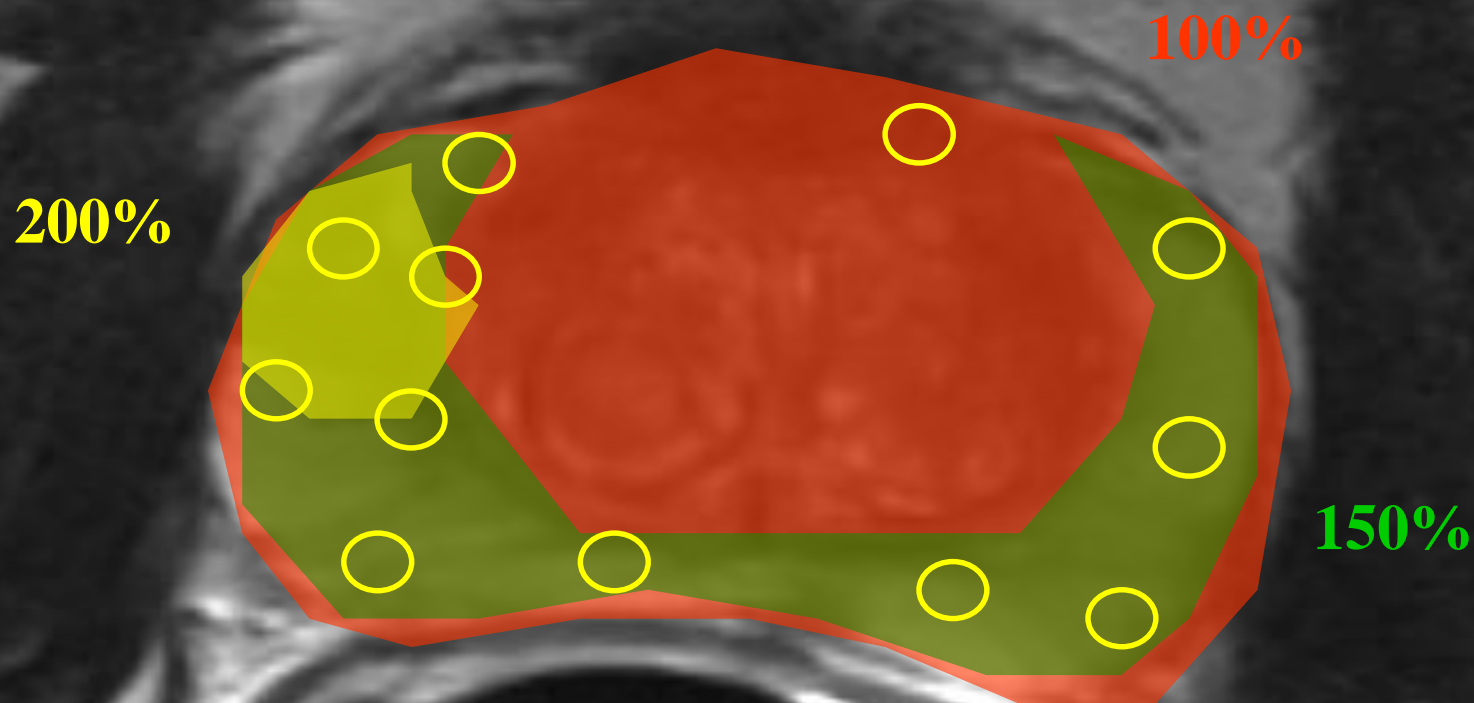
MR imaging before treatment (T2)

(a) central lobe, (b) peripheral zone, (c) tumor, (d) prostate.



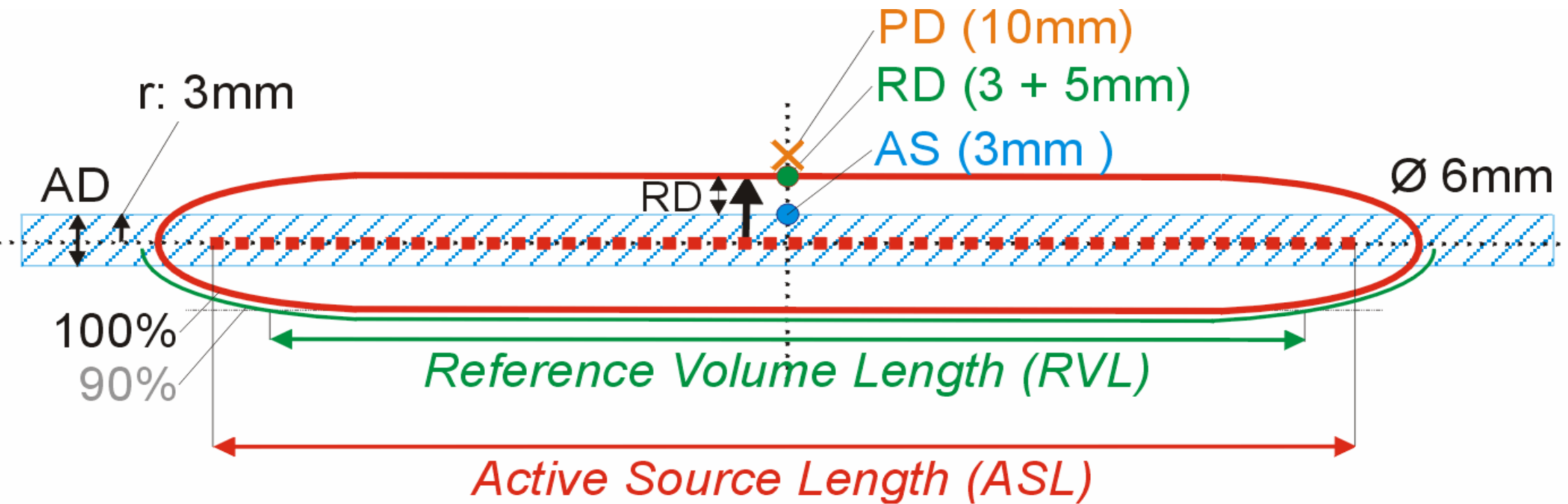
Definition of target volumes and dose

CTV1 CTV2 CTV3



Intraluminal Brachytherapy

Reference Isodose Length / Reference Volume Length

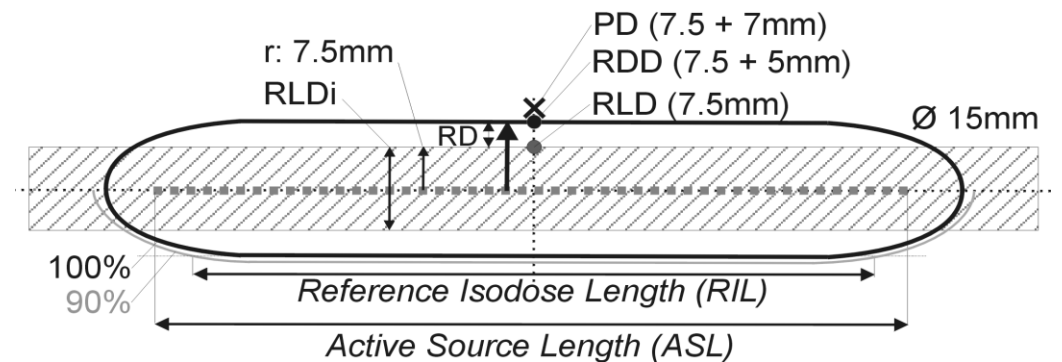
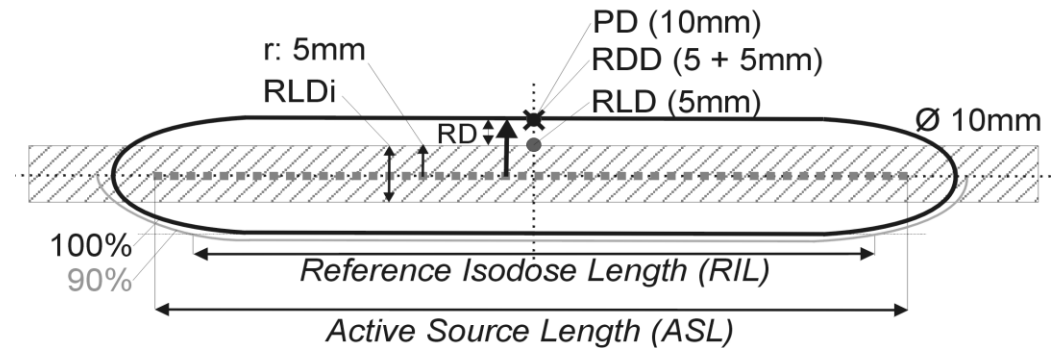
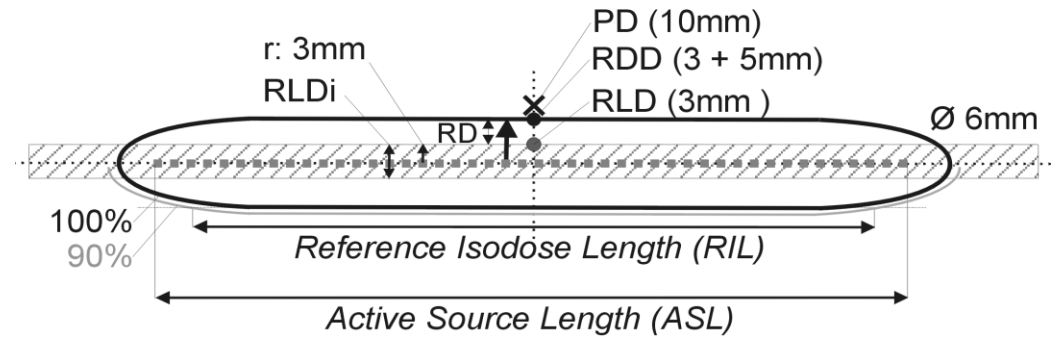


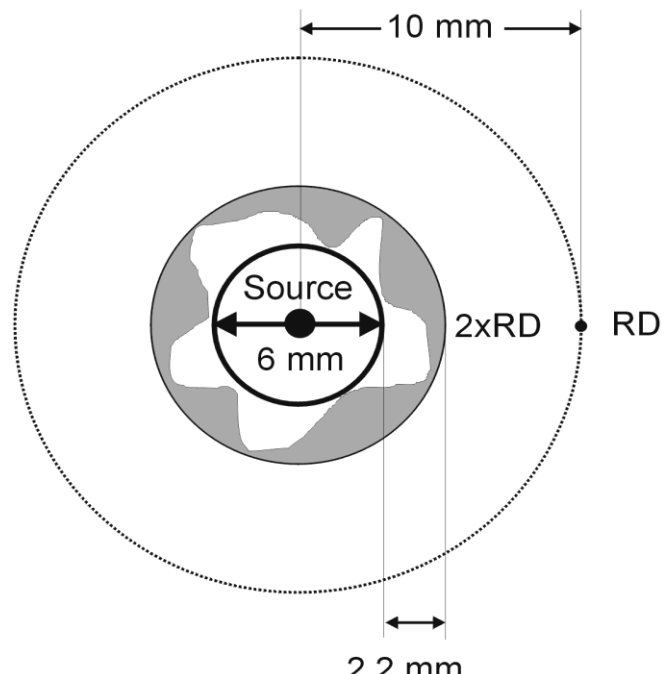
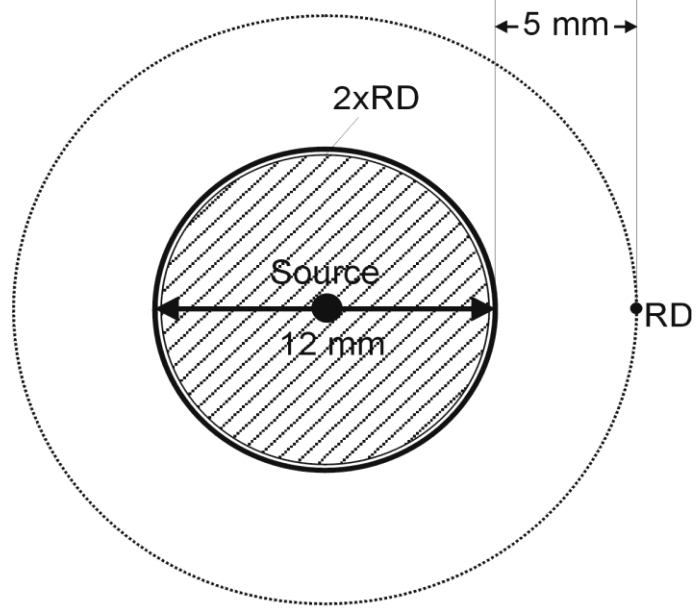
Reporting Endoluminal Treatments (example: Oesophagus)

<i>PD</i>	<i>Prescribed Dose</i>
<i>RDD</i>	<i>Reference Depth Dose</i>
<i>RLD</i>	<i>Reference Lumen Dose</i>
<i>RLDi</i>	<i>Reference Lumen Diameter</i>
<i>RD</i>	<i>Reference Depth</i>

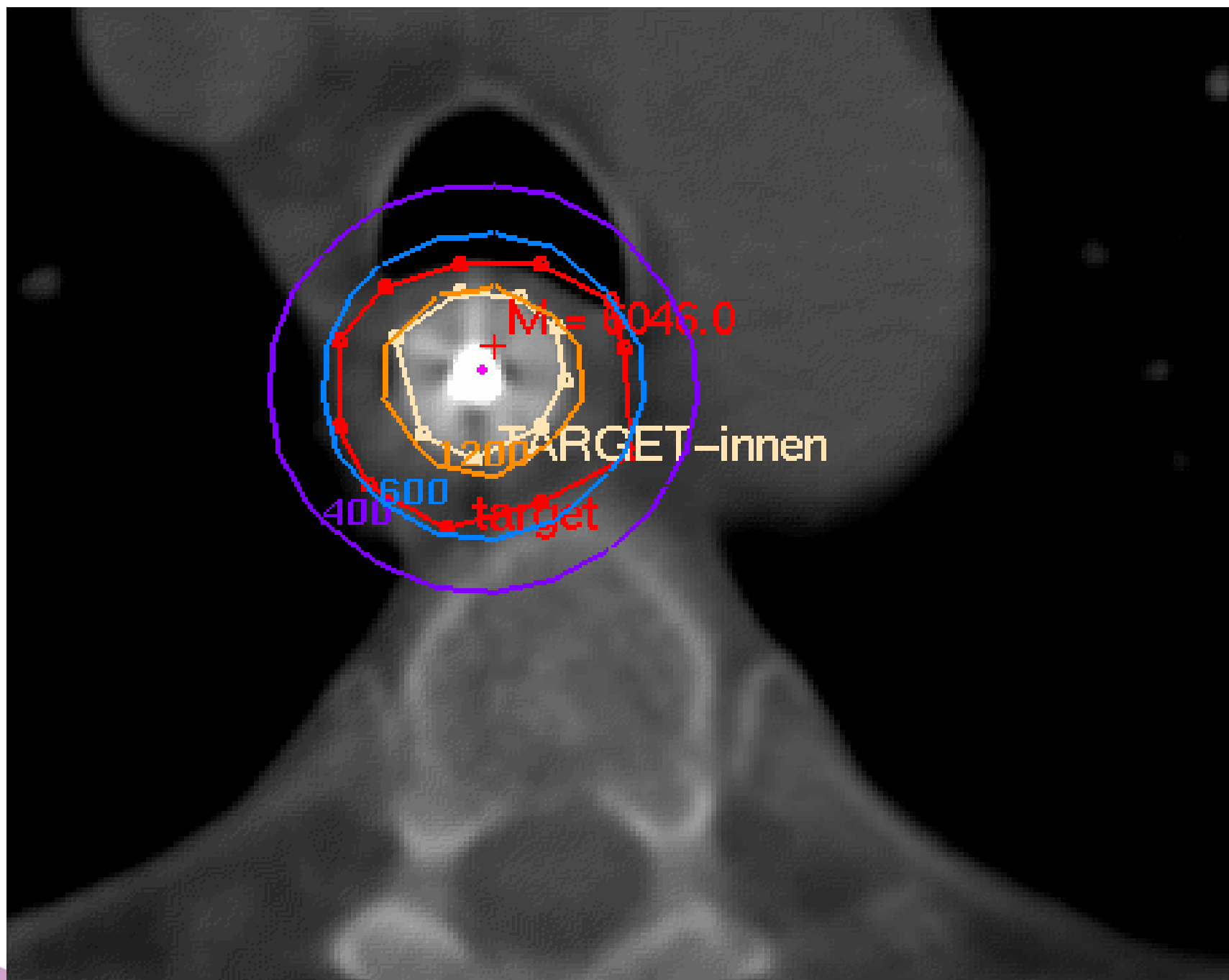
ASL *Active Source Length*
defined as the entire length of the radioactive source arrangement or the distance between first and last dwell position.

RIL *Reference Isodose Length*
defined as the length at reference depth enclosed by 90% of the reference depth dose





Dose distribution in endoluminal brachytherapy



Breast Brachytherapy

No clear guidelines by now

Target coverage (D90, V100)

High dose volumes (V150, V200)

Index values (DNR, DHI, COIN)

Skin dose

Need for common terminology

Planning aim dose

- Set of dose and dose/volume constraints for a treatment
 - 4 x 7 Gy to D_{90} to achieve 84 Gy EQD2 to D_{90} for HR CTV in cervix (EBRT+BT)
 - 145 Gy to D_{90} for prostate LDR
 - 8 x 4 Gy to D_{90} for breast APBI

Prescribed dose

- Finally accepted treatment plan (which is assumed to be delivered to an individual patient)

Delivered dose

- Actually delivered dose to the individual patient

Conclusion

Concepts and terminology for
prescribing
recording and reporting

In a level concept:

- Level 1 - *Minimum standard for reporting*
- Level 2 - *Advanced standard for reporting*
- Level 3 - *Research oriented reporting*

Thanks for your attention!

PHYSICAL - BIOLOGICAL DOCUMENTATION OF GYNAECOLOGICAL HDR BT

PATIENT , ID-number

tumour entity

cervix ca

EXTERNAL BEAM THERAPY

dose per fraction
fractions without central shield
fractions with central shield
total dose

1,8
25
45,0

TUMOUR

$D_{iso} [\alpha/\beta=10Gy]$
44,3
0,0
44,3

OAR

$D_{iso} [\alpha/\beta=3Gy]$
43,2
0,0
43,2

FIGO, TNM

IIB
cT2b pN0

GTV at diag.

88 cm³

chemoth.

cisplatin

BRACHYTHERAPY

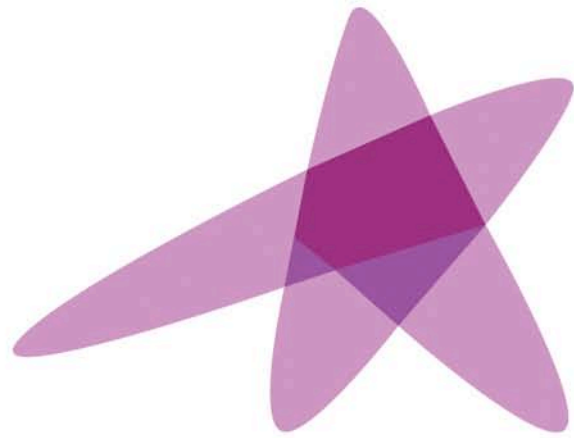
F 1 F 2 F 3 F 4 F 5 F 6

date							dose values in Gy	
TRAK [cGy at 1m]	0,54	0,49	0,47	0,44			1,94	
prescribed dose PD	7	7	7	7				
$PD_{iso} [\alpha/\beta=10Gy]$	9,9	9,9	9,9	9,9	0,0	0,0	39,7	83,9
volume of PD [cm ³]	121,1	106,9	97,7	89,5			103,8	11,7
PDx2	14,0	14,0	14,0	14,0	0,0	0,0		
$PDx2_{iso} [\alpha/\beta=10Gy]$	28,0	28,0	28,0	28,0	0,0	0,0	112,0	156,3
volume of PDx2 [cm ³]	41,6	33	30	26,1			32,7	5,7
pres. point level (A / My / [mm])	A	A	A	A				
pres. point [mm _{left} / mm _{right}]	22 / -22	A	A	19 / -19				
dose to + A left	7,6	7,1	6,7	6,5				
$A_{left} - D_{iso} [\alpha/\beta=10Gy]$	11,1	10,1	9,3	8,9	0,0	0,0	39,5	83,8
dose to - A right	7,8	6,9	7,3	6,7				
$A_{right} - D_{iso} [\alpha/\beta=10Gy]$	11,6	9,7	10,5	9,3	0,0	0,0	41,1	85,4
dose to A mean	7,7	7,0	7,0	6,6	0,0	0,0		
$A_{mean} - D_{iso} [\alpha/\beta=10Gy]$	11,4	9,9	9,9	9,1	0,0	0,0	40,3	84,6

GTV [cm ³]	8,8	7,8	5,5	6,1			7,1	1,3
D 100 = MTD	9,3	8,9	6,9	6,2				
$D 100_{iso} [\alpha/\beta=10Gy]$	15,0	14,0	9,7	8,4	0,0	0,0	47,1	91,3
D 90	13,3	12,0	11,7	10,6				
$D 90_{iso} [\alpha/\beta=10Gy]$	25,8	22,0	21,2	18,2	0,0	0,0	87,2	131,4
V 100 = volume of PD [%]	100,0%	100,0%	99,9%	99,1%			99,8%	0,4%

CTV [cm ³]	53,5	51,5	40	40,4			46,4	6,2
D 100 = MTD	5,0	5,0	3,5	3,8				
$D 100_{iso} [\alpha/\beta=10Gy]$	6,3	6,3	3,9	4,4	0,0	0,0	20,8	65,1
D 90	8,1	7,0	6,9	6,4				
$D 90_{iso} [\alpha/\beta=10Gy]$	12,2	9,9	9,7	8,7	0,0	0,0	40,6	84,8
V 100 = volume of PD [%]	95,9%	90,4%	89,3%	86,8%			90,6%	3,3%
volume of mean A-dose [%]	92,7%	90,4%	89,3%	88,9%			90,3%	1,5%

Vienna, 29 May – 1 June 2016



ESTRO
School

Advanced Brachytherapy Physics

Optimization and Inverse Planning

Dimos Baltas, Ph.D., Prof.

Division of Medical Physics

Department of Radiation Oncology, Medical Center - University of Freiburg

Faculty of Medicine, University of Freiburg, Germany

and

German Cancer Consortium (DKTK), Partner Site Freiburg, Germany

E-mail: dimos.baltas@uniklinik-freiburg.de

List of Content

- **Introduction on Dose Optimisation**
- **Forward Planning**
- **Inverse Optimisation and Planning**

Introduction on Dose Optimization

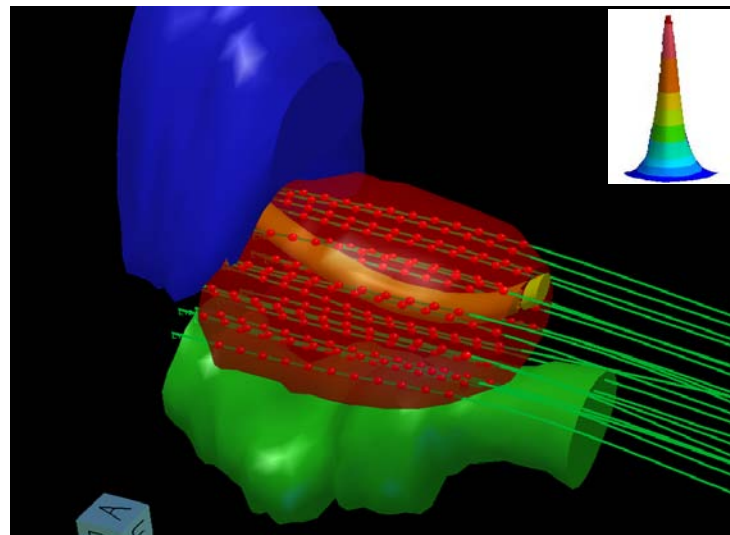


Bridge "inverter" between China and Hong Kong, since the traffic flows in Hong Kong on the left.

Introduction on Dose Optimisation

The Mapping process or The *Dose Operator*:

From Source/Energy
Fluence Distribution Ψ



$$D = \Psi \cdot A$$



To Dose Distribution D



A is the energy absorption per unit mass (dose) and unit energy fluence
Operator or the *Energy Absorption Operator*

Introduction on Dose Optimisation

The Mapping process or The *Dose Operator*:

A dose distribution D is *achievable*, if there exist a source/energy fluence distribution Ψ that is able to generate it!

- The dose space $\{D\}$ defines the space of all *physically achievable* dose distributions
- The source/energy fluence space $\{\Psi\}$ defines the space of all *physically possible* source/energy fluence distributions

Introduction on Dose Optimisation

While the determination of D from Ψ , the solution of the so-called forward problem, is always possible, the inverse problem, i.e. determination of Ψ for a specified D is not always possible.

The forward problem is the *dose calculation* problem for which a unique solution exists.

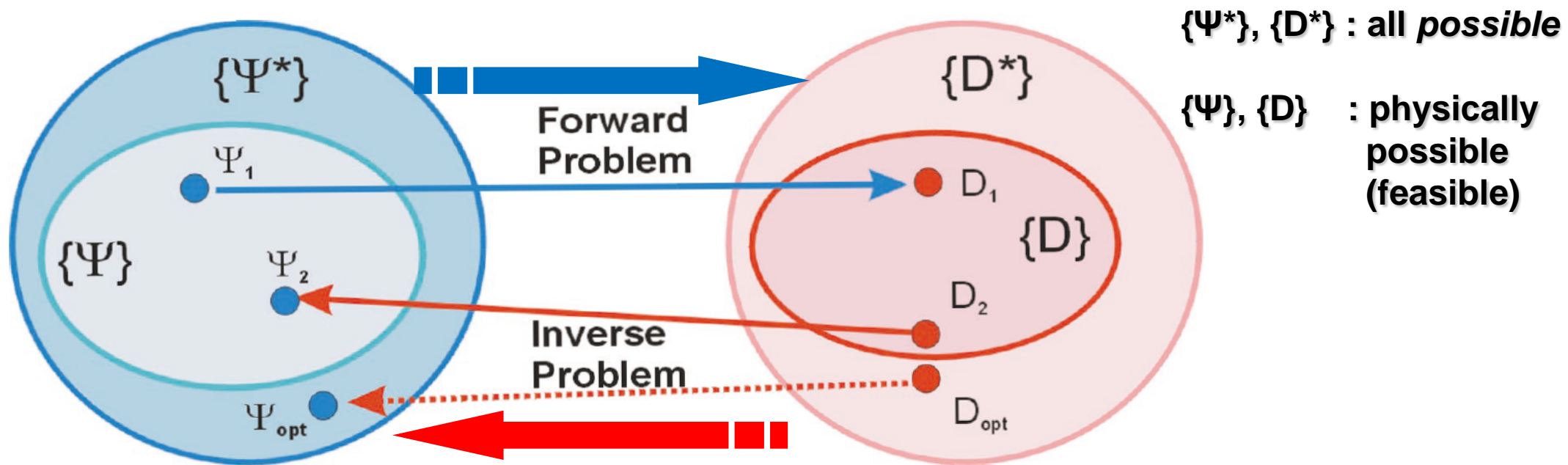


Figure 1. Forward and inverse problem in radiotherapy: The sets $\{\Psi^*\}$ and $\{D^*\}$ are all possible fluence and dose distributions respectively which include the corresponding physical possible distributions $\{\Psi\}$ and $\{D\}$. The determination of a fluence distribution from a desired optimal dose distribution D_{opt} is not always possible, such as for the two physical possible dose distributions D_1 and D_2 because the corresponding fluence distribution Ψ_{opt} may not be an element of $\{\Psi\}$

Introduction on Dose Optimisation

$$\{\Psi\} \rightarrow \{D\} : \quad D = \Psi \cdot A$$

As an analytical solution for Ψ cannot be (always) obtained we consider the *Inverse Problem* to determine Ψ for a desired D equivalent to determine:

- (a) the position and number of catheters
- (b) the position and number of source dwell positions (SDPs) or sources
- (c) the source dwell times

such that the obtained dose distribution D is as close as possible to the desired one.

This process is called *Inverse Optimisation* or *Inverse Planning*.

Introduction on Dose Optimisation

The Mapping process or The *Dose Operator*:

$$\{\Psi\} \rightarrow \{D\} : \quad D = \Psi \cdot A$$

A is the energy absorption per unit mass (dose) and unit energy fluence Operator or the *Energy Absorption Operator*

In other words, **A** is the *dosimetric Kernel*



$$A(\vec{r}) = \frac{\dot{D}(\vec{r})}{S_K} = \frac{\dot{D}(r, \theta)}{S_K} = \Lambda \cdot \frac{G_L(r, \theta)}{G_L(r_0, \theta_0)} \cdot g_L(r) \cdot F(r, \theta)$$

Introduction on Dose Optimisation

The Mapping process or The *Dose Operator*:

$$D = \Psi \cdot A$$

Ψ is the Source/Energy Fluence Distribution

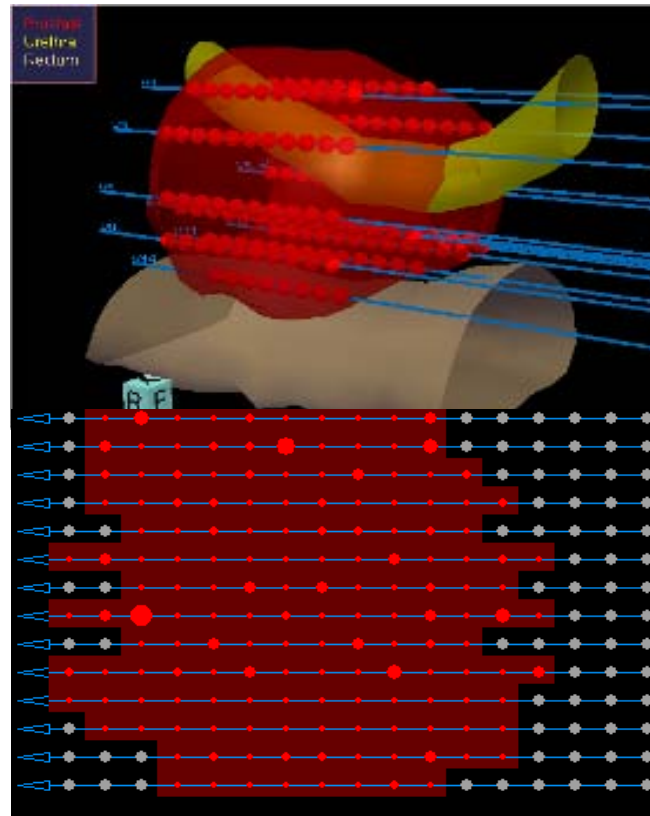
Ψ is for a single stepping source delivery system (afterloader) the Source Propagation Function

$$\{\vec{r}\}$$

$$\Psi(\vec{r}) = F(\{\vec{r}\}, \{S_K t\})$$

$$\{S_K \cdot t\} =$$

$$S_K \cdot \{t\}$$



Spatial

and

Strength/Time
Pattern

Introduction on Dose Optimisation

The Mapping process or The *Dose Operator*:

$$D = \Psi \cdot A$$

A is the energy absorption per unit mass (dose) and unit energy fluence Operator or the *Energy Absorption Operator*

Ψ is for a single stepping source delivery system (afterloader) the *Source Propagation Function*

$$\left. \begin{aligned} A(\vec{r}) &= \frac{\dot{D}(\vec{r})}{S_K} \\ \Psi(\vec{r}) &= F(\{\vec{r}\}, \{t\}) = \sum_{i=1}^{N_{ASDPs}} S_{k,i} t_i \delta(\vec{r} - \vec{r}_i) \end{aligned} \right\} \begin{aligned} D(\vec{r}) &= \sum_{i=1}^{N_{ASDPs}} S_{k,i} t_i A(\vec{r} - \vec{r}_i) \\ \text{or} \\ D(\vec{r}) &= \int_{-\infty}^{+\infty} \Psi(\vec{r}') A(\vec{r} - \vec{r}') d\nu \end{aligned}$$

With N_{ASDPs} the total number of active source dwell positions at positions r_i and dwell times t_i .

Introduction on Dose Optimisation

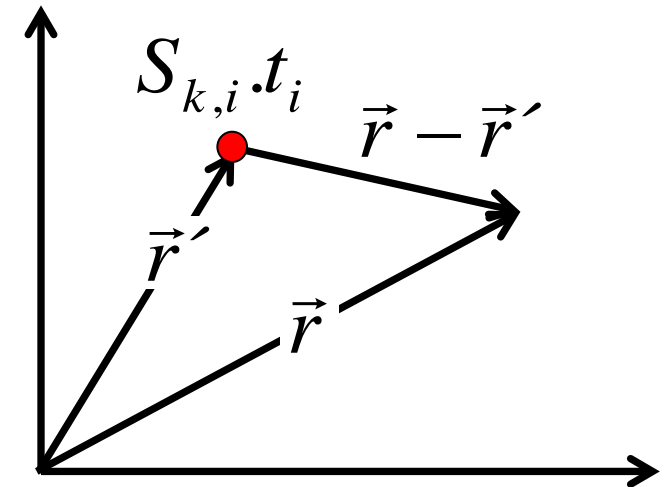
The Mapping process or The *Dose Operator*:

$$D = \Psi \cdot A$$

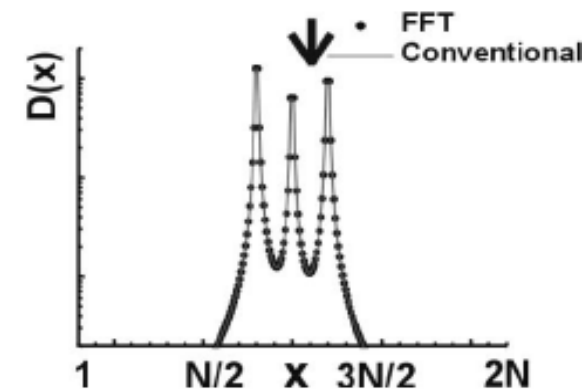
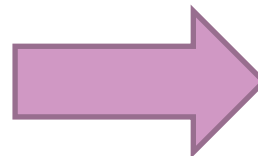
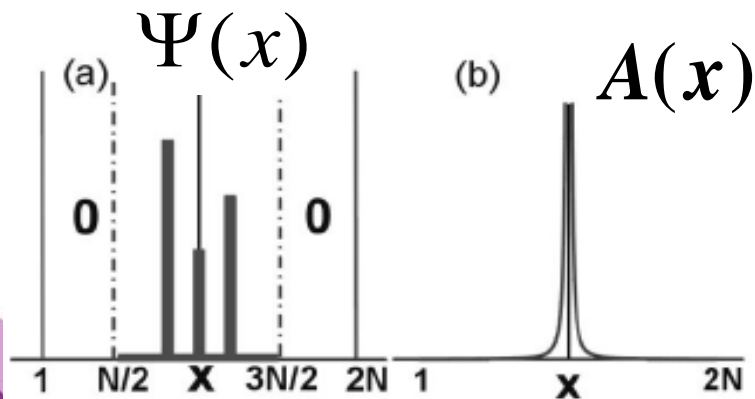
$$D(\vec{r}) = \sum_{i=1}^{N_{ASDPs}} S_{K,i} t_i A(\vec{r} - \vec{r}_i)$$

or

$$D(\vec{r}) = \int_{-\infty}^{+\infty} \Psi(\vec{r} \wedge) A(\vec{r} - \vec{r}') dv$$



Example for the 1D simplification



List of Content

- Introduction on Dose Optimisation
- **Forward Planning**
- Inverse Optimisation and Planning

Introduction on Dose Optimisation

While the determination of D from Ψ , the solution of the so-called forward problem, is *always* possible the inverse problem, i.e. determination of Ψ for a given D is not always possible.

The forward problem is the *dose calculation* problem for which a unique solution exists.

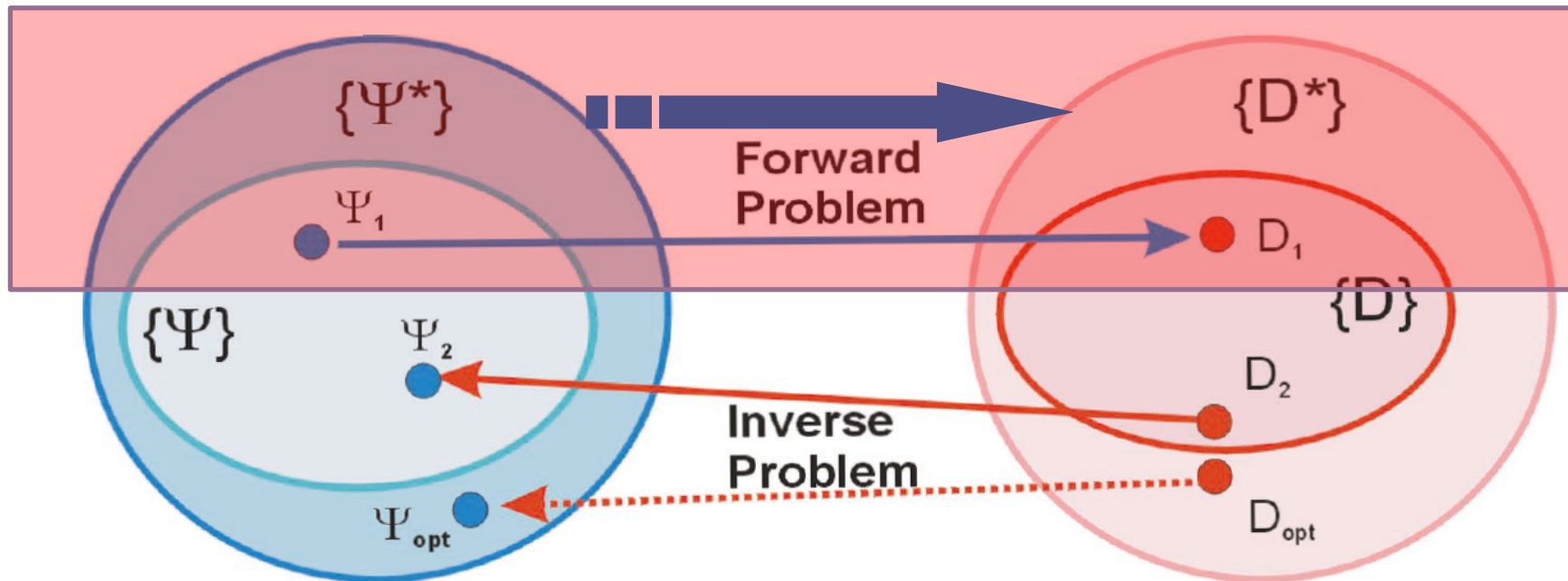
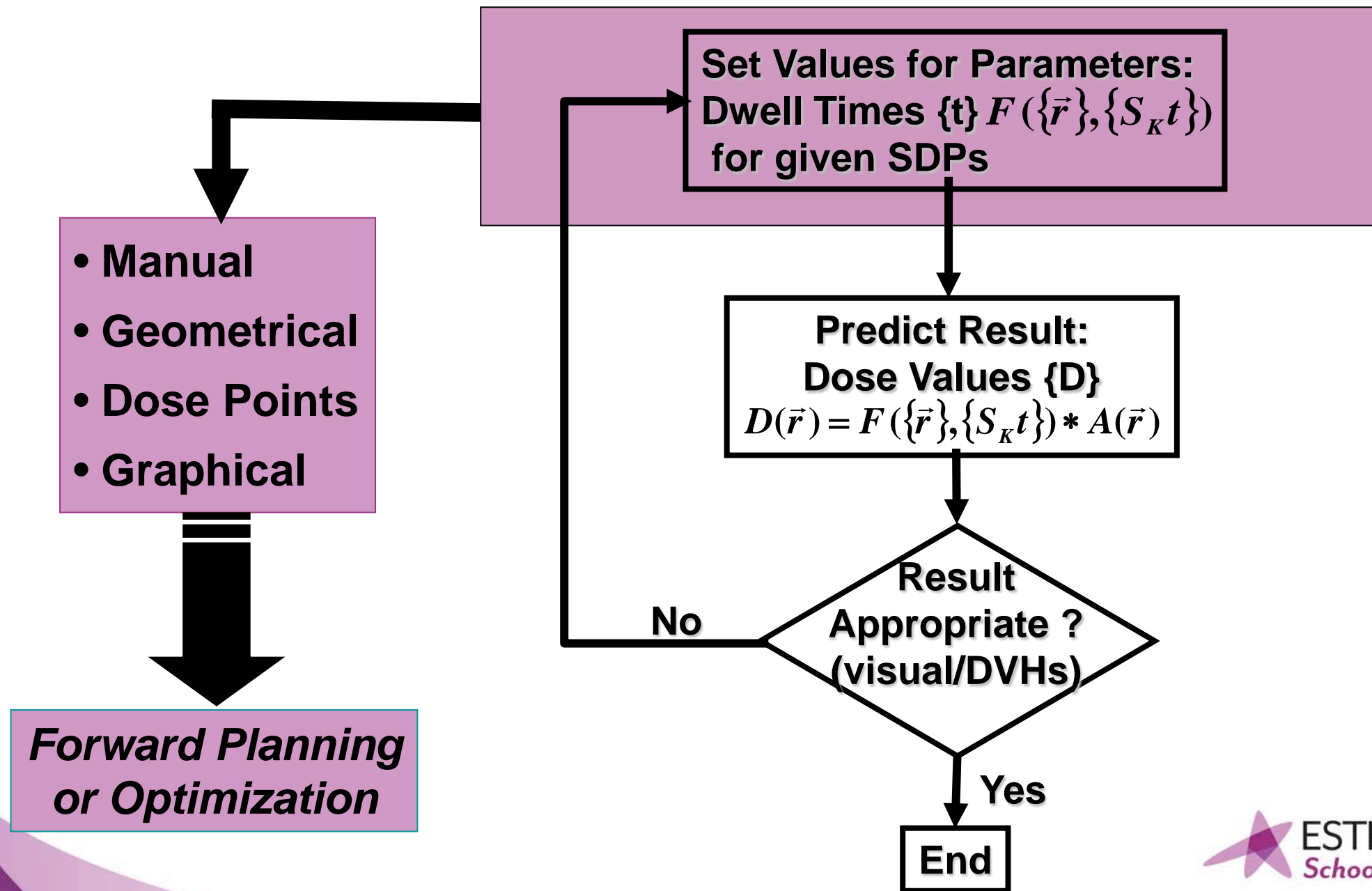


Figure 1. Forward and inverse problem in radiotherapy: The sets $\{\Psi^*\}$ and $\{D^*\}$ are all possible fluence and dose distributions respectively which include the corresponding physical possible distributions $\{\Psi\}$ and $\{D\}$. The determination of a fluence distribution from a desired optimal dose distribution D_{opt} is not always possible, such as for the two physical possible dose distributions D_1 and D_2 because the corresponding fluence distribution Ψ_{opt} may not be an element of $\{\Psi\}$

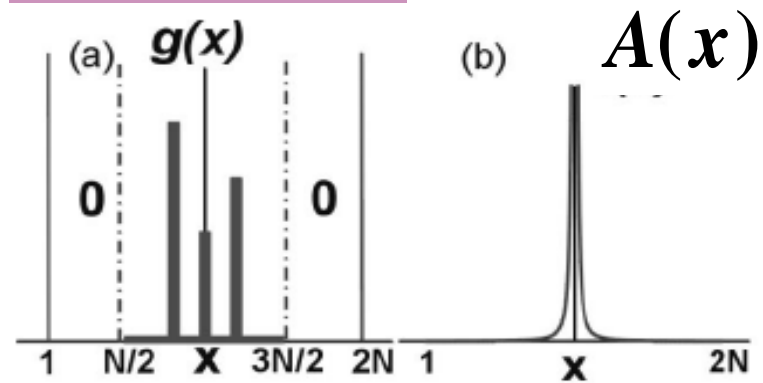
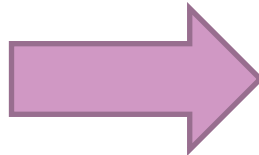
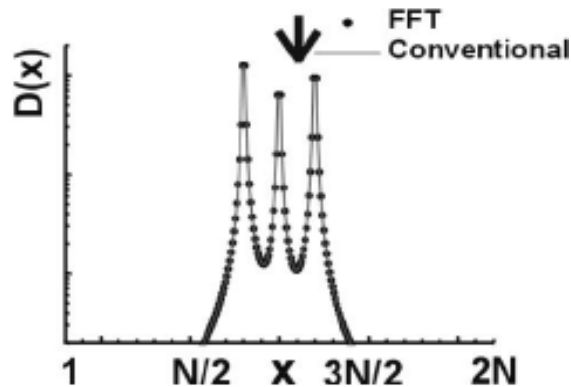
The “Forward Planning” in Brachytherapy (1990 – 1999)



List of Content

- Introduction on Dose Optimisation
- Forward Planning
- Inverse Optimisation and Planning

$$\Psi(x) = ???$$



Introduction on Dose Optimisation

The “Inverse Planning & Optimisation”

$$D = \Psi \cdot A$$

As an analytical solution cannot be (always) obtained we consider the *Inverse Problem* to determine the position and number of catheters, the position and number of source dwell positions (SDPs), and the source dwell times, such that the obtained dose distribution approaches as much as possible the desired one via an *Optimisation Process*.

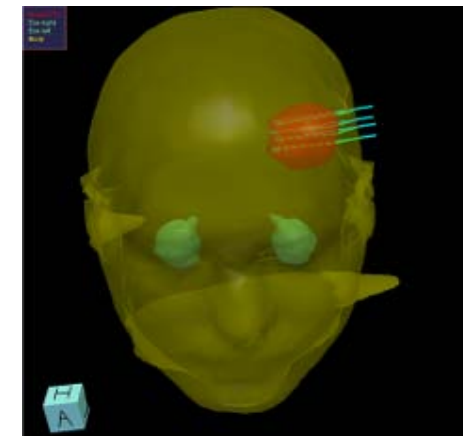
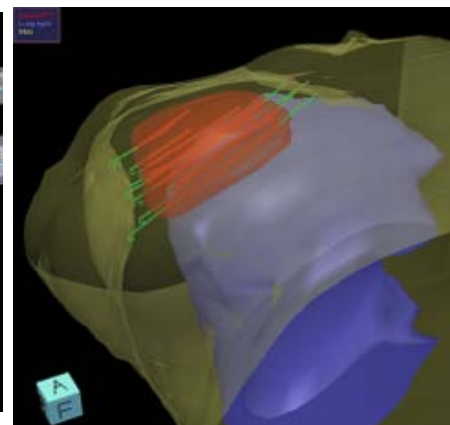
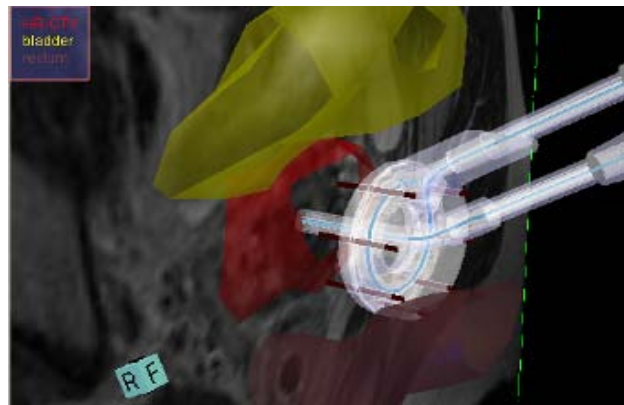
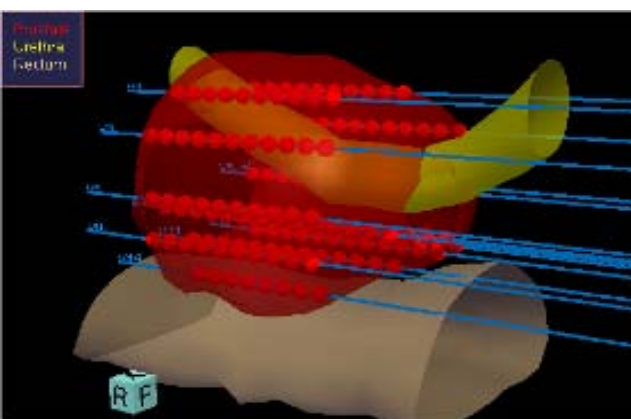
This process is called *Inverse Optimisation* or *Inverse Planning*.

Inverse Optimisation and Planning (2000 – today)

It presupposes the availability of:

- A complete 3D Source Dwell Position model (Catheters/Applicators)
- A complete 3D anatomy model
VOIs: Target(s), OARs
- The Desired Dose Distribution

Morphology

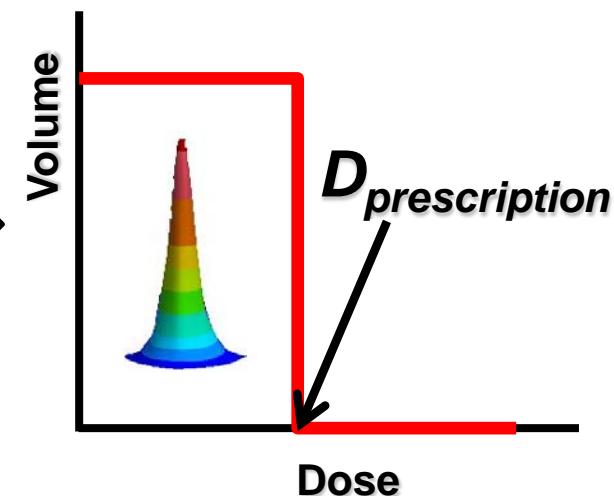
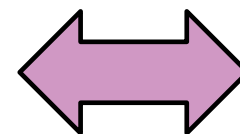


Inverse Optimisation and Planning (2000 – today)

Desired Dose Distribution:

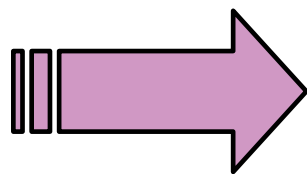
Even if the “*ideal*” dose distribution can be easily defined:

$$D(\vec{r}) = \begin{cases} D_{prescription} & \forall \vec{r} \in \text{PTV} \\ 0 & \forall \vec{r} \notin \text{PTV} \end{cases}$$



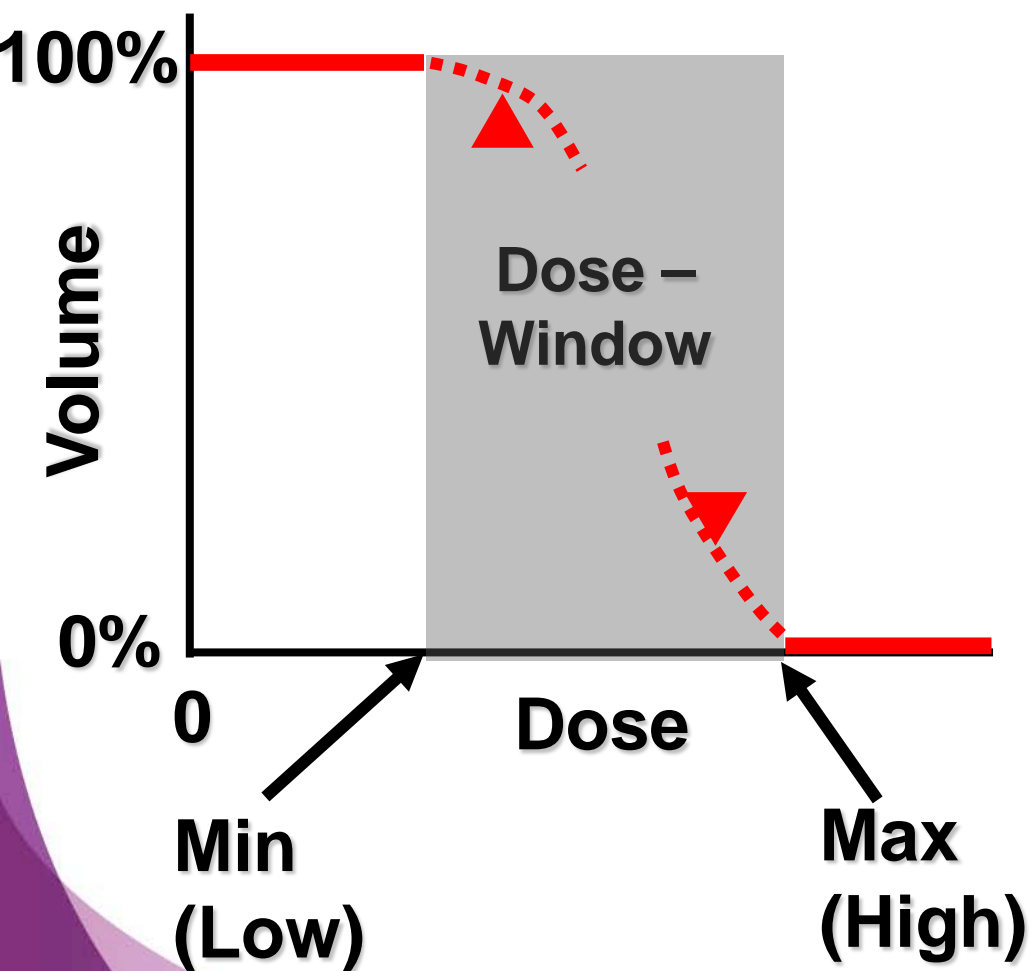
due to the “nature” of the dosimetric Kernel $A(r)$, $D \in \{D^*\}$ as defined here does not belong to the *Physically* achievable dose distributions $D \notin \{D\}$.

“Desired” Dose Distribution



Define Dose Window for Target(s) & OAR(s)

Desired Dose Distribution:



Dose - Volume – Pairs D_v
for GTVs, CTV/PTV,
OARs

➔ $V = 0\% \Rightarrow D_{\max} = D_H$

➔ $V = 100\% \Rightarrow D_{\min} = D_L$

The Desired Dose Distribution for the *Inverse Optimisation Process* is then defined as $\{D_v\}$, and/or $\{V_D\}$ *desired value sets*.

Inverse Optimisation and Planning (2000 – today)

Objectives and Objective Functions:

The selected and defined Dose-Volume parameters, usually D_v , for the inverse optimisation process define the *Objectives* of the optimisation.

The measure of how well these values are achieved defines the “Metrics” – the *Objective Functions* of the optimisation methodology (algorithm).

A natural measure quantifying the similarity of a dose distribution at N sampling points with dose values d_i to the corresponding desired dose values d_i^* is a distance measure. A common measure is the L_p norm:

$$L_p = \left\{ \sum_{i=1}^N (d_i - d_i^*)^p \right\}^{1/p}$$

For $p = 2$, i.e. L_2 we have the Euclidean distance.

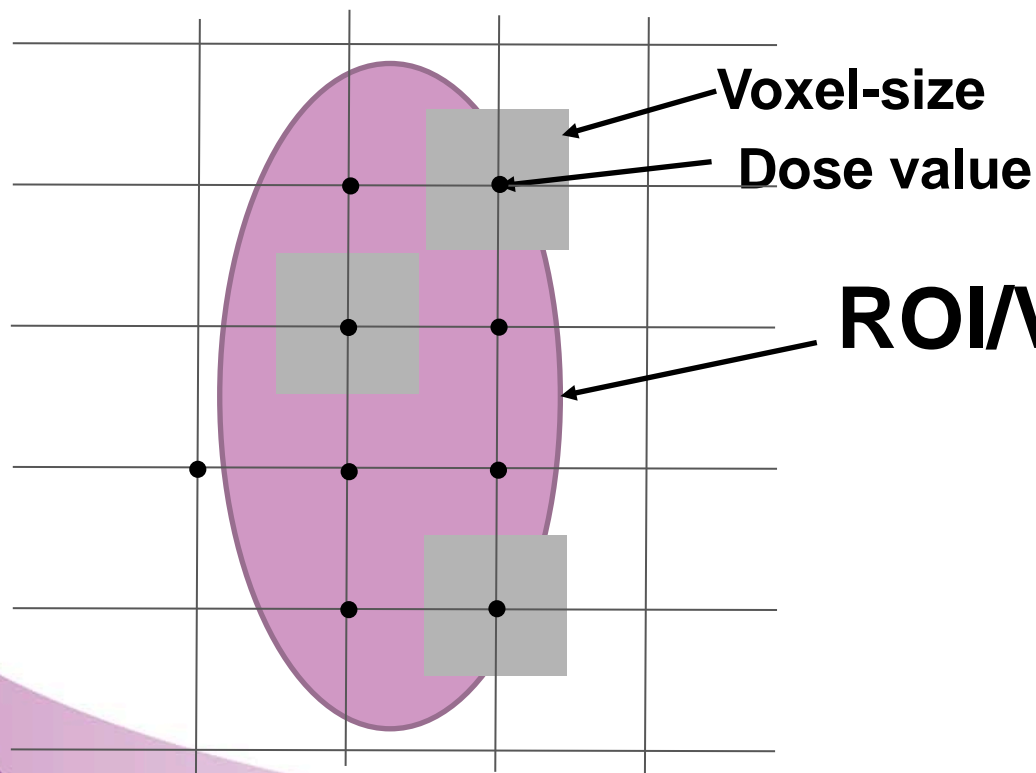
Inverse Optimization and Planning (2000 – today)

Attention:

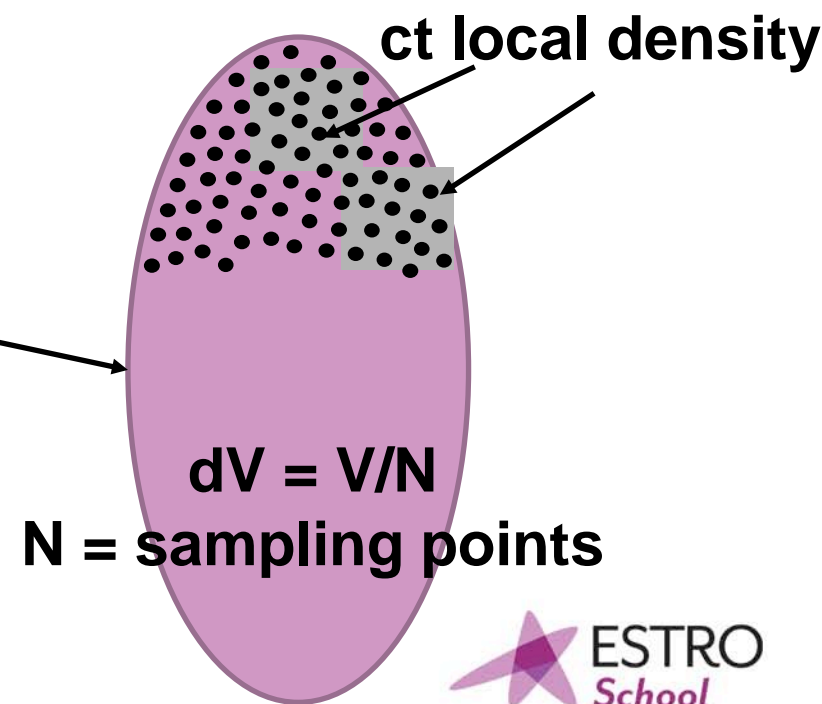
The dose distribution is analysed on the basis of a finite number of dose points, the sampling points. The sampling method can be:

- regular 3D grid (dose grid) or
- random (quasi) sampling or ↙
- geometry/implant adapted ↘

Grid-based Method



Random-Sampling Method



Inverse Optimisation and Planning (2000 – today)

General Form of an *Objective Function*

Low-Objective
 D_L for V_{Low}

$$f_i = \frac{1}{N_i} \sum_{j=1}^{N_i} \left[\Theta(D_L^i - d_j^i(\mathbf{x})) [D_L^i - d_j^i(\mathbf{x})]^p \right]$$

High-Objective
 D_H for V_{High}

$$f_i = \frac{1}{N_i} \sum_{j=1}^{N_i} \left[\Theta(d_j^i(\mathbf{x}) - D_H^i) [d_j^i(\mathbf{x}) - D_H^i]^p \right]$$

d_j^i is the dose at the j^{th} -sampling point for the i^{th} -objective function:

$$d_j^i(\mathbf{x}) = \sum_{k=1}^{N_{cath}} \sum_{l=1}^{N_{ASDP}^k} x_{lk}^2 S_{K,lk} \tilde{d}_{jkl}^i$$

Catheters/
Needles/
Applicators

Active SDPs

Dwell time $t_{lk} = x_{lk}^2$

Adjustable parameters

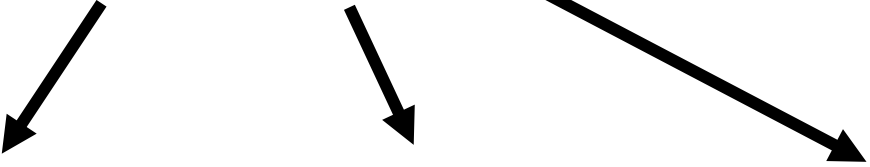
$$D(\vec{r}) = \int_{-\infty}^{+\infty} \Psi(\vec{r}') A(\vec{r} - \vec{r}') dv$$

Inverse Optimisation and Planning (2000 – today)

General Form of an *Objective Function*

d_j^i is the dose at the j^{th} -sampling point for the i^{th} -objective function:

$$d_j^i(\mathbf{x}) = \sum_{k=1}^{N_{cath}} \sum_{l=1}^{N_{ASDP}^k} x_{lk}^2 S_{K, lk} \tilde{d}_{jkl}^i$$


Catheters Active SDPs Dwell time t_{lk}

- $x_{lk}^2 = t_{lk}$ to avoid negative (non-physical) dwell time values t_{lk}
- \tilde{d}_{jkl}^i can (should) be calculated in a pre-processing step and are then available in a sense of a Look-Up-Table for the optimisation process. Implementations in this way (HIPO) make optimiser independent of the dose calculation engine considered (**TG 43, MC-LUTs, BS, CC, other Engines**)

Inverse Optimisation and Planning (2000 – today)

General Form of an *Objective Function*

$$f_i = \frac{1}{N_i} \sum_{j=1}^{N_i} \left[\Theta(D_L^i - d_j^i(\mathbf{x})) [D_L^i - d_j^i(\mathbf{x})]^p \right]$$

Transition Function Θ :

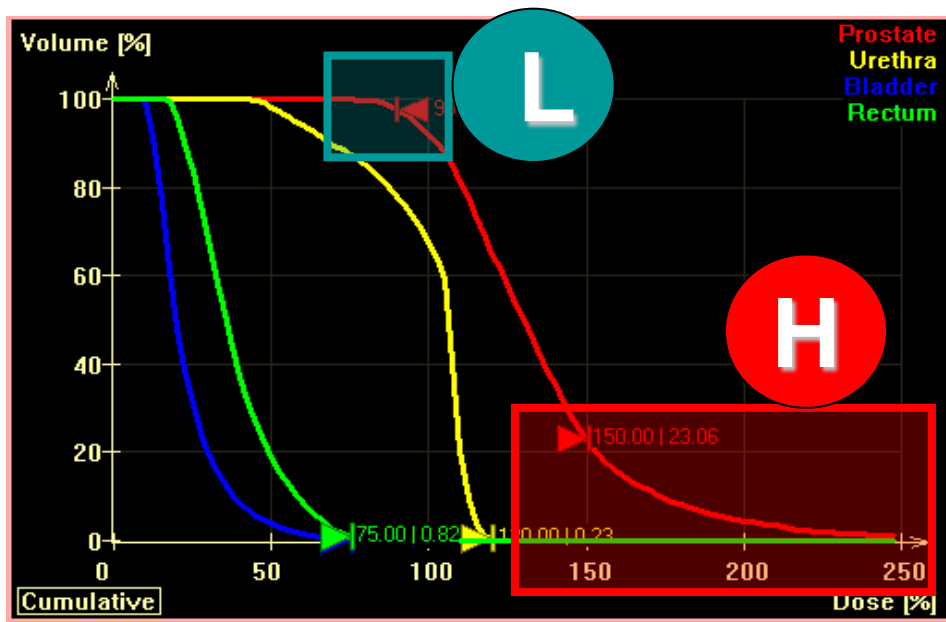
$$\Theta(y) \left\{ \begin{array}{l} \Theta_1(y) = \begin{cases} 0, & y < 0 \\ 1, & y \geq 0 \end{cases} \Rightarrow \text{linear} \\ \Theta_2(y) = 0.5[1 + \tanh(by)] \Rightarrow \text{non-linear} \end{array} \right.$$

Linear: Solution utilizing **Linear Programming (exact solver)**
or **stochastic/probabilistic numerical solvers**

Non-Linear: **deterministic numerical solvers**

Inverse Optimisation and Planning (2000 – today)

General Form of an *Objective Function* and DVH



Low-Objective for PTV

$D_L = D_V$ for $V_{100\%}$

$$f_i = \frac{1}{N_i} \sum_{j=1}^{N_i} \left[\Theta(D_L^i - d_j^i(\mathbf{x})) [D_L^i - d_j^i(\mathbf{x})]^p \right]$$



High-Objective for PTV


$D_H = D_V$ for $V_{0\%}$

$$f_i = \frac{1}{N_i} \sum_{j=1}^{N_i} \left[\Theta(d_j^i(\mathbf{x}) - D_H^i) [d_j^i(\mathbf{x}) - D_H^i]^p \right]$$


Inverse Optimisation and Planning (2000 – today)

General Form of an Objective Function: The norm factor p

Low-Objective
 D_L

$$f_i = \frac{1}{N_i} \sum_{j=1}^{N_i} \left[\Theta(D_L^i - d_j^i(\mathbf{x})) [D_L^i - d_j^i(\mathbf{x})]^p \right]$$


High-Objective
 D_H

$$f_i = \frac{1}{N_i} \sum_{j=1}^{N_i} \left[\Theta(d_j^i(\mathbf{x}) - D_H^i) [d_j^i(\mathbf{x}) - D_H^i]^p \right]$$


The Norm Factor p

- $p = 0$: Volume counting for deviation
- 1 : Linear weight proportional to deviation
- 2 : Variance (square-weighted) based Objective Function

Inverse Optimisation and Planning (2000 – today)

General

Optimising the values of the *Objective Functions* results to *Optimisation of the 3D Dose Distribution*.

Due to the fact that in general *Objective Functions* are defined as over-dosages (High-Objective) or under-dosage(s) (Low-Objective), *Optimisation of an Objective Function value means Minimization of its value (ideally 0) by adjusting the independent parameter values $\{ t \}$.*

Inverse Optimisation and Planning (2000 – today)

A short Introduction into the *Multiobjective (MO)* Problem ...

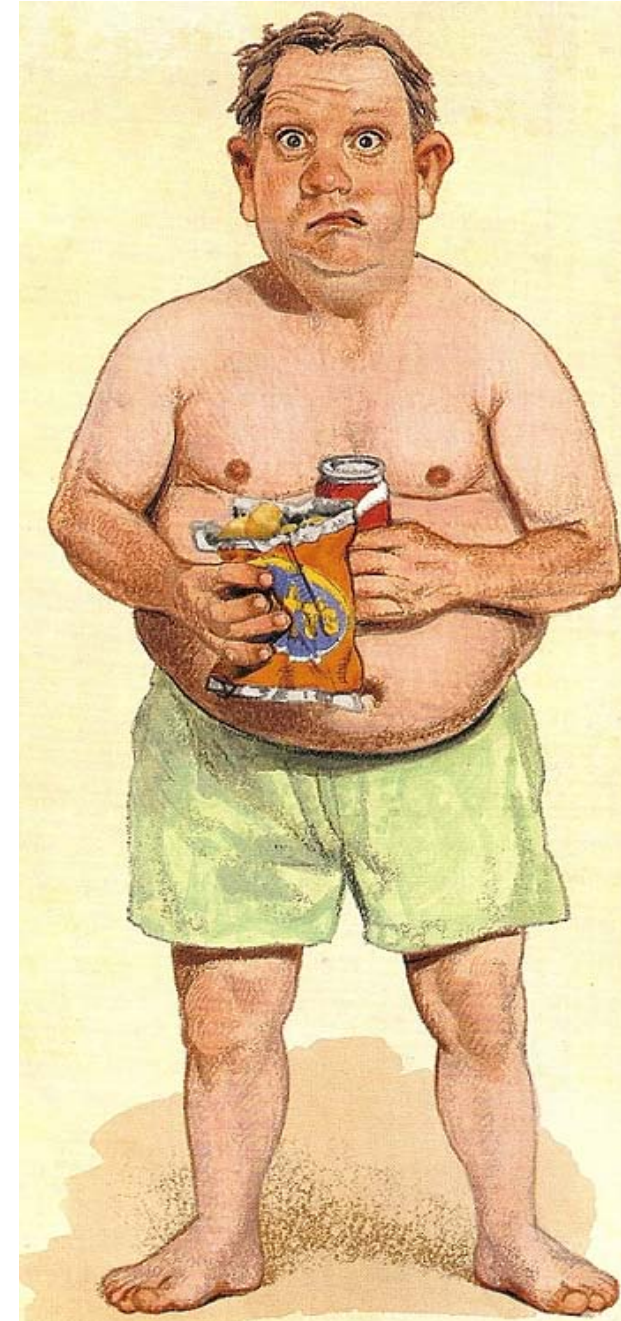


Fig.4. Homo adipositus

Inverse Optimisation and Planning (2000 – today)

Facts

Inverse Optimisation and Planning for brachytherapy has to consider several ***Objectives*** and is thus a ***Multiobjective (MO)*** problem.

We have ***competing Objectives***. Increasing the dose in the Target will increase the dose outside it.

A trade-off between the ***Objectives*** exist and we never have a situation in which all the ***Objectives*** can be in the best possible way satisfied ***simultaneously***.

Inverse Optimisation and Planning

A Multi-Objective (MO) Problem

Dominance & Pareto Front

A plan/solution x_1 **dominates** a plan/solution x_2 *if and only if* the two following conditions are true:

- x_1 is no worse than x_2 in all objectives, i.e. $f_j(x_1) \leq f_j(x_2) \quad \forall j=1, \dots, M$.
- x_1 is strictly better than x_2 in at least one objective, i.e. $f_j(x_1) < f_j(x_2)$ for at least one $j \in \{1, \dots, M\}$.

Among a set of solutions P , the **non-dominated set of solutions P'** are those that **are not dominated** by any other member of the set P : **The Pareto Optimal Set**.

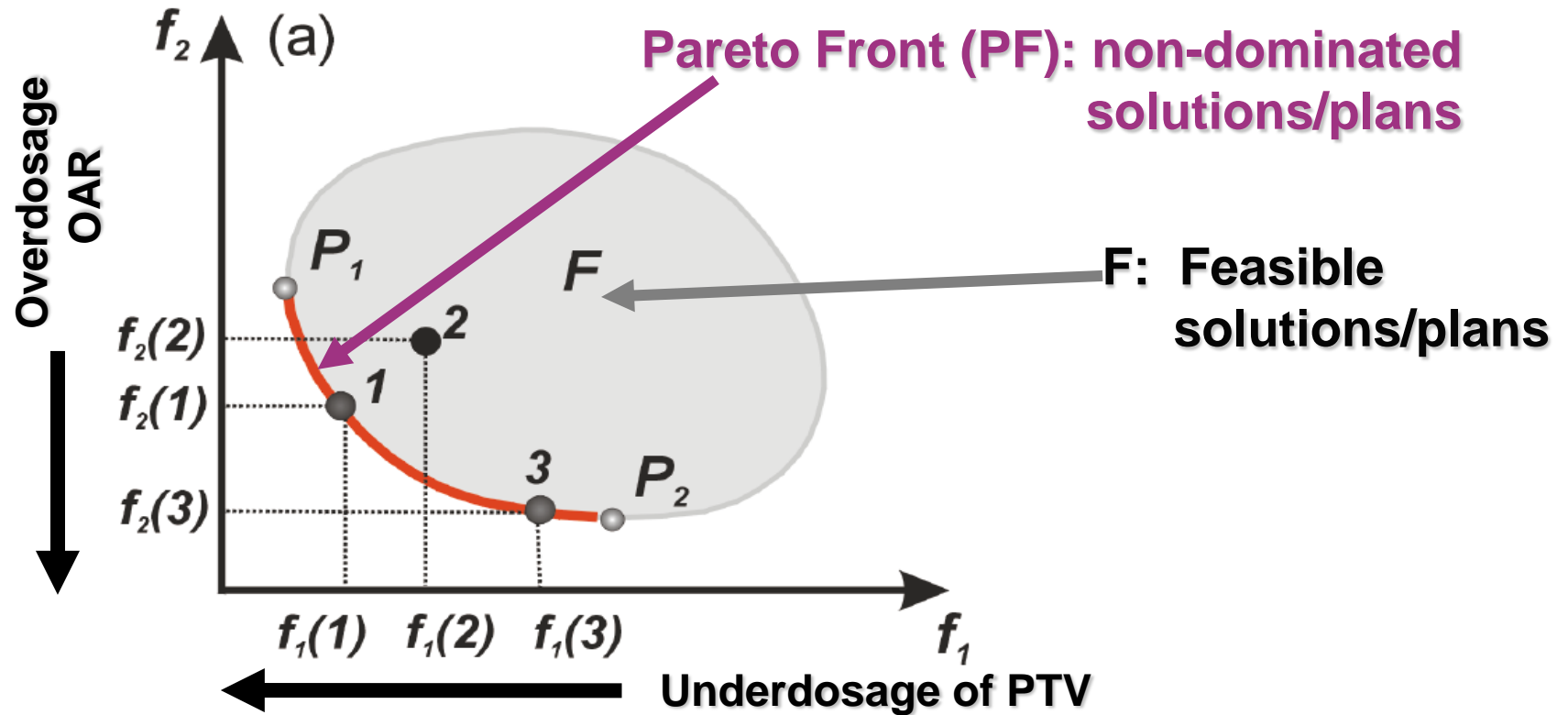
When the set P is the entire feasible search space then the set P' is called **the global Pareto Optimal Set**.

The image $f(x)$ of the **Pareto Optimal Set** is called the **Pareto Front (PF)**.

The **Pareto Optimal Set** is defined in the **parameter space**, while the **Pareto Front** is defined in the **Objective Space**.

Inverse Optimisation and Planning

A Multi-Objective (MO) Problem



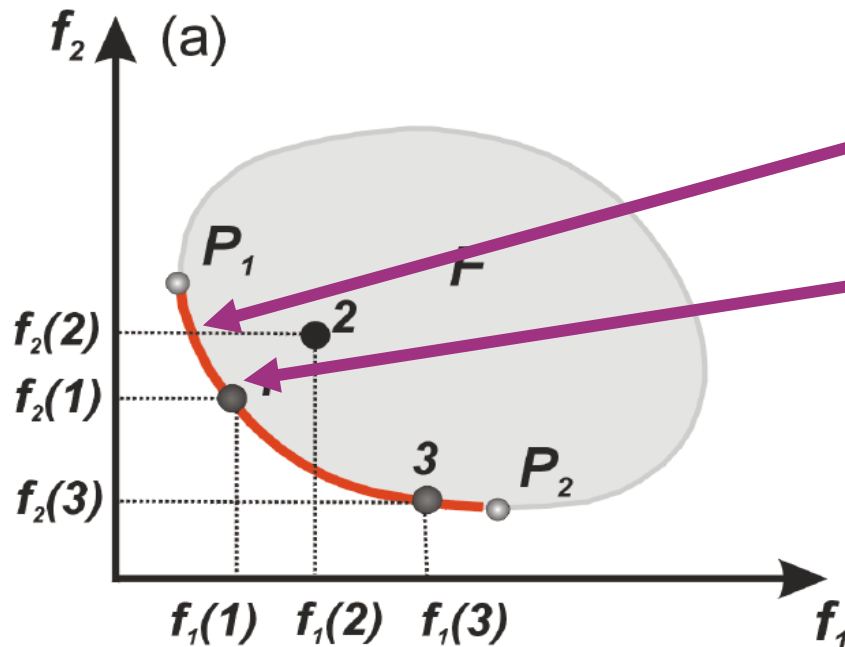
Example of a **bi-objective space** (f_1, f_2). We assume as mentioned already the minimization problem.

The **Pareto Front** is the boundary between the points P_1 and P_2 of the **feasible set** F . Solutions 1 and 3 are **non-dominated Pareto optimal solutions**. Solution 2 is **not Pareto Optimal** as solution 1 has simultaneously smaller values for both objectives. There is no reason why solution 2 should be accepted rather than solution 1. Therefore the aim of MO optimisation is to obtain a representative set of non-dominated solutions.

Inverse Optimisation and Planning

A Multi-Objective (MO) Problem

The *Multiobjective Optimisation (MO)* consists of two main Steps:



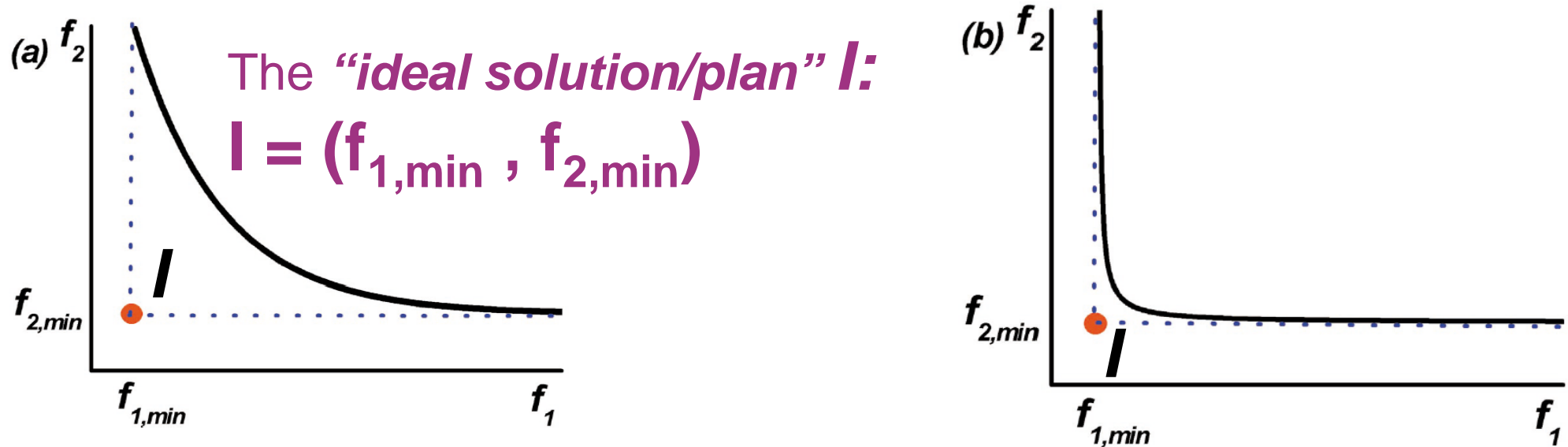
1. Estimation/Localisation of the *Pareto Front* (*Optimisation*)
2. Selection of the *most appropriate Plan* (*Decision*)

Some issues:

- Computationally intensive (time)
- Decision Tools (expertise)

Inverse Optimisation and Planning

A Multi-Objective (MO) Problem



Examples of a Pareto Front

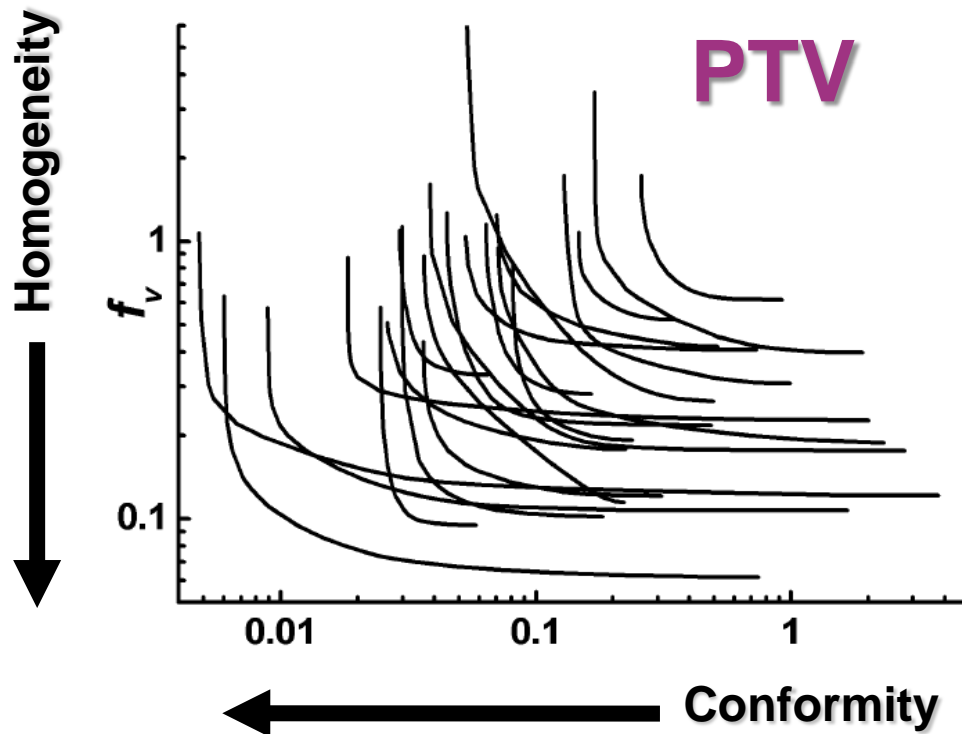
Left: there is **a strong trade-off** between the objectives/ objective functions f_1 and f_2 . The smaller the f_1 value is that we want the larger is the corresponding f_2 value. The “ideal point/plan” I lies far away from the front. There is a high dependence on the selection of the f_1 value.

Right: there is **a weak trade-off** between the objectives/ objective functions f_1 and f_2 . It is possible to optimise (minimise) the f_1 significant and close to the “ideal point/plan” I . Only very close to I we observe a rapid increase of f_2 . This is a case where for a set of parameters we can obtain simultaneously almost individual optimal values for f_1 and f_2

Inverse Optimisation and Planning

A Multi-Objective (MO) Problem

Bi-Objective Pareto Fronts obtained for **22 prostate implants**. The variety shows that a single objective optimization with constant importance factors does not give always a good result. In general a strong trade-off is observed. *

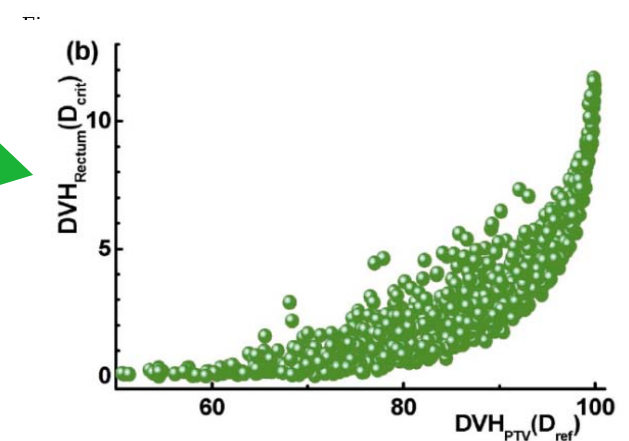
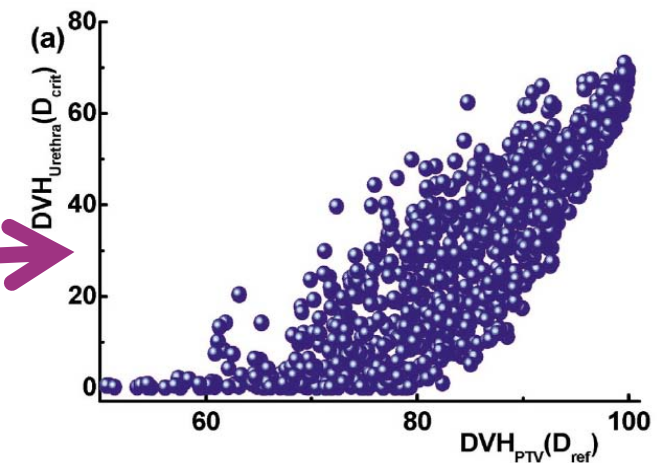
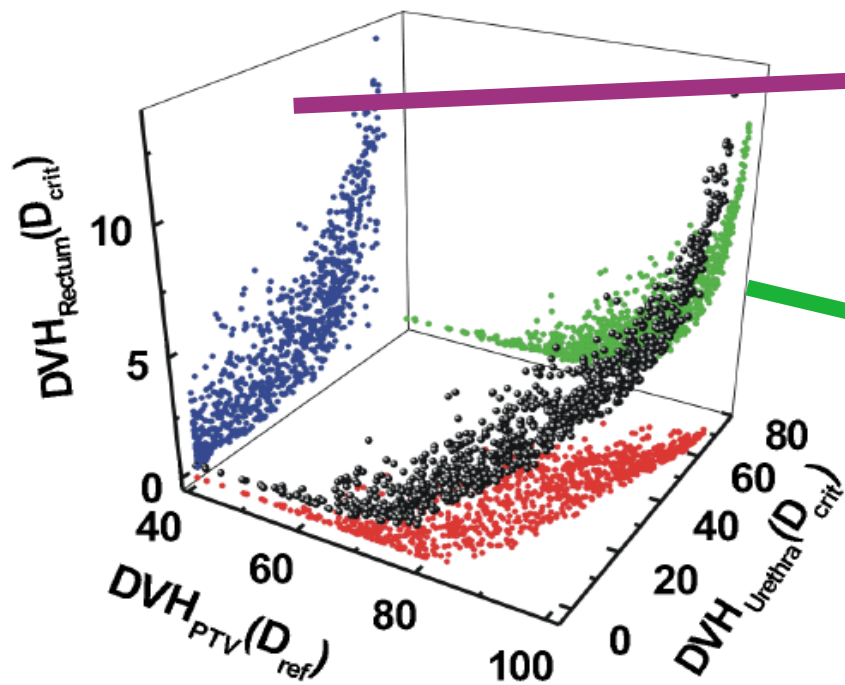


Example of a Pareto Front: there is **a strong trade-off** between the objectives/ objective functions f_1 and f_2 . The smaller the f_1 value is that we want the larger is the corresponding f_2 value. The “**ideal point/plan**” I lies far away from the front. There is a high dependence on the selection of the f_1 value.

*Lahanas, Milickovic, Baltas, Zamboglou: “Application of Multiobjective Evolutionary Algorithms for Dose Optimization Problems in Brachytherapy”, EMO 2001, LNCS 1993, 574-587, 2001.

Inverse Optimisation and Planning

A Multi-Objective (MO) Problem



Trade-off between three objectives (objective functions) for a prostate implant:

f_1 : PTV coverage, f_2 : urethra overdose and f_3 : rectum overdose.

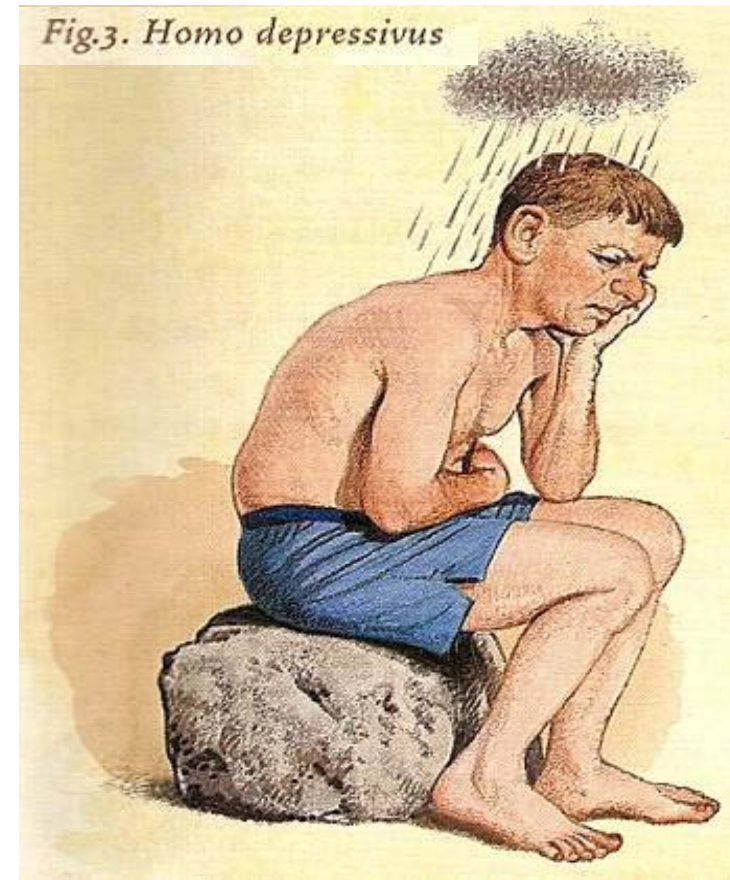
There resulting **three two-dimensional projections** are shown. These show the **trade-off** between two objectives in each case.

While for two objectives a solution very close to the optimal can be found, this becomes more difficult as more objectives are considered. **The complexity of the Pareto Front increases rapidly with the number of objectives / objective functions.**

Inverse Optimisation and Planning (2000 – today)

Facts

Although inverse Optimisation and Planning is a MO-Optimisation problem the majority of available Optimisation Algorithms in brachytherapy are *Single Objective Optimisation Algorithms*.



Inverse Optimisation and Planning (2000 – today)

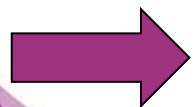
Create a single Objective Function via *weighted Aggregation*

The M **objective functions** f_m are combined into a **single objective function** f , by using a **weighted sum (aggregation)** of all objectives:

$$f = \sum_{m=1}^M w_m f_m = f(\{\vec{r}\}, \{t\}, \{w\})$$

w_m : the **Importance Factors (IFs)** for the individual **Objective Functions** f_m or **Penalties** for the **penalisation** of the **violation** of the **individual objectives**.

These are considered as a measure of the significance of each of the objectives/objective functions in the optimisation process.



The optimisation process equals then the minimisation of the **Aggregated Objective Function** f .

Inverse Optimisation and Planning (2000 – today)

Create a single Objective Function via *weighted Aggregation*

The minimisation of the Aggregated Objective Function f can be interpreted as finding the value f for which the line with slope $-w_1/w_2$ just touches the boundary of F as it proceeds outwards from the origin.

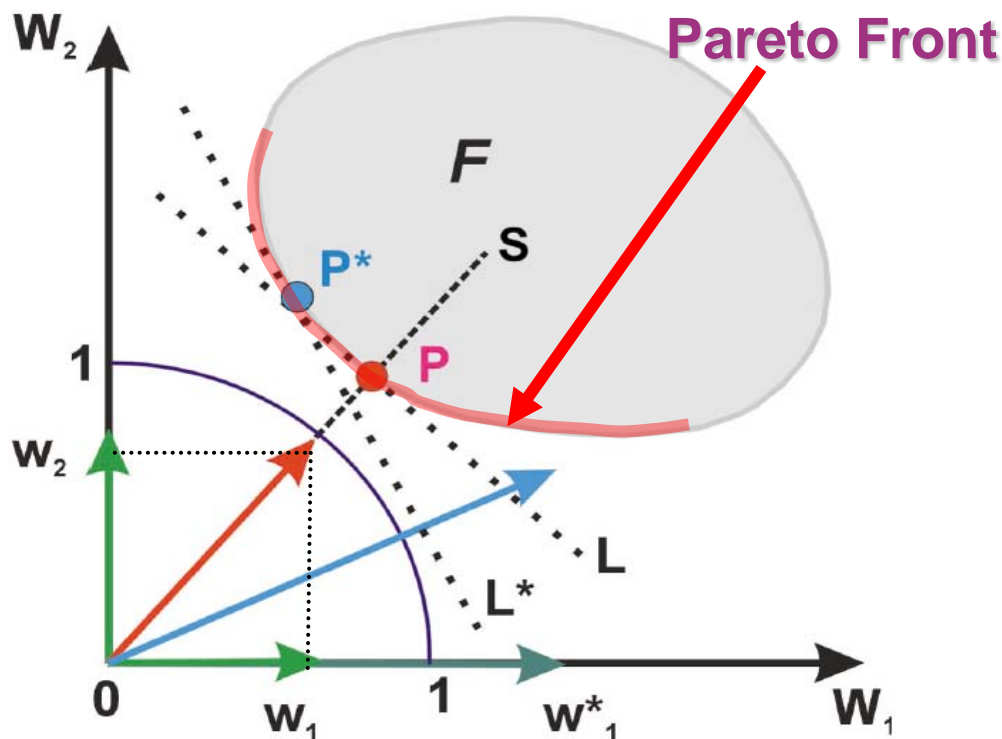


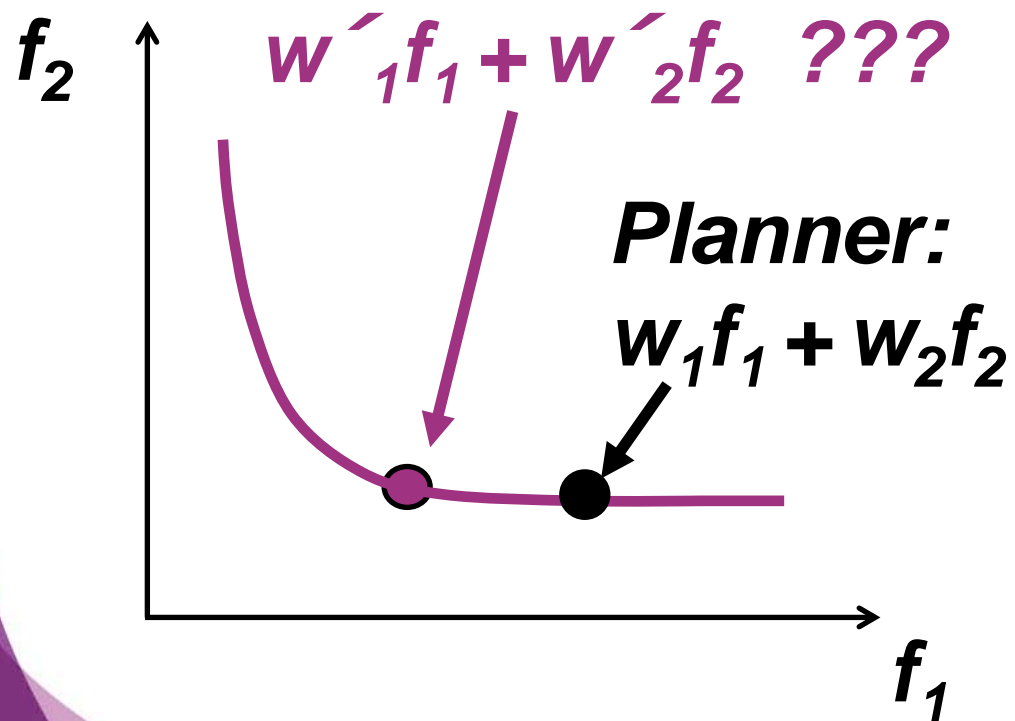
Figure 3. Single objective weighted sum optimization $w_1f_1 + w_2f_2$ for a bi-objective problem. For a given set of weights the vector sum of w_1, w_2 , if we consider these as vectors, specifies a direction \mathbf{S} shown by the dashed line. The optimization provides a solution which is the point P of a line L perpendicular to the direction \mathbf{S} that will touch the Pareto front as the line is moved away from the origin along \mathbf{S} . Solution P^* will be obtained if we replace w_1 by a larger weight w_1^* . The axes are $W_1 = w_1 \times f_1, W_2 = w_2 \times f_2$.

Inverse Optimisation and Planning (2000 – today)

Create a single Objective Function via *weighted Aggregation*

The plan/solution which is obtained in the *Weighted Aggregation* approach depends on the shape of the *Pareto Front* and the *importance factors/penalties* used.

Planner is not aware if there exist a better “*choice*” on the *Pareto Front* just next door!



Empirically estimated penalisation schemes, found to result to „good“ dose distributions are usually saved as *presets / protocols / class solutions* and can be used as starting points for the individual patient plan optimisation process.

Inverse Optimisation and Planning (2000 – today)

Facts

Planner freedom is limited due to:

- **The particular implemented Algorithm, since it defines the kind of Objectives and Objective Functions can be considered**

But keep in mind: This is Nothing different to IMRT!

Inverse Optimisation and Planning (2000 – today)

Objectives and Objective Functions

Diversity in considering:

- *Underdosage – Low Dose Limit D_L*
 - Targets (GTVs, CTVs, PTV)
 - Surface and/or volume

- *Overdosage – High Dose Limit D_H*
 - Targets (GTVs, CTVs, PTV)
 - OARs
 - Surface and/or volume

- *Artificial VOI e.g. Normal Tissue (NT)*
 - *Overdosage – High Dose Limit D_H*
 - ?

Inverse Optimisation and Planning (2000 – today)

Numerical Solvers / Optimisers (minimisation of aggregated f)

Diversity in considering:

- *Exact Solver*
 - **Linear Programming (LP)** (e.g. Simplex)

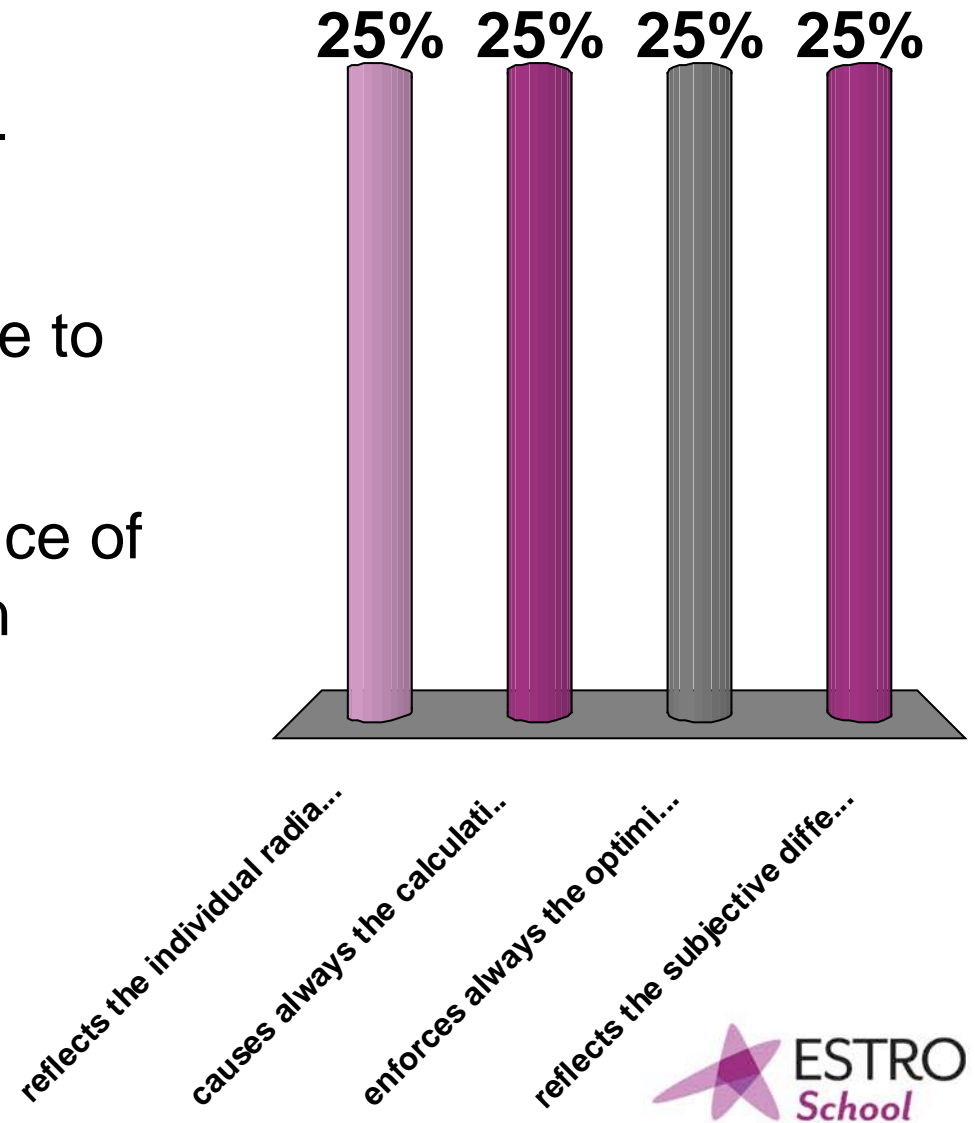
- *Deterministic*
 - **Gradient based** (e.g. Broyden-Fletcher-Goldfarb-Shanno-BFGS, L-BFGS, Fletcher-Reeves-Polak-Ribiere-FRPR, ...)
 - **Gradient-free** (e.g. Nelder-Mead Simplex Algorithm, ...)

- *Stochastic/Probabilistic*
 - **Simulating Annealing (SA)**
 - **Genetic/Evolutionary Algorithms (GA)**

All those solvers are based on iterative approaching of global minimum !!!

The penalisation of the individual objective functions:

- A. reflects the radiation sensitivity of the tissues and organs
- B. causes always the calculation of a sub-optimal dose distribution
- C. enforces always the optimisation engine to a non-good convergence
- D. reflects the subjective relative importance of the objectives towards calculation of an acceptable treatment plan



Inverse Optimisation and Planning (2000 – today)

A short Introduction into the *Topographic Inverse Optimisation* and Planning *TOP* ...

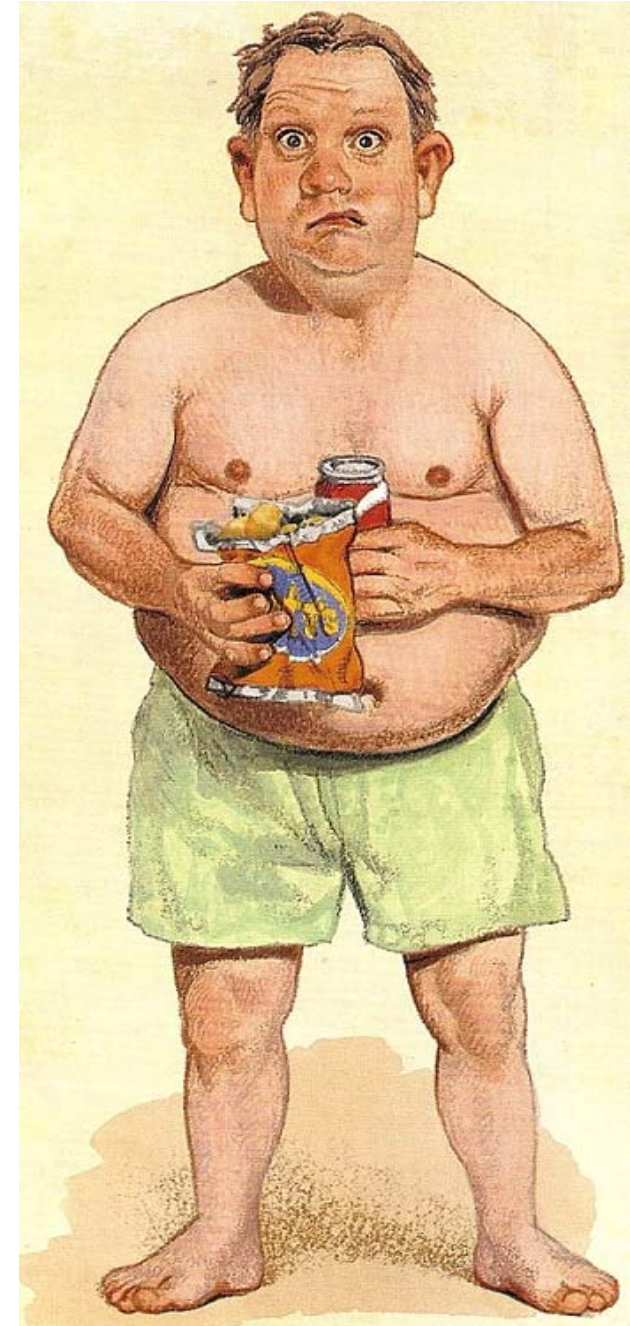


Fig.4. Homo adipositus

Inverse Optimisation and Planning: Topography based (TOP)

TOP: Additional not morphology (VOIs, DVHs) based Features, and/or local History:

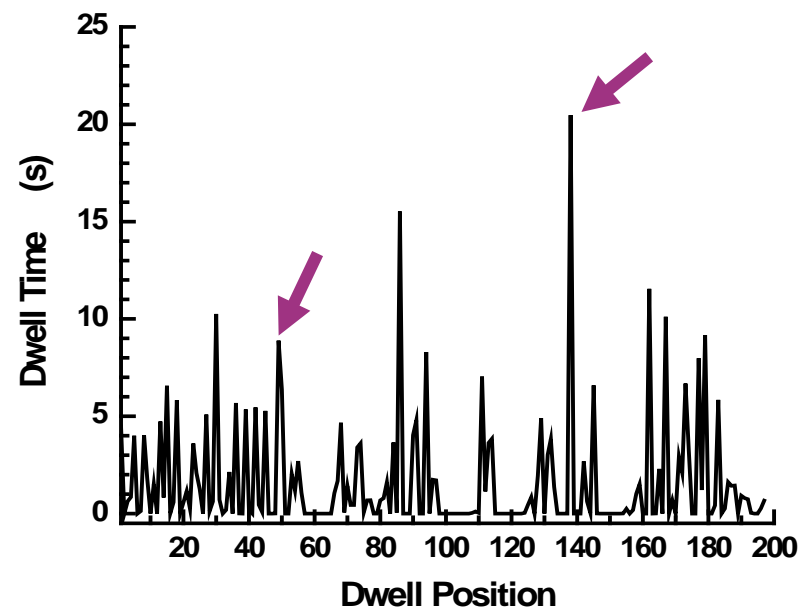
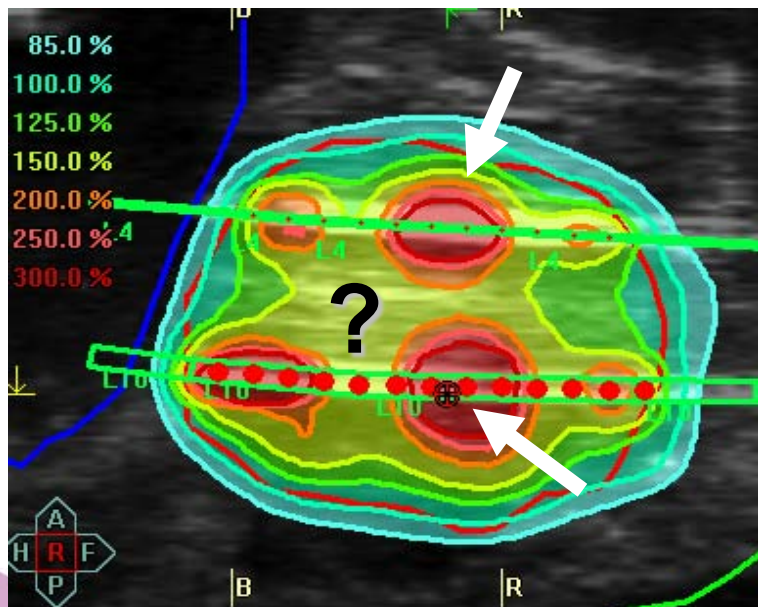
- **Dwell Time Modulation Restriction (MR)**
(Smoothness of Source Movement)

Inverse Optimisation and Planning

Topography based (TOP) : MR

Independently of the used Inverse Optimization Algorithm it is not an uncommon result for HDR implants that there exist a few very dominating Dwell positions where the largest part of the total dwell time is spent.

This leads obviously to a *selective extension of high dose volumes* around such dwell positions. If there is *no information available* about its necessity (e.g. location of a GTV/IDL), then it is reasonable to investigate whether this can be avoided.



Inverse Optimisation and Planning

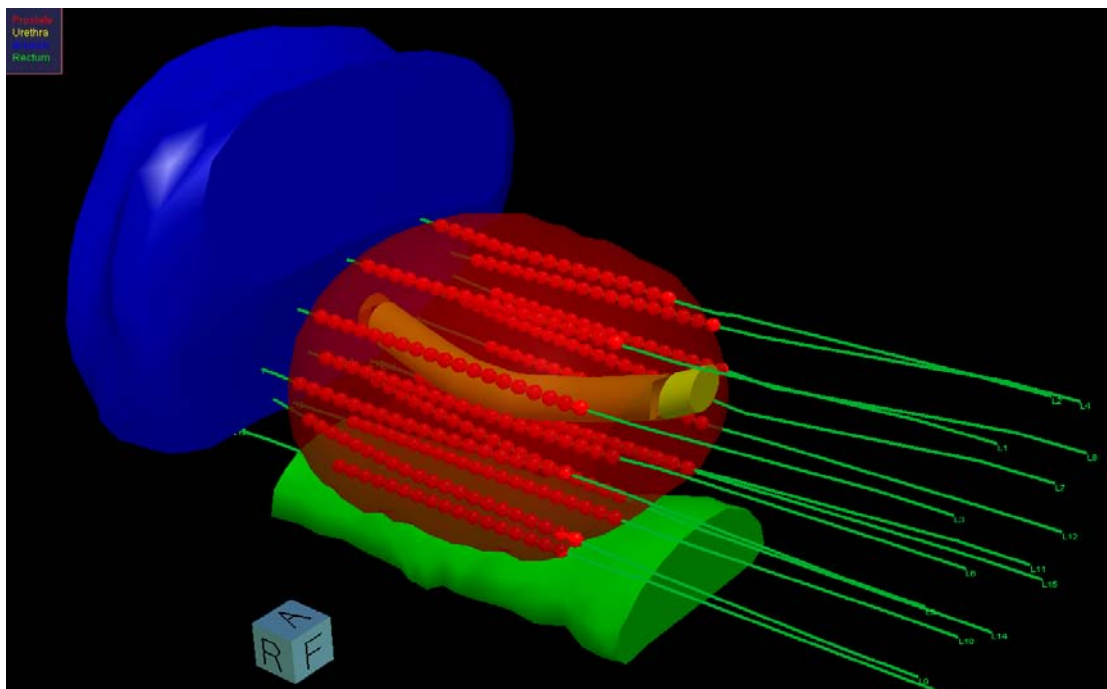
Topography based (TOP) : MR

Dwell Time *Modulation Restriction (MR)* - *Smoothness of Source Movement* - can be achieved by considering Dwell Time (Modulation) related *Objective Functions*:

- *Overall* Dwell Time
- *Smoothness* of Dwell Time Modulation within Catheters
- *Pseudo*: Restricting the maximal possible Dwell Time per Source Dwell Position

Topographic Optimisation (TOP)

MR: Modulation Restriction*



PTV = CTV 1 = 78 cm³

15 x Catheters

282 x ASDPs

3.6 ASDPs / cm³

6 x Objectives/Objective Functions

4,000 Dose Sampling Points

DVHO optimization settings

VDI Settings

Name	Type	Class	Dose limit [%]	Dose limit [cGy]	Imp. factor
<input checked="" type="checkbox"/> Normal Tissue	External	External	120.00	1380.00	8.000
<input checked="" type="checkbox"/> Prostate-Low	CTV1	Prostate	100.00	1150.00	20.000
<input checked="" type="checkbox"/> Prostate-High	CTV1	Prostate	150.00	1725.00	5.000
<input checked="" type="checkbox"/> Urethra	OAR	Urethra	120.00	1380.00	10.000
<input checked="" type="checkbox"/> Bladder	OAR	Bladder	75.00	862.50	10.000

Normal Tissue External External 120.00 1380.00 8.000

Dwell time gradient restr.
0.00 0.00 1.00

ASDPs outside target
 Consider ASDPs outside target

Convergence Settings
 Standard
 High Accuracy
Max. Iterations: 1000

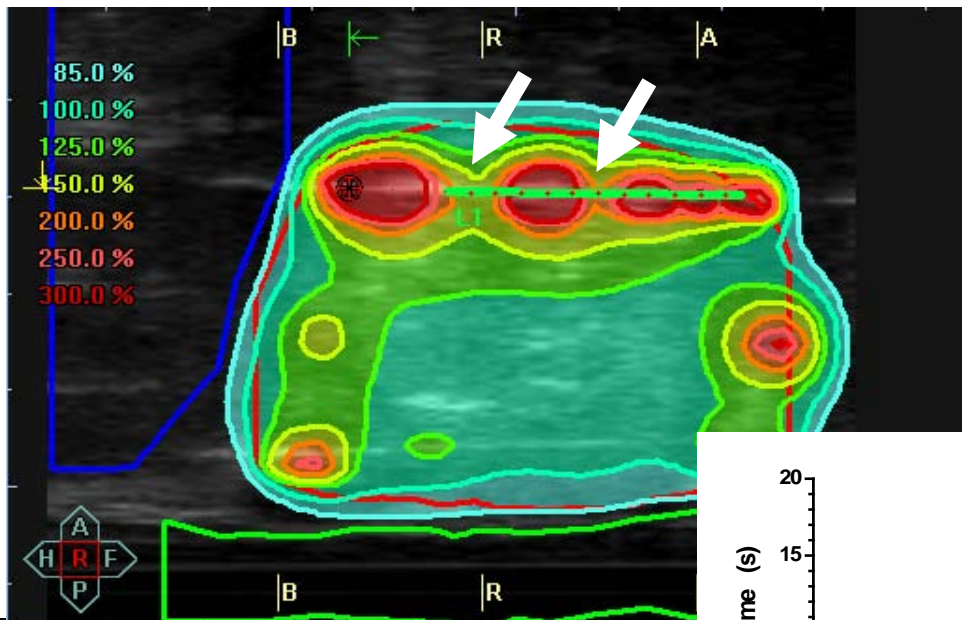
Apply and run OK Cancel

* Using HIPO (Pi-Medical Ltd) implementation in Oncentra Brachy & OcP (Nucletron B.V.)

Topographic Optimisation (TOP)

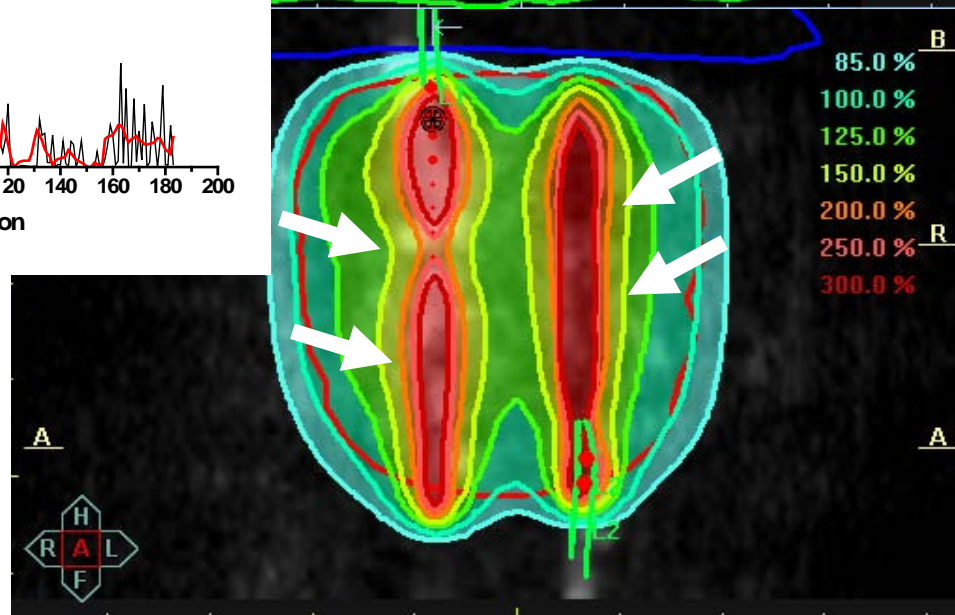
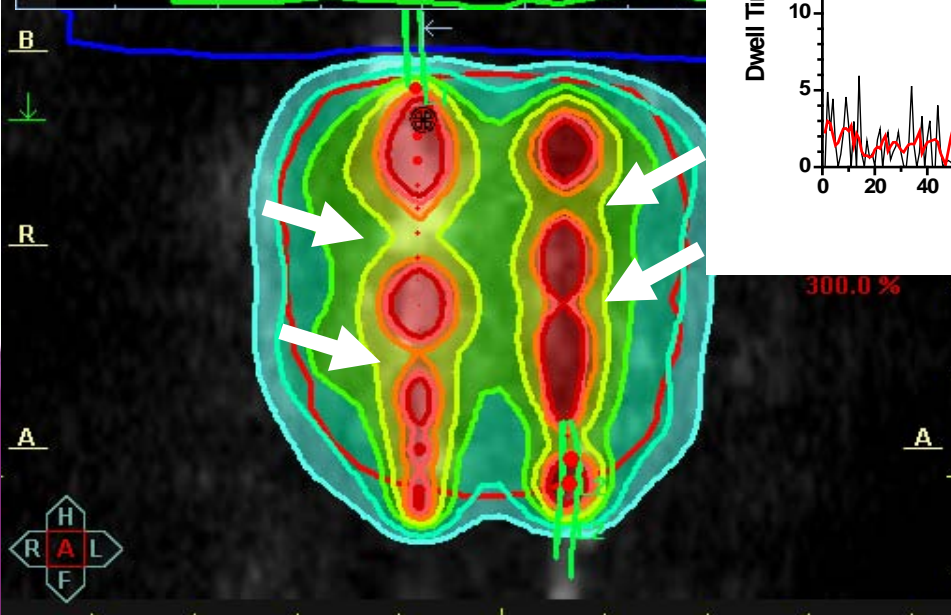
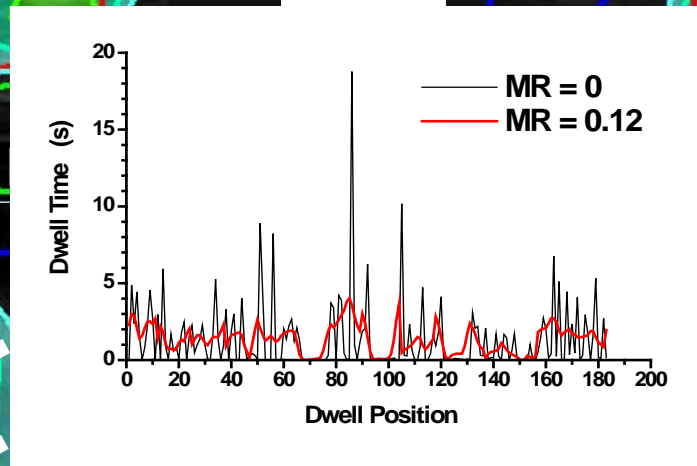
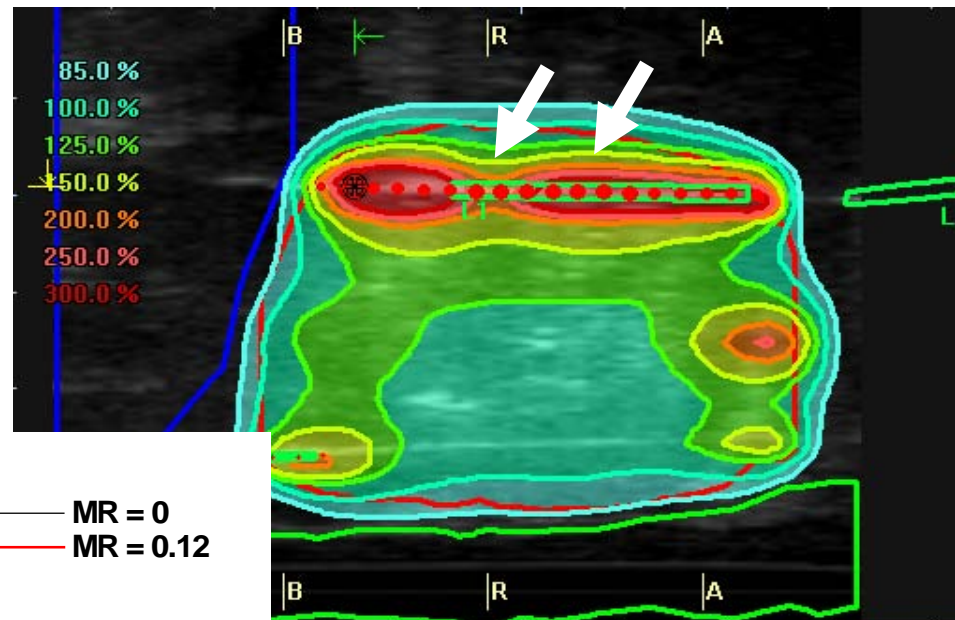
Modulation/Gradient Restriction

Parameter = 0.0



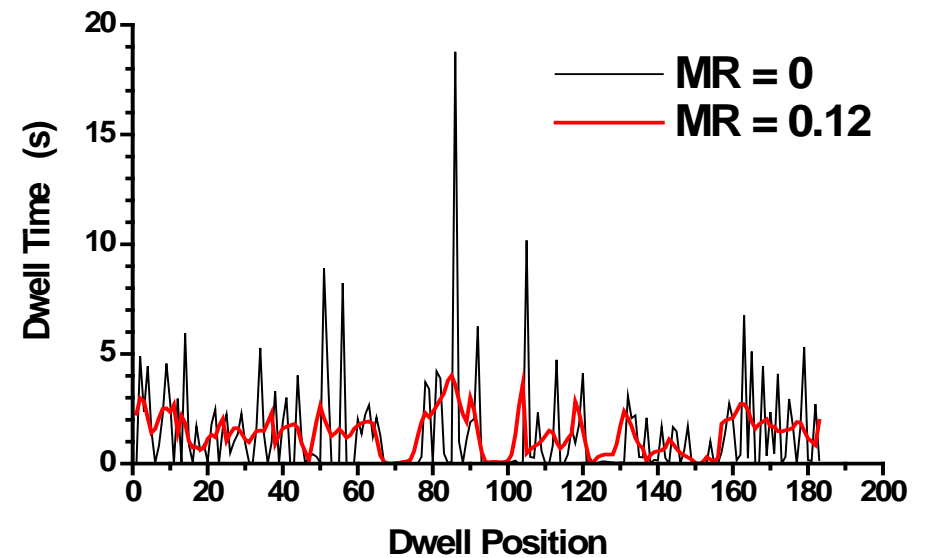
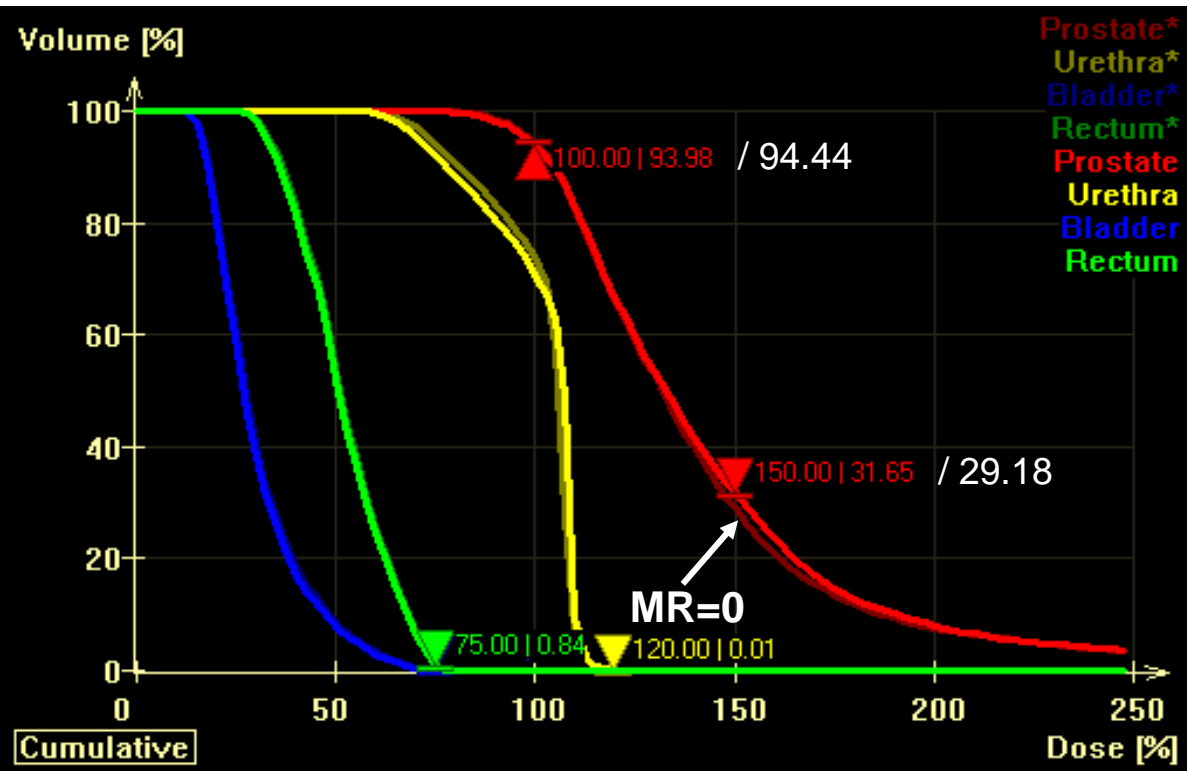
Modulation/Gradient Restriction

Parameter = 0.12



Topographic Optimisation (TOP)

MR: Modulation Restriction*



Total Dwell Time: 686.4 s \Rightarrow 675.3 s (-1.6%)

COIN: 0.884 \Rightarrow 0.888

Inverse Optimisation and Planning: Topography based (TOP)

- “..local History”: Pre-delivered Dose Part of Implant

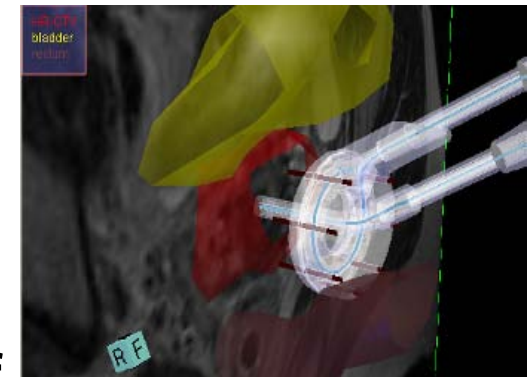
$$f_i = \frac{1}{N_i} \sum_{j=1}^{N_i} \left[\Theta(D_L^i - d_j^i(\mathbf{x})) [D_L^i - d_j^i(\mathbf{x})]^p \right]$$

$$f_i = \frac{1}{N_i} \sum_{j=1}^{N_i} \left[\Theta(d_j^i(\mathbf{x}) - D_H^i) [d_j^i(\mathbf{x}) - D_H^i]^p \right]$$

$d_j^i(\mathbf{x})$ has a “History”.

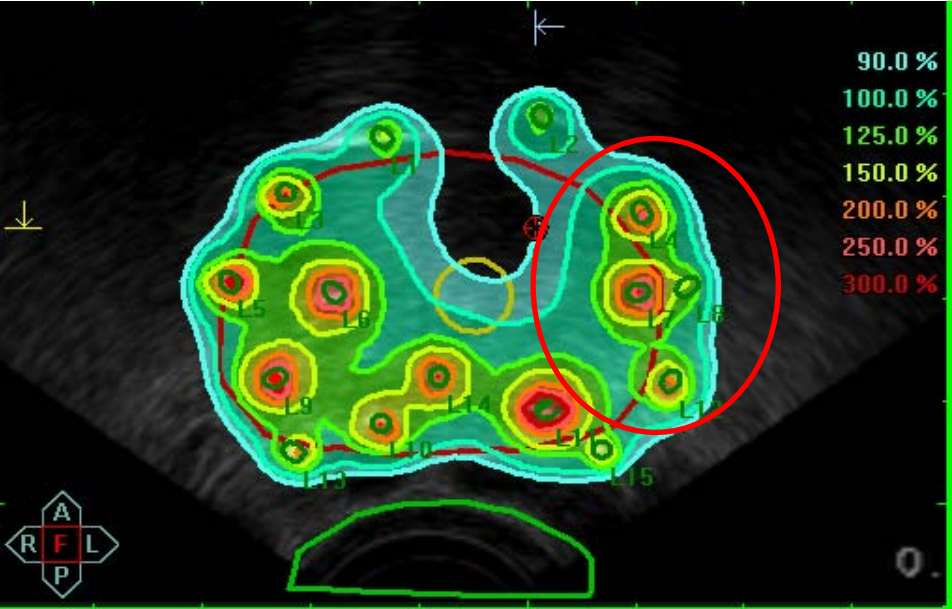
“History”:

- Pre-delivered Dose (previous Implants or ERT)
- Fixed contribution of a part of the implant
(Fixed contribution form Ring + Tandem & TOP of additional interstitial needles)

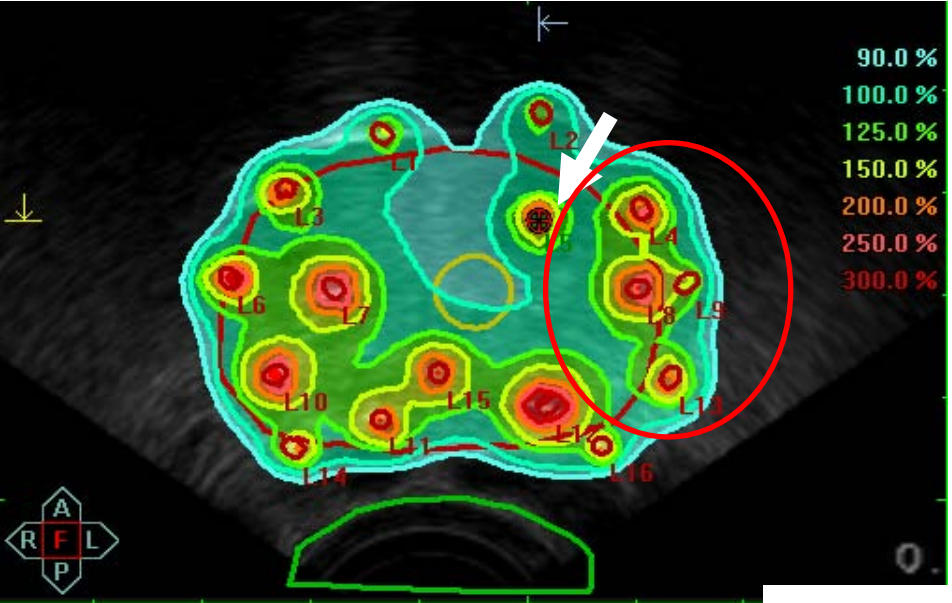
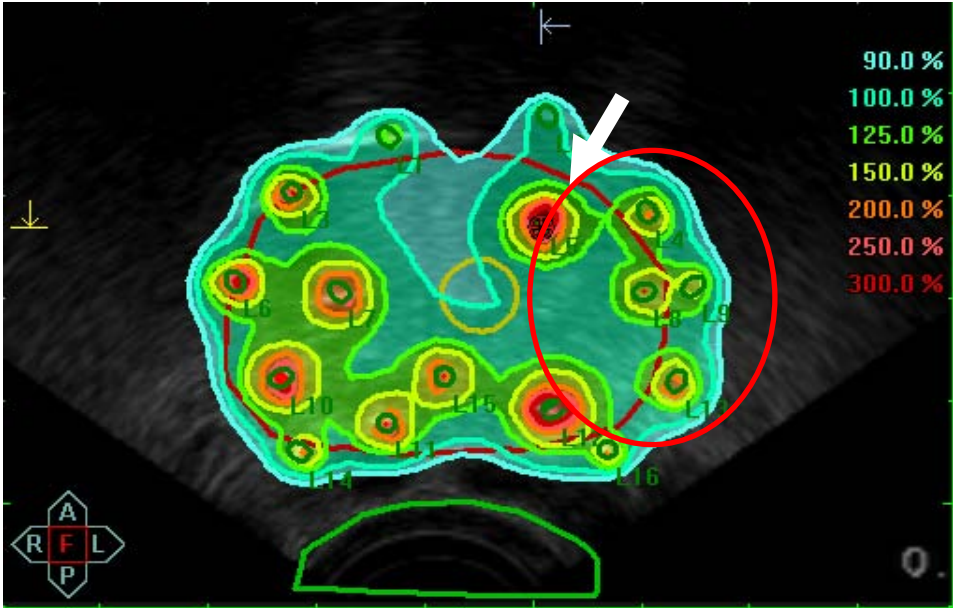


TOP: Topographic Optimisation

(A) Only 15 Catheters



(B) 15 + 1 Catheters, freely optimized

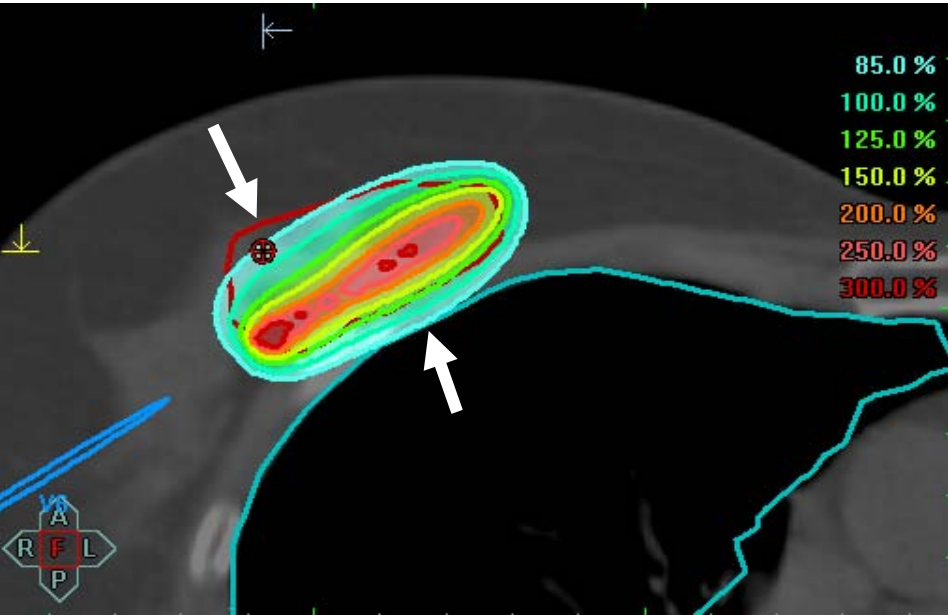


(C) 15 + 1 Catheters, TOP:
Dwell times for (A) “frozen”
Additional Catheter used for
Local Dwell Time Adjustment

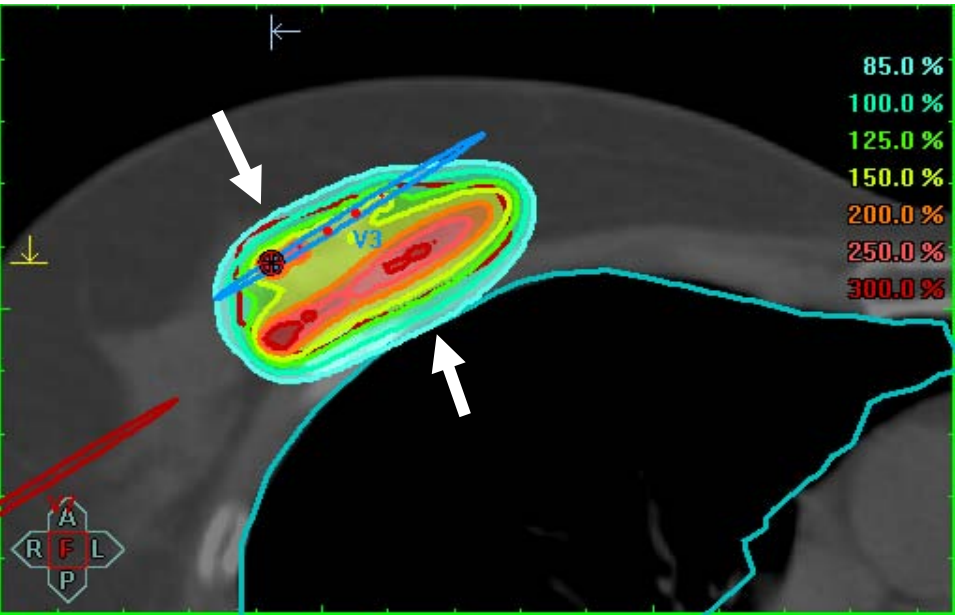
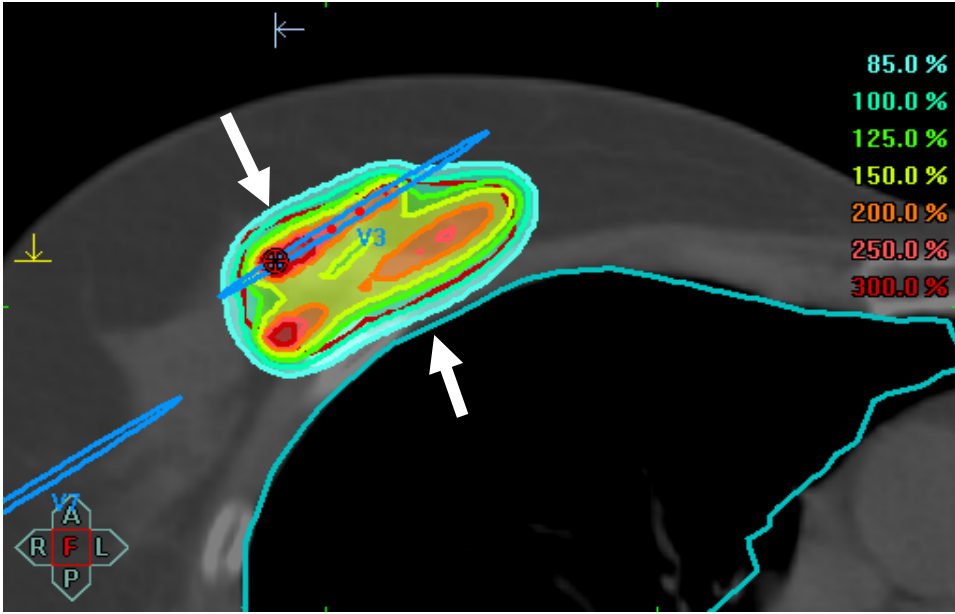
* Using HIPO (Pi-Medical Ltd) implementation in Oncentra Brachy & OcP (Nucletron B.V.)

TOP: Topographic Optimisation

(A) Only 8 Catheters



(B) 8 + 1 Catheters, freely optimized



(C) 8 + 1 Catheters, TOP:
Dwell times for (A) “frozen”
Additional Catheter used for
Local Dwell Time Adjustment

* Using HIPO (Pi-Medical Ltd) implementation in Oncentra Brachy & OcP (Nucletron B.V.)

List of Content

- Introduction on Dose Optimisation
- Forward Planning
- **Inverse** Optimisation and **Planning**

Introduction on Dose Optimisation

$$D = \Psi \cdot A$$

As an analytical solution for Ψ cannot be (always) obtained we consider the *Inverse Problem* to determine Ψ for a desired D equivalent to determine:

- (a) the position and number of catheters
- (b) the position and number of source dwell positions (SDPs) or sources
- (c) the source dwell times

such that the obtained dose distribution D is as close as possible to the desired one.

This process is called *Inverse Optimisation* or *Inverse Planning*.

Inverse Optimisation and Planning (2000 – today)

It presupposes the availability of:

- A complete 3D anatomy model
VOIs: Target(s), OARs
- The Desired Dose Distribution

} Morphology



Introduction on Dose Optimisation

This process is called *Inverse Optimisation* or *Inverse Planning*.

In general, it includes clinical constraints such as:

- (a) a realistic range of number of catheters or sources/source dwells and the possible positions and orientations of the catheters
- (b) clinical implantation rules/settings
- (c) anatomical constraints

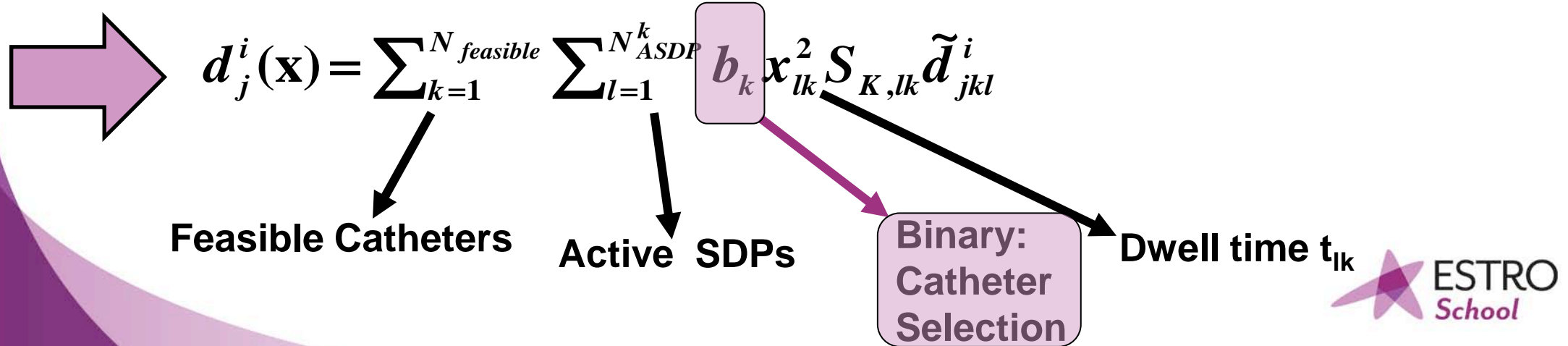
It is the procedure where the *ideal implant is imaged in a virtual environment*.

Inverse Planning: Discretisation Case

General Form of an Objective Function *incl. Catheters*

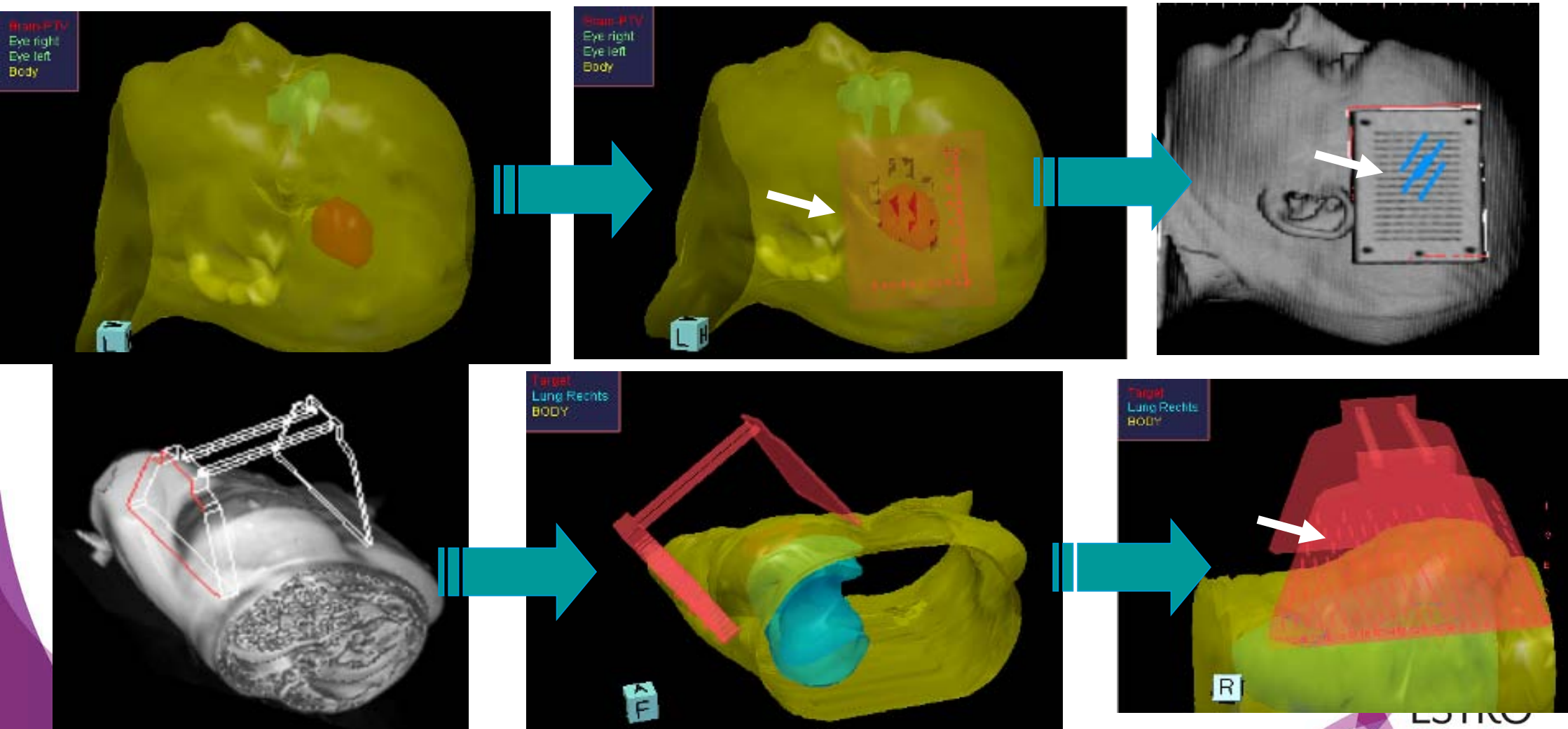
$$\left. \begin{aligned}
 \text{Low } f_i &= \frac{1}{N_i} \sum_{j=1}^{N_i} \left[\Theta(D_L^i - d_j^i(\mathbf{x})) [D_L^i - d_j^i(\mathbf{x})]^p \right] \\
 \text{High } f_i &= \frac{1}{N_i} \sum_{j=1}^{N_i} \left[\Theta(d_j^i(\mathbf{x}) - D_H^i) [d_j^i(\mathbf{x}) - D_H^i]^p \right]
 \end{aligned} \right\} f = \sum_{m=1}^M w_m f_m$$

d_j^i is the dose at the j^{th} -sampling point for the i^{th} -objective function:



Inverse Planning:

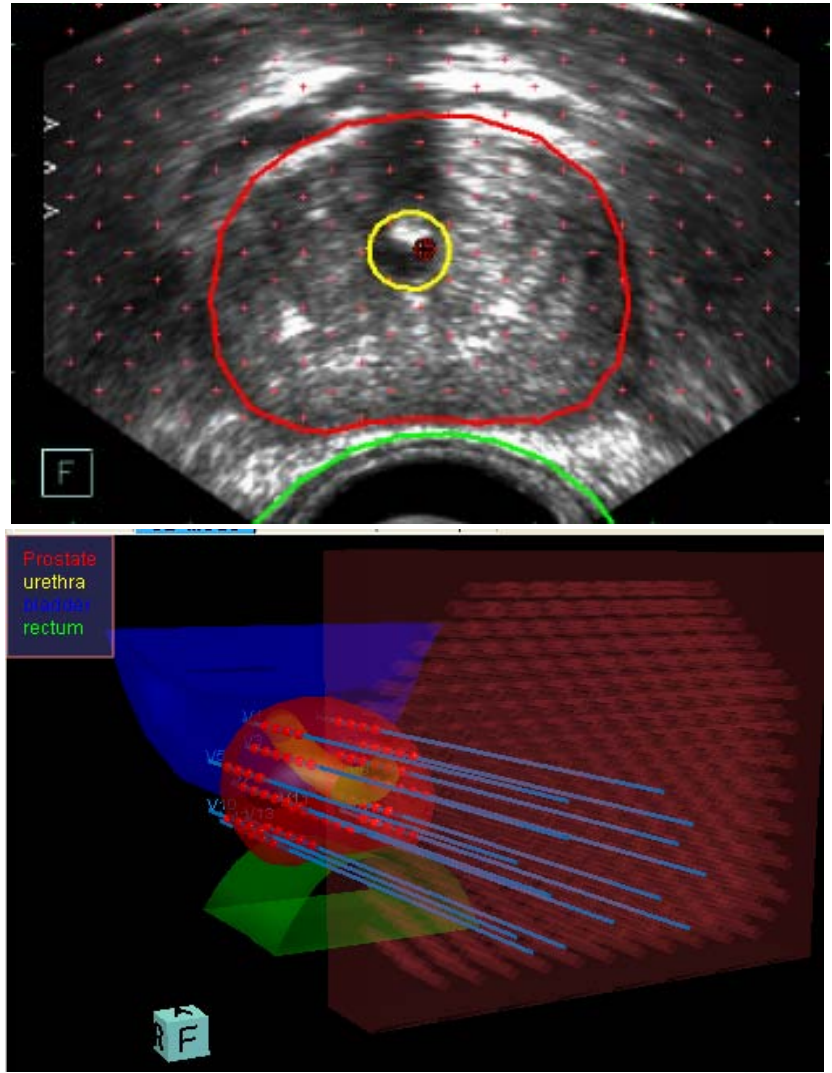
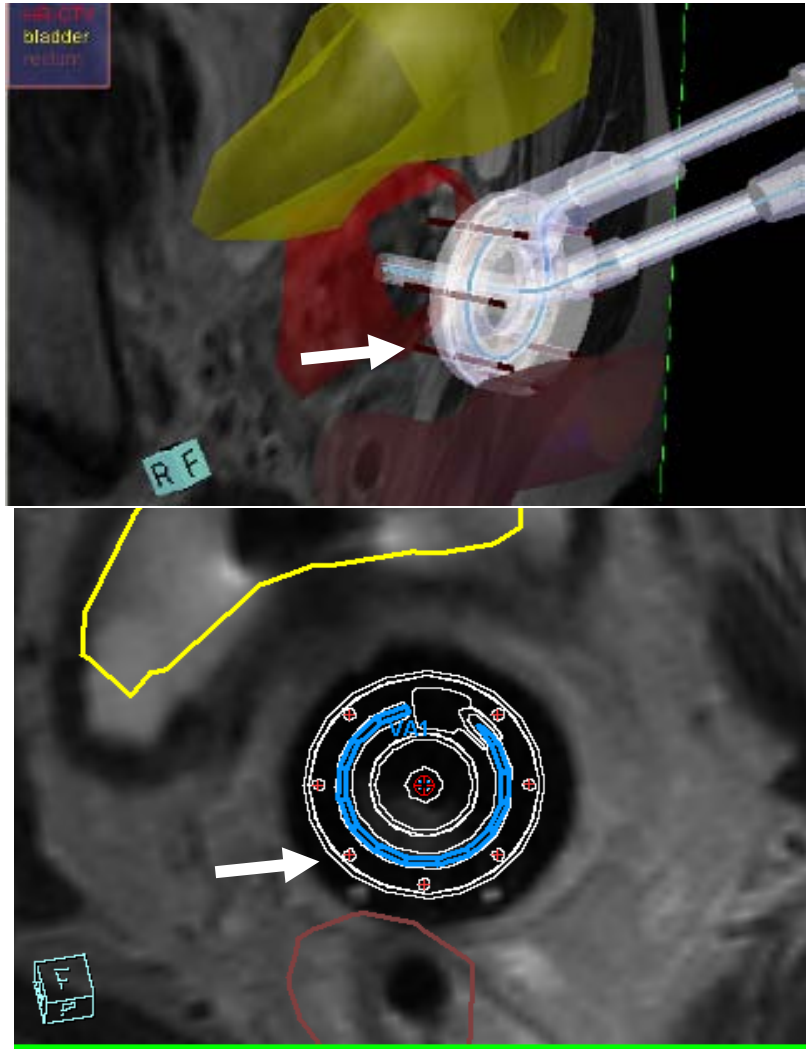
The automatic placement of an adequate number of catheters/applicators / needles based on dosimetric objectives and constraints is solvable in clinically acceptable time only after *discretisation*:



Inverse Planning:

The automatic placement of an adequate number of catheters/applicators / needles based on dosimetric objectives and constraints is solvable in clinically acceptable time only after *discretisation*:

Cervix-Ca: Applicator + Needles
Data by courtesy of University of Vienna



Prostate, 3D-U/S based

Overview of Commercially available Inverse Optimisation and Planning Tools for HDR BRT

Company RTP	Optimiser (HDR)	Objectives / Functions	Artificial VOI NT & Objective	Automatic Catheter Placement	Numerical Solver	TOP	Dwell Time (DT) Modulation Control
BEBIG HDR Plus Vs. 3.0.5	---	Aggregation: Low and High	only user-defined and added to OFs	No	Stochastic FSA	Yes DT	DT Homogeneity Error Weight & Total DT
Nucletron, ELEKTA Oncentra Brachy Vs. 4.3	IPSA	Aggregation: Low and High	automatically defined & added as OF	No	Stochastic FSA	Yes DT	DT Gradient
Nucletron, ELEKTA Oncentra Brachy Vs. 4.3 & OcP	HIPO	Aggregation: Low and High	automatically defined & added as OF	YES (Discretisation Case)	Deterministic L-BFGS & Heuristic/ Stochastic for Catheters	Yes DT & pre-delivered	DT Gradient Modulation Restriction
VARIAN Brachy-Vision Vs. 10 +	AVOL	Aggregation: Low and High incl. Basal Dose	automatically defined user option for OF	No	Deterministic Nelder-Mead Simplex Algorithm	Yes DT	Max./Min DT Constraints Gradient restriction

Inverse Optimisation and Planning: Perspectives

- **Radiobiology Based Inverse Planning & Optimisation**
 - **EUD, gEUD, TCP/NTCP, ...**
 - **Inhomogeneous Cancer Tissue Characteristics (Hypoxic areas, etc..)**

- **Robustness (Machine Uncertainties, ...)**

Literature I

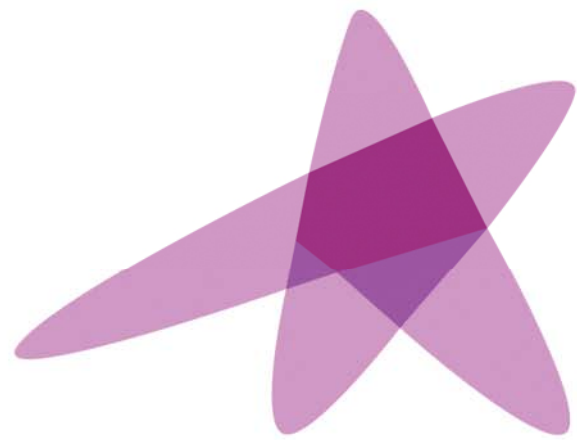
- G. Edmundson, "Geometry based optimization for stepping source implants," in Brachytherapy HDR and LDR, edited by A. A. Martinez, C. G. Orton, and R. F. Mould ~Nucletron, Columbia, 1990
- Van der Laarse and T. P. E. Prins, "Introduction to HDR brachytherapy optimisation," in Brachytherapy from Radium to Optimization, edited by R. F. Mould, J. Batterman, A. A. Martinez, and B. L. Speiser, Nucletron International, Veenendaal, The Netherlands, 1994, pp. 331–351.
- Y. Yu and M. C. Schell, "A genetic algorithm for the optimization of prostate implants," Med. Phys. 23, 2085–2091, 1996
- Kneschaurek P, Schiessl W and Wehrmann R Volume-based dose optimization in brachytherapy Int. J. Radiat. Oncol. Biol. Phys. 45 811–5, 1999
- Baltas, C. Kolotas, K. Geramani, R. F. Mould, G. Ioannidis, M. Kekchidi, and N. Zamboglou, "A conformal index COIN to evaluate implant quality and dose specifications in brachytherapy," Int. J. Radiat. Oncol., Biol., Phys. 40, 512–524 ~1998
- Lahanas, M., Baltas, D., Zamboglou, N.: Anatomy-based three-dimensional dose optimization in brachytherapy using multiobjective genetic algorithms. Med. Phys., 26, No. 9, 1904-1918, 1999.
- Lahanas, M., Milickovic, N., Baltas, D., Zamboglou, N.: Application of Multiobjective Evolutionary Algorithms for Dose Optimization in Brachytherapy. E. Zitzler et al. (Eds.): EMO 2001, LNCS 1993, 574-587, 2001
- Milickovic, N., Lahanas, M., Baltas, D., Zamboglou, N.: Comparison of Evolutionary and Deterministic Multiobjective Algorithms for Dose Optimization in Brachytherapy. E. Zitzler et al. (Eds.): EMO 2001, LNCS 1993, 167-180, 2001
- Lessard, E., & Pouliot, J. (2001). Inverse planning anatomy-based dose optimization for HDR brachytherapy of the prostate using fast simulated annealing algorithm and dedicated objective function. Medical Physics, 25(5), 773-779.
- Milickovic, N., Lahanas, M., Papagianopoulou, M., Zamboglou, N., Baltas, D.: Multiobjective anatomy-based dose optimization for HDR-brachytherapy with constraint free deterministic algorithms. Phys. Med. Biol., 47(13), 2263-2280, 2002
- Lahanas, M., Baltas, D., Zamboglou, N.: A hybrid evolutionary algorithm for multi-objective anatomy-based optimization in high-dose-rate brachytherapy. Phys. Med. Biol., 48, 399-415, 2003.
- Lahanas, M., Baltas, D., Giannouli, S.: Global convergence analysis of fast multi-objective gradient-based dose optimization algorithms for high-dose-rate brachytherapy. Phys. Med. Biol., 48, 599-617, 2003
- Jozsef, G., Streeter, O. E., & Astrahan, M. A. (2003). The use of linear programming in optimization of HDR implant dose distributions. Medical Physics, 30(5), 751-760.
- Lahanas, M., Karouzakis, K., Giannouli, S., Mould, R.F., Baltas, D.: Inverse planning in brachytherapy from radium to high dose rate ¹⁹²Iridium afterloading. NOWOTWORRY Journal of Oncology, 54 No 6, 535–546, 2004.
- Karabis, A., Giannouli, S., Baltas, D.: HIPO: A hybrid inverse treatment planning optimization algorithm in HDR brachytherapy. Radiother. Oncol., 76, Supplement 2, 29, 2005.

Literature II

- De Witt, K. D., Hsu, I.-C. J., Speight, J., Weinberg, V. K., Lessard, E., & Pouliot, J. (2005). 3D inverse treatment planning for the tandem and ovoid applicator in cervical cancer. *International Journal of Radiation Oncology, Biology, Physics*, 63(4), 1270-1274.
- Sumida, I., Shiomi, H., Yoshioka, Y., Inoue, T., Lessard, E., Hsu, I.-C. J., & Pouliot, J. (2006). Optimization of dose distribution for HDR brachytherapy of the prostate using attraction-repulsion model. *International Journal of Radiation Oncology, Biology, Physics*, 64(2), 643-649.
- Alterovitz, R., Lessard, E., Pouliot, J., Hsu, I.-C. J., O'Brien, J. F., & Goldberg, K. (2006). Optimization of HDR brachytherapy dose distributions using linear programming with penalty costs. *Medical Physics*, 33(11), 4012-4019.
- Baltas, D., & Zamboglou, N. (2006). 2D and 3D planning in brachytherapy. In W. Schlegel, T. Bortfeld, & A. L. Grosu (Eds.), *New technologies in radiation oncology* (pp. 237-254). New York: Springer.
- Jacob, D., Raben, A., Sarkar, A., Grimm, J., & Simpson, L. (2008). Anatomy-based inverse planning simulated annealing optimization in high-dose-rate prostate brachytherapy: Significant dosimetric advantage over other optimization techniques. *International Journal of Radiation Oncology, Biology, Physics*, 72(3), 820-872.
- Kim, Y., Hsu, I.-C. J., Lessard, E., Kurhanewicz, J., Noworolsky, S. M., & Pouliot, J. (2008). Class solution in inverse planned HDR prostate brachytherapy for dose escalation of DIL defined by combined MRI/MRSI. *Radiotherapy and Oncology*, 88, 148-155.
- Karabis, A., Belotti, P., & Baltas, D. (2009). Optimization of catheter position and dwell time in prostate HDR brachytherapy using HIPO and linear programming. *Proceedings of the 11th International Congress of the IUPESM (World Congress on Medical Physics and Biomedical Engineering)*, 25 (1), 612-615, doi: 10.1007/978-3-642-03474-9 172.
- Trnková, P., Pötter, R., Baltas, D., Karabis, A., Fidarova, E., Dimopoulos, J., Georg, D., Kirisits, C.: New inverse planning technology for image-guided cervical cancer brachytherapy: Description and evaluation within a clinical frame. *Radiother. Oncol.*, 93, 331-340, 2009.
- Mavroidis, P., Katsilieri, Z., Kefala, V., Milickovic, N., Papanikolaou, N., Karabis, A., Zamboglou, N., Baltas, D. Radiobiological evaluation of the influence of dwell time modulation restriction in HIPO optimized HDR prostate brachytherapy implants. *J Contemp Brachyther* Vol 2, No 3: 117-128, 2010.
- Jamema, S. V., Kirisits, C., Mahantshetty, U., Trnková, P., Deshpande, D. D., Shrivastava, S. K., & Pötter, R. (2010). Comparison of DVH parameters and loading patterns of standard loading, manual and inverse optimization for intracavitary brachytherapy on a subset of tandem/ovoid cases. *Radiotherapy and Oncology*, 97, 501-506.
- De Boeck Liesje, Belien Jeroen, Egyed Wendy. "Dose Optimisation in HDR brachytherapy: A literature review of quantitative models". HUB Research Papers 2011/32, Economics & Management, December 2011.
- Dinkla A.M., van der Laarse R., Koedooder K., Kok H.P., van Wieringen N., Pieters B.R., Bel A. Novel tools for stepping source brachytherapy treatment planning: Enhanced geometrical optimization and interactive inverse planning. *Medical Physics* 42 (1), 348-353, 2015.
- Dinkla A.M., van der Laarse R., Kaljouw E., Pieters B.R., Koedooder K., van Wieringen N., Bel A. A comparison of inverse optimization algorithms for HDR/PDR prostate brachytherapy treatment planning. *Brachytherapy* 14, 279-288, 2015.

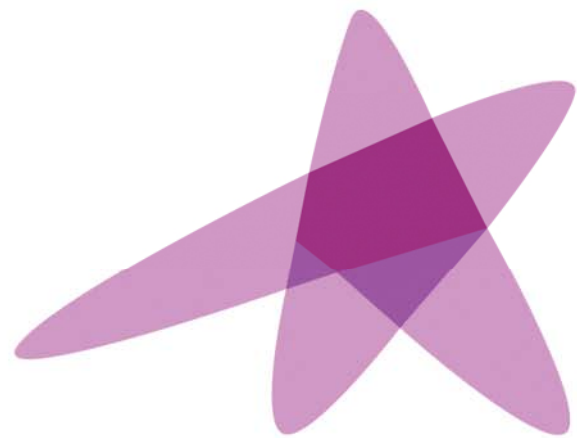


**Thank you very much
for your Attention !**



ESTRO

School



ESTRO
School

Advanced Brachytherapy Physics

Source Strength Determinations in Brachytherapy

Prof. Mark J. Rivard, Ph.D., FAAPM

Advanced Brachytherapy Physics, 29 May – 1 June, 2016



Disclosures

There are no conflicts-of-interest to report.

Opinions herein are solely those of the presenter, and are not meant to be interpreted as societal guidance.

Specific commercial equipment, instruments, and materials are listed to fully describe the necessary procedures. Such identification does not imply endorsement by the presenter, nor that these products are necessarily the best available for these purposes.

Learning Objectives

1. Accepted standard units for brachytherapy source strength
2. Source calibration traceability and standards labs
3. Calibration methods and techniques
4. Calibration uncertainties
5. Future calibrations

Photon Sources Examined

	High Energy	Low Energy
High Dose Rate	^{192}Ir , ^{60}Co	electronic (x rays)
Low Dose Rate	^{137}Cs	^{125}I , ^{103}Pd , ^{131}Cs

2004 AAPM TG-43U1

Brachytherapy Dosimetry Formalism

RAKR nearly identical to air-kerma strength S_K (distance specification)

$$\dot{D}(r, \theta) = S_K \cdot \Lambda \cdot \frac{G_L(r, \theta)}{G_L(r_0, \theta_0)} \cdot g_L(r) \cdot F(r, \theta)$$

$\dot{D}(r, \theta)$ dose rate to water in water at point $P(r, \theta)$

S_K air-kerma strength

Λ dose-rate constant

$g_L(r)$ radial dose function

$G_L(r, \theta)$ geometry function (line-source approximation)

$F(r, \theta)$ 2D anisotropy function

Brachytherapy Source Strength

Only the reference air kerma rate (RAKR) K_R is a quantity that is traceable to a standards laboratory (i.e., NMI or PSDL)

RAKR defined as kerma rate to air @ 1 meter
in vacuo, corrected for attenuation/scatter

RAKR defined on the source transverse-plane for photons with $E > \delta$
 δ threshold is dependent on source calibration protocol

RAKR has units Gy/s, also Gy/h or $\mu\text{Gy/s}$ (unit conversion - convenience)

mg Ra, mgRaEq, mCi (apparent activity), Bq **are not traceable quantities**

Obsolete units: mg Ra, mgRaEq, mCi (apparent activity), Bq

The Good Olde Days

Archives of Dermatology and Syphilology

VOLUME 45

APRIL 1942

NUMBER 4

COPYRIGHT, 1942, BY THE AMERICAN MEDICAL ASSOCIATION

THRESHOLD ERYTHEMA DOSE OF ROENTGEN RAYS

II. AN EXPERIMENTAL INVESTIGATION OF VARIOUS ASPECTS OF THE ERYTHEMA REACTION AND A NEW CLINICAL CRITERION FOR THE STANDARD THRESHOLD ERYTHEMA REACTION

JOHN C. BELISARIO, M.B., CH.M.
SYDNEY, AUSTRALIA

In the first paper¹ of this series Pugh and I reported the results of an investigation of the various magnitudes of the dose in roentgens reported in the literature as being equivalent to the erythema dose and also the variation in this dose in actual clinical use in Australia, the United States and England.

In order to obtain a more complete picture of the various clinical aspects of the erythema reaction the extensive experimental program herein reported was carried out.

A new criterion of the threshold erythema reaction is proposed and defined, which, it is believed, would greatly increase the degree of accuracy with which different workers could correlate their observations by avoiding the necessity for judging the degree of the reaction. A number of tests were performed before a suitable portion of the body could be chosen as a standard location for the tests, and the question of the effect of the quality of the radiation was also investigated.

Black Death



All Authorities Agree on Correct Unit

(1974) NCRP Report 41

(1983) French Cmte on ionizing Radiation Measurements

(1984) British Cmte on Radiation Units and Measurements

(1985) ICRU Report 38: Dose and volume specification for reporting intracavitary therapy in gynecology

(1987) AAPM TG-32: Specification of brachytherapy source strength

(1997) ICRU Report 58: Dose and volume specification for reporting interstitial brachytherapy

(2004) ESTRO Booklet 8: A practical guide to quality control of brachytherapy equipment

etc., etc., etc.

ICRU, GEC-ESTRO, and AAPM explicitly **recommend against** A_{app}

NRC Information Notice 2009-17

“The NRC has received reports of numerous medical events caused by errors in confusing the units of source strength in the specification of sources—specifically, units of air-kerma strength and apparent activity in units of millicurie (mCi).”

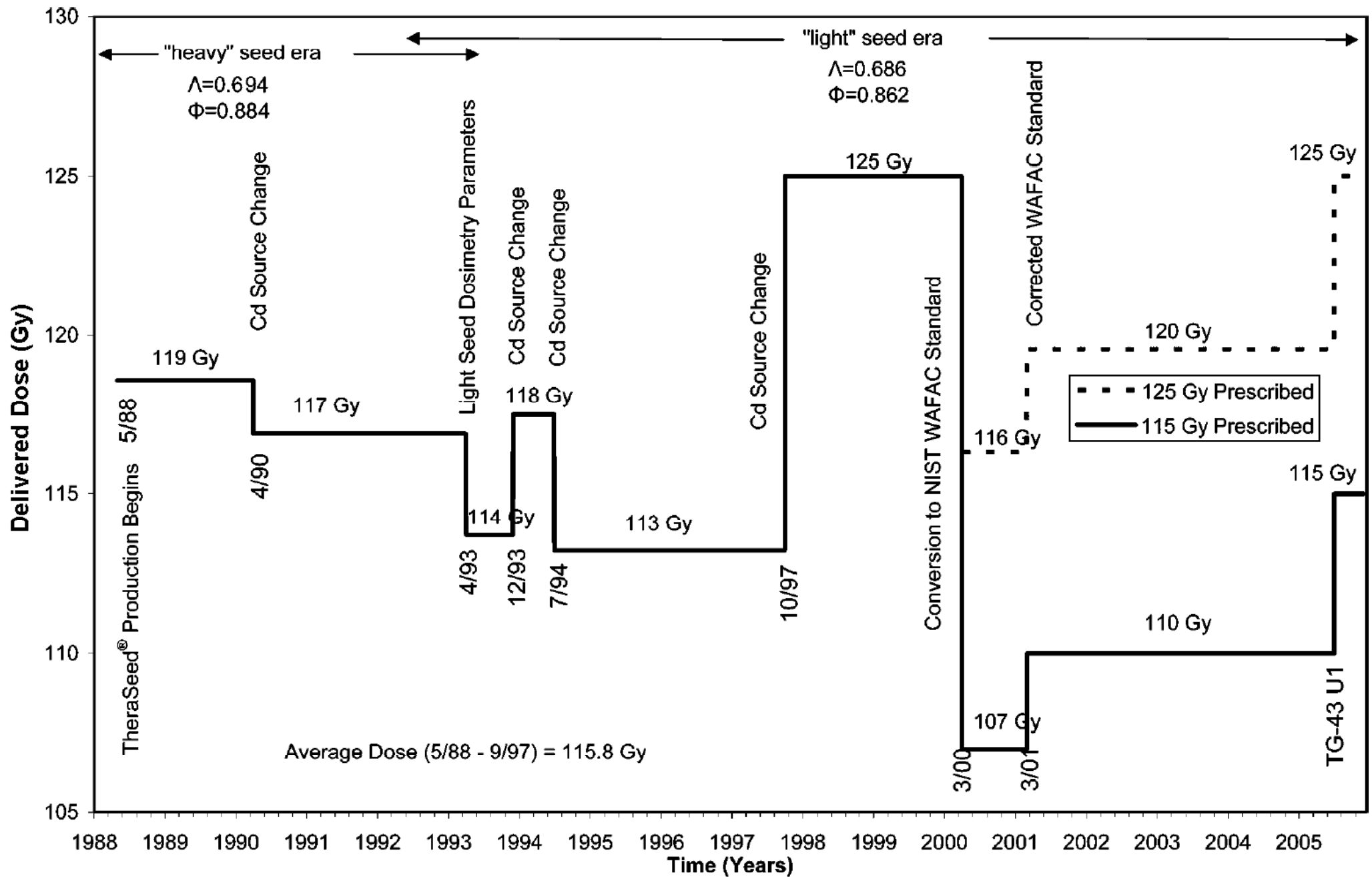
“human error caused all these events”

27% overdose errors with ^{125}I

78% overdose errors with ^{192}Ir

use of apparent activity for brachytherapy sources is
unsafe and inexcusable

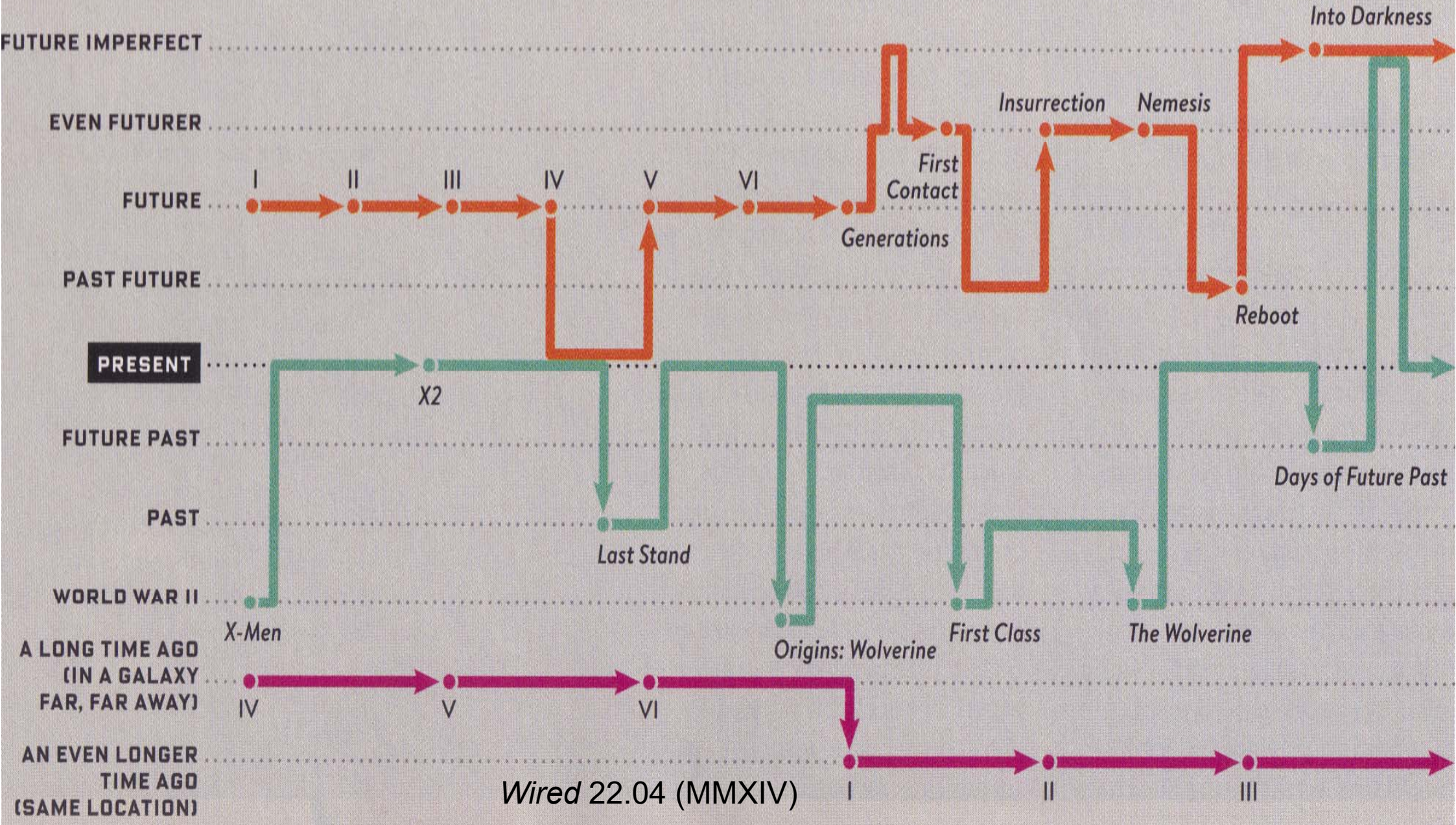
Influence of Missing Calibration on ^{103}Pd Dosage



Impact of Missing Time Calibration on Movies

Sci-Fi Movie Franchises (Location Along Time Continuum)

- STAR TREK
- X-MEN
- STAR WARS



Uncertainty is a Quantitative Measure of Quality

AAPM + ESTRO TG-138 Report

Medical Physics

A dosimetric uncertainty analysis for photon-emitting brachytherapy sources: Report of AAPM Task Group No. 138 and GEC-ESTRO

This report addresses uncertainties pertaining to brachytherapy single-source dosimetry preceding clinical use. The International Organization for Standardization (ISO) Guide to the Expression of Uncertainty in Measurement (GUM) and the National Institute of Standards and Technology (NIST) Technical Note 1297 are taken as reference standards for uncertainty formalism. Uncertainties in using detectors to measure or utilizing Monte Carlo methods to estimate brachytherapy dose distributions are provided with discussion of the components intrinsic to the overall dosimetric assessment. Uncertainties provided are based on published observations and cited when available. The uncertainty propagation from the primary calibration standard through transfer to the clinic for air-kerma strength is covered first. Uncertainties in each of the brachytherapy dosimetry parameters of the TG-43 formalism are then explored, ending with transfer to the clinic and recommended approaches. Dosimetric uncertainties during treatment delivery are considered briefly but are not included in the detailed analysis. For low- and high-energy brachytherapy sources of low dose rate and high dose rate, a combined dosimetric uncertainty $<5\%$ ($k=1$) is estimated, which is consistent with prior literature estimates. Recommendations are provided for clinical medical physicists, dosimetry investigators, and source and treatment planning system manufacturers. These recommendations include the use of the GUM and NIST reports, a requirement of constancy of manufacturer source design, dosimetry investigator guidelines, provision of the lowest uncertainty for patient treatment dosimetry, and the establishment of an action level based on dosimetric uncertainty. These recommendations reflect the guidance of the American Association of Physicists in Medicine (AAPM) and the Groupe Européen de Curiethérapie–European Society for Therapeutic Radiology and Oncology (GEC-ESTRO) for their members and may also be used as guidance to manufacturers and regulatory agencies in developing good manufacturing practices for sources used in routine clinical treatments.

Methodology for Uncertainty Estimation

Guide to Expression of Uncertainty in Measurement
ISO GUM (2010) precision \neq accuracy

Type A (statistical: standard deviation of results)

Type B (non-Type A uncertainties)

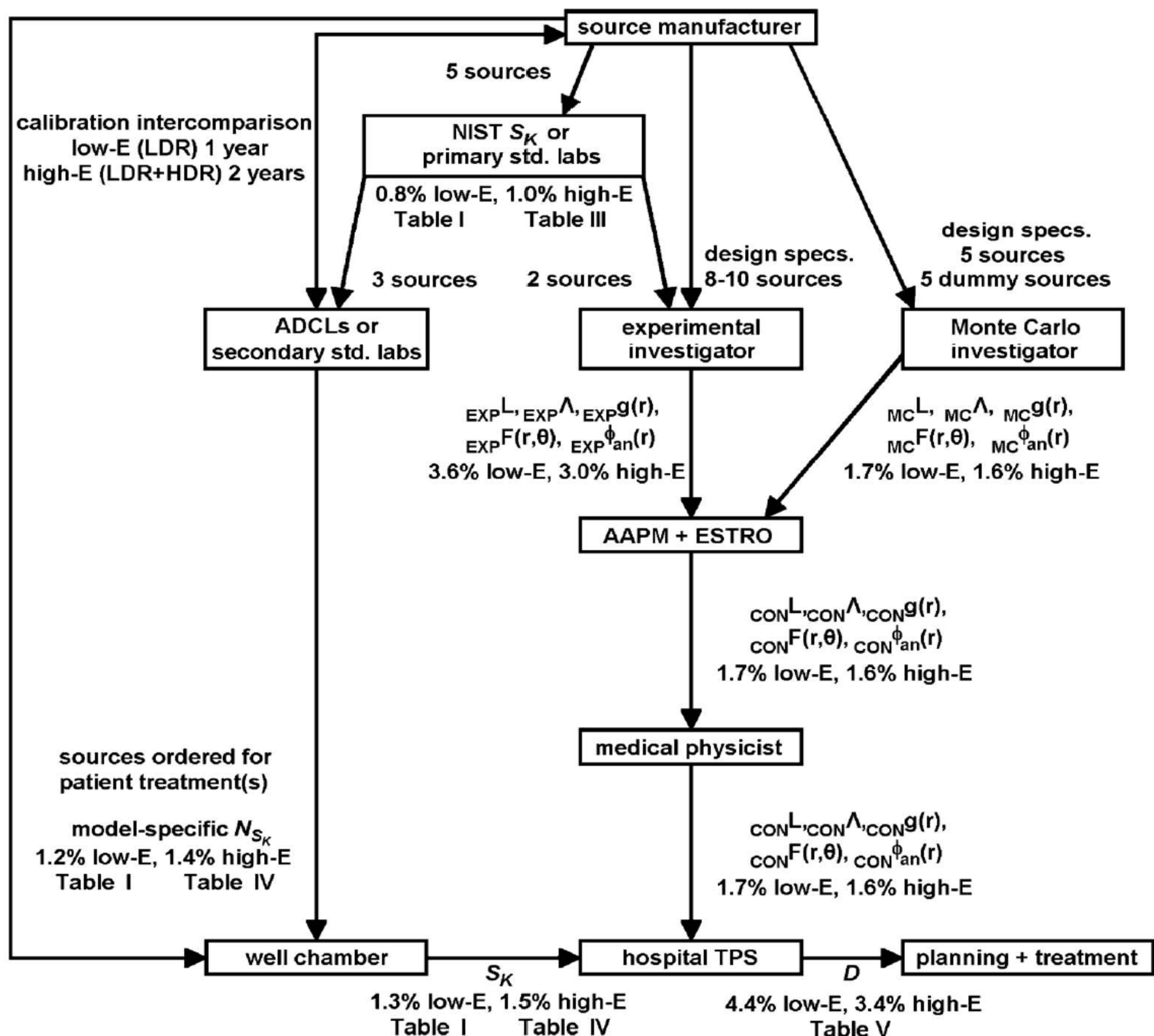
Law of Propagation of Uncertainty (no covariations)

TG-138 applies principles for expressing brachytherapy
dosimetric uncertainties

expanded uncertainty, $k = 2$ (95.45% confidence, 21/22)

special case for large # DOF

$k = t$ -factor otherwise with covariations



Low-Energy Calibration Uncertainty

Table I Propagation of best practice uncertainties ($k = 1$ unless stated otherwise) associated with the transfer of air-kerma strength from NIST through the ADCL to the clinic for LDR low-energy brachytherapy sources.

Row	Measurement description	Quantity (units)	Relative propagated uncertainty (%)
1	NIST WAFAC calibration	$S_{K,NIST}$ (U)	0.8
2	ADCL well ion chamber calibration	$S_{K,NIST} / I_{ADCL}$ (U / A)	0.9
3	ADCL calibration of source from manufacturer	$S_{K,ADCL}$ (U)	1.1
4	ADCL calibration of clinic well ion chamber	$S_{K,ADCL} / I_{CLINIC}$ (U / A)	1.2
5	Clinic measures source air-kerma strength	$S_{K,CLINIC}$ (U)	1.3
	Expanded uncertainty ($k = 2$)	$S_{K,CLINIC}$ (U)	2.6

Table II Propagation of best practice uncertainties ($k = 1$ unless stated otherwise) associated with the transfer of the air-kerma strength standard from NIST to the manufacturer for LDR low-energy brachytherapy sources.

Row	Measurement description	Quantity (units)	Relative propagated uncertainty (%)
1	NIST WAFAC calibration	$S_{K,NIST}$ (U)	0.8
2	Manufacturer well ion chamber calibration	$S_{K,NIST} / I_M$ (U / A)	0.9
3	Manufacturer calibration of QA source	$S_{K,M}$ (U)	1.1
4	Manufacturer instrument calibration for assay	$S_{K,M} / I_M$ (U / A)	1.2
5	Manufacturer assays production sources	$S_{K,M}$ (U)	1.3
6	Manufacturer places sources in 2% or 7% bins	$S_{K,Mbin}$ (U)	1.4 or 2.4
	Expanded uncertainty ($k = 2$)	$S_{K,Mbin}$ (U)	2.8 or 4.8

High-Energy Calibration Uncertainty

Table III Propagation of “best practice” uncertainties associated with the transfer of air-kerma strength from NIST through the ADCL to the clinic for **LDR high-energy** brachytherapy sources. Well chamber measurement uncertainty is estimated to be 0.5 %.

Step	Measurement description	Quantity (units)	Relative propagated uncertainty (%)
1	NIST calibration	$S_{K,NIST}$ (U)	1.0
2	ADCL well ion chamber calibration	$S_{K,NIST} / I_{ADCL}$ (U / A)	1.1
3	ADCL calibration of source from manufacturer	$S_{K,ADCL}$ (U)	1.2
4	ADCL calibration of clinic well ion chamber	$S_{K,ADCL} / I_{CLINIC}$ (U / A)	1.3
5	Clinic measures source air-kerma strength	$S_{K,CLINIC}$ (U)	1.4
	Expanded uncertainty ($k = 2$)	$S_{K,CLINIC}$ (U)	2.8

Table IV Propagation of “best practice” uncertainties associated with the transfer of air-kerma strength from a traceable NIST coefficient from the ADCL to the clinic for **HDR high-energy** brachytherapy sources.

Step	Measurement description	Quantity (units)	Relative propagated uncertainty (%)
1	ADCL calibration	$S_{K,NIST}$ (U)	1.1
2	ADCL well ion chamber calibration	$S_{K,NIST} / I_{ADCL}$ (U / A)	1.2
3	ADCL calibration of source from manufacturer	$S_{K,ADCL}$ (U)	1.3
4	ADCL calibration of clinic well ion chamber	$S_{K,ADCL} / I_{CLINIC}$ (U / A)	1.4
5	Clinic measures source air-kerma strength	$S_{K,CLINIC}$ (U)	1.5
	Expanded uncertainty ($k = 2$)	$S_{K,CLINIC}$ (U)	2.9

Summary of TG-138 Report

- AAPM + ESTRO recommend GUM methods for expressing dosimetric uncertainties
- precision \neq accuracy
- Type A (statistical: standard deviation of results)
Type B (non-Type A uncertainties)
- low-E (8.7%, $k=2$) high-E (6.8%, $k=2$)
- expanded uncertainty, $k=2$ (95% confidence 21/22)
- pre-Tx recommendations: S_K , exp, MC, vendors
- clinical practice uncertainties are larger

AAPM Calibration Recommendations

Medical Physics

Third-party brachytherapy source calibrations and physicist responsibilities: Report of the AAPM Low Energy Brachytherapy Source Calibration Working Group

Compiling and clarifying recommendations established by previous AAPM Task Groups 40, 56, and 64 were among the working group's charges, which also included the role of third-party handlers to perform loading and assay of sources. This document presents working group findings on the responsibilities of the institutional medical physicist and a clarification of the existing AAPM recommendations in the assay of brachytherapy sources. The AAPM leaves it to the discretion of the institutional medical physicist whether the manufacturer's or institutional physicist's measured value should be used in performing dosimetry calculations.

AAPM Calibration Recommendations

TABLE I. Quantities of brachytherapy sources to be assayed by the end-user physicist.

Source form	number to be assayed
All loose sources, nonsterile	$\geq 10\%$ of total or 10 seeds, whichever is larger.
Nonsterile cartridges	$\geq 10\%$ of total via whole cartridge assay or via single sources.
Mixture of nonsterile loose sources and sterile assemblies	Loose sources amounting to $\geq 10\%$ of the total order or ten seeds, whichever is larger.
Sterile source assemblies	$\geq 10\%$ of assemblies via sterile well chamber inserts or quantitative image analysis. Alternatively, order and assay nonsterile loose seeds equal to 5% of the total or five seeds, whichever is fewer.
Strands	$\geq 10\%$ of total or two strands, whichever is larger, using single-seed calibration coefficient (see Ref. 15). Alternatively, order and assay nonstranded loose seeds equal to 5% of the total or five seeds, whichever is fewer.

^aEach source-strength grouping in an order should be sampled. If the number of sources in a strength group is < 10 , the entire group should be assayed.

AAPM Calibration Recommendations

TABLE II. Actions to be taken by the physicist at the end-using institution based on the sample size assayed and the relative difference, ΔS_K , found between the manufacturer's source strength certificate and the assay by the physicist at the using institution.^a

Sample size for assay of sources by end-user medical physicist	ΔS_K	action by medical physicist
Individual source as part of an order of ≥ 10 sources ^b	$\Delta S_K \leq 6\%$	Nothing further.
	$\Delta S_K > 6\%$	Consult with the radiation oncologist regarding use of the outlier source: Dependent on the radionuclide, intended target, source packaging, and the availability of extra sources.
$\geq 10\%$ but $< 100\%$ of order, or batch measurements of individual sterile strands, cartridges or preloaded needles	$\Delta S_K \leq 3\%$	Nothing further.
	$5\% \geq \Delta S_K > 3\%$	Investigate source of discrepancy or increase the sample size.
	$\Delta S_K > 5\%$	Consult with manufacturer to resolve differences or increase the sample size. For assays performed in the operating room, consult with the radiation oncologist regarding whether to use the measured source strength or to average with the manufacturer's value.
100% of order, or batch measurements of each and every individual sterile strand, cartridge or preloaded needle	$\Delta S_K \leq 3\%$	Nothing further.
	$5\% \geq \Delta S_K > 3\%$	Investigate source of discrepancy.
	$\Delta S_K > 5\%$	Consult with manufacturer to resolve differences. For assays performed in the operating room, consult with the radiation oncologist regarding the consequences of proceeding with the implant using the measured source strength.

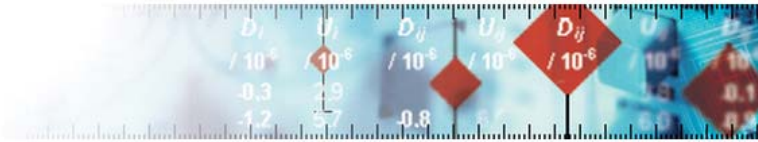
^aAssay results obtained at sites other than the end-user institution should not replace the source strength value on the manufacturer's certificate. The source strength value to be used in planning may be either that stated on the manufacturer's certificate or the value determined by institutional medical physicist when the difference is $\geq 5\%$.

^bFor orders consisting of < 10 sources, the action threshold is $\Delta S_K > 5\%$ for individual sources.

Calibration and Measurement Capabilities Ionizing Radiation



Bureau International des Poids et Mesures



[Home](#)

[Key and supplementary comparisons](#)

[Calibration and Measurement Capabilities - CMCs](#)

[Home](#) > [CMCs Search](#) > [RI search form](#) > [CMC descriptions](#)

CMCs - Result of the search



Physics

- [Acoustics, Ultrasound, Vibration](#)
- [Electricity and Magnetism](#)
- [Length](#)
- [Mass and related quantities](#)
- [Photometry and Radiometry](#)
- [Ionizing Radiation](#)
- [Thermometry](#)
- [Time and Frequency](#)

Chemistry

- [Chemistry](#)

Traceability to the SI through the BIPM

- [BIPM calibration and measurement services](#)

Related links

- [KCDB Statistics](#)
- [KCDB FAQs](#)
- [KCDB Reports](#)
- [CIPM MRA](#)
- [JCRB](#)
- [Find my NMI](#)
- [Metrologia](#)

Contact us

- BIPM.KCDB@bipm.org

Calibration and Measurement Capabilities Ionizing Radiation

Result of the search

→ Your selection : Dosimetry, Reference air kerma rate

17 summary CMC descriptions match your selection. Please select one or more CMCs, then click on 'view' to access more information.

Select	Quantity	Source	Country	NMI	RMO
<input type="checkbox"/>	Reference air kerma rate	Cs-137	Cuba	CPHR	COOMET
<input type="checkbox"/>	Reference air kerma rate	Ir-192	France	LNE	EURAMET
<input type="checkbox"/>	Reference air kerma rate	Co-60	Germany	PTB	EURAMET
<input type="checkbox"/>	Reference air kerma rate	Ir-192	Germany	PTB	EURAMET
<input type="checkbox"/>	Reference air kerma rate	I-125	Germany	PTB	EURAMET
<input type="checkbox"/>	Reference air kerma rate	Cs-137	Greece	IRCL/GAEC-EIM	EURAMET
<input type="checkbox"/>	Reference air kerma rate	Ir-192	Greece	IRCL/GAEC-EIM	EURAMET
<input type="checkbox"/>	Reference air kerma rate	Ir-192	Italy	ENEA-INMRI	EURAMET
<input type="checkbox"/>	Reference air kerma rate	Cs-137	Korea, Republic of	KRISS	APMP
<input type="checkbox"/>	Reference air kerma rate	Ir-192	Netherlands	VSL	EURAMET
<input type="checkbox"/>	Reference air kerma rate	Ir-192	Russian Federation	VNIIM	COOMET
<input type="checkbox"/>	Reference air kerma rate	Co-60	Slovakia	SMU	EURAMET
<input type="checkbox"/>	Reference air kerma rate	Cs-137	Slovakia	SMU	EURAMET
<input type="checkbox"/>	Reference air kerma rate	Cs-137	United States	NIST	SIM
<input type="checkbox"/>	Reference air kerma rate	Ir-192	United States	NIST	SIM
<input type="checkbox"/>	Reference air kerma rate	I-125	United States	NIST	SIM
<input type="checkbox"/>	Reference air kerma rate	Pd-103	United States	NIST	SIM

US: National Institute of Standards and Technology



[NIST Home](#) > [PML](#) > [Radiation Physics Division](#) > [Dosimetry Group](#) > Calibration of Low-Energy Photon Brachytherapy Sources

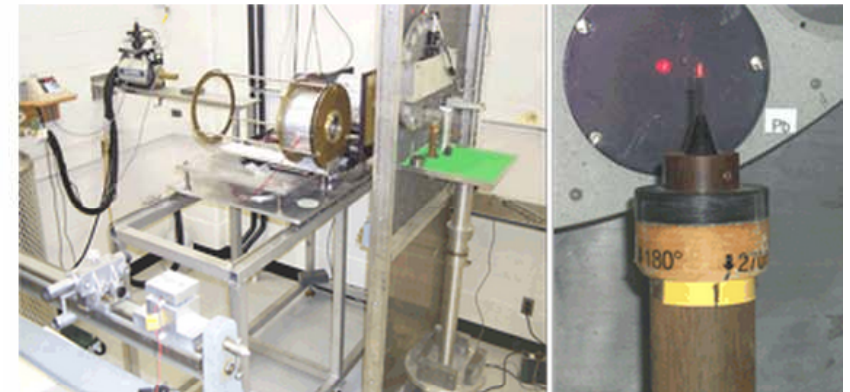
Calibration of Low-Energy Photon Brachytherapy Sources

Summary:

Small radioactive "seed" sources used in prostate brachytherapy, containing the radionuclide ^{103}Pd , ^{125}I , or ^{131}Cs , are calibrated in terms of air-kerma strength using the NIST Wide-Angle Free-Air Chamber (WAFAC). The WAFAC is an automated, free-air ionization chamber with a variable volume, allowing corrections to be made for passage of the beam through non-air-equivalent electrodes.

Description:

Since 1999, over 1,000 seeds of more than 40 different designs from 18 manufacturers have been calibrated using the WAFAC. On-site characterization at seed manufacturing plants for quality control, as well as at therapy clinics for treatment planning, relies on well-ionization chamber measurements. Following the primary standard measurement of air-kerma strength, the responses of several well-ionization chambers to the various seed sources are determined. The ratio of air-kerma strength to well-chamber response yields a calibration coefficient for the well-ionization chamber for a given seed type. Such calibration coefficients enable well-ionization chambers to be employed at therapy clinics for verification of seed air-kerma strength, which is used to calculate dose rates to ensure effective treatment planning. To understand the relationship between well-ionization chamber response and WAFAC-measured air-kerma strength for prostate brachytherapy seeds, emergent x-ray spectra are measured with a high-purity germanium (HPGe) spectrometer.



Photograph by: Michael G. Mitch

Lead Organizational Unit:

PML

Staff:

[Dosimetry Group](#)

[Michael G. Mitch](#)

[Jason S. Walia](#)

NIST: WAFAC (Low-E Sources)

Table 6b. Correction factors for measurements made with the automated WAFAC, assuming a source-to-aperture distance of 30 cm

Correction factor	For:	Currently implemented values		Values from the analyses presented in the text					
		¹²⁵ I	¹⁰³ Pd	¹²⁵ I	¹²⁵ I + Ag Kx	¹²⁵ I + Ag Kx	¹²⁵ I + Ag Kx	¹²⁵ I + Pd Kx	¹⁰³ Pd
1 k_{decay}	Correction to reference date, $T_{1/2}(\text{d})$	59.43	16.991	59.40	59.40	59.40	59.40	59.40	16.991
2 k_{sat}	Recombination inside WAFAC	<1.004	<1.004	<1.004	<1.004	<1.004	<1.004	<1.004	<1.004
3 k_{foil}	Attenuation in filter	1.0295	1.0738	1.0320	1.0342	1.0358	1.0394	1.0417	1.0776
4 $k_{\text{att-WAFAC}}$	Aperture-to-WAFAC air attenuation	1.0042	1.0079	1.0048	1.0050	1.0051	1.0055	1.0057	1.0089
5 $k_{\text{att-SA}}$	Source-to-aperture air attenuation	1.0125	1.0240	1.0143	1.0149	1.0153	1.0163	1.0170	1.0267
6 k_{invsq}	Inverse-square correction for aperture	1.0089	1.0089	1.0089	1.0089	1.0089	1.0089	1.0089	1.0089
7 k_{humidity}	Humidity correction	0.9982	0.9981	0.9979	0.9979	0.9979	0.9979	0.9979	0.9979
8 $k_{\text{int-scatt}}$	In-chamber photon-scatter correction	0.9966	0.9962	0.9968	0.9968	0.9968	0.9967	0.9967	0.9964
9 k_{stem}	Source-holder stem-scatter correction	0.9985	0.9985	0.9985	0.9985	0.9985	0.9985	0.9985	0.9985
10 k_{elec}	In-chamber electron-loss correction	1.0	1.0	1.0	1.0	1.0	1.0	1.0	1.0
11 k_{pen}	Aperture penetration	0.9999	0.9999	0.9999	0.9999	0.9999	0.9999	0.9999	0.9997
12 $k_{\text{ext-scatt}}$	External photon-scatter correction	1.0	1.0	0.9947	0.9947	0.9947	0.9947	0.9947	0.9945
Πk_{3-12}		1.0489	1.1100	1.0483	1.0513	1.0535	1.0585	1.0618	1.1116
	Percent change			-0.06	+0.23	+0.44	+0.92	+1.23	+0.14

NIST: WAFAC (Low-E Sources)

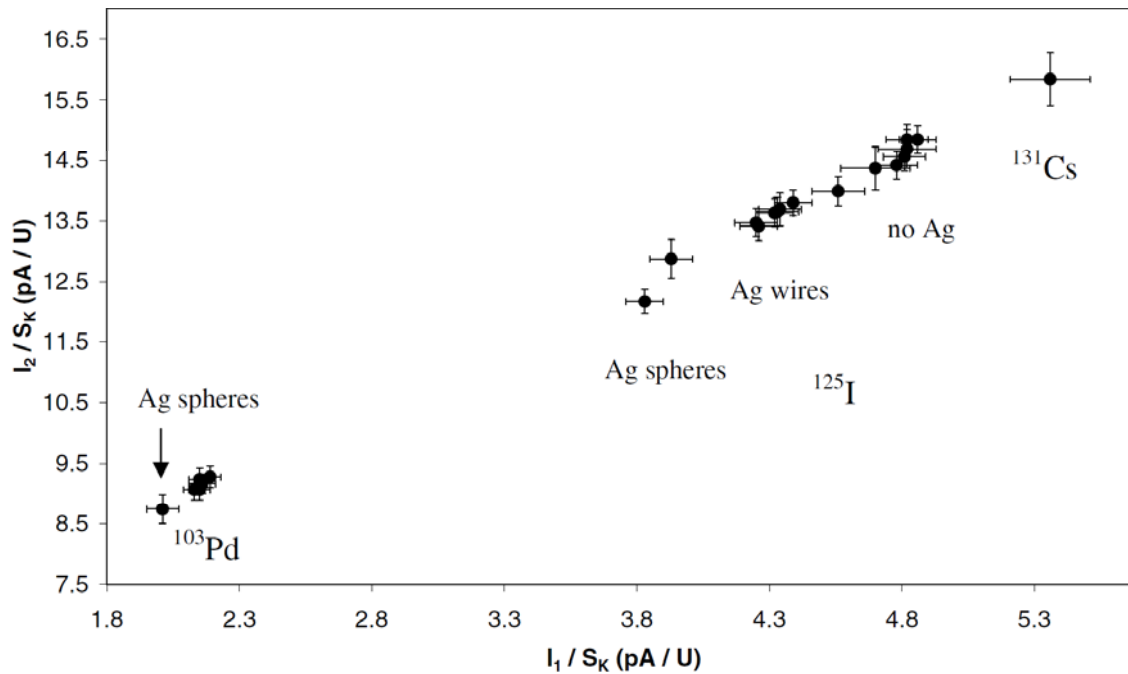
Table 7. Estimated relative standard uncertainties in the determination of air-kerma strength from prostate seeds using the WAFAC

Component	For:	Type A	Relative standard uncertainty, %	
			¹²⁵ I	¹⁰³ Pd
$I_{\text{net,diff}}$	Net current	s_I^a	0.06	0.06
W/e	Mean energy per ion pair		0.15	0.15
ρ_0	Air density		0.03	0.03
d	Source-aperture distance		0.24	0.24
V_{eff}	Effective volume	0.11	0.01	0.01
k_{decay}	Correction to reference date, $T_{1/2}$ (d)		0.02 ^b	0.08 ^b
k_{sat}	Recombination inside WAFAC		0.05	0.05
k_{foil}	Attenuation in filter		0.61	0.51
$k_{\text{att-WAFAC}}$	Aperture-to-WAFAC air attenuation		0.08	0.10
$k_{\text{att-SA}}$	Source-to-aperture air attenuation		0.24	0.31
k_{invsq}	Inverse-square correction for aperture		0.01	0.01
k_{humidity}	Humidity correction		0.07	0.07
$k_{\text{int-scatt}}$	In-chamber photon scatter correction		0.07	0.07
k_{stem}	Source-holder stem-scatter correction		0.05	0.05
k_{elec}	In-chamber electron-loss correction		0.05	0.05
k_{pen}	Aperture penetration		0.02	0.08
$k_{\text{ext-scatt}}$	External photon scatter correction		0.17	0.19
Combined			0.754	0.719

^a Determined as the standard deviation of the mean of the net current.

^b Assuming time from the reference date is no more than ≈ 15 days.

NIST: WAFAC (Low-E Sources)



Correlation of the response coefficients of two well-ionization chambers for various ^{103}Pd , ^{125}I and ^{131}Cs source

	Value	$s_i/\%$	$u_j/\%$
Net current, I_{net}		s_1	0.06
\bar{W}/e	33.97 J C ⁻¹	—	0.15
Air density, ρ_{air}	1.196 mg cm ⁻³	—	0.03
Aperture distance, d		—	0.24
Effective chamber volume, V_{eff}		0.11	0.01
Decay correction, k_1	$T_{1/2} = 59.43$ d	—	0.02
Recombination, k_2	< 1.004	—	0.05
Attenuation in filter, k_3	1.0295	—	0.61
Air attenuation in WAFAC, k_4	1.0042	—	0.08
Source–aperture attenuation, k_5	1.0125	—	0.24
Inverse-square correction, k_6	1.0089	—	0.01
Humidity, k_7	0.9982	—	0.07
In-chamber photon scatter, k_8	0.9966	—	0.07
Source-holder scatter, k_9	0.9985	—	0.05
Electron loss, k_{10}	1.0	—	0.05
Aperture penetration, k_{11}	0.9999	—	0.02
External photon scatter, k_{12}	1.0	—	0.17
Combined uncertainty			$(s_1^2 + 0.762^2)^{1/2}$

NIST: Electronic Brachytherapy

NIST | NIST Time | NIST Home | About NIST | Contact Us | A-Z Site Index | Search

Physical Measurement Laboratory

About PML | Publications | Topic/Subject Areas | Products/Services | News/Multimedia | Programs/Projects | Facilities

NIST Home > PML > Radiation Physics Division > Dosimetry Group > Calibrations of a Miniature X-ray Source Used for Electronic Brachytherapy

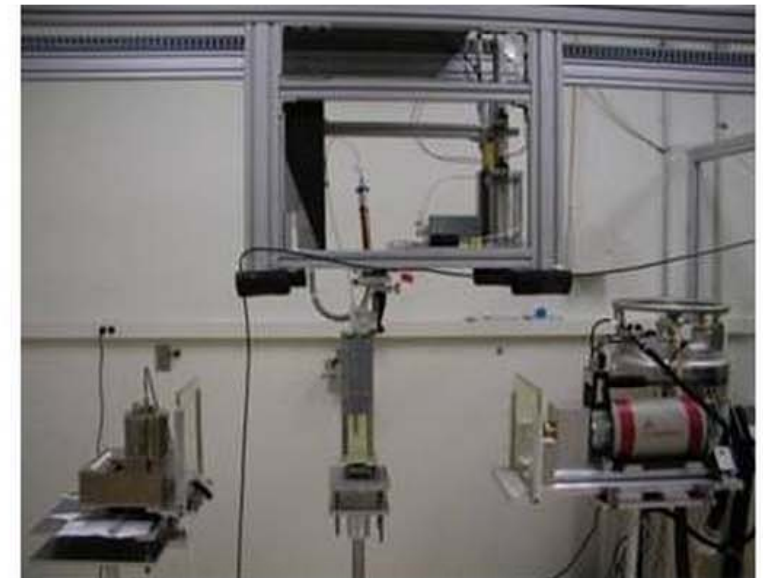
Calibrations of a Miniature X-ray Source Used for Electronic Brachytherapy

Summary:

A new laboratory dedicated to establishing a national primary air-kerma rate standard for Xoft's AXXENT™ miniature x-ray source has been fabricated. The Xoft source was designed to provide low-energy xrays (< 50 keV) for use in brachytherapy.

Description:

The Xoft source was designed to provide low-energy x-rays (< 50 keV) for use in brachytherapy. The air-kerma rate is being directly realized through use of the Lamperti free-air chamber, which was compared with another national x-ray standard with these sources. A high-purity germanium (HPGe) x-ray spectrometer is used to monitor the energy spectrum of the beam in real time, as well as provide necessary input data for Monte Carlo calculations of correction factors for the free-air chamber. To account for spatial anisotropy of emissions, the free-air chamber and spectrometer are rotated about the long axis of the x-ray tube during measurements. The response of well-ionization chambers to the x-ray sources is being studied in preparation for the development of a measurement assurance program for the dissemination of the new NIST standard to Accredited Dosimetry Calibration Laboratories (ADCLs). The ADCLs are accredited by the American Association of Physicists in Medicine (AAPM), and calibrate radiation measuring instruments for use in therapy clinics.



Xoft AXXENT (tm) electronic brachytherapy source in NIST Laboratory. (Photograph by: Michael G. Mitch)

- Homepage
- About PTB
- Structure**
- Thematic tours
- What's new
- Publications
- Jobs/Training
- Services
- Technology Transfer
- Forschung in Europa

Dosimetry

Structure > Abt. 6 Ionisierende Strahlung > Measurement and calibration capabilities > Dosimetry

Photon radiation

Reference air kerma rate

Contact person: Dr. H.-J. Selbach, *Phone:* +49 531 592 6220, *Fax:* +49 531 592 6405

Description	Details
γ-radiation (Ir-192)	
γ-radiation (Co-60)	

PTB: RAKR Capabilities

3.1 Weitergabe der Einheiten im gesetzlichen Messwesen

U_r Relative erweiterte Messunsicherheit, die sich aus der Standardmessunsicherheit durch Multiplikation mit dem Erweiterungsfaktor $k = 2$ ergibt. Sie wurde gemäß dem "Guide to the Expression of Uncertainty in Measurement" (ISO, 1995) ermittelt. Der Wert der Messgröße liegt im Regelfall mit einer Wahrscheinlichkeit von annähernd 95 % im zugeordneten Werteintervall.

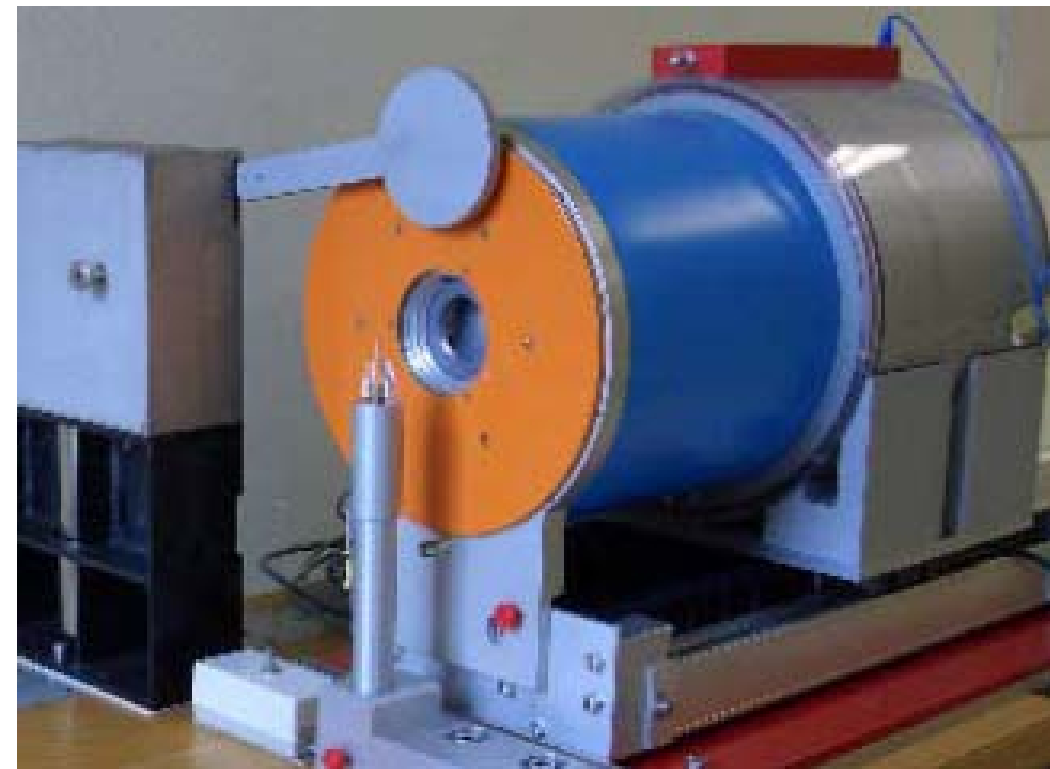
Einträge in "The BIPM key comparison database (KCDB)", <http://www.bipm.org>

Bezeichnung	Calibration or Measurement Service			Messbereich Measurand level or range			Messbedingungen Measurement conditions		U_r in %	Arbeitsanweisung	Zuständig	Aufgabe	Bemerkung
	Service identification	Messgröße Quantity	Instrument or Artifact	Instrument Type or Method	Min Min	Max Max	Einheit Unit	Parameter Parameter		Spezifikation Specification	Work instruction	Responsible	Task
EUR-RAD-PTB-1001	Absorbed dose rate to water	Dosemeter	Conversion coefficient, PMMA phantom	2,0E-04	2,0E-02	Gy s ⁻¹	X-rays 10 kV to 50 kV	10 kV to 40 kV DIN 6809/4 1988	2,8	AA-6200-001	6.2	09	Approved on 15 November 2010
EUR-RAD-PTB-1002	Absorbed dose rate to water	Dosemeter	Conversion coefficient, PMMA phantom	2,0E-04	2,0E-02	Gy s ⁻¹	X-rays 50 kV to 420 kV	50 kV to 100 kV DIN 6809/4 1988	2,8	AA-6200-001	6.2	09	Approved on 15 November 2010
EUR-RAD-PTB-1003	Absorbed dose rate to water	Dosemeter	Secondary standard in a water phantom	2,0E-04	2,0E-03	Gy s ⁻¹	X-rays 50 kV to 420 kV	100 kV to 300 kV DIN 6809/5 1996	2,1	AA-6200-001	6.2	09	Approved on 15 November 2010
EUR-RAD-PTB-1004	Absorbed dose rate to water	Dosemeter	Calibration in water phantom, reference field	2,0E-03	2,0E-02	Gy s ⁻¹	Co-60	DIN 6800/2 2008	0,5	AA-6200-010	6.2	08	Approved on 15 November 2010
EUR-RAD-PTB-1005	Reference air kerma rate	Ir-192 source (HDR, PDR, wire)	Transfer chamber calibrated with primary cavity chamber	1,0E-04	1,0E-01	Gy h ⁻¹	air kerma free in air at 1 m	DIN 6800/2 2008	1,8	AA-6200-022	6.2	11, 12	Approved on 15 November 2010
EUR-RAD-PTB-1006	Reference air kerma rate	Well-type chamber ionization chamber	Ir-192 reference field	1,0E-04	1,0E-01	Gy h ⁻¹	air kerma free in air	DIN 6800/2 2008	2,0	AA-6200-022	6.2	11, 12	Approved on 15 November 2010
EUR-RAD-PTB-1007	Reference air kerma rate	Co-60 HDR-source	Transfer chamber calibrated with primary cavity chamber	1,0E-04	1,0E-01	Gy h ⁻¹	air kerma free in air	DIN 6800/2 2008	1,5	AA-6200-022	6.2	11, 12	Approved on 15 November 2010
EUR-RAD-PTB-1008	Reference air kerma rate	Well-type chamber ionization chamber	Co-60 reference field	1,0E-04	1,0E-01	Gy h ⁻¹	air kerma free in air	DIN 6800/2 2008	1,7	AA-6200-022	6.2	11, 12	Approved on 15 November 2010
EUR-RAD-PTB-1009	Reference air kerma rate	I-125	Calibration using primary standard extrapolation chamber	1,0E-06	1,0E-04	Gy h ⁻¹	air kerma free in air	AAPM TG43	1,8	AA-6200-025	6.2	11, 12	Approved on 15 November 2010
EUR-RAD-PTB-1010	Reference air kerma rate	Well-type chamber	I-125 reference field	1,0E-06	1,0E-04	Gy h ⁻¹	air kerma free in air	AAPM TG43	2,0	AA-6200-025	6.2	11, 12	Approved on 15 November 2010

PTB: Grossvolumen Extrapolationskammer (GROVEX)

Electrode separation	50 mm	100 mm	150 mm	200 mm
Correction factor	1.0000	1.0001	1.0002	1.0003

Cause of the uncertainty	$u \times 100$	Degree of freedom	Index
Ionization current measurement (reproducibility)	0.5	100	32.6%
Electrode separation	0.06	50	0.4%
Air density and humidity	0.05	50	0.3%
Electrode area	0.5	50	33.0%
Source-to-measurement point distance	0.035	∞	0.2%
Incomplete ion collection	0.03	∞	0.1%
Attenuation in the Al-filter	0.5	∞	27.8%
Attenuation in the entrance window	0.12	∞	1.7%
Attenuation and scatter between source and entrance window	0.12	∞	1.7%
Attenuation and scatter in the chamber volume	0.12	∞	1.7%
Source holder	0.06	∞	0.4%
Combined uncertainty ($k = 1$)	0.9		
Uncertainty U ($k = 2$)	1.8		



Seed	PTB	UW	NIST	GROVEX	GROVEX
	GROVEX	VAFAC	WAFAC	VAFAC	WAFAC
	$\mu\text{Gy h}^{-1}$	$\mu\text{Gy h}^{-1}$	$\mu\text{Gy h}^{-1}$		
^{103}Pd No 1	26.307	26.389	26.4	0.997	0.997
^{103}Pd No 2	26.327	26.380	26.44	0.998	0.996
^{103}Pd No 3	27.973	26.951	26.90	1.001	1.003
^{125}I No 1	17.288	17.138	17.16	1.009	1.007
^{125}I No 2	12.191	12.226	12.25	0.997	0.995
^{125}I No 3	17.093	17.053	17.18	1.002	0.995

PTB: GROVEX II (Low-E Sources)

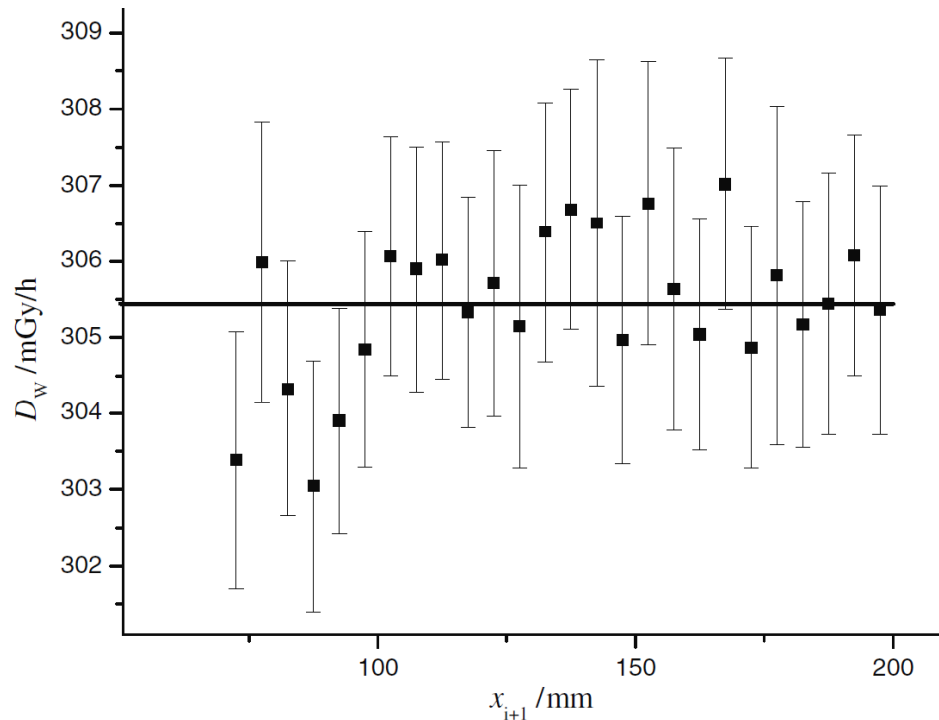


Figure 4. Results of a single extrapolation chamber measurement of an I-125 seed (BEBIG Symmetra I25.S16).

Table 2. Uncertainty budget of the absorbed-dose-rate to water \dot{D}_w .

Quantity	$(\Delta U/U) \times 100$	Index $\times 100$
r	0.2	6.7
k_{div}	0.1	8.3
A	0.5	14.7
k_{inv}	0.4	9.5
SYS_{EXP}	0.9	47.6
STAT_{EXP}	0.3	12.1
k_{hold}	0.1	0.2
k_{sat}	0.1	0.8
Total	1.3	$k = 1$

With a value of 1.3%, the total uncertainty is well below the targeted value of 2%.

As the next step, the measuring device will be optimized for routine measurements so that a calibration service can be started in the near future.

HDR and LDR brachytherapy

Calibration Service for ^{192}Ir High Dose Rate (HDR) Brachytherapy Dosimeters

NPL's ^{192}Ir HDR brachytherapy calibration service is for ionisation chambers used as secondary standards or instruments required for measurement of the greatest accuracy. Calibration of either an ionisation chamber alone or of a complete system including an electrometer is available.

Service Features

- Calibration directly against the NPL air kerma primary standard
- Reference air kerma rate (RAKR) of the ^{192}Ir source up to 50 mGy/h

Specification and Availability

- Calibration of well-type (re-entrant) chambers suitable for HDR sources
- Calibration of thimble chambers with customer provided calibration jig
- Electrometer calibration (charge or current calibration)
- Calibrations are normally carried out in spring, and are undertaken using a microSelectron ^{192}Ir HDR source
- Calibration conforms to IPEM Code of Practice (2010)



Well chambers



Thimble chamber calibration jig

For more information, please contact [Thorsten Sander](#) or our [Radiation Dosimetry Team](#)

Calibration Service for Low Dose Rate (LDR) Brachytherapy Sources

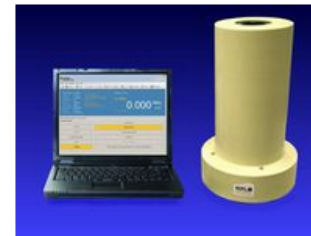
NPL's LDR brachytherapy service includes the calibration of ^{125}I seeds and ^{192}Ir wires and pins. The sources are calibrated with the Fidelis secondary standard radionuclide calibrator.

Service Features

- Source calibration traceable to the NPL air kerma primary standard

Specification and availability

- Source calibrations in terms of $\mu\text{Gy/h}$ at 1 m or MBq
- Calibration of ^{125}I seeds and ^{192}Ir wires and pins, including ^{125}I seeds (e.g. IMC 6711 OncoSeedTM, IMC 7000 RAPIDStrandTM) and ^{192}Ir wires and pins (e.g. Amersham ICW-series)
- Calibrations of other source types/configurations possible
- Calibrations are available by arrangement throughout the year



Fidelis secondary standard radionuclide calibrator

NPL: HDR ^{192}Ir Graphite Calorimetry

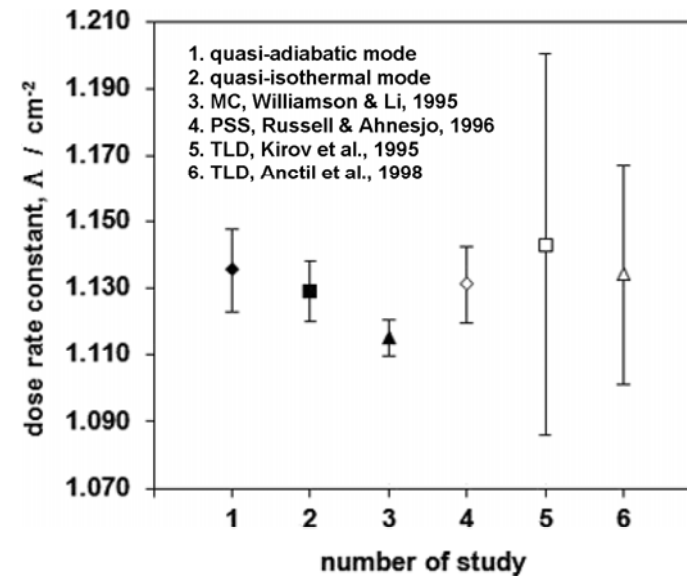
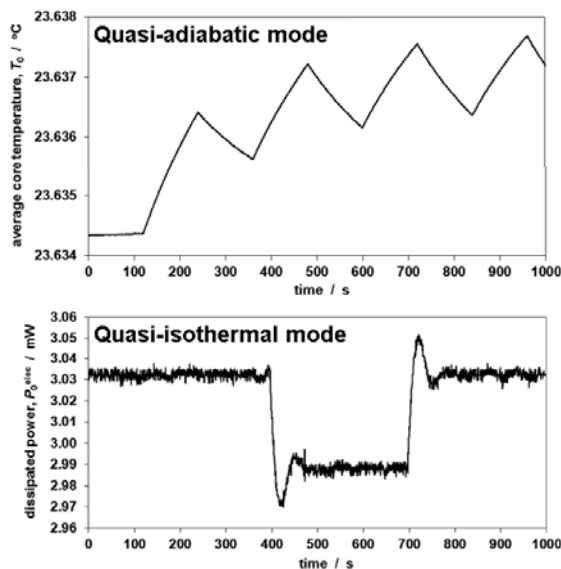
Table 2. Uncertainty budget of the HDR brachytherapy calorimeter for quasi-adiabatic absorbed dose rate measurements.

Quantity	Relative standard uncertainties	
	100 × Type A	100 × Type B
Repeatability of dT_0/dt measurements	0.60	—
Thermistor calibration	—	0.10
Heat transfer correction factor, $k_{\text{ht},q-a}$	—	0.50
Specific heat capacity of core, c_p	—	0.50
Radial source position	—	0.10
Vertical source position	—	0.10
Transient time	—	0.05
MC calculated perturbation correction factors	0.10	0.10
Graphite-to-water conversion	—	0.35
Quadratic summation	0.61	0.82
Combined relative standard uncertainty in $\dot{D}_{w,1\text{cm}}$	1.02	

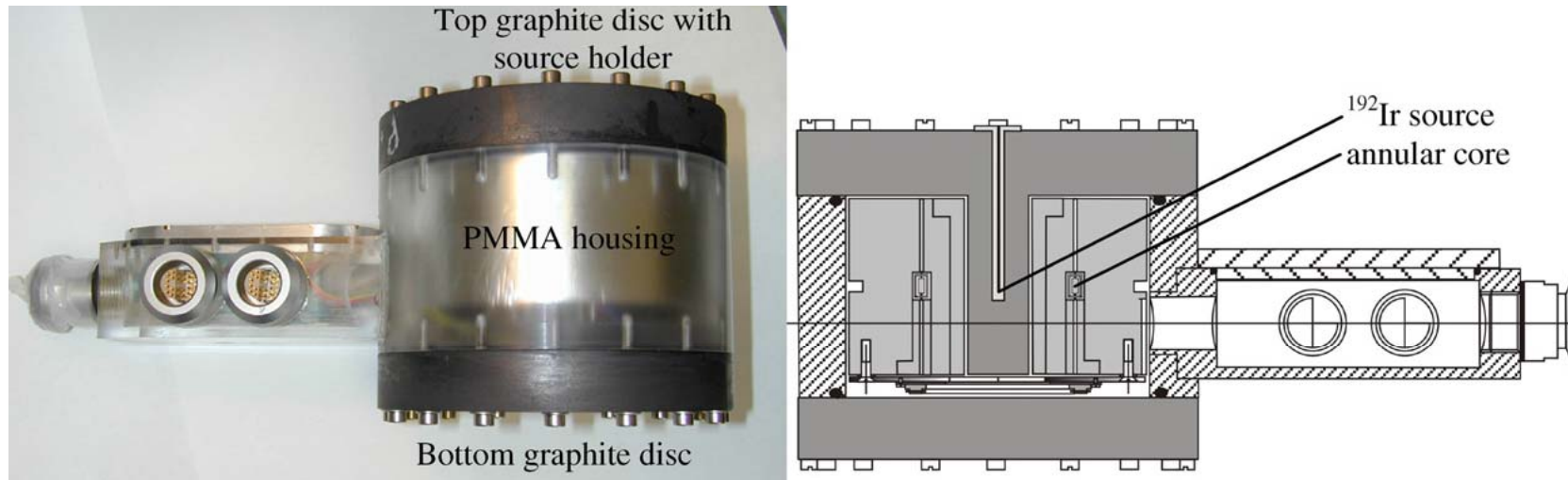
Table 3. Uncertainty budget of the HDR brachytherapy calorimeter for quasi-isothermal absorbed dose rate measurements.

Quantity	Relative standard uncertainties	
	100 × Type A	100 × Type B
Repeatability of ΔP_0^{elec} measurements	0.20	—
Stability of power supplies	—	0.05
Heat transfer correction factor, $k_{\text{ht},q-i}$	—	0.50
Mass of core, m_0	—	0.10
Radial source position	—	0.10
Vertical source position	—	0.10
MC calculated perturbation correction factors	0.10	0.10
Graphite-to-water conversion	—	0.35
Quadratic summation	0.22	0.64
Combined relative standard uncertainty in $\dot{D}_{w,1\text{cm}}$	0.68	

$$\dot{D}_{w,1\text{cm}} = -\frac{\Delta P_0^{\text{elec}}}{m_0} k_{\text{ht},q-i} k_{\text{gr}/w} k_{\text{volavg}} k_{\text{imp}} k_{\text{gap}} k_{\text{inh}} k_{\text{fullscat}}$$



Italy (ENEA-INMRI): HDR ^{192}Ir Graphite Calorimetry



$$\dot{D}_{w, 1 \text{ cm}} = \frac{f_c k_{qa} k_{gap} k_{fs} k_{vol \text{ avg}} k_{gw} k_{sh}}{m}$$

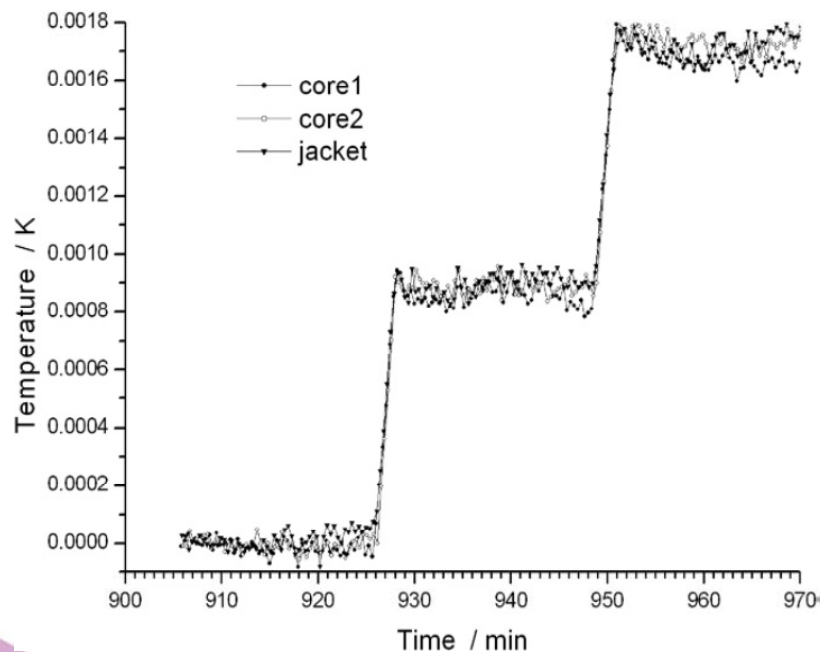
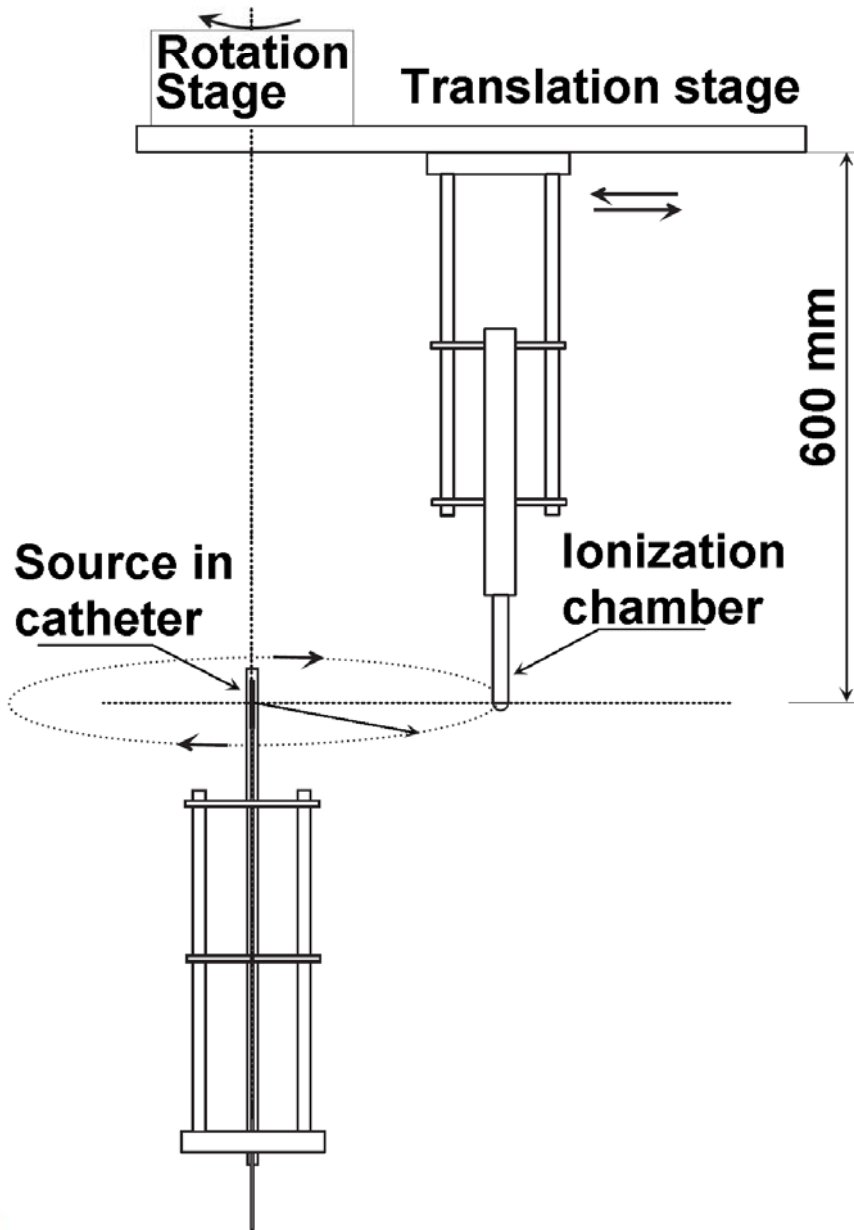


Table 1. Relative standard uncertainty for the determination of D_w .

Quantity	Value	Relative standard uncertainty	
		100 s_i	100 u_j
$-f_c/(\Delta\Omega/\Omega) \text{ s}^{-1}$	1.073×10^{-6}	1.11	0.10
$-k_{qa}/(J/(\Delta\Omega/\Omega))$	52.09	0.59	0.15
$-k_{gap}$	0.998	0.14	0.15
$-k_{fs}$	1.020	0.20	0.15
$-k_{vol \text{ avg}}$	1.004	0.15	0.15
$-k_{gw}$	6.890	0.12	0.15
$-k_{sh}$	0.997	—	0.10
$-m/g$	2.767	—	0.15
Measurement time /s	120	—	0.2
Source positioning		—	0.18
Quadratic summation		1.30	0.48
Combined relative standard uncertainty of \dot{D}_w ($1.418 \times 10^{-1} \text{ Gy s}^{-1}$)			1.38

France: LNE–LNHB HDR ^{192}Ir Calibration



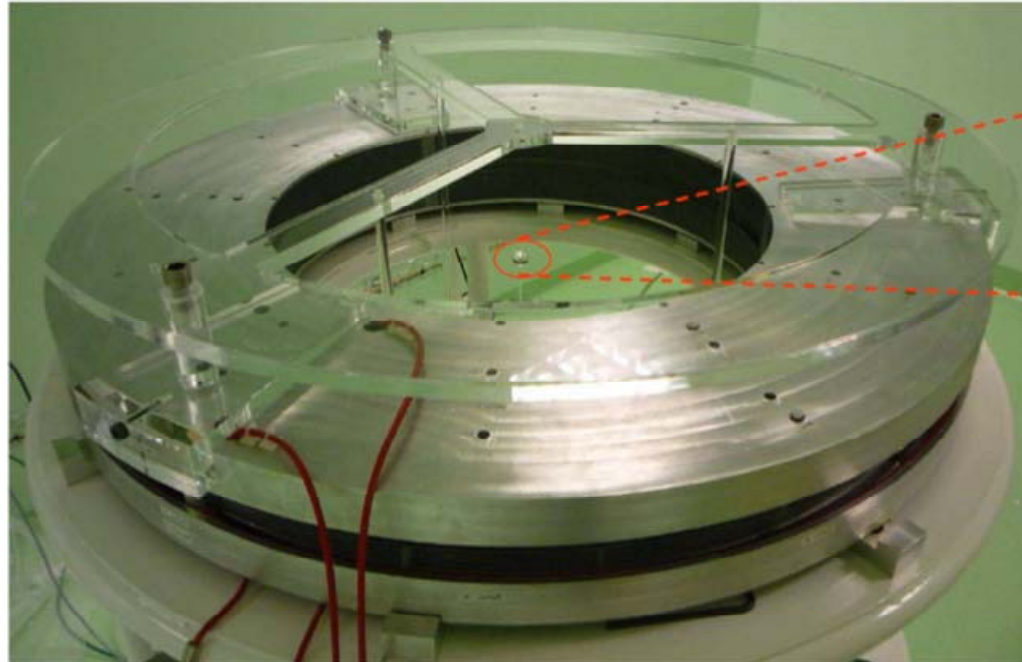
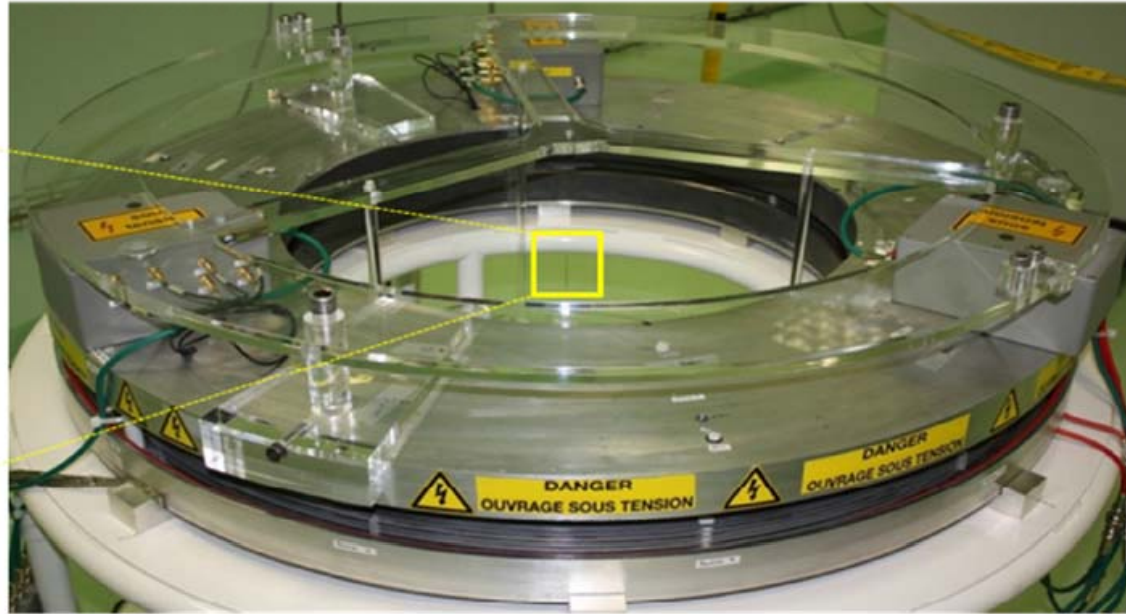
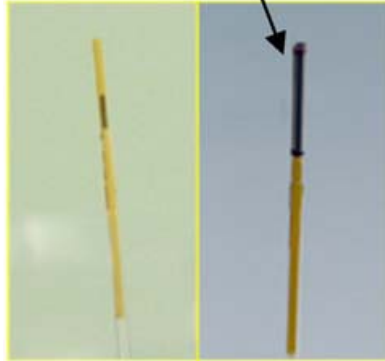
Uncertainty budget for a typical routine well-type chamber calibration (LNHB).

	Value	Relative standard uncertainty (%)	
		Type A	Type B
$\dot{K}_R(0)(\text{Gy h}^{-1} (1 \text{ m}))$	3.239×10^{-2}	–	0.60
$I (\text{A})$	3.1441×10^{-8}	<0.01	0.20
k_{dec}	1.07790	–	<0.01
k_{rec}	1.0005	<0.01	0.03
Combined standard uncertainty			0.63
Expanded uncertainty ($k = 2$)			1.3

Ionization chamber	UWADCL	LNHB	Discrepancy (%)
Nucletron 077.091 (S/N 25324)	9.421×10^5	9.432×10^5	–0.12
Standard Imaging HDR1000+ (S/N A002231)	4.652×10^5	4.665×10^5	–0.28
Standard Imaging HDR1000+ (S/N A032012)	4.659×10^5	4.669×10^5	–0.22

LNE-LNHB: ^{125}I Air-Kerma and Absorbed Dose to Water

Aluminum tube
to remove Ti K
X-rays



Iodine seed at the
centre of the 1 cm
PMMA sphere.

Sweden: HDR ^{192}Ir Calibration Audit

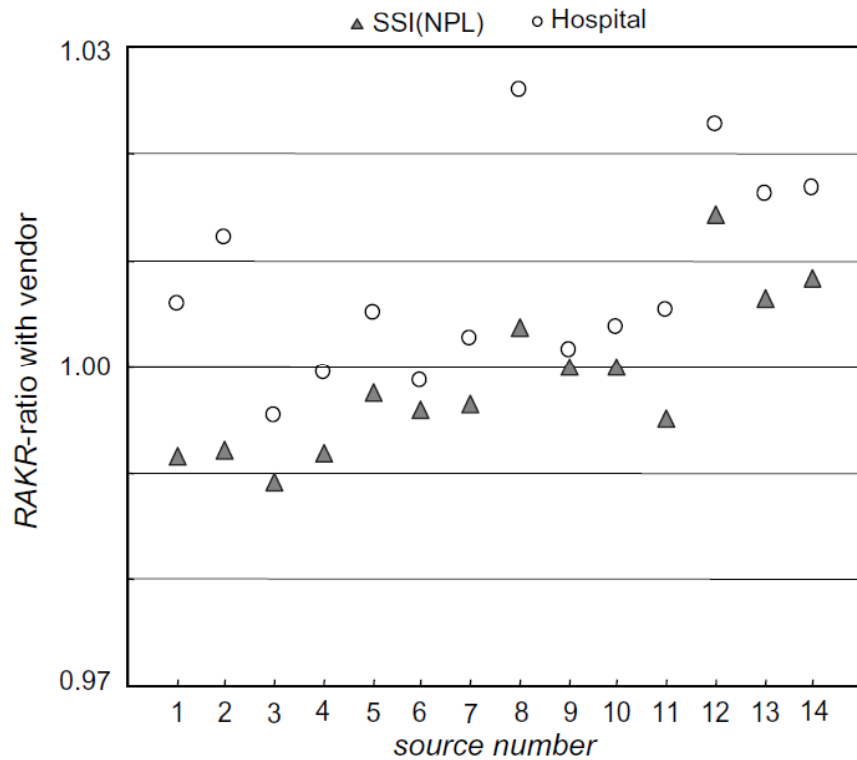


Fig. 4. Ratios of SSI- and hospital-determined *RAKR* values, respectively, to the corresponding values on vendor certificates.

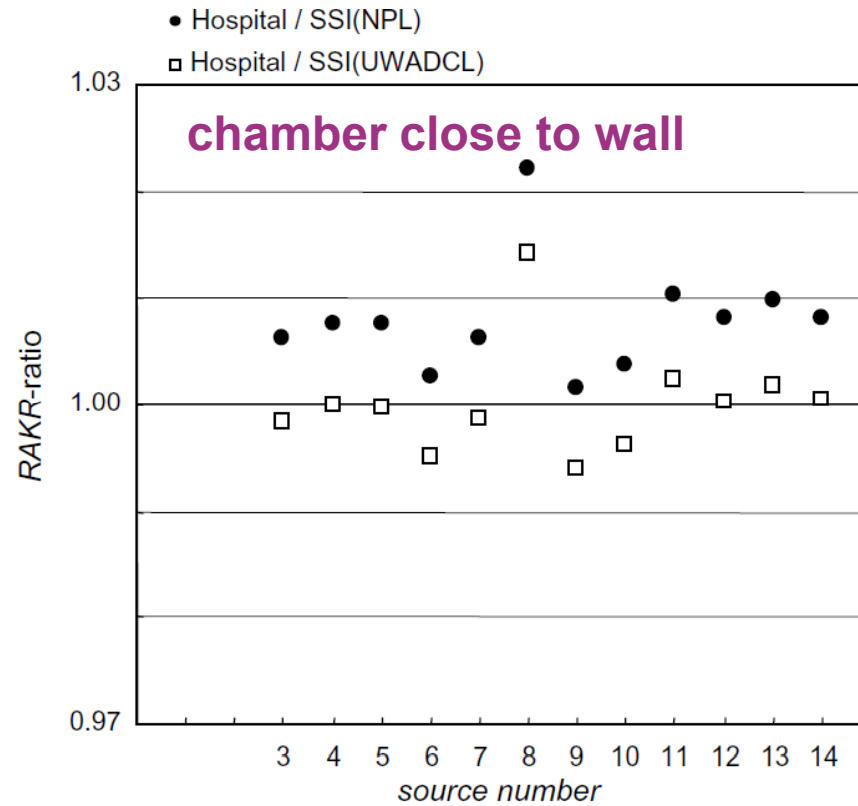


Fig. 5. Comparing ratios of the *RAKR* determined by the hospitals to those determined by SSI using either the NPL- or the UWADCL-calibration factor.

The well-type chamber of the Swedish Secondary Standard Laboratory is traceable to the HDR ^{192}Ir primary standard at NPL, and all Swedish hospitals use well-type chambers fulfilling recommendations for use in brachytherapy.

Calibration of photon and beta ray sources used in brachytherapy

*Guidelines on standardized procedures at
Secondary Standards Dosimetry Laboratories (SSDLs) and hospitals*



INTERNATIONAL ATOMIC ENERGY AGENCY

IAEA

March 2002

Chapter 5: Calibration at the SSDL and Hospital Level

5.1. Establishment of standards for photon and intravascular sources

5.1.1. Traceability in calibrations at SSDLs

The recommended detector is an appropriately calibrated well type chamber. The preferred traceability method is to have the well type chamber calibrated against the primary standard at the PSDL. Calibrations at an ADCL or the IAEA Dosimetry Laboratory can serve as an alternative. This calibration should be carried out for each radionuclide and source type to be used.

5.1.2. Traceability in calibrations at hospitals

It is recommended that for brachytherapy sources be calibrated with an appropriately calibrated well type chamber. For traceability, the well type chamber should be calibrated at the SSDL (or ADCL).

Chapter 5: Calibration at the SSDL and Hospital Level

5.2. Maintenance of standards for photon sources and intravascular sources

Well type chambers should be recalibrated regularly. SSDL recalibrations at ^{137}Cs quality can be made at a PSDL or the IAEA Dosimetry Laboratory.

5.3. Maintenance of standards for ^{192}Ir quality

Upon calibrating well type chambers every 2 years with HDR ^{192}Ir sources, some chamber types have shown calibration factor constancy to within 0.5%, and chamber-to-chamber variation of the ratio of HDR ^{192}Ir source calibration to ^{137}Cs and ^{60}Co also within 0.5%. Thus, a practical solution for checking a well chamber HDR ^{192}Ir source calibration factor is for the physicist to monitor chamber response throughout its lifetime by bracketing the ^{192}Ir average energy of 397 keV with ^{137}Cs and ^{241}Am sources.

Chapter 5: Calibration at the SSDL and Hospital Level

5.5. Guidance on constancy limits for well type chambers

Chamber output stability should be checked at least 4 times per year. If the calibration factor from ^{137}Cs re-calibrations, and periodic constancy checks, remain the same within 1% for high-energy photon sources, or within 1.5% for low-energy photon sources, it can reasonably be assumed that the calibration factor for other sources has not changed. Recalibration is recommended if it is observed that response changes by more than the limits given above.

5.6. Electrometer to be used

IEC 60731 describes desired characteristics of electrometers. They also shall be capable of measuring up to $0.2 \mu\text{A}$ for HDR sources and have a signal resolution of 0.1%. For LDR sources, signal resolution should be $\leq 10 \text{ fA}$ or less; this may be achieved by charge resolution of 0.2 pC when used in charge integration mode. It may be necessary to have two electrometers to cover the full range of brachytherapy sources to be calibrated.

Chapter 6: Calibration Using Free In-air Measurements

6.1. General

The free in-air measurement technique cannot be used for low-energy sources due to air-kerma calibration factor uncertainties, low air-kerma rates, and uncertainties due to air humidity. For long-lived radionuclides, e.g., ^{137}Cs , a source can be a working standard.

$$K_R = N_K \cdot (M_u/t) \cdot k_{\text{air}} \cdot k_{\text{scatt}} \cdot k_n \left(d/d_{\text{ref}} \right)^2$$

6.2. Formalism for reference air kerma rate

K_R reference air kerma rate

N_K chamber air kerma calibration factor at desired photon energy

M_U measured charge, corrected for T, P, recombination, transit error

t time for collecting charge

k_{scat} correction for room scatter

k_n correction factor for non-uniform electron fluence within the cavity

d measurement distance from source center to chamber center

d_{ref} reference measurement distance (i.e., 1 meter)

Chapter 6: Calibration Using Free In-air Measurements

6.3. Ionization chambers to be used

For HDR sources, chambers volumes $> 0.5 \text{ cm}^3$ can be used (e.g. Baldwin-Farmer 0.6 cm^3 chamber). For LDR sources, chamber volumes up to $1,000 \text{ cm}^3$ may be used for sufficient signal, but have large non-uniformity correction factor uncertainties. For ^{192}Ir , chambers should have air-kerma calibration factors vary less than 5% between ^{60}Co and 60 keV.

6.4. Air kerma calibration of ionization chambers

6.5. Correction factors for free in-air measurements

6.6. Uncertainty of free in-air calibration

etc., etc.

Chapter 7: Calibrations Using Well Type Chambers

7.1. General guidance

7.2. Calibration of SSDL reference sources

7.3. Calibration of hospital's well type chamber

The hospital's well chamber system is calibrated at the SSDL using the SSDL reference source. The response curve, spacer and insert, ion recombination, atmospheric communication, and air kerma calibration are checked.

7.4. Calibration of hospital's non-standard ^{137}Cs sources

7.5. Guidance for some special cases

7.6. Calibration of source trains

7.7. Traceability of ^{137}Cs source calibrations

etc., etc.

2004 ESTRO Booklet 8

A PRACTICAL GUIDE TO QUALITY CONTROL OF BRACHYTHERAPY EQUIPMENT
EUROPEAN SOCIETY FOR THERAPEUTIC RADIOLOGY AND ONCOLOGY

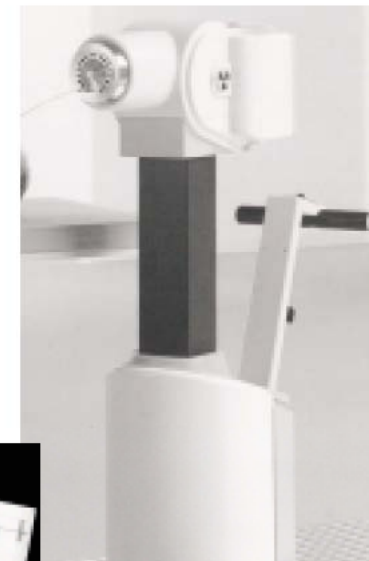
ESTRO 



*Supported by the EU
"Europe against Cancer" Programme
Grant Agreements N°SPC.2002480 / S12.322029*

*Edited by
Jack Venselaar
José Pérez-Calatayud*

A PRACTICAL GUIDE TO QUALITY CONTROL OF BRACHYTHERAPY EQUIPMENT



Chapter 3: Calibration of Brachytherapy Sources

3.3 In-air measurement technique

3.4 Calibration using well type chambers

3.5 Calibration using solid phantoms

Measurements in solid phantoms are not suitable for low-energy sources.

3.6 Relative measurements

Readings of consecutive source deliveries can be compared and deviations larger than 3% or 5% should be investigated. Serious incidents may be identified before treatment.

Chapter 9.2 on TPS Commissioning

9.2.6 Influence of shields, missing tissue, and inhomogeneities (abridged)

Presently, only simple correction algorithms are applied in some TPS. The effect of these algorithms must be verified and documented.

yes

Published shielding or tissue inhomogeneity data are based on MC.

yes

Validation of these MC data should be done by comparing with measured data, such as those obtained using TLD or small ionisation chambers.

ouch!

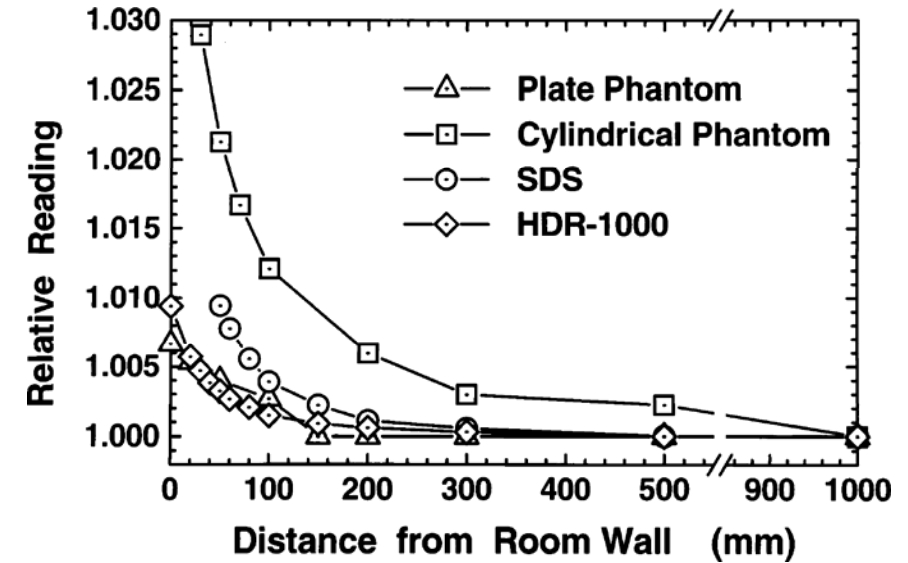
Algorithms are under development to account for scatter conditions and tissue inhomogeneities.

yes

Validation of these algorithms should be done in a similar way to the method used for checking the shielding algorithms.

ouch!

Comparison of RAKR Measurement Methods



Calibration system	Reference air kerma rate $\text{mGy}\cdot\text{h}^{-1}$ at 1m	Deviation from PTB
PTB	19.52	0.0%
HDR-1000	19.57	+0.3%
SDS	19.60	+0.4%
Cylindrical phantom	19.56	+0.2%

Adequate measurement precision (within 0.5%) using well chambers and Farmer chambers in-air or in-plastic phantoms.

UK IPEM Code of Practice for HDR ^{192}Ir RAKR

$$\dot{K}_R = I_{\text{raw}} \cdot f_{\text{elec}} \cdot k_{\text{dec}} \cdot k_{\text{Tp}} \cdot k_{\text{ion}} \cdot k_{\text{sg}} \cdot N_{\dot{K}_R}$$

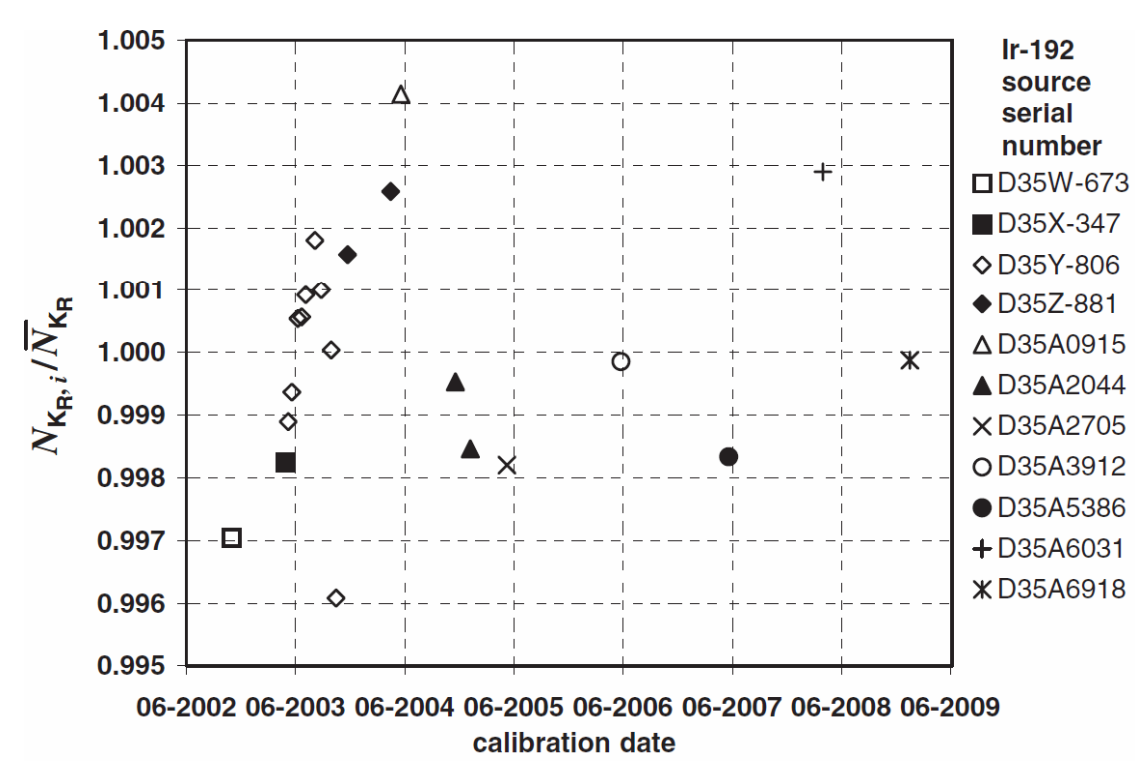


Figure 1. The graph shows the calibration history of a Standard Imaging 1000 Plus well chamber over 7 years. Calibrations were carried out with 11 different Nucletron microSelectron-v1 (classic) HDR ^{192}Ir brachytherapy sources. The maximum variation of all calibration coefficients, $N_{KR,i}$, determined between 2002 and 2009 was found to be $\pm 0.4\%$ of the running mean, \bar{N}_{KR} .

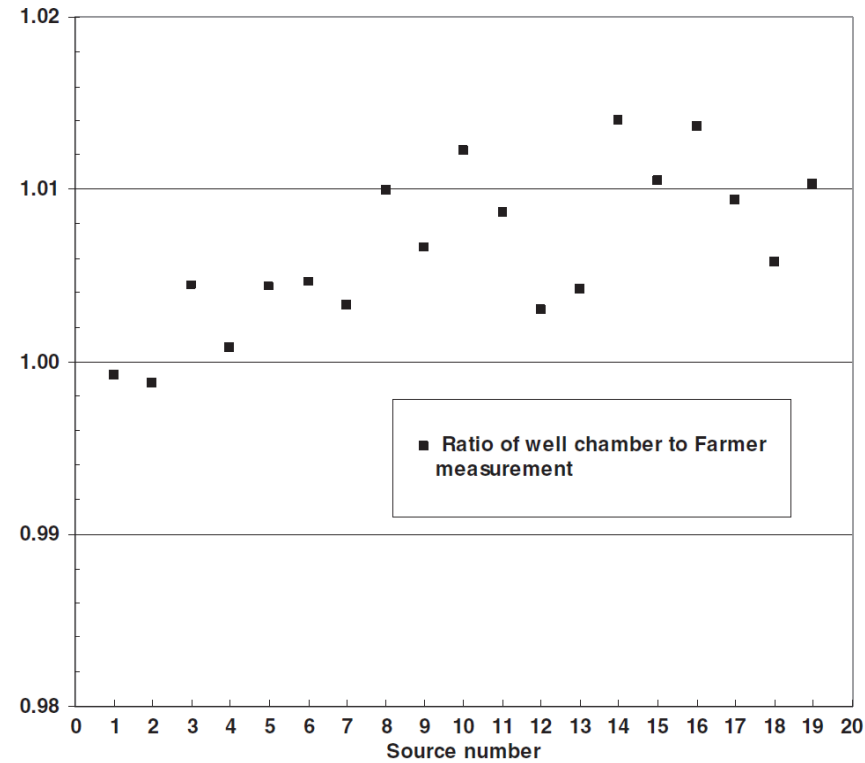
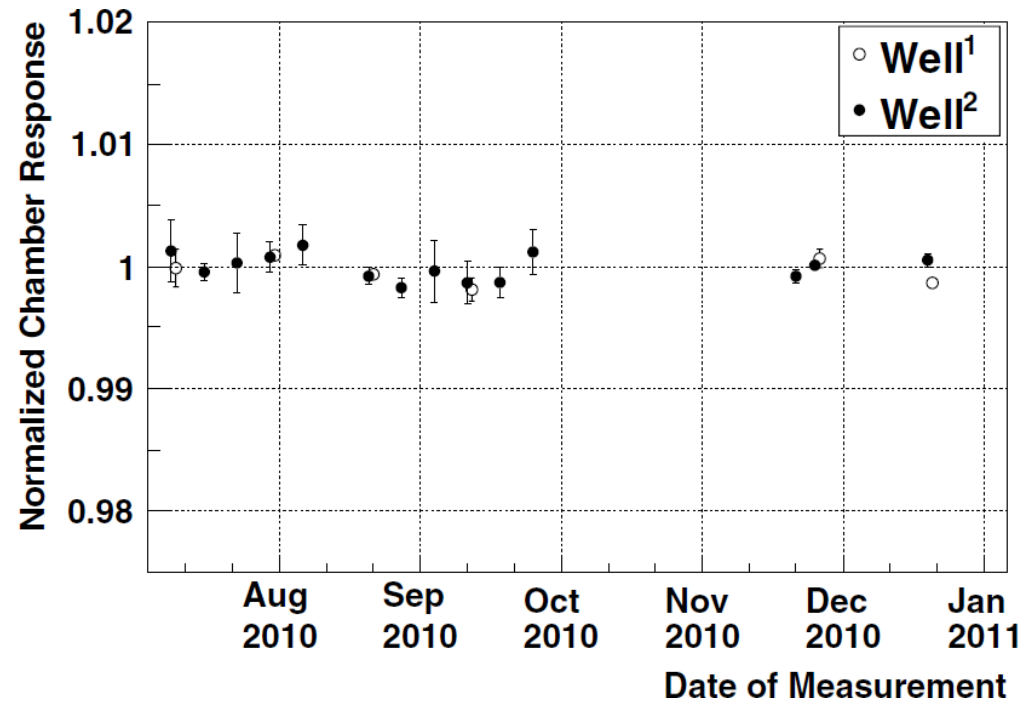
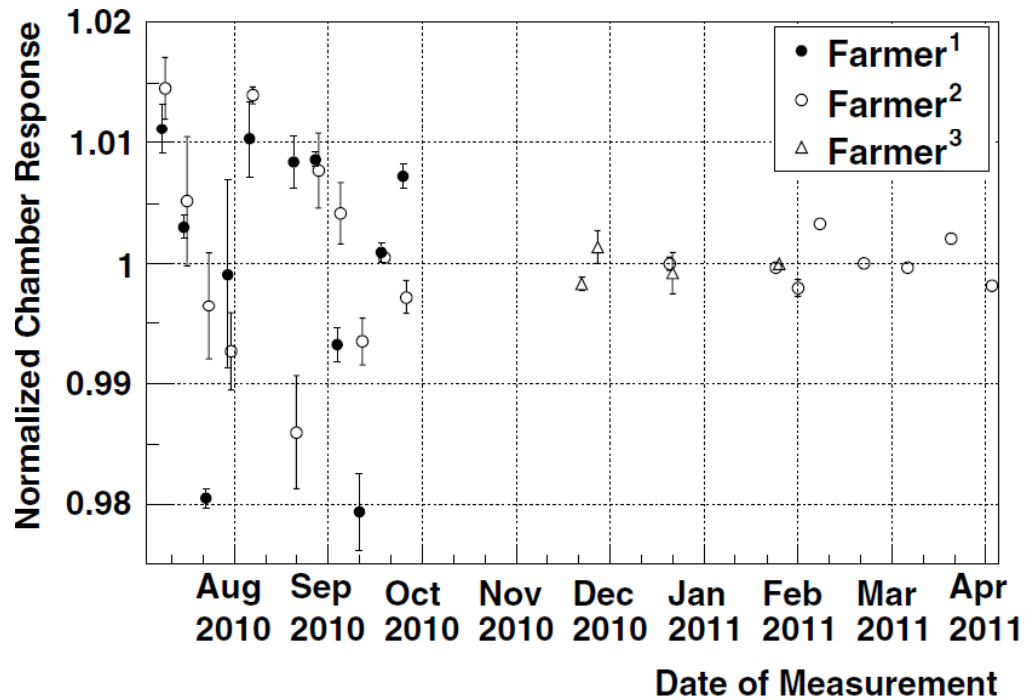


Figure B1. Reference air kerma rate (RAKR) comparison between a Standard Imaging 1000 Plus well chamber, calibrated using the new COP, and a Farmer chamber, calibrated at 280 kVp according to the old 1992 BIR/IPSM recommendations.

This COP aims to eliminate systematic differences between users, and reduce uncertainties by recommending the well chamber method of source calibration over the previously recommended (Aird *et al.*, 1993) Farmer method.

Implementation of UK IPEM Code of Practice



Improved measurement precision using well chambers instead of Farmer chambers.

Custom Room-Scatter Correction Factors

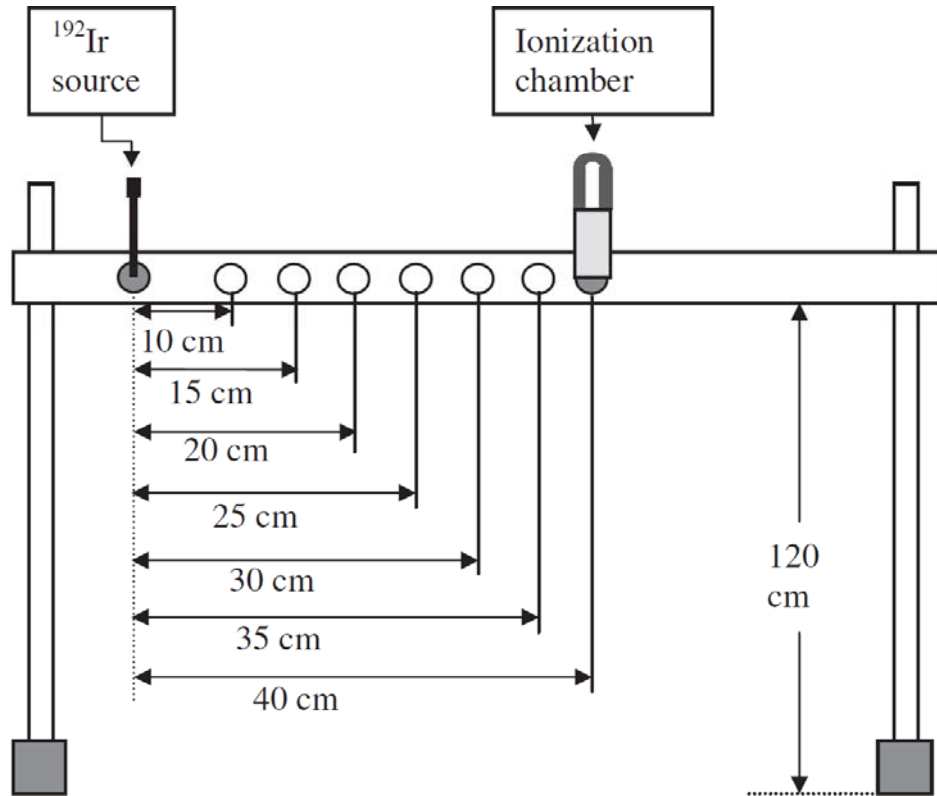


Fig. 1. Schematic cross-sectional view of the experimental arrangement used to measure the signal of the ionization chamber at seven different distances.

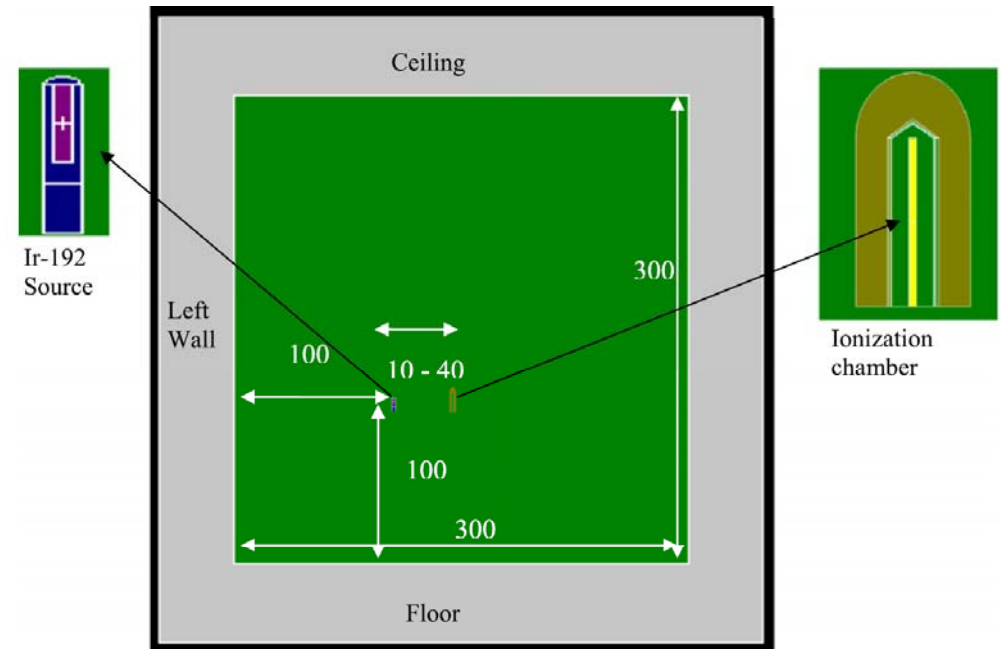


Fig. 2. MCNP Plot of the cross-sectional view of the problem geometry showing locations of the ^{192}Ir source and ionization chamber (all dimensions are in cm).

Monte Carlo calculations of K_{SC} (for f calculation) produced better agreement to analytical calculations than to Selvam et al. (2001).

RAKR for LDR ^{137}Cs

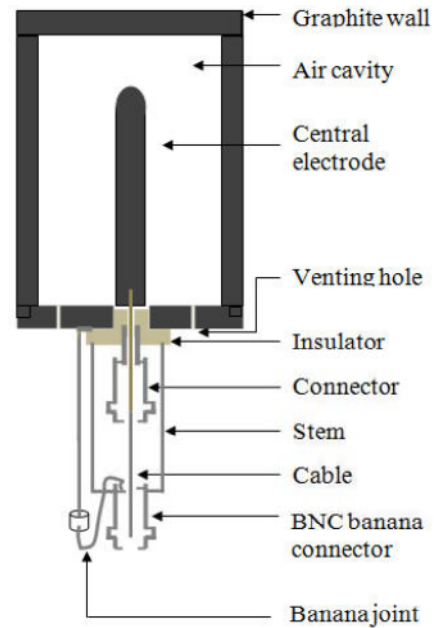
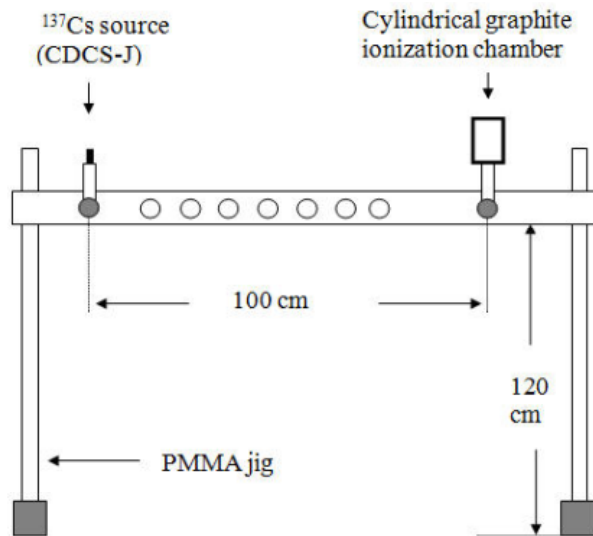


TABLE 3. Uncertainty in experimental determination of air kerma calibration coefficient (N_K) of the cylindrical graphite ionization chamber.

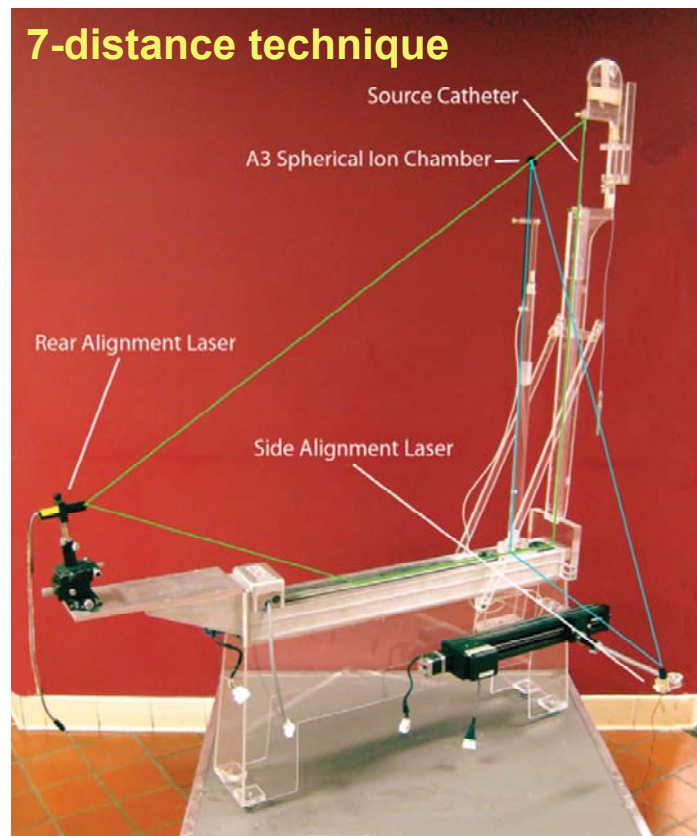
Uncertainty Components	Relative Standard Uncertainty (%)	
	Type A	Type B
Charge collection reproducibility	0.1	
Electrometer calibration		0.2
Leakage (Chamber + electrometer)		0.05
Temperature pressure correction factor (ktp)	0.2	
Timer accuracy	0.1	
Positional accuracy and reproducibility	0.2	
Room scatter correction factor (ksc)	0.12	
Ion recombination correction factor (krecom)		0.04
Nonuniformity correction factor (kn)		0.4
Air attenuation correction factor (katt)		0.1
RAKR of the ^{137}Cs source		1.0
Combined standard uncertainty ($k = 1$)	1.15 %	
Expanded uncertainty ($k = 2$)	2.3 %	

Good agreement (1.07%) between measured and MC-simulated N_K values.

US RAKR Standard for HDR ^{192}Ir

TABLE VI. HDR 1000 Plus inverse well chamber calibration coefficient Monte Carlo simulation summary.

Source model	pA/U (MCNP5)	Percent difference from existing classic Nucletron standard (%)
Classic Nucletron	2.074	—
Nucletron microSelectron V2	2.080	0.29
GammaMed	2.075	0.08
VariSource VS2000	2.114	1.79
Flexisource	2.084	0.48
Average	2.085	N/A



RAKR agreement across labs within ~ 1%.

TABLE VIII. Uncertainty analysis for transfer from standard well chamber to customer well chamber. Analysis was performed using the guidelines of NIST Technical Note 1297.

Parameter	Type A (%)	Type B (%)
Exradin A3 CHAMBER		
Charge	0.05	0.05
Air density	0	0.02
Ionic recombination	0	0
Beam divergence	0	0.1
Air attenuation/scatter	0	0.04
NIST N_K calibration coefficient	0	0.7
ELECTROMETER		
Electrometer calibration coefficient	0	0.11
Timing error	0	0.005
MEASUREMENT REPRODUCIBILITY		
Independent trial standard deviation	0.43	0
CALCULATION		
Interpolation for N_K	0	0.25
Solution algorithm	0	0.2
Time (half life)	0	0.03
Quadratic sum	0.433	0.812
Seven-distance method uncertainty $k = 1$		0.920
Source model effects		0.96
Customer chamber $k = 1$		0.309
Customer electrometer $k = 1$		0.166
Quadratic sum ADCL calibration $k = 1$		1.38
Quadratic sum ADCL calibration $k = 2$		2.75

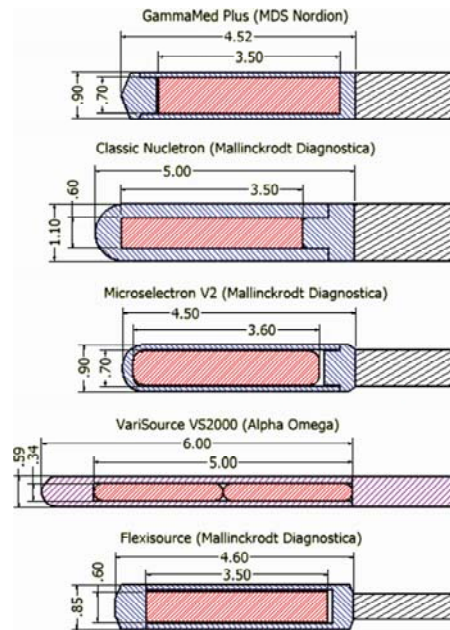
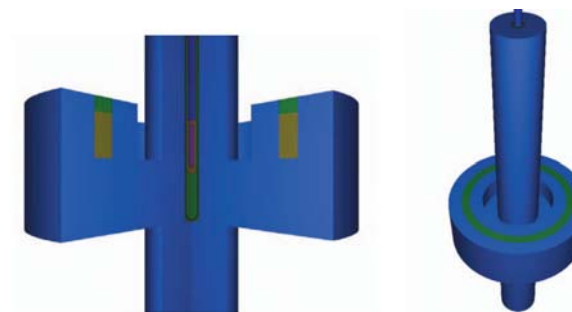


TABLE VII. International comparison results.

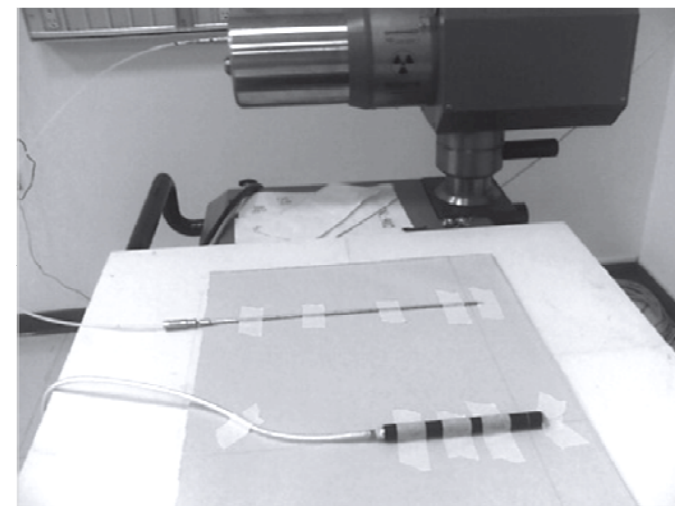
Well chamber model	UWADCL (10^2 Gy/C)	LNHB (10^2 Gy/C)	NPL (10^2 Gy/C)	Ratio UWADCL/LNHB	Ratio UWADCL/NPL
Nucletron 077.091 (S/N 25324)	2.617	2.592	2.584	1.010	1.013
Standard Imaging HDR 1000 Plus (S/N A002231)	1.294	1.285	1.280	1.006	1.010

New HDR ^{192}Ir Calibration Methods. Are They Needed?

Austerlitz, et al., Determination of absorbed dose in water at the reference point $D(r_0, \theta_0)$ for an ^{192}Ir HDR brachytherapy source using a Fricke system. *Med Phys* 35, 5360-5365 (2008).

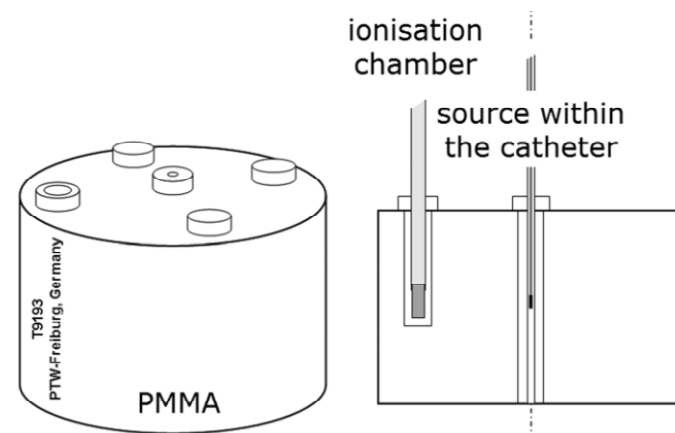


Chang, et al., An innovative method for ^{192}Ir HDR calibration by farmer chamber, V-film, and solid phantom. *NIM-A* 646, 192-196 (2011).



Fourie and Crabtree, A technique for calibrating a high dose rate ^{192}Ir brachytherapy source. *Australas Phys Eng Sci Med* 35, 85-92 (2012).

Kaulich, et al., Direct reference air-kerma rate calibration of ^{192}Ir for a thimble-type ionization chamber in a cylindrical solid phantom. *Metrologia* 49, S241-S245 (2012).



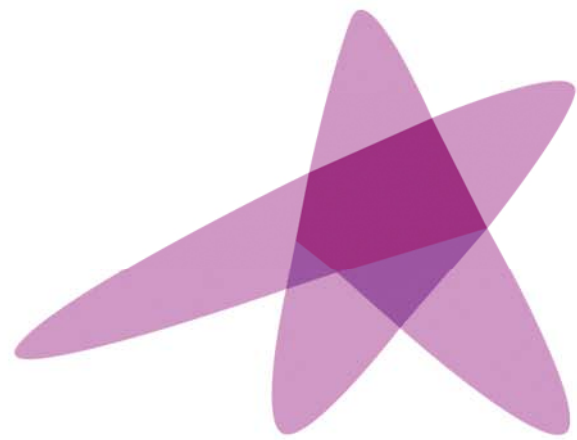
etc., etc.

Take Home Message

1. Independent assay of RAKR from the manufacturer is required.
2. Calibration methods are established for all brachytherapy sources.
3. Calibration infrastructure (i.e., SSDL availability) is variable.
4. Future improvements forthcoming in calibration methods and infrastructure.

Further Reading

- Aird, et al. BIR & IPSM, London, UK, 1993.
- Aubineau-Lanière, et al. Metrologia 2012;49:S189-92.
- Awunor, et al. Phys Med Biol 2011;56:5397-410.
- Bidmead, et al. Phys Med Biol 2010;55:3145-59.
- Butler, et al. Med Phys 2008;35:3860-5.
- DeWerd, et al. Med Phys 2011;38:782-801.
- Douysett, et al. Phys Med Biol 2005;50:1961-78.
- Douysett, et al. Phys Med Biol 2008;53:N85-97.
- Goetsch, et al. Med Phys 1991;18:462-67.
- Goetsch, et al. Intl J Radiat Oncol, Biol, Phys 1992;24:167-70.
- IAEA, TECDOC 1079, IAEA, Vienna, Austria, 1999.
- IAEA, TECDOC 1274, IAEA, Vienna, Austria, 2002.
- ICRU, ICRU Report 58, Bethesda, MD, 1997.
- Kumar et al. Appl Radiat Oncol 2012;70:282-9.
- Mainegra-Hing and Rogers, Med Phys 2006;33:3340-7.
- Nath, et al. AAPM TG-32, Melville, NY, 1987.
- Rasmussen, et al. Med Phys 2008;35:1483-8.
- Rasmussen, et al. Med Phys 2011;38:6721-9.
- Sander, et al. Metrologia 2012;49:S184-8.
- Sarfehnia, et al. Med Phys 2007;34:4957-61.
- Schneider. Metrologia 2012;49:S198-202.
- Selbach, et al. Metrologia 2008;45:422-8.
- Seltzer, et al. J Res NIST 2003;108:337-58.
- Soares, et al. Metrologia 2009;46:S80-98.
- Stump, et al. Med Phys 2002;29:1483-8.



ESTRO

School

Advanced Brachytherapy Physics

Vienna, 29 May – 1 June 2016

Experimental dosimetry in brachytherapy

P. Papagiannis, PhD
Medical Physics Laboratory
Medical School
National & Kapodistrian University of Athens

(no conflict of interest to disclose)

Objectives:

After this lecture the attendants should:

- have a clear understanding of:
 - dosimeter selection criteria & brachytherapy dosimetry challenges
- be familiar with:
 - a general terminology introduced to describe dosimeter characteristics
 - a general formalism for absorbed dose measurement
 - the key properties & operational features of utilized dosimeters
(mainly TLD and radiochromic Film)
- be informed of:
 - current trends
 - relevant literature
 - sources for further reading

Experimental dosimetry in brachytherapy

WHY...?

“theory is an interpolation of experiment”

(J.H. Hubbell in: X-Ray Spectrom. 28(4), 215–223, 1999)

Experimental dosimetry is needed for:

- **establishing source reference dose rate distributions**
(for clinical TG43-based TP)
- **commissioning and QA testing of TPS**
(planned dose is accurate)
- **dose verification in phantom or “in-vivo”**
(planned dose is accurately delivered)

Experimental dosimetry:

Use of a detector (dosimeter) providing a measurable signal that is of a known relationship with the absorbed dose in its volume

- The relationship between signal and dose is known for absolute dosimeters (calorimeters, ion chambers & Fricke gels)
- All other dosimeters must be **calibrated** relative to an absolute one in a beam quality Q_0 , to obtain the **absorbed dose sensitivity**:

$$S_{AD,w}(Q_0) = \frac{M(Q_0)}{D_w(Q_0)}$$

or equivalently the **calibration coefficient**:

$$N_{AD,w}(Q_0) = \frac{D_w(Q_0)}{M(Q_0)}$$

- Dose to a medium in the absence of the detector (water) is of interest
 - The calibration must be traceable to international standards

* The terminology used in this lecture is that introduced in:

Rogers & Cygler (Eds), Clinical dosimetry measurements in radiotherapy (2009 AAPM Summer School), Monograph No. 34, Medical Physics Publishing 2011

Dosimeter characteristics/requirements :

- (1) **Sensitivity:** must be high enough for low dose rate measurements. If the sensitivity is too high, it may cause rapid saturation at high dose rate
- (2) Adequate **dose range** and (preferably) **linearity of the response** as a function of accumulated dose
- (3) **Insensitivity of response to influence quantities** (dose rate, temperature, pressure, directional effect, accumulated dose, etc.): response should be independent, or variation should be known or measurable in order to perform adequate correction
- (4) **Energy response:** preferably independence of response as a function of energy
- (5) **Repeatability:** stability for repeated measurements over a short period of time
& **Reproducibility:** stability of material, construction, etc. over a long period of time
- (6) **Accuracy/precision:** the derivation of the dose from the dosimeter response must be possible with minimum uncertainty, but the requirements may differ for different applications

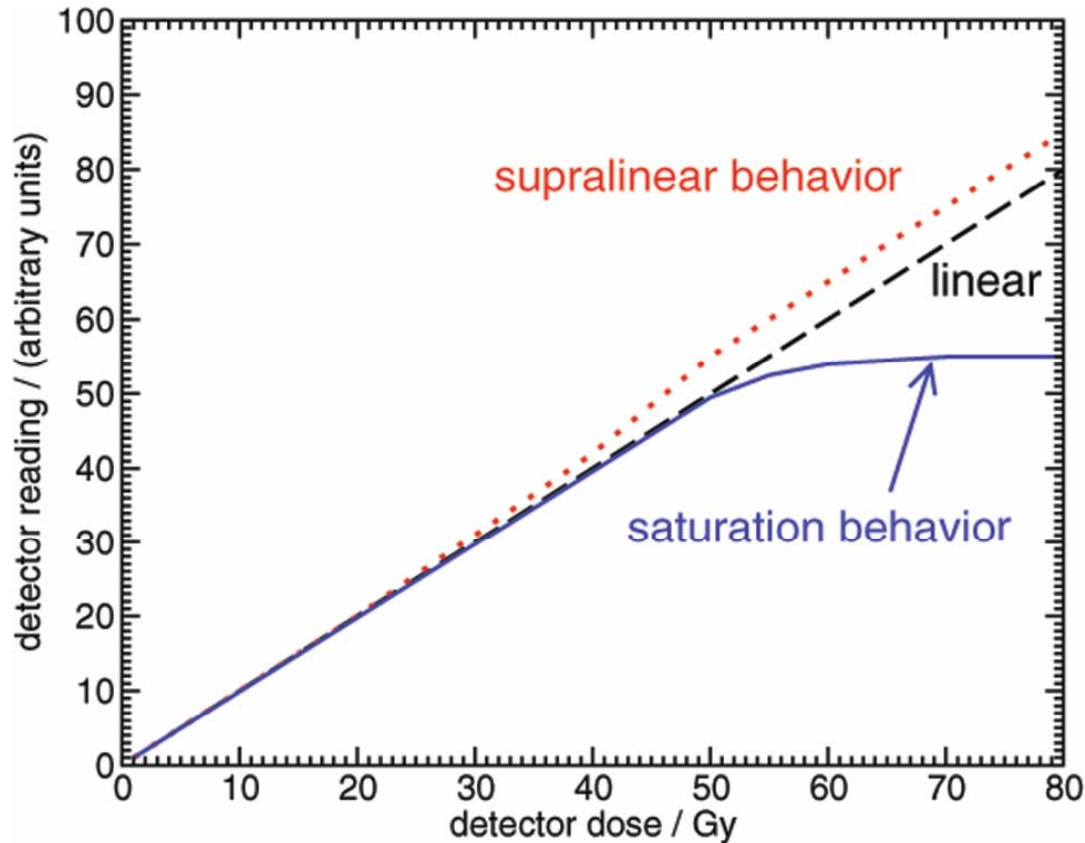
Quoted from:

Mayles, Nahum, Rosenwald (Eds): Handbook of radiotherapy physics: theory and practice,

© 2007 by Taylor & Francis Group LLC



Dose range / linearity / saturation:



$$D_{\text{det}}(D) = k_l (M(D)) \propto M(D)$$

where: k_l is the **intrinsic linearity** (normalized to 1 @ some D_0) and α relates D_0 to $M(D_0)$

- Detector response is linear if k_l is 1 for any D , $M(D)$
- !!!This is not always the case!!!

Figure from:

Rogers & Cygler (Eds), Clinical dosimetry measurements in radiotherapy (2009 AAPM Summer School), Monograph No. 34, Medical Physics Publishing 2011

Influence quantities:

A series of correction factors must be applied (if appropriate) to correct the dosimeter reading for any measurement condition affecting it

In example:

- environmental conditions

- background correction:

$$k_{bkgd} = \left(1 - \frac{M_{bkgd}}{M}\right)$$

- dose rate dependence:

$$M'(\dot{D}) = k_{dr}(M(\dot{D}))M(\dot{D})$$

Sensitivity, calibration & energy response:

Our calibration coeff. (inverse of dosimeter A.D. sensitivity)
actually comprises 2 parts:

$$N_{AD,w}(Q) = \frac{D_w(Q)}{M(Q)} = \frac{D_w(Q)}{D_{\text{det}}(Q)} \frac{D_{\text{det}}(Q)}{M(Q)} = f(Q)k_{bq}(Q)$$

- we define the **absorbed dose energy dependence** of the detector as the ratio of dose to water per unit dose to the detector at a given beam quality,

$$f(Q) = \frac{D_w(Q)}{D_{\text{det}}(Q)}$$

- We define the **intrinsic energy dependence** of the detector as the ratio of dose required to be absorbed to produce a unit signal

$$k_{bq}(Q) = \frac{D_{\text{det}}(Q)}{M(Q)}$$

Sensitivity, calibration & energy response:

Our calibration coeff. (inverse of dosimeter A.D. sensitivity)
actually comprises 2 parts:

$$N_{AD,w}(Q) = \frac{D_w(Q)}{M(Q)} = \frac{D_w(Q)}{D_{\text{det}}(Q)} \frac{D_{\text{det}}(Q)}{M(Q)} = f(Q)k_{bq}(Q)$$

- we define the **absorbed dose energy dependence** of the detector as the ratio of dose to water per unit dose to the detector at a given beam quality,

$$f(Q) = \frac{D_w(Q)}{D_{\text{det}}(Q)}$$

This depends on physical properties and radiation quality (cross sections) and detector geometry. It can be calculated via MC!

- We define the **intrinsic energy dependence** of the detector as the ratio of dose required to be absorbed to produce a unit signal

$$k_{bq}(Q) = \frac{D_{\text{det}}(Q)}{M(Q)}$$

This depends mainly on the physical process underlying the conversion of dose to the measured signal (and hence LET). It can only be measured!

Practical significance of $f(Q)$, $k_{bq}(Q)$

- f^{rel} or $k^{rel} > 1 \Rightarrow$ detector under-responds ...!
 f^{rel} or $k^{rel} < 1 \Rightarrow$ detector over-responds ...!

- Using a detector at a quality Q different than calibration (Q_0):

$$\begin{aligned} D_w(Q) &= M(Q_0) * \prod_i (\text{corr. factor})_i N_{AD,w}(Q_0) \frac{N_{AD,w}(Q)}{N_{AD,w}(Q_0)} = \\ &= M(Q_0) * \prod_i (\text{corr. factor})_i N_{AD,w}(Q_0) \frac{f(Q)}{f(Q_0)} \frac{k_{bq}(Q)}{k_{bq}(Q_0)} = \\ &= M(Q_0) * \prod_i (\text{corr. factor})_i N_{AD,w}(Q_0) f^{rel}(Q, Q_0) k_{bq}^{rel}(Q, Q_0) \end{aligned}$$

f^{rel}, k_{bq}^{rel} cannot be generally assumed energy independent

f^{rel} must be calculated

k_{bq}^{rel} must be measured

or taken from the literature for **matching** exp. conditions (Q , Q_0 , detector make, size, set up, ...)

Dosimeter characteristics/requirements :

- (1) Sensitivity:** must be high enough for low dose rate measurements. If the sensitivity is too high, it may cause rapid saturation at high dose rate
- (2) Adequate dose range** and (preferably) **linearity of the response** as a function of accumulated dose
- (3) Insensitivity of response to influence quantities** (dose rate, temperature, pressure, directional effect, accumulated dose, etc.): response should be independent, or variation should be known or measurable in order to perform adequate correction
- (4) Energy response:** preferably independence of response as a function of energy
- (5) Repeatability:** stability for repeated measurements over a short period of time
& Reproducibility: stability of material, construction, etc. over a long period of time
- (6) Accuracy/precision:** the derivation of the dose from the dosimeter response must be possible with minimum uncertainty, but the requirements may differ for different applications

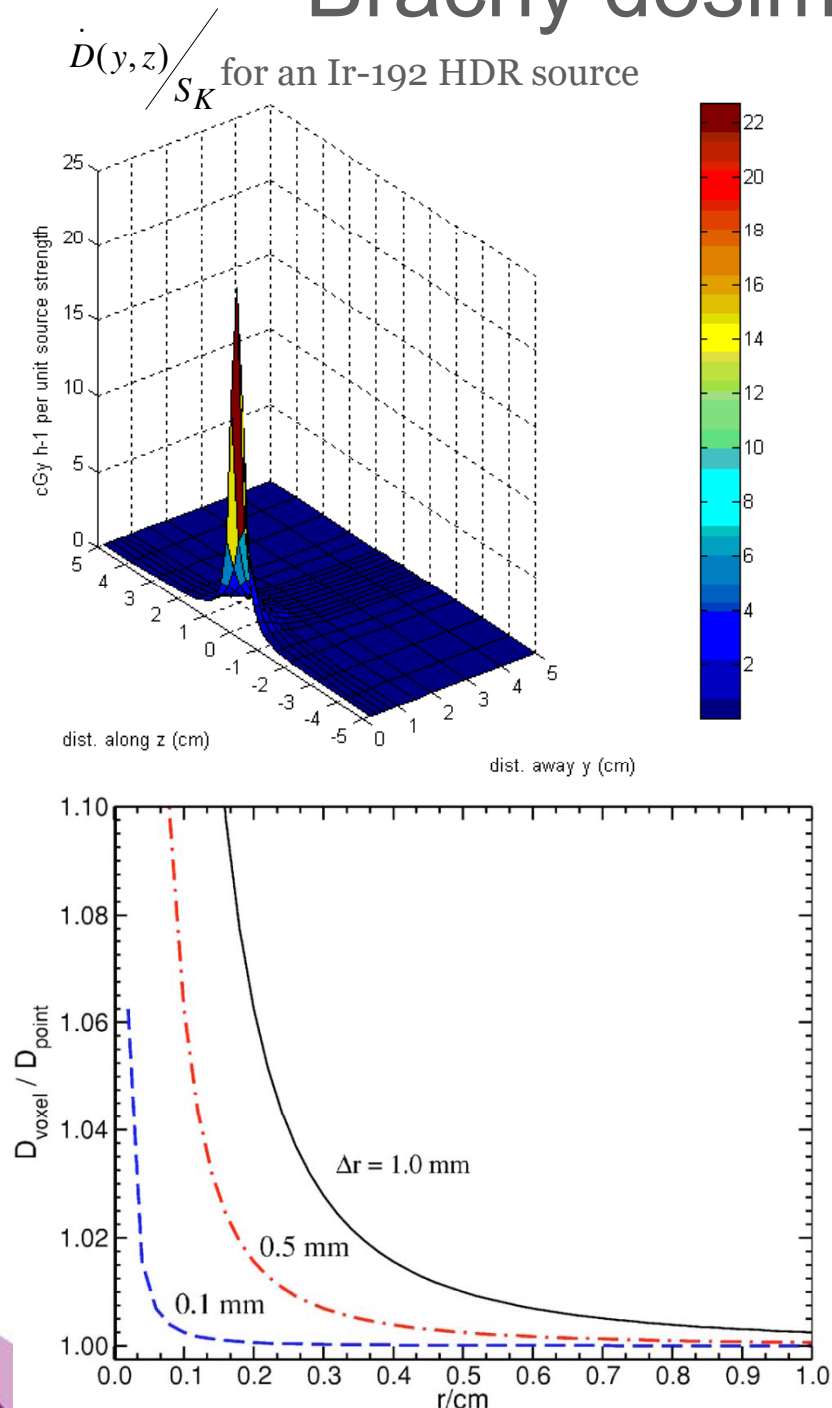
Quoted from:

Mayles, Nahum, Rosenwald (Eds): Handbook of radiotherapy physics: theory and practice,

© 2007 by Taylor & Francis Group LLC



Brachy dosimetry is challenging ...



Dose rate varies from ~ 20 Gy/s @ $(0.5\text{cm}, 90^\circ)$ from an Ir-192 HDR source to ~ 2 $\mu\text{Gy/s}$ @ $(5\text{cm}, 90^\circ)$ from an I-125 LDR source

Sensitivity high for low uncertainty, dose range high, (preferably) with $k_1=k_{\text{dr}}=1$

Spatial dose gradient is high (i.e. $\sim 25\%/mm$ in the radial direction @ $(0.5\text{cm}, 90^\circ)$ from an Ir-192 HDR source)

Volume must be small, positional accuracy is very important

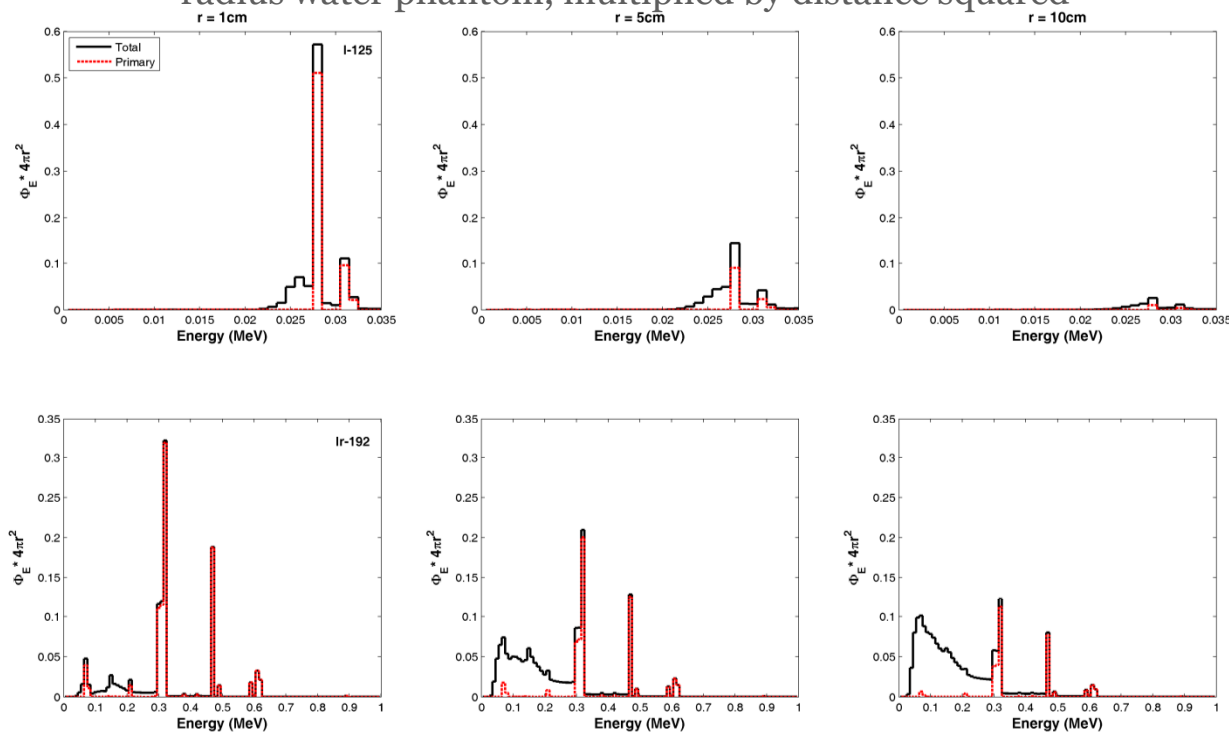
(1% rel. uncert. in $D(1\text{cm}, 90^\circ)$ requires 0.05mm uncertainty in r , assuming $1/r^2$ dose dependence since: $\frac{\sigma_D}{D} = 2 \frac{\sigma_r}{r}$)

If solid phantoms are used to increase positional accuracy a correction is required from $D_{w,\text{phant}}$ to $D_{w,w}$ at each meas. position

Figure from: Taylor, Yegin, Rogers, Med. Phys. 34(2) 445 (2007)

Brachytherapy Q is source/position dependent...

photon fluence vs distance per starting particle emitted from a point 125I (top) and 192Ir (bottom) source centered in a 15cm radius water phantom, multiplied by distance squared



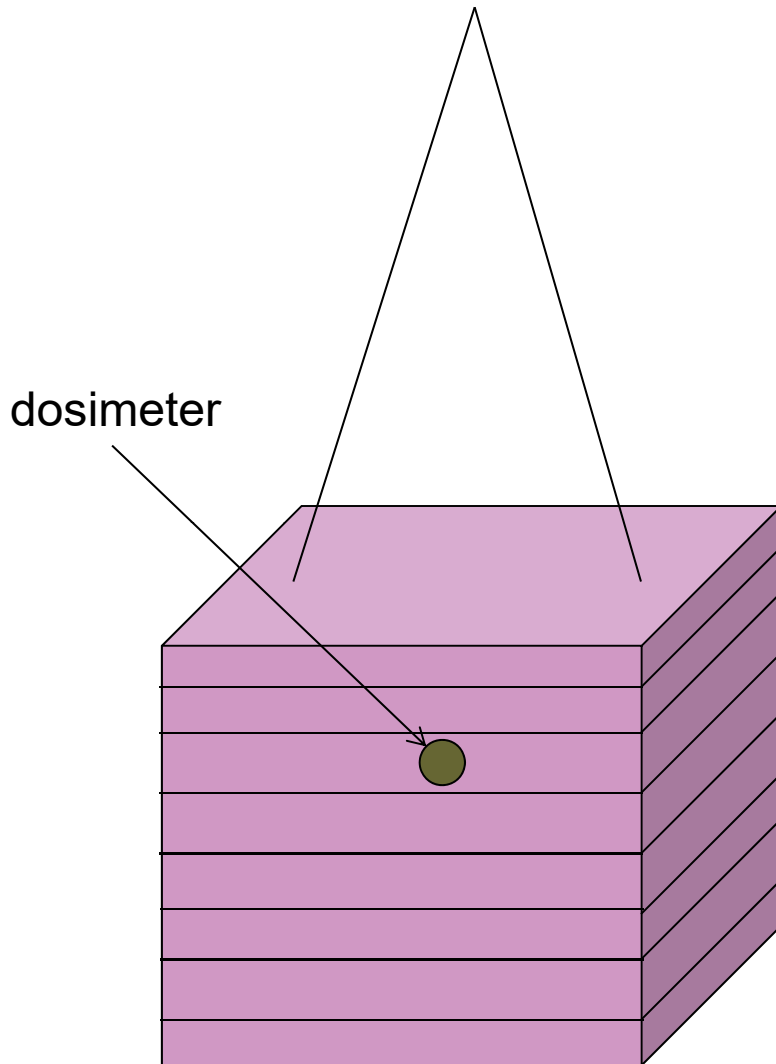
f^{rel}, k_{bq}^{rel} may be considerable
(especially for low E)

BUT

- They are source dependent (source materials)
- and position dependent (source spectra vary with distance, angle)

especially for high Z detectors

Beam quality: Q_0
(Co-60 or MV linac photon beam)



Calibration:

!!! Calibration uncertainty will be propagated as a type B unc. component to experimental results !!!

Absorbed dose sensitivity calibration

$$S_{AD,w}(Q_0) = \frac{M(Q_0)}{D_w(Q_0)} = \frac{1}{N_{AD,w}(Q_0)}$$

is usually performed using a Linac

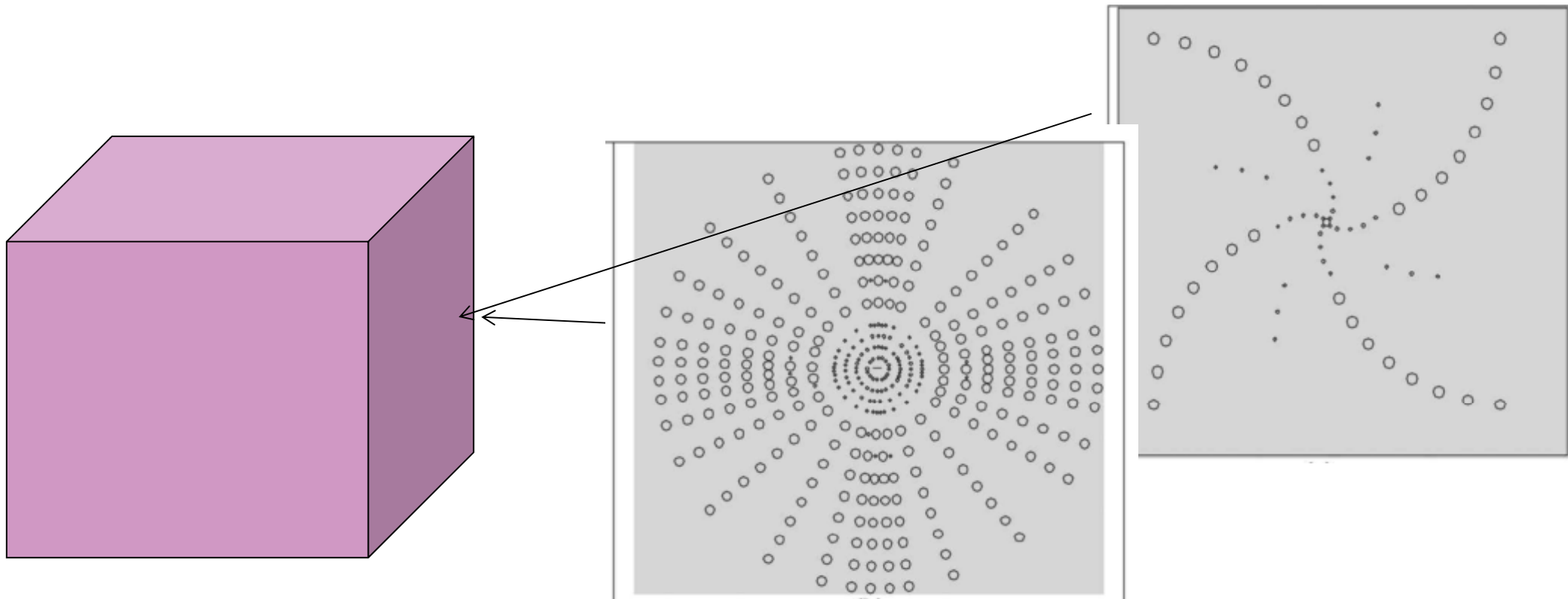
where:

$M(Q_0)$ is the dosimeter reading

$D_w(Q_0)$ is dose to water at the point of measurement in the absence of the detector obtained using an established reference dosimetry protocol (e.g. TRS398) and an ion chamber with a dose to water calibration traceable to international standards

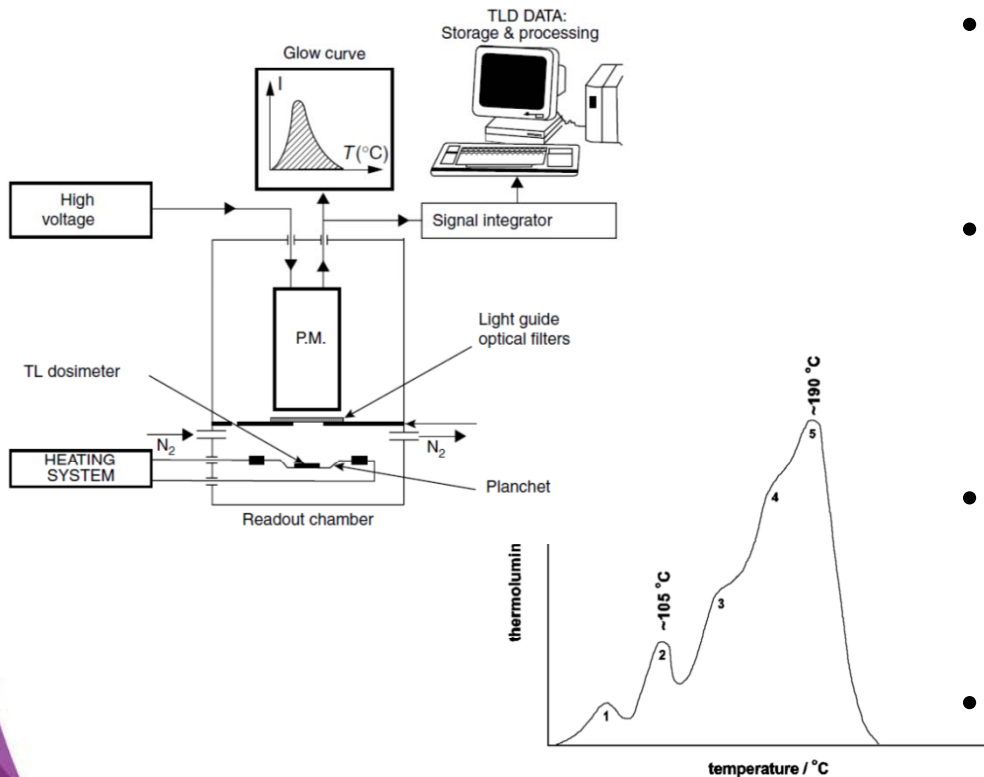
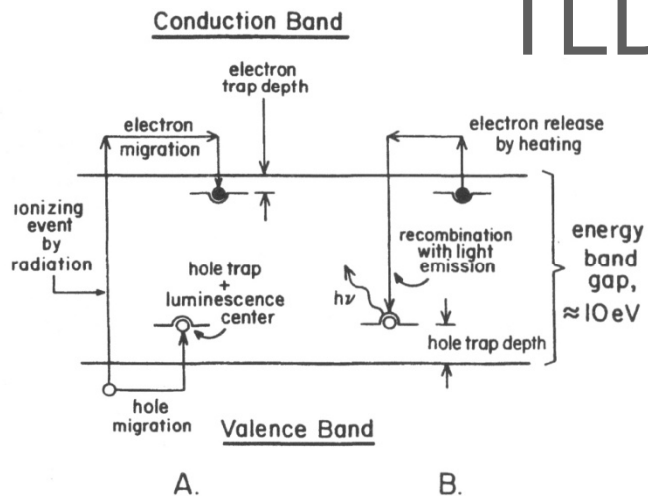
Let us do single source dosimetry (TG-43 characterization of a source)

using TLD as is traditionally done in the literature.



Figures from: Rogers & Cygler (Eds), *Clinical dosimetry measurements in radiotherapy* (2009 AAPM Summer School), Monograph No. 34, Medical Physics Publishing 2011

TLD: basic principles



- In imperfect crystals (i.e. TLD100: LiF doped with Mg and Ti in trace amounts) part of the energy absorbed by ionising radiation is stored and re-emitted upon heating in the form of light. Light is detected and correlated to the absorbed dose.
- Stored energy is in the form of the fraction of e^- freed by irradiation, that is trapped in a metastable energy state.
- When the crystal is heated, part of these e^- recombine with holes trapped in luminescence centers and emit light (thermo-luminescence, TL)
- The curve of TL output versus temperature (glow curve) shows peaks characteristic of trap energy depths in the crystal
- Besides TL crystal, glow curve shape varies with heating rate & max temperature

TLD: sensitivity/linearity

Material	Photoelectric Effect Z_{eff}	Compton Effect e^-/g	Density g/cm^3
Silicon (diodes) ^a	14	3×10^{23}	2.33
LiF (Mg, Ti) ^b	8.14	2.79×10^{23}	2.64
LiF (Mg, Ti, Na) ^b	8.14	2.79×10^{23}	2.64
Li ₂ B ₄ O ₇ :Mn ^b	7.4	2.92×10^{23}	2.30
Li ₂ B ₄ O ₇ :Cu ^c	7.4	2.92×10^{23}	2.30
CaSO ₄ :Mn ^b	15.3	3.02×10^{23}	2.61
CaSO ₄ :Dy ^b	15.3	3.03×10^{23}	2.61
CaF ₂ :Mn ^b	16.3	2.95×10^{23}	3.18
CaF ₂ :Dy ^b	16.3	2.95×10^{23}	3.18
Air ^d	7.64	3.03×10^{23}	1.293×10^{-3}
Water ^d	7.42	3.34×10^{23}	1.00
Fat ^d	5.92	3.48×10^{23}	0.91
Muscle ^d	7.42	3.36×10^{23}	1.04
Bone ^d	14	3×10^{23}	1.01–1.60

- TLD is effective in terms of interacting with photons in the brachytherapy E range
- The TL mechanism however is inefficient
- About 0.04% of TLD absorbed dose is emitted as TL energy per unit mass
- Individual TLD calibration is required as well as meticulous care in reproducible conditions of use to ensure precision/accuracy
- TLD dynamic dose range is wide. It comprises a linear D region followed by a region of supra-linearity and, eventually, saturation
- Linearity cannot be assumed and has to be measured by irradiating TLD groups in graded doses in the region of interest

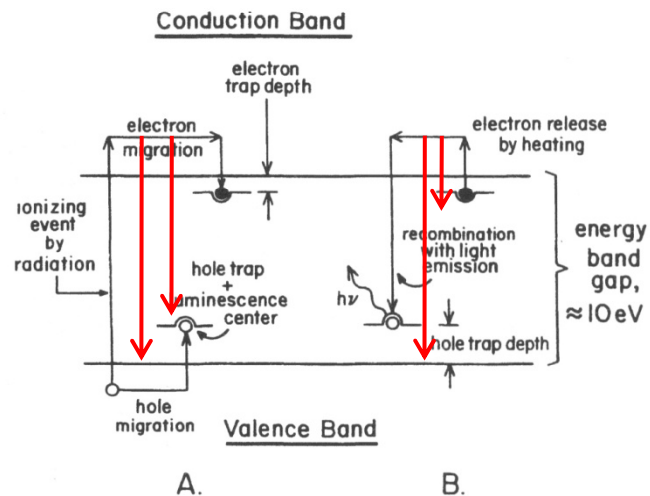


Table from: Mayles, Nahum, Rosenwald (Eds): Handbook of radiotherapy physics: theory and practice, © 2007 by Taylor & Francis Group LLC

TLD: influence factors

- TLD response is not significantly affected from environmental conditions (normal room temperatures, moderate exposure to light).

BUT

Traps are not stable @ room temperatures and annealing @ 400 °C for 1 h is required to ensure trap stability.

Fading can affect low T peaks. This can be mitigated by eliminating corresponding traps (annealing @ 80 °C for 24 h pre-irradiation) or emptying them before readout (annealing @ 100 °C for 2 h pre-irradiation and 10 min post-irradiation)

- background correction is necessary for PM dark current and TL non-related to D (the latter is reduced with N₂ gas purging during readout)
 - TLD response is dose rate independent

General formalism

$$\bullet \frac{\dot{D}_{w,w}(Q)}{S_K} = \frac{M(Q) * k_{bkgd} * k_l * g(t)}{S_K} * N_{AD,w}(Q_0) \frac{N_{AD,w}(Q)}{N_{AD,w}(Q_0)} * p_{phant} =$$

$$\frac{M(Q) * k_{bkgd} * k_l * g(t)}{S_K} * N_{AD,w}(Q_0) * k_{bq}^{rel} * f^{rel} * p_{phant}$$

Where: $g(t) = \frac{\lambda}{\exp[-\lambda(t_{start} - t_{cal})][1 - \exp(-\lambda\Delta t_{exp})]}$

and $p_{phant} = \frac{D_{w,w}(Q)}{D_{w,phant}(Q)}$ can be calculated using MC

I need to measure: $M, N_{AD,w}(Q_0),$ corrections $k_l,$ and $k_{bq},$
 calculate: $g(t), f, p_{phant},$
 and know: $S_K,$

with as low an uncertainty as possible!

Uncertainty requirements for single source dosimetry

In their methodological recommendations for measuring dosimetry parameters:

- TG-43U1* advises on using a dosimeter system with sufficient precision and accuracy to permit dose-rate estimations with combined 1σ Type A uncertainty $<5\%$ and 1σ Type B uncertainty $<7\%$ for a total 1σ uncertainty $<9\%$ for LE sources
- Joint AAPM-ESTRO report** advises on using a dosimeter system with sufficient precision and accuracy to permit dose-rate estimations with $k=1$ Type A (statistical) uncertainties 3% and $k=1$ Type B uncertainties 6%

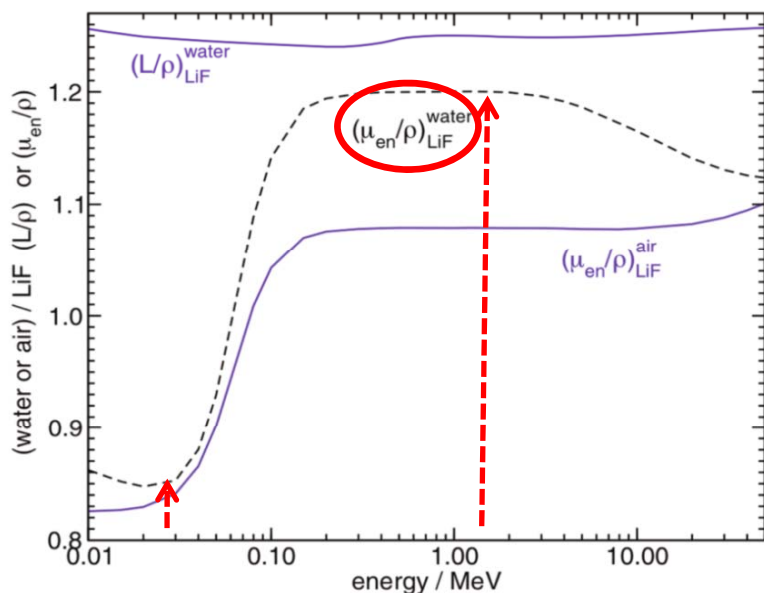
* Rivard et al., 2004. Update of AAPM Task Group No. 43 Report: A revised AAPM protocol for brachytherapy dose calculations. Med. Phys. 31(3), p.633.

** Perez-Calatayud et al., 2012. Dose calculation for photon-emitting brachytherapy sources with average energy higher than 50 keV: report of the AAPM and ESTRO. Med. Phys. 39(5), p.2904

TLD: absorbed dose energy dependence

$$f^{rel}(Q, Q_0) = \frac{D_w(Q)/D_{TLD}(Q)}{D_w(Q_0)/D_{TLD}(Q_0)}$$

$$f^{rel}(Q, Q_0) = \frac{(\mu_{en}/\rho)_{TLD}^w(Q)}{(\mu_{en}/\rho)_{TLD}^w(Q_0)} \approx 0.7$$



- TLD dose changes more than water at $Q \ll Q_0$ due to higher Z than water, so $f^{rel} < 1$
- Assuming TLD is a large cavity (dimensions large compared to max. e^- range & small compared to photon m.f.p.):

for LDR sources relative to Co-60.

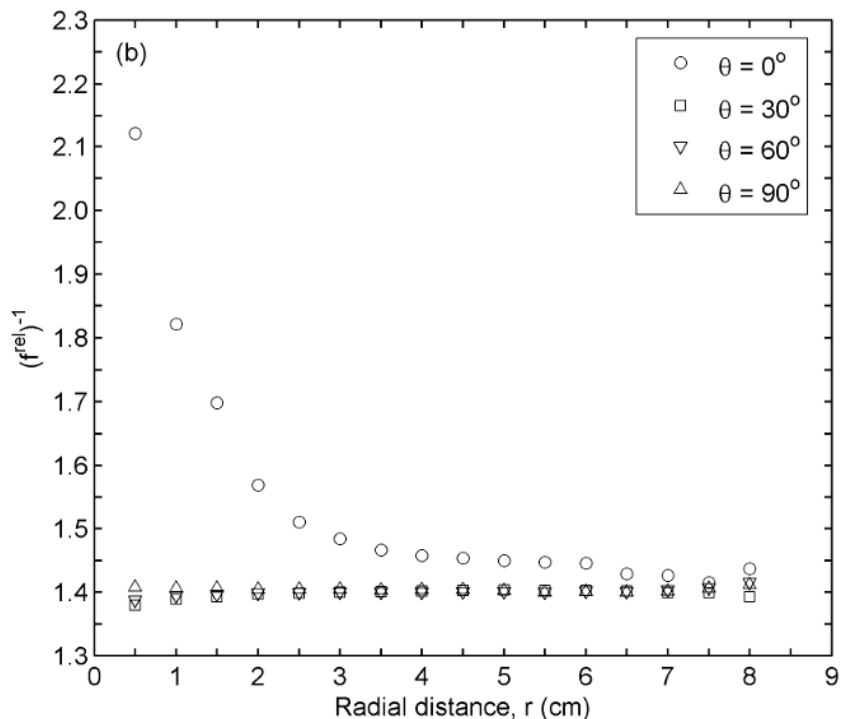
This is only an approximation.

- MC is used to account for:
- photon spectra @ each point in Q, Q_0
- TLD attenuation,
- v. averaging
- cavity corrections, ... etc.

See: Rodriguez and Rogers, Med. Phys. 41(11) p. 114301 (2014) for an excellent review...!

TLD: absorbed dose energy dependence

$$f^{rel}(Q, Q_0) = \frac{D_w(Q)/D_{TLD}(Q)}{D_w(Q_0)/D_{TLD}(Q_0)}$$



Best practice example for I-125 dosimetry with 6 MV linac calibration:

- f^{rel} is close to 0.7 but varies with point around the source
- Uncertainties: Type A=0.56%, type B=1%

Neglecting f^{rel} would introduce a type B uncertainty (dose overestimation) of 40%...!

Moutsatsos et al. Experimental determination of the Task Group-43 dosimetric parameters of the new I25.S17plus (125)I brachytherapy source, *Brachytherapy*, 13(6), 618 (2014).

TLD: intrinsic energy dependence

$$k_{bq}^{rel}(Q, Q_0) = \frac{D_{TLD}(Q)/M(Q)}{D_{TLD}(Q_0)/M(Q_0)}$$

Tochilin et al. 1968

Values normalized to Co-60

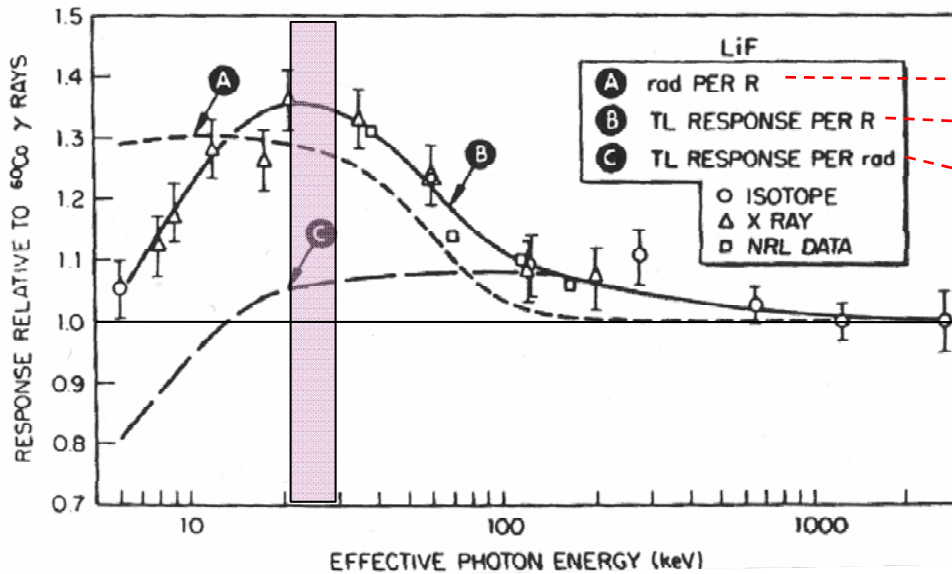


Figure from: Attix: Introduction to radiological physics and radiation dosimetry, © 2004 by Wiley-VCH Verlag GmbH & Co

$$\frac{M}{X} \rightarrow \left(\frac{D_{TLD}}{X} \right)_{large-cavity}$$

$$B:C \rightarrow \frac{1}{k_{bq}}$$

It was well known that dose to TLD to produce a unit signal decreases as energy decreases and LET increases

i.e.: $k_{bq}^{rel} < 1$ @ the brachy energies

or equivalently: TLD over-responds (more signal per unit dose) at lower energies due to LET increase

TLD: intrinsic energy dependence

$$k_{bq}^{rel}(Q, Q_0) = \frac{D_{TLD}(Q)/M(Q)}{D_{TLD}(Q_0)/M(Q_0)}$$

- In the light of studies indicating $k_{bq}^{rel} = 1$ within experimental uncertainties (i.e. Das et al 1996) k_{bq} was disregarded by most experimentalists

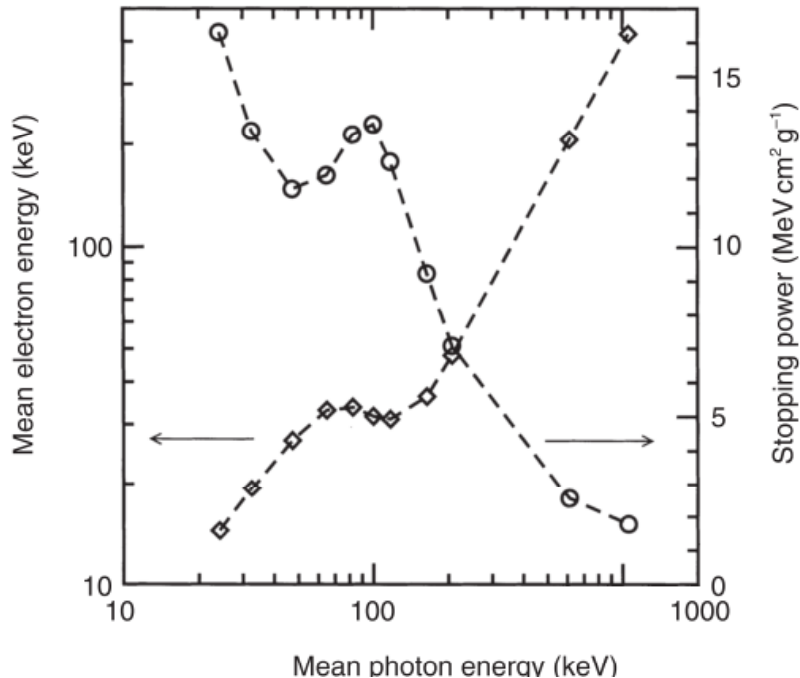


Figure from: Davis et al, Radiation Protection Dosimetry Vol. 106, No. 1, pp. 33–43 (2003)

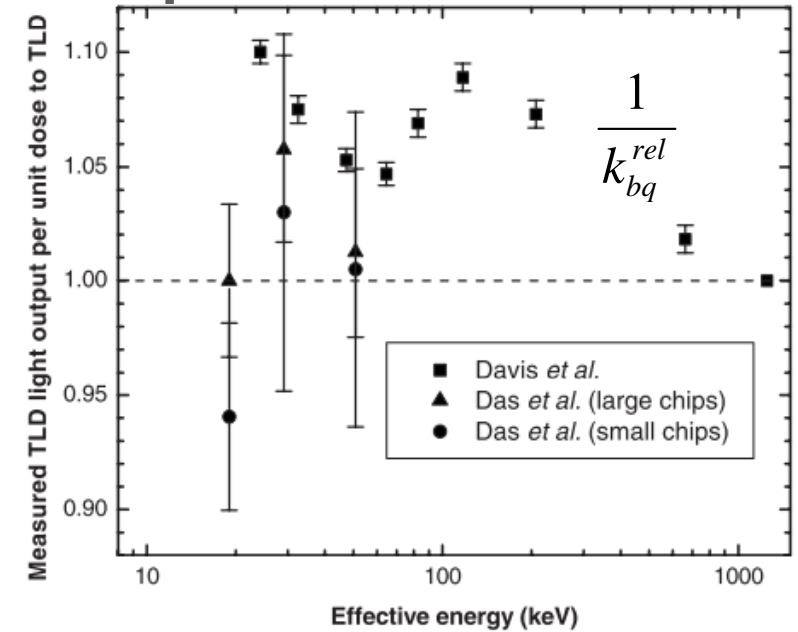


Figure from: Nunn et al, Med. Phys. 38(8) 1859 (2008)

- Until Davis et al (2003) measured TLD100 over-response at low E due to LET increase and the race to determine k_{bq} was on ...!

TLD: intrinsic energy dependence

$$k_{bq}^{rel}(Q, Q_0) = \frac{D_{TLD}(Q)/M(Q)}{D_{TLD}(Q_0)/M(Q_0)}$$

- Davis et al. k_{bq}^{rel} down to 0.9 (0.6 % Type A uncertainty, $k=1$, x-ray beams, LiF:Mg,Ti).
- Nunn et al. k_{bq}^{rel} down to 0.885 (3.5% combined standard uncertainty, $k=1$, x-ray beams, LiF:Mg,Ti).
- Carlsson Tedgren et al. k_{bq} down to 0.935 (1.9% combined standard uncertainty, $k=1$, x-ray beams, LiF:Mg,Ti). They also discussed potential differences due to TLD handling and formulation, and expressed concern regarding the applicability of determinations obtained using x-ray beams to other photon fields.
- Reed et al. $k_{bq}^{rel} = 0.883 \pm 0.011$ (I-125), 0.870 ± 0.012 (I-125 w. Ag), 0.871 ± 0.013 (Pd-103) (combined standard uncertainties, $k=1$ LiF:Mg,Ti).
- Rodriguez and Rogers minimized the difference between Λ measurements in the literature and MC calculations and arrived at $k_{bq}^{rel} = 0.931 \pm 0.013$ (I-125) and 0.922 ± 0.022 (Pd-103).

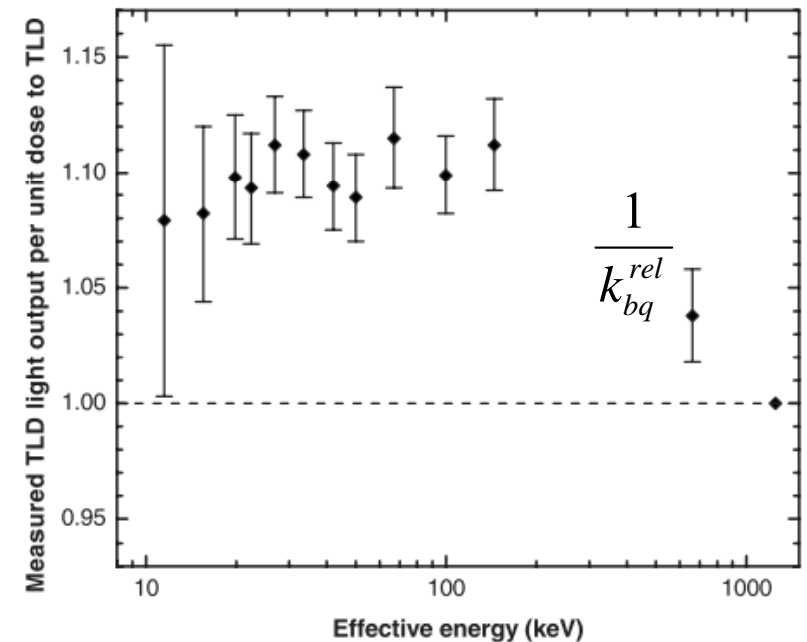


Figure from: Nunn et al, Med. Phys. 38(8) 1859 (2008)

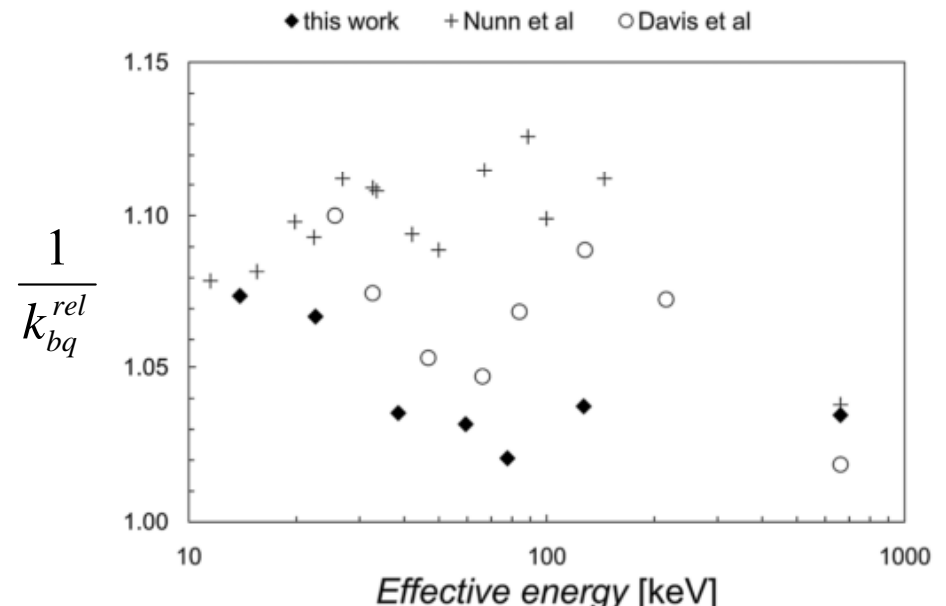


Figure from: Carlsson Tedgren et al, Med. Phys. 38(10) 3839 (2011)

TLD: intrinsic energy dependence

$$k_{bq}^{rel}(Q, Q_0) = \frac{D_{TLD}(Q)/M(Q)}{D_{TLD}(Q_0)/M(Q_0)}$$

- k_{bq}^{rel} is in the order of 0.90 ± 0.05 to 0.935 ± 0.03 for I-125 and Pd-103
- This correction appears to be protocol and TLD make specific.
- A correction might be needed for HE sources as well
(Joint AAPM-ESTRO report suggests $k_{bq}^{rel} = 1$) but for Ir-192 Carlsson et al. (Med. Phys. 39(2), 1133. 2012) suggests $k_{bq}^{rel} = 0.95$ but with increased uncertainties (3.5%, k=1).

$$P_{phant} = \frac{D_{w,w}(Q)}{D_{w,phant}(Q)}$$

Phantom correction

- Plastics fabricated for water equivalence in MV beams used as phantom material (solid water 457-Gamex, white water RW3-PTW, plastic water CIRS)
- Williamson (1991) first noted the need for a P_{phant} correction

TABLE II. Percent atomic composition (by weight) and densities of phantoms.^a

Atomic species	Water	PMMA	WT1	RW-1
H	11.2	8.0	8.1	13.2
C	...	60.0	67.2	79.4
N	2.4	...
O	88.8	32.0	19.9	3.8
Ca	2.3	2.7
Mg	0.9
Cl	0.1	...
Density (g cm ⁻³)	1.00	1.17	1.015 ^b	0.97

Table from: Luxton, Med. Phys. 21(5), 631 (1994)

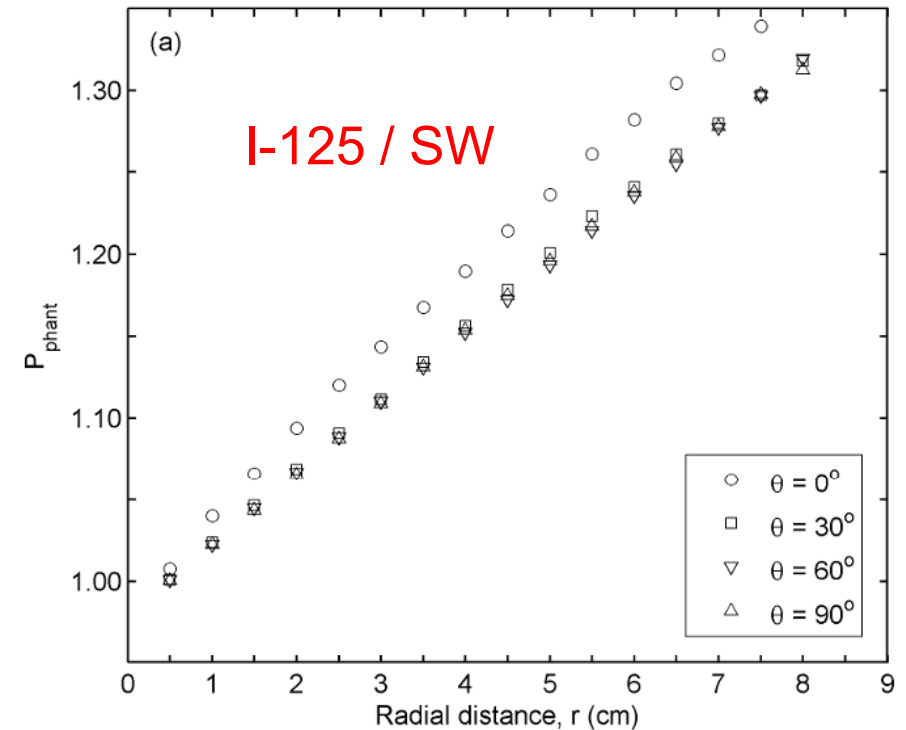
$$P_{phant} = \frac{D_{w,w}(Q)}{D_{w,phant}(Q)}$$

Phantom correction

- P_{phant} increases with distance due to increased density and increased attenuation from %Ca content
- There might also be a minor θ dependence

TABLE II. Percent atomic composition (by weight) and densities of phantoms.^a

Atomic species	Water	PMMA	WT1	RW-1
H	11.2	8.0	8.1	13.2
C	...	60.0	67.2	79.4
N	2.4	...
O	88.8	32.0	19.9	3.8
Ca	2.3	2.7
Mg	0.9
Cl	0.1	...
Density (g cm ⁻³)	1.00	1.17	1.015 ^b	0.97



$$P_{phant} = \frac{D_{w,w}(Q)}{D_{w,phant}(Q)}$$

Phantom correction

- Phantom material MUST be checked for density variation and composition (Ca or other high Z content variation that can be up to 30%) to minimize type B uncertainty.

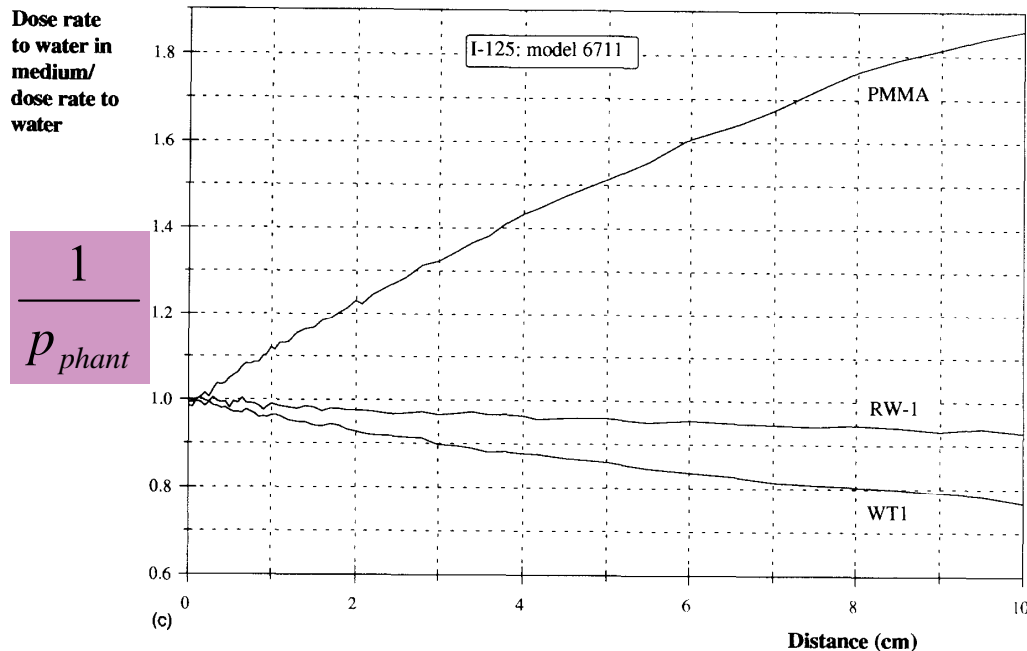


Figure from: Luxton, Med. Phys. 21(5), 631 (1994)

- High purity plastics (PMMA, polystyrene) might be preferable since P_{phant} deviation from unity is greater for LE source dosimetry BUT type B uncertainty of the correction will be lower.

TLD: uncertainty budget

Table 1

Analysis of the uncertainty associated with TLD results for the dose-rate constant of the I25.S17plus brachytherapy source

Component	Type A (%)	Type B (%)
Average of repetitive measurements	3.22 ^a	—
TLD dose calibration	0.48	1.21
Relative intrinsic energy dependence, k_{bq}^{rel}		2.50
Phantom material correction factor, P_{phant}	0.14	2.46
Relative absorbed dose energy dependence, f^{rel}	0.56	1.0
TLD-source relative positioning		0.6
Source strength, S_K		0.78 ^b
Quadratic sum	3.31	3.97
Combined total uncertainty ($k = 1$)	5.16 ^c	

TLD = thermoluminescent dosimeter.

Random or statistical effects are described with type A uncertainties, whereas type B uncertainties account for nonstatistical discrepancies. The tabulated values correspond to the National Institute of Standards and Technology—calibrated seed.

^a 3.20%, 5.90%, and 3.44% for seed 1, 2, and 3, respectively.

^b 1% for seed 1, 2, and 3.

^c 5.19%, 7.18%, and 5.34% for seed 1, 2, and 3, respectively.

In summary:

- TLD remains the standard method for single source exp. dosimetry (both LE,HE)
- Methodological recommendations are included in TG43U1 (Rivard et al. 2004), Joint AAPM-ESTRO report (Perez-Calatayud et al, 2012) and refs therein
- At minimum calculate your f^{rel} correction using MC and including TLD att./volume and p_{phant} as a function of (r,θ) . These are significant for LE and less for HE.
- What you don't know (phantom composition, density, etc) goes in your uncertainty budget!
- Overall uncertainty for LE is high mainly due to k_{bq}^{rel} uncertainty. Dose rate constants measured are on average ~5% higher than MC and hence the recommendation for equally averaged, consensus values in TG43U1 (Rivard et al. 2004)
- A dosimeter with reduced uncertainty would be welcome!

Alternatives to TLD

- 1D systems used for single source dosimetry and especially QA: ion chambers, alanine, OSLDs, PSDs, i.e:

Araki, F. et al., 2013. Measurement of absorbed dose-to-water for an HDR (192)Ir source with ionization chambers in a sandwich setup. *Med. Phys.*, 40(9), p.092101.

Sarfehnia, A., Kawrakow, I. & Seuntjens, J., 2010. Direct measurement of absorbed dose to water in HDR [sup 192]Ir brachytherapy: Water calorimetry, ionization chamber, Gafchromic film, and TG-43. *Med. Phys.*, 37(4), p.1924.

Adolfsson, E. et al., 2010. Response of lithium formate EPR dosimeters at photon energies relevant to the dosimetry of brachytherapy. *Med. Phys.*, 37(9), p.4946.

Schaeken, B. et al., 2011. Experimental determination of the energy response of alanine pellets in the high dose rate 192Ir spectrum. *PMB*, 56(20), pp.6625–34.

Kolbun, N. et al., 2010. Experimental determination of the radial dose distribution in high gradient regions around 192Ir wires: comparison of electron paramagnetic resonance imaging, films, and Monte Carlo simulations. *Med. Phys.*, 37(10), pp.5448–55.

Chiu-Tsao, S.-T., Medich, D. & Munro, J., 2008. The use of new GAFCHROMIC EBT film for [sup 125]I seed dosimetry in Solid Water phantom. *Med. Phys.*, 35(8), p.3787.

Aldelaijan, S. et al., 2011. Radiochromic film dosimetry of HDR (192)Ir source radiation fields. *Med. Phys.*, 38(11), pp.6074–83.

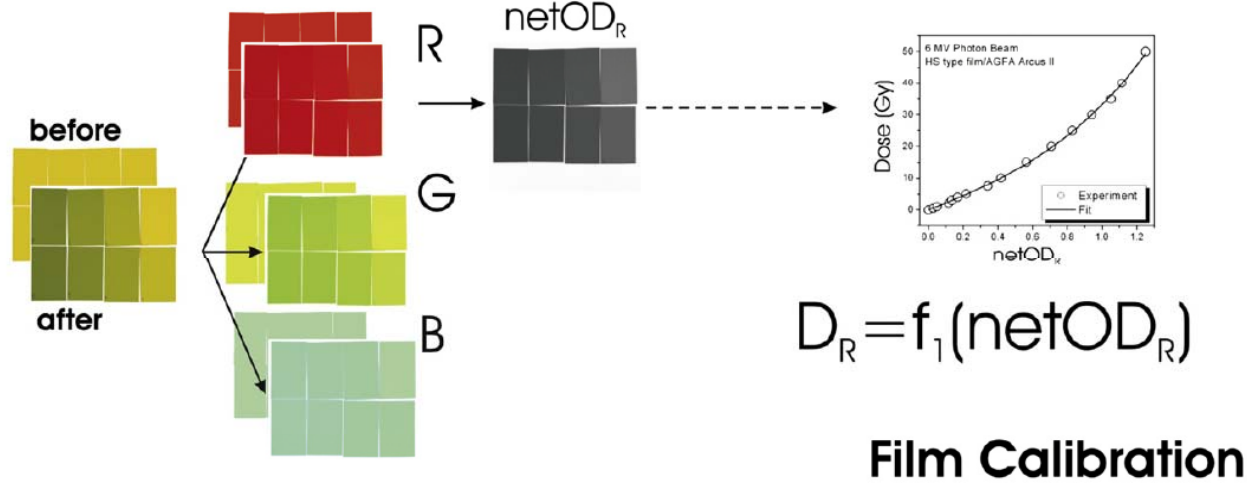
Palmer, A.L. et al., 2013. Comparison of methods for the measurement of radiation dose distributions in high dose rate (HDR) brachytherapy: Ge-doped optical fiber, EBT3 Gafchromic film, and PRESAGE® radiochromic plastic. *Med. Phys.*, 40(6), p.061707.

Palmer, A.L., Lee, C., et al., 2013. Design and implementation of a film dosimetry audit tool for comparison of planned and delivered dose distributions in high dose rate (HDR) brachytherapy. *PMB*, 58(19), pp.6623–40.

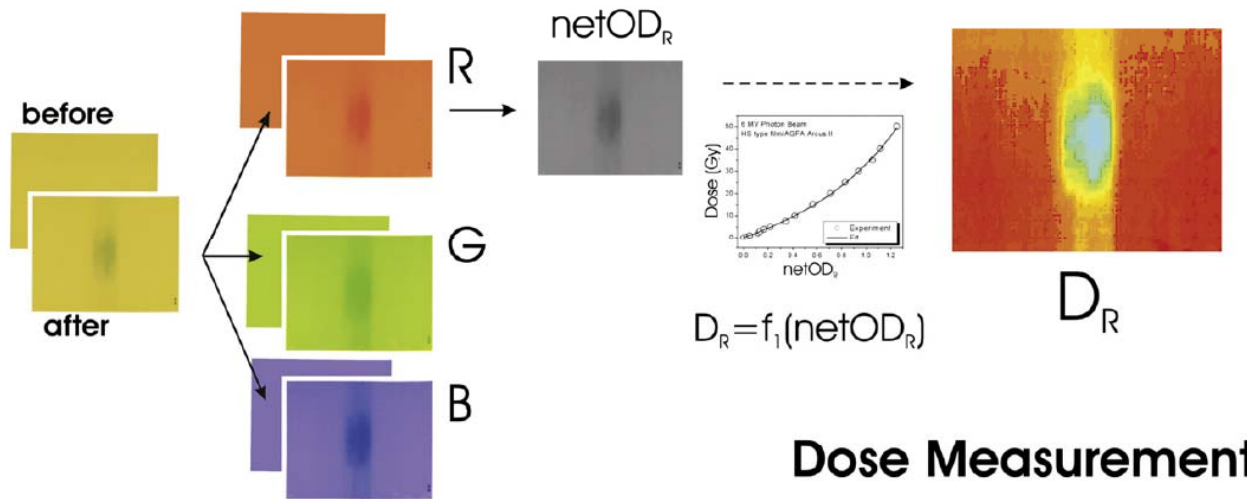
Palmer, A.L., Nisbet, A. & Bradley, D., 2013. Verification of high dose rate brachytherapy dose distributions with EBT3 Gafchromic film quality control techniques. *PMB*, 58(3), pp.497–511.

- OSLDs, PSDs and alanines are also used for in-vivo and will be reviewed in the next lecture.
- Due to spatial measurement resolution, other limitations, and level of development TLD remains the method of choice for single source dosimetry.
- What about 2D dosimetry using radiochromic films ...?

Radiochromic films: basic principles



Film Calibration



Dose Measurement

- Diacetylene molecules in a gelatin matrix coated on a polyester base
- Radiation induces polymerization of diacetylene molecules to form polydiacetylene dye polymers (self-developing)
- These are blue in color and cause light absorbance in the red part of the visible spectrum
- The change in net OD is measured using flat-bed scanners employing broad band visible light sources, and correlated to dose

Radiochromic films: types

Different types of Radiochromic™ films are available that differ in construction and characteristics:

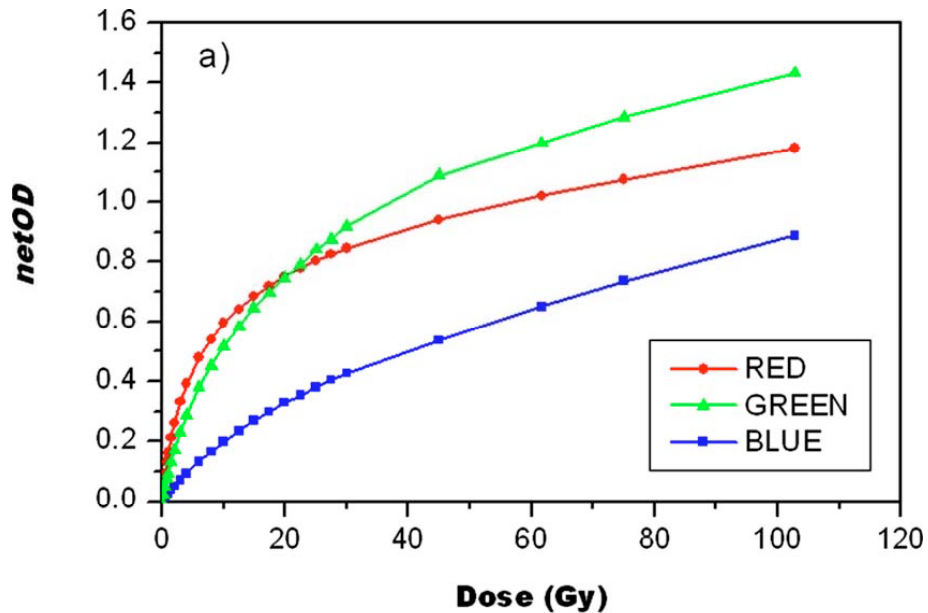
- EBT3 film for measuring patient dosimetry for IMRT plan verification.
- EBT-XD for the measurement of absorbed doses of ionizing radiation suited for high-energy photons.
- RTQA2 film for routine machine QA, such as radiation field / light field testing.
- MD-V3 films for measuring medium- to high-dose patient dosimetry.
- HD-V2 film for high-dose dosimetry work such as gamma Knife and SRS

2011: EBT-3 symmetric construction (126µm poly-30µm emulsion-126µm poly)
+ anti-Newton ring coating

Radiochromic films: influence factors

- There is post-irradiation signal growth that depends on t (log, 5% per decade) and T . A $k_{t,T}(t,T,D)$ correction must be applied OR films are kept @ stable T for (at least 8h) 24h before scanning.
- Background signal from an un-irradiated control film of the same batch and size, handled in the same way as the exp. films must be subtracted pixel-by-pixel to account for base OD and absorbance changes due to environmental conditions (T , visible light, humidity, scanning light, etc.) and obtain net OD change
- Film non-uniformity correction, $k_{nu}(x,y)$, is important. A double exposure technique with pixel-by-pixel subtraction or average pixel value subtraction (small films) must be employed.
- Alternatively, a triple channel technique has been developed (Micke et al, Multichannel film dosimetry with nonuniformity correction, *Med. Phys.* 38(5) 2523, 2011) and commercially available (FilmQA Pro software, Ashland-former ISP).
- There is also reader non-uniformity and films should always be read at the same scanner bed location to avoid application of a $k_{pos(x,y)}$ correction
 - Film response is dose rate independent!
 - Films can be used in water!

EBT films: sensitivity/linearity



- Sensitivity is film, scanner, protocol, and dose dependent
- It is non linear and different for all RGB channels

$$O.D. = -\log \frac{a + bD}{c + D}$$

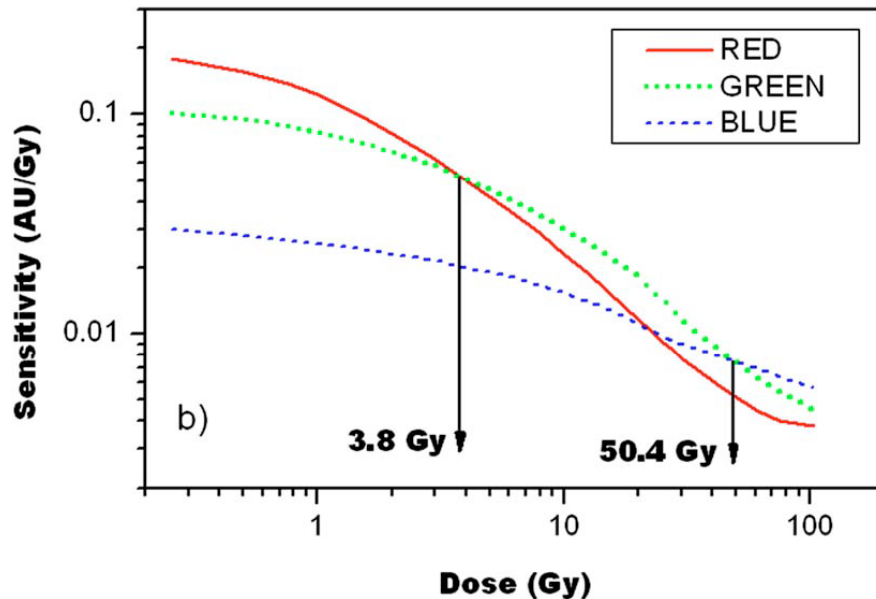
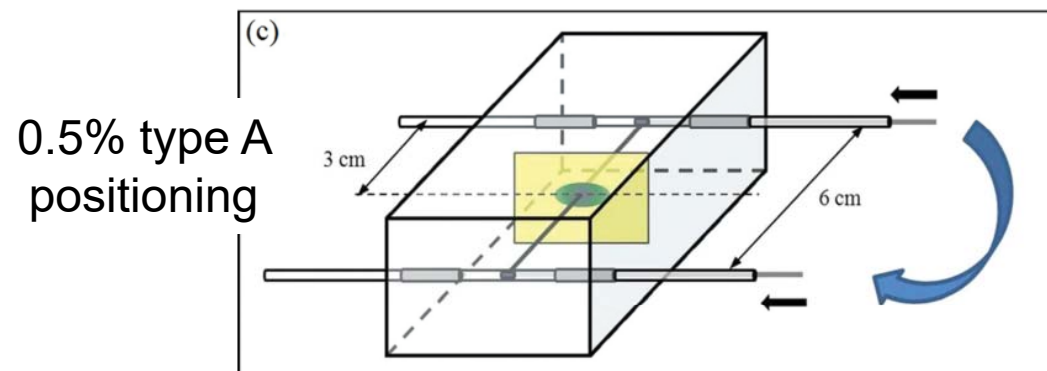


Figure from: Devic, Physica Medica 27(3) 122 (2011)

Radiochromic films: rel. E response

$$f^{rel}(Q, Q_0) = \frac{D_w(Q)/D_{TLD}(Q)}{D_w(Q_0)/D_{TLD}(Q_0)} \quad k_{bq}^{rel}(Q, Q_0) = \frac{D_{TLD}(Q)/M(Q)}{D_{TLD}(Q_0)/M(Q_0)}$$

- Arjomandy et al (2010) found the relative sensitivity of EBT2 relatively small (within $k=1$ uncert. 4.5%) from MV to 75kV_p
- Brown et al (2012) used synchrotron mono-chromatic x-rays and found up to 3% dose under-response ($f^{rel} k_{bq}^{rel} = 0.97$) at low E (25-35 keV)
- Bekerat et al (2014) indicate no relative energy dependence of EBT3 films between Ir-192 and Co-60 (albeit for 3cm film-source distance in a parallel-opposed Ir-192 HDR irradiation setup)
- The same authors report an over response ($f^{rel} k_{bq}^{rel} < 1$) of about $16\% \pm 4\%$ and an under response ($f^{rel} k_{bq}^{rel} > 1$) of about $27\% \pm 4\%$ for EBT3 irradiated in x-ray beams of average energies about 40 keV and 20 keV, respectively, relative to Co-60.



Radiochromic films: precision/accuracy

- Chiu-Tsao et al. (2008) used EBT for I-125 seed dosimetry in Solid Water with a calibration from a I-125 seed (uncertainty due to solid water not included)

TABLE IV. Uncertainty analysis for the dose rate constant.

Average uncertainty in NOD from experimental film scanning for a single data point	Type A	3.3%				
N (number of data points) at 1 cm along the transverse axis			144	(red)	176	(green)
Average uncertainty in NOD from experimental film scanning for N data points	Type A	$3.3\% / \sqrt{N-1}$	0.28%	(red)	0.25%	(green)
Uncertainty in conversion to dose (Table III)	Type B		6.6%	(red)	6.7%	(green)
Uncertainty in seed's air kerma strength, S_k (incorporating uncertainty in half life)	Type B		1.6%			
Total uncertainty in dose rate constant			6.8%	(red)	6.9%	(green)

TABLE III. Uncertainty in conversion from optical density to dose in the calibration procedure.

Average uncertainty in NOD from calibration film scanning	Type A	3.3%			
Uncertainty in calibration standard of air kerma strength, S_k (incorporating uncertainty in half life)	Type B	1.6%			
Uncertainty in positioning	Type B	5%			
Uncertainty in using fit to convert NOD to dose, σ_{fit}	Type B	2.3%	(red)	2.6%	(green)
Total conversion uncertainty		6.6%	(red)	6.7%	(green)

In summary:

- Radiochromic films close to maturity for brachytherapy dosimetry
BUT
- Further work is needed for their full relative energy response characterization
- Due to calibration uncertainty (rel. high and dose dependent) and influence factors they are reserved mainly for relative dosimetry in QA and D verification

3D dosimeters...?

Figure from: Rogers & Cygler (Eds), *Clinical dosimetry measurements in radiotherapy (2009 AAPM Summer School), Monograph No. 34, Medical Physics Publishing 2011*

- radiation-induced chemical change in a gel matrix can be mapped in 3D using MRI or optical CT

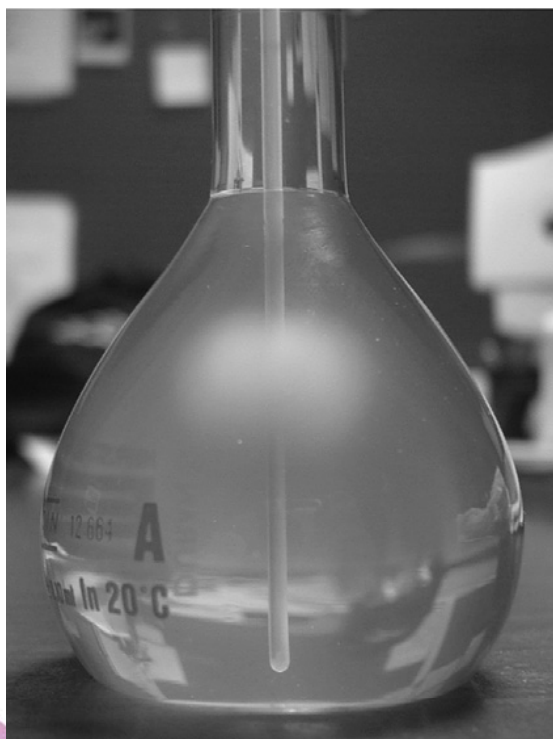
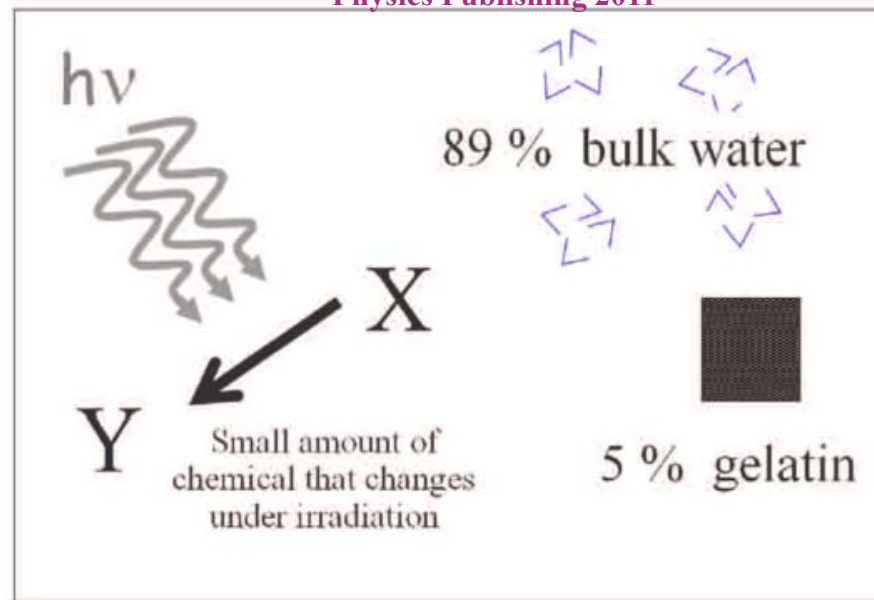


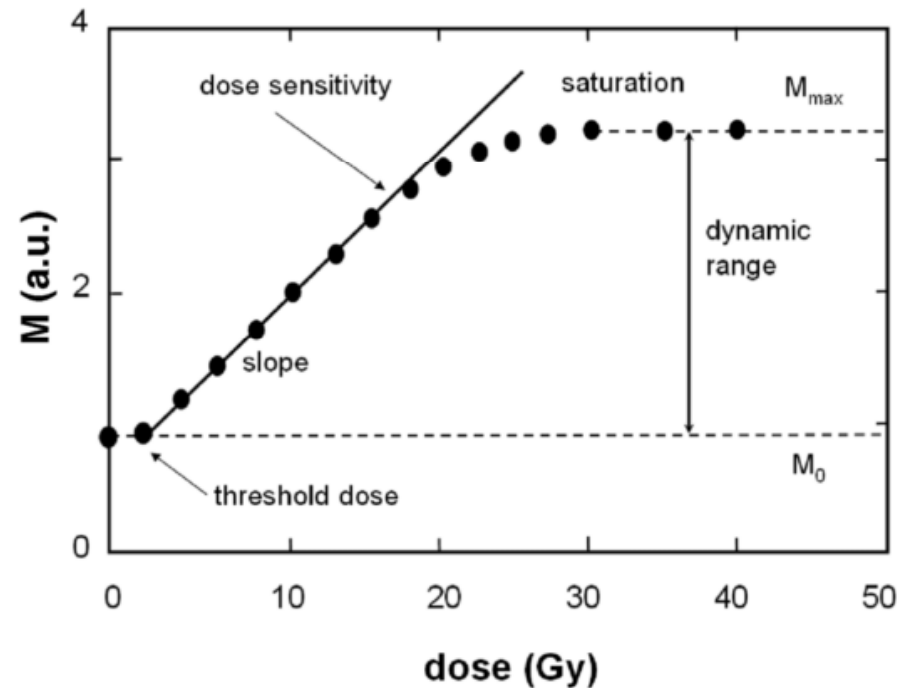
Figure from: Baltas, Sakelliou, Zamboglou (Eds), *The Physics of modern brachytherapy for oncology*, Taylor & Francis Books Inc, 2006

- polymer gels: Custom made with organic co-monomers
- Truview/Clearview gels (Modus Medical devices Inc.): xylenol orange organic reagent
- PRESAGE (Heuris Inc.): color forming leucodye + initiator within a polyurethane matrix (not a gel)

3D dosimeters

Advantages

- Dosimeter is the phantom (negligible to small p_{phant} depending on type)
- 3D character facilitates concurrent measurements and processing for minimizing positional and type A uncertainty
- negligible to small f^{rel} (depending on type)
- No dose rate dependence (except for methacrylic acid based gels-MAGIC & PRESAGE at very low dose rates)



Disadvantages

- Sensitivity varies with type and batch
- $k^{\text{rel}}_{\text{bq}}$ can be significant for some dosimeters @ low E
- 3D character augments influences and problems similar to that of films increasing type B uncertainty

Example polymer gels

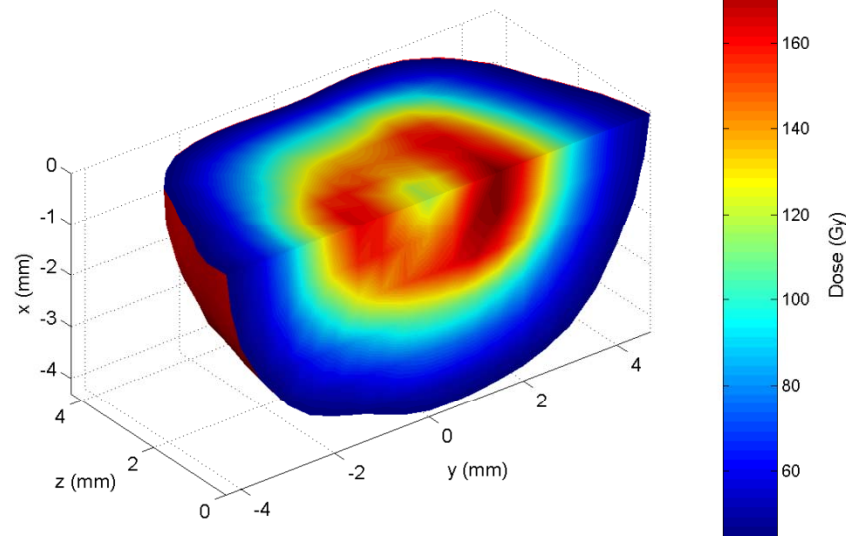
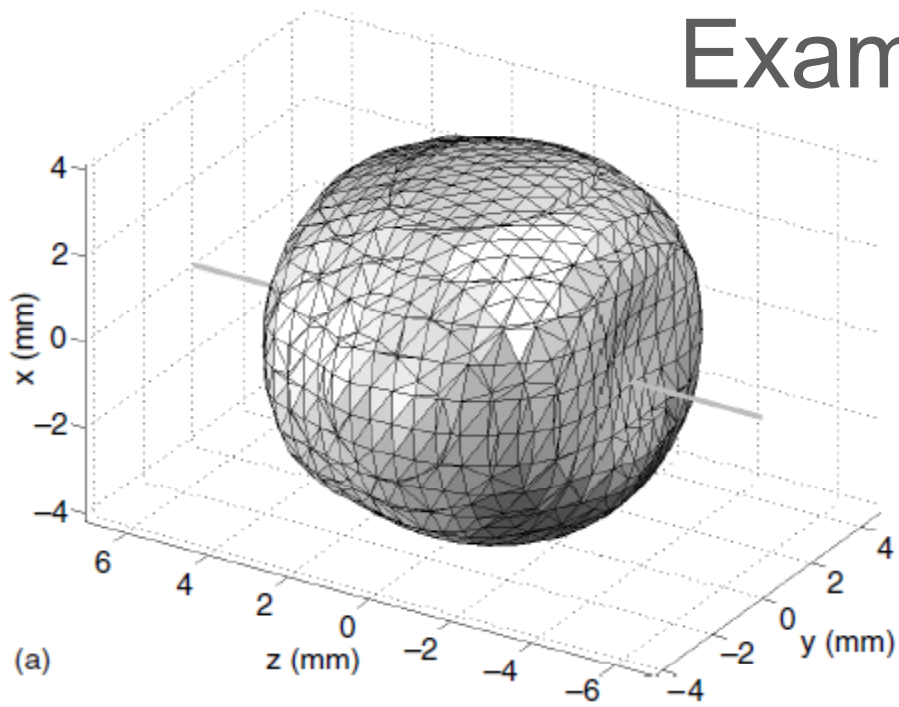
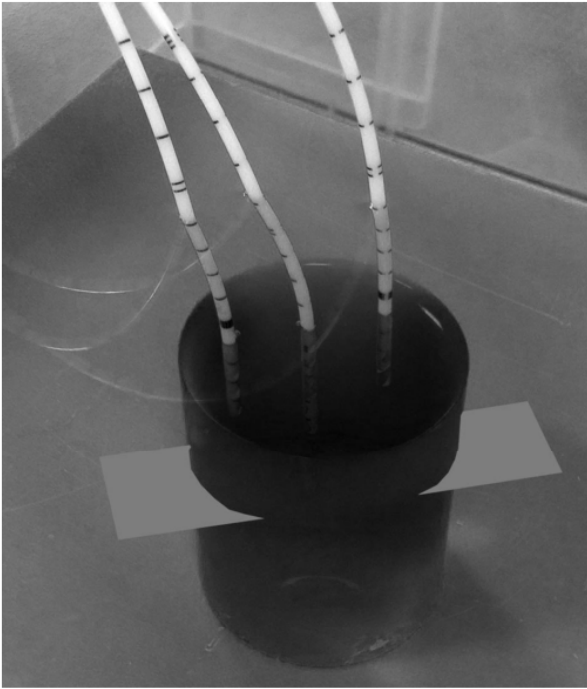


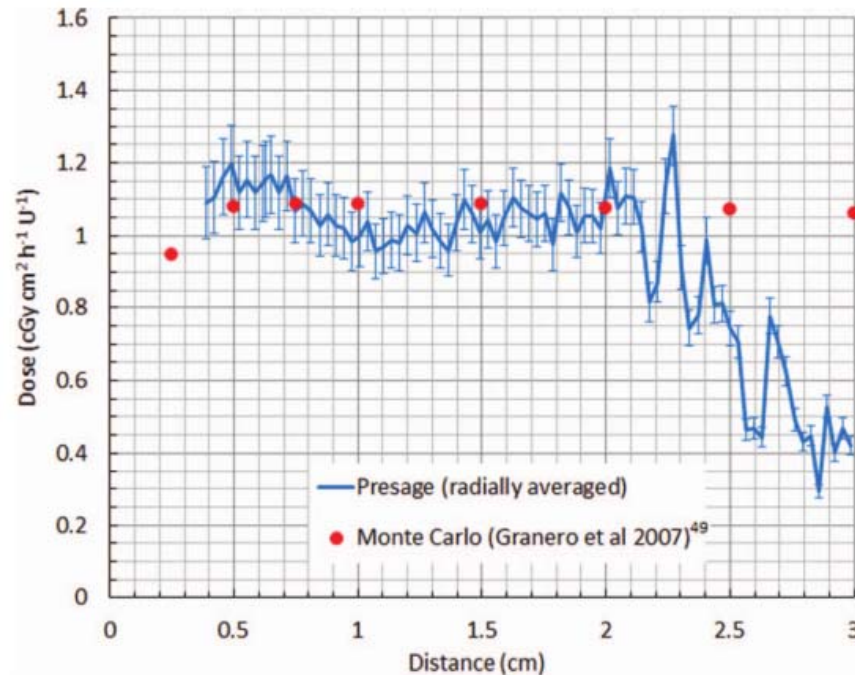
Fig. 1. A picture of the PABIG gel irradiated with two seeds (top: I25.S17, bottom: I25.S06) for a time period of 26 days.

Figures from: Baltas, Sakelliou, Zamboglou (Eds), The Physics of modern brachytherapy for oncology, Taylor & Francis Books Inc, 2006

Example PRESAGE

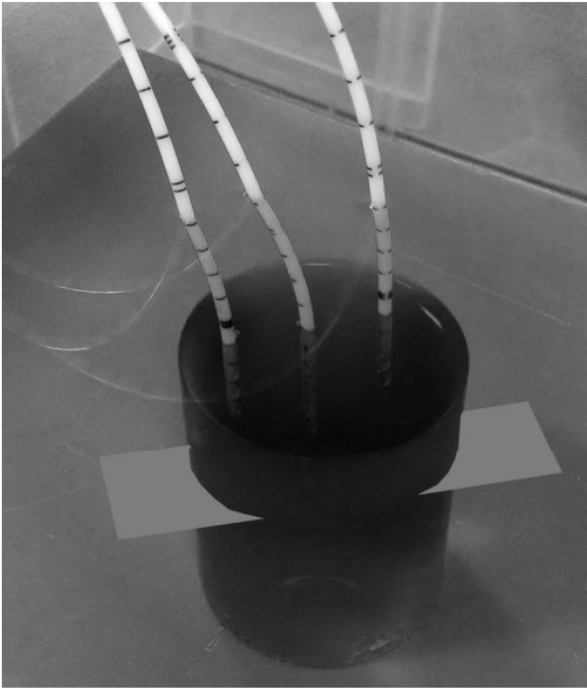


- Palmer et al. Ir-192 HDR dosimetry in TG-43 conditions

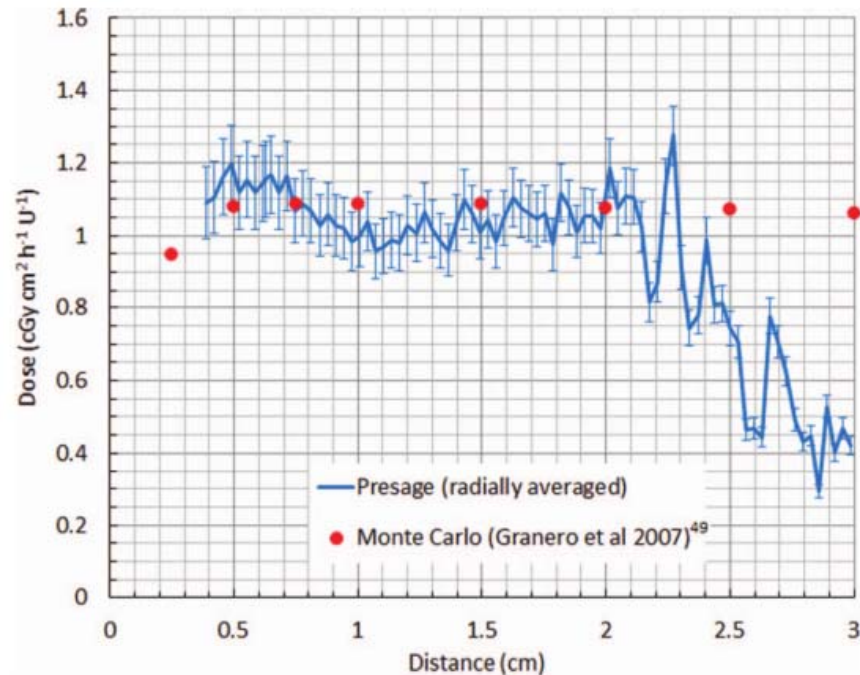


Pictures from: Palmer et al, Med. Phys. 40, 061707 (2013)

Example PRESAGE

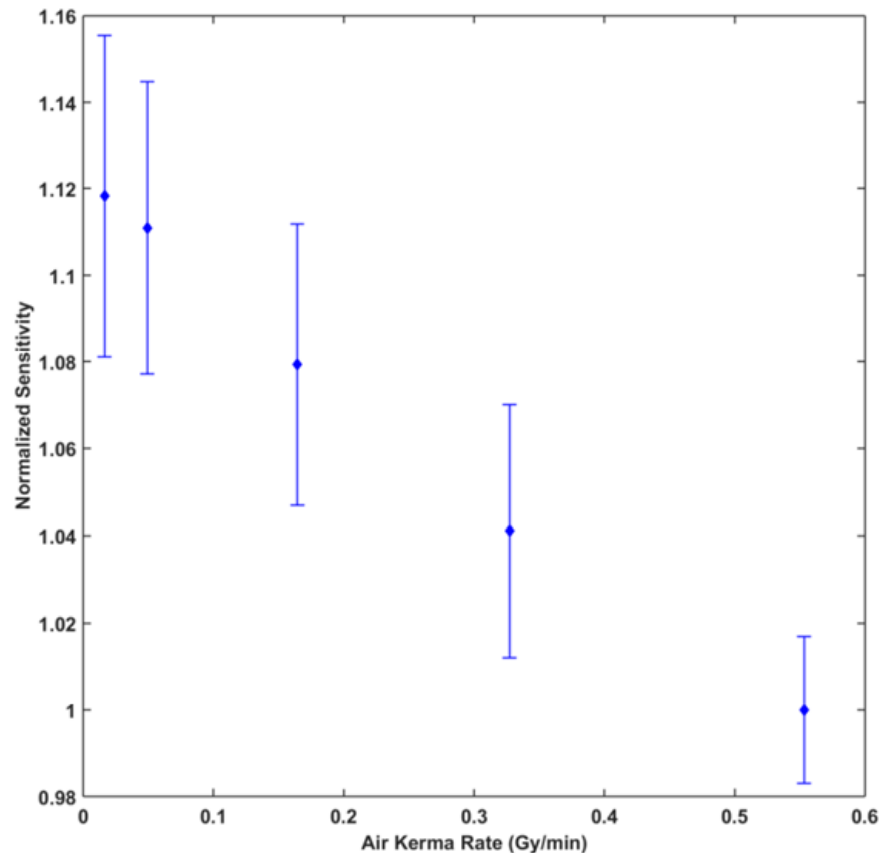


- Palmer et al. Ir-192 HDR dosimetry in TG-43 conditions



Pictures from: Palmer et al, Med. Phys. 40, 061707 (2013)

Example PRESAGE

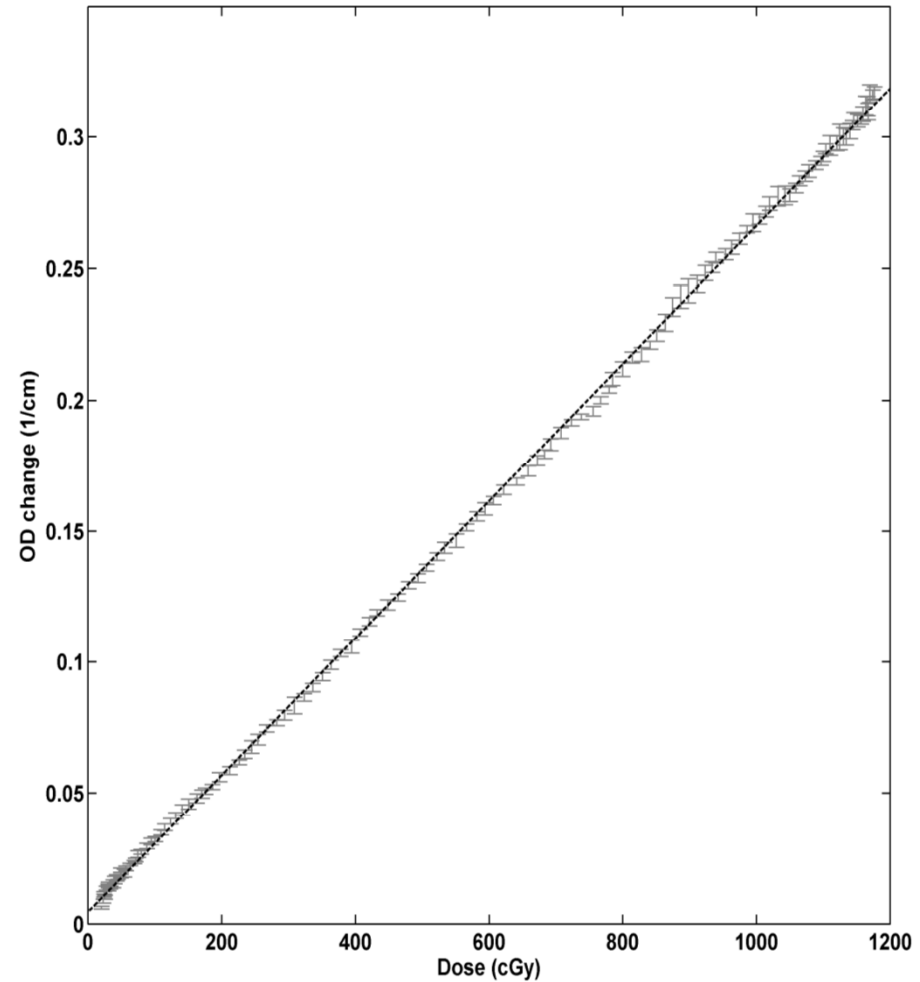
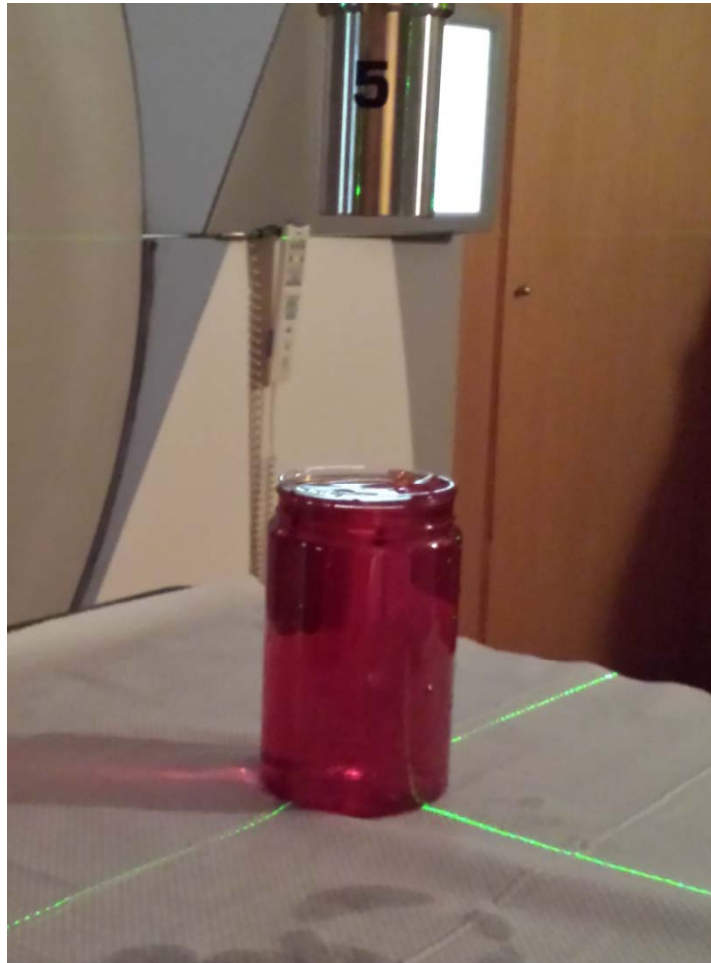


Private data:
relative response variation
with dose rates
encountered outside the
PTV in HDR brachy,
measured with PRESAGE
cuvettes

Figure 5: Normalized air kerma sensitivity as a function of air kerma rate, measured using PRESAGE cuvette samples from the same batch as the experimental and calibration PRESAGE dosimeters of this work. Data presented for each air kerma rate correspond to the average from 3 cuvettes at the same distance from an ^{192}Ir HDR source in a single irradiation and corresponding standard deviation of the mean.

Example Truview: private data

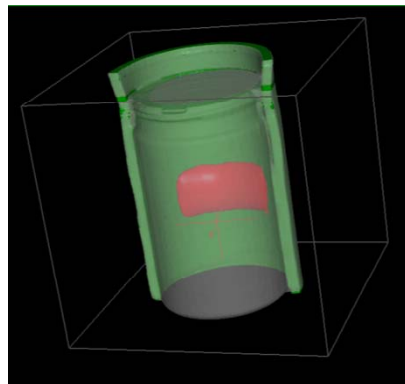
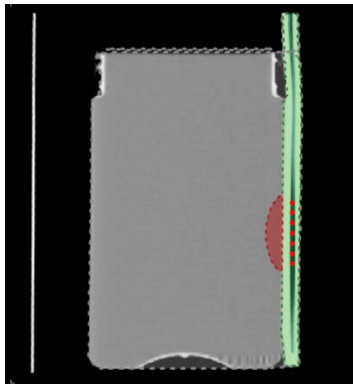
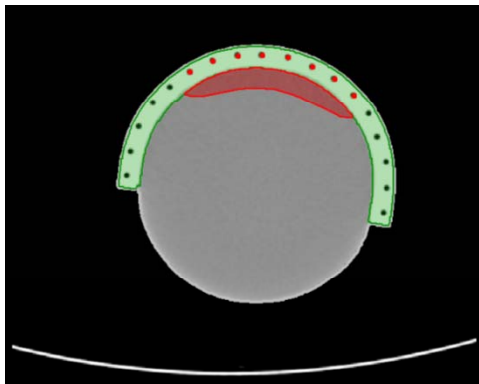
calibration



Example Truview: private data



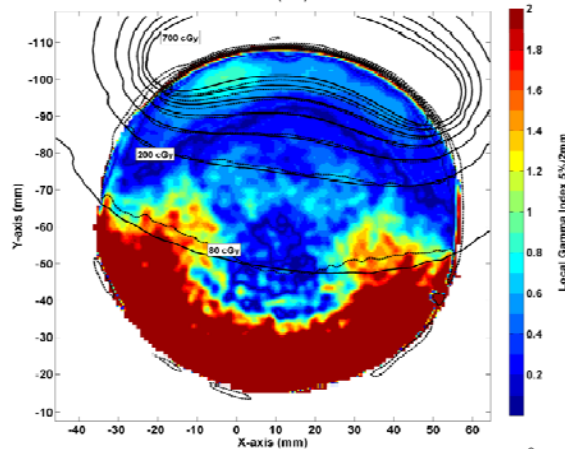
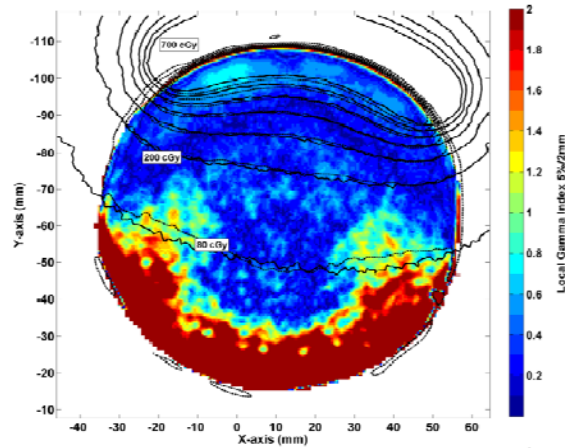
Set up and planning
(8 Gy to an arbitrary PTV
using geometrical
optimization)



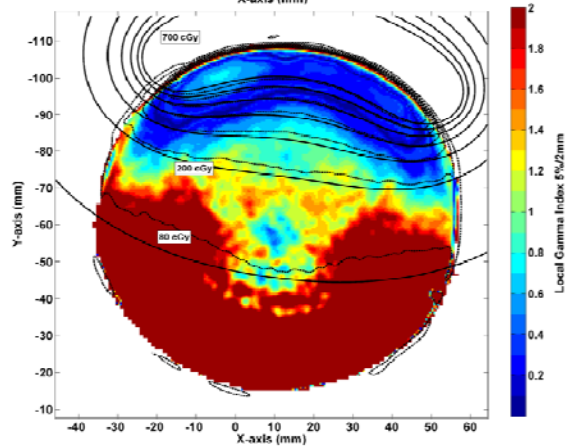
Example Truview: private data

Gamma index maps (2mm/5%) :

MC versus Truview



ACE versus Truview



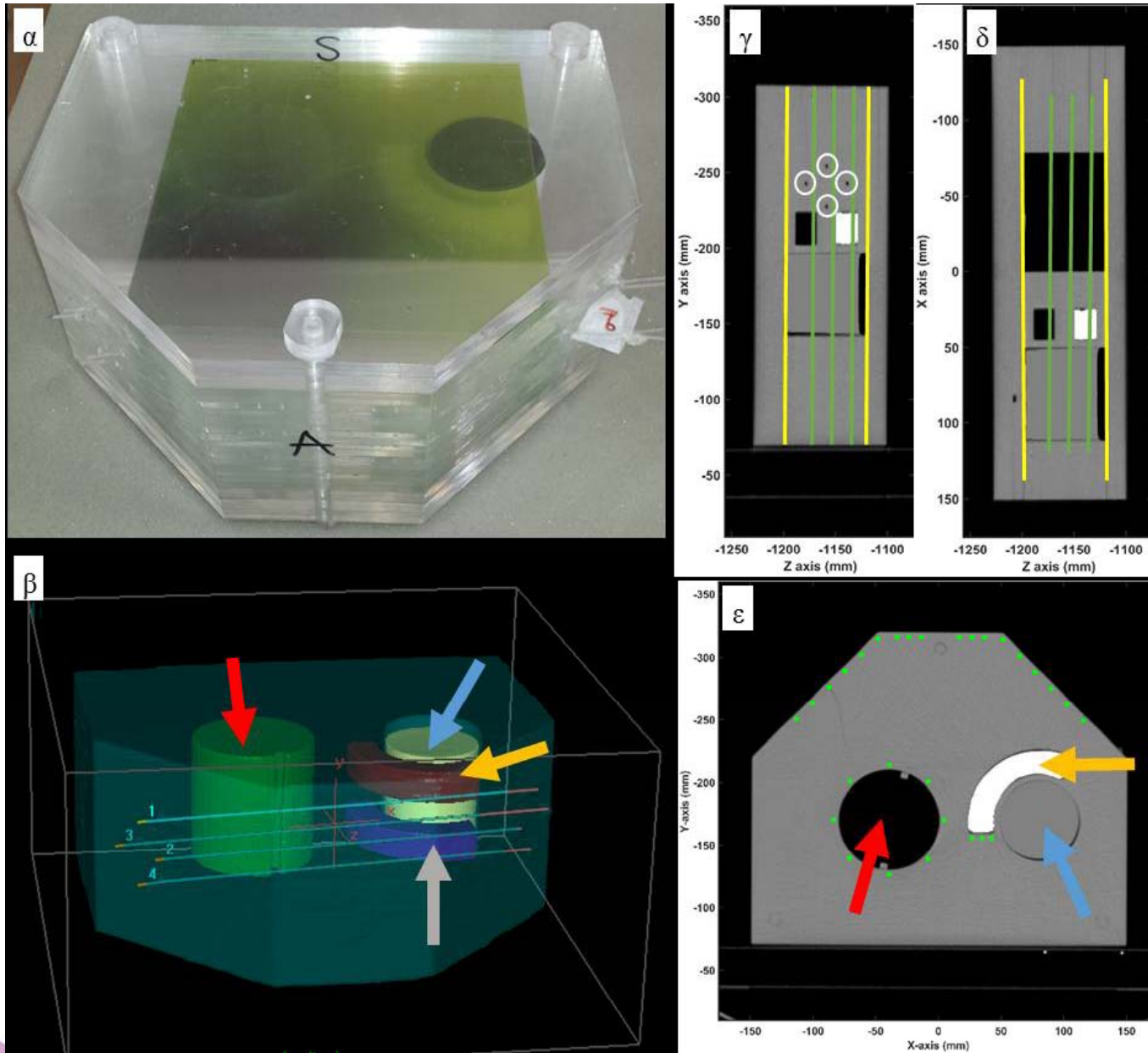
TG-43 vs Truview

Example commissioning/dose verification

- Laborious...!
- No single, ideal, system exists
- Registration of measured and calculated dose distributions comes into play

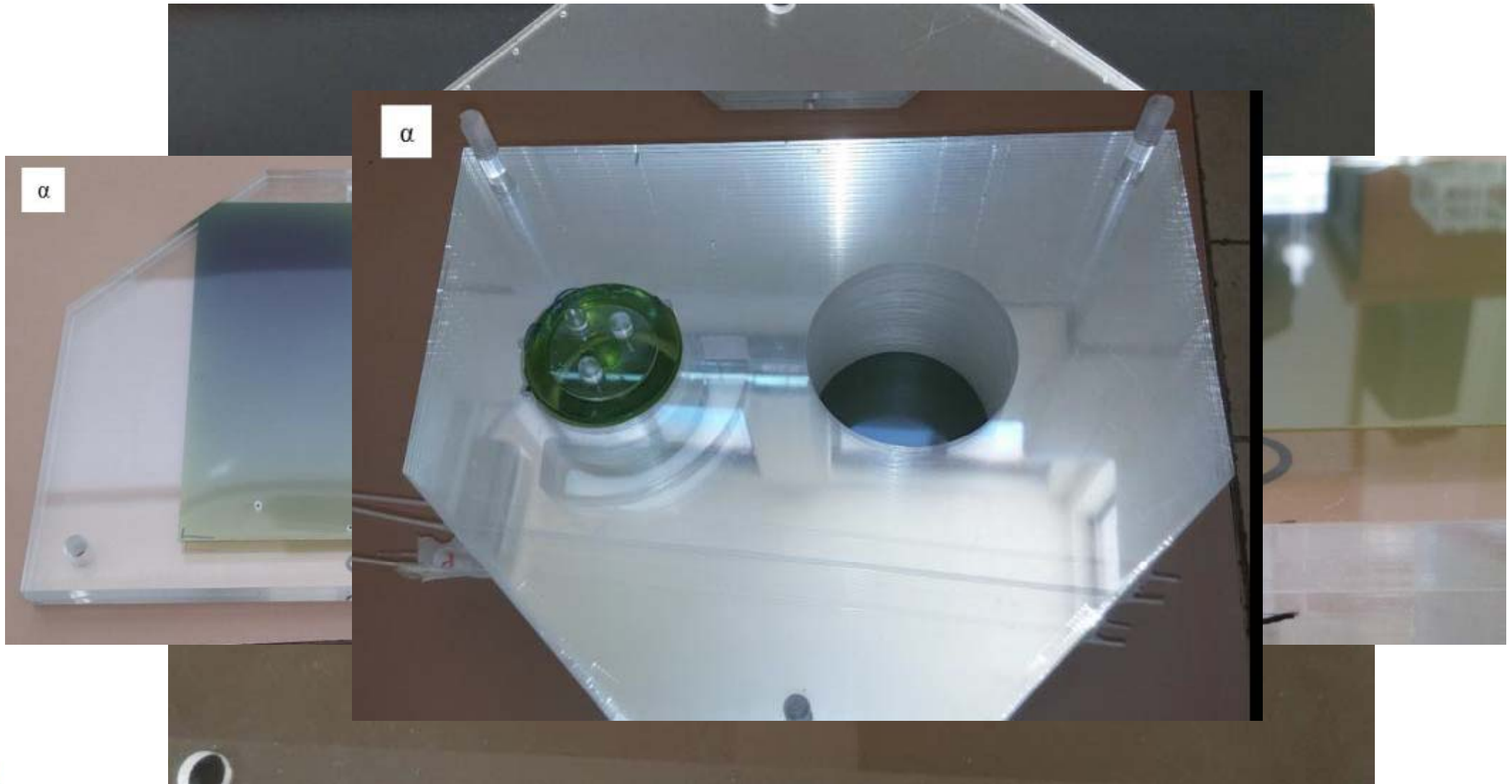
Still there is a way to verify calculations, albeit, within the experimental uncertainties

Example commissioning/dose verification



- Private data: experimental dosimetry for the validation of MBDCA results for Ir-192 HDR

Example commissioning/dose verification



Example commissioning/dose verification

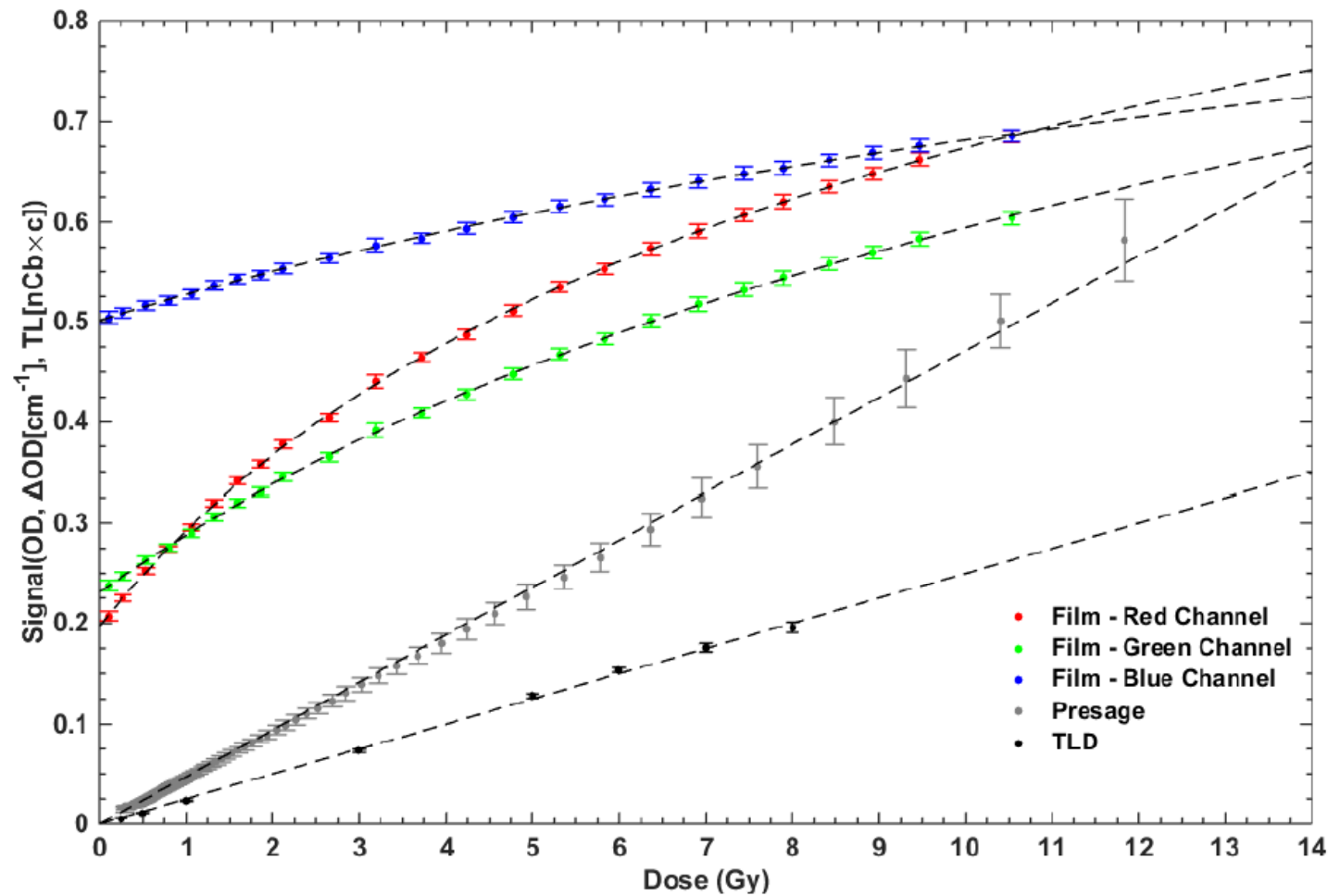


Figure 2: Absorbed dose sensitivity calibration data and calibration curves for the three dosimetric systems used in this work. TLD readings were scaled using a factor $c=52 \times 10^3$.

Dosimetric System	Source of Uncertainty	Spatial Uncertainty (mm)		Dosimetric Uncertainty (%)		Ref.
		Type B	Type A	Type B	Type A	
TLDs	Detector position	0.5				
	Catheter reconstruction	0.5				
	Calibration				1.51	
	Reference light correction factor			1.81		
	Absorbed dose sensitivity correction			4.28		
	f^{rel}			Position dependent: 1.8 - 3.8		
	Source air kerma strength				1.50	37
	Combined Uncertainty (k=1)	0.71		4.98 - 6.00	2.13	
	Total standard (k=1)	0.71		5.4 - 6.4		
	Total expanded (k=2)	-		10.8 - 12.7		
EBT3 films	Registration	1.5				
	Catheter reconstruction	0.5				
	Scanner reproducibility			0.25		38, 39
	OD measurement reproducibility			0.30		
	Scanner homogeneity				0.20	38, 39
	Film calibration				Dose dependent: 1.9 - 6.2	
	Source air kerma strength				1.50	37
	$(S_{col}/\rho)_{PMMA,w}$				0.5	16
	Combined Uncertainty (k=1)	1.58		0.39	2.48 - 6.40	
	Total standard (k=1)	1.58		2.5 - 6.4		
Total expanded (k=2)	-		5.0 - 12.8			
PRESAGE	Registration	2.5				
	Catheter reconstruction	0.5				
	Optical-CT readout reproducibility			2.50		
	Calibration				1.54	
	Source air kerma strength				1.50	37
	Temperature variations (± 0.5 °C)				0.85	22
	Temporal stability				2.00	22
	Intradosimetric consistency				2.00	23
	Intrabatch reproducibility				2.00	22
	Combined Uncertainty (k=1)	2.55		2.50	4.16	
	Total standard (k=1)	2.55		4.85		
	Total expanded (k=2)	-		9.7		

Example commissioning /dose verification

Example commissioning/dose verification

Table 2: Gamma Index test pass rates for the comparison of calculations and corresponding TLD measurements using the latter as the reference data, as a function of TLD position in the phantom. Distance-to-agreement and dose difference passing criteria were 6% local reference dose and 1 mm, respectively.

Proximal inhomogeneity	GI pass rate	
	ACE	MC
Phantom boundary	39/ 54	54/54
Air cylinder	20 / 23	21/23
Teflon insert	3 / 3	3/3
Air insert	3 / 3	3/3

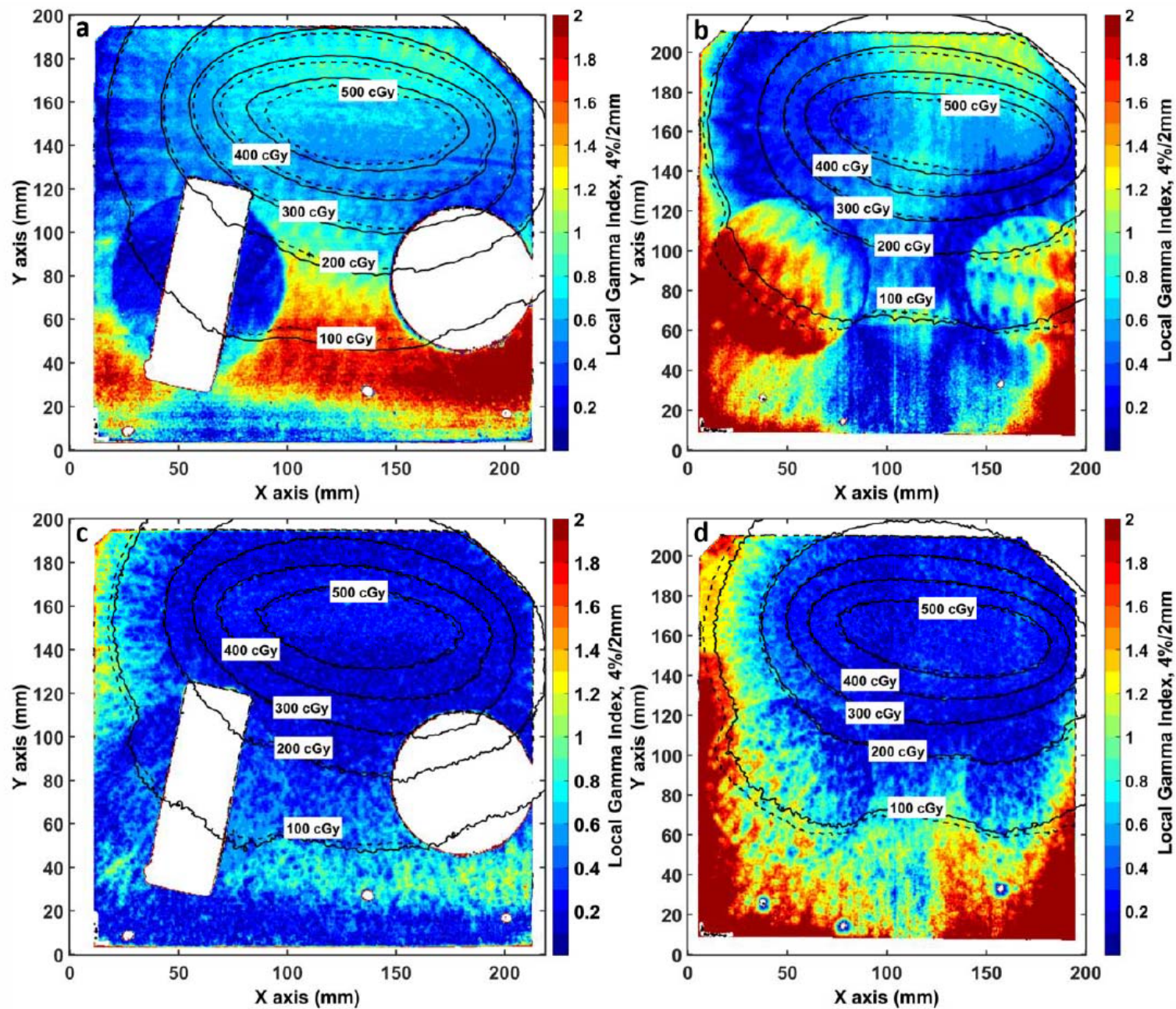
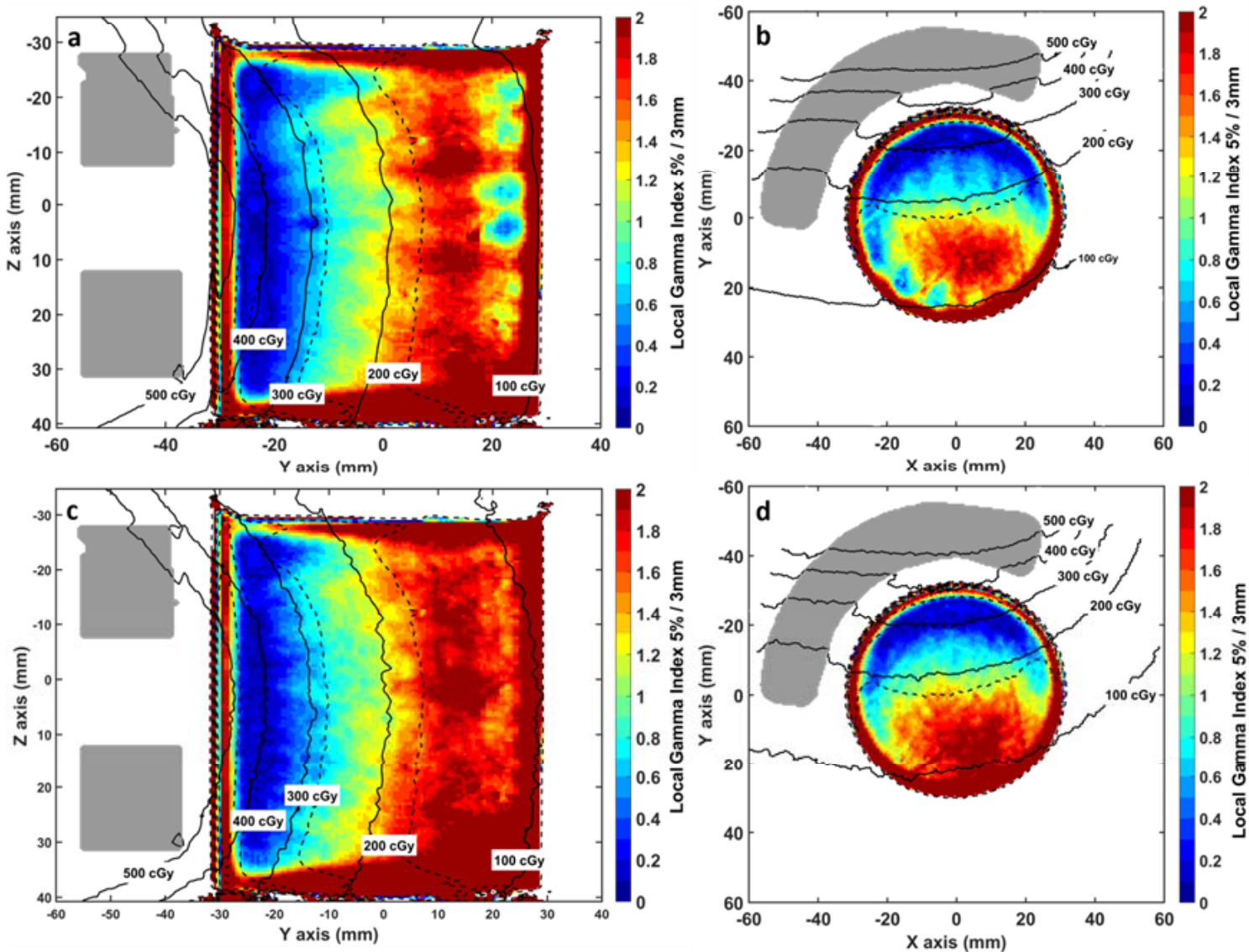


Figure 3: Gamma index maps (4%, 2mm) for Film1 (right) and Film2 (left) with measured (dashed lines) and calculated (solid lines) isodoses. (a-b), Film – ACE, (c-d) Film – MC.

Example
commissioning
/dose verification



Example
commissioning
/dose verification

Figure 4: Sagittal (left) and axial (right) slices of gamma index maps (5%, 3mm) for PRESAGE with measured (dashed lines) and calculated (solid lines) isodoses. (a-b) PRESAGE-ACE. (c-d) PRESAGE-MC.

Further reading ...

- Rogers & Cygler (Eds), Clinical dosimetry measurements in radiotherapy (2009 AAPM Summer School), Monograph No. 34, Medical Physics Publishing 2011
- Baltas, Sakelliou, Zamboglou (Eds), The Physics of modern brachytherapy for oncology, Taylor & Francis Books Inc, 2006
- Rivard, M.J. et al., 2004. Update of AAPM Task Group No. 43 Report: A revised AAPM protocol for brachytherapy dose calculations. Medical Physics, 31(3), p.633.
- Perez-Calatayud, J. et al., 2012. Dose calculation for photon-emitting brachytherapy sources with average energy higher than 50 keV: report of the AAPM and ESTRO. Medical physics, 39(5), pp.2904–29.

and references cited herein

Further reading ...

•References cited in this lecture:

- Adolfsson, E. et al., 2010. Response of lithium formate EPR dosimeters at photon energies relevant to the dosimetry of brachytherapy. *Med. Phys.*, 37(9), p.4946.
- Aldelaijan, S., Mohammed, H., Tomic, N., Liang, L.-H., Deblois, F., Sarfehnia, A., ... Devic, S. (2011). Radiochromic film dosimetry of HDR (192)Ir source radiation fields. *Medical Physics*, 38(11), 6074–83.
- Araki, F. et al., 2013. Measurement of absorbed dose-to-water for an HDR (192)Ir source with ionization chambers in a sandwich setup. *Med. Phys.*, 40(9), p.092101.
- Brown, T. a D., Hogstrom, K. R., Alvarez, D., Matthews, K. L., Ham, K., & Dugas, J. P. (2012). Dose-response curve of EBT, EBT2, and EBT3 radiochromic films to synchrotron-produced monochromatic x-ray beams. *Medical Physics*, 39(12), 7412–7.
- Chiu-Tsao, S.-T., Medich, D. & Munro, J., 2008. The use of new GAFCHROMIC EBT film for [¹²⁵I] seed dosimetry in Solid Water phantom. *Med. Phys.*, 35(8), p.3787.
- Davis, S. D., Ross, C. K., Mobit, P. N., Van der Zwan, L., Chase, W. J., & Shortt, K. R. (2003). The response of lif thermoluminescence dosimeters to photon beams in the energy range from 30 kV x rays to 60Co gamma rays. *Radiation Protection Dosimetry*, 106(1), 33–43.
- Devic, S. (2011). Radiochromic film dosimetry: past, present, and future. *Physica Medica : PM : An International Journal Devoted to the Applications of Physics to Medicine and Biology : Official Journal of the Italian Association of Biomedical Physics (AIFB)*, 27(3), 122–34.
- Kennedy, R. M., Davis, S. D., Micka, J. A., & DeWerd, L. A. (2010). Experimental and Monte Carlo determination of the TG-43 dosimetric parameters for the model 9011 THINSeed brachytherapy source. *Medical Physics*, 37(4), 1681–8.
- Kolbun, N. et al., 2010. Experimental determination of the radial dose distribution in high gradient regions around 192Ir wires: comparison of electron paramagnetic resonance imaging, films, and Monte Carlo simulations. *Med. Phys.*, 37(10), pp.5448–55.
- Luxton, G. (1999). Comparison of radiation dosimetry in water and in solid phantom materials for I-125 and Pd-103 brachytherapy sources: EGS4 Monte Carlo study. *Medical Physics*, 21(5), 631.
- Nunn, A. A., Davis, S. D., Micka, J. A., & Dewerd, L. A. (2010). LiF : Mg , Ti TLD response as a function of photon energy for moderately filtered x-ray spectra in the range of 20 – 250 kVp relative to C 60 o LiF : Mg , Ti TLD response as a function of photon energy for moderately filtered x-ray spectra in the range of, 1859(2008).
- Palmer, A.L. et al., 2013. Comparison of methods for the measurement of radiation dose distributions in high dose rate (HDR) brachytherapy: Ge-doped optical fiber, EBT3 Gafchromic film, and PRESAGE® radiochromic plastic. *Med. Phys.*, 40(6), p.061707.
- Palmer, A.L., Lee, C., et al., 2013. Design and implementation of a film dosimetry audit tool for comparison of planned and delivered dose distributions in high dose rate (HDR) brachytherapy. *PMB*, 58(19), pp.6623–40.
- Palmer, A.L., Nisbet, A. & Bradley, D., 2013. Verification of high dose rate brachytherapy dose distributions with EBT3 Gafchromic film quality control techniques. *PMB*, 58(3), pp.497–511.
- Papagiannis, P., Pantelis, E., Georgiou, E., Karaiskos, P., Angelopoulos, A., Sakelliou, L., ... Seimenis, I. (2006). Polymer gel dosimetry for the TG-43 dosimetric characterization of a new 125I interstitial brachytherapy seed. *PMB*, 51(8), 2101–11.
- Patel, N. S., Chiu-Tsao, S.-T., Williamson, J. F., Fan, P., Duckworth, T., Shasha, D., & Harrison, L. B. (2001). Thermoluminescent dosimetry of the Symmetra™ [¹²⁵I] model I25.S06 interstitial brachytherapy seed. *Medical Physics*, 28(8), 1761.
- Sarfehnia, A., Kawrakow, I. & Seuntjens, J., 2010. Direct measurement of absorbed dose to water in HDR [¹⁹²Ir] brachytherapy: Water calorimetry, ionization chamber, Gafchromic film, and TG-43. *Med. Phys.*, 37(4), p.1924.
- Schaecken, B. et al., 2011. Experimental determination of the energy response of alanine pellets in the high dose rate 192Ir spectrum. *PMB*, 56(20), pp.6625–34.
- Tedgren, A. C., Hedman, A., Grindborg, J.-E., & Carlsson, G. A. (2011). Response of LiF:Mg,Ti thermoluminescent dosimeters at photon energies relevant to the dosimetry of brachytherapy (<1 MeV). *Medical Physics*, 38(10), 5539–50.
- Tello, V. M. (1995). How water equivalent are water-equivalent solid materials for output calibration of photon and electron beams? *Medical Physics*, 22(7), 1177.

Vienna, 29 May – 1 June 2016



Advanced Brachytherapy Physics

Treatment Delivery Verification

Dimos Baltas, Ph.D., Prof.

Division of Medical Physics

Department of Radiation Oncology, Medical Center - University of Freiburg

Faculty of Medicine, University of Freiburg, Germany

and

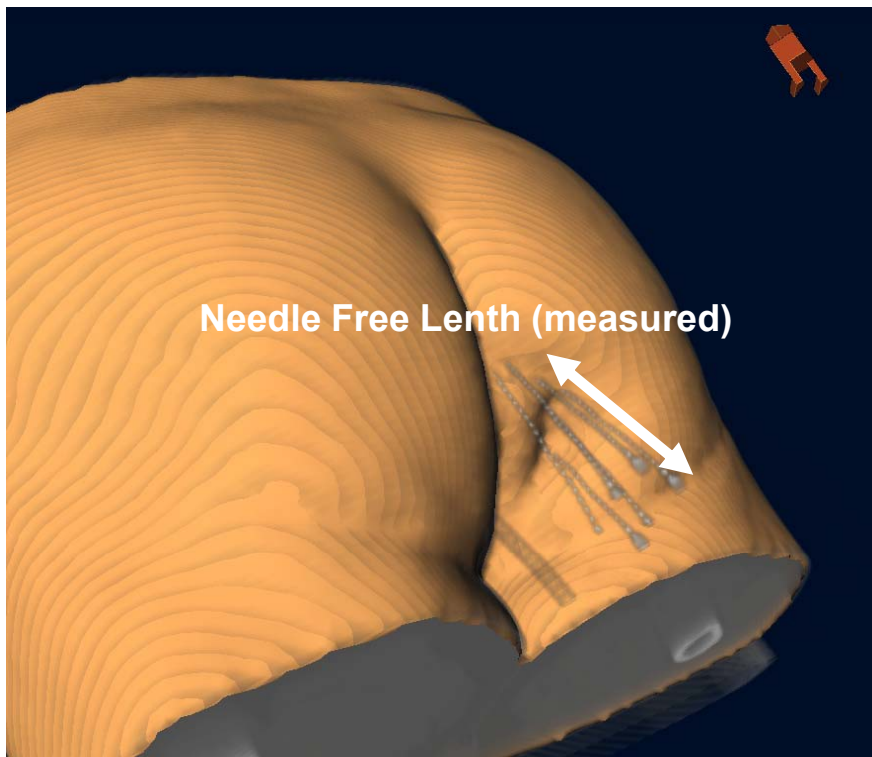
German Cancer Consortium (DKTK), Partner Site Freiburg, Germany

[E-mail: dimos.baltas@uniklinik-freiburg.de](mailto:dimos.baltas@uniklinik-freiburg.de)

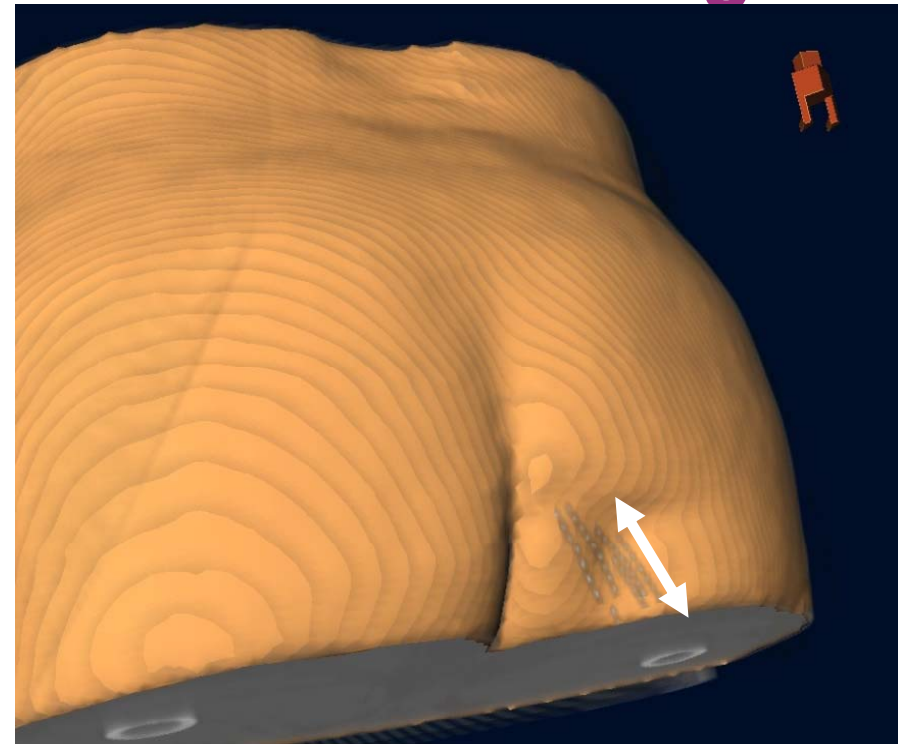
Modern Brachytherapy: Treatment Verification – An Example

■ The planned treatment delivery

CT-Verification



CT-Planning



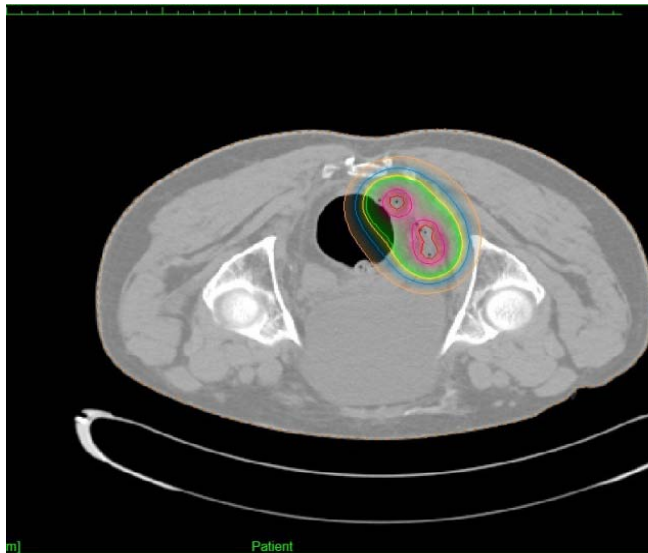
Needle free length

- measured after implantation and before CT-imaging
- controlled before each fraction

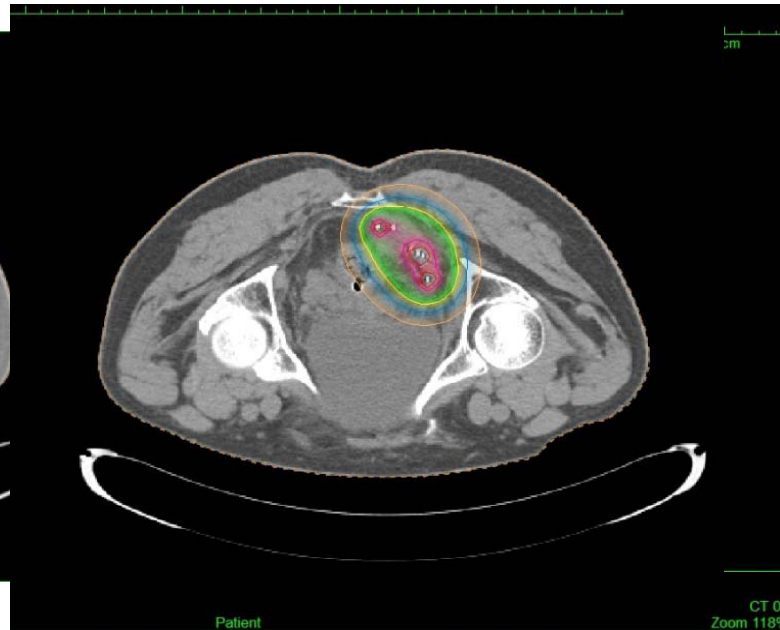
Modern Brachytherapy: Treatment Verification – An Example

- *Delivered Treatment versus Planned Treatment*

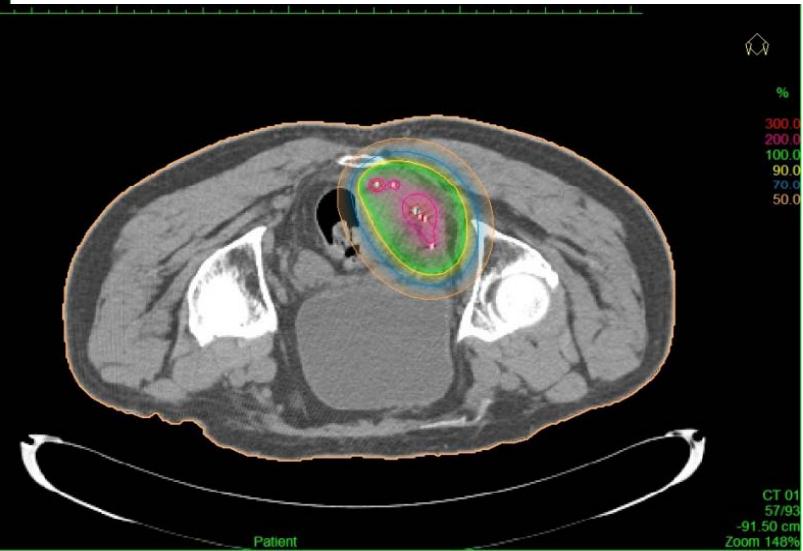
CT-Verification I



CT-Verification II



CT-Planning



Modern Brachytherapy: Treatment Delivery Verification

■ *Delivered Treatment versus Planned Treatment*

Currently we assume that:

- The geometry and location of the implanted catheters
- The connection of channels to implanted catheters
- The length of the channels
- The source movement patterns (dwell positions and dwell times) within the implanted catheters
- The patient anatomy at the relevant location

are during treatment delivery exact as considered and planned in the RTP.

BRT *versus* ERT Similarities and Differences

Dosimetric Kernel

→
(Spot)

Particles



Delivery Technology

→
(Modulation, Dose-Volume-Prescription)

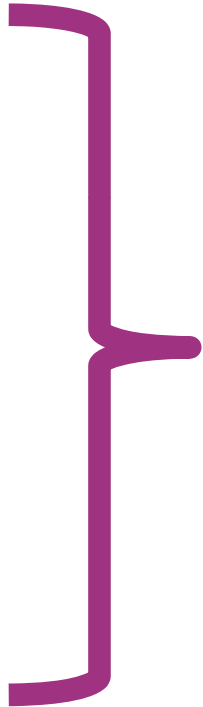
IMRT (X, P)



Dose Distribution

→
(Inhomogeneity)

SRS / SBRT



BRT *versus* ERT Similarities and Differences

■ *The Localization Process*

- 3D-Localization of the relevant Anatomy (as in ERT)
- 3D-Localization of the implanted catheters (“Beams”)
- Co-Registration of Anatomy and implanted catheters

BRT *versus* ERT Similarities and Differences

- **Beam Delivery System in BRT**

Beam = Catheter/Needle/Applicator

MLC Settings = Source moving patterns within applicator

Monitor Units = Dwell Times

Thus “beams” become for BRT *patient-dependent parameters*, that requires 3D reconstruction (Localization: Imaging, ...) and registration to anatomy

BRT *versus* ERT Similarities and Differences

- **Verification**

We mean the process of proof that we deliver the dose we planned to the tissue (3D) within a specific accuracy and precision level.

- **BRT (HDR)**

In opposite to ERT our dose delivery system (stepping source within implanted catheters) depends on the specific patient implant geometry (anatomy).

This is not the case for ERT, where the performance of the dose delivery system (MLC, Dose Rate, Energy, Gantry Angle, Collimator Angle & Couch Settings) is independent of the specific patient.

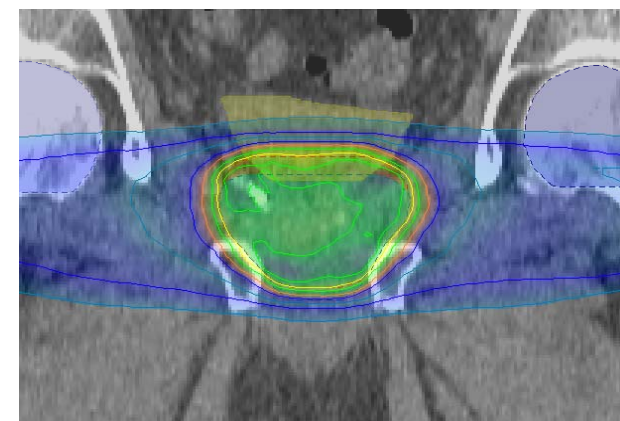
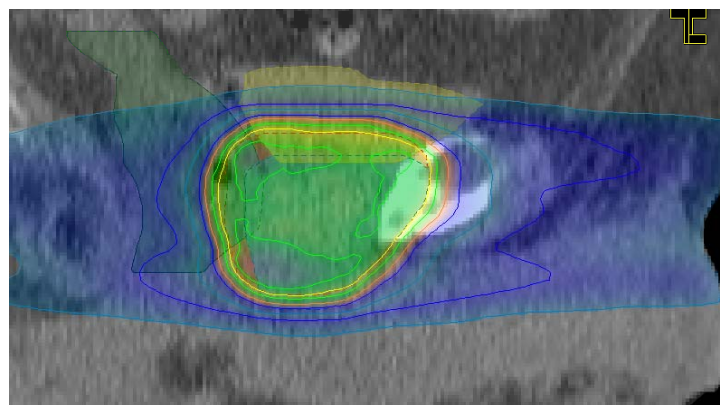
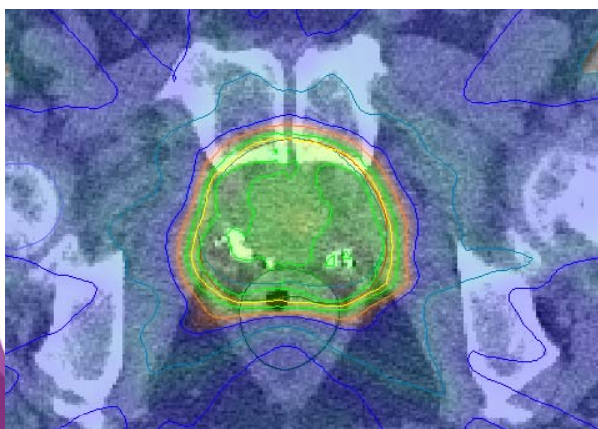
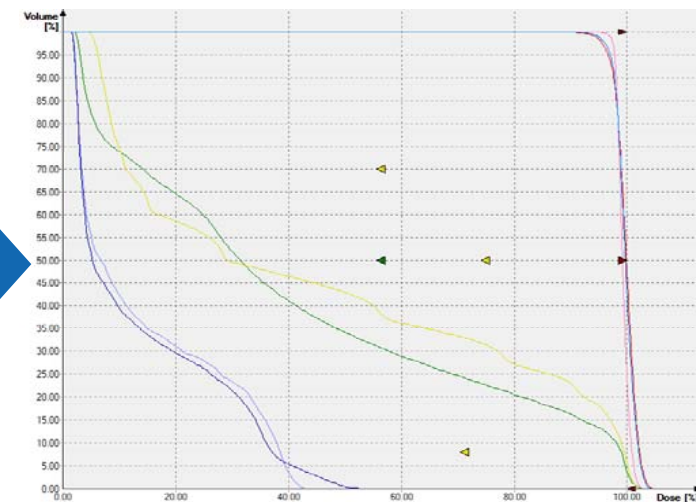
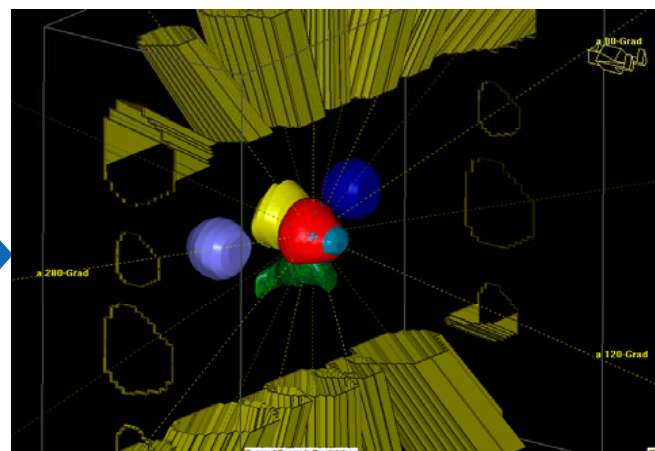
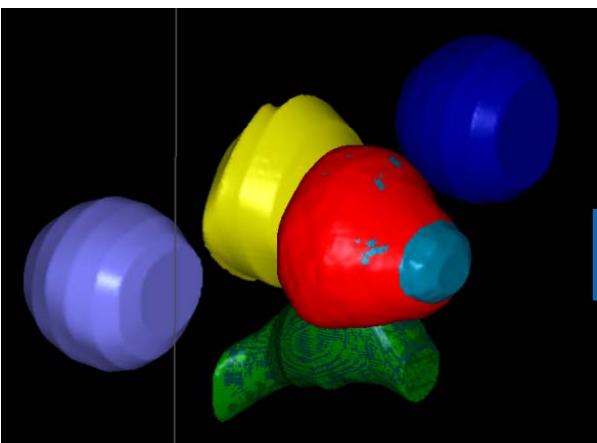
Where are we today in ERT?

- **Verification of individual RT-Plan via 2D/3D measurements:
RTP(Phantom) + Machine as an Off-Line
Pre-Treatment-Procedure**
- **Dose Reconstruction in Patient Anatomy utilising
Off-Line 3D-measurements: RTP + Machine**
- **3D-Dose Verification in Patient-customized Phantom
Off-Line 3D-measurement: RTP + Machine + Set-Up**
- **Real-Time Fluence Measurement during Treatment and Dose
Reconstruction**
- ...

Towards Dose - Reconstruction

Where are we today in ERT?

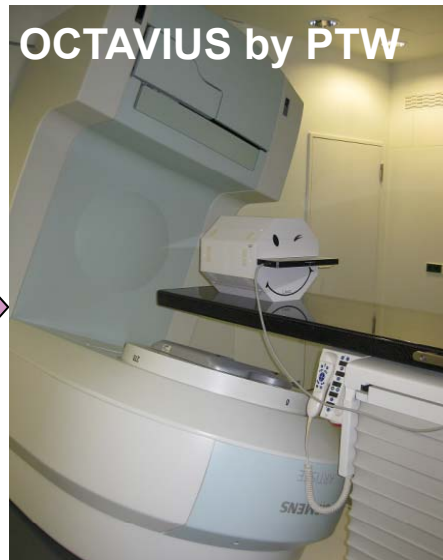
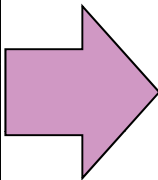
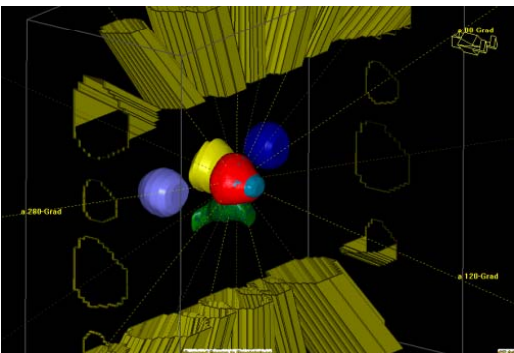
Example of a PCA-IMRT Offline Pre-Treatment Procedure: RTP(Phantom) + Machine



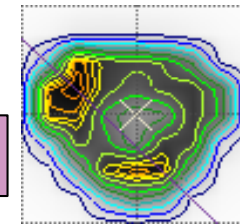
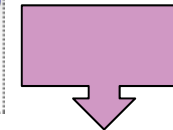
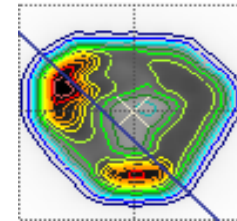
Where are we today in ERT?

Example of a PCA-IMRT Offline Pre-Treatment Procedure: RTP(Phantom) + Machine

RTP: Automatic transfer to phantom geometry

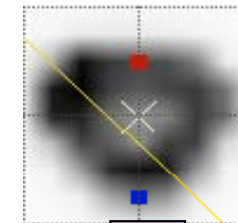


RTP



Meas.

Compare

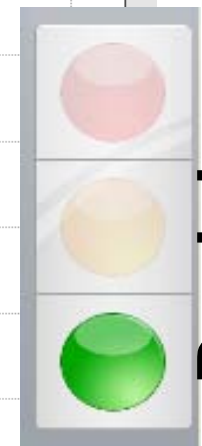
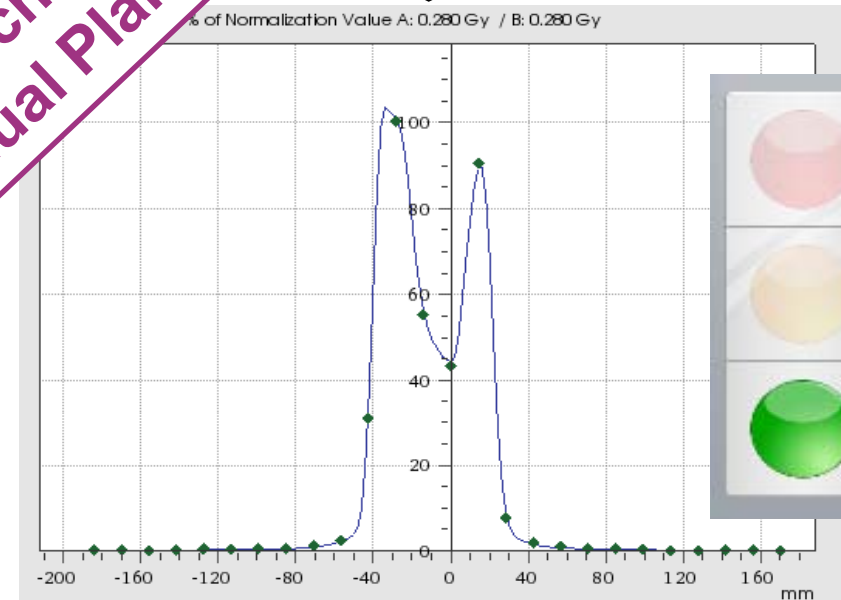
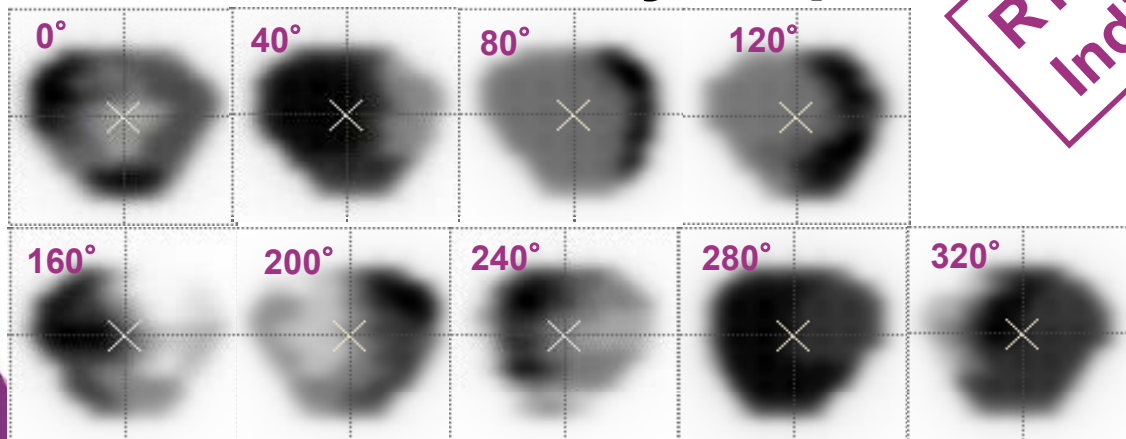


Gamma-3D



RTP + Machine:
Individual Plan

Fluence / Intensity Maps



Decision

Where are we today in ERT?

Example of Dose Reconstruction in Patient Anatomy utilising Off-Line 3D-measurements: RTP + Machine

White Paper

October 2013

D913.200.06/00

PTW

Dose reconstruction in the OCTAVIUS 4D phantom and in the patient without using dose information from the TPS

B. Allgaier, E. Schüle, J. Würfel

PTW-Freiburg Physikalisch-Technische Werkstätten Dr. Pöchlau GmbH
Lörracher Straße 7, 79115 Freiburg, Germany

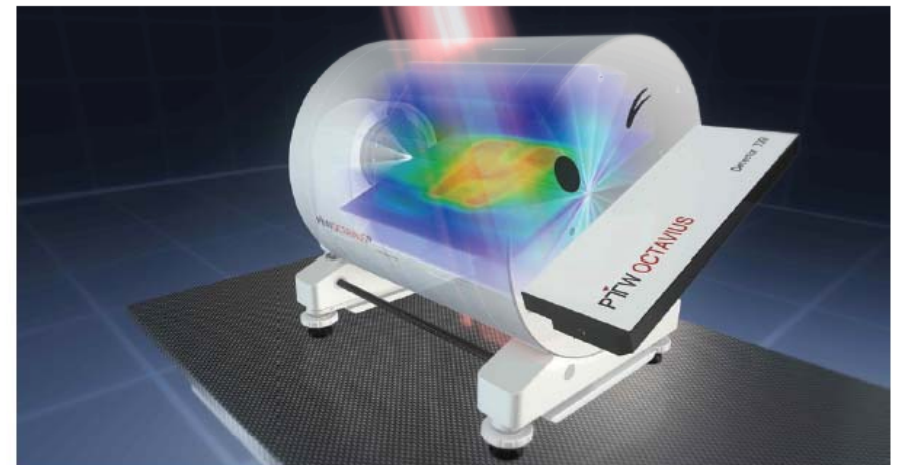
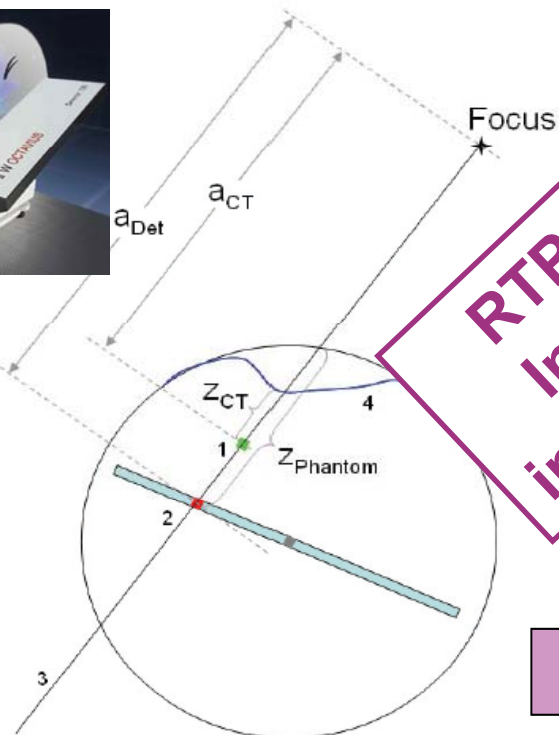
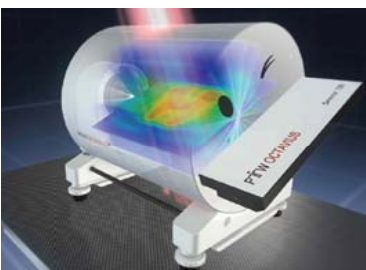


Fig. 1 The OCTAVIUS 4D system. The detector panel is inserted in a cylindrical phantom that rotates synchronously with the gantry. Detector panels with different spatial resolutions are available. The Detector 729 features 10 mm resolution, the central region of the Detector 1000^{SRS} features 2.5 mm.

Where are we today in ERT?

Example of Dose Reconstruction in Patient Anatomy utilising Off-Line 3D-measurements: RTP + Machine



**RTP + Machine:
Individual Plan
in Patient Geometry**

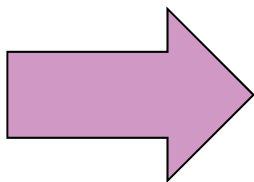


Fig. 2 OCTAVIUS 4D phantom with ray line (3) through focus and current detector (2), not to scale. The contour (4) is the patient surface from the CT image. The current detector measures the dose D_{Det} at the water-equivalent depth $z_{Phantom}$. The algorithm reconstructs the dose D_{CT} for the current voxel (1) at the water-equivalent depth z_{CT} in the CT image. a_{Det} and a_{CT} are geometrical distances from the focus to the current detector and to the current voxel, respectively.

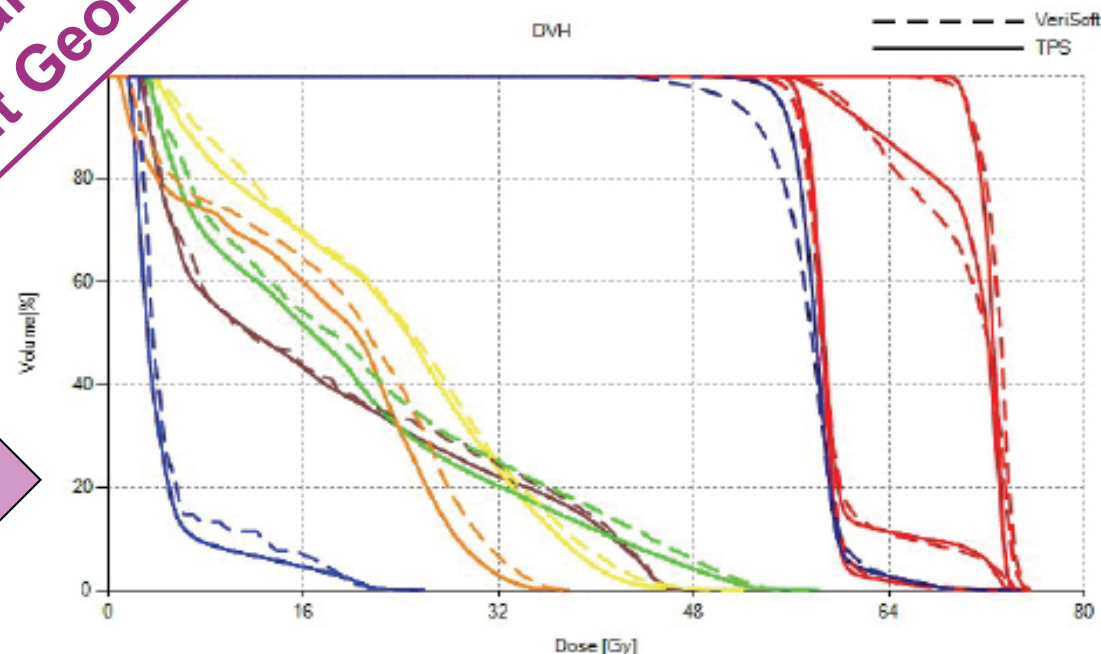
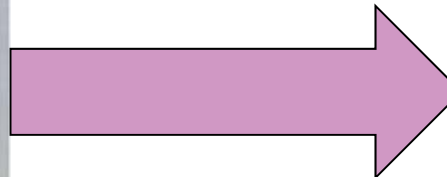
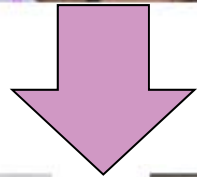
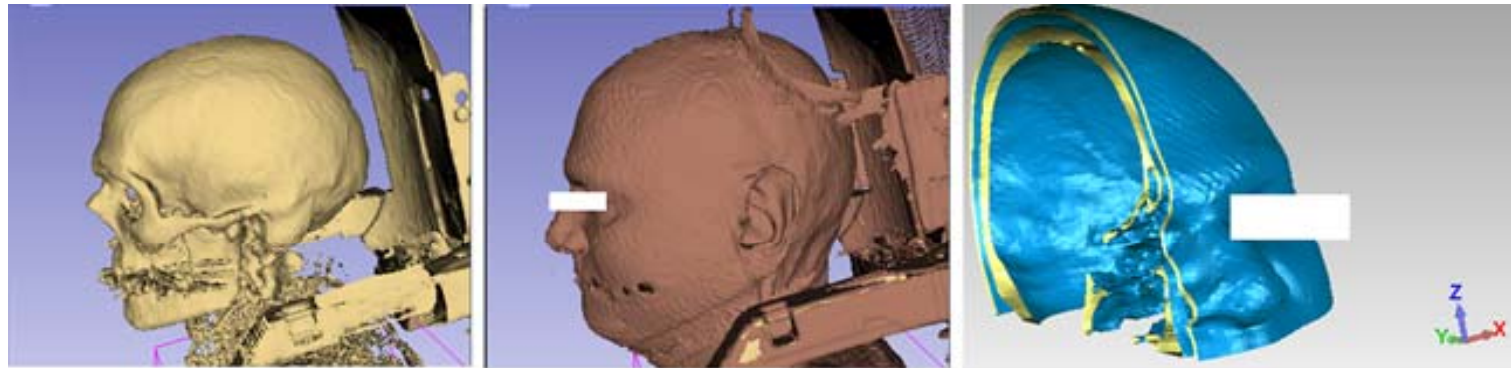


Fig. 3 Dose volume histograms in the patient's geometry determined by OCTAVIUS 4D (dashed lines) and by the TPS (solid lines)

Where are we today in ERT?

Example of 3D-Dose Verification in
Patient-customized Phantom:

Off-Line 3D-measurement: RTP + Machine + Set-Up

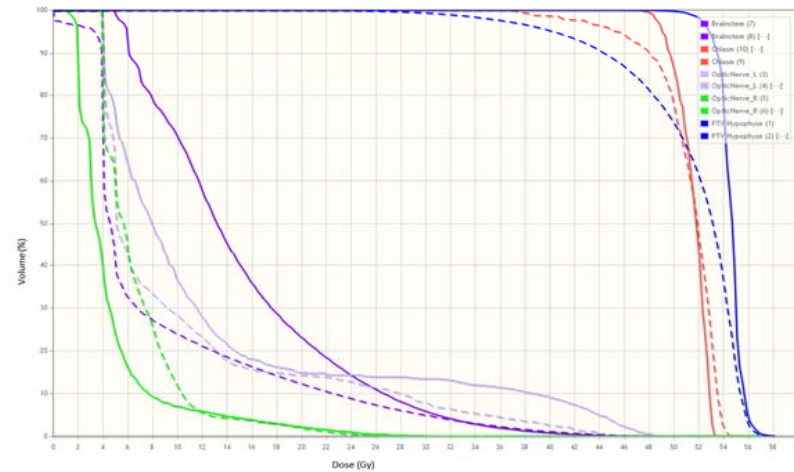


Where are we today in ERT?

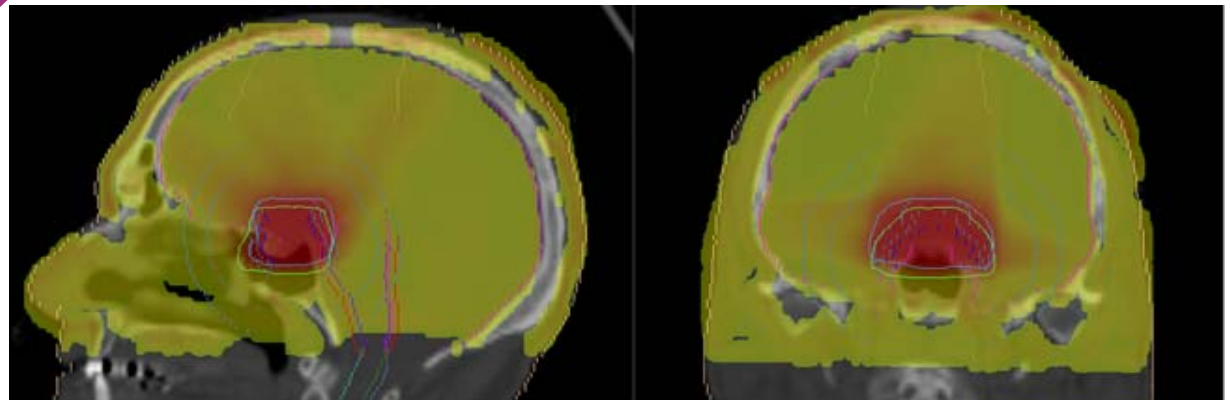
Example of 3D-Dose Verification in

Patient-customized Phantom:

Off-Line 3D-measurement: RTP + Machine + Set-Up



RTP + Machine + Set-Up:
Individual Plan
in Patient Geometry



Where are we today in ERT?

Example of Real-Time Fluence Measurement during Treatment and Dose Reconstruction: RTP + Machine + Set-Up + Patient



Two Years of Clinical Experience with DAVID –
A Translucent Multi-Wire Detector for On-Line Verification of
Patient Treatments

B. Poppe¹⁺², H.K. Looe¹⁺², A. Rühmann¹⁺², Y. Upphoff², K. Willborn²
and D. Harder³

¹WG Medical Radiation Physics, Carl von Ossietzky University, Oldenburg Germany

²Pius-Hospital, Oldenburg, Germany

³Prof. emer., University of Göttingen, Germany

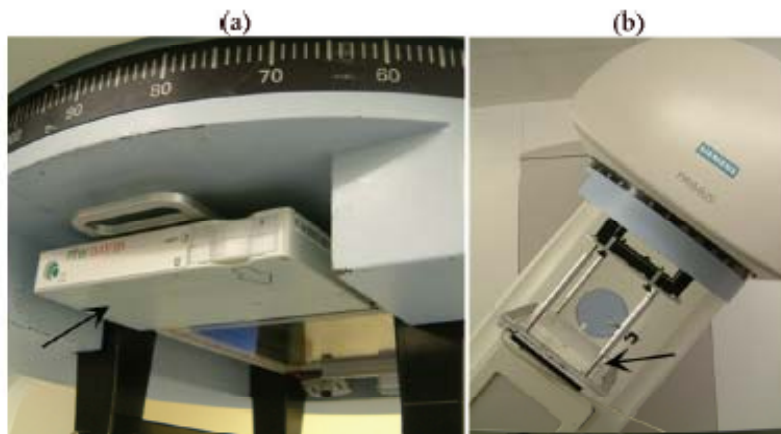


Fig. 1. (a) The DAVID transmission detector array, serving for permanent supervision of the MLC, at its operation position in the accessory holder of the Siemens PRIMUS accelerator. (b) The 2D-ARRAY, serving for daily accelerator checks and dosimetric plan verification, at its operation position in the gantry mount of the Siemens PRIMUS accelerator.

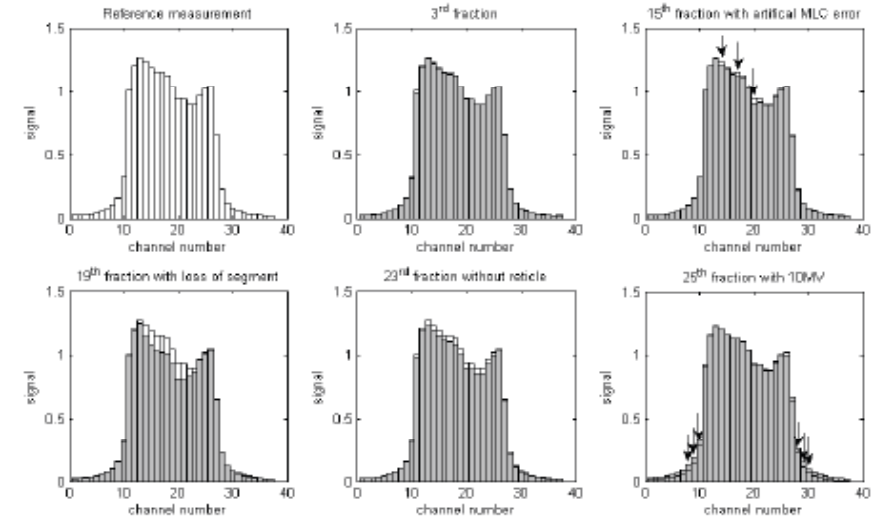
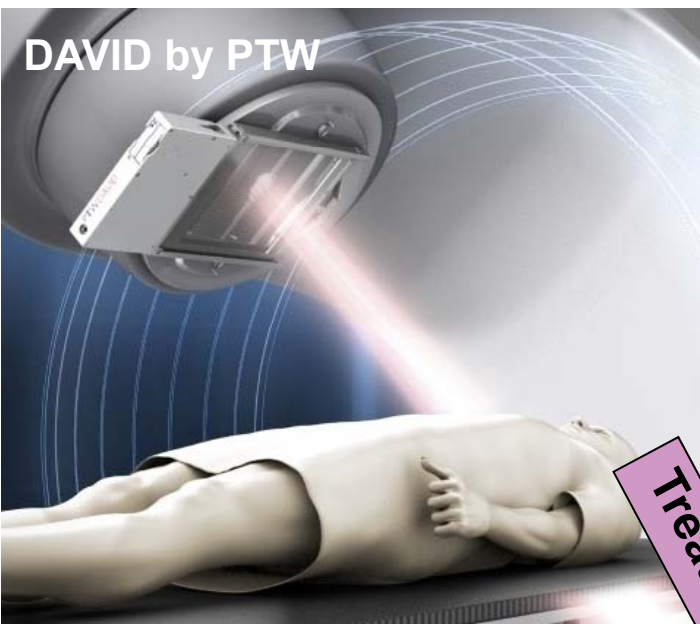


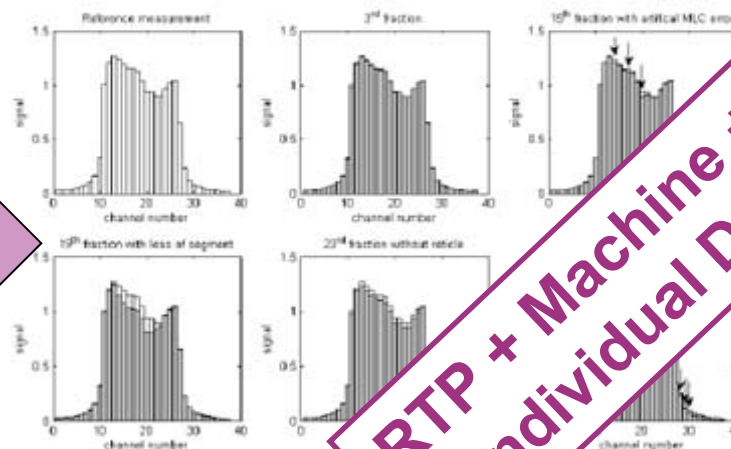
Fig. 2 Examples of the measured DAVID channel signals at gantry angle 0° for some selected fractions. Artificial errors, introduced in the 15th, 19th, 23rd and 25th fraction, were detected as deviations from the reference signals. Figure taken from (3).

Where are we today in ERT?

Example of Real-Time Fluence Measurement during Treatment and Dose Reconstruction: RTP + Machine + Set-Up + Patient

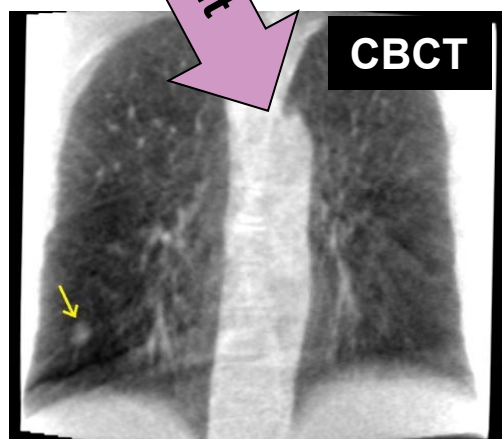


delivered



RTP + Machine + Set-Up + Patient:
Individual Delivered Treatment

Treatment



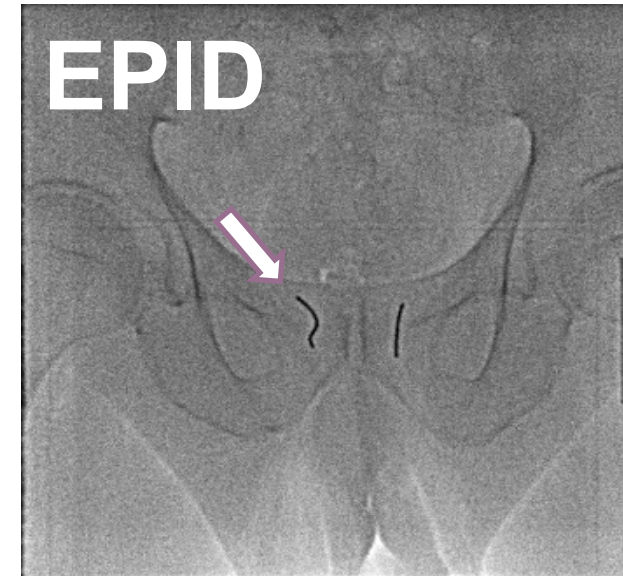
RTP



Where are we today in ERT?

Example of Anatomy (Target) based Verification of Positioning:

Patient (PTV) + Machine + Set-Up + ... (Targeting)



BRT *versus* ERT Similarities and Differences

■ The Verification Process

- What is the “DRR” in BRT?**
- What is the “BEV” in BRT?**
- What is the “EPID” in BRT?**
- What is the “Fiducial” in BRT?**
- What is the “measurable Beam Fluence” in BRT?**
- What is the “Fingerprint” of a “Beam-Delivery” in BRT?**
- What is the “individual plan verification process” in BRT?**
- ???**

BRT *versus* ERT Similarities and Differences

■ The Verification Process

The majority of those tools and/or processes *are not defined at all or are not implemented or are not part* of the current clinical treatment planning and treatment delivery procedure (RTP)!

BRT *versus* ERT Similarities and Differences

■ The Verification Process: ERT

DRR: Beam \leftrightarrow Anatomy

Fields	Dose Prescription	Plan Objectives	Optimization Objectives	Dose Statistics	Calculation Models	Plan Sum				
Fractionation Id	Dose / Fraction [Gy]	Number of Fractions	Total Dose [Gy]	Target Volume	Primary Reference Point [Volume]	Total Dose at Primary [Gy]	Relative Dose at Primary [%]	Prescribed Percentage [%]	Plan Normalization Mode	Plan Normalization Value [%]
F1	1.800	33	59.400	ThCa	ThCa [ThCa]	59.400	100.0	100.0	No plan normalization	10

Modern Brachytherapy: Treatment Delivery Verification

■ *Delivered Treatment versus Planned Treatment*

Currently we assume that:

- The geometry and location of the implanted catheters
- The connection of channels to implanted catheters
- The length of the channels
- The source movement patterns (dwell positions and dwell times) within the implanted catheters
- The patient anatomy at the relevant location

are during treatment delivery exact as considered and planned in the RTP.

A general Concept of Verification in BRT: Computational Verification CoVer

Dose Planned = Dose Delivered ? can not completely be answered w/o incorporating in-situ imaging and 3D-localization techniques!
If the *performance* of our BRT-MLC, thus the correct stepping with the correct dwell time pattern (fluence) at the correct geometrical configuration (the analogue of Gantry, Collimator, Couch Set-Up) is the appropriate (planned) can be most probably answered by applying *Computational Techniques*.

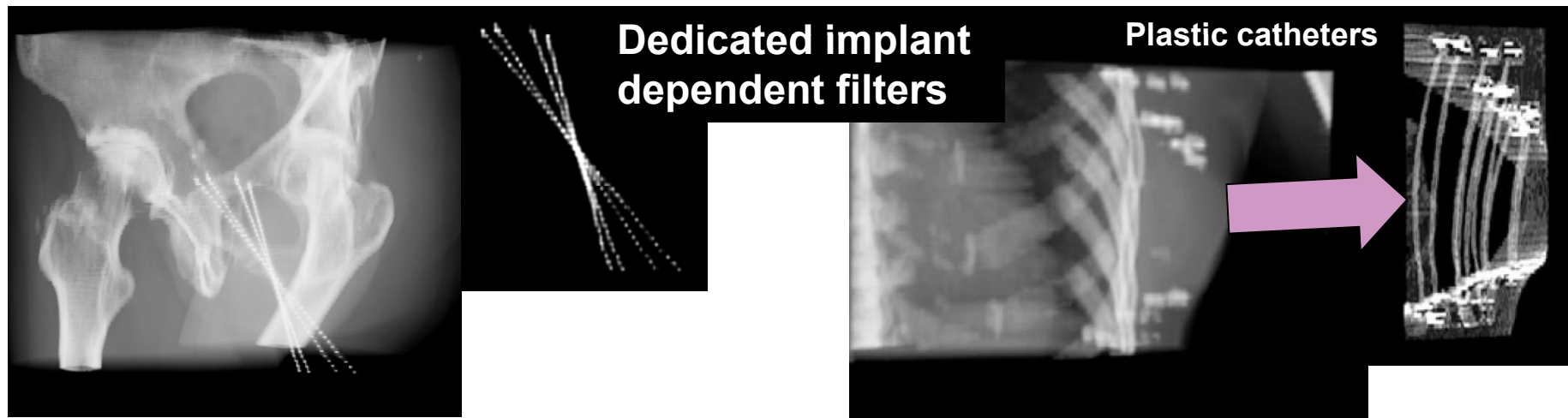
***Computational*, since in BRT we have to compute firstly and on the top issues similar to a DRR, an EPID, or a Fluence profile (the Finger-Print ?), which currently are not part of our standard RTP-procedure (as it is the case in ERT-RTP-Process).**

A general Concept of Verification in BRT:

- **Computational Methods (*Software*)**
- **System Implementation (*Hardware*)**
- **Integration (*Brainware*)**

A general Concept of Verification in BRT: Computational Verification Cover

- **Dedicated DRRs for Localisation and Verification purposes**
N x different ?



Milickovic N., Baltas D, et al. "CT imaging based digitally reconstructed radiographs and their application in brachytherapy", Phys. Med. Biol. 45, 2000

**Integrated in the RTPs + DICOM Export (SC) to
Imaging-based Verification Systems**

A general Concept of Verification in BRT: Computational Verification Cover

■ The “finger print” or the measurable fluence of a treatment

(1) Compute time-resolved information (dose-rate, dose, etc..)

that can be considered as the *reference* information for an *on-line* (in-vivo) verification process. This could be the *analogon* to DRR or **fluence profile** in ERT and could be considered as the “Finger-Print” of the treatment delivery (?):

- per channel / catheter
- whole treatment plan
- including uncertainties
 - » Implant-specific
 - » Treatment Device-specific
 - » Measurement system-specific
 - » ???

Integrated in the RTPs
+ Export to
Measurement-based
Verification Systems

■ The “finger print” or the measurable fluence of a treatment

Compute time-resolved information (dose-rate, dose, etc..)

Time-resolved *in vivo* luminescence dosimetry for online error detect in pulsed dose-rate brachytherapy

Claus E. Andersen^{a)}

Radiation Research Division, Risø National Laboratory for Sustainable Energy, Technical University of Denmark, DK-4000 Roskilde, Denmark

Søren Kynde Nielsen

Department of Medical Physics, Aarhus University Hospital, DK-8000 Århus C, Denmark

Jacob Christian Lindegaard

Department of Oncology, Aarhus University Hospital, DK-8000 Århus C, Denmark

Kari Tanderup

Department of Medical Physics, Aarhus University Hospital, DK-8000 Århus C, Denmark

(Received 7 May 2009; revised 17 August 2009; accepted for publication 5 September 2009; published 6 October 2009)

In vivo dosimetry in brachytherapy

Kari Tanderup^{a)}

Department of Oncology, Aarhus University Hospital, Aarhus 8000, Denmark and Department of Clinical Medicine, Aarhus University, Aarhus 8000, Denmark

Sam Beddar

Department of Radiation Oncology, The University of Texas MD Anderson Cancer Center, Houston, Texas 77030

Claus E. Andersen and Gustavo Kertzsch

Center of Nuclear Technologies, Technical University of Denmark, Roskilde 4000, Denmark

Joanna E. Cygler

Department of Physics, The Ottawa Hospital Cancer Centre, Ottawa, Ontario K1H 8L6, Canada

(Received 15 January 2013; revised 12 April 2013; accepted for publication 16 April 2013; published 25 June 2013)

In vivo dosimetry (IVD) has been used in brachytherapy (BT) for decades with a number of different detectors and measurement technologies. However, IVD in BT has been subject to certain difficulties and complexities, in particular due to challenges of the high-gradient BT dose distribution and the large range of dose and dose rate. Due to these challenges, the sensitivity and specificity toward error detection has been limited, and IVD has mainly been restricted to detection of gross errors. Given these factors, routine use of IVD is currently limited in many departments. Although the impact of potential errors may be detrimental since treatments are typically administered in large fractions and with high-gradient-dose-distributions, BT is usually delivered without independent verification of the treatment delivery. This Vision 20/20 paper encourages improvements within BT safety by developments of IVD into an effective method of independent treatment verification. © 2013 American Association of Physicists in Medicine. [<http://dx.doi.org/10.1118/1.4810943>]

Key words: *in vivo* dosimetry, brachytherapy, treatment errors, quality assurance

A phantom study of an *in vivo* dosimetry system using plastic scintillation detectors for real-time verification of ¹⁹²Ir HDR brachytherapy

Francois Therriault-Proulx

Department of Radiation Physics, The University of Texas MD Anderson Cancer Center, Houston, Texas 77030 and Département de Physique, de Génie Physique et d'Optique, Université Laval, Québec, Québec G1K 7P4, Canada

Tina M. Briere and Firas Mourtada

Department of Radiation Physics, The University of Texas MD Anderson Cancer Center, Houston, Texas 77030

Sylviane Aubin

Département de Radio-Oncologie, Hôtel-Dieu de Québec, Centre Hospitalier Universitaire de Québec, Québec, Québec G1R 2J6, Canada

Sam Beddar^{a)}

Department of Radiation Physics, The University of Texas MD Anderson Cancer Center, Houston, Texas 77030

Luc Beaulieu

Département de Physique, de Génie Physique et d'Optique, Université Laval, Québec, Québec G1K 7P4, Canada and Département de Radio-Oncologie, Hôtel-Dieu de Québec, Centre Hospitalier Universitaire de Québec, Québec, Québec G1R 2J6, Canada

(Received 3 October 2010; revised 22 February 2011; accepted for publication 9 March 2011; published 5 May 2011)

Adaptive error detection for HDR/PDR brachytherapy: Guidance for decision making during real-time *in vivo* point dosimetry

Gustavo Kertzsch^{a)} and Claus E. Andersen^{b)}

Center for Nuclear Technologies, Technical University of Denmark, DTU Nutech, Frederiksborgvej 399, DK-4000 Roskilde, Denmark

Kari Tanderup^{c)}

Department of Oncology, Aarhus University Hospital and Institute of Clinical Medicine, Aarhus University, Norrebrogade 44, DK-8000 Aarhus, Denmark

(Received 15 October 2013; revised 5 March 2014; accepted for publication 23 March 2014; published 14 April 2014)

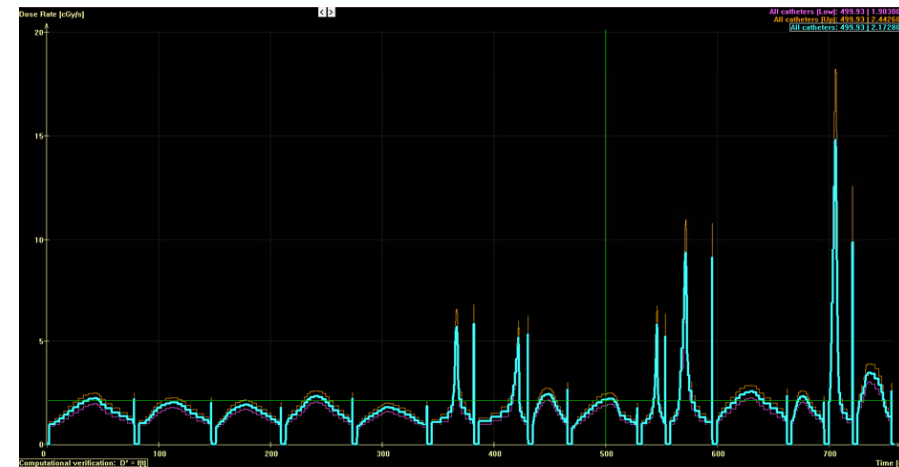
A general Concept of Verification in BRT: Computational Verification Cover

(2a) Where to be computed?

- **Single position *versus* Multiple Positions**
- **1D-Array**
- **2D-Array**
- **Measuring System-dependent**

(2b) How to be computed?

- **Time-resolved**
- **Channel & Dwell Position resolved**
- **Whole Treatment Plan**
- **Dedicated Verification Plan**
- **Workflow & Verification System-dependent**



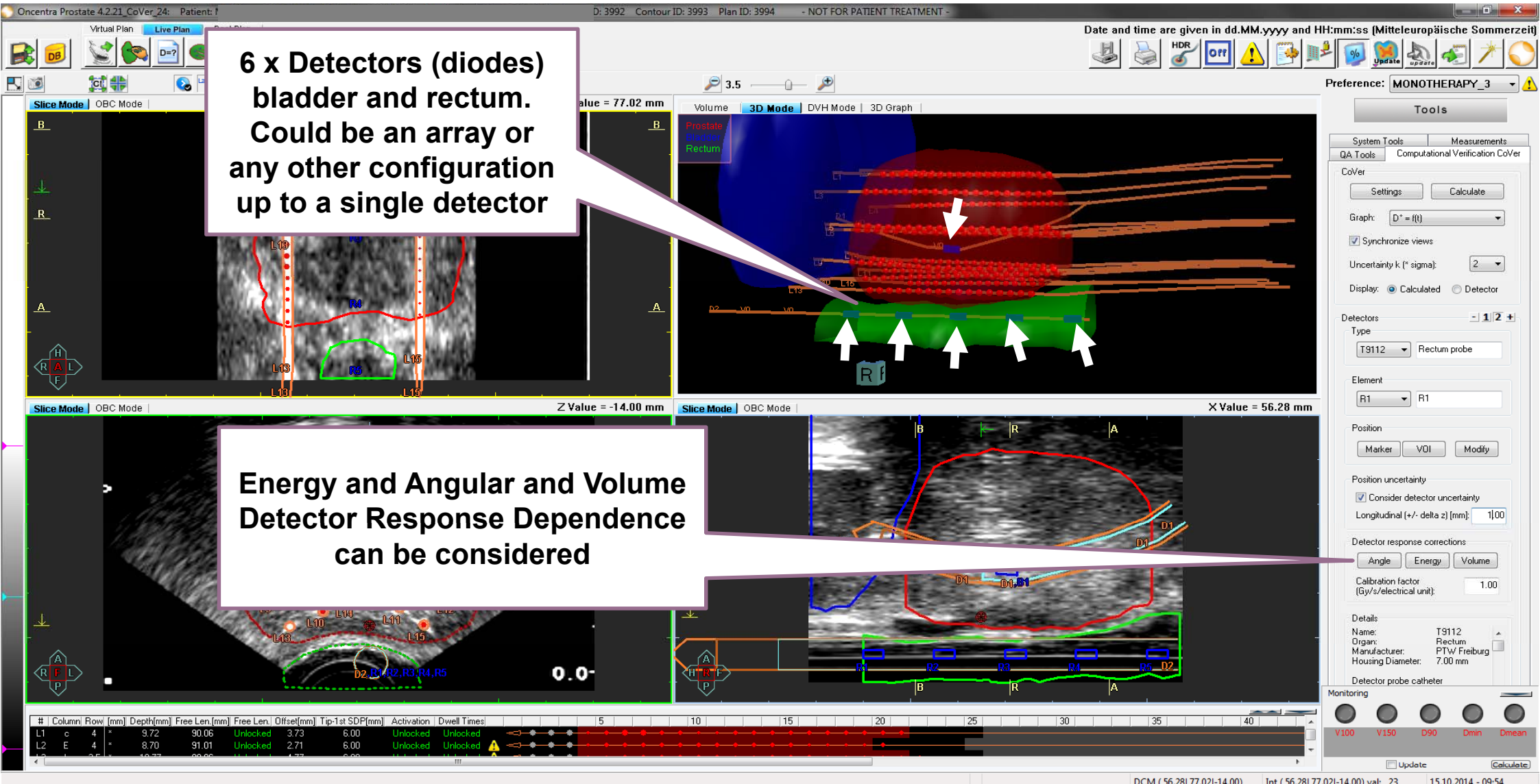
A general Concept of Verification in BRT: Computational Verification Cover

**(3) Map firstly *Computed to Measurable*
“Treatment-Finger-Print”, e.g. time- and/or channel/ADP-
resolved Dose or Dose Rate**

To be computed considering

- **Measuring System / Detector System characteristics**
 - » **Volume effect/response**
 - » **Directional response**
 - » **Energy response (distance)**
 - » **Temperature Response**
 - » **???**
- **Measuring System / Detector System related uncertainties**

A general Concept of Verification in BRT: Computational Verification Cover – A Prototype



6 x Detectors (diodes) bladder and rectum. Could be an array or any other configuration up to a single detector

Energy and Angular and Volume Detector Response Dependence can be considered

A general Concept of Verification in BRT: Computational Verification Cover – A Prototype

The screenshot displays the Oncentra Prostate 4.2.21 CoVer software interface. The main window shows a 3D model of a prostate with catheters and a detector probe. A settings dialog for 'Computational Verification CoVer settings' is open, showing parameters for source movement and uncertainty. A detailed view of a detector probe (T9112 Rectum probe) is shown on the right, with its parameters and a graph of dose rate over time.

Computational Verification CoVer settings

Parameters settings for source movement

Source driving

- Calculate dose for source driving:
- Drive-out [mm/s]: 467.00
- Drive-in [mm/s]: 467.00
- Stepping [mm/s]: 54.00
- Consider connecting tube: Only the last [mm]: 50.00
- Adjust dwell times for source transit

Simulation timer

Time interval [s]: 0.05

Timer start point:

- Drive out
- 1st ASDP

- Use afterloader time resolution

Storage and retrieval

Save Load OK Cancel

Parameter settings for uncertainty

Source position uncertainty

- Consider source uncertainty
- Longitudinal (+/- delta z) [mm]: 1.00

Other calculation uncertainties for k = 1

- Consider other calculation uncertainties:
- Source strength [%]: 2.00
- Treatment planning / dose calculation [%]: 3.00
- Medium dosimetric corrections [%]: 1.00
- Catheter reconstruction [%]: 1.00
- US-based 2D/3D-imaging overall effect [%]: 2.00
- Total dosimetric uncertainty [%]: 4.36

Detector Probe Parameters (T9112 Rectum probe)

Graph: $D^* = f(t)$

- Synchronise views
- Uncertainty k (* sigma): 2
- Display: Calculated Detector

Detectors: T9112 Rectum probe

Type: T9112

Element: R1

Position: R1

Position uncertainty

- Consider detector uncertainty
- Longitudinal (+/- delta z) [mm]: 1.00

Detector response corrections

Angle Energy Volume

Calibration factor (Gy/s/electrical unit): 1.00

Details

Name: T9112
Organ: Rectum
Manufacturer: PTW Freiburg
Housing Diameter: 7.00 mm

Detector probe catheter

Monitoring

Update Calculate

DCM (56.28|77.02|-14.00) Int (56.28|77.02|-14.00) val: 23 15.10.2014 - 09:54

A general Concept of Verification in BRT: Computational Verification Cover – A Prototype

Source Position corresponding to the time-point during treatment delivery time shown in graph

Time resolved Dose Rate at the position of Detector B1 w/o considering detector uncertainties

Detailed view of information for the specific time moment (X-axis of graph) in treatment plan delivery!

System Tools: Measurements, QA Tools, Computational Verification CoVer

CoVer Settings: Settings, Calculate

Graph: $D^* = f(t)$

Synchronize views

Uncertainty k ("sigma"): 2

Display: Calculated Detector

Detectors: T9111, Bladder tube

Element: B1, B1

Position: Marker, VOI, Modify

Position uncertainty: Consider detector uncertainty

Longitudinal (+/- delta z) [mm]: 1.00

Detector response corrections: Angle, Energy, Volume

Calibration factor (Gy/s/electrical unit): 1.00

Details: Name: T9111, Organ: Urethra, Manufacturer: PTW/Freiburg, Housing Diameter: 4.75 mm

Detector probe catheter: V100, V150, D90, Dmin, Dmean

Monitoring: Update

Settings

Settings	Total time [s]	Cath. time [s]	Type	ASDP	Pos. X [mm]	Pos. Y [mm]	Pos. Z [mm]	D* [cGy/s]	Std dev. [cGy/s]	D* (Low) [cGy/s]	D* (Up) [cGy/s]	D [cGy]	Std dev. [cGy]	D (Low) [cGy]	D (Up) [cGy]
499.350	31.450	ASDP	9-14	35.85	71.08	-26.74	2.17	0.13	1.90	2.44	46.46	3.05	40.36	52.56	
499.400	31.500	ASDP	9-14	35.85	71.08	-26.74	2.17	0.13	1.90	2.44	46.57	3.06	40.45	52.68	
499.450	31.550	ASDP	9-14	35.85	71.08	-26.74	2.17	0.13	1.90	2.44	46.68	3.06	40.55	52.80	
499.500	31.600	ASDP	9-14	35.85	71.08	-26.74	2.17	0.13	1.90	2.44	46.78	3.07	40.64	52.93	
499.550	31.650	ASDP	9-14	35.85	71.08	-26.74	2.17	0.13	1.90	2.44	46.89	3.08	40.74	53.05	
499.600	31.700	ASDP	9-14	35.85	71.08	-26.74	2.17	0.13	1.90	2.44	47.00	3.08	40.83	53.17	
499.650	31.750	ASDP	9-14	35.85	71.08	-26.74	2.17	0.13	1.90	2.44	47.11	3.09	40.93	53.29	

Computational Verification CoVer

Dose Detector Export Close

Catheter: L9 [B-1.5] - source: A14 DCM (35.85) 71.08|-26.74) Int (35.85) 71.08|-26.74) val: 161 15.10.2014 - 10:26

A general Concept of Verification in BRT: Computational Verification Cover

(4) Map *Computed Measurable* to *Measured* *“Treatment-Finger-Print”*, e.g. time- and/or channel/ADP- resolved Dose or Dose Rate

- **Consideration of actual “performance” of the measuring system/device**
- **Update of localization**
- **???**

(5) **Dedicated tools for (live and/or off-line):**

- **Pattern-analysis (e.g. AEDA*)**
- **Prediction**
- **Decision**
- **alert generation and interfacing**

*Kertzscher et al., 2014

A general Concept of Verification in BRT:

- **Computational Methods (*Software*)**
- **System Implementation (*Hardware*)**
- **Integration (*Brainware*)**

A general Concept of Verification in BRT: Hardware - Detectors

TABLE III. Characteristics of detectors and dosimetry systems of importance for precise routine IVD in brachytherapy. The items are rated according to: advantageous (++), good (+), and inconvenient (-).

	TLD	Diode	MOSFET	Alanine	RL	PSD
Size	+	+/-	+ /+++	-	++	++
Sensitivity	+	++	+	-	++	+ /+++
Energy dependence	+	-	-	+	-	++
Angular dependence	++	-	+	+	++	++
Dynamic range	++	++	+	-	++	++
Calibration	+	++	++	-	+/-	+ /+++
procedures, QA, stability, robustness, size of system, ease of operation						
Commercial availability	++	++	++	++	-	+
Online dosimetry	-	++	+	-	++	++
Main advantages	No cables, well studied system	Commercial systems at reasonable price, well studied system	Small size, commercial system at reasonable price	Limited energy dependence, no cables	Small size, high sensitivity	Small size, no angular and energy dependence, sensitivity
Main disadvantages	Tedious procedures for calibration and readout, not online dosimetry	Angular and energy dependence	Limited life of detectors, energy dependence	Not sensitive to low doses, tedious procedures for calibration and readout, not online dosimetry, expensive readout equipment not available in clinics	Needs frequent recalibration, stem effect, not commercially available	Stem effect

Energy-, Angular-, Temperature-, Volume-dependence: Computational methods in RTP !

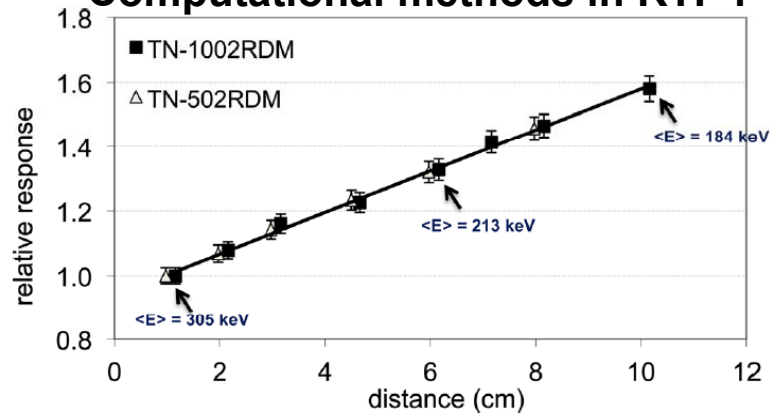


FIG. 6. Variation of the MOSFET response with distance for two detectors, normalized to 1 cm distance. The mean photon energies in PMMA are given for distance of 1, 6, and 10 cm.

B. Reniers, G. Landry, R. Eichner, A. Hallil, F. Verhaegen, *Med. Phys.* 39 (4), 1925-1935, 2012

**Most probably it is a sufficient requirement for the time-resolved –based systems:
 Have a stable response/behaviour over the period of signal acquisition (usually 10-30 min)
 Be small enough to be entered into catheters/applicators/**

A general Concept of Verification in BRT: System Implementation – Hardware: Imaging / EPID

A method for verification of treatment delivery in HDR prostate brachytherapy using a flat panel detector for both imaging and source tracking

Ryan L. Smith^{a)}

*Alfred Health Radiation Oncology, The Alfred Hospital, Melbourne, VIC 3004, Australia
and School of Science, RMIT University, Melbourne, VIC 3000, Australia*

Annette Haworth

*School of Science, RMIT University, Melbourne, VIC 3000, Australia and Physical Sciences,
Peter MacCallum Cancer Centre, East Melbourne, VIC 3002, Australia*

Vanessa Panettieri

Alfred Health Radiation Oncology, The Alfred Hospital, Melbourne, VIC 3004, Australia

Jeremy L. Millar and Rick D. Franich

*Alfred Health Radiation Oncology, The Alfred Hospital, Melbourne, VIC 3004, Australia
and School of Science, RMIT University, Melbourne, VIC 3000, Australia*

(Received 13 January 2016; revised 21 March 2016; accepted for publication 3 April 2016;
published 20 April 2016)

2439

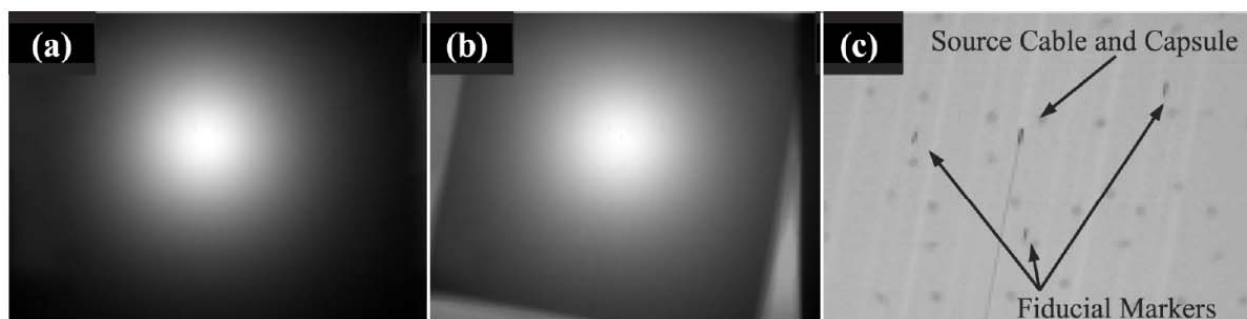


FIG. 5. (a) The captured exposure of the ^{192}Ir source using the FPD. (b) The simultaneous FPD exposure of the ^{192}Ir source and the projection image of the phantom. (c) The result of subtraction of (a) from (b), magnified view to show the physical source capsule used for independent position verification. The source cable, voids from the other empty catheters, and fiducial markers are also visible.

A general Concept of Verification in BRT:

Computational Verification CoVer

Dose Planned = Dose Delivered ? can not completely be answered w/o incorporating in-situ imaging and 3D-localization techniques!

If the *performance* of our BRT-MLC, thus the correct stepping with the correct dwell time pattern (fluence) at the correct geometrical configuration (the analogue of Gantry, Collimator, Couch Set-Up) is the appropriate (planned) can be most probably answered by applying *Computational Techniques*.

Computational, since in BRT we have to compute firstly and on the top issues similar to a DRR, an EPID, or a Fluence profile (the Finger-Print ?), which currently are not part of our standard RTP-procedure (as it is the case in ERT-RTP-Process).

A general Concept of Verification in BRT:

- **Computational Methods (*Software*)**
- **System Implementation (*Hardware*)**
- **Integration (*Brainware*)**

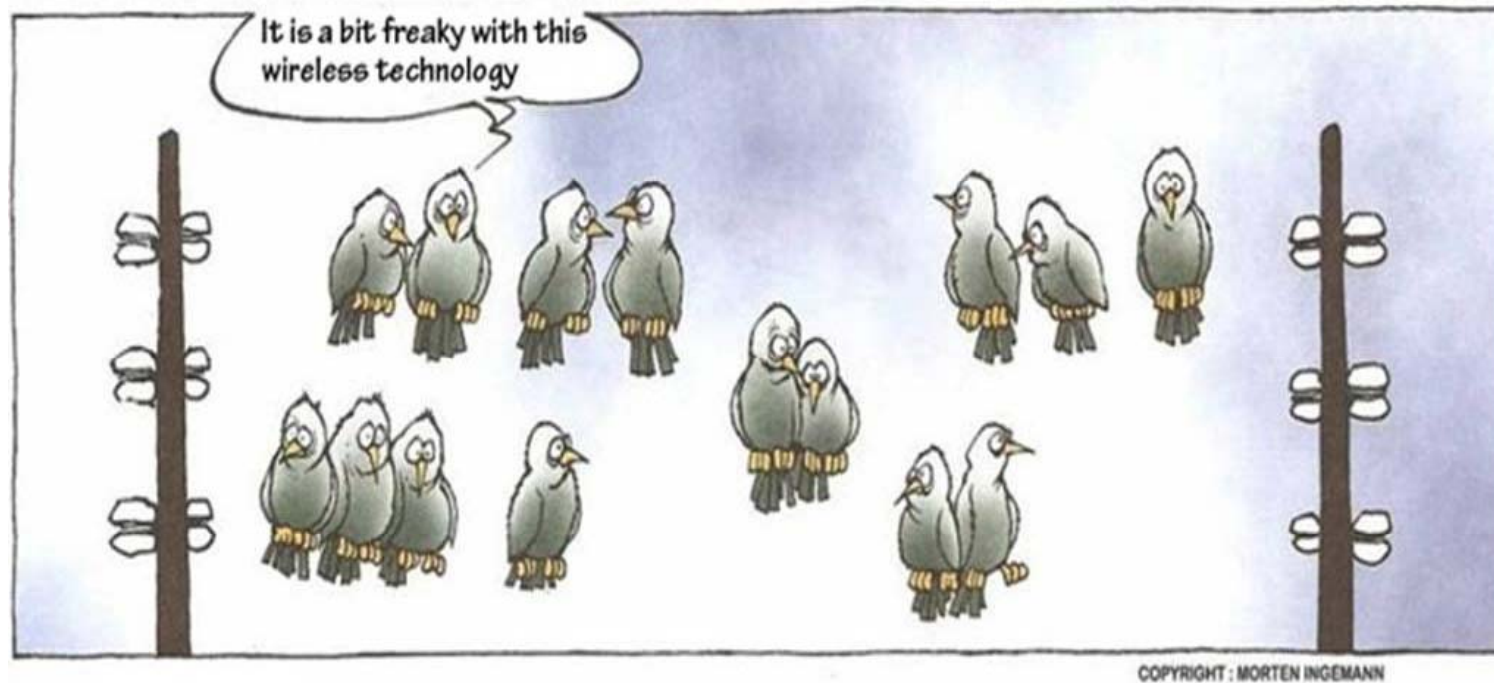
A general Concept of Verification in BRT: Integration (*Brainware*)

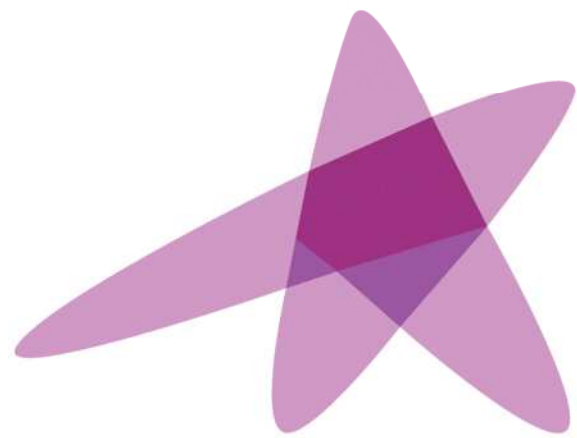
To Do

- **Interface to Afterloading device**
 - Synchronization of “time-axis” - Triggering
 - Synchronization of “system-status”
 - Interlock-Interface
 - ???
- **Standardized Interface to:**
 - Afterloaders
 - Detectors / Detector Systems



Thank you very much for your Attention





ESTRO

School



UNIVERSITÉ
LAVAL



In Vivo Dosimetry (IVD)

Prof. Luc Beaulieu, Ph.D., FAAPM

*1- Département de physique, de génie physique et d'optique, et
Centre de recherche sur le cancer, Université Laval, Canada*

*2- Département de radio-oncologie et Centre de recherche du CHU
de Québec, CHU de Québec, Canada*

Vienna, May 29 – June 1 2016



Disclosures

- I am leading a research effort to develop scintillator-based dosimeters
- I hold patents related to scintillation dosimetry
- My institution has a licensing agreement with Standard Imaging

Learning Objectives

- Context surrounding IVD in brachytherapy.
- Overview of the tools available, their performances and limitations for IVD in brachytherapy.
- Know the key challenges associated with IVD in brachytherapy.
- Provide a “skeleton framework” to set-up an IVD in your clinic → Pointers

In-Vivo Dosimetry

- Dose measurement(s) performed while the Tx. is proceeding
 - Within catheters
 - Intracavity
 - Surface

 - Not necessarily in real-time...

In-Vivo Dosimetry

“In vivo dosimetry (IVD) is in use in external beam radiotherapy (EBRT) to detect major errors, to assess clinically relevant differences between planned and delivered dose, to record dose received by individual patients, and to fulfill legal requirements”

- In vivo dosimetry in external beam radiotherapy. Mijnheer et al, Med. Phys 2013 (Vision 20/20)

In-Vivo Dosimetry

“The initial motivation for performing IVD in BT was mainly to assess doses to organs at risk (OAR) by direct measurements, because precise evaluation of OAR doses was difficult without 3D dose treatment planning.”

- In vivo dosimetry in brachytherapy. Tanderup et al, Med. Phys 2013 (Vision 20/20)

Vanguard your IRA to keep more of your money.

Open a Vanguard IRA today.

© 2011 The Vanguard Group, Inc. All rights reserved. Vanguard Marketing Corporation, Distributor. Obtain prospectus



June 20, 2009

SIGN IN TO E-MAIL FEEDBACK

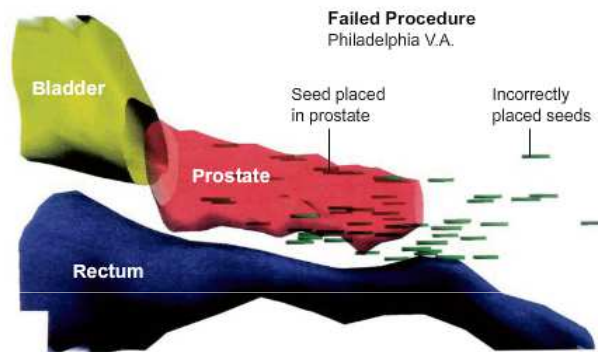
Failed Prostate Procedures at the Philadelphia V.A.

Investigators from the Nuclear Regulatory Commission have found that from 2002 to 2008, a cancer unit at the Philadelphia V.A. botched 92 of 116 brachytherapy procedures. A look at how the procedure is commonly performed.

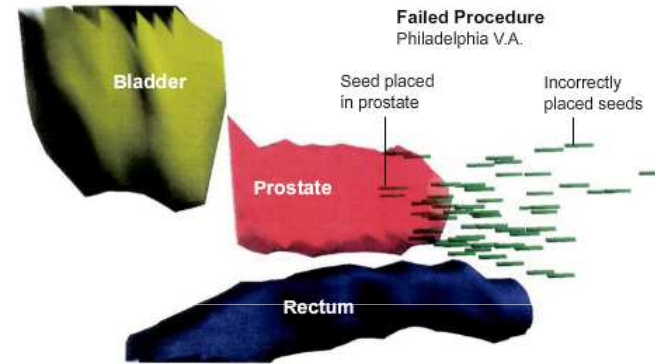
1 2 3 4 5 6 7 8 9 10 NEXT

What went wrong at the Philadelphia V.A.

These computer-generated images, part of a presentation produced by the Nuclear Regulatory Commission, show two specific patients who received the treatment. The images show the major organs, with the surrounding tissue rendered as white. Seeds that are implanted in or near the bladder or rectum can cause undue damage to otherwise healthy organs.



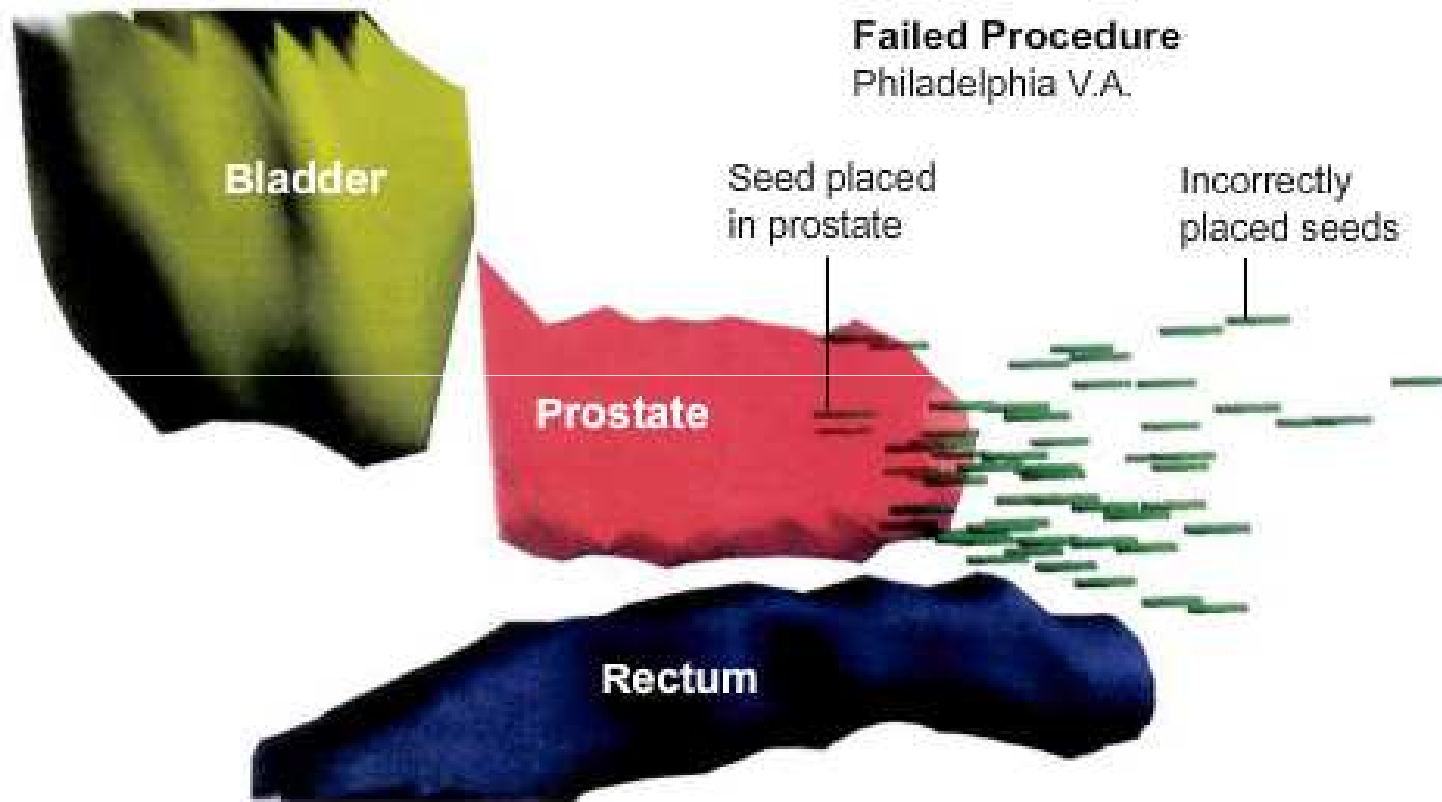
Here some of the radioactive seeds were implanted near the patient's rectum, potentially causing damage to that organ. In addition, the patient's prostate received only 43 gray of the 160 prescribed by the doctor.



In this case, nearly all of the seeds have been placed outside of the prostate, in the perineum. Of the prescribed dose of 160 gray, the prostate received only 24. This means that the patient's prostate cancer was only minimally treated by the procedure.

Sources: Dr. Adam P. Dicker and Dr. Yan Yu, Jefferson Medical College of Thomas Jefferson University; The Nuclear Regulatory Commission

Graham Roberts/The New York Times



In this case, nearly all of the seeds have been placed outside of the prostate, in the perineum. Of the prescribed dose of 160 gray, the prostate received only 24. This means that the patient's prostate cancer was only minimally treated by the procedure.

Source: New Yorks Times

Do you perform IVD in your clinics?

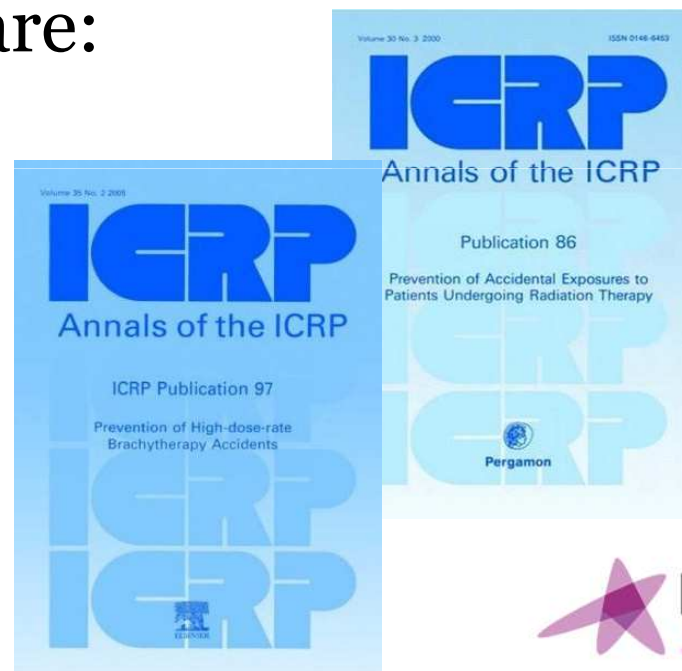
- a) Yes for all cases
- b) Yes for selected cases
- c) No

Contents

- Why IVD in brachytherapy?
- Tools and clinical experiences
- Challenges or “the physics is killing me”
- NextGen IVD tools
- Some pointers...

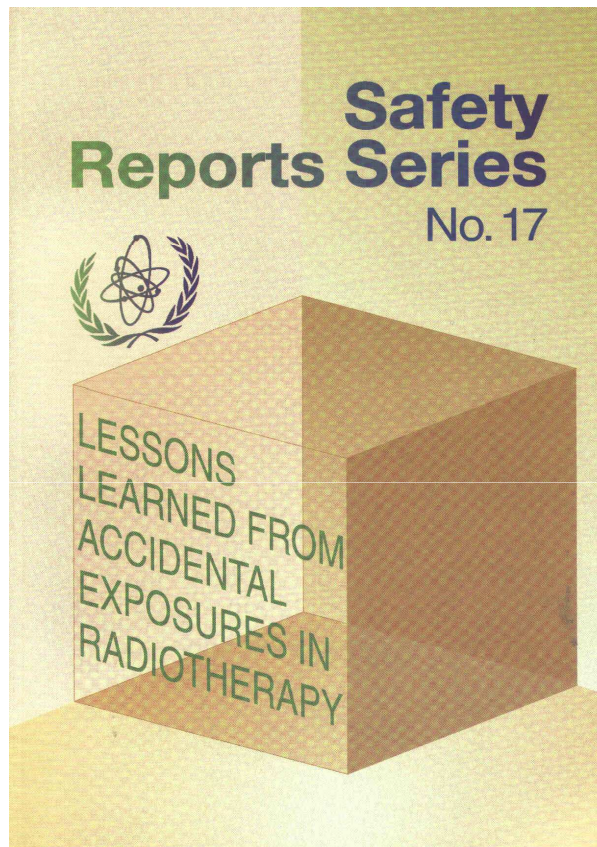
Why in vivo dosimetry?

- Prevent, rare but major accidents
 - *Brachytherapy procedures are performed without the safeguards of Record and Verify systems.*
- Human errors are the main cause of inadequate brachytherapy dose delivery, although mechanical failures occur as well. Examples are:
 - exchanged guide tubes;
 - misadjusted applicators;
 - reconstruction errors;
 - mechanical errors.



Why in vivo dosimetry?

- About 1/3 of the reported incidents in this IAEA booklet refer to brachytherapy!



Why in vivo dosimetry?

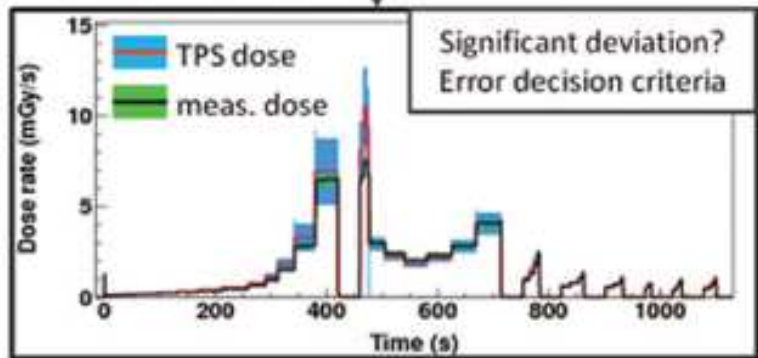
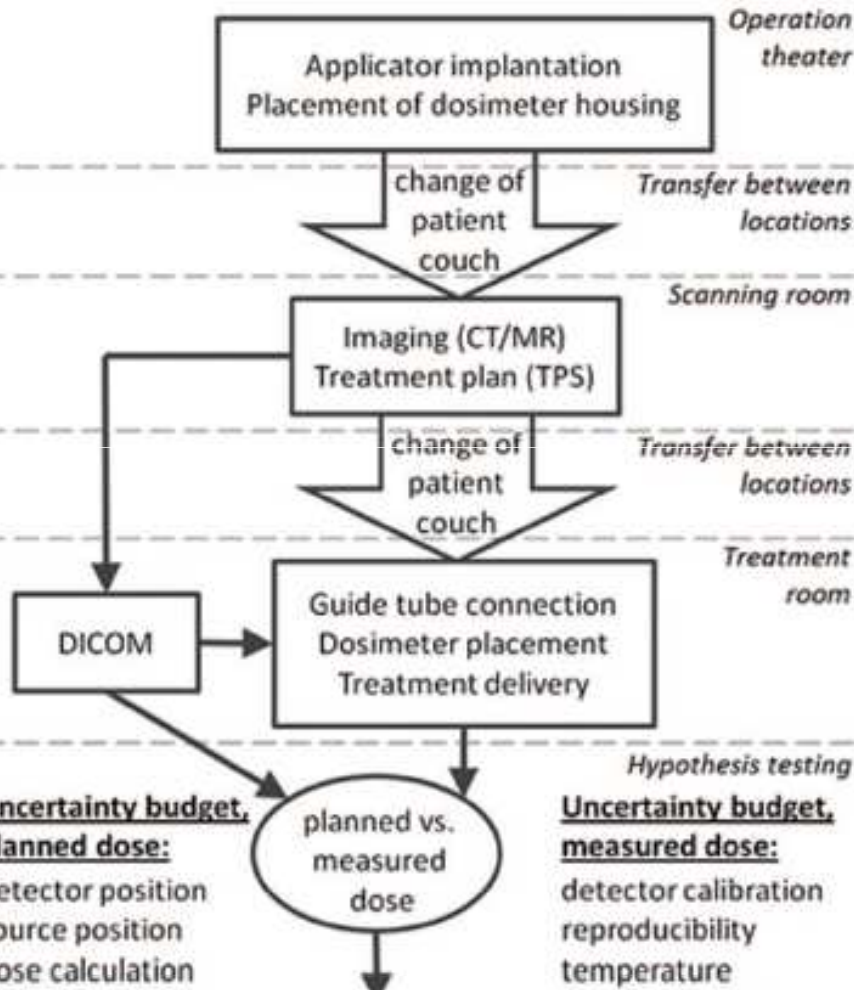
- Planned = delivered ?
 - Learning curve
 - Small number of fractions with increasing doses
 - Organ movement or deformation during treatment delivery
 - Organ swelling (LDR/PDR) or relative organ-catheter motion (HDR – multiple fractions)

Potential sources of error

- unstable fixation of dosimeter housing & applicators
- modified applicator & probe positions
- mis-reconstruction of applicators, fusion errors
- erroneous source-indexer length
- modified applicator & probe positions
- guide tube connection errors
- position drifts for dosimeter & applicators
- machine malfunction
- patient-DICOM mismatch
- Type I or II error
- Inaccurate TPS dose calc.
- inaccurate dosim. accuracy, e.g. erroneous calibration

- Necessary assumptions:
- patient-DICOM match
 - accuracy of dose calculation & measurements, and of their uncertainties
 - dosimeter, targets & OARs at original positions

Image guided brachytherapy workflow (example)



Interrupt (or terminate) treatment

Tanderup et al.
Vision 20/20.
Med. Phys. 2013

Why in vivo dosimetry?

- commissioning of new treatment technique – “in vivo” in phantom;
- Quality control of patient treatments;
- Confirmation of delivered dose (proof of good Tx);
- Used for inter-comparisons and audit systems.

Why in vivo dosimetry?

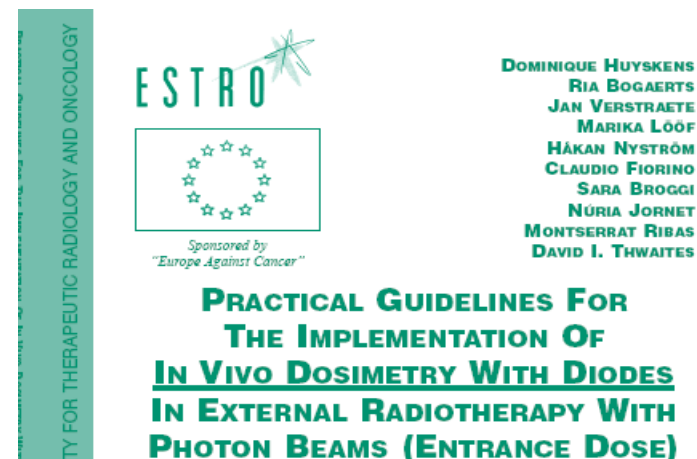
- Support for the use of in-vivo dosimetry by (inter)national bodies
- Legal obligation in many countries

Key questions!

- What do we want to know?
- What do we need to measure?

Guidance?

- ESTRO- the basic philosophy includes routine in-vivo dosimetry as an important chain in Quality Control of radiotherapy including brachytherapy;



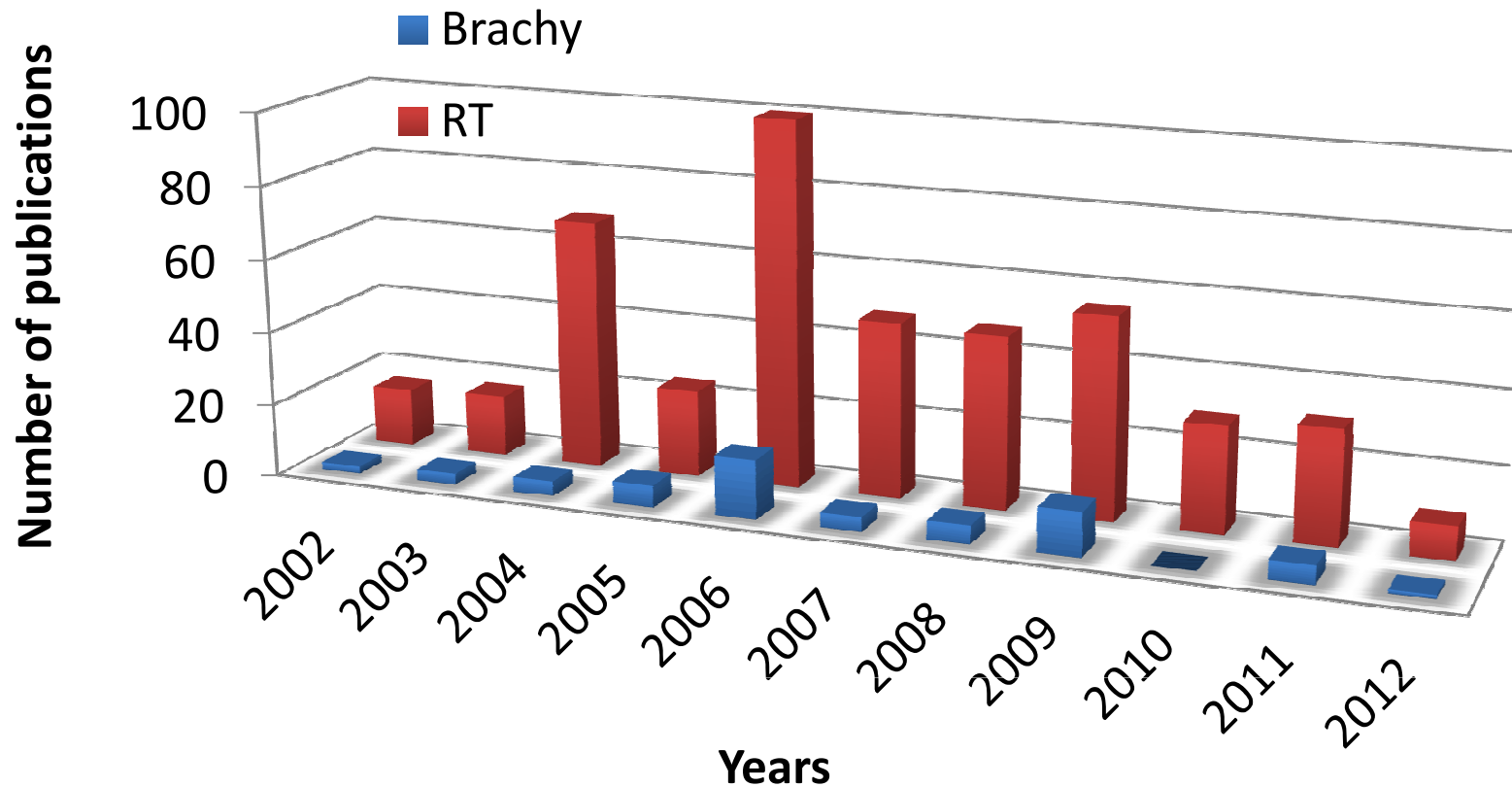
- IAEA – in a mission to improve the accuracy and safety of radiotherapy in developing countries;
- AAPM – TG-62 in a recommendation on the use of diode dosimetry in external beam radiotherapy (AAPM 2005).

What about Brachytherapy?

Key References

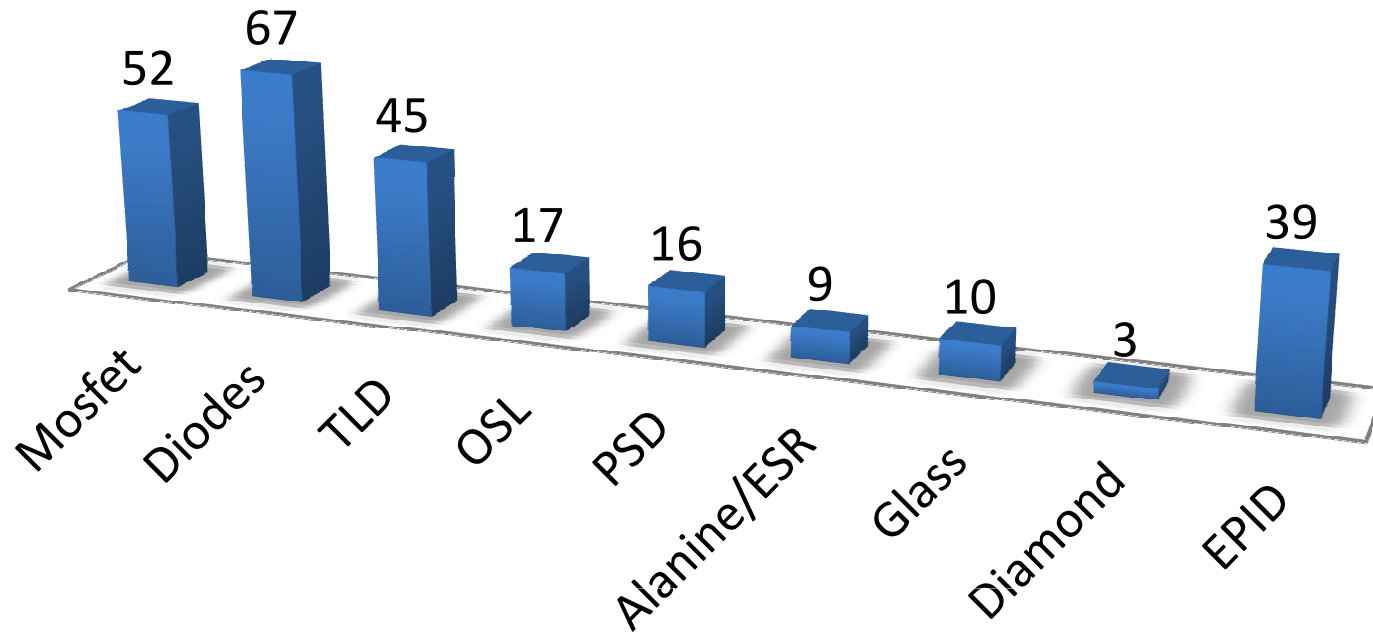
- Comprehensive Brachytherapy: physical and clinical aspect. JLM Venselaar, D Baltas, AS Meigooni and P.J. Hoskin. CRC Press, Taylor & Francis, 2013.
 - In particular Chapters 25: In Vivo Dosimetry in Brachytherapy by Cygler J. et al
- Brachytherapy physics, 2ed, AAPM monograph #31, 2005.
- In vivo dosimetry in brachytherapy. Tanderup K, Beddar S, Andersen C E, Kertzscher G and Cygler J E. Med. Phys. 40 (2013) 070902 - Vision 20/20 manuscript
- In vivo dosimetry: trends and prospects for brachytherapy. Kertzscher G, Rosenfeld A, Beddar S, Tanderup K and Cygler J E. Br. J. Radiol. 87 (2014) 20140206
- **Time-resolved in vivo luminescence dosimetry for online error detection in pulsed dose-rate brachytherapy. Andersen C E, Nielsen S K, Lindegaard J C and Tanderup K. Med. Phys. 36 (2009) 5033–43**
- A dosimetric uncertainty analysis for photon-emitting brachytherapy sources: Report of AAPM Task Group No. 138 and GEC-ESTRO. DeWerd L A, Ibbott G S, Meigooni A S, Mitch M G, Rivard M J, Stump K E, Thomadsen B R and Venselaar J L M 2011 *Med. Phys.* **38** 782–801

How common is this?



Source: PubMed, March 5th 2012: “in vivo dosimetry” AND “<Modality>” AND “<Year>”

Available Dosimeters (All)



Source: PubMed, March 5th 2012: “in vivo dosimetry” AND “<Detector>”

Contents

- Why IVD in brachytherapy?
- Tools and clinical experiences
- Challenges or “the physics is killing me”
- NextGen IVD tools
- Some pointers...

TABLE III. Characteristics of detectors and dosimetry systems of importance for precise routine IVD in brachytherapy. The items are rated according to: advantageous (++), good (+), and inconvenient (-).

	TLD	Diode	MOSFET	Alanine	RL	PSD
Size	+	+/-	+ /+++	-	++	++
Sensitivity	+	++	+	-	++	+ /+++
Energy dependence	+	-	-	+	-	++
Angular dependence	++	-	+	+	++	++
Dynamic range	++	++	+	-	++	++
Calibration	+	++	++	-	- /+	+ /+++
procedures, QA, stability, robustness, size of system, ease of operation						
Commercial availability	++	++	++	++	-	+
Online dosimetry	-	++	+	-	++	++
Main advantages	No cables, well studied system	Commercial systems at reasonable price, well studied system	Small size, commercial system at reasonable price	Limited energy dependence, no cables	Small size, high sensitivity	Small size, no angular and energy dependence, sensitivity
Main disadvantages	Tedious procedures for calibration and readout, not online dosimetry	Angular and energy dependence	Limited life of detectors, energy dependence	Not sensitive to low doses, tedious procedures for calibration and readout, not online dosimetry, expensive readout equipment not available in clinics	Needs frequent recalibration, stem effect, not commercially available	Stem effect

The Dosimeters

- TLDs



The Dosimeters

- TLDS
 - Prostate, Urethral and Rectal dose in HDR prostate implants
 - Brezovich IA et al., Med Phys 27, 2000;
 - Anagnostopoulos G et al., IJROBP 57, 2003;
 - Das R et al, Australas Phys Eng Sci Med. 2007;
 - Toye W et al, Rad Onc 91, 2008
 - Between 10 and 20 TLDS

The Dosimeters

- TLDs

Table 1
Experimental uncertainty in recorded TLD doses is presented with a confidence level of 68%

Uncertainty	Urethra (%)	Rectum (%)
<i>Measurement uncertainties</i>		
Linac calibration	1.5	1.5
Dose response of TLDs	5	5
<i>Positional</i>		
C-arm films & digitization	5	3
<i>TPS uncertainties</i>		
Source strength	5	5
Dose calculation algorithm	<1	<1
Total Uncertainty in difference between measurement and TPS	9	8

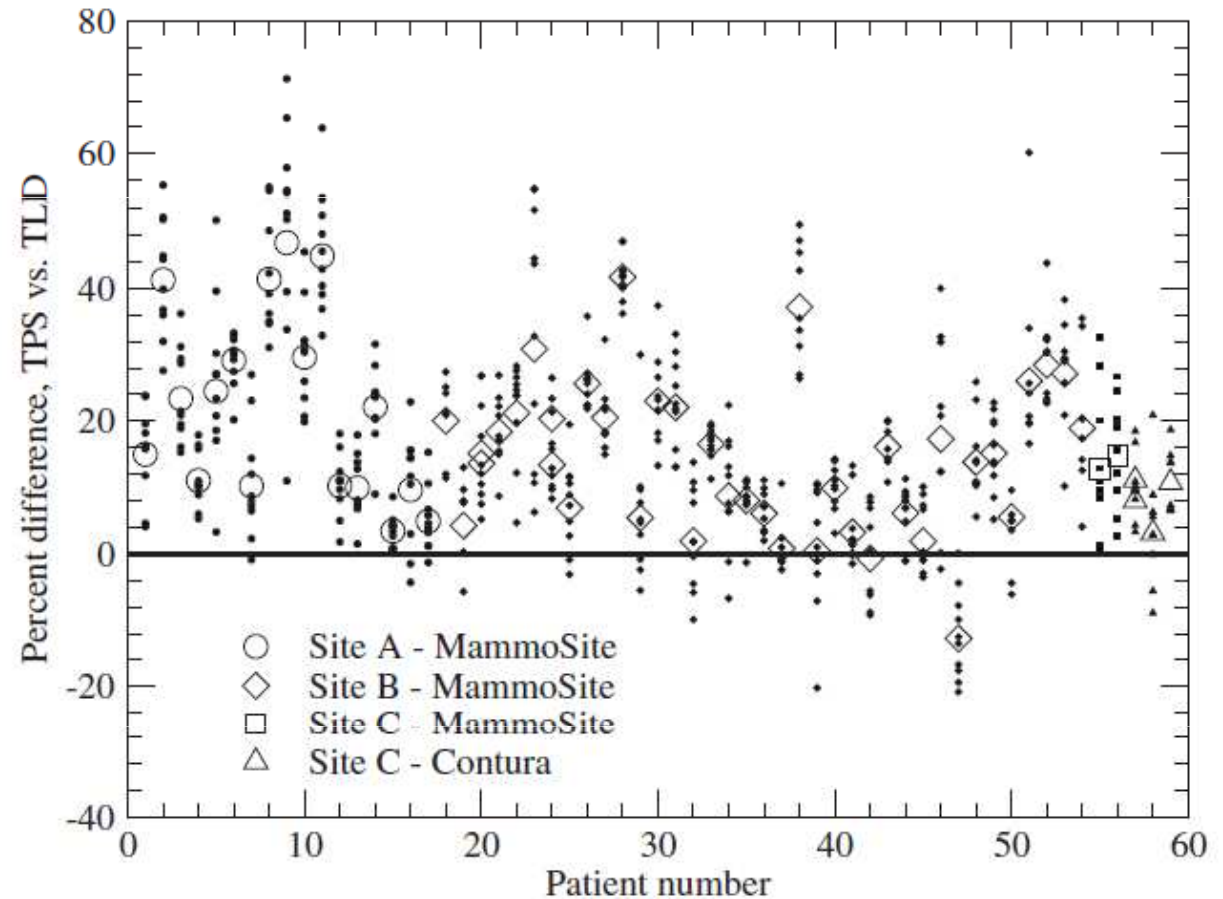
The dose uncertainty due to urethral and rectal TLD position has been estimated from the standard deviation in dose associated with the average shift correction of 4 mm.

- Flag dose delivery error of > 10%
 - Uncertainty about 10%
- Action level at 20%
 - 1/3 of case further investigated

Toye W et al, Rad Onc 91, 2008

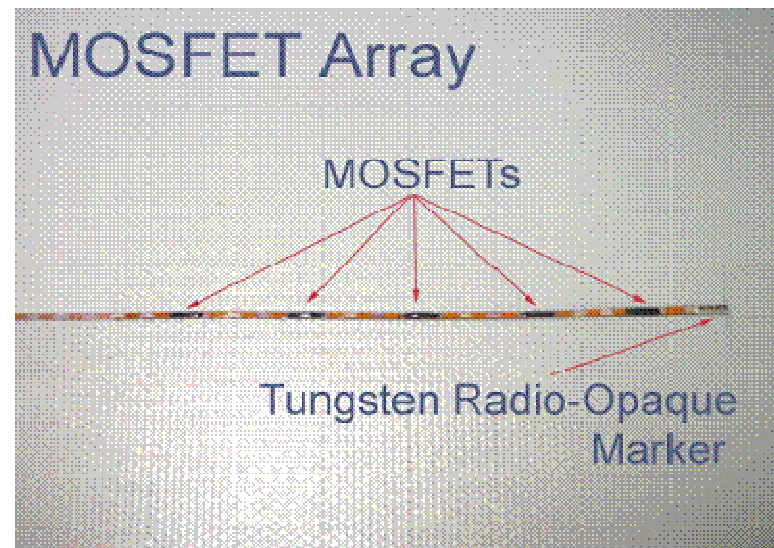
The Dosimeters

- Skin dose in breast HDR tx
 - Raffi JA et al, Med Phys 37 (2010)
- Average 16% deviation (59 cases) if TG-43
- Within 3% if advanced dose calculation (e.g. MC, Acuros)



The Dosimeters

- MOSFETs

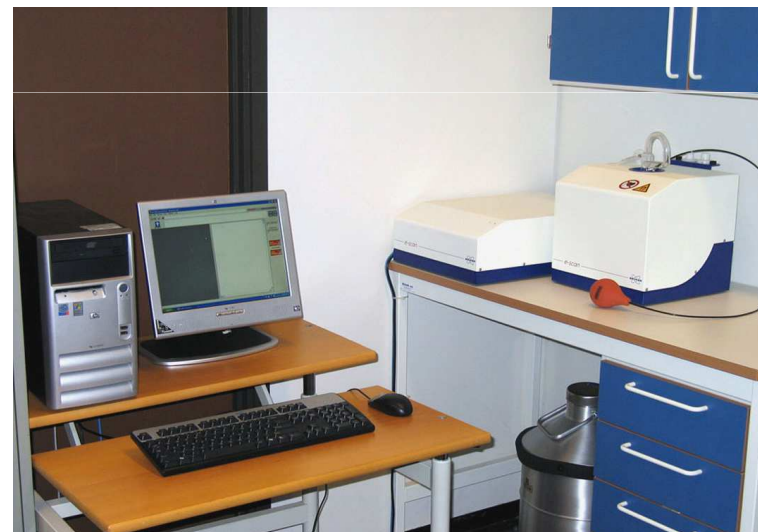
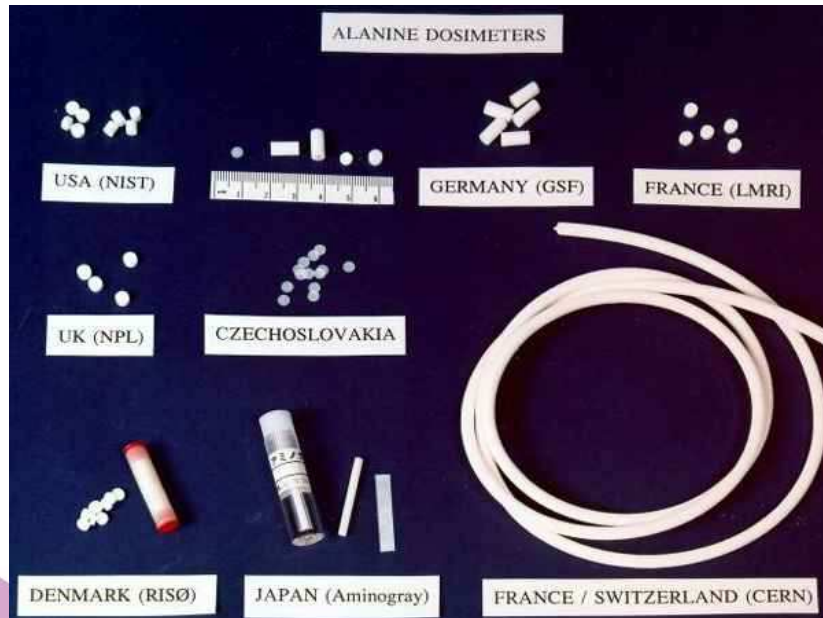
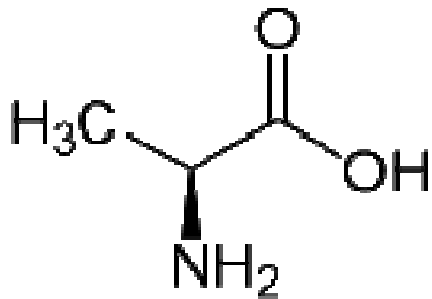


The Dosimeters

- MOSFETs (real-time!)
 - Urethral dose in seed implants
 - Cygler JE et al, Rad Onc 80, 2006 (single)
 - Bloemen-van Gurp E et al, IJROBP 73, 2009 (array)
 - High sensitivity MOSFET; calibration with ^{125}I seeds
 - Uncertainties (ideal situation): 8% (1σ)
 - Action level $\pm 16\%$ or 2σ

The Dosimeters

- Alanine (amino acid) / EPR / ESR



The Dosimeters

- Alanine (amino acid) / EPR / ESR
 - GYN (^{137}Cs)
 - Schultka K et al., Rad. Prot. Dos 120 (200
 - Average difference with planning 10%
 - Detector volume too large
- Alanine (amino acid) / EPR / ESR
 - Urethra dose in prostate HDR: Phantom Study
 - Anthon M et al., PMB 54 (2009)
 - Uncertainty of 5% at 1σ
 - exclude source strength uncertainty of 5%

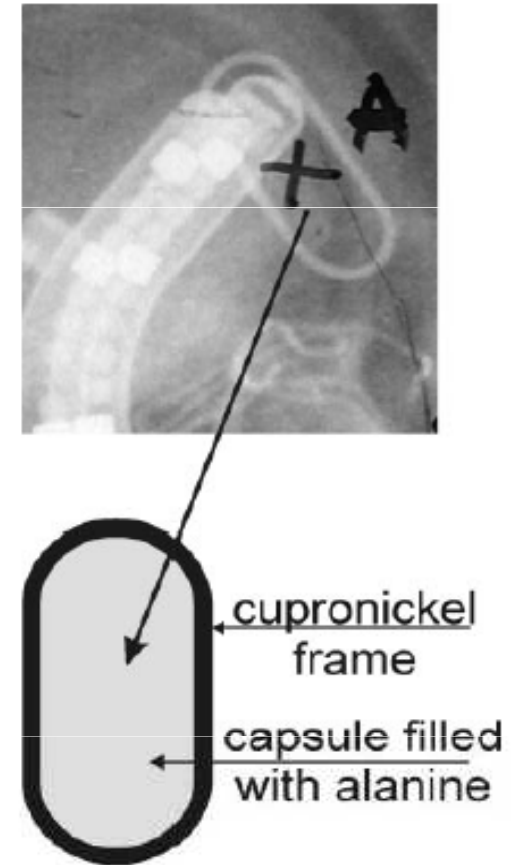


Figure 1. Visualisation of a detector on radiograph used for treatment planning. The cross marks the central point of the detector in which the dose was calculated by RTP.

The Dosimeters

- Diodes (real-time)
 - e.g. PTW 9112 (five diodes array)



The Dosimeters

- Diodes: PTW 9112 (5) and 9113 (1)
 - Cervix
 - Alecu R and Alecu M. Med Phys 26 (1999)
 - Agreement with TPS within 15%
 - Waldhäusl C et al., Rad Onc 77 (2005)
 - Phantom: uncertainty of diode measurements of 7% (1σ)
 - Clinical action level of $\pm 10\%$
 - 36 out of 55 cases need further investigation
 - » 19 > 20% rectal dose
 - » 6 > 20% bladder dose

The Dosimeters

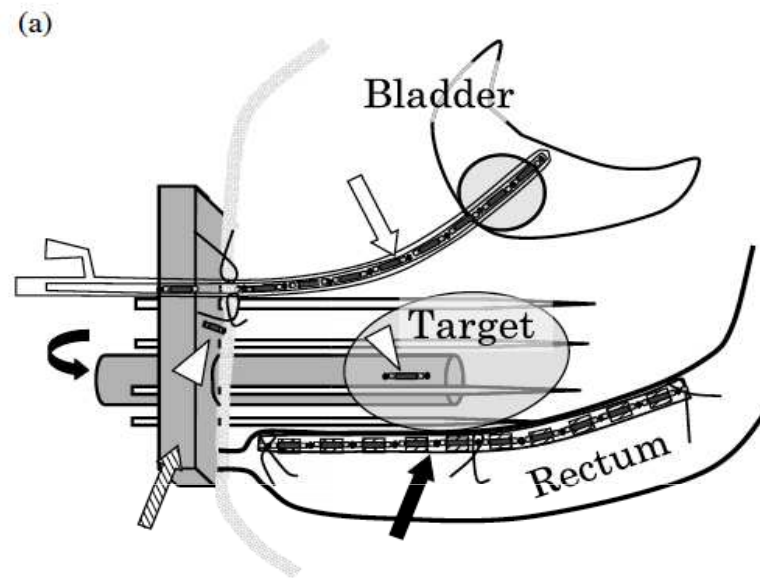
- Diodes

“...diodes allow performing in-vivo measurements, provided that the position of the diodes relative to the reference points are determined accurately”

- Waldhäusl C et al., Rad Onc 77 (2005)

The Dosimeters

- Radiophotoluminescent glass dosimeter
 - Dose Ace (Japan): UV stimulation of silver phosphate



Takayuki et al., IJROBP 2008

The Dosimeters

- Radiophotoluminescent glass dosimeter
 - Pioneers work: Roswit B, et al. Radiology 97 (1970) “In vivo radiation dosimetry. Review of a 12-year experience.”
 - Prostate: Takayuki et al., IJROBP 70 (2008) and Hsu SM et al., Med Phys 35 (2008)
 - GYN: Takayuki et al., IJROBP 70 (2008)
 - H&N Brachy: Takayuki et al., IJROBP 61 (2005)

The Dosimeters

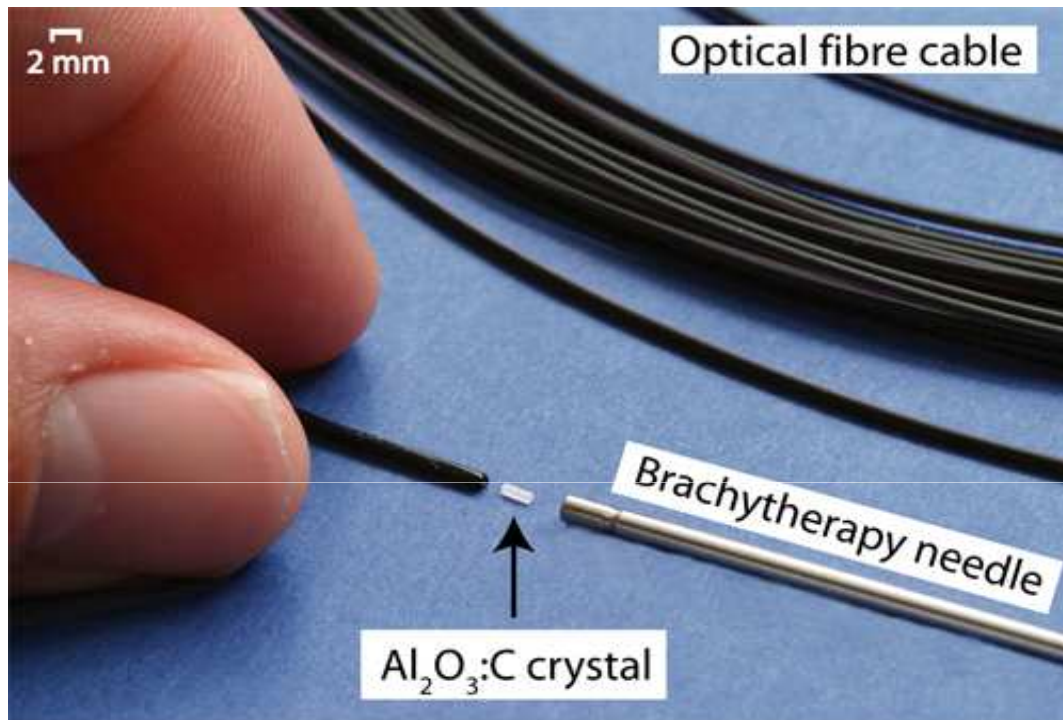
- Radiophotoluminescent glass dosimeter
 - Prostate (26 cases): Takayuki et al., IJROBP 70 (2008) and Hsu SM et al., Med Phys 35 (2008)
 - GYN (35 cases): Takayuki et al., IJROBP 70 (2008)
 - H&N Brachy (61 cases): Takayuki et al., IJROBP 61 (2005)

The Dosimeters

- Radiophotoluminescent glass dosimeter
 - Takayuki et al., IJROBP 70 (2008)
 - Deviations of more than 20% seen
 - Motions
 - Inhomogeneities

The Dosimeters

- Real-time OSL reading
 - Anderson's group



The Dosimeters

- Real-time OSL reading
 - Cervix/PDR: Anderson CE et al., Med Phys 36 (2011)
 - OSL measurements uncertainty 5% (1σ)
 - ★ Displacement errors are distance dependent
 - ★ Factor of 10 more likely to detector an error (like tube interchange) if time-resolved measurements.

The Dosimeters

- Plastic Scintillation (real-time) Dosimeters
 - BrachyFOD + PTW OPTIDOS (Lambert J, PMB 2006)
 - BC400, similar design as Beddar et al from 1992...

5508

J Lambert *et al*

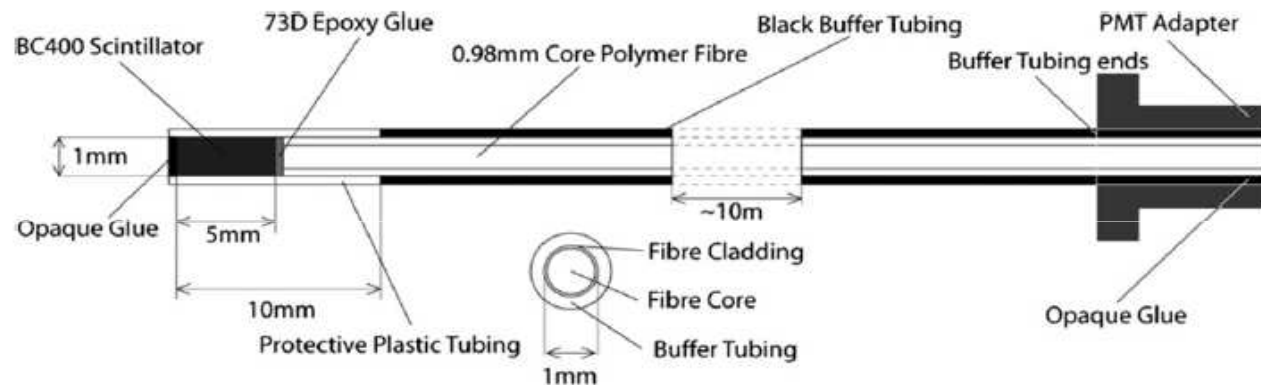


Figure 1. The design of the *BrachyFOD*TM. Two sizes were manufactured, one as shown in the figure and the other with a scintillator and fibre diameter of 0.5 mm and a scintillator length of 4 mm.

The Dosimeters

- Plastic Scintillating Fiber Dosimeters
 - Laval/MD Anderson design with Cerenkov correction



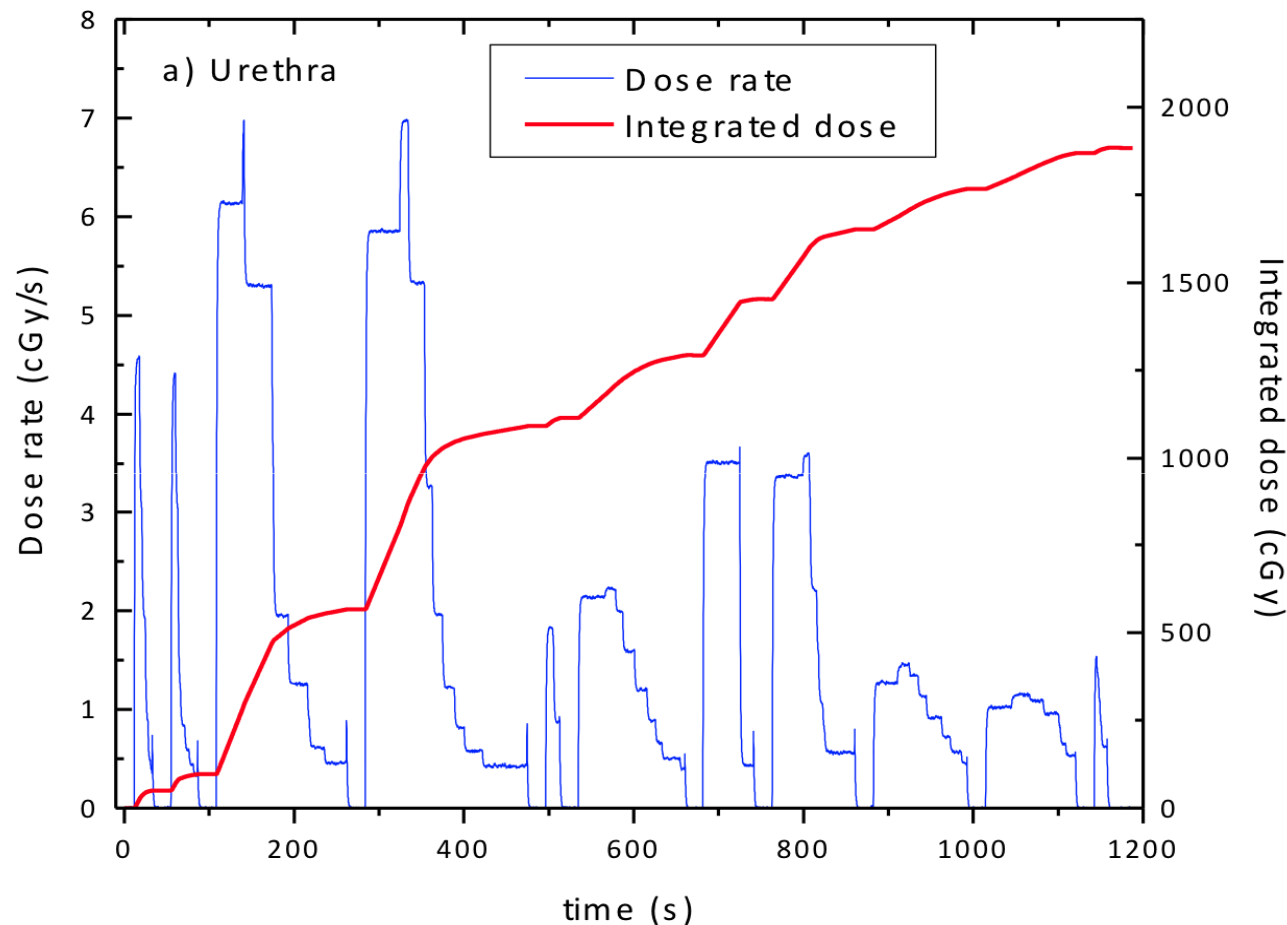
The Dosimeters

- Plastic Scintillating Fiber Dosimeters
 - Urethral dose (prostate HDR)
 - SUCHOWERSKA N, IJROBP 79 (2011)
 - 1 Measurements points with imaging (pt marker)
 - Average deviations without imaging 9%, max 67%.
 - Max. deviation with imaging 9%.

The Dosimeters

- Real-time IVD

- Whole tx, per catheter or per dwell-positions (Theriault-Proulx et al, Med Phys 2011)



Summary of Clinical IVD Studies

Table 9.1. A summary of clinical brachytherapy in vivo dosimetry studies.

Dosimeter	Study	Site	Action Level / Comment	Uncertainty (1 σ)
TLD	Brezovich et al(Brezovich <i>et al</i> 2000)	Prostate, Urethra,	Action level: 20% generally,	8-10%;
	Anagnostopoulos et al(Anagnostopoulos <i>et al</i> 2003)	rectal dose,		
	Das et al(Das <i>et al</i> 2007)			
	Toye W et al(Toye <i>et al</i> 2008)			
	Raffi et al(Raffi <i>et al</i> 2010)	skin (breast)		<3% (TLD uncertainty budget)
MOSFET	Cygler et al(Cygler <i>et al</i> 2006)	Urethra (prostate seed implants)	Action level: 16%	8%
Alanine /ESR	Schultka et al(Schultka <i>et al</i> 2006)	GYN (¹³⁷ Cs)	Detector volume too large; Difference with planning 10+%	None provided
	Anton et al(Anton <i>et al</i> 2009)	Urethra (prostate HDR)		5% (excl. source strength uncertainty)
Diodes	Alecu and Alecu(Alecu and Alecu 1999)	Cervix	Agreement with TPS within 15%	None provided
	Waldhäusl C et al(Waldhäusl <i>et al</i> 2005)	Cervix	Action level: 10% (36/55 cases needs further investigation)	7%
	Seymour et al(Seymour <i>et al</i> 2011)	Rectum (Prostate HDR)	95% measurements within 20%	9.8% (meas. only)

Beaulieu et al.
Chapter 9
Emerging
Brachytherapy
Technology

Emerging Technologies in Brachytherapy
William Y. Song, Kari Tanderup, Bradley Pieters

Hardback
\$199.95

February 26, 2017 **Forthcoming** by CRC Press
Reference - 304 Pages - 30 Color & 170 B/W Illustrations
ISBN 9781498736527 - CAT# K26490
Series: Series in Medical Physics and Biomedical Engineering

Beaulieu et al.
Chapter 9
Emerging
Brachytherapy
Technology

Glass Dosimeters	Takayuki et al(Nose <i>et al</i> 2008)	Prostate	Deviations of more than 20% seen.	None provided
	Hsu et al(Hsu <i>et al</i> 2008)	GYN		
	Takayuki et al(Nose <i>et al</i> 2008)	H&N		
OSLD "NanoDot"	Sharma and Jursinic(Sharma and Jursinic 2013)	GYN,Breast	-4.4% to 6.5% difference to AcurosDV	None provided
Real-time OSL	Andersen et al(Andersen <i>et al</i> 2009)	Cervix (PDR)	Errors detection are distance dependent; Time-resolved measurements are better	5%
Plastic Scintillation Dosimeters	Suchowerska et al(Suchowerska <i>et al</i> 2011)	Urethra (prostate HDR)	Maximum deviation without imaging 67%;	None provided
			maximum deviation with imaging 9%	
MOSkin	Carrara et al(Carrara <i>et al</i> 2016)	Rectum (Prostate HDR)		None provided
	Qi et al(Qi <i>et al</i> 2012)	Nasopharynx	Action level: 20%	2.5% (MOSkin uncertainty budget)

Emerging Technologies in Brachytherapy
William Y. Song, Kari Tanderup, Bradley Pieters

Hardback
\$199.95

February 26, 2017 **Forthcoming** by CRC Press
Reference - 304 Pages - 30 Color & 170 B/W Illustrations
ISBN 9781498736527 - CAT# K26490
Series: Series in Medical Physics and Biomedical Engineering



Lesson learned

- IVD in brachytherapy has only demonstrated its ability to detect gross errors
 - Above 10 to 20% depending on sites (dosimeters, isotopes, TPS, ...)

Contents

- Why IVD in brachytherapy?
- Tools and clinical experiences
- Challenges or “the physics is killing me”
- NextGen IVD tools
- Some pointers...

You cannot beat the house!

DeWerd et al, AAPM/ESTRO TG138

TABLE IV. Propagation of best practice uncertainties ($k=1$ unless stated otherwise) associated with the transfer of air-kerma strength from a traceable NIST coefficient from the ADCL to the clinic for HDR high-energy brachytherapy sources.

Row	Measurement description	Quantity (units)	Relative propagated uncertainty (%)
1	A		
2	ADCL well		
3	ADCL calibration		
4	ADCL calibration		
5	Clinic measurement		
	Expanded		

TABLE V. Propagation of best practice uncertainties ($k=1$ unless stated otherwise) in dose at 1 cm on the transverse plane associated with source-strength measurements at the clinic, brachytherapy dose measurements or simulation estimates, and treatment planning system dataset interpolation for low-energy (*low-E*) and high-energy (*high-E*) brachytherapy sources as relating to values presented in Fig. 1.

Row	Uncertainty component	Relative propagated uncertainty (%)	
		<i>low-E</i>	<i>high-E</i>
1	S_K measurements from row 5 of Tables I and IV	1.3	1.5
2	Measured dose	3.6	3.0
3	Monte Carlo dose estimate	1.7	1.6
4	TPS interpolation uncertainties	3.8	2.6
5	Total dose calculation uncertainty	4.4	3.4
	Expanded uncertainty ($k=2$)	8.7	6.8

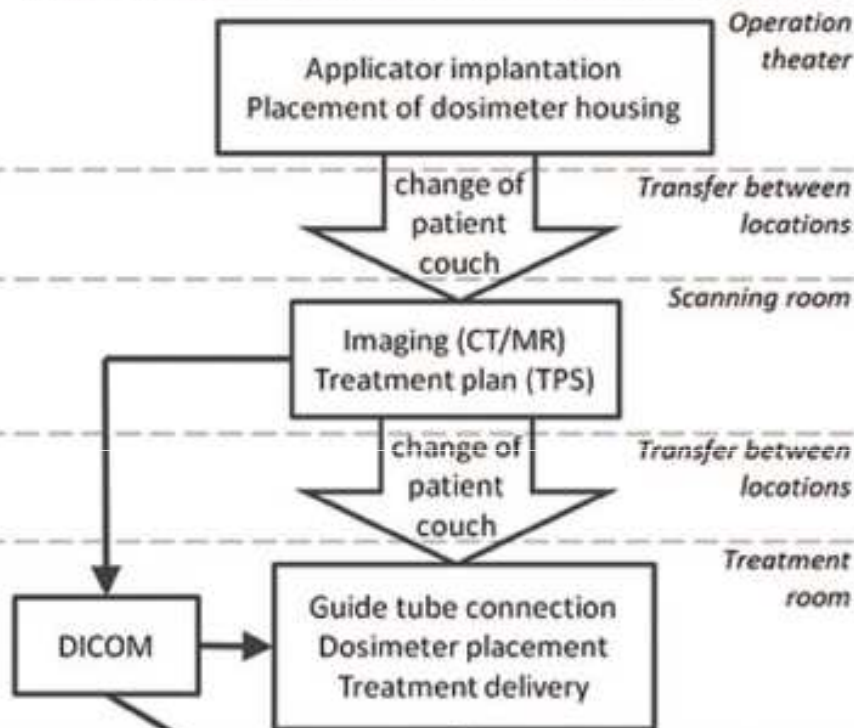
Potential sources of error

- unstable fixation of dosimeter housing & applicators
- modified applicator & probe positions
- mis-reconstruction of applicators, fusion errors
- erroneous source-indexer length
- modified applicator & probe positions
- guide tube connection errors
- position drifts for dosimeter & applicators
- machine malfunction
- patient-DICOM mismatch

- Type I or II error
- inaccurate TPS dose calc.
- inaccurate dosim. accuracy, e.g. erroneous calibration

- Necessary assumptions:
- patient-DICOM match
 - accuracy of dose calculation & measurements, and of their uncertainties
 - dosimeter, targets & OARs at original positions

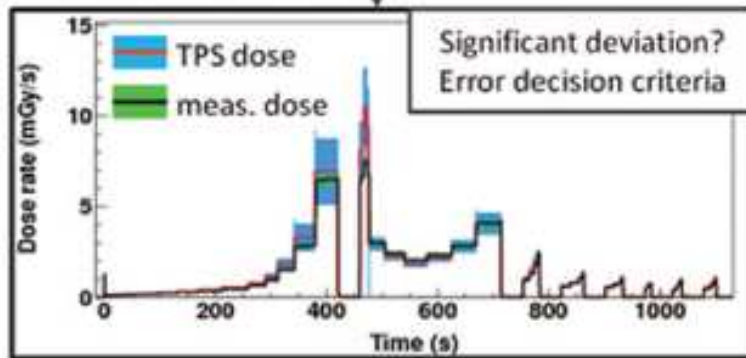
Image guided brachytherapy workflow (example)



Uncertainty budget, planned dose:
 detector position
 source position
 dose calculation

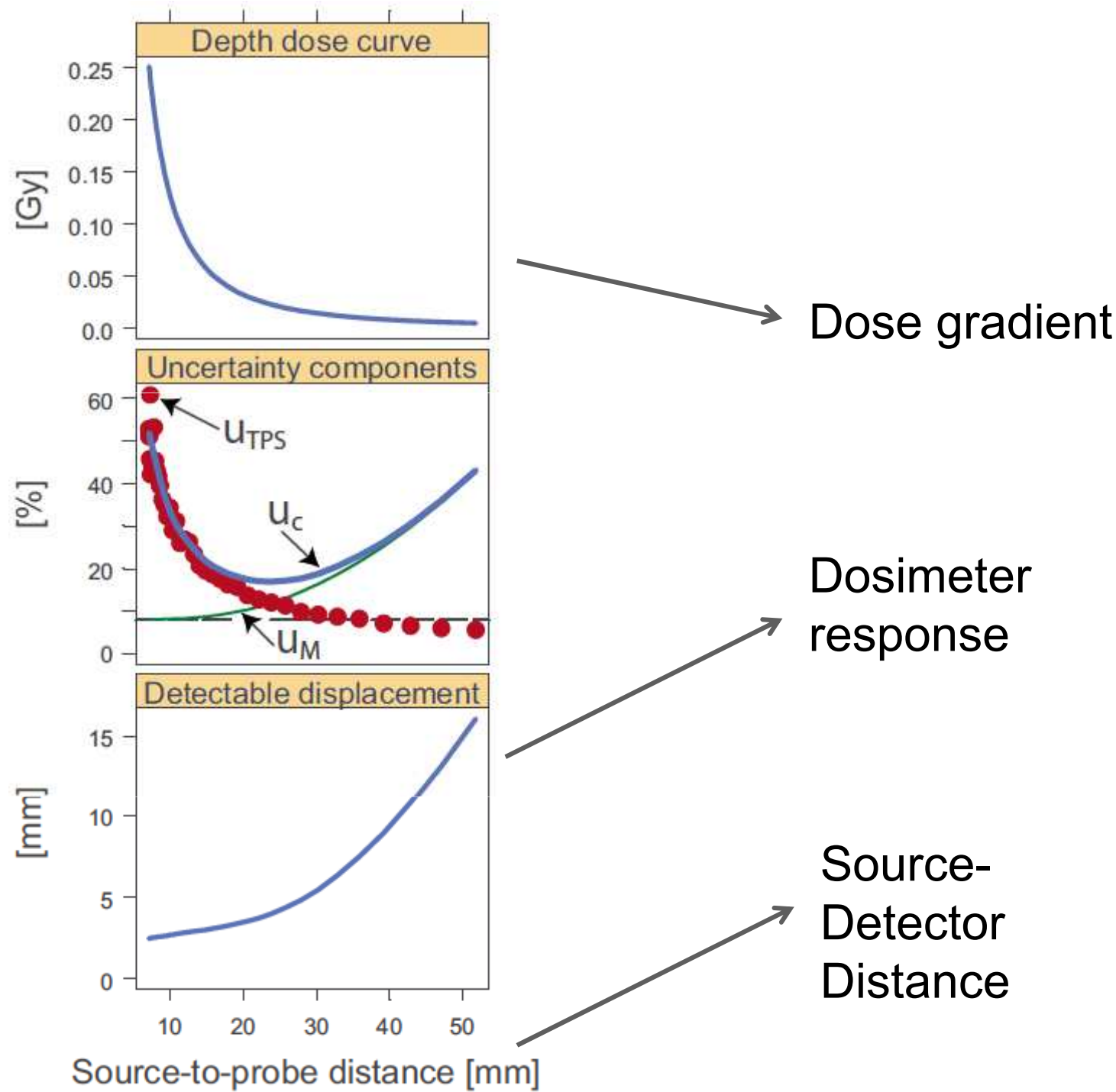
planned vs. measured dose

Uncertainty budget, measured dose:
 detector calibration
 reproducibility
 temperature



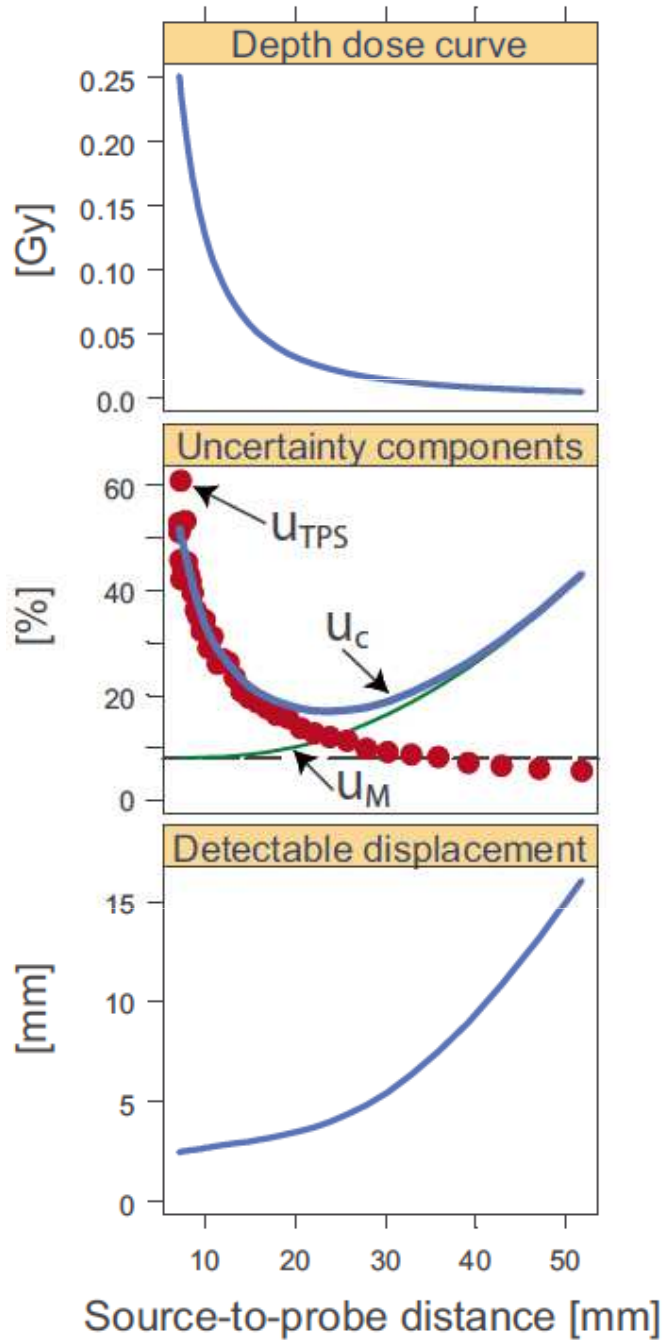
Interrupt (or terminate) treatment

Tanderup et al.
 Vision 20/20.
 Med. Phys. 2013

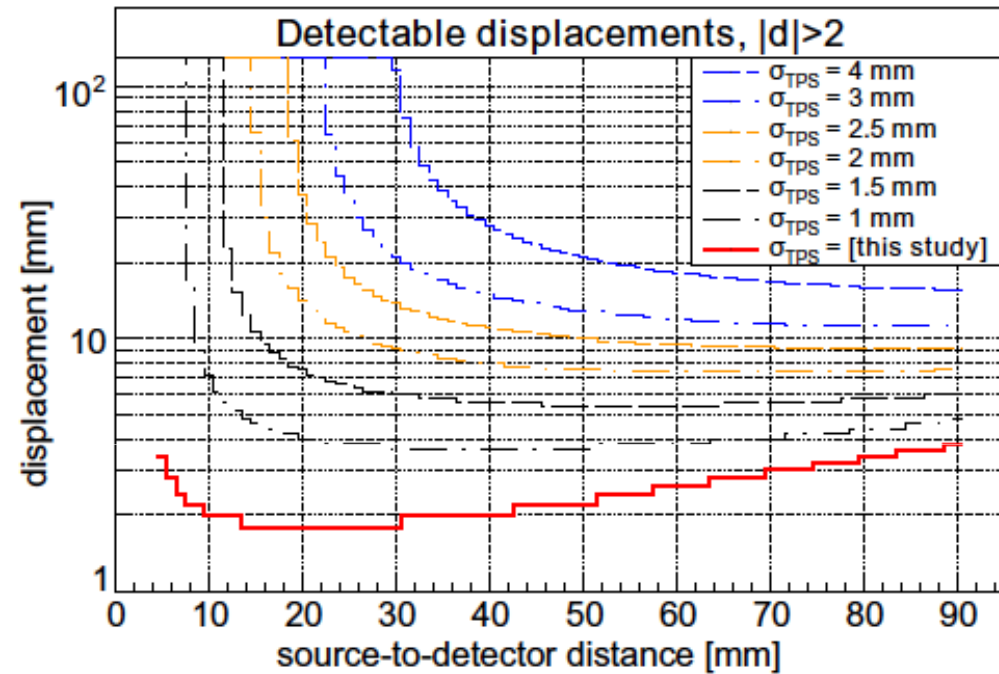


Source-Detector Distance “problem”

1. Displacement of the dosimeter relative to plan position
 - a) Organ-induced displacement
 - b) Manipulation error (digitization, displacement before measurements...)
2. Displacement of source position(s) relative to plan position(s)
 - a) Displacement of one or more catheters or an applicator, including rotation for certain applicators.
 - b) Organ-induced displacement
 - c) Manipulation error (wrong transfer tube connection...)
3. Combination of the above two i.e. source and sensor displacements
 - a) Perfectly in sync: no effect on dose measured but effect on dose delivered
 - b) Out of sync
4. Organ-related change that does not impact the relative distances but organ dosimetry (e.g. swelling, deformation, ...)

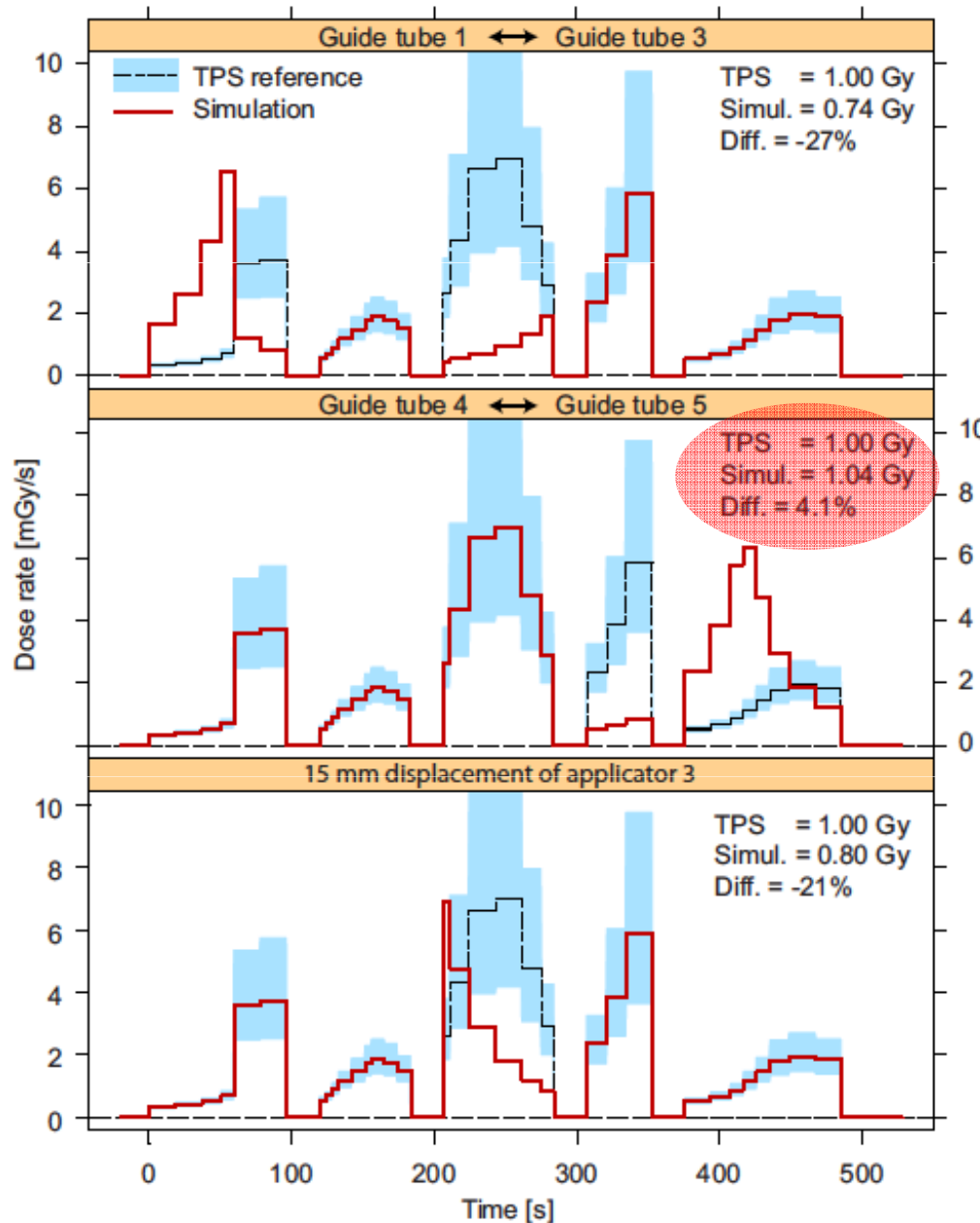


$$d = \frac{D_M - D_{TPS}}{\sqrt{u_M^2 + u_{TPS}^2}}$$



Kertzscher et al *Radiother. Oncol.* **100** (2011) 456–62

Time-Resolved IVD

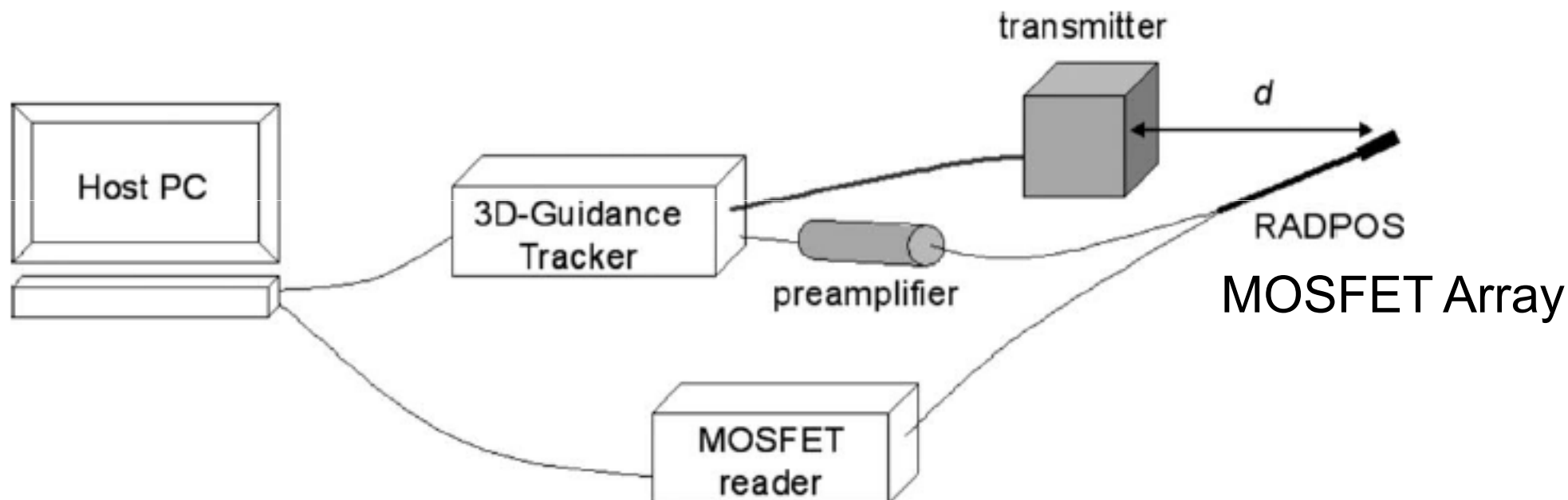


Only time-resolved

Contents

- Why IVD in brachytherapy?
- Tools and clinical experiences
- Challenges or “the physics is killing me”
- **NextGen IVD tools**
- Some pointers...

Next Generation Tools

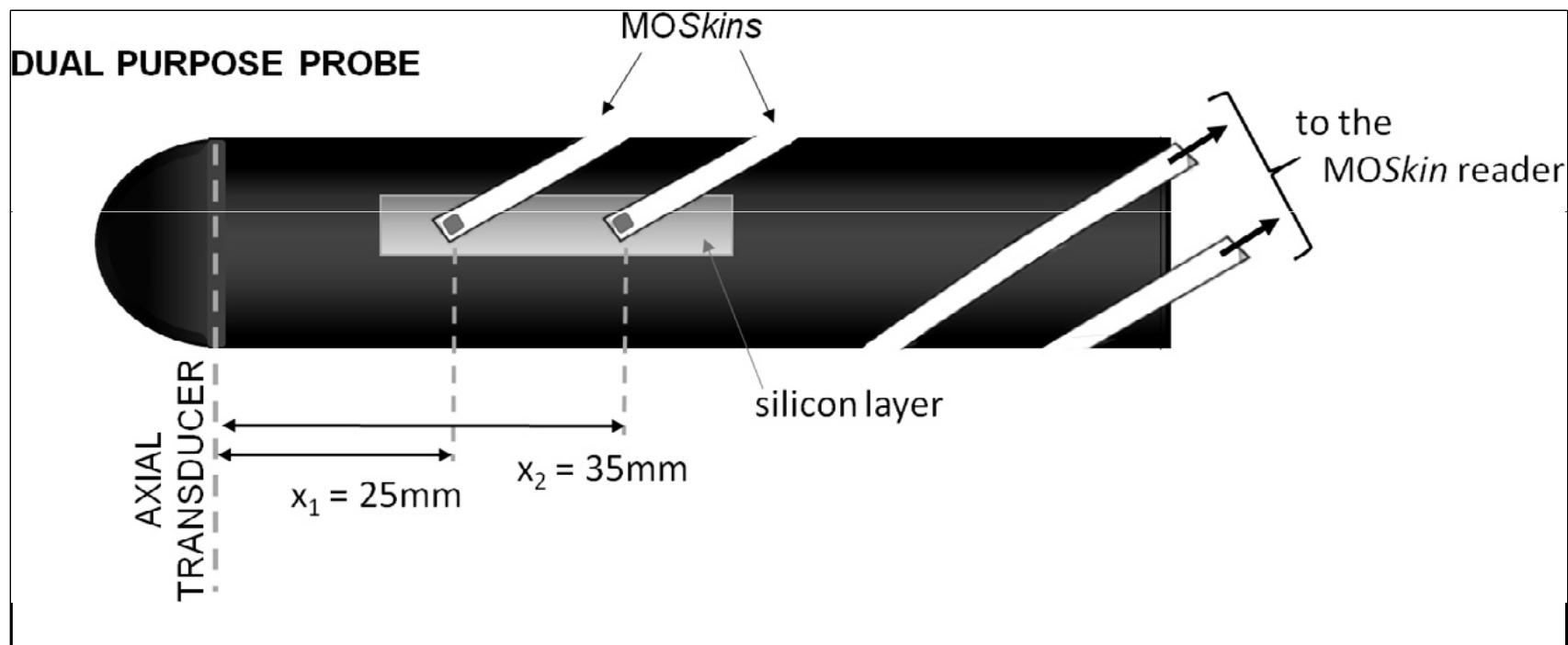


MORE ON TRACKING TECHNOLOGY TOMORROW

Cherpak A J, Cygler J E, E C and Perry G 2014 Real-time measurement of urethral dose and position during permanent seed implantation for prostate brachytherapy. - PubMed - NCBI Brachytherapy 13 169–77

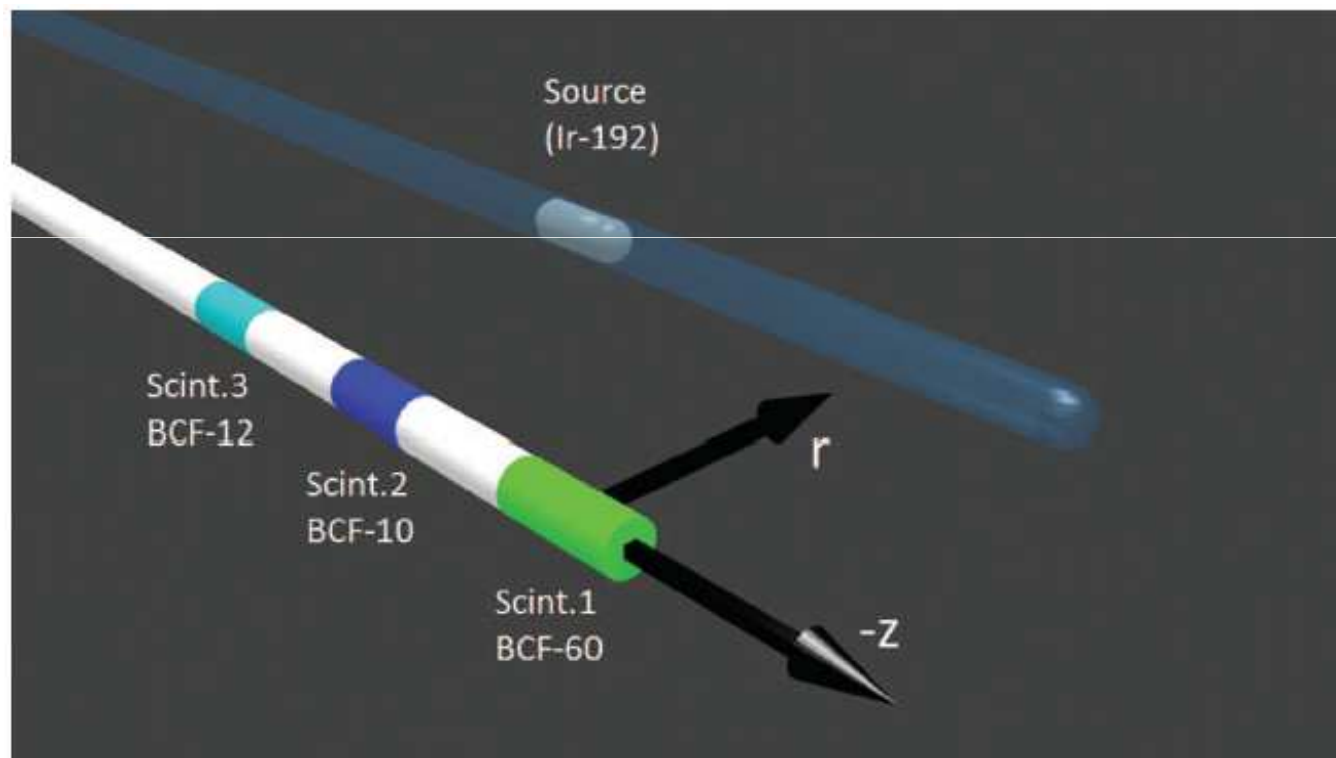
Cherpak A, Ding W, Hallil A and Cygler J E 2009 Evaluation of a novel 4D in vivo dosimetry system Med. Phys. 36 1672

Next Generation Tools



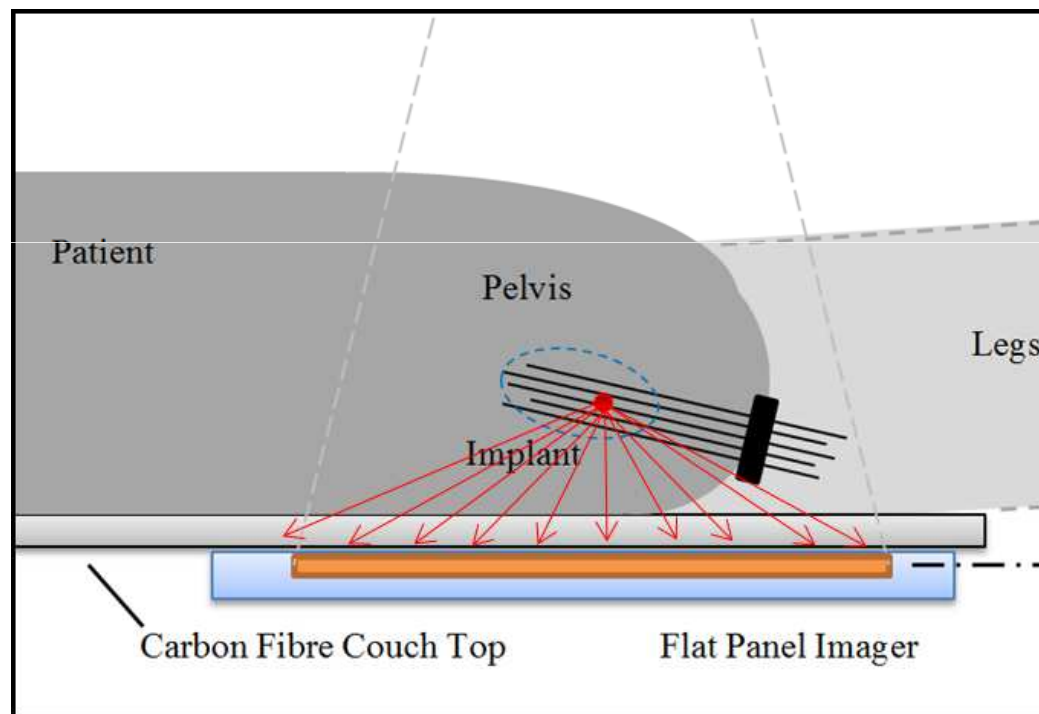
Carrara et al 2016 In vivo rectal wall measurements during HDR prostate brachytherapy with MOSkin dosimeters integrated on a trans-rectal US probe: Comparison with planned and reconstructed doses. *Radiother. Oncol.* **118** 148–53

Next Generation Tools



Therriault-Proulx F, Beddar S and Beaulieu L 2013 On the use of a single-fiber multipoint plastic scintillation detector for ^{192}Ir high-dose-rate brachytherapy Med. Phys. 40 062101

Next Generation Tools



Smith R L, Taylor M L, McDermott L N, Haworth A, Millar J L and Franich R D 2013 Source position verification and dosimetry in HDR brachytherapy using an EPID. Med. Phys. 40 111706

Smith R L, Haworth A, Panettieri V, Millar J L and Franich R D 2016 A method for verification of treatment delivery in HDR prostate brachytherapy using a flat panel detector for both imaging and source tracking. Med. Phys. 43 2435–42

Contents

- Why IVD in brachytherapy?
- Tools and clinical experiences
- Challenges or “the physics is killing me”
- NextGen IVD tools
- Some pointers...

To do before usage!

- Get to know your IVD tool(s)
 - No dosimeters is perfect
 - Expected performance in controlled conditions
 - Establish the uncertainty budget
 - Limitations
 - Explore characteristics (dependence): energy, angular, temperature, ...
 - Detection thresholds (dose, dose rate, known displacements)
 - ...

To do before usage!

- Plan to use imaging – think position(s)
- Take into account TPS limitation
 - Use MBDCA if available.

Consider the following:

- Use time-resolved measurements whenever possible
 - Use more than 1 measurement points if possible
 - Nakano T, Suchowerska N, Bilek M M, McKenzie D R, Ng N and Kron T 2003 High dose-rate brachytherapy source localization: positional resolution using a diamond detector. *Phys. Med. Biol.* 48 2133–46
 - Therriault-Proulx F, Beddar S and Beaulieu L 2013 On the use of a single-fiber multipoint plastic scintillation detector for ^{192}Ir high-dose-rate brachytherapy *Med. Phys.* 40 062101
 - Track your IV dosimeters in real-time if possible

Back to our key questions...

- Is IVD really the most appropriate tools for the task(s) you are trying to achieve?

Table 9.3 Table adapted from Tanderup *et al.* (2013) recast in term of potentially appropriate technology for the test to be performed.

Quality item	Typical quality test	Appropriate technology
Source calibration	Independent source calibration in the department	Well chamber
Afterloader source positioning and dwell time (nonpatient specific)	Autoradiography, commissioning of applicators, other source stepping and dwell time QA	- Films (position) - Well Chamber (time) - Flat Panel (possible for both)
Afterloader malfunction	Unpredictable afterloader malfunction is difficult to target with general QA.	- Real-time feedback <ul style="list-style-type: none"> o IVD o Flat Panel
Patient identification	Manual check	Not relevant
Correct treatment plan	Manual check	Checksum and similar independent software validation tools is the more efficient
Intra- and interfraction organ/applicator movement	Reimaging performed just before treatment delivery can in some cases be used to assess organ or tumor dose in image-guided BT.	- For organ motion: real-time imaging if possible - Applicator motion: real-time tracking of the applicator or 3D source tracking within the applicator (EM, optical, Flat Panel) - IVD could be relevant depending on decoupling between applicator and dosimeters
Applicator reconstruction and fusion errors	Manual check	- IVD relevant to catch error during treatment - Pre-delivery or real-time imaging - Independent applicator/channel reconstruction technology (e.g. EM tracking)
Applicator length/source-indexer length	Manual check	- IVD relevant to catch error during treatment - Flat Panel technology - EM tracking (if link to the afterloader drive wire)
Source step size (patient specific)	Manual check	- IVD relevant to catch error during treatment - Flat Panel technology
Interchanged guide tubes	Manual check	- IVD relevant to catch error during treatment - Flat Panel technology - EM tracking (if link to the afterloader drive wire)
Recording of dose	General QA related to dose calculation in the TPS	- IVD only direct mean to measure the real delivered dose - Flat Panel (dose engine needed, not direct)

Beaulieu et al. Chapter 9 Emerging Brachytherapy Technology

Emerging Technologies in Brachytherapy

William Y. Song, Kari Tanderup, Bradley Pieters

Hardback
\$199.95

February 26, 2017 **Forthcoming** by CRC Press
Reference - 304 Pages - 30 Color & 170 B/W Illustrations
ISBN 9781498736527 - CAT# K26490
Series: Series in Medical Physics and Biomedical Engineering

Conclusion

- IVD has a role in brachytherapy
 - Remains the only way to measure the delivered dose to OARs and target.
- Execution in a clinical setting requires a high level expertise and background preparation
 - It is more difficult than measuring S_k
- Commercial implementation of appropriate tools needed
 - Tracking
 - Better software (Intelligent, variable action level)

Vienna, 29.5.-1.6.2016



**Advanced Brachytherapy
Physics**

Clinical Impact of Uncertainties in Brachytherapy

Nicole Nesvacil
Medical University of Vienna



Disclosure:

Medical University of Vienna receives financial and equipment support for training and research activities from Nucletron, an Elekta Company and Varian Medical

Advanced Brachytherapy Physics, 29.5.-1.6.2016



Terminology

Planning aim dose

- Set of dose and dose/volume constraints for a treatment
 - 4 x 7 Gy to D_{90} to achieve 84 Gy EQD2 to D_{90} for CTV_{HR} in cervix (EBRT+BT)
 - 145 Gy to D_{90} for prostate LDR
 - 8 x 4 Gy to D_{90} for breast APBI

Prescribed dose = reported dose (input dose for dose-response analysis)

- Finally accepted treatment plan (which is assumed to be delivered to an individual patient)

Delivered dose = dose that produces observable effect (input effect for dose response analysis)

- Actually delivered dose to the individual patient

From ICRU 89

Example for fractionated brachytherapy

A center performs 4 fractions with the same treatment plan.

The mean prescribed D_{90} is 7 Gy per fraction.

What is the uncertainty in dose delivery due to target volume and OAR changes compared to the treatment plan?

Raw data

Prescribed D_{90} values in Gy

	Fraction 1	Fraction 2	Fraction 3	Fraction 4
Patient 1	7,0	7,0	7,0	7,0
Patient 2	6,5	6,5	6,5	6,5
Patient 3	7,9	7,9	7,9	7,9
Patient 4	6,7	6,7	6,7	6,7
Patient 5	6,8	6,8	6,8	6,8
Patient 6	8,1	8,1	8,1	8,1
Patient 7	7,5	7,5	7,5	7,5
Patient 8	6,4	6,4	6,4	6,4
Patient 9	6,2	6,2	6,2	6,2
Patient 10	7,0	7,0	7,0	7,0

Raw data

Delivered D_{90} values in Gy

	Fraction 1	Fraction 2	Fraction 3	Fraction 4
Patient 1	7,0	5,4	6,1	6,2
Patient 2	6,5	6,9	7,0	6,5
Patient 3	7,9	7,8	7,7	8,5
Patient 4	6,7	8,3	8,5	10,2
Patient 5	6,8	7,1	5,9	5,5
Patient 6	8,1	8,3	6,5	7,4
Patient 7	7,5	7,1	7,3	6,5
Patient 8	6,4	6,7	6,7	6,0
Patient 9	6,2	4,7	5,8	5,4
Patient 10	7,0	7,9	8,5	10,1

Results - Study 1 – Total physical dose

The mean prescribed D_{90} is

28 Gy (4 x 7 Gy)

The mean delivered D_{90} is

28.3 Gy

This means on average a 1 % deviation.

Results - Study 2 – Difference per fraction

The mean difference of prescribed dose to delivered dose per fraction is

0.1 Gy

This means on average a 1 % deviation.

Results – Study 3 – Difference per fraction

The mean absolute difference of prescribed dose to delivered dose per fraction is

0.7 Gy

This means on average a 10 % deviation.

Results – Study 4 – Difference per fraction

The mean difference of prescribed dose to delivered dose per fraction is

0.1 Gy (1%) systematic uncertainty

One standard deviation

0.9 Gy (13 %) random uncertainty

Results – Study 5 – Difference in total EQD2

The total prescribed dose including 45 Gy EBRT in

EQD2 is

84.2 Gy EQD2

The delivered dose is

84.8 Gy EQD2

Mean difference is 0.6 Gy (< 1%)

Results - Study 6 – Difference in total EQD2

The total prescribed dose including 45 Gy EBRT in

EQD2 is

84.2 Gy EQD2

The delivered dose is

84.8 Gy EQD2

Mean difference is 0.6 Gy (< 1%)

One standard deviation is 3.5 %

BRAPHYQS





Radiotherapy and Oncology

Volume 110, Issue 1, January 2014, Pages 199–212



Guidelines

Review of clinical brachytherapy uncertainties: Analysis guidelines of GEC-ESTRO and the AAPM ☆

Christian Kirisits^a,  , Mark J. Rivard^b, Dimos Baltas^c, Facundo Ballester^d, Marisol De Brabandere^e, Rob van der Laarse^f, Yury Niatsetski^g, Panagiotis Papagiannis^h, Taran Paulsen Hellebust^{i, j}, Jose Perez-Calatayud^k, Kari Tanderup^l, Jack L.M. Venselaar^m, Frank-André Siebertⁿ

 **Show more**

doi:10.1016/j.radonc.2013.11.002

[Get rights and content](#)

Open Access funded by Austrian Science Fund (FWF)

Need for common terminology

Errors

- Mainly resulting in systematic deviations
 - Wrong source strength in afterloader unit
 - Wrong offset for applicator tip to first dwell position
 - Wrong catheter connections, etc...

Need for common terminology

Uncertainties

- Type A (statistical)
- Type B (everything else)

Analyze and present systematic effects
(target volume shrinkage, edema causing applicator shifts)

Analyze and present normal distributed effects
(random catheter shifts, reconstruction with finite slice thickness)

Need for common terminology

Variations

- Known effects which can be predicted.
 - E.g. bladder filling can have an impact on dose to bladder or bowel
 - Prostate swelling influences the D_{90} – if the variations over time are known the delivered dose can be predicted

Examples

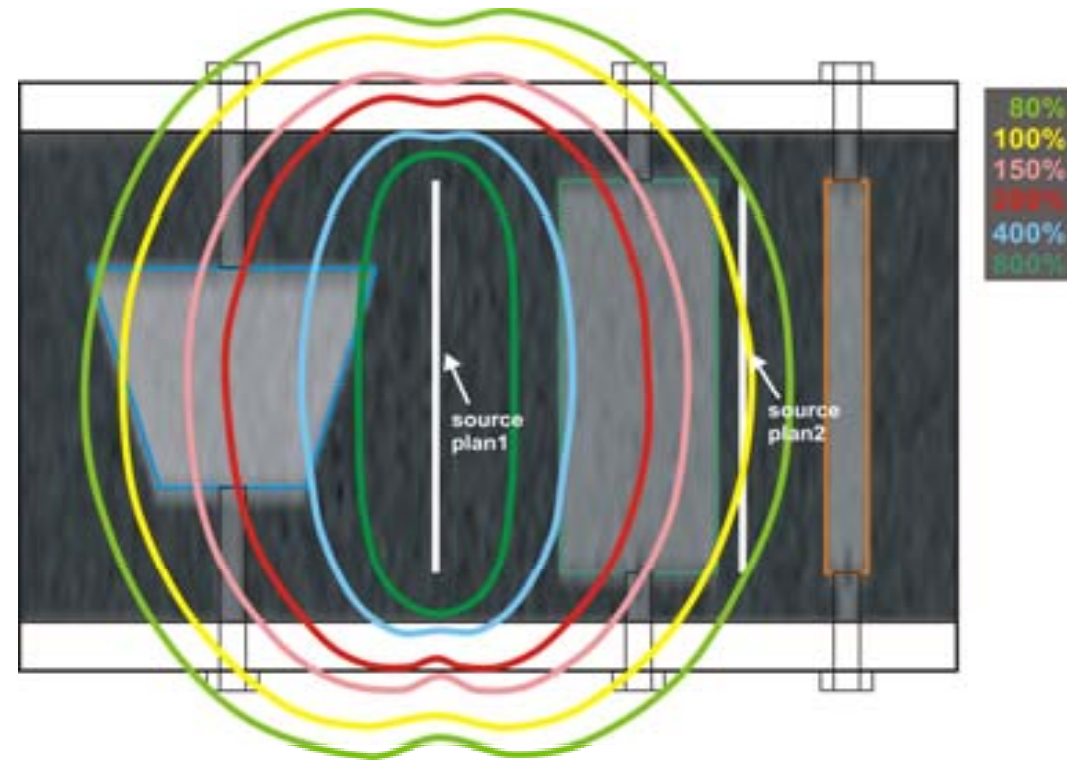


Deviations of DVH parameters

Inter-TPS variation

Large Cylinder Cone

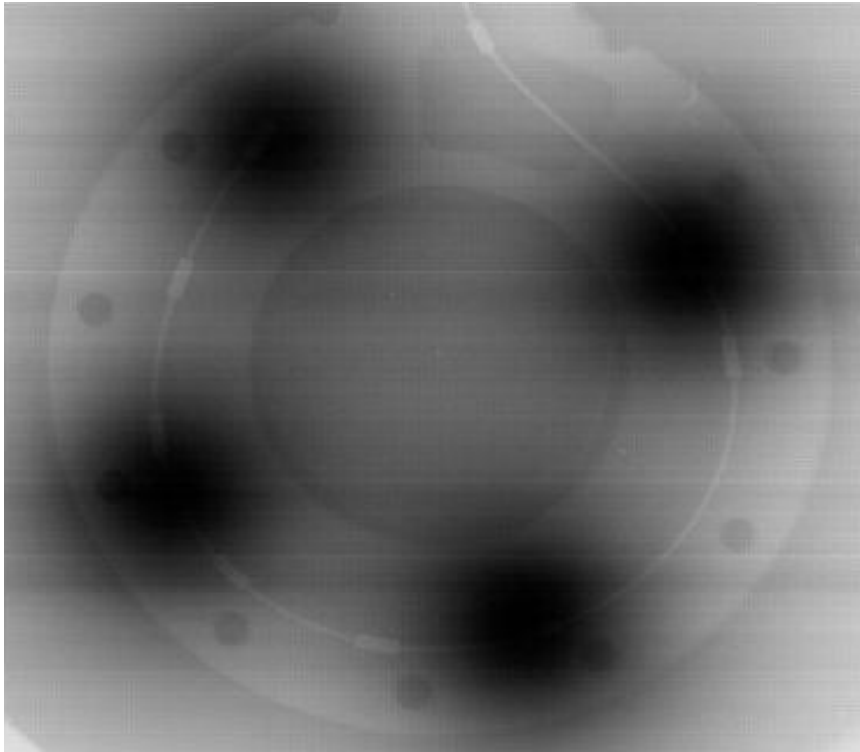
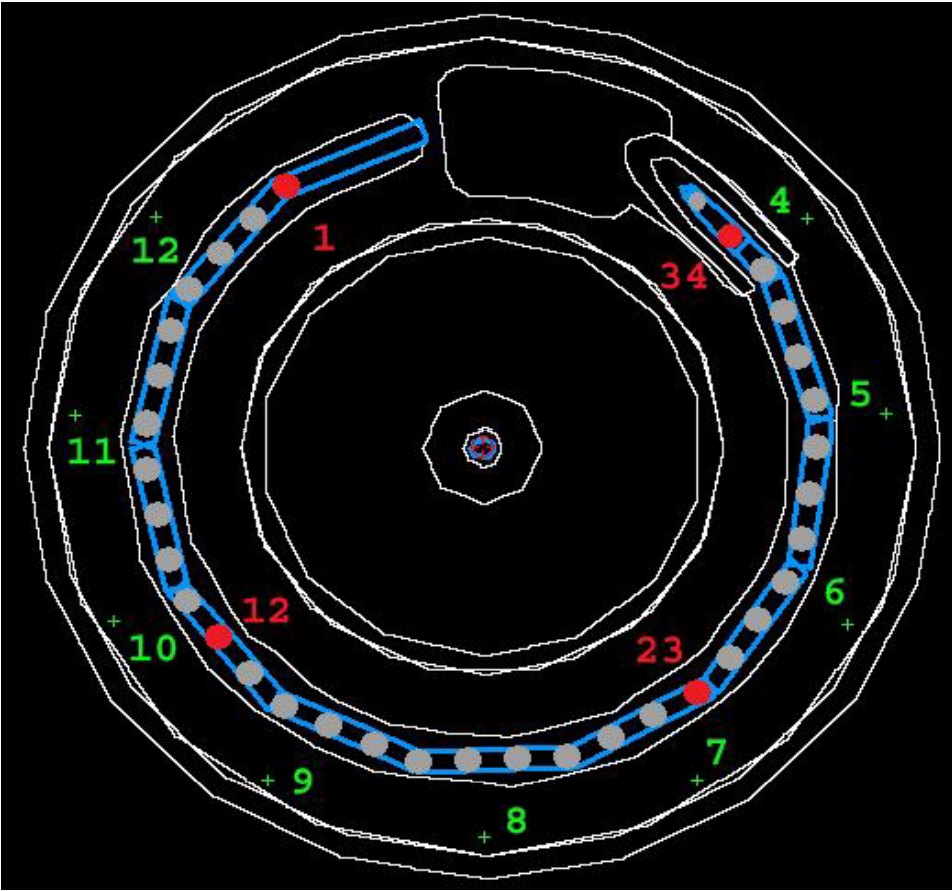
$D_{0.1cc}$ 1 SD	3%	3%
D_{2cc} 1 SD	1%	5%



ESTRO BRAPHYQS DVH subgroup

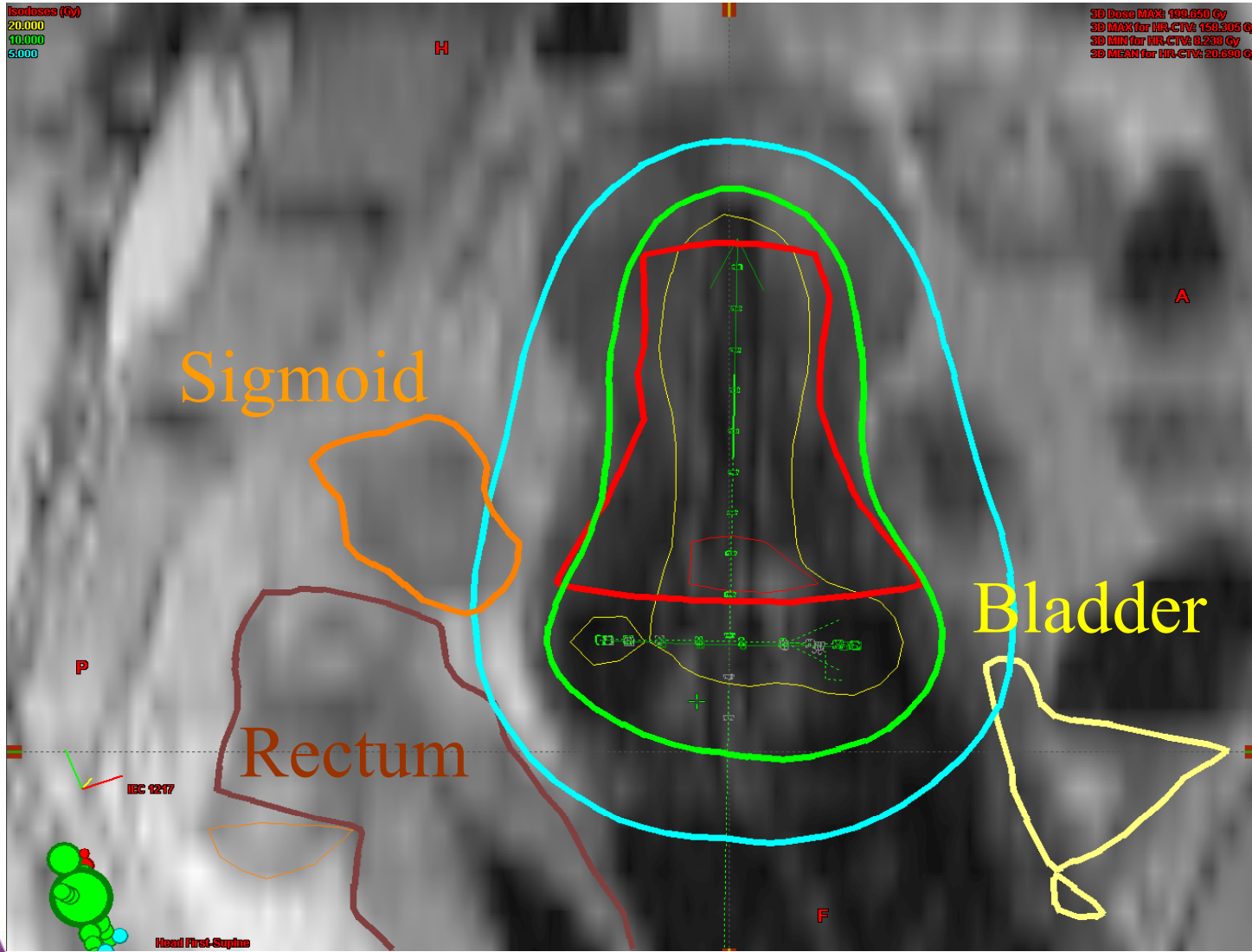
Kirisits et al. R&O 2007

Autoradiography



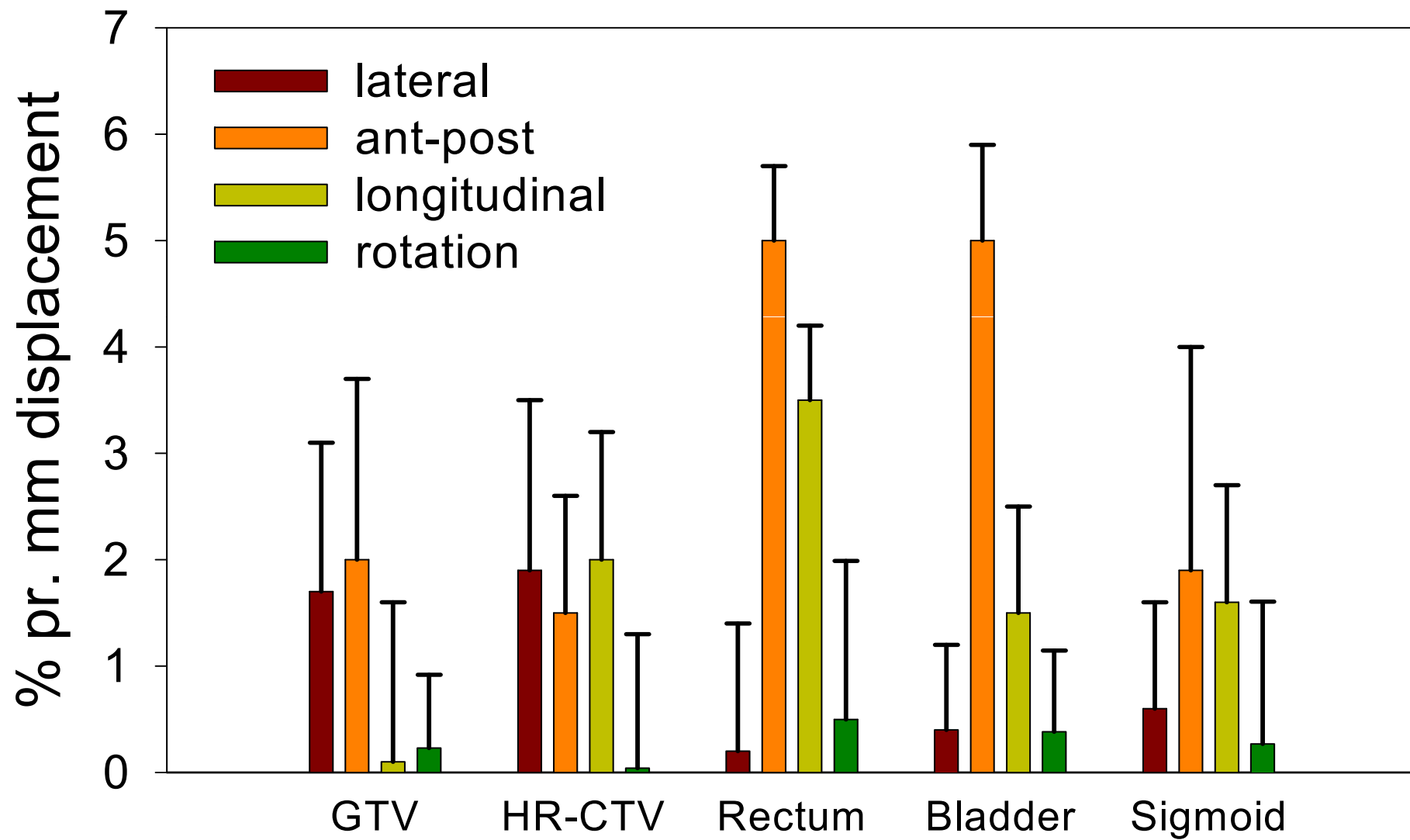
DVH parameter	± 2.5 mm	± 5.0 mm
CTV D ₉₀	$\pm 2\%$	-4% to +3%
CTV D ₁₀₀	-3% to +2%	-7% to +3%
GTV D ₉₀	$\pm 2\%$	-5% to +4%
GTV D ₁₀₀	$\pm 4\%$	-8% to +6%
Bladder D _{2cm³}	$\pm 3\%$	-5% to +7%
Rectum D _{2cm³}	$\pm 5\%$	-8% to +11%
Sigmoid D _{2cm³}	-3% to +2%	$\pm 4\%$

Stability of DVH



↑
Uncertainty of
cranio-caudal
applicator
positioning
↓

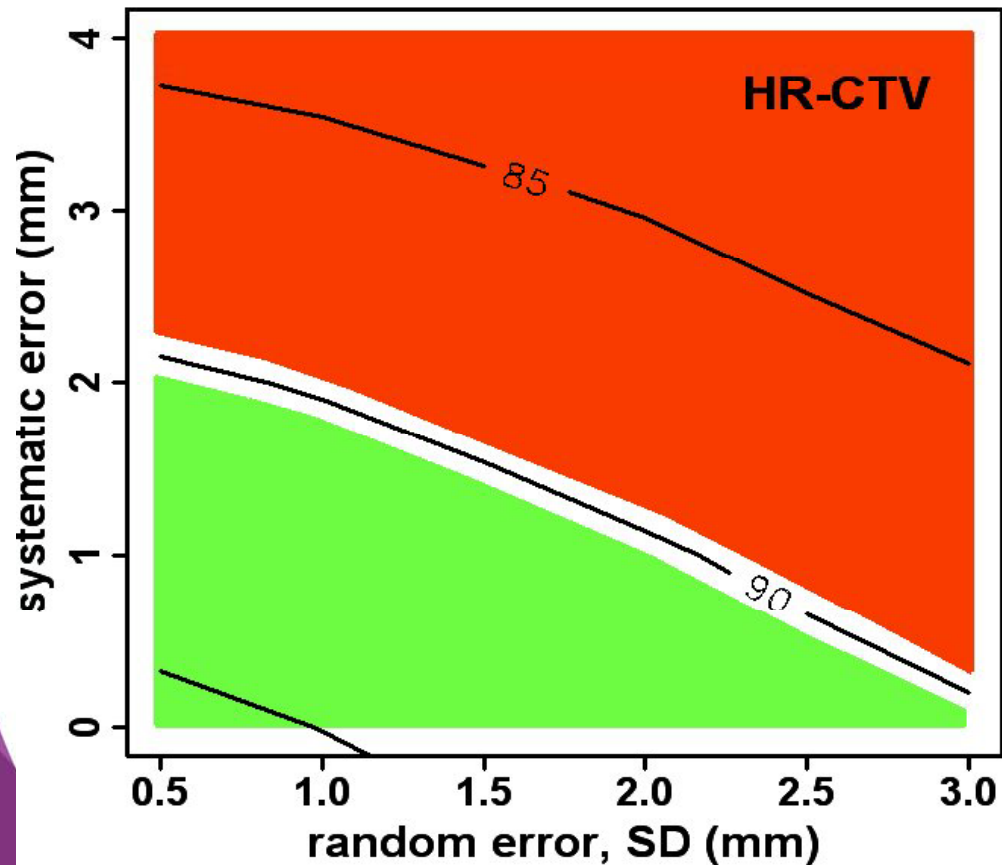
Mean DVH shifts (%)



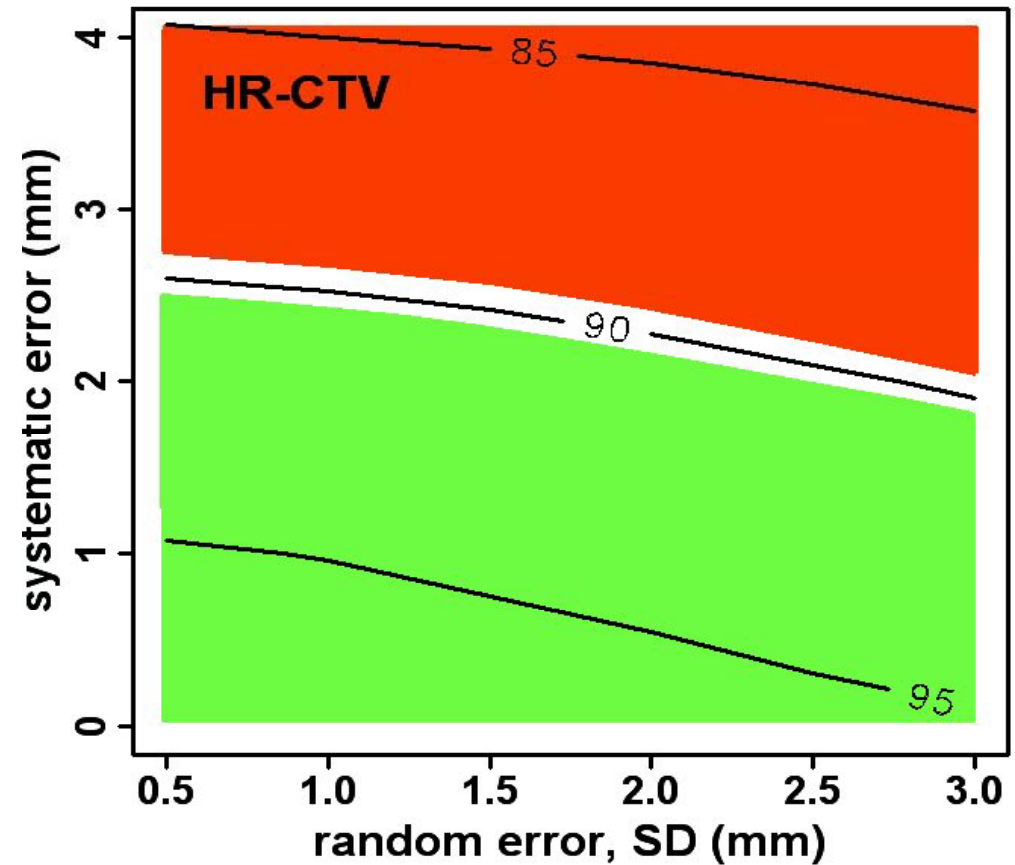
Delivered dose relative to TPS value for 90% of the patients

Reconstruction errors in longitudinal direction

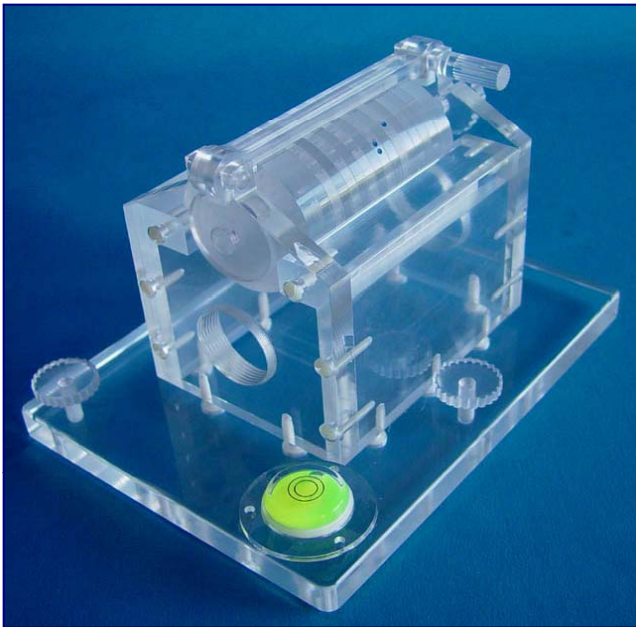
1 fraction



4 fractions



Accuracy of source localisation



CT phantom (solid)

Siebert et al. R&O 2007

- ◆ reconstruction uncertainty (1 SD)
 - < **1.4 mm** for 4-5 mm scans
 - < **1.0 mm** for 2-3 mm scans



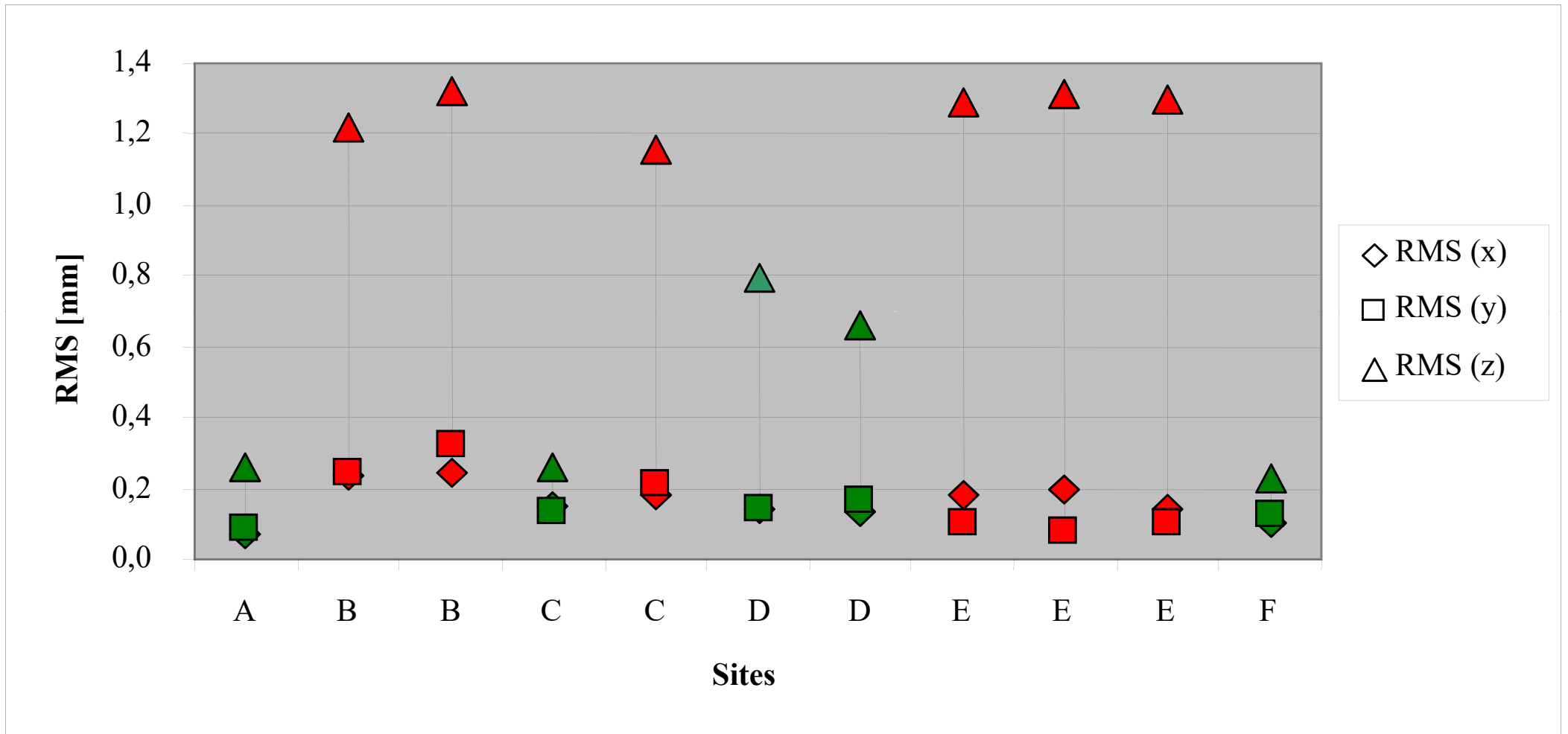
MRI / CT phantom (agarose gel)

De Brabandere et al. R&O 2006

- ◆ uncertainties for MRI slightly larger than for CT
- ◆ reconstruction uncertainty
 - < **2 mm** for 3-5 mm scans

See also *DeBrabandere et al. Brachyther 2013*

Results CT – multicenter study



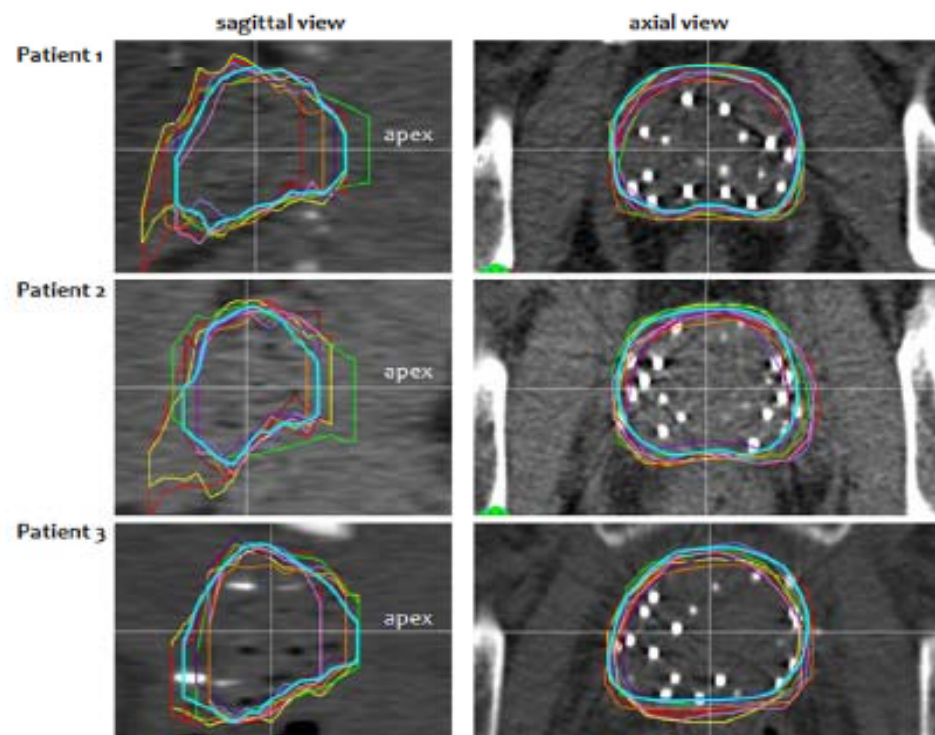
Slice thickness or Index: 4 / 5 mm

Slice thickness or Index: 2 / 3 mm

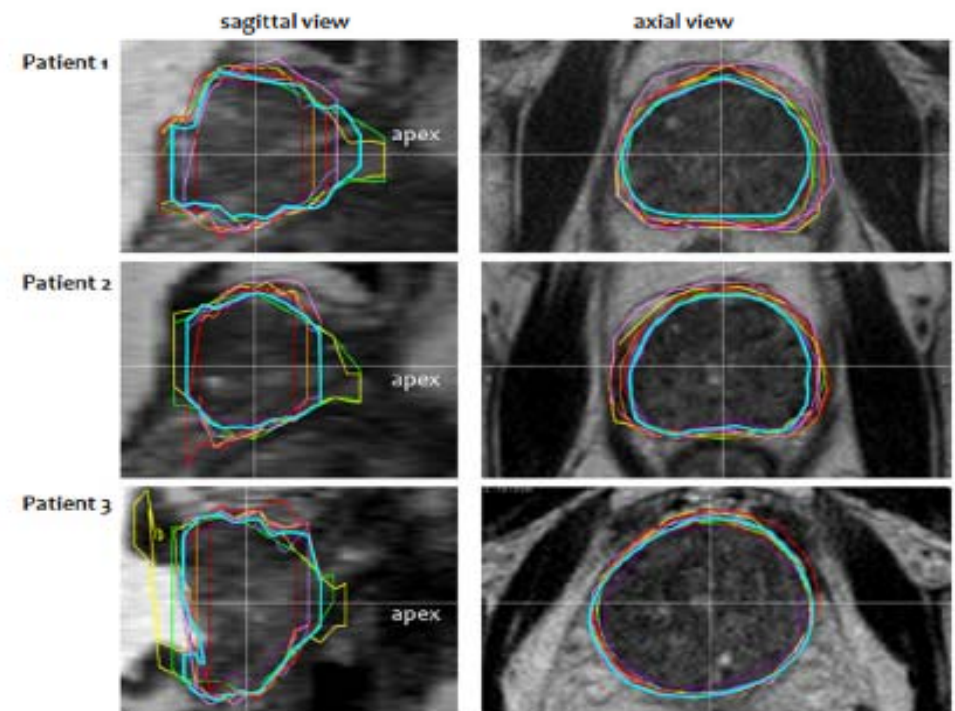
Interobserver variability study

De Brabandere et al, R&O 2012

(a) CT based contouring



(b) T2 based contouring





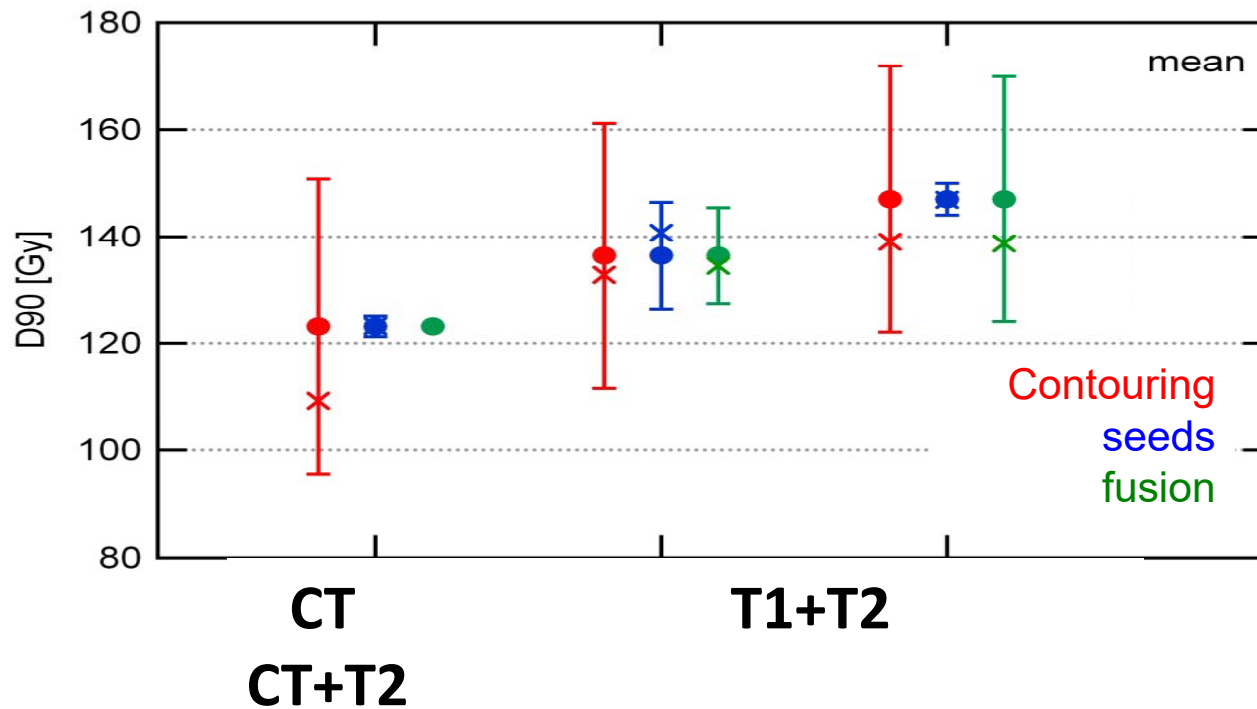
Prostate brachytherapy

Prostate post-implant dosimetry: Interobserver variability in seed localisation, contouring and fusion

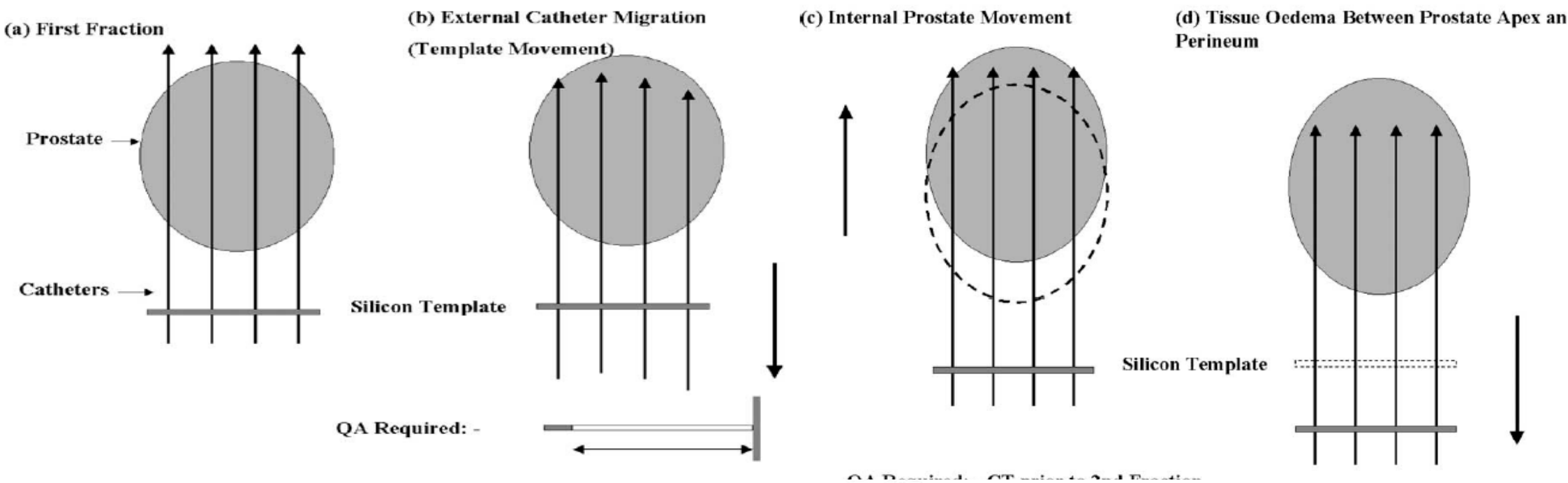
Marisol De Brabandere^{a,*}, Peter Hoskin^b, Karin Haustermans^a, Frank Van den Heuvel^a, Frank-André Siebert^c

^aUniversity Hospital Gasthuisberg, Leuven, Belgium; ^bMount Vernon Cancer Centre, Middlesex, UK; ^cUniversity Hospital of Schleswig-Holstein, Kiel, Germany

Mean 3 patients

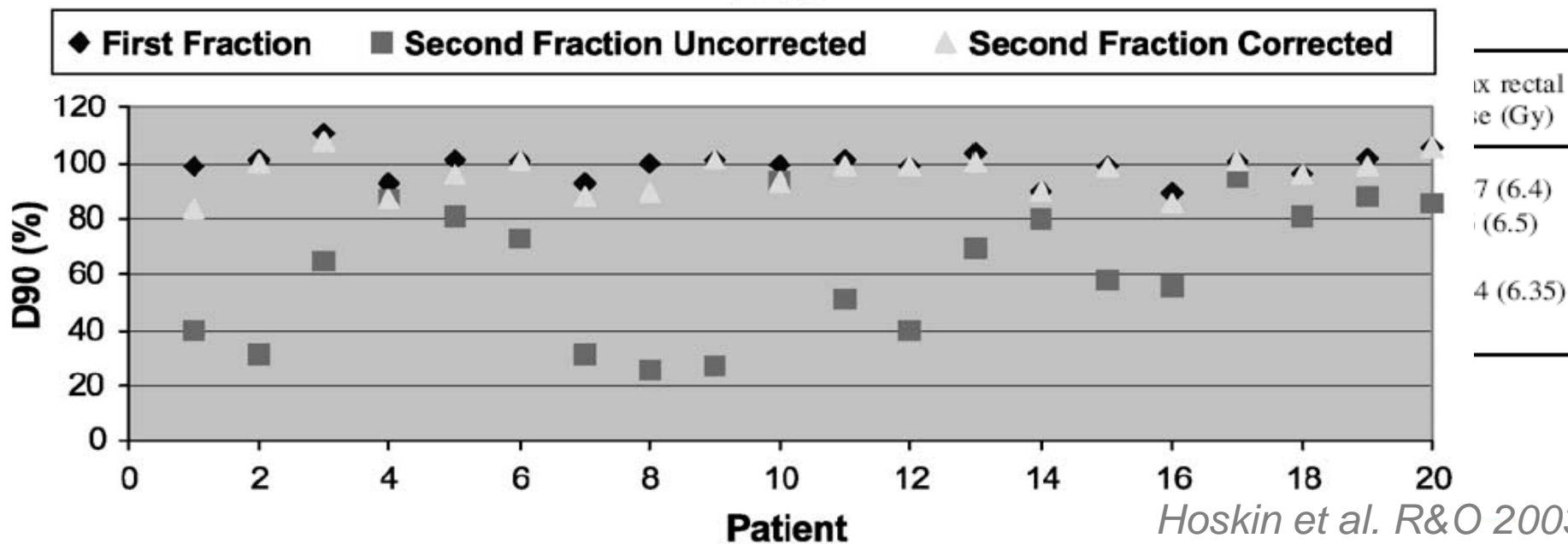


HDR afterloading BT for prostate cancer: catheter and gland movement between fractions



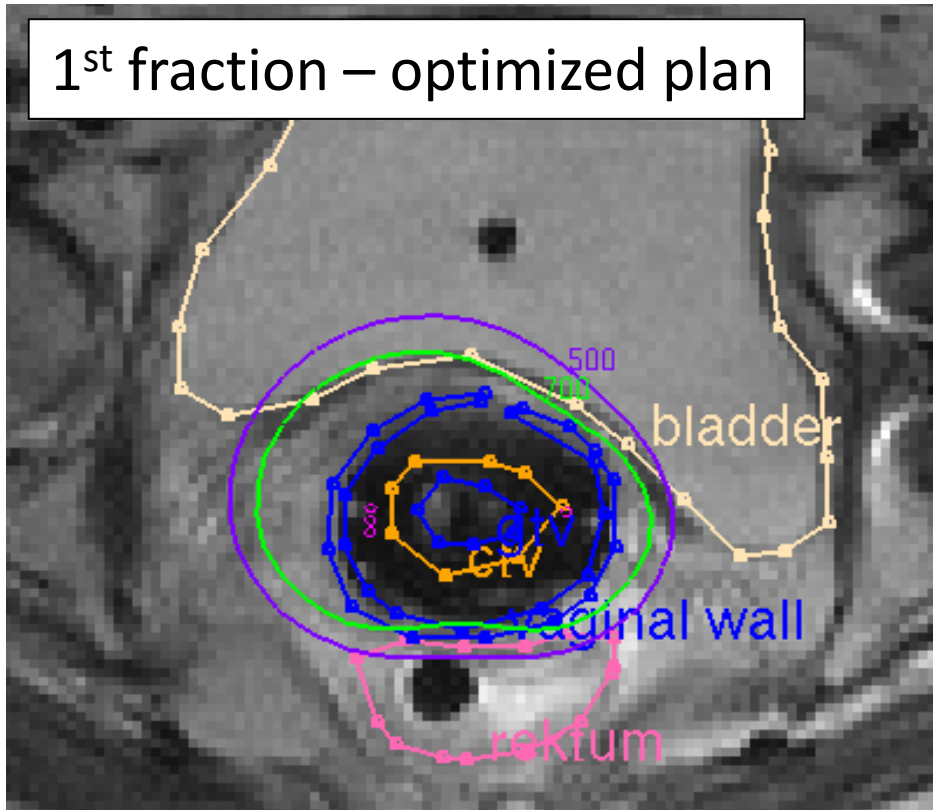
Mean (median) value

First fraction
Second fraction no
corrective action
Second fraction after
corrective action

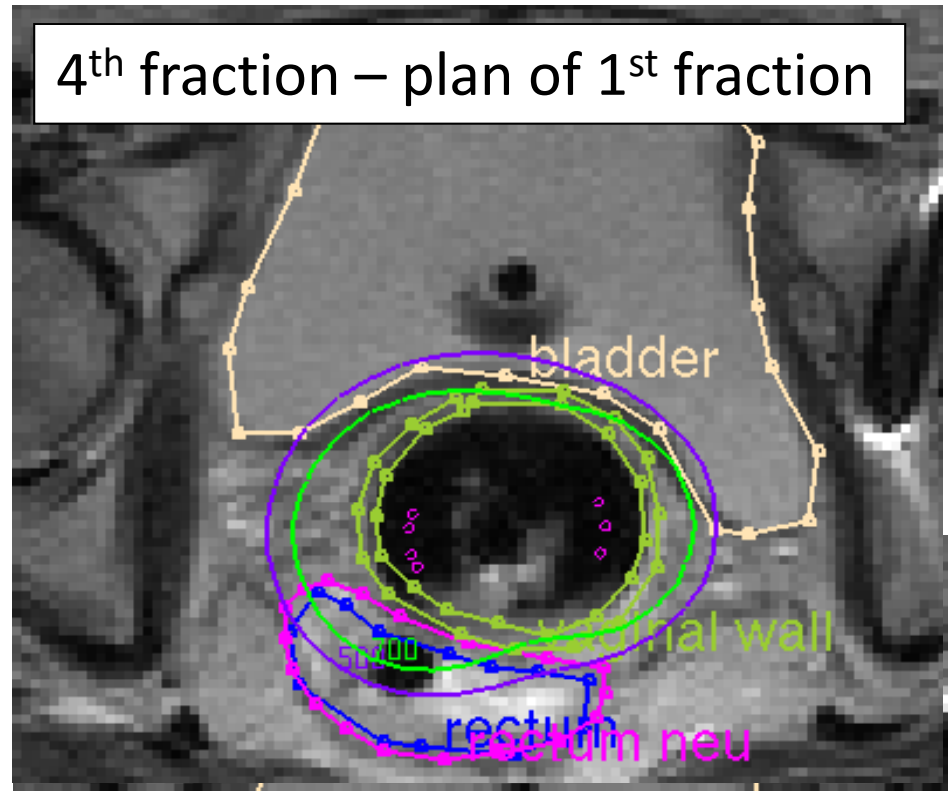


Interapplication variation

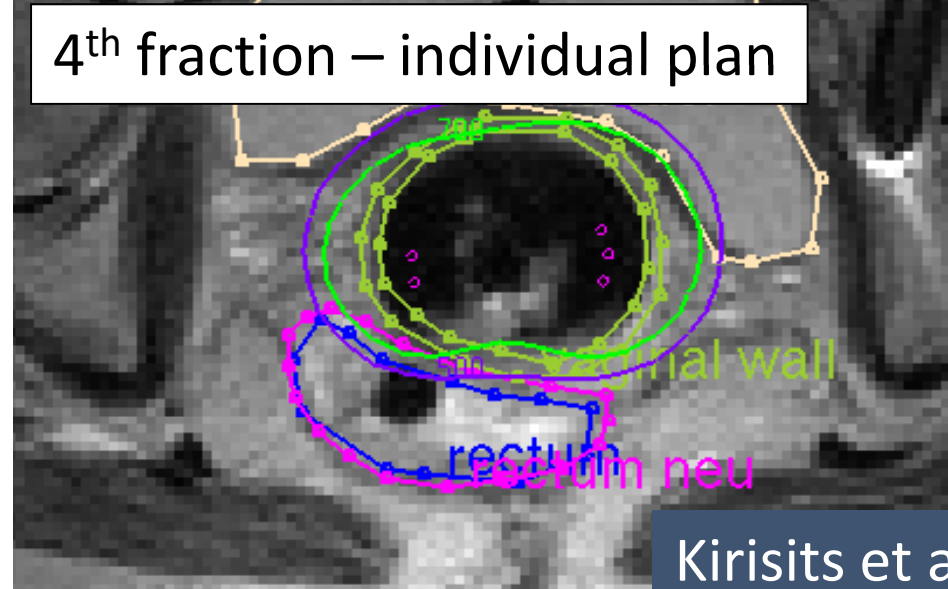
1st fraction – optimized plan



4th fraction – plan of 1st fraction



4th fraction – individual plan



Rectum	D_{2cc} [Gy]	ICRU [Gy]
1 st fraction	4.7	3.3
4 th fraction		
plan of 1 st frac.	8.3	6.5
individual plan	4.9	3.6

Application variation in fractionated HDR GYN BT

(Kirisits et al. 2006)

Mean differences between single plan for all implantations to individual plan for each implantation

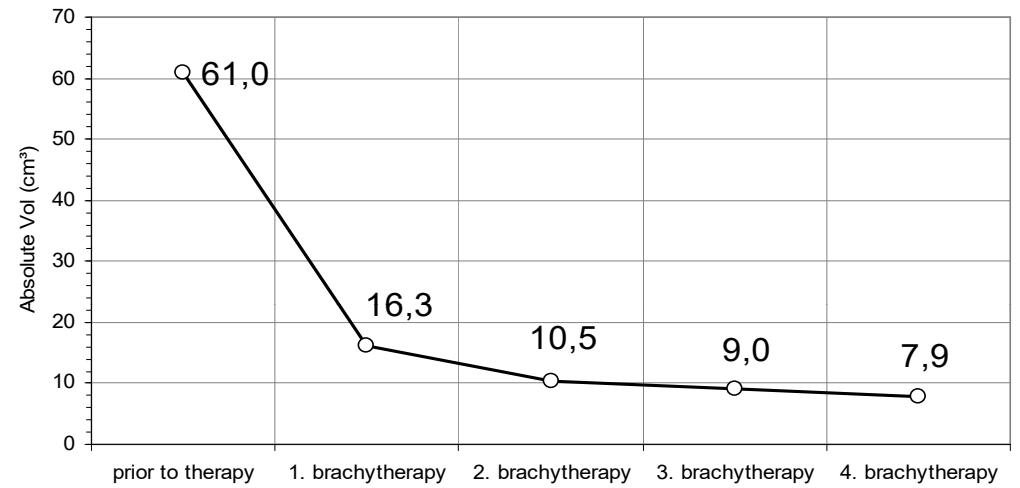
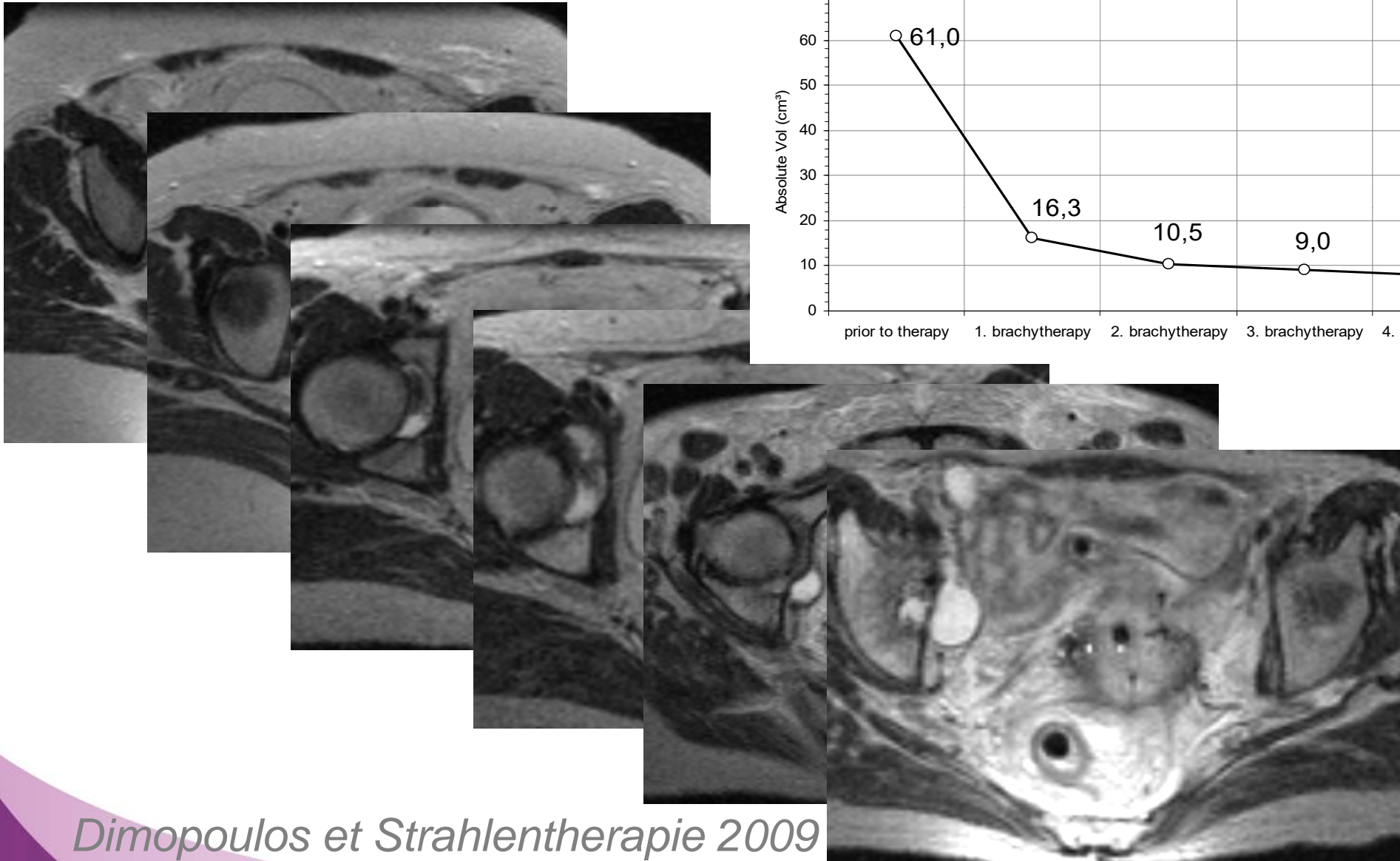
5.9 Gy for D_{90} CTV_{HR}

(14 % for BT dose only, 7 % including EBRT)

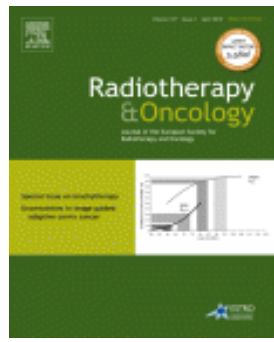
Much higher compared to interfraction study:

BT applied already during EBRT! (shrinkage)

MRI: Initial tumour extension (3D RT) pattern of response (4D RT) for adaptive MRI based planning



Expected interfraction variations for cervix BT



2013, R&O 107

Target

should remain fixed relative to applicator

Rectum:

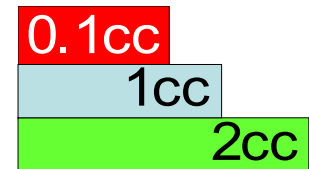
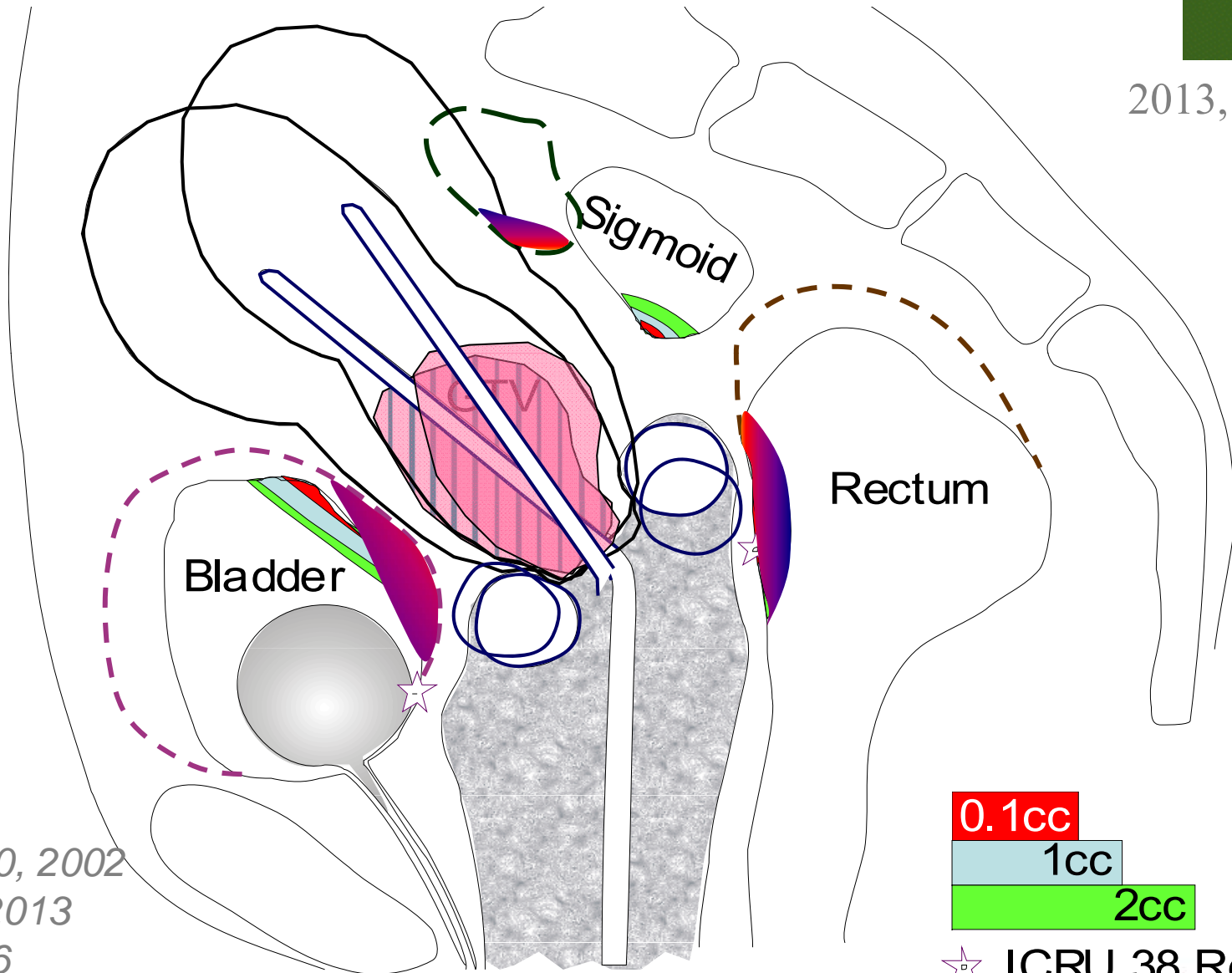
may slightly change in location and fill with gas

Bladder:

use of bladder filling protocols

Sigmoid:

might change its location



☆ ICRU 38 Ref. Points
ESTRO
School

Hellebust et al. R&O 60, 2002

Lang et al. R&O 107, 2013

Kirisits et al. R&O 2006

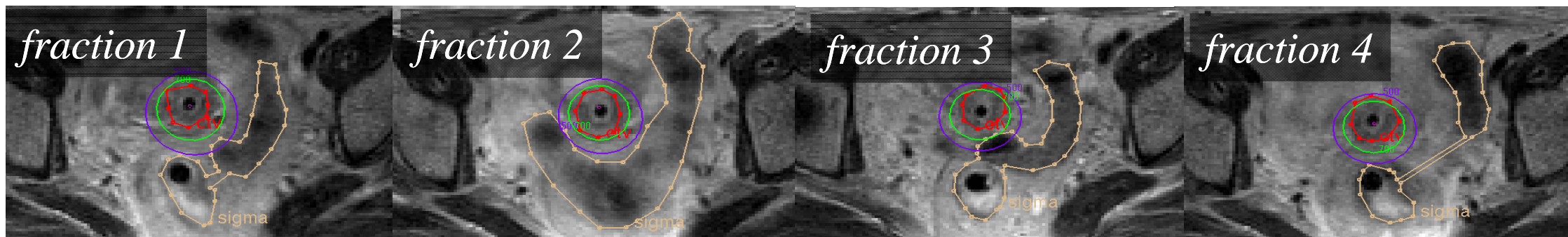
Nesvacil et al. R&O 107, 2013

Tanderup et al. R&O 107, 2013 (and references therein)

Inter-/intrafraction variation in cervix cancer BT







1 plan evaluated for images at different time points.

Anatomical changes between irradiations may lead to large random dosimetric uncertainties



© Lang et al. 2013, Radiother Oncol 107



#	patients	treatment	fractions	time range	Image type	images	variation
1	21	HDR	4	18-20 hrs	MRI	84	Intra-app. 
2	21	HDR	3	5 hrs	MRI	72	Intra-app. 
3	9	PDR	2 x 29 / 32	22 hrs	MRI	36	Intra-app. 
4	14	HDR	5	1-22 days	CT	69	Inter-app. 
5	27	HDR	4	7-10 days	MRI	54	Inter-app. 
6	31	PDR	2 x 20	1 week	MRI	62	Inter-app. 

123 patients

5 h – 3 weeks

377

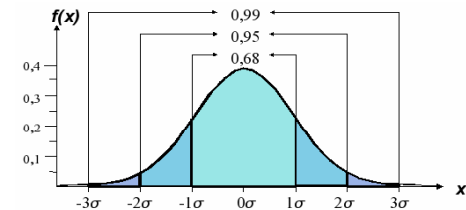
3 + 3

Multicenter Center study of inter-/intrafraction variations for target and OARs in cervix BT

	$\Delta D_{2\text{cm}^3}$ between 2 acquisitions [%] (fixed plan, variable anatomy)									ΔD_{90} [%] (fixed plan, variable anatomy)		
	bladder			rectum			sigmoid/bowel			CTV _{HR}		
	Mean	median	SD	mean	median	SD	mean	median	SD	mean	median	SD
total	2.7	1.5	20.3%	4.5	4.1	22.0%	1.6	-0.9	26.8%	-1.1	-1.7	13.1%
Intraapplication	1.3	1.5	17.7	3.8	2.3	20.5	-2.3	-3.7	23.5	-2.5	-4.3	10.8
interapplication	3.9	0.0	22.3	5.8	5.2	23.2	6.8	3.7	30.2	0.4	-0.8	15.1

Random uncertainties (1SD) of physical dose per BT fraction can be

- ~ 10% for CTV_{HR} D₉₀
(contouring uncertainty (*Petric, Hellebust R&O 2013*))
- ~ 20% for bladder, rectum D_{2cm³}
- ~ 30% for sigmoid D_{2cm³}



No correlation with time between images was detected!

Conclusion: As long as there is no direct imaging and dose reporting at the time of irradiation (online imaging, verification), we have to expect 20-30% dosimetric uncertainty for D_{2cm³} for OARs for each fraction, between prescribed and delivered dose.

Example for HDR intracavitary Cervix brachytherapy – per fraction

<u>Category</u>	<u>Optimum level</u>	<u>Assumptions</u>
Source strength	2%	PSDL traceable calibrations
Treatment planning	3%	Reference data with the appropriate bin width is used
Medium dosimetric corrections	1%	Applicator without shielding and CTV inside pelvis (concerning for scatter)
Dose delivery including registration of applicator geometry to anatomy	4%	Accurate QA concept for commissioning and constancy checks, especially for source positioning and applicator/source path geometry, appropriate imaging techniques, applicator libraries
Interfraction/Intrafraction changes	11%	For one treatment plan per applicator insertion but several subsequent fractions – check for major deviations in subsequent fractions
Total dosimetric uncertainty for one single fraction	12%	

Difference on uncertainty per fraction to uncertainty for total dose

For normal distributions the number of subsequent fractions (observations) results in compensation of variations

$$1 / \sqrt{N}$$

including constant EBRT results in

$$1 / 2$$

So 13% per fraction can be 3.5% for total dose

Example for HDR intracavitary Cervix brachytherapy – total dose 4 fractions

Category	Optimum level	Assumptions
Source strength	2%	PSDL traceable calibrations
Treatment planning	3%	Reference data with the appropriate bin width is used
Medium dosimetric corrections	1%	Applicator without shielding and CTV inside pelvis (concerning for scatter)
Dose delivery including registration of applicator geometry to anatomy	$1 / \sqrt{N}$	Accurate QA concept for commissioning and constancy checks, especially for source positioning and applicator/source path geometry, appropriate imaging techniques, applicator libraries
	4% → 2%	
Interfraction/Intrafraction changes	$1 / \sqrt{N}$	For one treatment plan per applicator insertion but several subsequent fractions –
	11% → 6%	
Total dosimetric uncertainty for entire BT	7%	

Example for LDR prostate brachytherapy

<u>Category</u>	<u>Optimum level</u>	<u>Assumptions</u>
Source strength	3%	PSDL traceable calibrations
Treatment planning	4%	Reference data with the appropriate bin width is used
Medium dosimetric Corrections	5%	A general prostate tissue is considered, but no consideration is given for calcifications (or their composition) in the patient
Inter-seed attenuation	4%	An advanced dose calculation formalism may indicate source models and orientations cause the largest effects
Treatment delivery imaging	2%	US QA performed according to AAPM TG-128
Anatomy changes between dose delivery and post-implant imaging	7%	Post-implant (day 0) imaging using CT, with a scalar correction factor for edema correction
Total dosimetric uncertainty	11%	

Example for US-based HDR prostate brachytherapy

<u>Category</u>	<u>Optimum level</u>	<u>Assumptions</u>
Source strength	2%	PSDL traceable calibrations.
Treatment planning	3%	Reference data with the appropriate bin width.
Medium corrections	1%	Full scatter conditions in the pelvic region and for the prostate location are assumed.
Catheter reconstruction and source positioning accuracy	2%	Assuming usage of dedicated catheter reconstruction tools (0.7 mm) and 1.0 mm source positioning accuracy
US-imaging overall effect	2%	US QA performed according to AAPM TG-128 report.
Changes of catheter geometry	2%	Assuming that new image acquisition and treatment plan calculation before each fraction.
Total dosimetric uncertainty	5%	For treatment delivery without patient movement and changes in the lithotomic set-up and with the US probe at the position of the acquisition

Example for HDR ^{192}Ir BT source for breast balloon applicator

<u>Category</u>	<u>Optimum level</u>	<u>Assumptions</u>
Source strength	2%	PSDL traceable calibrations.
Treatment planning	3%	Reference data with the appropriate bin width.
Medium dosimetric corrections	3%	Balloon filled with standard level of contrast agent, no consideration or composition of chestwall, lung, or breast.
Scatter dosimetric corrections	7%	A non-scalar correction for skin dose is needed, and will require an advanced dose calculation formalism to properly account for radiation scatter conditions in the patient.
Dose delivery including registration of applicator geometry to anatomy	7%	Accurate QA concept for commissioning and constancy checks, especially for source positioning and applicator/ source path geometry, appropriate imaging techniques (either small slice thickness, 3D sequences or combination of different slice orientations), applicator characterization.

Example for HDR ^{192}Ir BT source for breast balloon applicator

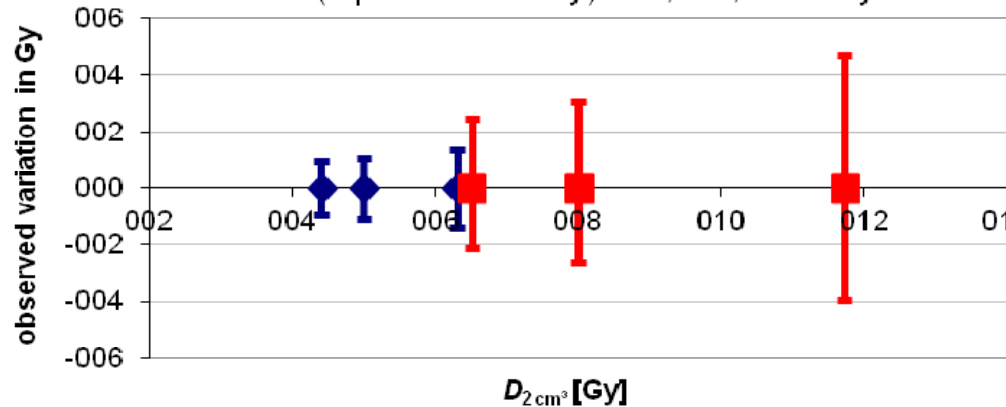
<u>Category</u>	<u>Optimum level</u>	<u>Assumptions</u>
Interfraction/Intrafraction changes between imaging and dose delivery	7%*	For one treatment plan per applicator insertion and measures to detect major variations for subsequent fractions.
Total dosimetric uncertainty	13%	For treatment delivered with the same BT source.

*Estimated value based on expert discussion

Translating random uncertainties to EQD2: single Fx

Example HDR : OAR, variation 22% physical dose

- ◆ physical dose: 4.4, 5.0, 6.3 Gy
- EQD2 (alpha/beta=3 Gy): 6.5, 8.0, 11.7 Gy

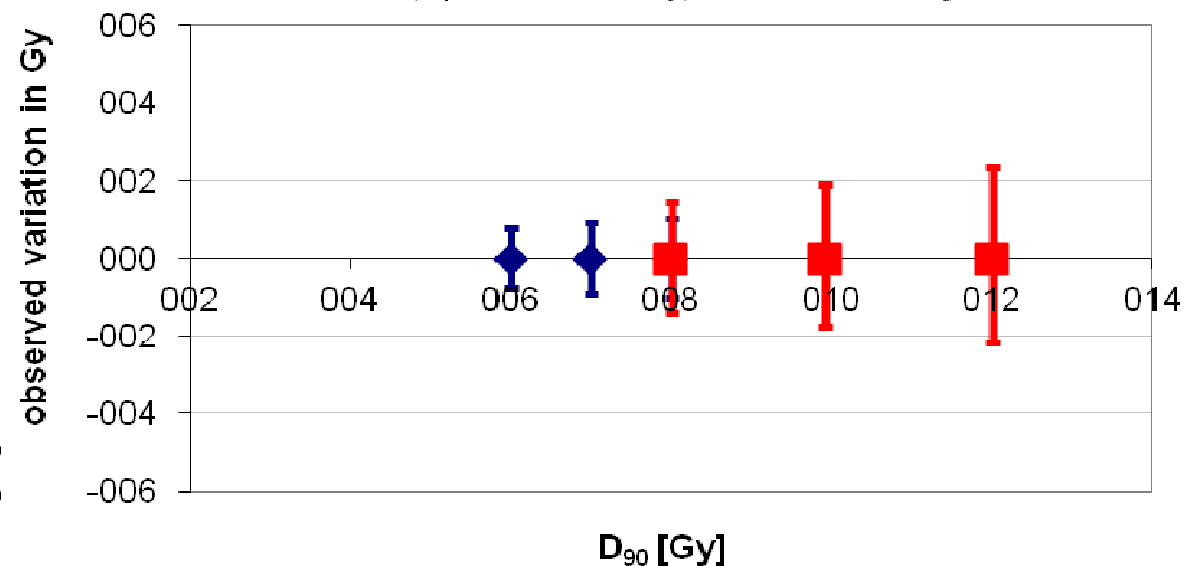


asymmetrical EQD2 error bars

OAR
(SD 22%)

Example HDR : HR CTV, variation 13% physical dose

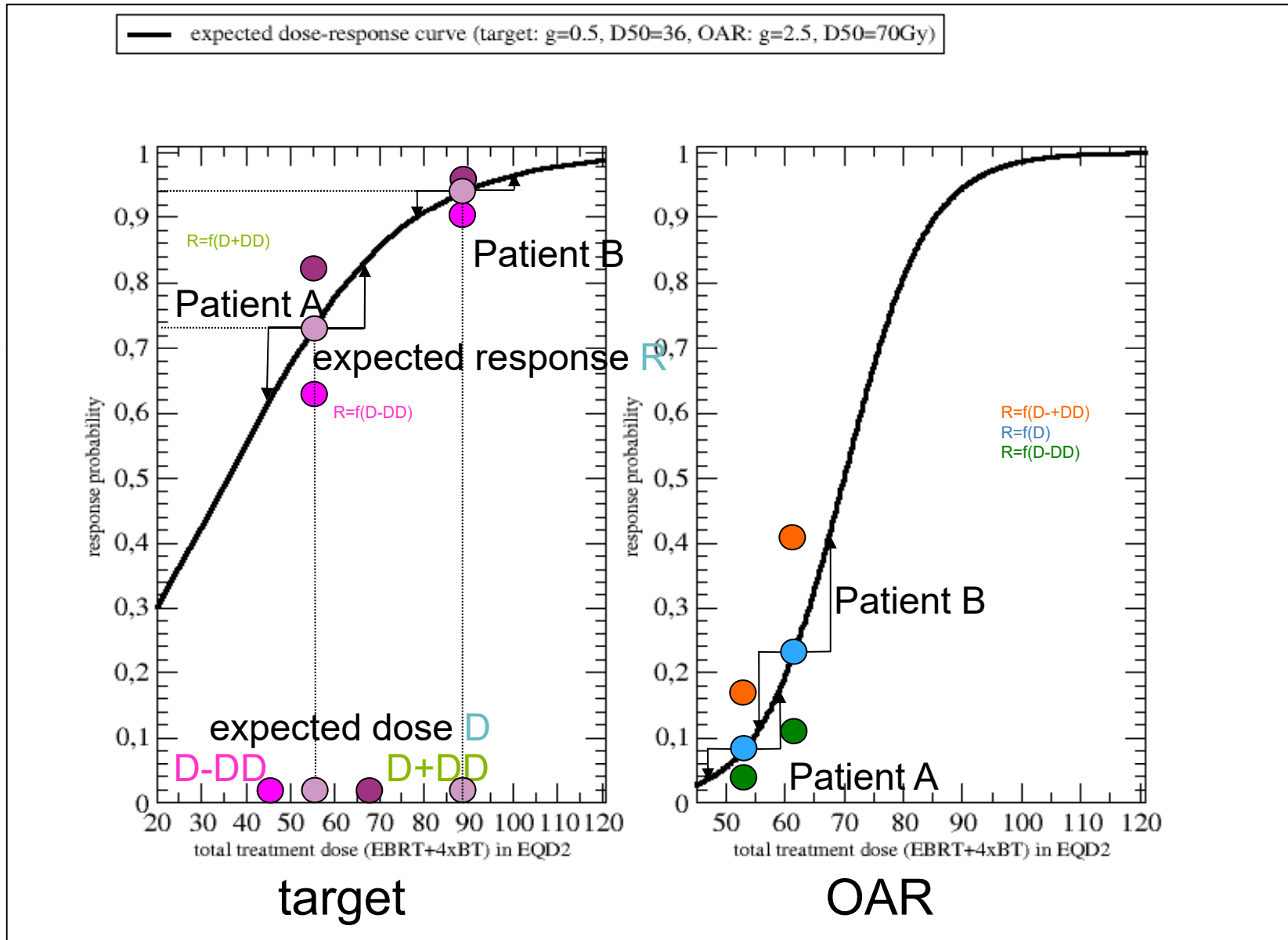
- ◆ physical dose: 6.0, 7.0, 8.0 Gy
- EQD2 (alpha/beta=10 Gy): 8.0, 9.9, 12.0 Gy



CTV_{HR}
(SD 13%)

The effect on the total treatment dose depends on the fractionation scheme!
The PDR uncertainties per pulse are currently unknown because of low time resolution of observations.

Examples for real dose-response curves and effect of random uncertainty for total dose (EQD2)

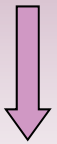


Examples for real dose-response curves and effect of random uncertainty for total dose (EQD2)

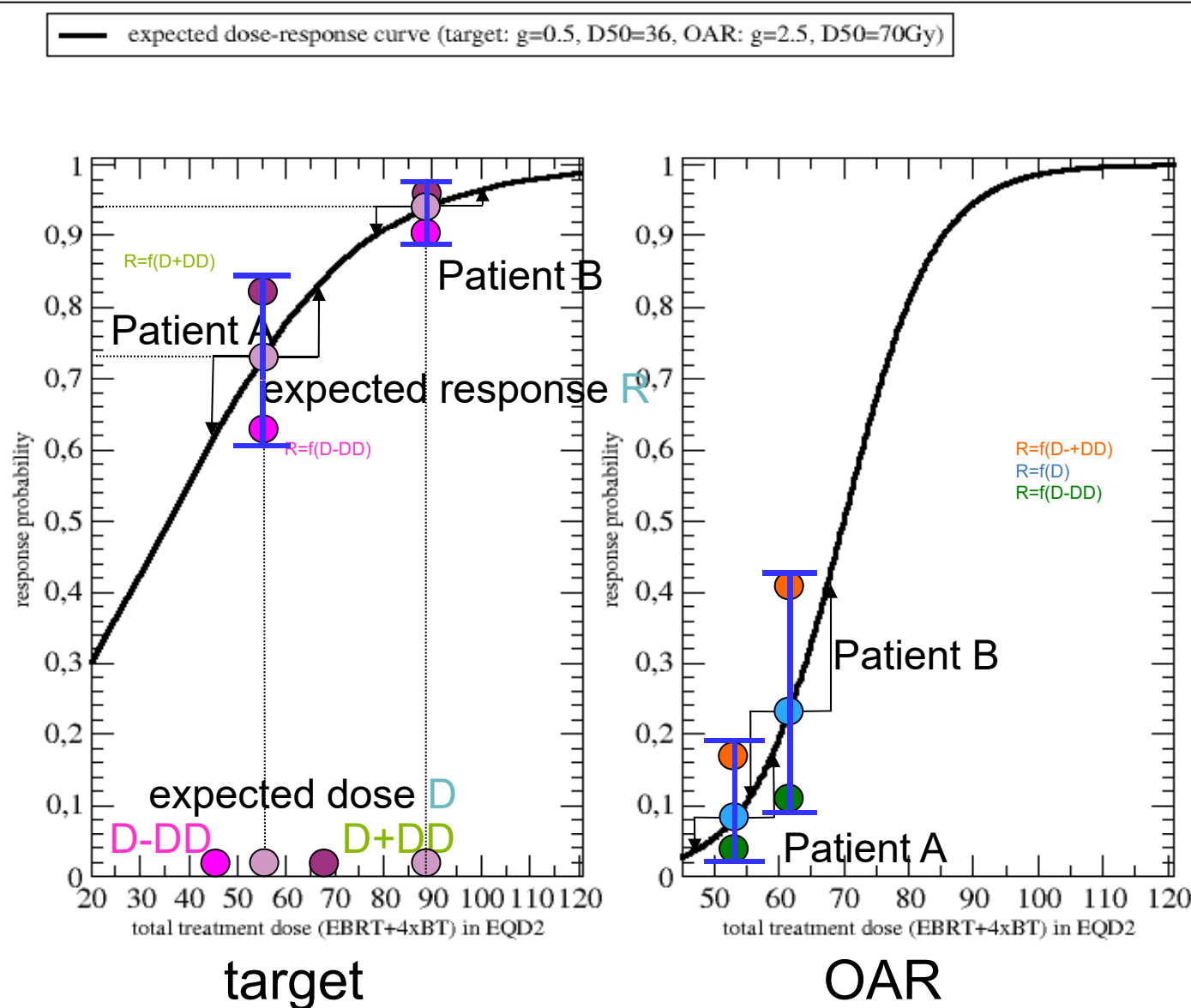
Uncertainties of physical fraction dose



translated to total dose EQD2

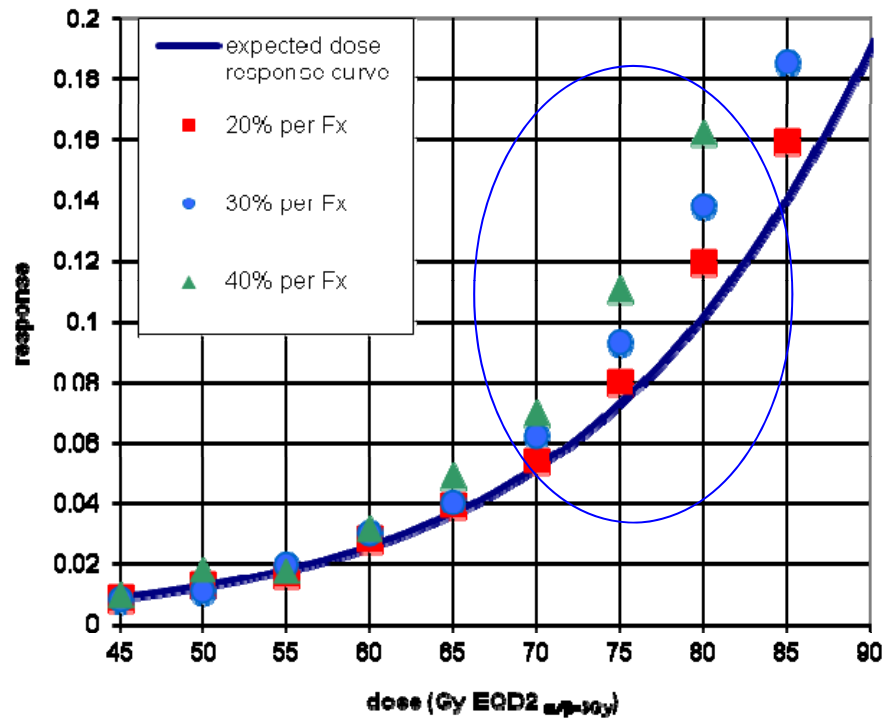


to uncertainty in response probability

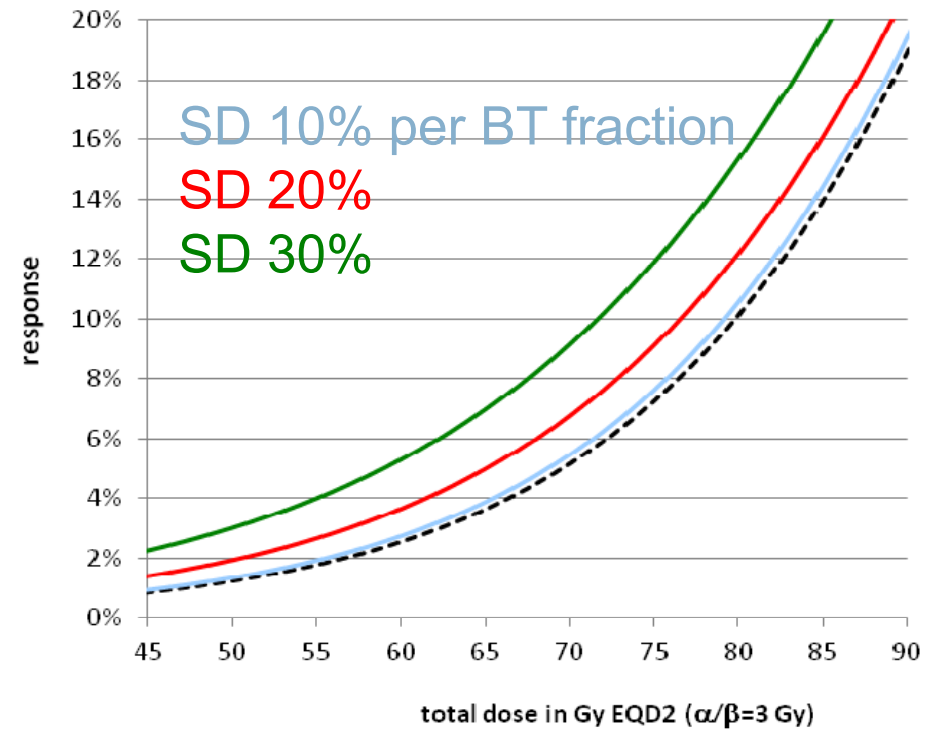


Effect of random dosimetric uncertainty (SD) on mean simulated dose-response data for OAR $D_{2\text{cm}^3}$

Simulated patient data



Calculated dose-response curve for simulated patients (SPSS)

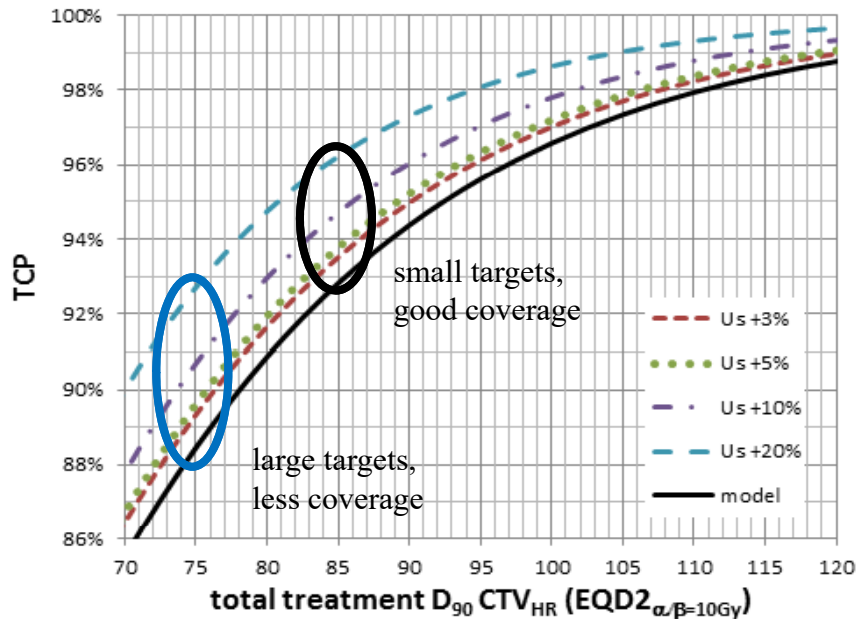


Increasing offset with increasing dose and increasing random dosimetric uncertainty:
2-3 % for SD 20% and 30% around rectum dose constraint level

Systematic dosimetric uncertainties

Systematic inter-/intra fraction variations for MRI-based cervix BT (Nesvacil et al. 2013, R&O 107):

e.g. $\Delta D_{90} < +3\%/fx \Rightarrow$ „observed“ local control @85 Gy 1% higher than model prediction

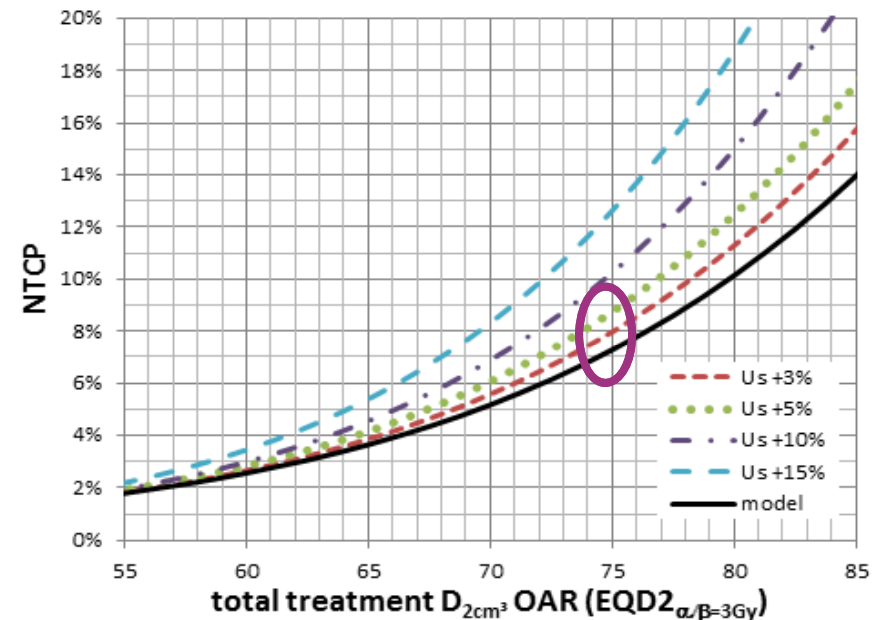


Systematically larger contours on CT vs. MRI \Rightarrow underestimation of D_{90} by CT contours (e.g. Viswanathan et al. 2007, IJROBP 68):

e.g. i) $\Delta D_{90} = +10\%/fx \Rightarrow$ 2% overestimation of local control @ 85 Gy

ii) $\Delta D_{90} = +20\%/fx \Rightarrow$ 3.5% overestimation of local control @ 85 Gy

systematic underestimation of rectum D_{2cm^3} : rectum probe (iv. dosimetry) stays inside - rectum always fills with gas in between image acquisition and treatment $\rightarrow D_{2cm^3}$ is systematically higher for each fraction

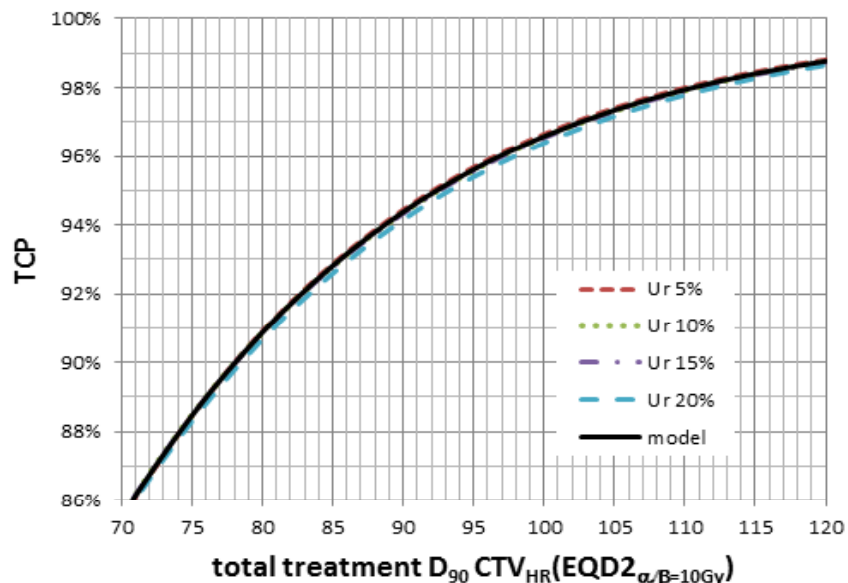


e.g. i) $\Delta D_{2cm^3} = +3\%/fx \Rightarrow$ observed morbidity @75Gy 1% higher than model prediction

ii) $\Delta D_{2cm^3} = +5\%/fx \Rightarrow$ observed morbidity @75 Gy is 2% higher than model prediction

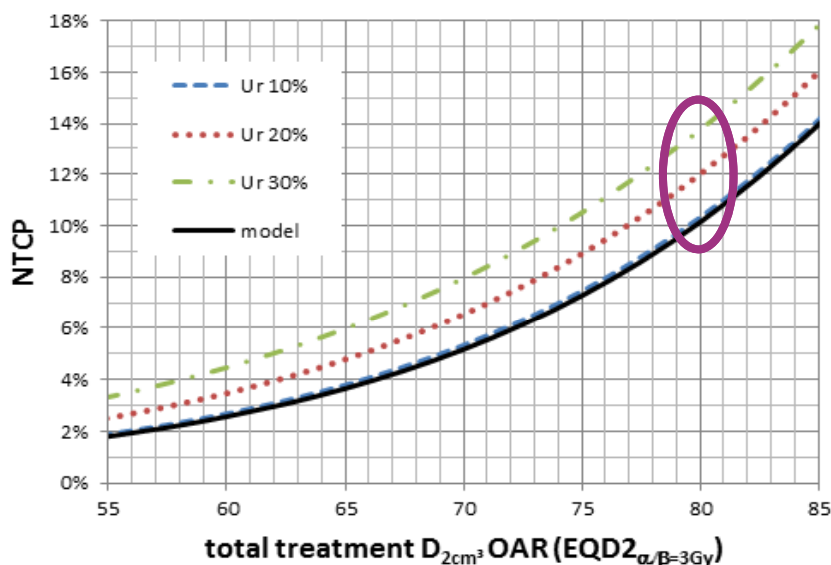
Example: random uncertainties for target OAR

Random variation of target D₉₀,
e.g. random inter-observer variation



For target – differences in TCP < 0.5%

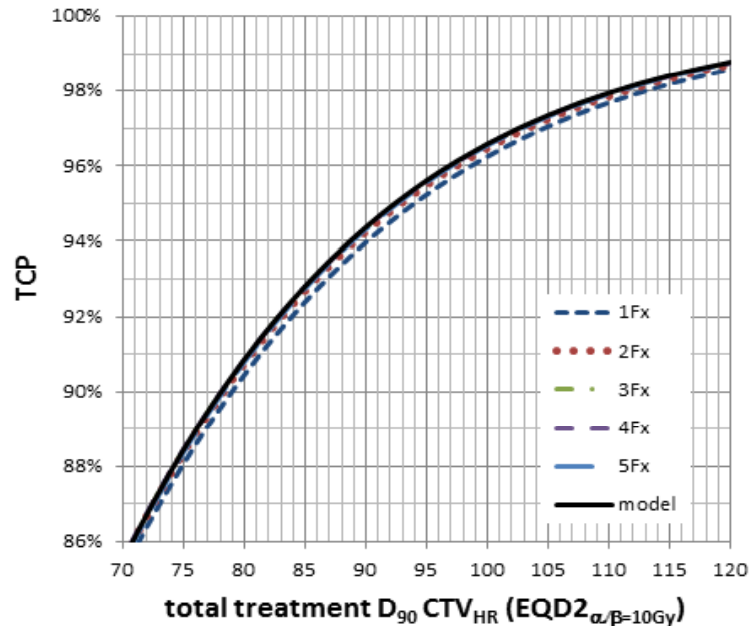
Random variation of rectum D_{2cm³}
e.g. random intra-/inter-fraction variation of
organ position or shape



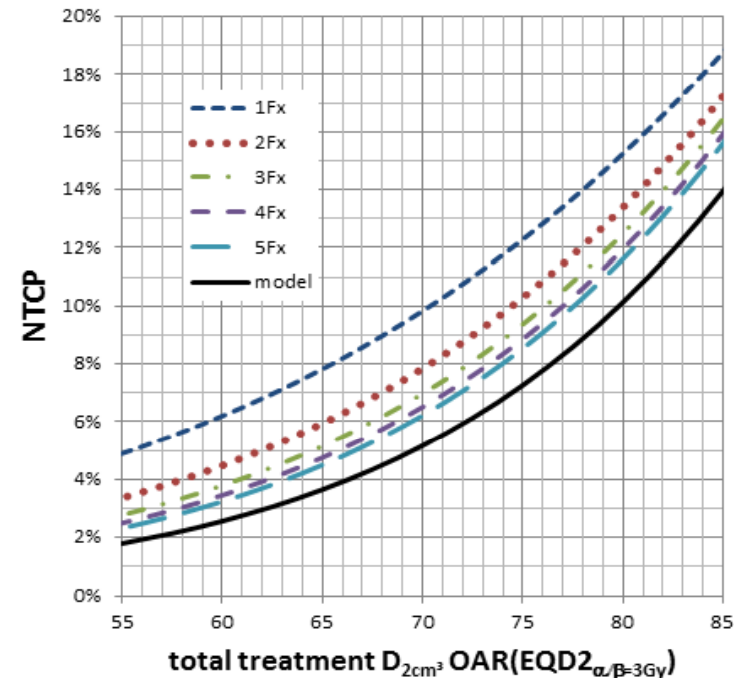
- $\Delta D_{2cm^3} = \pm 10\%/fx$ -> observed morbidity 7.5 %
(vs 7.3% model prediction)
- $\Delta D_{2cm^3} = \pm 20\%/fx$ -> observed morbidity 8.9 %
- $\Delta D_{2cm^3} = \pm 30\%/fx$ -> observed morbidity 10.5 %
- Model prediction: 10.5% NTCP@ 80Gy EQD2

Example: influence of the number of BT Fx

Random uncertainties and dose response for different fractionation schemes



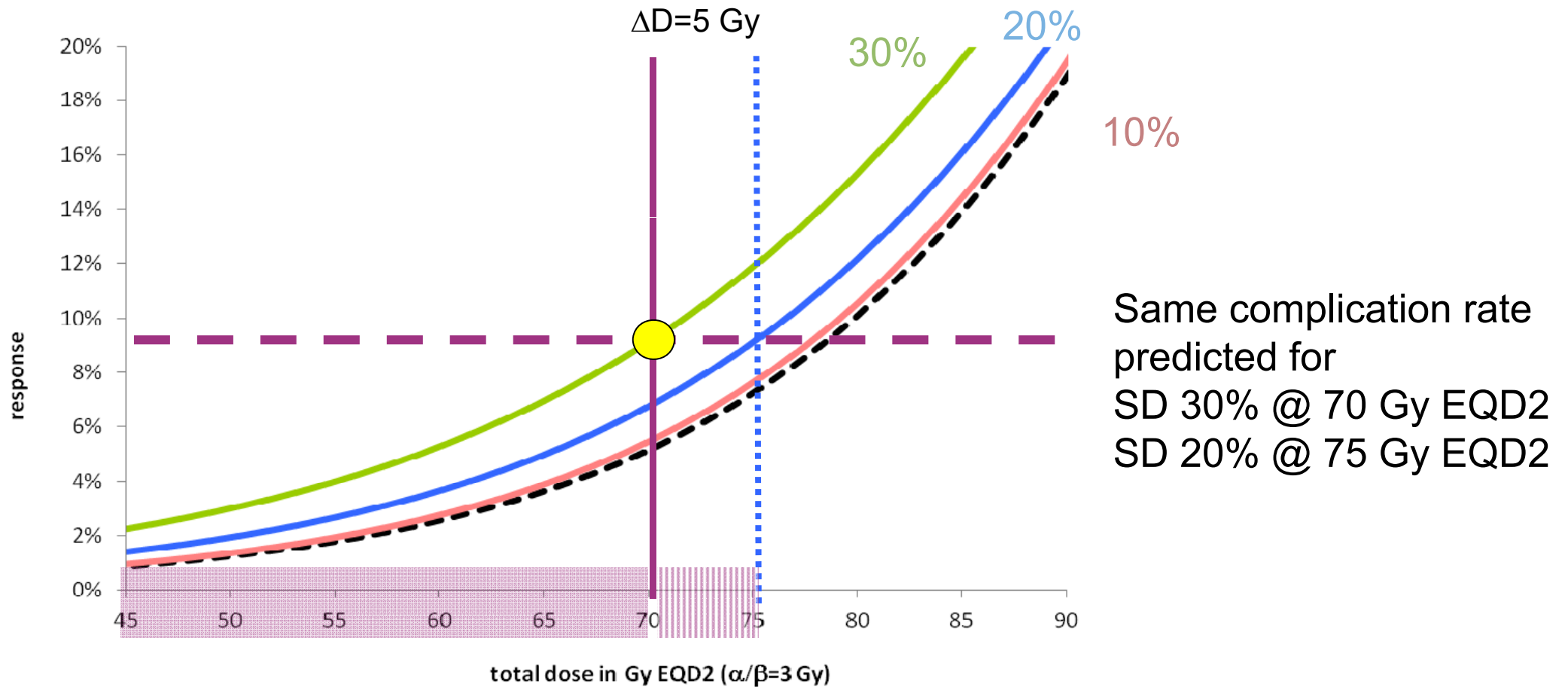
For target: using 1 Fx vs 2-5Fx results in ~0.5% lower tumour control probability than predicted by model



Example: random uncertainty $\Delta D_{2cm^3} = \pm 20\%/fx$:

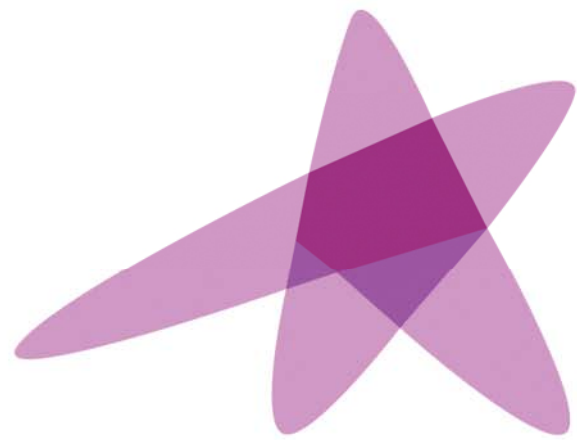
- nFx=5 => observed morbidity @75Gy 8.5%
- nFx=4 => observed morbidity @75Gy 8.9%
- nFx=3 => observed morbidity @75Gy 9.4%
- nFx=2 => observed morbidity @75Gy 10.3%
- nFx=1 => observed morbidity @75Gy 12.3%

Increasing OAR dose constraints by reducing uncertainties



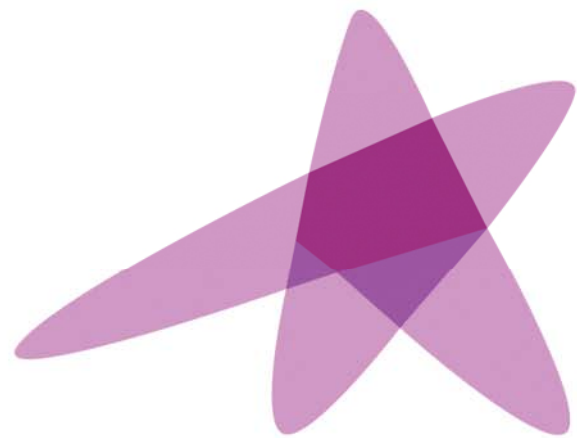
Clinician could consider relaxing the OAR dose constraint for this case, if it were possible to decrease large random uncertainties in the workflow!

"Can reduction of uncertainties in cervix cancer brachytherapy potentially improve clinical outcome?" Nesvacil et al. 2016, submitted to R&O



ESTRO

School



ESTRO
School

Advanced Brachytherapy Physics

Elements for a Quality Management Program in Brachytherapy

Prof. Mark J. Rivard, Ph.D., FAAPM

Advanced Brachytherapy Physics, 29 May – 1 June, 2016



Disclosures

The are no conflicts-of-interest to report.

Opinions herein are solely those of the presenter, and are not meant to be interpreted as societal guidance.

Specific commercial equipment, instruments, and materials are listed to fully describe the necessary procedures. Such identification does not imply endorsement by the presenter, nor that these products are necessarily the best available for these purposes.

Special thanks is extended to Bruce Thomadsen as the source for many of the slides in this presentation.

2013 AAPM Summer School

Quality and Safety in Radiotherapy: Learning the New Approaches in TG 100 and Beyond

June 16 - 20 • Colorado College • Colorado Springs, Colorado

Home

General Information

Program Information

Registration & Housing

Getting There

Contact Us

Welcome!



<http://www.aapm.org/meetings/2013SS/>



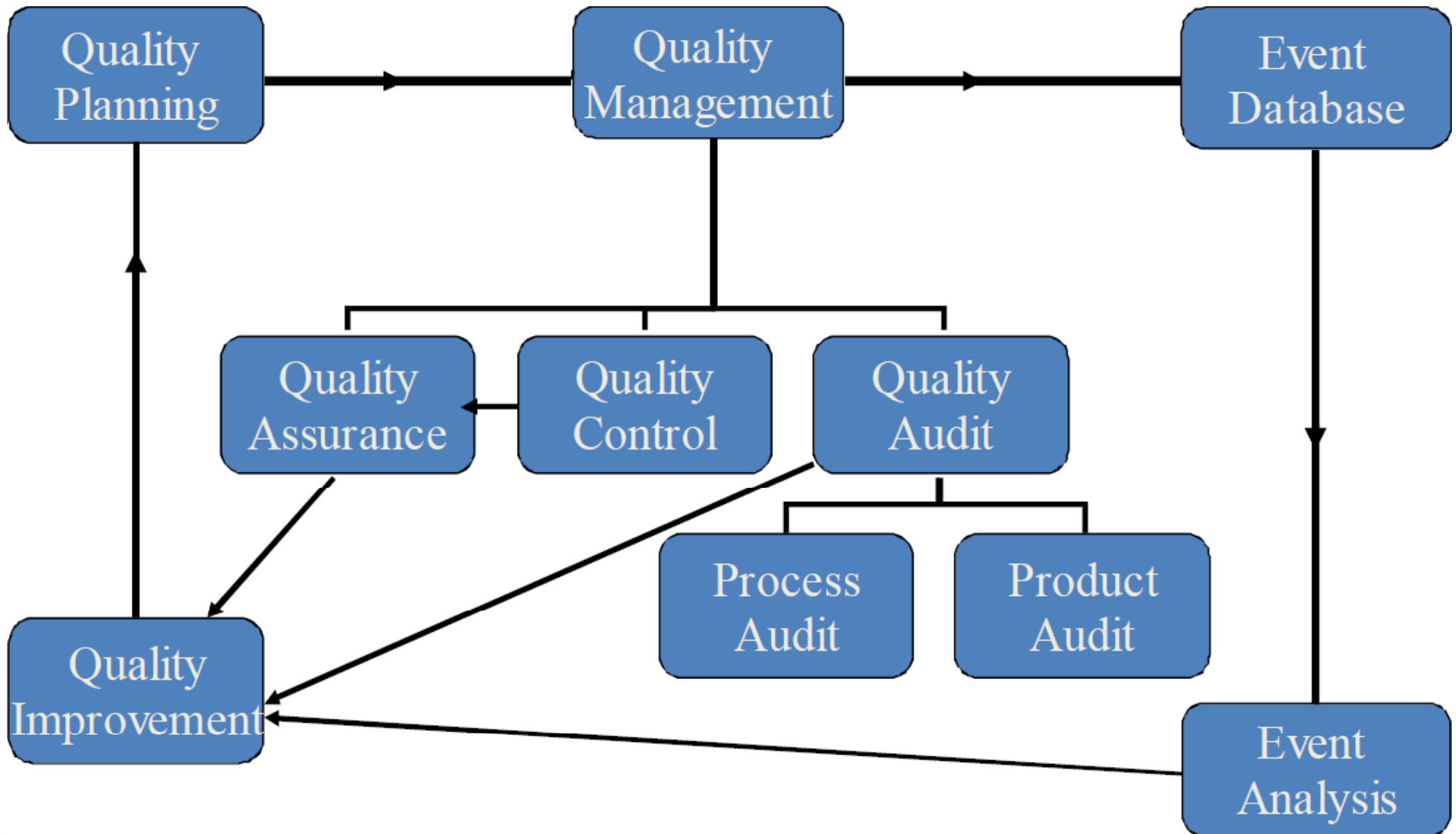
Learning Objectives

1. Definitions, terminology, and accepted nomenclature
2. Pre-purchase preparations and installation
3. Acceptance testing requires formalization
4. Commissioning a brachytherapy program
5. Example forms for clinical practice

Learning Objectives

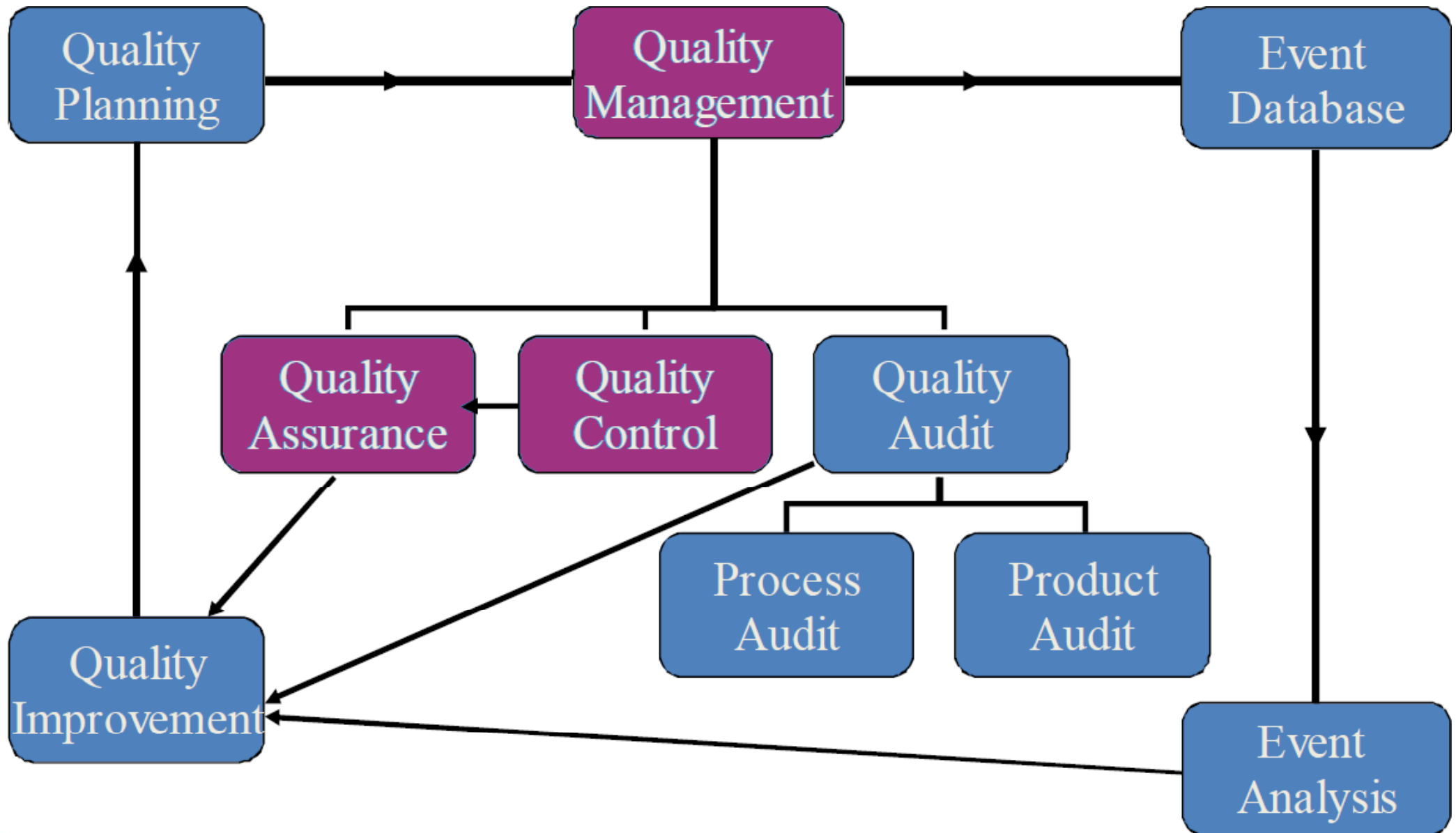
1. Definitions, terminology, and accepted nomenclature
2. Pre-purchase preparations and installation
3. Acceptance testing requires formalization
4. Commissioning a brachytherapy program
5. Example forms for clinical practice

QMP Schema



slide courtesy of Bruce Thomadsen

QMP Presentation Focus



QMP Philosophy

- Devise the QMP mission

patients will be treated safely, accurately, and efficiently
as defined by Rx, regulations, and societal standards

equipment + patient + staff + culture = success

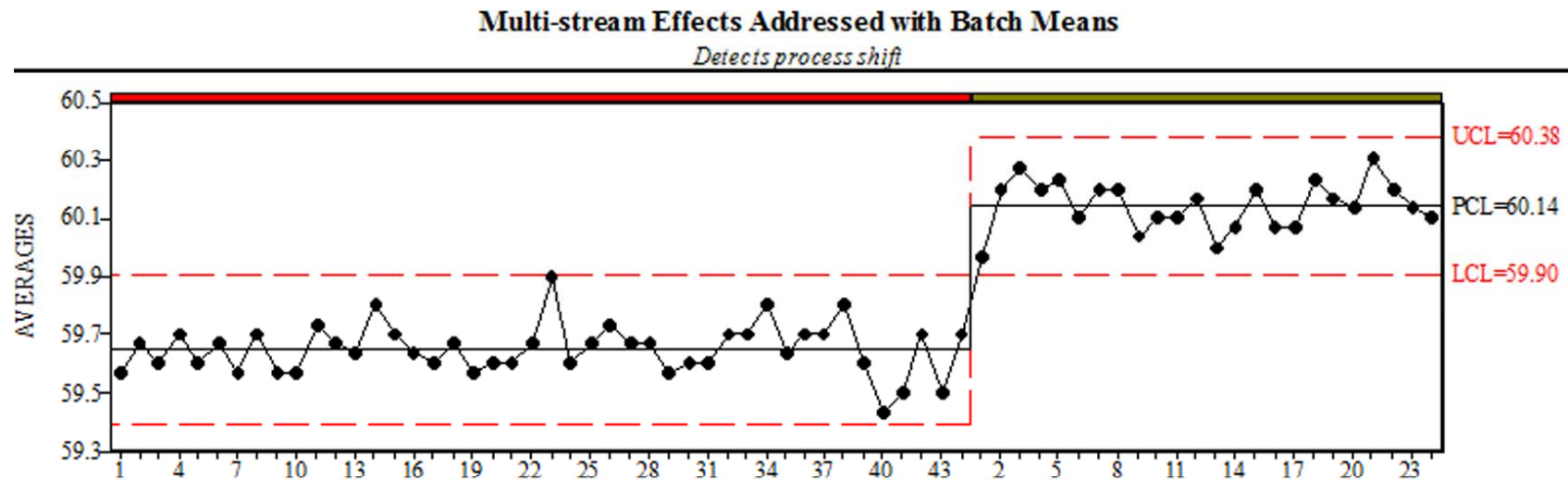
Shewhart: Father of Statistical Quality Control

Walter Andrew Shewhart (1891–1967)

1917: Ph.D. in Physics, University of California, Berkeley

1918: Joined Western Electric Company (supplier to AT&T)

1924: Invented the Control Diagram



1924-1932: Initiated study on sensitivity of worker productivity to light
Improvements were later attributed to management attention

Deming: Father of PDSA

William Edwards Deming (1900–1996)

1926: Ph.D. in Mathematical Physics, Yale University

1927: Employed by USDA and met Walter Shewhart
Applied statistics to industrial production methods



A system must be managed. It will not manage itself.

1943: Deming Cycle

Plan or design an experiment

Do the experiment by performing the steps

Study the results by analyzing the information

Act on decisions based upon the analyzed results



Fault Tree Analysis

Developed in 1961 at Bell Laboratories by H. A. Watson

Launch Control Safety Study for Intercontinental Ballistic Missile

Translation of system failure behavior into visual diagram and logic model

Visual model portrays system relationships and root cause pathways

Logic model provides qualitative & quantitative system evaluation

Utilizes Boolean algebra and probability theory

FTA popularized by US tragedies: Apollo 1 fire (1967), Three Mile Island nuclear meltdown (1979), Space Shuttle Challenger (1986)

FTA provides top-down risk assessment, FMEA is a bottom-up approach

US Military Procedures



assistdocs.com
U.S. Department of Defense

Database Last Updated: 02-MAY-2014

[New Search](#) | [What's New](#) | [Site Overview](#) | [ASSIST](#)

Basic Search → Results → Document Details

Document ID: MIL-P-1629

Overview

Title: PROCEDURES FOR PERFORMING A FAILURE MODE, EFFECTS AND CRITICALITY ANALYSIS

Scope: Scope information has not been recorded for this document

Document Status: Canceled

Doc Date: 09-NOV-1949

FSC/Area: 8405

Dist Stmt: See below

Doc Category: Detail Specification

Responsibilities

Lead Standardization Activity: CT DLA Troop Support - Clothing & Textile Items of Supply

Preparing Activity: GL U.S. Army Soldier Systems Center

Army Custodian: GL U.S. Army Soldier Systems Center

OFFICE OF MANNED
SPACE FLIGHT

APOLLO PROGRAM

**PROCEDURE
FOR
FAILURE MODE, EFFECTS, AND
CRITICALITY ANALYSIS
(FMECA)**

AUGUST 1966



REPRODUCED BY
NATIONAL TECHNICAL
INFORMATION SERVICE
U.S. DEPARTMENT OF COMMERCE
SPRINGFIELD, VA. 22161

NATIONAL AERONAUTICS AND SPACE ADMINISTRATION
WASHINGTON, D.C. 20546

First Known Paper on Brachytherapy Risk Analysis

Intl. J. Radiation Oncology, Biology, Physics

Analysis of treatment delivery errors in brachytherapy using formal risk analysis techniques

Purpose: To identify hazardous situations in treatments, analyze the nature of errors committed, and assess the value of several analysis techniques.

Methods and Materials: The study applied several risk analysis techniques to brachytherapy events (misadministrations) reported to the U.S. Nuclear Regulatory Commission and the International Atomic Energy Agency.

Results:

- (1) Events usually have multiple causes.
- (2) Failure to consider human performance in the design of equipment led to a large fraction of the events.
- (3) Verification procedures often were ineffectual.
- (4) Many events followed the failure of persons involved to detect that the situation was abnormal, often even though many indications pointed to that fact. Once the event was identified, the response often included actions appropriate for normal conditions, but inappropriate for the conditions of the event.
- (5) Events tended to happen most with actions having the least time available.
- (6) Lack of training and procedures covering unusual conditions frequently contributed to events.
- (7) New procedures or new persons joining a case in the middle present increased hazards.

Conclusion: Risk analysis tools common in industry provide useful information for error reduction in medical settings, although not as effectively, and modification of such techniques could improve their efficacy.

Numerous Opportunities for Errors

Table 3. Summary of the branches of the fault tree for high-dose-rate brachytherapy misadministrations, tracing backward to the initiating errors, with the frequency of errors along each branch indicated

Result of error	Major process	General category	Subcategory	Type of initial error
Wrong dose distribution or site 0.98 (43/44)	Treatment planning error 0.30 (13/44)	Localization 0.07 (3/44)		Improper simulation: >Marker misinterpretation 0.05 (2/44) Digitization error: >Entry error: Localization 0.07 (3/44) >>Digitization not follow protocol 0.02 (1/44) Calculation error: >Wrong input data 0.02 (1/44)
		Dosimetry error 0.23 (10/44)	Source strength 0.07 (3/44)	Erroneous source strength data: >Failure to enter or alter data 0.07 (3/44)
			Dose calculation 0.16 (7/44)	Incorrect data entry for calculation 0.02 (1/44) Wrong dose: >Incorrect dose entry 0.05 (2/44) Wrong position of dose distribution: >Inaccurate source position entry 0.05 (2/44) Dose specified to the wrong point 0.05 (2/44) Poor techniques 0.05 (2/44) Equipment failure 0.02 (1/44)
	Treatment implementation 0.68 (30/44)	Applicator shifted in patient 0.07 (3/44)	Applicator shifts >Patient movement >>Failure of securing mechanism 0.07 (3/44)	
		Applicator connection 0.05 (2/44)	Incorrect guide tubes 0.02 (1/44)	Applicator connected to through the wrong transfer tube type 0.02 (1/44)
			Wrong channel 0.02 (1/44)	Applicator connected incorrectly 0.02 (1/44)
		Treatment programming error 0.48 (21/44)	Manual programming error 0.48 (21/44)	Transcription error 0.41 (17/44)
				Data transposition 0.02 (1/44) Interpretation error 0.07 (3/44)
	Treatment delivery error: >Source fails to progress 0.10 (4/44)	Drive mechanism fails 0.05 (2/44)	Mechanical malfunction 0.02 (1/44) Kink in catheter 0.02 (1/44)	
	Wrong patient treated 0.02 (1/44)	Source disconnect 0.05 (2/44)		

Recent Paper on Brachytherapy FMEA

Failure modes and effects analysis applied to high-dose-rate brachytherapy treatment planning

D. Allan Wilkinson*, Matthew D. Kolar

Department of Radiation Oncology, Cleveland Clinic, Cleveland, OH

PURPOSE: To apply failure modes and effects analysis to high-dose-rate treatment planning to identify the most likely and significant sources of error in the process.

METHODS: We have made a list of 25 failure modes grouped into six categories (imaging, catheter reconstruction, dwell position activity, dose points/normalization, optimization/dose, and evaluation). Each mode was rated on a one to five scale for severity, likelihood of occurrence, and probability of escaping detection. An overall ranking was formed from the product of the three scores. The authors assigned scores independently and the resulting rankings were averaged. We also analyzed 44 reported medical events related to high-dose-rate treatment planning listed on the Nuclear Regulatory Commission Web site and compared them with our own rankings.

RESULTS: Failure modes associated with image sets, catheter reconstruction, indexer length, and incorrect dose points had the highest ranking in our analysis (scores higher than 20). The most often cited failure modes in the Nuclear Regulatory Commission reports examined were indexer length (20/44) and incorrect dose points (6/44). Several of our high-ranking modes are not associated with reported events.

CONCLUSION: It is a useful exercise to identify failure modes locally and analyze the efficacy of the local quality assurance program. Comparison with nationally reported failures can help direct the local analysis, but the absence or small number of reports for failure modes with a high score may be owing to low detectability. Such modes obviously cannot be ignored. © 2013 American Brachytherapy Society. Published by Elsevier Inc. All rights reserved.

Keywords: Failure modes; High-dose-rate brachytherapy; Treatment planning

Further Adoption of FMEA

1960s US civil aviation, automotive, and food industries

1970s Petroleum, plastics, waste water, and software industries

1980s ...

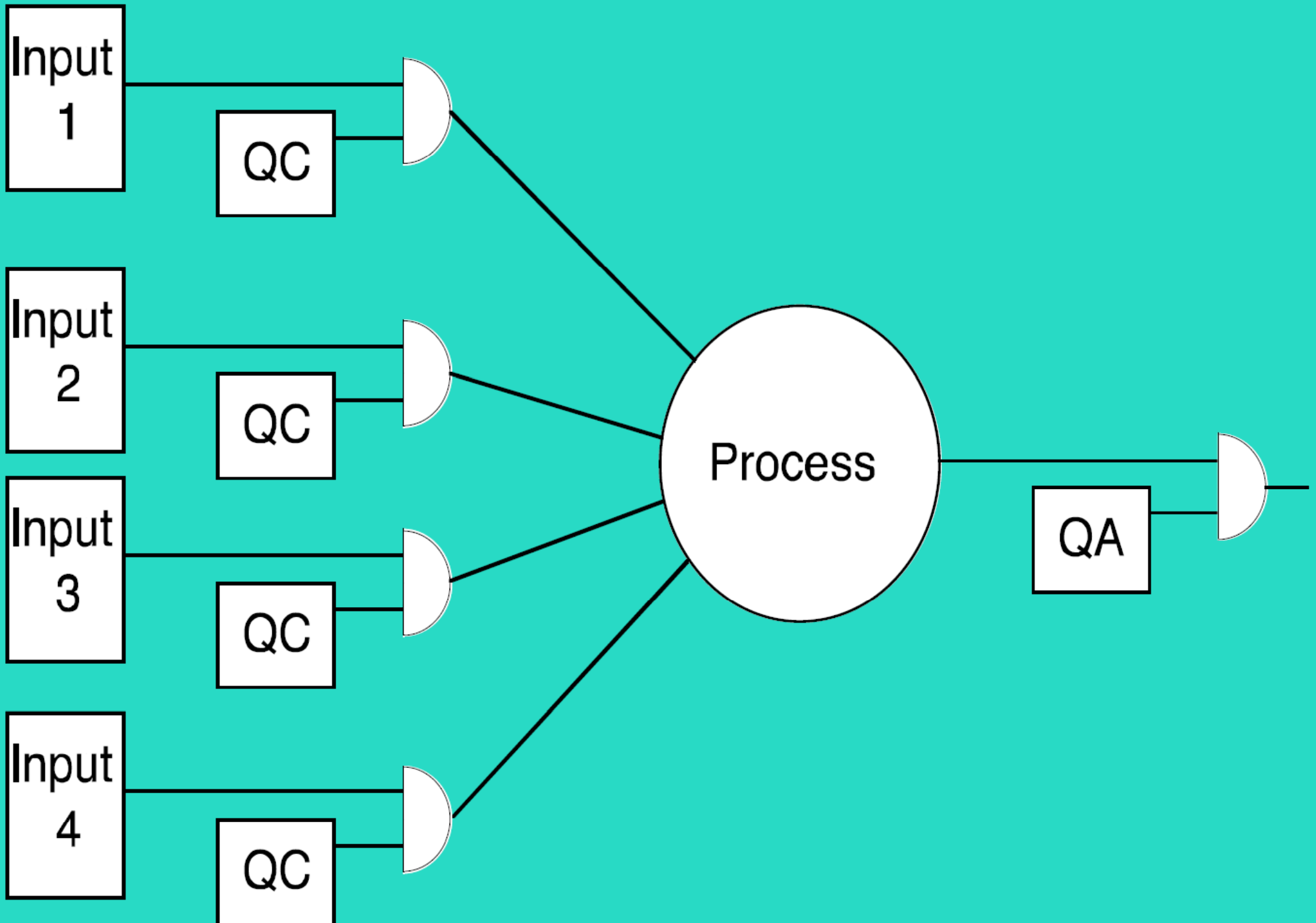
1990s ...

2000s Radiation oncology (brachytherapy)

Key Concepts

- Quality Management Program (QMP)
 - *ALL* activities **designed to contribute to process quality**
- Quality Assurance (QA) non-patient tests
 - activities that **measure the quality level** of a process
- Quality Control (QC) patient treatment checks
 - activities that **force specific qualities** onto a process

Quality Controls vs. Quality Assurance



ISO 900X and Quality Management

ISO 9000

A series of standards that define, establish, and maintain an effective QA system for manufacturing and service industries.

ISO 9001

Requirements for organizations wishing to meet the ISO 9000 standard

Reported benefits

1. Improve efficiencies and effective operations
2. Increases customer satisfaction and retention
3. Reduces audits
4. Enhances marketing
5. Improves employee motivation, awareness, and morale
6. Promotes international trade
7. Increases profit
8. Reduces waste and increases productivity
9. Common tool for standardization

Appropriate for large scale industries, not individual clinics

Learning Objectives

1. Definitions, terminology, and accepted nomenclature
2. Pre-purchase preparations and installation
3. Acceptance testing requires formalization
4. Commissioning a brachytherapy program
5. Example forms for clinical practice

Pre-Installation Preparations

- Assist administrators to create a realistic business plan
 - prepare for reimbursement fluctuations
 - include QA equipment and dummy markers
 - budget for regular training for new staff and facility upkeep
- Plan disease site(s): GYN, breast, prostate, skin, etc.
 - consider future potential for treating additional disease sites
 - balance desires for growth with a dash of realism
- Review potential manufacturer system specifications, installation requirements, and clinical integration
- RAU-to-R&V connectivity is available with newer systems

Pre-Installation Preparations

- Physical layout
 - location of electrical/telephone/network connections, interconnectivity with linac interlocks, special gases, closed loop AV system
 - consider imaging proximity and position RAU near imaging (dept CT, US, MRI?) or OR, maybe not in RadOnc center proper
- Regulatory aspects
 - vault design (primary/scatter/maze/door) ala NCRP 147/151/155, acceptable exposure levels, workflow
 - enhanced security measures, source controls, staff bkgnd checks
 - approval for n sources and max individual/total Ci (not RAKR)
 - broadscope license need not name individuals
- Visit established centers, contact colleagues, phone a friend

Learning Objectives

1. Definitions, terminology, and accepted nomenclature
2. Pre-purchase preparations and installation
3. Acceptance testing requires formalization
4. Commissioning a brachytherapy program
5. Example forms for clinical practice

Acceptance Testing: General

- Acceptance testing results set baseline for clinical use
- Usually no formal ATP form as for linacs
- Performance evaluation of system within manu. specs
- Re-perform annually to ensure system stability

Acceptance Testing: Applicators & Source

- Make electronic inventory of all hardware and disposables
- Applicators
 - confirm dimensions and serial numbers
 - confirm applicator shielding magnitude and shape
 - check connecting tubes and other ancillary equipment
- Source
 - validate source-to-dummy marker coincidence
 - superposition: transmission radiograph & autoradiograph
 - use electronic imaging tools if no radiochromic film
- Determine source strength (covered on Day 3)

Acceptance Testing: TPS

- AAPM TG-53 and TG-43 reports are good resources
- Verify functionality of dose, dwell time, and Tx time calculations
- High-level check of single-source isodose distributions
- Understanding of plan rotation matrix and coordinate recon

Acceptance Testing: TPS

- Accuracy of electronic data transfer to TCS/RAU
- Evaluate optimization software
 - develop reference dataset for accuracy & constancy
- DVH and implant figures of merit
- End-to-end testing
 - general functionality of entire system
 - identify QMP weaknesses by using items incorrectly

Acceptance Testing: General

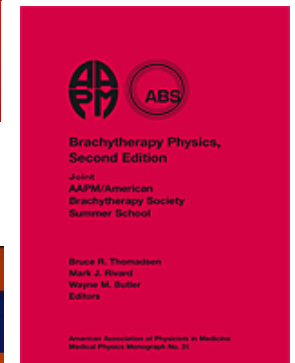
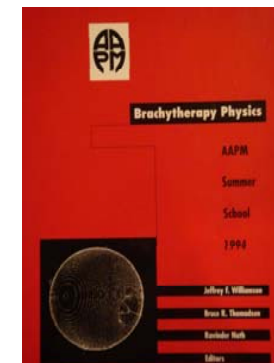
- Field service engineer provides system familiarization
- Test all components and features the time is now
- Ignore pressure to hurry and sign form
- Technical understanding of equipment is your responsibility

Learning Objectives

1. Definitions, terminology, and accepted nomenclature
2. Pre-purchase preparations and installation
3. Acceptance testing requires formalization
4. Commissioning a brachytherapy program
5. Example forms for clinical practice

References for Brachytherapy Commissioning

- Consider AAPM Task Group Reports and Guidance
 - TG-41 Remote Afterloading Technology (1993)
 - TG-43 Brachytherapy Dosimetry Formalism (1995)
 - TG-56 Code of Practice for Brachytherapy (1997)
 - TG-59 High Dose Rate Tx Delivery (1998)
 - AAPM/ESTRO HEBD Report #229 (2012)
- Consider AAPM Summer School texts
 - 1994 Chapters 28, 30, 31, 32
 - 2005 Chapters 6, 7, 11, 22, 32, 48
- Consider Bruce Thomadsen's 1999 text "Achieving Quality in Brachytherapy"



Commissioning: General

- Medical Event notification plan and action levels
- Patient/personnel radiation safety plan
- Patient positioning standards and contingencies
- Use of dummy markers, contrast agents, and imaging system settings to visualize disease/applicator/markers
- Form creation
 - WD (disease-site specific)
 - daily QA (performed by therapist under physicist supervision)
 - Tx runsheet QC
 - new source QA (TPS backup, TCS backup)
 - annual QA, rigorously check applicators and TPS data

Commissioning: General

- Establish disease-specific clinical standards to minimize “medical arts” and to follow ABS/ESTRO guidelines
- Create policies-and-procedures, have staff read, provide feedback, and document understanding (annually)
- Establish workflow for all processes: identify tasks, frequency, needed resources, responsible party(s)
- Develop safety standards and clinic-specific FMEAs, share results with all stakeholders
- Staff training on HDR system (RAU, applicators, and TPS) usage, emergency procedures, and common expectations

Commissioning: RAU

- Master all aspects of TCS functionality
- Document logic chain of RAU safety interlocks
- Determine timer linearity
- Understand emergency buttons, warnings, and error codes
- Demonstrate well chamber stability

Commissioning: Source

- Absorbed dose measurements not performed in the clinic
 - detector response sensitive to photon spectrum
 - dose falloff sensitive to medium composition
 - influence of positioning, attenuation, and scatter
 - no AAPM protocol for absorbed dose measurements
- Source form, inventory, wipe test documentation
- Understand eBT output variations for same source model

Commissioning: Source

- Validate source/dummy marker coincidence
- Source positional accuracy
- eBT source output stability
 - overall / global
 - spatial dependence (spectral changes)
- Demonstrate well chamber stability

Source Strength Measurements

- All HDR ^{192}Ir sources can have RAKR measured by physicist
- Using PSDL traceably-calibrated equipment for RAKR measurement
- For the eBT sources, only the Axxent has direct traceability to PSDL
- INTRABEAM and esteya sources do not yet have direct traceability
 - physicist may use AAPM TG-61 calibration method if they know the electron scatter/absorber thickness and the HVL for their device

Commissioning: Applicators

- Inventory all applicators
- Document sterilization procedures/responsibilities
- Determine intra-applicator source positioning
- Determine source/marker congruence in applicator

Commissioning: Applicators

- Validate dimensions (c.f., TPS applicator library info)
- Applicator performance evaluation (e.g., T&R)
- Confirm applicator/marker compatibility
- Establish standard imaging protocols (Day 2)

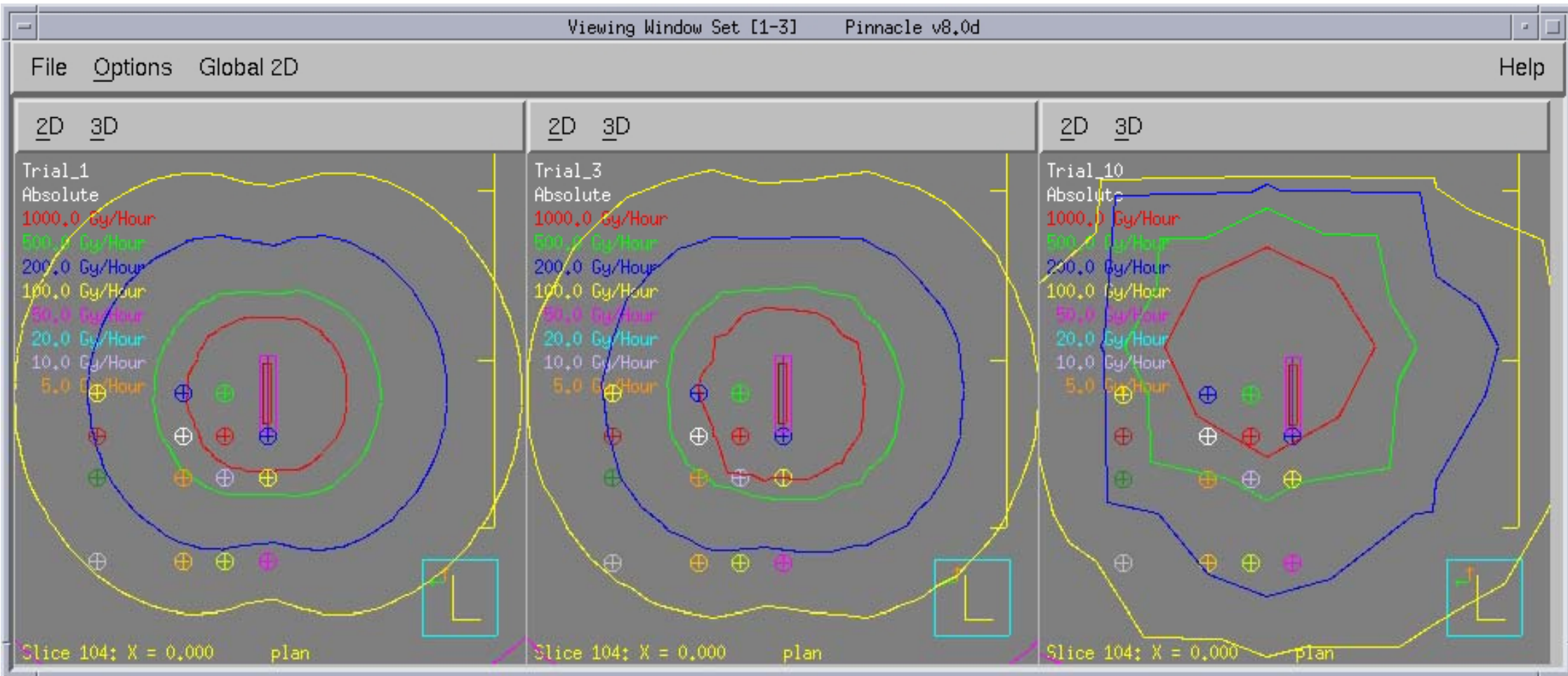
Commissioning: TPS

- Establish dose calc methods
 - imaging slice thickness, dummy marker usage, step size, optimization type and parameter ranges
- Compare TPS TG-43 dosimetry parameters to reference dataset or publication(s)
- Compare TPS dose calcs to TG-43 hand calcs
 - devise independent (secondary) dose calculation method
 - MBDCA covered on Day 1
- Commission source over required radii and polar angles

Commissioning: TPS

- AAPM TG-53 and TG-43 reports are good resources
- Evaluate data transfer between TPS and TCS/RAU
- Compare system performance range with TPS data
- Recommission TPS following all upgrades
- For advanced dose calculation modules, read carefully the TG-186 report for specific commissioning tasks (Day 1)

Commissioning: TPS



eBT Commissioning Specifics

- Consider AAPM Task Group Reports and Guidance
 - TG-43 Brachytherapy Dosimetry Formalism
 - TG-56 Code of Practice for Brachytherapy
 - TG-59 High Dose Rate Tx Delivery
 - TG-182 Recommendations on eBT Quality Management
 - 2008 AAPM (Butler *et al.*) Low-energy Source Calibrations
 - 2008 ASTRO Emerging Technology Cmte: Electronic Brachytherapy
- Need comparisons of measured and calculated dose distributions, and consensus datasets
- HDR breast commissioning by Hiatt et al. JACMP (2008)

Learning Objectives

1. Definitions, terminology, and accepted nomenclature
2. Pre-purchase preparations and installation
3. Acceptance testing requires formalization
4. Commissioning a brachytherapy program
5. Example forms for clinical practice

Philosophy on Forms

- Forms should be dynamic, constant improvements
- Use electronic forms, minimize paper usage (scan the paper!)
- Use mathematical tools (e.g., Excel) for non-patient data
- Data mining permits analysis across broad timescales
- Consider action levels beyond societal guidance
- Take high-level perspective on why to perform QA tasks

Example Daily HDR ¹⁹²Ir QA Form (upper)

Nucletron V2 MicroSelectron Remote Afterloader, Model # 105.088-03 Serial # 31743
Source is manufactured by QSA Global, model 105.002.

On each treatment day, the treating therapist will test the following system components and initial at the right indicating that the test was performed and that the result was within normal ranges. Any deviations must be promptly reported to a physicist.

1. Are the TV monitors at the control console operational (focus/zoom/pan)? _____
2. Is the intercom operational (2-way communications)? _____
3. Does the radiation survey meter function (battery check)? _____
4. Is the emergency basket stocked and the emergency storage container in place?
_____ [forceps/tongs, scissors, suture removal kit, and “CAUTION RADIATION AREA” tape] _____
5. Are the source guide tubes free of kinks, etc? _____
6. Did control console pass self-diagnostic checks when key switch is first turned? _____
7. Is the emergency STOP button in the treatment room (near emergency basket) operational?
_____ [verify illumination of the red “Reset” light , lower left of console] _____
8. Is the emergency STOP button on the HDR unit operational?
_____ [verify illumination of the red “Reset” light , lower left of console] _____

Attach source position check ruler to channel 2 (**incorrect channel**). Turn on ceiling light and adjust TV camera so that check ruler is clearly visible. Run: Daily QA, DQA patient to set the dummy source end to 1435 mm, and active source end to 1330 and 1430 mm. On the left side of the screen will be depicted a pre-Treatment Record

9. Are the date and time correct (within 5 minutes compared to local PC)? _____
10. Is the source strength on the printout within 0.020 cGy m²/h of the logbook activity? _____

Example Daily HDR ^{192}Ir QA Form (lower)

11. Confirm program and dwell times, press START to initiate treatment, and verify that Error Code 14 appears on the screen and that the source is not extended out of the safe. _____

Attach the source position check ruler to channel 1 (**correct channel**). Press START to initiate treatment.

12. Does the distal end of the dummy source goto 1435 ± 1 mm, and active source end goto 1330 ± 1 mm (dwell position 35) and 1430 ± 1 mm (dwell position 15)? _____

While the source is dwelling at dwell position 15 (nominally 1430 mm), check the door light, door interlock, interrupt button, and console emergency stop button. The source end should return to dwell position 15 after each restart.

13. Is the “HDR IN USE” door light on, and does the radiation area monitor function (red light)? _____

14. Is the door interlock operational? _____

15. Does the interrupt button on the console function properly? _____

16. Does the emergency STOP button on the treatment console promptly retract the source and emit an audible alarm and display the status on the screen?

_____ [verify illumination of the red “*Reset*” light , lower left of console] _____

Name: _____ Signature: _____ Date: _____

Example HDR ¹⁹²Ir Treatment QC Form (upper)

Patient Name: _____
 Medical Record #: _____
 Radiation Oncologist: _____

Treatment Date: _____
 Fraction #: _____
 RTT name: _____

*****generally

Pre-Treatment Time Out

- | | initials | performed by |
|---|----------|--------------|
| 1. Daily check performed on Nucletron microSelectron HDR unit. | _____ | RTT |
| 2. Confirm the presence of Emergency Source Storage Safe (Pb bailout pig). | _____ | RTT |
| 3. Connect catheters to treatment device and LOCK WHEELS to V2 unit. | _____ | RTT |
| 4. Informed Consent signed & dated, confirm Patient ID using 2 approved methods. | _____ | RTT |
| 5. Verification of radionuclide, treatment site & side, and total fraction dose. | _____ | RTT |
| 6. Written Directive completed and signed by physician Authorized User. | _____ | RTT |
| 7. Treatment plan and isodose plan signed by physician Authorized User. | _____ | RTT |
| 8. Confirm that calculations were checked by an Authorized Medical Physicist. | _____ | RTT |
| 9. Physician Authorized User and Physicist sign & date the Pre-Treatment Record. | _____ | RTT |
| 10. Perform radiation survey of patient body surface near proposed treatment site. _____ mR/h _____ | | MP |
| 11. Agreement of catheter-to-indexer routing sequence with the treatment plan. | _____ | MP |
| 12. Time Out Completed | _____ | RTT |
| 13. Confirm Authorized Physician and Physicist are within audible range of normal speech. | _____ | RTT |

Example HDR ¹⁹²Ir Treatment QC Form (lower)

During Treatment

14. Confirm radiation area monitor function (flash red) during treatment. _____ RTT

After Treatment

15. Physician Authorized User and Physicist sign & date the Treatment Record. _____ RTT

16. Using the Ludlum, model 14C serial # 99941, survey the following locations (a through e):

- a) Background reading outside the treatment room _____ mR/h
- b) Treatment unit external surface, at the trefoil (radioactive material) symbol _____ mR/h
- c) Connector and applicator apparatus _____ mR/h
- d) Full length of the catheter guide tube _____ mR/h
- e) Patient body surface near the treatment site prior to removal from the room _____ mR/h

Radiation surveys performed by authorized Medical Physicist. _____ MP

17. Compare pre- and post-treatment surveys to assess possibility of contamination. _____ MP

Does comparison of readings (items 10 & 16e) indicate contamination? (YES or NO) _____ MP

If YES, ask RTT to contact Health Physics and start Emergency Procedures

18. Record patient radiation survey information in the HDR Patient Survey Logbook. _____ MP

19. Were there any unintended deviations from the Written Directive ? (YES or NO) _____ MP

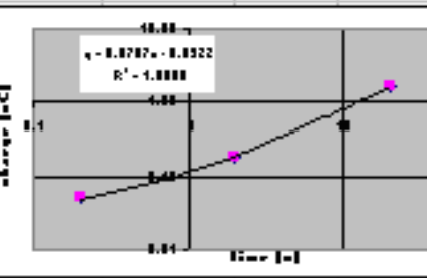
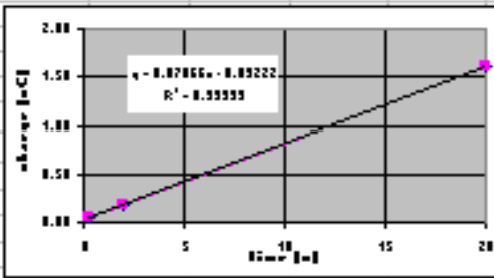
If YES, explain in detail (greater than 10% deviation is a recordable event):

20. QMP Reviewer Name _____ Signature/Date _____ MP

21. File this form in the patient's RadOnc paper chart and complete the billing. _____ MP

Example HDR ¹⁹²Ir Source Exchange Form (a)

1	date: *****										medical physicist(s): Mark Rivard										
2	ventional (not MR/CT) GYN connectors and ACD device L=1286mm																				
3	5	9	13	17	21	25	29	33	37	41	45	10 mm stepsize									
4	1.0	1.0	1.0	1.0	1.0	1.0	1.0	1.0	1.0	1.0	1.0										
5	1.0	1.0	1.0	1.0	1.0	1.0	1.0	1.0	1.0	1.0	1.0										
6	1.0	1.0	1.0	1.0	1.0	1.0	1.0	1.0	1.0	1.0	1.0										
7	GOOD	NA Update daily check program, treatment plans for ongoing patients, and 2 decay tables with new length L.																			
8	homogeneity on film GOOD or BAD ?										GOOD										
9	mechanical integrity of all applicators, connectors, and guide tubes based on visual inspection																				
10	Notes: start stop																				
11	110.7%	27:24.8	29:26.9																		
12	time	122.17	GOOD	Nucletron TCS time		121.6	seconds (> 100 s)														
13	22.5	°C	press.	1000		mbar	1.015	CTP	20												
14	2	0.2	20	2	0.2	toffset	-0.407	GOOD													
15	0.1879	0.85232	1.08837	0.18752	0.84725	R ²	0.99999	GOOD													
16	8:43 AM	reproducibility		0.1%	0.3%	GOOD	GOOD														
17	21	20	19	18	17	16	15	14													
18	1450.0	1452.5	1455.0	1457.5	1460.0	1462.5	1465.0	1467.5													
19	77.95	78.19	78.36	78.47	78.52	78.49	78.41	78.27													
20	imum reading	78.52	[nA]	HDR-1000 * C _{well} (cal'd 8/19/2010)				0.5047	mGy m ² h ⁻¹ nA ⁻¹												
21	decay factor	1.0034	F _{HDR}	6517A electrometer#2 C _{EL} (cal'd 7/9/2010)				1.000	A/Rdg 200 nA scale	February-07	-0.452	0.99999									
22	...S _x = ...Rdg * ...F * C _u * C _{...u} * C _u							40.4	mGy m ² h ⁻¹	May-07	-0.430	0.99999									
23	measured air kerma strength							4.0358	cGy m ² h ⁻¹	August-07	-0.438	0.99998									
24	Manu. cal date			January 17, 2012			43.84	mGy m ² h ⁻¹	#####	-0.442	0.99998										
25	F _{HDR}	done?	Cal ratio				1.010	GOOD	February-08	-0.440	0.99999										
26	YES	update source strength (H _{EMC} S _x) in microSelectron treatment console (Maintenance, Source Calibration)																			
27	YES	make 2 new decay tables and post at the planning workstation and in HDR console logbook																			
28	YES	update source strength (NEMC S _x) in the PLATO v.14.3 planning system (passwd=platobps)																			
29	YES	end-to-end test using VagCyl.xls file with new S _x and T _x time																			
30											May-09	-0.449	0.99999								
31											August-09	-0.421	1.00000								
32	IR Cs-137 insert, HDR-1000+, +300.0V, Filter(100)										#####	-0.408	1.00000								
33	speed: HIACCURACY										-0.438	0.99999	AVG								
34											0.013	0.00001	STDEV								
35											-0.424	-0.408	0.99998	MIN							
36											-0.451	-0.452	1.00000	MAX							
37	H.L. (days)	leakage	+0.00025	nA			0.0403223 0.00002 3 SIGMA														
38																					
39	...S _x = Rdg * C _u * C _{...u} * C _u							118.31	mGy m ² h ⁻¹												
40																					
41	days	decay	calc'd	ratio	C _{well}																
42	0	1.000	118.31	100.0%	-5.457E+11																
43	35	0.994	119.01	100.5%	-5.457E+11																
44	169	0.989	119.57	100.6%	-5.457E+11																
45	186	0.988	119.70	100.7%	-5.457E+11																
46	1901	0.887	133.34	99.7%	-5.484E+11																
47	2072	0.878	134.78	99.2%	-5.484E+11																
48	2349	0.863	137.15	100.2%	-5.484E+11																



Example HDR ¹⁹²Ir Source Exchange Form (a1)

	A	B	C	D	E	F	G	H	I	J	K	L	M	N	O	P	
1	HDR Quarterly QA				date:	1/27/12 8:43 AM	medical physicist(s):	Mark Rivard									
2	LOCALIZATION with 3 conventional (not MR/CT) GYN connectors and ACD device L=1286mm																
3	Position	1	5	9	13	17	21	25	29	33	37	41	45	10 mm stepsize			
4	CATH1 Shift [X mm]	1.0	1.0	1.0	1.0	1.0	1.0	1.0	1.0	1.0	1.0	1.0	1.0				
5	CATH2 Shift [X mm]	1.0	1.0	1.0	1.0	1.0	1.0	1.0	1.0	1.0	1.0	1.0	1.0				
6	CATH3 Shift [X mm]	1.0	1.0	1.0	1.0	1.0	1.0	1.0	1.0	1.0	1.0	1.0	1.0				
7	Shift _{AVG} [X.X mm]	1.0	GOOD	NA	Update daily check program, treatment plans for ongoing patients, and 2 decay tables with new length												
8	AUTORADIOGRAPH	Is source homogeneity on film GOOD or BAD ? GOOD															
9	Check mechanical integrity of all applicators, connectors, and guide tubes based on visual inspection													OK			
12								start	stop								
13								27:24.8	29:26.9								
14	TIMER ACCURACY	Measured time					122.17	GOOD	Nucletron TCS time			121.6	seconds (> 100 s)				
15	TIMER LINEARITY	temp		22.5 °C		press.		1000 mbar			1.015	C _{TP}	20 s				
16	t _{DWELL} [s]	20	2	0.2	20	2	0.2	t _{OFFSET}	-0.407			GOOD					
17	Reading [uC]	1.60416	0.18673	0.05232	1.60697	0.18752	0.04725	R ²	0.99999			GOOD					
18								ratios to first reading		99.8%	99.6%	110.7%					
20	SOURCE STRENGTH	time	8:43 AM			reproducibility		0.1%	0.3%	GOOD	GOOD						
21	position	22	21	20	19	18	17	16	15	14							
22	Length [mm]	1447.5	1450.0	1452.5	1455.0	1457.5	1460.0	1462.5	1465.0	1467.5							
23	Reading [nA]	77.54	77.95	78.19	78.36	78.47	78.52	78.49	78.41	78.27							
24	maximum reading		78.52 [nA]			HDR-1000 + C _{WELL} (cal'd 8/19/2010)					0.5047	mGy m ² h ⁻¹ nA ⁻¹					
25	decay factor		1.0034 F _{NEMC}			6517A electrometer#2 C _{EL} (cal'd 7/9/2010)					1.000	A/Rdg	200 nA scale				
26											NEMC S _K = MAX Rdg x NEMC F x C _{TP} x C _{WELL} x C _{EL}						
27	S_K COMPARISON											40.4	mGy m ² h ⁻¹				
28	Source ID	D36E-0374			Manu. cal date		January 17, 2012			43.84		mGy m ² h ⁻¹					
29	decay factor	0.912	F _{MANU}	done?								Cal ratio	1.010	GOOD			
30	YES update source strength (NEMC S _K) in microSelectron treatment console (Maintenance, Source Calibration)																
31	YES make 2 new decay tables and post at the planning workstation and in HDR console logbook																
32	YES update source strength (NEMC S _K) in the PLATO v.14.3 planning system (passwd=platobps)																
33	YES end-to-end test using VagCyl.xls file with new S _K and Tx time																

Example HDR ¹⁹²Ir Source Exchange Form (a2)

32	Cs-137 constancy check, LDR Cs-137 insert, HDR-1000+, +300.0V, Filter(100)						
33	align dots, eyelet/color face up	speed: HIACCURACY					
34	s# 3M 25 01554						
35	LDR Cs-137					-0.2136	20 nA setting
36	μGy.m ² /h/A						
37	-5.457E+11	11,018	H.L. (days)	leakage	+0.00025	nA	
38	C _{WELL} cal'd 8/24/2010						
39	NEMC S _K = Rdg x C _{TP} x C _{WELL} x C _{EL}					118.31	mGy m ² h ⁻¹
40							
41		S _K	days	decay	calc'd	ratio	C _{WELL}
42	1/27/2012	118.31	0	1.000	118.31	100.0%	-5.457E+11
43	10/24/2011	118.38	95	0.994	119.01	100.5%	-5.457E+11
44	8/11/2011	118.90	169	0.989	119.57	100.6%	-5.457E+11
45	7/25/2011	118.88	186	0.988	119.70	100.7%	-5.457E+11
46	11/13/2006	133.80	1901	0.887	133.34	99.7%	-5.484E+11
47	5/26/2006	135.90	2072	0.878	134.78	99.2%	-5.484E+11
48	8/22/2005	136.90	2349	0.863	137.15	100.2%	-5.484E+11
49						100.1%	avg
50						0.6%	stdev
51							

Example HDR ¹⁹²Ir Source Exchange Form (b)

1	SAFETY CHECKS		YES or NO		
2	1	HDR RAL ¹⁹² Ir alarms activate following AC power failure simulation (error code 104)?	YES		
3	2	Door Primalert functions with AC power off using extended HDR ¹⁹² Ir source?	YES	covers Daily #14	
4	3	Interrupt button on the console functions with display of elapsed treatment time?	YES	covers Daily #15	
5	4	Emergency STOP (on console) functions with display of elapsed treatment time?	YES	covers Daily #17	
6	5	Door interlock functions with display of elapsed treatment time?	YES	covers Daily #16	
7	6	Survey meter battery check and constancy check OK?	YES	covers Daily #4	
8	7	Was survey meter calibrated within 365 days ? (If not, notify Health Physics)	YES		
9	8	Are Emergency Procedures in the HDR Manual?	YES		
10	9	Is error 13 detected when indexer ring is not latched?	YES		
11	10	Is error 14 detected when interstitial interconnect tube is not inserted?	YES	covers Daily #12	
12	11	Is error 33 detected when interstitial interconnect tube is installed without catheter present?	YES		
13	12	Review of daily checks since last physics QA?	YES		
14					
15	Additional Notes (if needed):				
16					
17					
18			date:	1/27/2012	
19			inits:	MJR	
20					
21					
22					
23					
24					
25					

Example HDR ¹⁹²Ir Source Exchange Form (c)

	DAILY CHECKS	YES or NO	
1			
2	1 Are the TV monitors at the control console operational?	YES	
3	2 Is the intercom (audio) operational?	YES	
4	3 Does the radiation area monitor function?	YES	
5	4 Does the radiation survey meter (s# 99941) function?	YES	do prior page, 6
6	5 Is the emergency basket stocked and the emergency storage container in place?	YES	
7	6 Are the source guide tubes free of kinks, etc?	YES	
8	7 Did control console pass self-diagnostic tests when key switch is first turned?	YES	
9	8 Is the emergency STOP button in the treatment room operational?	YES	
10	9 Is the emergency STOP button on the HDR unit operational?	YES	
11	10 Is the Tx console date (exact) and time (within 5 minutes) correct?	YES	
12	11 Is the source strength on the printout within 0.020 cGy m ² /h of the posted activity?	YES	
13	12 Confirm program and dwell times, press START to initiate treatment, and verify that Error Code 14 appears on the screen and that the source is not extended out of the	YES	do prior page, 10
14	13 For L=1498 and 5 mm step size, does the distal end of the dummy source goto 1435 mm, and the active source end to 1330 mm (dwell 35) and 1430 mm (dwell 15) within 1 mm?	YES	
15	14 Is the "HDR IN USE" door light on?	YES	do prior page, 2
16	15 Does the interrupt button on the console function properly?	YES	do prior page, 3
17	16 Is the door interlock operational?	YES	do prior page, 5
18	17 Is the emergency STOP button on the treatment console operational?	YES	do prior page, 4
19			
20		date:	1/27/2012
21		inits:	MJR
22			
23			
24			
25			
26			

Example HDR ¹⁹²Ir Source Exchange Form (d)

1	HDR ¹⁹² Ir source D36E-0374					
2	73.83 day HL	Strength (cGy m ² /h)		Strength (cGy m ² /h)		
3	date	MIDNIGHT	NOON	date	MIDNIGHT	NOON
4	1/27/2012	4.036	4.017	3/17/2012	2.524	2.512
5	1/28/2012	3.998	3.979	3/18/2012	2.500	2.489
6	1/29/2012	3.961	3.942	3/19/2012	2.477	2.465
7	1/30/2012	3.924	3.905	3/20/2012	2.454	2.442
8	1/31/2012	3.887	3.869	3/21/2012	2.431	2.419
9	2/1/2012	3.851	3.833	3/22/2012	2.408	2.397
10	2/2/2012	3.815	3.797	3/23/2012	2.386	2.374
11	2/3/2012	3.779	3.761	3/24/2012	2.363	2.352
12	2/4/2012	3.744	3.726	3/25/2012	2.341	2.330
13	2/5/2012	3.709	3.691	3/26/2012	2.319	2.308
14	2/6/2012	3.674	3.657	3/27/2012	2.298	2.287
15	2/7/2012	3.640	3.623	3/28/2012	2.276	2.266
16	2/8/2012	3.606	3.589	3/29/2012	2.255	2.244
17	2/9/2012	3.572	3.555	3/30/2012	2.234	2.223
18	2/10/2012	3.539	3.522	3/31/2012	2.213	2.203
19	2/11/2012	3.506	3.489	4/1/2012	2.192	2.182
20	2/12/2012	3.473	3.457	4/2/2012	2.172	2.162
21	2/13/2012	3.440	3.424	4/3/2012	2.152	2.141
22	2/14/2012	3.408	3.392	4/4/2012	2.131	2.121
23	2/15/2012	3.376	3.361	4/5/2012	2.112	2.102
24	2/16/2012	3.345	3.329	4/6/2012	2.092	2.082
25	2/17/2012	3.314	3.298	4/7/2012	2.072	2.063

Example Manufacturer Calibration Form: HDR ¹⁹²Ir

Certificate For Sealed Sources

Issue Date: 2012-01-16 ⁽¹⁾

Product Code:

REF	105002
SN	D36E-0374
LOT	HDR011312

Serial no. Transport Container: 2392C6
Serial no. Check Cable: N/A
Certificate Number: FUwNz U0J0r v3V6G ad2vp 60

Source Specification

Reference Air Kerma Rate: 43.84 mGy h⁻¹ +/- 5% at 1m ⁽²⁾
Measurement Reference Date: 2012-01-17 18:00 CET ⁽¹⁾
Apparent Activity: 398 GBq (10.8 Ci) at measurement reference date. ^(3,4)

Source Type: MICROSELECTRON-HDR
Capsule dimensions: 0.9 mm diameter, 4.5 mm length
Source pellet dimensions: 0.6 mm diameter, 3.5 mm length
Source pellet form: Solid Iridium
Radionuclide: Ir-192
Encapsulation: single
Capsule material: stainless steel, AISI 316L
ISO Classification: ISO/99/C63211
Special form certificate number: D/0070/S-96

Quality Control

Laser Weld Visual Check: Passed
Source Capsule Integrity (15 N pull test): Passed
Leakage Test: Passed ⁽⁵⁾
Surface Contamination test: < 185 Bq (5 nCi) ⁽⁶⁾

The undersigned, authorized officer of QSA Global, Inc. certifies that this source complies with the requirements of ISO2919 and that all of the information given in this certificate is true and correct.

Quality Assurance



⁽¹⁾ Date Format yyyy-mm-dd.

⁽²⁾ Confidence level of 99.7%.

⁽³⁾ The apparent activity is determined by applying a conversion factor (0.110 mGy m²h⁻¹GBq⁻¹) to the measured gamma radiation output of the sealed source determined with a calibrated instrument. The instrument is traceable to the National Institute of Standards & Technology. (NIST)

⁽⁴⁾ The apparent activity is the Iridium-192 activity; other radionuclides not detectable.

⁽⁵⁾ Leakage test method according to ISO9978 method Liquid nitrogen bubble test (6.2.4).

⁽⁶⁾ Surface contamination test according to ISO9978 method Wet wipe test (5.3.1).

⁽⁷⁾ The quality assurance system of QSA Global Inc. is certified by Lloyd's Register Quality Assurance (LRQA) according to ISO 9001 and ISO 13485.



QSA GLOBAL

40 North Avenue Burlington, MA 01803 1(781) 272-2000

Example Manufacturer Calibration Form: HDR ^{192}Ir

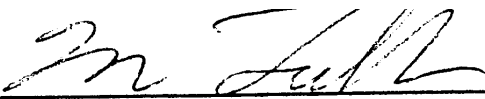
Source Specification

Reference Air Kerma Rate: 43.84 mGy h⁻¹ +/- 5% at 1m (2)

Measurement Reference Date: 2012-01-17 18:00 CET (1)

Apparent Activity: 398 GBq (10.8 Ci) at measurement reference date. (3,4)

Quality Assurance



(1) Date Format yyyy-mm-dd.

(2) Confidence level of 99.7%. **k = 3**

(3) The apparent activity is determined by applying a conversion factor (0.110 mGy m² h⁻¹ GBq⁻¹) to the measured gamma radiation output of the sealed source determined with a calibrated instrument. The instrument is traceable to the National Institute of Standards & Technology. (NIST)

Take Home Message

- QMP is a complex, systems concept
- QMP contains many familiar items – coordination is key
- Many societal guidelines available for brachytherapy QMP elements
- QMP should be specific to equipment and department
 - no “template” QMP, only guidance
 - regular, independent departmental review is desirable
- Forms help formalize QMP goals and make tasks consistent
- e-forms provide robust documentation, but can be altered
- Balance tension of form constancy and form advancements
- TG-100 and international error databases may alter current QMP focus

Further Reading

Nath, et al. Med Phys 1997;24:1557-98.

Thomadsen, 1999. Achieving Quality in Brachytherapy

Thomadsen, Williamson, Rivard, and Meigooni. Med Phys 2008;35:4708-23.

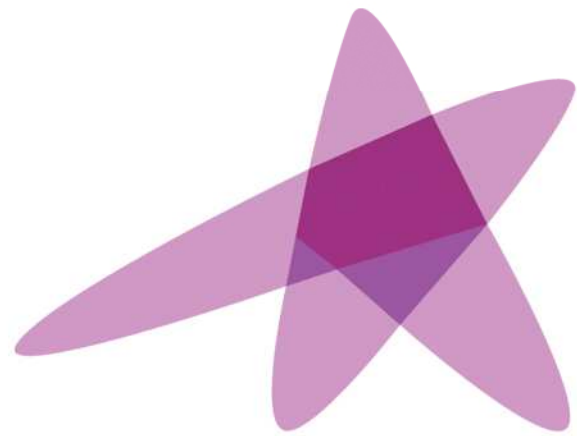
Thomadsen, et al. Prac Radiat Oncol 2014;4:65-70.

Venselaar and Perez-Calatayud, 2004. ESTRO Booklet 8.

Acknowledgements

Bruce Thomadsen, University of Wisconsin, USA





ESTRO

School



UNIVERSITÉ
LAVAL



Future Perspectives I: Tracking Technologies in Brachytherapy

Prof. Luc Beaulieu, Ph.D., FAAPM

*1- Département de physique, de génie physique et d'optique, et
Centre de recherche sur le cancer, Université Laval, Canada*

*2- Département de radio-oncologie et Centre de recherche du CHU
de Québec, CHU de Québec, Canada*

Vienna, May 29 – June 1 2016



Disclosures

- I am actively involved in the development of tracking systems for brachytherapy
- I hold research contracts and grants with:
 - Canada's NSERC Industrial Research Chair
 - Elekta
 - Philips

Learning Objectives

- Tracking technologies for brachytherapy
 - What are they?
 - How they work?
- Provide examples of use
- Discuss other potential applications

Tracking → Real-time Guidance



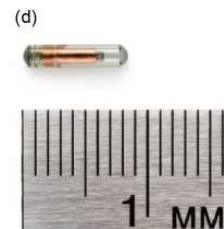
Tracking in Brachytherapy?

- Position of needle, catheter or applicator in real-time
 - Angulation/rotation
 - On the fly decision -> replanning
- Automated, fast and accurate channel reconstruction
 - Wrong connection between transfer tube and afterloader
- Potentially tracking organ motion/deformation
- Enabling new brachytherapy and interventional procedures

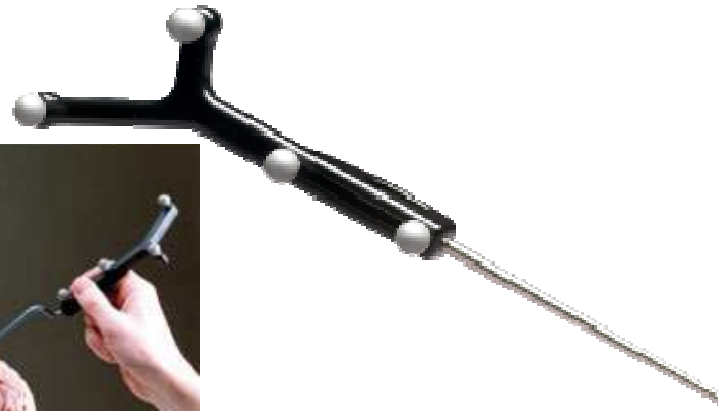
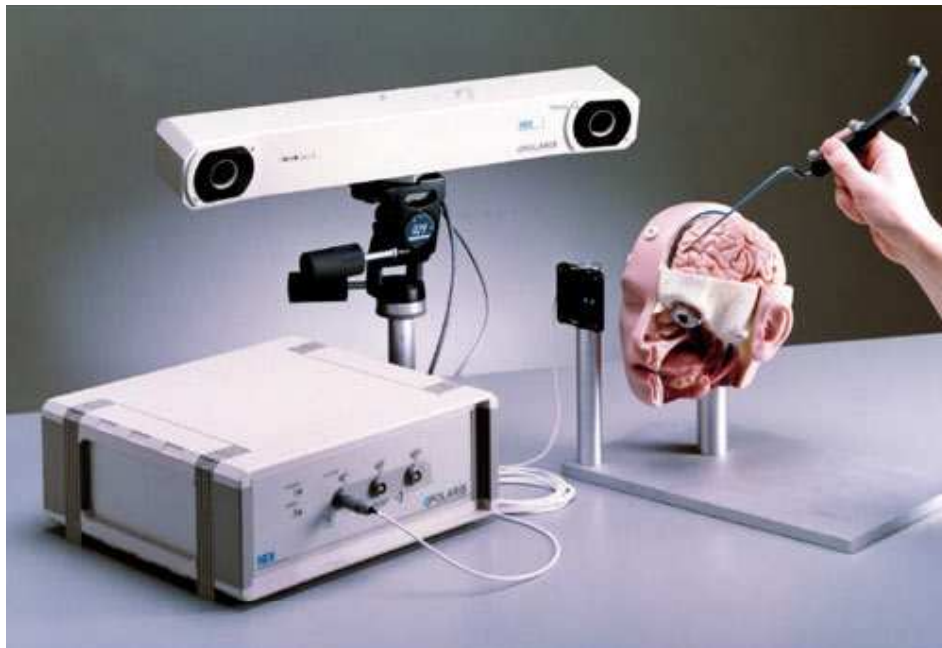
Potential Technologies

- Image-based tracking: CT, MR or US
- Real-time tracking
 - Optical IR tracking
 - Camera-based (Xbox style!)
 - EM tracking
 - Optical Fiber Shape Sensing (Bragg Grating)
- MR with active coils
- ...

Tracking in RT



IR/Optical Tracking



Limited to line of sight

- Same for white light camera

Potential Technologies

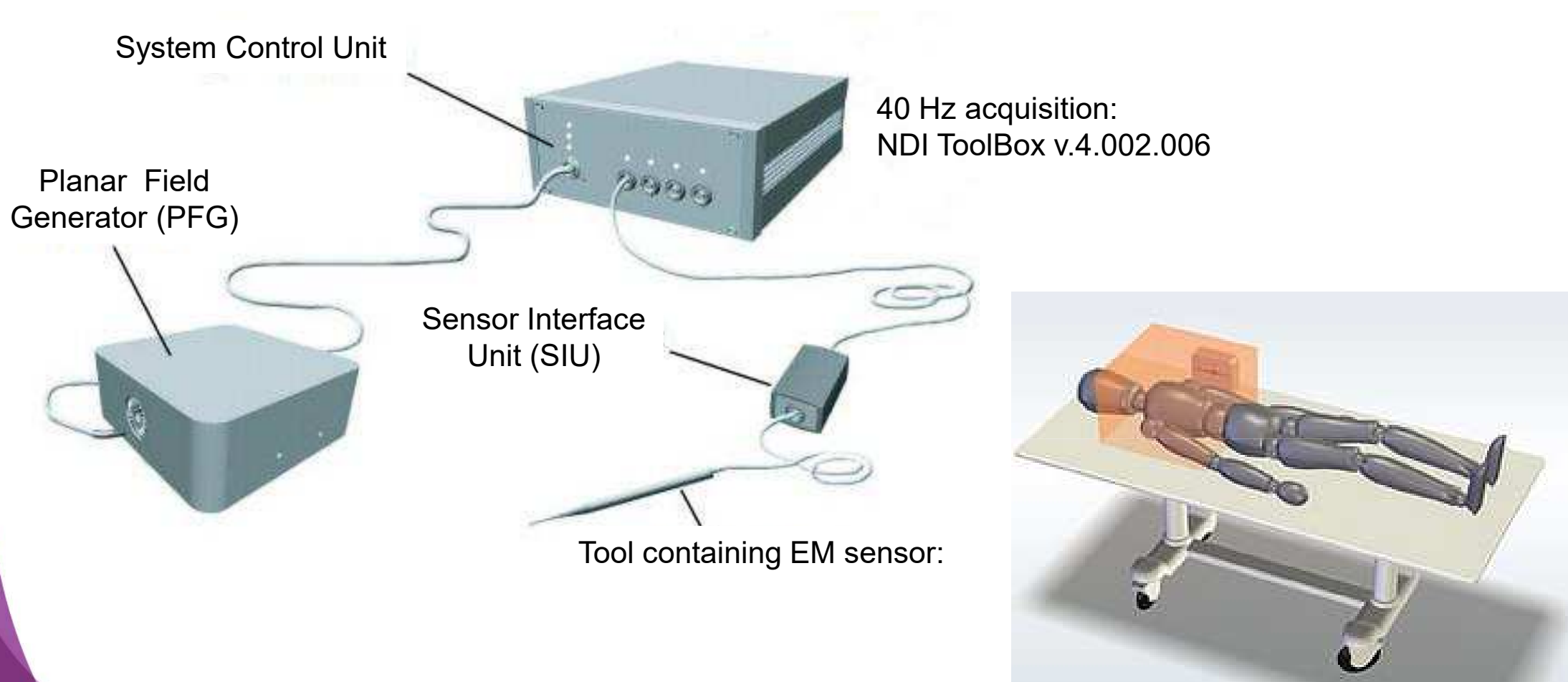
- Real-time tracking – no line of sight needed
 - EM tracking (CT and US compatible)
 - Optical Fiber Bragg Grating (CT, US and MR-compatible)
 - <https://www.nasa.gov/feature/fiber-optic-sensing>

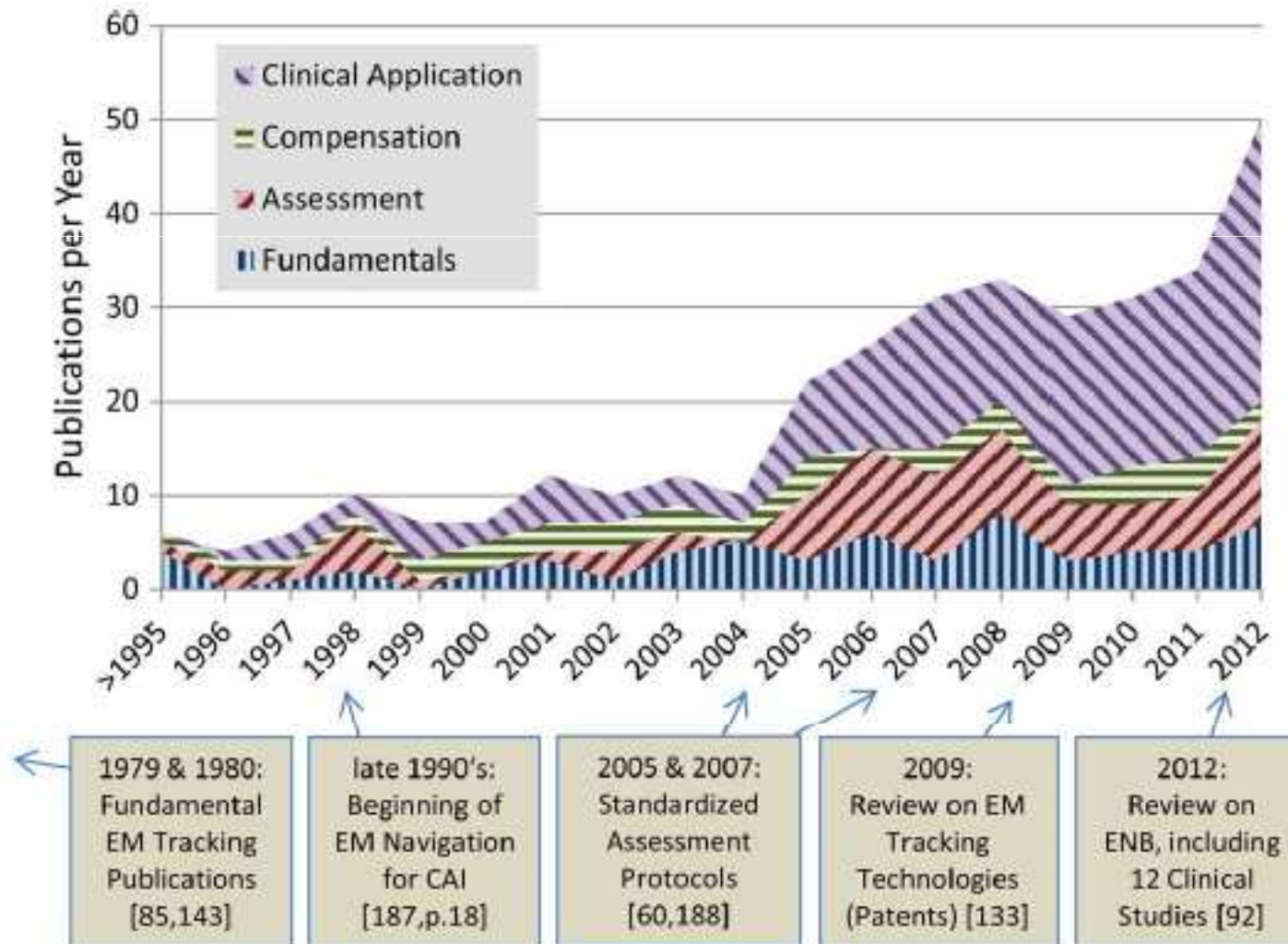
Electromagnetic tracking system (EMTS)

- **Electromagnetic Tracking in Medicine—A Review of Technology, Validation, and Applications.** Franz et al., IEEE Transactions on Medical Imaging **33** (2014)
- **Electromagnetic tracking for catheter reconstruction in ultrasound-guided high-dose-rate brachytherapy of the prostate.** Bharat S, Kung C, Dehghan E, Ravi A, Venugopal N, Bonillas A, Stanton D and Kruecker J. Brachytherapy 13 (2014) 640–50
- **EM-Navigated Catheter Placement for Gynecologic Brachytherapy: An Accuracy Study.** Mehrtash A, Damato A, Pernelle G, Barber L, Farhat N, Viswanathan A, Cormack R and Kapur T. Proc Soc Photo Opt Instrum Eng (2014) 9036 90361F
- **A system to use electromagnetic tracking for the quality assurance of brachytherapy catheter digitization.** Damato A L, Viswanathan A N, Don S M, Hansen J L and Cormack R A. Med. Phys. 41 (2014) 101702
- **Fast, automatic, and accurate catheter reconstruction in HDR brachytherapy using an electromagnetic 3D tracking system.** Poulin E, Racine E, Binnekamp D and Beaulieu L. Med. Phys. **42** (2015) 1227–32
- **Performance and suitability assessment of a real-time 3D electromagnetic needle tracking system for interstitial brachytherapy.** Boutaleb S, Racine E, Fillion O, Bonillas A, Hauvast G, Binnekamp D and Beaulieu L. J Contemp Brachytherapy 7 (2015) 280–9

Electromagnetic tracking system (EMTS)

Example: Aurora[®] V2 from Northern Digital Inc. (Ontario, Canada)





From Franz et al, 2014

EMTS Technologies

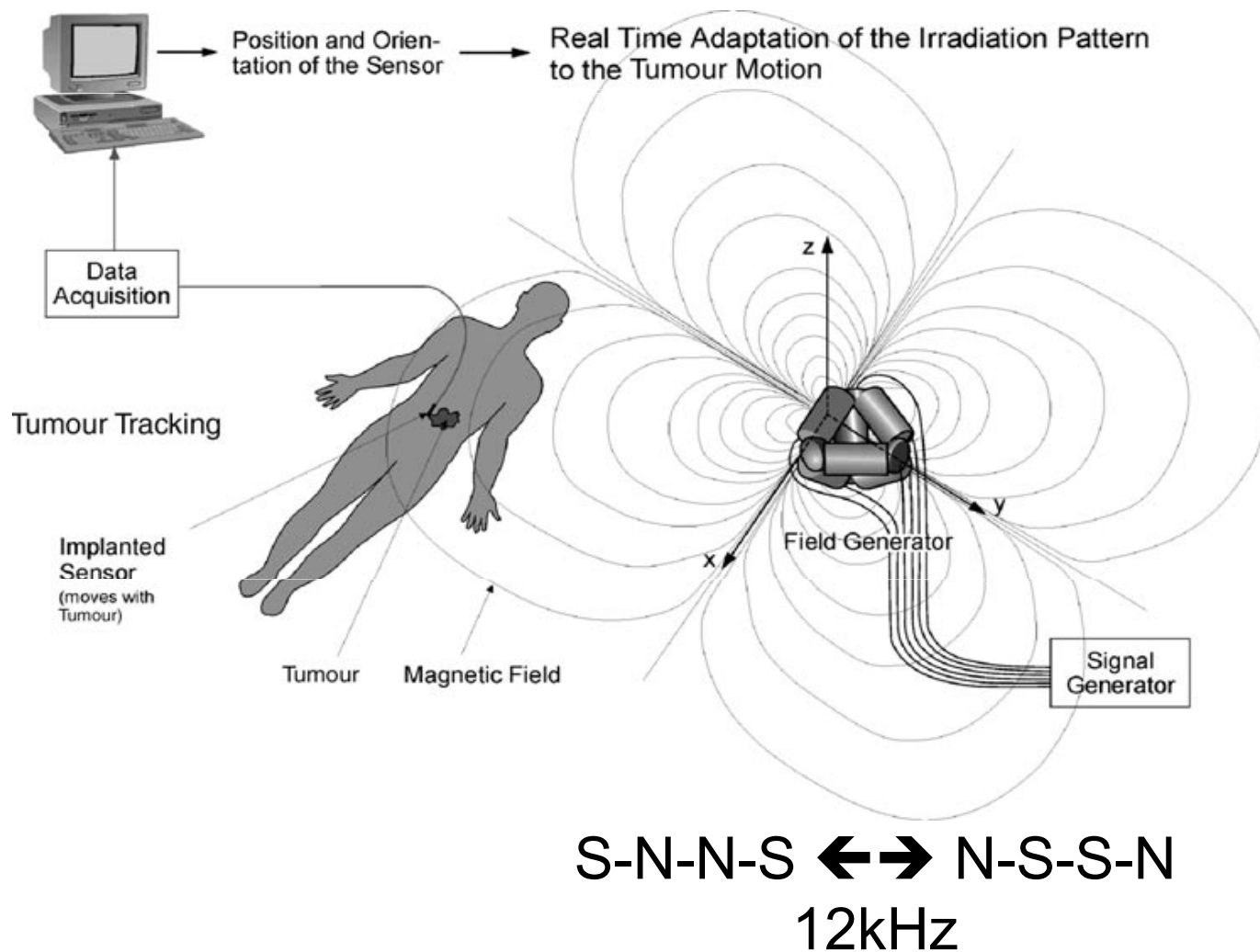
TABLE I
TYPES OF FIELD GENERATORS

Type	Typical Properties	Examples
Standard	Range: ca. 1 m, Size: cube-shaped, ca. 10–30 cm	NDI Tetrahedon FG [34], NDI Planar FG [117, p.6], Ascension Mid Range [117], Polhemus Standard FG [34], Medtronic AxiEM FG [146]
Flat	Range: ca. 1 m, Size: flat, ca. 50×40 cm	NDI Tabletop FG [102], NDI Window FG [207], Ascension Flat FG [117, p.5], SuperDimension location board [145], Biosense Webster location pad [144]
Mobile	Range: ca. 0.2 m, Size: small, < ca. 10 cm	NDI Compact FG [39], NDI Handheld FG [142], Ascension Short Range FG [143], Polhemus Short Ranger [147], Smith&Nephew Donut FG [58], Cortrak Receiver Unit [81]
Long Range	Range: ca. 5 m, Size: ca. 50×50 cm	Polhemus Long Ranger [147]

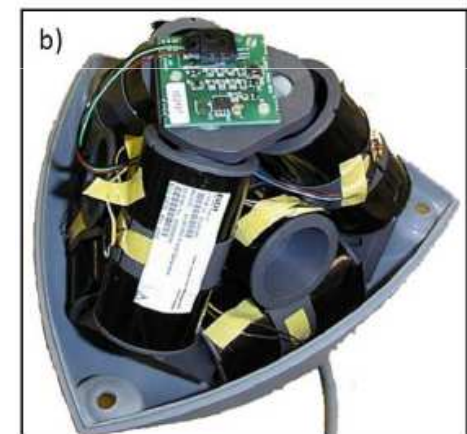
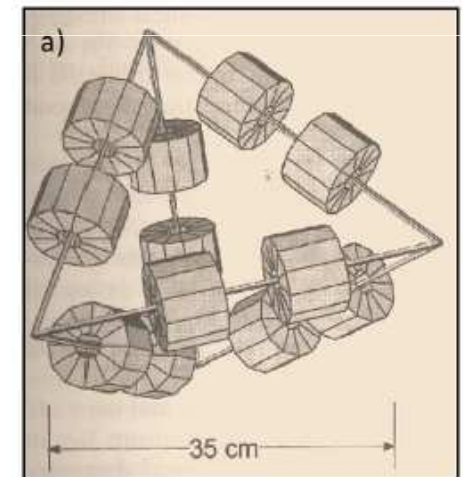
From Franz et al, 2014

Planar field generator - AC

- NDI Aurora system (théorie Seiler *et al.* PMB 2000)



Six differential coils



Planar field generator - AC

- Sensor = induction coil
- Alternating current of ± 2 A at 12 kHz for 3.3 ms each differential coil will create 6 different voltages at the sensor
- If 5DOF needle: 6 measurements and 5 unknown
- If 6DOF: 2 sensor coils

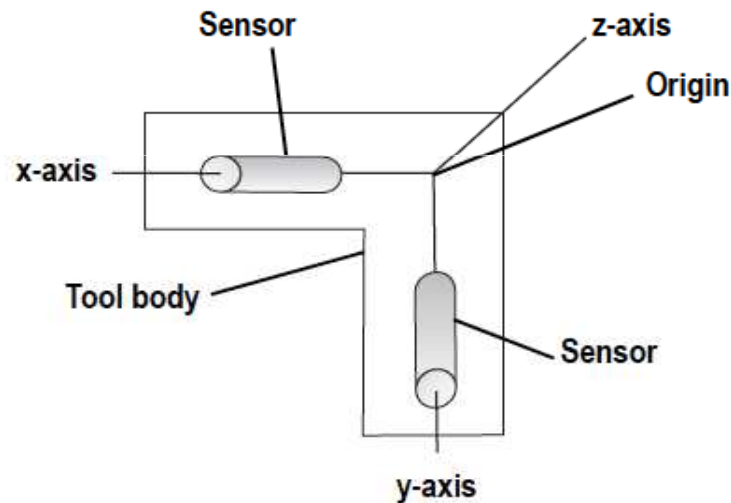


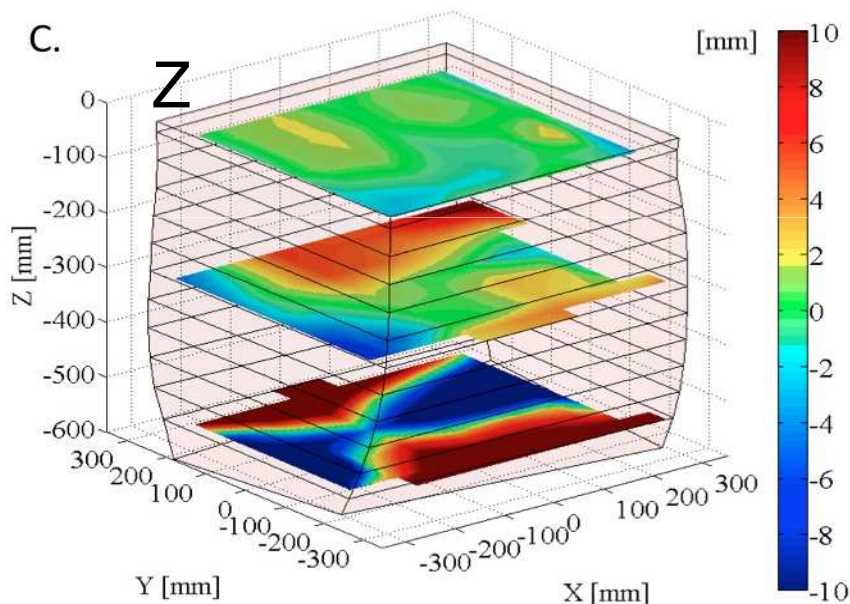
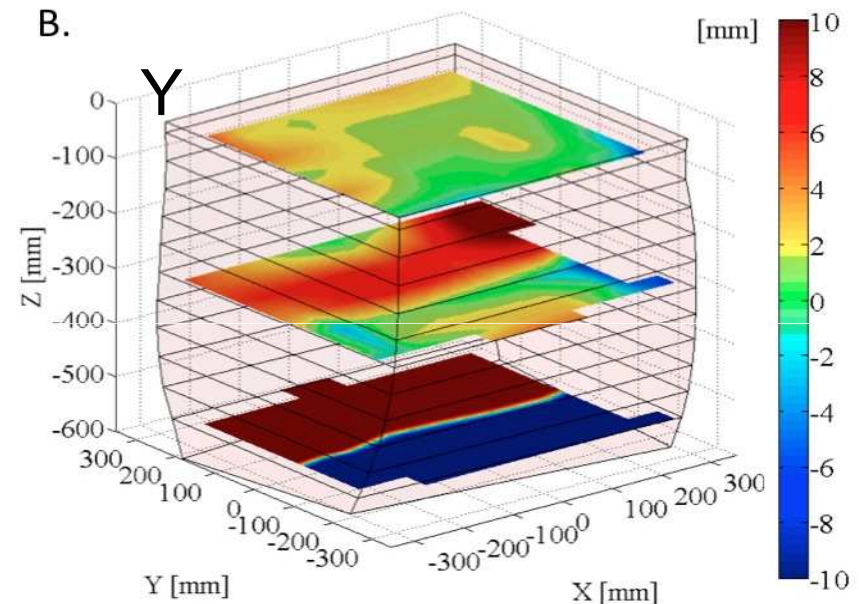
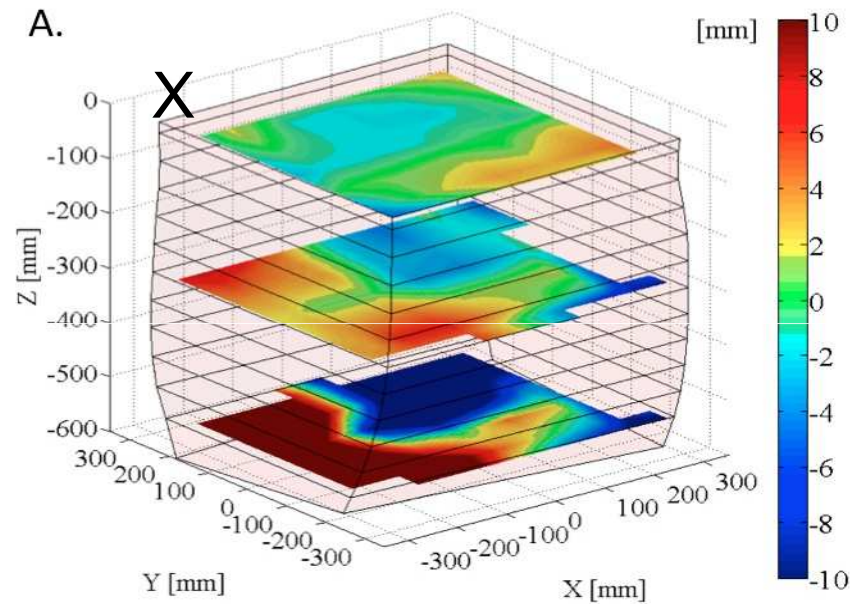
Figure 5-5 Sample 6DOF Tool

TABLE III
ASSESSMENT STUDY RESULTS

(a) **Standardized assessment according to Hummel *et al.* [61]:** Shows the mean RMS error over 90 positions as precision (Prec.) and the mean error of 161 measured 5 cm distances between these points as positional accuracy (Acc.). The rotational accuracy (Rot.) is given as the mean error of thirty-one 11.5° measurements for two axes, because 5 DoF sensors were used for most assessments.

<i>System</i> FG	Environment	Ref.	Pos. [mm]		Rot. [°]
			Prec.	Acc.	
<i>NDI Aurora</i>					
Planar FG	Laboratory	[59]	0.17	0.25	0.2/0.9
	Laboratory	[102]	0.20	0.80	1.2/1.0
	CT Suite	[102]	0.18	4.40	1.2/1.0
	X-Ray Suite	[15]	-	1.31	-
Tabletop FG	Laboratory	[102]	0.05	0.30	0.8/0.7
	CT Suite	[102]	0.05	0.90	0.8/0.7
Compact FG	Laboratory	[102]	0.05	0.50	1.0/0.8
	CT Suite	[102]	0.06	0.50	1.0/0.8
	US probes	[39]	<0.2	<2.5	<3
<i>Ascension microBird</i>					
Mid Range FG	Laboratory	[61]	0.14	0.69	0.04
<i>Ascension 3D Guidance</i>					
Mid Range FG	Laboratory	[117]	0.15	0.24	.05/.06
Flat FG	Laboratory	[117]	0.20	0.18	.02/.02

Detection Volume



- Detection volume if not perfectly cubic
- Deviation from expected positions increase with distance (Z) and close to edges (X,Y plane)
 - ± 1 mm in the first 30 cm
 - ± 10 mm at 55 cm
 - Angle $< 2\%$ first 30 cm
 - +8 to -10% at 55 cm

Brachytherapy Clinical Settings

Electromagnetic tracking for catheter reconstruction in ultrasound-guided high-dose-rate brachytherapy of the prostate

Shyam Bharat^{1,*}, Cynthia Kung¹, Ehsan Dehghan¹, Ananth Ravi², Niranjana Venugopal², Antonio Bonillas¹, Doug Stanton¹, Jochen Kruecker¹

¹*Department of Ultrasound Imaging and Interventions, Philips Research North America, Briarcliff Manor, NY*

²*Department of Radiation Oncology, Sunnybrook Health Sciences Center, Toronto, ON, Canada*

Brachytherapy **13** 640–50

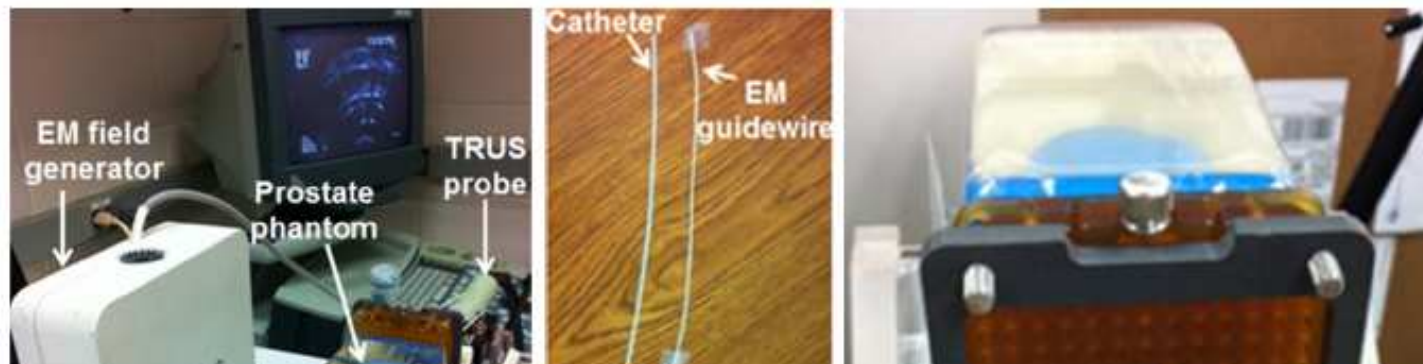
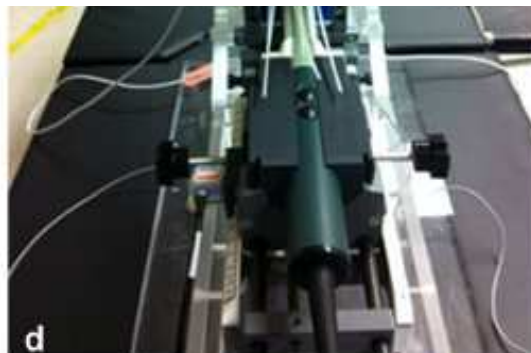


Table 6
Performance accuracy of EM catheter mapping system in the OR environment

	In-plane discrepancy (mm)			Out-of-plane discrepancy (mm)		
	Mean	Standard deviation	Maximum	Mean	Standard deviation	Maximum
EM vs. TRUS (in OR)						
Calibrating and testing in a “low distortion” environment	0.4	0.2	1	0.8	0.4	1.7
Calibrating in a “low distortion” environment and testing in distorting environment	1	0.2	1.5	1.1	0.8	1.9
Calibrating in a “low distortion” environment and testing in distorting environment, after updating the calibration in the distorting environment	0.3	0.2	1.1	1.1	0.8	1.9
Calibrating and testing in distorting environment	0.6	0.3	1.5	0.4	0.2	0.6

EM = electromagnetic; OR = operating room; TRUS = transrectal ultrasound.

In the OR, a “low distortion” environment refers to the absence of clinical equipment other than the treatment table and the ultrasound system near the testing area. A distorting environment refers to an environment that includes the presence of other clinically used brachytherapy equipment, such as leg stirrups, stepper holder, treatment planning computer, treatment afterloader, instrument table, and others, in their typical positions.



Interim Summary

- Needs to be used within the first 30 cm of the field generator
- Needle parallel to the field generator yield better angular accuracy
- Field generator generate heat: not under the patient
- Interference seen only for CRT monitor and bulky metallic arms (not shown)
 - Insensitive to US probe and needles/catheters

What can you do with this?

- Follow needles, catheters or an applicators in space (up to 6 DOF) in real-time (40 Hz)
 - Insertion guidance
 - Automatically reconstruct catheter/ applicator channels
 - Direct link to real-time imaging
 - Direct link to a optimization engine (background replanning)
 - ...

Auto. Catheter reconstruction

Fast, automatic, and accurate catheter reconstruction in HDR brachytherapy using an electromagnetic 3D tracking system

Eric Poulin and Emmanuel Racine

Département de physique, de génie physique et d'optique et Centre de recherche sur le cancer de l'Université Laval, Université Laval, Québec, Québec G1V 0A6, Canada and Département de radio-oncologie et Axe Oncologie du Centre de recherche du CHU de Québec, CHU de Québec, 11 Côte du Palais, Québec, Québec G1R 2J6, Canada

Dirk Binnekamp

Integrated Clinical Solutions & Marketing, Philips Healthcare, Veenpluis 4-6, Best 5680 DA, The Netherlands

Luc Beaulieu^{a)}

Département de physique, de génie physique et d'optique et Centre de recherche sur le cancer de l'Université Laval, Université Laval, Québec, Québec G1V 0A6, Canada and Département de radio-oncologie et Axe Oncologie du Centre de recherche du CHU de Québec, CHU de Québec, 11 Côte du Palais, Québec, Québec G1R 2J6, Canada

(Received 8 May 2014; revised 9 January 2015; accepted for publication 26 January 2015; published 18 February 2015)

Purpose: In high dose rate brachytherapy (HDR-B), current catheter reconstruction protocols are relatively slow and error prone. The purpose of this technical note is to evaluate the accuracy and the robustness of an electromagnetic (EM) tracking system for automated and real-time catheter reconstruction.

Methods: For this preclinical study, a total of ten catheters were inserted in gelatin phantoms with different trajectories. Catheters were reconstructed using a 18G biopsy needle, used as an EM stylet and equipped with a miniaturized sensor, and the second generation Aurora[®] Planar Field Generator from Northern Digital Inc. The Aurora EM system provides position and orientation value with precisions of 0.7 mm and 0.2°, respectively. Phantoms were also scanned using a μ CT (GE Healthcare) and Philips Big Bore clinical computed tomography (CT) system with a spatial resolution of 89 μ m and 2 mm, respectively. Reconstructions using the EM stylet were compared to μ CT and CT. To assess the robustness of the EM reconstruction, five catheters were reconstructed twice and compared.

Results: Reconstruction time for one catheter was 10 s, leading to a total reconstruction time inferior to 3 min for a typical 17-catheter implant. When compared to the μ CT, the mean EM tip identification error was 0.69 ± 0.29 mm while the CT error was 1.08 ± 0.67 mm. The mean 3D distance error was found to be 0.66 ± 0.33 mm and 1.08 ± 0.72 mm for the EM and CT, respectively. EM 3D catheter trajectories were found to be more accurate. A maximum difference of less than 0.6 mm was found between successive EM reconstructions.

Conclusions: The EM reconstruction was found to be more accurate and precise than the conventional methods used for catheter reconstruction in HDR-B. This approach can be applied to any type of catheters and applicators. © 2015 American Association of Physicists in Medicine. [<http://dx.doi.org/10.1118/1.4908011>]

Proof of concept

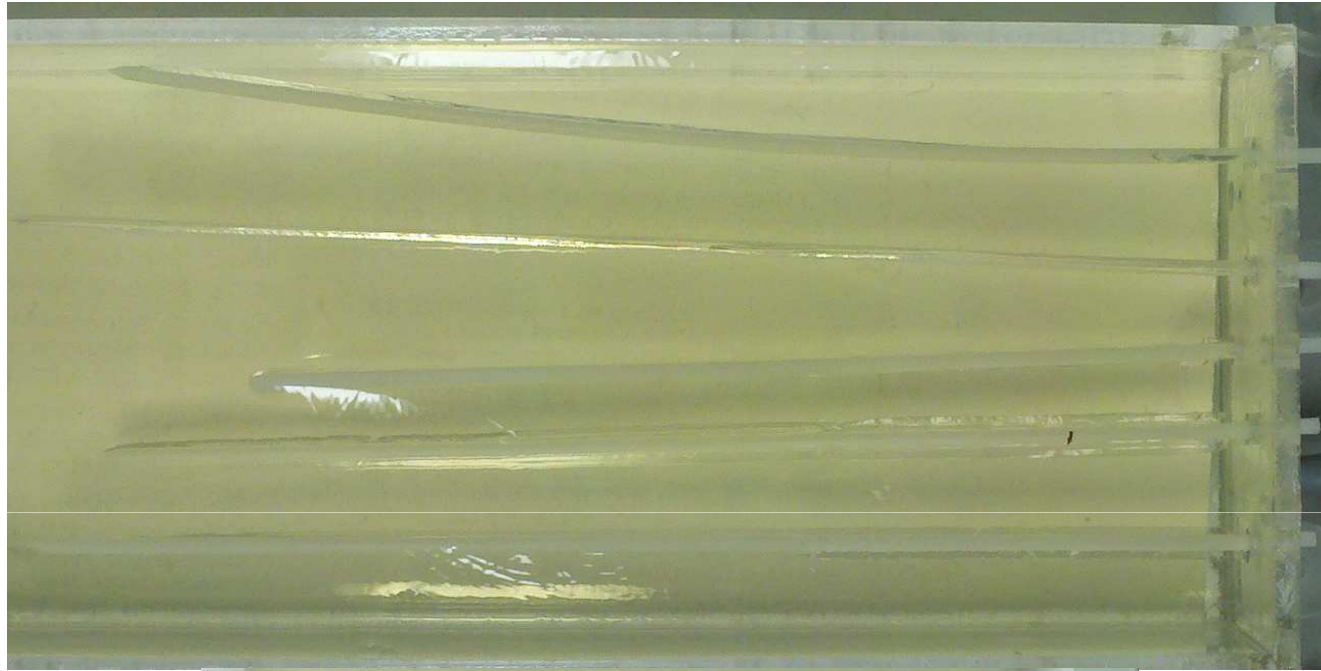
Fast (< 10 s par channel)

More precise than CT

Can do much more than what has been tested in this paper...

Auto. Catheter reconstruction

- 10 catheters were inserted in gelatin phantoms with different trajectories.

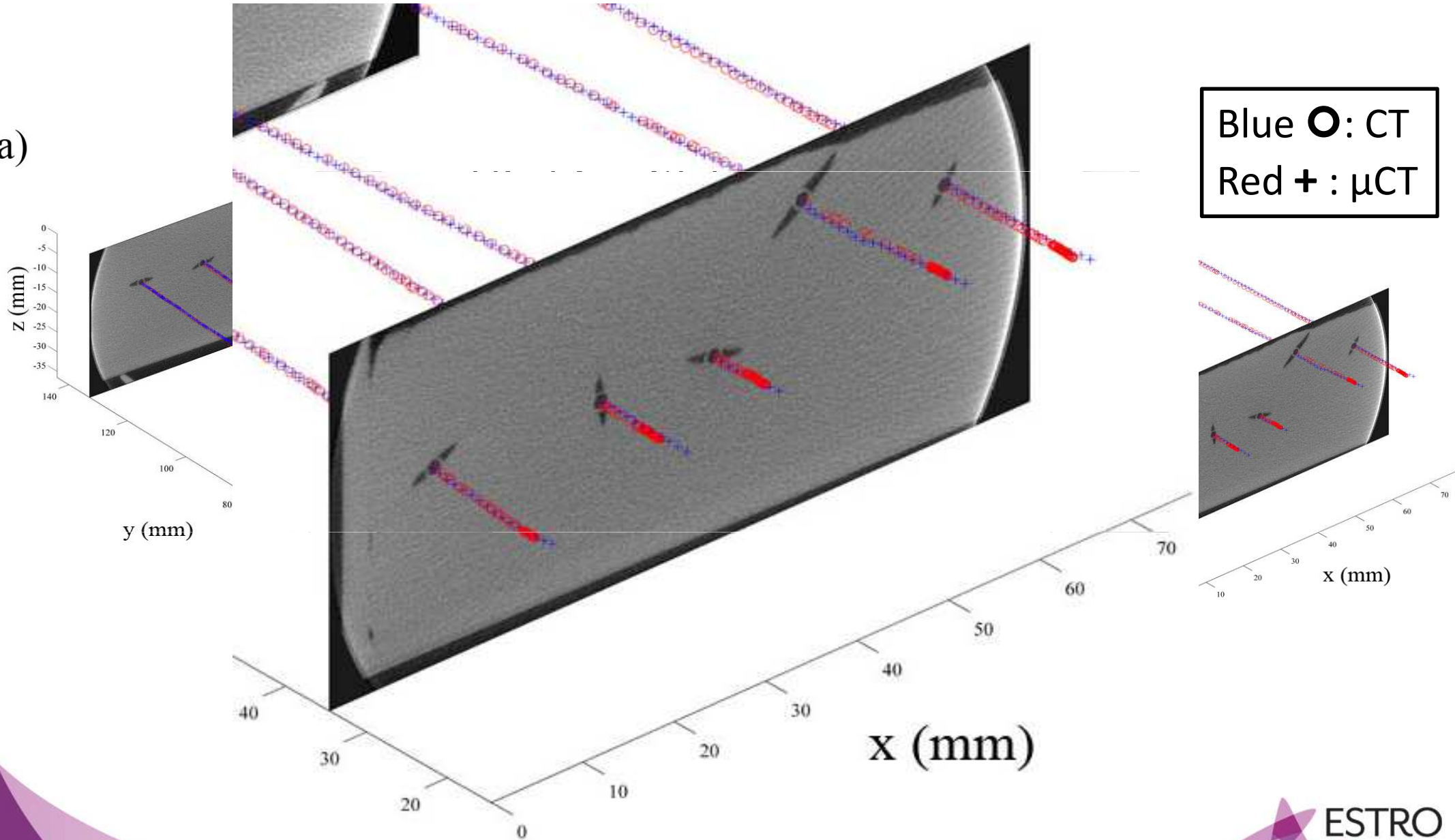


Auto. Catheter reconstruction

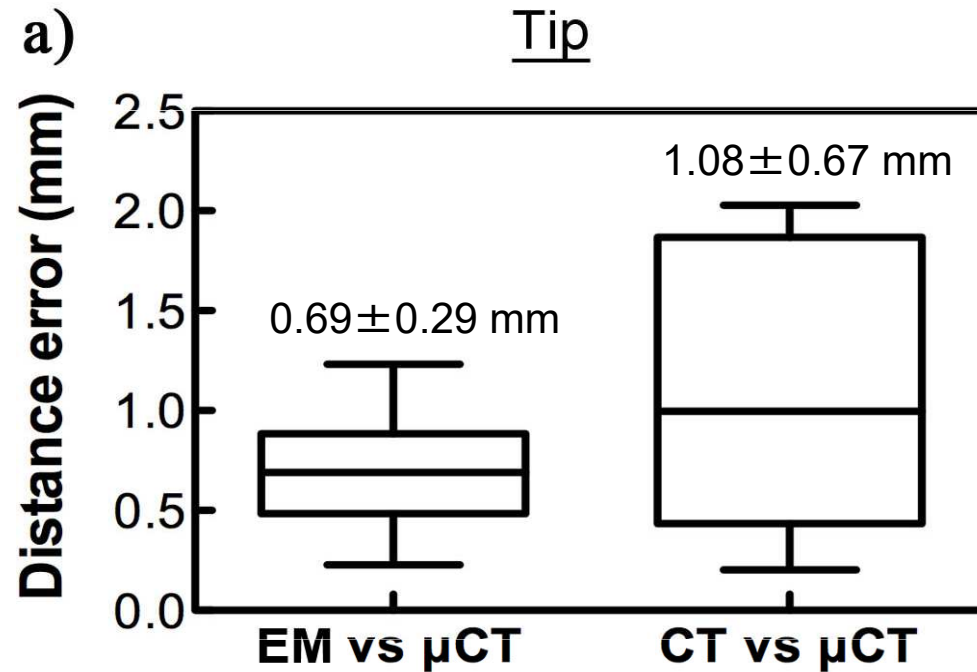
- EM reconstructions at 40 Hz
- μ CT reconstruction (GE) at 89 μm (reference)
- CT reconstructions (Philips BigBore) at 2 mm
- Reconstructions using the EM stylet were compared to μ CT and CT (3D distances used; tips as reference).
- To assess the robustness of the EM reconstruction, by reconstructing catheters multiple times.

Auto. Catheter reconstruction

a)



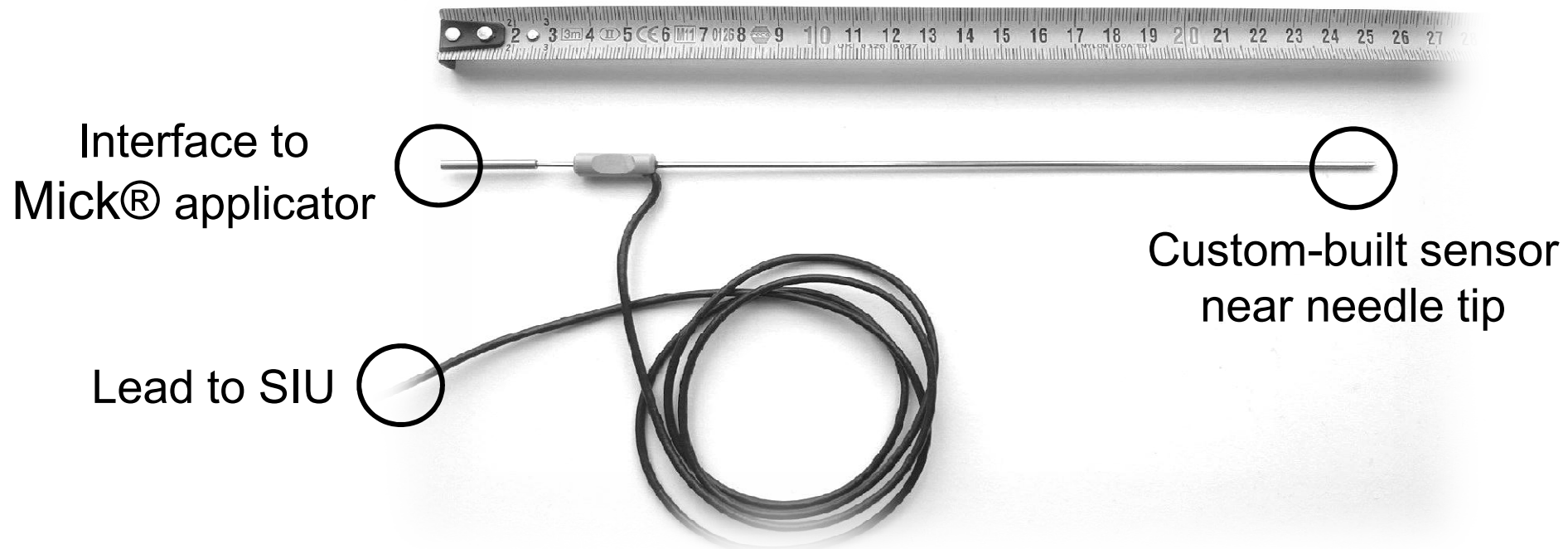
Auto. Catheter reconstruction



Unpaired Student t-test show statistically significance difference
Poulin et al, Medical Physics 2015;42(3):1227–32.

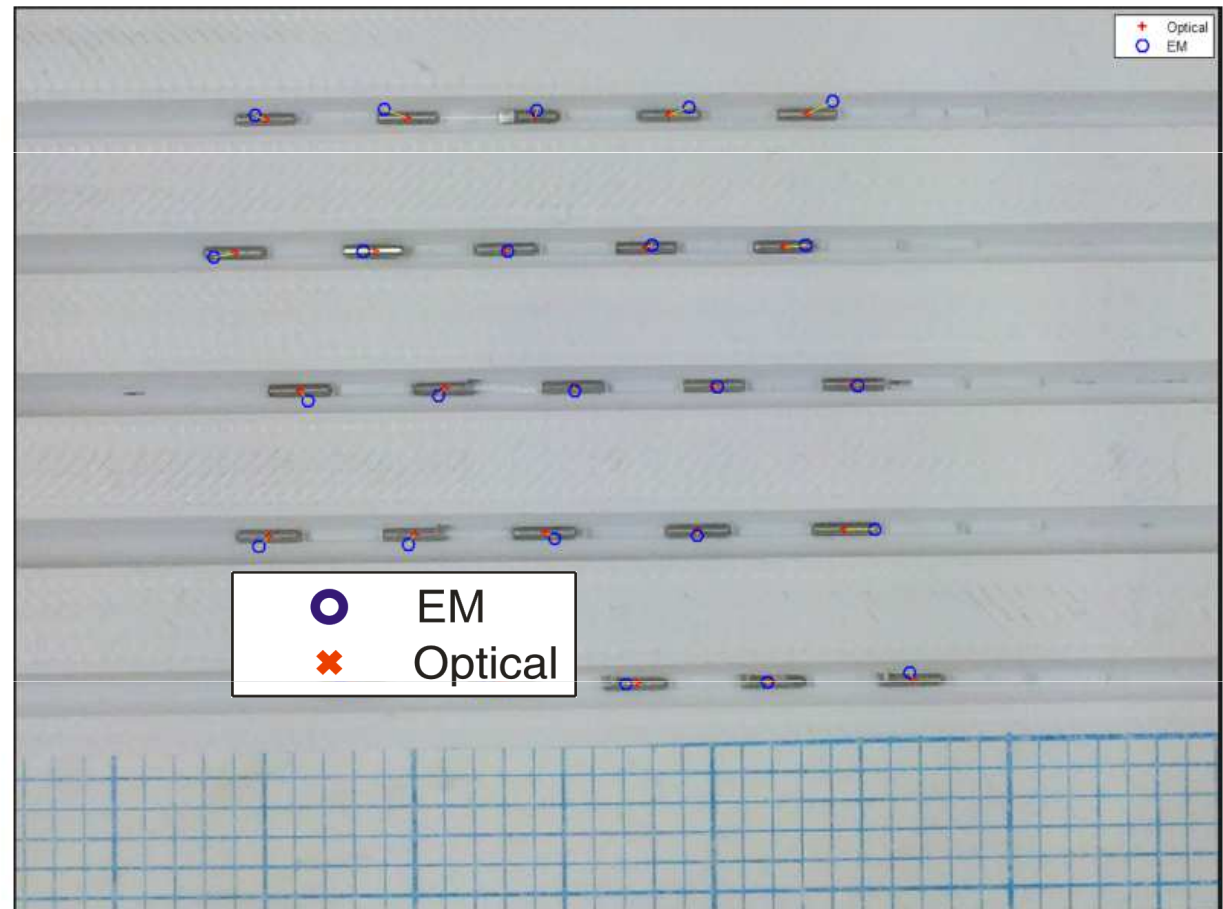
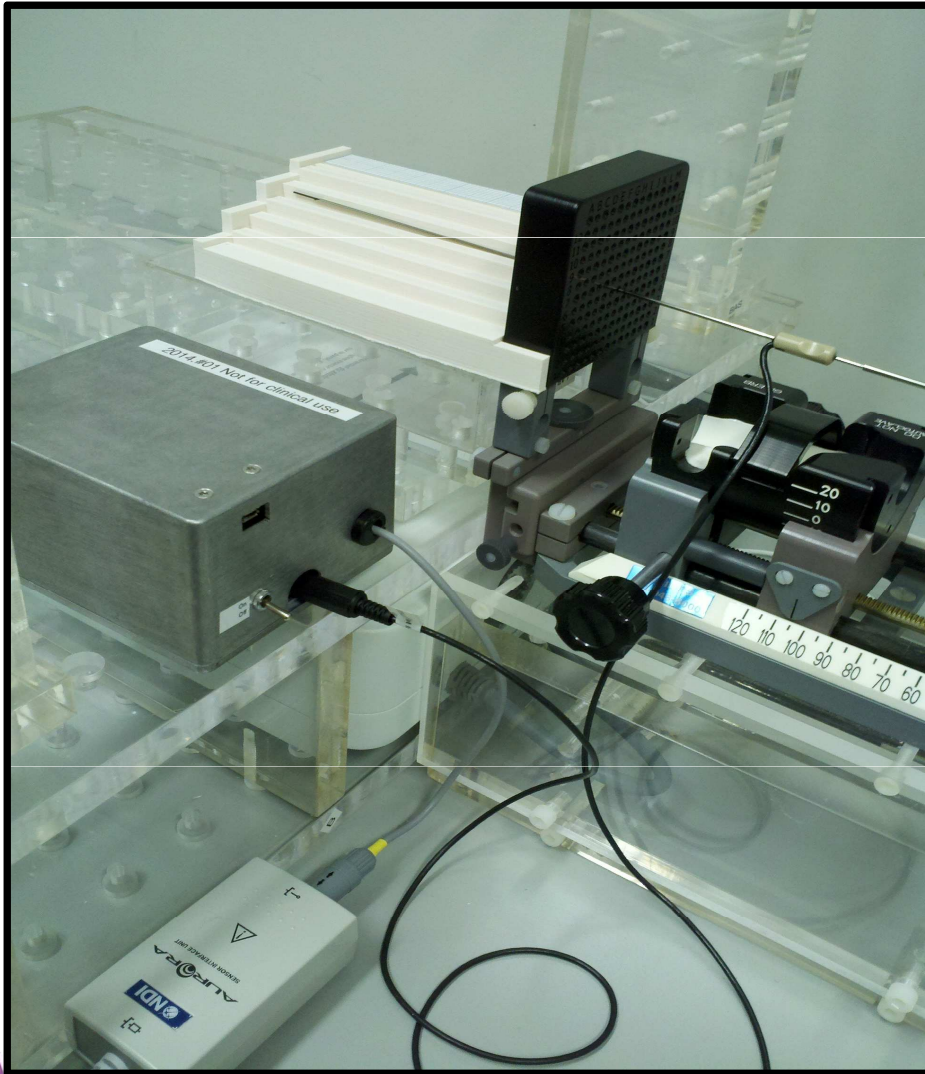
Seed drop position

A hollow brachytherapy electromagnetic needle prototype was recently developed by Philips Healthcare.



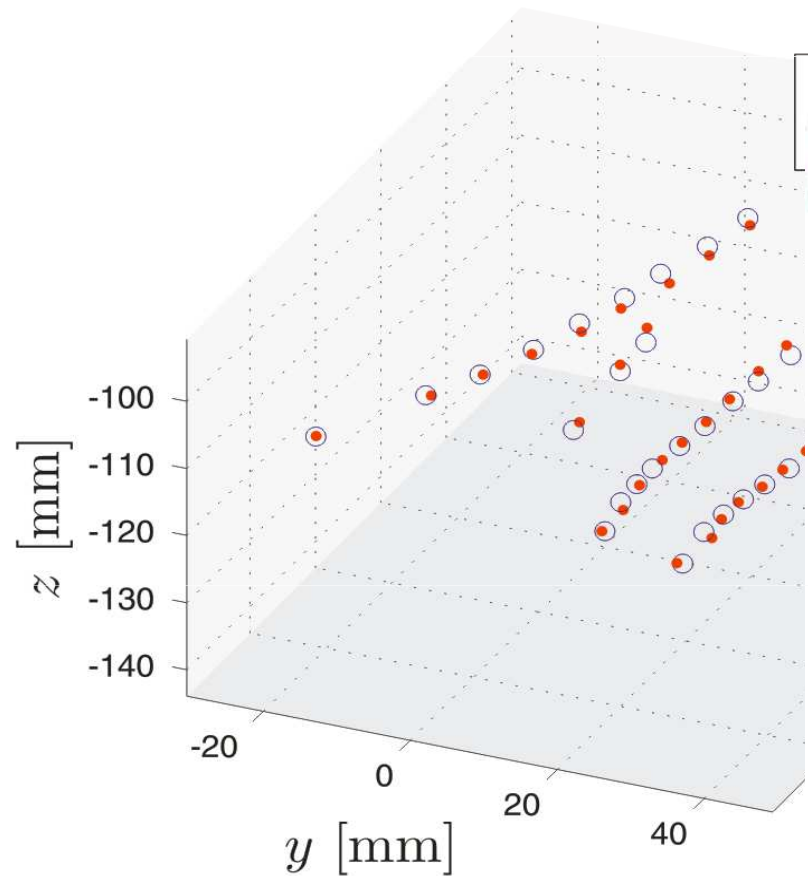
- ✓ Detects seed drops by exploiting local changes of electromagnetic properties in the medium.
- ✓ Preserves standard tacking capabilities.

Automated Seed Detection



Seed drop position

Registration of detected seed distributions. True seed positions were obtained from a μ CT scan (GE, 89 μ m slice thickness).

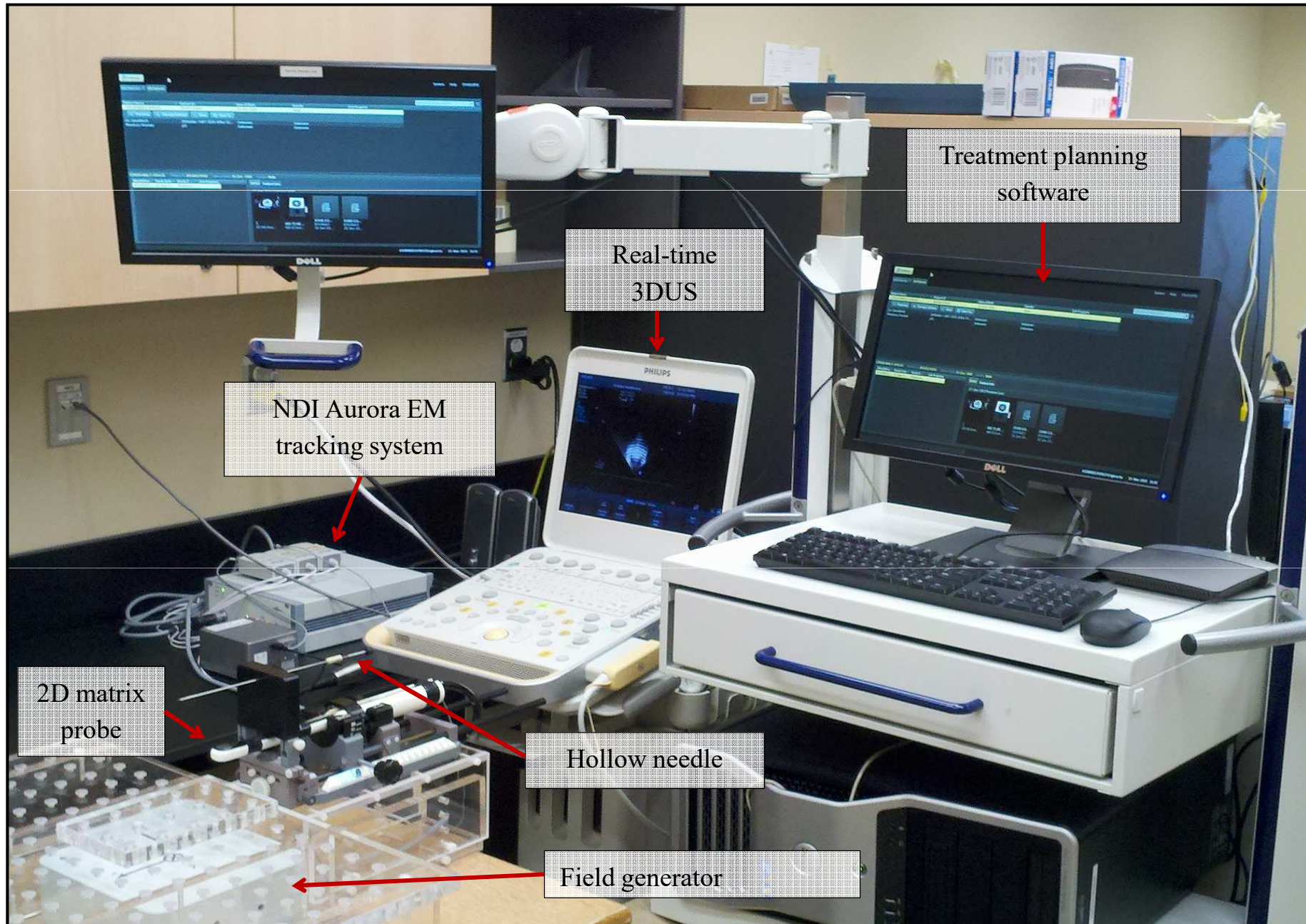


• μ -CT

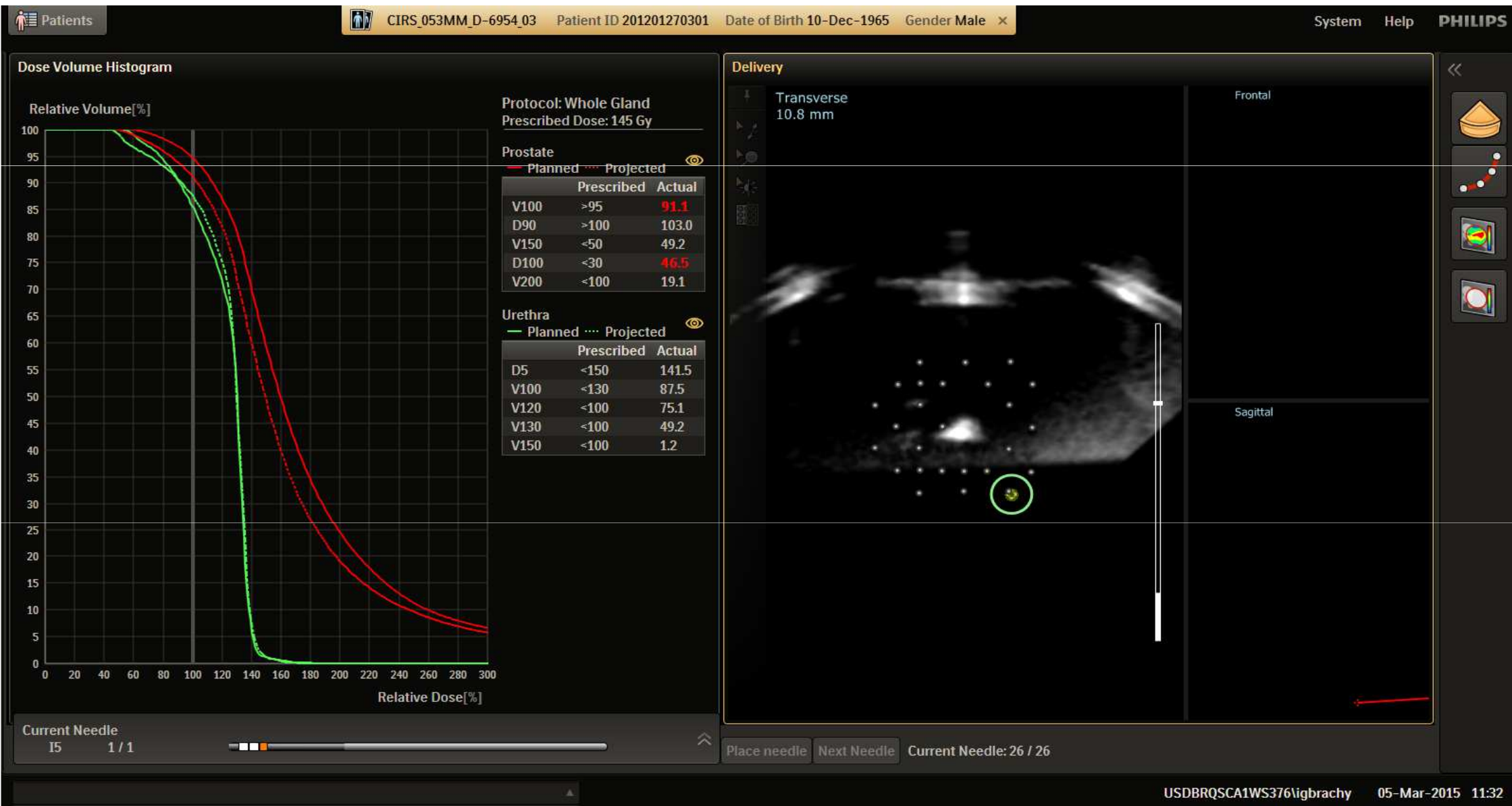
TABLE III. Statistics of the seed drop position estimates for the 3D characterization experiment.

	Error measurements [mm]			
	Minimum	Maximum	Average	Std dev.
$ e_x $	$0.0^{+0.1}_{-0.0}$	$0.6^{+0.5}_{-0.1}$	$0.2^{+0.5}_{-0.2}$	$0.1^{+0.3}_{-0.1}$
$ e_y $	$0.0^{+0.2}_{-0.0}$	$0.7^{+0.5}_{-0.2}$	$0.2^{+0.5}_{-0.2}$	$0.1^{+0.3}_{-0.1}$
$ e_z $	$0.1^{+1.0}_{-0.1}$	$2.1^{+1.0}_{-1.1}$	$0.4^{+1.0}_{-0.4}$	$0.4^{+0.5}_{-0.2}$
e_{3D}	$0.1^{+1.0}_{-0.1}$	$2.1^{+1.1}_{-0.8}$	$0.6^{+1.2}_{-0.5}$	$0.4^{+0.7}_{-0.2}$

Real-time EM Tracking System



Delivery and Feedback Loop



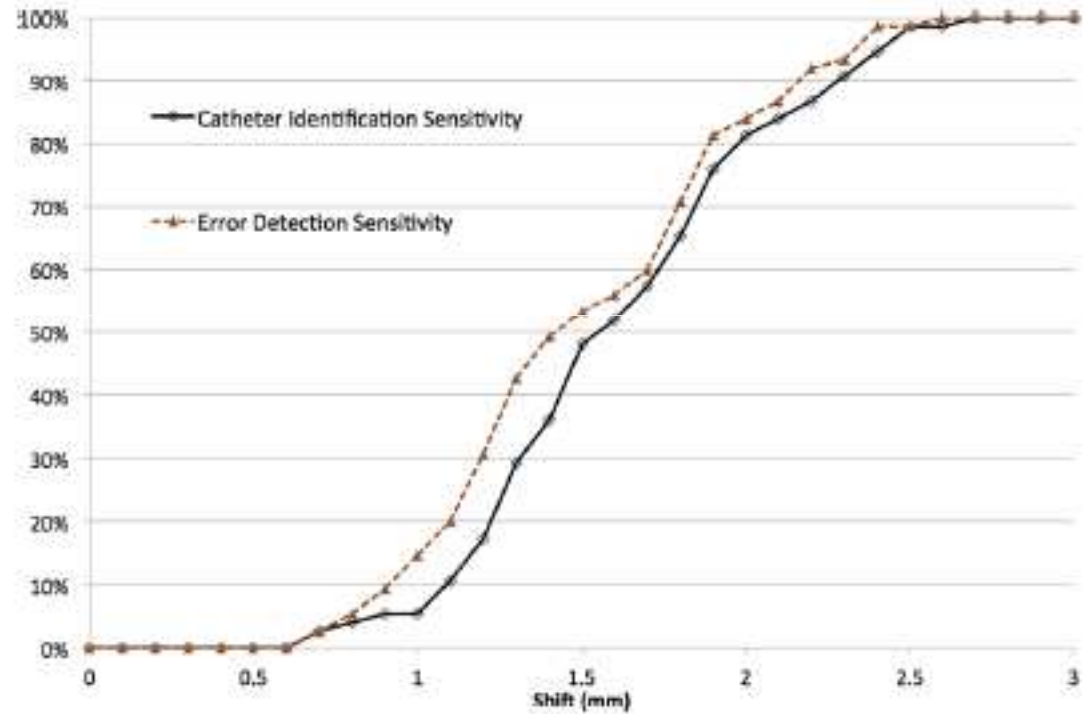
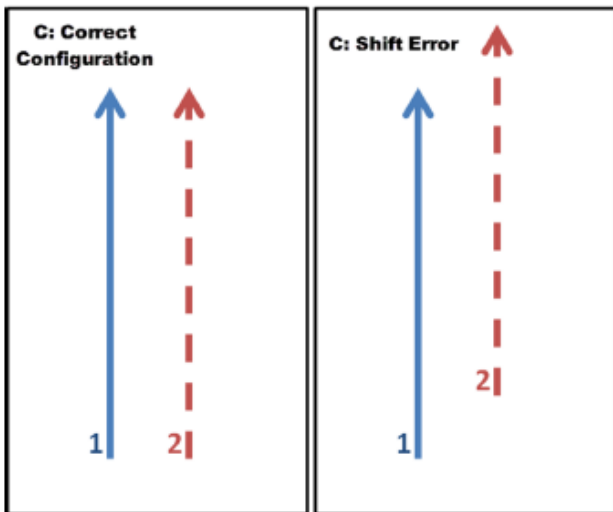
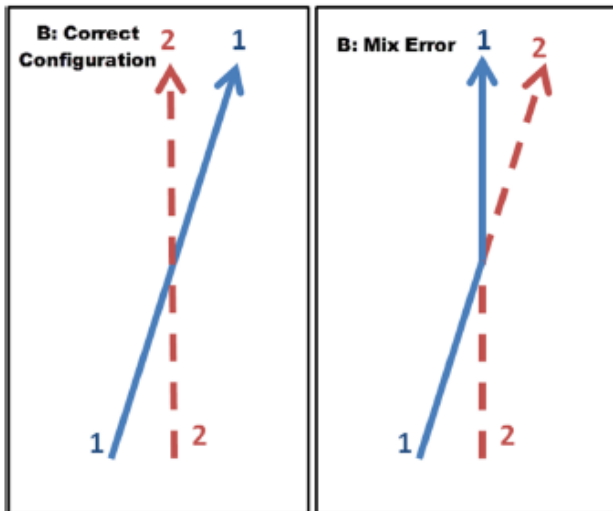
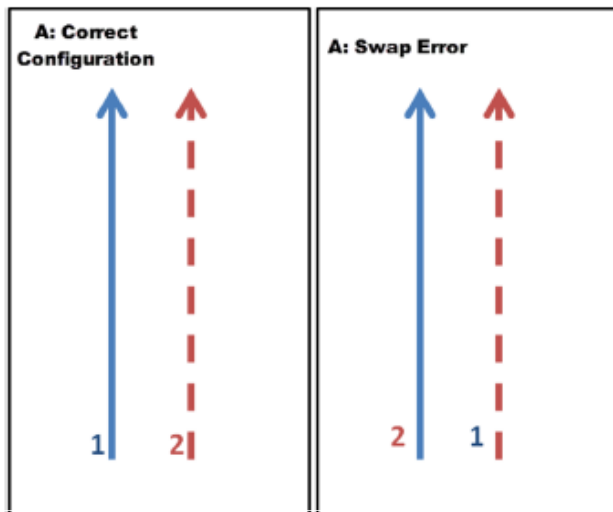


FIG. 5. Catheter identification and error-detection sensitivity as a function of shift size. Error-detection specificity was 100% for all shift sizes, and catheter-identification specificity was 100% for shifts ≥ 2.7 mm and $>99.7\%$ for all shifts.

Damato et al. *Med. Phys.* **41** 101702

Doing more?

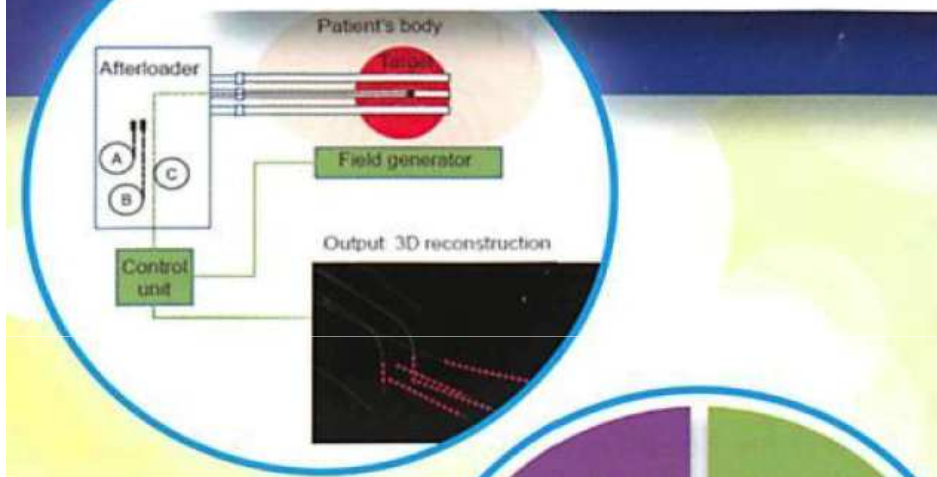
Flexitron 3rd DriveWire?



- Automated applicator/catheter reconstruction
- Online channel set-up QA

Treatment certainty

Adding certainty to safety by ensuring accurate delivery of the planned dose to both the target and the organs at risk.



Another possibility:
Embedded in-vivo dosimeter

Vision 2020 BrachyNext meeting, Miami 2014

Optical Tracking

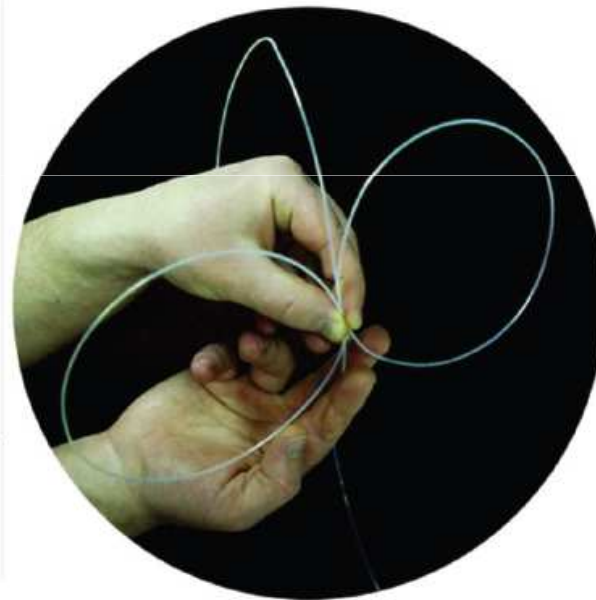
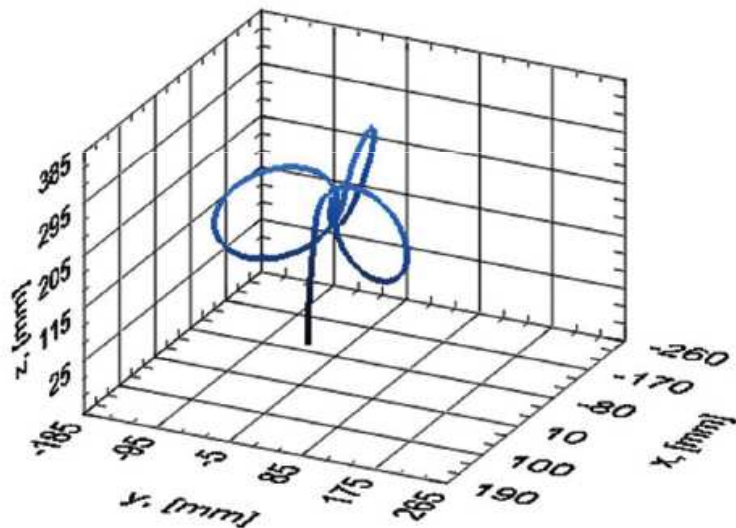
Fiber Shape Sensing

- **REVIEW ARTICLE: In-fibre Bragg grating sensors** *Measurement Science and Technology*. Rao Y-J. **8** (1997) 355–75
- **Optical Fiber-Based MR-Compatible Sensors for Medical Applications: An Overview**. Fabrizio Taffoni , Domenico Formica , Paola Saccomandi, Giovanni Di Pino and Emiliano Schena. *Sensors* 13 (2013), 14105-14120
- **Optical in-fiber bragg grating sensor systems for medical applications**. Y. J. Rao, D. J. Webb, D. A. Jackson, L. Zhang, and I. Bennion. *Journal of biomedical optics* 3 (1998), 38–44
- **3D flexible needle steering in soft-tissue phantoms using Fiber Bragg Grating sensors**. Abayazid M, Kemp M and Misra S. *ICRA (2013)* 5843–9
- **Real-Time Estimation of Three-Dimensional Needle Shape and Deflection for MRI-Guided Interventions**. Yong-Lae Park, Santhi Elayaperumal, Bruce Daniel, Seok Chang Ryu, Mihye Shin, Joan Savall, Richard J. Black, Behzad Moslehi, and Mark R. Cutkosky. *IEEE/ASME Transactions on Mechatronics* 15 (2010) 906 – 915

Fiber-optics Shape Sensing

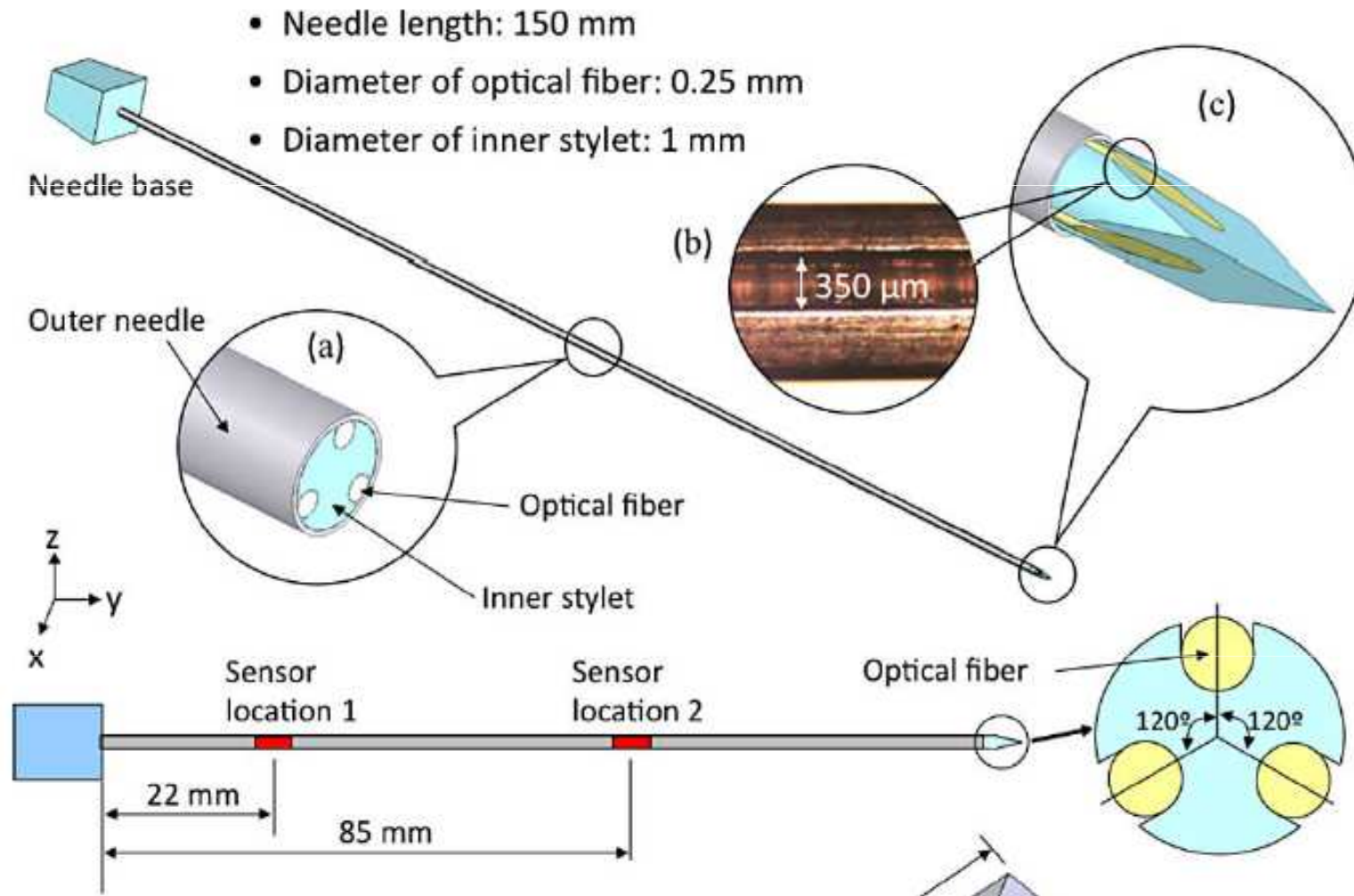
Fiber Bragg Grating (FBG)

- Down to 80 μm diameter fiber
- Femtoseconds laser
- 3 or more FBG etched within the fiber at various location along the needle or catheter or ...



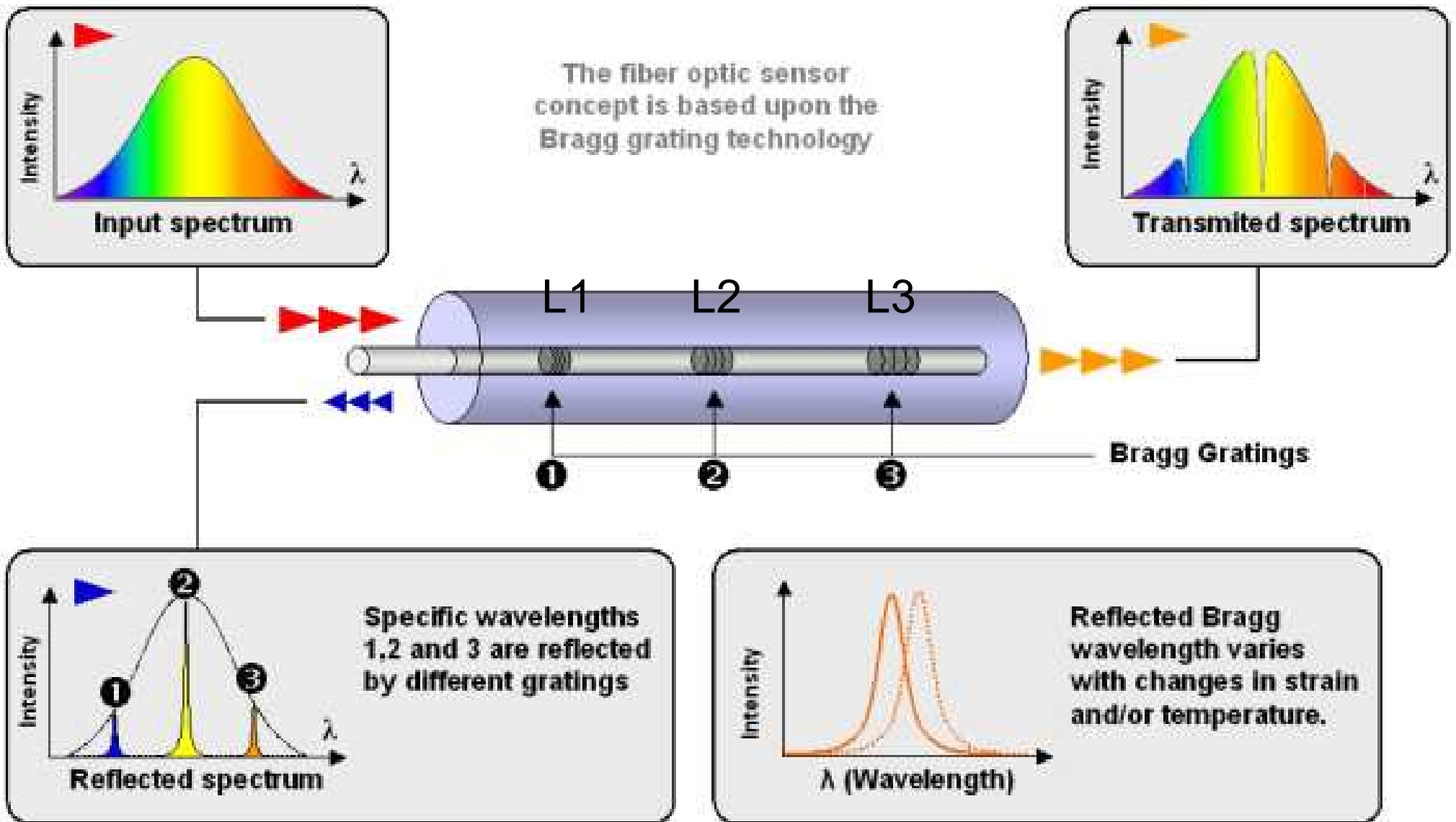
Credit: NASA

Fiber-optics Shape Sensing



Park et al, IEEE/ASME (2010); Tiffoni et al, Sensor (2013)

The fiber optic sensor concept is based upon the Bragg grating technology



$$\frac{\Delta\lambda_i}{\lambda_i} = k_s \varepsilon + k_T \Delta T$$

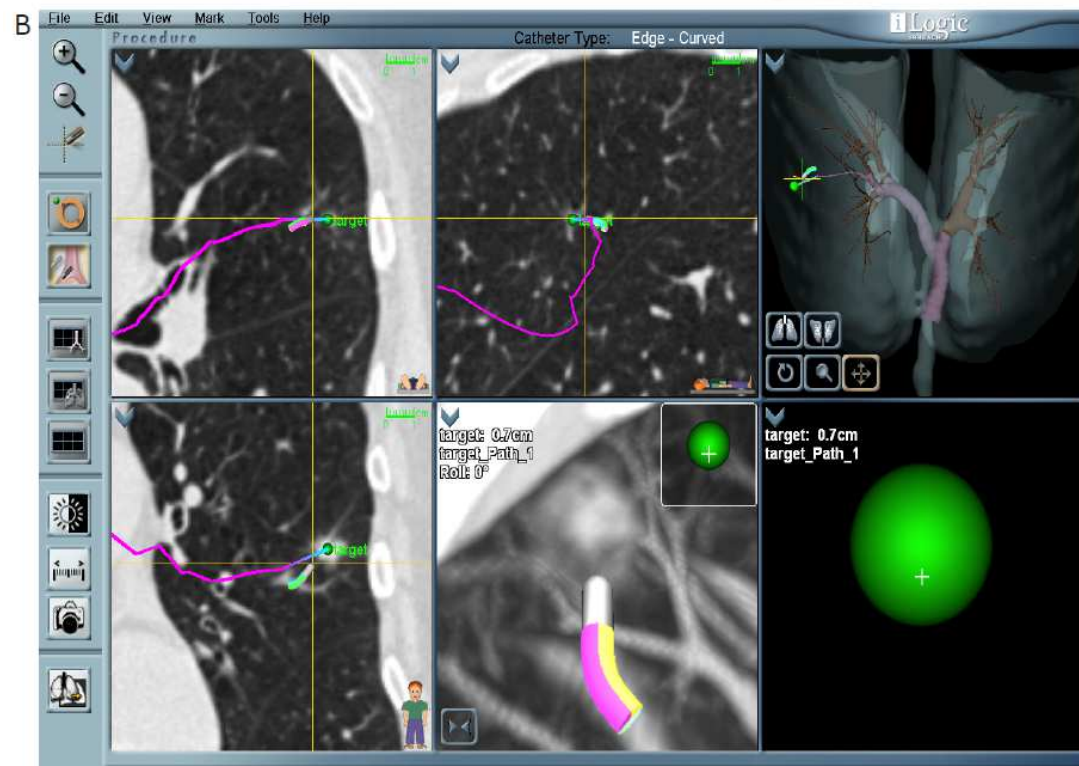
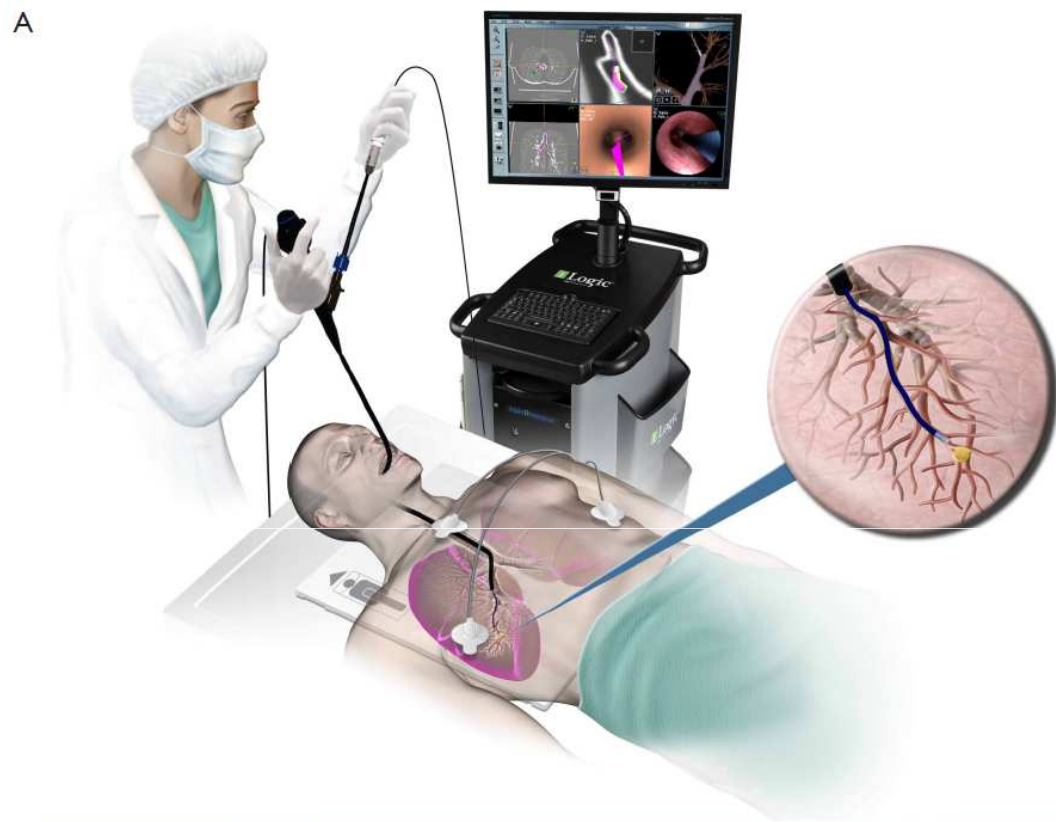
ε : strain

ΔT : temperature change

k : coefficients

Table 1. Performances and medical applications for MR-compatible FBG sensors.

Reference	Sensing Element	Measurand	Application Field	Characteristics
Rao <i>et al.</i> , 1998 [18]	FBG	Temperature	Hyperthermic treatment	Accuracy ≈ 0.8 °C, range 20 °C–60 °C, Resolution ≈ 0.2 °C
Webb <i>et al.</i> , 2000 [20]	FBG	Temperature	Hyperthermic treatment	Resolution ≈ 0.2 °C
Sacomandi <i>et al.</i> , 2012–2013 [21,22]	FBG	Temperature	Hyperthermic treatment	Range up to 80 °C
Schena <i>et al.</i> , 2013 [23]	FBG	Temperature	Hyperthermic treatment	Range 20 °C–80 °C, sensitivity ≈ 8.4 pm·°C ⁻¹
Gowardhan <i>et al.</i> , 2007 [24]	FBG	Temperature	Cryotherapy	Minimum value ≈ -60 °C
Samset <i>et al.</i> , 2005 [25]	FBG	Temperature	Cryotherapy	Range -195 °C–100 °C
Weherle <i>et al.</i> , 2001 [26]	FBG	Inspiratory volume	Respiratory monitoring	Range 60 mL–500 mL, Frequency up to 10 Hz
Witt <i>et al.</i> , 2012 [27]	FBG	Thoracic movements	Respiratory monitoring	/
De jonckheere <i>et al.</i> , 2007 [28]	FBG	Strain	Respiratory monitoring	/
D'Angelo <i>et al.</i> , 2008 [29]	FBG	Strain	Respiratory monitoring	/
Grillet <i>et al.</i> , 2007–2008 [30,31]	FBG	Strain	Respiratory monitoring	Strain up to 41.2%, Sensitivity ≈ 0.35 nm·% ⁻¹ , Accuracy ≈ 0.1 %
Silva <i>et al.</i> , 2011 [32]	FBG	Respiratory/heart rate (HR)/(RR)	Respiratory and cardiac monitoring	





UMC Utrecht

MR compatibility of Fiber Bragg Gratings (FBG)-based sensing for real-time needle tracking

M. Borot de Battisti¹, B. Denis de Senneville^{2,3}, M. Maenhout¹,
G. Hautvast⁴, D. Binnekamp⁴, J.J.W. Lagendijk¹, M. van
Vulpen¹, M.A. Moerland¹

¹University Medical Center Utrecht, Dept. of Radiotherapy, Utrecht, The Netherlands

²University Medical Center Utrecht, Imaging Division, Utrecht, The Netherlands

³University of Bordeaux, UMR 5251 CNRS, Bordeaux, France

⁴Philips Group Innovation - Biomedical Systems, Eindhoven, The Netherlands

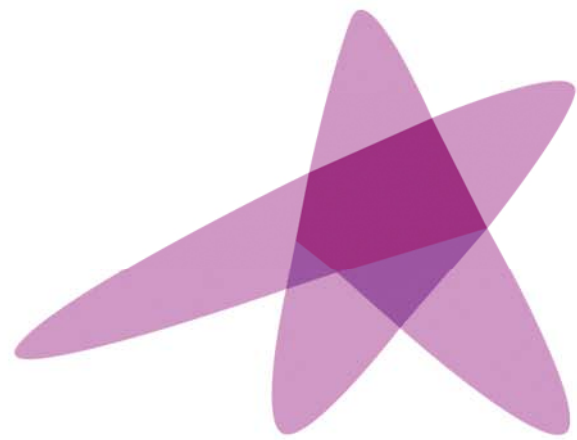
Real-time Tracking Technologies

They are coming

- Real-time position/angulation of needle, catheter or applicator (intelligent!)
- Fast and accurate HDR channel reconst. and tips
- Real-time tracking of seed drop location

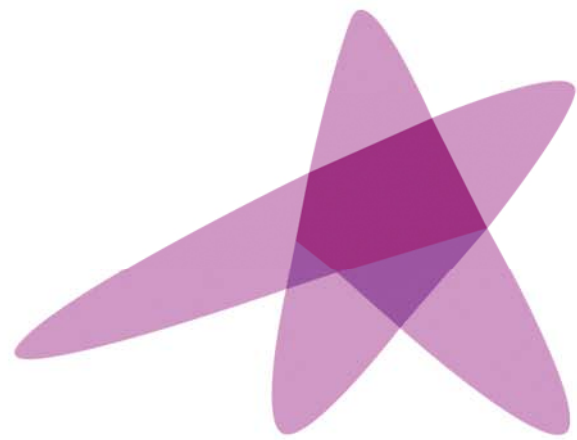
Could be incorporated in specific workflows

- Automated imaging plane display
- Real-time continuous dosimetry and replanning (Seed)
- QA of channel (reconstr., swapped, ...)



ESTRO

School



ESTRO
School

Advanced Brachytherapy Physics

Perspective on Future Progress for Brachytherapy Physics and Technological Advancements: Radionuclides and Novel Applicators

Prof. Mark J. Rivard, Ph.D., FAAPM

Advanced Brachytherapy Physics, 29 May – 1 June, 2016



Disclosures

Dr. Rivard serves as a consultant to CivaTech Oncology and a minor shareholder to Advanced Radiation Therapy, LLC

Opinions herein are solely those of the presenter, and are not meant to be interpreted as societal guidance.

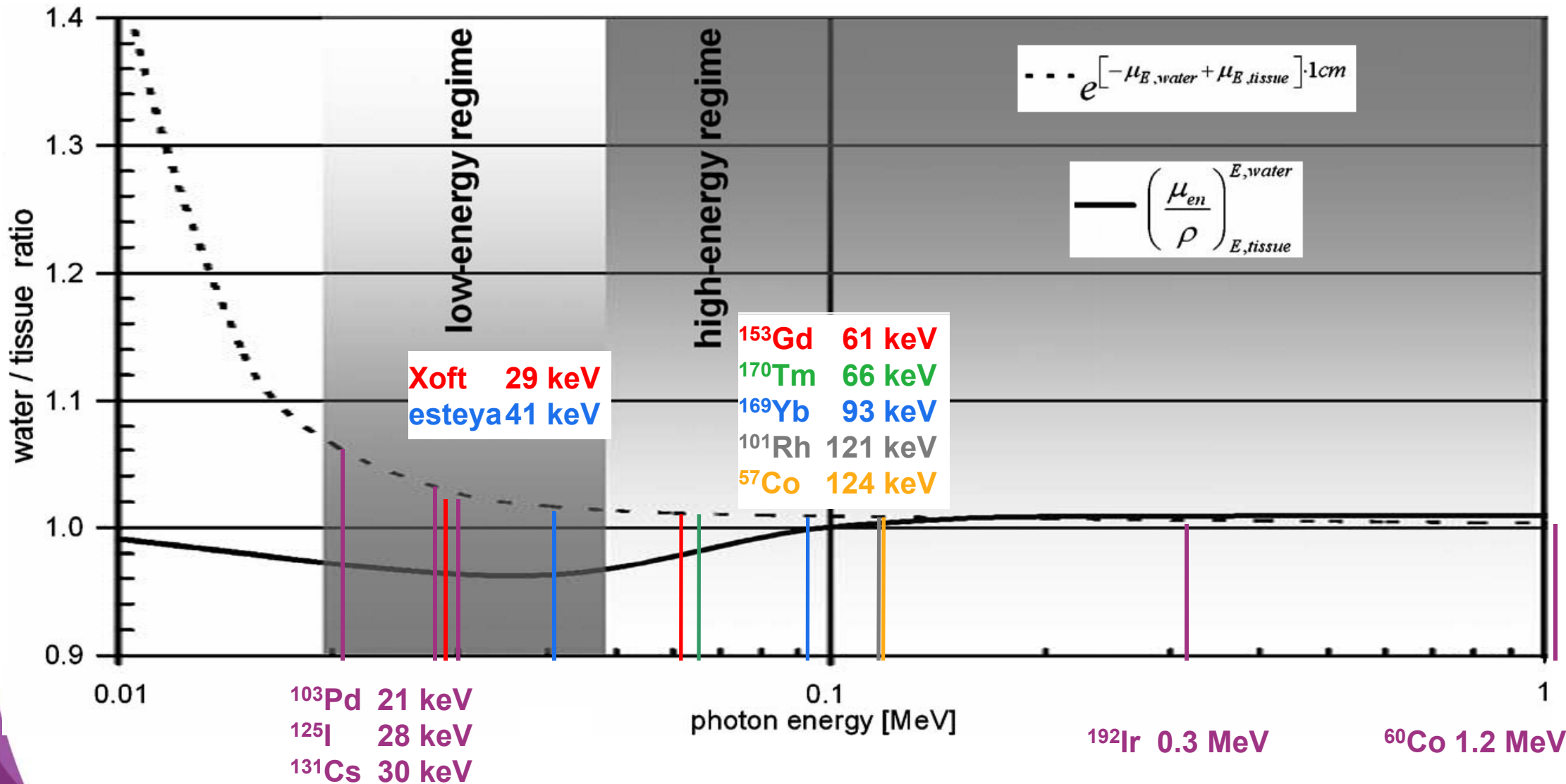
Specific commercial equipment, instruments, and materials are listed to fully describe the necessary procedures. Such identification does not imply endorsement by the presenter, nor that these products are necessarily the best available for these purposes.

Learning Objectives

1. Examine radiological properties of current and potential radionuclides. Consider if these differences will be clinically meaningful.
2. Learn about current novel BT sources and applicators and possibilities. Consider if these differences will be clinically meaningful.

New BT Radionuclides: Mean Photon Energy

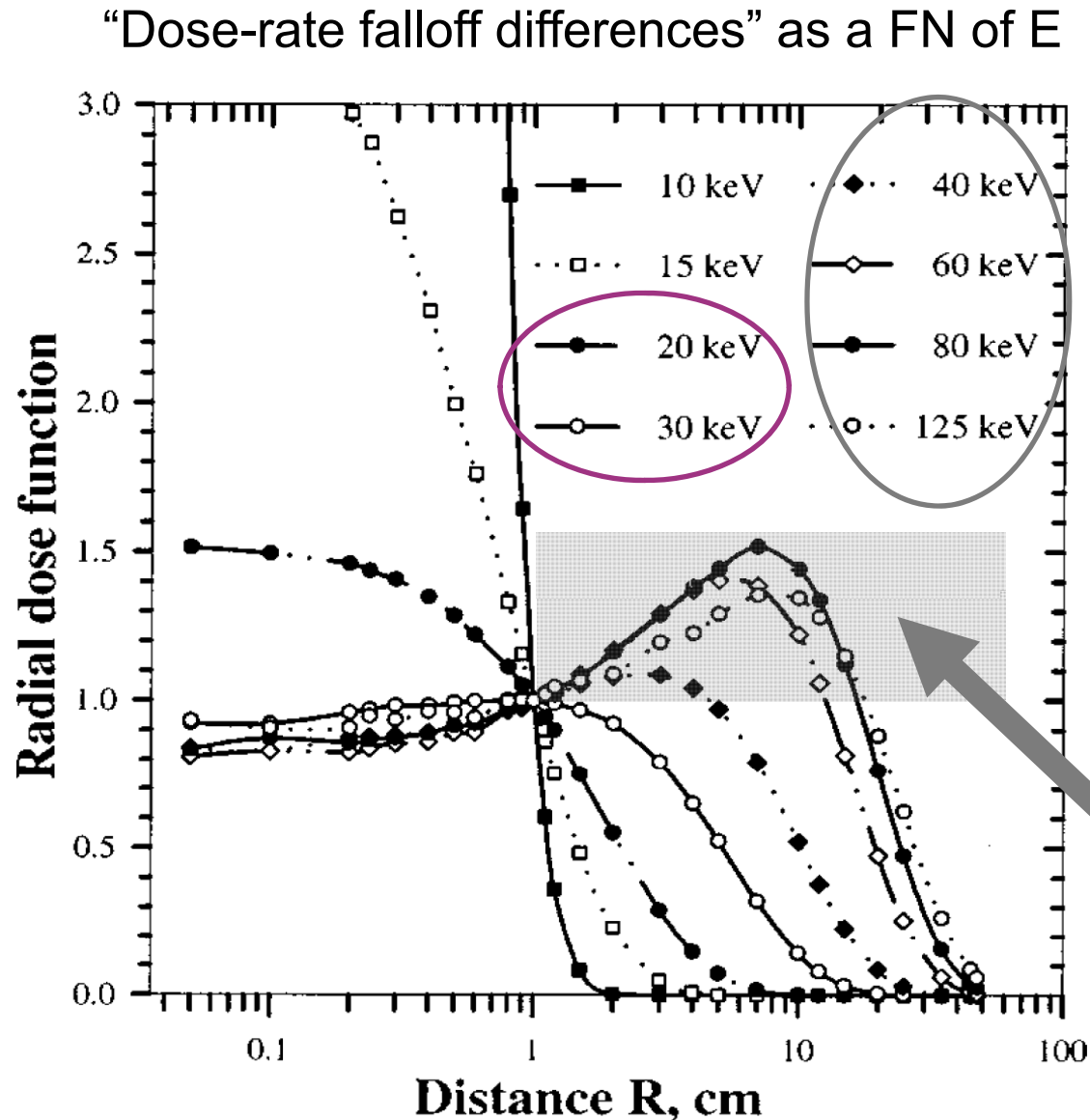
- How sensitive is dosimetry for novel radionuclides and eBT to material heterogeneities (and general differences with TG-43)?



New BT Radionuclides

established
low-E sources

^{103}Pd 21 keV
 ^{125}I 28 keV
 ^{131}Cs 30 keV

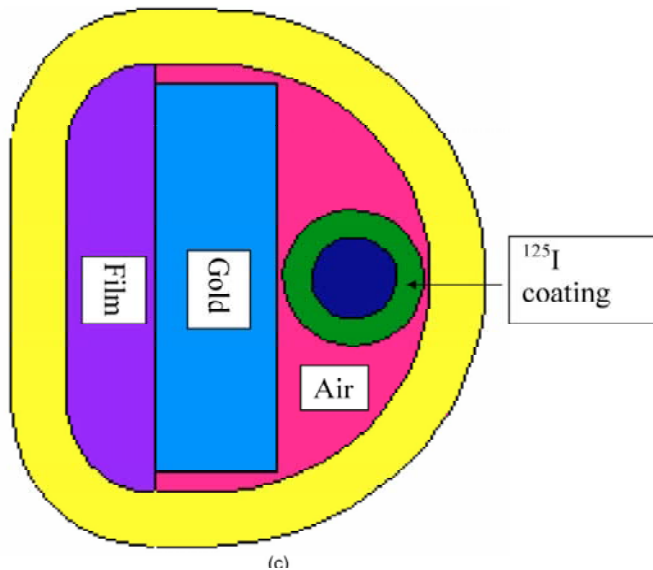
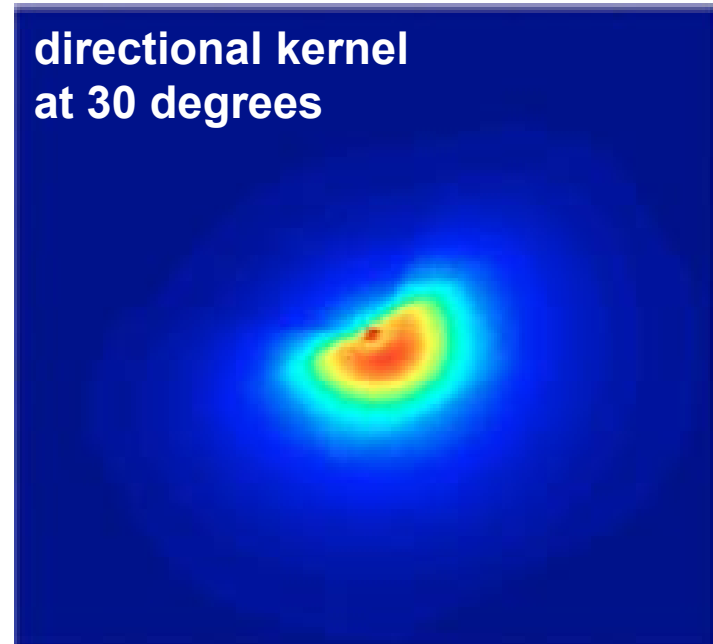
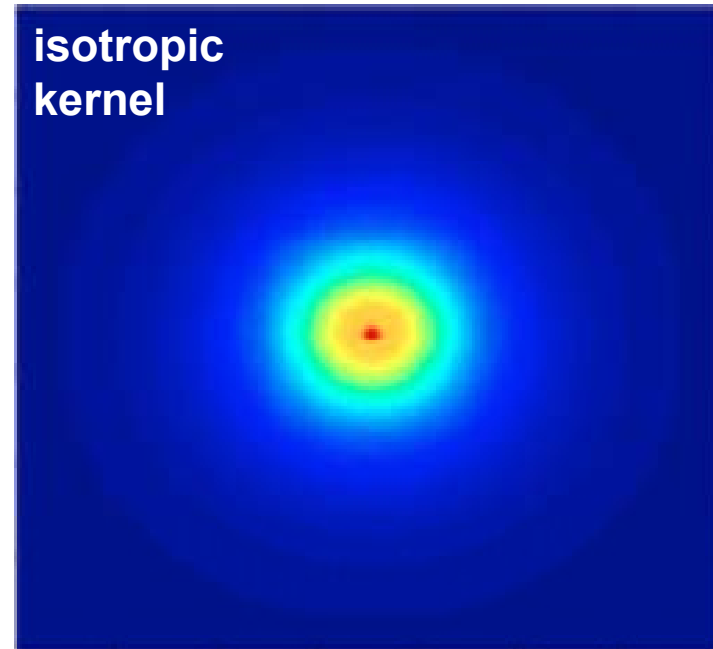
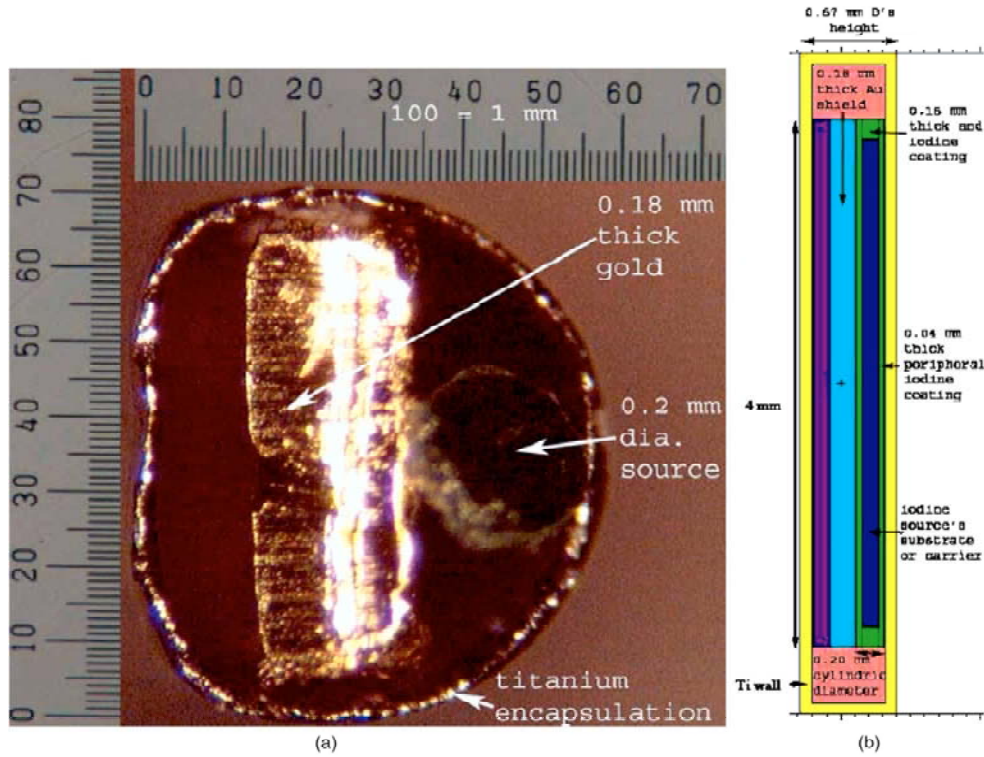


novel
sources

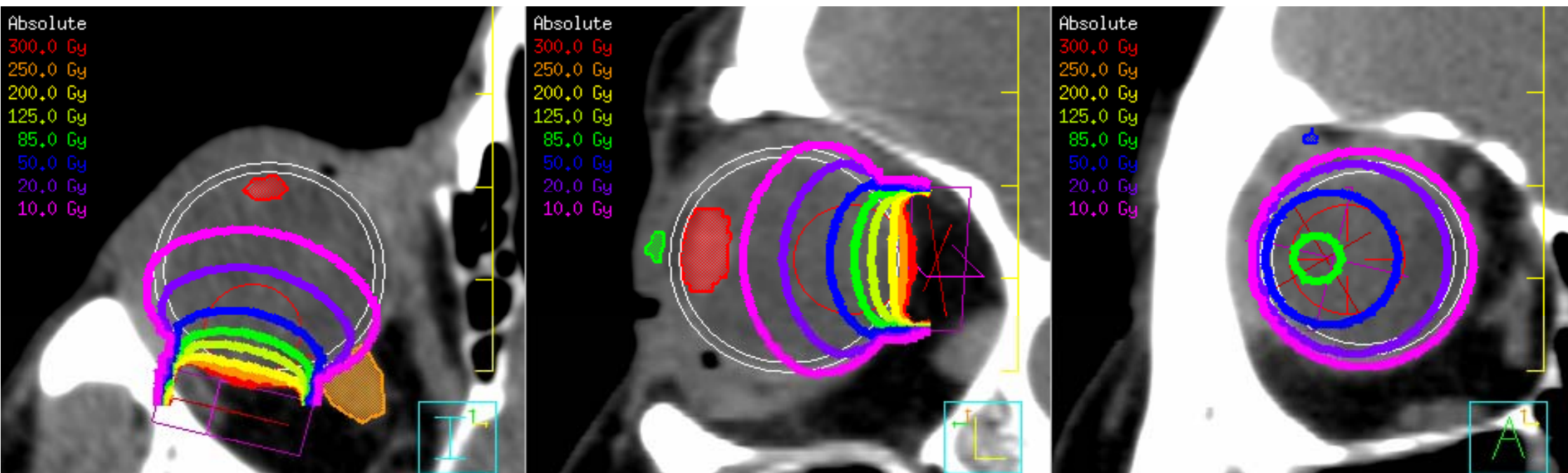
Xoft 29 keV
esteya 41 keV
 ^{153}Gd 61 keV
 ^{170}Tm 66 keV
 ^{169}Yb 93 keV
 ^{101}Rh 121 keV
 ^{57}Co 124 keV

dose increase
due to
radiation scatter

Extreme BT Shielding: LDR ^{125}I

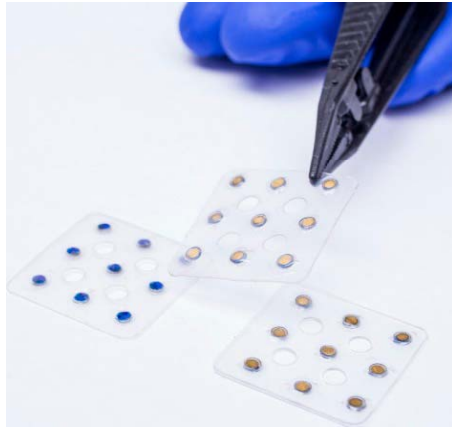


Extreme BT Shielding: LDR ^{125}I



Rivard, et al., *Med. Phys.* 36, 1968-1975 (2009)

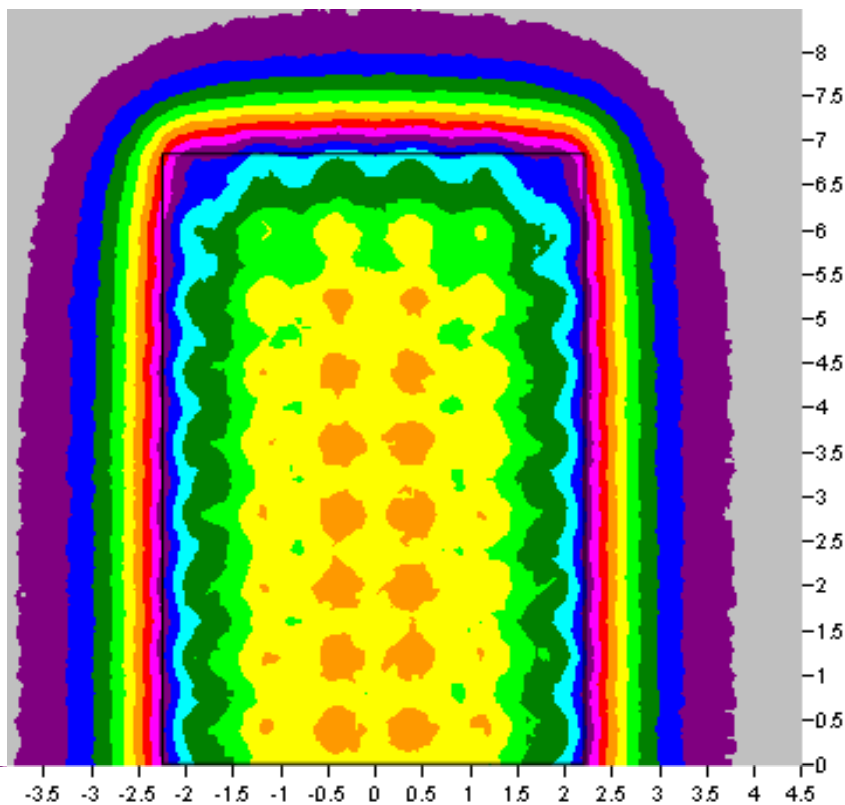
Extreme BT Shielding: LDR ^{103}Pd



CivaSheet

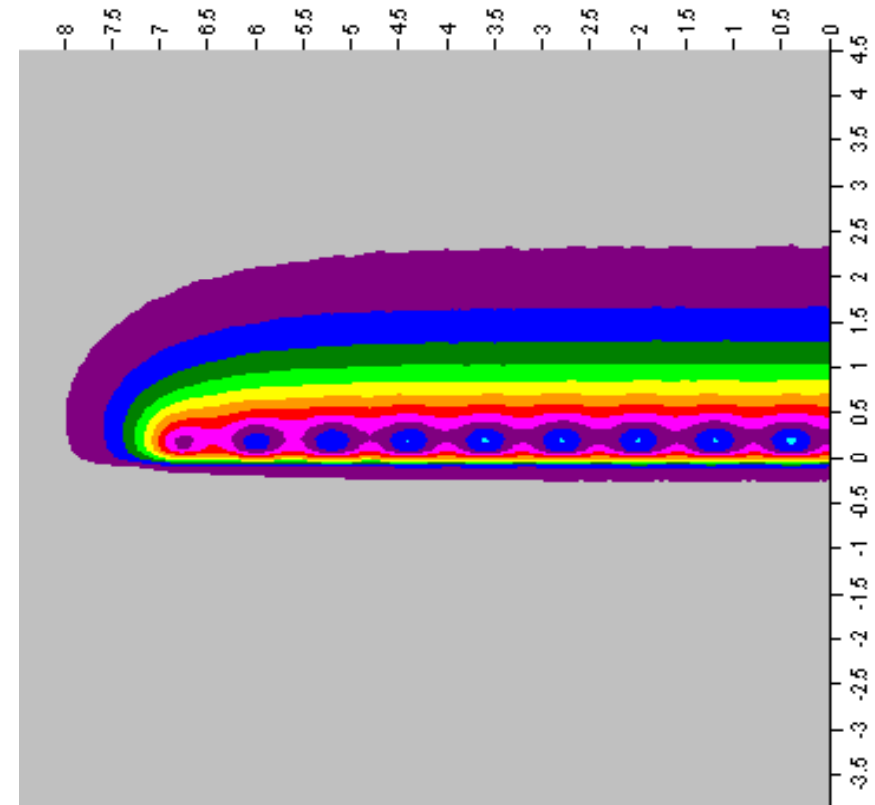
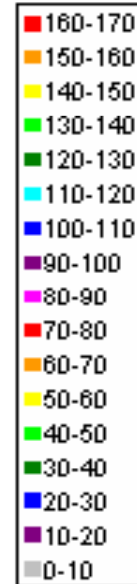


2.5 mm diam.



0.5 cm from front surface

Dose

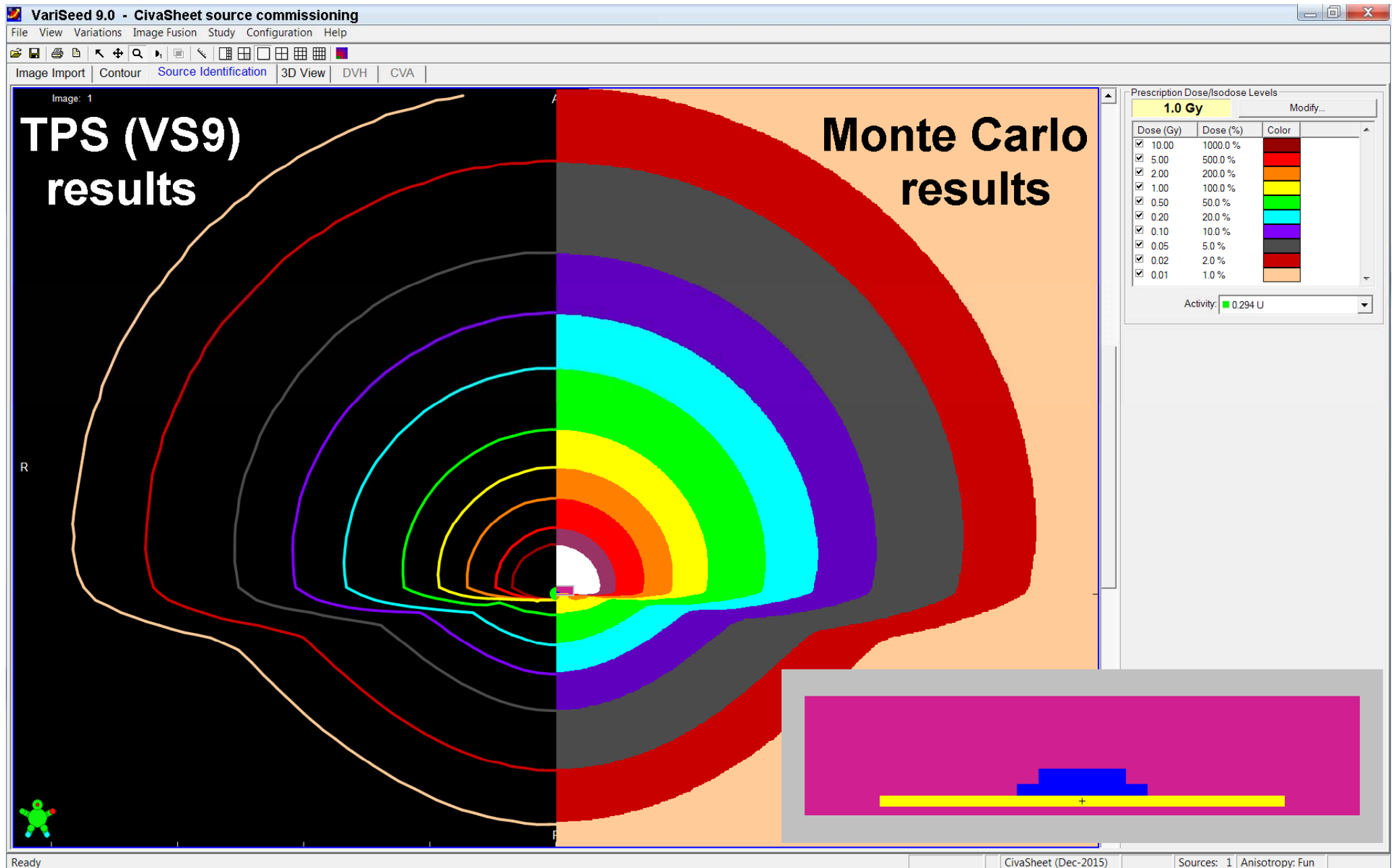


lateral view



Rivard, et al., work in progress

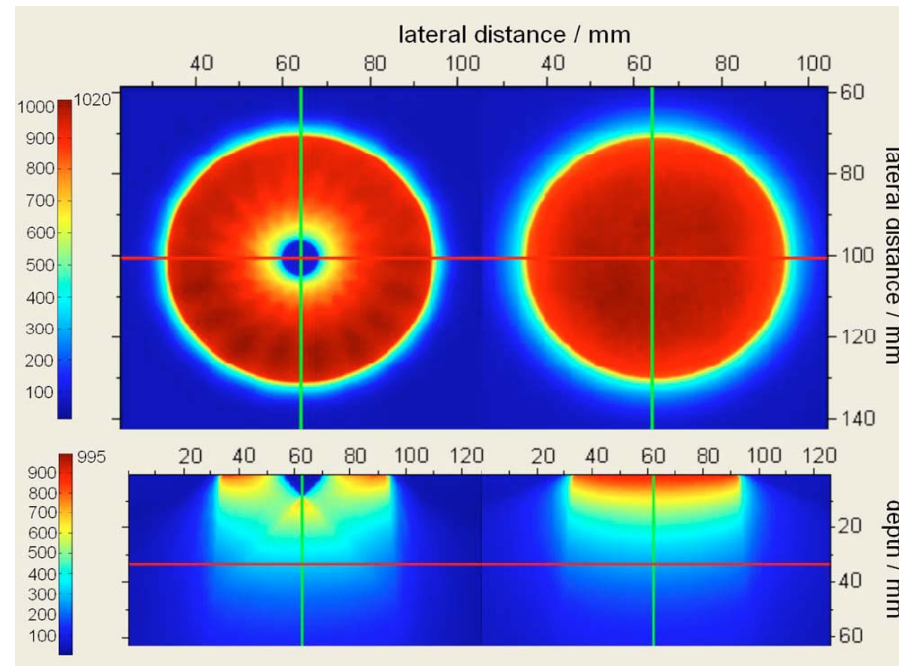
Extreme BT Shielding: LDR ^{103}Pd



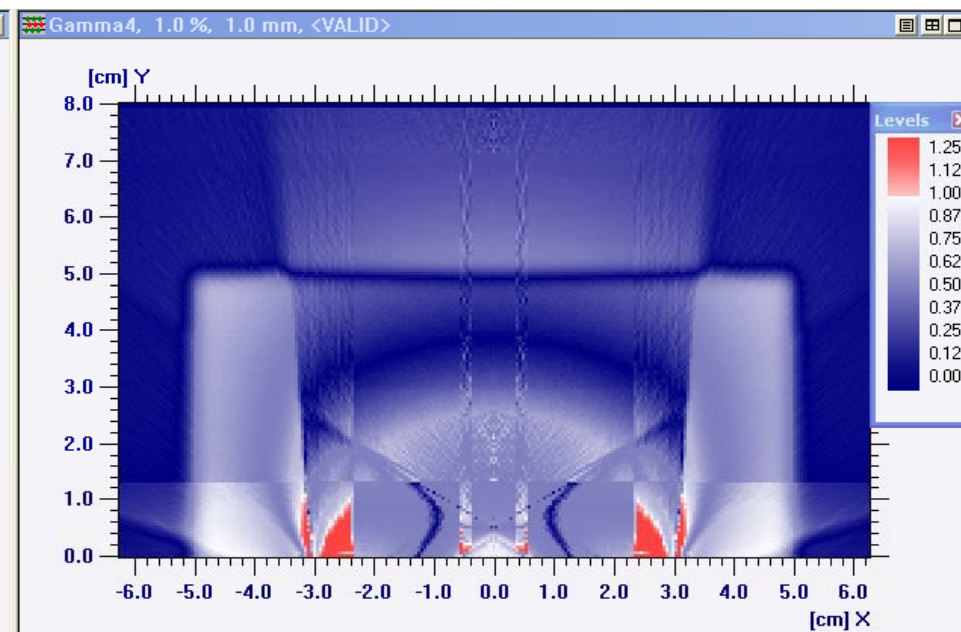
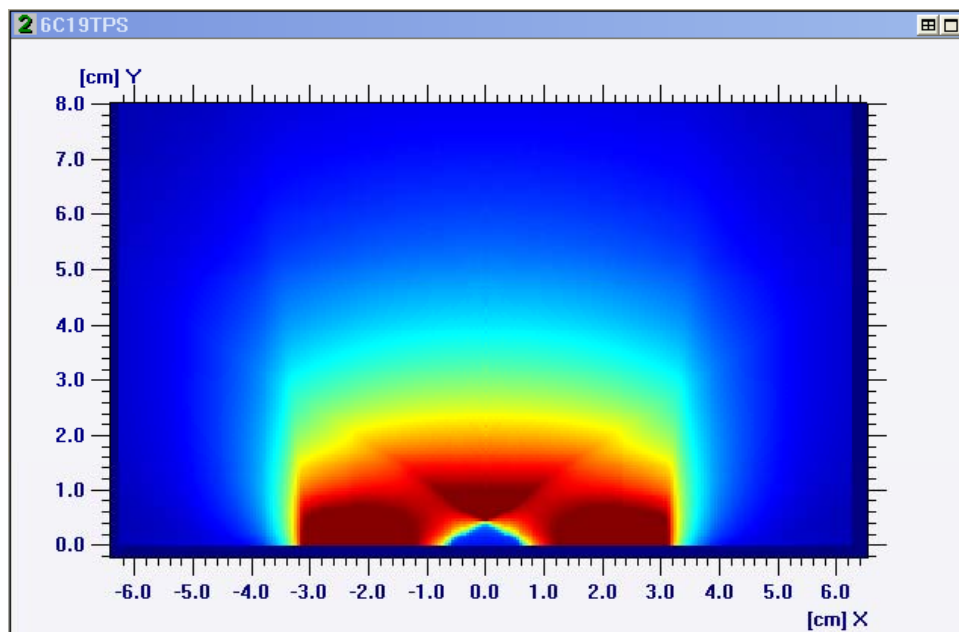
Rivard, et al., work in progress

Extreme BT Shielding: HDR ^{192}Ir

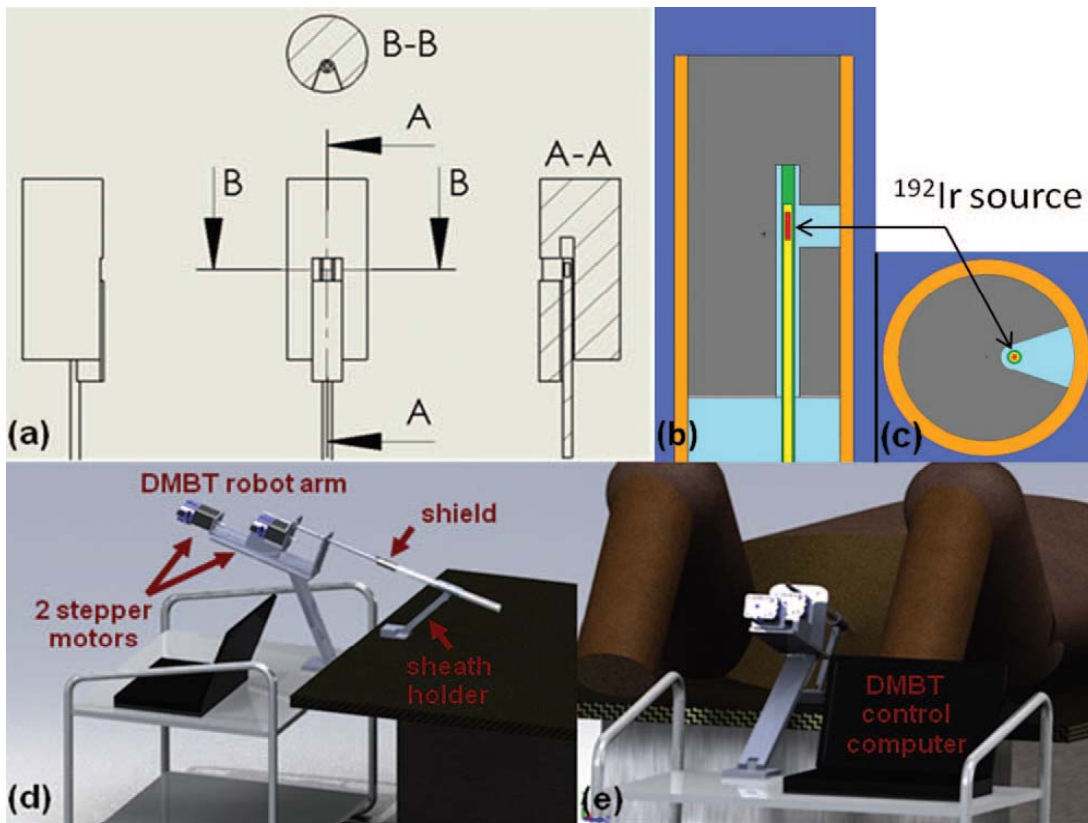
AccuBoost: non-invasive breast BT



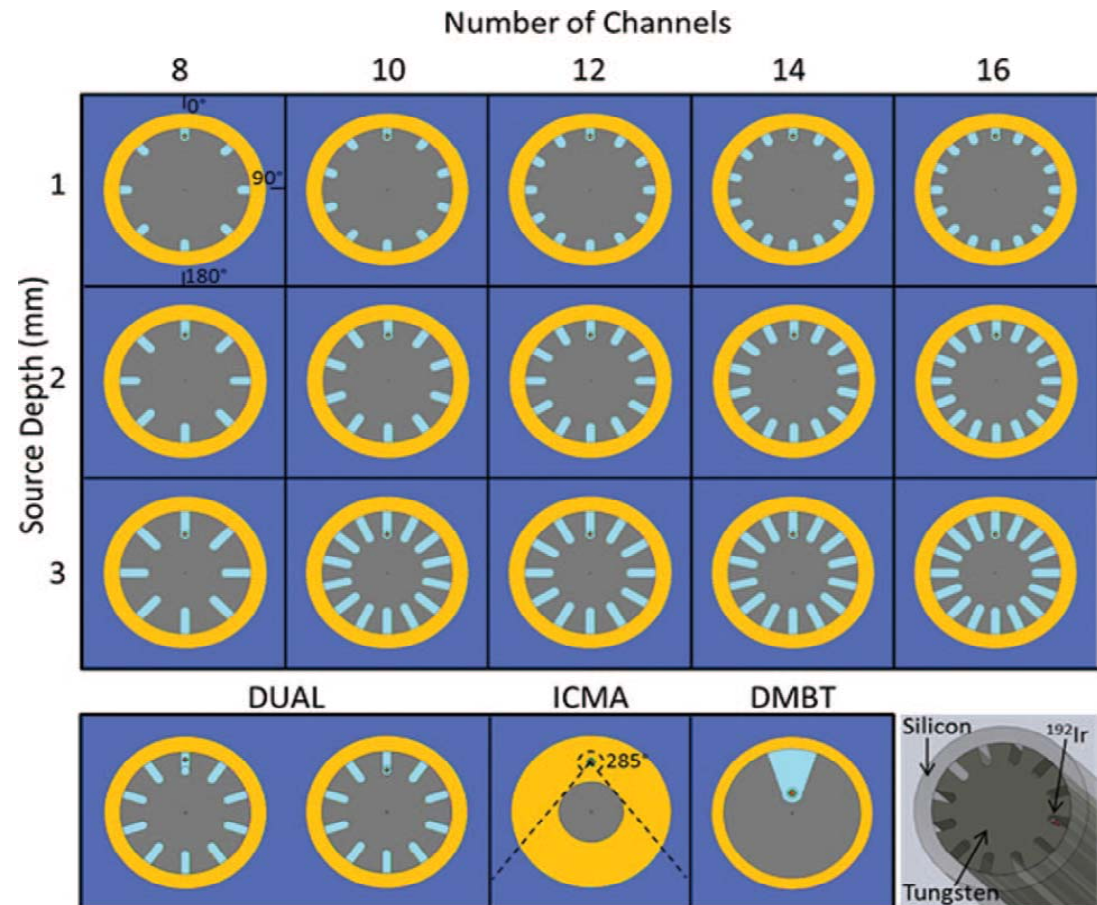
Yang, et al., *Med. Phys.* 38, 1519-1525 (2011) Yang and Rivard, *Med. Phys.* 37, 5665-5671 (2010)



Extreme BT Shielding: HDR ^{192}Ir

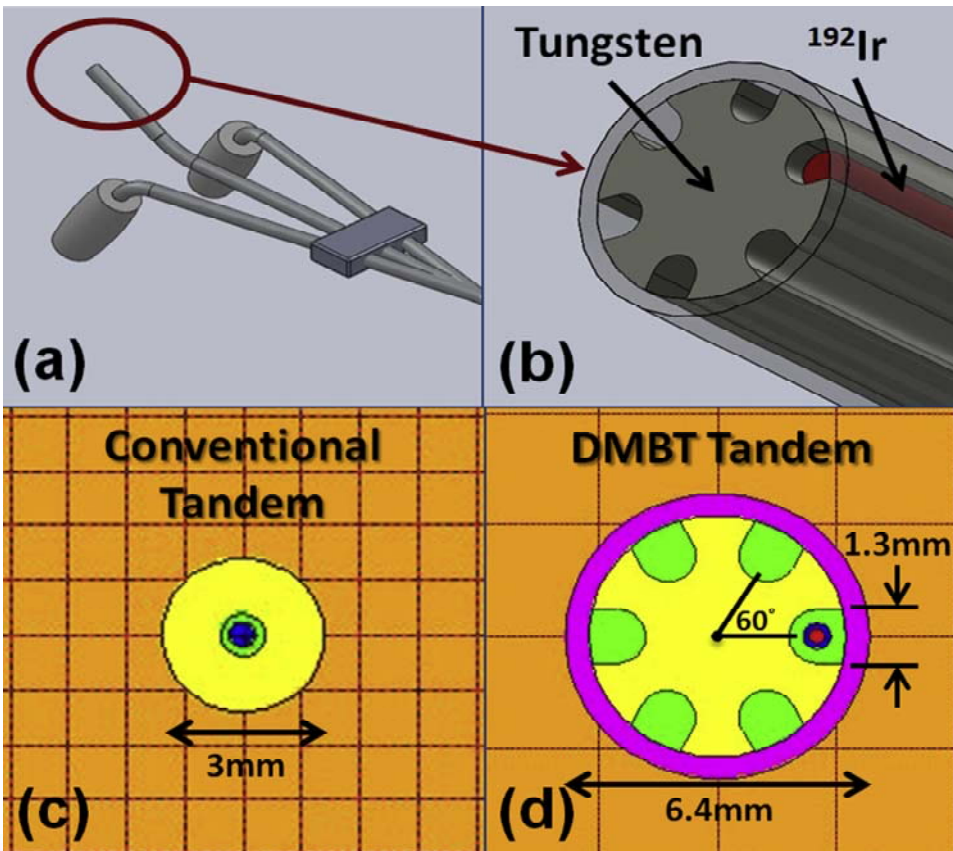


Webster, et al., *Med. Phys.* 40, 011718 (2013)

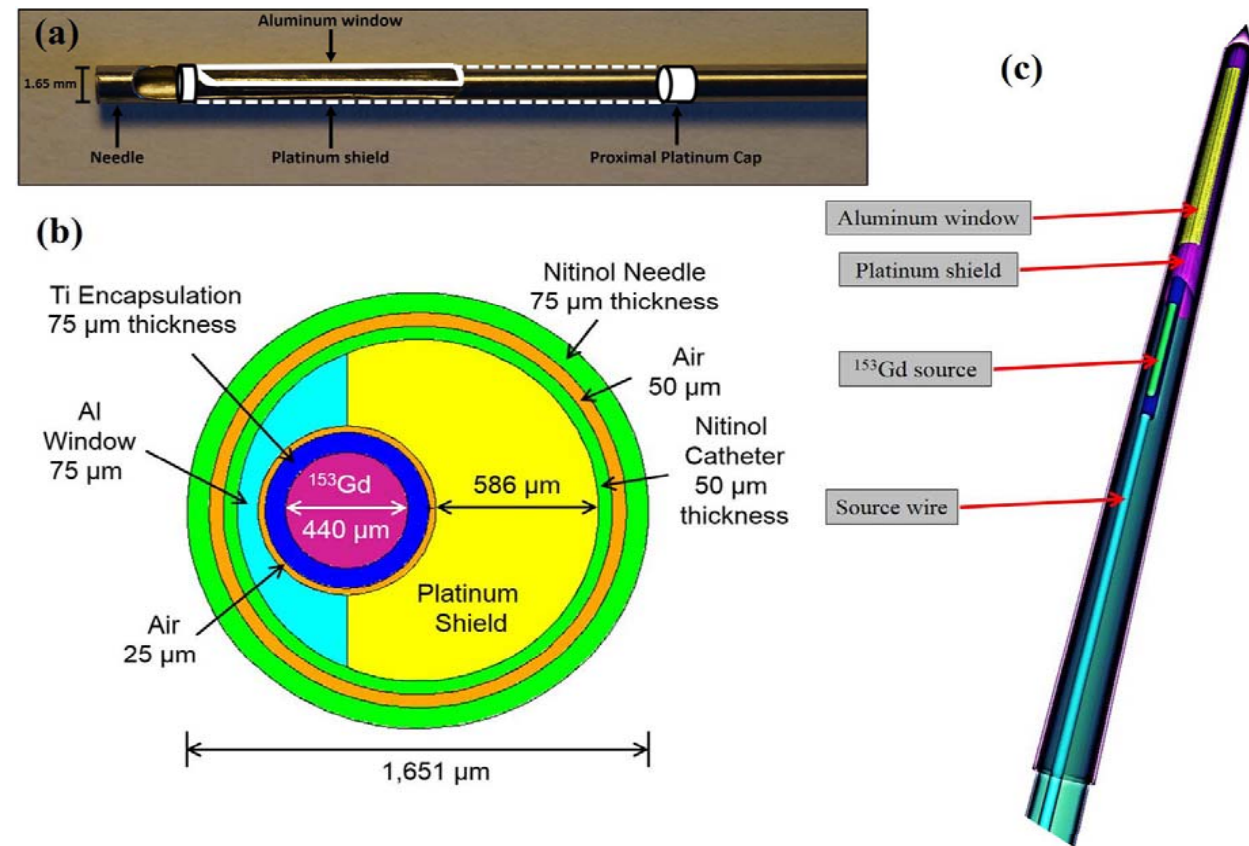


Webster, et al., *Med. Phys.* 40, 091704 (2013)

Extreme BT Shielding: HDR ^{192}Ir or ^{153}Gd

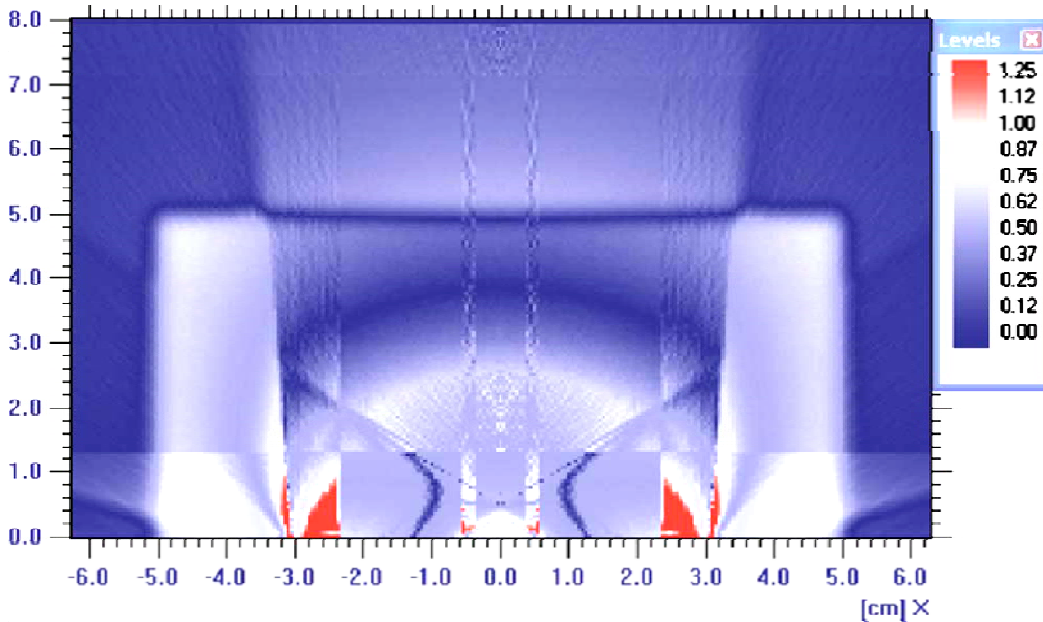
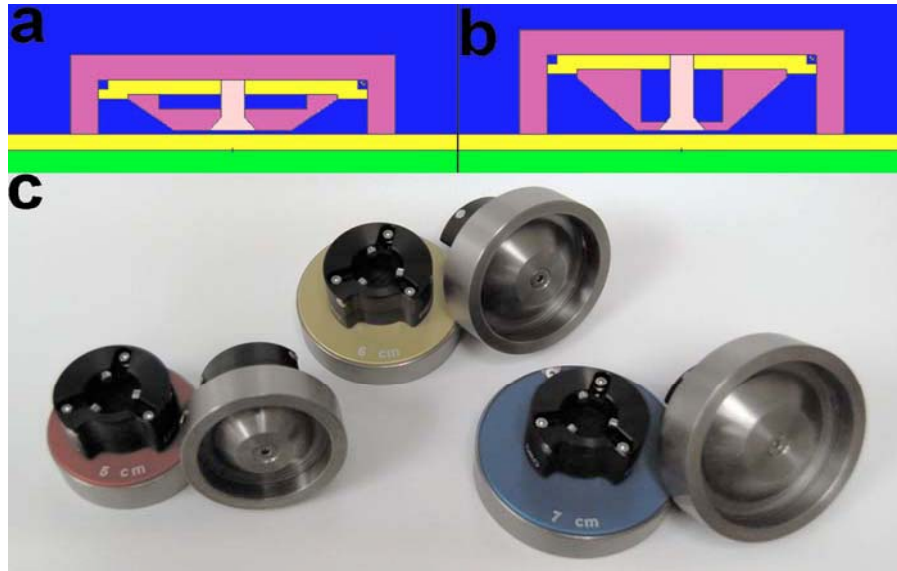


Han, et al., *IJROBP* 89, 666-673 (2014)



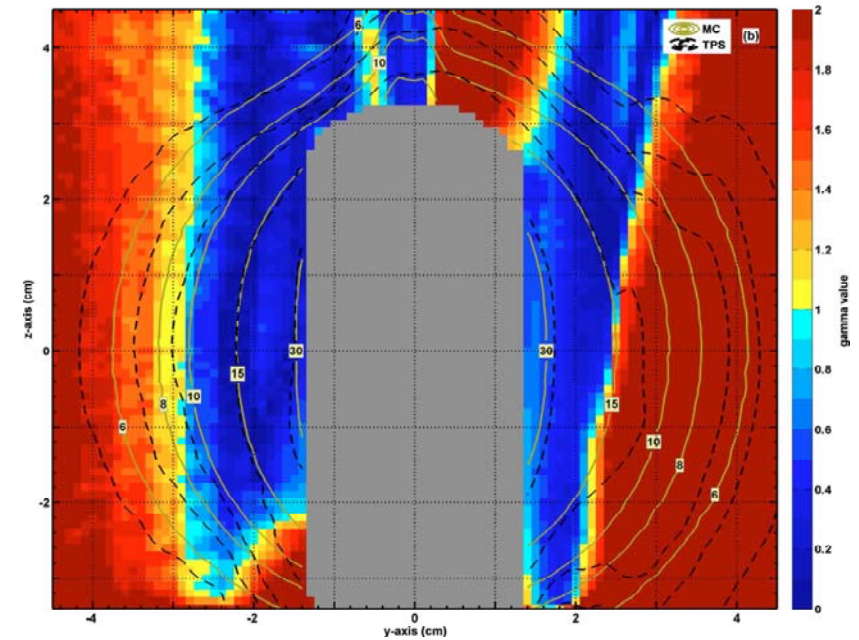
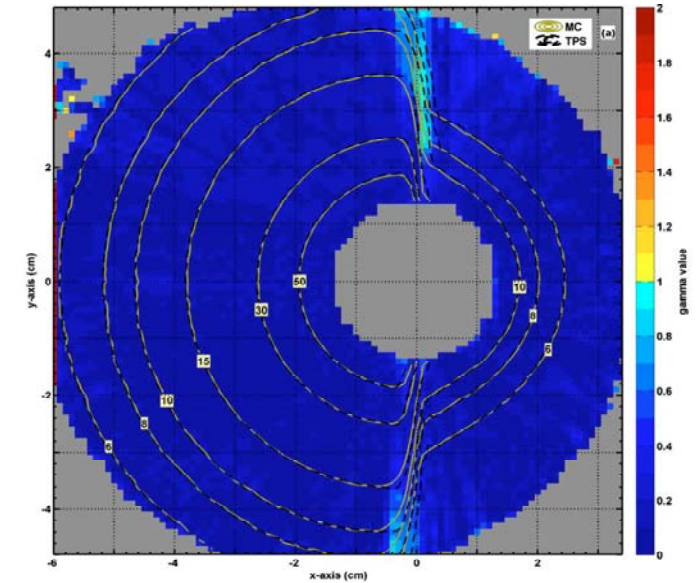
Adams, et al., *Med. Phys.* 41, 051703 (2014)

Need New TPS Evaluation Criteria



1% and 1 mm

Yang, et al., *Med. Phys.* (2011)



5% and 2 mm

Petrokokkinos, et al., *Med. Phys.* (2011)

What Would Olaf Do?



Summary

- new sources (radionuclides and eBT) fall in the energy range sensitive to scatter, requiring advanced BT dose calculations
- new sources and applicators have significant shielding, not compatible with current TPS based on simple TG-43
- commercially available (Acuros BV and Oncentra ACE) for ^{192}Ir (and academic-based TPS) can accurately calculate BT dose
- current and ongoing societal guidance for advanced BT dose calcs



... earn their trust